VOLUME 26 / NUMBER 20
OCTOBER 23, 1988
ACC. NOS. N88-26289 TO N88-27146

STAR
AN ABSTRACT JOURNAL

Scientific and Technical Aerospace Reports

PRODUCED BY THE
SCIENTIFIC AND TECHNICAL
INFORMATION
DIVISION

NASA

NATIONAL AERONAUTICS AND SPACE ADMINISTRATION

WHAT YOU CAN DO FOR *STAR*

All users of this abstract service are urged to forward reports to be considered for announcement in *STAR*. This will aid NASA in its efforts to provide the fullest possible coverage of all scientific and technical publications that might support aeronautics and space research and development. If you have prepared relevant reports (other than those that you will transmit to NASA, DoD, or DOE through the usual contract- or grant-reporting channels), please send them for consideration to the NASA Scientific and Technical Information Facility, P.O. Box 8757, B.W.I. Airport, Maryland 21240.

Reprints of journal articles, book chapters, and conference papers are also welcome. These will be considered for announcement in *STAR's* companion journal, *International Aerospace Abstracts.*

You may specify a particular source to be included in a report announcement if you wish; otherwise the report will be placed on public sale at the National Technical Information Service. Copyrighted publications will be announced but not distributed or sold.

PURCHASE OF *STAR*

The semimonthly issues are available for sale by the Superintendent of Documents, U.S. Government Printing Office, Washington, D.C. 20402.

PUBLISHED BY:

UNITED STATES GOVERNMENT
NATIONAL AERONAUTICS AND SPACE ADMINISTRATION
SCIENTIFIC AND TECHNICAL INFORMATION DIVISION
Scientific and Technical Aerospace Reports, Volume 26, is prepared by the NASA Scientific and Technical Information Facility operated for the National Aeronautics and Space Administration by RMS Associates.

The Administrator of the National Aeronautics and Space Administration has determined that the publication of this periodical is necessary in the transaction of the public business required by law of this Agency. Use of funds for printing this periodical has been approved by the Director of the Office of Management and Budget through March 22, 1989.

US ISSN 0036-8741

INTRODUCTION

Scientific and Technical Aerospace Reports (STAR) is a major component of a comprehensive National Aeronautics and Space Administration information system covering aeronautics, space, and supporting disciplines. *STAR* is issued on the 8th and 23rd of each month and announces current publications of the following types:

- NASA, NASA contractor, and NASA grantee reports
- Reports issued by other U.S. Government Agencies, domestic and foreign institutions, universities, and private firms
- Translations in report form
- NASA-owned patents and patent applications
- Dissertations and theses

Journal, book, and conference literature, cover-to-cover journal translations, and certain foreign dissertations are announced in a companion journal, *International Aerospace Abstracts (IAA)*, available on subscription from the American Institute of Aeronautics and Astronautics, Technical Information Service, 555 West 57th Street, 12th Floor, New York, New York 10019.

SUBJECT SCOPE

Subject scope of *STAR*, and *IAA* includes all aspects of aeronautics and space research and development, supporting basic and applied research, and applications. Aerospace aspects of earth resources, energy development, conservation, oceanography, environmental protection, urban transportation, and other topics of high national priority are also covered.

OTHER NASA PUBLICATIONS

Other NASA publications and information services are described in the publication, *The NASA Scientific and Technical Information System ... and How to Use It*, available without charge from the NASA Scientific and Technical Information Facility, P.O. Box 8757, B.W.I. Airport, Maryland 21240.

HOW TO USE *STAR* SUBJECT CATEGORIES

STAR is categorized by 10 major subject divisions divided into 76 specific subject categories and one general category/division. The major subject divisions are listed in the Table of Contents, together with a note for each that defines its scope and provides any cross-references. For example:

AERONAUTICS

Includes aeronautics (general); aerodynamics; air transportation and safety; aircraft communications and navigation; aircraft design, testing and performance; aircraft instrumentation; aircraft propulsion and power; aircraft stability and control; and research and support facilities (air).

For related information see also *Astronautics*.

Each major division is further divided into as many as nine specific categories, which are identified by category numbers.

Abstracts in *STAR* are grouped by specific category, the categories appearing in sequential order. Category breaks in the abstract section are identified by the category number and title, and a scope note. Cross-references to other categories are provided as appropriate. For example:

02 AERODYNAMICS

Includes aerodynamics of bodies, combinations, wings, rotors, and control surfaces; and internal flow in ducts and turbomachinery.

For related information see also *34 Fluid Mechanics and Heat Transfer.*

CROSS-REFERENCES

Individual *STAR* abstracts are not ordinarily cross-referenced, except for certain conference reports or book translations that have had separate abstracts written for their component papers or chapters. Citations and abstracts of the components follow immediately after those of the parent document. When the subject content of a component differs sufficiently from the general content of the parent, a cross-reference citation also is printed at the end of the category to which it normally would have been assigned if it were independent.

DOCUMENTS ON MICROFICHE

Documents on microfiche[1] are designated by a pound sign (#) following the accession number. The pound sign is used without regard to the source or quality of the microfiche.

AVAILABILITIES

One or more sources from which a document announced in *STAR* is available to the public is given in each citation. The most commonly indicated sources and their acronyms or abbreviations are listed below. If the publication is available from a source other than those listed, the publisher and his address will be displayed on the availability line or in combination with the corporate source line.

Avail: NTIS. Sold by the National Technical Information Service. Prices for hard copy (HC) and microfiche (MF) are indicated by a price code following the letters HC or MF in the *STAR* citation. Current values for the price codes are given in the tables on page vii.

Initially distributed microfiche under the NTIS SRIM (Selected Research in Microfiche) is available at greatly reduced unit prices. For this service and for information concerning subscription to NASA printed reports, consult the NTIS Subscription Section, Springfield, Va. 22161.

NOTE ON ORDERING DOCUMENTS: When ordering NASA publications (those followed by the * symbol), use the N accession number. NASA patent applications (only the specifications are offered) should be ordered by the US-Patent-Appl-SN number. Non-NASA publications (no asterisk) should be ordered by the AD, PB, or other *report number* shown on the last line of the citation, not by the N accession number. It is also advisable to cite the title and other bibliographic identification.

Avail: SOD (or GPO). Sold by the Superintendent of Documents, U.S. Government Printing Office, in hard copy. The current price and order number are given following the availability line. (NTIS will fill microfiche requests, as indicated above, for those documents identified by a # symbol.)

(1) A microfiche is a transparent sheet of film, 105 by 148 mm in size, containing as many as 60 to 98 pages of information reduced to micro images (not to exceed 26:1 reduction).

Avail: BLL (formerly NLL): British Library Lending Division, Boston Spa, Wetherby, Yorkshire, England. Photocopies available from this organization at the price shown. (If none is given, inquiry should be addressed to the BLL.)

Avail: DOE Depository Libraries. Organizations in U.S. cities and abroad that maintain collections of Department of Energy reports, usually in microfiche form, are listed in *Energy Research Abstracts*. Services available from the DOE and its depositories are described in a booklet, *DOE Technical Information Center - Its Functions and Services* (TID-4660), which may be obtained without charge from the DOE Technical Information Center.

Avail: ESDU. Pricing information on specific data, computer programs, and details on ESDU topic categories can be obtained from ESDU International Ltd. Requesters in North America should use the Virginia address while all other requesters should use the London address, both of which are on page vi.

Avail: Fachinformationszentrum, Karlsruhe. Sold by the Fachinformationszentrum Energie, Physik, Mathematik GMBH, Eggenstein Leopoldshafen, Federal Republic of Germany, at the price shown in deutschmarks (DM).

Avail: HMSO. Publications of Her Majesty's Stationery Office are sold in the U.S. by Pendragon House, Inc. (PHI), Redwood City, California. The U.S. price (including a service and mailing charge) is given, or a conversion table may be obtained from PHI.

Avail: NASA Public Document Rooms. Documents so indicated may be examined at or purchased from the National Aeronautics and Space Administration, Public Documents Room (Room 126), 600 Independence Ave., S.W., Washington, D.C. 20546, or public document rooms located at each of the NASA research centers, the NASA Space Technology Laboratories, and the NASA Pasadena Office at the Jet Propulsion Laboratory.

Avail: Univ. Microfilms. Documents so indicated are dissertations selected from *Dissertation Abstracts* and are sold by University Microfilms as xerographic copy (HC) and microfilm. All requests should cite the author and the Order Number as they appear in the citation.

Avail: US Patent and Trademark Office. Sold by Commissioner of Patents and Trademarks, U.S. Patent and Trademark Office, at the standard price of $1.50 each, postage free. (See discussion of NASA patents and patent applications below.)

Avail: (US Sales Only). These foreign documents are available to users within the United States from the National Technical Information Service (NTIS). They are available to users outside the United States through the International Nuclear Information Service (INIS) representative in their country, or by applying directly to the issuing organization.

Avail: USGS. Originals of many reports from the U.S. Geological Survey, which may contain color illustrations, or otherwise may not have the quality of illustrations preserved in the microfiche or facsimile reproduction, may be examined by the public at the libraries of the USGS field offices whose addresses are listed in this Introduction. The libraries may be queried concerning the availability of specific documents and the possible utilization of local copying services, such as color reproduction.

Avail: Issuing Activity, or Corporate Author, or no indication of availability. Inquiries as to the availability of these documents should be addressed to the organization shown in the citation as the corporate author of the document.

NASA PATENTS AND PATENT APPLICATIONS

Patents and patent applications owned by NASA are announced in *STAR* under appropriate subject categories and are referenced in the *STAR* indexes. In the Report/Accession Number Index, patents are indexed by the NASA Case Number (which appears in lieu of the report number in other indexes), the U.S. Patent Number, the U.S. Patent Application Serial Number, and the U.S. Patent Class. Patent applications for which patents have not yet been issued are indexed by the NASA Case Number and the U.S. Patent Application Serial Number.

NASA *patent application specifications* are sold in paper copy by the National Technical Information Service at price code A02. Microfiche are sold at price code A01. The US-Patent-Appl-SN- number should be used in ordering either paper copy or microfiche from NTIS. Printed copies of *patents* (which are not microfiched) are available for purchase at $1.50 per copy from:

Commissioner of Patents and Trademarks
U.S. Patent and Trademark Office
Washington, D.C. 20231

When ordering patents, the U.S. Patent Number should be used, and payment must be remitted in advance, preferably by money order or check payable to the Commissioner of Patents and Trademarks. Prepaid purchase coupons for ordering are also available from the Patent and Trademark Office. The patents and patent applications announced in *STAR* are owned by NASA and are available for royalty-free licensing. Requests for licensing terms and further information should be addressed to:

Associate General Counsel for Intellectual Property/Code GP
National Aeronautics and Space Administration
Washington, D.C. 20546

ELIGIBILITY AND REGISTRATION FOR NASA INFORMATION PRODUCTS AND SERVICES

A variety of services is available to organizations of the following types that have registered with NASA to receive specific services or products:

1. NASA offices, research centers, contractors, subcontractors, grantees, and consultants;
2. Other U.S. Government agencies and their contractors;
3. Libraries in the United States that have arrangements with NASA to maintain collections of NASA documents for public reference;
4. Other organizations in the United States having a need for NASA documents in work related to aeronautics and space research;
5. Organizations abroad that have established reciprocal document exchange arrangements with NASA.

Only the central service points or central points of document acquisition and control within qualified organizations are eligible to register for NASA products and services. Domestic organizations that may be eligible to receive various classes of NASA publications and services should address their requests for registration or for further information to:

NASA Scientific and Technical Information Facility
ATTN: Registration Activity
P.O. Box 8757
B.W.I. Airport, Maryland 21240

Organizations abroad should direct requests to the same address, but to the attention of: International Exchange Program.

AVAILABILITY OF *STAR* ABSTRACTS ON MICROFICHE

Microfiche of the abstract sections of this issue and other issues of *STAR* are available on annual subscription from NTIS as PB88-911300, Attn: Subscriptions, 5285 Port Royal Road, Springfield, Virginia 22161. Annual subscription rates are $70.00 North America; $140.00 foreign. Abstract sections for previous years retroactive to 1964 are available at the current rates. Microfiche for individual *STAR* issue abstract sections are not available.

PUBLIC COLLECTIONS OF NASA DOCUMENTS

DOMESTIC: NASA and NASA-sponsored documents and a large number of aerospace publications are available to the public for reference purposes at the library maintained by the American Institute of Aeronautics and Astronautics, Technical Information Service, 555 West 57th Street, 12th Floor, New York, New York 10019

EUROPEAN: An extensive collection of NASA and NASA-sponsored publications is maintained by the British Library Lending Division, Boston Spa, Wetherby, Yorkshire, England for public access. The British Library Lending Division also has available many of the non-NASA publications cited in *STAR*. European requesters may purchase facsimile copy or microfiche of NASA and NASA-sponsored documents, those identified by both the symbols # and * from ESA - Information Retrieval Service European Space Agency, 8-10 rue Mario-Nikis, 75738 Paris CEDEX 15, France.

FEDERAL DEPOSITORY LIBRARY PROGRAM

In order to provide the general public with greater access to U.S. Government publications, Congress established the Federal Depository Library Program under the Government Printing Office (GPO), with 50 regional depositories responsible for permanent retention of material, inter-library loan, and reference services. At least one copy of nearly every NASA and NASA-sponsored publication, either in printed or microfiche format, is received and retained by the 50 regional depositories. A list of the regional GPO libraries, arranged alphabetically by state, appears on the inside back cover. These libraries are *not* sales outlets. A local library can contact a Regional Depository to help locate specific reports, or direct contact may be made by an individual.

ADDRESSES OF ORGANIZATIONS

American Institute of Aeronautics and Astronautics
Technical Information Service
555 West 57th Street, 12th Floor
New York, New York 10019

British Library Lending Division,
Boston Spa, Wetherby, Yorkshire,
England

Commissioner of Patents and Trademarks
U.S. Patent and Trademark Office
Washington, D.C. 20231

Department of Energy
Technical Information Center
P.O. Box 62
Oak Ridge, Tennessee 37830

ESA-Information Retrieval Service
ESRIN
Via Galileo Galilei
00044 Frascati (Rome) Italy

ESDU International, Ltd.
1495 Chain Bridge Road
McLean, Virginia 22101

ESDU International, Ltd.
251-259 Regent Street
London, W1R 7AD, England

Fachinformationszentrum Energie, Physik, Mathematik GMBH
7514 Eggenstein Leopoldshafen
Federal Republic of Germany

Her Majesty's Stationery Office
P.O. Box 569, S.E. 1
London, England

NASA Scientific and Technical Information Facility
P.O. Box 8757
B.W.I. Airport, Maryland 21240

National Aeronautics and Space Administration
Scientific and Technical Information Division (NTT-1)
Washington, D.C. 20546

National Technical Information Service
5285 Port Royal Road
Springfield, Virginia 22161

Pendragon House, Inc.
899 Broadway Avenue
Redwood City, California 94063

Superintendent of Documents
U.S. Government Printing Office
Washington, D.C. 20402

University Microfilms
A Xerox Company
300 North Zeeb Road
Ann Arbor, Michigan 48106

University Microfilms, Ltd.
Tylers Green
London, England

U.S. Geological Survey Library
National Center - MS 950
12201 Sunrise Valley Drive
Reston, Virginia 22092

U.S. Geological Survey Library
2255 North Gemini Drive
Flagstaff, Arizona 86001

U.S. Geological Survey
345 Middlefield Road
Menlo Park, California 94025

U.S. Geological Survey Library
Box 25046
Denver Federal Center, MS914
Denver, Colorado 80225

NTIS PRICE SCHEDULES

(Effective January 1, 1988)

Schedule A
STANDARD PRICE DOCUMENTS AND MICROFICHE

PRICE CODE	NORTH AMERICAN PRICE	FOREIGN PRICE
A01	$ 6.95	$13.90
A02	9.95	19.90
A03	12.95	25.90
A04-A05	14.95	29.90
A06-A09	19.95	39.90
A10-A13	25.95	51.90
A14-A17	32.95	65.90
A18-A21	38.95	77.90
A22-A25	44.95	89.90
A99	*	*
NO1	49.50	89.90
NO2	48.00	80.00

Schedule E
EXCEPTION PRICE DOCUMENTS AND MICROFICHE

PRICE CODE	NORTH AMERICAN PRICE	FOREIGN PRICE
E01	$ 8.50	17.00
E02	11.00	22.00
E03	12.00	24.00
E04	14.50	29.00
E05	16.50	33.00
E06	19.00	38.00
E07	21.50	43.00
E08	24.00	48.00
E09	26.50	53.00
E10	29.00	58.00
E11	31.50	63.00
E12	34.00	68.00
E13	36.50	73.00
E14	39.50	79.00
E15	43.00	86.00
E16	47.00	94.00
E17	51.00	102.00
E18	55.00	110.00
E19	61.00	122.00
E20	71.00	142.00
E99	*	*

* Contact NTIS for price quote.

IMPORTANT NOTICE

NTIS Shipping and Handling Charges
U.S., Canada, Mexico — ADD $3.00 per TOTAL ORDER
All Other Countries — ADD $4.00 per TOTAL ORDER

Exceptions — Does NOT apply to:
ORDERS REQUESTING NTIS RUSH HANDLING
ORDERS FOR SUBSCRIPTION OR STANDING ORDER PRODUCTS *ONLY*

NOTE: Each additional delivery address on an order requires a separate shipping and handling charge.

VOLUME 26 NUMBER 20 / OCTOBER 23, 1988

TABLE OF CONTENTS

AERONAUTICS

Includes aeronautics (general); aerodynamics; air transportation and safety; aircraft communications and navigation; aircraft design, testing and performance; aircraft instrumentation; aircraft propulsion and power; aircraft stability and control; and research and support facilities (air).

For related information see also *Astronautics.*

01 AERONAUTICS (GENERAL) 2745

02 AERODYNAMICS 2751

Includes aerodynamics of bodies, combinations, wings, rotors, and control surfaces; and internal flow in ducts and turbomachinery.

For related information see also *34 Fluid Mechanics and Heat Transfer*

03 AIR TRANSPORTATION AND SAFETY 2755

Includes passenger and cargo air transport operations; and aircraft accidents.

For related information see also *16 Space Transportation* and *85 Urban Technology and Transportation.*

04 AIRCRAFT COMMUNICATIONS AND NAVIGATION 2756

Includes digital and voice communication with aircraft; air navigation systems (satellite and ground based); and air traffic control.

For related information see also *17 Space Communications, Spacecraft Communications, Command and Tracking* and *32 Communications and Radar.*

05 AIRCRAFT DESIGN, TESTING AND PERFORMANCE 2757

Includes aircraft simulation technology.

For related information see also *18 Spacecraft Design, Testing and Performance* and *39 Structural Mechanics.* For land transportation vehicles see *85 Urban Technology and Transportation.*

06 AIRCRAFT INSTRUMENTATION 2760

Includes cockpit and cabin display devices; and flight instruments.

For related information see also *19 Spacecraft Instrumentation* and *35 Instrumentation and Photography.*

07 AIRCRAFT PROPULSION AND POWER 2760

Includes prime propulsion systems and systems components, e.g., gas turbine engines and compressors; and onboard auxiliary power plants for aircraft.

For related information see also *20 Spacecraft Propulsion and Power, 28 Propellants and Fuels,* and *44 Energy Production and Conversion.*

08 AIRCRAFT STABILITY AND CONTROL 2761

Includes aircraft handling qualities; piloting; flight controls; and autopilots.

For related information see also *05 Aircraft Design, Testing and Performance.*

09 RESEARCH AND SUPPORT FACILITIES (AIR) 2762

Includes airports, hangars and runways; aircraft repair and overhaul facilities; wind tunnels; shock tubes; and aircraft engine test stands.

For related information see also *14 Ground Support Systems and Facilities (Space).*

ASTRONAUTICS

Includes astronautics (general); astrodynamics; ground support systems and facilities (space); launch vehicles and space vehicles; space transportation; space communications, spacecraft communications, command and tracking; spacecraft design, testing and performance; spacecraft instrumentation; and spacecraft propulsion and power.

For related information see also *Aeronautics*

12 ASTRONAUTICS (GENERAL) 2762

For extraterrestrial exploration see *91 Lunar and Planetary Exploration.*

13 ASTRODYNAMICS N.A.

Includes powered and free-flight trajectories; and orbital and launching dynamics.

14 GROUND SUPPORT SYSTEMS AND FACILITIES (SPACE) 2763

Includes launch complexes, research and production facilities; ground support equipment, e.g., mobile transporters; and simulators.

For related information see also *09 Research and Support Facilities (Air).*

15 LAUNCH VEHICLES AND SPACE VEHICLES N.A.

Includes boosters; operating problems of launch/space vehicle systems; and reusable vehicles.

For related information see also *20 Spacecraft Propulsion and Power.*

16 SPACE TRANSPORTATION 2764

Includes passenger and cargo space transportation, e.g., shuttle operations; and space rescue techniques.

For related information see also *03 Air Transportation and Safety* and *18 Spacecraft Design, Testing and Performance.* For space suits see *54 Man/System Technology and Life Support.*

17 SPACE COMMUNICATIONS, SPACECRAFT COMMUNICATIONS, COMMAND AND TRACKING N.A.

Includes telemetry; space communications networks; astronavigation and guidance; and radio blackout.

For related information see also *04 Aircraft Communications and Navigation* and *32 Communications and Radar.*

18 SPACECRAFT DESIGN, TESTING AND PERFORMANCE 2764

Includes satellites; space platforms; space stations; spacecraft systems and components such as thermal and environmental controls; and attitude controls.

For life support systems see *54 Man/System Technology and Life Support.* For related information see also *05 Aircraft Design, Testing and Performance, 39 Structural Mechanics,* and *16 Space Transportation.*

19 SPACECRAFT INSTRUMENTATION N.A.

For related information see also *06 Aircraft Instrumentation* and *35 Instrumentation and Photography.*

20 SPACECRAFT PROPULSION AND POWER 2766

Includes main propulsion systems and components, e.g. rocket engines; and spacecraft auxiliary power sources.

For related information see also *07 Aircraft Propulsion and Power, 28 Propellants and Fuels, 44 Energy Production and Conversion,* and *15 Launch Vehicles and Space Vehicles.*

CHEMISTRY AND MATERIALS

Includes chemistry and materials (general); composite materials; inorganic and physical chemistry; metallic materials; nonmetallic materials; propellants and fuels; and materials processing.

23 CHEMISTRY AND MATERIALS (GENERAL) 2767

24 COMPOSITE MATERIALS 2767

Includes physical, chemical, and mechanical properties of laminates and other composite materials.

For ceramic materials see *27 Nonmetallic Materials.*

25 INORGANIC AND PHYSICAL CHEMISTRY 2768

Includes chemical analysis, e.g., chromatography; combustion theory; electrochemistry; and photochemistry.

For related information see also *77 Thermodynamics and Statistical Physics.*

26 METALLIC MATERIALS 2771

Includes physical, chemical, and mechanical properties of metals, e.g., corrosion; and metallurgy.

27 NONMETALLIC MATERIALS 2776

Includes physical, chemical, and mechanical properties of plastics, elastomers, lubricants, polymers, textiles, adhesives, and ceramic materials.

For composite materials see *24 Composite Materials.*

28 PROPELLANTS AND FUELS 2780

Includes rocket propellants, igniters and oxidizers; their storage and handling procedures; and aircraft fuels.

For related information see also *07 Aircraft Propulsion and Power, 20 Spacecraft Propulsion and Power,* and *44 Energy Production and Conversion.*

29 MATERIALS PROCESSING 2782

Includes space-based development of products and processes for commercial application.

For biological materials see *55 Space Biology.*

ENGINEERING

Includes engineering (general); communications and radar; electronics and electrical engineering; fluid mechanics and heat transfer; instrumentation and photography; lasers and masers; mechanical engineering; quality assurance and reliability; and structural mechanics.

For related information see also *Physics.*

31 ENGINEERING (GENERAL) 2782

Includes vacuum technology; control engineering; display engineering; cryogenics; and fire prevention.

32 COMMUNICATIONS AND RADAR 2788

Includes radar; land and global communications; communications theory; and optical communications.

For related information see also *04 Aircraft Communications and Navigation* and *17 Space Communications, Spacecraft Communications, Command and Tracking.* For search and rescue see *03 Air Transportation and Safety,* and *16 Space Transportation.*

33 ELECTRONICS AND ELECTRICAL ENGINEERING 2793

Includes test equipment and maintainability; components, e.g., tunnel diodes and transistors; microminiaturization; and integrated circuitry.

For related information see also *60 Computer Operations and Hardware* and *76 Solid-State Physics.*

34 FLUID MECHANICS AND HEAT TRANSFER 2797

Includes boundary layers; hydrodynamics; fluidics; mass transfer and ablation cooling.

For related information see also *02 Aerodynamics* and *77 Thermodynamics and Statistical Physics.*

35 INSTRUMENTATION AND PHOTOGRAPHY 2805

Includes remote sensors; measuring instruments and gages; detectors; cameras and photographic supplies; and holography.

For aerial photography see *43 Earth Resources and Remote Sensing.* For related information see also *06 Aircraft Instrumentation* and *19 Spacecraft Instrumentation.*

36 LASERS AND MASERS 2806

Includes parametric amplifiers.

For related information see also *76 Solid-State Physics.*

37 MECHANICAL ENGINEERING 2808

Includes auxiliary systems (nonpower); machine elements and processes; and mechanical equipment.

38 QUALITY ASSURANCE AND RELIABILITY 2812

Includes product sampling procedures and techniques; and quality control.

39 STRUCTURAL MECHANICS 2812

Includes structural element design and weight analysis; fatigue; and thermal stress.

For applications see *05 Aircraft Design, Testing and Performance* and *18 Spacecraft Design, Testing and Performance.*

GEOSCIENCES

Includes geosciences (general); earth resources and remote sensing; energy production and conversion; environment pollution; geophysics; meteorology and climatology; and oceanography.

For related information see also *Space Sciences.*

42 GEOSCIENCES (GENERAL) N.A.

43 EARTH RESOURCES AND REMOTE SENSING 2816

Includes remote sensing of earth resources by aircraft and spacecraft; photogrammetry; and aerial photography.

For instrumentation see *35 Instrumentation and Photography.*

44 ENERGY PRODUCTION AND CONVERSION 2818

Includes specific energy conversion systems, e.g., fuel cells; global sources of energy; geophysical conversion; and windpower.

For related information see also *07 Aircraft Propulsion and Power, 20 Spacecraft Propulsion and Power,* and *28 Propellants and Fuels.*

45 ENVIRONMENT POLLUTION 2821

Includes atmospheric, noise, thermal, and water pollution.

46 GEOPHYSICS 2823

Includes aeronomy; upper and lower atmosphere studies; ionospheric and magnetospheric physics; and geomagnetism.

For space radiation see *93 Space Radiation.*

47 METEOROLOGY AND CLIMATOLOGY 2825

Includes weather forecasting and modification.

48 OCEANOGRAPHY 2828

Includes biological, dynamic, and physical oceanography; and marine resources.

For related information see also *43 Earth Resources and Remote Sensing.*

LIFE SCIENCES

Includes life sciences (general); aerospace medicine; behavioral sciences; man/system technology and life support; and space biology.

51 LIFE SCIENCES (GENERAL) 2829

52 AEROSPACE MEDICINE 2831

Includes physiological factors; biological effects of radiation; and effects of weightlessness on man and animals.

53 BEHAVIORAL SCIENCES 2832

Includes psychological factors; individual and group behavior; crew training and evaluation; and psychiatric research.

54 MAN/SYSTEM TECHNOLOGY AND LIFE SUPPORT 2833

Includes human engineering; biotechnology; and space suits and protective clothing.

For related information see also *16 Space Transportation.*

55 SPACE BIOLOGY N.A.

Includes exobiology; planetary biology; and extraterrestrial life.

MATHEMATICAL AND COMPUTER SCIENCES

Includes mathematical and computer sciences (general); computer operations and hardware; computer programming and software; computer systems; cybernetics; numerical analysis; statistics and probability; systems analysis; and theoretical mathematics.

59 MATHEMATICAL AND COMPUTER SCIENCES (GENERAL) N.A.

60 COMPUTER OPERATIONS AND HARDWARE 2834

Includes hardware for computer graphics, firmware, and data processing.

For components see *33 Electronics and Electrical Engineering.*

61 COMPUTER PROGRAMMING AND SOFTWARE 2836

Includes computer programs, routines, algorithms, and specific applications, e.g., CAD/CAM.

62 COMPUTER SYSTEMS 2841

Includes computer networks and special application computer systems.

63 CYBERNETICS 2842

Includes feedback and control theory, artificial intelligence, robotics and expert systems.

For related information see also *54 Man/System Technology and Life Support.*

64 NUMERICAL ANALYSIS 2843

Includes iteration, difference equations, and numerical approximation.

65 STATISTICS AND PROBABILITY 2846

Includes data sampling and smoothing; Monte Carlo method; and stochastic processes.

66 SYSTEMS ANALYSIS 2847

Includes mathematical modeling; network analysis; and operations research.

67 THEORETICAL MATHEMATICS 2848

Includes topology and number theory.

PHYSICS

Includes physics (general); acoustics; atomic and molecular physics; nuclear and high-energy physics; optics; plasma physics; solid-state physics; and thermodynamics and statistical physics.

For related information see also *Engineering.*

70 PHYSICS (GENERAL) 2848

For precision time and time interval (PTTI) see *35 Instrumentation and Photography;* for geophysics, astrophysics or solar physics see *46 Geophysics, 90 Astrophysics,* or *92 Solar Physics.*

71 ACOUSTICS 2848
Includes sound generation, transmission, and attenuation.
For noise pollution see *45 Environment Pollution.*

72 ATOMIC AND MOLECULAR PHYSICS 2850
Includes atomic structure, electron properties, and molecular spectra.

73 NUCLEAR AND HIGH-ENERGY PHYSICS 2852
Includes elementary and nuclear particles; and reactor theory.
For space radiation see *93 Space Radiation.*

74 OPTICS 2853
Includes light phenomena and optical devices.
For lasers see *36 Lasers and Masers.*

75 PLASMA PHYSICS 2855
Includes magnetohydrodynamics and plasma fusion.
For ionospheric plasmas see *46 Geophysics.* For space plasmas see *90 Astrophysics.*

76 SOLID-STATE PHYSICS 2861
Includes superconductivity.
For related information see also *33 Electronics and Electrical Engineering* and *36 Lasers and Masers.*

77 THERMODYNAMICS AND STATISTICAL PHYSICS 2880
Includes quantum mechanics; theoretical physics; and Bose and Fermi statistics.
For related information see also *25 Inorganic and Physical Chemistry* and *34 Fluid Mechanics and Heat Transfer.*

SOCIAL SCIENCES

Includes social sciences (general); administration and management; documentation and information science; economics and cost analysis; law, political science, and space policy; and urban technology and transportation.

80 SOCIAL SCIENCES (GENERAL) 2881
Includes educational matters.

81 ADMINISTRATION AND MANAGEMENT 2881
Includes management planning and research.

82 DOCUMENTATION AND INFORMATION SCIENCE 2881
Includes information management; information storage and retrieval technology; technical writing; graphic arts; and micrography.
For computer documentation see *61 Computer Programming and Software.*

83 ECONOMICS AND COST ANALYSIS 2882
Includes cost effectiveness studies.

84 LAW, POLITICAL SCIENCE AND SPACE POLICY 2883
Includes NASA appropriation hearings; aviation law; space law and policy; international law; international cooperation; and patent policy.

85 URBAN TECHNOLOGY AND TRANSPORTATION 2883
Includes applications of space technology to urban problems; technology transfer; technology assessment; and surface and mass transportation.
For related information see *03 Air Transportation and Safety, 16 Space Transportation,* and *44 Energy Production and Conversion.*

SPACE SCIENCES

Includes space sciences (general); astronomy; astrophysics; lunar and planetary exploration; solar physics; and space radiation.
For related information see also *Geosciences.*

88 SPACE SCIENCES (GENERAL) 2883

89 ASTRONOMY 2883
Includes radio, gamma-ray, and infrared astronomy; and astrometry.

90 ASTROPHYSICS 2884
Includes cosmology; celestial mechanics; space plasmas; and interstellar and interplanetary gases and dust.
For related information see also *75 Plasma Physics.*

91 LUNAR AND PLANETARY EXPLORATION 2885
Includes planetology; and manned and unmanned flights.
For spacecraft design or space stations see *18 Spacecraft Design, Testing and Performance.*

92 SOLAR PHYSICS 2886
Includes solar activity, solar flares, solar radiation and sunspots.
For related information see *93 Space Radiation.*

93 SPACE RADIATION 2886
Includes cosmic radiation; and inner and outer earth's radiation belts.
For biological effects of radiation see *52 Aerospace Medicine.* For theory see *73 Nuclear and High-Energy Physics.*

GENERAL

Includes aeronautical, astronautical, and space science related histories, biographies, and pertinent reports too broad for categorization; histories or broad overviews of NASA programs.

99 GENERAL N.A.

Note: N.A. means that no abstracts were assigned to this category for this issue.

SUBJECT INDEX I-1
PERSONAL AUTHOR INDEX I-49
CORPORATE SOURCE INDEX I-57
CONTRACT NUMBER INDEX I-69
REPORT/ACCESSION NUMBER INDEX I-71

TYPICAL CITATION AND ABSTRACT

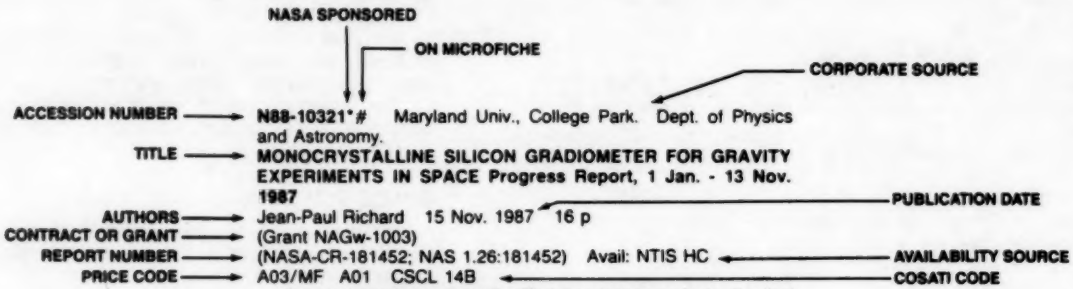

A very important research effort has been made in the last decade in the field of high precision measurement with laser instrumentation. The development of a space borne gradiometer operating at a high sensitivity level using laser measurement of the distance between proof mass over a short base line of order one meter is discussed. Two aspects of laser technology make it a promising tool for gradiometry measurements: quantum limited accuracy and absolute distance measurements. The quantum limit associated with laser instrumentation was formulated. The relevant quantum and classical sources of errors in laser measurements were reviewed and corresponding laser performance requirements for gradient measurements were evaluated. Some mechanical quality factor measurements were made on simple resonant monocrystalline silicon suspensions. It was discovered that the use of zero derivative restoring forces to position the gradiometer test masses will dramatically reduce the gradiometer temperature control requirements. A laser beam side injection scheme was discovered which permits rejection of common mode accelerations. These concepts are briefly discussed. Author

VOLUME 26 NUMBER 20/ OCTOBER 23, 1988

Scientific and Technical Aerospace Reports

A Semimonthly Publication of the National Aeronautics and Space Administration

01 AERONAUTICS (GENERAL)

N88-26289*# Puerto Rico Univ., Mayaguez.
THE ROLE OF AVIATION TECHNOLOGY IN THE CARIBBEAN BASIN Final Report, Sep. 1987 - Jul. 1988
Robert W. Smith [1988] 99 p
(Contract NCC2-496)
(NASA-CR-183069; NAS 1.26:183069) Avail: NTIS HC A05/MF A01 CSCL 01A

Aviation technology can play a significant role in the development of the countries of the Caribbean Basin. A variety of applications of rotorcraft in the region, the benefits, both economic and political which can result from utilization of rotorcraft in both a public service and commercial role are presented. A computer simulation of rotorcraft used as emergency medical vehicles is applied to compare and evaluate the advantages of using rotorcraft technology such as civil derivatives of the new tiltrotor. It is concluded that by using a civil derivative of the tiltrotor, significant improvements can be obtained in the level of health service in the region. The potential for cargo and passenger transport applications are currently being investigated and a second computer simulation is being developed to be used to evaluate the potential benefits to be derived from such applications. Author

N88-26290# National Aerospace Lab., Tokyo (Japan).
PROCEEDINGS OF THE 5TH NAL SYMPOSIUM ON AIRCRAFT COMPUTATIONAL AERODYNAMICS
Nov. 1987 259 p In ENGLISH and JAPANESE Symposium held in Tokyo, Japan, 25-26 Jun. 1987 Original contains color illustrations
(NAL-SP-8; ISSN-0452-2982) Avail: NTIS HC A12/MF A01

The complete proceedings of the 5th NAL Symposium on Aircraft Computational Aerodynamics are presented. Representative titles are: On the NAL Numerical Simulator System; Numerical Simulations of Aerodynamical Contribution of Flow about a Spaceplane-type Configuration; Numerical Simulation of Flow around a Shuttle Orbiter; A Rarefied Gas Numerical Wind Tunnel; A Numerical Analysis of Flow Characteristics in Laser Propulsion Systems; Numerical Simulation of Hydrogen Jets; On Symmetric Total Variation Diminishing Schemes; Relaxation Scheme for Compressible Flows; and Grid Generation of a Helicopter Rotary Wing. Only the titles and abstracts are translated. For individual titles, see N88-26291 through N88-26327.

N88-26291# National Aerospace Lab., Tokyo (Japan).
ON THE NAL NUMERICAL SIMULATOR SYSTEM **c09**
Hajime Miyoshi and Masahiro Fukuda *In its* Proceedings of the 5th NAL Symposium on Aircraft Computational Aerodynamics Nov. 1987 p 1-11 In JAPANESE; ENGLISH summary Original contains color illustrations (For primary document see N88-26290 20-01)
Avail: NTIS HC A12/MF A01

The Numerical Simulator System installed at NAL Computational Sciences Division is working well for computational research activities. Description is given of the background and the course of the system installation, the illustration of the system configuration and utilization, and the examples of advanced computational results. The factors affecting the progress of the Research Computational Fluid Dynamics, primarily supercomputer hardware, are mentioned. Author

N88-26292*# National Aeronautics and Space Administration. Ames Research Center, Moffett Field, Calif.
NUMERICAL SIMULATIONS OF AERODYNAMIC CONTRIBUTION OF FLOWS ABOUT A SPACE-PLANE-TYPE CONFIGURATION **c02**
Kisa Matsushima, Susume Takanashi, Kozo Fujii (National Aerospace Lab., Tokyo, Japan), and Shigeru Obayashi *In* National Aerospace Lab., Proceedings of the 5th NAL Symposium on Aircraft Computational Aerodynamics Nov. 1987 p 13-18 In JAPANESE; ENGLISH summary (For primary document see N88-26290 20-01)
Avail: NTIS HC A12/MF A01 CSCL 01B

The slightly supersonic viscous flow about the spaceplane under development at the National Aerospace Lab. in Japan was simulated numerically using the LU-ADI algorithm. The wind tunnel testing for the same plane also was conducted with parallel processing. The simulation was used to capture the phenomena which have a great deal of influence on the aerodynamic force and efficiency but it is difficult to capture by experiments. It includes more accurate representation of vortical flows with high angles of attack of an aircraft. The spaceplane shape geometry simulated is the simplified model of the real spaceplane, which is a combination of a flat and slender body and a double delta type wing. The comparison between experimental results and numerical ones will be done in the future. Author

N88-26293# National Aerospace Lab., Tokyo (Japan).
NUMERICAL SIMULATIONS OF FLOW AROUND SHUTTLE ORBITER **c02**
Satoru Ogawa, Tomiko Ishiguro, and Yoko Takakura (Fujitsu Ltd., Tokyo, Japan) *In its* Proceedings of the 5th NAL Symposium on Aircraft Computational Aerodynamics Nov. 1987 p 19-28 In JAPANESE; ENGLISH summary (For primary document see N88-26290 20-01)
Avail: NTIS HC A12/MF A01

Numerical simulations of flow around shuttle orbiter are performed by solving the 3-D Euler equations. A numerical grid is generated for the whole configuration of shuttle orbiter by using equations of mesh line orthogonality and cell volume which form a hyperbolic partial differential equation system. To increase the applicability of the hyperbolic grid generation scheme, the second metric tensor is used for the determination of cell volume, and the 1-D elastic model is used to relax the orthogonality condition of two coordinate lines. The transonic and supersonic flows around the shuttle orbiter are solved by using the Harten-Yee type Total Variation Diminishing scheme. It is shown that the results of numerical flow simulation using the present method is reasonable. Author

N88-26294# National Aerospace Lab., Tokyo (Japan).
FINITE ELEMENT ANALYSIS OF INCOMPRESSIBLE VISCOUS FLOW AROUND MULTI-ELEMENT AEROFOILS **c02**
Masashi Shigemi *In its* Proceedings of the 5th NAL Symposium on Aircraft Computational Aerodynamics Nov. 1987 p 29-35 In JAPANESE; ENGLISH summary (For primary document see

N88-26290 20-01)
Avail: NTIS HC A12/MF A01

The Navier-Stokes equation was solved by the finite element method to simulate the laminar flow around airfoils. The concept of the penalty function method was introduced in the finite element method to simplify the implication of the incompressibility constraint. The streamline upwind Petrov-Galerkin method was also incorporated to avoid the numerical oscillation in the velocity field, which is known to appear when a simple finite element formulation is applied to flow problems in high Reynolds number region. Three examples (flow around a symmetric airfoil with zero angle of attack, flow around an airfoil which is known to show the laminar leading edge separation when the Reynolds number is fairly low, and flow around an airfoil with flap) were chosen to test the stability of the formulation developed. Results are presented and discussed. Author

N88-26295# Kyoto Univ. (Japan). Dept. of Aeronautical Engineering.
NUMERICAL SIMULATIONS OF ASTROPHYSICAL JETS c02
Takuya Matsuda, Ryuji Ishii, Yoshikuni Umeda, Atsuhiko Yasuda, Keisuke Sawada, and Eiji Shima (Kawasaki Heavy Industries Ltd., Kobe, Japan) *In* National Aerospace Lab., Proceedings of the 5th NAL Symposium on Aircraft Computational Aerodynamics Nov. 1987 p 37-42 In JAPANESE; ENGLISH summary (For primary document see N88-26290 20-01)
Avail: NTIS HC A12/MF A01

Propagation of astrophysical jets was investigated numerically by using the Osher method which has a second order of accuracy in space and time. The characteristic structures of them, i.e., a beam, a lobe, a working surface and a cocoon, were successfully simulated. It was found that those structures were very sensitive to the density ratio (gas density of the jet at the effective nozzle exit divided by that of the ambient). Herein, the ambient gas condition first introduced by the authors was applied on all the numerical boundaries. The numerical results have clearly shown that the ambient gas condition is better than the pressure condition adopted, for example, by Norman et al. The ambient gas condition can be widely applied to other problems with numerical boundaries. Author

N88-26296# Nagoya Univ. (Japan).
NUMERICAL CALCULATION OF SUPERSONIC FLOW BY THE PNS EQUATIONS c02
Michiru Yasuhara and Yoshiaki Nakamura *In* National Aerospace Lab., Proceedings of the 5th NAL Symposium on Aircraft Computational Aerodynamics Nov. 1987 p 43-48 In JAPANESE; ENGLISH summary (For primary document see N88-26290 20-01)
Avail: NTIS HC A12/MF A01

The Parabolized Navier-Stokes equation is studied. The PNS equations were used in order to reduce CPU time. The calculation time was reduced to some thousands as much as the thin layer Navier-Stokes equations. Two cases were calculated; one was a hemispheric cylinder, and the other is a hemispherical elliptic cylinder at an angle of attack. The first case was compared with the time dependent thin layer NS equations. The comparison between them was good. The second case showed clear effect of attack angle such as the turn of flow from the lower surface to the upper surface. Author

N88-26297# Fuji Heavy Industries Ltd., Utsunomiya (Japan).
NAVIER-STOKES ANALYSIS OF TRANSONIC TRANSPORT AIRCRAFT EMPENNAGE c02
Yasuhiro Koshioka, Keisuke Kamo, and Kanichi Amano (Japan Aircraft Development Corp., Tokyo.) *In* National Aerospace Lab., Proceedings of the 5th NAL Symposium on Aircraft Computational Aerodynamics Nov. 1987 p 47-54 In JAPANESE; ENGLISH summary (For primary document see N88-26290 20-01)
Avail: NTIS HC A12/MF A01

Flow field simulations over transonic transport aircraft empennage were carried out based on 3-D Navier-Stokes equations. The computations were done for the flow fields of various Mach numbers and angles of attack to investigate the variation of the lift curve slope with Mach number at low angle of attack, and the variation of the lift coefficient with angle of attack at low Mach number. The values of lift curve slope obtained by the computations show good agreement with those by experiments. The difference between computations and experiments looks a little large about lift coefficient versus angle of attack. Author

N88-26298# Kyoto Univ. (Japan). Dept. of Engineering.
NUMERICAL SOLUTIONS OF THE EULER EQUATIONS FOR THE FLOW FIELD AROUND COUNTER-ROTATING PROPELLERS c02
Makoto Kobayakawa and Masahiro Nakao (Mitsubishi Heavy-Industries Ltd., Tokyo, Japan) *In* National Aerospace Lab., Proceedings of the 5th NAL Symposium on Aircraft Computational Aerodynamics Nov. 1987 p 55-63 In JAPANESE; ENGLISH summary Original language document was announced in IAA as A88-13544 (For primary document see N88-26290 20-01)
Avail: NTIS HC A12/MF A01

In order to investigate the flow field around the ATP through numerical methods for its optimal design, 3-D Euler equations are most prominent. The flow field around counterrotating propellers in advancing 0.8 Mach is obtained. Two spaces including front and rear blades are solved separately. The interaction between both blades are taken into the calculation by the connecting surfaces. The noniterative implicit ADI scheme is used in order to solve Euler equations. The periodic steady and averaged steady solutions are obtained. The latter is simplified by averaging the variables at the connecting surface. This shortens the calculation time to 1/3 compared with the periodic steady analysis which simulates the relative motion of the blades exactly. Numerical calculations are performed for two counter rotating ATP's with SR-1 and SR-3 blades. Both results show that they are similar to each other, and the propeller efficiencies increase compared with single rotating ATP with same blades. Author

N88-26299# Kyoto Univ. (Japan). Dept. of Aeronautical Engineering.
NUMERICAL SIMULATION OF SUPERSONIC FREE-JETS c02
Ryuji Ishii, Takuya Matsuda, Yoshikuni Umeda, Atsuhiko Yasuda, Keisuke Sawada, and Eiji Shima (Kawasaki Heavy Industries Ltd., Kobe, Japan) *In* National Aerospace Lab., Proceedings of the 5th NAL Symposium on Aircraft Computational Aerodynamics Nov. 1987 p 65-71 In JAPANESE; ENGLISH summary (For primary document see N88-26290 20-01)
Avail: NTIS HC A12/MF A01

Axisymmetric underexpanded supersonic jets are investigated numerically. A time dependent technique is applied to solve the Euler equations for a compressible ideal gas. The characteristics of Mach disk obtained by the calculations are compared with the experiments and a good agreement is obtained. It is shown that the global jet structure with a nearly regular shock pattern which is stable and steady itself, is destabilized by the vortex rings (Kelvin-Helmholtz roll-up) on the jet boundary. These vortices produce shocks inside the jet, which are convected downstream with eddies. This strongly suggests that a time dependent or a time converged solution cannot be expected without making a suitable time averaging of the time dependent solutions. Other important instabilities are also investigated. Author

N88-26300# Tokyo Univ. (Japan). Inst. of Computational Fluid Dynamics.
COMPUTATION OF FLOW AROUND NACA0012 AIRFOIL AT HIGH ANGLE OF ATTACK c02
Yoshifumi Shida and Kunio Kuwahara *In* National Aerospace Lab., Proceedings of the 5th NAL Symposium on Aircraft Computational Aerodynamics Nov. 1987 p 73-79 In JAPANESE; ENGLISH summary Previously announced in IAA as A87-42448 (For primary document see N88-26290 20-01)
Avail: NTIS HC A12/MF A01

Transonic flow around an NACA0012 airfoil at high angle of

attack is simulated by solving the 2-D Navier-Stokes equations. The block pentadiagonal matrix scheme is employed. Periodic phenomena of shock wave vortex interaction are observed. For comparison, computation of subsonic flow was done. Small vortices are observed between the leading edge and the center of the chord. Author

N88-26301# National Aerospace Lab., Tokyo (Japan).
AERODYNAMIC SIMULATION FOR COMPLETE ASKA AIRCRAFT CONFIGURATION **c02**
Susumu Takanashi and Keisuke Sawada (Kawasaki Heavy Industries Ltd., Kobe, Japan) *In its* Proceedings of the 5th NAL Symposium on Aircraft Computational Aerodynamics Nov. 1987 p 81-84 In JAPANESE; ENGLISH summary (For primary document see N88-26290 20-01)
Avail: NTIS HC A12/MF A01

A numerical simulation of transonic flows over a complete STOL ASKA aricraft configuration is carried out. A computational grid system is constructed using the algebraic multiblock method. The Euler equations are numerically solved by the upwind finite volume scheme. Author

N88-26302*# National Aeronautics and Space Administration. Ames Research Center, Moffett Field, Calif.
NUMERICAL SIMULATION OF VISCOUS FLOWS OVER TRANSONIC AIRCRAFT CONFIGURATIONS **c02**
Susumu Takanashi, Masahiro Yoshida, Kozo Fujii, Kisa Matsushima (Fujitsu Ltd., Tokyo, Japan), and Shigeru Obayashi *In* National Aerospace Lab., Proceedings of the 5th NAL Symposium on Aircraft Computational Aerodynamics Nov. 1987 p 85-89 In JAPANESE; ENGLISH summary (For primary document see N88-26290 20-01)
Avail: NTIS HC A12/MF A01 CSCL 01A

Numerical simulation of compressible viscous flow fields is carried out for a transonic transport configuration. A single structured grid system is constructed using analytical transformations such as conformal mapping, shearing, twisting, rotating, clustering, stretching transformations. The Reynolds averaged, thin layer Navier-Stokes equations are solved on a supercomputer, FACOM VP-400, using the LU-ADI factorization method. Author

N88-26303# National Aerospace Lab., Tokyo (Japan).
CALCULATIONS OF UNSTEADY AERODYNAMICS FOR A FULL AIRCRAFT CONFIGURATION USING BOUNDARY ELEMENT METHOD **c02**
Mitsunori Yanagizawa, Toshiyuki Morita, and Shigefumi Tatsumi (Mitsubishi Heavy-Industries Ltd., Tokyo, Japan) *In its* Proceedings of the 5th NAL Symposium on Aircraft Computational Aerodynamics Nov. 1987 p 91-101 In JAPANESE; ENGLISH summary (For primary document see N88-26290 20-01)
Avail: NTIS HC A12/MF A01

A boundary element method is presented for determining aerodynamic loadings on arbitrary configurations in oscillatory subsonic flow. Formulas (modified Morino's method) are given for the unsteady pressure distributions or unsteady force experienced in subsonic flow by the wing-store combination, oscillating in the torsional oscillations about a fixed axis parallel to the span and other oscillating modes (flapping, plunging). Interference effects from an underwing pylon store were analyzed. The method is finally verified through comparison with experiment for the model at angles of attack from -5 to +5 degrees, and reduced frequencies from 0.65 to 1.3 at low subsonic flow. Author

N88-26304# National Aerospace Lab., Tokyo (Japan).
RAREFIED GAS NUMERICAL WIND TUNNEL 3: UNIVERSAL CODE FOR THREE DIMENSIONAL BODIES **c02**
Katsuhisa Koura, Kinuyo Nakamura, Toshio Isobe, Kazuyo Suematsu, Masayuki Hatakeyama, and Toshiyuki Shimoji (Facom Hitac Co. Ltd., Japan) *In its* Proceedings of the 5th NAL Symposium on Aircraft Computational Aerodynamics Nov. 1987 p 103-107 In JAPANESE; ENGLISH summary (For primary document see N88-26290 20-01)
Avail: NTIS HC A12/MF A01

The rarefied gas numerical wind tunnel is under construction using the null-collision direct simulation Monte Carlo method. It is confirmed that the universal code (RGNWT) for 3-D bodies is valid for general use. The vectorized code (RGNWTV) for the NAL NS system is successfully in progress. Author

N88-26305# Nissan Motor Co. Ltd., Tokyo (Japan).
A NUMERICAL ANALYSIS OF FLOW CHARACTERISTICS IN LASER PROPULSION SYSTEM **c36**
Toru Shimada and Takashi Abe (Tokyo Univ., Japan) *In* National Aerospace Lab., Proceedings of the 5th NAL Symposium on Aircraft Computational Aerodynamics Nov. 1987 p 109-114 In JAPANESE; ENGLISH summary (For primary document see N88-26290 20-01)
Avail: NTIS HC A12/MF A01

For the purpose of the system design of the laser thermal propulsion experiment chamber, a numerical simulation was conducted using a quasi-two dimensional axisymmetric mathematical model of Glumb and Krier. In order to simplify the local laser intensity calculation, a computational grid of which one coordinate family is made run along the laser beam was chosen. Calculations were carried out for various values of mass flow rate and laser incident power. Qualitative understanding was obtained in regard with the dependency of the laser beam absorption rate on these parameters. Author

N88-26306# National Aerospace Lab., Kakuda (Japan).
ANALYSIS OF FLOW THROUGH PUMP OF LARGE ROCKET ENGINE **c20**
Hitoshi Yamada and Yoshiaki Watanabe *In* National Aerospace Lab., Proceedings of the 5th NAL Symposium on Aircraft Computational Aerodynamics Nov. 1987 p 115-119 In JAPANESE; ENGLISH summary (For primary document see N88-26290 20-01)
Avail: NTIS HC A12/MF A01

A liquid turbopump consists of a main pump, a preburner pump, and a single stage impulse turbine. In order to design a high pressure and a high efficiency pump, it is necessary to analyze the pump blade passage flows in detail, using a three dimensional flow analysis method. The design method and the experiment is described, which was carried out using liquid nitrogen and liquid oxygen at a NAL turbopump test facility. The design method presented combines a streamline analysis and a blade-to-blade analysis. The predicted pump head coefficients are in reasonable agreement with the experimental results considering the pump efficiency. Because a large amount of input data is usually necessary to calculate three dimensional flows, a method of calculating blade shapes correctly by giving two blade angles at the impeller inlet and outlet is developed. Author

N88-26307# Iwaki Meisei Univ. (Japan).
NUMERICAL SIMULATION OF IGNITION OF HYDROGEN JET IN HOT AIR **c25**
Fumio Takayama, Shirou Taki, Toshitaka Fujiwara, Koichi Hayashi, and Akira Sakurai (Tokyo Denki Univ., Japan) *In* National Aerospace Lab., Proceedings of the 5th NAL Symposium on Aircraft Computational Aerodynamics Nov. 1987 p 121-127 In JAPANESE; ENGLISH summary Previously announced in IAA as A87-33954 (For primary document see N88-26290 20-01)
Avail: NTIS HC A12/MF A01

The nonsteady aspects of mixing and ignition of hydrogen jets injected into air heated by rapid compression was studied. A numerical model for hydrogen jets undergoing chemical reaction is developed on the basis of experimental findings. Basic equations of a chemically reactive, multicomponent, axisymmetric, viscous and heat conducting gas flow are discretized by the application of the second order explicit MacCormack method and the Flux Corrected Transport smoothing technique. General patterns of the computed density distribution of the jet in its early stages compare favorable with the corresponding experimental results deduced from

Schlieren photographs. The ignition time measured by the amount of water production in the computation is generally consistent with that of hydrogen jet in the experiments. Author

N88-26308# Tohoku Univ., Sendai (Japan). Inst. of High Speed Mechanics.
NUMERICAL SIMULATION OF THE SHOCK TUBE FLOWS BY TVD SCHEME **c34**
Katsuhiro Itoh and Kazuyoshi Takayama *In* National Aerospace Lab., Proceedings of the 5th NAL Symposium on Aircraft Computational Aerodynamics Nov. 1987 p 129-136 In JAPANESE; ENGLISH summary (For primary document see N88-26290 20-01)
Avail: NTIS HC A12/MF A01

A computational and experimental investigation is presented of unsteady transonic flow over an elliptical cylinder and an NACA0012 airfoil in a shock tube. To simulate the unsteady transonic shock tube flow, a Total Variation Diminishing finite difference scheme is applied to Navier-Stokes equations. The complicated unsteady transonic flow accompanied by shock waves was successfully simulated with a high resolution. The computational isopycnics are consistent with those of the interferograms. Author

N88-26309# National Aerospace Lab., Tokyo (Japan).
NUMERICAL CALCULATION OF THREE DIMENSIONAL FLOW BY TVD SCHEME **c02**
Tomiko Ishiguro, Satoru Ogawa, and Yoko Takakura (Fujitsu Ltd., Tokyo, Japan) *In its* Proceedings of the 5th NAL Symposium on Aircraft Computational Aerodynamics Nov. 1987 p 137-146 In JAPANESE; ENGLISH summary (For primary document see N88-26290 20-01)
Avail: NTIS HC A12/MF A01

Numerical simulations of flow around three dimensional complex configurations are performed by solving both the Euler and the Navier-Stokes equations. Recent Total Variation Diminishing schemes are used for two problems: (1) Subsonic transonic supersonic flow around a shuttle orbiter; and (2) Hypersonic inviscid viscous flow in a scramjet inlet. It is shown that the results of numerical flow simulation using the present methods are reasonable. Author

N88-26310# National Aerospace Lab., Tokyo (Japan).
NUMERICAL ANALYSIS OF THREE DIMENSIONAL CASCADE FLOW BY SOLVING NAVIER-STOKES EQUATIONS **c34**
Osamu Nozaki, Kazuhiro Nakahashi, and Atsuhiro Tamura *In its* Proceedings of the 5th NAL Symposium on Aircraft Computational Aerodynamics Nov. 1987 p 147-156 In JAPANESE; ENGLISH summary (For primary document see N88-26290 20-01)
Avail: NTIS HC A12/MF A01

Three dimensional viscous flow fields in two different types of cascades, such as turbine nozzle and fan blades, were numerically simulated by solving the Navier-Stokes equations. For the turbine nozzle flows, computed flow patterns on a vane in stationary and rotating frames, and on a differently stacked vane were compared. In a fundamental case, the computed results showed good agreement with experimental data. Three dimensional flow separations as well as secondary flows caused by passage vortices could be predicted and effectively visualized using surface oil flow and streamline techniques, which were useful methods for three dimensional flow representation. Author

N88-26311# Tokyo Metropolitan Univ. (Japan). Coll. of Aeronautical Engineering.
SIMULATION OF AXISYMMETRIC FLOW WITH H2O2 REACTIONS **c34**
Shizui Watanabe *In* National Aerospace Lab., Proceedings of the 5th NAL Symposium on Aircraft Computational Aerodynamics Nov. 1987 p 157-160 In JAPANESE; ENGLISH summary (For primary document see N88-26290 20-01)
Avail: NTIS HC A12/MF A01

A simulation method of the conservation equations of fluid dynamics including transport properties and chemical kinetics is presented. It is constructed as follows: First, conservation equations are solved by a Newton-Raphson type iterative method; then velocities and mass fluxes are determined; second, species diffusion equations and enthalpy diffusion terms are evaluated explicitly; third, chemical kinetic equations are solved implicitly, then thermodynamic quantities and each molarity of chemical species are determined. For chemical kinetics, 9 chemical species and 22 elementary reactions are used. This simulation method is applied to analyze hydrogen jet into heat oxygen and argon mixture. Author

N88-26312# National Aerospace Lab., Tokyo (Japan).
NUMERICAL ANALYSIS OF DUCT FLOW USING THREE-DIMENSIONAL PARABOLIZED NAVIER-STOKES EQUATION **c34**
Kazuo Kikuchi and Atsuhiro Tamura *In its* Proceedings of the 5th NAL Symposium on Aircraft Computational Aerodynamics Nov. 1987 p 159-168 In JAPANESE; ENGLISH summary (For primary document see N88-26290 20-01)
Avail: NTIS HC A12/MF A01

The validity of a numerical solution procedure developed by Kikuchi and Tamura about three dimensional viscous compressible flow fields based on parabolized Navier-Stokes equations is examined by comparing the results of two experiments. The calculations for three dimensional flow fields in curved pipe and S-type duct with circular cross sections were carried out. Qualitatively good numerical results were obtained. The discrepancies between the numerical and experimental results seem to be caused by inaccurate inlet conditions which were not explicitly designated in the experiments. Author

N88-26313# Kawasaki Heavy Industries Ltd., Kagamihara (Japan).
THE ROLE OF COMPUTATIONAL FLUID DYNAMICS IN AERONAUTICAL ENGINEERING (5): IMPROVEMENTS AND APPLICATIONS OF IMPLICIT TVD FINITE VOLUME CODE **c34**
Eiji Shima, Kenji Yoshida, and Kanichi Amano (Japan Aircraft Development Corp., Tokyo.) *In* National Aerospace Lab., Proceedings of the 5th NAL Symposium on Aircraft Computational Aerodynamics Nov. 1987 p 169-175 In JAPANESE; ENGLISH summary (For primary document see N88-26290 20-01)
Avail: NTIS HC A12/MF A01

An automatic grid generator for multiple element airfoils was developed and the existing implicit TVD (Total Variation Diminishing) finite volume code was improved in both accuracy and efficiency, in order to make the Navier-Stokes solver a practical design tool for high lift devices. Utilizing these codes, Navier-Stokes analysis of the single slotted flap was carried out. The automatic grid generator utilizes the elliptic equation solver using the finite difference method combined with the panel method. The flow field is divided into subregions by the dividing stream lines which is calculated by the panel method and the computational grid in each subregion is generated by solving the elliptic equations. To obtain a high accuracy on a rapidly stretching grid, the flow solver uses the TVD formulation containing a explicit treatment of nonuniform grid spacing. Converging rate and numerical stability of the flow solver is augmented by the relaxation approach using Symmetric Point Gauss Seidel method in matrix inversion process which is necessary for an implicit scheme. Author

N88-26314# Mitsubishi Heavy-Industries Ltd., Tokyo (Japan).
EXTENSIVE VERIFICATION OF BLADE-TO-BLADE FLOW CODE BASED ON DENTON SCHEME **c07**
Tomihiko Sato, Sunao Aoki, and Hedetaka Mori *In* National Aerospace Lab., Proceedings of the 5th NAL Symposium on Aircraft Computational Aerodynamics Nov. 1987 p 178-181 In JAPANESE; ENGLISH summary (For primary document see N88-26290 20-01)
Avail: NTIS HC A12/MF A01

The Denton time marching blade-to-blade computer aided interactive code is attractive as it is fast and can handle mixed subsonic-supersonic flows. Code control variables are calibrated

from the user's point of view. Factors affecting computing costs and accuracy are investigated, and the know how necessary to operate the code efficiently is discussed. Next, comparisons of calculated and experimental results are presented. Calculated surface Mach number distributions are compared with experimental data obtained from two dimensional cascade tests for 23 cascades. For the nozzles, excellent agreement is obtained if the flows are fully subsonic, or transonic with weak shock boundary layer interaction. For the blades, very good agreement is also obtained if the blades have moderate blade reaction and viscous effects are small. Satisfactory results are obtained for suction surface diffusion, even at off-design inlet conditions, if absolute values of incidence angle are less than 10 degrees. Author

N88-26315# Ishikawajima-Harima Heavy Industries Co. Ltd., Tokyo (Japan).
APPLICATION OF COMPUTATIONAL FLUID DYNAMICS TO DESIGN OF COMPRESSOR CASCADE **c34**
Teiichi Tamaki, Kaoru Chiba, Atsushi Shimizu, and Kenji Kobayashi *In* National Aerospace Lab., Proceedings of the 5th NAL Symposium on Aircraft Computational Aerodynamics Nov. 1987 p 183-189 In JAPANESE; ENGLISH summary (For primary document see N88-26290 20-01)
Avail: NTIS HC A12/MF A01

One of the most important problems for the gas turbine design engineers is to estimate the compressor and turbine cascade flow conditions. However, an efficient cascade design tool can be obtained with computational fluid dynamics. The results of numerical simulation were compared with some cascade experiments. A full potential analysis scheme with boundary layer correction was in good agreement with two dimensional stational and rotational transonic cascade measurements. A controlled diffusion cascade designed with the new design procedure was tested and shown to have a good performance. Author

N88-26316# Kawasaki Heavy Industries Ltd., Kagamihara (Japan).
ON THE ACCURACY OF UPWIND BIASED FINITE VOLUME METHOD **c02**
Keisuke Sawada and Susumu Takanashi *In* National Aerospace Lab., Proceedings of the 5th NAL Symposium on Aircraft Computational Aerodynamics Nov. 1987 p 191-195 In JAPANESE; ENGLISH summary (For primary document see N88-26290 20-01)
Avail: NTIS HC A12/MF A01

An improvement of the spatial accuracy of an upwind biased finite volume scheme adopting a preprocessing approach is investigated. In the preprocessing approach, the cell face values of the dependent variables are estimated with a higher order spatial accuracy at first, usually based on the Taylor expansion in the computational space, then numerical fluxes are determined by an appropriate method such as an upwind scheme. A sufficient grid smoothness in the physical space is implicitly assumed when the Taylor expansion is applied to find the averaged slopes in the computational space. This can lead to a possible generation of numerical errors on the skewed grid system. In the present study, the distribution of conservative variables are fit in the physical space with an accuracy of up to a third order, then the average slopes in each cell is found. Numerical experiments are compared with various methods of finding the relevant averaged slopes including the present one. Author

N88-26317# National Aerospace Lab., Tokyo (Japan).
AN IMPLICIT, HIGH ORDER ACCURATE, UPWIND SCHEME FOR UNSTEADY EULER EQUATIONS **c34**
Kenichi Matsuno *In its* Proceedings of the 5th NAL Symposium on Aircraft Computational Aerodynamics Nov. 1987 p 197-200 In JAPANESE; ENGLISH summary (For primary document see N88-26290 20-01)
Avail: NTIS HC A12/MF A01

A new implicit finite difference scheme for unsteady Euler equations is proposed. The quantities of the order of the square of the time step are employed as unknowns of the scheme, which produces a delta-square form of the algorithm. The present scheme has second order time accuracy without iteration. The iteration proces in the algorithm, which the scheme has as an option, improves the numerical accuracy and robustness. Numerical experiments show that the present scheme is very good not only for unsteady problems but also for steady problems. Author

N88-26318# National Aerospace Lab., Tokyo (Japan).
ON THE PROPAGATING SPEED IN DIFFERENCE APPROXIMATIONS FOR CONSERVATION LAWS **c64**
Hideaki Aiso *In its* Proceedings of the 5th NAL Symposium on Aircraft Computational Aerodynamics Nov. 1987 p 201-207 In JAPANESE; ENGLISH summary (For primary document see N88-26290 20-01)
Avail: NTIS HC A12/MF A01

There are various ways of analyzing or estimating finite difference approximations for differential equations. A way of analyzing finite difference approximations is proposed from the point of view of propagation phenomena of conservation laws. Characteristics of conservation laws may be considered as routes on which small perturbations propagate. On the other hand, difference equations approximating conservation laws have no concept of characteristics. But it is natural to think that propagation of a small perturbation in the difference approximation must have some resemblance with that in the original conservation law. A condition for propagation phenomena of finite difference approximations to conservation laws is proposed, and this condition imposes some compatibility with characteristics of the original conservation laws. The analysis based on this condition leads to the fact that, among explicit 3 point conservative difference approximations, only the upstream difference approximation satisfies completely this condition. This fact may explain the importance of upstream finite difference approximations with a stronger theoretical foundation. Author

N88-26319# National Aerospace Lab., Tokyo (Japan).
ON SYMMETRIC TVD SCHEMES Abstract Only **c34**
Takayuki Aki *In its* Proceedings of the 5th NAL Symposium on Aircraft Computational Aerodynamics Nov. 1987 p 209 In JAPANESE; ENGLISH summary (For primary document see N88-26290 20-01)
Avail: NTIS HC A12/MF A01

An overview is presented for a construction of a class of shock capturing difference methods. The scope of the overview extends over not only to explicit but also to implicit methods. Special emphasis is on the concepts underlying the construction method rather than the techniques in practice, because practical schemes obtainable by applying the present method is of wider variety than those obtained in the state-of-the-art developments. Some results of practical applications of the present method are reviewed. Author

N88-26320# Fujitsu Ltd., Tokyo (Japan).
ON THE STATIONARY SOLUTIONS OF THREE-DIMENSIONAL EULER EQUATIONS BY THE TVD DIFFERENCE SCHEMES **c34**
Yoko Takakura, Tomiko Ishiguro, and Satoru Ogawa (National Aerospace Lab., Tokyo, Japan) *In* National Aerospace Lab., Proceedings of the 5th NAL Symposium on Aircraft Computational Aerodynamics Nov. 1987 p 211-216 In JAPANESE; ENGLISH summary (For primary document see N88-26290 20-01)
Avail: NTIS HC A12/MF A01

Numerical estimations are performed for an improved Total Variation Diminishing (TVD) schemes (Harten-Yee and Chakravarthy-Osher numerical fluxes) and also for the classical schemes with artificial dissipation models (Beam-Warming and Obayashi numerical fluxes) through a series of numerical experiments for three dimensional inviscid flows around the ONERA M6 wing. Numerical experiments indicate that the two TVD numerical fluxes are excellent in the points that they capture shock waves without numerical oscillations and rapid expansions sharply and that they have the robustness and the self-adjusting mechanisms regarding the numerical viscosity. On the other hand

the Obayashi numerical flux is not capable of capturing the rapid expansions sharply like the Beam Warming nunerical flux, although the former captures the shock waves without numerical oscillations. Author

N88-26321# National Aerospace Lab., Tokyo (Japan).
NUMERICAL SIMULATION OF TRANSITION TO TURBULENCE IN PLANE POISEUILLE FLOW BY A SPECTRAL METHOD **c02**
Kiyoshi Yamamoto and Iwao Hosokawa (Iwate Univ., Morioka, Japan) *In its* Proceedings of the 5th NAL Symposium on Aircraft Computational Aerodynamics Nov. 1987 p 217-223 In JAPANESE; ENGLISH summary (For primary document see N88-26290 20-01)
Avail: NTIS HC A12/MF A01

Direct numerical simulation of the transition process from laminar to turbulent plane Poiseuille flow is carried out using a new computing method derived from the Fourier spectral method. The subcritical nonlinear instability for a three dimensional small disturbance, which is induced by the basic flow plus the two dimensional finite amplitude T-S wave, is investigated at a Reynolds number, 5000. The two distinct secondary instability mechanisms, the peak-valley splitting and the resonance interaction between T-S wave and a pair of subharmonic oblique waves, are obtained depending on a slight difference being in the initially given three dimensional small disturbances. The mechanisms correspond to the experimental observation in the boundary layer on a flat plate. The transition is accelerated by the growing three dimensional disturbances and the turbulent flow obtained agrees well with the experimental observation. Author

N88-26322# Ministry of Transportation, Tokyo (Japan). Ship Research Inst.
NUMERICAL SIMULATION OF TURBULENT FLOW USING THE EXPONENTIAL EXPRESSION OF k-EPSILON EQUATION **c02**
Munehiko Hinatsu and Yoshiaki Kodama *In* National Aerospace Lab., Proceedings of the 5th NAL Symposium on Aircraft Computational Aerodynamics Nov. 1987 p 225-232 In JAPANESE; ENGLISH summary (For primary document see N88-26290 20-01)
Avail: NTIS HC A12/MF A01

A numerical simulation is presented of a turbulent flow around a wing section by use of kappa-epsilon turbulence model. In order to assure the positiveness of kappa and epsilon, the exponential expression of kappa-epsilon is used. IAF method is adopted as a computational scheme. A new treatment for the boundary condition on the wing surface is devised. A turbulent flow around NACA0012 wing section with 5 deg angle of attack at Re = 10 to the 6th power is simulated. Author

N88-26323# Chiba Univ. (Japan). Faculty of Engineering.
RELAXATION SCHEME FOR COMPRESSIBLE FLOWS **c02**
Nobuhide Nishikawa and Akira Suzuki *In* National Aerospace Lab., Proceedings of the 5th NAL Symposium on Aircraft Computational Aerodynamics Nov. 1987 p 233-239 In JAPANESE; ENGLISH summary (For primary document see N88-26290 20-01)
Avail: NTIS HC A12/MF A01

The flow structure of compressible flows over a circular hump or spherical blunt body are numerically analyzed by Line Gauss Seidel relaxation algorithm including verification of the available studies. For compressible flow the Euler equation on transformed coordinate is expressed as a delta form and time linearization to the system of conservation reduced to the unfactored expression together with flux splitting. The lines for which Gauss Seidel system is applied are chosen parallel to oncoming flow direction. The CFL number can be chosen dramatically large and the number of iterations until convergence in time marching problem is about 10 especially for supersonic flows. Author

N88-26324# Keio Univ., Tokyo (Japan). Faculty of Science and Technology.
THE MODIFIED-FLUID-IN-CELL METHOD TO WHICH ADAPTIVE MESH AND MULTIGRID WERE APPLIED **c02**
Ikuo Ono, Kentaro Motoda, Eriya Kanai, and Tsuneyo Ando *In* National Aerospace Lab., Proceedings of the 5th NAL Symposium on Aircraft Computational Aerodynamics Nov. 1987 p 241-246 In JAPANESE; ENGLISH summary (For primary document see N88-26290 20-01)
Avail: NTIS HC A12/MF A01

When the compressible flow field including shock wave are numerically analyzed, the solution diverges because of the discontinuity of shock. If modified-Fluid-in-Cell method is used, the discontinuity is artificially smoothed and the flow field is analyzed stably. Stability and accuracy of the solution depend on a mesh system in the analysis by modified Fluid-in-Cell method. A new algorithm is proposed in order to decrease the influence of a mesh system and the calculation time. It includes Adaptive Mesh Method and Multigrid Method. Using the adaptive Mesh Method makes it possible to calculate the flow field without the influence of a mesh system. When a fine mesh is used to get a highly accurate solution, much more steps and computational time are necessary. So Multigrid Method is used in the present algorithm. Calculation of a supersonic flow field around a blunt nosed body is carried out. In comparison with previous methods, it takes less calculation time and good calculation results are obtained with respect to the shock wave and pressure contours. Author

N88-26325# Tsukuba Univ., Ibaraki (Japan). Inst. of Engineering Mechanics.
GRID GENERATION OF A HELICOPTER ROTARY-WING **c02**
Alain Carcasses and Y. Yoshizawa *In* National Aerospace Lab., Proceedings of the 5th NAL Symposium on Aircraft Computational Aerodynamics Nov. 1987 p 247-253 In JAPANESE; ENGLISH summary (For primary document see N88-26290 20-01)
Avail: NTIS HC A12/MF A01

A method of elliptic grid generation for a helicopter rotary wing is proposed. Flexibility of several flight conditions of helicopters is emphasized. The elliptic grid is reduced to the method of solution of a large scale simultaneous equations. Three dimensional grid points are rearranged into one dimensional vectors, of which components are all the grid points in a surface of generated curvilinear coordinates. The SOR method is applied to the one dimensional vectors in a checker board manner, and the conjugate gradient method is used to solve each equation. In the range of test calculations, the proposed method is satisfactory from the viewpoints of numerical calculations. More efficiency, however, would be required for the grid generation in a large scale of calculation. Author

N88-26326# Tokyo Metropolitan Univ. (Japan). Coll. of Aeronautical Engineering.
THEORY OF NUMERICAL INFORMATION ENVIRONMENT AND ITS APPLICATIONS **c82**
Masayuki Hatakeyama *In* National Aerospace Lab., Proceedings of the 5th NAL Symposium on Aircraft Computational Aerodynamics Nov. 1987 p 255-259 In JAPANESE; ENGLISH summary (For primary document see N88-26290 20-01)
Avail: NTIS HC A12/MF A01

A concept of Numerical Information Environment (NIE) is proposed along with its actual method of system constitution. The NIE was studied and developed to store, analyze and simulate a large scale numerical data and information of a target interactively and iteratively. First, a global concept of Numerical Information, and Numerical Information World are defined. To establish and operate the NIE, a concept of Software Bus and its actual programming method were developed on the basis of the World. The Software Bus system always plays the role of a distributing center of all the numerical data and information, and is also a general method to transmit them among the modules in the NIE and between the processes in the UNIX. By using the software bus system, any kind of direct numerical simulation or analyses programs can be mounted on the software Bus system. To get a

view of the database oriented system, a Bus View system was developed with the aid of a graphic system. An application system named Dynamic DB System is described. Author

N88-26327# Fujitsu Ltd., Kawasaki (Japan).
CELLULAR ARRAY PROCESSOR CAP AND ITS APPLICATION TO COMPUTER GRAPHICS c61
Hiroyuki Sato, Kouichi Murakami, Morio Ikesaka, Hiroaki Ishihata, and Mitsuo Ishii *In* National Aerospace Lab., Proceedings of the 5th NAL Symposium on Aircraft Computational Aerodynamics Nov. 1987 p 262-271 In JAPANESE; ENGLISH summary Original contains color illustrations (For primary document see N88-26290 20-01)
Avail: NTIS HC A12/MF A01

A general purpose highly parallel computer Cellular Array Processor (CAP) was developed. The CAP consists of 64 processors configured in a two dimensional array. Communication between cells is done in two ways: Global communication using a common bus and local communication using intercell communication lines. Each cell has video memory for subimage storage. A frame of image data distributed to many cells is displayed directly on a monitor through the video bus. A multitask real time operating system called Cell Monitor was developed for efficient parallel processing. The CAP was applied to computer graphics. High quality image generation using ray tracing is efficiently performed on the CAP. Performance in ray tracing with 64 cells reaches 80 percent of Fujitsu's M-380 main frame computer. Author

N88-26328*# National Aeronautics and Space Administration. Lewis Research Center, Cleveland, Ohio.
FIBER OPTICS FOR ADVANCED AIRCRAFT
Robert J. Baumbick 1988 13 p Presented at the Fiber Optics, Optoelectronics and Laser Applications International Symposium and Exhibition, Boston, Mass., 6-9 Sep. 1988; sponsored by the Society of Photo-Optical Instrumentation Engineers
(NASA-TM-101294; E-4276; NAS 1.15:101294) Avail: NTIS HC A03/MF A01 CSCL 01B

The increased use of composites makes the digital control more susceptible to electromagnetic effects. In order to provide the protection to the digital control additional shielding will be required as well as protective circuitry for the electronics. This results in increased weight and reduced reliability. The advantages that fiber optic technology provides for advanced aircraft applications is recognized. The use of optical signals to carry information between the aircraft and the control module provides immunity from contamination by electromagnetic sources as well as other important benefits such as reduced weight and volume resulting from the elimination of the shielding and the replacement of metal conductors with low weight glass fibers. In 1975 NASA began work to develop passive optical sensors for use with fiber optics in aircraft control systems. The problem now is to choose the best optical sensor concepts and evaluate them for use. In 1985 NASA and DOD entered into a joint program, Fiber Optic Control System Integration (FOCSI), to look at optical technology specifically for use in advanced aircraft systems. The results of this program are discussed. The conclusion of the study indicated that the use of fiber optic technology in advanced aircraft systems is feasible and desirable. The study pointed to a lack of available sensors from vendors capable of operating in the adverse environments of advanced aircraft. Author

02 AERODYNAMICS

Includes aerodynamics of bodies, combinations, wings, rotors, and control surfaces; and internal flow in ducts and turbomachinery.

For related information see also *34 Fluid Mechanics and Heat Transfer.*

N88-26329# Tokyo Univ. (Japan). Inst. of Space and Astronautical Science.
HIGH SPEED AND HIGH ANGLE OF ATTACK WIND TUNNEL TEST RESULTS OF THE WINGED SPACE VEHICLE C-2
Yoshifumi Inatani, Kiyoshi Sato, and Keiichi Karashima Oct. 1987 36 p
(ISAS-RN-623; ISSN-0285-6808) Avail: NTIS HC A03/MF A01

Wind tunnel test results of the Winged Space Vehicle executed in 1984 and 1985 at the National Aerospace Laboratory in Tokyo are discussed. The test was conducted and supported by the Working Group for the Development of a Winged Space Vehicle at the Institute of Space and Astronautical Science (ISAS) to obtain the aerodynamic characteristics of the vehicle recently studied in a preliminary aerodynamic design phase. In the present study, attention has been paid to both longitudinal and lateral/directional stability and controllability at high angles of attack at the high speeds encountered at atmospheric reentry. Test results are summarized in terms of aerodynamic coefficients and their derivatives. Detailed discussions are made to reveal the relations between vehicle configuration and aerodynamic characteristics of the vehicle. Author

N88-26330# Tokyo Univ. (Japan). Inst. of Space and Astronautical Science.
ON THE DYNAMIC BEHAVIOR OF BALLOON DURING ITS LAUNCH; APPLICATION OF PANEL METHOD AND EXTENSION TO UNSTEADY PROBLEM
Yoshifumi Inatani Jul. 1987 25 p
(ISAS-RN-622; ISSN-0285-6808) Avail: NTIS HC A03/MF A01

The boundary integral method (Panel method) has been applied and extended to investigate the unsteady problem in which body shape is deformed dynamically due to flow effects inside or outside the body. Such an unsteady effect has been represented by use of an extension of the conventional panel method. The interaction between the deformation of the body and the flow field is represented as a Virtual Mass Matrix, and the motion of the body surface and the flow field are solved by tracing the control points distributed on the body surface. Integral relations of the singularity distributed on the panel are also presented. Techniques developed are applied to the dynamic simulation of a balloon launching. A series of simulation studies was carried out and the deformation of the balloon during its launch has been followed. The dynamic behavior of the balloon during launching and the load history of the balloon membrane are obtained. Author

N88-26331# Georgia Inst. of Tech., Atlanta.
WALL INTERFERENCE ASSESSMENT/CORRECTION OF DATA FROM TESTS OF A CAST 10-2/DOA 2 AIRFOIL IN THE LANGLEY 0.3-m TRANSONIC CRYOGENIC TUNNEL M.S. Thesis
Clyde R. Gumbert May 1988 68 p
Avail: NTIS HC A04/MF A01

A Wall Interference Assessment/Correction (WIAC) procedure developed for the 8- by 24-inch slotted wall airfoil test section of the Langley 0.3-m Transonic Cryogenic Tunnel was applied to data from three tests of the CAST 10-2/DOA 2 airfoil. The uncorrected data from these tests contained dissimilarities attributable to different model sizes and differences in test section conditions. It is shown that the upstream flow angle required as a boundary condition in the WIAC code can be deduced from the first pass through the correction code by considering the front of the model to be a flow angle probe. It is also shown that a model aspect ratio factor such as that proposed by Murthy is required to more properly account for the sidewall boundary layer contribution to the blockage interference and hence the Mach number correction. The resulting angle of attack and Mach number

corrections make data from the three tests collapse over most of the range of Mach number and Reynolds number where the tests overlap. Author

N88-26332*# Texas A&M Univ., College Station. Dept. of Aerospace Engineering.
AN INITIAL INVESTIGATION INTO METHODS OF COMPUTING TRANSONIC AERODYNAMIC SENSITIVITY COEFFICIENTS Semiannual Progress Report, 1 Jan. - 30 Jun. 1988
Leland A. Carlson Jul. 1988 138 p
(Grant NAG1-793)
(NASA-CR-183061; NAS 1.26:183061; TAMRF-5802-88-02)
Avail: NTIS HC A07/MF A01 CSCL 01A

The initial effort was concentrated on developing the quasi-analytical approach for two-dimensional transonic flow. To keep the problem computationally efficient and straightforward, only the two-dimensional flow was considered and the problem was modeled using the transonic small perturbation equation. B.G.

N88-26333# International Centre for Theoretical Physics, Trieste (Italy).
FINITE ELEMENT APPROXIMATION TO A MODEL PROBLEM OF TRANSONIC FLOW
S. Tangmanee Dec. 1986 23 p
(DE88-701835; IC-86/346) Avail: NTIS (US Sales Only) HC A03/MF A01

A model problem of transonic flow, the Tricomi equation, contained in IR sup 2 bounded by the rectangular curve boundary is posed in the form of symmetric positive differential equations. The finite element method is then applied. When the triangulation of omega-bar is made of quadrilaterals and the approximation space is the Lagrange polynomial, we get the error estimates. DOE

N88-26334# McDonnell-Douglas Corp., Long Beach, Calif.
IMPROVED POTENTIAL FLOW COMPUTATIONAL METHODS WITH EULER CORRECTIONS FOR AIRFOIL AND WING/BODY DESIGN Final Report, 15 Sep. 1985 - 15 Sep. 1987
L. T. Chen and T. Q. Dang 30 Sep. 1987 60 p
(Contract N00167-85-C-0134; W23-03)
(AD-A192303; MDC-K0445; DTRC-AD-CR-01-87) Avail: NTIS HC A04/MF A01 CSCL 01A

The development of two and three dimensional Euler correction methods based on the Clebsch transformation is described. In these methods, the velocity field is decomposed into irrotational and rotational parts. A multi-grid full potential method based on both the finite difference and finite volume formulations is modified to solve for the rotational part. Two approaches are developed to solve for the rotational field. The approximate Euler-Clebsch approach assumes the entropy is convected along mesh lines, while the exact Euler-Clebsch approach solves the convection of entropy numerically along streamlines. The two approaches agree well in the airfoil application. Only the approximate Euler-Clebsch approach is employed in the three dimensional calculations. A study of finite difference and finite volume formulations of the full potential equation is also included. Solutions are presented for various airfoils, wings and an F-14 wing/body and are compared with results of the full potential and the time marching Euler methods. GRA

N88-26335*# Stanford Univ., Calif. Dept. of Aeronautics and Astronautics.
NUMERICAL STUDY OF DELTA WING LEADING EDGE BLOWING
David Yeh, Domingo Tavella, and Leonard Roberts Jul. 1988 130 p
(Contract NCC2-341)
(NASA-CR-183101; NAS 1.26:183101; JIAA-TR-86) Avail: NTIS HC A07/MF A01 CSCL 01A

Spanwise and tangential leading edge blowing as a means of controlling the position and strength of the leading edge vortices are studied by numerical solution of the three-dimensional Navier-Stokes equations. The leading edge jet is simulated by defining a permeable boundary, corresponding to the jet slot, where suitable boundary conditions are implemented. Numerical results are shown to compare favorably with experimental measurements. It is found that the use of spanwise leading edge blowing at moderate angle of attack magnifies the size and strength of the leading edge vortices, and moves the vortex cores outboard and upward. The increase in lift primarily comes from the greater nonlinear vortex lift. However, spanwise blowing causes earlier vortex breakdown, thus decreasing the stall angle. The effects of tangential blowing at low to moderate angles of attack tend to reduce the pressure peaks associated with leading edge vortices and to increase the suction peak around the leading edge, so that the integrated value of the surface pressure remains about the same. Tangential leading edge blowing in post-stall conditions is shown to re-establish vortical flow and delay vortex bursting, thus increasing C sub L sub max and stall angle. Author

N88-26336*# Sverdrup Technology, Inc., Cleveland, Ohio.
HIGH SPEED INLET CALCULATIONS WITH REAL GAS EFFECTS Final Report
William J. Coirier Jul. 1988 8 p Presented at the 24th Joint Propulsion Conference, Boston, Mass., 11-13 Jul. 1988; sponsored in part by AIAA, ASME, SAE and ASEE
(Contract NAS3-24105)
(NASA-CR-182167; E-4287; NAS 1.26:182167; AIAA-88-3076)
Avail: NTIS HC A02/MF A01 CSCL 01A

A 2-D steady-state Navier-Stokes solver has been upgraded to include the effects of frozen and equilibrium air chemistry for applications to high speed flight vehicles. To provide a computationally economical first order approximation to the high temperature physics, variable thermodynamic data is used for the chemically frozen mode to allow for a variation with temperature of the air specific heats and enthalpy. For calculations involving air in chemical equilibrium, a specially modified version of the NASA Lewis Chemical Equilibrium Code, CEC, is used to compute the chemical composition and resultant thermochemical properties. The upgraded solver is demonstrated by comparing results from calorically perfect (C sub p=constant), thermally perfect (frozen) and equilibrium air calculations for a variety of geometries, and flight Mach numbers. Author

N88-26337*# National Aeronautics and Space Administration, Washington, D.C.
LUDWIG PRANDTL COLLECTED TREATISES ON APPLIED MECHANICS, HYDRO- AND AERODYNAMICS, PART 1
Walter Tollmien, Hermann Schlichting, and Henry Goertler Jul. 1988 50 p Transl. into ENGLISH from Ludwig Prandtl Gesammelte Abhandlungen zur Angewandten Mechanik, Hydro- und Aerodynamik, Erster Teil. Berlin (Federal Republic of Germany), Springer-Verlag, 1961 p 254-289 Transl. by SCITRAN, Inc., Santa Barbara, Calif.
(Contract NASw-4307)
(NASA-TT-20316; NAS 1.77:20316) Avail: NTIS HC A03/MF A01 CSCL 01A

The manifold peculiarities of the laws of air resistance are able to support entirely satisfactorily the aerodynamic theory of air resistance explained here. The shape of the rear portion of the body is in many instances more important for resistance than the shape of the front section. By means of appropriate design, the resistance of aircraft bodies and similar vehicles can be reduced to close to theoretical value zero. Author

N88-26338*# National Aeronautics and Space Administration, Washington, D.C.
LUDWIG PRANDTL COLLECTED TREATISES ON APPLIED MECHANICS, HYDRO- AND AERODYNAMICS, PART 2, IV INTERFACES AND RESISTANCE
Walter Tolmien, Hermann Schlichting, and Henry Goertler Jul. 1988 14 p Transl. into ENGLISH from Ludwig Prandtl Gesammelte Abhandlungen zur Angewandten Mechanik, Hydro- und Aerodynamik, Zweiter Teil. Ueber Fluessigkeitsbewegung bei Sehr Kleiner Reibung, Berlin (Fed. Republic of Germany),

Springer-Verlag, 1961 p 575-584 Transl. by SCITRAN, Inc., Santa Barbara, Calif.
(Contract NASw-4307)
(NASA-TT-20315; NAS 1.77:20315) Avail: NTIS HC A03/MF A01 CSCL 01A

This study describes tests and confirmation of the theories of Ludwig Prandtl concerning hydrodynamics, aerodynamics, interfaces, and drag. Author

N88-26339# Institut Franco-Allemand de Recherches, St. Louis (France).
INFLUENCE OF REAR BODY GEOMETRY ON THE VELOCITY CHARACTERISTICS OF THE NEAR WAKE [INFLUENCE DE LA GEOMETRIE DE L'ARRIERE-CORPS SUR LES CARACTERISTIQUES DE LA VITESSE DU PROCHE SILLAGE]
C. Berner and V. Petitdemange 24 Jun. 1988 26 p In FRENCH Original contains color illustrations
(ISL-R-113/87; ETN-88-92734) Avail: NTIS HC A03/MF A01

A two-dimensional laser Doppler velocimeter was used to study the influence of an axisymmetric body on near wake velocity fields. The axial velocity components, the axial turbulent intensity, and the turbulent kinetic energy are measured in the domain of subsonic compressible flow. As expected, rear body geometry has a considerable influence on the wake velocity characteristics. The separation point is a function of Mach number. At constant Mach number the size of recirculation zones diminishes when angle and distance increase. ESA

N88-26340*# National Aeronautics and Space Administration. Lewis Research Center, Cleveland, Ohio.
A DIAGONALLY INVERTED LU IMPLICIT MULTIGRID SCHEME
Jeffrey W. Yokota, David A. Caughey (Cornell Univ., Ithaca, N.Y.), and Rodrick V. Chima 1988 11 p Presented at the 1st National Fluid Dynamics Congress, Cincinnati, Ohio, 24-28 Jul. 1988; sponsored by AIAA, ASME, ASCE, SIAM and APS
(NASA-TM-100911; E-4163; NAS 1.15:100911; AIAA-88-3567) Avail: NTIS HC A03/MF A01 CSCL 01A

A new Diagonally Inverted LU Implicit scheme is developed within the framework of the multigrid method for the 3-D unsteady Euler equations. The matrix systems that are to be inverted in the LU scheme are treated by local diagonalizing transformations that decouple them into systems of scalar equations. Unlike the Diagonalized ADI method, the time accuracy of the LU scheme is not reduced since the diagonalization procedure does not destroy time conservation. Even more importantly, this diagonalization significantly reduces the computational effort required to solve the LU approximation and therefore transforms it into a more efficient method of numerically solving the 3-D Euler equations. Author

N88-26341# National Aerospace Lab., Amsterdam (Netherlands).
CALCULATION OF 2-D UNSTEADY TRANSONIC FULL POTENTIAL FLOW ABOUT OSCILLATING AIRFOILS BY TWO COMPLEMENTARY APPROACHES
H. Schippers and M. H. L. Hounjet 1986 16 p Presented at the 4th AIAA Applied Aerodynamics Conference, 9-11 Jun. 1986, San Diego, Calif. Previously announced in IAA as A86-49586 Sponsored by Nederlands Inst. voor Vliegtuigontwikkeling en Ruimtevaart, Delft
(PB88-127519; NLR-MP-86035-U) Avail: NTIS HC E03/MF E01; copy not available from STI Facility CSCL 01A

Results of 2-D unsteady transonic flow calculations for AGARD standard aeroelastic configurations are presented, which were obtained by numerical methods for the solution of the unsteady full potential equation. Two complementary methods were applied to oscillating transonic flow about thick blunt-nosed airfoils: (1) the time-integration TULIPS method; and (2) the time-linearized FIRANC method. The calculations were performed for the subsonic and transonic flow about the supercritical NLR 7301 airfoil, both undergoing sinusoidal pitching oscillations. The results of both methods are extensively compared. GRA

N88-26342*# National Aeronautics and Space Administration. Ames Research Center, Moffett Field, Calif.
VORTEX METHODS FOR SEPARATED FLOWS
Philippe R. Spalart Jun. 1988 66 p
(NASA-TM-100068; A-88097; NAS 1.15:100068) Avail: NTIS HC A04/MF A01 CSCL 01A

The numerical solution of the Euler or Navier-Stokes equations by Lagrangian vortex methods is discussed. The mathematical background is presented in an elementary fashion and includes the relationship with traditional point-vortex studies, the convergence to smooth solutions of the Euler equations, and the essential differences between two- and three-dimensional cases. The difficulties in extending the method to viscous or compressible flows are explained. The overlap with the excellent review articles available is kept to a minimum and more emphasis is placed on the area of expertise, namely two-dimensional flows around bluff bodies. When solid walls are present, complete mathematical models are not available and a more heuristic attitude must be adopted. The imposition of inviscid and viscous boundary conditions without conformal mappings or image vortices and the creation of vorticity along solid walls are examined in detail. Methods for boundary-layer treatment and the question of the Kutta condition are discussed. Practical aspects and tips helpful in creating a method that really works are explained. The topics include the robustness of the method and the assessment of accuracy, vortex-core profiles, timemarching schemes, numerical dissipation, and efficient programming. Calculations of flows past streamlined or bluff bodies are used as examples when appropriate. Author

N88-26343*# Florida Univ., Gainesville. Dept. of Engineering Science, Mechanics and Aerospace Engineering.
THE DETERMINATION OF THE TOPOLOGICAL STRUCTURE OF SKIN FRICTION LINES ON A RECTANGULAR WING-BODY COMBINATION
Leslie A. Yates and Richard L. Fearn Aug. 1988 13 p
(Grant NAG1-368)
(NASA-CR-4168; NAS 1.26:4168) Avail: NTIS HC A03/MF A01 CSCL 01A

A short tutorial in the application of topological ideas to the intepretation of oil flow patterns is presented. Topological concepts such as critical points, phase portraits, topological stability, and indexing are discussed. These concepts are used in an ordered procedure to construct phase portraits of skin friction lines with oil flow patterns for a wing-body combination and two angles of attack. The relationship between the skin friction phase portrait and planar cuts of the velocity field is also discussed. Author

N88-26292*# National Aeronautics and Space Administration. Ames Research Center, Moffett Field, Calif.
NUMERICAL SIMULATIONS OF AERODYNAMIC CONTRIBUTION OF FLOWS ABOUT A SPACE-PLANE-TYPE CONFIGURATION
Kisa Matsushima, Susume Takanashi, Kozo Fujii (National Aerospace Lab., Tokyo, Japan), and Shigeru Obayashi *In* National Aerospace Lab., Proceedings of the 5th NAL Symposium on Aircraft Computational Aerodynamics Nov. 1987 p 13-18 In JAPANESE; ENGLISH summary (For primary document see N88-26290 20-01)
Avail: NTIS HC A12/MF A01 CSCL 01B

N88-26293# National Aerospace Lab., Tokyo (Japan).
NUMERICAL SIMULATIONS OF FLOW AROUND SHUTTLE ORBITER
Satoru Ogawa, Tomiko Ishiguro, and Yoko Takakura (Fujitsu Ltd., Tokyo, Japan) *In its* Proceedings of the 5th NAL Symposium on Aircraft Computational Aerodynamics Nov. 1987 p 19-28 In JAPANESE; ENGLISH summary (For primary document see N88-26290 20-01)
Avail: NTIS HC A12/MF A01

N88-26294# National Aerospace Lab., Tokyo (Japan).
FINITE ELEMENT ANALYSIS OF INCOMPRESSIBLE VISCOUS FLOW AROUND MULTI-ELEMENT AEROFOILS

Masashi Shigemi *In its* Proceedings of the 5th NAL Symposium on Aircraft Computational Aerodynamics Nov. 1987 p 29-35 In JAPANESE; ENGLISH summary (For primary document see N88-26290 20-01)
Avail: NTIS HC A12/MF A01

N88-26295# Kyoto Univ. (Japan). Dept. of Aeronautical Engineering.
NUMERICAL SIMULATIONS OF ASTROPHYSICAL JETS
Takuya Matsuda, Ryuji Ishii, Yoshikuni Umeda, Atsuhiko Yasuda, Keisuke Sawada, and Eiji Shima (Kawasaki Heavy Industries Ltd., Kobe, Japan) *In* National Aerospace Lab., Proceedings of the 5th NAL Symposium on Aircraft Computational Aerodynamics Nov. 1987 p 37-42 In JAPANESE; ENGLISH summary (For primary document see N88-26290 20-01)
Avail: NTIS HC A12/MF A01

N88-26296# Nagoya Univ. (Japan).
NUMERICAL CALCULATION OF SUPERSONIC FLOW BY THE PNS EQUATIONS
Michiru Yasuhara and Yoshiaki Nakamura *In* National Aerospace Lab., Proceedings of the 5th NAL Symposium on Aircraft Computational Aerodynamics Nov. 1987 p 43-48 In JAPANESE; ENGLISH summary (For primary document see N88-26290 20-01)
Avail: NTIS HC A12/MF A01

N88-26297# Fuji Heavy Industries Ltd., Utsunomiya (Japan).
NAVIER-STOKES ANALYSIS OF TRANSONIC TRANSPORT AIRCRAFT EMPENNAGE
Yasuhiro Koshioka, Keisuke Kamo, and Kanichi Amano (Japan Aircraft Development Corp., Tokyo.) *In* National Aerospace Lab., Proceedings of the 5th NAL Symposium on Aircraft Computational Aerodynamics Nov. 1987 p 47-54 In JAPANESE; ENGLISH summary (For primary document see N88-26290 20-01)
Avail: NTIS HC A12/MF A01

N88-26298# Kyoto Univ. (Japan). Dept. of Engineering.
NUMERICAL SOLUTIONS OF THE EULER EQUATIONS FOR THE FLOW FIELD AROUND COUNTER-ROTATING PROPELLERS
Makoto Kobayakawa and Masahiro Nakao (Mitsubishi Heavy-Industries Ltd., Tokyo, Japan) *In* National Aerospace Lab., Proceedings of the 5th NAL Symposium on Aircraft Computational Aerodynamics Nov. 1987 p 55-63 In JAPANESE; ENGLISH summary Original language document was announced in IAA as A88-13544 (For primary document see N88-26290 20-01)
Avail: NTIS HC A12/MF A01

N88-26299# Kyoto Univ. (Japan). Dept. of Aeronautical Engineering.
NUMERICAL SIMULATION OF SUPERSONIC FREE-JETS
Ryuji Ishii, Takuya Matsuda, Yoshikuni Umeda, Atsuhiko Yasuda, Keisuke Sawada, and Eiji Shima (Kawasaki Heavy Industries Ltd., Kobe, Japan) *In* National Aerospace Lab., Proceedings of the 5th NAL Symposium on Aircraft Computational Aerodynamics Nov. 1987 p 65-71 In JAPANESE; ENGLISH summary (For primary document see N88-26290 20-01)
Avail: NTIS HC A12/MF A01

N88-26300# Tokyo Univ. (Japan). Inst. of Computational Fluid Dynamics.
COMPUTATION OF FLOW AROUND NACA0012 AIRFOIL AT HIGH ANGLE OF ATTACK
Yoshifumi Shida and Kunio Kuwahara *In* National Aerospace Lab., Proceedings of the 5th NAL Symposium on Aircraft Computational Aerodynamics Nov. 1987 p 73-79 In JAPANESE; ENGLISH summary Previously announced in IAA as A87-42448 (For primary document see N88-26290 20-01)
Avail: NTIS HC A12/MF A01

N88-26301# National Aerospace Lab., Tokyo (Japan).
AERODYNAMIC SIMULATION FOR COMPLETE ASKA AIRCRAFT CONFIGURATION
Susumu Takanashi and Keisuke Sawada (Kawasaki Heavy Industries Ltd., Kobe, Japan) *In its* Proceedings of the 5th NAL Symposium on Aircraft Computational Aerodynamics Nov. 1987 p 81-84 In JAPANESE; ENGLISH summary (For primary document see N88-26290 20-01)
Avail: NTIS HC A12/MF A01

N88-26302*# National Aeronautics and Space Administration. Ames Research Center, Moffett Field, Calif.
NUMERICAL SIMULATION OF VISCOUS FLOWS OVER TRANSONIC AIRCRAFT CONFIGURATIONS
Susumu Takanashi, Masahiro Yoshida, Kozo Fujii, Kisa Matsushima (Fujitsu Ltd., Tokyo, Japan), and Shigeru Obayashi *In* National Aerospace Lab., Proceedings of the 5th NAL Symposium on Aircraft Computational Aerodynamics Nov. 1987 p 85-89 In JAPANESE; ENGLISH summary (For primary document see N88-26290 20-01)
Avail: NTIS HC A12/MF A01 CSCL 01A

N88-26303# National Aerospace Lab., Tokyo (Japan).
CALCULATIONS OF UNSTEADY AERODYNAMICS FOR A FULL AIRCRAFT CONFIGURATION USING BOUNDARY ELEMENT METHOD
Mitsunori Yanagizawa, Toshiyuki Morita, and Shigefumi Tatsumi (Mitsubishi Heavy-Industries Ltd., Tokyo, Japan) *In its* Proceedings of the 5th NAL Symposium on Aircraft Computational Aerodynamics Nov. 1987 p 91-101 In JAPANESE; ENGLISH summary (For primary document see N88-26290 20-01)
Avail: NTIS HC A12/MF A01

N88-26304# National Aerospace Lab., Tokyo (Japan).
RAREFIED GAS NUMERICAL WIND TUNNEL 3: UNIVERSAL CODE FOR THREE DIMENSIONAL BODIES
Katsuhisa Koura, Kinuyo Nakamura, Toshio Isobe, Kazuyo Suematsu, Masayuki Hatakeyama, and Toshiyuki Shimoji (Facom Hitac Co. Ltd., Japan) *In its* Proceedings of the 5th NAL Symposium on Aircraft Computational Aerodynamics Nov. 1987 p 103-107 In JAPANESE; ENGLISH summary (For primary document see N88-26290 20-01)
Avail: NTIS HC A12/MF A01

N88-26309# National Aerospace Lab., Tokyo (Japan).
NUMERICAL CALCULATION OF THREE DIMENSIONAL FLOW BY TVD SCHEME
Tomiko Ishiguro, Satoru Ogawa, and Yoko Takakura (Fujitsu Ltd., Tokyo, Japan) *In its* Proceedings of the 5th NAL Symposium on Aircraft Computational Aerodynamics Nov. 1987 p 137-146 In JAPANESE; ENGLISH summary (For primary document see N88-26290 20-01)
Avail: NTIS HC A12/MF A01

N88-26316# Kawasaki Heavy Industries Ltd., Kagamihara (Japan).
ON THE ACCURACY OF UPWIND BIASED FINITE VOLUME METHOD
Keisuke Sawada and Susumu Takanashi *In* National Aerospace Lab., Proceedings of the 5th NAL Symposium on Aircraft Computational Aerodynamics Nov. 1987 p 191-195 In JAPANESE; ENGLISH summary (For primary document see N88-26290 20-01)
Avail: NTIS HC A12/MF A01

N88-26321# National Aerospace Lab., Tokyo (Japan).
NUMERICAL SIMULATION OF TRANSITION TO TURBULENCE IN PLANE POISEUILLE FLOW BY A SPECTRAL METHOD
Kiyoshi Yamamoto and Iwao Hosokawa (Iwate Univ., Morioka, Japan) *In its* Proceedings of the 5th NAL Symposium on Aircraft Computational Aerodynamics Nov. 1987 p 217-223 In JAPANESE; ENGLISH summary (For primary document see N88-26290 20-01)
Avail: NTIS HC A12/MF A01

N88-26322# Ministry of Transportation, Tokyo (Japan). Ship Research Inst.
NUMERICAL SIMULATION OF TURBULENT FLOW USING THE EXPONENTIAL EXPRESSION OF k-EPSILON EQUATION
Munehiko Hinatsu and Yoshiaki Kodama *In* National Aerospace Lab., Proceedings of the 5th NAL Symposium on Aircraft Computational Aerodynamics Nov. 1987 p 225-232 In JAPANESE; ENGLISH summary (For primary document see N88-26290 20-01)
Avail: NTIS HC A12/MF A01

N88-26323# Chiba Univ. (Japan). Faculty of Engineering.
RELAXATION SCHEME FOR COMPRESSIBLE FLOWS
Nobuhide Nishikawa and Akira Suzuki *In* National Aerospace Lab., Proceedings of the 5th NAL Symposium on Aircraft Computational Aerodynamics Nov. 1987 p 233-239 In JAPANESE; ENGLISH summary (For primary document see N88-26290 20-01)
Avail: NTIS HC A12/MF A01

N88-26324# Keio Univ., Tokyo (Japan). Faculty of Science and Technology.
THE MODIFIED-FLUID-IN-CELL METHOD TO WHICH ADAPTIVE MESH AND MULTIGRID WERE APPLIED
Ikuo Ono, Kentaro Motoda, Eriya Kanai, and Tsuneyo Ando *In* National Aerospace Lab., Proceedings of the 5th NAL Symposium on Aircraft Computational Aerodynamics Nov. 1987 p 241-246 In JAPANESE; ENGLISH summary (For primary document see N88-26290 20-01)
Avail: NTIS HC A12/MF A01

N88-26325# Tsukuba Univ., Ibaraki (Japan). Inst. of Engineering Mechanics.
GRID GENERATION OF A HELICOPTER ROTARY-WING
Alain Carcasses and Y. Yoshizawa *In* National Aerospace Lab., Proceedings of the 5th NAL Symposium on Aircraft Computational Aerodynamics Nov. 1987 p 247-253 In JAPANESE; ENGLISH summary (For primary document see N88-26290 20-01)
Avail: NTIS HC A12/MF A01

03 AIR TRANSPORTATION AND SAFETY

Includes passenger and cargo air transport operations; and aircraft accidents.

For related information see also *16 Space Transportation* and *85 Urban Technology and Transportation.*

N88-26344*# National Aeronautics and Space Administration. Langley Research Center, Hampton, Va.
INFLUENCE OF WIND SHEAR ON THE AERODYNAMIC CHARACTERISTICS OF AIRPLANES
Dan D. Vicroy Aug. 1988 62 p Sponsored by NASA, Washington, D.C. and DOT, Washington, D.C.
(NASA-TP-2827; L-16439; NAS 1.60:2827; DOT/FAA/PS-88/15) Avail: NTIS HC A04/MF A01 CSCL 01C

The aerodynamic effect of shear flow through a series of sensitivity studies of the wind velocity gradients and wing planform geometry parameters is investigated and characterized. The wind shear effect is computed using a modified vortex-lattice computer program and characterized through the formulation of wind shear aerodynamic coefficients. The magnitudes if the aerodynamic effects are demonstrated by computation of the resultant change in the aerodynamics of a conventional wing and horizontal stability configuration on a fixed flight path through a simulated microburst. The results indicate that as much as 20 percent of the control authority of the airplane may be required to counteract the wind-shear-induced forces and moments in the microburst environment. Author

N88-26345# National Transportation Safety Board, Washington, D. C.
AIRCRAFT ACCIDENT REPORT: JOE FOSTER EXCAVATING, INC., BELL 206B, N49606, IN-FLIGHT COLLISION WITH TREES, ALAMO, CALIFORNIA, AUGUST 3, 1986
2 May 1988 27 p
(PB88-910405; NTSB-AAR-88-04) Avail: NTIS HC A03/MF A01 CSCL 01C

On August 3, 1986, at 1235 Pacific daylight saving time, a Bell 206B helicopter, N49606, owned and operated by Joe Foster Excavating, Inc., Danville, California, crashed in a wooded area in Alamo, California, while circling a residence. Visual meteorological conditions prevailed at the time. The pilot and passenger, the owner of the helicopter, sustained fatal injuries; the helicopter was destroyed. The National Transportation Safety Board determines that the probable cause of this accident was the pilot's incapacitation resulting from a myocardial event. Contributing to the cause of the accident was the pilot's failure to comply with the provisions of both his medical and pilot certificates and the inadequate procedures used by the Federal Air Surgeon to medically recertify the pilot. Author

N88-26346# National Transportation Safety Board, Washington, D. C.
AIRCRAFT ACCIDENT REPORT: MIDAIR COLLISION OF SKYWEST AIRLINES SWEARINGEN METRO 2, N163SW, AND MOONEY M20, N6485U, KEARNS, UTAH, JANUARY 15, 1987
15 Mar. 1988 71 p
(PB88-910404; NTSB-AAR-88-03) Avail: NTIS HC A04/MF A01 CSCL 01C

On January 15, 1987, at about 1252 mountain standard time, SkyWest flight 1834, a Swearingen SA-226TC (METRO 2), and a Mooney M20 collided in flight over Kearns, Utah, in visual meteorological conditions. The two pilots and six passengers aboard the METRO 2 and the two pilots aboard the Mooney were killed in the accident which occurred within the confines of the Salt Lake City airport radar service area. The National Transportation Safety Board determines that the probable cause of this accident was lack of navigational vigilance by the Mooney instructor pilot which led to the unauthorized intrusion into the Salt Lake City airport radar service area. Contributing to the accident were the absence of a mode-C transponder on the Mooney airplane and the limitations of the air traffic control system to provide collision protection under the circumstances of this accident. Author

N88-26347*# Princeton Univ., N. J. Dept. of Mechanical and Aerospace Engineering.
INTELLIGENT GUIDANCE AND CONTROL FOR WIND SHEAR ENCOUNTER Biannual Progress Report
Robert F. Stengel 21 Jul. 1988 101 p
(Grant NAG1-834)
(NASA-CR-183060; NAS 1.26:183060; PR-150-6549-1) Avail: NTIS HC A06/MF A01 CSCL 01C

The principal objective is to develop methods for assessing the likelihood of wind shear encounter, for deciding what flight path to pursue, and for using the aircraft's full potential for combating wind shear. This study requires the definition of both deterministic and statistical techniques for fusing internal and external information, for making go/no-go decisions, and for generating commands to the aircraft's cockpit displays and autopilot for both manually controlled and automatic flight. The program has begun with the development of a real-time expert system for pilot aiding that is based on the results of the FAA Windshear Training Aids Program. A two-volume manual that presents an overview, pilot guide, training program, and substantiating data provides guidelines for this initial development. The Expert System to Avoid Wind Shear (ESAWS) currently contains over 140 rules and is coded in the LISP programming language for implementation on a Symbolics 3670 LISP machine. Author

N88-26348*# Structural Semantics, Palo Alto, Calif.
CHECKLIST INTERRUPTION AND RESUMPTION: A LINGUISTIC STUDY Final Report
Charlotte Linde and Joseph Goguen Jul. 1987 34 p
(Contract NAS2-11052)
(NASA-CR-177460; NAS 1.26:177460) Avail: NTIS HC A03/MF A01 CSCL 01C

This study forms part of a project investigating the relationships among the formal structure of aviation procedures, the ways in which the crew members are taught to execute them, and the ways in which thet are actually performed in flight. Specifically, this report examines the interactions between the performance of checklists and interruptions, considering both interruptions by radio communications and by other crew members. The data consists of 14 crews' performance of a full mission simulation of a higher ratio of checklist speech acts to all speech acts within the span of the performance of the checklist. Further, it is not number of interruptions but length of interruptions which is associated with crew performance quality. Use of explicit holds is also associated with crew performance. Author

N88-26349*# Structural Semantics, Palo Alto, Calif.
COMMUNICATION TRAINING FOR AIRCREWS: A REVIEW OF THEORETICAL AND PRAGMATIC ASPECTS OF TRAINING PROGRAM DESIGN Final Report
Charlotte Linde, Joseph Goguen, and Linda Devenish Jun. 1987 56 p
(Contract NAS2-12379)
(NASA-CR-177459; NAS 1.26:177459) Avail: NTIS HC A04/MF A01 CSCL 01C

This study is the final report of a project studying methods of communications training applicable to both civilian and military aviation personnel, including multiperson teams or single pilot fixed wing or rotary wing aircraft. A review is provided of a number of theories proposed as relevant for producing training materials for improved communications. Criteria are given for evaluating the applicability of training programs to the aviation environment, and these criteria are applied to United Airlines' Resources Management Training, as well as to a number of commercially available general purpose training programs. The report considers in detail assertiveness training and grid management training, examining their theoretical background and attempts made to validate their effectiveness. It was found that there are substantive difficulties in assessing the effectiveness of both training programs, as well as problems with the theories underlying them. However, because the aviation environment offers unique advantages for studying the effectiveness of communications training, recommendations are made on the design of appropriate training programs and on procedures that might be used to validate them. Author

N88-26350# Boeing Commercial Airplane Co., Seattle, Wash.
ENHANCED EMERGENCY SMOKE VENTING Final Report
Elliott L. Maylor Jul. 1988 96 p
(Contract DTFA03-87-C-00038)
(DOT/FAA/CT-88/22) Avail: NTIS HC A05/MF A01

This study evaluated two concepts modifying the air conditioning systems of large commercial airplanes to enhance the venting of smoke that may be continuously injected into the passenger cabin during inflight fire emergencies. Data from past fire accidents and airplane tests provided a basis for creating four fire/smoke scenarios and deriving five sets of equations to predict the smoke venting effectiveness of current airplanes and the proposed concepts. Concept A would modify the air conditioning packs by adding high flow modes with dual outflow valves and Concept B would add ram air ventilation with an added dump valve. The estimated costs to incorporate Concept A or B in the U.S. fleet were about 381 or 587 million dollars, respectively. The effectiveness equations predicted that both concepts would provide only slightly significant smoke venting enhancement. Furthermore, the study showed that both concepts would have been negated by reported crew actions and/or fire damage in past fires. It was concluded that current U.S. fleet airplanes will keep a majority of the passenger cabin free of smoke during inflight fires while the air conditioning systems are kept operating. Author

04 AIRCRAFT COMMUNICATIONS AND NAVIGATION

Includes digital and voice communication with aircraft; air navigation systems (satellite and ground based); and air traffic control.

For related information see also *17 Space Communications, Spacecraft Communications, Command and Tracking* and *Communications and Radar.*

N88-26351# Sandia National Labs., Albuquerque, N. Mex.
SIMPLE 2-D NAVIGATION FOR WHEELED VEHICLES
P. R. Klarer 1988 20 p Presented at the 15th AUVS Annual Technical Symposium, San Diego, Calif., 6 Jun. 1988
(Contract DE-AC04-76DP-00789)
(DE88-007115; SAND-88-0540C; CONF-880689-1) Avail: NTIS HC A03/MF A01

This paper describes a simple algorithm to perform navigation in a two-dimensional world model. The algorithm utilizes a simple geometric approach which is first applied to a bicycle. The equations are then expanded to apply to 3- and 4-wheeled vehicles with conventional steering mechanism (such as the Ackerman steering geometry in the 4-wheeled case). Calculations for omnidirectional robots which utilize differential odometry and differential drive are described as well. Practical considerations and sources of error are discussed, as are possible extensions of this method to a three-dimensional world model. DOE

N88-26352# Oak Ridge National Lab., Tenn.
TREATMENT OF SYSTEMATIC ERRORS IN THE PROCESSING OF WIDE ANGLE SONAR SENSOR DATA FOR ROBOTIC NAVIGATION
M. Beckerman and E. M. Oblow Apr. 1988 30 p
(Contract DE-AC05-84OR-21400)
(DE88-008961; ORNL/TM-10763; CESAR-88/07) Avail: NTIS HC A03/MF A01

A methodology has been developed for the treatment of systematic errors which arise in the processing of sparse sensor data. We present a detailed application of this methodology to the construction from wide-angle sonar sensor data of navigation maps for use in autonomous robotic navigation. In the methodology we introduce a four-valued labelling scheme and a simple logic for label combination. The four labels, conflict, occupied, empty and unknown, are used to mark the cells of the navigation maps; the logic allows for the rapid updating of these maps as new information is acquired. The systematic errors are treated by relabelling conflicting pixel assignments. Most of the new labels are obtained from analyses of the characteristic patterns of conflict which arise during the information processing. The remaining labels are determined by imposing an elementary consistent-labelling condition. DOE

N88-26353# Eurocontrol Experimental Centre, Bretigny (France).
STATISTICAL PROPERTIES OF REAL TIME EVENTS IN AN ATC (AIR TRAFFIC CONTROL) SYSTEM
H. P. Englmeier and P. Hunt Jun. 1987 28 p
(PB88-118781; EEC-205) Avail: NTIS HC E04/MF E04; copy not available from STI Facility CSCL 17G

The analysis of the flow of data in a processing system concerning air traffic control is described. It was found that the frequency of events or interrupts when expressed as a function of the time interval between two consecutive events or interrupts follows a lognormal distribution or a superposition of several lognormal distributions. The analysis, the validity of the results, the theoretical background and possible applications for real time systems are treated. Author

N88-26354# Air Command and Staff Coll., Maxwell AFB, Ala.
NAVSTAR GLOBAL POSITIONING SYSTEM
Rudolph T. Schwab Apr. 1988 23 p
(AD-A192609; ACSC-88-2355) Avail: NTIS HC A03/MF A01 CSCL 17G

The NAVSTAR Global Positioning System (GPS) is an all-weather, jam-resistant, continuous-operation, space-based, passive radio navigation and positioning system. The GPS consists of three segments: the Space Segment, the Control Segment, and the User Segment. The United States Armed Forces will purchase over 20,000 GPS user sets, with the US Army buying 6,000 sets. This article for publication will provide the Army soldier with an understanding of the capabilities and limitations of GPS. The article includes a short history on why GPS was developed, discusses the three GPS segments, and provides examples on how GPS will enhance US Army operations. GRA

N88-26355# Technische Hogeschool, Delft (Netherlands). Afdeling Geodesie.
POSITION AND VELOCITY DETERMINATION USING A GLOBAL POSITIONING SYSTEM: AN OUTLINE Thesis [POSITIE- EN SNELHEIDSBEPALING M.B.V. G.P.S.: EEN SCHETS]
O. J. Kikstra Feb. 1987 89 p In DUTCH
(B8735052; ETN-88-92429) Avail: NTIS HC A05/MF A01

A part of the software for a moving sequential Global Positioning System (GPS) receiver was developed. The principles of GPS and of the moving receiver are explained. The data emitted by the satellite are described. The prediction program that calculates the position of the satellite with respect to the receiver, the expected satellite configuration, and the expected Doppler shift of the emitted signal, starting from NASA data or satellite data, is described. The data processing program, based on a Kalman filter approximation, is presented. Advice for modifications in the programs is given. ESA

N88-26356# Technische Hogeschool, Delft (Netherlands). Vakgroep Mathematische en Physische Geodaesie.
RESEARCH PROJECT LORAN-C OF THE GEOMETRIC SERVICE OF THE MINISTRY OF PUBLIC WORKS Thesis [ONDERZOEK LORAN-C BIJ DE MEETKUNDIGE DIENST VAN RIJKSWATERSTAAT]
J. P. H. Chatrou May 1987 62 p In DUTCH Original contains color illustrations
(B8735055; ETN-88-92472) Avail: NTIS HC A04/MF A01

The data from the radio position finding system Loran-C were analyzed from a geodetic point of view. The system and its components are introduced. The signal analysis and the differential application of Loran-C are presented. The emphasis was on the development of software for signal processing, as well as on user friendliness and robustness. The results of practical tests show that Loran-C allows navigation in a large area. The pseudo-circular mode gives better results than the hyperbolic one. The dynamic model is important for quality improvement with a filter. The reliability can be improved by differential use, with the monitor station as close as possible to the user. ESA

N88-26357# Technische Hogeschool, Delft (Netherlands).
THE SERCEL TR5S GLOBAL POSITIONING SYSTEM (GPS) RECEIVER Thesis [SERCEL TR55 GPS ONTVANGER. MEETPRINCIPE'S EN RESULTATEN]
G. M. LammertsvanBueren May 1987 57 p In DUTCH
(ETN-88-92473) Avail: NTIS HC A04/MF A01

The Sercel TR5S measuring procedures are presented. The GPS measurements, single-point position finding using pseudo-range measurements, and cumulative phase observations to improve the precision of pseudo-range measurements are outlined. The remaining differences between range variations measured with pseudo-range and phase observations are less than 2 m in 30 min. The smoothed-pseudo-range principle is presented. The measurement of baseline using phase observations of the Sercel receiver is explained. The results of phase observations are bad (differences of up to 37 m) because the baselines are very long (240 to 650 km) and the effects of ionosphere and troposphere are not corrected. The results of pseudo-range calculations are good: accuracy of 2 ppm is obtained under favorable circumstances. ESA

N88-26358# National Aerospace Lab., Amsterdam (Netherlands). Informatics Div.
A POSITIONING SYSTEM BASED ON NAVSAT
N. M. deReus, G. Moek, and G. J. Olsder (Technische Hogeschool, Delft, Netherlands) 24 Feb. 1987 38 p Submitted for publication
(NLR-MP-87018-U; B8803893; ETN-88-92610) Avail: NTIS HC A03/MF A01

The user position estimator of the NAVSAT system is described. Motion of the users is modelled by splines. The estimation procedure is based on the extended Kalman filter approach. The estimator was included in a NAVSAT system simulator. Various designs with respect to number of satellites, accuracy of the clocks, magnitude of modelling errors, and order of the spline approximation used, can be evaluated using this simulator. Results of two runs with the filter are presented. Based on second order spline approximations of the user trajectory, absolute position accuracies of a few meters are obtained. Using third order splines does not give better results; this may depend on the particular user trajectories simulated and on the fact that noise on these trajectories only influences the acceleration directly (and not the velocity or third derivatives of the position). The estimation of Regional Center clock biases works reasonably well. ESA

N88-26359*# Texas Instruments, Inc., Plano, Tex. Defense Systems and Electronics Group.
SPACECRAFT APPLICATIONS OF ADVANCED GLOBAL POSITIONING SYSTEM TECHNOLOGY Final Report
15 Jun. 1988 77 p
(Contract NAS9-17781)
(NASA-CR-172063; NAS 1.26:172063; U1-780130-F) Avail: NTIS HC A05/MF A01 CSCL 17G

This is the final report on the Texas Instruments Incorporated (TI) simulations study of Spacecraft Application of Advanced Global Positioning System (GPS) Technology. This work was conducted for the NASA Johnson Space Center (JSC) under contract NAS9-17781. GPS, in addition to its baselined capability as a highly accurate spacecraft navigation system, can provide traffic control, attitude control, structural control, and uniform time base. In Phase 1 of this program, another contractor investigated the potential of GPS in these four areas and compared GPS to other techniques. This contract was for the Phase 2 effort, to study the performance of GPS for these spacecraft applications through computer simulations. TI had previously developed simulation programs for GPS differential navigation and attitude measurement. These programs were adapted for these specific spacecraft applications. In addition, TI has extensive expertise in the design and production of advanced GPS receivers, including space-qualified GPS receivers. We have drawn on this background to augment the simulation results in the system level overview, which is Section 2 of this report. Author

05 AIRCRAFT DESIGN, TESTING AND PERFORMANCE

Includes aircraft simulation technology.

For related information see also *18 Spacecraft Design, Testing and Performance* and *39 Structural Mechanics*. For land transportation vehicles see *85 Urban Technology and Transportation*.

N88-26360*# Lockheed Aeronautical Systems Co., Marietta, Ga.
PROPFAN TEST ASSESSMENT TESTBED AIRCRAFT STABILITY AND CONTROL/PERFORMANCE 1/9-SCALE WIND TUNNEL TESTS Final Report
B. H. Little, Jr., K. H. Tomlin, A. S. Aljabri, and C. A. Mason

May 1988 157 p
(Contract NAS3-24339)
(NASA-CR-182121; NAS 1.26:182121; LG88ER0056) Avail: NTIS HC A08/MF A01 CSCL 01C

One-ninth scale wind tunnel model tests of the Propfan Test Assessment (PTA) aircraft were performed in three different NASA facilities. Wing and propfan nacelle static pressures, model forces and moments, and flow field at the propfan plane were measured in these tests. Tests started in June 1985 and were completed in January 1987. These data were needed to assure PTA safety of flight, predict PTA performance, and validate analytical codes that will be used to predict flow fields in which the propfan will operate. Author

N88-26361*# National Aeronautics and Space Administration. Hugh L. Dryden Flight Research Facility, Edwards, Calif.
FLIGHT RESEARCH AND TESTING
Terrill W. Putnam and Theodore G. Ayers Jun. 1988 24 p Presented at the Transonic Symposium, Hampton, Va., Apr. 1988
(NASA-TM-100439; H-1483; NAS 1.15:100439) Avail: NTIS HC A03/MF A01 CSCL 01C

Flight research and testing form a critical link in the aeronautic R and D chain. Brilliant concepts, elegant theories, and even sophisticated ground tests of flight vehicles are not sufficient to prove beyond doubt that an unproven aeronautical concept will actually perform as predicted. Flight research and testing provide the ultimate proof that an idea or concept performs as expected. Ever since the Wright brothers, flight research and testing have been the crucible in which aeronautical concepts have advanced and been proven to the point that engineers and companies have been willing to stake their future to produce and design new aircraft. This is still true today, as shown by the development of the experimental X-30 aerospace plane. The Dryden Flight Research Center (Ames-Dryden) continues to be involved in a number of flight research programs that require understanding and characterization of the total airplane in all the aeronautical disciplines, for example the X-29. Other programs such as the F-14 variable-sweep transition flight experiment have focused on a single concept or discipline. Ames-Dryden also continues to conduct flight and ground based experiments to improve and expand the ability to test and evaluate advanced aeronautical concepts. A review of significant aeronautical flight research programs and experiments is presented to illustrate both the progress made and the challenges to come. Author

N88-26362# Advisory Group for Aerospace Research and Development, Neuilly-Sur-Seine (France).
FLIGHT MECHANICS PANEL SYMPOSIUM ON ROTORCRAFT DESIGN FOR OPERATIONS: TECHNICAL EVALUATION REPORT
F. Reina (Agusta Sistemi S.p.A., Varese, Italy) Mar. 1988 17 p Symposium held in Amsterdam, Netherlands, 13-16 Oct. 1986
(AGARD-AR-243; ISBN-92-835-0450-X) Copyright Avail: NTIS HC A03/MF A01

The expanding roles of the helicopter and the intensified threat perceived by its potential users have led to proposals for future rotorcraft with characteristics significantly different from existing types. The resulting rapid evolution of rotorcraft configurations, in response to user demands, now requires a translation into design criteria to permit the aerospace research and development community to provide appropriate and cost effective responses to these demands. The objective of this symposium is to explore the impact of operational needs on the evolution of rotorcraft design and to identify priorities and neglected topics. Three specific issues are central to this problem: (1) the translation of operational mission requirements into design criteria; (2) the evaluation of techniques to incorporate user defined needs into the design and methods of test and verification; and (3) the identification of design areas where unusual or new user needs are demanding special or radical features. All papers were obtained by invitation. The Conference Proceedings, commissioned by the AGARD Flight Mechanics Panel are published separately as AGARD CP 423. This Advisory Report was prepared at the request of the Flight Mechanics Panel of AGARD. Author

N88-26363# Naval Postgraduate School, Monterey, Calif.
THE EFFECT OF A TURBULENT AIRSTREAM ON A VERTICALLY-LAUNCHED MISSILE AT HIGH ANGLES OF ATTACK M.S. Thesis
Donald P. Roane, Jr. Dec. 1987 72 p
(AD-A192408) Avail: NTIS HC A04/MF A01 CSCL 16B

The purpose of this thesis is to initiate an investigation of the response of a shipboard surface-to-air missile launched vertically into a region of turbulence at high angles of attack. A review was conducted on the effects of asymmetric vortices, turbulent flowfields, and the marine atmospheric environment on a slender body of revolution. Turbulence mapping of a wind tunnel with installed turbulence-generating grids was conducted using hot-wire anemometry. The resultant turbulence intensities and length scales were analyzed as a function of the downstream distance and the grid mesh-width/bar-diameter ratio. Turbulence intensity was found to decrease, while the length scale increased, with increasing distance from the generating grid. Both the turbulence intensity and length scale increased with an increase in the grid bar diameter. GRA

N88-26364# Deutsche Airbus G.m.b.H., Munich (West Germany).
AIRBUS 1987: SUCCESS IN EUROPE [AIRBUS 1987 - ERFOLG IN EUROPA]
1987 36 p In GERMAN
(ETN-88-92099) Avail: NTIS HC A03/MF A01

The European Airbus-program initiated in 1969 with emphasis on the 6 Airbus versions from A300 to A340-300 is reviewed. Data concern dimensions performance, capacity, weight and flight length. Advantages and main aerodynamic and flight characteristics of each model are given. ESA

N88-26365# Societe Nationale Industrielle Aerospatiale, Suresnes (France). Direction Centrale de la Qualite.
SENSITIVITY TO CRACK INITIATION IN THICK ASSEMBLIES. TEST REPORT 48-444 [SENSIBILITE DE DETECTION DE CRIQUES DANS LES ASSEMBLAGES EPAIS. PROCES-VERBAL 48-444]
J. Odorico and D. Lecuru 10 Feb. 1987 27 p In FRENCH
(Contract STPA-85-96-032)
(Rept-48-444; ETN-88-92147) Avail: NTIS HC A03/MF A01

The safe detection values for cracks starting at bolt holes in aluminum plates thicker than 5 mm is studied. The choice and preparation of the assembly to be controlled are discussed. A control procedure based on low frequency (200 Hz) eddy currents is described. The study of an Airbus structural element shows that the estimates of crack length distribution are in accordance with the measurements. ESA

N88-26366# National Aerospace Lab., Amsterdam (Netherlands). Flight Div.
TRAJECTORY MEASUREMENT OF THE FOKKER 100 AIRCRAFT DURING AUTOLAND TESTING
R. Krijn and J. C. T. vanderVeen 6 Feb. 1986 16 p Presented at the 1986 Aerospace Industries/Test Measurement Symposium, Seattle, Wash., 5-8 May 1986 Sponsored by the Netherlands Agency for Aerospace Programs
(NLR-MP-86010-U; B8803803; ETN-88-92602) Avail: NTIS HC A03/MF A01

An accurate, fast, and flexible trajectory measurement system was developed for the automatic landing trials of the Fokker 100 prototype. The system combines the photogrammetrical forward-looking camera method with inertial navigation. Accuracy is 0.3 m standard deviation along track, and 0.15 m cross track and height. Turnaround time is less than 12 hr, and location can be changed at 24 hr notice. ESA

N88-26367*# Boeing Vertol Co., Philadelphia, Pa.
HOVER PERFORMANCE TESTS OF BASELINE METAL AND ADVANCED TECHNOLOGY BLADE (ATB) ROTOR SYSTEMS FOR THE XV-15 TILT ROTOR AIRCRAFT Final Report
K. Bartie, H. Alexander, M. McVeigh, S. LaMon, and H. Bishop Oct. 1986 151 p
(Contract NAS2-11250)
(NASA-CR-177436; NAS 1.26:177436; D210-12380-1) Avail: NTIS HC A08/MF A01 CSCL 01C

Rotor hover performance data were obtained for two full-scale rotor systems designed for the XV-15 Tilt Rotor Research Aircraft. One rotor employed the rectangular planform metal blades (rotor solidity = 0.089) which were used on the initial flight configuration of the XV-15. The second rotor configuration examined the nonlinear taper, composite-construction, Advanced Technology Blade (ATB), (rotor solidity = 0.10) designed to replace the metal blades on the XV-15. Variations of the baseline ATB tip and cuff shapes were also tested. A new six-component rotor force and moment balance designed to obtain highly accurate data over a broad range of thrust and torque conditions is described. The test data are presented in nondimensional coefficient form for the performance results, and in dimensional form for the steady and alternating loads. Some wake and acoustic data are also shown.
Author

N88-26520# Deutsche Forschungs- und Versuchsanstalt fuer Luft- und Raumfahrt, Brunswick (West Germany). Inst. fuer Flugmechanik.
FLIGHT VEHICLE SYSTEM IDENTIFICATION: STATUS AND PROSPECTS
P. G. Hamel *In its* System Identification in Vehicle Dynamics 1987 p 51-90 (For primary document see N88-26518 20-31)
Avail: NTIS HC A18/MF A01; DFVLR, VB-PL-DO, 90 60 58, 5000 Cologne, Fed. Republic of Germany, 109 Deutsche marks

N88-26525# Centre d'Etudes et de Recherches, Toulouse (France). Dept. d'Automatique.
MULTIVARIABLE IDENTIFICATION OF A FLEXIBLE TRANSPORT AIRCRAFT
M. Clique, G. Monnier, M. Labarrere, A. Bucharles, and J. L. Pac (Ecole Nationale Superieure de l'Aeronautique et de l'Espace, Toulouse, France) *In* DFVLR, System Identification in Vehicle Dynamics 1987 p 173-192 (For primary document see N88-26518 20-31)
Avail: NTIS HC A18/MF A01; DFVLR, VB-PL-DO, 90 60 58, 5000 Cologne, Fed. Republic of Germany, 109 Deutsche marks

N88-26526# Deutsche Forschungs- und Versuchsanstalt fuer Luft- und Raumfahrt, Brunswick (West Germany). Inst. fuer Flugmechanik.
A TWO-POINT AERODYNAMIC MODEL FOR IDENTIFICATION [EIN 2-PUNKT-AERODYNAMIKMODELL FUER DIE IDENTIFIZIERUNG]
W. Moennich *In its* System Identification in Vehicle Dynamics 1987 p 193-207 In GERMAN (For primary document see N88-26518 20-31)
Avail: NTIS HC A18/MF A01; DFVLR, VB-PL-DO, 90 60 58, 5000 Cologne, Fed. Republic of Germany, 109 Deutsche marks

N88-26527# Deutsche Forschungs- und Versuchsanstalt fuer Luft- und Raumfahrt, Brunswick (West Germany). Inst. fuer Flugmechanik.
THE IDENTIFICATION OF THE DIRECT LIFT CONTROL FLAP SYSTEM OF THE RESEARCH AIRCRAFT ATTAS [ZUR IDENTIFIZIERUNG DES DLC-KLAPPENSYSTEMS DES FORSCHUNGSFLUGZEUGS ATTAS]
D. Rohlf and W. Moennich *In its* System Identification in Vehicle Dynamics 1987 p 209-222 In GERMAN (For primary document see N88-26518 20-31)
Avail: NTIS HC A18/MF A01; DFVLR, VB-PL-DO, 90 60 58, 5000 Cologne, Fed. Republic of Germany, 109 Deutsche marks

N88-26528# Deutsche Forschungs- und Versuchsanstalt fuer Luft- und Raumfahrt, Brunswick (West Germany). Inst. fuer Flugmechanik.
PARAMETRIC ESTIMATION OF AERODYNAMIC NONLINEARITIES IN ROLLING MOMENT DUE TO SIDESLIP USING MAXIMUM LIKELIHOOD METHOD
R. V. Jategaonkar *In its* System Identification in Vehicle Dynamics 1987 p 223-234 (For primary document see N88-26518 20-31)
Avail: NTIS HC A18/MF A01; DFVLR, VB-PL-DO, 90 60 58, 5000 Cologne, Fed. Republic of Germany, 109 Deutsche marks

N88-26529# Deutsche Forschungs- und Versuchsanstalt fuer Luft- und Raumfahrt, Brunswick (West Germany). Inst. fuer Flugfuehrung.
FLIGHT TEST PREPARATION AND MEASURING DATA VALIDATION FOR PARAMETER IDENTIFICATION [FLUGVERSUCHSVORBEREITUNG UND MESSDATENUEBERPRUEUNG FUER DIE PARAMETER-IDENTIFIKATION]
K.-O. Proskawetz *In its* System Identification in Vehicle Dynamics 1987 p 235-249 In GERMAN (For primary document see N88-26518 20-31)
Avail: NTIS HC A18/MF A01; DFVLR, VB-PL-DO, 90 60 58, 5000 Cologne, Fed. Republic of Germany, 109 Deutsche marks

N88-26530# Technische Hogeschool, Delft (Netherlands).
A NEW METHOD FOR THE ESTIMATION OF AIRCRAFT INERTIA CHARACTERISTICS
R. C. deJong and J. A. Mulder *In* DFVLR, System Identification in Vehicle Dynamics 1987 p 251-265 (For primary document see N88-26518 20-31)
Avail: NTIS HC A18/MF A01; DFVLR, VB-PL-DO, 90 60 58, 5000 Cologne, Fed. Republic of Germany, 109 Deutsche marks

N88-26532# Deutsche Forschungs- und Versuchsanstalt fuer Luft- und Raumfahrt, Brunswick (West Germany). Inst. fuer Flugmechanik.
UTILIZATION OF IDENTIFICATION METHODS IN THE TIME AND FREQUENCY DOMAIN FOR THE DETERMINATION OF THE XV-15 (TILT-ROTOR) DYNAMICS FOR LATERAL MOTION IN HOVER FLIGHT [ANWENDUNG VON IDENTIFIZIERUNGSVERFAHREN IM ZEIT- UND FREQUENZBEREICH ZUR BESTIMMUNG DER XV-15 (TILT-ROTOR) DYNAMIK FUER DIE SEITENBEWEGUNG IM SCHWEBEFLUG]
J. Kaletka and M. B. Tischler (Army Aviation Research and Development Command, Moffett Field, Calif.) *In its* System Identification in Vehicle Dynamics 1987 p 287-307 In GERMAN; ENGLISH summary (For primary document see N88-26518 20-31)
Avail: NTIS HC A18/MF A01; DFVLR, VB-PL-DO, 90 60 58, 5000 Cologne, Fed. Republic of Germany, 109 Deutsche marks

N88-26533# Deutsche Forschungs- und Versuchsanstalt fuer Luft- und Raumfahrt, Brunswick (West Germany). Inst. for Flight Mechanics.
APPLICATION OF COMPLEMENTARY PARAMETER IDENTIFICATION TECHNIQUES TO FLIGHT TEST DATA OF A TRANSPORT AIRCRAFT
B. Krag, M. Labarrere, G. W. Foster, and J. H. Breeman (National Aerospace Lab., Amsterdam, Netherlands) *In* DFVLR, System Identification in Vehicle Dynamics 1987 p 309-342 (For primary document see N88-26518 20-31)
Avail: NTIS HC A18/MF A01; DFVLR, VB-PL-DO, 90 60 58, 5000 Cologne, Fed. Republic of Germany, 109 Deutsche marks

06 AIRCRAFT INSTRUMENTATION

Includes cockpit and cabin display devices; and flight instruments.

For related information see also *19 Spacecraft Instrumentation* and *35 Instrumentation and Photography.*

N88-26368# National Aerospace Lab., Amsterdam (Netherlands). Flight Div.
DEVELOPMENT OF AN AIRBORNE FACILITY FOR ADVANCED AVIONICS RESEARCH
N. vanDriel 1 Mar. 1987 17 p Presented at the 53rd AGARD Avionics Panel Symposium, Las Vegas, Nev., 27 Apr. - 1 May 1987 Previously announced in IAA as A88-23801
(NLR-MP-87012-U; B8803804; ETN-88-92607) Avail: NTIS HC A03/MF A01

A program to equip an aircraft with avionics research instruments is outlined. A Fairchild Metro 2 will be equipped with a programmable electronic flight instrument system (EFIS), programmable flight management computer (FMC), programmable flight control computer, Navstar GPS, microwave landing system (MLS), and a digital data link. Applications of the system include: research on MLS approaches (e.g., interception angles, segment lengths and orientations, equipment requirements); research on the use of EFIS, for conventional and unconventional presentations; research on the use of digital data links; research on the use of FMC's; and research on the use of satellite navigation systems especially for RNAV operations and approaches. ESA

07 AIRCRAFT PROPULSION AND POWER

Includes prime propulsion systems and systems components, e.g., gas turbine engines and compressors; and onboard auxilliary power plants for aircraft.

For related information see also *20 Spacecraft Propulsion and Power, 28 Propellants and Fuels,* and *44 Energy Production and Conversion.*

N88-26369# Argonne National Lab., Ill.
AN EFFICIENT COMPUTATIONAL TOOL FOR RAMJET COMBUSTOR RESEARCH
S. P. Vanka, J. L. Krazinski, and A. S. Nejad 1988 14 p Presented at the 26th AIAA Aerospace conference, Reno, Nev., 10 Jan. 1988
(Contract W-31-109-eng-38)
(DE88-010034; CONF-880139-4; AIAA-88-0060) Avail: NTIS HC A03/MF A01

A multigrid based calculation procedure is presented for the efficient solution of the time-averaged equations of a turbulent elliptic reacting flow. The equations are solved on a non-orthogonal curvilinear coordinate system. The physical models currently incorporated are a two equation k-epsilon turbulence model, a four-step chemical kinetics mechanism, and a Lagrangian particle tracking procedure applicable for dilute sprays. Demonstration calculations are presented to illustrate the performance of the calculation procedure for a ramjet dump combustor configuration. DOE

N88-26370# Commission of the European Communities (Luxembourg).
GUIDE TO THE CONTROL OF HIGH TEMPERATURE CORROSION AND PROTECTION OF GAS TURBINE MATERIALS
C. DuretThual, R. Morbioli, and P. Steinmetz 1986 120 p
(PB88-107412; EUR-10682-EN; ISBN-92-825-6541-6) Avail: NTIS HC E05/MF E05; copy not available from STI Facility CSCL 21E

Components of hot sections in gas turbines are subjected to severe thermomechanical cycles and operate in complex environments which depend on the type of machine and conditions of use. The aim of the work is to show how to control hot corrosion processes or to decrease corrosion attack which affects these components. Some basic knowledge is given on hot corrosion so that the users can orientate themselves towards a solution. The background of the problem of the basic corrosion processes is covered along with the way to study them, the materials and coatings currently used for blades and vanes, the effect of environment and coating on components' mechanical properties and finally the prevention of corrosion and solutions for the future. Author

N88-26371# Pratt and Whitney Aircraft, West Palm Beach, Fla. Engineering Div.
ENGINE COMPONENT RETIREMENT FOR CAUSE. VOLUME 1: EXECUTIVE SUMMARY Final Report, Aug. 1980 - Nov. 1986
John A. Harris, Jr. Aug. 1987 60 p
(Contract F33615-80-C-5160)
(AD-A192730; PWA-FR-18301-Vol-1; AFWAL-TR-87-4069-Vol-1)
Avail: NTIS HC A04/MF A01 CSCL 21E

This program developed and integrated materials behavior characteristics, component life analysis, nondestructive evaluation and cost-risk technology to establish and demonstrate the retirement for cause maintenance concept as it applies to rotating components of military gas turbine engines. As such it provides the basis for elimination of classical time or cyclic limits currently imposed for retirement of gas turbine rotor components by substituting a life management system in which each individual component is retired from service when the unique, economical safe life of that component is exhausted. The methodology was demonstrated on and validated for the U.S. Air Force F100 engine's rotor components and has been implemented on that engine system by the USAF Air Logistics Command. Use of Retirement for Cause is projected to result in life cycle cost savings in excess of $1 billion for that engine system. The Retirement for Cause methodology developed is generic, and may be applied to not only other gas turbine engines, but to components of any life limited system. GRA

N88-26372# Technische Univ., Munich (West Germany). Lehrstuhl fuer Flugantriebe.
STRUCTURAL OPTIMIZATION OF FIBER COMPOSITE TURBOMACHINE BLADES Ph.D. Thesis [ZUR STRUKTUROPTIMIERUNG VON FASERVERBUND-TURBOMASCHINENSCHAUFELN]
Gerd Berchtold 1987 104 p In GERMAN
(ETN-88-92351) Avail: NTIS HC A06/MF A01

An optimization procedure based on the combination of existing procedures is presented with emphasis on its effectiveness for the analysis of large finite element structures without the use of variable reducing methods. Computation speed elevation and data storage space reduction lead to application of this procedure on minicomputers. Two test examples of fiber composite optimization are proposed: a square section tubular structure and optimization of a compressor blade with determination of the finite element network subjected to external loads in the case of isotropic and anisotropic material properties. ESA

N88-26373# National Aerospace Lab., Amsterdam (Netherlands). Structures and Materials Div.
CORROSION PREVENTION IN GAS TURBINES
A. J. A. Mom 13 May 1987 36 p In DUTCH; ENGLISH summary Presented at the Corrosiedag 1986 van de NCC-sector Energie, Arnhem, Netherlands, 16 Sep. 1986
(NLR-MP-87029-U; B8805308; ETN-88-92611) Avail: NTIS HC A03/MF A01

Corrosion prevention and reduction in gas turbines is discussed. Preventative measures concentrate on the environment in the gas turbine, using filters, washing, scouring with rice husks, choice of fuel. Corrosion can be mitigated by the use of coatings or other materials. Good corrosion prevention requires developing an integral plan whereby the effects of the various preventive measures and the costs entailed are reviewed and considered as a whole. ESA

N88-26314# Mitsubishi Heavy-Industries Ltd., Tokyo (Japan).
EXTENSIVE VERIFICATION OF BLADE-TO-BLADE FLOW CODE BASED ON DENTON SCHEME
Tomihiko Sato, Sunao Aoki, and Hedetaka Mori *In* National Aerospace Lab., Proceedings of the 5th NAL Symposium on Aircraft Computational Aerodynamics Nov. 1987 p 178-181 In JAPANESE; ENGLISH summary (For primary document see N88-26290 20-01)
Avail: NTIS HC A12/MF A01

08 AIRCRAFT STABILITY AND CONTROL

Includes aircraft handling qualities; piloting; flight controls; and autopilots.

For related information see also *05 Aircraft Design, Testing and Performance.*

N88-26374*# National Aeronautics and Space Administration. Langley Research Center, Hampton, Va.
LOW-SPEED WIND-TUNNEL TEST OF A STOL SUPERSONIC-CRUISE FIGHTER CONCEPT
Paul L. Coe, Jr. and Donald R. Riley Jul. 1988 43 p
(NASA-TM-4050; L-16422; NAS 1.15:4050) Avail: NTIS HC A03/MF A01 CSCL 01C

A wind-tunnel investigation was conducted to examine the low-speed static stability and control characteristics of a 0.10 scale model of a STOL supersonic cruise fighter concept. The concept, referred to as a twin boom fighter, was designed as a STOL aircraft capable of efficient long range supersonic cruise. The configuration name is derived from the long twin booms extending aft of the engine to the twin vertical tails which support a high center horizontal tail. The propulsion system features a two dimensional thrust vectoring exhaust nozzle which is located so that the nozzle hinge line is near the aircraft center of gravity. This arrangement is intended to allow large thrust vector angles to be used to obtain significant values of powered lift, while minimizing pitching moment trim changes. Low speed stability and control information was obtained over an angle of attack range including the stall. A study of jet induced power effects was included. Author

N88-26375 Princeton Univ., N. J.
CONTROL OF FLIGHT THROUGH MICROBURST WIND SHEAR USING DETERMINISTIC TRAJECTORY OPTIMIZATION Ph.D. Thesis
Mark Lockwood Psiaki 1987 392 p
Avail: Univ. Microfilms Order No. DA8800331

Aircraft control strategies that minimize the hazard of longitudinal flight through microburst wind shear are developed and analyzed, principally using deterministic trajectory optimization and to a lesser extent using classical control. The purpose is to determine the ultimate limits to safe performance in a microburst and develop control strategies that achieve such performance. Several tragic microburst-related accidents have demonstrated the need for improved control strategies. Over 1,100 optimal trajectories were computed for jet transport and general aviation aircraft flying through idealized and actual microbursts. They were generated using a Successive Quadratic Programs trajectory optimization algorithm, which directly handles inequality constraints. Qualitative aspects of the best strategies provide a composite picture of good control in a microburst. Variations of the optimal performance with microburst type, intensity, length scale, and location define safe-performance limits. These studies provide guidelines for design and evaluation of practical microburst-encounter control laws. Controllers should replicate the pitch steering and throttle strategies found in the composite picture of good control. Evaluation should include frequency response analysis and comparison of closed-loop safe-performance limits with optimal limits. Dissert. Abstr.

N88-26376*# National Aeronautics and Space Administration. Lewis Research Center, Cleveland, Ohio.
COMPUTER SIMULATION OF A SINGLE PILOT FLYING A MODERN HIGH-PERFORMANCE HELICOPTER
Mark E. Zipf, William G. Vogt, Marlin H. Mickle, Ronald G. Hoelzeman, Fei Kai, and James R. Mihaloew (Pittsburgh Univ., Pa.) Jul. 1988 25 p
(Grant NAG3-729)
(NASA-TM-100182; E-3759; NAS 1.15:100182) Avail: NTIS HC A03/MF A01 CSCL 01C

Presented is a computer simulation of a human response pilot model able to execute operational flight maneuvers and vehicle stabilization of a modern high-performance helicopter. Low-order, single-variable, human response mechanisms, integrated to form a multivariable pilot structure, provide a comprehensive operational control over the vehicle. Evaluations of the integrated pilot were performed by direct insertion into a nonlinear, total-force simulation environment provided by NASA Lewis. Comparisons between the integrated pilot structure and single-variable pilot mechanisms are presented. Static and dynamically alterable configurations of the pilot structure are introduced to simulate pilot activities during vehicle maneuvers. These configurations, in conjunction with higher level, decision-making processes, are considered for use where guidance and navigational procedures, operational mode transfers, and resource sharing are required. Author

N88-26377*# National Aeronautics and Space Administration. Lewis Research Center, Cleveland, Ohio.
COMPUTER SIMULATION OF MULTIPLE PILOTS FLYING A MODERN HIGH PERFORMANCE HELICOPTER
Mark E. Zipf, William G. Vogt, Marlin H. Mickle, Ronald G. Hoelzeman, Fei Kai, and James R. Mihaloew (Pittsburgh Univ., Pa.) Jul. 1988 32 p
(Grant NAG3-729)
(NASA-TM-100183; E-3760; NAS 1.15:100183) Avail: NTIS HC A03/MF A01 CSCL 01C

A computer simulation of a human response pilot mechanism within the flight control loop of a high-performance modern helicopter is presented. A human response mechanism, implemented by a low order, linear transfer function, is used in a decoupled single variable configuration that exploits the dominant vehicle characteristics by associating cockpit controls and instrumentation with specific vehicle dynamics. Low order helicopter models obtained from evaluations of the time and frequency domain responses of a nonlinear simulation model, provided by NASA Lewis Research Center, are presented and considered in the discussion of the pilot development. Pilot responses and reactions to test maneuvers are presented and discussed. Higher level implementation, using the pilot mechanisms, are discussed and considered for their use in a comprehensive control structure. Author

N88-26378*# National Aeronautics and Space Administration. Ames Research Center, Moffett Field, Calif.
A HIGH FIDELITY REAL-TIME SIMULATION OF A SMALL TURBOSHAFT ENGINE
Mark G. Ballin Jul. 1988 95 p
(NASA-TM-100991; A-88151; NAS 1.15:100991) Avail: NTIS HC A05/MF A01 CSCL 21E

A high-fidelity component-type model and real-time digital simulation of the General Electric T700-GE-700 turboshaft engine were developed for use with current generation real-time blade-element rotor helicopter simulations. A control system model based on the specification fuel control system used in the UH-60A Black Hawk helicopter is also presented. The modeling assumptions and real-time digital implementation methods particular to the simulation of small turboshaft engines are described. The validity of the simulation is demonstrated by comparison with analysis-oriented simulations developed by the manufacturer, available test data, and flight-test time histories. Author

N88-26524# York Univ. (England). Dept. of Electronics.
FREQUENCY DOMAIN IDENTIFICATION OF THE DYNAMICS OF A SCALED REMOTELY-PILOTED HELICOPTER
P. Young and R. J. Patton *In* DFVLR, System Identification in Vehicle Dynamics 1987 p 153-172 Sponsored by the United Kingdom Science and Engineering Research Council and the United Kingdom Ministry of Defence (For primary document see N88-26518 20-31)
Avail: NTIS HC A18/MF A01; DFVLR, VB-PL-DO, 90 60 58, 5000 Cologne, Fed. Republic of Germany, 109 Deutsche marks

N88-26535# Technische Univ., Brunswick (West Germany). Inst. fuer Regelungstechnik.
NONLINEAR IDENTIFICATION OF AN AIRCRAFT FOR THE DIRECT CALCULATION OF AN ANTICIPATORY CONTROL [NICHTLINEARE IDENTIFIZIERUNG EINES FLUGZEUGS ZUR DIREKTEN BERECHNUNG EINER VORSTEUERUNG]
M. Haverland and U. Lindemann *In* DFVLR, System Identification in Vehicle Dynamics 1987 p 363-374 In GERMAN (For primary document see N88-26518 20-31)
Avail: NTIS HC A18/MF A01; DFVLR, VB-PL-DO, 90 60 58, 5000 Cologne, Fed. Republic of Germany, 109 Deutsche marks

09 RESEARCH AND SUPPORT FACILITIES (AIR)

Includes airports, hangars and runways; aircraft repair and overhaul facilities; wind tunnels; shock tubes; and aircraft engine test stands.

For related information see also *14 Ground Support Systems and Facilities (Space).*

N88-26379# Air Force Human Resources Lab., Brooks AFB, Tex.
FLIGHT SIMULATOR: FIELD OF VIEW UTILIZED IN PERFORMING TACTICAL MANEUVERS Final Report, Jan. 1983 - Dec. 1984
Linda A. Wiekhorst and Frank T. Vaccaro Apr. 1988 26 p Supersedes AFHRL-TP-86-29
(AD-A192412; AFHRL-TP-87-50; AFHRL-TP-86-29) Avail: NTIS HC A03/MF A01 CSCL 05F

This paper documents the field of view (FOV) utilized by experienced fighter pilots when performing specified portions of air-to-air and air-to-ground maneuvers. The FOV measurements were taken in the Simulator for Air-to-Air Combat (SAAC) and the Advanced Simulator for Pilot Training (ASPT). During the air-to-ground data collection, measurements were also taken while subjects performed the same tasks with a limited field of view (LFOV). Results of the data collected indicate that the FOV utilized varied widely between air-to-air and air-to-ground maneuvers. In nearly all cases, the FOV utilized for air-to-air maneuvers was symmetrical and that for air-to-ground maneuvers was skewed to one side. When air-to-ground tasks were performed in an LFOV, significantly poorer bomb scores and significantly higher release altitudes were found when compared to wide-FOV performance. A noticeable performance change in the LFOV condition was a tendency of the pilots to turn tighter into the target. The true effect of this change in flight path still needs to be investigated. Specifying one optimal LFOV for all maneuvers to be performed or trained in an operational flight simulator would be difficult if both cost and performance were to be considered. The variability of the FOV leads to the conclusion that placement of LFOV will be an important decision when considering what tasks will be performed. Full training implications cannot be determined until further transfer-of-training experiments are completed. GRA

N88-26380# Naval Postgraduate School, Monterey, Calif.
ANALYSIS OF GAS TURBINE TEST CELL NUMBER 1, LEMOORE NAVAL AIR STATION, CALIFORNIA M.S. Thesis
Kevin D. Smith Dec. 1987 136 p
(AD-A192870) Avail: NTIS HC A07/MF A01 CSCL 01C

A three-dimensional numerical analysis of Gas Turbine Test Cell 1 at Lemoore Naval Air Station, California, is given. The Parabolic, Hyperbolic, or Elliptic Numerical Integration Code (PHOENICS) is used to determine the steady-state aerothermal characteristics within the test cell during the full power run-up of a GE F404 gas turbine engine (afterburner in operation). The method in which PHOENICS arrives at a solution is discussed as well as how the code was applied to this problem. The solution of the problem is presented in tabular form and the results are discussed. Recommendations for the future application of PHOENICS to this project are given. GRA

N88-26381*# National Aeronautics and Space Administration, Washington, D.C.
SURFACE TEMPERATURE THERMAL FLUXMETERS FOR SHOCK TUBES
Jean Maulard Aug. 1988 75 p Transl. into ENGLISH from La Recherche Aerospatiale (France), no. 26, Sep. - Oct. 1968 p 39-60 Original language document was announced in IAA as A69-12876 Transl. by Scientific Translation Service, Santa Barbara, Calif.
(Contract NASw-4307)
(NASA-TT-20319; NAS 1.77:20319; ONERA-TP-648) Avail: NTIS HC A04/MF A01 CSCL 14B

This article reviews the principle of the surface temperature thermal fluxmeter which is generally used for measurements in shock tubes. Pickups of this type are described; they were built and experimented upon at ONERA and enable heat flux measurements either on the wall or at the impact point of hemispherical models. The calibration of these fluxmeters raises a delicate problem and the processes used are dealt with in an in-depth study. Author

N88-26291# National Aerospace Lab., Tokyo (Japan).
ON THE NAL NUMERICAL SIMULATOR SYSTEM
Hajime Miyoshi and Masahiro Fukuda *In its* Proceedings of the 5th NAL Symposium on Aircraft Computational Aerodynamics Nov. 1987 p 1-11 In JAPANESE; ENGLISH summary Original contains color illustrations (For primary document see N88-26290 20-01)
Avail: NTIS HC A12/MF A01

12 ASTRONAUTICS (GENERAL)

For extraterrestrial exploration see *91 Lunar and Planetary Exploration.*

N88-26382# Los Alamos National Lab., N. Mex. Earth and Space Science Div.
A BASIS OF SETTLEMENT: ECONOMIC FOUNDATIONS OF PERMANENT PIONEER COMMUNITIES
Eric M. Jones 1988 17 p Presented at the NASA Symposium on Lunar Bases and Space Activities of the 21st Century, Houston, Tex., 5 Apr. 1988
(Contract W-7405-eng-36)
(DE88-010907; LA-UR-88-1110-Rev; CONF-8804104-1-Rev; Paper-LBS-88-016) Avail: NTIS HC A03/MF A01

High transport costs will dominate the pattern of lunar development. During the earliest phases, when lunar facilities consist of a research and resource development complex with staff serving tours of a few months, transport costs will encourage local production of food, fuel, and building materials. Once these capabilities are in place and the number of personnel grows to a few hundred, staff rotation might well dominate transport budgets. At that point it would make economic sense to encourage some members of staff to become permanent residents. By analogy with early British settlement in Australia, a vigorous private sector economy could emerge if the lunar organization provided quasi-export earning through its role as the community's major employer and as the major buyer of locally-produced goods. By providing such a market for goods and services, the lunar organization would not only provide a means whereby permanent residents would support themselves but could also accelerate the

process of replacing imported goods with local manufactures, thereby reducing the cost of operations. By analogy with recent Alaskan experience, if the resource development activity started making money from sales to orbital customers, severance taxes and or royalty payments could also provide means by which a lunar community could support itself. DOE

13 ASTRODYNAMICS

Includes powered and free-flight trajectories; and orbital and launching dynamics.

No abstracts in this category.

14 GROUND SUPPORT SYSTEMS AND FACILITIES (SPACE)

Includes launch complexes, research and production facilities; ground support equipment, e.g., mobile transporters; and simulators.

For related information see also *09 Research and Support Facilities (Air).*

N88-26383# Los Alamos National Lab., N. Mex.
REAMING EXPERIMENTS FOR THE LETHALITY TEST SYSTEM
D. Hooten and P. Stanley 1988 5 p Presented at the 4th Symposium on Electromagnetic Launch Technology, Austin, Tex., 12 Apr. 1988
(Contract W-7405-eng-36)
(DE88-007902; LA-UR-88-782; CONF-880478-8) Avail: NTIS HC A02/MF A01

Various reaming techniques were tried for use on the barrel of the Lethality Test System railgun. This report covers the successes and failures of the reamers and the techniques that were tried. DOE

N88-26384# Los Alamos National Lab., N. Mex.
WHY PLASMA ARMATURE RAILGUNS DON'T WORK (AND WHAT CAN BE DONE ABOUT IT)
J. V. Parker 1988 9 p Presented at the 4th Symposium on Electromagnetic Launch Technology, Austin, Tex., 12 Apr. 1988
(Contract W-7405-eng-36)
(DE88-007900; LA-UR-88-789; CONF-880478-9) Avail: NTIS HC A02/MF A01

Plasma armature railguns have failed to achieve the high velocities predicted in the early 1980's. Only a few experiments in the last decade have exceeded the velocity of 5.9 km/s obtained by Rashleigh and Marshall in their pioneering plasma armature experiments. The apparent barrier at 6 to 7 km/s results from viscous and ablation drag on neutral and ionized material in the railgun bore. It has taken almost five years to understand and demonstrate clearly the inter-relation of ablation, viscous drag, and arc restrike. In the light of this improved understanding, it is time to examine the future potential of plasma armature railguns. There is little reason to hope that conventional railguns will exceed a velocity of 8 to 10 km/s. New approaches based on reducing the amount of material entering the bore or eliminating electrical conduction appear promising. Based on current understanding a velocity of 20 to 25 km/s appears possible using either advanced materials or novel railgun power systems. DOE

N88-26385# National Aeronautics and Space Administration. Lewis Research Center, Cleveland, Ohio.
APPLICATION OF SUPERCONDUCTING TECHNOLOGY TO EARTH-TO-ORBIT ELECTROMAGNETIC LAUNCH SYSTEMS
J. R. Hull (Argonne National Lab., Ill.) and L. M. Carney 1988 15 p Presented at the Conference on Superconductivity and Applications, Buffalo, N.Y., 18 Apr. 1988 Prepared in cooperation with National Aeronautics and Space Administration, Cleveland, OH.
(Contract W-31109-eng-38)
(NASA-TM-101134; NAS 1.15:101134; DE88-009955; CONF-880466-1) Avail: NTIS HC A03/MF A01

Benefits may occur by incorporating superconductors, both existing and those currently under development, in one or more parts of a large-scale electromagnetic launch (EML) system that is capable of delivering payloads from the surface of the Earth to space. The use of superconductors for many of the EML components results in lower system losses; consequently, reductions in the size and number of energy storage devices are possible. Applied high-temperature superconductivity may eventually enable novel design concepts for energy distribution and switching. All of these technical improvements have the potential to reduce system complexity and lower payload launch costs. DOE

N88-26386# Argonne National Lab., Ill.
APPLICATION OF SUPERCONDUCTING TECHNOLOGY TO EARTH-TO-ORBIT ELECTROMAGNETIC LAUNCH SYSTEMS
L. M. Carney 28 Jun. 1988 29 p Presented at the 4th Symposium on Electromagnetic Launch Technology, Austin, Tex., 12 Apr. 1988
(Contract W-31109-eng-38)
(DE88-010022; CONF-880478-13) Avail: NTIS HC A03/MF A01

This paper explores the potential benefits that may occur as a result of incorporating superconductors, both existing and those currently under development, in one or more parts of a large-scale electromagnetic launch system that is capable of delivering payloads from the earth's or lunar surface to space. Analysis indicates that superconducting components result in significant cost reductions for both rail and coaxial accelerator designs. DOE

N88-26387*# National Aeronautics and Space Administration. Marshall Space Flight Center, Huntsville, Ala.
ANALYSIS OF THE PERFORMANCE OF THE SPACE ULTRAVACUUM RESEARCH FACILITY IN ATTACHED AND FREE-FLYER MODE
Robert J. Naumann Mar. 1988 30 p
(NASA-TM-100325; NAS 1.15:100325) Avail: NTIS HC A03/MF A01 CSCL 14B

The old concept of using the wake of a spacecraft to obtain an ultrahigh vacuum is revisited with a somewhat different emphasis. Since it is possible to configure a wake shield so that a surface of interest does not subtend any walls that could become contaminated, it appears that it should be possible to achieve a contamination-free, ultrahigh vacuum capability with infinite pumping speed even in the presence of high heat loads and moderate gas loads. With the new interest in developing thin films with precision controlled synthetic microstructures such as superlattices, mixed metal oxide high temperature superconductors, rare-earth magneto-optical devices, and nano-crystalline alloys, the ability to work with a variety of different materials without cross contamination should be of significance. This paper analyzes the performance of the conceptual design for a Space Ultravacuum Research Facility (SURF), both in a Shuttle-attached mode and as a free-flyer. It is shown that even in the Shuttle-attached mode, it should be possible to obtain vacuum levels equivalent to 10 to the -10 Torr with O and N2 as the primary constituents. This should be sufficient to demonstrate the feasibility of the concept, particularly the infinite pumping speed and virtual elimination of contamination aspects. As a free-flyer the SURF will be limited primarily by the gas load associated with the process being performed. For chemical beam epitaxy (CBE) it is shown that equivalent vacuum levels of 10 to the -14 Torr should be possible at 300 km. Author

15 LAUNCH VEHICLES AND SPACE VEHICLES

Includes boosters; operating problems of launch/space vehicle systems; and reusable vehicles.

For related information see also *20 Spacecraft Propulsion and Power.*

No abstracts in this category.

16 SPACE TRANSPORTATION

Includes passenger and cargo space transportation, e.g., shuttle operations; and space rescue techniques.

For related information see also *03 Air Transportation and Safety* and *18 Spacecraft Design, Testing and Performance.* For space suits see *54 Man/System Technology and Life Support.*

N88-26388# Air Command and Staff Coll., Maxwell AFB, Ala.
BOOK ANALYSIS. CHALLENGER: A MAJOR MALFUNCTION
Thomas M. Hall Apr. 1988 25 p
(AD-A192458; ACSC-88-1135) Avail: NTIS HC A03/MF A01 CSCL 22E

This report analyzes Challenger: A Major Malfunction by Malcolm McConnell, which covers the history of the space shuttle program from its design through the Challenger accident. McConnell attempts to show that the design of the shuttle was compromised by cost considerations, how politics influenced shuttle acquisition and operations, and how pressure to fly compromised safety. With minor exceptions, the book is a faithful account of the factors which caused the Challenger accident, and is recommended to Air Force/DOD readers. GRA

17 SPACE COMM., SPACECRAFT COMM., COMMAND & TRACKING

Includes telemetry; space communications networks; astronavigation and guidance; and radio blackout.

For related information see also *04 Aircraft Communications and Navigation* and *32 Communications and Radar.*

No abstracts in this category.

18 SPACECRAFT DESIGN, TESTING AND PERFORMANCE

Includes satellites; space platforms; space stations; spacecraft systems and components such as thermal and environmental controls; and attitude controls.

For life support systems see *54 Man/System Technology and Life Support.* For related information see also *05 Aircraft Design, Testing and Performance, 39 Structural Mechanics,* and *16 Space Transportation.*

N88-26389*# National Aeronautics and Space Administration. Goddard Space Flight Center, Greenbelt, Md.
DESIGN AND TESTING OF A HIGH POWER SPACECRAFT THERMAL MANAGEMENT SYSTEM
Michael E. McCabe, Jr., Jentung Ku, and Steve Benner (TS Infosystems, Lanham, Md.) Jun. 1988 109 p Sponsored in part by AF
(Contract NAS5-28626)
(NASA-TM-4051; Rept-88B0167; NAS 1.15:4051) Avail: NTIS HC A06/MF A01 CSCL 22B

The design and test results are presented of an ammonia hybrid capillary pumped loop thermal control system which could be used for heat acquisition and transport on future large space platforms and attached payloads, such as those associated with the NASA Space Station. The High Power Spacecraft Thermal Management System (HPSTM) can operate as either a passive, capillary pumped two phase thermal control system, or, when additional pressure head is required, as a mechanically pumped loop. Testing has shown that in the capillary mode, the HPSTM evaporators can acquire a total heat load of between 600 W and 24 kW, transported over 10 meters, at a maximum heat flux density of 4.3 W/sq cm. With the mechanical pump circulating the ammonia, a heat acquisition potential of 52 kW was demonstrated for 15 minutes without an evaporator failure. These results represent a significant improvement over the maximum transport capability previously displayed in other capillary systems. The HPSTM system still retains the proven capillary capabilities of heat load sharing and flow control between evaporator plates, rapid power cycling, and nonuniform heating in both the capillary and hybrid operating modes. Author

N88-26390# Groningen Rijksuniversiteit (Netherlands). Subfaculteit Wiskunde en Informatica.
L(SUB INFINITY SYMBOL)-APPROXIMATIONS OF COMPLEX FUNCTIONS AND ROBUST CONTROLLERS FOR LARGE FLEXIBLE SPACE STRUCTURES
R. F. Curtain 1987 24 p
(PB88-186226; TW-281) Avail: NTIS HC A03/MF A01 CSCL 22B

A survey is presented of a theory for a frequency domain design of robust controllers for infinite dimensional systems using L sub infinity approximations. Applications to large flexible space structures are discussed. Author

N88-26391# Lawrence Livermore National Lab., Calif.
A SIMULATION OF POST BOOST VEHICLE DEPLOYMENT OF MULTIPLE REENTRY VEHICLES
P. L. Sholl Apr. 1988 32 p
(Contract W-7405-eng-48)
(DE88-009537; UCID-21389) Avail: NTIS HC A03/MF A01

This report summarizes the equations and assumptions used to develop the model for PBV (Post Boost Vehicle) deployment of multiple reentry vehicles for the Block 1 and Block 2 simulation effort by the R-program Weapons Concept Group. DOE

N88-26392# Los Alamos National Lab., N. Mex.
HEAT PUMP AUGMENTED RADIATORS FOR SPACECRAFT THERMAL MANAGEMENT
M. A. Merrigan and R. S. Reid 1988 24 p Presented at the 5th Symposium on Space Nuclear Power Systems, Albuquerque, N. Mex., 11 Jan. 1988
(Contract W-7405-eng-36)
(DE88-007890; LA-UR-88-847; CONF-880122-10) Avail: NTIS HC A03/MF A01

Because future space missions will require heat rejection subsystems having megawatt capacity, the development of lightweight heat rejection techniques is desirable. Closed systems for waste heat rejection in space are radiative and their capacity is proportional to the fourth power of absolute temperature. Reductions in the surface area and therefore, in the mass of a space radiator are possible by increasing the heat rejection temperature above the temperature of the thermal source. One proposed method of increasing the heat rejection temperature uses a heat pump powered by a cyclic heat engine operating at a temperature above the waste heat source. This heat pumping technique reduces the required direct radiator surface area, but it introduces mass penalties associated with its power supply and its heat rejection system. The use of a heat pump augmented heat rejection system will generally be practical if it reduces the total radiator mass requirement over a suitable baseline design.

The mass penalties of the heat pump augmented radiator over a baseline (a flat plate radiator) are considered in this analysis.
DOE

N88-26393# Oak Ridge National Lab., Tenn.
HEAT PUMP AUGMENTED RADIATOR FOR LOW-TEMPERATURE SPACE APPLICATIONS
M. Olszewski and U. Rockenfeller 1988 20 p Presented at the 23rd Intersociety Energy Conversion Engineering Conference, Denver, Colo., 31 Jul. 1988 Prepared in cooperation with Rocky Research Corp., Boulder City, Nev.
(Contract DE-AC05-84OR-21400)
(DE88-008369; CONF-880702-2) Avail: NTIS HC A03/MF A01

Closed-cycle, space-based heat rejection systems depend solely on radiation to achieve their heat dissipation function. Since the payload heat rejection temperature is typically 50 K above that of the radiation sink in near earth orbit, the size and mass of these systems can be appreciable. Size (and potentially mass) reductions are achievable by increasing the rejection temperature via a heat pump. Two heat pump concepts were examined to determine if radiator area reductions could be realized without increasing the mass of the heat rejection system. The first was a conventional, electrically-driven vapor compression system. The second is an innovative concept using a solid-vapor adsorption system driven by reject heat from the prime power system. The mass and radiator area of the heat pump radiator systems were compared to that of a radiator only system to determine the merit of the heat pump concepts. Results for the compressor system indicated that the mass minimum occured at a temperature lift of about 50 K and radiator area reductions of 35 percent were realized. With a radiator specific mass of 10 kgm^2, the heat pump system is 15 percent higher than the radiator only baseline system.
DOE

N88-26394*# National Aeronautics and Space Administration. Langley Research Center, Hampton, Va.
PYROTECHNIC SYSTEM FAILURES: CAUSES AND PREVENTION
Laurence J. Bement Jun. 1988 42 p
(NASA-TM-100633; NAS 1.15:100633) Avail: NTIS HC A01/MF A01 CSCL 19A

Although pyrotechnics have successfully accomplished many critical mechanical spacecraft functions, such as ignition, severance, jettisoning and valving (excluding propulsion), failures continue to occur. Provided is a listing of 84 failures of pyrotechnic hardware with completed design over a 23-year period, compiled informally by experts from every NASA Center, as well as the Air Force Space Division and the Naval Surface Warfare Center. Analyses are presented as to when and where these failures occurred, their technical source or cause, followed by the reasons why and how these kinds of failures persist. The major contributor is a fundamental lack of understanding of the functional mechanisms of pyrotechnic devices and systems, followed by not recognizing pyrotechnics as an engineering technology, insufficient manpower with hands-on experience, too few test facilities, and inadequate guidelines and specifications for design, development, qualification and acceptance. Recommendations are made on both a managerial and technical basis to prevent failures, increase reliability, improve existing and future designs, and develop the technology to meet future requirements. Author

N88-26395# Physical Sciences, Inc., Andover, Mass.
THE USE OF LIQUID FILMS FOR SPACECRAFT SURVIVABILITY TO LASER RADIATION Final Report
Gelb 15 May 1987 3 p
(Contract F49620-84-C-0102)
(AD-A192954; AFOSR-88-0304TR) Avail: NTIS HC A02/MF A01 CSCL 07D

This contains the results of a program to investigate the concept of liquid film protection of spacecraft materials from laser interaction. The liquid film protection concept consists of using a reflective thin film coating over a graphitic substrate to reduce the absorbed laser energy and hence the degree of damage caused by the laser interaction. The required properties of thin film are: (1) it liquifies at temperatures substantially below that for substantial substrate vaporization; (2) its vaporization temperature is much higher than the substrate; and (3) the liquified film must allow the passage of substrate vaporization products through it without destroying the film coherence. GRA

N88-26396# Aerospace Corp., El Segundo, Calif. Space Sciences Lab.
A SEVERE SPACECRAFT-CHARGING EVENT ON SCATHA IN SEPTEMBER 1982
H. C. Koons, P. F. Mizera, J. L. Roeder, and J. F. Fennell 5 Feb. 1988 30 p
(Contract F04701-85-C-0086)
(AD-A193007; TR-0086A(2940-06)-6; SD-TR-88-12) Avail: NTIS HC A03/MF A01 CSCL 22B

On September 22, 1982, 29 large amplitude electrostatic discharges were detected by the Pulse Analyzer onboard the SCATHA satellite. Seventeen of these pulses exceeded the maximum voltage discrimination level, which was set to 7.4 volts. This was the worst instance of electrostatic discharges encountered to date by the SCATHA satellite. Three different spacecraft anomalies occurred on SCATHA that day, the most serious being a two-minute loss of data. During this same time period, the Surface Potential Monitor experiment aboard the satellite measured the largest differential surface charging observed in the data since the satellite's launch in January 1979. GRA

N88-26397*# Bionetics Corp., Hampton, Va.
SOME OPERATIONAL ASPECTS OF A ROTATING ADVANCED-TECHNOLOGY SPACE STATION FOR THE YEAR 2025 Contractor Report, May - Nov. 1987
M. J. Queijo, A. J. Butterfield, W. F. Cuddihy, C. B. King, R. W. Stone, J. R. Wrobel, and P. A. Garn Jun. 1988 313 p
(Contract NAS1-18267)
(NASA-CR-181617; NAS 1.26:181617) Avail: NTIS HC A14/MF A01 CSCL 22B

The study of an Advanced Technology Space Station which would utilize the capabilities of subsystems projected for the time frame of the years 2000 to 2025 is discussed. The study includes tradeoffs of nuclear versus solar dynamic power systems that produce power outputs of 2.5 megawatts and analyses of the dynamics of the spacecraft of which portions are rotated for artificial gravity. The design considerations for the support of a manned Mars mission from low Earth orbit are addressed. The studies extend to on-board manufacturing, internal gas composition effects, and locomotion and material transfer under artificial gravity forces. The report concludes with an assessment of technology requirements for the Advanced Technology Space Station.
Author

N88-26398* National Aeronautics and Space Administration. Lyndon B. Johnson Space Center, Houston, Tex.
MOBILE REMOTE MANIPULATOR SYSTEM FOR A TETRAHEDRAL TRUSS Patent
Clarence J. Wesselski, inventor (to NASA) and William C. Schneider, inventor (to NASA) 19 Jul. 1988 15 p Filed 5 Sep. 1986 Supersedes N87-15260 (25 - 07, p 0875) Sponsored by NASA
(NASA-Case-MSC-20985-1; US-Patent-4,757,767; US-Patent-Appl-SN-904134; US-Patent-Class-104-49; US-Patent-Class-104-35; US-Patent-Class-104-172.1; US-Patent-Class-244-159) Avail: US Patent and Trademark Office CSCL 05H

The mobile remote manipulator system (MRMS) was initially developed for transit about the trusses of the delta space station; however, it can be utilized just as easily for transit about the trusses of the dual keel station. The MRMS is comprised of a mobile platform having a rail system formed of transversely disposed T-shaped tracks, which engage with guide pins located at the nodes of the trusses. The guide pins form a grid and the tracks are so designed as to permit travel in either of two orthogonal directions. The present invention provides a near-uniform traversing

velocity with minimal dynamic loading on the system. Pivoting changers move the platform from one face to another.
Official Gazette of the U.S. Patent and Trademark Office

N88-26513# Mitsubishi Electric Co., Amagasaki (Japan).
NUTATIONAL STABILITY OF A SATELLITE EQUIPPED WITH AN ACTIVE MAGNETIC MOMENTUM WHEEL
Masao Inoue, Kazuo Tsuchiya, Atsushi Nakajima, and Chikara Murakami (Tokyo Metropolitan Univ., Japan) *In* Tokyo Univ., The Proceedings of the Symposium on Mechanics for Space Flight 1987 Mar. 1988 p 127-136 (For primary document see N88-26499 20-31)
Avail: NTIS HC A07/MF A01

N88-26514# Nippon Electric Co. Ltd., Yokohama (Japan). Space Development Div.
DYNAMICS OF SATELLITES WITH RADIAL WIRE ANTENNAS
Motoki Hinada, Ichiro Nakatani, Keiken Ninomiya, Noboru Muranaka, Takakazu Namera, Masahi Uo, and Naoto Ogura *In* Tokyo Univ., The Proceedings of the Symposium on Mechanics for Space Flight 1987 Mar. 1988 p 137-147 (For primary document see N88-26499 20-31)
Avail: NTIS HC A07/MF A01

19 SPACECRAFT INSTRUMENTATION

For related information see also *06 Aircraft Instrumentation* and *35 Instrumentation and Photography.*

No abstracts in this category.

20 SPACECRAFT PROPULSION AND POWER

Includes main propulsion systems and components, e.g., rocket engines; and spacecraft auxilliary power sources.

For related information see also *07 Aircraft Propulsion and Power, 28 Propellants and Fuels, 44 Energy Production and Conversion,* and *15 Launch Vehicles and Space Vehicles.*

N88-26399# Naval Postgraduate School, Monterey, Calif.
AN INTERACTIVE COMPUTER CODE FOR PRELIMINARY DESIGN OF SOLID PROPELLANT ROCKET MOTORS M.S. Thesis
Chung-I. Yuan Dec. 1987 92 p
(AD-A192869) Avail: NTIS HC A05/MF A01 CSCL 21H

An interactive computer code for the preliminary design of solid propellant rocket motors (SPRMD) was successfully developed and its use was demonstrated through a design example. SPRMD was written in FORTRAN for use on an IBM PC/AT. It combined several existing codes (MICROPEP, GRAINS, ROCKET, etc.) and used the performance loss estimation methods suggested by the AGARD Propulsion and Energetics Panel for aluminized propellants. GRA

N88-26400# Air Force Astronautics Lab., Edwards AFB, Calif.
ENVIRONMENTAL MONITORING OF A TITAN 34D 5 1/2 SEGMENT SOLID ROCKET MOTOR STATIC FIRING Final Report, Feb. - Jul. 1987
Graham W. Rinehart and Daniel D. Berlinrut Mar. 1988 63 p
(AD-A192975; AFAL-TR-88-029) Avail: NTIS HC A04/MF A01 CSCL 21H

On 15 June 1987 a full-scale 5 1/2 segment Titan 34D solid rocket motor was static fired at the Air Force Astronautics Laboratory, Edwards AFB, CA. An environmental monitoring program was initiated to assure protection of test personnel and compliance with environmental restrictions. A protocol for monitoring densely populated closed environments was developed and initiated in the Control Center. Realtime monitoring of gaseous hydrogen chloride and analysis of preserved collections of hydrochloric acid depositions was performed. Revolatilization chamber experiments were performed to predict and study the strength of acidic off-gassing. Results of the program indicate that the personnel and equipment involved in the test were adequately protected and no significant environmental impact occurred as a result of the motor firing. GRA

N88-26401*# National Aeronautics and Space Administration. Lewis Research Center, Cleveland, Ohio.
A REUSABLE ROCKET ENGINE INTELLIGENT CONTROL
Walter C. Merrill and Carl F. Lorenzo Jul. 1988 11 p Presented at the 24th Joint Propulsion Conference, Boston, Mass., 11-13 Jul. 1988; sponsored in part by AIAA, ASME, SAE, and ASEE
(NASA-TM-100963; E-4256; NAS 1.15:100963; AIAA-88-3114)
Avail: NTIS HC A03/MF A01 CSCL 21H

An intelligent control system for reusable space propulsion systems for future launch vehicles is described. The system description includes a framework for the design. The framework consists of an execution level with high-speed control and diagnostics, and a coordination level which marries expert system concepts with traditional control. A comparison is made between air breathing and rocket engine control concepts to assess the relative levels of development and to determine the applicability of air breathing control concepts to future reusable rocket engine systems. Author

N88-26402*# National Aeronautics and Space Administration. Lewis Research Center, Cleveland, Ohio.
ADVANCED PHOTOVOLTAIC POWER SYSTEM TECHNOLOGY FOR LUNAR BASE APPLICATIONS
David J. Brinker and Dennis J. Flood 1988 10 p Presented at the Lunar Bases and Space Activities in the 21st Century Symposium, Houston, Tex., 5-7 Apr. 1988; sponsored by NASA, AIAA, Lunar and Planetary Inst., American Geophysical Unions, ANS, ASCE, Space Studies Inst. and National Space Society
(NASA-TM-100965; E-4258; NAS 1.15:100965) Avail: NTIS HC A02/MF A01 CSCL 21H

Advanced photovoltaic/electrochemical (batteries or regenerative fuel cells for storage) power system options for a lunar base are discussed and compared. Estimated system masses are compared with those projected for the SP-100 nuclear system. The results of the comparison are quantified in terms of the mass saved in a scenario which assembles the initial base elements in Low Earth Orbit (LEO) and launches from there to the lunar surface. A brief summary is given of advances in photovoltaic/electrochemical power system technologies currently under development in the NASA/OAST program. A description of the planned focussed technology program for surface power in the new Pathfinder initiative is also provided. Author

N88-26403*# Calspan Field Services, Inc., Arnold AFS, Tenn.
THE EFFECTS OF RCS JET FIRING ON THE ISOLATED ORBITER AND MATED COAST PHASES OF THE GLIDE RETURN TO LAUNCH SITE MANEUVER AT MACH NUMBER 6 (IA302B) Final Report, 16 Nov. - 12 Dec. 1987
L. V. Garrett, T. D. Buchanan, and P. E. Fryberger Apr. 1988 74 p Prepared in cooperation with Arnold Engineering Development Center, Arnold AFS, Tenn. Sponsored by NASA
(NASA-CR-180223; NAS 1.26:180223; AEDC-TSR-88-V7) Avail: NTIS HC A04/MF A01 CSCL 21H

An updated Space Shuttle aerodynamic data base was obtained in Tunnel B for two phases of the Glide Return to Launch Site (GRTLS) abort maneuver. One-and-a-quarter percent scale models of the Space Shuttle Orbiter and External Tank were used to measure the effects of various combinations of Reaction Control System (RCS) jet thrusters at Mach number 6. The angle-of-attack range for the isolated orbiter was -10 to 15 deg at sideslip angles from -5 to 10 deg during Phase 1 of testing. The angle-of-attack range for the mated orbiter and external tank was -5 to 15 deg with sideslip angles of -2 to 5 deg during Phase 2. The test was

conducted at a unit Reynolds number of 0.75 million per foot.
Author

N88-26306# National Aerospace Lab., Kakuda (Japan).
ANALYSIS OF FLOW THROUGH PUMP OF LARGE ROCKET ENGINE
Hitoshi Yamada and Yoshiaki Watanabe *In* National Aerospace Lab., Proceedings of the 5th NAL Symposium on Aircraft Computational Aerodynamics Nov. 1987 p 115-119 In JAPANESE; ENGLISH summary (For primary document see N88-26290 20-01)
Avail: NTIS HC A12/MF A01

23 CHEMISTRY AND MATERIALS (GENERAL)

N88-26404* National Aeronautics and Space Administration. Lewis Research Center, Cleveland, Ohio.
SUBSTITUTED 1,1,1-TRIARYL-2,2,2-TRIFLUOROETHANES AND PROCESSES FOR THEIR SYNTHESIS Patent
William B. Alston, inventor (to NASA) and Roy F. Gratz, inventor (to NASA) 19 Jul. 1988 12 p Filed 29 Oct. 1986 Supersedes N87-14432 (25 - 06, p 0739) Sponsored by NASA
(NASA-Case-LEW-14345-1; US-Patent-4,758,380; US-Patent-Appl-SN-924474; US-Patent-Class-260-389; US-Patent-Class-260-386; US-Patent-Class-260-395; US-Patent-Class-549-241) Avail: US Patent and Trademark Office CSCL 07A

Synthetic procedures are described for tetraalkyls, tetraacids and dianhydrides substituted 1,1,1-triaryl-2,2,2-trifluoroethanes which comprises: (1) 1,1-bis(dialkylaryl)-1 aryl-2,2,2-trifluoroethane; (2) 1,1-bis(dicarboxyaryl)-1 aryl-2,2,2-trifluoroethane; or (3) cyclic dianhydride or diamine of 1,1-bis(dialkylary)-1 aryl-2,2,2,-trifluoroethanes.
Official Gazette of the U.S. Patent and Trademark Office

24 COMPOSITE MATERIALS

Includes physical, chemical, and mechanical properties of laminates and other composite materials.
For ceramic materials see *27 Nonmetallic Materials*.

N88-26405 George Washington Univ., Washington, D.C.
STIFFNESS DEGRADATION OF COMPOSITE LAMINATES Ph.D. Thesis
Se Hoon Yang 1987 386 p
Avail: Univ. Microfilms Order No. DA8725939

The reduction of stiffness is an important measure of fatigue damage in composite laminates. A residual stiffness degradation model is proposed from which the statistical distribution of the residual stiffness of composite laminates in service can be predicted. Since the stiffness can be measured nondestructively in service, several analytical methods were proposed to predict the stiffness degradation of a particular composite component in service. These include the method of linear regression analysis, a Bayesian approach and a time series analysis. The stiffness at fatigue failure is referred to as the failure stiffness and its criterion is postulated. Based on such a postulated criterion and the residual stiffness degradation model, the statistical distribution of the fatigue life is derived. Experiments were conducted on graphite/epoxy laminates to generate statistically significant data for evaluating the proposed analytical models. Dissert. Abstr.

N88-26406# Virginia Polytechnic Inst. and State Univ., Blacksburg. Dept. of Materials Engineering Science.
INSTABILITY-RELATED DELAMINATION GROWTH OF EMBEDDED AND EDGE DELAMINATIONS Ph.D. Thesis
John D. Whitcomb May 1988 200 p
Avail: NTIS HC A09/MF A01

Compressive loads can cause local buckling in composite laminates that have a near surface delamination. This buckling causes load redistribution and secondary loads, which in turn cause interlaminar stresses and delamination growth. The goal of this research was to enhance the understanding of this instability-related delamination growth in laminates containing either an embedded or an edge delamination. Author

N88-26407*# Clemson Univ., S.C. Advanced Engineering Fibers Lab.
THERMOPLASTIC COATING OF CARBON FIBERS Annual Report, 1987 - 1988
D. D. Edie, G. C. Lickfield, M. J. Drews, M. S. Ellison, L. E. Allen, J. R. McCollum, and H. L. Thomas 23 Jul. 1988 13 p
(Grant NAG1-680)
(NASA-CR-183067; NAS 1.26:183067) Avail: NTIS HC A03/MF A01 CSCL 11D

Now that quantities of prepreg were made on the thermoplastic coating line, they are being formed into both textile preform structures and directly into composite samples. The textile preforms include both woven and knitted structures which will be thermoformed into a finished part. In order to determine if the matrix resin is properly adhering to the fibers or if voids are being formed in the coating process, the tensile strength and modulus of these samples will be tested. The matrix uniformity of matrix distribution in these samples is also being determined using an image analyzer. Author

N88-26408# California Univ., Berkeley. Lawrence Berkeley Lab.
SINTERING OF THE HETEROGENEOUS MGO COMPACTS Ph.D. Thesis
Mark Kin-Fu Lin Apr. 1988 109 p
(Contract DE-AC03-76SF-00098)
(DE88-010357; LBL-25165) Avail: NTIS HC A06/MF A01

This study explores the optimum sintering schedule for an agglomerate compact. Various pertinent models have been proposed to assess the influence of the multimodal pore size distributions on the overall densification kinetics and the effect of temperature on the sintered microstructure. A thorough investigation of the sintering behavior and microstructural evolution for the heterogeneous MgO compact has been performed. The enhancements of the densification rate, the grain growth rate, and the increase in interpore spacing while sintering the heterogeneous compacts have been observed in this study. High-temperature sintering tends to produce a heterogeneous structure, and many pores are trapped within the grains. Low-temperature sintering is advantageous to produce a more homogeneous structure. 2-step sintering, combining a pre-treatment at low temperature (i.e., the homogenization treatment) with subsequent high temperature sintering, is proposed as an optimum sintering schedule for the agglomerated compact. DOE

N88-26409# Oak Ridge National Lab., Tenn.
INTERFACE MODIFICATION IN NICALON (TRADEMARK)/SiC COMPOSITES
R. A. Lowden and D. P. Stinton 1988 28 p Presented at the 12th Annual Conference on Composites and Advanced Ceramic Materials, Cocoa Beach, Fla., 20 Jan. 1988
(Contract DE-AC05-84OR-21400)
(DE88-009708; CONF-880118-5) Avail: NTIS HC A03/MF A01

Improved mechanical behavior in Nicalon/SiC composites has been produced by controlling the interfacial bond through coating of the fibers with thin films before densification. Varying degrees of bonding have been achieved with different coating materials and film thicknesses. The effects of bonding on fiber pull-out, and thus mechanical behavior, have been investigated. Fiber-matrix bond strengths have been semi-quantitatively evaluated using indentation methods and a simple tensile test. Electron microscopy and surface analysis were utilized to characterize interface compositions and structures. These results have been used to further examine fiber-matrix interfaces and their influence on mechanical behavior. DOE

N88-26410# Aerospace Corp., El Segundo, Calif. Materials Sciences Lab.
ELECTRICAL RESISTIVITY OF CARBON-CARBON COMPOSITES
Phillip I. Gold 1 Feb. 1988 16 p
(Contract F04701-85-C-0086)
(AD-A193006; TR-0086A(2935-06)-4; SD-TR-88-10) Avail: NTIS HC A03/MF A01 CSCL 11D

A simple four-point method for measuring the resistivity of carbon-carbon composite billets was developed. Measurements compare favorably with previously published results. GRA

N88-26411# Wright State Univ., Dayton, Ohio.
HIGH TEMPERATURE TESTING OF C/C (CARBON/CARBON) COMPOSITES Final Report, Jul. 1986 - Sep. 1987
Parvis Dadras 12 Dec. 1987 8 p
(Grant AF AFOSR-0224-86)
(AD-A193012; AFOSR-88-0309TR) Avail: NTIS HC A02/MF A01 CSCL 11D

A high temperature vacuum furnace for across-ply testing of carbon/carbon composites has been installed. This furnace has a double-walled water-jacketed vacuum chamber and is equipped with a 30 kVA variable output transformer, semi-automatic vacuum system, a digital temperature controller programmer, a two-color optical pyrometer, various thermocouples, and a digital data acquisition system. This furnace has been installed on an existing Model 1123 Instron, and heating to 2200 C has been accomplished. Graphite toolings have been prepared, and across-ply tensile testing to 1700 C has been conducted. GRA

N88-26412# Drexel Univ., Philadelphia, Pa. Dept. of Mechanical Engineering and Mechanics.
COMPUTATION EQUIPMENT FOR DAMAGE SIMULATION IN LAMINATED COMPOSITES Final Report, 1 Oct. 1986 - 30 Sep. 1987
A. S. Wang 25 Feb. 1988 9 p
(Grant AF AFOSR-0013-87)
(AD-A193013; TR-5; AFOSR-88-0311TR) Avail: NTIS HC A02/MF A01 CSCL 12E

This report describes the MicroVAX II based computational equipment funded by the Air Force Office of Scientific Research and installed at Drexel University. This equipment is dedicated exclusively for computational mechanics for composites materials research. Owing to its large computing capacity and availability to perform intensive computational tasks at substantially lower unit cost, this equipment has caused positive impacts on current AFOSR programs and other research work conducted at Drexel University. In short, this computational equipment has already enhanced the quality and the quantity of composite materials research at Drexel University. GRA

N88-26413*# Texas A&M Univ., College Station. Dept. of Aerospace Engineering.
A MICROMECHANICS MODEL OF THE STIFFNESS AND STRENGTH OF LAMINATES WITH FIBER WAVINESS
Charles E. Harris and Jong-Won Lee Jul. 1988 102 p
(Grant NAG1-711)
(NASA-CR-181670; NAS 1.26:181670) Avail: NTIS HC A06/MF A01 CSCL 11D

A mathematical model based on the Euler-Bernoulli beam theory is proposed for predicting the effective Young's moduli of piecewise isotropic composite laminates with local ply curvatures in the main load-carrying layers. Strains in corrugated layers, In-Phase layers, Out-of-Phase layers are predicted for various geometries and material configurations by assuming matrix layers as elastic foundations of different spring constants. The effective Young's moduli measured from corrugated aluminum specimens and aluminum/epoxy specimens with In-Phase and Out-of-Phase wavy patterns coincide very well with the model predictions. Moire fringe analysis of an In-Phase specimen and an Out-of-Phase specimen are also presented confirming the main assumption of the model related to the elastic constraint due to the matrix layers. The present model is also compared with the experimental results and other models, including the micro-buckling models, published in the literature. The results of the present study show that even a very small scale local ply curvature produces a noticeable effect on the mechanical constitutive behavior of a laminated composite. Author

N88-26414# Centre National de la Recherche Scientifique, Montpellier (France). Lab. de Science des Materiaux Vitreux.
MANUFACTURING OF A CERAMIC-CERAMIC COMPOSITE MATRIX USING THE SOL-GEL PROCEDURE Final Report [ELABORATION D'UNE MATRICE POUR COMPOSITES CERAMIQUE-CERAMIQUE PAR LA VOIE SOL-GEL]
G. Larnac and J. Phalippou Sep. 1987 50 p In FRENCH
(Contract DRET-85-183)
(ETN-88-92157) Avail: NTIS HC A03/MF A01

The preparation of high density gels and thermal processing of the Li2O-Al2O3-SiO2 ceramic system is studied. This type of material would be an ideal matrix for ceramic matrix composites. The limit processing temperature was chosen at 1300 C. The synthesis was done following a prehydrolysis procedure from tetrahydrosilane, sec-Al butyrate and lithium nitrate. Recrystallization and ternary diagram characteristics are discussed. The mechanical properties of materials obtained using the procedure are similar to those reported using melting and recrystallization. ESA

25 INORGANIC AND PHYSICAL CHEMISTRY

Includes chemical analysis, e.g., chromatography; combustion theory; electrochemistry; and photochemistry.

For related information see also *77 Thermodynamics and Statistical Physics.*.

N88-26415# Pennsylvania Univ., Philadelphia. Dept. of Materials Science and Engineering.
THE PROTONIC BETA DOUBLE PRIME ALUMINAS: PREPARATION, STABILITY, CONDUCTIVITY AND STRUCTURE Final Report, 1 Mar. 1984 - 31 Aug. 1986
G. C. Farrington 19 Mar. 1988 28 p
(Contract DE-AC02-80ER-10597)
(DE88-008442; DOE/ER-10597/1) Avail: NTIS HC A03/MF A01

The preparation, thermal stability, conductivity, and structures of the various protonic beta aluminas are investigated. The following issues were addressed: (1) why does a mixed ammoniumhydronium composition form when sodium beta alumina undergoes ion exchange in ammonium nitrate and what determines the relative proportions of ammonium and hydronium ions in the structure; (2) what is the thermal stability of the compound; and (3) what is the conductivity of ammoniumhydronium beta alumina and how is it influenced by composition. Data demonstrate that composition, thermal stability, and ionic conductivity in ammoniumhydronium beta alumina are closely related. Proportions of ammonium and hydronium are variable and depend on the duration of the ion-exchange process. Eventually, however, a steady-state composition is achieved. This composition corresponds to a particular and rather elegant ordered arrangement of ammonium ions, hydronium ions, and vacancies in the structure. In addition and in contrast to previous work, it was found that water and ammonia evolve from ammoniumhydronium beta alumina in discrete steps below 350 C. Water is lost from the structure between 150 to 250 C with an enthalpy of 10 kcal/mole. The loss of ammonia occurs at 250 to 300 C with an enthalpy of 19 kcal/mole. Below 300 C, the thermal decomposition of ammoniumhydronium beta alumina is reversible. The conductivity of single crystals of ammoniumhydronium beta alumina (steady-state composition) obeys an Arrhenius relationship below 200 C with an activation energy of 0.26 eV (sigma = 10 to the -3 (Omega-cm sup-1) at 25 C). Thermal annealing at 280 C causes the conductivity to fall into the range observed for samples of hydronium beta alumina. DOE

N88-26416# Case Western Reserve Univ., Cleveland, Ohio. Dept. of Chemical Engineering.
IN SITU SPECTROSCOPIC STUDIES OF TRANSITION METAL MACROCYCLES AS CATALYSTS FOR THE ELECTROCHEMICAL REDUCTION OF OXYGEN Annual Report, Dec. 1986 - Nov. 1987
D. A. Scherson and E. B. Yeager Apr. 1988 35 p
(Contract GRI-5086-260-1403)
(PB88-203195; GRI-88/0066) Avail: NTIS HC A03/MF A01 CSCL 07D

The vibrational, electronic, and structural properties of transition metal macrocycles adsorbed on electrode surfaces are investigated with an array of in situ spectroscopic techniques. These include potential difference FTIR, electrochemically modulated infrared spectroscopy, EMIRS, electromodulated reflection absorption spectroscopy in the UV-visable spectral region, Mossbauer spectroscopy in the transmission, and conversion electron modes and x-ray absorption fine structure. The information arising from the use of these techniques is being complemented by conventional electrochemical measurements, and scanning tunneling microscopy as a means of imaging transition metal macrocycles adsorbed on metal surfaces including infrared, ultraviolet visible, Mossbauer and x-ray absorption fine structure. These studies are aimed at gaining a basic understanding of the factors that control the electrocatalytic activity of transition metal macrocycles adsorbed on electrode surfaces for the electrochemical reduction of dioxygen. Author

N88-26417# Technische Hogeschool, Delft (Netherlands). Dept. of Aerospace Engineering.
COMBUSTION OF PMMA (POLYMETHYLMETHACRYLATE), PE (POLYETHYLENE) AND PS (POLYSTYRENE) IN A RAMJET
C. W. M. vanderGeld, P. A. O. G. Korting, and T. Wijchers Apr. 1987 75 p Prepared in cooperation with Prins Maurits Lab. TNO, Rijswijk, Netherlands
(PB88-186572; SFCC/Pub-42; LR-514; PML-1987-C-18) Avail: NTIS HC A04/MF A01 CSCL 21B

The combustion behavior of polymethyl methacrylate (PMMA), polyethylene (PE) and polystyrene (PS) was investigated in a connected pipe test facility. Instantaneous and local regression rates were determined. Spectroscopy was applied. Main issues of the present investigation are the establishing and understanding of the most important phenomena that control or emanate from the combustion of a cylindrical solid fuel with a rearward facing step. Main utilization is for solid fuel ramjets, safe burning of toxic waste and hot gas generators. During the investigation attention was focussed on regression rate, efficiency, temperatures, and soot production. Author

N88-26418# Argonne National Lab., Ill.
LASER FLUORESCENCE SPECTROSCOPY OF ZINC NEUTRALS ORIGINATING FROM LASER-IRRADIATED AND ION-BOMBARDED ZINC SULFIDE AND ZINC SURFACES
H. F. Arlinghaus, W. F. Calaway, C. E. Young, M. J. Pellin, D. M. Gruen, and L. L. Chase Feb. 1988 12 p Presented at the Boulder Damage Symposium, Boulder, Colo., 26 Oct. 1987 Prepared in cooperation with Lawrence Livermore National Lab., Calif.
(Contracts W-7405-eng-48; W-31-109-eng-38)
(DE88-008037; UCRL-98168; CONF-8710165-13) Avail: NTIS HC A03/MF A01

Time-Of-Flight (TOF) measurements, employing high-resolution Laser-induced Fluorescence Spectroscopy (LFS) as a probe, have been used to measure the yield and velocity distribution of Zn atoms ejected from a ZnS single crystal under irradiation by 308 nm photons. By comparison with the known ion sputtering yield for pure zinc, the absolute yield was determined to be 10 to the 10th atoms/pulse at a laser fluence of 30 mJ/sq cm. The velocity distribution of the Zn atoms could be fitted by a Maxwell-Boltzmann distribution, having a characteristic temperature of 2360 K. In addition, Doppler-shift techniques have been combined with TOF measurements in order to separate prompt from delayed emission of ablated atoms, as well as to probe possible molecular or cluster fragmentation. The results obtained suggest the possibility of molecular or cluster emission from ZnS. DOE

N88-26419# Sandia National Labs., Albuquerque, N. Mex.
EXPERIMENTAL AND THEORETICAL ANALYSIS OF THE RADIATIVE TRANSFER WITHIN A SOOTY POOL FIRE
R. S. Longenbaugh and L. K. Matthews Feb. 1988 141 p Prepared in cooperation with New Mexico State Univ., Las Cruces
(Contract DE-AC04-76DP-00789)
(DE88-007099; SAND-86-0083; TTC-0642) Avail: NTIS HC A07/MF A01

Numerous models are available for characterizing the radiation heat transfer environment within a sooty pool fire. Usually, these models contain a number of unknown parameters (i.e., extinction coefficient and absorption coefficient) which correspond to physical properties of the fire environment. The objective of this work is to provide quantitative estimates of the unknown parameters, using experimental data obtained from a large scale pool fire (9.1 m x 18.3 m) and nonlinear parameter estimation techniques. This work is part of an effort to evaluate the effects of a sooty pool fire on shipping containers transporting radioactive materials. In some unusual accident situations a container may be completely engulfed in flames, so it is important to understand the radiation effects on a container. Since radiation plays a dominant role in the total energy balance, radiation effects are the main thrust of this study. The radiation-to-convection ratio is on the order of four or five to one. This ratio has been suggested by other authors and is confirmed by the current work. During the course of this work, it was determined that the large scale pool fire was absorption dominant. Therefore, scattering was neglected and a one parameter model was developed. Mean absorption coefficients ranged between 0.006/cm and 0.017/cm. DOE

N88-26420# Cornell Univ., Ithaca, N.Y. Dept. of Materials Science and Engineering.
SURFACE PHASES AND THEIR INFLUENCE ON METAL-OXIDE INTERFACES Progress Report, 1 Aug. 1987 - 1 Apr. 1988
J. M. Blakely Mar. 1988 4 p
(Contract DE-FG02-87ER-45328)
(DE88-007938; DOE/ER-45328/1) Avail: NTIS HC A02/MF A01

The first part of the program has been devoted to design of equipment and technique development. A UHV system has been redesigned for this project. Experiments on the modification of atomically stepped surfaces of Ni by submonolayer sulphur coverages have been started during the grant period. Progress has been made in the area of scanning tunneling microscopy to be used in connection with the study of surface phase morphology. DOE

N88-26421# Oak Ridge National Lab., Tenn.
METHOD FOR THE ISOTOPICALLY SELECTIVE DETECTION OF INERT GASES
M. G. Payne Apr. 1988 5 p Presented at the 4th International Symposium on Resonance Ionization Spectroscopy and its Applications, Gaithersburg, Md., 10 Apr. 1988
(Contract DE-AC05-84OR-21400)
(TI88-008370; CONF-880435-6) Avail: NTIS HC A02/MF A01

A method for the detection of inert gases is described. This technique differs from the original Oak Ridge National Laboratory approach by obtaining isotopic selectivity by both mass analysis and laser spectroscopy. DOE

N88-26422# Los Alamos National Lab., N. Mex.
ULTRAVIOLET IMAGING OF HYDROGEN FLAMES
G. J. Yates, M. Wilke, and N. King 1988 9 p Presented at SPIE's Technical Symposium on Optics, Electro-optics and Sensors, Orlando, Fla., 4 Apr. 1988
(Contract W-7405-eng-36)
(DE88-009152; LA-UR-88-1121; CONF-880462-7) Avail: NTIS HC A02/MF A01

We have assembled an ultraviolet-sensitive intensified camera

for observing hydrogen combustion by imaging the OH, Lambda Sigma (+) bandhead emissions near 309 nm. The camera consists of a quartz and CaF achromat lense-coupled to an ultraviolet image intensifier which is in turn fiber-coupled to a Focus Projection Scan (FPS) vidicon. The emission band is selected with interference filters which serve to discriminate against background. The camera provides optical gain of 100 to 1000 and is capable of being shuttered at nanosecond speeds and of being framed at over 600 frames per second. We present data from observations of test flames in air at standard RS-170 video rates with varying background conditions. Enhanced images using background subtraction are presented. Finally, we discuss the use of polarizaton effects to further discrimine against sky background. This work began as a feasibility study to investigate ultraviolet technology to detect hydrogen fires for the NASA space program. DOE

N88-26423# Massachusetts Inst. of Tech., Cambridge. Dept. of Mechanical Engineering.
MODELLING OF PREMIXED COMBUSTION USING A THIN FLAME SHEET AND THE EFFECT OF THE HYDRODYNAMIC INSTABILITY
A. F. Ghoniem and O. M. Knio 1987 54 p
(Contract DE-AC04-81AL-16310)
(DE88-009467; DOE/AL-16310/T2) Avail: NTIS HC A04/MF A01

A dynamic thin flame model that introduces the effect of flame structure on the burning velocity is described and appropriate numerical schemes are constructed to obtain solutions in configurations with available experimental data for validation. Using this model, the role of the hydrodynamic instability, which arises due to the imbalance between the flow and the local burning velocities, on the evolution of the flame front and the pressure history during the combustion of premixed gases in confined chambers is investigated. It is shown that the hydrodynamic instability plays an important role and that accurate modeling can only be achieved if the stabilizing effect due to flame curvature is included in the formulation. The problem is relevant to the modeling of combustion in engines, pressure rise due to confined explosion, and the analysis of processes governed by flame-flow interactions. Results provide an interpretation for phenomena associated with large scale distortion of flames and shed light on their underlying mechanism. DOE

N88-26424# San Diego State Univ., Calif. Dept. of Electrical and Computer Engineering.
ELECTRON-IMPACT-IONIZATION AND ELECTRON-ATTACHMENT CROSS SECTIONS OF RADICALS IMPORTANT IN TRANSIENT GASEOUS DISCHARGES Annual Report, 1 Sep. 1986 - 31 Dec. 1987
Long C. Lee, Dong P. Wang, and Santosh K. Srivastava 5 Feb. 1988 53 p
(Contract N00014-86-K-0558)
(AD-A192248) Avail: NTIS HC A04/MF A01 CSCL 07D

In this research program, an apparatus using electron beam, laser beam and molecular beam has been constructed to measure the electron-impact-ionization cross sections and electron-attachment cross sections of radicals that are abundant in electrical discharge media. The electron excitation cross sections of radicals are very little known. The radical data are needed for understanding the microscopic processes of electrical discharges and for designing gaseous discharge switches. High power gaseous discharge switches are currently needed for the development of inductive-energy-storage systems, high power lasers, and particle beam experiments. GRA

N88-26425# Spectra Technology, Inc., Bellevue, Wash.
RARE GAS HALIDE (RGH) KINETICS Final Report
Wayne D. Kimura Feb. 1988 153 p
(Contract N00014-85-C-0843)
(AD-A192352; C-11-333) Avail: NTIS HC A08/MF A01 CSCL 07B

As a result of the measurements performed during this program and the refinements made to the computer model, our understanding of xenon chloride (XeCl) kinetics has increased dramatically. Qualitatively, one might state that our understanding of XeCl is now comparable to the other major excimers. Much of the mystery associated with the XeCl kinetics has been lifted. For example, significant vibrational excitation of HCl appears to be occurring as indirectly indicated by the behavior of the electron density. The exact character of the electron energy distribution and its affect on the kinetics is now better understood. The distribution is not entirely Maxwellian, as was generally assumed by models before this work. Instead, only the low energy distribution (the distribution below the ionization energy of xenon) is Maxwellian; the high energy distribution is non-Maxwellian. Ultimately, the interest is in improving the performance of XeCl lasers, in particular, scaling them to longer pulse lengths. As mentioned earlier, control of halogen depletion is crucial for achieving long pulse lengths. GRA

N88-26426# Purdue Univ., West Lafayette, Ind. Dept. of Chemistry.
A SIMULATION ANALYSIS OF ERRORS IN THE MEASUREMENT OF STANDARD ELECTROCHEMICAL RATE CONSTANTS FROM PHASE-SELECTIVE IMPEDANCE DATA Technical Report, 1 Oct. 1986 - 30 Sep. 1987
D. F. Milner and M. J. Weaver 30 Sep. 1987 21 p
(Contract N00014-86-K-0556)
(AD-A192739; TR-63) Avail: NTIS HC A03/MF A01 CSCL 07D

A digital simulation analysis is presented of the coupled effects of solution resistance and lock in amplifier damping upon the evaluation of standard rate constants for rapid electrode reactions using phase-selective AC impedance measurements with positive-feedback iR compensation. These two effects combine to yield apparent (i.e. measured) rate constants, evaluated using the conventional frequency-dependent analysis,that are generally smaller than the actual values. The extent to which these systematic errors depend on experimental conditions is explored for various values of the uncompensated and specific solution resistances, the amplifier filter time constant, the double layer capacitance and other relevant parameters. A simple scheme employing these simulations is outlined by which the actual values can be extracted from apparent measurements. Some experimental verification of these effects is also presented. GRA

N88-26427# Purdue Univ., West Lafayette, Ind. Dept. of Chemistry.
THE INFLUENCE OF UNCOMPENSATED SOLUTION RESISTANCE ON THE DETERMINATION AND STANDARD ELECTROCHEMICAL RATE CONSTANTS USING CYCLIC VOLTAMMETRY AND SOME COMPARISONS WITH AC VOLTAMMETRY Technical Report No. 68, 1 Oct. 1986 - 30 Sep. 1987
David F. Milner and Michael J. Weaver 25 Sep. 1987 34 p
(Contract N00014-86-K-0556)
(AD-A192825) Avail: NTIS HC A03/MF A01 CSCL 07D

A digital simulation analysis is presented of the deleterious effects of uncompensated solution resistance, Rus, upon the evaluation of standard rate constants, k2ob, using cyclic voltammetry. The results are expressed in terms of systematic deviations of apparent measured rate constants, k2ob(app), evaluated in the conventional manner without regard for Rus, from the corresponding actual values, k2ob (true), as a function of Rus and other experimental parameters. Attention is focused on the effects of altering the electrode area and the double-layer capacitance upon the extent of the deviations between kob (app) and ksob (true), and on comparisons with corresponding simulated results obtained from phase-selective ac impedance data. GRA

N88-26428# Purdue Univ., West Lafayette, Ind.
ASYNCHRONOUS OPTICAL SAMPLING FOR LASER-BASED COMBUSTION DIAGNOSTICS IN HIGH PRESSURE FLAMES Annual Report, 15 Dec. 1986 - 14 Dec. 1987
Galen B. King, Normand M. Laurendeau, and Fred E. Lytle 20 Jan. 1988 22 p

(Grant AF AFOSR-0323-84)
(AD-A192920; AFOSR-88-0297TR) Avail: NTIS HC A03/MF A01 CSCL 21B

This report describes progress on the development of a new laser based combustion diagnostic for the quantitative measurement of both major and minor species in high pressure flames. The technique, Asynchronous Optical Sampling (ASOPS), is a state-of-the-art improvement in picosecond pump/probe spectroscopy. The timing parameters for the current ASOPS instrument are described and consideration is given to the optimization of these parameters. The first ASOPS measurements in a combustion environment have been made on atomic sodium. These measurements are compared with laser induced fluorescence measurements to demonstrate the viability of ASOPS as a combustion diagnostic. GRA

N88-26429# Georgia Inst. of Tech., Atlanta. School of Aerospace Engineering.
HETEROGENEOUS DIFFUSION FLAME STABILIZATION Final Report, Oct. 1983 - Sep. 1987
Warren C. Strahle and Jechiel I. Jagoda 29 Nov. 1987 12 p
(Grant AF AFOSR-0356-83)
(AD-A193014; AFOSR-88-0328TR) Avail: NTIS HC A03/MF A01 CSCL 21B

Analytical modelling and several experimental diagnostics were applied to an experimental flow in a two-dimensional subsonic windtunnel with a backward facing step and provision for injection of inerts and combustibles through the porous floor behind the step. The analytical techniques were based on a two equation model of turbulence with several variants of near wall models and numerical approaches. Conventional experimental techniques, where applicable in the cold flow, included hot film and pitot anemometry. Laser - based diagnostics in the cold and hot flows for velocity and species concentration measurements (both mean and instantaneous) included laser velocimetry in two components and Rayleigh molecular scattering. GRA

N88-26430*# National Aeronautics and Space Administration. Lewis Research Center, Cleveland, Ohio.
PERFORMANCE OF LIGHTWEIGHT NICKEL ELECTRODES
Doris L. Britton [1988] 8 p Presented at the 33rd International Power Sources Symposium, Cherry Hill, N.J., 13-16 Jun. 1988; sponsored by the Dept. of the Army
(NASA-TM-100958; E-4252; NAS 1.15:100958) Avail: NTIS HC A02/MF A01 CSCL 07D

The NASA Lewis Research Center is currently developing nickel electrodes for nickel-hydrogen (Ni-H2) batteries. These electrodes are lighter in weight and have higher energy densities than the heavier state-of-the-art (SOA) sintered nickel electrodes. In the present approach, lightweight materials or plaques are used as conductive supports for the nickel hydroxide active material. These plaques (fiber and felt, nickel plated plastic and graphite) are commercial products that are fabricated into nickel electrodes by electrochemically impregnating them with active material. Evaluation is performed in half cells structured in the bipolar configuration. Initial performance tests include capacity measurements at five discharge levels, C/2, 1.0C 1.37C, 2.0C and 2.74C. The electrodes that pass the initial tests are life cycle tested in a low Earth orbit regime at 80 percent depth of discharge. Different formulations of nickel fiber materials obtained from several manufacturers are currently being tested as possible candidates for nickel electrodes. One particular lightweight fiber mat electrode has accumulated over 3000 cycles to date, with stable capacity and voltage. Life and performance data of this electrode were investigated and presented. Good dimensional stability and active material adherence have been demonstrated in electrodes made from this lightweight plaque. Author

N88-26431*# National Aeronautics and Space Administration, Washington, D.C.
IGNITION AND FLAME SPREAD OF PMMA
K. Akita and T. Hirano Jul. 1988 20 p Transl. into ENGLISH from Saigai no Kenkyu (Japan), v. 11, 1979 p 291-297 Transl. by SCITRAN, Inc., Santa Barbara, Calif.
(Contract NASw-4307)
(NASA-TT-20290; NAS 1.77:20290) Avail: NTIS HC A03/MF A01 CSCL 21B

A discussion on the environmental effects on ignition and flame spread of combustible polymeric material which are used for building structures, based on recent work on ignition and flame spread of polymethylmethacrylate (PMMA). Several problems generated from the discussion are pointed out. Author

N88-26432# Technische Univ., Munich (West Germany). Lehrstuhl fuer Thermodynamik.
DYNAMICS AND STABILITY OF COMBUSTION DRIVEN SELF OSCILLATIONS IN PRESENCE OF VARIOUS FREQUENCIES. EXTENSIVE STABILITY CRITERIA Ph.D. Thesis [DYNAMIK UND STABILITAET SELBSTERREGTER VERBRENNUNGSSCHWINGUNGEN BEIM AUFTRETEN MEHRERER FREQUENZEN. EIN ERWEITERTES STABILITAETSKRITERIUM]
Walter Lang 1986 138 p In GERMAN Sponsored by Stiftung Volkswagenwerk, Hanover, Fed. Republic of Germany
(ETN-88-92123) Avail: NTIS HC A07/MF A01

Oscillations induced by the action of an acoustic wave in combustion chamber and in the flame are studied on a laboratory burner. For premixed flames various flame holders are experimented. The oscillation process is determined by measurement of acoustic pressure, acoustic velocity by laser doppler anemometer, and energy production with a photomultiplier. For each type of frequency, stability criteria are established. ESA

N88-26433# Ecole Nationale Superieure de Mecanique et d'Aerotechnique, Poitiers (France). Lab. d'Energetique et de Detonique.
STUDY OF THE LOCAL BEHAVIOR OF A FLAME Final Report [ETUDE DU COMPORTEMENT LOCAL D'UNE FLAMME]
P. Cambray, B. Deshaies, and G. Joulin 1988 70 p In FRENCH
(Contract DRET-85-130)
(ETN-88-92300) Avail: NTIS HC A04/MF A01

The behavior of axisymmetric C3H8-O2-N2 flames of adjustable length impinging on flat obstacles is studied. The flow was measured using Doppler laser anemometry and a tomographic laser device which allowed the visualization of a flame meridian cross-section. Experimental and theoretical determinations of the Markstein number for 100 flame configurations are given. Laws characterizing the flame behavior are presented. Once the Markstein number is measured, these laws are applicable to the given mixtures in other flame dynamics problems, including turbulent flames. ESA

N88-26307# Iwaki Meisei Univ. (Japan).
NUMERICAL SIMULATION OF IGNITION OF HYDROGEN JET IN HOT AIR
Fumio Takayama, Shirou Taki, Toshitaka Fujiwara, Koichi Hayashi, and Akira Sakurai (Tokyo Denki Univ., Japan) *In* National Aerospace Lab., Proceedings of the 5th NAL Symposium on Aircraft Computational Aerodynamics Nov. 1987 p 121-127 In JAPANESE; ENGLISH summary Previously announced in IAA as A87-33954 (For primary document see N88-26290 20-01)
Avail: NTIS HC A12/MF A01

26 METALLIC MATERIALS

Includes physical, chemical, and mechanical properties of metals, e.g., corrosion; and metallurgy.

N88-26434 Cincinnati Univ., Ohio.
A CONSTITUTIVE MODEL WITH DAMAGE FOR HIGH-TEMPERATURE SUPERALLOYS Ph.D. Thesis
James Allen Sherwood 1987 171 p
Avail: Univ. Microfilms Order No. DA8729260

The purpose is to develop a physically based constitutive equation that includes damage for use in multiaxial stress analysis. Material damage arising during creep and cyclic loadings in homogeneous isotopic nickel-base superalloys is examined. Inelastic and elastic effects were included in the modeling. The basic model is described, and the governing equations are presented. The inelastic strain rate equation, which resembles the exponential law proposed by Bodner, involves an empirical function of the accumulated inelastic strain. This function represents the accumulation of damage in the metallic continuum. The proposed models are developed for the three-dimensional case and can be made to include thermal dependence by varying the material constants as a function of temperature. However, because of the limited data base, the model is only applied to isothermal uniaxial tensile, creep, and cyclic loadings. Approximate times for the initiation of tertiary creep and number of cycles to fatigue failure are determined by numerical integration of the governing equations, which use material constants determined from experimental data. Behavior of the model is compared with experimental results. Finally, recommendations and conclusions are given.
Dissert. Abstr.

N88-26435# Oak Ridge National Lab., Tenn.
PHASE STABILITY AND ALLOY DESIGN OF ORDERED INTERMETALLICS
C. T. Liu 1987 15 p Presented at the NATO Advanced Study Institute on Alloy Phase Stability, Crete, Greece, 14 Jun. 1987
(Contract DE-AC05-84OR-21400)
(DE88-007479; CONF-8706103-8) Avail: NTIS HC A03/MF A01

Recent research on phase stability and grain boundary structure in ordered intermetallics is summarized. Ordered intermetallics have many attractive high-temperature properties; however, low ductility and brittle fracture limit their use for structural applications. Embrittlement in intermetallics is mainly caused by low-crystal symmetry and insufficient number of slip systems, poor cleavage strength, and intrinsic and extrinsic grain-boundary weakness. Experimental studies of ordered phase stability and grain-boundary structure have led to substantial improvement in the ductility and fracture toughness of several ordered intermetallics, including (Co,Fe)3V, (Ni,Fe)3V, (Co,Ni,Fe)3V, Fe3Al, Ni3Al, Ni3Ga, and Ni3Si. At present, the control of ordered structures and grain-boundary properties is mainly based on some empirical and/or phenomenological relationship. First-principle calculations have advanced to the stage that they are able to help us to understand the electron structure and phase stability and to design ductile ordered intermetallic alloys for structural use at elevated temperatures.
DOE

N88-26436*# National Aeronautics and Space Administration. Lewis Research Center, Cleveland, Ohio.
ACCELERATED FATIGUE CRACK GROWTH BEHAVIOR OF PWA 1480 SINGLE CRYSTAL ALLOY AND ITS DEPENDENCE ON THE DEFORMATION MODE
Jack Telesman and Louis J. Ghosn (Cleveland State Univ., Ohio.) Jun. 1988 16 p Proposed for presentation at the 6th International Conference on Superalloys, Seven Springs, Pa., 18-22 Sep. 1988; sponsored by the American Inst. of Mining, Metallurgical and Petroleum Engineers
(NASA-TM-100943; E-4231; NAS 1.15:100943) Avail: NTIS HC A03/MF A01 CSCL 11F

An investigation of the fatigue crack growth (FCG) behavior of PWA 1480 single crystal nickel base superalloy was conducted. Typical Paris region behavior was observed above a delta K of 8 MPa sq rt of m. However, below that stress intensity range, the alloy exhibited highly unusual behavior. This behavior consisted of a region where the crack growth rate became essentially independent of the applied stress intensity. The transition in the FCG behavior was related to a change in the observed crack growth mechanisms. In the Paris region, fatigue failure occurred along (111) facets; however, at the lower stress intensities, (001) fatigue failure was observed. A mechanism was proposed, based on barriers to dislocation motion, to explain the changes in the observed FCG behavior. The FCG data were also evaluated in terms of a recently proposed stress intensity parameter, K sub rss. This parameter, based on the resolved shear stresses on the slip planes, quantified the crack driving force as well as the mode I delta K, and at the same time was also able to predict the microscopic crack path under different stress states.
Author

N88-26437# Oak Ridge National Lab., Tenn.
INITIAL DEVELOPMENT OF HIGH-TEMPERATURE TITANIUM SILICIDE ALLOYS
C. T. Liu, E. H. Lee, and T. J. Henson Jan. 1988 31 p
(Contract DE-AC05-84OR-21400)
(DE88-007860; ORNL-6435) Avail: NTIS HC A03/MF A01

Mechanical and metallurgical properties of Ti5Si3 and its alloys were studied for the purpose of developing high-temperature silicides for structural use. Titanium silicides are extremely hard and brittle. Microcracks that formed transgranularly were observed in the silicide and its alloys, indicating a poor cleavage strength for Ti3Si5. Microalloying with boron and carbon gave no apparent beneficial effect. The tendency for cracking can be reduced by lowering the silicon content or by alloying with 2 to 4 percent Cr and 4 percent Zr. In particular, almost no cracks were observed in the alloy Ti-33Si-4Zr-4Cr (at. percent). Titanium silicide has a hardness of 980 dph. The hardness shows a slight increase with zirconium additions and a decrease with chromium additions. Tensile tests indicate that the silicide and its alloys are brittle even at 1000 C. All alloys fractured with a strength less than 100 MPa. Among the silicides tested, the alloys containing 4 to 8 percent Cr have better fracture strength. The fracture mode of the silicide alloys is mainly transgranular with a cleavage appearance. The silicides showed basically a parabolic oxidation rate at 800 C, with an oxidation rate higher by an order of magnitude than that of nickel aluminides.
DOE

N88-26438# Los Alamos National Lab., N. Mex.
GLASS FORMING RANGES OF AMORPHOUS ALLOYS
R. B. Schwarz 1988 10 p Presented at the International Symposium on Nonequilibrium Solid Phase of Metals and Alloys, Kyoto, Japan, 14 Mar. 1988
(Contract W-7405-eng-36)
(DE88-007897; LA-UR-88-809; CONF-880310-1) Avail: NTIS HC A02/MF A01

Two main methods of synthesis of amorphous metallic alloys are based on the rapid solidification of molten alloys and on isothermal solid state reactions between pure metals. We discuss recent calculations for the glass forming range for both techniques and we compare the predicted homogeneity ranges of the amorphous phase with experiments.
DOE

N88-26439# Helsinki Univ. of Technology, Espoo (Finland). Lab. of Engineering Materials.
PLASTIC DEFORMATION AND ROUGHNESS OF FREE METAL SURFACES Ph.D. Thesis
A. E. Valkonen 1988 513 p Prepared in cooperation with Ohio State Univ., Columbus
(Grant NSF DMR-83-11620)
(PB88-196621; MTR-1/88; ISBN-951-754-400-6) Avail: NTIS HC A22/MF A01 CSCL 11F

The overall goal of the work is to develop a strong basis for a subsequent research program the purpose of which is to provide detailed experimental analyses of the interactions between localized plastic deformation and surface roughness in different metals and alloys subjected to various deformation histories. The main specific goals of this work are to: (1) develop a framework for understanding the nature of surface roughness as based on the random process theory; (2) develop a framework for understanding the laser light based surface roughness measurement methods by means of the rough surface scattering theory of electromagnetic radiation; (3) describe the present state of the art of stylus profilometry and laser light scattering methods in the area of surface roughness measurement.
GRA

N88-26440# International Centre for Theoretical Physics, Trieste (Italy).
PRECIPITATION STUDY BY ELECTRICAL RESISTIVITY MEASUREMENT IN Ni-Al ALLOYS
M. I. Ansari Jul. 1987 9 p
(DE88-701877; IC-87/135) Avail: NTIS (US Sales Only) HC A02/MF A01

Results of a resistomatric study of an Ni-13.1 at. percent Al alloy show that the initial increase in resistivity can be related to the segregation of solute atoms into smaller coherent clusters or zones, during aging after quenching, in a wide temperature range. Furthermore, the Al solute concentrations in equilibrium with gamma-prime precipitates in this alloy are also investigated. DOE

N88-26441# International Centre for Theoretical Physics, Trieste (Italy).
ABNORMAL DIFFUSION OF VACANCIES IN METALS
Huilong Zhu and Zuqia Huang Jun. 1987 15 p
(DE88-701880; IC-87/138) Avail: NTIS (US Sales Only) HC A03/MF A01

The vacancy-concentration effect on the vacancy-migration-energy and the behaviour of divacancies were considered in deriving a formula for the vacancy-current in bcc metals. It turns out that vacancies will migrate in the direction of increasing concentration, when the concentration is greater than some critical value determined by a reasonable physical condition. The method in this paper can be extended easily to other metals. DOE

N88-26442# Oak Ridge National Lab., Tenn.
REDUCED-ACTIVATION AUSTENITIC STAINLESS STEELS: THE Fe-Cr-C SYSTEM
R. L. Klueh and P. J. Maziasz 1988 28 p Presented at the 14th International Symposium on Effects of Radiation on Materials, Andover, Mass., 27 Jun. 1988
(Contract DE-AC05-84OR-21400)
(DE88-008091; CONF-880613-2) Avail: NTIS HC A03/MF A01

Nickel-free manganese-stabilized steels are being developed for fusion-reactor applications. As the first part of this effort, the austenite-stable region in the Fe-Mn-Cr-C system was determined. Results indicated that the Schaeffler diagram developed for Fe-Ni-Cr-C alloys cannot be used to predict the constituents expected for high-manganese steels. This is true because manganese is not as strong an austenite stabilizer relative to delta-ferrite formation as predicted by the diagram, but it is a stronger austenite stabilizer relative to martensite than predicted. Therefore, the austenite-stable region for Ne-Mn-Cr-C alloys occurs at lower chromium and higher combinations of manganese and carbon than predicted by the Schaeffler diagram. Development of a manganese-stabilized stainless steel should be possible in the composition range of 20 to 25 percent Mn, 10 to 15 percent Cr, and 0.01 to 0.25 percent C. Tensile behavior of an Fe-20 percent Mn-12 percent Cr-0.25 percent C alloy was determined. The strength and ductility of this possible base composition was comparable to type 316 stainless steel in both the solution-annealed and cold-worked condition. DOE

N88-26443# Auburn Univ., Ala.
HELIUM INDUCED DEGRADATION IN THE WELDABILITY OF AN AUSTENITIC STAINLESS STEEL
H. T. Lin, S. H. Goods, M. L. Grossbeck, and B. A. Chinl 1988 30 p Presented at the 14th International Symposium on Effects of Radiation on Materials, Andover, Mass., 27 Jun. 1988 Prepared in cooperation with Sandia National Labs., Livermore, Calif. and ORNL, Tenn.
(Contract DE-AC05-84OR-21400)
(DE88-009062; CONF-880613-4) Avail: NTIS HC A03/MF A01

Autogenous gas tungsten arc welding was performed on He-doped type 316 stainless steel. Helium was uniformly implanted in the material using the tritium trick to levels of 27 and 105 appm. Severe intergranular cracking occurred in both fusion and heat-affected zones. Microstructural observations of fusion zone indicated that the pore size, degree of porosity, and tendency to form cracks increased with increasing helium concentration. Scanning electron microscopy showed that cracking in He-doped materials was due to the precipitation of helium bubbles on grain boundaries and dentrite interfaces. Results of the present study demonstrate that the use of conventional welding techniques to repair materials degraded by exposure to radiation may be difficult if the irradiation results in the generation of even rather small amounts of helium. DOE

N88-26444# Cornell Univ., Ithaca, N.Y. Dept. of Materials Science and Engineering.
GRAIN BOUNDARY STRUCTURE IN Ni3Al
R. A. D. Mackenzie, M. D. Vaudin, and S. L. Sass Jul. 1987 7 p Presented at the Conference on Interface Science and Engineering, Lake Placid, N.Y., 12 Jul. 1987
(Contract DE-FG02-85ER-45211)
(DE88-009164; DOE/ER-45211/4; CONF-870793-7; MSC-6186) Avail: NTIS HC A02/MF A01

The influence of boron segregation and non-stochiometry on grain boundary structure in Ni3Al was studied by transmission and scanning electron microscopy techniques. Small angle twist and tilt boundaries were produced by hot pressing misoriented single crystals of both doped and undoped materials. Dislocation structures were observed in both bicrystal and polycrystal grain boundaries. In most cases the grain boundary dislocations were found to have the expected a(100) Burgers vector, however, in one case dislocations with Burgers vector a2(110) dislocations have been observed. Using a SEM diffraction technique the frequency of occurrence of grain boundary types was examined and found to be unchanged by the addition of boron. DOE

N88-26445# Michigan Technological Univ., Houghton. Dept. of Metallurgical Engineering.
THE EFFECTS OF GRADIENTS ON BOUNDARY STABILITY Progress Report, 1 Jul. 1987 - 31 Mar. 1988
S. A. Hackney, M. R. Plichta, and J. K. Lee 1988 21 p
(Contract DE-FG02-87ER-45315)
(DE88-009592; DOE/ER-45315/1) Avail: NTIS HC A03/MF A01

This report discusses effects that will change grain boundary stability. In particular, morphological transitions and thermotransport induced grain boundary migration are briefly mentioned. DOE

N88-26446# Massachusetts Inst. of Tech., Cambridge. Dept. of Materials Science and Engineering.
GRAIN BOUNDARIES Annual Report
R. W. Balluffi and P. D. Bristowe 28 Apr. 1988 10 p
(Contract DE-FG02-87ER-45310)
(DE88-009889; DOE/ER-45310/8) Avail: NTIS HC A02

The present document is a progress report describing the work accomplished on the study of the grain boundaries of gold. The research that was proposed initially for this period consisted of studies of the atomistic structure of grain boundaries by means of combined X-ray diffraction and computer modeling and of grain boundary phase transitions by electron microscopy and computer modeling. Progress has been made on both of these areas which is described in more detail. A list of reports describing the research completely during the first year is presented. DOE

N88-26447# Dartmouth Coll., Hanover, N.H. School of Engineering.
THE STRUCTURE AND PROPERTIES OF GRAIN BOUNDARIES IN B2 ORDERED ALLOYS
I. Baker Apr. 1988 14 p
(Contract DE-FG02-87ER-45311)
(DE88-009890; DOE/ER-45311/T1) Avail: NTIS HC A03/MF A01

During this period we have produced fine-grained alloys of FeAl and NiAl which span the respective phase fields of these materials. We have: (1) initiated mechanical testing of the FeAl alloys as a function of grain size, which confirms that the yield strength decreases with increasing deviation from stoichiometry;

(2) initiated grain growth studies of the FeAl alloys, whose preliminary results suggest that grain growth is more rapid in off-stoichiometric compositions; (3) successfully prepared thin foils of NiAl alloys and iron-rich FeAl alloys for transmission electron microscopy; (4) initiated an Atom Probe Field Ion Microscope study of the grain boundary chemistry of NiAl; (5) attempted to study boundary chemistry in NiAl and studied grain boundary chemistry in Ni3Al using Auger electron spectroscopy; and (6) performed a short oxidation study of FeAl, which shows that oxidation rate increases with increasing iron content in FeAl. DOE

N88-26448# Argonne National Lab., Ill.
EFFECT OF DOUBLE LAYER STRUCTURE ON THE DETERMINATION OF CORROSION RATES FROM POLARIZATION MEASUREMENTS
Z. Nagy and P. F. Schultz 1988 9 p Presented at the Electrochemical Society Spring Meeting, Atlanta, Ga., 15 May 1988
(Contract W-31109-eng-38)
(DE88-010097; CONF-880549-2) Avail: NTIS HC A03/MF A01

The effect of the double layer structure is seldom considered in the electrochemical measurements of corrosion rates. Polarization equations of corroding metals can be corrected for the effect of the double layer using the classical Frumkin correction of electrode kinetics. This corrected polarization equation can be used to generate synthetic data which, in turn, permit the calculation of the error caused by the neglect of the double layer effect in the electrochemical corrosion rate determinations. While the error depends on many parameters, the two dominating factors are the concentration of the solution and the potential of the corroding metal with respect to the potential of zero change (pzc). The error will be negligible (less than 10 percent) if the solution concentration is at least 0.1 molar or the corrosion potential is at least + or - 0.25 V from the pzc. The error can be very large, many hundreds or thousands of percents, unless at least one of the above conditions is met, and the appearance of the polarization curves will have no clear indication of the unreliability of the measurement. Under these conditions, the electrochemical measurements should be supplemented with other types of corrosion rate determinations, or a correction can be made if the double layer parameters are known. DOE

N88-26449# Los Alamos National Lab., N. Mex.
A NUMERICAL STUDY OF RAYLEIGH-TAYLOR INSTABILITY IN ALUMINUM AND STEEL PLATES
B. J. Daly Mar. 1988 31 p
(Contract W-7405-eng-36)
(DE88-010475; LA-11192-MS) Avail: NTIS HC A03/MF A01

The SCRAM code is applied to the study of Rayleigh-Taylor instability in metal plates, and comparisons of these computer results are made with experimental data for 1100-O aluminum, 6061-T6 aluminum and 304 stainless steel. Various models for the pressure, temperature, and strain-rate dependencies of the flow stress are compared in the computer calculations. The coefficients that are required in these models to give good agreement with the experimental results are generally close to values that were determined from previous experimental comparisons. The sensitivity of the computed results to modeling parameters, to variations in the hardening modulus, and to the amplitude and wavelength of the perturbations in the plate surface is examined. Very little growth in amplitude occurs if either the initial amplitude or the wavelength is sufficiently small. The growth rate increases monotonically with increasing initial amplitude. There appears to exist a wavelength of maximum growth, such that the growth rate increases rapidly with wavelength up to this wavelength, but then decreases slowly as the wavelength is further increased. DOE

N88-26450# Argonne National Lab., Ill.
THE ADHERENCE OF NICKEL OXIDE ON NICKEL DURING HIGH TEMPERATURE OXIDATION
Yung Y. Liu and K. Natesan Mar. 1988 12 p Presented at the Adhesion in Solids, Reno, Nev., 5 Apr. 1988
(Contract W-31109-eng-38)
(DE88-011194; CONF-8804117-2; CONF-8804117-2) Avail: NTIS HC A03/MF A01

A combined experimental/analytical study is being conducted to investigate the fundamental nature of adherence of oxide scales formed on metals during high-temperature oxidation. Isothermal oxidation experiments were conducted on high-purity nickel (Ni 270) specimens in air at temperatures of up to 1200 C. None of the experiments resulted in physical separation of nickel oxide scales from nickel substrate, even though substantial amounts of porosity were found in scales close to the scale/metal interfaces. The results of numerical and analytical calculations of stresses in the NiO/Ni system suggest that metal and oxide plasticities play a role in the experimental observations. DOE

N88-26451# Naval Postgraduate School, Monterey, Calif.
OPTIMIZING SUPERPLASTIC RESPONSE IN LITHIUM CONTAINING ALUMINUM-MAGNESIUM ALLOYS M.S. Thesis
Ian G. Munro Dec. 1987 93 p
(AD-A192217) Avail: NTIS HC A05/MF A01 CSCL 11F

Four lithium containing Al-Mg-Zr alloys, containing 6 to 8 wt. pct. Mg, 0.5 to 2 wt. pct. Li, and 0.15 to 0.25 wt. pct. Zr. were studied with a view to maximizing superplastic ductilities. Differential scanning calorimetry was employed to assist in the characterization of the microstructures and to determine the solvi of the constituent second phases. These data were used to aid in the choice of thermomechanical processing parameters previously applied to Al-Mg alloys containing 10 wt. pct. magnesium. The superplastic response of the alloys was evaluated over a range of temperatures (275 C to 350 C) and a range of strain rates (10 to the minus 5 power 0.1 sec-1). Elongations in excess of 1000 percent at 300 C and .01.7 sec-1 strain rate were obtained in a Al-8Mg-1Li-0.15Zr (wt. pct.) alloy. Transmission electron microscope investigations of the microstructure before and after superplastic deformation revealed that the volume fraction of second phase was predominantly responsible for structural stability. GRA

N88-26452# Southwest Research Inst., San Antonio, Tex.
STUDY OF THE INFLUENCE OF METALLURGICAL FACTORS ON FATIGUE AND FRACTURE OF AEROSPACE STRUCTURAL MATERIALS Annual Report, 1 Jan. 1987 - 31 Dec. 1987
James Lankford, David L. Davidson, Kwai S. Chan, and Gerald R. Leverant 31 Jan. 1988 34 p
(Contract F49620-86-C-0024)
(AD-A192909; SWRI-06-8972/2; AFOSR-88-0294TR) Avail: NTIS HC A03/MF A01 CSCL 11F

This report summarizes the results of a two-phase study involving (1) experimental characterization and analytical modeling of fatigue crack tip micromechanics in aerospace structural aluminum alloys, and (2) identification and modeling of key microstructural factors controlling fracture in aluminum-iron-x alloys. Dynamic load cycling within the SEM and stereoimaging strain analysis have been used to characterize crack opening loads, strains, and effective stress intensity (delta/Keff) values for large and small cracks in a variety of alloys; both constant amplitude and overload/underload situations were studied. It was found that delta/Keff based on local crack tip opening load was not an adequate crack growth rate correlating factor. Instead, it was necessary to use a new driving force term which includes both closure and local crack tip plasticity. The latter was computed by calculating delta/J integrals within the crack tip plastic zone using local crack tip strain data obtained via high resolution SEM of loaded and unloaded cracks. GRA

N88-26453*# National Aeronautics and Space Administration, Washington, D.C.
THE T-T-T CURVE IN Cu-Cr ALLOY
Hisashi Suzuki and Motohiro Kanno Jun. 1988 15 p Transl. into ENGLISH from Nippon Kinzuki Gakkaishi (Japan), v. 35, no. 5, 1981 p 434-439 Transl. by SCITRAN, Inc., Santa Barbara, Calif. Original document was prepared by Tokyo Univ., Japan

(Contract NASw-4307)
(NASA-TT-20167; NAS 1.77:20167) Avail: NTIS HC A03/MF A01 CSCL 11F

As the Cu-Cr alloy is known to be very quench-sensitive, the isothermal transformation curve was studied by other investigators. In this report, experiments to confirm the shape of the curve (having two noses) were carried out. The reason why the curve shows two noses was also investigated on the basis of observations of transmission electron micrographs of the aged structures. Results obtained were as follows: (1) a remarkable heterogeneous precipitation was observed on dislocation lines and on grain boundaries when the alloy was aged directly at high temperatures; (2) the two noses at high and low temperature in the T-T-T curve were confirmed to be due to heterogeneous precipitations at those temperatures, respectively; (3) however, when the alloy was quenched and normally aged, the pseudo T-T-T curve was of the ordinary C type, probably due to the homogeneous precipitation caused by the stabilization of vacancy clusters; and (4) generally, in the alloys of simple and homogeneous precipitation types, the T-T-T curves were considered to show two or more noses contrary to the single nose as expected. Author

N88-26454*# National Aeronautics and Space Administration, Washington, D.C.
THE INFLUENCE OF FOREIGN PARTICLES ON BEARING METALS
Sanae Mori Jun. 1988 20 p Transl. into ENGLISH from Japan Society of Lubrication Engineers Journal, v. 17, 1972, p 741-746 Transl. by SCITRAN, Inc., Santa Barbara, Calif.
(Contract NASw-4307)
(NASA-TT-20155; NAS 1.77:20155) Avail: NTIS HC A03/MF A01 CSCL 11F

Incidents of damage to automobile engine bearings caused by foreign particles are discussed. Granular materials can cause cracks and intrusions into soft bearing surfaces, leaving scratches in the bearing metals. Author

N88-26455*# National Aeronautics and Space Administration, Washington, D.C.
SHAPE MEMORY ALLOYS: NEW MATERIALS FOR FUTURE ENGINEERING
E. Hornbogen Jul. 1988 20 p Transl. into ENGLISH from Legierungen mit Formgedaechtnis: Neue Werkstoffe fuer die Technik der Zukunft, Berlin (Federal Republic of Germany), v. 41, no. 5, 1987 p 488-493 Transl. by SCITRAN, Inc., Santa Barbara, Calif. Original document was prepared by Ruhr Univ., Bochum
(Contract NASw-4307)
(NASA-TT-20193; NAS 1.77:20193) Avail: NTIS HC A03/MF A01 CSCL 11F

Shape memory is a new material property. An alloy which experiences relative severe plastic deformation resumes its original shape again after heating by 10 to 100 C. Besides simple shape memory, in similar alloys there is the second effect where the change in shape is caused exclusively by little temperature change. In pseudo-elasticity, the alloy exhibits a rubber-like behavior, i.e., large, reversible deformation at little change in tension. Beta Cu and beta NiTi alloys have been used in practice. The probability is that soon alloys based on Fe will become available. Recently increasing applications for this alloy were found in various areas of technology, even medical technology. A review with 24 references is given, including properties, production, applications and fundamental principles of the shape memory effect. Author

N88-26456# Institut National Polytechnique, Grenoble (France). Lab. de Thermodynamique et Physico-Chimie Metallurgique.
FATIGUE OF LITHIUM-ALUMINUM ALLOYS: AN EXAMPLE OF LOCALIZATION OF THE PLASTIC DEFORMATION Ph.D. Thesis [FATIGUE DES ALLIAGES BINAIRES ALUMINIUM-LITHIUM: UN EXEMPLE DE LOCALISATION DE LA DEFORMATION PLASTIQUE]
Yves Brechet 1987 229 p In FRENCH
(ETN-88-92309) Avail: NTIS HC A11/MF A01

The fatigue behavior of Li-Al alloys is studied using scanning electron microscope, transmission electron microscope, and X-ray difusion analysis. The fault structure evolution under stress is studied in situ. The existence of precipitate redisolution is demonstrated for the low Li concentration bands. A model for the phase transition induced by plastic deformation is proposed. A model to explain the localization of plastic fatigue deformation is also presented. ESA

N88-26457# Technische Univ., Munich (West Germany). Lehrstuhl fuer Metallurgie und Metallkunde.
INVESTIGATION OF STRUCTURE AND SURFACE STATE EFFECT ON HYDROGEN EMBRITTLEMENT OF STEELS, UNDER CONSIDERATION OF ACOUSTIC EMISSION ANALYSIS Ph.D. Thesis [UNTERSUCHUNGEN ZUM EINFLUSS DES GEFUEGE- UND OBERFLAECHENZUSTANDS AUF DIE WASSERSTOFFVERSPROEDUNG VON STAEHLEN UNTER EINBEZIEHUNG DER SCHALLEMISSIONSANALYSE]
Martin Ernst Max Kock 1987 169 p In GERMAN Sponsored by Forschungsvereinigung Antriebstechnik e.V., Fed. Republic of Germany, Arbeitsgemeinschaft industrieller Forschungsvereinigungen, Fed. Republic of Germany
(ETN-88-92350) Avail: NTIS HC A08/MF A01

Materials used in the engine industry like 50 CrV4, 16MnCr5 and 100 Cr6 are studied for their hydrogen embrittlement behavior during tensile and flexion tests coupled with acoustic emission analysis. The test procedure is based on the variation of hydrogen concentration distribution after hydrogen absorption by the material and the detection of microcracks by acoustic emission. The rise of hardness and material strength improves the resistance to hydrogen embrittlement for a given heat treatment procedure. Material structure is examined by hydrogen analysis, and metallographic and fractographic investigations. ESA

N88-26458# Technische Hogeschool, Delft (Netherlands). Dept. of Aerospace Engineering.
CORROSION IN AIRCRAFT STRUCTURES. PART 1: TEXT [CORROSIE VAN VLIEGTUIGCONSTRUCTIFS. DEEL 1: TEKST]
H. F. deJong Jun. 1987 123 p In DUTCH
(LR-527-Pt-1; B8733279; ETN-88-92467) Avail: NTIS HC A06/MF A01

The relation between aircraft manufacturer and aircraft user with respect to corrosion, and the economic and safety aspects of corrosion are presented. Corrosion theory aspects are explained. Electrode reaction kinetics are treated. The corrosion of metals and alloys in acid, neutral and strongly alkaline media, as well as the significance of pH-diagrams are discussed. The different kinds of corrosion occurring in aircraft structures are overviewed. The different forms of local corrosion are presented. ESA

N88-26459# Technische Hogeschool, Delft (Netherlands). Dept. of Aerospace Engineering.
CORROSION IN AIRCRAFT STRUCTURES. PART 2: FIGURES [CORROSIE VAN VLIEGTUIGCONSTRUCTIES. DEEL 2: FIGURES]
H. E. deJong Jun. 1986 53 p In DUTCH
(LR-527-Pt-2; B8733281; ETN-88-92468) Avail: NTIS HC A04/MF A01

Graphs, tables, drawings, and photographs illustrating aircraft corrosion are presented. ESA

N88-26460# California Univ., Berkeley. Lawrence Berkeley Lab.
THE PREPARATION OF MECHANICALLY ALLOYED POWDERS FOR TEM (TRANSMISSION ELECTRON MICROSCOPY) EXAMINATION
E. A. Kamenetzky, M. Wall, R. Castro, and L. E. Tanner 12 Feb. 1988 7 p Presented at the Fall Meeting of the Materials Research Society, Boston, Mass., 30 Nov. 1987 Prepared in cooperation with Lawrence Livermore National Lab., Calif.
(Contracts W-7405-eng-48; DE-AC03-76SF-00098)
(DE88-008043; UCRL-98230; CONF-871124-99) Avail: NTIS HC A02/MF A01

Transmission electron microscopy (TEM) specimens of mechanically alloyed elemental Ni and Nb powders are prepared by a new procedure. The alloyed powders are mixed with smaller Al powder and fill an aluminum ring (3 mm outer diameter). This composite is cold pressed together with the Al powders taking most of the deformation. The compacted specimen can be mechanically thinned. Electropolishing and ion milling can then proceed by standard methods with special precautions to minimize differential polishing or milling rates. Microstructural aspects of the formation of an amorphous phase by high-energy ball milling these powders have been studied. After 6 h each particle transforms to a heterogeneous layered composite of particles of one element in the matrix of the other. Particle size ranges from 15 nm to 90 nm. Mechanical alloying for 36 h results in the formation of an apparently uniform phase interspersed with a few small (4 nm to 30 nm) elemental crystalline particles. DOE

N88-26461# Oak Ridge National Lab., Tenn.
NICKEL ALUMINIDES: A NEW FAMILY OF NICKEL + ALUMINUM ALLOYS FEATURING SIMPLE COMPOSITION, LOW DENSITY, EXCELLENT OXIDATION RESISTANCE AND HIGH YIELD STRENGTH THAT INCREASES WITH TEMPERATURE
1988 10 p
(Contract DE-AC05-84OR-21400)
(DE88-010692; ORNL/M-548) Avail: NTIS HC A02/MF A01

The three alloys presented in this brochure are based on the intermetallic compound Ni3Al. Ni3Al is brittle, but by changing the composition to Ni76Al24 and adding approximately 200 ppM boron the alloy becomes ductile. The strength of these alloys depends entirely on the behavior of the ordered crystal structure and the grain size. Larger grain size favors good high temperature strength and fine grain size favors good low temperature strength. An unusual feature of the strength is that in annealed material the yield stress increases with test temperature up to about 800 C. Nickel aluminides display excellent oxidation and corrosion resistance characteristics which can be further enhanced with simple additives. Forming and processing can be accomplished by a variety of methods. Molten aluminides can be formed into ingots, castings, and near net shapes by several different processes. Nickel Aluminides can also be produced and consolidated from powder. Both cast and powder ingots, sheet, tube hollows, and rod can be further processed in several ways. DOE

27 NONMETALLIC MATERIALS

Includes physical, chemical, and mechanical properties of plastics, elastomers, lubricants, polymers, textiles, adhesives, and ceramic materials.

For composite materials see *24 Composite Materials*.

N88-26462*# National Aeronautics and Space Administration, Washington, D.C.
PRODUCTION OF POWDERED SODIUM HYDRIDE WITH LARGE SPECIFIC SURFACE BY THE CATALYZED REACTION OF MOLTEN SODIUM WITH HYDROGEN-1
Vladimir Prochazka, Petr Kriz, and Jaroslav Tlaskal Jul. 1988 20 p Transl. into ENGLISH from Chemicky Prymysl (USSR), v. 23, no. 12, 1973 p 615-620 Transl. by SCITRAN, Inc., Santa Barbara, Calif. Original document prepared by Research Inst. of Inorganic Chemistry, CSAV, Prague, Czechoslovakia
(Contract NASw-4703)
(NASA-TT-20185; NAS 1.77:20185) Avail: NTIS HC A03/MF A01 CSCL 11G

Published data and experiments were used to provide alternatives and recommendations for suitable equipment in the production of powdered sodium hydride with large specific surface. From the data concerning the effects of the quantity of carbon monoxide, which is a precursor of catalysts, on the reaction rate, rate constants, specific surface and the resultant purity of sodium hydride, it appears that the magnitude and specific surface increases with increasing quantities of precursor of catalyst, but there is a concomitant build up of impurities and the rate constant of the reaction decreases. The rate constant increases by increasing temperature and pressure. The appropriate reaction conditions, production procedures and equipment will be determined by the requirements for product purity, magnitude of specific surface and rate of reaction. Such decisions will be necessary for working with sodium and hydrogen at elevated temperatures and pressures. Author

N88-26463# Solar Turbines International, San Diego, Calif.
DEVELOPMENT OF PROTECTIVE COATINGS FOR CERAMIC TUBULAR COMPONENTS Topical Report, Mar. 1986 - Dec. 1987
M. vanRoode and J. R. Price Dec. 1987 101 p
(Contract GRI-5086-232-1233)
(PB88-197165; SR87-R-5334-12; GRI-88/0005) Avail: NTIS HC A06/MF A01 CSCL 11B

Process technology was developed for the deposition of adherent ceramic oxide coatings on silicon based substrates for corrosion protection of ceramic heat exchanger tube operating in aluminum remelters. Single and multilayer coatings of mullite, zircon, alumina, yttria and yttria stabilized zirconia remained adherent and intact after isothermal heat treatment at 1093 C/120 hrs followed by cyclic heat treatment between 1010 and 371 C (60 one hr cycles). Ten optimized coating compositions were deposited on alpha-SiC and SCRB-210 tubes for environmental exposure testing in a simulated aluminum remelt environment. An aluminum reclamation simulator was designed, constructed, and installed under the program. A computer simulation study was undertaken to characterize the gas phase chemistry in the aluminum remelt environment and to predict the nature of the corrosion products at the silicon based tube surfaces. Mechanical properties of coated and uncoated tube specimens were determined. Author

N88-26464*# North Carolina State Univ., Raleigh. Dept. of Textile Chemistry.
THE CRYSTALLIZATION OF TOUGH THERMOPLASTIC RESINS IN THE PRESENCE OF CARBON FIBERS Technical Report, year endings 31 Dec. 1986
Michael H. Theil [1988] 120 p
(Grant NAG1-525)
(NASA-CR-182984; NAS 1.26:182984) Avail: NTIS HC A06/MF A01 CSCL 11C

The presence of carbon fibers increased the crystallization rates of both PEEK and PPS thermoplastic polymers. The effect was most pronounced at higher crystallization temperatures. Isothermal crystallization rates were analyzed by applying classical phenomenological nucleation theory. Unusually high values of the so-called Avrami exponent were found for neat PEEK. Isothermal crystallization of PEEK and PPS polymers produced crystalline samples having a wide variety of melting temperatures. The melting as observed by differential scanning calorimetry occurred as dual endotherms which were called primary (higher temperature) and secondary melting peaks. Each primary peak accounted for most of the crystallinity present. The secondary peaks represented the melting of crystallites formed later than those attributable to the primary endotherms. The presence of carbon fibers increased the thermal stability of both PEEK and PPS crystallites as manifested by higher temperatures for the primary melting peaks. This may be attributable to increased crystallite size, greater crystallite perfection, and/or favorable modification of the crystallite interface. Over the range studied, crystallization temperature strongly influenced the positions of the secondary peaks but not the primary peaks. Author

N88-26465# Sandia National Labs., Albuquerque, N. Mex.
ELECTROPHORETIC COATINGS. PART 1: SANDIA APPLICATIONS
D. J. Sharp and J. K. G. Panitz 1988 15 p Presented at the AT and T Task Group 5 Meeting, Albuquerque, N. Mex., 22 Mar. 1988

(Contract DE-AC04-76DP-00789)
(DE88-008666; SAND-88-0318C; CONF-880383-1) Avail: NTIS HC A03/MF A01

Electrophoretic (electrocoating) technology provides capabilities for deposition of a broad range of dielectric materials. Many modern electrophoretic coating resins are designed to deposit at the anode. The resins are commonly synthesized by maleinizing the organic backbone to introduce carboxylate groups (RCOO(sup -)). These materials may then be electrochemically deposited as colloidal species suspended in a liquid. Colloidal particles which do not normally deposit electrophoretially by themselves may be adsorbed onto polymers or other electrophoretically active charged species, i.e., ionic detergents, thereby providing a vehicle for transport and deposition. With the proper choice of these intermediaries which may be either allowed to remain in the deposit or removed by oxidative firing, etc., a broad range of materials become coating candidates. We also report on variations in electrocoating technology which permit deposition of composite high thermal conductivity dielectric coatings for photovoltaic concentrator arrays, adhesive-dielectric coatings, aluminum oxidestyrene-acrylate dielectric films for acapcitor applications, submicron-thick, free-standing, polymer films, fluorocarbon binder tribological coatings, and radiation hardening coatings. DOE

N88-26466# National Bureau of Standards, Boulder, Colo. Chemical Engineering Science Div.
THERMAL CONDUCTIVITY OF SELECTED FOAMS AND SYSTEMS FROM 100 TO 300 K Final Report, May - Jul. 1986
L. L. Sparks, W. P. Dube, and A. J. Slifka Jan. 1988 56 p
(PB88-201553; NBSIR-88/3086) Avail: NTIS HC A04/MF A01 CSCL 11C

The apparent thermal conductivity of five insulating materials was determined in the nominal temperature range from 100 to 300 K (-280 to 80 F). A guarded-hot-plate apparatus was used and the testing environment was dry nitrogen gas at near ambient pressure. One specimen was retested in a vacuum environment. Three of the specimens were neat ploymethacrylimide (PMA) foams with nominal densities of 51 and 71 kg/cu m (3.2 and 4.4 lb/cu ft.). Other specimens tested were a polyurethane foam sprayed on an aluminum substrate and a sandwich construction specimen utilizing PMA foam of normal density 110 kg/cu m (6.9 lb/cu ft). The results in nitrogen gas show the expected conductivity increase with increasing density. The observed conductivity of 0.67 Pa (5 micrometers of Hg) is significantly lower than that in ambient-pressure nitrogen gas. The large relative difference may ne due to increased thermal resistance at the plate-specimen boundaries. GRA

N88-26467# Sandia National Labs., Albuquerque, N. Mex.
THE EFFECTS OF HERTZIAN STRESS AND TEST AMBIENT ON THE FRICTION COEFFICIENT OF MsS2 COATINGS
L. E. Pope and J. K. G. Panitz 1988 15 p Presented at the 15th International Conference on Metallurgical Coatings, San Diego, Calif., 11 Apr. 1988
(Contract DE-AC04-76DP-00789)
(DE88-008118; SAND-87-2588C; CONF-880488-1) Avail: NTIS HC A03/MF A01

Rf sputter deposited MoS2 coatings on 304 stainless steel substrates have been evaluated for different deposition and different storage conditions. For air testing, the friction coefficient of all of the MoS2 coatings decreased with increasing Hertzian stress up to an intermediate stress and was constant for still higher stresses. A lower friction coefficient occurred for samples stored in the lower relative humidity ambient. The constant friction coefficient with increasing stress regime initiated at a lower Hertzian stress for 2 percent relative humidity storage. The MoS2 films were predominantly crystalline; however, a small amount of amorphous material was present. The coatings with the larger amount of amorphous material had the larger friction coefficient. Testing in ultrahigh vacuum lowered the friction coefficient relative to testing in air for both relative humidities, but this testing did not recover all of the increase in friction coefficient for air testing that was attributed to high humidity storage. The coatings had all orientations, but the basal planes were predominantly perpendicular to the substrate surface. The sulfur to molybdenum ratio did not decrease significantly with high humidity storage, although the crystallographic orientation of the films were similar. Hence, these results indicate that factors in addition to orientation affect the oxidation of MoS2 films. DOE

N88-26468# Tennessee Univ., Knoxville.
DUAL MECHANISM BIFUNCTIONAL POLYMERS: DESIGN, SYNTHESIS AND APPLICATION OF A NEW CATEGORY OF METAL ION COMPLEXING AGENTS Progress Report, 1 Aug. 1987 - 31 Jul. 1988
S. D. Alexandratos Apr. 1988 10 p
(Contract DE-FG05-86ER-13591)
(DE88-008233; DOE/ER-13591/2) Avail: NTIS HC A02/MF A01

Ionic recognition between a polymer and an ion can yield a highly specific separation agent for the recovery of target ions in dilute solutions. Reactive polymers named dual mechanism bifunctional polymers consist of polymers which interact with ions via two different mechanisms through two different groups. Research during the current period has focused on metal ion studies with the Class 2 phosphonic acid/phosphonate ester resins, the development of a new Class 2 resin involving pseudocrown ether moieties, and introduction of the Class 3 ion exchange/precipitation resins. DOE

N88-26469# Oak Ridge National Lab., Tenn.
APPLICATION OF ELECTRON MICROSCOPY FOR THE ANALYSIS OF THE MECHANICAL BEHAVIOR OF ADVANCED CERAMICS
V. J. Tennery, L. F. Allard, T. A. Nolan, and M. H. Rawlins 1988 8 p Presented at the 33rd International Gas Turbine Conference and Exhibit, Amsterdam, Netherlands, 5 Jun. 1988
(Contract DE-AC05-84OR-21400)
(DE88-005049; CONF-880607-1) Avail: NTIS HC A02

The microstructure and fracture surfaces of two commercially available silicon nitride ceramics have been characterized using techniques of scanning and analytical transmission electron microscopy. These results have been correlated to mechanical property data (obtained from static and dynamic fatigue tests using four-point flexural test methods both at room temperature and at elevated temperature). For one of the materials, the results clarified failure mechanisms. For the other, the results showed how processing variables can affect microstructure (and thus mechanical behavior), and emphasized particularly that mechanical tests of billet-derived specimens may be unreliable in predicting the mechanical behavior of production components. DOE

N88-26470# Oak Ridge National Lab., Tenn.
A STUDY OF SOLVENT EFFECTS ON THE SYNTHESIS OF PURE COMPONENT AND COMPOSITE CERAMIC POWDERS BY METAL ALKOXIDE HYDROLYSIS
M. T. Harris, C. H. Byers, and R. R. Brunson 1988 8 p Presented at the Spring Meeting of the Materials Research Society, Reno, Nev., 4 Apr. 1988
(Contract DE-AC05-84OR-21400)
(DE88-008381; CONF-880408-9; CONF-880408) Avail: NTIS HC A02/MF A01

The production of ceramics having high density, low porosity, and fine grains requires the use of high-purity metal oxide powders that consist of particles of uniform shape, size, and composition. Metal Alkoxide hydrolysis is an attractive method for the synthesis of high-purity metal oxide particles. The nature of the precipitate formed is affected by the solvent. This present study investigates the growth kinetics and characteristics of metal oxide particles (i.e., ZrO2 and TiO2) that are produced in various alcohol solvents (ethanol, 1-butanol, 2-butanol, and tert-butyl alcohol). Results are also presented for the synthesis of uniform homogeneous composite metal oxide particles (i.e., Y2O3-ZrO2 and ZrO2-TiO2) by low-temperature metal alkoxide hydrolysis. DOE

N88-26471# Washington Univ., Seattle. Dept. of Chemistry.
FUNDAMENTAL STUDIES OF ELASTOMERS Annual Report, 16 Feb. 1987 - 15 Mar. 1988
B. E. Eichinger 15 Mar. 1988 16 p
(Contract DE-FG06-84ER-45123)
(DE88-009679; DOE/ER-45123/4) Avail: NTIS HC A03/MF A01

This progress report describes work in the three areas of (1) computer simulation, (2) theory of the shape distribution of polymer chains, and (3) synthetic projects on elastomers. Areas of study include: the influence of chain scission on the radiation cure of polyethylene; crosslinking in urethane formation; calculations on spherical distributions for linear and circular chains; gel synthesis; derivitization of commercial elastomers to incorporate acetyl-acetone; synthesis of polysilylenes; polymerization of a strained bicyclic olefin. DOE

N88-26472# Argonne National Lab., Ill.
OBSERVATIONS ON RESIDUAL STRESSES IN CERAMIC COMPOSITES BY NEUTRON DIFFRACTION TECHNIQUES
S. Majumdar, D. S. Kupperman, and J. P. Singh Feb. 1988 32 p Presented at the 12th Annual Conference on Composites and Advanced Ceramic Materials, Cocoa Beach, Fla., 20 Jan. 1988
(Contract W-31-109-eng-38)
(DE88-009937; CONF-880118-8; CONF-880118) Avail: NTIS HC A03/MF A01

This paper presents a comparison between the residual thermal stresses and strains, developed during cooling of a ceramic-ceramic (SiC--Al2O3) composite, determined by analytical methods and by an experimental neutron diffraction technique. Because the coefficient of thermal contraction of the matrix (Al2O3) is greater than that of the residual stresses were determined by using two self-consistent models. In the first, a plane strain composite cylinder model, the fibers are approximated as infinitely long circular cylinders. In the second, due to Eshelby, the fibers are approximated as ellipsoids (specialized to prolate spheroids in this case). The two models give almost identical estimates of the stresses and strains in the fibers. The interpretation of the measured strains in the fibers by neutron scattering has some uncertainty because of the lack of a clearly defined crystal structure of SiC. However, in general, the measured and calculated strains are reasonably close. DOE

N88-26473# Illinois Univ., Chicago. Dept. of Radiology.
APPLICATION OF MAGNIFICATION XERORADIOGRAPHY TO ADVANCED CERAMICS
R. J. Kriz and W. A. Ellingson (Argonne National Lab., Ill.) Feb. 1988 19 p Presented at the 12th Annual Conference on Composites and Advanced Ceramic Materials, Cocoa Beach, Fla., 20 Jan. 1988 Prepared in cooperation with Argonne National Lab., IL.
(Contract W-31109-eng-38)
(DE88-009965; CONF-880118-6; CONF-880118) Avail: NTIS HC A03/MF A01

Low-density inclusions and voids in ceramics present a detection problem to X-ray imaging because of the relatively low contrast in the resulting image. An X-ray imaging technique called xeroradiography has been in use for medical applications for detecting calcifications (low-density inclusions) in breast tissue. The method has a built-in edge enhancement. We have applied this technique to green and densified Si3N4 specimens and have shown initial improvements over other X-ray methods in detection of seeded defects. DOE

N88-26474# Massachusetts General Hospital, Boston. Radiology Dept.
DETERMINATION OF BINDER DISTRIBUTIONS IN GREEN-STATE CERAMICS BY NMR IMAGING
L. Garrido, J. L. Ackerman, W. A. Ellingson, and J. D. Weyand Mar. 1988 16 p Presented at the 12th Annual Conference on Composites and Advanced Ceramic Materials, Cocoa Beach, Fla., 20 Jan. 1988 Prepared in cooperation with Argonne National Lab., Ill; Aluminum Co. of America, Alcoa Center, Pa.
(Contract W-31109-eng-38)
(DE88-009990; CONF-880118-7) Avail: NTIS HC A03/MF A01

The manufacture of reliable high performance structural ceramics requires a good understanding of the different steps involved in the process. The presence of nonuniformities in the distribution of the polymeric binder could give rise to local fluctuations of density that could produce failure of the ceramic piece. Specimens prepared from Al2O3 with 15 and 2.5 percent w/w binder were imaged using NMR in order to measure binder distribution maps. Results show that NMR imaging could be a useful technique to nondestructively evaluate the quality of green-state specimens. DOE

N88-26475# Argonne National Lab., Ill.
THE OUTLOOK FOR CERAMICS IN HEAT ENGINES, 1990-2010: RESULTS OF A WORLDWIDE DELPHI SURVEY
R. P. Larsen and A. D. Vyas 1988 24 p Presented at the Worldwide Perspective on the Status of Ceramics for Heat Engines, Detroit, Mich., 29 Feb. 1988
(Contract W-31109-eng-38)
(DE88-010075; CONF-880279-1) Avail: NTIS HC A03/MF A01

A study is described that was conducted to provide a realistic technical and economic assessment of the use of advanced ceramic materials technology for heat engines in transportation applications. Key results from a worldwide Delphi survey are presented on the expected timing and rate of market development for ceramic engine components and engines. These results show that, by the mid 1990s, a substantial number of ceramic engine components will be in production and ceramic-intensive engines will be introduced. Also presented in the study are benefits and barriers to the use of ceramic technology in heat engines and other relevant factors influencing its rate of adoption. A modeling approach is presented that uses the survey data to produce a series of market penetration curves for individual ceramic engine components for light- and heavy-duty applications under different scenarios. Finally, the conditions required for rapid market development of ceramic technology for heat engines are discussed. DOE

N88-26476# Florida Univ., Gainesville.
SYNTHESIS OF MODEL POLYMERS AND RELATED STRUCTURES IN SUPPORT OF VINYL MONOMER GRAFTING STUDIES Progress Report, 1 Jul. 1987 - 30 Jun. 1988
T. E. Hogen-Esch and G. B. Butler 1988 9 p
(Contract DE-FG05-84ER-45104)
(DE88-010245; DOE/ER-45104/3) Avail: NTIS HC A02/MF A01

Objectives of the present program include the synthesis, structural characterization and properties of cellulose-based water-soluble graft copolymers and other copolymers capable of effectively enhancing the viscosity of their aqueous solutions. In support of this program we plan the synthesis of a number of water-soluble well defined block- or star block colopymers capable of effectively viscosifying their solutions through reversible crosslinking. In order to understand the effects on the rheology of branching or cyclization in the above systems, we also plan the synthesis of water-soluble cyclic- and star polymers. DOE

N88-26477# Tennessee Univ., Knoxville. Dept. of Chemistry.
STATISTICAL MECHANICS OF POLYMER SYSTEMS Annual Report
J. Kovac 1 May 1988 11 p
(Contract DE-FG05-84ER-45114)
(DE88-011172; DOE/ER-45114/5) Avail: NTIS HC A03/MF A01

This project involves two different, but complementary, efforts. The first is the development and application of dynamic Monte Carlo computer simulation techniques for the study of polymer dynamics. The second is the study of equilibrium and nonequilibrium aspects of the glass transition. Progress has been made in both areas during the previous year. DOE

N88-26478# Argonne National Lab., Ill.
CHARACTERIZATION OF COATING WEAR PHENOMENA IN NITRIDE AND CARBIDE COATED TOOL INSERTS
G. R. Fenske, N. Kaufherr, R. H. Lee, B. M. Kramer, R. F. Bunshah, and W. D. Sproul (Northwestern Univ., Evanston, Ill.) 1988 14 p Presented at the 15th International Conference on Metallurgical Coatings, San Diego, Calif., 11 Apr. 1988
(Contract W-31109-eng-38)
(DE88-011196; CONF-880488-5; CONF-880488) Avail: NTIS HC A03

Hard nitride- and carbide- coatings of Ti, Zr, and Hf were deposited on T-15 cutting tool inserts using high-rate reactive sputtering (HRRS) and Activated Reactive Evaporation (ARE) processes. The coated inserts were subjected to a series of metal cutting tests to evaluate their performance and to compare their relative ranking with wear model predictions. The cutting tests indicated the coated inserts outperformed uncoated inserts. However, their ranking based on measured lifetime (to reach a 0.003 in. crater depth) did not agree with predicted wear model predictions. Subsequently, a series of short-term cutting tests were initiated to study the wear behavior of the coatings during the early stages of the wear process when the coating was still intact. Post-test examination of the inserts suggest that the predominant wear mechanism was not due to abrasion or thermochemical dissolution as predicted by the model, but was a result of substrate softening followed by microfracture of the coating. The substrate softening is attributed to the severe cutting conditions (325 sfpm under dry cutting conditions) used in the cutting tests. DOE

N88-26479# Oak Ridge National Lab., Tenn.
FACTORS INFLUENCING THE TOUGHENING BEHAVIOR OF WHISKER REINFORCED CERAMICS
P. F. Becher, Chung-Hway Hsueh, P. Angelini, and T. N. Tiegs 1988 9 p Presented at the International Conference on Whisker- and Fiber-toughened Ceramics, Oak Ridge, Tenn., 7 Jun. 1988
(Contract DE-AC05-84OR-21400)
(DE88-011396; CONF-8806103-1) Avail: NTIS HC A02/MF A01

Whisker reinforced ceramics exhibit substantial improvements in fracture toughness and other mechanical properties as compared to the unreinforced ceramics. In many of the whisker reinforced ceramics, enhanced toughness is derived from bridging of the crack by the strong whiskers. An analysis of the whisker bridging contribution reveals that the toughness is a function of the whisker strength, radius, and volume content, the ratio of the Young's modulus of the composite to that of the whisker, and the ratio of the fracture energy of the matrix to that of the whisker-matrix interface. Recent studies show that the analysis based on whisker bridging quantitatively describes the experimentally observed toughening that results from whisker reinforcement. DOE

N88-26480# Rockwell International Corp., Thousand Oaks, Calif. Science Center.
THE EFFECTS OF THIN COMPRESSIVE FILMS ON INDENTATION FRACTURE TOUGHNESS MEASUREMENTS
P. H. Kobrin and A. B. Harker 1988 17 p
(Contract N00014-85-C-0140)
(AD-A192243) Avail: NTIS HC A03/MF A01 CSCL 11C

Thin compressive films have been shown to decrease the lengths of radial cracks produced by a Vickers indentation in a variety of nonmetallic materials. The intrinsic stress of submicron thick films deposited by reactive ion beam sputtering was measured by a cantilever technique. The change in the apparent identation fracture toughness of the coated material was correlated with film thickness and stress, identation load, and the nature of the substrate. GRA

N88-26481*# National Aeronautics and Space Administration. Langley Research Center, Hampton, Va.
INITIAL ADHESIVE SCREENING OF NOVEL POLYAMIDE-IMIDES AND THEIR COPOLYMERS
Donald J. Progar and James F. Dezern Aug. 1988 21 p
(NASA-TM-100641; NAS 1.15:100641) Avail: NTIS HC A03/MF A01 CSCL 11C

Continued interest by the research community in thermally stable, tough, high temperature adhesives has resulted in the investigation by Langley Research Center of two linear aromatic polyamide-imide (PAI) homopolymers and two linear aromatic PAI copolymers. The homopolymers were made with either 3,3'=DABA or 4,4'-DABA and BTDA. The two polymers were prepared with a monomer ratio of 0.75 DABP:0.25 DABA:1.00 BTDA. These aromatic PAIs possess high thermal stability because of intermolecular hydrogen bonding and chain stiffness. Lap shear strength (LSS) was the main criteria used to evaluate the polymers as adhesives. LSS of bonded Ti-6Al-4V was determined at room temperature (RT), 177, 204 and 232 C. The glass transition temperature and the type of bond failure were also determined. The best LSS values of the four adhesive systems investigated were obtained with the PAI copolymer identified in the report as LARC-TPI (25 percent 3,3'-DABA); however, it did not produce LSSs nearly as high as LARC-TPI. The poor flow properties observed appear to be due to a combination of high molecular weight and the increased interchain electronic interactions associated with the amide group. Author

N88-26482*# National Aeronautics and Space Administration. Lewis Research Center, Cleveland, Ohio.
FRACTURE RESISTANCE OF A TiB2 PARTICLE/SiC MATRIX COMPOSITE AT ELEVATED TEMPERATURE
Michael G. Jenkins, Jonathan A. Salem, and Srinivasa G. Seshadri Jun. 1988 18 p
(NASA-TM-100967; E-3842-1; NAS 1.15:100967) Avail: NTIS HC A03/MF A01 CSCL 11C

The fracture resistance of a comercial TiB2 particle/SiC matrix composite was evaluated at temperatures ranging from 20 to 1400 C. A laser interferometric strain gauge (LISG) was used to continuously monitor the crack mouth opening displacement (CMOD) of the chevron-notched and straight-notched, three-point bend specimens used. Crack growth resistance curves (R-curves) were determined from the load versus displacement curves and displacement calibrations. Fracture toughness, work-of-fracture, and R-curve levels were found to decrease with increasing temperature. Microstructure, fracture surface, and oxidation coat were examined to explain the fracture behavior. Author

N88-26483*# National Aeronautics and Space Administration, Washington, D.C.
REFRACTORY MATERIALS OF ZIRCONATE. PART 2: SYNTHESIS AND SOME PROPERTIES OF STRONTIUM, ZIRCONATE, CALCIUM ZIRCONATE AND BARIUM ZIRCONATE
Tsutomo Okubo, Osamu Yonemochi, Kazuo Nakamura, and Minoru Maeda Jun. 1988 17 p Transl. into ENGLISH from Nagoya Kogyo Gijutsu Shikensho Hohoku (Japan), v. 24, no. 10, 1975 p 271-277 Transl. by SCITRAN, Inc., Santa Barbara, Calif.
(Contract NASw-4307)
(NASA-TT-20186; NAS 1.77:20186) Avail: NTIS HC A03/MF A01 CSCL 11C

Chemical compounds SrZrO3, CaZrO3, and BaZrO3 were synthesized by solid reaction and arc fusion, and their properties examined. Results were as follows: (1) in the synthesis of CaZrO3 by solid reaction, ZrO2 solid solution with cubic form was produced, which then changed into CaZrO3; (2) the BaZrO3 was a cubic form and did not show any transformation, while SrZrO3 and CaZrO3 with an orthorhombic form transformed to a cubic form at high temperature; and (3) the solubility of BaZrO3 in acid and its vaporization rate at a high temperature were greater than those of zirconates. Author

N88-26484*# National Aeronautics and Space Administration, Washington, D.C.
RESISTANCE OF POLYAMIDE-6 AGAINST LONG TIME EFFECTS OF VARIOUS MEDIA AT VARIOUS TEMPERATURES
W. Debski and M. Przylecka Aug. 1988 15 p Transl. into ENGLISH from Bestandigkeit von Polyamid-6 Gegen Langzeitige

Einwirkung Verschiedener Medien bei Verschiedenen Temperaturen, (Poznan, Poland) Plaste und Kautschuk, V. 21, no. 11, Nov. 1974 p 828-833 Presented at the High Polymers Meeting, Karl Marx Stadt (German Democratic Republic), 10-12 Sep. 1973 Transl. by SCITRAN, Inc., Santa Barbara, Calif. Original document was prepared by Research and Development Center for Plastic Working Plaso-Proplast, Poznan, Poland
(Contract NASw-4307)
(NASA-TT-20297; NAS 1.77:20297) Avail: NTIS HC A03/MF A01 CSCL 11C

During the first phase of tempering of polyamide-6, there are temporary changes which are apparently related to the lamella structure of the material. Test specimens at high temperature show that the mechanical properties of polyamide-6 are changed permanently, and mostly at 80 C. From the results of density tests and X-ray analysis, it follows that these changes depend on environmental influences and differ in gaseous and liquid media. The results of the test specimens of the mechanical properties as a function of temperature and the medium give information about the practical applications of polyamide-6. Author

N88-26485# Fraunhofer Inst. fuer Werkstoffmechanik, Freiburg (West Germany).
IRREVERSIBLE DEFORMATIONS DURING FRACTURE IN POLYMERS Final Report [IRREVERSIBLE DEFORMATIONEN IN POLYMEREN BEIM BRUCHVORGANG]
L. Koenczoel Jun. 1986 10 p In GERMAN
(Contract DFG-Ko/883/1-1)
(W-7/86; ETN-88-92100) Avail: NTIS HC A02/MF A01

Theoretical and experimental studies on the accumulation of damage by crack propagation in polymers are presented. The application of the crack layer theory to fatigue crack propagation in polymethyl methacrylate is valid for the description of energy related effects of fatigue crack propagation in thermoplastics submitted to multiple crazing and large deformations. Deformations and crack growth in thermoplastics can be examined by acoustic emission especially in the case of short glass fiber reinforced polyvinylchloride, polystyrol, and during the crystallization of polymers. Failure phenomena are revealed by density and intensity modifications of the acoustic emission. ESA

N88-26486# Societe Europeenne de Propulsion, Bordeaux (France). Div. Propulsion a Poudre et Composites.
HIGH TEMPERATURE RESINS FOR INJECTION. HIGH TEMPERATURE PRE-IMPREGNATED Final Report [RESINES HAUTE TEMPERATURE POUR INJECTION. PREIMPREGNES HAUTE TEMPERATURE]
P. Taveau and J. A. Moreau 13 Nov. 1986 100 p In FRENCH
(Contract DRET-84-439)
(RC-648676; ETN-88-92155) Avail: NTIS HC A05/MF A01

The injection of liquid resins on dry carbon fiber structures is studied, testing 14 commercial resins of epoxy maleic-imide and PSP types. Only seven were accepted for further hot aging tests. Pre-impregnated structures were also studied. After 2000 hr at 200 C the order of conservation of properties is polyimide-epoxy-PSP. ESA

N88-26487# Centre d'Etudes et de Recherches, Toulouse (France). Dept. d'Etudes et de Recherches en Micro-Ondes.
POLYMERIZATION OF EPOXY MATRIX COMPOSITES USING PULSED MICROWAVES Final Report [POLYMERISATION PAR ENERGIE MICRO-ONDE EN REGIME IMPULSIONNEL DE COMPOSITES A MATRIX EPOXY]
Henri Jullien, Michel Delmotte, Francois-Marie Thuillier, Henri Valot, D. Boulonnais, D. Sailleau (Institut National de Recherche Chemique Applique, Paris, France), Alain Priou, and Serge Aussudre Dec. 1986 167 p In FRENCH
(Contract DRET-85-002)
(CERT-3/1324-MO; ETN-88-92162) Avail: NTIS HC A08/MF A01

The effect of pulsed microwave polymerization on the chemical reaction of epoxy matrix composites and resulting mechanical properties is investigated. A form factor of 5 at a frequency of 2450 MHz was employed. The measurement techniques include infrared spectrometry and fluorescence thermometry. The generation of an intermediate specific chemical species is supposed, though it is not identified. The resulting composite materials show an increase of mechanical characteristics of 10 percent with total polymerization cycle. ESA

N88-26488# Pau Univ. (France). Lab. de Chimie Organique Physique.
STRUCTURAL STUDY OF IMPREGNATING RESINS OF TGMDA/DDS TYPE [ETUDE STRUCTURALE DES RESINES D'IMPREGNATION DU TYPE TGMDA/DDS]
M. F. Grenier-Loustalot and P. Grenier 1987 153 p In FRENCH
(Contract DRET-85-34-355-00470501)
(ETN-88-92167) Avail: NTIS HC A08/MF A01

The molten amine-epoxy system reactions and kinetics are studied. The analytical methods include quantitative chemical analysis, infrared absorption spectroscopy, high resolution nuclear magnetic resonance, and microcalorimetry. It is shown that the reactivity of the N-(epoxy)2 group with aromatic amines is controlled by the presence of impurities and by the introduction of a methyl group in the ortho position of the benzene cycle. The presence of prepolymers partially epoxydized and including chlorine and secondary amines groups is demonstrated. ESA

N88-26489# Oak Ridge National Lab., Tenn.
CERAMIC TECHNOLOGY FOR ADVANCED HEAT ENGINES PROGRAM DATA BASE Summary Report
M. K. Booker 1988 94 p
(Contract DE-AC05-84OR-21400)
(DE88-008954; ORNL/M-462) Avail: NTIS HC A05/MF A01

A large amount and wide variety of data on the behavior of advanced ceramic materials is currently being generated within the Ceramic Technology for Advanced Heat Engines Program. This paper summarizes efforts to date to develop a computer data base system for the management of those data. The system is based on the use of desktop microcomputers, which provides a maximum of efficiency, economy, and convenience in the operation of the system. DOE

28 PROPELLANTS AND FUELS

Includes rocket propellants, igniters, and oxidizers; their storage and handling procedures; and aircraft fuels.

For related information see also *07 Aircraft Propulsion and Power, 20 Spacecraft Propulsion and Power,* and *44 Energy Production and Conversion.*

N88-26490# Materials Research Labs., Melbourne (Australia).
GRANULATION OF PYROTECHNIC TRACER COMPOSITION R284T
M. A. Wilson Mar. 1988 16 p
(MRL-TN-528; AR-005-208) Avail: NTIS HC A03/MF A01

Materials Research Laboratory has developed a method to improve the handling characteristics of the pyrotechnic tracer composition R248T made at Explosives Factory Maribyrnong (EFM). The modification was required to enable the automatic loading, at Ammunition Factory, Footscray (AFF), of 7.62 mm tracer bullets for Army. Previous attempts to improve the physical properties of the composition by the addition of a small percentage of flow modifier had proved unsuccessful. MRL investigated a number of alternative methods using granulation techniques to improve the flow properties of this batch. This technical note describes these methods, and the assistance given to EFM to further develop the most appropriate process for the manufacture of this tracer composition. Author

N88-26491# Los Alamos National Lab., N. Mex.
NUMERICAL MODELING OF THE EFFECT OF PARTICLE SIZE OF EXPLOSIVES ON SHOCK INITIATION PROPERTIES

C. L. Mader and J. D. Kershner Mar. 1988 22 p
(Contract W-7405-eng-36)
(DE88-010479; LA-11239-MS) Avail: NTIS HC A03/MF A01

The three-dimensional Eulerian reactive hydrodynamic code 3DE has been used to investigate the effects of particle size and the resulting void or hole size on the shock initiation of heterogeneous explosive charges of TNT. Shocks interacting with TNT containing various hole sizes have been modeled. The void fraction was held at 0.5 percent while the spherical hole sizes were varied from 0.5- to 0.0005-mm radius, and the TNT was shocked to 12.5 GPa. As the hole size was varied from 0.5 to 0.05 mm, the explosive became more sensitive to shock as the hole size decreased, and the number of hot spots increased. When the hole size was decreased to 0.0005 mm, a 12.5-GPa shock wave failed to build toward propagating detonation because the resulting hot spots were cooled by side rarefactions before appreciable decomposition occurred. At the same density, the most shock-sensitive explosive will be that with particle sizes between coarse and extremely fine material. DOE

N88-26492# North Dakota Univ., Grand Forks. School of Engineering and Mines.
FEASIBILITY OF PRODUCING JET FUEL FROM GPGP (GREAT PLAINS GASIFICATION PLANT) BY-PRODUCTS Quarterly Report, 17 Aug. - 16 Nov. 1987
W. G. Willson, C. L. Knudson, and J. R. Rindt 1987 48 p
(Contract DE-AC22-87PC-90016)
(DE88-010233; DOE/PC-90016/T2) Avail: NTIS HC A04/MF A01

The technical and economic feasibility of producing aviation turbine fuel from by-product streams of the Great Plains Gasification Plant (GPGP) in Beulah, ND, is assessed. A secondary goal of the project is to assess the conversion of the by-product streams into a new, higher-density aviation fuel. GPGP currently produces 150 MM SCFD of synthetic natural gas from 16,000 tpd of North Dakota lignite. In addition the plant generates three liquid hydrocarbon streams : 730 barrels per day (BPD) naphtha, 880 BPD phenols, and 3200 BPD tar/oil. Work at the University of North Dakota Energy and Mineral Research Center has focused on two tasks performed in support of these objectives. The first task consisted of a detailed analysis of the by-product streams under consideration. Of the three streams, the tar oil stream is the largest and shows the most promise for upgrading to aviation turbine fuel. Detailed characterization data on the tar/oil were presented in the previous quarterly. A true boiling point (TBP) distillation was performed on the GPGP phenol stream, yielding nine fractions which were characterized using NMR, GC, and GC/MS. The second task involves an engineering evaluation of by-product upgrading. Two methods are under investigation for the production of aviation fuel: single-stage, in which heteroatom removal and hydrogenation are accomplished in a single step, and two-stage, in which the heteroatoms are removed in the first-stage, and hydrogenation occurs during the second stage. Hydrogenation was improved by increased pressure and temperature, although the measured effect on aromatic content awaits further analyses. Data indicates that, to achieve complete nitrogen and sulfur removal, the preferred operating conditions are temperatures of 610 to 645 F and pressures of at least 2000 psig. DOE

N88-26493# Naval Civil Engineering Lab., Port Hueneme, Calif.
BIODEGRADATION OF JP-5 AVIATION FUEL BY SUBSURFACE MICROBIAL COMMUNITIES Progress Report, 1 Jan. - 15 Mar. 1987
Charles M. Swindoll 1988 17 p
(AD-A192743) Avail: NTIS HC A03/MF A01 CSCL 21D

Leakage of the aviation fuels JP-5, JP-4 and AVGAS from storage tanks has resulted in a severe environmental insult to a Naval fuel farm and adjacent areas. As part of the reclamation effort, the indigenous microorganisms are being characterized. This information will be used to optimize the bioreclamation of the site. Approximately 60 aerobic microorganisms, including more than 40 bacteria, 6 actinomycetes and 10 fungi have been isolated from soil contaminated with aviation fuels and adjacent noncontaminated soil. All isolated bacteria were able to grow on JP-5 as their sole carbon source. Most of the bacteria from the contaminated sites were small, gram negative rods, while most bacteria from the noncontaminated site were gram positive rods. All of these microorganisms would be expected to contribute to the bioremediation of the contaminated site. GRA

N88-26494# Fluorochem, Inc., Azusa, Calif.
RESEARCH IN ENERGETIC COMPOUNDS Final Report, 1 Jan. 1978 - 31 Dec. 1987
T. A. Archibald, L. C. Garver, A. A. Malik, F. O. Bonsu, and D. D. Tzeng 9 Feb. 1988 79 p
(Contract N00014-78-C-0147)
(AD-A192953; ONR-2-10) Avail: NTIS HC A05/MF A01 CSCL 07C

Alternate routes to 1,1,3,3-tetranitrocyclobutane were investigated. Attempts to nitrate or dephenylate 1,3-dinitro-2,4-diphenylcylobutane were unsuccessful. Ethyl 1,3-dinitrocyclobutane-1-carboxylate, obtained from ethyl bicyclo(1.1.0)butane-1-carboxylate and dinitrogen tetroxide, was treated with silver nitrate, sodium nitrite and base to give 1,1,3,3-tetra-nitrocyclobutane in 10 to 22 percent yield. 3,3-Dinitrocyclobutanecarboxylic acid, obtained via ethyl 3-oxocyclobutane-1-carboxylate oxime, was subjected to a Curtius reaction, conversion of the isocyanate to the amine, and oxidation to give, 1,1,3-trinitrocyclobutane. This compound decomposed under oxidative nitration conditions. Attempts to oxidize 3,3-dinitrocyclobutanol, obtained from the amine, were unsuccessful. 3,3-Dinitrocyclobutane-1,1-dicarboxylic acid was prepared from diethyl 3-oxocyclobutane-1,1-dicarboxylate. GRA

N88-26495*# Jet Propulsion Lab., California Inst. of Tech., Pasadena.
ANTIMISTING KEROSENE: LOW TEMPERATURE DEGRADATION AND BLENDING Final Report, Jun. 1983 - Aug. 1985
A. Yavrouian, P. Parikh, and V. Sarohia Jun. 1988 57 p
(Contracts NAS7-100; DTFA03-80-A-00215)
(NASA-CR-182725; JPL-Pub-D-5518; NAS 1.26:182725; DOT/FAA/CT-86/3) Avail: NTIS HC A04/MF A01 CSCL 21D

The inline filtration characteristics of freshly blended and degraded antimisting fuels (AMK) at low temperature are examined. A needle valve degrader was modified to include partial recirculation of degraded fuel and heat addition in the bypass loop. A pressure drop across the needle valve of up to 4,000 psi was used. The pressure drop across a 325 mesh filter screen placed inline with the degrader and directly downstream of the needle valve was measured as a function of time for different values of pressure drop across the needle valve. A volume flux of 1 gpm/sq in was employed based on the frontal area of the screen. It was found that, at ambient temperatures, freshly blended AMK fuel could be degraded using a single pass degradation at 4,000 psi pressure drop across the needle valve to give acceptable filterability performance. At fuel temperatures below -20 C, degradation becomes increasingly difficult and a single pass technique results in unacceptable filtration performance. Recirculation of a fraction of the degraded fuel and heat addition in the bypass loop improved low temperature degradation performance. The problem is addressed of blending the AMK additive with Jet A at various base fuel temperatures. Author

N88-26496# Lawrence Livermore National Lab., Calif.
ROCKET-PROPELLANT BURN TESTS OF SILICIDE-COATED NIOBIUM AND TANTALUM
P. G. Curtis, O. H. Krikorian, and F. H. Helm 20 Apr. 1988 33 p
(Contract W-7405-eng-48)
(DE88-010729; UCID-21395) Avail: NTIS HC A03/MF A01

Coatings designed to protect refractory metals in fire situations were tested on niobium and tantalum in a furnace and in a rocket-fuel flame. The best performance was obtained from

Cr-Si-type silicide coatings applied by the pack-cementation process. The main mode of failure of the coated parts was corrosion by molten stainless steel rather than oxidation. DOE

29 MATERIALS PROCESSING

Includes space-based development of products and processes for commercial applications.
For biological materials see *55 Space Biology.*

N88-26497*# Case Western Reserve Univ., Cleveland, Ohio.
INDUSTRIAL PROCESSES INFLUENCED BY GRAVITY Final Report
Simon Ostrach Jun. 1988 47 p
(Contract C-21066-G)
(NASA-CR-182140; NAS 1.26:182140) Avail: NTIS HC A03/MF A01 CSCL 22A

In considering new directions for low gravity research with particular regard to broadening the number and types of industrial involvements, it is noted that transport phenomena play a vital role in diverse processes in the chemical, pharmaceutical, food, and biotech industries. Relatively little attention has been given to the role of gravity in such processes. Accordingly, numerous industrial processes and phenomena are identified which involve gravity and/or surface tension forces. Phase separations and mixing are examples that will be significantly different in low gravity conditions. A basis is presented for expanding the scope of the low gravity research program and the potential benefits of such research is indicated. Author

N88-26498*# Intersonics, Inc., Northbrook, Ill.
PROGRAM FOR THE FEASIBILITY OF DEVELOPING A HIGH PRESSURE ACOUSTIC LEVITATOR Final Contractor Report
Charles A. Rey, Dennis R. Merkley, and Gregory R. Hammarlund Jul. 1988 49 p
(Contract NAS3-25115)
(NASA-CR-182154; NAS 1.26:182154) Avail: NTIS HC A03/MF A01 CSCL 22A

This is the final report for the program for the feasibility of developing a high-pressure acoustic levitator (HPAL). It includes work performed during the period from February 15, 1987 to October 26, 1987. The program was conducted for NASA under contract number NAS3-25115. The HPAL would be used for containerless processing of materials in the 1-g Earth environment. Results show that the use of increased gas pressure produces higher sound pressure levels. The harmonics produced by the acoustic source are also reduced. This provides an improvement in the capabilities of acoustic levitation in 1-g. The reported processing capabilities are directly limited by the design of the Medium Pressure Acoustic Levitator used for this study. Data show that sufficient acoustic intensities can be obtained to levitate and process a specimen of density 5 g/cu cm at 1500 C. However, it is recommended that a working engineering model of the HPAL be developed. The model would be used to establish the maximum operating parameters of furnace temperature and sample density. Author

31 ENGINEERING (GENERAL)

Includes vacuum technology; control engineering; display engineering; cryogenics; and fire prevention.

N88-26499# Tokyo Univ. (Japan). Inst. of Space and Astronautical Science.
THE PROCEEDINGS OF THE SYMPOSIUM ON MECHANICS FOR SPACE FLIGHT 1987
K. Oshima, ed. Mar. 1988 146 p Symposium held in Tokyo, Japan, 18-20 Nov. 1987
(ISAS-SP-6; ISSN-0288-433X) Avail: NTIS HC A07/MF A01

The proceedings of the symposium are presented and aimed at the scientific information exchange concerning the mechanics for space flight among research scientists and engineers of related fields of technology. The sessions were entitled: Vortical Flows; Numerical Fluid Dynamics; Hypersonic Flows, Heat Pipe Engineering; and Guidance and Control for Space Flight. Fifteen of the 32 papers presented at the conference are presented. For individual titles, see N88-26500 through N88-26514.

N88-26500# Tokyo Univ. (Japan). Dept. of Aeronautical Engineering.
NUMERICAL ANALYSIS OF RECONNECTION OF VORTEX RINGS **c34**
H. L. Chen and K. Oshima *In its* The Proceedings of the Symposium on Mechanics for Space Flight 1987 Mar. 1988 p 3-12 (For primary document see N88-26499 20-31)
Avail: NTIS HC A07/MF A01

The interaction, especially the reconnection, of two vortex rings taking into account the viscous effect, was analyzed. A computational code was developed for the three-dimensional, time-dependent incompressible Navier-Stokes equations and applied to the generation process of vortex rings and the interaction of them which are traveling along the parallel axes. These processes were successfully simulated and the results obtained agree with experimental results. Author

N88-26501# Tokyo Univ. (Japan). Inst. of Space and Astronautical Science.
VORTEX FILAMENT SIMULATION FOR THE CROSSLINKING RINGS **c34**
Akiko Yamashita and Yuko Oshima (Ochanomizu Women's Univ., Tokyo, Japan) *In its* The Proceedings of the Symposium on Mechanics for Space Flight 1987 Mar. 1988 p 13-18 (For primary document see N88-26499 20-31)
Avail: NTIS HC A07/MF A01

When two vortex rings are arranged side by side coplanerly, they approach each other and join to one large ring due to their interaction. This process was numerically simulated using a three-dimensional vortex filament method. One vortex ring which has vorticity within the core was approximated by a bundle of seven vortex filament rings. Each pair of filaments were crosslinked in turn until a large vortex ring formed. Author

N88-26502# Ochanomizu Women's Univ., Tokyo (Japan). Faculty of Science.
CROSSLINKING OF TWO VORTEX RINGS SIDE BY SIDE **c34**
Yuko Oshima and Naoki Izutsu (Tokyo Univ., Japan) *In* Tokyo Univ., The Proceedings of the Symposium on Mechanics for Space Flight 1987 Mar. 1988 p 19-27 (For primary document see N88-26499 20-31)
Avail: NTIS HC A07/MF A01

Mechanism of crosslinking of two vortex rings was investigated experimentally. Phase locked measurements of velocity using x-type hot wire were carried out over the whole flow field at point by point, and time-dependent vorticity fields were deduced. Also, the flow fields were visualized by Schlieren method. It is found that a new pair of vortex tubes are created connecting the interacting vortex rings and they grow up gradually while the vorticity intensities of the main rings decreases. This is considered as kind of bridging phenomenon of the vortex tubes, proposed by Kida and Takaoka in their numerical simulation. Author

N88-26503# Tokyo Univ. (Japan).
TURBULENCE TRANSITION IN A CIRCULAR PIPE **c34**
Yoshio Ishii and Hidesada Kannda (IBM Japan.) *In its* The Proceedings of the Symposium on Mechanics for Space Flight 1987 Mar. 1988 p 29-36 (For primary document see N88-26499 20-31)
Avail: NTIS HC A07/MF A01

Experimental observation and numerical simulation of transition flow in a pipe were carried out at various Reynolds numbers with several kinds of disturbance at the entrance. In the experiment, a tracer method was adapted to observe the transition phenomena, and, in the numerical simulation, stream function vorticity

formulation was applied to simulate the appearance of turbulence. These results have shown fairly good agreement between the experiment and the numerical simulation. Author

N88-26504# Gunma Univ., Maebashi (Japan). Faculty of Engineering.
ABSORPTION CHARACTERISTICS OF SI3N4 ABLATION LAYER PLASMA **c75**
Hiroyuki Shirai *In* Tokyo Univ., The Proceedings of the Symposium on Mechanics for Space Flight 1987 Mar. 1988 p 37-45 (For primary document see N88-26499 20-31)
Avail: NTIS HC A07/MF A01

The equilibrium composition and spectral absorption coefficient of Si3N4 ablation layer plasmas were calculated for temperature of 3000 to 9000 K, layer thickness of 0 to 0.5 cm, and pressure of 2 to 5 atm. In the calculation of radiation, molecular bands, atomic lines and continuum processes are included. These results are applied to a simple shock layer model to assess the effectiveness of the ablation layers for a blockage of high temperature radiation from a stagnation shock layer composed of hydrogen and helium. The results show that the photoionization process of a Si atom is mainly responsible for blocking the radiation, and that the Si3N4 ablation layer is very effective in reducing the radiative heating due to high energy photons. Author

N88-26505# Miyazaki Univ. (Japan). Dept. of Applied Physics.
THERMOSTATISTICAL ESTIMATIONS OF VAPOR-STATE MOLECULES AFFECTED BY GRAVITY IN A HEAT PIPE **c34**
Kanji Etori *In* Tokyo Univ., The Proceedings of the Symposium on Mechanics for Space Flight 1987 Mar. 1988 p 47-54 (For primary document see N88-26499 20-31)
Avail: NTIS HC A07/MF A01

Some thermodynamical properties of vapor state molecules in a heat pipe are analytically examined in an unsteady quasi-thermoequilibrium state. First, as a analytical procedure, the Hamiltonian of a gas molecule is formulated as the sum of those energies of the translation, the intermolecular interaction, the rotation, the vibration and the work with respect to the ensemble average of an unsteady velocity of a vapor state molecule in a gravity. The partition function and the free energy in this system are secondly introduced by using the Hamiltonian. According to the thermodynamical relations, the entropy and the specific heat per mol of the vapor state molecules are derived from the free energy and are finally estimated to examine the shifts affected by the gravity from the conventional values which do not include any gravitational term. Author

N88-26506# Ibaraki Univ., Hitachi (Japan).
AN EXPERIMENTAL INVESTIGATION OF TRANSIENT CHARACTERISTICS IN A GRAVITY-ASSISTED HEAT PIPE **c34**
F. Kaminaga, N. Tsuyuzaki, T. Saito (Japan Atomic Energy Research Inst., Tokyo.), M. Konno, and Y. Okamoto *In* Tokyo Univ., The Proceedings of the Symposium on Mechanics for Space Flight 1987 Mar. 1988 p 55-60 (For primary document see N88-26499 20-31)
Avail: NTIS HC A07/MF A01

Transient characteristics of a wickless gravity assisted heat pipe are investigated experimentally for a rapid temperature change of an evaporator section by submerging in a hot water bath. The results indicate that at high water bath temperature, response time of the heat pipe is kept in a few seconds, but at low temperature it is on the order of minutes and considerable temperature fluctuations are caused by a bumping. Author

N88-26507# Nippon Inst. of Tech. (Japan).
HEAT TRANSFER OF MESH-WICK HEAT-PIPES (BOTTOM HEAT MODE) **c34**
Yoshio Ikeda and Sadayuki Onuma *In* Tokyo Univ., The Proceedings of the Symposium on Mechanics for Space Flight 1987 Mar. 1988 p 61-76 (For primary document see N88-26499 20-31)
Avail: NTIS HC A07/MF A01

A heat pipe in which the working fluid circulates by gravity need not contain a wick; this type of heat pipe can be examined as a thermosiphon. For better moistening inside the evaporating zone and improvement of flooding or entrainment, wicks of groove type are often used. The performance of the metal wick of the copper ethanol heat pipe is examined by investigating the effect of inclination and volume of enclosed fluid on thermal resistance. In modeling the thermal resistance of the heat pipe, it is assumed that, in the evaporating zone, the surplus fluid beyond the volume required for a complete circulation with full depth of fluid film is stagnant and the thickness of the wick contributes the thermal resistance and that, in the condensation zone, the equivalent wick thickness to the depth of circulating fluid film accounts for the thermal resistance. In calculating the porosity, permeability and effective thermal conductivity of the wick, the equations including the normalized clearance are used. Since heat pipes generally contain surplus fluid beyond the porous volume of the wick, the depth calculated by the equations of the Nusselt's condensation theory is added to the depth of fluid film in the range beyond the wick. Author

N88-26508# Osaka Univ. (Japan). Dept. of Aeronautical Engineering.
AN ARRANGING METHOD ON L/D OF TWO-PHASE CLOSED THERMOSYPHONS **c34**
Takayoshi Matsuoka, Kanji Negishi, Ken-ichi Kaneko, Masao Hirashima, Yuuji Nishikawa, and Masakazu Taguchi (Takuma Research and Development Co. Ltd., Dojima, Japan) *In* Tokyo Univ., The Proceedings of the Symposium on Mechanics for Space Flight 1987 Mar. 1988 p 77-86 (For primary document see N88-26499 20-31)
Avail: NTIS HC A07/MF A01

There were many papers reporting the deviation of heat transfer characteristics of two-phase closed thermosyphons on the change of the length (L) and diameter (D). Almost all the papers have, however, explained only qualitative characteristics and scarcely deduced an empirical formula. A method of arranging the L and D was derived from the experimental results of corrugated thermosyphons with different L and D. The temperature profiles were calculated with a good agreement with the experimental results. Author

N88-26509# Tsukuba Univ., Ibaraki (Japan). Inst. of Engineering Mechanics.
A STATISTICAL TREATMENT OF ACCELERATED LIFE TEST DATA FOR COPPER-WATER HEAT PIPES **c34**
M. Murakami, K. Arai, and Y. Kojima (Fujitsu Ltd., Kawasaki, Japan) *In* Tokyo Univ., The Proceedings of the Symposium on Mechanics for Space Flight 1987 Mar. 1988 p 87-98 (For primary document see N88-26499 20-31)
Avail: NTIS HC A07/MF A01

A statistical method is proposed to treat accelerated life test data conducted at several elevated temperatures for a sufficient number of commercially available Cu-water heat pipes to predict the operation life. The temperature distribution measurements periodically carried out yield both data sets concerning the temperature drop and the gas column length as measures of noncondensible gas accumulation. The gas analysis with a mass spectrometer is also carried out to obtain the gas quantity data. A method of unified regression analysis to take account of the acceleration factor resulted from a number of elevated test temperatures is proposed to establish a method to predict the long term performance degradation from life test data. The mutual correlations among three kinds of data sets are also discussed. Author

N88-26510# Toshiba Corp., Tokyo (Japan).
FORCED-CONVECTIVE BOILING IN SMALL DIAMETER TUBE **c34**
Yoshiro Miyazaki, Yoshio Kuriyma, and Masao Furukawa (National Space Development Agency, Tokyo, Japan) *In* Tokyo Univ., The Proceedings of the Symposium on Mechanics for Space Flight

1987 Mar. 1988 p 99-105 (For primary document see N88-26499 20-31)
Avail: NTIS HC A07/MF A01

A straight bare tube type evaporator was tested in order to evaluate its feasibility on space applications. Two categories of flow regimes were observed during the test. One flow regime indicated a high pressure loss and a slight temperature decrease along the flow direction, and the test results showed a fairly good agreement with the analytical results obtained using a nucleat boiling model. Whereas, the other flow regime showed a contrasting feature of low pressure loss and abrupt temperature rise along the flow direction. In this case also the results obtained on the basis of the analytical model of film boiling showed a fairly good agreement with the experimental results of heat transfer characteristics. Author

N88-26511# Takuma Research and Development Co. Ltd., Dojima (Japan).
CHARACTERISTICS OF LONG SIZE THERMOSYPHONS MADE OF CORRUGATED TUBE **c34**
Masao Hirashima, Yuuji Nishikawa, Masakazu Taguchi, Kanji Negishi, Ken-ichi Kanero, and Takayoshi Matsuoka (Osaka Univ., Japan) *In* Tokyo Univ., The Proceedings of the Symposium on Mechanics for Space Flight 1987 Mar. 1988 p 107-113 (For primary document see N88-26499 20-31)
Avail: NTIS HC A07/MF A01

Two-phase closed thermosyphons made of corrugated tube operating in the gravitational field have different characteristics in comparison with that of smooth tube in some items. The cause depends on the accumulated working fluid in the concave space of corrugated tube which tends to induce a dry out phenomenon in the evaporator section. The difference of these characteristics between thermosyphons of corrugated tube and smooth tube seems to amplify with the increment of the length of the thermosyphon. The temperature distribution along the axis of thermosyphon, the heat transport and the heat transfer coefficient as a function of the inclination angle at a fill charge ratio 50 percent of the working fluid were obtained by the experiments and discussed herein. A correlating equation of the heat transfer coefficient was deduced also from the experiments. Author

N88-26512# Shanghai Inst. of Energy (China).
AN ANALYSIS OF GAS-STEAM TOTAL POWER RECOVERY ENERGY SYSTEM **c44**
Zhi-Guang Ling *In* Tokyo Univ., The Proceedings of the Symposium on Mechanics for Space Flight 1987 Mar. 1988 p 115-125 (For primary document see N88-26499 20-31)
Avail: NTIS HC A07/MF A01

The main idea of the suggested total power recovery energy system is to conduct the steam generated from the waste heat boiler to mix with the exhausted gas and form a gas steam mixed working medium in the system. In order to explain the feasibility of the proposed system, a comparison is made between this system and the conventional system of generating electricity by passing the steam through steam turbine and compressor, i.e., a tandem gas-steam combined cycle. A complete description and analysis of the proposed system is given along with results and conclusions. E.R.

N88-26513# Mitsubishi Electric Co., Amagasaki (Japan).
NUTATIONAL STABILITY OF A SATELLITE EQUIPPED WITH AN ACTIVE MAGNETIC MOMENTUM WHEEL **c18**
Masao Inoue, Kazuo Tsuchiya, Atsushi Nakajima, and Chikara Murakami (Tokyo Metropolitan Univ., Japan) *In* Tokyo Univ., The Proceedings of the Symposium on Mechanics for Space Flight 1987 Mar. 1988 p 127-136 (For primary document see N88-26499 20-31)
Avail: NTIS HC A07/MF A01

The influence of the magnetically suspended rotor on the satellite motion is studied. Although cross feedbacks in the magnetic bearing provide stability margin to the rotor gyroscopic motion, they may destabilize the satellite nutation. Stability analyses of the dynamical interaction between the satellite and the magnetically suspended rotor whose controller used three types of (proportional, integral and derivative) cross feedbacks were performed. The results indicated that they had significant effects on the rotor and the satellite motion. Author

N88-26514# Nippon Electric Co. Ltd., Yokohama (Japan). Space Development Div.
DYNAMICS OF SATELLITES WITH RADIAL WIRE ANTENNAS **c18**
Motoki Hinada, Ichiro Nakatani, Keiken Ninomiya, Noboru Muranaka, Takakazu Namera, Masahi Uo, and Naoto Ogura *In* Tokyo Univ., The Proceedings of the Symposium on Mechanics for Space Flight 1987 Mar. 1988 p 137-147 (For primary document see N88-26499 20-31)
Avail: NTIS HC A07/MF A01

An analysis is given for the dynamics of a spinning satellite with four radial wire antennas. In this analysis, a generalized model is used, in which, mass properties of wire antennas are not equal and antennas' attachment points on the satellite have some amounts of offsets from the satellite CG (center of gravity) plane. Each antenna is modeled as a physical pendulum. They have two degrees of freedom: in spin plane and out of plane motion. Lagrangian with 14 degrees of freedom is obtained, and then equations of motion are derived. A set of equations can be divided into three groups. From a modal analysis for each group, the effects of wire antennas asymmetry and their offsets on the satellite attitude motion is revealed. Numerical simulation results of GEOTALL satellite are also given. Author

N88-26515# Technion - Israel Inst. of Tech., Haifa. Dept. of Aeronautical Engineering.
VERTICAL SHIP MOTIONS AND SEA LOADS CONSIDERING NONLINEAR EFFECTS Ph.D. Thesis - Feb. 1984
I. Shacham and T. Weller Dec. 1986 150 p
(TAE-592) Avail: NTIS HC A07/MF A01

A mathematical model dealing with vertical motions and longitudinal strength of a ship, whose shape deviates from the linear theory assumptions, was developed. The model includes nonlinear effects stemming from ship flexibility, widening of side walls in the waterline region and ship bottom emersion. The model also considers coupling between ship response and exciting forces (hydroelastic). Based on the mathematical model equations, a computer program was written to calculate the motions and stresses, developed in a prescribed ship hull sailing at a given speed and course in a given sinusoidal type sea. Calculations obtained for a fast patrol boat and an aircraft carrier featured by a large bow flare, demonstrated very good agreement, both qualitatively and quantitatively, with results measured in sea trials. The method of solution proposed resulted in a time saving computer program, which can be applied effectively for a parametric study of the many factors which affect the whipping phenomenon. The program can also be used as an auxiliary tool at the design stage of new ships and for the determination of sailing envelopes of existing ships. B.G.

N88-26516# Rockwell International Corp., Golden, Colo.
A FINITE ELEMENT ANALYSIS FOR THE HYDROFORMING OF ALUMINUM
S. M. Lepi, L. K. Hayer, J. L. Krankota, and F. E. Gibbs 19 Feb. 1988 16 p
(Contract DE-AC04-76DP-03533)
(DE88-008050; RFP-4208) Avail: NTIS HC A03/MF A01

Finite element modeling of an aluminum hydroforming process, using MARC finite element software, is being investigated at Rocky Flats to aid in process development. The purpose of this analysis was to determine how well MARC predicts the final dimensions of an aluminum part formed with a VERSON hydrostatic forming press. A two dimensional, axisymmetric model was created using MENTAT mesh generating software and analyzed with MARC on a VAX 8800 mainframe computer. The analysis predicted part thickness within a five percent error band. Based upon these findings, future analyses will be conducted to optimize hydroforming process parameters. DOE

N88-26517# Naval Postgraduate School, Monterey, Calif.
ELECTRODYNAMIC DRIVER FOR THE SPACE THERMOACOUSTIC REFRIGERATOR (STAR) M.S. Thesis
Michele Fitzpatrick Mar. 1988 187 p
(AD-A192337; AD-E801594) Avail: NTIS HC A09/MF A01 CSCL 13A

The objective of the STAR project is to test and space qualify a new continuous cycle cryogenic refrigeration system for cooling of sensors and electronics which is based upon the newly discovered thermoacoustic heat pumping effect. The new refrigerator has no sliding seals, a cycle frequency of about 300 hz, and uses acoustic resonance to enhance the overall power density and efficiency. This thesis is concerned specifically with the design and testing of the electrodynamic transducer which is responsible for the electro-acoustic power conversion. A computer model of the driver/resonator system is presented along with the techniques for measurement of the electrical and mechanical parameters used as input for the model is presented along with the techniques for measurement of the electrical and mechanical parameters used as input for the model. A final driver design (including dimensional drawings) utilizing a modified JBL 2450J neodymium-iron-boron compression driver and associated leak tight electrical feed-throughs, microphone, accelerometer, pressure gage pressure housing, and resonator interface is provided. GRA

N88-26518# Deutsche Forschungs- und Versuchsanstalt fuer Luft- und Raumfahrt, Brunswick (West Germany). Inst. fuer Flugmechanik.
SYSTEM IDENTIFICATION IN VEHICLE DYNAMICS
Rudolf Brockhaus, ed. and Karl-Friedrich Doherr, ed. (Technische Hochschule, Darmstadt, West Germany) 1987 402 p Partly in GERMAN and ENGLISH Proceedings of the Symposium on Sicherheit im Luftverkehr, Brunswick, Fed. Republic of Germany, 10-11 Mar. 1987
(DFVLR-Mitt-87-22; ISSN-0176-7739; ETN-88-92314) Avail: NTIS HC A18/MF A01; DFVLR, VB-PL-DO, 90 60 58, 5000 Cologne, Fed. Republic of Germany, 109 Deutsche marks

Parameter estimation of dynamical systems, flight vehicle system identification, modeling and parameter identification of motor vehicles, and simulation models for the dynamics of track vehicle systems are reviewed. In frequency domain identification, vehicle dynamics, dynamics of a scaled remotely piloted helicopter, and the multivariate identification of a flexible transport aircraft are treated. As examples of applications of the maximum likelihood identification method, a two-point aerodynamic model, the identification of a direct-lift-control flap system, the parameter estimation of aerodynamic nonlinearities, flight test data validation, and aircraft inertia characteristics estimation are presented. Transport dynamics, dynamics of lateral motion in hover flight, and flight path reconstruction, are discussed. A passenger simulation is outlined. For individual titles, see N88-26519 through N88-26536.

N88-26519# Technische Hochschule, Darmstadt (West Germany). Inst. fuer Regelungstechnik.
PARAMETER ESTIMATION OF DYNAMICAL SYSTEMS **c61**
R. Isermann *In* DFVLR, System Identification in Vehicle Dynamics 1987 p 9-49 In GERMAN; ENGLISH summary (For primary document see N88-26518 20-31)
Avail: NTIS HC A18/MF A01; DFVLR, VB-PL-DO, 90 60 58, 5000 Cologne, Fed. Republic of Germany, 109 Deutsche marks

Identification of dynamical systems, and the characteristic features of various methods are considered. The parameter estimation of systems with time-discrete signals is presented. The least squares method and the maximum likelihood method are described. Parameter estimation for systems with time-continuous signals is presented. It is shown how parameter estimation methods are applied to time-variant, multivariable, and nonlinear systems. Recursive estimation algorithms suitable for on-line applications in real-time, are emphasized. ESA

N88-26520# Deutsche Forschungs- und Versuchsanstalt fuer Luft- und Raumfahrt, Brunswick (West Germany). Inst. fuer Flugmechanik.
FLIGHT VEHICLE SYSTEM IDENTIFICATION: STATUS AND PROSPECTS **c05**
P. G. Hamel *In its* System Identification in Vehicle Dynamics 1987 p 51-90 (For primary document see N88-26518 20-31)
Avail: NTIS HC A18/MF A01; DFVLR, VB-PL-DO, 90 60 58, 5000 Cologne, Fed. Republic of Germany, 109 Deutsche marks

The state of the art of flight vehicle parameter identification techniques from flight test data is reviewed. Model structure aspects for basic and highly augmented airframes are emphasized. Results on system identification related to highly augmented flight vehicles as well as to high angle-of-attack maneuvers are presented. ESA

N88-26521# Stuttgart Univ. (West Germany). Inst. fuer Mechanik.
MODELING AND PARAMETER IDENTIFICATION OF MOTOR VEHICLES [MODELLBILDUNG UND PARAMETERIDENTIFIKATION BEI KRAFTFAHRZEUGEN] **c37**
W. Schiehlen *In* DFVLR, System Identification in Vehicle Dynamics 1987 p 91-102 In GERMAN (For primary document see N88-26518 20-31)
Avail: NTIS HC A18/MF A01; DFVLR, VB-PL-DO, 90 60 58, 5000 Cologne, Fed. Republic of Germany, 109 Deutsche marks

The modeling and parameter identification of motor vehicles is treated with a view to the investigation of vibrations. The vehicle model is derived from the method of multibody systems. The road is considered as rigid. The parameter identification uses frequency response covariance methods. ESA

N88-26522# Deutsche Forschungs- und Versuchsanstalt fuer Luft- und Raumfahrt, Oberpfaffenhofen (West Germany). Inst. fuer Dynamik der FLugsysteme.
SIMULATION MODELS FOR THE DYNAMICS OF TRACKED VEHICLE SYSTEMS: STATE-OF-THE-ART AND OPEN PROBLEMS **c37**
W. Kortuem and J. Jaschinski *In its* System Identification in Vehicle Dynamics 1987 p 103-140 (For primary document see N88-26518 20-31)
Avail: NTIS HC A18/MF A01; DFVLR, VB-PL-DO, 90 60 58, 5000 Cologne, Fed. Republic of Germany, 109 Deutsche marks

The use of simulation models for track ground transportation systems for the velocity range between 300 and 500 km/hr is discussed. The role of system dynamics for track vehicles is outlined. The dynamic modeling of track vehicles, in particular wheel/rail systems is explained. The MEDYNA general program for model assembling and simulation is presented. Identification activities within wheel/rail research are described. The role of identification for high-speed ground transportation system dynamics is outlined. ESA

N88-26523# Technische Hochschule, Darmstadt (West Germany). Fachbereich Regelsystemtheorie.
VEHICLE DYNAMICS: IDENTIFICATION IN THE FREQUENCY DOMAIN [FAHRZEUGDYNAMIK: IDENTIFIKATION IM FREQUENZBEREICH] **c37**
V. Tews *In* DFVLR, System Identification in Vehicle Dynamics 1987 p 141-152 In GERMAN; ENGLISH summary (For primary document see N88-26518 20-31)
Avail: NTIS HC A18/MF A01; DFVLR, VB-PL-DO, 90 60 58, 5000 Cologne, Fed. Republic of Germany, 109 Deutsche marks

A method to identify the behavior of nonlinear systems in the frequency domain was developed. If random signals are used as inputs the resulting frequency response is also a random signal due to the nonlinear effects. For composite frequency input signals, satisfying requirements on their phase angles, each spectral line is shown to be approximately a normally distributed random variable, the mean value of which is a linearized system, optimal in a mean-squares sense. The variance can be calculated via the ordinary coherence function. This approach was extended to multivariable systems. Using the multiple coherence, conditioned

power spectral densities and partial coherence, the variation areas for each of the elements in the frequency response matrix can be calculated, even in the presence of correlated inputs. The application of this method to vehicle dynamics is illustrated by an axle undergoing random excitation on a test bench. ESA

N88-26524# York Univ. (England). Dept. of Electronics.
FREQUENCY DOMAIN IDENTIFICATION OF THE DYNAMICS OF A SCALED REMOTELY-PILOTED HELICOPTER **c08**
P. Young and R. J. Patton *In* DFVLR, System Identification in Vehicle Dynamics 1987 p 153-172 Sponsored by the United Kingdom Science and Engineering Research Council and the United Kingdom Ministry of Defence (For primary document see N88-26518 20-31)
Avail: NTIS HC A18/MF A01; DFVLR, VB-PL-DO, 90 60 58, 5000 Cologne, Fed. Republic of Germany, 109 Deutsche marks

A linear digital simulation of a radio-controlled model helicopter was performed to evaluate the validity of applying frequency domain identification to structural estimation of a complex nonlinear system. The control and telemetry systems, the sensors and the associated signal conditioning developed for the radio-controlled helicopter facility are described. Sine-wave frequency sweeps were applied to each input in turn to excite all the dominant modes of the system, and the time series data were analyzed to obtain the system transfer functions. The closed-loop transfer functions are found by least-squares curve fitting, and the poles and zeros are determined for each case. Comparing these modes with the corresponding elements in the transfer function matrix obtained from the Levernier algorithm gives results which demonstrate the usefulness of the frequency domain approach in identification. ESA

N88-26525# Centre d'Etudes et de Recherches, Toulouse (France). Dept. d'Automatique.
MULTIVARIABLE IDENTIFICATION OF A FLEXIBLE TRANSPORT AIRCRAFT **c05**
M. Clique, G. Monnier, M. Labarrere, A. Bucharles, and J. L. Pac (Ecole Nationale Superieure de l'Aeronautique et de l'Espace, Toulouse, France) *In* DFVLR, System Identification in Vehicle Dynamics 1987 p 173-192 (For primary document see N88-26518 20-31)
Avail: NTIS HC A18/MF A01; DFVLR, VB-PL-DO, 90 60 58, 5000 Cologne, Fed. Republic of Germany, 109 Deutsche marks

A method for the identification of multivariable linear systems is presented. Fourier analysis was used to obtain power spectral densities from measured signals and to compute each transfer function in the frequency domain. The modes of the system were located using Steiglitz identification techniques for the different input-output pairs. The proposed algorithm leads to the determination of a multivariable state space representation. The application to a flexible transport aircraft is given; the results show that the proposed method is adapted to multi-input, multi-output systems. ESA

N88-26526# Deutsche Forschungs- und Versuchsanstalt fuer Luft- und Raumfahrt, Brunswick (West Germany). Inst. fuer Flugmechanik.
A TWO-POINT AERODYNAMIC MODEL FOR IDENTIFICATION [EIN 2-PUNKT-AERODYNAMIKMODELL FUER DIE IDENTIFIZIERUNG] **c05**
W. Moennich *In its* System Identification in Vehicle Dynamics 1987 p 193-207 In GERMAN (For primary document see N88-26518 20-31)
Avail: NTIS HC A18/MF A01; DFVLR, VB-PL-DO, 90 60 58, 5000 Cologne, Fed. Republic of Germany, 109 Deutsche marks

An aerodynamic model for the identification of lateral aircraft motion using maximum likelihood identification programs is presented, in which airfoil/fuselage and the horizontal tail surface are separated (two-point model). This separation allows one to consider several nonlinearities. The model takes into account elevator, elevator trimming, and direct lift control flap input signals as well as thrust effects on aerodynamics (interference between driving jet and horizontal tail surface). The method can be applied to all fixed-wing aircraft if compressibility effects can be neglected. The results show that a good or very good adaptation of the identification model output to the flight test measuring signals is obtained. The standard deviation of the identified parameters is so small that the reliability of the results can be considered as good. ESA

N88-26527# Deutsche Forschungs- und Versuchsanstalt fuer Luft- und Raumfahrt, Brunswick (West Germany). Inst. fuer Flugmechanik.
THE IDENTIFICATION OF THE DIRECT LIFT CONTROL FLAP SYSTEM OF THE RESEARCH AIRCRAFT ATTAS [ZUR IDENTIFIZIERUNG DES DLC-KLAPPENSYSTEMS DES FORSCHUNGSFLUGZEUGS ATTAS] **c05**
D. Rohlf and W. Moennich *In its* System Identification in Vehicle Dynamics 1987 p 209-222 In GERMAN (For primary document see N88-26518 20-31)
Avail: NTIS HC A18/MF A01; DFVLR, VB-PL-DO, 90 60 58, 5000 Cologne, Fed. Republic of Germany, 109 Deutsche marks

A simple replacement model for the direct lift control (DLC) flap control system was developed, and the DLC-flap efficiency of three landing flap positions was determined with a view to the identification of the ATTAS DLC-flap system. Starting from flight test data, a linear transfer behavior of second order in the frequency domain was determined; this model was extended by taking into account nonlinearities. The DLC-flap efficiencies were identified together with all other system parameters. Good adaptations to the time evolution, as well as small scatter in the identified parameters are obtained. The effect of the DLC-flap on buoyancy, drag, and pitching moment was determined as a function of the landing flap position. ESA

N88-26528# Deutsche Forschungs- und Versuchsanstalt fuer Luft- und Raumfahrt, Brunswick (West Germany). Inst. fuer Flugmechanik.
PARAMETRIC ESTIMATION OF AERODYNAMIC NONLINEARITIES IN ROLLING MOMENT DUE TO SIDESLIP USING MAXIMUM LIKELIHOOD METHOD **c05**
R. V. Jategaonkar *In its* System Identification in Vehicle Dynamics 1987 p 223-234 (For primary document see N88-26518 20-31)
Avail: NTIS HC A18/MF A01; DFVLR, VB-PL-DO, 90 60 58, 5000 Cologne, Fed. Republic of Germany, 109 Deutsche marks

The utility of nonlinear maximum likelihood procedures for unconventional problems of estimating discontinuous complex aerodynamic nonlinearities is treated. It is demonstrated that a maximum likelihood procedure in which the need for explicit sensitivity equations is overcome by approximating the sensitivity coefficients through a numerical procedure can handle conveniently different general nonlinear system models. As examples cubic nonlinearity and aerodynamic hysteresis, characterized by a discontinuous relationship in rolling moment due to sideslip, which can possibly lead to uncommanded roll oscillations in aircraft motion, were identified from the simulated responses. ESA

N88-26529# Deutsche Forschungs- und Versuchsanstalt fuer Luft- und Raumfahrt, Brunswick (West Germany). Inst. fuer Flugfuehrung.
FLIGHT TEST PREPARATION AND MEASURING DATA VALIDATION FOR PARAMETER IDENTIFICATION [FLUGVERSUCHSVORBEREITUNG UND MESSDATENUEBERPRUEUNG FUER DIE PARAMETER-IDENTIFIKATION] **c05**
K.-O. Proskawetz *In its* System Identification in Vehicle Dynamics 1987 p 235-249 In GERMAN (For primary document see N88-26518 20-31)
Avail: NTIS HC A18/MF A01; DFVLR, VB-PL-DO, 90 60 58, 5000 Cologne, Fed. Republic of Germany, 109 Deutsche marks

Flight test preparation and flight test data validation are explained. Using the results of the process analysis, the excitation signals are optimized, the regulating variables are fixed, and the flight tests are planned. After the flight tests, the compatibility of the test data among each other is checked using a maximum

likelihood identification program for nonlinear systems, and the errors are corrected. The procedure can also be applied to other domains of aircraft engineering in order to guarantee a high parameter estimation quality. ESA

N88-26530# Technische Hogeschool, Delft (Netherlands).
A NEW METHOD FOR THE ESTIMATION OF AIRCRAFT INERTIA CHARACTERISTICS **c05**
R. C. deJong and J. A. Mulder *In* DFVLR, System Identification in Vehicle Dynamics 1987 p 251-265 (For primary document see N88-26518 20-31)
Avail: NTIS HC A18/MF A01; DFVLR, VB-PL-DO, 90 60 58, 5000 Cologne, Fed. Republic of Germany, 109 Deutsche marks

A method for the experimental determination of the aircraft center of gravity and the moments and products of inertia is presented and evaluated. The method is based on the application of statistical parameter estimation techniques to the analysis of multidegree of freedom oscillations using a high accuracy instrumentation system. A suspension rig, in which the aircraft can simultaneously rotate about the pitch and yaw axis and translate along the roll and pitch-axis was used to demonstrate the validity of the method. Inertia moments, inertia products, and the three coordinates of the center of gravity are simultaneously estimated from measurements of a single oscillation. The experiment is less time-consuming than previous methods, since no separate center-of-gravity nor rig reconfigurations are needed. ESA

N88-26531# Daimler-Benz A.G., Stuttgart (West Germany).
IDENTIFICATION METHODS FOR TRANSPORT DYNAMICAL INVESTIGATIONS [IDENTIFIKATIONSMETHODEN FUER FAHRDYNAMISCHE UNTERSUCHUNGEN] **c37**
W. Reichelt *In* DFVLR, System Identification in Vehicle Dynamics 1987 p 267-286 In GERMAN (For primary document see N88-26518 20-31)
Avail: NTIS HC A18/MF A01; DFVLR, VB-PL-DO, 90 60 58, 5000 Cologne, Fed. Republic of Germany, 109 Deutsche marks

The suitability of the identification theory for transport dynamics was investigated, by the determination of the yaw transfer function from driving test data using digital computers. Identification methods from the time and frequency domain were used. The significance of the applied excitation signals (step, pulse, stochastic) is explained. The frequency domain method shows by far the best agreement with the measured frequency response, due to the better excitation by the stochastic input signal. ESA

N88-26532# Deutsche Forschungs- und Versuchsanstalt fuer Luft- und Raumfahrt, Brunswick (West Germany). Inst. fuer Flugmechanik.
UTILIZATION OF IDENTIFICATION METHODS IN THE TIME AND FREQUENCY DOMAIN FOR THE DETERMINATION OF THE XV-15 (TILT-ROTOR) DYNAMICS FOR LATERAL MOTION IN HOVER FLIGHT [ANWENDUNG VON IDENTIFIZIERUNGSVERFAHREN IM ZEIT- UND FREQUENZBEREICH ZUR BESTIMMUNG DER XV-15 (TILT-ROTOR) DYNAMIK FUER DIE SEITENBEWEGUNG IM SCHWEBEFLUG] **c05**
J. Kaletka and M. B. Tischler (Army Aviation Research and Development Command, Moffett Field, Calif.) *In its* System Identification in Vehicle Dynamics 1987 p 287-307 In GERMAN; ENGLISH summary (For primary document see N88-26518 20-31)
Avail: NTIS HC A18/MF A01; DFVLR, VB-PL-DO, 90 60 58, 5000 Cologne, Fed. Republic of Germany, 109 Deutsche marks

Mathematical models for the open loop dynamics of the XV-15 aircraft (tilt-rotor) were developed from flight test data using the frequency domain identification and the time domain identification approaches. The flight tests and the evaluation of test results are described. The results from the two approaches compare favorably. However, the differences clearly demonstrate the effects of the inherent weighting of each individual technique; they also indicate the relative strengths and weaknesses of the approaches. Based on the results a proposal for a coordinated system identification approach, using the advantages of both methods is given. ESA

N88-26533# Deutsche Forschungs- und Versuchsanstalt fuer Luft- und Raumfahrt, Brunswick (West Germany). Inst. for Flight Mechanics.
APPLICATION OF COMPLEMENTARY PARAMETER IDENTIFICATION TECHNIQUES TO FLIGHT TEST DATA OF A TRANSPORT AIRCRAFT **c05**
B. Krag, M. Labarrere, G. W. Foster, and J. H. Breeman (National Aerospace Lab., Amsterdam, Netherlands) *In* DFVLR, System Identification in Vehicle Dynamics 1987 p 309-342 (For primary document see N88-26518 20-31)
Avail: NTIS HC A18/MF A01; DFVLR, VB-PL-DO, 90 60 58, 5000 Cologne, Fed. Republic of Germany, 109 Deutsche marks

The experience gained from the application of different parameter identification techniques to the same set of flight test data is presented. The basic equations in the techniques used (maximum likelihood estimates and Kalman filter technique) are presented. The results of flight path reconstruction and parameter identification are discussed. It is shown that differences in the results can be attributed to the different models. ESA

N88-26534# Krauss-Maffei A.G., Munich (West Germany).
IDENTIFICATION OF LATERAL OPERATION DYNAMICS OF RAIL VEHICLES USING ROLL TEST STAND TESTS [IDENTIFIZIERUNG DER LATERALEN LAUFDYNAMIK VON SCHIENENFAHRZEUGEN DURCH ROLLPRUEFSTANDSVERSUCHE] **c37**
K. Heym *In* DFVLR, System Identification in Vehicle Dynamics 1987 p 343-361 In GERMAN (For primary document see N88-26518 20-31)
Avail: NTIS HC A18/MF A01; DFVLR, VB-PL-DO, 90 60 58, 5000 Cologne, Fed. Republic of Germany, 109 Deutsche marks

Identification tests were performed on a roll test stand in order to verify physical and mathematical models for nonlinear operation dynamics. It is shown that the model approaches give a good qualitative description of all the relevant effects in the stability and perturbation behavior during drive with low traction. This is very probably also valid for the railroad section behavior. Simulation programs which allow a significant reduction of the economic risks in the construction of expensive prototypes were developed. The roll test stand reduces the railroad section test to a minimum. ESA

N88-26535# Technische Univ., Brunswick (West Germany). Inst. fuer Regelungstechnik.
NONLINEAR IDENTIFICATION OF AN AIRCRAFT FOR THE DIRECT CALCULATION OF AN ANTICIPATORY CONTROL [NICHTLINEARE IDENTIFIZIERUNG EINES FLUGZEUGS ZUR DIREKTEN BERECHNUNG EINER VORSTEUERUNG] **c08**
M. Haverland and U. Lindemann *In* DFVLR, System Identification in Vehicle Dynamics 1987 p 363-374 In GERMAN (For primary document see N88-26518 20-31)
Avail: NTIS HC A18/MF A01; DFVLR, VB-PL-DO, 90 60 58, 5000 Cologne, Fed. Republic of Germany, 109 Deutsche marks

Using the example of the identification and control of an aircraft, a predictive control method for nonlinear sections is presented. In many cases a linear controller is not sufficient for the control of nonlinear sections, but the combination of a linear controller and predictive control gives better results. The proposed method allows the determination of predictive control coefficients directly from measured quantities. It is shown that the coefficients build up quickly, allowing to follow section parameter variations and providing a high safety level. The method can be used for the identification of nonlinear systems that can be described by a model that is linear in the coefficients. Dynamic effects can also be taken into account. ESA

N88-26536# Volkswagen A.G., Wolfsburg (West Germany).
PARAMETER IDENTIFICATION OF THE PASSENGER SIMULATION MODEL MADYMO: METHODS AND EXPERIENCE [PARAMETERIDENTIFIKATION DES INSASSENSIMULATIONSMODELLS MADYMO: METHODEN UND ERFAHRUNGEN] **c37**
R. Zobel, H.-G. Bock, and Th. Reiners (Bonn Univ., West Germany) *In* DFVLR, System Identification in Vehicle Dynamics 1987 p 375-399 In GERMAN (For primary document see N88-26518 20-31)
Avail: NTIS HC A18/MF A01; DFVLR, VB-PL-DO, 90 60 58, 5000 Cologne, Fed. Republic of Germany, 109 Deutsche marks

The evolution of the delay in the passenger motion was determined from the evolution of the delay of the vehicle cell using the simulation model MADYMO. This is a flexible program for the calculation of the motion of a dummy passenger. The dummy consists of segments with a tree structure and connected with joints. The computer program itself provides the accompanying differential equation, which makes it flexible with respect to changes in the dummy. The high degree of modeling possiilities imposes high requirements on measuring techniques for the determination of characteristics. Statistical tests are often required for the description of dynamic phenomena. Therefore an automatic maximum likelihood as well as multipurpose parameter identification method was used. ESA

N88-26537# Technische Hogeschool, Delft (Netherlands). Dept. of Aerospace Engineering.
TECHNICAL INSTRUCTIONS FOR A CONTROL OPERATING SYSTEM OF THE GAS FLOW INSTALLATION FOR THE SOLID FUEL COMBUSTION CHAMBER [TECHNISCHE GEBRUIKSAANWIJZING VOOR HET REGEL/BEDIENINGSSYSTEEM VAN DE GASTOEVOERINSTALLATIE VOOR DE VASTE BRANDSTOF VERBRANDINGSKAMER]
J. Versmissen and R. P. vandenBerg Jan. 1987 278 p In DUTCH Prepared in cooperation with Prins Maurits Lab. TNO, Rijswijk, Netherlands Sponsored in cooperation with Technische Hogeschool, Delft, Netherlands
(Contracts STW-DLR-11.0120; PEO-90753.140)
(LR-507; PML-1987-C1; SFCC-30; B8733285; ETN-88-92455)
Avail: NTIS HC A13/MF A01

Operating instruction for a solid fuel combustion chamber control system are given. The technical realization of the system is described. The operation of the different components is explained with a view to maintenance and possible extension: control panel, flow chart panel, safety unit, interfaces, compressor, solid state relay box, firing unit, thermocouple conditioning unit, reorders, tap and valve signals, simulation unit, switching panel, video timer interface, and computer system. ESA

N88-26538# Helsinki Univ. (Finland). Lab. of Engineering Materials.
EVALUATION OF ENGINEERING LEAK BEFORE BREAK ASSESSMENT METHODS BY PIPING TESTS
H. Talja May 1987 27 p
(PB88-126982; Rept-1/87; ISBN-951-754-195-3) Avail: NTIS HC E03/MF E01; copy not available from STI Facility CSCL 13B

Battelle's method is a simple and feasible tool for assessing leakage before breaks occur in ductile piping components. The applicability and reliability of the method are assessed by evaluating a number of piping tests performed by the Imatra Power Company. Furthermore, a simple method for calculating upper and lower bounds for leak areas is discussed. GRA

N88-26539*# National Aeronautics and Space Administration. Lewis Research Center, Cleveland, Ohio.
REDUCING ADHESION AND AGGLOMERATION WITHIN A CLOUD OF COMBUSTIBLE PARTICLES
Howard D. Ross Jul. 1988 42 p
(NASA-TM-100902; E-4082; NAS 1.15:100902) Avail: NTIS HC A03/MF A01 CSCL 21B

The study of combustible particle clouds inside flame tubes is of fundamental scientific interest as well as a practical concern. Only the suspended concentration is important to the combustion process, so that assurances must be provided that a minimum of particles adheres to the tube wall. This paper demonstrates experimentally the ability to minimize adhesion and agglomeration of acoustically-mixed lycopodium particles within a 5-cm diameter lexan flame tube. The area density of particles (ADP) adhering to the wall of bare lexan tubes was measured at greater than 100 particles/sq mm. The nature of adhesion was found to be clearly electrostatic, with the ADP level aggravated by increased mixing time, vigor, and the concentration of particles. Increases in the conductivity of the air and the tube wall did not affect ADP levels substantially. However, the observed adhesion was reduced to less than 10 p/sq mm when the air was ionized by use of an alpha emitter mounted on the inner walls of the flame tube. Author

32 COMMUNICATIONS AND RADAR

Includes radar; land and global communications; communications theory; and optical communications.

For related information see also *04 Aircraft Communications and Navigation* and *17 Space Communications, Spacecraft Communications, Command and Tracking.* For search and rescue see *03 Air Transportation and Safety,* and *16 Space Transportation.*

N88-26540# Army Test and Evaluation Command, Aberdeen Proving Ground, Md.
DIGITAL COMMUNICATION TRANSMITTER AND RECEIVER TEST PROCEDURES Final Report
15 Jan. 1988 73 p Supersedes N87-17980
(AD-A191218; ITOP-6-2-246) Avail: NTIS HC A04/MF A01 CSCL 25E

This ITOP outlines the test methods used in evaluating the performance and characteristics of general types of transmitters and receivers used for the transmission and reception of digital data, to include single and multichannel devices. The test methods serve as a guide in determining the overall efficiency of such equipment as a function of their design and their recorded performance. This ITOP is limited to methods for observing the operation of test receivers, transmitters, and transceivers under test as major components. It does not consider testing of the human factors or the maintainability aspects of the equipment. The described test procedures are not intended for testing spread spectrum systems. GRA

N88-26541*# National Aeronautics and Space Administration. Pasadena Office, Calif.
DATA VOLUME REDUCTION FOR IMAGING RADAR POLARIMETRY Patent Application
Howard A. Zebker, inventor (to NASA), Daniel N. Held, inventor (to NASA), Jakob J. vanZyl, inventor (to NASA), Pascale C. Dubois, inventor (to NASA), and Lynne Norikane, inventor (to NASA) (Jet Propulsion Lab., California Inst. of Tech., Pasadena.) 5 Apr. 1988 26 p
(Contract NAS7-918)
(NASA-Case-NPO-17184-1-CU; NAS 1.71:NPO-17184-1-CU; US-Patent-Appl-SN-195225) Avail: NTIS HC A03/MF A01 CSCL 17I

Two alternative methods are presented for digital reduction of synthetic aperture multipolarized radar data using scattering matrices, or using Stokes matrices, of four consecutive along-track pixels to produce averaged data for generating a synthetic polarization image. NASA

N88-26542 Pennsylvania Univ., Philadelphia.
MICROWAVE IMAGE UNDERSTANDING AND ITS APPLICATION TO RADAR CROSS SECTION MANAGEMENT Ph.D. Thesis

Hsueh-Jyh Li 1987 258 p
Avail: Univ. Microfilms Order No. DA8725182

The basic scattering properties of a perfectly conducting object are briefly reviewed. In the high frequency region, the scattered field of a complex shaped object can be attributed to a combination of several mechanisms. The advent of high resolution radar enables the consideration of each scattering mechanism separately. The microwave image of a conducting object is interpreted from a new approach, based on the understanding of the scattering mechanism and the image reconstruction algorithm. The connection between various scattering mechanisms and their reconstructed images is then established. Several numerical and experimental examples were included to support this interpretative approach. The algorithm to extrapolate the available data into the mission bands is developed. The term, diaphanization, defined as the technique of reducing RCS and the technique of obscuring an image is introduced. The RCS management is considered not only from a detection perspective, namely the reduction of the target's RCS to elude radar detection, but also from the image point of view where disguising of a target's appearance to impede recognition by an imaging radar is sought. The procedure which employs microwave diversity imaging to diaphanize a target over prescribed spectral and angular windows is given and the robustness of the diversity imaging system to the Gaussian noise is demonstrated. Tradiational techniques for reducing the RCS are applied to RCS magnagement studies. Dissert. Abstr.

N88-26543 George Washington Univ., Washington, D.C.
MULTI-TARGET TRACKING ALGORITHMS FOR CLUTTERED ENVIRONMENTS Ph.D. Thesis
Marco Antonio Mayor 1987 212 p
Avail: Univ. Microfilms Order No. DA8801953

Commercial and military surveillance systems must provide continuous and reliable position information for all targets in the surveillance space in the presence of false returns. These false detections may be produced by unwanted terrain clutter returns and noise sources. To accomplish this task successfully, detection and continuous track of all targets in the surveillance space is required. Two algorithms that allow the tracking of multiple maneuvering and non-maneuvering targets in cluttered environments are presented. The first algorithm describes a general approach for initiating, maintaining, and terminating maneuvering and non-maneuvering targets in cluttered environments. To accomplish this, the method splits the target trajectory when more than one measurement is found in the track validation region and requires multiple scans to confirm true target trajectories and eliminate unlikely tracks. The second tracking approach does not require multiple scans, but instead uses all the available measurement data at each sampling time to update the target track. Simulation results for both algorithms are presented. The results demonstrate good tracking performance for various maneuvering and non-maneuvering target scenarios in cluttered and clear environments. In addition, the exponentially weighted probabilistic data association (EPDA) method is compared to the standard probabilistic data association (PDA) algorithm. The EPDA was shown to have superior tracking performance over the standard PDA method. Dissert. Abstr.

N88-26544*# National Aeronautics and Space Administration. Goddard Space Flight Center, Greenbelt, Md.
THE ROLE OF SPACE BORNE IMAGING RADARS IN ENVIRONMENTAL MONITORING: SOME SHUTTLE IMAGING RADAR RESULTS IN ASIA
M. Imhoff and C. Vermillion Nov. 1986 24 p
(NASA-TM-101175; NAS 1.15:101175) Avail: NTIS HC A03/MF A01 CSCL 17I

The synoptic view afforded by orbiting Earth sensors can be extremely valuable for resource evaluation, environmental monitoring and development planning. For many regions of the world, however, cloud cover has prevented the acquisition of remotely sensed data during the most environmentally stressful periods of the year. This paper discusses how synthetic aperture imaging radar can be used to provide valuable data about the condition of the Earth's surface during periods of bad weather. Examples are given of applications using data from the Shuttle Imaging Radars (SIR) A and B for agriculture land use and crop condition assessment, monsoon flood boundary and flood damage assessment, water resource monitoring and terrain modeling, coastal forest mapping and vegetation penetration, and coastal development monitoring. Recent SIR-B results in Bangladesh are emphasized, radar system basics are reviewed and future SAR systems discussed. Author

N88-26545*# Arizona State Univ., Tempe. Dept. of Electrical and Computer Engineering.
SCATTERING PATTERNS OF DIHEDRAL CORNER REFLECTORS WITH IMPEDANCE SURFACE IMPEDANCES
Semiannual Report, 1 Feb. - 31 Jul. 1988
Constantine A. Balanis, Timothy Griesser, and Kefeng Liu [1988] 29 p
(Grant NAG1-562)
(NASA-CR-183078; NAS 1.26:183078) Avail: NTIS HC A03/MF A01 CSCL 20N

The radar cross section patterns of lossy dihedral corner reflectors are calculated using a uniform geometrical theory of diffraction for impedance surfaces. All terms of up to third order reflections are considered for patterns in the principal plane. The surface waves are included whenever they exist for reactive surface impedances. The dihedral corner reflectors examined have right, obtuse, and acute interior angles, and patterns over the entire 360 deg azimuthal plane are calculated. The surface impedances can be different on the four faces of the dihedral corner reflector; however, the surface impedance must be uniform over each face. Computed cross sections are compared with a moment method technique for a dielectric/ferrite absorber coating on a metallic corner reflector. The analysis of the dihedral corner reflector is important because it demonstrates many of the important scattering contributors of complex targets including both interior and exterior wedge diffraction, half-plane diffraction, and dominant multiple reflections and diffractions. Author

N88-26546# Helsinki Univ. of Technology, Espoo (Finland). Electromagnetics Lab.
APPLICATION OF MOMENT ITERATION METHOD (MIM) TO ELECTROMAGNETIC FIELD COMPUTATION
I. V. Lindell and K. I. Nikoskinen Feb. 1988 19 p
(PB88-194139; ISBN-951-754-405-7; Rept-23) Avail: NTIS HC A03/MF A01 CSCL 20N

The well known method of moments is transformed into a very general iterational form called moment iteration method (MIM), which can be applied to problems involving large or complicated bodies. It is shown that other iterational methods applied in the literature can be conceived as special cases of MIM. The convergence of MIM is not automatic, but it is obtained through acceptance of only such iterational steps which reduce the residual norm. The generality of the method gives possibilities for different strategies of computation. Two examples are considered with two different strategies: one applying zooming expansion functions whose scale decreases during the iteration process, the other one applying statistical method of choosing the expansion functions. Since MIM does not involve orthogonalization processes for choosen expansion functions, the method is simpler and suitable to small computers for which the computing time requirement is not of prime importance. Author

N88-26547# Technische Hogeschool, Delft (Netherlands). Afd. der Elektrotechniek.
NEW HYBRID METHOD FOR SOLVING TIME-DOMAIN INTEGRAL EQUATIONS (ONE-DIMENSIONAL SCATTERING PROBLEMS)
R. Wiemans Dec. 1987 41 p
(PB88-186192; Rept-1987-27) Avail: NTIS HC A03/MF A01 CSCL 20N

A fast and accurate method is presented for solving electromagnetic, time domain, direct scattering problems. Both theory and numerical implementations are discussed. The theory

is explained on the basis of scattering problems for a inhomogeneous, lossy dielectric slab embedded in vacuum. For this one dimensional situation, a recurrent scheme can be derived. Then the theory is extended to a more general case; namely, scattering problems for a slab in between two homogeneous, lossless half-spaces. Finally, some representative numerical results are presented. Author

N88-26548# Lawrence Livermore National Lab., Calif.
PROCEEDINGS OF THE ARRAY SIGNAL PROCESSING SYMPOSIUM: TREATY VERIFICATION PROGRAM
D. B. Harris, comp. Feb. 1988 359 p Symposium held in Livermore, Calif., 14 Jul. 1987; sponsored by DOE/DOE/LLNL
(Contract W-7405-eng-48)
(DE88-008346; CONF-8707152-Vugraphs) Avail: NTIS HC A16/MF A01

A common theme underlying the research these groups conduct is the use of propagating waves to detect, locate, image or otherwise identify features of the environment significant to their applications. The applications considered in this symposium are verification of nuclear test ban treaties, non-destructive evaluation (NDE) of manufactured components, and sonar and electromagnetic target acquisition and tracking. These proceedings cover just the first two topics. In these applications, arrays of sensors are used to detect propagating waves and to measure the characteristics that permit interpretation. The reason for using sensors arrays, which are inherently more expensive than single sensor systems, is twofold. By combining the signals from multiple sensors, it is usually possible to suppress unwanted noise, which permtis detection and analysis of weaker signals. Secondly, in complicated situations in which many waves are present, arrays make it possible to separate the waves and to measure their individual characteristics (direction, velocity, etc.). Other systems (such as three-component sensors in the seismic application) can perform these functions to some extent, but none are so effective and versatile as arrays. The objectives of test ban treaty verification are to detect, locate and identify underground nuclear explosions, and to discriminate them from earthquakes and conventional chemical explosions. Two physical modes of treaty verification are considered: monitoring with arrays of seismic stations (solid earth propagation), and monitoring with arrays of acoustic (infrasound) stations (atmospheric propagation). The majority of the presentations represented in these proceeding address various aspects of the seismic verification problem. DOE

N88-26549# Sandia National Labs., Albuquerque, N. Mex.
HIGH BANDWIDTH OPTOELECTRONIC SIGNAL LINK FOR USE IN AN EMP (ELECTROMAGNETIC PULSE) PLUS RADIATION ENVIRONMENT
P. Garcia 1988 5 p Presented at the 10th Annual Ideas in Science and Electronics Exposition, Albuquerque, N. Mex., 10 May 1988
(Contract DE-AC04-76DP-00789)
(DE88-009254; SAND-87-3081C; CONF-880579-4) Avail: NTIS HC A02/MF A01

Electronic systems which must operate in an electromagnetic pulse (EMP) environment are often enclosed in a conducting box, or Faraday enclosure. The conducting walls must have apertures to allow communications with systems outside the enclosure. EMP leakage is minimized when the aperture diameter is small and has finite thickness. Optical signals, because of their short wavelength, can efficiently traverse apertures that are highly attenuating to EMP signals. A communication link consisting of a GaAlAs laser diode source and a photodiode detector is well-suited to this application. DOE

N88-26550# Lawrence Livermore National Lab., Calif.
A MAXIMUM ENTROPY SOLUTION FOR THE UNDERDETERMINED ELECTROMAGNETIC FIELD WITHIN A VOLUME
R. M. Bevensee Feb. 1988 6 p Presented at the IEEE Antennas and Propagation International Symposium, Syracuse, N.Y., 6 Jun. 1988
(Contract W-7405-eng-48)
(DE88-007020; UCRL-98245; CONF-880658-2) Avail: NTIS HC A02/MF A01

We wish to estimate the sinusoidal electric field within a volume V (sub c), subject to constraints of measured electric field at certain points and zero tangential electric field at others. The field is expanded in a set of K solenoidal and perhaps irrotational modes with unknown amplitudes, defined within the convenient dashed volume V (sub e). Since the number of complex data in the three spatial directions, considerably less than the number of complex amplitudes K, this is an underdetermined problem. We present its Gibbs Maximum Entropy (GME) solution. DOE

N88-26551# Lawrence Livermore National Lab., Calif.
MAXWELL3: A 3D FINITE ELEMENT ELECTROMAGNETIC MODELING CODE
J. B. Grant 15 Apr. 1988 41 p
(Contract W-7405-eng-48)
(DE88-010602; UCID-21285) Avail: NTIS HC A03/MF A01

The simulation of electromagnetic coupling and scattering has grown in importance in recent years due to the vulnerability of integrated circuits to EMI. More specifically, there is a need for simulating electromagnetic scattering from, and coupling to, three dimensional objects. To satisfy the need for accurate, time domain modeling of 3D electromagnetic coupling and scattering MAXWELL3 was developed. The numerical method chosen requires the discretization of the model with a mesh generator. MAXWELL3 then uses the mesh and computes the time domain electric and magnetic fields by integrating Maxwell's curl equations. The output from MAXWELL3 can then be used with a post processor to get the desired information in a graphical form. MAXWELL3 is a linear, time domain, finite element code designed for simulation of electromagnetic fields interacting with three dimensional objects. The discretized model is defined by a collection of homogeneous, isotropic hexahedral elements (six faced, eight noded bricks) which need not correspond to a logically regular grid. Because the elements are not restricted to rectangular boxes, the problem space boundaries and interior surfaces can be of arbitrary shape. DOE

N88-26552# Virginia Univ., Charlottesville. Dept. of Electrical Engineering.
A RANDOM ACCESS ALGORITHM FOR ENVIRONMENTS WITH CAPTURE AND LIMITED FEEDBACK CAPABILITIES Technical Report, 1 Sep. 1986 - 31 Aug. 1988
P. Papantoni-Kazakos and Daniel F. Lyons Mar. 1988 24 p
(Contract N00014-86-K-0742)
(AD-A192233; UVA/525415/EE88/111) Avail: NTIS HC A03/MF A01 CSCL 25B

We consider synchronous packet radio systems, deploying spread-spectrum encoding. In such systems, capture events occur, where in the presence of k simultaneous packet transmissions, a single packet is captured with probability P(k). We adopt the case where P(k) = p q to the (k-1) power, k = or or greater than 1, for some system probabilities p and q, where ternary feedback per slot is available, where in the event of capture the identity of the captured packet is not revealed, and where capture in the presence of a single packet transmission and capture in the presence of multiple transmissions are not distinguishable events. For the above system, we present and analyze a full sensing window random access algorithm. Due to the system model considered, the algorithm inevitably induces losses. Its performance characteristics are the fraction of lost traffic and the per successfully transmitted packet expected delays. We compute the values of those characteristics, for various values of the system and the algorithmic parameters, and for the limit Poisson user model. The algorithm can attain low delays while simultaneously inducing relatively few losses. GRA

N88-26553# Systems Engineering Labs., Inc., Greenbelt, Md.
STOCHASTIC MODELING OF EM SCATTERING FROM FOLIAGE Interim Report, Oct. 1985 - Oct. 1986
Gilmore Blankenship Dec. 1987 68 p

(Contract F19628-85-C-0180)
(AD-A192258; RADC-TR-87-257) Avail: NTIS HC A04/MF A01 CSCL 17I

During the first year of this project, we focussed on the development and evaluation of analytical methods for the description of scattering and absorption of electromagnetic radiation by dense foliage. Three different techniques are discussed in this report. The T-matrix approach to multiple scattering represents the field at an individual scattering center in terms of an equivalent field produced by the other scatterers. It supports several natural approximations for this equivalent field which take multiple scattering processes into account at various levels of detail. The homogenization method is a technique for the derivation of an equivalent representation of the scattering process in terms of an asymptotic analysis of Maxwell's equations in the limit as the separation between the scattering centers approaches zero. Bounds for the effective parameter representations are also discussed. There has been some very interesting recent work in this area on the classical work of Hashin and Shtrikman. We summarize aspects of this work that relate to the problem of scattering in foliage. GRA

N88-26554# Naval Ocean Systems Center, San Diego, Calif.
ANTENNA HEIGHTS FOR THE OPTIMUM UTILIZATION OF THE OCEANIC EVAPORATION DUCT. PART 3: RESULTS FROM THE MEDITERRANEAN MEASUREMENTS, VOLUME 2
J. H. Richter and H. V. Hitney Jan. 1988 291 p
(AD-A192311; AD-E801594; NOSC/TD-1209-Pt-3-Vol-2) Avail: NTIS HC A13/MF A01 CSCL 04B

Extensive evaporation ducting measurements were conducted in the Eastern Mediterranean. The purpose of the measurements was to provide data for model validations and to determine if existing climatologies could be used for estimating the probability of occurrence for evaporation ducting conditions. GRA

N88-26555# Naval Ocean Systems Center, San Diego, Calif.
ANTENNA HEIGHTS FOR THE OPTIMUM UTILIZATION OF THE OCEANIC EVAPORATION DUCT. PART 1: RESULTS FROM THE PACIFIC MEASUREMENTS. PART 2: RESULTS FROM THE KEY WEST MEASUREMENTS, VOLUME 1
J. H. Richter and H. V. Hitney Jan. 1988 220 p
(AD-A192358; NOSC/TD-1209-Pt-1/2-Vol-1) Avail: NTIS HC A10/MF A01 CSCL 20N

Extensive evaporation ducting measurements were conducted over a period of 1 year in the Southern California offshore area and for 2 weeks between Key West and the Marquesas Keys. The purpose of the measurements was to provide data for model validations and to determine if existing climatologies could be used for estimating the probability of occurrence for evaporation ducting conditions. GRA

N88-26556# Air Command and Staff Coll., Maxwell AFB, Ala.
THE USE OF COMMERCIAL OFF-THE-SHELF EQUIPMENT AND ITS IMPACT ON C3 (COMMAND, CONTROL AND COMMUNICATIONS EMP (ELECTROMAGNETIC PULSE) SURVIVABILITY
Melvin D. Hoke, Jr. Apr. 1988 36 p
(AD-A192614; ACSC-88-1250) Avail: NTIS HC A03/MF A01 CSCL 15E

The President's Blue Ribbon Commission on Defense Management has recommended that the military should make greater use of off-the-shelf components, systems, and services (also know as Non-Developmental Items or NDI). This recommendation, if blindly implemented, could have an adverse impact on the survivability of critical command, control, and communications assets. The study evaluates how the electromagnetic pulse (EMP) survivability of a strategic, time-urgent, fixed, ground-based, Command, Control, and Communications (C3) facility would be impacted by the use of off-the-shelf C3 equipments. The study concludes that to have a quantifiable measure of confidence in the facility's EMP survivability, the piece of off-the-shelf equipment under consideration will first have to be subjected to some degree of EMP testing. GRA

N88-26557# Sol Telecommunications Services, Inc., McLean, Va.
RESEARCH IN ELECTROMAGNETIC SHIELDING THEORY. PART1. SHIELDING BY RECTANGULAR ENCLOSURES Final Report, May 1986 - Mar. 1988
Richard L. Monroe 31 Mar. 1988 164 p
(Contract DAAL02-86-C-0052; DA Proj. 1L1-62120-AH-25)
(AD-A192881; HDL-CR-88-052-1) Avail: NTIS HC A08/MF A01 CSCL 09G

General expressions for the electric and magnetic fields at any point inside slotted and continuous, rectangular enclosures exposed to arbitrary external, time harmonic source fields are obtained under the assumption that the enclosures are constructed from good conductors and the slot is small compared to the wavelength of the source field. These expressions consist of infinite series summed over the TE waveguide modes where each term is the product of one or more mode functions and a Fourier coefficient that depends on the spatial variation of the source magnetic field. The Fourier coefficients were evaluated in closed form for two cases: the outside surface of the slot exposed to a spatially uniform magnetic field and the outside surface of one wall of the continuous enclosure exposed to a spatially uniform magnetic field. Frequency domain calculations based on these expressions showed that for frequencies below the enclosure cutoff frequency, the magnetic field at all locations inside a typical slotted enclosure is independent of frequency. For the same range of frequencies the field inside a continuous enclosure is a monotonically decreasing function of frequency. At frequencies above cutoff, the fields in both slotted and continuous enclosures show very complex behavior associated with cavity resonances. GRA

N88-26558# Sol Telecommunications Services, Inc., McLean, Va.
RESEARCH IN ELECTROMAGNETIC SHIELDING THEORY. PART 2: EMP (ELECTROMAGNETIC PULSE) SIMULATION USING SMALL LOOPS Final Report, May 1986 - Mar. 1988
Richard L. Monroe 31 Mar. 1988 46 p
(Contract DAAL02-86-C-0052; DA Proj. 1L1-62120-AH-25)
(AD-A192882; HDL-CR-88-052-2) Avail: NTIS HC A03/MF A01 CSCL 09G

The feasibility of an EMP simulator consisting of a high voltage pulse generator driving a small loop antenna is investigated. It is shown that such a simulator could be used to make direct time domain measurements of the shielding effectiveness of small enclosures like the S280C tactical electronics shelter using a method analogous to the frequency domain technique employed in the small loop test described in MIL-STD-285 and IEEE-299. Specifications are given for a simulator that would reproduce the waveform, structure, and polarization of an EMP field over a 4 m2 plane surface with a peak field of 2.7 A/m. The simulator consists of a 2 MV generator with a 0.755 pf storage capacitor and a resistance of 331 ohms driving a 0.3 m square loop formed from conductors with 1 cm radii. In operation, the loop is oriented with its plane perpendicular to the surface of the enclosure and its center 2.5 m from that surface. GRA

N88-26559# Naval Ocean Systems Center, San Diego, Calif.
EFFECTS OF ATMOSPHERIC MODEL LAYERING ON LOWTRAN 6 CALCULATIONS OF 8-12 MICROMETERS NEAR-HORIZON SKY RADIANCES
F. G. Wollenweber Jan. 1988 11 p
(AD-A192969; NOSC/TD-1193) Avail: NTIS HC A03/MF A01 CSCL 04A

Measurements of 8- to 12-micrometer near-horizon sky radiances and meteorological parameters over the ocean near San Diego, California were used to evaluate the sky radiance algorithm of LOWTRAN 6. Discrepancies in measured and calculated sky radiances previously attributed to the neglect of multiple scattering effects of aerosols can be overcome by introducing additional low-level layers in the calculations of LOWTRAN 6. A comparison between radiance calculations using the single scattering, additive-layer approach and those using a

multiple scattering version of LOWTRAN 6 raises questions about the applicability of the multiple scattering approach in the far infrared region. GRA

N88-26560# Aerospace Corp., El Segundo, Calif. Electronics Research Lab.
COHERENT RF ERROR STATISTICS
R. B. Dybdal and R. H. Ott 1 Mar. 1988 34 p
(Contract F04701-85-C-0086)
(AD-A193002; TR-0086(6925-05)-1; SD-TR-88-07) Avail: NTIS HC A03/MF A01 CSCL 20N

RF error statistics for power, voltage, and phase have been developed under the assumptions that the error component is coherently related to the desired signal, its magnitude is constant, and that its phase is equally likely and uniformly distributed from 0 to 360 deg. The error statistics which result from these assumptions have non-zero mean values for power and voltage and standard deviations which differ significantly from those projected on the basis of Gaussian statistics for incoherent errors. These statistics will be applied to typical component errors which arise in an overall system error budget. GRA

N88-26561# Technische Univ., Berlin (West Germany). Fachbereich fuer Elektrotechnik.
SIGNAL PROCESSING IN DIGITAL SPEECH TRANSMISSION SYSTEMS Ph.D. Thesis [SIGNALAUFBEREITUNG IN DIGITALEN SPRACHUEBERTRAGUNGSSYSTEMEN]
Benedito G. AguiarNeto 1987 140 p In GERMAN Sponsored by the Deutsches Akademischen Austauschdienst
(ETN-88-92122) Avail: NTIS HC A07/MF A01

Acoustic noise suppression in speech environments by emitter signal processing and noise cancelling procedure is performed. Optimal filter theory and theory of short time spectral evaluation are used. Necessary statistical information on disturbance signals in speech signals by short time analysis are obtained. Optimal filter theory is based on Wiener-Kolmogoroff filtering techniques and spectral subtraction. Optimal filter impulse is determined by the minimum mean square error. ESA

N88-26562# Physics and Electronics Lab. TNO, The Hague (Netherlands).
ERROR PERFORMANCE OF VOICE BAND DATA SIGNALS WITH AN OVERLOADED DELTA MODULATOR
C. Eberwijn and Tj. H. Khoe Jan. 1987 12 p
(Contract A73/KL/035)
(FEL-1987-05; ETN-88-92567) Avail: NTIS HC A03/MF A01

Error measurements for digital transmission of voice band data signals in 2400 bit/sec four-phase shift keying signals in combination with an overloaded 16 kbs digitally controlled delta modulator are discussed. Overloading a delta codec (+2 dBm input level) results in an error improvement factor (measured channel bit error rate (BER) 16 kbs compare with injected trunk BER, 265 kbs) of 10 in the BER range of 0.0001 to 0.1. An input level of -24 dBm (point of highest signal to noise ratio and lowest BER within the normal range of input levels) results in a measured channel BER which almost equals the injected BER in the range of 0.0001 to 0.1. ESA

N88-26563# Physics and Electronics Lab. TNO, The Hague (Netherlands).
THE PERFORMANCE OF EUROCOM ERROR CORRECTION SCHEMES FOR DATA COMMUNICATIONS
E. N. deBrieder Jul. 1987 16 p
(Contract A82/KL/060)
(FEL-1987-56; ETN-88-92571) Avail: NTIS HC A03/MF A01

The behavior of forward error correction (FEC) was examined in an environment with different error levels, with error-injection on the trunk. The results of the FEC-measurement are compared with the theory. The FEC-measurement shows the performance of the Eurocom FEC-function. For a bit error rate (BER) of 0.01, the FEC-improvement factor is 10,000. The FEC-improvement factor is not contant, but depends on the injected BER. Lowering the BER results in an increase of the improvement factor. The uncommitted logic array operates according to the Eurocom class 1, 2 and 4 requirements. ESA

N88-26564# National Aerospace Lab., Amsterdam (Netherlands). Space/Informatics Div.
DOCUMENT TRANSFER BY A DIGITAL SATELLITE LINK
H. J. Simons, J. Dijk, and A. P. Verlijsdonk (Technische Hogeschool, Eindhoven, Netherlands) 13 Nov. 1986 9 p Presented at the Conference on New Systems and Services in Telecommunication, Luik, Belgium, 12-14 Nov. 1986 Sponsored by the Dutch Ministry of Education and Science
(NLR-MP-86071-U; B8805304; ETN-88-92605) Avail: NTIS HC A02/MF A01

The general user and system requirements for an electronic document delivery (EDD) system are specified and a protocol for a high-resolution EDD system by satellite is given. The proposed system is compatible with the APOLLO system concept for bulk data transfer via satellite, developed by the European Space Agency. Proposals for transmission experiments via the special services payload and the 20/30 GHz transponder of the OLYMPUS satellite are made. ESA

N88-26565*# Ohio State Univ., Columbus. ElectroScience Lab.
RADAR CROSS SECTION STUDIES/COMPACT RANGE RESEARCH Final Report
W. D. Burnside, A. K. Dominek, I. J. Gupta, E. H. Newman, P. H. Pathak, and L. Peters, Jr. Jun. 1988 66 p
(Grant NsG-1613)
(NASA-CR-183124; NAS 1.26:183124; ESL-716148-31) Avail: NTIS HC A04/MF A01 CSCL 17I

A summary is given of the achievements of NASA Grant NsG-1613 by Ohio State University from May 1, 1987 to April 30, 1988. The major topics covered are as follows: (1) electromagnetic scattering analysis; (2) indoor scattering measurement systems; (3) RCS control; (4) waveform processing techniques; (5) material scattering and design studies; (6) design and evaluation of design studies; and (7) antenna studies. Major progress has been made in each of these areas as verified by the numerous publications produced. Author

N88-26566*# National Aeronautics and Space Administration. Lewis Research Center, Cleveland, Ohio.
COSPAS/SARSAT 406-MHz EMERGENCY BEACON DIGITAL CONTROLLER
William D. Ivancic Jul. 1988 18 p
(NASA-TM-100859; E-4064; NAS 1.15:100859) Avail: NTIS HC A03/MF A01 CSCL 20N

The digital control portion of a low-cost 406-MHz COSPAS/SARSAT emergency beacon has been designed and breadboarded at the NASA Lewis Research Center. This report discusses the requirements and design tradeoffs of the digital controller and describes the hardware and software design, which is available only to United States citizens and companies. Author

N88-26567*# Texas Univ., Austin. Bureau of Engineering Research.
LASER RANGING DATA ANALYSIS Final Report, 1987
19 Aug. 1988 109 p
(Contract NAS5-27344; Grant NAG5-1021)
(NASA-CR-183115; NAS 1.26:183115) Avail: NTIS HC A06/MF A01 CSCL 17I

Near real-time Lageos laser ranging data are analyzed in terms of range bias, time bias, and internal precision, and estimates for earth orientation parameters X(sub p), Y(sub p), and UT1 are obtained. The results of these analyses are reported in a variety of formats. Copies of monthly summaries from November, 1986 through November, 1987 are included. B.G.

N88-26568* National Aeronautics and Space Administration. Lyndon B. Johnson Space Center, Houston, Tex.
METHOD AND APPARATUS FOR MEASURING DISTANCE Patent
Christopher L. Lichtenberg, inventor (to NASA), Paul W. Shores, inventor (to NASA), and Herbert S. Kobayashi, inventor (to NASA) 12 Jul. 1988 14 p Filed 20 Feb. 1986 Supersedes N86-24879 (24 - 15, p 2445) Sponsored by NASA
(NASA-Case-MSC-20912-1; US-Patent-4,757,315; US-Patent-Appl-SN-831193; US-Patent-Class-342-125; US-Patent-Class-342-43; US-Patent-Class-342-51; US-Patent-Class-342-127) Avail: US Patent and Trademark Office CSCL 17I

The invention employs a continuous wave radar technique and apparatus which can be used as a distance measuring system in the presence of background clutter by utilizing small passive transponders. A first continuous electromagnetic wave signal S sub 1 at a first frequency f sub 1 is transmitted from a first location. A transponder carried by a target object positioned at a second (remote) location receives the transmitted signal, phase-coherently divides the f sub 1 frequency and its phase, and re-transmits the transmitted signal as a second continuous electromagnetic wave signal S sub 2 at a lower frequency f sub 2 which is a subharmonic of f sub 1. The re-transmitted signal is received at the first location where a measurement of the phase difference is made between the signals S sub 1 and S sub 2, such measuremnt being indicative of the distance between the first and second locations.

Official Gazette of the U.S. Patent and Trademark Office

33 ELECTRONICS AND ELECTRICAL ENGINEERING

Includes test equipment and maintainability; components, e.g., tunnel diodes and transistors; microminiaturization; and integrated circuitry.

For related information see also *60 Computer Operations and Hardware* and *76 Solid-State Physics.*

N88-26569*# Hampton Inst., Va. Dept. of Physics.
EFFECTS OF COSMIC RAYS ON SINGLE EVENT UPSETS Annual Report
Calvin W. Lowe, Adebisi O. Oladipupo, and Demetrius D. Venable 14 Jul. 1988 45 p
(Grant NAG5-929)
(NASA-CR-183053; NAS 1.26:183053) Avail: NTIS HC A03/MF A01 CSCL 09C

The efforts at establishing a research program in space radiation effects are discussed. The research program has served as the basis for training several graduate students in an area of research that is of importance to NASA. In addition, technical support was provided for the Single Event Facility Group at Brookhaven National Laboratory. Author

N88-26570# Instituto de Pesquisas Espaciais, Sao Jose dos Campos (Brazil).
ANALYSIS OF NETWORKS WITH PARAMETERS S: GENERALIZATION OF JUNCTION MATRIX [ANALISE DE REDES COM PARAMETROS S: GENERALIZACAO DA MATRIZ DE LIGACAO]
Edson GusellaJunior May 1988 8 p In PORTUGESE Submitted for publication
(INPE-4535-PRE/1282) Avail: NTIS HC A02/MF A01

A generalization is presented of a junction matrix represented by OKOSHI (1) for analysis of networks of planar circuits with elements characterized by parameters of scattering, S. This generalization permits the connection of access of the elements in parallel, series, and other forms. Since parameters S exist in more conditions than parameters Z and Y, its use is convenient for network analysis, for dc of microwaves, where its use is sufficiently known. Author

N88-26571# Central Research Inst. of Electric Power Industry, Tokyo (Japan).
DEVELOPMENT OF EXTERNAL COOLING CRYO-RESISTIVE CABLE SYSTEMS. PART 2: INSULATION CHARACTERISTICS ON 66 kV RATED CRYO-RESISTIVE TESTING CABLE
Kaoru Ishihara, Shige Akita, Hiroshi Suzuki, Junichi Ogata, and Minoru Nemoto Aug. 1987 36 p In JAPANESE; ENGLISH summary
(DE88-770191; CRIE-T-86080-Pt-2) Avail: NTIS (US Sales Only) HC A03

Cryo-resistive cable system was tested to demonstrate dielectric characteristics. Dielectric characteristics of 66kV cryo-resistive cable at the start of immersion cooling in the liquid nitrogen were 2.25 specific dielectric constant and 0.18 percent dielectric loss which was less than 0.4 percent , the aimed value. Electrostatic capacity and dielectric loss tangent of dielectric characteristics under the applied voltage did not depend on the voltage and the dielectric loss was less than 0.4 percent through the temperature range from -170 to -190C. These values fulfilled the specifications on 275kV class cryo-resistive cable design. The tested cable passed the cable test on 66kV oil-filled cable (ac 90kV, 10 min), but broken down at ac 110kV on the way to endurance testing voltage 130kV. The breakdown occurred due to the mechanical damage of cable insulator by bending and thermal contraction of the cable. It is necessary from these facts to develop flexible cable terminal and joint which can absorb the contraction to realize 275kV cryo-resistive cable. (19 figs, 7 tabs, 15 refs). DOE

N88-26572# National Bureau of Standards, Gaithersburg, Md. Center for Electronics and Electrical Engineering.
CENTER FOR ELECTRONICS AND ELECTRICAL ENGINEERING TECHNICAL PUBLICATION ANNOUNCEMENTS COVERING CENTER PROGRAMS, JULY TO SEPTEMBER 1987
E. J. Walters Apr. 1988 27 p
(PB88-196530; NBSIR-88/3748) Avail: NTIS HC A03/MF A01 CSCL 09C

This is the fourteenth issue of a quarterly publication providing information on the technical work of the National Bureau of Standards Center for Electronics and Electrical Engineering. The issue of the Center for Electronics and Electrical Engineering Technical Publication Announcements covers the third quarter of calendar year 1987. Abstracts are provided by technical area for papers published this quarter. Author

N88-26573# Helsinki Univ. of Technology, Espoo (Finland). Electromagnetics Lab.
VARIATIONAL ANALYSIS OF DIELECTRICALLY LOADED MULTIDEPTH CORRUGATED WAVEGUIDES
M. I. Oskanen Jan. 1988 23 p
(PB88-193602; Rept-22; ISBN-951-754-389-1) Avail: NTIS HC A03/MF A01 CSCL 09C

Propagation behavior in a multidepth corrugated waveguide is analyzed. The analysis is based on the theory of nonstandard eigenvalues and variational methods. The method is tested for an empty dual-depth corrugated waveguide, which results have been previously calculated in the literature by using surface-impedance and space harmonic methods. These methods are summarized. Also some space harmonic formulas are rederived into the form where the fundamental surface admittance component is separated from the higher order terms. It is seen that with elementary trial functions very accurate dispersion relations can be obtained by the variational method. Encouraged by this, the method is then extended for a tri-depth guide operating in three different frequency bands, and for dielectrically loaded dual- and tri-depth guides. The latter appear encouraging because of their simpler fabrication techniques. GRA

N88-26574# California Univ., Berkeley. Lawrence Berkeley Lab.
AMBIENT TEMPERATURE SECONDARY LITHIUM BATTERIES USING LiAl LITHIUM INSERTION ANODES Final Report
K. M. Abraham Dec. 1987 40 p

(Contract DE-AC03-76SF-00098)
(DE88-008394; LBL-24647) Avail: NTIS HC A03/MF A01

The feasibility of using Li(sub x)Fe2O3, Li(sub x)WO2 and beta-LiAl as alternative anodes for ambient temperature secondary Li batteries was studied. A convenient procedure for the synthesis of these materials at normal temperature and pressure conditions has been developed. The electrochemical behavior of the alternative anode materials was studied in cells utilizing a TiS2 cathode and PC-LiClO4 electrolyte. While the lithiated oxides have exhibited good reversibility, their equivalent weights are too high for use in high energy density batteries. The experimentally determined value for the reversible Li capacity of Li(sub x)Wo2 indicated an equivalent weight of 370 for this anode. The corresponding value for Li6Fe2O3 was 201. The results obtained with the beta -LiAl, synthesized by the new procedure, were too limited to draw meaningful conclusions regarding its usefulness in practical cells. Amorphous V2O5, Cr3O8 and Li(sub x)CoO2 were evaluated as cathodes for possible use in conjunction with the alternative anodes. While the capacities of alpha-V2O5 and Cr3O8, of 2.4 LiV2O5 and 4.5 Li/Cr3O8, respectively, are attractive for practicel applications, these positive electrodes exhibited rather low rate capabilities. The performance of Li(sub x)CoO2 was inferior to the results previously reported for the cathode and might have been influenced by the electrolyte employed in our studies. DOE

N88-26575# Central Research Inst. of Electric Power Industry, Tokyo (Japan).
LOSS EVALUATION OF SELF-COMMUTATED POWER CONDITIONER FOR BATTERY ENERGY STORAGE SYSTEM
Tadao Ishikawa Jun. 1987 38 p In JAPANESE
(DE88-752075; CRIE-T-86032) Avail: NTIS (US Sales Only) HC A03/MF A01

Regarding the loss of the voltage-fed self-commutated type converter to be used for the battery energy storage system of magawatt class, its loss calculation formulas in conformity with the operating conditions of the converter are derived, and the operation control range of the converter taking into consideration the loss is also studied. Namely, as to the loss of the switching elements playing a very important role in the efficiency calculation of the converter, a new calculation method is derived that is capable of evaluating the loss more accurately and also corresponding to the variation of the operating conditions of the battery. This calculation method was applied to the simulator of the battery energy storage system in which actual machines were used as the models, and it was confirmed that the losses coincide well under whatever operating conditions. Moreover, to minimize the margin of the actual operating control conditions of the converter against such factors as the operating output of the storage system, the 1-5 characteristics in conformity with the charge and discharge of the battery, and the loss of the converter, the value of the range taking into consideration the loss has been calculated. DOE

N88-26576# Lawrence Livermore National Lab., Calif.
DEGRADATION OF BEAM BRIGHTNESS BY FIELD EMISSION FROM A CATHODE SHROUD
Y. J. Chen, J. K. Boyd, and W. C. Turner 15 Mar. 1988 25 p Presented at the Particle Beam Physics Topical Meeting, Baltimore, Md., 18 Apr. 1988
(Contract W-7405-eng-48)
(DE88-008345; UCRL-98043; CONF-880494-1) Avail: NTIS HC A03/MF A01

Degradation of beam brightness by field emission from the cathode shroud is studied by using particle-in-cell codes: DPC and ST. We find that emission from the space charge limited cathode is reduced due to the presence of the shroud electrons in the main beam. A scaling law for beam emittance is derived analytically. We find that emittance squared is linearly proportional to the fraction of beam current carried by field emitted electrons. The beam brightness is degraded by a factor of two when field emission electrons constitute 6.25 percent of the beam current. DOE

N88-26577# Lawrence Livermore National Lab., Calif.
A MODEL FOR INSULATED WIRES IN THE METHOD OF MOMENTS CODE NEC (NUMERICAL ELECTROMAGNETICS CODE)
G. J. Burke Jan. 1988 34 p
(Contract W-7405-eng-48)
(DE88-008920; UCID-21301) Avail: NTIS HC A03/MF A01

The numerical electromagnetics code (NEC) is a general purpose computer program for modeling antennas by the numerical solution of an integral equation. NEC solves an electric field integral equation for wire structures and a magnetic field integral equation for surfaces, and can evaluate the effect of an interface between air and a lossy half space by means of a reflection coefficient approximation or the rigorous solution involving Sommerfeld integrals. This report describes an extension of NEC to model an insulating sheath on wires in air or buried in a lossy half space including, if desired, the effect of the air-ground interface. DOE

N88-26578# Sandia National Labs., Albuquerque, N. Mex.
EXPLORATORY BATTERY TECHNOLOGY DEVELOPMENT AND TESTING REPORT FOR 1986
N. J. Magnani, R. P. Clark, J. W. Braithwaite, D. M. Bush, P. C. Butler, J. M. Freese, K. R. Grothaus, K. D. Murphy, and P. E. Shoemaker Feb. 1988 143 p
(Contract DE-AC04-76DP-00789)
(DE88-009870; SAND-87-3094) Avail: NTIS HC A07/MF A01

Sandia National Laboratories, Albuquerque, has been designated as Lead Center for the Exploratory Battery Technology Development and Testing Project, which is sponsored by the U.S. Department of Energy's Office of Energy Storage and Distribution. In this capacity, Sandia is responsible for the engineering development of advanced rechargeable batteries for both mobile and stationary energy-storage applications. This report details the technical achievements realized in pursuit of the Lead Center's goals during calendar year 1986. DOE

N88-26579# General Electric Co., Largo, Fla. Neutron Devices Dept.
A BIBLIOGRAPHY AND AUTHOR INDEX FOR ELECTRICAL DISCHARGES IN VACUUM (1897-1986)
H. C. Miller Mar. 1988 395 p
(Contract DE-AC04-76DP-00656)
(DE88-008744; GEPP-TIS-366e) Avail: NTIS HC A17/MF A01

This bibliography covers the field of electrical discharges in vacuum, comprising both electrical breakdown in vacuum and vacuum arcs. A brief reference review section lists some papers which would be helpful to the novice in this field. The bulk of this paper consists of bioliographic listings, arranged by year of publication and alphatectically by first author within each year. An author index refers one to all papers authored or coauthored by a particular person. There are 3483 papers listed through December 1986. DOE

N88-26580# Argonne National Lab., Ill.
MODELING AND THERMAL MANAGEMENT OF ADVANCED BATTERIES
J. Lee 1988 13 p Presented at the 3rd Annual Battery Conference on Applications and Advances, Long Beach, Calif., 12 Jan. 1988
(Contract W-31109-eng-38)
(DE88-010023; CONF-880133-3) Avail: NTIS HC A03/MF A01

Mathematical modeling has been an efficient and powerful tool for evaluating thermal behavior of batteries and electrochemical cells. In this paper, the methodology and applications of thermal modeling in various advanced battery systems are reviewed. Potential needs and extensions of battery thermal modeling are discussed. DOE

N88-26581# Argonne National Lab., Ill.
MOLTEN SALT ELECTROLYTES FOR HIGH-TEMPERATURE LITHIUM CELLS
D. R. Vissers, L. Redey, and T. D. Kaun 1988 3 p Presented at the 4th International Meeting on Lithium Batteries, Vancouver,

British Columbia, 23 May 1988
(Contract W-31109-eng-38)
(DE88-010058; CONF-880598-3) Avail: NTIS HC A02/MF A01

The high-temperature lithium cells under study at the Argonne National Laboratory (ANL) utilize either Li-Al, Li-Si, or Li-Al-Si negative electrodes; FeS, FeS2, or (Ni, Fe)S2 positive electrodes; and a molten salt electrolyte. The cells operate in the temperature range of 400-475 C, depending on the electrolyte composition and choice of positive electrode. At present, Gould Inc. is fabricating and testing prismatic Li-Al-SiFeS cells, and ANL is evaluating both cylindrical and prismatic designs for the Li-AlFeS2 cell. In the past, the bulk of the research and development effort on the lithium sulfide cells emphasized the Li-AlFeS over the Li-AlFeS2 system because of the poor capacity retention of the Li-AlFeS2 system and the cost of the current collector materials associated with the FeS2 electrode. However, because the Li-AlFeS2 system has the potential of yielding cells with higher specific energy and power than those obtainable with the Li-AlFeS system, it is now receiving greater attention. In the paper, we will review the importance of the molten salt electrolyte in the performance of the Li-AlFeS system and the recent breakthroughs in capacity retention achieved with this system. DOE

N88-26582# International Fuel Cells Corp., South Windsor, Conn.
PHOSPHORIC ACID ELECTRIC UTILITY FUEL CELL TECHNOLOGY DEVELOPMENT Technical Progress Report, quarter ending 31 Oct. 1987
1987 10 p
(Contract DE-AC21-83FE-60338)
(DE88-010187; DOE/FE-60338/2557; FCR-9206; TPR-33) Avail: NTIS HC A03

The Department of Energy has initiated this program to advance phosphoric acid electric utility cell stack technology and to reduce cell stack cost. The cell stack has a nominal 10-sq ft active area and operates at 120 psia/405 F. The program comprises six parallel phases, which culminate in a full-height, 10-sq ft stack verification test. The only active technical task under this program is Phase 6, Task 5-Operational Testing. The objective of this task is to conduct additional testing of the full-height 10-sq ft stack with a goal of reaching 3500 hours. DOE

N88-26583# SRI International Corp., Menlo Park, Calif.
DEVELOPMENT OF LIQUID METAL FIELD-EMISSION SOURCES FOR USE IN FAST REPETITIVE OPENING SWITCHES Final Technical Report, 1 Jul. 1986 - 31 Oct. 1987
Michael J. Coggiola Jan. 1988 79 p
(Contract N00014-86-K-0596)
(AD-A192230; SRI-MP-88-007) Avail: NTIS HC A05/MF A01 CSCL 09A

Liquid metal field-emission sources appear to have desirable characteristics as the active element of a high-current repetitive switch. The results we obtained indicate that many of the operational parameters of these devices can be controlled, although the mechanisms are not yet understood. In particular, the enhanced mode of operation found for the Gallium/Indium/Argon system gives very large, narrow current pulses by an unknown mechanism. The use of various diagnostics, including the dispersed optical emission, may provide some insight into these mechanisms. Additional research is required to determine the optimum configuration for a practical switch. The choice of metals, the diode geometry, and the triggering mechanism will need to be addressed before the liquid metal field-emission device can be incorporated into an active switch. GRA

N88-26584# Georgia Tech Research Inst., Atlanta.
INTEGRATED OPTOELECTRONIC CIRCUITS UTILIZING InGaAsP GROWN BY MOLECULAR BEAM EPITAXY (ERBIUM DOPING OF MBE GaAs) Final Report, 1 Apr. 1985 - 31 Dec. 1986
E. L. Meeks 1987 19 p
(Contract N00014-83-K-2017)
(AD-A192269) Avail: NTIS HC A03/MF A01 CSCL 09E

A study of erbium doping of Molecular Beam Epitaxy(MBE) grown gallium arsenide layers was initiated. In the present work, the low temperature photoluminescence of Er in GaAs was confirmed and the growth conditions necessary to produce Er doped layers were established. Secondary Ion Mass Spectrometry (SIMS) data on the MBE grown GaAs:Er doped layers confirm the presence of Er in the layers and the increase in Er doping with source temperature. Photoluminescence measurements on three samples of MBE grown GaAs: Er layers were very interesting. There is no evidence of any broad background which is observed in ion-implanted samples. The intense and sharply structured photoluminescence of MBE grown Er doped GaAs centered around 1.54 microns has been confirmed. GRA

N88-26585# Illinois Univ., Urbana. Electromagnetics Lab.
MICROWAVE AMPLIFIERS Final Report, 7 Sep. 1984 - 30 Sep. 1987
S. L. Chuang, S. W. Lee, S. M. Lee, and D. Ahn 25 Jan. 1988 147 p
(Contract F33615-84-K-1557)
(AD-A192974; AFWAL-TR-87-1144) Avail: NTIS HC A07/MF A01 CSCL 09A

A two-dimensional model for GaAs MESFET has been developed to study its linear and nonlinear microwave performances. The I-V characteristics curves for the intrinsic GaAs MESFET are obtained and compared with those for experimental measurements. Scattering parameters are calculated using the complete microwave model, which includes the intrinsic model and the parasitic elements, and compared with experimental findings. Reasonably good agreement between our calculation and the experimental measurements are obtained. Microwave nonlinear performances for a GaAs MESFET are simulated based on the large signal model. The microwave ouput signal in the time domain is simulated with two large input signals of different frequencies. Then the output power at the fundamental, first-order, second-order, and third-order harmonics are obtained. The power gains for the fundamental and the third-order spur at different bias points are calculated. Various HEMT models have been investigated. Three analytical models, the classical Fermi-Dirac, the two-level two-dimensional Electron Gas (2DEG) and the extended 2DEG models, are employed to study the electron concentration at the heterointerface where the electrons have very high mobility which is responsible for the ultra-fast transistor action due to the separation of electrons and ionized donors. GRA

N88-26586# Aerospace Corp., El Segundo, Calif. Electronics Research Lab.
JFET/SOS (JUNCTION FIELD-EFFECT TRANSISTOR/SILICON-ON-SAPPHIRE) DEVICES: GAMMA-RADIATION-INDUCED EFFECTS
Linda F. Halle, Thomas C. Zietlow, and Charles E. Barnes 1 Mar. 1988 29 p
(Contract F04701-85-C-0086)
(AD-A193001; TR-0086(6925-07)-3; SD-TR-88-17) Avail: NTIS HC A03/MF A01 CSCL 18G

Enhancement and depletion mode JFETs have been fabricated on silicon-on-sapphire substrates. When these devices are irradiated under bias with a Co-60 source, their drain currents increase, and their threshold voltages shift in such a way that the devices become more difficult to pinch off. These effects can be explained by positive charge trapping at the silicon/sapphire interface. Gate to drain leakage currents also increase, and can be traced to interface effects at the gate edges rather than to the passivating oxide. These effects were studied as a function of dose rate and postirradiation annealing. Deep-level transient spectroscopy (DLTS) was performed prior to and following both irradiation and anneal on both the gate-drain and gate-source p-n junctions. DLTS trap bands were observed whose characteristics depended on the depth of the depletion layer and on the total gamma dose received. The DLTS spectra suggest that a continuum of levels is responsible for the bands, and that the emission kinetics are influenced by band bending at the Si/sapphire interface. The major bands corresponded in temperature with steps in

capacitance-temperature curves. A correlation of these steps with the transistor characteristics suggests that channel pinch off can be influenced by capture and emission at deep centers. GRA

N88-26587# Aerospace Corp., El Segundo, Calif. Lab. Operations.
NICKEL HYDROGEN CELL POSITIVE-ELECTRODE STUDIES: COBALT SEGREGATION IN REDUCING ENVIRONMENTS
Albert H. Zimmerman 22 May 1987 44 p
(Contract F04701-85-C-0086)
(AD-A193025; TR-0086A(2945-01)-4; SD-TR-87-64) Avail: NTIS HC A03/MF A01 CSCL 09A

Nickel electrodes from nickel hydrogen battery cells that had exhibited anomalously low capacities have been tested. Electrode characterization tests showed that changes had occurred in the electrode active material to increase the charge and discharge voltages. The increased charge voltages resulted in a decrease in charge efficiency. These changes apparently resulted from storage of the cell at low voltage with excess hydrogen present in the cell. Chemical and physical analyses indicated that cobalt, a 10% additive in the nickel electrode active material, had undergone segregation from the active material to form a cobalt rich compound that is not normally present in the electrodes. This chemical change is felt to be largely responsible for the changes in electrode performance. A model for the processes causing cobalt segregation is described, and test results are presented to support the model. GRA

N88-26588# Institut National Polytechnique, Grenoble (France). Lab. d'Electromagnetisme, Micro-Ondes et Opto-Electronique.
STUDY AND IMPLEMENTATION OF ULTRAHIGH FREQUENCY COUPLING DEVICES USING THE FIN LINE TECHNOLOGY Ph.D. Thesis [ETUDE ET REALISATION DE COUPLEURS HYPERFREQUENCE EN TECHNOLOGIE LIGNE A AILETTES]
Eric Imbert 1988 127 p In FRENCH
(ETN-88-92307) Avail: NTIS HC A07/MF A01

Analytic procedures for computer aided design are presented. The resulting expressions are derived from a generalized spectral method. The specific characterization of each type of coupler is carried out experimentally and analytically. The types studied include the ring coupler, the hybrid coupler, and the branch-line coupler. ESA

N88-26589# Technische Univ., Munich (West Germany). Lehrstuhl fuer Energiewirtschaft und Kraftwerkstechnik.
COMPUTER CONTROLLED PROCEDURES FOR TRACTION BATTERY POWER PERFORMANCE TESTS Ph.D. Thesis [PROZESSRECHNERGESTUETZTES VERFAHREN ZUR PRUEFUNG DER LEISTUNGSERGIEBIGKETT VON TRAKTIONSBATTERIEN]
Ulrich Wagner 1987 131 p In GERMAN
(ETN-88-92352) Avail: NTIS HC A07/MF A01

Software and hardware design for test procedures of the main characteristics of electric vehicle battery systems adapted to various applications and comparison between systems on the same utilization are described. Electrochemical equations for the charge and discharge process of lead-acid batteries are reviewed. Definition of choice parameters for quality control, design of a computer controlled bench test equipment, determination of performance requirement limits, and simulation of practical charge-discharge cycles are developed. ESA

N88-26590# Technische Univ., Berlin (West Germany). Fachbereich fuer Elektrotechnik.
CONTRIBUTION TO SPEED REGULATION OF SMALL MOTORS WITH PHASE-LOCKED LOOPS Ph.D. Thesis [BEITRAG ZUR DREHZAHLREGELUNG VON KLEINMOTOREN MIT PHASENREGELKREISEN]
Weitang Zhang 1987 177 p In GERMAN
(ETN-88-92373) Avail: NTIS HC A09/MF A01

Nonlinear properties of phase-frequency detector (PFD-type 4) in phase-locked loop (PLL) motor regulation are investigated. Frequency and phase characteristic lines are given and a mathematical model for the PFD-type 4 is presented. The validity of the model is confirmed by simulation and experimental investigations. An improved PFD-type 5 is developed enabling a better behavior for the PLL motor control system. Theoretical and experimental results are compared with success. ESA

N88-26591# Technische Univ., Brunswick (West Germany). Fakultaet fuer Maschinenbau und Elektrotechnik.
EXTINCTION BEHAVIOR OF LOW VOLTAGE SWITCHING ARC UNDER CONSIDERATION OF CATHODIC COATINGS AND DYNAMIC ARC COLUMN Ph.D. Thesis [DAS STROMNULLDURCHGANGS-VERHALTEN VON NIEDERSPANNUNGS-SCHALTLICHTBOEGEN UNTER BERUECKSICHTIGUNG VON KATHODENSCHICHT UND DYNAMISCHER BOGENSAEULE]
Norbert Reimann 1987 138 p In GERMAN
(ETN-88-92384) Avail: NTIS HC A07/MF A01

Experimental study of two mechanisms of low voltage Ac-arc extinction conditions is described: the cathodic effect and the column cooling phenomena for electric currents between 350 A to 3.5 kA at 550 V. Cathodic effect is examined for two contact materials, one favorable (Ag/CdO) and one unfavorable (tungsten). Thermal behavior of the arc column is surveyed in air and SF6 environments. Combination effects of both types of extinction mechanisms are investigated by a mathematical model for various arc and switching parameters. Simulation computation is performed for the determination of extinction limits applied to real electric networks. ESA

N88-26592# Technische Univ., Brunswick (West Germany). Fakultaet fuer Maschinenbau und Elektrotechnik.
PERMANENT MAGNET EXCITATION OF AXIAL FLOW SYNCHRONOUS MACHINES WITH HIGH ROTATION MOMENT Ph.D. Thesis [DAUERMAGNETERREGTE AXIALFELDSYNCHRONMASCHINEN MIT HOHEM DREHMOMENT]
Rolf Mayer 1987 190 p In GERMAN
(ETN-88-92385) Avail: NTIS HC A09/MF A01

Computation of axial magnetic flux machines under consideration of radial dependant geometric, and electric and magnetic properties is presented. A three-dimensional permanent magnet flux model provides the conditions for the establishment of a programmable design algorithm. Analytical magnetic field study leads to the prediction of torque oscillations generated by harmonic effects of air gap field and permits their reduction. Calculus results obtained are used for the design and fabrication of a traction motor of 200 kW with a torque of 3.8 kNm at 500 t/min. ESA

N88-26593# Physics and Electronics Lab. TNO, The Hague (Netherlands).
AN INTEGRATED CIRCUIT FOR ERROR PROTECTION IN MODERN DATA COMMUNICATION SYSTEMS CONFORMING TO EUROCOM SPECIFICATIONS
P. C. A. M. Karsten Jun. 1987 23 p
(Contract A82/KL/060)
(FEL-1987-48; ETN-88-92570) Avail: NTIS HC A03/MF A01

The functional specification of an integrated circuit for error protection purposes on the physical level in accordance with the Eurocom data traffic requirements is described. The most important requirements of Eurocom D/1 within the data communication field that implies the interface between network or subscriber data equipment and the circuit switched network are summarized. This includes the application of the integrated circuit to realize the most important parts of these interfaces for all data classes, concerning synchronous and asynchronous data. The use of this interface in data equipment for network store and forward functions and in user data terminal equipment such as the Packet terminal is discussed. ESA

N88-26594# Lawrence Livermore National Lab., Calif.
CRYSTALLIZATION OF ALUMINUM HYDROXIDE IN THE ALUMINUM-AIR BATTERY: LITERATURE REVIEW, CRYSTALLIZER DESIGN AND RESULTS OF INTEGRATED SYSTEM TESTS
A. Maimoni 31 Mar. 1988 102 p
(Contract W-7405-eng-48)
(DE88-010510; UCRL-53843) Avail: NTIS HC A06/MF A01

The literature on aluminum trihydroxide crystallization is reviewed and the implications of crystallization on the design and performance of the aluminum-air battery are illustrated. Results of research on hydrargillite crystallization under battery operating conditions at Alcoa Laboratories, Alcan Kingston Laboratories, and Lawrence Livermore National Laboratory are summarized and are applied to the design of an electrolyte management system using lamella settlers for clarification of the electrolyte and product separation. The design principles were validated in a series of experiments that, for the first time in the aluminum-air program, demonstrated continuous operation of an integrated system consisting of cells, crystallizer, and a product-removal system. DOE

N88-26595*# Old Dominion Univ., Norfolk, Va. Dept. of Electrical and Computer Engineering.
MODELING AND OPTIMUM TIME PERFORMANCE FOR CONCURRENT PROCESSING Interim Report, May - Nov. 1987
Roland R. Mielke, John W. Stoughton, and Sukhamoy Som
Washington NASA Aug. 1988 48 p
(Grant NAG1-683)
(NASA-CR-4167; NAS 1.26:4167) Avail: NTIS HC A03/MF A01 CSCL 09C

The development of a new graph theoretic model for describing the relation between a decomposed algorithm and its execution in a data flow environment is presented. Called ATAMM, the model consists of a set of Petri net marked graphs useful for representing decision-free algorithms having large-grained, computationally complex primitive operations. Performance time measures which determine computing speed and throughput capacity are defined, and the ATAMM model is used to develop lower bounds for these times. A concurrent processing operating strategy for achieving optimum time performance is presented and illustrated by example. Author

N88-26596* National Aeronautics and Space Administration. Pasadena Office, Calif.
LOW NOISE CRYOGENIC DIELECTRIC RESONATOR OSCILLATOR Patent
G. John Dick, inventor (to NASA) (Jet Propulsion Lab., California Inst. of Tech., Pasadena.) 12 Jul. 1988 7 p Sponsored by NASA
(NASA-Case-NPO-17157-1-CU; US-Patent-4,757,278; US-Patent-Appl-SN-116810; US-Patent-Class-331-3; US-Patent-Class-331-94.1; US-Patent-Class-331-162) Avail: US Patent and Trademark Office CSCL 09A

A microwave oscillator is provided which can operate at a temperature of many degrees above absolute zero while providing very low phase noise that has heretofore generally required temperatures within a few degrees K. The oscillator includes a ring-shaped resonant element of ruby (sapphire plus chromium) or iron sapphire crystal, lying adjacent to a resonator element of sapphire, so that the regenerator element lies directly in the magnetic field of the resonator element. The resonator element is substantially devoid of contact with electrically conductive material. Microwave energy of a pump frequency (e.g., 31 GHz) is outputted from the regenerator element, while signal energy (e.g., 10 GHz) is outputted from the resonator element.
Official Gazette of the U.S. Patent and Trademark Office

34 FLUID MECHANICS AND HEAT TRANSFER

Includes boundary layers; hydrodynamics; fluidics; mass transfer; and ablation cooling.

For related information see also *02 Aerodynamics* and *77 Thermodynamics and Statistical Physics.*

N88-26597 Texas Univ., Austin.
NUMERICAL SOLUTION OF WEAK FORMS OF CONSERVATION LAWS ON OPTIMAL UNSTRUCTURED TRIANGULAR GRIDS Ph.D. Thesis
Stephen Ray Kennon 1987 144 p
Avail: Univ. Microfilms Order No. DA8728586

A class of finite element schemes for simulating convection-dominated flows is developed and analyzed. These methods are shown to be optimal in a certain well-defined sense of a model linear problem. The first scheme uses a special set of discontinuous trial functions to construct the finite element solution. It is shown that this scheme is L sub 2-optimal in the sense that the L sub 2-norm of the difference between the exact solution and the approximate solution is minimized with respect to these special trial functions. The second scheme uses continuous trial functions and discontinuous test functions. This scheme has the advantageous property that it produces nodally exact solutions when discontinuities are aligned with the computational grid. The concept of polynomial conservation laws is introduced as a generalization of the Euler equations governing compressible inviscid flows. The finite element schemes developed for the model linear problem are extended to the nonlinear polynomial conservation laws, and numerical examples are given for a problem governed by the Euler equations. In addition to the finite element schemes for convection-dominated flows, a method is developed for generating optimal triangular grids. Dissert. Abstr.

N88-26598# Tokyo Univ. (Japan). Inst. of Space and Astronautical Science.
A SHOCK-TUBE EXPERIMENT ON GASES MIXING PROCESSES ASSOCIATED WITH CO2/N2 MIXING GASDYNAMIC LASER
Hakuro Oguchi, Katsushi Funabiki, Shunitsu Sato, and Masahiro Hatakeyama Aug. 1986 16 p
(ISAS-RN-350) Avail: NTIS HC A03/MF A01

Synchronized operation of double shock tubes is made in nearly full automation. Recognizing the feasibility of the operation, a mixing process is studied of two different gases ejected from the separate nozzles after the respective shock compressions. The mass sampling probe developed for this experiment is used to detect the mole fraction distributions of gas species in the mixing region downstream from the nozzle exit. Test gases are CO2 and N2 whose mixture is used in the CO2/N2 gas-dynamic laser. Moreover, the effect of the gas-mixing process on small signal gain distributions is investigated. Author

N88-26599# Tokyo Univ. (Japan). Inst. of Space and Astronautical Science.
NAVIER-STOKES SIMULATION OF SHOCK-TUBE FLOWS OVER A WEDGE-TYPE STEP BY FINITE VOLUME METHOD
H. Oguchi, M. Hatakeyama, and O. Inoue Mar. 1988 9 p
(ISAS-RN-628; ISSN-0285-6808) Avail: NTIS HC A02/MF A01

Shock-tube flows over a wedge-type step are simulated numerically by the finite volume method with quadrilateral cells. The 2-D, time-dependent Navier-Stokes equations are solved. Time development of flow fields and pressure histories on walls are obtained and shown to be in good qualitative agreement with experiments. Author

N88-26600# Tokyo Univ. (Japan). Inst. of Space and Astronautical Science.
A NUMERICAL SIMULATION OF TWO-DIMENSIONAL TRANSIENT SHEAR FLOW

Yasuhiro Koshioka Mar. 1988 61 p
(ISAS-RN-627; ISSN-0285-6808) Avail: NTIS HC A04/MF A01

With emphasis on the effect of numerical accuracy of the scheme, a new algorithm is presented on the basis of an improvement of the Arakawa method, and numerical computation is made for the continuous, transient phenomena of a shear layer from a linear regime to a nonlinear one by the use of the Euler equations satisfying vorticity, energy, and enstrophy conservations. A comparison is made to clarify the validity of the present scheme applied to the transient phenomenon of a shear layer with an assumption of a monochronic disturbance, and detailed examination is made further on the change in flow field of the merging vortices. Author

N88-26601*# Washington Univ., Seattle. Dept. of Mechanical Engineering.
COMPRESSION CREEP OF FILAMENTARY COMPOSITES
D. L. Graesser and M. E. Tuttle Mar. 1988 120 p
(Grant NAG1-621)
(NASA-CR-182550; NAS 1.26:182550) Avail: NTIS HC A06/MF A01 CSCL 20D

Axial and transverse strain fields induced in composite laminates subjected to compressive creep loading were compared for several types of laminate layups. Unidirectional graphite/epoxy as well as multi-directional graphite/epoxy and graphite/PEEK layups were studied. Specimens with and without holes were tested. The specimens were subjected to compressive creep loading for a 10-hour period. In-plane displacements were measured using moire interferometry. A computer based data reduction scheme was developed which reduces the whole-field displacement fields obtained using moire to whole-field strain contour maps. Only slight viscoelastic response was observed in matrix-dominated laminates, except for one test in which catastrophic specimen failure occurred after a 16-hour period. In this case the specimen response was a complex combination of both viscoelastic and fracture mechanisms. No viscoelastic effects were observed for fiber-dominated laminates over the 10-hour creep time used. The experimental results for specimens with holes were compared with results obtained using a finite-element analysis. The comparison between experiment and theory was generally good. Overall strain distributions were very well predicted. The finite element analysis typically predicted slightly higher strain values at the edge of the hole, and slightly lower strain values at positions removed from the hole, than were observed experimentally. It is hypothesized that these discrepancies are due to nonlinear material behavior at the hole edge, which were not accounted for during the finite-element analysis. Author

N88-26602# Oklahoma Univ., Norman. School of Chemical Engineering and Materials Science.
DEVELOPMENT OF AN EQUATION OF STATE FOR COMPUTATION OF SUPERCOMPRESSIBILITY FACTORS, CRITICAL FLOW FACTORS AND OTHER PROPERTIES FOR WET, SOUR NATURAL GASES, SYNTHETIC GASES AND ADMIXTURES Final Report, Oct. 1984 - Sep. 1987
K. E. Starling, M. Mannan, J. L. Savidge, S. Sadasivan, and T. B. Reid Sep. 1987 217 p
(Contract GRI-5084-260-1010)
(PB88-202676; GRI-88/0001) Avail: NTIS HC A10/MF A01 CSCL 20D

The accurate compressibility/supercompressibility factor correlation for sweet/dry natural gases was extended to include water and hydrogen sulfide. In the temperature and pressure range where most custody transfers take place, the correlation is accurate within 0.1 percent or better in the supercompressibility factor. One conclusion reached is that a more extensive high quality PVT data base for wet/sour natural gases is needed to further test the correlation. The revised alternate characterization methods developed allow faster and simpler calculations resulting in large reductions in computer time when compared with the alternate characterization method presented in AGA Report no. 8. The equation of state method was applied for prediction of highly accurate sonic velocities and critical flow factors for use with sonic nozzles. The prediction of the sonic velocity is shown to be generally accurate within plus or minus 0.1 percent at reasonable operation conditions for sonic nozzles. The prediction of critical factors is also shown to be more accurate than the Johnson method. Author

N88-26603*# Alabama Univ., Huntsville. Dept. of Chemistry.
CRITICAL POINT WETTING DROP TOWER EXPERIMENT Semiannual Report
William F. Kaulker Jul. 1988 10 p
(Grant NAG8-511)
(NASA-CR-183062; NAS 1.26:183062) Avail: NTIS HC A02/MF A01 CSCL 20D

Experiments with the wetting behavior of immiscible fluids against the container below the critical temperature are being performed in the MSFC Drop Tower Facility. Microgravity conditions extending up to three seconds (of the 4.5 second drop) are generated for the experiment. Specimens consist of glass cylindrical ampoules partially filled with fluid phases. How the fluids develop the meniscus geometry as well as hot the fluid interfaces respond to the microgravity induced oscillations is recorded during the experiment with on-board cameras. Drops are made at various temperatures to determine the interfacial energy variation as a function of temperature. Author

N88-26604# Central Research Inst. of Electric Power Industry, Tokyo (Japan).
CHARACTERISTICS OF PRESSURE LOSS DURING FILTRATION USING A POROUS CERAMIC FILTER
Shigeo Ito, Masatoshi Watanabe, Hisao Makino, Tsutomu Nagayama, and Takashi Tanaka Apr. 1987 31 p In JAPANESE; ENGLISH summary
(DE88-752547; CRIE-W-86025) Avail: NTIS (US Sales Only) HC A03

Characteristics of pressure loss during filtration was studied using a porous ceramic filter (PF). Immediately after the filtration started, collected particles formed a thin layer on the PF surface, which was transferred to cake filtration. Pressure loss during filtration was expressed as the sum of the loss in the filter and that in the particle layer. The effect of plugged surface pores with fine particles was evaluated as the change of permeability. Increase rate of pressure loss during filtration was proportional to the particle concentration, 2.6 power of the filtration rate and square of the specific surface area. When the filtration rate became larger, however, the porosity decreased and pressure loss increased because the pressure gradient increased in the collected particle layer and the particle layer was compacted. It is necessary to elucidate the compacted properties of collected particle layer to estimate more accurately the pressure loss. DOE

N88-26605# Edgerton, Germeshausen and Grier, Inc., Idaho Falls, Idaho.
MAGNETIC HEAT PUMP DESIGN
L. D. Kirol and M. W. Dacus 1988 5 p Presented at IECEC '87, Philadelphia, Pa., 10 Aug. 1987
(Contract DE-AC07-76ID-01570)
(DE88-007730; EGG-M-12987; CONF-8708237-1) Avail: NTIS HC A02/MF A01

Heat pumps utilizing the magnetocaloric effect offer a potentially attractive alternative to conventional heat pumps and refrigerators. Many physical configurations of magnetic heat pumps are possible. Major classes include those requiring electrical energy input and those with mechanical energy input. Mechanical energy is used to move magnets, working material, or magnetic shielding. Each type of mechanical magnetic heat pump can be built in a rotary (recuperative) or reciprocal (regenerative) configuration. Machines with electrical energy input utilize modulation of the magnetic field to cause working material to execute the desired thermodynamic cycle, and can also be recuperative or regenerative. Recuperative rotary heat pumps in which working material is moved past stationary magnets is the preferred configuration. Regenerative devices suffer performance degradation from temperature change of regenerator material and mixing and conduction in the

regenerator. Field modulated cycles are not practical due to ac losses in superconducting magnets. Development of methods for recuperator fluid pumping is the major challenge in design of rotary recuperative devices. Several pumping options are presented, and the design of a bench scale heat pump described. DOE

N88-26606# Los Alamos National Lab., N. Mex.
FREELY EXPANDING DETONATION PRODUCTS: SCALING OF RATE PROCESSES
N. R. Greiner 1988 27 p Presented at the 19th International ICT Conference on Combustion and Detonation, Karlsruhe, Fed. Republic of Germany, 29 Jun. 1988
(Contract W-7405-eng-36)
(DE88-007827; LA-UR-88-963; CONF-880693-1) Avail: NTIS HC A03/MF A01

Using the Los Alamos reactive hydrodynamics code KIVA, calculations have been made to simulate the free expansion of cylinders of detonation products into a high vacuum. The emphasis of this paper is on the scaling of rate processes with cylinder size and initial conditions as a function of position in the expanding mass. The processes considered include diffusion, unimolecular decomposition, biomolecular radical reactions, and vibrational relaxation. The calculations also give time-dependent velocity fields; schlieren images; and profiles of density, pressure, and temperature. Many features of the calculations can be compared with experimental observations, including time-delayed schlieren and shadowgraph snapshots, time-dependent absorption spectra, and time-of-arrival profiles of molecular species. Some unexpected insights, such as the effect of the equation of state on the shape of the expanding plume and the effect of position on the rate of quenching, are discussed. These calculations are being used to interpret the available experimental data and to design future experiments. DOE

N88-26607# Oak Ridge National Lab., Tenn.
THE OAK RIDGE HEAT PUMP DESIGN MODEL: MARK 3 VERSION PROGRAM DOCUMENTATION
S. K. Fischer, C. K. Rice, and W. L. Jackson Mar. 1988 41 p
(Contract DE-AC05-84OR-21400)
(DE88-007863; ORNL/TM-10192) Avail: NTIS HC A03/MF A01

Oak Ridge National Laboratory (ORNL) is a leader in the development of analytical tools for the design of electrically driven, air-to-air heat pumps. Foremost among these tools is the ORNL Heat Pump Design Model, which can be used to predict the steady-state heating and cooling performance of an electrically driven, air-source heat pump. The ORNL Heat Pump Design Model has continued to evolve since the users' manual for the program, ORNL/CON-80/R1, was last revised in August 1983. This series of modifications to the heat pump model resulted in the Mark 3 Version, which is three to five times faster, easier to use, and more versatile than earlier versions and can be executed on a personal computer. The major changes made to earlier versions of the heat pump model relate to the organization of the input data, elimination of redundant calculations in the compressor and refrigerant property computations, improvement of the thermostatic expansion valve and capillary tube correlations, revision of output format, and modifications to enable the model to run on a personal computer. The Mark 3 version is a comprehensive, easy-to-use program for the simulation of an electrically driven, air-source heat pump. DOE

N88-26608# Central Research Inst. of Electric Power Industry, Tokyo (Japan).
DEVELOPMENT OF ADVANCED FLOW SIMULATION SYSTEM BY WATER FLOW MODEL. NEW METHOD OF VELOCITY MEASUREMENT USING CROSS-CORRELATION
Jun Inumaru, Toshio Abe, Toru Hisamatsu, and Toshiaki Hasegawa Jul. 1987 35 p In JAPANESE; ENGLISH summary
(DE88-753120; CRIE-W-86036) Avail: NTIS (US Sales Only) HC A03

In order to establish a high-load combustion technology, a velocity measurement with water flow model was investigated as well as its technical possibility. In this method, the flow is visualized by the incident slit beam on the water stream which contains a specific amount of tracer (minute air bubbles), by calculating the time delay (Tau-m) of the concentration signal at two points alogside the flow direction using a cross-correlation method, average flow rate (5) can be obtained from Tau-m and L (distance between the two points). Using a turbulent free jet for the flow rate measurement, average cross-sectional flow rate of the nozzle and Delta-t (data sampling interval), etc. were changed; possible range of flow rate measurement strongly depended on Delta-t; comparison with the measurement by a Laser Doppler Velocimeter indicated that the meaurement error got less even in the range near to the outer-edge of the jet if Delta-t and the filter operation were improved. This indicates the future possibility of application to a two dimensional flow field, and moreover to a three dimensional flow field by using slit beams with different wavelengths. DOE

N88-26609# Argonne National Lab., Ill.
MULTIGRID COMPUTATION OF PRACTICAL FLUID FLOWS AND HEAT TRANSFER
S. P. Vanka 1988 6 p Presented at the International Conference on Computational Engineering Science, Atlanta, Ga., 10 Apr. 1988
(Contract W-31-109-eng-38)
(TI88-010064; CONF-880438-6) Avail: NTIS HC A02/MF A01

The use of multigrid strategies can significantly accelerate the convergence of many current calculations of practical engineering flows with heat transfer, turbulence and chemical reaction. This lecture describes the author's recent research in this area. DOE

N88-26610# International Centre for Theoretical Physics, Trieste (Italy).
NONLINEAR EQUATION OF STATE EFFECTS AND THE MOMENTUM-DILUTION TRADE-OFF IN A TURBULENT BUOYANT JET
T. C. Ponce May 1987 25 p
(DE88-701839; IC-86/364) Avail: NTIS (US Sales Only) HC A03/MF A01

This paper presents the results of an investigation aimed at determining the effects of using a nonlinear equation of state (instead of a linearized one) in a mathematical model of an axisymmetric turbulent buoyant jet in a neutrally stratified ambient. It also seeks to establish criteria to determine whether a linear or nonlinear equation of state should be used in the numerical modelling of axisymmetric turbulent buoyant jets in a stagnant neutrally stratified ambient. The fluid flow equations derived for the fully developed flow field of a round turbulent buoyant jet, together with the nonlinear equations of state corresponding to various types of jets (e.g. hot water jets, hot air jets, saline water jets), are solved. The numerical solutions are compared to that of a similar jet model that uses a linearized equation of state in order to arrive at guidelines in using a linearized or nonlinear equation of state. These guidelines involve (1) the fluid medium to be used, (2) the property of the jet that gives rise to the buoyancy (e.g. temperature differences, concentration differences, etc.) and (3) the initial density parameter, d(sub O). The nonlinear equation of state is then applied to a hot water buoyant jet model to see whether the momentum-dilution trade-off observed in fitting the prediction of a hot water jet model using a linearized equation of state to the data would be diminished. Results show that a nonlinear equation of state greatly improves the data fitting process. DOE

N88-26611# Argonne National Lab., Ill.
USE OF DIRECT SOLVERS FOR MULTIDIMENSIONAL FLUID FLOW COMPUTATIONS
S. P. Vanka 1988 4 p Presented at the International Conference on Computational Engineering Science, Atlanta, Ga., 10 Apr. 1988
(Contract W-31109-eng-38)
(DE88-010063; CONF-880438-7) Avail: NTIS HC A02/MF A01

Direct solvers for the inversion of the linearized set of the

coupled Navier-Stokes equations are robust and can provide efficient solutions to practical flow problems in a few iterations. However, the required computer storage (and in some cases the CPU time) can be large, especially for three-dimensional flows. Techniques such as domain decomposition and plane-by-plane inversion are feasible but their performance in preserving the robustness is problem dependent and uncertain. This paper reviews some recent research in fluid flow computations using direct solvers. DOE

N88-26612# Southwest Research Inst., San Antonio, Tex.
EXPERIMENTS ON DENSELY-LOADED NON-NEWTONIAN SLURRIES IN LAMINAR AND TURBULENT PIPE FLOWS Quarterly Technical Progress Report
J. T. Park, R. J. Mannheimer, T. A. Grimley, and T. B. Morrow 26 May 1988 25 p
(Contract DE-FG22-86PC-90962)
(DE88-010579; DOE/PC-90962/T6; SWRI-06-1364; QTPR-6)
Avail: NTIS HC A03/MF A01

An experimental description of the flow structure of non-Newtonian slurries in the laminar, transitional, and full turbulent pipe flow regimes is the primary objective of this research. Measurements include rheological characterization of the fluid and local fluid velocity measurements with a Laser Doppler Velocimeter (LDV). Optical access to the flow is gained through a test section and model slurry which are both transparent. The model slurry is formulated from silica gel particles and hydrocarbon liquid mixture whose indices of refraction are matched so that light is not scattered from the particles. Experiments are being conducted in a large-scale pipe slurry. Flow measurements including turbulence quantities such as Reynolds stress were measured with a two-component two-color LDV. The present research indicates that non-Newtonian slurries are possible with concentrations of a few percent by weight of small particles whose sizes are two microns or less. A non-Newtonian slurry from small particles could maintain large particles (one millimeter size) at high concentrations in suspension almost indefinitely. Such a slurry would prevent particle fallout and its associated problems. DOE

N88-26613# Oak Ridge National Lab., Tenn.
BOUNDARY ELEMENT METHOD FOR CONTACT HEAT TRANSFER
L. J. Gray, A. L. Askew, and G. E. Giles Apr. 1988 17 p Presented at the European Boundary Element Meeting, Brussels, Belgium, 8 May 1988 Prepared in cooperation with Martin Marietta Energy Systems, Inc., Oak Ridge, Tenn.
(Contract DE-AC05-84OR-21400)
(DE88-011013; CONF-8805129-1) Avail: NTIS HC A03/MF A01

The (steady state) heat flow between two contacting solids is investigated utilizing an efficient new boundary element method for treating thin cavities. A significant advantage of this approach is that a (multidomain) decomposition of the region is avoided and the contact region remains an interior surface. Consequently, the discontinuous flux across the contact/non-contract boundary is not solved for directly and no special provisions for the singularity are required. These fluxes can be accurately obtained after the boundary integral equation has been solved and all boundary values are known. Calculations for a circular contact region are presented, and the results are compared against a known analytic solution. Since pevious work on this method has only considered interior cavities and the contact gap is a surface crack, the treatment of surface cracks will also be described. DOE

N88-26614# Manchester Univ. (England).
PULSED SPRAY STRUCTURE AND ATOMISATION TECHNIQUES Final Report, Nov. 1983 - Aug. 1987
A. J. Yule Aug. 1987 31 p
(Contract DAJA45-83-C-0061; DA Proj. 1L1-61102-BH-57)
(AD-A192280) Avail: NTIS HC A03/MF A01 CSCL 21B

The process of atomisation from diesel injectors is found to persist for a significant proportion of the spray length before impaction on the cylinder wall. Both aerodynamic shear and cavitation appear to be of importance for the liquid jet breakdown. In addition cyclic variations are found in the atomisation and penetration of sprays. The transient nature of the spray initial conditions can cause pile up and coagulation of droplets at the leading edge of the spray pulse for certain cases. Improved modeling of diesel injection requires recognition of these phenomena and this is supported by both modeling and experimental data which have been obtained under realistic engine conditions in a specially developed rig. GRA

N88-26615*# National Aeronautics and Space Administration, Washington, D.C.
EXPERIMENTAL INVESTIGATION OF TURBULENT FLOW IN SMOOTH AND LONGITUDINAL GROOVED TUBES
P. Nitschke May 1984 76 p Transl. into ENGLISH of Experimentelle Untersuchung der Turbulent Stroemung in Glatten und Laengsgerillten Rohren (Goettingen, Fed. Republic of Germany, Max-Planck Inst. fuer Stromungsforschung), 1983 Original language document was announced as N84-16510 Transl. by Kanner (Leo) Associates, Redwood City, Calif.
(Contract NASw-3541)
(NASA-TM-77480; NAS 1.15:77480) Avail: NTIS HC A05/MF A01 CSCL 20D

Turbulent flow in tubes with and without longitudinal grooves is examined. The discovery of fine grooves forming a sort of streamline pattern on the body of sharks led to the expectation that the grooves on a surface reduce the momentum change, and thus the drag. To test this thesis, drag law, velocity profile and the profile of the velocity fluctuation were determined. Results show that for moderate Reynolds numbers the drag coefficient for grooved tubes is about 3 percent smaller than that of the smooth tubes. At higher Reynolds numbers, however, the drag coefficient for grooved tubes becomes larger than that for smooth tubes. No significant differences in the velocity profiles between grooved tubes and smooth tubes are found. Author

N88-26616*# Sverdrup Technology, Inc., Cleveland, Ohio.
THREE-DIMENSIONAL VISCOUS FLOW COMPUTATIONS OF A CIRCULAR JET IN SUBSONIC AND SUPERSONIC CROSS FLOW Final Contractor Report
G. J. Harloff and J. K. Lytle Jul. 1988 14 p Presented at the 1st National Fluid Dynamics Congress, Cincinnati, Ohio, 24-28 Jul. 1988; sponsored by ASME
(Contract NAS3-25266)
(NASA-CR-182153; E-4223; NAS 1.26:182153) Avail: NTIS HC A03/MF A01 CSCL 20D

Three-dimensional viscous flow computations are presented for 90 deg injection angle jets in subsonic and supersonic cross flow. Comparisons with experimental data include jet centerline and vortex trajectories for the subsonic cross flow, and surface pressure measurement for the supersonic crossflow case. The vortices induced in the jet/freestream interaction are computed and illustrated. The vortices persist in subsonic flow and die out quickly in supersonic flow. The structure of the shocks in the unconfined supersonic flow is illustrated. Author

N88-26617*# National Aeronautics and Space Administration, Washington, D.C.
WAVE PROPAGATION IN LOCALLY ISOTROPIC TURBULENT MEDIUM WITH SMOOTHLY CHANGING CHARACTERISTICS
V. I. Tatarskiy Jul. 1988 9 p Transl. into ENGLISH from Doklady Akademii Nauk SSSR (USSR), v. 120, no. 2, 1985 p 289-292 Transl. by Scientific Translation Service, Santa Barbara, Calif.
(Contract NASw-4307)
(NASA-TT-20312; NAS 1.77:20312) Avail: NTIS HC A02/MF A01 CSCL 20D

Discussed are the problems of fluctuations in amplitude and phase of short waves propagating in a locally isotropic turbulent medium whose local statistical properties are the same along the entire wave propagation path. Author

N88-26618*# Old Dominion Univ., Norfolk, Va. Inst. for Computational and Applied Mechanics.
A STUDY OF FLOW SEPARATION IN TRANSONIC FLOW USING INVISCID AND VISCOUS COMPUTATIONAL FLUID DYNAMICS (CFD) SCHEMES
J. A. Rhodes, S. N. Tiwari, and E. vonLavante Apr. 1988 218 p
(Grant NAG1-363)
(NASA-CR-183119; NAS 1.26:183119; ODU/ICAM-88-102)
Avail: NTIS HC A10/MF A01 CSCL 20D

A comparison of flow separation in transonic flows is made using various computational schemes which solve the Euler and the Navier-Stokes equations of fluid mechanics. The flows examined are computed using several simple two-dimensional configurations including a backward facing step and a bump in a channel. Comparison of the results obtained using shock fitting and flux vector splitting methods are presented and the results obtained using the Euler codes are compared to results on the same configurations using a code which solves the Navier-Stokes equations. Author

N88-26619*# Mississippi State Univ., Mississippi State. Dept. of Aerospace Engineering.
IMPROVED 3-D TURBOMACHINERY CFD ALGORITHM Final Report, 1 Nov. 1986 - 15 May 1988
J. Mark Janus and David L. Whitfield Jun. 1988 56 p Prepared in cooperation with Scientific Research Associates, Inc., Glastonbury, Conn.
(Contract NAS8-36185)
(NASA-CR-179364; NAS 1.26:179364) Avail: NTIS HC A04/MF A01 CSCL 20D

The building blocks of a computer algorithm developed for the time-accurate flow analysis of rotating machines are described. The flow model is a finite volume method utilizing a high resolution approximate Riemann solver for interface flux definitions. This block LU implicit numerical scheme possesses apparent unconditional stability. Multi-block composite gridding is used to orderly partition the field into a specified arrangement. Block interfaces, including dynamic interfaces, are treated such as to mimic interior block communication. Special attention is given to the reduction of in-core memory requirements by placing the burden on secondary storage media. Broad applicability is implied, although the results presented are restricted to that of an even blade count configuration. Several other configurations are presently under investigation, the results of which will appear in subsequent publications. Author

N88-26620# Universitaet der Bundeswehr, Neubiberg (West Germany). Inst. fuer Thermodynamik.
ON MICROPHYSICAL PRINCIPLES OF THERMOFLUID DYNAMICS [UEBER DIE MIKROPHYSIKALISCHEN GRUNDLAGEN DER THERMOFLUIDDYNAMIK]
Dieter Straub Mar. 1987 278 p In GERMAN
(ETN-88-92095) Avail: NTIS HC A13/MF A01

An alternative theory of continuum physics is presented via a review of Boltzmann's theory, its fundamentals, and various aspects of its results. The ideas of Prigogine, the microphysics derived from them, and the defects they reveal in Boltzmann's theory are reviewed. ESA

N88-26621# Technische Univ., Munich (West Germany). Lehrstuhl fuer Apparate- und Anlagenbau Expermentelle Spannungsanalyse.
CROSS FLOW INDUCED VIBRATIONS IN TUBE BUNDLE BY DISPLACED AND MISALIGNED TUBE CONFIGURATIONS Ph.D. Thesis [STROEMUNGSINDUZIERTE SCHWINGUNGEN QUERANGESTROEMTER ROHRBUENDEL BEI VERSETZTER UND FLUCHTENDER ROHRANORDNUNG]
Hubert Troidl 1986 176 p In GERMAN
(ETN-88-92132) Avail: NTIS HC A09/MF A01

Fluid elastic instability of cross flow induced vibration is studied with evaluation of vibration amplitudes leading to buffeting and whirling of heat exchanger tubes in displaced and misaligned configurations. Digital test data processing and high speed cameras contribute to visualization of tube movements and fluid flow profiles. Tests are performed on aluminum and steel tubes in air and water flow for free and rigid tubes. ESA

N88-26622# Institut de Mecanique des Fluides de Marseille (France).
STUDY OF FLOW TRACER BEHAVIOR MODELS AND EXPERIMENTAL VALIDATION WITH MULTIPLE EXPOSURE HOLOGRAPHIC VELOCIMETRY [ETUDE DE MODELES DE COMPORTEMENT DE TRACEURS DANS UN ECOULEMENT ET LEUR VALIDATION EXPERIMENTALE PAR VELOCIMETRIE HOLOGRAPHIC A EXPOSITIONS MULTIPLES]
M. Dadi 4 Aug. 1987 160 p In FRENCH
(Contract DRET-84-003-5)
(IMFL-87/30; ETN-88-92159) Avail: NTIS HC A08/MF A01

Models describing the behavior of tracers are discussed and experimentally evaluated using the Gabor procedure for obtaining multiple holographic records. Low density and small diameter tracers are correctly predicted by all models, but high inertia tracers are best predicted by a semi-empirical model only. In all cases the drag viscous force is sufficient to describe the movement of the tracing particle around an obstacle. ESA

N88-26623# Centre d'Etudes et de Recherches, Toulouse (France).
COMPRESSIBLE BOUNDARY LAYERS Final Report [COUCHES LIMITES COMPRESSIBLES]
B. Aupoix, C. Eldem, and A. Lafon Jan. 1987 34 p In FRENCH
(Contract DRET-86-002)
(CERT-OA-13/5005-AYD; ETN-88-92164) Avail: NTIS HC A03/MF A01

The sensitivity of hypersonic boundary layers outside the zone of chemical equilibrium was studied. The effect of the wall catalysis, the reaction rates used, and wall temperature are shown. Model simplifications concerning the number of reactions included and the diffusion terms are validated. The development of a calculation method for boundary layers in chemical equilibrium allowed flow at the end of reentry to be studied, the boundary layer being able to become turbulent. A simplified integral method was reevaluated to allow rapid prediction of wall heat flux. ESA

N88-26624# Institut National Polytechnique, Grenoble (France).
STUDY OF A WATER-STEAM TWO PHASE FLOW IN A T-BRANCH Ph.D. Thesis [ETUDE DES ECOULEMENTS DIPHASIQUES EAU-VAPEUR DANS UN BRANCHEMENT EN TE]
Thierry Maciaszek (Ecole Nationale Superieure de Mecanique et d'Aerotechnique, Poitiers, France) 1987 254 p In FRENCH
(ETN-88-92306) Avail: NTIS HC A12/MF A01

A thermohydraulic model to describe the mixed water-steam behavior in a T-branch is proposed. The model is based on the energy, mass, and momentum balance equations. The method is described and the solutions obtained are compared to experiments. Problems studied include phase separation for stratified flow in the main duct and different branching possibilities. Laws describing phase separation are proposed. ESA

N88-26625# Stuttgart Univ. (West Germany). Inst. fuer Theoretische Physik.
STATIONARY, WAVE TYPE, AND CHAOS TYPE CONVECTION IN SPHERICAL SYMMETRY GEOMETRIES Ph.D. Thesis [STATIONAERE, WELLENARTIGE UND CHAOTISCHE KONVEKTION IN GEOMETRIEN MIT KUGELSYMMETRIE]
Rudolf Friedrich 1986 143 p In GERMAN
(ETN-88-92358) Avail: NTIS HC A07/MF A01

Geophysical and astrophysical fluid flow behavior is observed on a model between two concentric spheres surfaces in radial symmetry and gravitation field. A radial temperature drop in the fluid leads, as in the Bernard problem in fluid dynamics, to the rise of convection instability studied by linear stability theory. For the solution of the eigenvalue problems two possibilities are discussed: the Galerkin method, and the iteration procedure.

Eigenfunctions are classified by their transformation properties by a rotation of the coordinate system. Instability is studied as a function of the variation of the inner fluid boundary radius. Time dependant fluid flows are determined by application of Ginzburg-Landau equations. Stationary and periodical fluid flow behavior, wave type flow, quasi-periodical behavior, and chaos type flow behavior are considered. ESA

N88-26626# Technische Univ., Brunswick (West Germany). Fakultaet fuer Maschinenbau und Elektrotechnik.
INVESTIGATION ON REFRIGERANT R12 CRITICAL BOILING POINT IN NARROW FLOW PIPES CONSIDERED AS MODEL FLUID Ph.D. Thesis [UNTERSUCHUNG ZUM KRITISCHEN SIEDEZUSTAND IN ENGEN STROEMUNGSKANAELEN MIT DEM KAELTEMITTEL R12 ALS MODELLFLUID]
Thomas Mueller-Menzel 1987 134 p In GERMAN
(ETN-88-92374) Avail: NTIS HC A07/MF A01

Experimental investigations on critical heat flow rates in vertical upstream round tubes of small diameter in presence of high mass flow rates and pressures are described. Critical heat flux rates are studied on refrigerant R12 and a thermodynamical model is established, considering the phenomena of limiting quality and upstream boiling. The effects of vapor quality, pipe diameter and length, mass flow rate, and pressure on the formation of critical boiling are examined. Experimental data obtained with R12 are extrapolated on water conditions and presented in tables for 4 mm diameter pipes. ESA

N88-26627# National Aerospace Lab., Amsterdam (Netherlands). Informatics Div.
AXISYMMETRIC LIQUID SLOSHING UNDER LOW-G CONDITIONS: NUMERICAL SIMULATION METHOD (REFERENCE MANUAL)
A. E. P. Veldmann and M. E. S. Vogels 29 May 1986 85 p
(Contract NIVR-1860/1999)
(NLR-TR-86057-4; B8803896; ETN-88-92599) Avail: NTIS HC A05/MF A01

A mathematical model for the description of axisymmetric three-dimensional transient flow of a viscous liquid in a partially filled cylindrical container under low gravity conditions is presented. The model consists of the Navier-Stokes equations with no-slip condition at the solid boundaries, and with the continuity of stress condition at the free liquid boundary. The numerical method by which these equations are discretized and solved is a Eulerian finite difference method. It is a member of the Marker-and-Cell family in combination with the volume-of-fluid method for tracking in liquid region. The numerical method is implemented in a computer program SAVOF. The reference manual of SAVOF is presented. Possibilities of SAVOF with respect to the motion of the container and the large displacements of the liquid are demonstrated. ESA

N88-26628# National Aerospace Lab., Amsterdam (Netherlands). Informatics Div.
PRELIMINARY DESIGN AND ANALYSIS OF PROCEDURES FOR THE NUMERICAL GENERATION OF 3D BLOCK-STRUCTURED GRIDS
J. W. Boerstoel 13 Aug. 1986 80 p
(Contract NIVR-311.1-1101/01604N)
(NLR-TR-86102-U; B8803895; ETN-88-92601) Avail: NTIS HC A05/MF A01

Aproaches to grid generation are analyzed. A grid-generation procedure for complex aircraft configurations could be based on a combination of three subprocesses: decomposition of the flow domain into 100 hexahedronal blocks; trilinear transfinite interpolation to generate initial grid point distributions; and elliptic mesh-size tuning and smoothing. To get insight into this procedure, mathematical models of the subprocesses were worked out. The results of the analysis are technical concepts required or desirable in the grid-generation procedure. ESA

N88-26629# National Aerospace Lab., Amsterdam (Netherlands). Space/Informatics Div.
LIQUID MOTIONS IN PARTIALLY FILLED CONTAINERS: PRELIMINARY RESULTS OF THE D-1 MISSION
J. P. B. Vreeburg and M. E. S. Vogels 23 Jun. 1986 12 p Presented at the 26th COSPAR Conference, Toulouse, France, Jun.-Jul. 1986 Previously announced in IAA as A87-39838 Sponsored in cooperation with the Space Research Organization, Utrecht, Netherlands
(Contract NIVR-1999)
(NLR-MP-86042-U; B8805306; ETN-88-92603) Avail: NTIS HC A03/MF A01

Capillary liquid flow in transparent models of spacecraft tanks was studied in the Spacelab fluid physics module. A typical dimension in a container is 5 cm. Six experiment runs were conducted with liquid in a straight cylinder container with hemispherical ends. The flight results are recorded on cine film that is processed for photogrammetric data. The liquid (water) remained at one end of the container throughout the experiments and shows a stuck contact line with the wall (perspex). Since the liquid contained bubbles and the contact line was noncircular, interpretation of the results is not straightforward. For axisymmetric configuration, a computer program, SAVOF, was developed for numerical simulations of the liquid flow. The dependence of the lowest axisymmetric resonance of the liquid on the contact line (stuck) position was calculated both for a nonrotating and a rotating tank. The flight results are generally in line with the numerical results. ESA

N88-26630# Technische Hogeschool, Eindhoven (Netherlands).
DRAG REDUCTION OF TURBULENT BOUNDARY LAYERS BY MEANS OF GROOVED SURFACES Ph.D. Thesis
Cornelis Johannes Ad Pulles 1988 140 p Sponsored by the Netherlands Technology Foundation
(ETN-88-92618) Avail: NTIS HC A07/MF A01

The phenomenon that the friction factor of a flat plate can be decreased by coating the surface with small longitudinal grooves was studied. This phenomenon occurs in a turbulent boundary layer flow and apparently the grooves influence the eddies in the flow in such a way that the stress transport shows a 7 percent decrease. Water channel and wind tunnel measurements show the occurrence of drag reduction even at the low Reynolds numbers used in the method of hydrogen bubble visualization. The effects of the grooves on the turbulent burst frequency differ from the description in literature. Visualization experiments show that the grooves influence the flow only rather marginally. It is discussed how the ideas proposed in the literature are tenable in relation to the experimental findings. It appears that the most obvious ideas are not completely justified in their uncorrected version. ESA

N88-26631# Office National d'Etudes et de Recherches Aerospatiales, Paris (France).
SPECTRAL RESOLUTION OF THE NAVIER-STOKES EQUATIONS IN MULTI-DOMAIN CURVED COMPLEX GEOMETRIES Ph.D. Thesis - Paris VI Univ.
Brigitte Metivet 1987 181 p In FRENCH; ENGLISH summary
(ONERA-NT-1987-2; ISSN-0078-3781; ETN-88-92726) Avail: NTIS HC A09/MF A01

A spectral method for incompressible viscous fluids in cases involving nonperiodic boundary conditions and complex three-dimensional geometries is proposed. A finite difference time and collocation space scheme is used for digitizing the problem. Discrete velocity and pressure spaces fulfilling the inf-sup condition are chosen. The solution domain is divided into subdomains which can be mapped onto a cube. The patching method is related to the Schwarz algorithm. The convergence is discussed and expressions giving the approximation of the method are presented. ESA

N88-26632# Office National d'Etudes et de Recherches Aerospatiales, Paris (France).
PARALLELIZATION ON A MULTIPROCESSOR SYSTEM OF A SOLUTION METHOD FOR THE UNSTEADY NAVIER-STOKES EQUATIONS AT HIGH REYNOLDS NUMBERS Ph.D. Thesis - Paris VI Univ.
Laure Mane 1987 111 p In FRENCH; ENGLISH summary Report will be announced as translation (ESA-TT-1116) Original contains color illustrations
(ONERA-NT-1987-8; ISSN-0078-3781; ETN-88-92730) Avail: NTIS HC A06/MF A01

The numerical simulation on a shared memory multiprocessor of unsteady separated flows around a body is studied. The two-dimensional equations are solved in stream function and vorticity formulations. The method combines highly accurate finite difference schemes and alternating direction implicit techniques. The algorithm parallelization is based on splitting the computational domain into subdomains. The performances of the parallel code are presented. The results of the simulation of a pulse-started NACA 0012 airfoil for different angles of attack and Reynolds numbers up to 100,000 are presented. ESA

N88-26633# Institut Franco-Allemand de Recherches, St. Louis (France).
TREATMENT OF THE SEPARATED FLOW AROUND PROFILES (NONVISCOUS, INCOMPRESSIBLE, TWO DIMENSIONAL FLOW) BY THE SINGULARITIES METHOD [TRAITEMENT DE L'ECOULEMENT (NON VISQUEUX, INCOMPRESSIBLE, BIDIMENSIONNEL) AUTOUR DE PROFILS AVEC DECOLLEMENT PAR LA METHODE DES SINGULARITES]
M. Schaffar 3 Apr. 1987 67 p In FRENCH
(ISL-R-106/87; ETN-88-92732) Avail: NTIS HC A04/MF A01

The method is based on assuming linear vortices distributed over the profile divided in N segments. The wake is examined by means of turbulent layers. The profiles studied at variable incidence are described. The results depend on the procedures of wake analysis (layers with interpolation, point turbulence with or without vortex coalescence) and also on parameters such as the time step and the inertial flow around the profile. ESA

N88-26634*# National Aeronautics and Space Administration. Ames Research Center, Moffett Field, Calif.
A MICROCOMPUTER BASED FREQUENCY-DOMAIN PROCESSOR FOR LASER DOPPLER ANEMOMETRY
W. Clifton Horne and Desmond Adair Jul. 1988 7 p Presented at the 4th International Symposium on Applications of Laser Anemometry to Fluid Mechanics. Lisbon, Portugal, 11-14 Jul. 1988
(NASA-TM-100998; A-88173; NAS 1.15:100998) Avail: NTIS HC A02/MF A01 CSCL 20D

A prototype multi-channel laser Doppler anemometry (LDA) processor was assembled using a wideband transient recorder and a microcomputer with an array processor for fast Fourier transform (FFT) computations. The prototype instrument was used to acquire, process, and record signals from a three-component wind tunnel LDA system subject to various conditions of noise and flow turbulence. The recorded data was used to evaluate the effectiveness of burst acceptance criteria, processing algorithms, and selection of processing parameters such as record length. The recorded signals were also used to obtain comparative estimates of signal-to-noise ratio between time-domain and frequency-domain signal detection schemes. These comparisons show that the FFT processing scheme allows accurate processing of signals for which the signal-to-noise ratio is 10 to 15 dB less than is practical using counter processors. Author

N88-26635*# Universities Space Research Association, Huntsville, Ala. Structures and Dynamics Lab.
VELOCITY-PRESSURE INTEGRATED VERSUS PENALTY FINITE ELEMENT METHODS FOR HIGH REYNOLDS NUMBER FLOWS Final Report
Sang-Wook Kim Apr. 1988 62 p
(Contract NAS8-35918)
(NASA-CR-179357; NAS 1.26:179357) Avail: NTIS HC A04/MF A01 CSCL 20D

Velocity-pressure integrated and consistent penalty finite element computations of high Reynolds number, laminar flows are presented. In both of the methods, the pressure has been interpolated using linear shape functions for a triangular element. The triangular element is contained inside the bi-quadratic isoparametric element. It has been reported previously that the pressure interpolation method, when used in the velocity-pressure integrated method, yielded accurate computational results for high Reynolds number flows. It is shown that use of the same pressure interpolation method in the consistent penalty finite element method yielded accurate velocity and pressure fields which were comparable to those obtained using the velocity-pressure integrated method. Accuracy of the two finite element methods has been demonstrated by comparing the computational results with available experimental data and/or fine-grid finite difference computational results. Advantages and disadvantages of the two methods are discussed on the basis of accuracy and convergence nature. Example problems considered include a lid-driven cavity flow for Reynolds number of 10,000, a laminar backward-facing step flow, a laminar flow through a nest of cylinders, and a channel flow with an internal blockage. A finite element computer program (NSFLOW/P) for the 2-D, incompressible Navier-Stokes equations is also presented. Author

N88-26308# Tohoku Univ., Sendai (Japan). Inst. of High Speed Mechanics.
NUMERICAL SIMULATION OF THE SHOCK TUBE FLOWS BY TVD SCHEME
Katsuhiro Itoh and Kazuyoshi Takayama *In* National Aerospace Lab., Proceedings of the 5th NAL Symposium on Aircraft Computational Aerodynamics Nov. 1987 p 129-136 In JAPANESE; ENGLISH summary (For primary document see N88-26290 20-01)
Avail: NTIS HC A12/MF A01

N88-26310# National Aerospace Lab., Tokyo (Japan).
NUMERICAL ANALYSIS OF THREE DIMENSIONAL CASCADE FLOW BY SOLVING NAVIER-STOKES EQUATIONS
Osamu Nozaki, Kazuhiro Nakahashi, and Atsuhiro Tamura *In its* Proceedings of the 5th NAL Symposium on Aircraft Computational Aerodynamics Nov. 1987 p 147-156 In JAPANESE; ENGLISH summary (For primary document see N88-26290 20-01)
Avail: NTIS HC A12/MF A01

N88-26311# Tokyo Metropolitan Univ. (Japan). Coll. of Aeronautical Engineering.
SIMULATION OF AXISYMMETRIC FLOW WITH H2O2 REACTIONS
Shizui Watanabe *In* National Aerospace Lab., Proceedings of the 5th NAL Symposium on Aircraft Computational Aerodynamics Nov. 1987 p 157-160 In JAPANESE; ENGLISH summary (For primary document see N88-26290 20-01)
Avail: NTIS HC A12/MF A01

N88-26312# National Aerospace Lab., Tokyo (Japan).
NUMERICAL ANALYSIS OF DUCT FLOW USING THREE-DIMENSIONAL PARABOLIZED NAVIER-STOKES EQUATION
Kazuo Kikuchi and Atsuhiro Tamura *In its* Proceedings of the 5th NAL Symposium on Aircraft Computational Aerodynamics Nov. 1987 p 159-168 In JAPANESE; ENGLISH summary (For primary document see N88-26290 20-01)
Avail: NTIS HC A12/MF A01

N88-26313# Kawasaki Heavy Industries Ltd., Kagamihara (Japan).
THE ROLE OF COMPUTATIONAL FLUID DYNAMICS IN AERONAUTICAL ENGINEERING (5): IMPROVEMENTS AND APPLICATIONS OF IMPLICIT TVD FINITE VOLUME CODE
Eiji Shima, Kenji Yoshida, and Kanichi Amano (Japan Aircraft

Development Corp., Tokyo.) *In* National Aerospace Lab., Proceedings of the 5th NAL Symposium on Aircraft Computational Aerodynamics Nov. 1987 p 169-175 In JAPANESE; ENGLISH summary (For primary document see N88-26290 20-01)
Avail: NTIS HC A12/MF A01

N88-26315# Ishikawajima-Harima Heavy Industries Co. Ltd., Tokyo (Japan).
APPLICATION OF COMPUTATIONAL FLUID DYNAMICS TO DESIGN OF COMPRESSOR CASCADE
Teiichi Tamaki, Kaoru Chiba, Atsushi Shimizu, and Kenji Kobayashi *In* National Aerospace Lab., Proceedings of the 5th NAL Symposium on Aircraft Computational Aerodynamics Nov. 1987 p 183-189 In JAPANESE; ENGLISH summary (For primary document see N88-26290 20-01)
Avail: NTIS HC A12/MF A01

N88-26317# National Aerospace Lab., Tokyo (Japan).
AN IMPLICIT, HIGH ORDER ACCURATE, UPWIND SCHEME FOR UNSTEADY EULER EQUATIONS
Kenichi Matsuno *In its* Proceedings of the 5th NAL Symposium on Aircraft Computational Aerodynamics Nov. 1987 p 197-200 In JAPANESE; ENGLISH summary (For primary document see N88-26290 20-01)
Avail: NTIS HC A12/MF A01

N88-26319# National Aerospace Lab., Tokyo (Japan).
ON SYMMETRIC TVD SCHEMES Abstract Only
Takayuki Aki *In its* Proceedings of the 5th NAL Symposium on Aircraft Computational Aerodynamics Nov. 1987 p 209 In JAPANESE; ENGLISH summary (For primary document see N88-26290 20-01)
Avail: NTIS HC A12/MF A01

N88-26320# Fujitsu Ltd., Tokyo (Japan).
ON THE STATIONARY SOLUTIONS OF THREE-DIMENSIONAL EULER EQUATIONS BY THE TVD DIFFERENCE SCHEMES
Yoko Takakura, Tomiko Ishiguro, and Satoru Ogawa (National Aerospace Lab., Tokyo, Japan) *In* National Aerospace Lab., Proceedings of the 5th NAL Symposium on Aircraft Computational Aerodynamics Nov. 1987 p 211-216 In JAPANESE; ENGLISH summary (For primary document see N88-26290 20-01)
Avail: NTIS HC A12/MF A01

N88-26500# Tokyo Univ. (Japan). Dept. of Aeronautical Engineering.
NUMERICAL ANALYSIS OF RECONNECTION OF VORTEX RINGS
H. L. Chen and K. Oshima *In its* The Proceedings of the Symposium on Mechanics for Space Flight 1987 Mar. 1988 p 3-12 (For primary document see N88-26499 20-31)
Avail: NTIS HC A07/MF A01

N88-26501# Tokyo Univ. (Japan). Inst. of Space and Astronautical Science.
VORTEX FILAMENT SIMULATION FOR THE CROSSLINKING RINGS
Akiko Yamashita and Yuko Oshima (Ochanomizu Women's Univ., Tokyo, Japan) *In its* The Proceedings of the Symposium on Mechanics for Space Flight 1987 Mar. 1988 p 13-18 (For primary document see N88-26499 20-31)
Avail: NTIS HC A07/MF A01

N88-26502# Ochanomizu Women's Univ., Tokyo (Japan). Faculty of Science.
CROSSLINKING OF TWO VORTEX RINGS SIDE BY SIDE
Yuko Oshima and Naoki Izutsu (Tokyo Univ., Japan) *In* Tokyo Univ., The Proceedings of the Symposium on Mechanics for Space Flight 1987 Mar. 1988 p 19-27 (For primary document see N88-26499 20-31)
Avail: NTIS HC A07/MF A01

N88-26503# Tokyo Univ. (Japan).
TURBULENCE TRANSITION IN A CIRCULAR PIPE
Yoshio Ishii and Hidesada Kannda (IBM Japan.) *In its* The Proceedings of the Symposium on Mechanics for Space Flight 1987 Mar. 1988 p 29-36 (For primary document see N88-26499 20-31)
Avail: NTIS HC A07/MF A01

N88-26505# Miyazaki Univ. (Japan). Dept. of Applied Physics.
THERMOSTATISTICAL ESTIMATIONS OF VAPOR-STATE MOLECULES AFFECTED BY GRAVITY IN A HEAT PIPE
Kanji Etori *In* Tokyo Univ., The Proceedings of the Symposium on Mechanics for Space Flight 1987 Mar. 1988 p 47-54 (For primary document see N88-26499 20-31)
Avail: NTIS HC A07/MF A01

N88-26506# Ibaraki Univ., Hitachi (Japan).
AN EXPERIMENTAL INVESTIGATION OF TRANSIENT CHARACTERISTICS IN A GRAVITY-ASSISTED HEAT PIPE
F. Kaminaga, N. Tsuyuzaki, T. Saito (Japan Atomic Energy Research Inst., Tokyo.), M. Konno, and Y. Okamoto *In* Tokyo Univ., The Proceedings of the Symposium on Mechanics for Space Flight 1987 Mar. 1988 p 55-60 (For primary document see N88-26499 20-31)
Avail: NTIS HC A07/MF A01

N88-26507# Nippon Inst. of Tech. (Japan).
HEAT TRANSFER OF MESH-WICK HEAT-PIPES (BOTTOM HEAT MODE)
Yoshio Ikeda and Sadayuki Onuma *In* Tokyo Univ., The Proceedings of the Symposium on Mechanics for Space Flight 1987 Mar. 1988 p 61-76 (For primary document see N88-26499 20-31)
Avail: NTIS HC A07/MF A01

N88-26508# Osaka Univ. (Japan). Dept. of Aeronautical Engineering.
AN ARRANGING METHOD ON L/D OF TWO-PHASE CLOSED THERMOSYPHONS
Takayoshi Matsuoka, Kanji Negishi, Ken-ichi Kaneko, Masao Hirashima, Yuuji Nishikawa, and Masakazu Taguchi (Takuma Research and Development Co. Ltd., Dojima, Japan) *In* Tokyo Univ., The Proceedings of the Symposium on Mechanics for Space Flight 1987 Mar. 1988 p 77-86 (For primary document see N88-26499 20-31)
Avail: NTIS HC A07/MF A01

N88-26509# Tsukuba Univ., Ibaraki (Japan). Inst. of Engineering Mechanics.
A STATISTICAL TREATMENT OF ACCELERATED LIFE TEST DATA FOR COPPER-WATER HEAT PIPES
M. Murakami, K. Arai, and Y. Kojima (Fujitsu Ltd., Kawasaki, Japan) *In* Tokyo Univ., The Proceedings of the Symposium on Mechanics for Space Flight 1987 Mar. 1988 p 87-98 (For primary document see N88-26499 20-31)
Avail: NTIS HC A07/MF A01

N88-26510# Toshiba Corp., Tokyo (Japan).
FORCED-CONVECTIVE BOILING IN SMALL DIAMETER TUBE
Yoshiro Miyazaki, Yoshio Kuriyma, and Masao Furukawa (National Space Development Agency, Tokyo, Japan) *In* Tokyo Univ., The Proceedings of the Symposium on Mechanics for Space Flight 1987 Mar. 1988 p 99-105 (For primary document see N88-26499 20-31)
Avail: NTIS HC A07/MF A01

N88-26511# Takuma Research and Development Co. Ltd., Dojima (Japan).
CHARACTERISTICS OF LONG SIZE THERMOSYPHONS MADE OF CORRUGATED TUBE
Masao Hirashima, Yuuji Nishikawa, Masakazu Taguchi, Kanji Negishi, Ken-ichi Kanero, and Takayoshi Matsuoka (Osaka Univ., Japan) *In* Tokyo Univ., The Proceedings of the Symposium on Mechanics for Space Flight 1987 Mar. 1988 p 107-113 (For primary document see N88-26499 20-31)
Avail: NTIS HC A07/MF A01

35 INSTRUMENTATION AND PHOTOGRAPHY

Includes remote sensors; measuring instruments and gages; detectors; cameras and photographic supplies; and holography.

For aerial photography see *43 Earth Resources and Remote Sensing.* For related information see also *06 Aircraft Instrumentation,* and *19 Spacecraft Instrumentation.*

N88-26636 Michigan Univ., Ann Arbor.
INTERFEROMETRIC RECORDING OF HOLOGRAPHIC OPTICAL ELEMENTS USING PARTIALLY COHERENT LIGHT Ph.D. Thesis
Stacy Cuevas Leon 1987 143 p
Avail: Univ. Microfilms Order No. DA8801360

The invention of the laser along with the theory of off axis holography made the construction of holographic optics such as diffraction gratings, zone plates, and holographic mirrors quite convenient. One drawback of the laser, when used in the construction of holographic optical elements (HOEs) is coherent noise. Several techniques for constructing HOEs in light of reduced coherence are described. When the coherence of a laser source is reduced, coherent noise is suppressed. Classical and modern interferometers are described for use in the construction of HOEs. These interferometers generally operate in partially or totally incoherent light. The use of spatially incoherent light in transmission HOE construction is shown to be a significant improvement over the use of coherent light. Spatially incoherent and temporally incoherent transmission HOE forming systems are shown to have the ability to interfere a broad range of spherical wavefronts. They are capable of forming holographic zone plates with a wide variation of conjugate focal planes. Optical systems for the construction of reflection HOEs, in either spatially or temporally incoherent light, are described along with a transmission HOE forming system that operates in completely white light. The areas of possible research are discussed. Dissert. Abstr.

N88-26637# Los Alamos National Lab., N. Mex.
TIME-RESOLVED DOUBLY BENT CRYSTAL X-RAY SPECTROMETER
M. P. Hockaday, M. D. Wilke, R. L. Blake, J. Vaninetti, N. T. Gray, and P. T. Nedrow 1988 16 p Presented at the 7th Topical Conference on High Temperature Plasma Diagnostics, Napa, Calif., 13 Marc. 1988 Prepared in cooperation with EG and G Energy Measurements, Inc., Los Alamos, N. Mex.
(Contract W-7405-eng-36)
(DE88-007899; LA-UR-88-797; CONF-880364-14) Avail: NTIS HC A03/MF A01

X-ray spectroscopy is an essential tool in high temperature plasma research. We describe a time-resolved X-ray spectrometer suitable for measuring spectra in harsh environments common to many very high energy density laboratory plasma sources. The spectrometer consisted of a doubly curved Si(111) crystal diffraction element, a WL-1201 (ZnO:Ga) phosphor, a coherent fiber optic array, and two visible streak cameras. The spectrometer design described here has a minimum time resolution of 1.3 ns with 2.8 eV spectral resolution over a 200 eV wide bandpass in the 6-7 keV region of the spectrum. Complete system spectral throughput calibrations were done at the Cornell High Energy Synchrotron (CHESS). Details of the design and calibration results are presented. DOE

N88-26638# Oak Ridge Gaseous Diffusion Plant, Tenn. Enrichment Technology Applications Center.
EVALUATION OF THERMOPHOSPHOR TEMPERATURE TECHNIQUE Final Report
S. W. Allison Oct. 1987 23 p
(Contract DE-AC05-84OT-21400)
(DE88-007654; K/ETAC-38) Avail: NTIS HC A03/MF A01

For the past year the Enrichment Technology Applications Center (ETAC) of Martin Marietta Energy Systems has performed research and development on the thermographic phosphor method. The effort had two objectives: to provide a detailed error analysis for the thermal phosphor method for envisioned turbine applications; and to evaluate the technique in a laboratory environment in the 400 F to 700 F range by comparison with standard methods. This technique has the potential for solving a number of aerodynamic thermometry needs at the Arnold Engineering Development Center (AEDC). Results place the thermophosphor technique on a firmer practical base from which to launch into more advanced aerodynamic measurement applications. DOE

N88-26639# Air Force Weapons Lab., Kirtland AFB, N. Mex.
MICROWAVE CALIBRATION SYSTEM 2 Final Report, Mar. - Aug. 1987
K. Hendricks, G. DeMuth, and L. Torraca Apr. 1988 46 p
(AD-A192976; AFWL-TR-87-119) Avail: NTIS HC A03/MF A01 CSCL 14B

An expanded microwave calibration system is presented. This report discusses the process used to obtain a calibration for a detector, and the various hardware and software pieces for the system. Options available in using the system are presented. GRA

N88-26640# Edgerton, Germeshausen and Grier, Inc., Salem, Mass. Frequency Products Div.
TACTICAL RUBIDIUM FREQUENCY STANDARD (TRFS), VOLUME 1 Final Technical Report, Nov. 1983 - Dec. 1986
Thomas J. Lynch and William J. Riley Oct. 1987 129 p
(Contract F19628-83-C-0175)
(AD-A192981; RADC-TR-87-166-Vol-1) Avail: NTIS HC A07/MF A01 CSCL 14B

This report describes the accomplishments during a 3-year R&D program to design, develop, fabricate and evaluate two full scale engineering models of a Tactical Rubidium Frequency Standard (TRFS). The TRFS is a miniature atomic time and frequency source that is capable of operation in a harsh tactical military environment. In particular, it incorporates advances in miniaturization, ruggedness, fast warmup and high temperature operation that are required for aircraft applications. The report includes a detailed description of the TRFS design and the results of qualification tests on the two full scale engineering models. All program objectives were met. GRA

N88-26641*# National Aeronautics and Space Administration. Lewis Research Center, Cleveland, Ohio.
ACTIVE PHASE COMPENSATION SYSTEM FOR FIBER OPTIC HOLOGRAPHY
Carolyn R. Mercer and Glenn Beheim [1988] 8 p Prepared for presentation at the 32nd Annual International Technical Symposium on Optical and Optoelectronic Applied Science and Engineering, San Diego, Calif., 14-19 Aug., 1988; sponsored by Society of Photo-Optical Instrumentation Engineers
(NASA-TM-101295; E-4277; NAS 1.15:101295) Avail: NTIS HC A02/MF A01 CSCL 14B

Fiber optic delivery systems promise to extend the application of holography to severe environments by simplifying test configurations and permitting the laser to be remotely placed in a more benign location. However, the introduction of optical fiber leads to phase stability problems. Environmental effects cause the pathlengths of the fibers to change randomly, preventing the formation of stationary interference patterns which are required for holography. An active phase control system has been designed and used with an all-fiber optical system to stabilize the phase difference between light emitted from two fibers, and to step the phase difference by 90 deg without applying any constraints on the placement of the fibers. The accuracy of the phase steps is shown to be better than 0.02 deg., and a stable phase difference can be maintained for 30 min. This system can be applied to both conventional and electro-optic holography, as well as to any system where the maintenance of an accurate phase difference between two coherent beams is required. Author

N88-26642# Technische Univ., Munich (West Germany). Lehrstuhl fuer Nachrichtentechnik.
DISPLAY AND PROCESSING OF MULTIDIMENSIONAL SIGNALS WITH THE AID OF FRACTAL IMAGE SEQUENCES Ph.D. Thesis [DARSTELLUNG UND VERARBEITUNG HOEHERDIMENSIONALER SIGNALE MIT HILFE VON SCHNITTBILDSEQUENZEN]
Richard Bamler 1986 135 p In GERMAN
(ETN-88-92131) Avail: NTIS HC A07/MF A01

Dimensional reduction of multidimensional signals is performed by sequencing signals in 2D fractal images allowing a 2D processing. The fact that many nD signals exist already as 2D fractal image sequences is used. Mathematical models for fractal image sequences are given and examples of spatial-frequency representations of 2D signals illustrate how these sequences are obtained. ESA

N88-26643# Technische Hogeschool, Delft (Netherlands). Vakgroep Mathematische en Physische Geodesie.
TESTING OF A GRAVIMETER LCR G 785 Thesis [HET TESTEN VAN DE GRAVIMETER LCR G 785]
Pieter J. vanEss May 1987 53 p In DUTCH
(B8735061; ETN-88-92424) Avail: NTIS HC A04/MF A01

Measurements were performed and computer programs developed in order to test the drift of the gravimeter La Coste-Romberg Model G. Test measurements permitted determination of the accuracy of the instrument with respect to spring setting, flattening out, stopping, and gravimeter azimuth. The dynamic behavior of the gravimeter was analyzed with a view to microseism studies. The drift of the gravimeter was determined by tide measurements. ESA

N88-26644*# National Aeronautics and Space Administration. Lewis Research Center, Cleveland, Ohio.
FIBER OPTIC SENSORS WITH INTERNAL REFERENCING
Grigory Adamovsky and Duncan J. Maitland, IV (Cleveland State Univ., Ohio.) 1988 12 p Prepared for the Conference on Optical Testing and Metrology 2, Dearborn, Mich., 26-30 Jun. 1988; sponsored by the Society of Photo-Optical Instrumentation Engineers
(Contract NCC3-558)
(NASA-TM-100893; E-4134; NAS 1.15:100893) Avail: NTIS HC A03/MF A01 CSCL 14B

The main problem with amplitude modulating type sensors is that any variation in the intensity of the optical signal which occurs throughout the sensing system is interpreted by the photodetector as resulting from the sensor itself and is reflected as an error in the sensed parameter. To account for these errors, a referencing technique with the signal and reference channels separated in the time domain over the same fiber link can be used. Selected sensing and signal processing techniques involving temporally separated signal and referencing channels are described. A transition from the time into the frequency domain is also discussed. Experimental data are presented. Author

N88-26645*# National Aeronautics and Space Administration. Lewis Research Center, Cleveland, Ohio.
SMALL-DROPLET SPRAY MEASUREMENTS WITH A SCATTERED-LIGHT SCANNER
Robert D. Ingebo and Donald R. Buchele 1988 16 p Presented at the 2nd Symposium on Liquid Particle Size Measurement Techniques, Atlanta, Ga., 9-11 Nov. 1988; sponsored by the American Society for Testing and Materials
(NASA-TM-100973; E-4236; NAS 1.15:100973) Avail: NTIS HC A03/MF A01 CSCL 14B

Interacting two-phase flow through pneumatic two-fluid nozzles was investigated to determine the effect of nitrogen gas mass-velocity on the Sauter mean diameter of water sprays produced by the breakup of small diameter liquid-jets in high velocity gas streams. Tests were conducted primarily in the aerodynamic-stripping regime of liquid-jet atomization. It was found that the loss of droplets due to vaporization and dispersion had a marked effect on drop size measurements. A scattered-light scanner, developed at NASA Lewis Research Center was used to measure Sauter mean diameters, D sub 32, as small as 5 microns, which were correlated with nitrogen gas mass-velocity to give the following expression: D(sup -1)(sub 32) = 11.7(rho (sub n) V(sub n))(sup 1.33) where D sub 32 and p(sub n)V(sub n) are given in centimeters and g/sq cm-sec, respectively. The exponent 1.33 is the same as that predicted by atomizing theory for liquid-jet breakup in high velocity gas streams. Author

36 LASERS AND MASERS

Includes parametric amplifiers.
For related information see also *76 Solid-State Physics.*

N88-26646 Stanford Univ., Calif.
THE FREE-ELECTRON LASER: THEORETICAL INNOVATIONS AND GAS-LOADED EXPERIMENT Ph.D. Thesis
Thurmon Lawrence Deloney, II 1987 79 p
Avail: Univ. Microfilms Order No. DA8800923

Due to the improvements in technology and techniques, there is a renewed interest in the interactions of charged particle beams with periodic fields. The free-electron laser (FEL) and its kindred can theoretically generate coherent radiation from the microwave band through soft X-rays, with a single device being capable of a decade of wavelength tuning. In recent years, experimental devices have directly generated microwave, infrared, and visible wavelengths, while new ultraviolet systems are being developed. The problem with generating these shorter wavelengths in a standard Compton FEL is that the requirements on the electron beam energy and electron beam quality, or brightness, increases as the wavelength gets shorter. The gain of the FEL also falls with the wavelength. Two improvements in FELs are addressed: the dispersive FEL (DFEL) and the gas-loaded FEL (GFEL). The GFEL issues are addressed theoretically and some experimental results are presented, as well as the results of the DFEL simulation. Dissert. Abstr.

N88-26647# Stanford Linear Accelerator Center, Calif.
RESULTS FROM THE SLAC LASERTRON
J. J. Welch Jan. 1988 21 p
(Contract DE-AC03-76SF-00515)
(DE88-007816; SU-SLAC-PUB-4517) Avail: NTIS HC A03/MF A01

Rf power at 2856 MHz has been obtained from the SLAC proof of principle lasertron. Experiments show that the electron beam is well bunched when the laser beam is well dispersed, the voltage high, and the current density low. However, if any of the criteria is not met, space charge forces can cause significant debunching. The maximum beam power to rf power conversion efficiency was 12.3 percent , and the maximum rf power was 2 kW. Both maxima were obtained under the same operating conditions, at a beam voltage of 75 kV. When the maximum efficiency was obtained, it was limited by the poor match of the beam impedance to the cavity impedance. The rf measurements, the technical problems that limit available current and voltage, and the theory of the coupling between the beam and the cavity are discussed. DOE

N88-26648# Lawrence Livermore National Lab., Calif.
THE PROPAGATION OF IRRADIANCE MOMENTS OF AN ABERRATED, APODIZED FEL BEAM
M. R. Teague 29 Mar. 1988 13 p
(Contract W-7405-eng-48)
(DE88-008972; UCID-21304) Avail: NTIS HC A03/MF A01

It is pointed out that the size of the far field spot and its tranverse location may be found directly from the FEL output-plane irradiance and phase distribution. DOE

N88-26649# Central Research Inst. of Electric Power Industry, Tokyo (Japan).
LASER DIAGNOSTICS APPLIED TO ADVANCED COMBUSTION SYSTEMS

Toshihiko Nakata, Mikio Sato, and Kazuo Koyada Jun. 1987 42 p In JAPANESE: ENGLISH summary
(DE88-753119; CRIE-W-86035) Avail: NTIS (US Sales Only) HC A03

The existing systems can be classified into three systems as following; one corresponding to various types for the pulverized coals; one based on the application of spectroscopic analysis of the combustion flame; and one based on the temperature distribution measurement in the combustor using sonic measurement. These are, however, not satisfactory at the present stage, and the accurate measurement of important physical quantities (flow rate, temperature, gas concentration, etc.) which determine the state of combustion becomes more important. Recent laser measurement has a merit to allow direct measurement of the quantity of state without disturbing the combustion area, but such problems as laser beam attenuation and signal light evaluation, etc. must be solved. Hereafter it is important to conduct a comprehensive diagnosis on combusion on the basis of the combination of the past experience for developing a new system by constructing a highly reliable laser measuring system and utilizing the factor of temperature and flow rate, etc. DOE

N88-26650# Los Alamos National Lab., N. Mex.
LASER DESORPTION/ABLATION STUDIES BY RESONANCE IONIZATION MASS SPECTROMETRY
N. S. Nogar, R. C. Estler, M. W. Rowe (Texas A&M Univ., College Station.), B. L. Fearey, and C. M. Miller 1988 5 p Presented at the 4th International Symposium on Resonance Ionization Spectroscopy and its Applications, Gaithersburg, Md., 10 Apr. 1988 Prepared in cooperation with Fort Lewis Coll., Durango, CO.;Texas A and M Univ., College Station.
(Contract W-7405-eng-36)
(DE88-009124; LA-UR-88-1281; CONF-880435-12) Avail: NTIS HC A02/MF A01

Theory and results are presented for Resonance Ionization Mass Spectroscopy (RIMS) diagnostics of a variety of laser-materials interactions. DOE

N88-26651# New Mexico Univ., Albuquerque. Center for Advanced Studies.
THE CHIRPED-PULSE FREE-ELECTRON LASER Annual Performance Report, Sep. 1987 - Apr. 1988
G. T. Moore Apr. 1988 15 p
(Contract DE-AC04-76DP-00789)
(DE88-009289; DOE/ER-13788/1) Avail: NTIS HC A03/MF A01

A theoretical and numerical investigation is underway of pulsed free electron lasers in which there is a dependence of electron energy on the time of injection into the wiggler. The chirped FEL is investigated using an one-dimensional model, neglecting emittance. Diffraction is included only approximately by projection onto the fundamental Gaussian mode of a stable optical resonator. DOE

N88-26652# Argonne National Lab., Ill.
NOVEL MAGNETIC MATERIALS RESEARCH USING FREE ELECTRON LASERS
S. D. Bader Oct. 1987 5 p Presented at the Topical Meeting on Free-Electron Laser Applications in the Ultraviolet, Cloudcroft, N. Mex., 2 Mar. 1988
(Contract W-31109-eng-38)
(DE88-009989; CONF-880318-2) Avail: NTIS HC A02/MF A01

Synchrotron-radiation sources have dramatically increased the research capabilities of materials scientists. In the following, broad examples of magnetic materials research opportunities are considered. Order-of-magnitude estimates are then given of source flux and spin-polarized signal level for an undulator and an FEL source. The comparison illustrates the impact expected of FEL sources on magnetic materials research in the future. DOE

N88-26653# Los Alamos National Lab., N. Mex.
TRACKING A MONOCHROMATIC LIGHT SOURCE
L. Taylor, ed. and L. Schilling, ed. Jul. 1988 10 p
(Contract W-7405-eng-36)
(DE88-011260; LA-11312-MS) Avail: NTIS HC A02/MF A01

Experiments being planned by the Neutral Beam Technology Group of the Accelerator Technology Division will require the tracking of a monochromatic light source in space. Some general optical tracking problems are analyzed with an eye toward their application in the proposed Beam Experiments Aboard Rockets (BEAR) Program. This paper reports on a demonstration project intended as an initial step in fulfilling this requirement. DOE

N88-26654# Technische Univ., Munich (West Germany). Lehrstuhl fuer Allgemeine Elektrotechnik und Angewandte Elektrotechnik.
NEW SEMICONDUCTOR LASER STRUCTURE FOR AN OPTICAL COMMUNICATION SYSTEM Ph.D. Thesis [EINE NEUE HALBLEITERLASERSTRUKTUR FUER DIE OPTISCHE NACHRICHTENTECHNIK]
Gustav Mueller 1987 84 p In GERMAN
(ETN-88-92353) Avail: NTIS HC A05/MF A01

An InP/InGaAsP semiconductor injection laser structure suitable for optical communication in the wave emission range of 1.3 micron to 1.6 micron is described. Design and operation of bridge-contacted ridge-waveguide (BCRW) laser diodes are compared with other index guided semiconductor laser structures of simplified fabrication process. Lateral current limitation, lateral waveguiding, and longitudinal wave propagation are established. Fabrication technology is described for BCRW laser diodes and experimental results show the static emission properties independence of structure geometry. ESA

N88-26655# Lawrence Livermore National Lab., Calif.
HIGH SPATIAL FREQUENCY THERMAL BLOOMING INSTABILITY: A LINEAR STABILITY ANALYSIS
J. J. Barnard 29 Apr. 1988 24 p Presented at the Workshop on Physics of Directed Energy Propagation in the Atmosphere, Las Cruces, N. Mex., 29 Mar. 1988
(Contract W-7405-eng-48)
(DE88-010711; UCRL-98068; CONF-8803106-1) Avail: NTIS HC A03/MF A01

The fine-scale thermal blooming instability is shown to be affected by the laser pulse length. In this study, we calculate the asymptotic gain of a sinusoidal perturbation as a function of pulse length and perturbation wave number. We include the effects of viscosity, diffusion, and wind shear, and we heuristically estimate the effect of turbulence. We find that for short laser pulses, the small wave number perturbations are reduced due to acoustic effects. However, large wave number perturbations remain large and extend to a higher cutoff in wave number than in the long laser pulse limit. At wave numbers higher than this cutoff, thermal diffusion causes exponential decay of the perturbations. For long laser pulse length wind shear and turbulence limit perturbation growth. DOE

N88-26656# Lawrence Livermore National Lab., Calif.
OPTICAL COATINGS FOR HIGH AVERAGE POWER XeF LASERS Final Report
D. Milam, I. Thomas, J. Wilder, and D. George 16 Mar. 1988 50 p
(Contract W-7405-eng-48)
(DE88-011356; UCID-21349) Avail: NTIS HC A03/MF A01

Porous silica, calcium and magnesium fluorides were investigated for potential use as antireflective coatings for XeF lasers. Excellent optical properties were obtained for all types, and laser damage thresholds were in the range 18 to 25 J/sq cm at 350 nm for 25 ns pulses at 25 Hz pulse repetition frequency. Studies of the effects of the XeF laser environment on these coatings were incomplete. Three oxides, ZrO2, HfO2, and Ta2O5 were investigated as the high index components to be paired with low index porous SiO2 for highly reflective dielectric coatings. Single oxide layers had indices in the 1.7 to 1.8 range and HfO2 coatings had the highest damage threshold at about 5 J/sq cm. An unexpected problem arose on attempts to prepare multilayer

coatings. Stress in the coating after 6 to 8 layers had been put down, gave rise to crazing and peeling. This could not be avoided even on extending the curing process between coats. DOE

N88-26657# Lawrence Livermore National Lab., Calif.
MODEL FOR PULSE AMPLIFICATION BY A GASEOUS LASER AMPLIFIER
C. D. Boley and B. E. Warner 19 Oct. 1987 12 p Presented at the Optical Society of America Annual Meeting, Rochester, N.Y., 18 Oct. 1987
(Contract W-7405-eng-48)
(DE88-011729; UCRL-96753; CONF-871047-1) Avail: NTIS HC A03/MF A01

We have developed a computational model for pulse amplification by a pulsed electric discharge laser amplifier. We have applied the model to the copper vapor system, for which the oscillator has previously been modeled on a 0-D level and a 1-D level. The laser intensity transport equations are set up on a ray and are differenced with respect to the axial coordinate. Amplified spontaneous emission is handled similarly. Rate equations for the atomic levels are set up in each axial cell. The motion of the atoms is negligible on the nanosecond time scales of interest. The entire system of equations is advanced in time by a standard mathematical package. Working with a selection of input pulse shapes and energies, we have obtained predictions for the amplified signal as a function of time. We have also obtained results for related diagnostics such as the radiation profiles along the tube at selected times. DOE

N88-26305# Nissan Motor Co. Ltd., Tokyo (Japan).
A NUMERICAL ANALYSIS OF FLOW CHARACTERISTICS IN LASER PROPULSION SYSTEM
Toru Shimada and Takashi Abe (Tokyo Univ., Japan) *In* National Aerospace Lab., Proceedings of the 5th NAL Symposium on Aircraft Computational Aerodynamics Nov. 1987 p 109-114 In JAPANESE; ENGLISH summary (For primary document see N88-26290 20-01)
Avail: NTIS HC A12/MF A01

37 MECHANICAL ENGINEERING

Includes auxiliary systems (nonpower); machine elements and processes; and mechanical equipment.

N88-26658 Cleveland State Univ., Ohio.
DESIGN OF A CONTROLLER TO REDUCE RESIDUAL VIBRATION IN THE POSITIONING CONTROL OF FLEXIBLE ROBOTIC MANIPULATORS Ph.D. Thesis
Anthony Paul Messuri 1987 218 p
Avail: Univ. Microfilms Order No. DA8801079

Residual vibration refers to the structural vibrations which continue after the completion of a movement by a robotic manipulator from one position to another. These low-frequency vibrations occur at the damped natural frequencies of the system and require a fixed amount of time at the end of the movement to allow these unwanted vibrations to settle. The research effort is aimed at developing a control method which will reduce the residual vibration in a robotic manipulator while also reducing the time required to arrive at the desired final position. The application of this control method involves the design of a controller to test the structural dynamic characteristics of the robotic structure and analyze three characteristics in order to determine the natural frequencies of the system at the endpoint, and then design a control drive signal which reduces the input energy occurring at these natural frequencies. The accuracy with which the peak frequency is determined is shown to have a significant effect on the ability of the controller to reduce residual vibration. The software algorithms together with the capabilities of appropriate test equipment enable the controller to determine the peak frequency with a high degree of accuracy. The controleer was tested by using it to control a simple shaker system, a one-axis rotational system, and a commercial robotic manipulator. Dissert. Abstr.

N88-26659# Los Alamos National Lab., N. Mex.
FINITE ELEMENT WELDING COMPUTATIONS USING GENERAL PURPOSE NONLINEAR ANALYSIS CODES
L. A. VanGulick 1988 29 p Presented at the ASME Pressure Vessel and Piping Conference, Pittsburgh, Pa., 19 Jun. 1988
(Contract W-7405-eng-36)
(DE88-005398; LA-UR-88-313; CONF-880661-1) Avail: NTIS HC A03/MF A01

Parts being welded experience high local temperatures and severe thermal gradients which lead to large local stresses due to nonuniform thermal expansion and contraction. Unacceptable degradation of material mechanical properties, residual stresses, and changes in geometry can result. General purpose nonlinear finite element method analysis codes offer features which should facilitate their use for predicting welding temperatures, displacements, and stresses. A series of computations evaluating the use of general purpose codes for this purpose is described. Useful code features are identified and computational procedures to enhance solution accuracy suggested. DOE

N88-26660# Sandia National Labs., Albuquerque, N. Mex.
FORCE SERVO CONTROL OF A COMMERCIAL GANTRY ROBOT
B. J. Petterson and J. F. Jones 1988 10 p Presented at the Robots 12/Vision Conference, Detroit, Mich., 6 Jun. 1988
(Contract DE-AC04-76DP-00789)
(DE88-006649; SAND-87-2167C; CONF-880683-1) Avail: NTIS HC A02/MF A01

Sandia National Laboratories is investigating robotic handling of spent nuclear fuel shipping casks for the proposed geologic waste repositories. Robotic handling will impact not only the design of the transportation casks but also the overall design of the waste repository. A goal of robotic handling is reduction of personnel radiation exposure. One of the major technology development areas has been the integration of sensors into the control of the robot system to allow operation in semi-structured environments. In particular, a multiaxis force sensor is used to make robot trajectory corrections based on the contact forces between the robot and cask. DOE

N88-26661# Sandia National Labs., Albuquerque, N. Mex.
RRSAS (ROBOTIC RADIATION SURVEY AND ANALYSIS SYSTEM) PROJECT: A REAL TIME SENSOR DRIVEN ROBOTIC SYSTEM
Siegfried Th1nborg 1988 14 p Presented at the Robots 12/Vision Conference, Detroit, Mich., 6 Jun. 1988
(Contract DE-AC04-76DP-00789)
(DE88-006825; SAND-87-1994C; CONF-880683-2) Avail: NTIS HC A03/MF A01

A prototype robotic system developed to conduct radiation surveys on nuclear waste shipping casks is discussed. The system integrates sensing and model based control into the operation of a commercial gantry robot. This allows location of the cask, automatic development of radiation survey test plans, and execution of complete radiation surveys, including force controlled contact swiping at random locations on the cask surface. The robotic system incorporates data management and real-time graphical presentation of survey results. DOE

N88-26662# Edgerton, Germeshausen and Grier, Inc., Idaho Falls, Idaho.
PHYSICAL-CHEMICAL REACTIONS AT WELDING ARC/MOLTEN POOL INTERFACES Annual Report, FY 1986
J. F. Key and M. E. McIlwain Sep. 1987 41 p
(Contract DE-AC07-76ID-01570)
(DE88-007717; EGG-MS-7856) Avail: NTIS HC A03/MF A01

The arc heat source has been shown to have a strong influence on the characteristics of the molten weld pool and resulting weld bead morphology. The existence of nonequilibrium temperature distribution between arc species and the presence of metallic vapor in the arc plasma above the anode have been suggested to have an influence on the current distribution. These two influences have been investigated. A multi-fluid treatment of the arc to discern the

impact on the anode current distribution and transport properties by nonequilibrium temperature distribution between electrons and heavy species in the welding arc suggests that nonequilibrium has a pronounced influence on the transport properties. However, the resulting anode current distribution is only slightly perturbed. Results suggest that nonequilibrium between species in the interfacial region of the arc above the anode produces only a second-order influence on the anode current distribution. The presence of small amounts (5-10 percent) of manganese can significantly enhance the low temperature conductivity of the plasma. This results in broadening of the anode current distribution relative to that found when only argon is present in the arc. Attemps to develop optical and laser diagnostics for the interfacial region above the anode are reported. Results suggest that laser induced fluorescence has considerable merit for determining species distributions in the arc and possibly in the interfacial region.
DOE

N88-26663# Oak Ridge National Lab., Tenn.
SENSOR FUSION FOR ROBOT NAVIGATION
D. M. Jollay and R. E. Ricks 1988 19 p Presented at the 26th Annual Conference of the Association for Computing Machinery Southeast Region, Mobile, Ala., 21 Apr. 1988
(Contract DE-AC05-84OR-21400)
(DE88-008383; CONF-880499-1; CONF-880499) Avail: NTIS HC A03/MF A01

This paper demonstrates how a relatively simple vision analysis algorithm can be used in conjunction with sonar sensors to greatly improve the ability of the robot to perceive and accurately locate obstacles. So far, the system can only handle somewhat constrained environments: tall, rectangular, darker colored obstacles with well lighted, lighter colored walls forming the background. The intent was to demonstrate how a simple sensor fusion system can lead to great improvements in robot perception. The program is executed much more quickly than other more sophisticated 3D vision techniques. It is more reliable than if just one type of sensor were used. In addition, the robot, HERMIES-2, is capable of accurately maintaining its position and orientation in the navigation area. The navigation program is relatively inexpensive to implement, and is goal oriented. It allows relatively optimum paths to be found in a previously unexplored, potentially dynamic environment.
DOE

N88-26664# Lawrence Livermore National Lab., Calif.
DUCTILE-BRITTLE TRANSITION OF CUTTING BEHAVIOR IN DIAMOND TURNING OF SINGLE CRYSTAL SI
C. K. Syn, J. S. Taylor, R. R. Donaldson, and S. Shimada Jan. 1988 9 p Presented at the Annual Spring Meeting of the Japan Society of Precision Engineering, Kawasaki, Japan, 16 Mar. 1988 Prepared in cooperation with Osaka Univ., Japan
(Contract W-7405-eng-48)
(DE88-008890; UCRL-98100; CONF-880390-1) Avail: NTIS HC A02/MF A01

Diamond turning of single crystal silicon disks with round-nosed diamond tools has been studied by interrupting the turning and observing the surface of shoulders formed between the turned regions and original surface. The observation of such a shoulder surface reveals a distinct transition from the very smooth, crack-free zone on the top side of the shoulder. The location of the boundary between the two zones moves up or down or out of the shoulder depending on the feed rate, depth of cut, crystallographic orientation and cutting fluid. Such a distinct transition seems to indicate a change in the cutting mode or material removal process from ductile plastic deformation of the work material in front of the cutting tool to brittle crack propagation and fracture. The location of such a transition zone seems determined by the uncut chip thickness. Experimental details and possible explanations for cutting mode transition will be discussed in detail during the presentation.
DOE

N88-26665# Clemson Univ., S.C. Dept. of Electrical and Computer Engineering.
MOBILE ROBOT SURVIVAL
F. R. Sias, Jr. and F. Heckendorn 1988 5 p Presented at the Southeastcon '88 Conference and Exhibit, Knoxville, Tenn., 11 Apr. 1988 Prepared in cooperation with Du Point de Nemours (E. I.) and Co., Aiken, S.C.
(Contract DE-AC09-76SR-00001)
(DE88-009108; DP-MS-88-37; CONF-880433-5) Avail: NTIS HC A02/MF A01

Mobile robots designed for use in hazardous environments around nuclear reactors or nuclear power plants are subject to a number of threats that may severely damage or result in the loss of an expensive robot. If the radiation level is sufficiently high it will not be possible to send a man into the environment to correct the malfunction and the robot may not be recoverable. In order to protect a mobile robot in a hazardous radiation environment, it is first necessary to examine and classify all of the potential threats and then devise schemes to prevent or counteract each possible source of damage in a cost-effective manner. Some of the most obvious mobile robot threats include radiation damage to on-board electronics, non-recoverable attitude due to capsizing or suspension of the transport, damage due to robot or arm collision with objects, immobilization by obstructions, loss of control tether, and loss of robot power. Experience with a wheeled robot at the Dupont Savannah River Laboratory has demonstrated that it is readily possible to tip a robot over or to trap the robot arm in overhead objects when controlling it using cues only from an on-board video camera. This paper provides an analysis of the threats and examines possible solutions.
DOE

N88-26666# Sandia National Labs., Albuquerque, N. Mex.
INSTRUMENTATION FOR THE MEASUREMENT OF PENETRATOR DYNAMIC RESPONSE TO PERMIT FORCE ESTIMATION
V. I. Bateman May 1988 34 p
(Contract DE-AC04-76DP-00789)
(DE88-010608; SAND-87-0673) Avail: NTIS HC A03/MF A01

The general problem of penetrator instrumentation is discussed, and the advantages of strain gages for the field test environment are presented. The use of strain modes shapes to determine the best locations for strain gage installation is explained and applied to a geometrically simple bar whose mode shapes can be derived analytically. For more complex structures such as penetrators, a rationale is provided to derive strain mode shapes from an acceleration-based modal analysis. This rationale is used to determine the strain mode shapes using experimental data for a penetrator body.
DOE

N88-26667# Central Research Inst. of Electric Power Industry, Tokyo (Japan).
COMPUTATIONAL STUDY ON THERMAL EFFICIENCY OF CERAMIC GAS TURBINE
Toru Hisamatsu, Toshio Abe, Teruhide Hamamatsu, Kazuhiko Kawaike, Hiroshi Miyata, Shiro Iijima, and Ryoichiro Oshima Jun. 1987 21 p In JAPANESE; ENGLISH summary
(DE88-753114; CRIE-W-86015) Avail: NTIS (US Sales Only) HC A03

The effect on the thermal efficiency of combined cycle power plant by applying the ceramic gas turbine was analyzed. Stator vanes and moving blades were thought to relate the performance improvement, but from the reliability point of view, the analysis was made only to the ceramic stator vanes. In order to analyze the performance of only metal blades, only ceramic blades and their combination, inflowing process of cooling air was ascertained and cooling air quantity on the cooling characteristics was calculated. Ceramic blades were assumed to be able to use without air cooling within the applying temperature range. When the sending end efficiency of the present combined power plant using 1100 C class gas turbine was assumed as 44 percent , the increase of the sending end efficiency (absolute value) was expected to be about 2.5 percent when ceramic blades were applied to the first stage at the turbine inlet temperature of 1300°C, and about 3.2 percent when ceramic blades were applied to first and second stages.
DOE

N88-26668# Central Research Inst. of Electric Power Industry, Tokyo (Japan).
STUDY ON THE HEAT RESISTING AND COOLING PROPERTY OF THE CERAMICS-METAL HYBRID STATOR VANES
Toru Hisamatsu, Toshio Abe, Teruhide Hamamatsu, Hiroshi Miyata, Shiro Izima, Takahashi, Ichiro, and Ryoichiro Oshima Jun. 1987 28 p In JAPANESE; ENGLISH summary
(DE88-753117; CRIE-W-86033) Avail: NTIS (US Sales Only) HC A03

20 MW class gas turbine stator blade was designed and test-made. Combustion gas with temperature up to 1,600°C was flown to five wings in a row. Temperature of the metal core reduced its influence as the amount of the cooling air increased; in the case of s/s with maximum allowable temperature of 600°C, required amount of cooling air was found to be roughly 0.5 percent of the total amount of the compressed air (1/10 of the metal, air-cooled blades), which coincided with the results of analysis. Concerning the temperature distribution of the ceramic shell, big difference was found in the front edge surface (outer and inner); more temperature reduction was found at the rear edge of the blade at the time of shut-down. The results of analysis were the same as that of the heat impact test of the single ceramic body. It is hereafter desirable to consider the generation of the thermal stress amd to improve the shell structure. DOE

N88-26669# International Centre for Theoretical Physics, Trieste (Italy).
MAGNETOHYDRODYNAMIC SQUEEZE FILM
E. A. Hamza Jun. 1987 24 p
(DE88-701876; IC-87/134) Avail: NTIS (US Sales Only) HC A03/MF A01

The motion of an electrically conducting fluid film squeezed between two parallel disks in the presence of a magnetic field applied perpendicular to the disks is studied. Analytic solutions through use of a regular perturbation scheme are obtained. The results show that the electromagnetic forces increase the load carrying capacity considerably. DOE

N88-26670# Tennessee Univ., Knoxville. Dept. of Mechanical and Aerospace Engineering.
OPTIMIZATION OF PERFORMANCE CRITERIA WITH BOUNDED JOINT VELOCITIES FOR ROBOTS WITH ONE DEGREE OF REDUNDANCY
R. V. Dubey, J. A. Euler, and S. M. Babcock 1988 9 p Presented at the US-Japan Symposium on Flexible Automation, Minneapolis, Minn., 18 Jul. 1988 Prepared in cooperation with ORNL, Tenn.
(Contract DE-AC05-84OR-21400)
(DE88-003915; CONF-880721-1; CESAR-87/41) Avail: NTIS HC A03

Most kinematic control schemes for robots with redundant joints determine the joint motions for a desired end-effector trajectory such that a performance criterion is optimized. When the robot is in motion, it may reach a configuration in which the joint velocities required to optimize a performance criterion, while following a desired end-effector trajectory, may be extremely high. This problem is referred to as an algorithmic singularity. The control scheme presented in this paper avoids high joint velocities by compromising optimization of the performance criterion in the neighborhood of an algorithmic singularity. This scheme does not require the pseudoinverse of the Jacobian and thus, it is computationally efficient and well suited for real-time implementation. Unlike other control schemes, the robot is not required to be an optimum configuration at the starting point. The application of this scheme to a seven-degree-of-freedom manipulator at the Center for Engineering Systems Advanced Research (CESAR) is described. DOE

N88-26671# Argonne National Lab., Ill.
FLUID FLOW MODELING IN CASTING PROCESSES AND ITS IMPLICATIONS
W. T. Sha 1988 17 p Presented at the Modeling Control of Casting and Welding Processes Conference, Palm Coast, Fla., 17 Apr. 1988
(Contract W-31109-eng-38)
(DE88-010009; CONF-8804124-1) Avail: NTIS HC A03/MF A01

In recent years, mathematical modeling of casting processes has received increasing attention; however, very little work has been done on modeling of fluid flow of liquid melt. This paper discusses some important aspects and implications of fluid flow modeling pertinent to casting processes. The recent advances and projected progress of computer technology and numerical analysis have made is possible to begin to perform realistic simulations of the casting process in general and to model fluid flow of liquid melt in particular. Topics to be discussed include the (1) desirability of a computer system specifically for casting modeling, (2) need for efficient solution technique for fluid flow and user-friendly pre- and post-processors or user-interface package, and (3) development of both realistic constitutive relations and reliable material properties pertinent to castings. Fluid flow of liquid melt plays an important role in the design of the feed system and mold, solidification rate and pattern, gas entrainment, and segregation of alloy elements. DOE

N88-26672# Allied Bendix Aerospace, Kansas City, Mo.
GTAW CHARACTERIZATION FOR WELD PENETRATION ON 304L STAINLESS STEEL
J. P. Dereskiewicz May 1988 38 p
(Contract DE-AC04-76DP-00613)
(DE88-010611; BDX-613-3931) Avail: NTIS HC A03/MF A01

A statistical analysis determined flange thickness to be the most significant independent variable on weld penetration within the experimental range, followed by gap size and flange height. Step size was concluded to be insignificant on weld penetration in the experimental range from 0 to 0.020 in. When an optimized low heat input weld schedule was used, weld penetration was dependent upon flange thickness and flange height when gap size was less than 0.0075 in. and upon flange thickness and gap when gap size varied from 0.0075 to 0.015 in. Generally, as weld penetration increased, flange thickness and gap size decreased while flange height increased. Weld penetration could be predicted for various flange thicknesses, flange heights, and gaps by utilizing the factorial cube, surface response curves, topography maps, and weld penetration equations developed from this study. The 0.030-in. minimum weld penetration requirement could not be met throughout the tolerance range unless flange thickness was approximately 0.025 in. A technical effort is presently being pursued to characterize a cold wire feed gas tungsten arc system to enhance weld penetration and meet product drawing requirements. DOE

N88-26673# Southwest Research Inst., San Antonio, Tex. Belvoir Fuels and Lubricants Research Facility.
ANALYTICAL AND EXPERIMENTAL INVESTIGATION OF RINGLESS PISTON CONCEPT Interim Report, Sep. 1986 - Dec. 1987
Daniel W. Dickey and Charles D. Wood Dec. 1987 57 p
(Contracts DAAJ02-86-C-0030; DAAK70-85-C-0007)
(AD-A192835; BFLRF-247) Avail: NTIS HC A04/MF A01
CSCL 21G

The purpose of this project was to analytically and experimentally investigate the concept of a ringless piston internal combustion engine. A joint objective was to design, build, and test a ringless piston to improve ringless piston engine performance. A computer model was developed to predict ringed and ringless piston engine performance. Experimental performance data were then collected by operating a small, liquid cooled, two stroke gasoline engine with and without the piston ring on the stock aluminum and Southwest Research Institute prototype steel piston. The experimental performance data were then compared with the results of the computer model. The results showed that a piston engine can operate without piston rings. GRA

N88-26674# Naval Ocean Systems Center, San Diego, Calif.
LOCAL FREE-SPACE MAPPING AND PATH GUIDANCE FOR MOBILE ROBOTS Technical Report, Apr. - Oct. 1986

William T. Gex and Nancy L. Campbell Mar. 1988 22 p
(AD-A192970; NOSC/TD-1227) Avail: NTIS HC A03/MF A01
CSCL 17G

A method was developed of mapping the local environment in front of a ground vehicle that employs acoustic sensors. The extent of known free space is used to generate navigation points, in the form of a subgoal and avoidance points, which may be used by another process to generate a path. The map information is also used to steer the sensors to areas of the environment that require further investigation. Inconsistencies in sensor returns are resolved with multiple sensor scans. GRA

N88-26675*# Ohio State Univ., Columbus. Dept. of Mechanical Engineering.
A REVIEW OF GEAR HOUSING DYNAMICS AND ACOUSTICS LITERATURE Technical Report, Mar. - Dec. 1987
Rajendra Singh and Teik Chin Lim Jul. 1988 85 p
(Grant NAG3-773)
(NASA-CR-183110; NAS 1.26:183110) Avail: NTIS HC
A05/MF A01 CSCL 13I

A review of the available literature on gear housing vibration and noise reduction is presented. Analytical and experimental methodologies used for bearing dynamics, housing vibration and noise, mounts and suspensions, and the overall geared and housing system are discussed. Typical design guidelines as outlined by various investigators are given. Author

N88-26676# Stuttgart Univ. (West Germany). Inst. fuer Thermische Stroemungsmaschinen und Maschinenlaboratorium.
EXPERIMENTAL AND THEORETICAL STUDY OF THE DYNAMIC OPERATIONAL BEHAVIOR OF A THREE STAGE RADIAL COMPRESSOR Ph.D. Thesis [EXPERIMENTELLE UND THEORETISCHE UNTERSUCHUNG DES DYNAMISCHEN BETRIEBSVERHALTENS EINES DREISTUFIGEN RADIALVERDICHTERS]
Michael Loehle 1986 216 p In GERMAN
(ETN-88-92129) Avail: NTIS HC A10/MF A01

For the analysis of thermal and mechanical loads of a compressor during accidental events, rapid control processes, and transient operation, the dynamic response characteristics are investigated. Experimental tests on a three stage serial radial compressor indicate that by rapid acceleration the dynamic characteristics are different from stationary ones. In the case of periodic variations of the main control factors like mass flow and pressure, the dynamic characteristics curve has the form of a hysteresis. ESA

N88-26677# National Aerospace Lab., Amsterdam (Netherlands). Informatics Div.
AN INTRODUCTION TO ROBOT JOINT CONTROL METHODS
M. Kuijper 1 Aug. 1986 35 p
(NLR-TR-86080-U; B8803894; ETN-88-92600) Avail: NTIS HC
A03/MF A01

Control of robot joints based on servocontrol, hierarchical control, optimal control, nominal/perturbation control, nonlinear feedback control, and adaptive control is reviewed. The complexity of the model equation on which a control method should be based, depends upon the relevance of the dynamic coefficients. It seems likely that in the case of space-robots the model equation should be nonlinear, leading to control methods based on nominal/perturbation control, nonlinear feedback control, and adaptive control. ESA

N88-26678# National Aerospace Lab., Amsterdam (Netherlands). Space Div.
SIMULATION OF SPACE MANIPULATOR OPERATIONS (EUROSIM)
C. N. A. Pronk, A. Elfving, E. Ersu, and A. L. Lippay 13 Mar. 1987 10 p Presented at the Summer Computer Simulation Conference, Montreal, Quebec, 27-30 Jul. 1987
(Contract ESA-6482/85)
(NLR-MP-87017-U; B8805305; ETN-88-92609) Avail: NTIS HC
A02/MF A01

Definition and planning of application software for ESA's European Robotic Operations Simulator are reviewed. Simulation definition and test control software; overall system dynamic model; generic models for the in-orbit infrastructure, including spacecraft, environment, and payload; and mathematical models for the space manipulator system are discussed. A survey of existing models and software completed the requirements study. A plan for further development was specified. ESA

N88-26679*# National Aeronautics and Space Administration. Lewis Research Center, Cleveland, Ohio.
CONTACT FORCE HISTORY AND DYNAMIC RESPONSE DUE TO THE IMPACT OF A SOFT PROJECTILE
J. E. Grady Aug. 1988 23 p
(NASA-TM-100961; E-4035; NAS 1.15:100961) Avail: NTIS HC
A03/MF A01 CSCL 13I

A series of ballistic impact tests on several different instrumented targets was performed to characterize the dynamic contact force history resulting from the impact of a compliant projectile. The results show that the variation of contact force history with impact velocity does not follow the trends predicted by classical impact models. An empirical model was therefore developed to describe this behavior. This model was then used in a finite-element analysis to estimate the force history and calculate the resulting dynamic strain response in a transversely impacted composite laminate. Author

N88-26521# Stuttgart Univ. (West Germany). Inst. fuer Mechanik.
MODELING AND PARAMETER IDENTIFICATION OF MOTOR VEHICLES [MODELLBILDUNG UND PARAMETERIDENTIFIKATION BEI KRAFTFAHRZEUGEN]
W. Schiehlen *In* DFVLR, System Identification in Vehicle Dynamics 1987 p 91-102 In GERMAN (For primary document see N88-26518 20-31)
Avail: NTIS HC A18/MF A01; DFVLR, VB-PL-DO, 90 60 58, 5000 Cologne, Fed. Republic of Germany, 109 Deutsche marks

N88-26522# Deutsche Forschungs- und Versuchsanstalt fuer Luft- und Raumfahrt, Oberpfaffenhofen (West Germany). Inst. fuer Dynamik der FLugsysteme.
SIMULATION MODELS FOR THE DYNAMICS OF TRACKED VEHICLE SYSTEMS: STATE-OF-THE-ART AND OPEN PROBLEMS
W. Kortuem and J. Jaschinski *In its* System Identification in Vehicle Dynamics 1987 p 103-140 (For primary document see N88-26518 20-31)
Avail: NTIS HC A18/MF A01; DFVLR, VB-PL-DO, 90 60 58, 5000 Cologne, Fed. Republic of Germany, 109 Deutsche marks

N88-26523# Technische Hochschule, Darmstadt (West Germany). Fachbereich Regelsystemtheorie.
VEHICLE DYNAMICS: IDENTIFICATION IN THE FREQUENCY DOMAIN [FAHRZEUGDYNAMIK: IDENTIFIKATION IM FREQUENZBEREICH]
V. Tews *In* DFVLR, System Identification in Vehicle Dynamics 1987 p 141-152 In GERMAN; ENGLISH summary (For primary document see N88-26518 20-31)
Avail: NTIS HC A18/MF A01; DFVLR, VB-PL-DO, 90 60 58, 5000 Cologne, Fed. Republic of Germany, 109 Deutsche marks

N88-26531# Daimler-Benz A.G., Stuttgart (West Germany).
IDENTIFICATION METHODS FOR TRANSPORT DYNAMICAL INVESTIGATIONS [IDENTIFIKATIONSMETHODEN FUER FAHRDYNAMISCHE UNTERSUCHUNGEN]
W. Reichelt *In* DFVLR, System Identification in Vehicle Dynamics 1987 p 267-286 In GERMAN (For primary document see N88-26518 20-31)
Avail: NTIS HC A18/MF A01; DFVLR, VB-PL-DO, 90 60 58, 5000 Cologne, Fed. Republic of Germany, 109 Deutsche marks

N88-26534# Krauss-Maffei A.G., Munich (West Germany).
IDENTIFICATION OF LATERAL OPERATION DYNAMICS OF RAIL VEHICLES USING ROLL TEST STAND TESTS [IDENTIFIZIERUNG DER LATERALEN LAUFDYNAMIK VON SCHIENENFAHRZEUGEN DURCH ROLLPRUEFSTANDSVERSUCHE]
K. Heym *In* DFVLR, System Identification in Vehicle Dynamics 1987 p 343-361 In GERMAN (For primary document see N88-26518 20-31)
Avail: NTIS HC A18/MF A01; DFVLR, VB-PL-DO, 90 60 58, 5000 Cologne, Fed. Republic of Germany, 109 Deutsche marks

N88-26536# Volkswagen A.G., Wolfsburg (West Germany).
PARAMETER IDENTIFICATION OF THE PASSENGER SIMULATION MODEL MADYMO: METHODS AND EXPERIENCE [PARAMETERIDENTIFIKATION DES INSASSENSIMULATIONSMODELLS MADYMO: METHODEN UND ERFAHRUNGEN]
R. Zobel, H.-G. Bock, and Th. Reiners (Bonn Univ., West Germany) *In* DFVLR, System Identification in Vehicle Dynamics 1987 p 375-399 In GERMAN (For primary document see N88-26518 20-31)
Avail: NTIS HC A18/MF A01; DFVLR, VB-PL-DO, 90 60 58, 5000 Cologne, Fed. Republic of Germany, 109 Deutsche marks

38 QUALITY ASSURANCE AND RELIABILITY

Includes product sampling procedures and techniques; and quality control.

N88-26680# Sandia National Labs., Albuquerque, N. Mex.
MICROFOCUS X-RAY TECHNIQUES FOR FLAW LOCATION
J. W. Guthrie Mar. 1988 13 p
(Contract DE-AC04-76DP-00789)
(DE88-008636; SAND-88-0448) Avail: NTIS HC A03/MF A01

Two flaw location techniques are proposed using direct image magnifications from a microfocus X-ray system with less than or equal to 0.0004-in. focal spot and 10-160-kV capabilities. DOE

N88-26681# Sandia National Labs., Albuquerque, N. Mex.
DEVELOPMENT OF AN AUTOMATED X-RAY GAUGE FOR NONDESTRUCTIVE QUANTITATIVE ANALYSIS
W. D. Drotning Mar. 1988 56 p
(Contract DE-AC04-76DP-00789)
(DE88-008633; SAND-88-0119) Avail: NTIS HC A04/MF A01

This report describes an X-ray gauging system developed in the Materials Characterization Department at Sandia for nondestructive quantitative analysis. The automated device utilizes the transmission of low-energy X-rays through a material in order to measure the areal density of the material. If the material density is known, the X-ray gauge serves as a non-contacting thickness gauge, typically for micron-range dimensions. On the other hand, if the material thickness is known, X-ray gauging measurements yield the volume density of the material, so that quantitative chemical analysis may be achieved. Under some conditions, one material may be examined in the presence of another, making the gauge useful for examination of a thin coating on a substrate or of an element dispersed in a host matrix. Using digital rather than analog conversion techniques, measurement precision of 0.1 percent and accuracy near 0.5 percent have been achieved, with analytical correction for X-ray detection losses. The accuracy of the instrument has been demonstrated by comparison with chemical quantitative analysis techniques. Compared to chemical techniques, the X-ray gauge is faster, lower cost and nondestructive while maintaining measurement accuracy. In addition, accuracy has been demonstrated in analysis for elements for which calibration standards were not available. This feature offers a significant advantage over chemical analysis methods which require a known calibration standard for each element to be measured. The X-ray gauge thus provides a technique for rapid, accurate and automated nondestructive quantitative analysis of materials with minimal operator attention and sample handling. DOE

N88-26682# Los Alamos National Lab., N. Mex.
METHODS AND TECHNIQUES OF NDA (NONDESTRUCTIVE ASSAY)
T. D. Reilly 1988 41 p Presented at the Regional Training Course on State Systems of Accounting for and Control of Nuclear Materials, Rio de Janeiro, Brazil, 11 Apr. 1988
(Contract W-7405-eng-36)
(DE88-009145; LA-UR-88-1077; CONF-8804109-1) Avail: NTIS HC A03/MF A01

Nondestructive assay (NDA) refers to techniques and instruments developed to measure nuclear materials in the many forms in which they occur throughout the fuel cycle. These techniques were first developed to support nuclear safeguards inspections and nuclear material accountability; they are also used extensively for process and quality control. Most accountability measurements are based on analytical chemistry and require that a sample be drawn and analyzed destructively. Destructive analysis can not be applied to many of the product materials found in the fuel cycle, such as fuel rods and assemblies, because of their high monetary value. Also, many waste and scrap materials can not be adequately sampled for destructive analysis because of their heterogenous nature. This situation led to the development of nondestructive analysis techniques. This paper presents an overview of the major NDA techniques and instrumentation in use today. The instrumentation described below is now used frequently by safeguards inspectors and facility operators alike. DOE

N88-26683# Materialpruefungsanstalt, Stuttgart (West Germany).
PRINCIPLES OF A NONDESTRUCTIVE EVALUATION PROCESS FOR DAMAGE LOCATION, DAMAGE PROFILE, AND DAMAGE EXTENSION IN WELDED JOINTS BY RADIOMETRIC MEASUREMENTS [GRUNDLAGEN FUER EIN VERFAHREN ZUR ZERSTOERUNGSFREIEN BESTIMMUNG VON FEHLERLAGE, FEHLERGESTALT UND FEHLERABMESSUNGEN IN SCHWEISSNAEHTEN MITTELS RADIOMETRISCHER MESSUNGEN]
Wolfgang Wuensch Oct. 1986 160 p In GERMAN Sponsored by Bundesministeriums des Innern, Bonn, Fed. Republic of Germany
(MPA-86-02; ISSN-0721-4529; ETN-88-92092) Avail: NTIS HC A08/MF A01

A procedure for damage evaluation of welded joints of pipes and nuclear reactors with wall width up to 60 to 120 mm is described. The method is based on gamma radiation attenuation by metals and application of monoenergetic gamma rays. Experimental assembly includes an Ir-gamma radiation source, test sample inserted between two collimators, and NaI-detector. This nondestructive testing method improves visual flaw detection by direct measurement on the test sample allowing the quantitative evaluation of welded joint quality independently from the image assessment. ESA

39 STRUCTURAL MECHANICS

Includes structural element design and weight analysis; fatigue; and thermal stress.

For applications see *05 Aircraft Design, Testing and Performance* and *18 Spacecraft Design, Testing and Performance.*

N88-26684*# National Aeronautics and Space Administration. Langley Research Center, Hampton, Va.
THREE-DIMENSIONAL ANALYSIS OF A POSTBUCKLED EMBEDDED DELAMINATION
John D. Whitcomb Jul. 1988 26 p
(NASA-TP-2823; L-16453; NAS 1.60:2823) Avail: NTIS HC A03/MF A01 CSCL 20K

Delamination growth caused by local buckling of a delaminated

group of plies was investigated. Delamination growth was assumed to be governed by the strain energy release rates, G(1), G(2) and G(3). The strain energy release rates were calculated using a geometrically nonlinear three-dimensional finite element analysis. The program is described and several checks of the analysis are discussed. Based on a limited parametric study, the following conclusions were reached: (1) the problem is definitely mixed mode (in some cases G(1) is larger than G(2), for other cases the opposite is true); (2) in general, there is a large gradient in the strain energy release rates along the delamination front; (3) the locations of maximum G(1) and G(2) depend on the delamination shape and the applied strain; (4) the mode 3 component was negligible for all cases considered; and (5) the analysis predicted that parts of the delamination would overlap. The results presented did not impose contact constraints to prevent overlapping. Further work is needed to determine the effects of allowing the overlapping.
Author

N88-26685# Materials Research Labs., Melbourne (Australia).
AUSTRALIAN STRUCTURES RESPONSE EVALUATION: GROUND SHOCK AND AIR BLAST MEASUREMENTS FOR SITE INVESTIGATION SURVEY
Phillip Box Aug. 1987 91 p
(MRL-TN-526; AR-005-198) Avail: NTIS HC A05/MF A01

A site investigation survey was conducted during November 1986 as a preliminary requirement for the drafting of a trials plan associated with the proposed Australian Structures Response Evaluation Trials. The site near Woomera, South Australia, was formerly used by the European Launcher Development Organization during the 1960's. Ground shock and air blast measurements were conducted during the survey. This report details the instrumentation and the techniques used to make these measurements. An investigation into the response of the piezoelectric polymer transducers used during the survey is described and the results reported.
Author

N88-26686# Materials Research Labs., Melbourne (Australia).
ANALYSIS OF THE PERFORATION OF MONOLITHIC AND SIMPLE LAMINATE ALUMINIUM TARGETS AS A TEST OF ANALYTICAL DEFORMATION MODELS
R. L. Woodward and I. G. Crouch Apr. 1988 22 p
(MRL-R-1111; AR-005-219) Avail: NTIS HC A03/MF A01

Several models are used to estimate the ballistic limit velocities of homogeneous aluminum targets impacted by small caliber armor piercing projectiles and blunt fragment simulators. It is demonstrated that a careful use of the models, combined with an understanding of material failure mechanisms, enables good estimates of ballistic resistance to be made using the analytical techniques. One of the techniques is modified and adapted to the calibration of ballistic resistance of simple two plate aluminum laminates. Correlation of computations with empirical data demonstrates that the technique is a useful design tool in predicting the optimum relative thickness of the two plates and the laminate performance.
Author

N88-26687 Illinois Univ., Chicago.
SPATIAL DYNAMICS OF DEFORMABLE MULTIBODY SYSTEMS WITH VARIABLE KINEMATIC STRUCTURE Ph.D. Thesis
Che-Wei Chang 1987 171 p
Avail: Univ. Microfilms Order No. DA8726079

A Cartesian-based method for the spatial kinematic and dynamic analysis of deformable multibody systems that are subject to topology changes is presented. A pieced interval analysis scheme that accounts for the change in the spatial system topology due to the changes in the connectivity between bodies is developed. Deformable bodies in the system are discretized using the finite element method to characterize the system vibration. In order to maintain the generality of the formulation, Cartesian coordinates are used to identify the configuration of the body reference. This allows introducing general forcing functions and the additions and/or deletions of kinematic constraints. In control applications, however, it is desirable to determine the joint forces associated with the joint relative variables. The Cartesian variables are expressed in terms of the joint and elastic variables. The resulting kinematic relationships are then employed to determine the joint force associated with the joint variables.
Dissert. Abstr.

N88-26688*# Texas Univ., El Paso. Dept. of Mechanical and Industrial Engineering.
VIBRATION FREQUENCIES OF TAPERED BARS WITH NONCLASSICAL BOUNDARY CONDITIONS Final Report, 1 Jun. 1986 - 30 Jun. 1988
W. Lionel Craver, Jr. Jul. 1988 38 p
(Grant NAG9-146)
(NASA-CR-183059; NAS 1.26:183059) Avail: NTIS HC A03/MF A01 CSCL 20K

The goals for this research were revised and clarified. The goals are restated along with an evaluation of the accomplishment of the goal. All of the cases of the truncated-cone beams that were originally proposed to be solved were solved. A summary of these solutions is presented. Some cases of beams with unequal tapers were solved and are discussed.
B.G.

N88-26689# Brown Univ., Providence, R. I. Div. of Engineering.
FATIGUE CRACK GROWTH UNDER FAR-FIELD CYCLIC COMPRESSION Progress Report, Aug. 1987 - Apr. 1988
S. Suresh Apr. 1988 5 p
(Contract DE-FG02-84ER-45167)
(DE88-011215; DOE/ER-45167/8) Avail: NTIS HC A02/MF A01

Work carried out in this program has led to the theoretical and experimental understanding of stable fatigue crack propagation in brittle solids with a variety of constitutive behavior patterns. A unique feature of this research is that novel experimental results are substantiated in conjunction with detailed theoretical and/or numerical analysis of fracture behavior. Furthermore, the results of this work are finding immediate application in a wide variety of fracture test methods.
DOE

N88-26690# Los Alamos National Lab., N. Mex.
MICROSTRUCTURAL EFFECTS IN STATIC AND DYNAMIC NUMERICAL EXPERIMENTS
B. C. Trent 1988 9 p Presented at the 29th US Symposium on Rock Mechanics, Minneapolis, Minn., 13 Jun. 1988
(Contract W-7405-eng-36)
(DE88-004289; LA-UR-87-4218; CONF-880654-3) Avail: NTIS HC A02/MF A01

A numerical analysis of cemented granular material has been performed in order to better understand the relationship between the individual components of a rock matrix and the macroscopic constitutive response. A distinct element code was modified to allow interparticle bonding by incorporating appropriate elastic relationships. A modified Griffith criterion was utilized to initiate fracture within individual bonds. A number of quasi-static and dynamic numerical experiments are presented which show that realistic macroscopic behavior may be obtained without the use of phenomenological formulations such as plasticity.
DOE

N88-26691# Sandia National Labs., Albuquerque, N. Mex.
RANDOM VIBRATION ANALYSIS OF RATTLING STRUCTURES
T. L. Paez and T. L. Ernest 1987 7 p
(Contract DE-AC04-76DP-00789)
(DE88-007196; SAND-87-2676C) Avail: NTIS HC A02

An excitation-response model is developed for structural systems that have the potential for rattling response. The mathematical model is used to establish spectral relations for stationary random excitation and response, and the model is applied to a laboratory experiment. The spectral density and ordinary coherence characteristics of a system with rattling are developed. It is shown that the mathematical model can accurately reflect the features of randomly excited structural motion in a rattling structure.
DOE

N88-26692# International Centre for Theoretical Physics, Trieste (Italy).
IMAGE FORCE EXPRESSION FOR THE DISLOCATION NEAR A CRACK
S. J. Zhou and C. W. Lung Jul. 1987 18 p
(DE88-701894; IC-87/152) Avail: NTIS (US Sales Only) HC A03/MF A01

Using the conformal mapping technique, the image force expressions for the dislocation near an elliptic hole and a semielliptical (edge) hole have been derived respectively. Let the short axis of the ellipse approach zero, the finite length crack limit solution was obtained, which was in agreement with the result obtained by use of method of dislocation model for the crack.
DOE

N88-26693*# Old Dominion Univ., Norfolk, Va. Dept. of Civil Engineering.
EXPERIMENTAL AND THEORETICAL INVESTIGATION OF PASSIVE DAMPING CONCEPTS FOR MEMBER FORCED AND FREE VIBRATION Progress Report, period ending 31 Dec. 1987
Zia Razzaq and David W. Mykins Dec. 1987 125 p
(Grant NAG1-336)
(NASA-CR-183082; NAS 1.26:183082) Avail: NTIS HC A06/MF A01 CSCL 20K

Potential passive damping concepts for use in space structures are identified. The effectiveness of copper brush, wool swab, and silly putty in chamber dampers is investigated through natural vibration tests on a tubular aluminum member. The member ends have zero translation and possess partial rotational restraints. The silly putty in chamber dampers provide the maximum passive damping efficiency. Forced vibration tests are then conducted with one, two, and three damper chambers containing silly putty. Owing to the limitation of the vibrator used, the performance of these dampers could not be evaluated experimentally until the forcing function was disengaged. Nevertheless, their performance is evaluated through a forced dynamic finite element analysis conducted as a part of this investigation. The theoretical results based on experimentally obtained damping ratios indicate that the passive dampers are considerably more effective under member natural vibration than during forced vibration. Also, the maximum damping under forced vibration occurs at or near resonance.
Author

N88-26694*# California State Univ., Long Beach. Dept. of Mechanical Engineering.
STRESS CONCENTRATION AROUND CIRCULAR HOLE IN A COMPOSITE MATERIAL SPECIMEN REPRESENTATIVE OF THE X-29A FORWARD-SWEPT WING AIRCRAFT
Hsien-Yang Yeh Aug. 1988 22 p
(Contract NGT-05020412)
(NASA-CR-179435; H-1435; NAS 1.26:179435) Avail: NTIS HC A03/MF A01 CSCL 20K

The theory of anisotropic elasticity was used to evaluate the anisotropic stress concentration factors of a composite laminated plate containing a small circular hole. This advanced composite material was used to manufacture the X-29A forward swept wing. Observe that the usual isotropic material stress concentration factor is three. However, for composite material, it was found that the anisotropic stress concentration factor is no longer constant, and that the locations of maximum tangential stress points could shift by changing the fiber orientation with respect to the loading axis. The analysis showed that through the lamination process, the stress concentration factor could be drastically reduced, and therefore the structural performance could be improved. Both the mixture rule approach and the constant strain approach were used to calculate the stress concentration factor. The results predicted by the mixture rule approach were about 20 percent deviate from the experimental data. However, the results predicted by the constant strain approach matched the testing data very well. This showed the importance of the inplane shear effect on the evaluation of stress concentration factor for the X-29A composite plate.
Author

N88-26695# Advisory Group for Aerospace Research and Development, Neuilly-Sur-Seine (France).
AUTOMATED MEASUREMENT OF CRACK LENGTH AND LOAD LINE DISPLACEMENT AT ELEVATED TEMPERATURE
H. P. vanLeeuwen, F. F. Groep, L. Schra, and N. Dam (National Aerospace Lab., Emmeloord, Netherlands) Feb. 1988 14 p Presented at the 65th Meeting of the Structures and Materials Panel of AGARD, Cesme, Turkey, 4-9 Oct. 1987
(AGARD-R-751; ISBN-92-835-0446-1) Copyright Avail: NTIS HC A03/MF A01

Test results reported in the literature show that in creep cracking tests at elevated temperature under steady load, the crack growth rate correlates best with the contour integral C* (also called J*) in comparison to other possible parameters. In the case of the fatigue at elevated temperature, the crack growth rate correlates best with C* if cracking is predominantly time dependent. If, however, cracking is predominantly cycle dependent the crack growth rate correlates best with the range Delta J of the contour integral J. It is discussed that in such testing C* and J are fairly easily determined if, apart from load and crack length, the load line displacement is measured. A description is given of a test setup developed for elevated temperature creep cracking tests in which crack length was measured with the electrical potential drop method and load line displacement measured with two inductive transducers located inside the furnace. Measurement was automated with the aid of a personal computer which controlled the measurements and processed the results automatically. This setup can be adapted for elevated temperature fatigue testing.
Author

N88-26696# Ohio State Univ., Columbus. Research Foundation
RESEARCH ON THE KINETICS OF PHASE CHANGES IN SOLIDS
J. P. Hirth Feb. 1988 11 p
(Contract N00014-85-K-0196)
(AD-A192222; TR-5) Avail: NTIS HC A03/MF A01 CSCL 11F

A brief outline is presented of experimental observations and theoretical interpretations of hydrogen embrittlement of steels. Detailed results on the effect of precharged hydrogen on reduction in ductility of low-strength steels under plane strain loading are discussed. Under such conditions hydrogen is shown to degrade the steels by promoting plastic instability in the form of shear bands, lowering the critical strain for various events without changing the locally ductile mode of fracture.
GRA

N88-26697# Stanford Univ., Calif. Dept. of Applied Mechanics.
AN ASSESSMENT OF MODELLING TECHNIQUES FOR THE FINITE ELEMENT ANALYSIS OF REINFORCED CONCRETE PLATE AND SHELL STRUCTURES Final Report, Oct. 1985 - Sep. 1986
Thomas J. Hughes Feb. 1988 27 p
(Contract N62583-86-M-R195)
(AD-A192263; NCEL-CR-88.008) Avail: NTIS HC A03/MF A01 CSCL 11D

Currently employed modeling techniques used in the analysis of reinforced concrete plate and shell structures are assessed. Methodologies exhibiting shortcomings are identified. Particular attention is focused on strain softening, solution algorithms, reinforcement, and invariances. Recommendations concerning future work are made.
GRA

N88-26698# Pennsylvania State Univ., University Park. Communications and Space Sciences Lab.
FEB STRUCTURAL ANALYSIS, REVISION H
Charles L. Croskey 10 Feb. 1988 89 p
(AD-A192302; TN-1310-NR-01-Rev-H) Avail: NTIS HC A05/MF A01 CSCL 13M

The purpose of this analysis is to document the expected simple loads on the cold plate through the tie down blots around the perimeter of the FEB. Finite element analysis has been performed to determine the specific vibration modes and natural frequencies. The simple static analysis is also repeated when one bolt is missing.

Flange analysis of the baseplate is performed as well as analysis of the attachment and cross bracing of the internal modules. The underlying coldplate is assumed soft in that the net moments are assumed centered around the center of gravity of the FEB and the coldplate does not force any specific moment axis. Since all perimeter bolts on the 700 mm x 420 mm grid are used, 32 tie down bolts are used. For the analysis of the distribution of quasi-static loads on the tie down bolts, the FEB bottom plate will be assumed to be perfectly rigid around its perimeter. The thick-walled outer cover attaches to the FEB with the same bolt pattern, which contributes to the rigidity of the outer perimeter of the base plate. GRA

N88-26699# Naval Postgraduate School, Monterey, Calif.
VIBRATION RESPONSE OF CONSTRAINED VISCOELASTICALLY DAMPED PLATES: ANALYSES AND EXPERIMENTS M.S. Thesis
Gerald J. Maurer Dec. 1987 72 p
(AD-A192329; AD-E801594) Avail: NTIS HC A04/MF A01 CSCL 20K

The frequency response analysis of several constrained viscoelastically damped plates were performed with modifications to account for the frequency dependent properties of viscoelastic materials (loss factors and shear modulus) using MSC/NASTRAN. A modal strain energy approximation method was also applied to each plate. Comparisons of the frequency response analysis to the modal strain energy method were made for each plate structure. The experiments were performed on the plates to establish the base line data for the comparisons. The modal strain energy method frequency response plots showed good agreement with the frequency response analysis method plots for all plate structures analyzed. Plate structures with fewer natural frequencies in the frequency range investigated showed better agreement between the two prediction methods than the structures with more natural frequencies. GRA

N88-26700# Northwestern Univ., Evanston, Ill. Structural Mechanics Lab.
TIME-DOMAIN BOUNDARY ELEMENT ANALYSIS OF DYNAMIC NEAR-TIP FIELDS FOR IMPACT-LOADED COLLINEAR CRACKS Interim Report
C. Zhang and J. D. Achenbach Feb. 1988 36 p
(Contract N00014-85-K-0401)
(AD-A192930; NU-SML-TR-88-1) Avail: NTIS HC A03/MF A01 CSCL 20K

A time-domain boundary integral equation method has been developed to calculate elastodynamic fields generated by the incidence of stress (or displacement) pulses on single cracks and systems of two collinear cracks. The system of boundary integral equations has been cast in a form which is amenable to solution by the boundary element method in conjunction with a time-stepping technique. Particular attention has been devoted to dynamic overshoots of the stress intensity factors. Elastodynamic stress intensity factors for pulse incidence on a single crack have been computed as functions of time, and they have been compared with results of other authors. For collinear macrocrack-microcrack configurations the stress intensity factors at both tips of the macrocrack have been computed as functions of time for various values of the crack spacing and the relative size of the microcrack. GRA

N88-26701# Northwestern Univ., Evanston, Ill. Structural Mechanics Lab.
OFF-BOUNDARY APPROACH TO THE BOUNDARY ELEMENT METHOD Interim Report
J. D. Achenbach, G. E. Kechter, and Y.-L. Xu 15 Feb. 1988 23 p
(Contract N00014-85-K-0401)
(AD-A192931; NU-SML-TR-88-2) Avail: NTIS HC A03/MF A01 CSCL 20K

This paper is concerned with scattering of time-harmonic waves by compact inhomogeneities in an elastic solid. In the calculation procedure a boundary integral equation is solved numerically by the boundary element method (BEM). An alternative to the usual boundary element method is employed. The alternative approach is applicable to cavities or fixed rigid bodies of general shape located in linearly elastic, isotropic, homogeneous solids, but the specific results reported herein are for spherical cavities. The alternative approach eliminates the cumbersome singularities associated with the usual approach to BEM, and it also eliminates the problems encountered at the so called fictitious eigenfrequencies. GRA

N88-26702# Northwestern Univ., Evanston, Ill. Structural Mechanics Lab.
A NEW BOUNDARY INTEGRAL EQUATION FORMULATION FOR ELASTODYNAMIC AND ELASTOSTATIC CRACK ANALYSIS Interim Report
Ch. Zhang and J. D. Achenbach 15 Feb. 1988 34 p
(Contract N00014-85-K-0401)
(AD-A192967; NU-SML-TR-88-3) Avail: NTIS HC A03/MF A01 CSCL 20K

An elastodynamic conservation integral, the Jk integral, is employed to derive boundary integral equations for crack configurations, in a direct and natural way. These equations immediately have lower order singularities than the ones obtained in the conventional manner by the use of the Betti-Rayleigh reciprocity relation. This is an important advantage for the development of numerical procedures for solving the BIE's, and for an accurate calculation of the strains and stresses at internal points close to the crack faces. For curved cracks of arbitrary shape the BIE's presented here have simple forms, and they do not require integration by parts, as in the conventional formulation. For the dynamic case, the unknown quantities are the crack opening displacements and their derivatives (dislocation densities), while for the static case only the dislocation densities appear in the formulation. For plane cracks the boundary integral equations reduce to the ones obtained by other investigators. GRA

N88-26703# Karlsruhe Univ. (West Germany). Fakultaet fuer Maschinenbau.
DYNAMICAL STRESS CONCENTRATION PROBLEMS, FROM EVERY SIDE, BORDERED AND PERFORATED PLATES Ph.D. Thesis [DYNAMISCHE SPANNUNGSKONZENTRATIONSPROBLEME BEI ALLSEITS BERANDETEN, GELOCHTEN SCHEIBEN]
Mathias Maass 1986 128 p In GERMAN
(ETN-88-92128) Avail: NTIS HC A07/MF A01

Dynamic stress concentration in bordered and perforated plates is studied by linear elastodynamic equations, assuming a viscoelastic material behavior of the Voigt-Kelvin model. The Lamean equation with harmonic excitation is suitable for the analysis of four configurations of a hole in a plate: central hole in a circular plate, excentric hole in a circular plate, central circular hole and central ellipsoidal hole in rectangular plates. Numerical results indicate that dynamical stress are more important than the static ones. ESA

N88-26704# Technische Univ., Munich (West Germany). Lehrstuhl fuer Thermodynamik.
STUDY OF TEMPERATURE AND STRESS FIELDS OF TWO SLIDING CYLINDERS Ph.D. Thesis [BERECHNUNG DER TEMPERATUR- UND SPANNUNGSFELDER VON GLEIT-WAELZPAARUNGEN]
Hubertus Winkler 1986 168 p In GERMAN
(ETN-88-92134) Avail: NTIS HC A08/MF A01

Surface contact-zones of cylinders submitted to high mechanical and thermal loads are studied in the case of elastic and elastoplastic behavior. Analytical and numerical computations for the temperature and stress fields are presented. Three size effects of contact surfaces are considered: tape shaped contact zone, patch shaped contact zone, and large size contact. Due to the complexity of each application separate computer programs are developed for the complete computing of thermal and stress profiles. Critical phases of contact during the moving of cylinders

with the highest temperature gradients attained are determined. ESA

N88-26705# Centre National de la Recherche Scientifique, Marseilles (France). Lab. de Mecanique et d'Acoustique.
STRESS ANALYSIS USING INFRARED THERMOGRAPHY [ANALYSE DES CONTRAINTES PAR THERMOGRAPHIE INFRAROUGE]
1988 38 p In FRENCH
(Contract DRET-84-1183)
(ETN-88-92169) Avail: NTIS HC A03/MF A01

The implementation of a numerical interface of the video signals from the camera and the evaluation of the potential of thermography for different solid mechanics applications are discussed. While the numerical interface works correctly, the conclusion on the applications to laboratory studies is pessimistic, since the Hughes camera is inadequate to detect isotherms separated by less than 0.02 C. ESA

N88-26706# National Aerospace Lab., Amsterdam (Netherlands). Structures and Materials Div.
AUTOMATED MEASUREMENT OF CRACK LENGTH AND LOAD LINE DISPLACEMENT AT ELEVATED TEMPERATURE
H. P. vanLeeuwen, F. F. Groep, L. Schra, and N. Dam 20 Jul. 1987 10 p Presented at the 65th AGARD Structures and Materials Panel Meeting, Cesme, Turkey, Oct. 1987
(NLR-MP-87049-U; B8805303; ETN-88-92613) Avail: NTIS HC A02/MF A01

A test set-up was developed for high temperature creep cracking tests in which crack length is measured with the electrical potential drop method and load line displacement is measured with two inductive transducers located inside the furnace. Measurement was automated with the aid of a personal computer which controlled the measurements and processed the results automatically. This set-up can be adapted for high temperature fatigue testing. ESA

N88-26707# National Aerospace Lab., Amsterdam (Netherlands). Structures and Materials Div.
PREDICTION OF FATIGUE GROWTH
A. U. deKoning 1 Sep. 1987 47 p Presented at the Advanced Seminar on Fracture Mechanics ASFM6 on Assessment of Cracked Components by Fracture Mechanics, Ispra, Italy, 28 Sep.-2 Oct. 1987
(Contract ESA-5826/84-NL-PB(SC))
(NLR-MP-87052-U; B8805302; ETN-88-92614) Avail: NTIS HC A03/MF A01

The practical significance of fatigue crack growth life prediction is related to the service life, the inspection period, and the fracture control requirements. Fatigue crack growth in metallic materials is discussed. Effects such as chemical environment, short cracks, and crack closure on the growth rate are considered, as well as crack growth retardation and acceleration. Crack growth models for prediction of fatigue crack growth are evaluated. Experimental methods for determination of the material parameters involved in the models are described. Criteria for selection of software for prediction of fatigue crack growth are given. ESA

N88-26708# Office National d'Etudes et de Recherches Aerospatiales, Paris (France).
DAMAGE IN A PERFORATED GRAPHITE-EPOXY PLATE UNDER MONOTONIC, CYCLIC BIAXIAL LOADING Ph.D. Thesis - Univ. de Technologie de Compiegne
G. Inizan 1987 205 p In FRENCH; ENGLISH summary Report also be announced as translation (ESA-TT-1117)
(ONERA-NT-1987-5; ISSN-0078-3781; ETN-88-92729) Avail: NTIS HC A10/MF A01

Damage propagation in a graphite-epoxy composite plate is studied. Biaxial stress is induced by tensile loading in two perpendicular directions. A hole in the center localizes damage initiation. The main technique of damage investigation is penetrant-enhanced X-ray radiography. The results from a finite element program of damage propagation are compared with experimental data. The analysis predicts damage initiation load and its localization, damage propagation, and failure load. A convergence study shows that it is stable. Tests under cyclic biaxial loadings give reproducible damage propagation, depending on the load and the biaxial coefficient. ESA

N88-26709*# National Aeronautics and Space Administration. Ames Research Center, Moffett Field, Calif.
A GENERAL-PURPOSE APPROACH TO COMPUTER-AIDED DYNAMIC ANALYSIS OF A FLEXIBLE HELICOPTER
Om P. Agrawal (University of Southern Illinois, Carbondale.) Jul. 1988 27 p
(NASA-TM-101002; A-88183; NAS 1.15:101002) Avail: NTIS HC A03/MF A01 CSCL 20K

A general purpose mathematical formulation is described for dynamic analysis of a helicopter consisting of flexible and/or rigid bodies that undergo large translations and rotations. Rigid body and elastic sets of generalized coordinates are used. The rigid body coordinates define the location and the orientation of a body coordinate frame (global frame) with respect to an inertial frame. The elastic coordinates are introduced using a finite element approach in order to model flexible components. The compatibility conditions between two adjacent elements in a flexible body are imposed using a Boolean matrix, whereas the compatibility conditions between two adjacent bodies are imposed using the Lagrange multiplier approach. Since the form of the constraint equations depends upon the type of kinematic joint and involves only the generalized coordinates of the two participating elements, then a library of constraint elements can be developed to impose the kinematic constraint in an automated fashion. For the body constraints, the Lagrange multipliers yield the reaction forces and torques of the bodies at the joints. The virtual work approach is used to derive the equations of motion, which are a system of differential and algebraic equations that are highly nonlinear. The formulation presented is general and is compared with hard-wired formulations commonly used in helicopter analysis. Author

42 GEOSCIENCES (GENERAL)

No abstracts in this category.

43 EARTH RESOURCES AND REMOTE SENSING

Includes remote sensing of earth resources by aircraft and spacecraft; photogrammetry; and aerial photography.

For instrumentation see *35 Instrumentation and Photography.*

N88-26710*# Kansas Univ. Center for Research, Inc., Lawrence. Radar Systems and Remote Sensing Lab.
[SOURCES OF SCATTERING IN VEGETARIAN AND OTHER SURFACES AND OBJECTS] Final Report
R. K. Moore Jun. 1988 7 p
(Grant NAG5-271)
(NASA-CR-182975; NAS 1.26:182975; RSL-5870-5) Avail: NTIS HC A02/MF A01 CSCL 20N

The sources of scattering in vegetation and other surfaces and objects were studied. A special radar, SOURCESCAT, that could resolve a cylindrical volume 18 cm in diameter and 11 cm long was built. This system provided the first really fine-resolution measurements of radar backscatter from vegetation. The measurements showed that many of the assumptions used previously in modeling vegetation backscatter were false. Vegetation studied included various field crops, prairie grass, and various trees. Major differences were found in the roles of leaves, branches, stems, and trunks for different species. An artificial tree

was studied in the laboratory using the systems. The most significant findings were that the average radar volume scattering coefficient is independent of azimuth, and that slanting of the polarization vector can give useful information not available with ordinary vertical and horizontal polarization. A model for scattering from a single leaf was developed. This model, for the first time, took into account the presence of veins in leaves. The pattern of scatter from a leaf was shown quite different from that for which the veins are ignored. A list of publications and presentations resulting from this project are attached. B.G.

N88-26711*# Illinois Natural History Survey, Champaign.
INTERPRETING FOREST BIOME PRODUCTIVITY AND COVER UTILIZING NESTED SCALES OF IMAGE RESOLUTION AND BIOGEOGRAPHICAL ANALYSIS Final Report
Louis R. Iverson, Elizabeth A. Cook, Robin L. Graham, Jerry S. Olson, Thomas D. Frank, and Ke Ying 15 Jun. 1988 135 p Prepared in cooperation with Oak Ridge National Lab., Tenn.; Global Patterns Associates, Lenoir City, Tenn.; and Illinois Univ., Urbana
(Contract NAS5-28781)
(NASA-CR-183036; NAS 1.26:183036) Avail: NTIS HC A07/MF A01 CSCL 02F

The objective was to relate spectral imagery of varying resolution with ground-based data on forest productivity and cover, and to create models to predict regional estimates of forest productivity and cover with a quantifiable degree of accuracy. A three stage approach was outlined. In the first stage, a model was developed relating forest cover or productivity to TM surface reflectance values (TM/FOREST models). The TM/FOREST models were more accurate when biogeographic information regarding the landscape was either used to stratigy the landscape into more homogeneous units or incorporated directly into the TM/FOREST model. In the second stage, AVHRR/FOREST models that predicted forest cover and productivity on the basis of AVHRR band values were developed. The AVHRR/FOREST models had statistical properties similar to or better than those of the TM/FOREST models. In the third stage, the regional predictions were compared with the independent U.S. Forest Service (USFS) data. To do this regional forest cover and forest productivity maps were created using AVHRR scenes and the AVHRR/FOREST models. From the maps the county values of forest productivity and cover were calculated. It is apparent that the landscape has a strong influence on the success of the approach. An approach of using nested scales of imagery in conjunction with ground-based data can be successful in generating regional estimates of variables that are functionally related to some variable a sensor can detect. B.G.

N88-26712*# Oklahoma Univ., Norman. School of Meteorology.
HYDROLOGIC MODELS FOR LAND-ATMOSPHERE RETROSPECTIVE STUDIES OF THE USE OF LANDSAT AND AVHRR DATA Semiannual Report, 1 Oct. 1987 - 31 Mar. 1988
Claude E. Duchon, T. H. Lee Williams, and Arlin D. Nicks 2 Jun. 1988 2 p Sponsored by NASA
(NASA-CR-182861; NAS 1.26:182861) Avail: NTIS HC A02/MF A01 CSCL 08B

The use of a Geographic Information System (GIS) and LANDSAT analysis in conjunction with the Simulator for Water Resources on a Rural Basin (SWRRB) hydrologic model to examine the water balance on the Little Washita River basin is discussed. LANDSAT analysis was used to divide the basin into eight non-contiguous land covers or subareas: rangeland, grazed range, winter wheat, alfalfa/pasture, bare soil, water, woodland, and impervious land (roads, quarry). The use of a geographic information system allowed for the calculation of SWRRB model parameters in each subarea. Four data sets were constructed in order to compare SWRRB estimates of hydrologic processes using two methods of maximum LAI and two methods of watershed subdivision. Maximum LAI was determined from a continental scale map, which provided a value of 4.5 for the entire basin, and from its association with the type of land-cover (eight values). The two methods of watershed subdivision were determined according to drainage subbasin (four) and the eight land-covers. These data sets were used with the SWRRB model to obtain daily hydrologic estimates for 1985. The results of the one year analysis lead to the conclusion that the greater homogeneity of a land-cover subdivision provides better water yield estimates than those based on a drainage properties subdivision. B.G.

N88-26713 Stanford Univ., Calif.
IMAGE PYRAMID MOTION DETECTION APPLIED TO SEA ICE Ph.D. Thesis
Ramin Samadani 1987 195 p
Avail: Univ. Microfilms Order No. DA8801022

The automatic detection of motion from a sequence of images is studied. Motion detection is modeled as the determination of a vector mapping between successive images. Solutions for finding this vector mapping are outlined. In particular, image pyramid correlation algorithms are developed and then tested with synthetic aperture radar image of sea ice. Image pyramids are described, using the multirate systems concepts of decimation and interpolation, as systems with more than one sampling rate. An image pyramid motion detection algorithm is developed. First image pyramids are constructed from the original images. Corresponding features in the coarsest levels of the pyramids are then matched using correlations. The algorithm is tested using sea ice images taken three days apart and is found to generate vectors which are highly consistent with manually generated vectors for these same scenes. An image remapping and subtraction technique is developed as an alternative method for highlighting erroneous vectors. The algorithm also performs better compared to correlation without an image pyramid and pyramid correlations without the median filter. Variations of the pyramid motion detection algorithms are developed which allow control over the continuity of a spline interpolation. Dissert. Abstr.

N88-26714# Battelle Columbus Labs., Ohio.
REMOTE SENSING AND SATELLITE APPLICATIONS TO THE NEEDS OF THE GAS AND PIPELINE INDUSTRY
A. G. Mourad and T. J. Kuzma Oct. 1987 138 p
(Contract GRI-5087-271-1520)
(PB88-202668; GRI-87/0346) Avail: NTIS HC A07/MF A01 CSCL 08B

A survey of gas industry needs was made along with a literature search involving remote sensing techniques with possible applications to gas industry needs. A questionnaire was developed covering the areas of leak detection, right of way monitoring, pipeline location, pipeline conditions, exploration, and communications. The questionnaire was used to interview personnel from the gas industry, the Gas Research Institute, and consulting firms. The results from these inteviews indicate the most active areas of concern are monitoring the right of way, detecting leaks and pipeline conditions, and upgrading communication systems. The literature search indicated that many aspects of remote sensing and satellite technology could be applicable to the gas industry's needs. An overview of remote sensing was prepared, and specific techniques were outlined that could be utilized by the gas and pipeline industry. Some qualitive analyses of the remote sensing and satellite applications to the industry's needs were performed. Author

N88-26715# Pennsylvania State Univ., University Park. Environmental Resources Research Inst.
SURFACE HYDROLOGY, SEDIMENT TRANSPORT DYNAMICS AND REMOTE SENSING OF DISTURBED WATERSHEDS IN A HUMID TEMPERATE REGION Progress Report
1988 6 p
(Contract DE-FG02-87ER-60594)
(DE88-008719; DOE/ER-60594/1) Avail: NTIS HC A02/MF A01

The fundamental goal of this multilayer research effort is to quantify the temporal evolution of the hydrologic cycle on disturbed watersheds and construct a modular hydrologic model that uses, as primary input, variable quantities and types of remotely sensed

data sets in a Geographic Information System (GIS) format. The hypothesis to be tested states that the geomorphic evolution of disturbed watersheds which are in disequilibrium can be quantified with field data and subsequently modeled, utilizing both field-derived and remotely sensed data sets. DOE

N88-26716*# Oklahoma Univ., Norman. School of Meteorology.
HYDROLOGIC MODELS FOR LAND-ATMOSPHERE RETROSPECTIVE STUDIES OF THE USE OF LANDSAT AND AVHRR DATA Semiannual Report, 1 Oct. 1987 - 31 Mar. 1988
Claude E. Duchon, T. H. Lee Williams, and Arlin D. Nicks 2 Jun. 1988 2 p Sponsored by NASA
(NASA-CR-182862; NAS 1.26:182862) Avail: NTIS HC A02/MF A01 CSCL 04A

The use of a Geographic Information System (GIS) and LANDSAT analysis in conjunction with the Simulator for Water Resources on a Rural Basin (SWRRB) hydrologic model to examine the water balance on the Little Washita River basin is discussed. In the research completed to date LANDSAT analysis was used to divide the basin into eight non-contiguous land covers or sub areas. The use of a geographic informatin system allowed for the calculation of SWRRB model parameters in each subarea. Four data sets were constructed in order to compare SWRRB estimates of hydrologic processes using two methods of maximum LAI and two methods of watershed division. These data sets were used with the SWRRB model to obtain daily hydrologic estimates for 1985. B.G.

N88-26717# Gulf Weather Corp., Bay Saint Louis, Miss.
SATELLITE REMOTE SENSING OF THE WET BULB GLOBE TEMPERATURE HEAT STRESS INDEX, PHASE 2
F. J. Schatzle, J. D. Baldwin, S. A. Hsu, O. K. Huh, and F. W. Quirk 3 Dec. 1987 11 p
(Contract DAMD17-86-C-6004)
(AD-A192798) Avail: NTIS HC A03/MF A01 CSCL 04B

The Wet Bulb Globe Temperature (WBGT) is the basic parameter used by the U.S. Army to quantify heat stress. The index is computed as a weighted sum of dry bulb, wet bulb and black globe temperature measurements. During 1985, Gulf Weather Corporation received a Small Business Innovation Research (SBIR) Phase 1 contract form the U.S. Army Research Institute of Environmental Medicine to determine if the WBGT could be determined from information routinely available from U.S. weather satellites. Phase 1 efforts demonstrated relationships between dry bulb temperature and Advanced Very High Resolution Radiometer (AVHRR) data and between wet bulb temperature and the total precipitable water derivable from Tiros Operational Vertical Sounder (TOVS) data available from NOAA satellites. Algorithms for these relationship were developed. Phase 2 of the research was initiated in June 1987. Additional ground truth data were collected for further refinement of these algorithms. Data were collected in arid regions of the southwestern United States. Additional data for moist, vegetated areas will be collected in the summer of 1988. GRA

N88-26718# Technische Hogeschool, Delft (Netherlands). Center for Computer Graphics and Mapping.
THE TRANSITION FROM TRADITIONAL TO MODERN MAP REPRODUCTION [DE OVERGANG VAN TRADITIONELE NAAR MODERNE KAARTREPRODUKTIE]
A. J. Lalesse Nov. 1987 125 p In DUTCH Original contains color illustrations
(B8735128; ETN-88-92423) Avail: NTIS HC A06/MF A01

The question of how far the use of computers can replace the traditional reproduction techniques is treated. Traditional maps and maps produced with computers are discussed. Quality, quantity, flexibility, large- and small-scale maps; colors, apparatus, materials, text processing, production time, personnel, costs and profits, and phased automation are considered. It is concluded that computerized cartography will expand, that reproduction will be substantially influenced by the computer, but also that reproduction will continue to play an important role in cartography in the coming years. ESA

N88-26719# National Aerospace Lab., Amsterdam (Netherlands). Informatics Div.
GEOGRAPHICAL INFORMATION FOR DESIGN PURPOSES
T. D. deWitte 11 Feb. 1987 28 p IN DUTCH; ENGLISH summary
(NLR-MP-87014-U; B8803802; ETN-88-92608) Avail: NTIS HC A03/MF A01

The preparation and use of geographical information for design purposes are reviewed. Digital geographical information distinguishes structured and nonstructured information. Structured information concerns numerically ordered features. Nonstructured information concerns images of areas recorded by scanning maps. This led to a geographic information base, applied to a route-planning system for aircraft. Requirements with respect to information availability, up-to-dateness, accessibility are severe, so it is necessary to provide the system with dedicated application data bases. Two steps in designing a geographical information system are distinguished: a subsystem for the preparation of the application data bases, and a subsystem for the use of the geographical data. This system uses structured (e.g., terrain elevation) and nonstructured geographical information (digital map images). Digital maps can also be composed from structured information using the specific geographical features. ESA

N88-26720# National Research Inst. for Mathematical Sciences, Pretoria (South Africa).
GRAPHICAL COMMUNICATION AND SYMBOLISM IN A COMPUTERIZED CARTOGRAPHY AND MAP COMPILATION SYSTEM
C. F. Scheepers Jul. 1986 27 p
(PB88-124672; CSIR-TWISK-479) Avail: NTIS HC E05/MF E05; copy not available from STI Facility CSCL 08B

The document deals with the use of maps to convey graphic information, and with the implications for design and implementation strategies for computerized cartographic systems. It also addresses the aesthetic acceptability of computer-compiled maps. Specific applications in computational geometry include polygon hatching and the use of polygonal skeletons in automatic name placement. GRA

44 ENERGY PRODUCTION AND CONVERSION

Includes specific energy conversion systems, e.g., fuel cells; global sources of energy; geophysical conversion; and windpower.

For related information see also *07 Aircraft Propulsion and Power, 20 Spacecraft Propulsion and Power,* and *28 Propellants and Fuels.*

N88-26721# Electrotek Concepts, Inc., Knoxville, Tenn.
ANALYSIS OF THE ELECTRICAL CHARACTERISTICS OF A WESTINGHOUSE VARIABLE SPEED GENERATING SYSTEM FOR WIND TURBINE APPLICATIONS
J. I. Herrera and T. W. Reddoch Feb. 1988 57 p
(Contract DE-AC02-83CH-10093)
(DE88-001139; SERI/STR-217-3133) Avail: NTIS HC A04/MF A01

Variable speed electric generating technology can enhance the general use of wind energy in electric utility applications. This enhancement results from two characteristic properties of variable speed wind turbine generators: an improvement in drive train damping characteristics, which results in reduced structural loading on the entire wind turbine system, and an improvement in the overall efficiency by using a more sophisticated electrical generator. Electronic converter systems are the focus of this investigation, particularly the properties of a Westinghouse variable-speed, constant-frequency system with wound-rotor induction generator and a cycloconverter. Experience with solid-state converter systems in large wind turbines is extremely limited. This report presents measurements of electrical performances of the Westinghouse system and is limited to the terminal characteristics of the system.

Variable speed generating systems working effectively in utility applications will require a satisfactory interface between the turbine-generator pair and the utility network. The electrical testing described herein focuses largely on the interface characteristics of the generating system. A MOD-0 wind turbine was connected to a very strong system; thus, the voltage distortion was low and the total harmonic distortion in the utility voltage was less than 3 percent (within the 5 percent limit required by most utilities). The largest voltage component of a frequency below 60 Hz was 40 dB down from the 60-Hz component. DOE

N88-26722# Central Research Inst. of Electric Power Industry, Tokyo (Japan).
SURVEY ON UTILITY TECHNOLOGY OF A TIDAL AND OCEAN CURRENT ENERGY
Manabu Hirose, Masataka Kadoyu, and Hiroyoshi Tanaka Jun. 1987 68 p In JAPANESE
(DE88-770148; CRIE-U-86033) Avail: NTIS (US Sales Only) HC A04

A study is made to show the current technological levels in Japan and other nations regarding the conversion of tidal current or ocean current energy to electric power and to determine the latent energy quantities and energy-related characteristics of tidal and ocean currents. In Japan, relatively large-scale experiments made so far mostly used one of the following three types of devices: Savonius-wheel type, Darrieus-wheel type, and cross-flow-wheel type. Field experiments of tidal energy conversion have been performed at the Naruto and Kurushima Straits. The energy in the Kuroshio current is estimated at about 170 billion kWh per year. Ocean current energy does not undergo large seasonal variations. The total energy in major straits and channels in the Inland Sea and other sea areas to the west is estimated at about 124 billion kWh per year. Tidal current energy shows large seasonal variations, but it is possible to predict the changes. A survey is made to determine energy-related characteristics of a tidal current at Chichino-seto, Kagoshima Prefecture. At Chichino-seto, the flow velocity ranges from 0 to 2.2m/s, with a latent tidal current energy of about 70 kW, of which about 20 kW can actually be utilized. DOE

N88-26723# California Univ., Berkeley. Lawrence Berkeley Lab.
OXYGEN REDUCTION IN FUEL CELL ELECTROLYTES Ph.D. Thesis
K. A. Striebel, F. R. McLarnon, and E. J. Cairns Dec. 1987 244 p
(Contract DE-AC03-76SF-00098)
(DE88-008240; LBL-24340) Avail: NTIS HC A11/MF A01

Experimental and theoretical studies of oxygen reduction (OR) in novel acid and alkaline electrolytes on smooth and supported Pt have been carried out. Similar kinetically limited rates for OR were measured in the super-acid electrolytes trifluoromethane sulfonic acid (TFMSA) and tetrafluoroethane-1,2-disulfonic acid (TFEDSA), with the rotating disk electrode (RDE) technique at 23 C and pH = 1. A first-order dependence on O2 pressure was measured. The mechanism for OR on Pt in alkaline electrolytes is complicated by the concurrent oxidation and reduction of Pt. Rotating ring-disk electrode (RRDE) studies carried out with anodic and cathodic potential sweeps in 0.1 to 6.9 M KOH and 0.1 to 4.0 M K2CO3 revealed similar currents when corrected for O2 solubility differences. In dilute electrolytes, OR proceeds primarily through the 4-electron pathway to water, independent of pH. In KOH, the mechanism for Pt oxidation changes and the fraction of current yielding a peroxide product increases at 2 to 3 M. These changes were not observed in K2CO3. Porous gas diffusion electrodes (GDE) with supported Pt catalyst were studied in a special cell with low uncompensated solution resistance. Cyclic voltammograms yielded measurements of the wetted areas of carbon and Pt and the local electrolyte composition. GDE galvanostatic steady-state performance with 100 percent O2 was measured in 2 to 11 M KOH and 2 to 5.5 M K2CO2. Results suggest that OR on carbon contributes to the high currents in 6.9 M KOH at high overpotentials. In K2CO3, lower wetted areas and slow OH(-) ion transport are responsible for the poor performance when compared with KOH. Models for the steady-state operation of porous GDE's were developed. These models account for the diffusion and reaction of O2 and ionic transport in KOH and K2CO3. DOE

N88-26724# California Univ., Berkeley. Lawrence Berkeley Lab.
ELECTROCATALYSTS FOR OXYGEN ELECTRODES Final Report
E. Yeager Jan. 1988 123 p
(Contract DE-AC03-76SF-00098)
(DE88-008397; LBL-24788) Avail: NTIS HC A06/MF A01

The performance of low and moderate temperature fuel cells and rechargeable metal-air batteries is limited by the catalytic activity and life of the O2 electrocatalysts. The overall objective of this research has been the development of much more effective electrocatalysts for O2 reduction and generation, combining high catalytic activity with long-term stability in concentrated acid and alkaline electrolytes. Research emphasis is on achieving a fundamental understanding of O2 electrocatalysis. DOE

N88-26725# Arizona Univ., Tucson. Dept. of Biochemistry.
MECHANISMS OF PHOTOCHEMICAL ENERGY CONVERSION BY CHLOROPHYLL Progress Report, 1 Sep. 1987 - 1 May 1988
G. Tollin 1 May 1988 10 p
(Contract DE-FG02-86ER-13631)
(DE88-008763; DOE/ER-13631/2) Avail: NTIS HC A02/MF A01

This project involves laser flash photolysis studies of the mechanism of electron transfer reactions involving chlorophyll triplet state and various electron donor and acceptor species occuring in lipid bilayer vesicles. Through the use of fluorescent probes, we have shown that the electrostatic binding of cytochrome to positively-charged bilayer vesicles is accompanied by its intramembrane penetration. This supports our earlier studies which showed that binding led to quenching of chlorophyll triplets on both sides of the bilayer. That the bound cytochrome is mobile on the bilayer surface was demonstrated as the heme edge is not appreciably blocked from being reduced by reactants in the aqueous phase. In contrast to this, binding of plastocyanin to the bilayer does prevent electron transfer into the protein from the aqueous phase. Furthermore, the intrinsic reactivity of plastocyanin is increased by as much as six-fold upon binding to the membrane. We have also investigated the effects of electrostatic interactions on the kinetics, and the inside-outside asymmetry properties, of reactions between chlorophyll triplet and various small molecule acceptors in large unilamellar vesicles. Large effects were observed which could be interpreted in terms of charge-charge interactions between reactants, products and membrane components, as well as the existence of a spontaneous transmembrane electrical potential. DOE

N88-26726# Sandia National Labs., Albuquerque, N. Mex.
PHOTOVOLTAIC CONCENTRATOR TECHNOLOGY: RECENT RESULTS
E. C. Boes 1988 12 p Presented at the 8th European Photovoltaic Solar Energy Conference, Florence, Italy, 9 May 1988
(Contract DE-AC04-76DP-00789)
(DE88-009588; SAND-87-1730C; CONF-880513-1) Avail: NTIS HC A03/MF A01

This paper discusses the recent results in photovoltaic concentrator technology development. The major topics presented are a detailed description of current concentrator module development efforts, a summary of concentrator component development, and a discussion of the economics of photovoltaic concentrators in light of these activities and the higher concentrator cell efficiencies that have been demonstrated. DOE

N88-26727# California Univ., Berkeley. Lawrence Berkeley Lab.
DETERMINATION AND APPLICATION OF BIDIRECTIONAL SOLAR-OPTICAL PROPERTIES OF FENESTRATION SYSTEMS
K. Papamichael, J. Klems, and S. Selkowitz Mar. 1988 9 p Presented at Solar '88: American Solar Energy Society Annual Meeting and 13th National Passive Solar Conference, Cambridge, Mass., 18 Jun. 1988
(DE88-010364; LBL-25124; CONF-880615-3; CONF-880615) Avail: NTIS HC A02/MF A01

Accurate determination of the luminous and thermal performance of fenestration systems that incorporate optically complex components requires detailed knowledge of their radiant behavior. We describe a large scanning radiometer used to measure the bidirectional transmittance and reflectance of fenestration systems and components. We present examples of measured data obtained for simple non-specular samples. We describe a method of obtaining the overall properties of fenestration systems by calculation from scanning radiometer measurements of fenestration components. Finally, we describe the application of bidirectional solar-optical properties of fenestration systems to determine their luminous and thermal performance with respect to building energy consumption and occupants' comfort. We also discuss the advantages and limitations of the method, which appears to be promising. DOE

N88-26728# Central Research Inst. of Electric Power Industry, Tokyo (Japan).
THERMODYNAMIC ANALYSIS OF CHEMICAL HEAT STORAGE SYSTEM FOR HEAT PUMP
Michiyuki Saikawa, Tetsushiro Iwatsubo, and Teruhide Hamamatsu Sep. 1987 24 p In JAPANESE; ENGLISH summary
(DE88-753121; CRIE-W-87005) Avail: NTIS (US Sales Only) HC A03

In order to establish a performance index of chemical heat storage, a method of assessment was proposed wherein the action principles were adjusted as well as the examples of the application. In a chemical heat storage system wherein the exhaust heat at heat storage operation and the driving heat source at the exothermic operation and the compressor power are utilized, the driving force cannot be neglected; heat must be assessed not only by quantity but also by the temperature level (in other words by both heat and power). By examining the flow of enthalpy and the exergy using a method of exergy analysis, the characteristics of chemical heat storage was grasped, and it was found that exergy efficiency could be defined in various ways including the above-mentioned exhaust heat and the driving heat source. In other words, the definition should be made according to each case of the application. DOE

N88-26729# Department of Energy, Washington, D. C. Assistant Secretary for Conservation and Renewable Energy.
WIND ENERGY TECHNOLOGY: GENERATING POWER FROM THE WIND, A CURRENT AWARENESS BULLETIN
L. Smith, ed. and B. C. Steele, ed. Jan. 1988 25 p
(DE88-008292; DOE/WET-88-1) Avail: NTIS HC A03/MF A01

Wind Energy Technology: Generating Power from the Wind (WET) announces on a bimonthly basis the current worldwide information available on wind turbine concepts and design, including the basic science of wind turbine dynamics, as well as advanced components and systems research; wind turbine performance; ancillary wind turbine equipment, including system protection and interconnection devices; wind resource identification; wind turbine project planning and development; legal-institutional implications of wind energy conversion systems; and environmental aspects of wind turbines. This publication contains the abstracts of DOE reports, journal articles, conference papers, patents, theses, and monographs added to the Energy Data Base (EDB). DOE

N88-26730# Los Alamos National Lab., N. Mex.
PROSPECTS FOR HOT DRY ROCK IN THE FUTURE
M. E. Berger and H. D. Murphy 1988 10 p Presented at the DOE Geothermal Program Review, San Francisco, Calif., 19 Apr. 1988
(Contract W-7405-eng-36)
(DE88-010909; LA-UR-88-1261; CONF-880477-5) Avail: NTIS HC A02

The Hot Dry Rock (HDR) geothermal energy program is a renewable energy program that can contribute significantly to the nation's balanced and diversified energy mix. The program was reviewed five times in the past three years. Three of these reviews were done by the US Department of Energy (DOE) and a fourth was conducted by the National Research Council at the request of DOE. In addition, HDR was evaluated in the Energy Research Advisory Board's Solid Earth Sciences Report. Recent economic studies for HDR have been performed by Bechtel National, Inc., the Electric Power Research Institute, and the United Kingdom. These studies are reviewed in light of recent progress at Fenton Hill in reducing drilling costs, and mapping and in identifying drilling targets. All of the attention focused on HDR has resulted in evaluating the way in which HDR fits within the nation's energy mix and in estimating when HDR will contribute to energy security. To establish a framework for evaluating the future of HDR, the status and progress of HDR are reviewed and the remaining Fenton Hill program is outlined. Recommendations are also made for follow-on activities that will lead to achieving full development of HDR technologies in the appropriate time frame. DOE

N88-26731# Department of Energy, Washington, D. C. Office of the Deputy Assistant Secretary for Oil, Gas, Shale and Special Technologies.
FUEL CELL SYSTEMS PROGRAM PLAN: FISCAL YEAR 1988
May 1988 43 p
(DE88-011080; DOE/FE-0105) Avail: NTIS HC A03/MF A01

The DOE fuel cell program supports high-risk, high-payoff technology development. This provides industry with the capability to develop and apply fuel cell systems that use conventional and alternative hydrocarbon fuels. The principal DOE fuel cell program goal is to develop cost effective, efficient, and environmentally benign fuel cell systems which will operate on coal-based fuels (and dual fuels: coal and gas) in multiple end use sectors. In the near-term, and as an interim step in achieving this goal, distillate fuel and natural fuel cell system technologies will also be developed. This interim step is a logical progression to the more complex coal-fueled systems and provides a marketable gas-fueled technology. The specific near- to mid-term (mid-1990s) objectives are to develop the key fuel cell technology for phosphoric acid, molten carbonate, and solid oxide fuel cell systems, and to evaluate and conduct research on more advanced fuel cell concepts that would further improve technical and economic performance. Advanced fuel cell concepts may in the long-term (post 2000) offer potential for use in additional applications such as in the transportation and residential sectors. In these applications oil could be displaced by fuel cell systems using fuels derived from coal. DOE

N88-26732*# National Aeronautics and Space Administration. Lewis Research Center, Cleveland, Ohio.
THE DESIGN AND FABRICATION OF A STIRLING ENGINE HEAT EXCHANGER MODULE WITH AN INTEGRAL HEAT PIPE
Jeffrey G. Schreiber [1988] 11 p Presented at the 23rd Intersociety Energy Conversion Engineering Conference, Denver, Colorado, 31 Jul. - 5 Aug. 1988; sponsored in part by ASME, AIAA, ANS, SAE, IEEE, ACS and AIChE
(NASA-TM-101296; E-4101; NAS 1.15:101296) Avail: NTIS HC A03/MF A01 CSCL 10B

The conceptual design of a free-piston Stirling Space Engine (SSE) intended for space power applications has been generated. The engine was designed to produce 25 kW of electric power with heat supplied by a nuclear reactor. A novel heat exchanger module was designed to reduce the number of critical joints in the heat exchanger assembly while also incorporating a heat pipe as the link between the engine and the heat source. Two inexpensive verification tests are proposed. The SSE heat exchanger module is described and the operating conditions for

the module are outlined. The design process of the heat exchanger modules, including the sodium heat pipe, is briefly described. Similarities between the proposed SSE heat exchanger modules and the LeRC test modules for two test engines are presented. The benefits and weaknesses of using a sodium heat pipe to transport heat to a Stirling engine are discussed. Similarly, the problems encountered when using a true heat pipe, as opposed to a more simple reflux boiler, are described. The instruments incorporated into the modules and the test program are also outlined. Author

N88-26733# Technische Univ., Berlin (West Germany). Fachbereich fuer Elektrotechnik.
DEVELOPMENT OF A MODEL PROCEDURE FOR THE DETERMINATION OF VOLUME DIFFUSION LENGTHS BY TRANSIENT MEASUREMENTS ON MONOCRYSTAL SILICON SOLAR CELLS Ph.D. Thesis [ENTWICKLUNG EINES MODELLVERFAHRENS ZUR BESTIMMUNG DER VOLUMENDIFFUSIONSIONSLAENGEN IN DER BASIS MONOKRISTALLINER SILIZIUM-SOLARZELLEN AUS TRANSIENTEN MESSUNGEN]
Richard Kern 1987 129 p In GERMAN
(ETN-88-92119) Avail: NTIS HC A07/MF A01

Theoretical and experimental determination of diffusion lengths of minority carrier concentrations is performed, permitting the improvement of semiconductor material quality for monocrystal silicon solar cells. Transient tests and measurement curves after optical excitation with large or narrow band spectra and after electric injection of majority carriers provide concordant results for the diffusion lengths. ESA

N88-26734# Technische Univ., Munich (West Germany). Inst. fuer Anorganisch-Chemie.
PHOTOVOLTAIC CELLS WITH n-SILICON AND CONDUCTIVE POLYMERS Ph.D. Thesis [PHOTOVOLTAISCHE ZELLEN MIT N-SILICIUM UND LEITENDEN POLYMEREN]
Dieter Beckert 1986 101 p In GERMAN
(ETN-88-92133) Avail: NTIS HC A06/MF A01

Photoelectrochemical (PEC) cells on semiconductor cells with conductive polymers are studied to provide economical electrical energy with high energetic performance and long lifetime. Photocorrosion problems of the semiconductor in contact with the electrolyte are examined and various methods of stabilization of n-silicon are tested. The use of monocrystals in PEC-cells is compared with cheaper polycrystal materials. Characterization of photoelectrode materials is performed with photocurrent-voltage curves and intensity-time curves. Photoelectrodes passivation obtained by various coatings is determined. ESA

N88-26735# Electrotechnical Lab., Sakura (Japan).
PREPARATION TECHNOLOGY FOR THIN FILM SOLID ELECTROLYTE FUEL CELLS
A. Negishi 1987 13 p In JAPANESE Submitted for publication
(PB88-131925) Copyright Avail: NTIS HC E04 as PB88-131909; copy not available from STI Facility CSCL 10A

Thin film technology of solid electrolyte is described together with an outline of the theoretical aspect and unique advantages of solid electrolyte fuel cells, their structure and manufacture, and the present status of research and development in the field. GRA

N88-26736*# Jet Propulsion Lab., California Inst. of Tech., Pasadena.
ANALYTICAL DETERMINATION OF CRITICAL CRACK SIZE IN SOLAR CELLS
C. P. Chen 14 May 1988 32 p
(Contract NAS7-918)
(NASA-CR-183128; JPL-Publ-88-10; NAS 1.26:183128) Avail: NTIS HC A03/MF A01 CSCL 10A

Although solar cells usually have chips and cracks, no material specifications concerning the allowable crack size on solar cells are available for quality assurance and engineering design usage. Any material specifications that the cell manufacturers use were developed for cosmetic reasons that have no technical basis. Therefore, the Applied Solar Energy Corporation (ASEC) has sponsored a continuing program for the fracture mechanics evaluation of GaAs. Fracture mechanics concepts were utilized to develop an analytical model that can predict the critical crack size of solar cells. This model indicates that the edge cracks of a solar cell are more critical than its surface cracks. In addition, the model suggests that the material specifications on the allowable crack size used for Si solar cells should not be applied to GaAs solar cells. The analytical model was applied to Si and GaAs solar cells, but it would also be applicable to the semiconductor wafers of other materials, such as a GaAs thin film on a Ge substrate, using appropriate input data. Author

N88-26512# Shanghai Inst. of Energy (China).
AN ANALYSIS OF GAS-STEAM TOTAL POWER RECOVERY ENERGY SYSTEM
Zhi-Guang Ling *In* Tokyo Univ., The Proceedings of the Symposium on Mechanics for Space Flight 1987 Mar. 1988 p 115-125 (For primary document see N88-26499 20-31)
Avail: NTIS HC A07/MF A01

45 ENVIRONMENT POLLUTION

Includes atmospheric, noise, thermal, and water pollution.

N88-26737*# Smithsonian Astrophysical Observatory, Cambridge, Mass.
MEASUREMENT OF HO2 AND OTHER TRACE GASES IN THE STRATOSPHERE USING A HIGH RESOLUTION FAR-INFRARED SPECTROMETER AT 28 KM Semiannual Status Report, 1 Jan. 1987 - 30 Jun. 1988
Wesley A. Traub and Kelly V. Chance Jun. 1988 9 p
(Grant NsG-5175)
(NASA-CR-180400; NAS 1.26:180400; SASR-20; SASR-21; SASR-22) Avail: NTIS HC A02/MF A01 CSCL 13B

The major events and results to date of the ongoing program of measuring stratospheric composition by the technique of far-infrared Fourier-transform spectroscopy from a balloon-borne platform are reviewed. The highlights of this period were the two balloon flight campaigns which were performed at Palestine, Texas, both of which produced large amounts of scientifically useful data. Author

N88-26738# Department of Energy, Oak Ridge, Tenn.
ACID PRECIPITATION: A CURRENT AWARENESS BULLETIN
P. S. Blackburn, ed. Jan. 1988 59 p
(DE88-007987; DOE/APC-88-1) Avail: NTIS HC A04/MF A01

Acid Precipition (APC) announces on a monthly basis the current worldwide information on acid precipation and closely related subjects, including wet and dry deposition, long-range transport, environmental effects, modeling, and socioeconomic factors. This publication contains the abstracts of DOE reports, journal articles, conference papers, patents, theses, and monographs added to the Energy Data Base (EDB) during the past month. Also included are US information obtained through acquisition programs or interagency agreements and international agreements and international information obtained through the International Energy Agency's Energy Technology Data Exchange or government-to-government agreements. DOE

N88-26739# Research Triangle Inst., Research Triangle Park, N.C.
REVIEW OF METHODS FOR REMOTE SENSING OF ATMOSPHERIC EMISSIONS FROM STATIONARY SOURCES Final Report
M. L. Saeger, C. K. Sokol, S. J. Coffey, R. S. Wright, and W. E. Farthing Mar. 1988 98 p Prepared in cooperation with Southern Research Inst., Birmingham, Ala.

(Contract EPA-68-02-4442)
(PB88-190483; RTI/3744/04-01F; EPA/600/4-88/014) Avail: NTIS HC A05/MF A01 CSCL 13B

The report reviews the commercially available and developing technologies for the application of remote sensing to the measurement of source emissions. The term remote sensing technology, as applied in the report, means the detection or concentration measurement of trace atmospheric species by sensing the interaction of propagating electromagnetic energy and the specific constituent along the path of propagation. Many remote monitoring techniques are applicable to source measurements. The source of the energy can be natural or designed as part of the system. In general, passive techniques are easier to use and less expensive to purchase and operate than are the active systems. Active systems are, in general, more specific and more sensitive than the passive systems. Some active techniques provide the added advantage of range resolution, which is preferred for some types of measurement application. GRA

N88-26740# Oak Ridge National Lab., Tenn.
THE SEASONAL EXCHANGE OF CARBON DIOXIDE BETWEEN THE ATMOSPHERE AND THE TERRESTRIAL BIOSPHERE: EXTRAPOLATION FROM SITE-SPECIFIC MODELS TO REGIONAL MODELS
A. W. King, D. L. DeAngelis, and W. M. Post Dec. 1987 297 p
(Contract DE-AC05-84OR-21400)
(DE88-007870; ORNL/TM-10570) Avail: NTIS HC A13/MF A01

Ecological models of the seasonal exchange of carbon dioxide (CO2) between the atmosphere and the terrestrial biosphere are needed in the study of changes in atmospheric CO2 concentration. In response to this need, a set of site-specific models of seasonal terrestrial carbon dynamics was assembled from open-literature sources. The collection was chosen as a base for the development of biome-level models for each of the earth's principal terrestrial biomes or vegetation complexes. The primary disadvantage of this approach is the problem of extrapolating the site-specific models across large regions having considerable biotic, climatic, and edaphic heterogeneity. Two methods of extrapolation were tested. DOE

N88-26741# Pacific Northwest Labs., Richland, Wash. Atmospheric Sciences Dept.
OVERVIEW OF THE PRECP (PROCESSING OF EMISSIONS BY CLOUDS AND PRECIPITATION) PROGRAM
Jeremy M. Hales Feb. 1988 9 p Presented at the NAPAP Atmospheric Chemistry Task Group Review, Knoxville, Tenn., 13 Mar. 1988
(Contract DE-AC06-76RL-01830)
(DE88-008205; PNL-SA-15688; CONF-880351-3) Avail: NTIS HC A02/MF A01

The PRocessing of Emissions by Clouds and Precipitation (PRECP) Program addresses the scientific understanding and quantitative description of the physical and chemical storm processes that lead to deposition of pollutants to the earth's surface. These processes are primary determinants of source-receptor transport distances and of the chemical forms, concentrations, and wet-deposition loadings of pollutants at receptor sites. The importance of each of these features to NAPAP, both for policy analysis and for input to scientific studies of receptor response, are largely self-evident. A brief description of the program is presented. DOE

N88-26742# Central Research Inst. of Electric Power Industry, Tokyo (Japan).
DEVELOPMENT OF AN ATMOSPHERIC DIFFUSION EVALUATION METHOD INCORPORATING TOPOGRAPHICAL EFFECTS. PART 1: LITERATURE REVIEW OF ATMOSPHERIC DIFFUSION MODELS INCORPORATING TERRAIN EFFECTS
Yoichi Ichikawa and Sho Nishinomiya Aug. 1987 45 p In JAPANESE; ENGLISH summary
(DE88-753104; CRIE-T-86073-Pt-1) Avail: NTIS (US Sales Only) HC A03

Atmospheric diffusion models incorporating terrain effects were reviewed from many literatures. Gaussian trajectory plume models in which plume trajectories were assumed to progress linearly were widely used for flat areas. Many diffusion models incorporating terrain effects were proposed but could not be used practically. The plume model which had the physical basis was thought practical to predict plume trajectories and plume trajectories were in general predicted from the potential flow theory. It is necessary hereafter to examine the accuracy of the model prediction through field and wind tunnel experiments. The Lagrangian statistical trajectory models based on Markov chain relation etc. was effective to express the turbulent but it was difficult to treat topographical conditions appropriately with existing models. It is therefore necessary to develop newly so-called turbulent diffusion models, in which atmospheric turbulence can be incorporated. DOE

N88-26743# International Centre for Theoretical Physics, Trieste (Italy).
OUR CLIMATE IN DANGER
A. M. Choudhury Nov. 1987 20 p
(DE88-701824; IC-86/240) Avail: NTIS (US Sales Only) HC A03/MF A01

In this paper, the effect of the increase in the temperature of the earth's atmosphere as a consequence of the increase in the CO(sub 2) content and other trace gases has been reviewed. The results have been obtained by a number of model studies. The effect of the depletion of the ozone layer has also been considered. There is the horrific prediction that the global mean temperature of the earth will rise by about 3 deg. C and the antarctic ice will melt by the middle of the next century. As a result, the mean sea level will rise by several meters and this will make many cities and countries or part of countries vanish from the globe. As Bangladesh is a low deltaic region, it will be specially vulnerable. Model computations show that in some regions rainfall will increase whereas in other regions specially in the tropics, rainfall will decrease and desertification will increase. If this happens, mankind will be faced with a major disaster in history. Effect on the society in general and remedial measures have been discussed. DOE

N88-26744*# National Aeronautics and Space Administration. John F. Kennedy Space Center, Cocoa Beach, Fla.
SURVEY FOR LEAST BELL'S VIREO IN RIPARIAN HABITAT ON VANDENBERG AIR FORCE BASE, SANTA BARBARA COUNTY, CALIFORNIA
David R. Breininger (Bionetics Corp., Cocoa Beach, Fla.) Mar. 1988 30 p
(Contract NAS10-10285)
(NASA-TM-100984; NAS 1.15:100984; BIO-1) Avail: NTIS HC A03/MF A01 CSCL 13B

The least bell's vireo (Vireo bellii pusillus) was listed in 1986 as an endangered species by the U.S. Fish and Wildlife Service. Because of the possibility of the species existing on Vandenberg Air Force Base (VAFB), this survey was conducted to determine if they exist, and if so to prepare a distribution map of the species on the base. Major riparian areas were surveyed on foot for 17 days in April, May, and July 1987. No least bell's vireo were sighted; based on past studies, it is unlikely that there is a significant population on VAFB. There are, however, at least 13 other species of special concern that inhabit VAFB riparian woodlands. Most of these species have declined along the south coast of Santa Barbara County, and many have declined in much of the southern half of California. Riparian areas on VAFB are an important environmental resource for the southern half of California; many of these areas, however, show signs of degradation. Author

46 GEOPHYSICS

Includes aeronomy; upper and lower atmosphere studies; ionospheric and magnetospheric physics; and geomagnetism.

For space radiation see *93 Space Radiation.*

N88-26745*# Massachusetts Inst. of Tech., Cambridge. Dept. of Civil Engineering.

TRACER WATER TRANSPORT AND SUBGRID PRECIPITATION VARIATION WITHIN ATMOSPHERIC GENERAL CIRCULATION MODELS Interim Technical Report

Randal D. Koster, Peter S. Eagleson, and Wallace S. Broecker Mar. 1988 366 p

(Grant NAG5-743)

(NASA-CR-182897; NAS 1.26:182897; MIT-R88-06; MIT-317) Avail: NTIS HC A16/MF A01 CSCL 08G

A capability is developed for monitoring tracer water movement in the three-dimensional Goddard Institute for Space Science Atmospheric General Circulation Model (GCM). A typical experiment with the tracer water model follows water evaporating from selected grid squares and determines where this water first returns to the Earth's surface as precipitation or condensate, thereby providing information on the lateral scales of hydrological transport in the GCM. Through a comparison of model results with observations in nature, inferences can be drawn concerning real world water transport. Tests of the tracer water model include a comparison of simulated and observed vertically-integrated vapor flux fields and simulations of atomic tritium transport from the stratosphere to the oceans. The inter-annual variability of the tracer water model results is also examined. Author

N88-26746# Finnish Meteorological Inst., Helsinki.

ON THE GLOBAL RADIATION INCIDENT VARIOUSLY ORIENTATED SURFACES ON THE SOUTH COAST OF FINLAND

Bengt Tammelin, Maija Pietarinen, and Aulis Peltomaa 1987 75 p

(FMI-5) Avail: NTIS HC A04/MF A01

The amount of solar radiation (direct + diffuse + reflected) incident on surfaces of varying orientation has been investigated by means of an automatic observation station situated on the southern coast of Finland. Results from the first year of observations (1980 to 1981) show that the methods for estimating radiation incident on the surface walls used in Finland give results which clearly differ from those actually measured. In this report, the measured data are compared with results obtained from various radiation models. These tests show that the model in which diffuse and reflected radiation is assumed to be isotropic leads to better-than-average results compared to the use of the other tested calculation models. Author

N88-26747*# Houston Univ., Tex.

FINE-SCALE TRAVERSES IN CUMULATE ROCKS, STILLWATER COMPLEX: A LUNAR ANALOGUE STUDY Final Technical Report

Donald Elthon 29 Jul. 1988 7 p

(Grant NAG9-212)

(NASA-CR-183066; NAS 1.26:183066) Avail: NTIS HC A02/MF A01 CSCL 08G

The objective was to document finite-scale compositional variations in cumulate rocks from the Stillwater Complex in Montana and to interpret these data in the context of planetary magma fractionation processes such as those operative during the formation of the Earth's Moon. This research problem involved collecting samples in the Stillwater Complex and analyzing them by electron microprobe, X-ray fluorescence (XRF), and instrumental neutron activation analysis (INAA). The electron microprobe is used to determine the compositions of cumulus and intercumulus phases in the rocks, the XRF is used to determine the bulk-rock major element and trace element (Y, Sr, Rb, Zr, Ni, and Cr) abundances, and the INAA lab. is used to determine the trace element (Sc, Co, Cr, Ni, Ta, Hf, U, Th, and the REE) abundances of mineral separates and bulk rocks. B.G.

N88-26748# National Center for Atmospheric Research, Boulder, Colo. Climate and Global Dynamics Div.

CIRCULATION STATISTICS FROM SEASONAL AND PERPETUAL JANUARY AND JULY SIMULATIONS WITH THE NCAR (NATIONAL CENTER FOR ATMOSPHERIC RESEARCH) COMMUNITY CLIMATE MODEL (CCM1):R15

G. S. Williamson and D. L. Williamson Dec. 1987 198 p

(Grant NSF ATM-87-09659)

(PB88-192620; NCAR/TN-302-STR) Avail: NTIS HC A09/MF A01 CSCL 04A

Horizontal maps and meridional cross sections of selected circulation statistics are presented for 15 year seasonal and 1200 day perpetual January and July simulation with the 12 layer R15 version of the NCAR Community Climate Model (CCM1). These circulation statistics provide prospective model users with a brief, concise summary of the climate produced by the configuration of the model. The statistics are computed for the 90 day December, January, February and June, July, August periods of the 15 years of the seasonal runs. For the perpetual simulations they are computed for 90 day periods separated by 60 days to ensure reasonable independence, yielding eight samples. The statistics are presented in such a way as to easily allow direct comparison with the model's predecessor (CCMOB). They also allow direct comparison between the perpetual and seasonal simulations. Author

N88-26749# Central Research Inst. of Electric Power Industry, Tokyo (Japan).

WIND TUNNEL STUDY OF ATMOSPHERIC DIFFUSION IN UNSTABLE STRATIFIED BOUNDARY LAYER. PART 2: CHARACTERISTIC SCALE AND DIFFUSION

Koichi Sada, Shinji Kakishima, and Yoichi Ichikawa Aug. 1987 23 p In JAPANESE; ENGLISH summary

(DE88-753109; CRIE-T-86095-Pt-2) Avail: NTIS (US Sales Only) HC A03

In pursuit of clarifying turbulence statistics related with diffusion, a study on changes in characteristic scales in an air flow shifting from the neutral state to an unstable state in order to determine these characteristic scales and to determine the relations with the scales and diffusion processes in a wind tunnel. The vertical plume spread in the unstable state under the flat land condition is found to correspond to that in a semi-unstable state in the atmosphere. Measurements are made of tracer diffusion and speed disturbance under air flow conditions. It is shown that lateral plume spread distributions in the wind tunnel under neutral and unstable condition almost agree with each other when the characteristic scales are used for normalization. The characteristic scale shows a value 4-14 time as much as the time scale in the wind tunnel. This relation is also observed in the atmosphere. DOE

N88-26750# International Centre for Theoretical Physics, Trieste (Italy).

PROPAGATION OF INERNIO-ACOUSTIC GRAVITY WAVES IN A ROTATING AND RADIATING OPAQUE ATMOSPHERE

A. R. Bestman Jun. 1987 11 p

(DE88-701866; IC-87/123) Avail: NTIS (US Sales Only) HC A03/MF A01

The critical level for wave propagation is studied in the presence of radiation driven winds using a hydrodynamic model. As a result of the extremely complex nature of the problem, the galaxy is assumed opaque so that the optically thick gas approximation of radiation is invoked. Further the frequencies involved in the wave motion are taken fairly high so that the wave is essentially adiabatic. Despite these idealizations, the wave motion is governed by a fourth order ordinary differential equation with variable coefficients. The simplest configuration studied by the classical Frobenius method involves three waves which propagate across the critical level (regular singular point) attenuated, while the fourth is attenuated/amplified on crossing the critical level. This constitutes the well-known valve effect, which is enhanced by radiation. DOE

N88-26751# Birmingham Univ. (England).
ION AND ELECTRON INTERACTIONS OF ATMOSPHERIC IMPORTANCE Final Report, 1 Jul. 1986 - 30 Nov. 1987
David Smith and Nigel G. Adams 31 Dec. 1987 82 p
(Grant AF AFOSR-0095-82)
(AD-A192255; AFGL-TR-88-0021) Avail: NTIS HC A05/MF A01 CSCL 07D

The Variable-Temperature Flowing Afterglow/Langmuir Probe (VT-FALP) and the Variable-Temperature Selected Ion Flow Drift Tube (VT-SIFDT) apparatuses have been exploited to study (1) dissociative electron attachment to HBr and HI and reverse processes of associative detachment of Br- and I- with H atoms (2) secondary dissociative electron attachment reactions of the radicals CCl3 and CCl2Br formed in the primary dissociative electron attachment reactions of CCl4 and CCl3Br(3) dissociative recombination reactions of several positive ion species (4) the ternary association reactions of CH3+ ions with H2, N2 and CO as a function of the centre-of-mass interaction energy. GRA

N88-26752# Weston Observatory, Mass.
SURFACE DISTURBANCES PRODUCED BY LOW-LEVEL, SUBSONIC B-1 AIRCRAFT Scientific Report, Aug. 1986 - Aug. 1987
Francis A. Crowley and Joseph I. Blaney 15 Nov. 1987 45 p
(Contract F19628-86-C-0055)
(AD-A192257; AFGL-TR-87-0325; SR-1) Avail: NTIS HC A03/MF A01 CSCL 15C

Properties of infrasonic and seismic disturbances excited by low level, subsonic B-1 flights over the Arkansas River Valley near La Junta, Colorado are measured and studied for different wind conditions. The study emphasizes the role seismics and infrasonics might play to detect and track aircraft overflying a distributed network of pressured sensors and seismometers. The work concludes that carefully sited and calibrated seismic nodal elements, operating at low data rates, have a high potential to provide timely azimuth information for tracking. GRA

N88-26753# Lowell Univ., Mass. Center for Atmospheric Research.
HIGH LATITUDE IONOSPHERIC RADIO STUDIES Final Report, 3 May 1983 - 30 Sep. 1986
Bodo W. Reinisch, Klaus Bibl, Claude G. Dozois, Robert R. Gamache, and David F. Kitrosser Jan. 1988 165 p
(Contract F19628-83-C-0092)
(AD-A192270; ULRF-439/CAR; AFGL-TR-87-0056) Avail: NTIS HC A08/MF A01 CSCL 04A

Structure and dynamics of the ionosphere are explored under this contract by digital high-frequency sounding techniques. The research emphasizes the investigation of the auroral and subauroral ionosphere, but also includes studies on the polar cap and mid-latitude ionosphere. GRA

N88-26754# Boston Coll., Chestnut Hill, Mass.
ROCKET MEASUREMENTS WITHIN A POLAR CAP ARC: IONOSPHERIC MODELLING
Robert E. Sheehan 19 Nov. 1987 34 p
(Contract F19628-85-K-0051)
(AD-A192381; AFGL-TR-87-0326; SR-2) Avail: NTIS HC A03/MF A01 CSCL 04A

Precipitating electron fluxes measured over a polar cap, F-region auroral arc were input to an ionospheric model that calculates production rate and density profiles of various species. The model also finds the electron temperature and electric conductivities over a specified altitude range. Most model results compare favorably with rocket measurements taken near apogee over the arc. The actual electron temperature is underestimated by the model and the relative densities of some minor species do not agree. Model results show that initial density conditions in particular strongly affect the development of electron density enhancements produced by dynamic, short lived (15 min) fluxes of soft electrons. The neutral atmosphere chosen for the model also influences the electron density profile produced by soft fluxes. Such differences may play a role in the solar cycle dependence of density fluctuations that cause scintillations in the polar cap. GRA

N88-26755# Aerospace Corp., El Segundo, Calif. Space Sciences Lab.
ON THE CONJUGACY OF THE AURORA: HIGH AND LOW LATITUDES
P. F. Mizera, D. J. Gorney, and D. S. Evans 5 Feb. 1988 18 p
(Contract F04701-85-C-0086)
(AD-A193008; TR-0086A(2940-06)-4; SD-TR-88-09) Avail: NTIS HC A03/MF A01 CSCL 04A

On December 5, 1983 the polar orbiting satellites NOAA-7 and DMSP-F6, while in opposite hemispheres, each crossed a narrow structure of auroral electron precipitation at nearly the same Universal Time (UT) and at the same high magnetic-latitude, local time location. The Operational Line Scanner (OLS) image taken by DMSP-F6 of the northern polar region showed that this enhancement was associated with a sun-aligned arc (SAA) which extended poleward from the midnight sector auroral zone and passed across the polar cap very near to the magnetic pole. The DMSP-F6 plasma measurements showed particle precipitation at background levels in the regions adjacent to the SAA suggesting that those magnetic field lines connected to the interplanetary medium via the northern tail lobe. NOAA-7 observations show that the analogous precipitation structure in the southern hemisphere was embedded in a region of low intensity ion and electron precipitation which had the characteristics of the plasma sheet population. Comparisons between the boundaries of the lower latitude auroral zone precipitation and the electron distributions at those boundaries were also made. The results of these comparisons together with those made for the high altitude SAA argue for a high degree of inter-hemisphere conjugacy in the electron precipitation over a wide range of invariant magnetic latitudes. GRA

N88-26756# Iowa State Univ. of Science and Technology, Ames. Dept. of Physics.
WAVENUMBER SPECTRA FROM THIR 6.7 MICRON WATER VAPOR DATA
Gloria L. Manney and John L. Stanford [1988] 20 p
Avail: NTIS HC A03/MF A01

Wavenumber spectra from Nimbus-7 THIR 6.7 micron water vapor data are analyzed using series 4800 km long, in regions free of high clouds and frontal zones. In these regions, the brightness temperatures may be considered as temperatures on a water vapor isosteric (constant density) surface. Power above the noise can be extracted down to wavelengths of about 60 km. Fitting the power spectrum versus horizontal wavenumber, k, to a k sup -n power law for wavelengths from 60 to a few hundred kilometers gives slopes of n = 2.6 to 2.9, depending on the exact wavenumbers that are fitted. This type of data may prove useful in studying mesoscale phenomena if care is taken in its interpretation. Author

N88-26757# Royal Netherlands Meteorological Inst., De Bilt. Afdeling Fysische Meteorologie.
A CONTROL PROGRAM FOR GLOBAL RADIATION MEASUREMENTS [EEN CONTROLEPROGRAMMA VOOR GLOBALE STRALINGSMETINGEN]
W. R. Raaff and C. A. Velds 1987 24 p In DUTCH
(KNMI-TR-100; B8725693; ISSN-0169-1708; ETN-88-91805)
Copyright Avail: NTIS HC A03/MF A01

A control program for the detection of errors in global radiation measurement results was developed. The control program for the diurnal hourly values of astronomical factors, (time of sunrise and sunset, Sun altitude, and the radiation incident at the edge of the atmosphere) is explained and demonstrated with an example. The control of large inventories of radiation data is outlined. The computer program is enclosed. ESA

N88-26758# Cologne Univ. (West Germany). Inst. fuer Geophysik und Meteorologie.
DIFFUSION OF SLIGHT SOLAR INDUCED DISTURBANCES IN THE MIDDLE ATMOSPHERE [DIE AUSBREITUNG SCHWACHER SOLAR INDUZIERTER STOERUNGEN IN DER MITTLEREN ATMOSPHAERE]
Martin Dameris, A. Ebel, ed., F. M. Neubauer, ed., E. Raschke, ed., and P. Speth, ed. 1987 140 p In GERMAN
(Contract DFG-Eb-56/7-2.3)
(Mitt-53; ISSN-0069-5882; ETN-88-92346) Avail: NTIS HC A07/MF A01

Nimbus 6 satellite observations and static-morphologic investigations of global structure wave type disturbances correlated with solar activity during 2 to 40 day periods demonstrate that solar activity effects in the middle atmosphere are influenced by dynamical process. Middle atmosphere global system reaction effects on solar slight disturbances are studied and their generation by solar activity in temperature and pressure fields in the upper stratosphere are described. A 1D-numerical data model (0 to 80 km) and a global 3D-circulation model for stratosphere, mesosphere, and thermosphere (10 to 150 km) are used. Simulation results indicate that the intensity and morphology of slight disturbances effects in the middle atmosphere are mainly influenced by the prevalent wind conditions. ESA

N88-26759*# California Inst. of Tech., Pasadena. Seismological Lab.
EFFECTS OF A TEMPERATURE-DEPENDENT RHEOLOGY ON LARGE SCALE CONTINENTAL EXTENSION
Leslie J. Sonder and Philip C. England (Oxford Univ., England) 18 Aug. 1988 60 p
(Grant NAG5-842)
(NASA-CR-183117; NAS 1.26:183117) Avail: NTIS HC A04/MF A01 CSCL 08E

The effects of a temperature-dependent rheology on large-scale continental extension are investigated using a thin viscous sheet model. A vertically-averaged rheology is used that is consistent with laboratory experiments on power-law creep of olivine and that depends exponentially on temperature. Results of the calculations depend principally on two parameters: the Peclet number, which describes the relative rates of advection and diffusion of heat, and a dimensionless activation energy, which controls the temperature dependence of the rheology. At short times following the beginning of extension, deformation occurs with negligible change in temperature, so that only small changes in lithospheric strength occur due to attenuation of the lithosphere. However, after a certain critical time interval, thermal diffusion lowers temperatures in the lithosphere, strongly increasing lithospheric strength and slowing the rate of extension. This critical time depends principally on the Peclet number and is short compared with the thermal time constant of the lithosphere. The strength changes cause the locus of high extensional strain rates to shift with time from regions of high strain to regions of low strain. Results of the calculations are compared with observations from the Aegean, where maximum extensional strains are found in the south, near Crete, but maximum present-day strain rates are largest about 300 km further north. Author

N88-26760*# Universities Space Research Association, Huntsville, Ala.
THE NASA MARSHALL ENGINEERING THERMOSPHERE MODEL
Michael Philip Hickey Jul. 1988 40 p
(Contract NAS8-36400)
(NASA-CR-179359; NAS 1.26:179359) Avail: NTIS HC A03/MF A01 CSCL 04A

Described is the NASA Marshall Engineering Thermosphere (MET) Model, which is a modified version of the MFSC/J70 Orbital Atmospheric Density Model as currently used in the J70MM program at MSFC. The modifications to the MFSC/J70 model required for the MET model are described, graphical and numerical examples of the models are included, as is a listing of the MET model computer program. Major differences between the numerical output from the MET model and the MFSC/J70 model are discussed. Author

47 METEOROLOGY AND CLIMATOLOGY

Includes weather forecasting and modification.

N88-26761# National Oceanographic Data Center, Washington, D. C.
MARINERS WEATHER LOG, VOLUME 31, NUMBER 4, FALL 1987 Quarterly Report
1988 69 p
(PB88-173851) Avail: NTIS HC A04/MF A01 CSCL 04B

Topics addressed are: fog songs; buoy records; tropical cylcones of 1986; auroras; marine weather review for the north Pacific and north Atlantic Oceans; marine observations program; tips to the radio officer; and hurrican alley. GRA

N88-26762# Research Triangle Inst., Research Triangle Park, N.C.
PARAMETRIC METHODOLOGIES OF CLOUD VERTICAL TRANSPORT FOR ACID DEPOSITION MODELS
F. M. Vukovich and R. C. Haws Mar. 1988 309 p Sponsored by EPA, Research Triangle Park, N.C.
(EPA-68-02-4059)
(PB88-191374; EPA/600/3-88/011) Avail: NTIS HC A14/MF A01 CSCL 04B

A CUmulus VENTing (CUVENT) cloud module was developed that calculates the vertical flux of mass from the boundary layer to the cloud layer by an ensemble of nonprecipitating subgrid-scale air mass clouds. This model is integrated into the Regional Acid Deposition Model (RADM) and serves to establish the effect of cloud venting for the RADM. In the initial phase of this research, the basic cloud venting algorithm was established. CUVENT used the cloud model to calculate the vertical transport of mass due to the ensemble of nonprecipitating air mass convective clouds. The major effort was to design a parameterization scheme for the cloud model so that it may be incorporated into the RADM. This parameterization scheme used basic meteorological data such as pressure, temperature, humidity, surface heat flux, etc., to predict the convective cloud amount at cloud base and cloud distribution parameters. Author

N88-26763*# National Aeronautics and Space Administration. Goddard Space Flight Center, Greenbelt, Md.
METEOROLOGICAL ATLAS OF THE SOUTHERN HEMISPHERE LOWER STRATOSPHERE FOR AUGUST AND SEPTEMBER 1987
P. A. Newman, D. J. Lamich, M. Gelman (National Meteorological Center, Washington, D.C.), M. R. Schoeberl, W. Baker, and A. J. Krueger Jun. 1988 135 p
(NASA-TM-4049; Rept-88B0189; NAS 1.15:4049) Avail: NTIS HC A07/MF A01 CSCL 04B

Southern Hemisphere meteorological data for the months of August and September 1987 in the lower stratosphere are shown. National Meteorological Center (NMC) data, Total Ozone Mapping Spectrometer (TOMS) data, and Goddard Laboratory for Atmospheres (GLA) data are used to display polar stereographic projections of 200 to 100 mb vertical mean temperatures, 100 mb zonal mean geopotential height perturbations, total ozone, Ertel's potential vorticity (Epv), and 50 to 30 mb vertical mean temperatures. In addition, latitude height cross sections at 65 W of potential temperature, Epv, geostrophic isotachs, and temperature are also shown. Finally, a longitude height cross section at 65 S of temperature and geostrophic wind vectors is also shown. Author

N88-26764# Washington Univ., Seattle. Dept. of Atmospheric Sciences.
STUDIES OF THE MECHANISMS AND RATES WITH WHICH NITROGEN SPECIES ARE INCORPORATED INTO CLOUD WATER AND PRECIPITATION Final Report
D. A. Hegg and P. V. Hobbs Dec. 1987 56 p Sponsored by Coordinating Research Council, Inc., Atlanta, Ga.
(PB88-193065; CRC-APRAC-AP-7) Avail: NTIS HC A04/MF A01 CSCL 04B

The relationship between nitrate production and nitrate precursor reactants was examined. A data base was established on PAN, including vertical profiles in the atmosphere, which could be used to assess the transport and scavenging of PAN by precipitating systems. A rainband chemistry model was used to quantify the fluxes of odd-nitrogen species thru precipitating systems. Additional data sets were obtained by piggy-backing measurements of nitrogen species on the Genesis of Atlantic Lows Experiment field study. Author

N88-26765# National Oceanic and Atmospheric Administration, Seattle, Wash. Marine Environmental Lab.
NUMERICAL MODEL FOR THE COMPUTATION OF RADIANCE DISTRIBUTIONS IN NATURAL WATERS WITH WIND-ROUGHENED SURFACES
C. D. Mobley and R. W. Preisendorfer Jan. 1988 203 p Prepared in cooperation with Washington Univ., Seattle
(PB88-192703; NOAA-TM-ERL-PMEL-75; CONTRIB-813) Avail: NTIS HC A10/MF A01 CSCL 04B

This report is a repository of the details of derivation of a numerical procedure to determine the unpolarized radiance distribution as a function of depth, direction, and wavelength, in a natural hydrosol such as lake or sea. The input to the model consists of (1) the incidence radiance distribution at the air-water surface, (2) the state of randomness of the air-water surface as a function of wind speed, (3) the volume scattering and volume attenuation functions of the medium as a function of depth and wavelength, and (4) the type of bottom boundary. The model has an expandable library of derived quantities that are of use in various applications of optics to natural waters, such as marine biological studies, underwater visual search tasks, remote sensing, and climatology. GRA

N88-26766# Sandia National Labs., Albuquerque, N. Mex.
COMPUTER CONTROLLED DATA ACQUISITION SYSTEM FOR THE NASA 1986 ROCKET TRIGGERED LIGHTNING PROGRAM
J. P. Johnson, J. M. Arellano, R. T. Hasbrouck, and J. W. Lamb 1988 27 p Presented at the International Conference on Lightning and Static Electricity, Oklahoma City, Okla., 19 Apr. 1988 Prepared in cooperation with Lawrence Livermore National Lab., Calif.
(Contract DE-AC04-76DP-00789)
(DE88-008335; SAND-87-2521C; CONF-880493-1) Avail: NTIS HC A03/MF A01

The Lightning-Strike Object (LSO) for the NASA 1986 Rocket Triggered Lightning Program (RTLP-86) was provided jointly by Sandia National Laboratories and Lawrence Livermore National Laboratory. The LSO is a large Faraday-cage-like metal canister containing electronic equipment with an electrical cable extending to a lightning rod 7 m above the canister. The lightning attachment was to the cable outer shield, which was shorted to the inner conductor(s) at the top end of the cable. Transient limiters were employed on each conductor entering the canister. Measurements were made both inside and outside. Computer controlled digital oscilloscopes were chosen to handle the large amount of data and for a fast system response. Eight dual-channel oscilloscopes, a computer, printer, and plotter recorded lightning stroke current applied to the LSO and various voltage and current responses inside. Computer software was written specifically for the RTLP-86 to collect and store data from the oscilloscopes. Turn-around time for the instrumentation system was two to three minutes. Isolation from lightning induced currents and EMI was maintained through the use of nine fiber-optic data links between the sensors and the recording equipment housed in a metal building (actually a railroad caboose). Control and recording power was from a diesel generator located beside the caboose. Data was recorded from 22 lightning flashes containing more than 80 return strokes. The maximum peak stroke current was 52 kA. Typical data is presented. DOE

N88-26767# Lawrence Livermore National Lab., Calif.
AN INTERAGENCY WORKING GROUP ON LIGHTNING THREAT WARNING
R. T. Hasbrouck Jan. 1988 5 p Presented at the International Conference on Lightning and Static Electricity, Oklahoma City, Okla., 19 Apr. 1988
(Contract W-7405-eng-48)
(DE88-009828; UCRL-98006; CONF-880493-2) Avail: NTIS HC A02/MF A01

In a lightning environment, it is desirable to experience a thunderstorm without sustaining serious physical or economic loss. Properly implemented and maintained protection techniques go a long way toward minimizing or eliminating losses. However, activities that cannot be pracitcally protected must be temporarily curtailed during a lightning hazard period. Thus, some method for sensing the onset and departure of the hazard is required. Untimely curtailment or resumption of activities can place personnel and equipment in jeopardy, or result in excessive, and expensive, downtime. False alarms are equally undesirable. Presently, this need for a lightning warning system can be partially met through the use of a cloud-to-ground lightning detection and tracking system. Several manufacturers are installing these systems and the Federal government is seeking to coordinate them into a nationwide network. However, these systems do not provide lightning threat (pre-first-strike) warning. Techniques and equipment for producing such warnings exist, but until recently there has been no unified effort to consolidate the knowledge, standardize the requirements, and identify the problems of the various users. This paper will briefly describe the formation of an interagency working group which intends to specifically address such issues. DOE

N88-26768# Central Research Inst. of Electric Power Industry, Tokyo (Japan).
REMOTE SENSING OF TEMPERATURE PROFILES. PERFORMANCE TEST OF PASS
Yukio Akai and Sho Nishinomiya Aug. 1987 39 p In JAPANESE; ENGLISH summary
(DE88-753108; CRIE-T-86092) Avail: NTIS (US Sales Only) HC A03

In order for the rationalization of meteorological observation and cost reduction for the environmental assessment and in connection with the introduction of Radar Acoustic Sounding System (RASS), wherein the radars for the sonic and the radio waves were combined, its principle and the result of measurement are described. Measurement of the atmospheric temperature by RASS was similar to that by the conventional tower method on the low-layer radio zonde; the height of the inversion layer and occurence found in the SODAR echo pattern quite well coincided. Altitude of observation changed mainly by the wind velocity; observation was possible, 100 percent for the altitude up to 150 m at wind velocity below 14 m/s, and 80 percent for the altitude up to 300 m at wind velocity below 6m/s. It was found that, at low wind velocity where an atmospheric diffusion is problematic, observation was possible up to 500 m altitude, by which an application for the continuous observation of the inversion layer can be expected. DOE

N88-26769# International Centre for Theoretical Physics, Trieste (Italy).
PRESENT STATUS OF ARTIFICIAL RAIN MAKING
A. M. Choudhury Nov. 1987 12 p
(DE88-701823; IC-86/239) Avail: NTIS (US Sales Only) HC A03/MF A01

In this paper a review has been made of the present status of artificial rainmaking. The history of artificial rainmaking goes back to 1946 when Vincent Schaefer of the USA discovered the general

principles. During the last 40 years cloud seeding activities have stirred the imagination of scientists all over the world. If this could be carried out in an operational manner, mankind could have solved the problems of drought which threaten many parts of the globe with famine. However, though a lot of progress has been made in cloud physics, an operational rainmaking programme is yet far from reality. In some cases seeding increases the rainfall whereas in other cases a decrease in rainfall has been noticed. It would be necessary to approach the subject more thoroughly and systematically and while making experiments on rainmaking a proper experimental design should be carried out so that the results of such experiments could be evaluated scientifically. DOE

N88-26770# Los Alamos National Lab., N. Mex.
A RADAR STUDY OF THE INTERACTION BETWEEN LIGHTNING AND PRECIPITATION
D. N. Holden and C. W. Ulbrich 1988 10 p Presented at the 8th International Conference on Atmospheric Electricity, Uppsala, Sweden, 13 Jun. 1988 Prepared in cooperation with Clemson Univ., S.C.
(Contract W-7405-eng-48)
(DE88-009120; LA-UR-88-1328; CONF-8806113-1) Avail: NTIS HC A02/MF A01

A radar study was made of the interaction between lightning and precipitation with the 430 MHz Doppler radar at the Arecibo Observatory in Puerto Rico. On one occasion, the spectral power at Doppler velocities near that corresponding to the updraft increased substantially within a fraction of a second after a discharge was detected in the beam. Calculations were made to simulate the effect of an electric field change on mean Doppler velocity for a distribution of droplets in a thunderstorm. DOE

N88-26771# Naval Postgraduate School, Monterey, Calif.
SYNOPTIC PATTERNS RELATED TO TROPICAL CYCLONE RECURVATURE M.S. Thesis
Brett T. Sherman Mar. 1988 44 p
(AD-A192338; AD-E801594) Avail: NTIS HC A03/MF A01 CSCL 04B

Relative vorticity fields calculated from the U. S. Navy Operational Global Band Analysis are used to relate synoptic and storm parameters to the track of tropical cyclones in the western North Pacific Ocean. In this preliminary study, synoptic patterns are developed, described and discussed from the perspective of a pattern recognition technique to assist the forecasters at the Joint Typhoon Warning Center, Guam. The focus is on track turning motions to the left and right of the persistence track and on trying to accurately predict the point of the turn or recurvature in relation to the time evolution of the vorticity patterns. The developmental sample of storms indicates that there is potential for using synoptic patterns in the Global Band Analysis to guide the selection of the appropriate track aid in the 48 to 60 hour time range. Author (GRA)

N88-26772# Paris VI Univ. (France).
INFLUENCE OF STABLE STRATIFICATION ON ATMOSPHERIC TURBULENCE: AN EXPERIMENTAL CONTRIBUTION Ph.D. Thesis [INFLUENCE DE LA STRATIFICATION STABLE SUR LA TURBULENCE ATMOSPHERIQUE: UNE CONTRIBUTION EXPERIMENTALE]
Francis Dalaudier 1986 209 p In FRENCH
(ETN-88-92292) Avail: NTIS HC A10/MF A01

Local measurement completed with radar measurements were carried out to characterize atmospheric turbulence and its relation to stratification. The study scale is limited on the lower side by inertial turbulence, and on the higher side by gravity waves. A stratosphere-troposphere VHF radar was used. A wave model is developed to interpret turbulences at scales above 100 m. For scales under 10 m inertial turbulence is predominant. The interpretation of the intermediate scale turbulences is discussed. The relation of vertical profile velocity variation and vertical profile temperature variation is complex, and their spectra are not related by any simple expression. ESA

N88-26773# Cologne Univ. (West Germany). Inst. fuer Geophysik und Meteorologie.
DYNAMIC INTERACTION OF CONVECTIVE CUMULUS WITH LARGE-SCALE ENVIRONMENT [DYNAMISCHE WECHSELWIRKUNG DER CUMULUSKONVEKTION MIT IHRER GROSSSKALIGEN UMGEBUNG]
Winfried Koenig, A. Ebel, ed., F. M. Neubauer, ed., E. Raschke, ed., and P. Speth, ed. 1987 62 p In GERMAN; ENGLISH summary
(Mitt-55; ISSN-0069-5882; ETN-88-92348) Avail: NTIS HC A04/MF A01

Assuming convective clouds as independent plumes in the large-scale mean flow, the small scale effects on the vorticity budget are described by the momentum difference induced by the clouds at the boundary of the large-scale area. During periods of intense convective activities detrainment effects become important in the upper troposphere, while large-scale horizontal advection of vorticity is reduced in the middle layers. The comparison of the different contributions to the budget shows that the twisting effect plays a major role in the generation of vorticity in the cloud ensemble. Eddy effects in the large-scale budgets are mainly influenced by the cloud mass flux and the momentum difference between the cloud ensemble and the large-scale environment. For the determination of the cloud mass flux distribution established parameterization schemes can be used. The momentum of the cloud ensemble is investigated by deriving two different parameterization concepts: one approach deals with the generation of a vortex couplet induced by the tilting of horizontal vorticity components; another describes the drag effects of clouds in the large-scale flow. ESA

N88-26774# Cologne Univ. (West Germany). Inst. fuer Geophysik und Meteorologie.
WESTWARD MOVING ATMOSPHERIC WAVE DISTURBANCES OVER THE AFRICAN TROPICS: DYNAMIC AND ENERGETIC ASPECTS [WESTWAERTS WANDERNDE ATMOSPHAERISCHE WELLENSTOERUNGEN DER AFRIKANISCHE TROPEN: IHRE DYNAMIK UND ENERGETIK]
Bernhard Eberz, A. Ebel, ed., F. M. Neubauer, ed., E. Raschke, ed., and P. Speth, ed. 1987 90 p In GERMAN; ENGLISH summary Sponsored by BMFT, Bonn, Fed. Republic of Germany
(Mitt-57; ISSN-0069-5882; ETN-88-92349) Avail: NTIS HC A05/MF A01

The generation mechanism of six cases of easterly waves over the African region are discussed. This wave occurs in the summer months of the Northern Hemisphere and moves westward with a wavelength of 2500 to 3000 km and with a phase velocity of 7 deg per day. They are found directly north of the intertropical convergence zone (ITCZ). Decisive for their development is the existence of a strong baroclinic zone based on the contrast of hot desert air and cooler tropical air over the African continent, and as a result of these conditions the low African easterly jet in 700 to 600 hPa. The vorticity budget, the conversion term of Lorenz's energy cycle, and the necessary condition of barotropic instability are computed. The existence of two different types of easterly wave: northerly baroclinic waves with small vertical extension and southerly barotropic waves with cyclonic vorticity above 700 hPa is found. ESA

N88-26775# Mainz Univ. (West Germany). Fachbereich Physik.
AN EFFICIENT MODEL FOR CHANGES OF GLOBAL CLIMATE AND COMPOSITION OF THE ATMOSPHERE DUE TO HUMAN ACTIVITIES Ph.D. Thesis
Christoph Bruehl 1987 173 p In GERMAN; ENGLISH summary
(ETN-88-92359) Avail: NTIS HC A08/MF A01

An interactive climate-photochemistry-model is presented, for the study of global emission scenarios in a steady state atmosphere, as well as numerically efficient time-dependent simulation of the effects of the anthropogenically influenced gases CO2, CH4, N2O, NOx, CO and chlorofluorocarbons for time periods as long as centuries. The one-dimensional chemical diffusion model

computes the concentrations of 36 atmospheric constituents using photochemical data. The effects of the trace gases CH4, N2O, CF2Cl2, and CFCl3 on the infrared radiation budget are calculated. Scattering by air molecules, aerosol particles, and cloud droplets is included, using a very fine spectral resolution, important for the computation of photolysis rates. Parameterization of tropospheric lapse rates is obtained. The coupling with a simple ocean-model, to account for the timelag in the greenhouse effect induced temperature increase in the lower atmosphere due to heat transfer into the ocean is presented. The complete model computes a surface temperature increase of 2 K for the period 1860 to 2050, compared to 2.7 K without considering the ocean; CO2 contributes about half of these values. The change in the vertical ozone distribution due to chemical interactions with the man made gases influences substantially the temperatures in the stratosphere and troposphere. ESA

N88-26776# Lawrence Livermore National Lab., Calif.
WIND FLOW STUDY: JULY 1987 AND NOVEMBER-DECEMBER 1987
K. R. Chapman and F. J. Gouveia Jan. 1988 106 p
(Contract W-7405-eng-48)
(DE88-008969; UCID-21360) Avail: NTIS HC A06/MF A01

For a ten-day period in July 1987, two meteorological towers were used to evaluate wind flow and surface roughness in a grassy field west of Building 111 at LLNL. We recorded 512-s averages of wind speed and wind direction at one level and temperature at two levels to document local wind flow and thermal stability. These data show the wind direction during this data-collection period to be mostly from the southwest quadrant. Six anemometers were spaced logarithmically along a 2.5-m mast to measure vertical wind speed profiles. The average surface roughness calculated from these profiles under near-neutral atmospheric stability was 15.6 cm. For a five-week period in November and December 1987, we took additional wind speed measurements in the same field to further document wind flow. Wind direction and temperature data were collected at a 40-m tower near the northeast corner of the Laboratory. Additional profile and turbulence parameters were calculated with this data set: alpha, drag coefficient, and turbulent intensity. Variations and averages were analyzed, and averages for stability and wind direction categories are presented. DOE

N88-26777# Commission of the European Communities (Luxembourg).
THE 1985 METEOROLOGICAL YEARBOOK OF ISPRA (27TH)
G. Bollini, A. Galva, C. Gandino, and E. Porrati 1986 97 p
(PB88-125729; EUR-10570-IT) Copyright Avail: NTIS HC E04/MF E04; copy not available from STI Facility CSCL 04B

After a short description of the methods for measuring and elaborating on atmospheric phenomena, many tables and graphics for the meteorological year 1985 are reported. The measurements of solar irradiation are marked with the final hour following Italian winter time. GRA

N88-26778*# Washington Univ., Seattle. Coll. of Forest Resources.
EVALUATION OF SURFACE ENERGY AND RADIATION BALANCE SYSTEMS FOR FIFE
Leo J. Fritschen and Ping Qian 15 Aug. 1988 57 p
(Grant NAG5-901)
(NASA-CR-183118; NAS 1.26:183118) Avail: NTIS HC A04/MF A01 CSCL 04B

The energy balance and radiation balance components were determined at six sites during the First International Satellite Land Surface Climatology Project Field Experiment (FIFE) conducted south of Manhattan, Kansas during the summer of 1987. The objectives were: to determine the effect of slope and aspect, throughout a growing season, on the magnitude of the surface energy balance fluxes as determined by the Energy Balance Method (EBM); to investigate the calculation of the soil heat flux density at the surface as calculated from the heat capacity and the thermal conductivity equations; and to evaluate the performance of the Surface Energy and Radiation Balance System (SERBS). A total of 17 variables were monitored at each site. They included net, solar (up and down), total hemispherical (up and down), and diffuse radiation, soil temperature and heat flux density, air and wet bulb temperature gradients, wind speed and direction, and precipitation. A preliminary analysis of the data, for the season, indicate that variables including net radiation, air temperature, vapor pressure, and wind speed were quite similar at the sites even though the sites were as much as 16 km apart and represented four cardinal slopes and the top of a ridge. Author

48 OCEANOGRAPHY

Includes biological, dynamic, and physical oceanography; and marine resources.

For related information see also *43 Earth Resources and Remote Sensing.*

N88-26779# National Academy of Sciences - National Research Council, Washington, D. C. Ad Hoc Committee on Antarctic Physical and Chemical Oceanography.
PHYSICAL OCEANOGRAPHY AND TRACER CHEMISTRY OF THE SOUTHERN OCEAN
1988 140 p
(Contract DE-FG01-84ER-60266)
(DE88-006852; DOE/ER-60266/T2) Avail: NTIS HC A07/MF A01

This report considers technical and scientific developments and research questions in studies of the Southern Ocean since its predecessor, Southern Ocean Dynamics--A Strategy for Scientific Exploration 1973-1983 was published. The summary lists key research questions in Southern Ocean oceanography. Chapter 1 describes how Southern Ocean research has evolved to provide the basis for timely research toward more directed objectives. Chapter 2 recommends four research programs, encompassing many of the specific recommendations that follow. Appendix A provides the scientific background and Reference/Bibliography list for this report for: on air-sea-ice interaction; the Antarctic Circumpolar Current; water mass conversion; chemical tracer oceanography; and numerical modeling of the Southern Ocean. Appendix B describes the satellite-based observation systems expected to be active during the next decade. Appendix C is a list of relevant reports published during 1981-1987. DOE

N88-26780# National Oceanic and Atmospheric Administration, Seattle, Wash. Marine Environmental Lab.
EIGENMATRIX REPRESENTATIONS OF RADIANCE DISTRIBUTIONS IN LAYERED NATURAL WATERS WITH WIND-ROUGHENED SURFACES
R. W. Preisendorfer Jan. 1988 101 p
(PB88-188701; NOAA-TM-ERL-PMEL-76) Avail: NTIS HC A06/MF A01 CSCL 08C

The report develops analytic, closed-form solutions for radiance distributions in natural waters such as lakes and seas.The solutions are valid in layered waterbodies for which each layer has inherent optical properties (absorption and scattering functions) which are independent of depth within that layer. The water body is assumed free of internal light sources. The effects of a wind-blown air-sea surface are included. The work extends to the radiance level certain results which were previously known to hold for irradiances. The eigenmatrix formalism developed here is convenient for nmuerical computation of radiance distributions, given the inherent optical properties of the water and the desired boundary conditions of the water surface and bottom (the direct problem). Moreover, the formalism suggests an algorithm for solving the inverse problem: the determination of the inherent optical properties from measurements of the radiance distribution within a water body. GRA

N88-26781 Technische Hogeschool, Delft (Netherlands). Onderafdeling der Wiskunde en Informatica.
FULLY IMPLICIT SPLITTING METHOD FOR ACCURATE TIDAL COMPUTATIONS

P. Wilders, T. L. vanStijn, G. S. Stelling, and G. A. Fokkema 1987 41 p Prepared in cooperation with Rijkswaterstaat, The Hague, Netherlands and Philips International B.V., Eindhoven, Netherlands
(PB88-183637; Rept-87-75) Copyright Avail: Issuing Activity CSCL 08C

Often industrial codes for the numerical integration of the 2-D shallow water equations are based on an Alternating Method Implicit method. However, for large time steps these codes suffer from inaccuracies when dealing with a complex geometry or bathymetry. This reduces the performance considerably. In the paper, a new method is presented in which these inaccuracies are absent, even for large time steps. The method is a fully implicit time-integration method. In order to obtain linear systems that can be solved efficiently, the authors introduce a time-splitting method. The resulting linear system are solved iteratively by using the preconditioned Conjugate Gradients Squared method. GRA

N88-26782# Alaska Univ., Fairbanks. Geophysical Inst.
ARCTIC ICE ISLAND AND SEA ICE MOVEMENTS AND MECHANICAL PROPERTIES Quarterly Report No. 14, 1 Jan. - 31 Mar. 1987
W. M. Sackinger and M. O. Jeffries 1987 31 p
(Contract DE-AC21-83MC-20037)
(DE88-004267; DOE/MC-20037/T1) Avail: NTIS HC A03/MF A01

The research program on ice islands has four elements: (1) through the use of satellite imagery, historical records, and aerial photography, to establish a time history of all of the Arctic ice shelves, and thus an historically verified source for ice islands; (2) to establish postioning buoys on the known existing ice islands to track their trajectories daily and to telemeter daily barometer pressure and temperature, via System Argos; (3) to calculate geostrophic winds from global pressure maps and barometric pressure data from the buoys, and relate the observed ice island trajectories to the winds and the internal pack ice forces; (4) to construct a model for ice island motion which will enable a determination of the probability of interaction between ice islands and offshore structures, and which will be verified by comparsion with the experimentally observed trajectory data. Research activities covered in the fourteenth quarter include; ice islands (buoy operation and ice island motion); and mechanical properties of sea spray ice bonds to structures. DOE

N88-26783# Woods Hole Oceanographic Institution, Mass.
PREDICTION OF CONTINENTAL SHELF SEDIMENT TRANSPORT USING A THEORETICAL MODEL OF THE WAVE-CURRENT BOUNDARY LAYER Ph.D. Thesis
Margaret R. Goud Aug. 1987 214 p
(Contract N00014-86-K-0061; Grant NSF OCE-84-03249)
(AD-A192272; WHOI-88-4) Avail: NTIS HC A10/MF A01 CSCL 08H

This thesis presents an application of the Grant-Madsen-Glenn bottom boundary layer model (Grant and Madsen, 1979; Glenn and Grant, 1987) to predictions of sediment transport on the continental shelf. The analysis is a two-stage process. Via numerical experiment, we explore the sensitivity of sediment transport to variations in model parameters and assumptions. A notable result is the enhancement of suspended sediment stratification due to wave boundary layer effects. When sediment stratification is neglected under conditions of suspended sediment stratification due to wave boundary layer effects. When sediment stratification is neglected under conditions of suspended sediment stratification due to wave boundary layer effects. When sediment stratification is neglected under conditions of large wave bottom velocities concentration predictions can be more than an order of magnitude higher than any observed during storm conditions on the continental shelf. A number limitations to application emerged from the analysis. Solutions to the stratified model are not uniquely determined under a number of cases of interest, potentially leading to gross inaccuracies in the prediction of sediment load and transport. Load and sediment transport in the outer Ekman Layer, beyond the region of emphasis for the model, can be as large or larger than the near-bottom estimates in some cases; such results suggest directions for improvement in the theoretical model. GRA

N88-26784# Woods Hole Oceanographic Institution, Mass.
STABILITY OF A COASTAL UPWELLING FRONT OVER TOPOGRAPHY Ph.D. Thesis
John A. Barth Oct. 1987 190 p
(Contract N00014-84-C-0134; Grant NSF OCE-84-08563)
(AD-A192354; WHOI-87-48) Avail: NTIS HC A09/MF A01 CSCL 08C

A two-layer shallow water equation model is used to investigate the linear stability of a coastal upwelling front. The model features a surface front near a coastal boundary and bottom topography which is an arbitrary function of the cross-shelf coordinate. By combining the various conversation statements for the global properties of the system, a general stability theorem is established which allows the a priori determination of the stability of a coast upwelling front. Unstable waves are found for the modelled coastal upwelling front. The unstable wave motions are frontally-trapped and dominant in the upper layer. The wave propagates phase in the direction of the basic state flow and the primary energy conversion is via baroclinic instability. The effect of varying the model parameters is presented. Moving the front closer than Rossby Radii to the coastal boundary results in a decrease in the growth rate of the fastest growing wave. Increasing the overall vertical shear of the basic state flow, by either decreasing the lower layer depth or increasing the steepness of the interface, results in an increase in the growth of the fastest growing wave. A bottom sloping in the same sense as the interface results in a decrease of the growth rates and along front wavenumbers of the unstable waves in the system. Linearized bottom friction is included in the stability model and results in a decrease in the growth rates of the unstable waves by extracting energy from the system. GRA

51 LIFE SCIENCES (GENERAL)

N88-26785# Joint Publications Research Service, Arlington, Va.
JPRS REPORT: SCIENCE AND TECHNOLOGY. USSR: LIFE SCIENCES
10 Jun. 1988 32 p Transl. into ENGLISH from various Russian articles
(JPRS-ULS-88-009) Avail: NTIS HC A03/MF A01

Translated abstracts and articles from various USSR books and journals are presented under the general heading of Life Sciences. Various subheadings are: Aerospace Medicine; Agricultural Science; Biochemistry; Biophysics; Immunology; Laser Bioeffects; Molecular Biology; Pharmacology, Toxicology; Physiology; and Public Health. Abstracts from Aerospace Medicine and Physiology are of particular interest to NASA. For individual titles, see N88-26786 through N88-26790.

N88-26786# Joint Publications Research Service, Arlington, Va.
EFFECT OF WEIGHTLESSNESS ON BRAIN DEVELOPMENT (RESULTS OF FLIGHT OF PREGNANT RATS ON KOSMOS-1514 BIOSATELLITE AND STUDY OF SUBSEQUENT DEVELOPMENT OF THEIR PROGENY ON EARTH Abstract Only
S. N. Olenev, A. R. Danilov, T. A. Kryuchkova, L. M. Sorokina, and I. B. Krasnov *In its* JPRS Report: Science and Technology. USSR: Life Sciences 10 Jun. 1988 p 1 Transl. into ENGLISH from Arkhiv Anatomii, Gistologii i Embriologii (Leningrad, USSR), v. 93, no. 9, Sep. 1987 p 20-27 (For primary document see N88-26785 20-51)
Avail: NTIS HC A03/MF A01

Materials obtained from the biosatellite Kosmos-1514 were used to determine whether or not weightlessness causes changes in brain development in rats and, if so, what processes are responsible and what are the consequences of these changes during further

development on earth. The rats were under conditions of weightlessness on the 13th day of pregnancy and were in flight for 6 days. Some fetal material was taken immediately after landing and some was taken on the 15th, 30th and 90th day of development, and this material was compared to fetal material of rats kept on earth. Morphological processes such as reproduction, migration, neuronal differentiation, growth of processes, establishment of nervous connection and vascularization developed rather completely during weightlessness and brief acceleration upon landing. The rat experiencing weightlessness showed a change in development of the cerebral capillaries; there were more of them and they were thinner. Changes in migration rate of cells were evident from study of the cortical plate formation. Macroscopic examination of fixed brain pieces showed no appreciable differences between the experimental rats and control rats.

Author

N88-26787# Joint Publications Research Service, Arlington, Va.
SIGNIFICANCE OF SENSORY SIGNAL PHASE MISMATCH IN MECHANISMS OF MOTION SICKNESS DEVELOPMENT Abstract Only **c52**
O. A. Vorobyev *In its* JPRS Report: Science and Technology. USSR: Life Sciences 10 Jun. 1988 p 1 Transl. into ENGLISH from Izvestiya Akademii Nauk SSSR, Seriya Biologicheskaya (Moscow, USSR), no. 5, Sep. - Oct. 1987 p 753-761 (For primary document see N88-26785 20-51)
Avail: NTIS HC A03/MF A01

A study of features of combined stimulation of vestibular and extrapyrimidal structures under complex dynamic conditions, which produces motion sickness, with use of materials from the author's research and from the literature, is described and discussed. The study included electronystagmographic study of 6 males during performance of 3 versions of a test of the continuous effect of Coriolis accelerations. The study of the effect on man of angular, linear and Coriolis acceleration and opticokinetic stimuli confirmed that the susceptibility to motion sickness under complex dynamic conditions is determined predominantly by the degree of phase mismatch of sensory signals of different analyzer systems. Types of motion sickness were examined from these positions. It was found that motion sickness results from volumetric excitation in the central nervous system, spreading to the higher autonomic centers, which may occur according to the holographic principle of conversion of sensory signals with phase heterogeneity. This suggests that phase mismatch of sensory signals play a major part in development of motion sickness.

Author

N88-26788# Joint Publications Research Service, Arlington, Va.
BIORHYTHMS OF BINOCULAR VISION Abstract Only **c52**
T. P. Teterina, V. V. Volkov, and L. P. Kochetkova *In its* JPRS Report: Science and Technology. USSR: Life Sciences 10 Jun. 1988 p 15 Transl. into ENGLISH from Fiziologiya Cheloveka (Moscow, USSR), v. 13, no. 5, Sep. - Oct. 1987 p 779-782 Original language document was announced in IAA as A88-18033 (For primary document see N88-26785 20-51)
Avail: NTIS HC A03/MF A01

The biorhythms of monocular perception in the processes of binocular fixation were investigated together with the effects of the subjects' age and physical load on the rhythms. It was found that, during binocular fixation of an immobile object in free space, there takes place a rhythmic synchronous alternation of the monocular perceptions by each of the two eyes. Average rhythm frequency in subjects with normal binocular vision was found to be 10.9 + or - 0.3/min, with a period duration of about 4.78/sec and a monocular phase duration of between a fraction of a second and 1 to 3 seconds. Monocular rhythm frequency varied during the 24 hr period, being lowest in the morning and highest around 6 PM. The rhythm frequency was found to be also affected by the age of an individual, being higher in young adults than in children aged 10 to 14 years, and by exercise, which increased the rhythm frequency.

E.R.

N88-26789# Joint Publications Research Service, Arlington, Va.
METHOD FOR OBSERVING CHANGES IN FUNCTIONAL STATE OF HUMAN OPERATOR Abstract Only **c52**
B. M. Vladimirskiy and L. A. Vlaskina *In its* JPRS Report: Science and Technology. USSR: Life Sciences 10 Jun. 1988 p 16 Transl. into ENGLISH from Fiziologiya Cheloveka (Moscow, USSR), v. 13, no. 5, Sep. - Oct. 1987 p 863-865 (For primary document see N88-26785 20-51)
Avail: NTIS HC A03/MF A01

A method of diagnosing the functional state of a human operator was developed and checked experimentally. Correlation coefficients of instantaneous values of EEG amplitude, recorded in three symmetric zones of the cerebral cortex, served as starting material. Correlation coefficients (4 to 6 out of 15 possible) which differed the most in their mean values during transition from one functional state to another were used. Construction of a correlation coefficient matrix for correlation coefficient values selected at the preceding stage and subsequent analysis of the main components revealed change of functional state with great accuracy. Indicators of time-space organization of EEG activity revealed in the diagnosis were individually stable and can be used to construct psychophysiologic portraits of specific operators. Tracking the functional state of a human operator during fatigue development was used to check the effectiveness of the method.

Author

N88-26790# Joint Publications Research Service, Arlington, Va.
RESPIRATION AND OXYGEN TENSION IN THE BLOOD OF ANIMALS EXPOSED TO HIGH PRESSURES Abstract Only
F. P. Tulbayeva *In its* JPRS Report: Science and Technology. USSR: Life Sciences 10 Jun. 1988 p 16-17 Transl. into ENGLISH from Izvestiya Akademii Nauk Kazakhskoy SSR, Seriya Biologicheskaya (Alma-Ata, USSR), no. 4, Jul. - Aug. 1987 p 74-77 (For primary document see N88-26785 20-51)
Avail: NTIS HC A03/MF A01

A study is presented of the dynamics of the respiratory function and oxygen tension in arterial and venous blood in animals during time spent in a nitrogen-oxygen mixture under high pressure. The experiments were performed on 12 male rabbits exposed for two hrs to a normoxic nitrogen-oxygen mixture under a pressure of 40 kgf/sq cm. Respiration frequency and volume per minute decreased sharply during the course of 2 hrs exposure to high pressure. Oxygen tension in both arterial and venous blood gradually decreased over the same time. Survival time of the animals varied, but all died from asphyxia during the course of the experiment. It is suggested that the high density of the gas being breathed increased respiration resistance, causing a decrease in pulmonary ventilation and resultant oxygen deficiency.

Author

N88-26791# Gas Research Inst., Chicago, Ill. Chemical Technology Div.
PHOTOSYNTHETIC WATER SPLITTING Annual Report, 1987
E. Greenbaum Jan. 1988 36 p
(Contracts DE-AC05-84OR-21400; GRI-5883-260-0880)
(DE88-007809; ORNL/TM-10704; GRI-88/0044) Avail: NTIS HC A03/MF A01

This document is an annual report of photosynthetic water splitting for the production of hydrogen and oxygen. Unicellular green algae are capable of evolving molecular hydrogen in the presence of carbon dioxide. Controlling factors that determine hydrogen evolution are either temperature or light intensity. Also, mutants of the green alga Chlamydomonas are capable of evolving hydrogen in the presence of carbon dioxide. The significance of these discoveries is that the presence of carbon dioxide (or bicarbonate) is a key factor in determining the activity of the Photosystem 2 water splitting complex. Second, a new advance in oxygen sensor technology has been made that, for the first time, allows the absolute measurement of photosynthetically evolved oxygen from a single colony of microalgae growing on a solidified agar medium. The key aspect of this electrochemical sensor is the utilization of ultra-pure potassium hydroxide as the electrolyte and a recognition of the role that electrolyte impurities play in contributing to base line noise.

DOE

N88-26792# Pacific Northwest Labs., Richland, Wash.
INTERACTION OF BIOLOGICAL SYSTEMS WITH STATIC AND ELF ELECTRIC AND MAGNETIC FIELDS
L. E. Anderson, ed., B. J. Kelman, ed., and R. J. Weigel, ed. 1987 540 p Presented at the 23rd Hanford Life Sciences Symposium, Richland, Wash., 2 Oct. 1984
(Contract DE-AC06-76RL-01830)
(DE88-007951; CONF-841041) Avail: NTIS HC A23/MF A01

Although background levels of atmospheric electric and geomagnetic field levels are extremely low, over the past several decades, human beings and other life forms on this planet have been subjected to a dramatically changing electromagnetic milieu. An exponential increase in exposure to electromagnetic fields has occurred, largely because of such technological advances as the growth of electrical power generation and transmission systems, the increased use of wireless communications, and the use of radar. In addition, electromagnetic field generating devices have proliferated in industrial plants, office buildings, homes, public transportation systems, and elsewhere. Although significant increases have occurred in electromagnetic field strenghths spanning all frequency ranges, this symposium addresses only the impact of these fields at static and extremely low frequencies (ELF), primarily 50 and 60 Hz. This volume contains the proceedings of the symposium entitled Interaction of biological systems with static and ELF electric and magnetic fields . The purpose of the symposium was to provide a forum for discussions of all aspects of research on the interaction of static and ELF electromagnetic fields with biological systems. These systems include simple biophysical models, cell and organ preparations, whole animals, and man. Dosimetry, exposure system design, and artifacts in ELF bioeffects research were also addressed, along with current investigations that examine fundamental mechanisms of interactions between the fields and biological processes. Papers are indexed separately. DOE

N88-26793# Argonne National Lab., Ill.
MODELING THE PRIMARY EVENTS OF PHOTOSYNTHESIS USING CHLOROPHYLL CONTAINING FIXED DISTANCE DONOR-ACCEPTOR MOLECULES
M. R. Wasielewski, D. G. Johnson, and W. A. Svec 1988 4 p Presented at the US-Japan Information Exchange Seminar, Kyoto, Japan, 8 Jan. 1988
(Contract W-31-109-eng-38)
(DE88-010033; CONF-880181-1) Avail: NTIS HC A02/MF A01

Two specific questions that we addressed are: how does the dimeric primary electron donor in photosynthetic proteins initiate charge separation, and how do electron transfer reactions from chlorophylls to quinones depend on free energy of reaction and the surrounding medium. DOE

N88-26794# Yale Univ., New Haven, Conn. Dept. of Ophthalmology and Visual Science.
REGULATORY BIOCHEMICAL AND METABOLIC RESPONSES IN PHOTORECEPTORS Final Report, 1 Jul. 1984 - 30 Sep. 1987
Peter J. Stein Nov. 1987 41 p
(Grant AF AFOSR-0171-84)
(AD-A192898; AFOSR-88-0567TR) Avail: NTIS HC A03/MF A01 CSCL 06A

Studies of near infrared light scattering changes in disk membrane suspensions reveal three novel phenomena. The light induced scattering changes observed in the presence of Guanosine triphosphate and Cyclic guanosine monophosphate were produced by aggregation/disaggregation of the membrane vesicles. This aggregation/disaggregation process was correlated with activation of phosphodiesterase and a change in its apparent solubility. That is, PDE became more tightly bound to the membrane when it was activated. We have begun preliminary studies of near infrared scattering signals in the isolated retina. In this preliminary work, we have observed that IBMX, an inhibitor of phosphodiesterase activity, profoundly affects the infrared light scattering signal in the isolated retina. It seems likely that the in vitro and in vivo signals may share a common origin. In a separate series of experiments, we have purified opsin, the apoprotein of the visual pigment protein, and reconstituted it into phospholipid vesicles. We used patch clamp recording to demonstrate that the purified, reconstituted protein exhibits cGMP-activated single channel activity. These results suggest that opsin, in addition to performing its function as the receptor molecule, may be the light-sensitive pore in the plasma membrane of the rod outer segment. GRA

N88-26795*# National Aeronautics and Space Administration. John F. Kennedy Space Center, Cocoa Beach, Fla.
VEGETATION STUDIES ON VANDENBERG AIR FORCE BASE, CALIFORNIA
Paul A. Schmalzer, Diana E. Hickson, and C. Ross Hinkle (Bionetics Corp., Cocoa Beach, Fla.) Mar. 1988 484 p
(Contract NAS10-10285)
(NASA-TM-100985; NAS 1.15:100985) Avail: NTIS HC A21/MF A01 CSCL 06B

Vandenburg Air Force Base, located in coastal central California with an area of 98,400 ac, contains resources of considerable biological significance. Available information on the vegetation and flora of Vandenburg is summarized and new data collected in this project are presented. A bibliography of 621 references dealing with vegetation and related topics related to Vanderburg was compiled from computer and manual literature searches and a review of past studies of the base. A preliminary floristic list of 642 taxa representing 311 genera and 80 families was compiled from past studies and plants identified in the vegetation sampling conducted in this project. Fifty-two special interest plant species are known to occur or were suggested to occur. Vegetation was sampled using permanent plots and transects in all major plant communities including chaparral, Bishop pine forest, tanbark oak forest, annual grassland, oak woodland, coastal sage scrub, purple sage scrub, coastal dune scrub, coastal dunes, box elder riparian woodland, will riparian woodland, freshwater marsh, salt marsh, and seasonal wetlands. Comparison of the new vegetation data to the compostie San Diego State University data does not indicate major changes in most communities since the original study. Recommendations are made for additional studies needed to maintain and extend the environmental data base and for management actions to improve resource protection. Author

52 AEROSPACE MEDICINE

Includes physiological factors; biological effects of radiation; and effects of weightlessness on man and animals.

N88-26796# Helsinki Univ. of Technology, Espoo (Finland). Low Temperature Lab.
AUDITORY EVOKED MAGNETIC FIELDS IN MAN
J. Maekelae 1988 68 p
(PB88-193446; ISBN-951-754-430-8) Avail: NTIS HC A04/MF A01 CSCL 06S

In understanding responses to complex stimuli, required to illuminate properties unique to human Central Nervous System, it is useful to understand responses to simpler forms of the stimuli. Noise bursts, frequency and amplitude modulations, and constant frequency quasiperiodic sounds are acoustic constituents of speech. Magnetic responses to such stimuli are described. In order to analyze the neural sources of auditory evoked responses and to clarify the functional properties of the human supratemporal auditory cortex, auditory evoked magnetic fields to different stimuli were studied in healthy humans and in one deaf patient with a cochlear implant. Author

N88-26797# Brookhaven National Lab., Upton, N. Y.
ACUTE RADIATION SYNDRONES AND THEIR MANAGEMENT
E. P. Cronkite 1988 36 p Presented at the International Conference on Biological Effects of Large Doses of Ionizing and Non-ionizing Radiation, Hangzhou, People's Republic of China, 26 Mar. 1988
(Contract DE-AC02-76CH-00016)

(DE88-009839; BNL-41186; CONF-880394-2) Avail: NTIS HC A03/MF A01

Radiation syndromes produced by large doses of ionizing radiation are divided into three general groups depending on dose of radiation and time after exposure. The CNS syndrome requires many thousands of rad, appears in minutes to hours, and kills within hours to days. The GIS appears after doses of a few hundred to 2000 rad. It is characterized by nausea, vomiting, diarrhea, and disturbances of water and electrolyte metabolism. It has a high mortality in the first week after exposure. Survivors will then experience the HS as a result of marrow aplasia. Depending on dose, survival is possible with antibiotic and transfusion therapy. The relationship of granulocyte depression to mortality in dogs and human beings is illustrated. The role of depth dose pattern of mortality of radiation exposure is described and used as an indication of why air exposure doses may be misleading. The therapy of radiation injury is described based on antibiotics, transfusion therapy, and use of molecular regulators. The limited role of matched allogenic bone marrow transplants is discussed. DOE

N88-26798# State Univ. of New York at Buffalo, Amherst.
THE INTERACTION OF SENSORY AND PERCEPTUAL VARIABLES: SPATIAL, TEMPORAL AND ORIENTATION RESPONSE TO FIGURE AND GROUND Final Report, 1 Jun. 1984 - 31 Aug. 1987
Naomi Weisstein 25 Feb. 1988 34 p
(Grant AF AFOSR-0115-84)
(AD-A192897; AFOSR-88-0282TR) Avail: NTIS HC A03/MF A01 CSCL 05H

Numerous experimental observations support the principal investigator's conjecture that human visual segmentation of figure and ground is partly determined by properties of the visual scene. Support derives from observations that: figure and ground occupy different perceptual depth planes; perceived differences of depth are necessary for figure-ground segmentation; patches of an image are assigned to depth planes partly on the basis of their relative spatial frequency content, temporal frequency content (distinguished from perceived velocity), and retinal disparity. Details of these and other experiments are included with discussion and references. GRA

N88-26799# Technische Univ., Munich (West Germany). Flugmedizinischen Inst. Fuerstenfeldbruck.
DOES DIHYDROERGOTAMINE USED IN THERAPEUTICAL DOSES INFLUENCE THE PHYSICAL AND PSYCHOMOTOR PERFORMANCE OF YOUNG PILOTS OR OTHER TRAFFIC DRIVERS SUBJECTED TO HYPOTONIA? Ph.D. Thesis [BEEINFLUSST DIHYDROERGOTAMIN IN THERAPEUTISCH GEBRAEUCHLICHEN DOSEN DIE PHYSISCHE UND PSYCHOMOTORISCHE LEISTUNGSFAEHIGKEIT ZUR HYPOTONIE NEIGENDER JUGENDLICHER PILOTEN ODER SONSTIGER VERKEHRSTEILNEHMER?]
Kurt Poemp 1986 63 p In GERMAN
(ETN-88-92136) Avail: NTIS HC A04/MF A01

Dihydroergotamine retard is studied on human physical and psychomotor performance in clinical tests relative to its action on orthostatic symptoms. Results on 23 young pilots with orthostatic misregulation indicates that this medicine improves physical performance without negative effects on psychomotricity. This medicine is well adapted to pilots and drivers. ESA

N88-26800* NASA Scientific and Technical Information Facility, Baltimore-Washington International Airport, Md. 21240.
AEROSPACE MEDICINE AND BIOLOGY: A CONTINUING BIBLIOGRAPHY WITH INDEXES (SUPPLEMENT 313)
Aug. 1988 73 p
(NASA-SP-7011(313); NAS 1.21:7011(313)) Avail: NTIS HC A05 CSCL 06E

This bibliography lists 227 reports, articles, and other documents introduced into the NASA scientific and technical information system in July, 1988. Author

N88-26787# Joint Publications Research Service, Arlington, Va.
SIGNIFICANCE OF SENSORY SIGNAL PHASE MISMATCH IN MECHANISMS OF MOTION SICKNESS DEVELOPMENT Abstract Only
O. A. Vorobyev *In its* JPRS Report: Science and Technology. USSR: Life Sciences 10 Jun. 1988 p 1 Transl. into ENGLISH from Izvestiya Akademii Nauk SSSR, Seriya Biologicheskaya (Moscow, USSR), no. 5, Sep. - Oct. 1987 p 753-761 (For primary document see N88-26785 20-51)
Avail: NTIS HC A03/MF A01

N88-26788# Joint Publications Research Service, Arlington, Va.
BIORHYTHMS OF BINOCULAR VISION Abstract Only
T. P. Teterina, V. V. Volkov, and L. P. Kochetkova *In its* JPRS Report: Science and Technology. USSR: Life Sciences 10 Jun. 1988 p 15 Transl. into ENGLISH from Fiziologiya Cheloveka (Moscow, USSR), v. 13, no. 5, Sep. - Oct. 1987 p 779-782 Original language document was announced in IAA as A88-18033 (For primary document see N88-26785 20-51)
Avail: NTIS HC A03/MF A01

N88-26789# Joint Publications Research Service, Arlington, Va.
METHOD FOR OBSERVING CHANGES IN FUNCTIONAL STATE OF HUMAN OPERATOR Abstract Only
B. M. Vladimirskiy and L. A. Vlaskina *In its* JPRS Report: Science and Technology. USSR: Life Sciences 10 Jun. 1988 p 16 Transl. into ENGLISH from Fiziologiya Cheloveka (Moscow, USSR), v. 13, no. 5, Sep. - Oct. 1987 p 863-865 (For primary document see N88-26785 20-51)
Avail: NTIS HC A03/MF A01

53 BEHAVIORAL SCIENCES

Includes psychological factors; individual and group behavior; crew training and evaluation; and psychiatric research.

N88-26801# Pittsburgh Univ., Pa. Learning Research and Development Center.
INFERENCE AND DISCOVERY IN AN EXPLORATORY LABORATORY Technical Report, 1984 - 1987
Valerie Shute, Robert Glaser, and Kalyani Raghavan Feb. 1988 89 p
(Contract N00014-84-K-0542; RR0-4206)
(AD-A192231; UPITT/LRDC/ONR/KBC-10) Avail: NTIS HC A05/MF A01 CSCL 05H

This paper describes the results of a study done as part of a research program investigating the use of computer-based laboratories to support self-paced discovery learning in domains like microeconomics, electricity, and light refraction. Program objectives include maximizing the laboratories' effectiveness in helping students learn content knowledge, as well as identifying and coaching effective inference and discovery behaviors. This study with the microeconomics discovery laboratory demonstrates that computer-based laboratories can help students learn targeted concepts. In addition, the study identifies the inductive reasoning strategies used in the microeconomics discovery world by first-year university students, and compares the strategies of more and less successful learners. GRA

N88-26802# Bolt, Beranek, and Newman, Inc., Cambridge, Mass.
PLANS FOR DISCOURSE
Barbara J. Grosz and Candace L. Sidner 1 Feb. 1988 35 p
(Contract N00014-85-C-0079)
(AD-A192242; BBN-6728) Avail: NTIS HC A03/MF A01 CSCL 05H

Discourses are fundamentally instances of collaboration behavior. We propose a model of the collaborative plans of agents achieving joint goals and illustrate the role of these plans in discourses. Three types of collaborative plans, called Shared Plans, are formulated for joint goals requiring simultaneous, conjoined or

sequential actions on the part of the agents who participate in the plans and the discourse; a fourth type of Shared Plan is presented for the circumstance where two agents communicate, but only one acts. GRA

N88-26803# South Carolina Univ., Columbia. Dept. of Psychology.
WORKING MEMORY CAPACITY: AN INDIVIDUAL DIFFERENCES APPROACH Annual Technical Report, 1 Jan. 1987 - 1 Jan. 1988
Randall W. Engle 11 Feb. 1988 65 p
(Grant AF AFOSR-0069-87)
(AD-A192359; AFOSR-88-0265TR) Avail: NTIS HC A04/MF A01 CSCL 05H

Five experiments are described that study the relationship between measures of working memory and reading comprehension. Two experiments investigated whether the complex span measure must be similar to the reading comprehension task to be predictive of comprehension. The correlation found between reading comprehension and two reading-related complex spans was similar to those found between two arithmetic-related complex spans and comprehension. The relationship remained significant when quantitative skills were factored out. The simple digit and word spans (measured without a background task) did NOT correlate with reading comprehension. The complex span/comprehension correlations were a function of the difficulty of the background task. When the difficulty level of the reading-related or arithmetic-related background tasks was moderate, the span/comprehension correlations were higher in magnitude than when the background tasks were simple or very difficult. The third experiment showed that if serial recall was required in the span tasks, simple word span did significantly predict reading comprehension but not as well as the sentence span. The fourth experiment showed that the ordering of list lengths in the span tasks had little influence on the correlation between span scores and comprehension. The fifth experiment is the first in a series investigating variables whether variables that influence simple word span also influence the sentence word span. GRA

N88-26804# Air Command and Staff Coll., Maxwell AFB, Ala.
USAF FLYING SCREENING: FIRST STEP ON THE ROAD TO WINGS
Stefan Eisen, Jr. Apr. 1988 49 p
(AD-A192613; ACSC-88-0850) Avail: NTIS HC A03/MF A01 CSCL 05I

The current high attrition rate in USAF pilot training is partly due to high potential eliminees entering the training system. This study examines the flight screening programs of West Germany, Great Britain, Canada, Israel, and the US Navy, and makes observations on significant features in each of the programs. Recommendations are made based on lifting the best features from each program and integrating them into the current USAF flying screening program. By improving the screening process, fewer high potential eliminees will enter the USAF pilot training system, leading to a lower attrition rate. GRA

N88-26805# Carnegie-Mellon Univ., Pittsburgh, Pa. Dept. of Psychology.
THE ROLE OF WORKING MEMORY IN LANGUAGE COMPREHENSION
Patricia A. Carpenter and Marcel A. Just Feb. 1988 33 p
(Contract N00014-85-K-0584; RR0-4206)
(AD-A192721; ONR-88-1) Avail: NTIS HC A03/MF A01 CSCL 05H

This chapter provides an account of the transient computational and storage demands that typically arise during comprehension, and of the information management policies that attempt to satisfy those demands. The chapter describes a number of recent studies that examine the trading relation between between computation and storage in working memory during language comprehension. Comprehension processes tend to minimize storage requirements by minimizing the number of partial products that have to be stored. The minimization is accomplished by immediately digesting as much of the information from the text as possible (what we have called the immediacy of processing), rather than using a wait-and-see strategy. A second focus is on the differences among individuals in their ability to maintain information in working memory during comprehension. Such individual differences in working memory capacity are closely related to large and stable individual differences in reading comprehension ability. GRA

N88-26806# Centre d'Etudes et de Recherches de Medecine Aerospatiale, Paris (France). Div. de Psychophysiologie de la Perception Visuelle.
PRELIMINARY STUDY WITHIN A PROJECT FOR THE DEVELOPMENT OF INTELLIGENT ASSISTANCE TO PILOTING: FORMAL DESCRIPTION OF COMBAT PILOT EXPERTISE AND IMPLEMENTATION OF AN INTERACTIVE SYSTEM TO REPRESENT OPERATIONS [ETUDE PRELIMINAIRE DANS LE CADRE DU DEVELOPPEMENT D'AIDES INTELLIGENTES AU PILOTAGE: FORMALISATION DE L'EXPERTISE D'UN PILOTE DE COMBAT ET MAQUETTAGE D'UN SYSTEME INTERACTIF DE REPRESENTATIONS OPERATIONNELLES]
R. Amalberti, C. Valot, and J.-P. Menu Dec. 1987 143 p In FRENCH
(Contract DRET-86-1021)
(CERMA-87-31; ETN-88-92543) Avail: NTIS HC A07/MF A01

In order to explore the mental functions of combat pilots a psychological analysis was performed including a thorough questioning leading to the implementation of general laws describing the organization of knowledge and behavior in real combat situations. The implementation of a computer aid system for the flight phase confirms that a simplified display has a negative effect since it affects the pilot's trust in system capacities. ESA

54 MAN/SYSTEM TECHNOLOGY AND LIFE SUPPORT

Includes human engineering; biotechnology; and space suits and protective clothing.

For related information see also *16 Space Transportation.*

N88-26807*# Life Systems, Inc., Cleveland, Ohio.
ADVANCED LIFE SUPPORT CONTROL/MONITOR INSTRUMENTATION CONCEPTS FOR FLIGHT APPLICATION Final Report, Nov. 1983 - Jun. 1985
D. B. Heppner, M. J. Dahlhausen, and R. B. Fell Mar. 1986 73 p
(Contract NAS2-11758)
(NASA-CR-177378; NAS 1.26:177378; LSI-TR-596-28) Avail: NTIS HC A04/MF A01 CSCL 05H

Development of regenerative Environmental Control/Life Support Systems requires instrumentation characteristics which evolve with successive development phases. As the development phase moves toward flight hardware, the system availability becomes an important design aspect which requires high reliability and maintainability. This program was directed toward instrumentation designs which incorporate features compatible with anticipated flight requirements. The first task consisted of the design, fabrication and test of a Performance Diagnostic Unit. In interfacing with a subsystem's instrumentation, the Performance Diagnostic Unit is capable of determining faulty operation and components within a subsystem, perform on-line diagnostics of what maintenance is needed and accept historical status on subsystem performance as such information is retained in the memory of a subsystem's computerized controller. The second focus was development and demonstration of analog signal conditioning concepts which reduce the weight, power, volume, cost and maintenance and improve the reliability of this key assembly of advanced life support instrumentation. The approach was to develop a generic set of signal conditioning elements or cards which can be configured to fit various subsystems. Four generic sensor signal conditioning cards were identified as being

required to handle more than 90 percent of the sensors encountered in life support systems. Under company funding, these were detail designed, built and successfully tested. Author

N88-26808# Midwest Systems Research, Inc., Dayton, Ohio.
A COCKPIT NATURAL LANGUAGE STUDY - SELECTED TRANSCRIPTS Final Report, Oct. 1986 - Dec. 1987
Ronald L. Small, Dan E. Flory, Michael P. Munger, David T. Williamson, and Bryon T. Hollis Apr. 1988 310 p
(Contract F33615-85-C-3623)
(AD-A192972; AFWAL-TR-88-3009) Avail: NTIS HC A14/MF A01 CSCL 01C

This third report on the Cockpit Natural Language (CNL) study contains a brief description of the purpose and methodology of the CNL study, a section on lessons learned, scenario situation descriptions, a glossary and transcripts from 9 of the 54 pilots interviewed. Pilot comments cover the issues and implementation details of automation, displays, voice interaction and artificially-intelligent computer aids. Lessons learned from the CNL study include (1) Voice interaction is best employed as a new channel of information transfer, not just as a backup mode for manual or visual channels. (2) Pilot-cockpit voice interaction requires a shared information context between the pilot and the cockpit's computer in order to ensure that pilot commands are properly understood and executed. (3) Role-playing works (even with a low-fidelity cockpit simulation) when extracting valuable information from a pilot community. And (4), voice-activated computer messages should not replace pilot-to-pilot communications (radio calls, hand signals, etc.). GRA

N88-26809# Crew Systems Consultants, Yellow Springs, Ohio.
IMPROVEMENT OF HEAD-UP DISPLAY STANDARDS. VOLUME 1: HEAD-UP DISPLAY DESIGN GUIDE, APPENDIX Final Report, 10 Oct. 1984 - 15 Jun. 1987
Richard L. Newman Sep. 1987 139 p
(Contract F33615-85-C-3602)
(AD-A192973; TR-87-15-Vol-1; AFWAL-TR-87-3055-Vol-1) Avail: NTIS HC A07/MF A01 CSCL 01D

A design guide for Head-Up Displays (HUDs) has been prepared to assist the HUD engineer by providing in one source a list of design criteria for HUDs. The criteria are based on a review of existing HUD specifications and HUD research. GRA

N88-26810# Katholieke Universiteit, Nijmegen (Netherlands). Psychologisch Lab.
DIRECT MANIPULATION AND THE DESIGN OF USER INTERFACES
P. Desain Dec. 1986 41 p
(PB88-126354; Rept-87-FU-01) Avail: NTIS HC E03/MF E01; copy not available from STI Facility CSCL 05H

An approach to user interfaces is described from a cognitive engineering point of view. A model of task representations within the user is given, together with complexity measures of the transitions between the representations. Two main approaches to user interface design are compared: the conversational method and the model world method. Some of their strong and weak points are explained, in connection with their most sophisticated examples; natural languages and direct manipulation, it turns out that in many respects they are complementary to each other. GRA

55 SPACE BIOLOGY

Includes exobiology; planetary biology; and extraterrestrial life.

No abstracts in this category.

59 MATHEMATICAL AND COMPUTER SCIENCES (GENERAL)

No abstracts in this category.

60 COMPUTER OPERATIONS AND HARDWARE

Includes hardware for computer graphics, firmware, and data processing.

For components see *33 Electronics and Electrical Engineering.*

N88-26811 New South Wales Univ., Kensington (Australia). Dept. of Computer Science.
THE UMAC SIMULATOR Abstract Only. M.S. Thesis
Viriya Upatising May 1987 76 p
Avail: Issuing Activity

The UMAC is a microprogrammed computer. The UMAC architecture comprises standard bit-sliced technology. The UMAC simulator and translator were developed as a teaching tool to help in learnig more about the concept of microprogramming and hardware emulation. A microassembler language was developed for the machine along with a translator compiling program which converts it into microcode, and a bit-by-bit simulator. The simulator and translator were written in the standard C programming language, and currently can be run on an IBM PC and on any computer with the UNIX operating system. The architecture of the UMAC computer is investigated and the usage and syntax of the translator and simulator are discussed. The implementation of the translator and simulator is also discussed. Author

N88-26812# Lawrence Livermore National Lab., Calif.
COMPUTER SCIENCE RESEARCH, 1987: COMPUTATION DIRECTORATE
J. R. McGraw, ed. and K. F. Grupe, ed. 1987 159 p
(Contract W-7405-eng-48)
(DE88-008637; UCID-20664-87) Avail: NTIS HC A08/MF A01

The topics of research presented here reflect our view of the broad range of issues we need to address in support of our computing environment. Large-scale Scientific Computations represents one of our newest ventures. The goal is to more closely link expertise in the problem domains (e.g., fluid dynamics) with expertise in sophisticated numerical methods, thus allowing for a broader range of solution strategies to get better answers. Parallel Numerical Algorithms focuses more tightly on the development and analysis of numerical techniques for use in parallel computing situations. Issues here include the solution of extremely large partial differential equations, matrix solution techniques, and Monte Carlo programming techniques. In the area of General Numerical Algorithms we recognize the need for a significant amount of research on numerics without the additional complexity of parallelism. This area includes work on partial differential equations, ordinary differential equations, interpolation, and a variety of statistical analysis. Parallel Systems Software addresses issues related to going from a parallel algorithm to its correct and efficient implementation on a particular system. Distributed Operating Systems and Networks describes our efforts to provide a very flexible environment for users to access a diverse set of machines and services in an efficient and simple manner. Expert Systems Software covers another relatively new and expanding area. We are looking at various ways that knowledge engineering ideas can reduce development time for writing new code systems and improve our control over experimental processes. In the section on General Purpose Software we include several projects that span a wide range of topics. The last section, Technology Information Systems,

reports the status of a special effort to provide sophisticated methods for allowing users to access remote information centers. DOE

N88-26813# Los Alamos National Lab., N. Mex.
THE PERFORMANCE OF THE NEC SX-2 AND CRAY X-MP SUPERCOMPUTERS
O. M. Lubeck, J. W. Moore, and R. Mendez 1987 14 p Prepared in cooperation with Naval Postgraduate School, Monterey, Calif.
(Contract W-7405-eng-36)
(DE88-009177; LA-UR-87-227) Avail: NTIS HC A03/MF A01

Since our first article on the Japanese supercomputers appeared in the December 1985 issue of Computer, we have conducted additional benchmarks of the new NEC SX-2 vector processor. We present these new results for the SX-2 and updated timings of the X-MP/48. DOE

N88-26814# Michigan State Univ., East Lansing. Dept. of Computer Science.
RELAY APPROACH MESSAGE ROUTING IN HYPERCUBE MULTIPROCESSORS
Y. Lan, L. M. Ni, and A. H. Esfahanian 1988 9 p Presented at the 3rd. International Conference on Supercomputing, Boston, Mass., 15 May 1988 Prepared in cooperation with Argonne National Lab., Ill.
(Contract W-31109-eng-38)
(DE88-009973; CONF-880567-6) Avail: NTIS HC A02/MF A01

A relay approach message routing for hypercube multiprocessors is proposed which is able to forward a received message immediately after the address fields of the message are received if the outgoing channels are not blocked. The relay message routing can significantly reduce the communication latency compared with the store-and-forward message routing. Based on the relay approach, a distributed routing mechanism which is able to handle unicast, multicast, and broadcast interprocessor communications is proposed. These three types of interprocessor communication are modeled as an Optimal Multicast Tree problem which can guarantee a minimum message delivery time. Network traffic is minimized for the cases of unicast and broadcast and close to minimum for the case of multicast. A hardware router design based on the proposed distributed relay routing is discussed. DOE

N88-26815# University Coll., London (England). Dept. of Computer Science.
RESEARCH IN COMPUTER SCIENCE 1985/6
Dec. 1986 48 p
(PB88-113840; UCL-CS-TR-125) Avail: NTIS HC E05/MF E05; copy not available from STI Facility CSCL 09B

Summaries are given of research projects in: Distributed systems; Communications and networks; Functional programming; Software engineering; Artificial intelligence; Image processing; Distributed database systems; and Geometrical architecture for multimedia information systems. Author

N88-26816# Stanford Univ., Calif. Computer Systems Lab.
RESEARCH IN VLSI COMPUTER SYSTEMS Progress Report, Apr. - Oct. 1987
John Hennessy Oct. 1987 17 p
(Contracts MDA903-83-C-0335; N00014-87-K-0828)
(AD-A192915) Avail: NTIS HC A03/MF A01 CSCL 12F

This report summarizes progress in the DARPA funded projects in the areas of multiprocessor architecture and software, and computer-aided design from April 1987 to October 1987. The major areas under investigation have included: analysis and synthesis design aids, high performance chip design, multiprocessor and VLSI computer architectures. The major research problems are introduced and progress is discussed; the Appendix contains a list of published research papers from these projects. GRA

N88-26817# Institute for Water Resources, Fort Belvoir, Va.
MANAGING MICROCOMPUTER APPLICATIONS: A PRIMER AND GUIDE TO GOOD PRACTICE
Richard M. Males and Michael R. Walsh Mar. 1988 92 p
(AD-A192992; IWR-88-R-3) Avail: NTIS HC A05/MF A01 CSCL 12F

This report has a dual purpose. First, the report is a primer for managers to help them understand the potential impacts of the microcomputer on organization and staff productivity. The most common types of microcomputer software are described and basic types of applications developed by planners are discussed. Second, the report is a guide for managers faced with managing the use of microcomputers and the development of applications by their staff and others. A process for managing the development of corporate applications is presented. The report is directed at a non-computer professional audience, i.e. managers within the Corps who have a technical background, but may not be microcomputer users themselves, and have as part of their responsibility the management of individuals and/or projects in which microcomputers are used. The report is designed primarily to raise awareness of the need for, and the methods of, management of microcomputer applications. Outline formats are often used, and key ideas are highlighted. It is hoped that this format will communicate the key concpts better than a more traditional report. GRA

N88-26818# Technische Univ., Berlin (West Germany). Fachbereich fuer Informatik.
DESIGN OF HIGH PERFORMANCE MICROCOMPUTERS FOR NUMERICAL DATA PROCESSING Ph.D. Thesis [REALISIERUNGSPRINZIPIEN VON MIKRORECHNERN HOHER NUMERISCHER LEISTUNG]
Ulrich Bruening 1987 170 p In GERMAN
(ETN-88-92371) Avail: NTIS HC A08/MF A01

Criteria and performance of computers for numerical processing applications are reviewed with emphasis on performance improvement possibilities. Parallel computer architectures and link structures for multicomputer architecture are described. To attain high speed data processing the suitable storage organizations are analyzed and their effectiveness evaluated. Pipeline processing is considered relative to its influence on other information processing components. A computer architecture design with eight parallel data type computers is proposed. On the basis of this architecture, development possibilities are outlined. ESA

N88-26819# Center for Mathematics and Computer Science, Amsterdam (Netherlands). Dept. of Computer Science/Dept. of Algorithms and Architecture.
SIMPLE MULTIREADER REGISTERS USING TIME-STAMP SCHEMES
Amos Israeli, Ming Li (Harvard Univ., Cambridge, Mass.), and Paul M. B. Vitanyi Nov. 1987 11 p Submitted for publication
(Grants NSF DCR-83-01766; NSF DCR-86-06366; N00014-85-K-0445)
(CWI-CS-R8758; B8805681; ETN-88-92591) Copyright Avail: NTIS HC A03/MF A01

The theory of time-stamp schemes is used to implement an atomic 1-writer n-reader variable (register) from n sq atomic 1-writer 1-reader variables, using bounded time-stamps. The number of time-stamps needed is (2n+2) sq, so this scheme uses O(n sq log n) control bits altogether. The construction is simple, transparent, and optimal in worst-case number of control bits per subvariable. A similar scheme that uses only 2-bit variables written by readers, and 2n-bit variables written by the writer is given. This uses altogether O(n sq) control bits altogether. This scheme is optimal in worst-case overal number of control bits. Apart from being optimal in several ways, the constructions add an intuitive dimension to algorithms for this problem. ESA

61 COMPUTER PROGRAMMING AND SOFTWARE

Includes computer programs, routines, alogorithms, and specific applications, e.g., CAD/CAM.

N88-26820# Joint Inst. for Nuclear Research, Dubna (USSR). Lab. of Computing Techniques and Automation.
AUTOMATED SYSTEM FOR MATHEMATICAL PROCESSING OF THE DATA FROM A HYBRID SPECTROMETER
A. U. Abdurakhimov, Ya. Balgasuren, N. A. Buzdavina, N. N. Govorun, V. S. Goman, V. G. Ivanov, A. T. Matyushin, L. S. Okhrimenko, and I. S. Saitov 1986 6 p In RUSSIAN; ENGLISH summary
(DE87-702995; JINR-R-10-86-612) Avail: NTIS (US Sales Only)HC 02/MF A01

An automated system for hybrid spectrometer data mathematical processing is described. The system provides for automatic processing by chains of programs and preliminary analysis of computer results. The system operation was tested in modelling the p-d events. DOE

N88-26821# Princeton Univ., N. J. Dept. of Statistics.
TUNING A MAJOR PART OF A CLUSTERING ALGORITHM
Katherine M. Hansen and John W. Tukey Feb. 1988 64 p
(Contract DAAL03-86-K-0073)
(AD-A191446; TR-294; ARO-23360.8-MA) Avail: NTIS HC A04/MF A01 CSCL 12C

Most proposals for clustering algorithms have been based on introspection. Few proposed algorithms have had their performance studied. This approach involves: (1) striving to avoid comparing distances on remote parts of the data (because metrics deserve only minimum trust), and (2) using a stochastically defined test bed to measure, and where possible understand, the performance of an evolving algorithm, with the intent of using our understanding to modify it in such a way as to improve its performance. This test bed involves 3 circular Gaussian samples, of size 50 each, centered at the vertices of an equilateral triangle of side t(sigma). Its use assumes that a 3-group answer is being sought. Thus the only concern is with a part of the clustering process. Our early algorithms begin to misbehave in the range 5 is less than or = t is less than or = 7. Our successive steps of improvement work at smaller and smaller t. The last version we have tried still performs usefully (median misclassification about 16 percent) at t = 2.7, where knowledge of three populations would only let us hold misclassification to a median of 13.3 percent. Comparison with a Gaussian maximum likelihood algorithm on the same set of triple samples shows only slightly better performance than for our algorithm. GRA

N88-26822 New South Wales Univ., Kensington (Australia). School of Electrical Engineering and Computer Science.
A MULTIPROCESS OPERATING SYSTEM FOR 16 BIT MICROCOMPUTERS OR PORTING UNIX (TRADEMARK) TO A NS32016 WITH ENHANCEMENTS M.S. Thesis Abstract Only
Lucy Chubb 1987 142 p
Avail: Issuing Activity

How the Unix operating system version 7 was ported to a microcomputer based on the NS32016 CPU and associated slave processors is described. The port had several aims: to get a working kernel running on the NS32016, to implement paged virtual memory, to change the representation of processes so that the address space of each running process corresponds to a file in a directory created for that purpose, and investigate any further developments which such changes might make possible. Preparation for the port required making sure that the appropriate hardware and software tools were available and familiarization with the source code of Unix. After deciding what modifications were required the port proceeded by designing, coding and testing the changes. The kernel is now essentially complete. Finally, a number of extensions to the operating system based on the changes made to the representation of processes and the implementation of paged virtual memory are proposed and discussed. These extensions allow a simpler implementation of text sharing and the ability for processes to map files into their virtual space. Author

N88-26823*# Illinois Univ., Urbana. Dept. of Computer Science.
CORRECTNESS CRITERIA FOR PROCESS MIGRATION
Chin Lu and J. W. S. Liu 22 Feb. 1987 11 p Submitted for publication Sponsored in part by AT and T Information Systems
(Grant NAG1-613)
(NASA-CR-182939; NAS 1.26:182939) Avail: NTIS HC A03/MF A01 CSCL 09B

Two correctness criteria, the state consistency criterion and the property consistency criterion for process migration are discussed. The state machine approach is used to model the interactions between a user process and its environment. These criteria are defined in terms of the model. The idea of environment view was introduced to distinguish what a user process observes about its environment from what its environment state really is and argue that a consistent view of the environment must be maintained for every migrating process. Author

N88-26824# Instituto de Pesquisas Espaciais, Sao Jose dos Campos (Brazil).
THE KNOWLEDGE BASED AUTOMATIC EXTRACTION OF THE MACHINABLE SURFACES FOR AUTOMATIC CAD-CAM SYSTEM
Valter Rodrigues and Marcos Regis Vescovi May 1988 10 p Prepared for presentation at the 3rd Congresso Latino Americano de Automatica, Vina del Mar, Chile, 3-7 Oct. 1988
(INPE-4542-PRE/1288) Avail: NTIS HC A02/MF A01

The goal of this work is to automate the CAD-CAM system for turning operations. Considering that the manufacturing process cycle has five computational steps: (1) Computer Aided Parts Design; (2) Recognition and Extraction of Surfaces (CAD-CAM Link); 30 Computer-Automated Process Planning (CAPP); (4) Programming; and (5) Plan Execution, this paper describes how to use the knowledge-based system concept to model the second and third steps. For the machining operation in these steps the production rules for knowledge representation were used. The interpretation of the geometric model (B-REPS system) give the machinable surfaces and its associated process. The integration of manufacturing processes leads the sequence from turning operations to process planning. Author

N88-26825*# TAI Corp., Huntsville, Ala.
[COMMON DATA FORMAT (CDF) TO STORE IMAGES] Final Report
Loy W. Shreve, II Jul. 1988 4 p
(Contract NAS8-36992)
(NASA-CR-179366; NAS 1.26:179366) Avail: NTIS HC A02/MF A01 CSCL 09B

The original goal of this study was to allow free interchange of images between the HGS and other analytical tools available to NASA. Originally conceived as a collection of individual computer programs that could individually convert any format image to any other format and transfer images via several routes, NASA elected to adopt a Common Data Format (CDF) to store images. This allowed the storage of all images in one format on the NASA EADS. Most of the individual programs were then combined and placed in a user friendly menu-driven system that allows free interchange of image formats within EADS (Sun Workstation), HGS, and Omnicon systems. Additional software and hardware was supplied that allows physical transfer of the formatted images throughout these systems and to external systems. Author

N88-26826# Lawrence Livermore National Lab., Calif.
SEGMERGE: A SCANLINE VISIBLE SURFACE ALGORITHM WITH ADAPTIVE SPAN SELECTION AND INEXPENSIVE ANTIALIASING
T. Balch Mar. 1988 11 p
(Contract W-7405-eng-48)
(DE88-009186; UCID-21350) Avail: NTIS HC A03/MF A01

Spanning scanline algorithms are efficient because they take advantage of scanline and span coherence. An entire horizontal span can be declared visible at once, thus avoiding comparisons at each pixel. It is important that the number of spans be minimized because depth comparisons are made at each one. This paper presents two new techniques for scanline visible surface rendering: first, a span selection method which minimizes the number of spans and discards invisible segments; second, an inexpensive antialiasing method. It will be shown that subpixel sampling for antialiasing requiring N times more work for point sampling algorithms can be done with only N times more work for spanning scanline algorithms. DOE

N88-26827# Los Alamos National Lab., N. Mex.
XDATAP
H. M. Fisher Mar. 1988 79 p
(Contract W-7405-eng-36)
(DE88-007161; LA-11155-MS) Avail: NTIS HC A05/MF A01

XDATAP is a device-independent, versatile, interactive, graphics utility whose esential function is the plotting of cross-section data. The code is based on DISSPLA Graphics and may also be run using a command file. While the original intent of the code was to compare cross sections in A Compact ENDF format with ENDF Evaluated Nuclear Data Files, presently the code is useful as a data diagnostic tool, that is, for the review, examination, comparison, and plotting of cross-section data. The code is also very useful as a general plotting utility for those users interested in examining other types of data. XDATAP is capable of representing a variety of reaction types of MTs, for example, total, elastic scattering, (n,2n), (n,en), (n,f), heating data, nubar data, producing pie diagrams, color plots, etc., manipulating data in several different formats contained on a variety of Nuclear Data Libraries (MCNP, ENDF, ENDL, Random Multigrooup, etc). DOE

N88-26828# Brookhaven National Lab., Upton, N. Y.
FASTRUN PHASE SEQUENCER DESCRIPTOR LANGUAGE (PDL)
D. Sweely 20 Jan. 1988 14 p
(Contract DE-AC02-76CH-00016)
(DE88-007966; BNL-40991) Avail: NTIS HC A03

After hand-coding several revisions of the FASTRUN phase commands, the need for a high level description of commands became obvious. The Phase Descriptor Language (PDL) was designed to streamline the revision process and provide clearer documentation of command sequencing in FASTRUN. The key element in the PDL is the phase compiler. This complier reads the high level code and outputs a Motorola source file that can be assembled using commercial software. This complier is written in the C programming language and executes on the IBM AT software development station. DOE

N88-26829# Argonne National Lab., Ill.
COMPUTING SMALL SINGULAR VALUES OF BIDIAGONAL MATRICES WITH GUARANTEED HIGH RELATIVE ACCURACY: LAPACK WORKING NOTE NUMBER 3
J. Demmel and W. Kahan Feb. 1988 44 p
(Contract W-31-109-eng-38)
(DE88-008465; ANL/MCS-TM-110) Avail: NTIS HC A03/MF A01

Computing the singular values of a bidiagonal matrix is the final phase of the standard algorithm for the singular value decomposition of a general matrix. We present a new algorithm which computes all the singular values of a bidiagonal matrix to high relative accuracy independent of their magnitudes. In contrast, the standard algorithm for bidiagonal matrices may compute small singular values with no relative accuracy at all. Numerical experiments show that the new algorithm is comparable in speed to the standard algorithm, and frequently faster. We also show how to accurately compute tiny eigenvalues of some classes of symmetric tridiagonal matrices using the same technique. DOE

N88-26830# Illinois Univ., Urbana. Dept. of Computer Science.
A PRACTICAL SHIFTED ADAMS ALGORITHM
Hon-Wah Tam Mar. 1988 35 p
(Contract DE-FG02-87ER-25026)
(DE88-008573; DOE/ER-25026/20; UIUCDCS-R-88-1420; UILU-ENG-88-1725) Avail: NTIS HC A03/MF A01

This is a continuation of the study of the shifted Adams method. A previous report has suggested that the shifted Adams method might be more effective than the Adams method on nonstiff ordinary differential equations. A variable stepsize variable order Adams algorithm has been incorporated in the code ODE. This report generalizes this algorithm to the shifted Adams method. The generalized algorithm is implemented in a new code EFODE. DOE

N88-26831# Bradford Univ. (England). Postgraduate School of Electrical and Electronic Engineering.
INTERACTIVE COMPUTER PROGRAMME FOR THE ANALYSIS OF A TWO-WAY WILKINSON DIVIDER/COMBINER
M. R. Mgombelo and J. G. Gardiner Jun. 1987 25 p Prepared in cooperation with Dar es Salaam Univ., Tanzania
(PB88-105424; UB/PSEEE/RR-396) Avail: NTIS HC E03/MF E03; copy not available from STI Facility CSCL 09B

The two-way Wilkinson divider/combiner has acquired a lot of popularity in equal power division and combination of signals since its invention in 1969, because of its modest useful frequency bandwidth. The development of a computer program to analyze the network, useful characteristics, and the values of characteristics when the bandwidth of operation is known, is presented. A listing of the FORTRAN program is included. Author

N88-26832# University of Southern California, Marina del Rey. Information Sciences Inst.
SIMS: SINGLE INTERFACE TO MULTIPLE SYSTEMS
Jasmina Pavlin and Raymond L. Bates Feb. 1988 26 p
(Contract MDA903-81-C-0335)
(AD-A192264; ISI/RR-88-200) Avail: NTIS HC A03/MF A01 CSCL 12E

This report describes the Single Interface to Multiple Systems (SIMS) project, which is developing a tool to automatically invoke services to perform the tasks of information systems users. Most of these tasks involve multiple software servers that differ vastly in their functional capabilities, their view of the world, and their input and output languages (e.g., databases and expert systems). Before a user can determine if a server can perform the required task, he must first understand the language and services provided by each server, and then express the task in the terms used by the server. In contrast, SIMS allows the user to specify a task in a service-independent language. Our approach is dynamic in that SIMS determines which server will satisfy the request when the task is defined. SIMS performs logical integration, where the servers remain separate, but a common model makes them appear as if they were providing a single virtual service. Logical and dynamic integration allow the system of which SIMS is a part to be more easily designed and maintained. GRA

N88-26833# Odyssey Research Associates, Inc., Ithaca, N.Y.
NEBULA SUPPORT SOFTWARE Final Technical Report, Sep. 1984 - Jun. 1987
Abraham Shenker, Leonard Silver, and George Gesslein Oct. 1987 19 p
(Contract F30602-84-C-0182)
(AD-A192281; RADC-TR-87-179) Avail: NTIS HC A03/MF A01 CSCL 12E

This is the final report for the Nebula Support Software contract. It provides a Unix-based capability on the VAX-11/780 which supported the development of software targeted for execution on the Nebula computer operating under the control of a native Unix system. This effort consisted of two tasks - the first was the retarget of the System 5 c-compiler and c-library to the Nebula Instruction Set Architecture (ISA), and the second was the port of the System 5 kernel to the Nebula Brassboard System developed by CDC. The code generated by the retargeted c-compiler will be run on the Nebula simulator and on the RADC Brassboard implementation of the Nebula ISA. GRA

N88-26834# Georgia Inst. of Tech., Atlanta. Production and Distribution Research Center.
CONDITIONS FOR FINITE CONVERGENCE OF ALGORITHMS FOR NONLINEAR PROGRAMS AND VARIATIONAL INEQUALITIES
Faiz A. Al-Khayyal and Jerzy Kyparisis Jan. 1988 25 p Prepared in cooperation with Florida International Univ., Miami
(Contract N00014-86-K-0173)
(AD-A192355; PDRC-88-01) Avail: NTIS HC A03/MF A01 CSCL 12D

Algorithms for nonlinear programming and variational inequality problems are, in general, only guaranteed to converge in the limit to a Karush-Kuhn-Tucker point, in the case of nonlinear programs, or a solution in the case of variational inequalities. In this paper we derive sufficient conditions for nonlinear programs and variational inequalities such that any convergent algorithm can be modified to guarantee finite convergence to a solution. Our conditions are more general than existing results and, in addition, have wider applicability. Moreover, we note that our sufficient conditions are close to the related necessary conditions, and show by counterexamples that our main nondegeneracy assumptions cannot be relaxed. GRA

N88-26835# Mission Research Corp., Albuquerque, N. Mex.
COMPUTER PROGRAMS FOR HIGH-CURRENT BEAM TRANSPORT IN ACCELERATORS
Brendan B. Godfrey Dec. 1987 28 p Prepared in cooperation with Science Applications International Corp., La Jolla, Calif.
(Contract N60921-85-C-0044)
(AD-A192356; AMRC-R-1012) Avail: NTIS HC A03/MF A01 CSCL 20G

Numerical techniques exist for modeling particle beam dynamics in high current accelerators at several levels of fidelity. Equilibria can be determined with beam envelope codes, particle ray-tracing, Vlasov equilibrium solvers, and single-disk particle codes. The linear stability of these equilibria is addressed with dispersion relations solved numerically, linearized PIC codes, and single- and multi-component beam centroid programs. Beam nonlinear dynamics are investigated with multidimensional PIC codes employing either the complete electromagnetic field equations or various approximations to them. Each of these options is discussed, and several examples are provided. GRA

N88-26836# Naval Postgraduate School, Monterey, Calif.
EDITFONT: AN INTERACTIVE FONT EDITING SYSTEM M.S. Thesis
Hector J. Olivera, Chen T. Wu, and Michael J. Zyda Jan. 1988 62 p
(AD-A192373; NPS52-88-001) Avail: NTIS HC A04/MF A01 CSCL 12E

The major goal of this work has been the development and implementation of an interactive bit mapped font editor that enables the graphics programmer to create different fonts and icons for use in application programs. The font editor, called editfont, has been implemented on the Silicon Graphics, Inc. IRIS workstation. Editfont consists of approximately 3500 lines of code, including the program documentation. Fonts created by editfont can be retrieved from disk and high level routines implemented with the IRIS graphics library. One feature of the system is the capacity for font extraction from a picture. The steps for font generation via font extraction are explained in detail. File formats, data structures and routines used by the system are also described. Software and hardware limitations of the system are outlined, as well as possible future extensions. GRA

N88-26837# Air Command and Staff Coll., Maxwell AFB, Ala.
COMPUTER-AIDED WRITING
David A. King Apr. 1988 81 p
(AD-A192516; ACSC-88-1465) Avail: NTIS HC A05/MF A01 CSCL 05F

The production of written communications is an important and time-consuming activity for most professional organizations. Computer-aided writing offers great potential for increased productivity, quality, and convenience. In addition to word processors, Computer-Aided Writing (CAW) tools include outline processors and prompting programs, electronic dictionaries, style and grammar checkers, logic analyzers, on-line information systems for research, disk-based references, commenting and review software, desktop publishing and typesetting systems, and hypertext systems. The purpose of this research report is to survey the field of Computer-Aided Writing (CAW) tools for use on IBM-compatible Personal Computer (PC) systems. The information presented in this report is intended to acquaint computer resource managers and prospective CAW users with current PC-based CAW technology. Based on an extensive review of recent PC literature and hands-on evaluation of selected CAW products, this report discusses various categories of CAW tools, utility of current products, prospects for future developments, and selection and planning criteria. The report also specifically addresses the application of CAW technology at the Air Command and Staff College (ACSC) which is the sponsor of this project. GRA

N88-26838# Carnegie-Mellon Univ., Pittsburgh, Pa. Management Sciences Research Group.
A MATROID ALGORITHM AND ITS APPLICATION TO THE EFFICIENT SOLUTION OF TWO OPTIMIZATION PROBLEMS ON GRAPHS, REVISION Management Sciences Research Report
Carl Brezovec, Gerard Cornuejols, and Fred Glover Feb. 1988 27 p
(Contract N00014-85-K-0198; Grant NSF ECS-86-01660)
(AD-A192709; MSSR-534(R); WP-29-86-87-Rev) Avail: NTIS HC A03/MF A01 CSCL 12A

The problem of finding a minimum weight base B of a matroid is addressed when, in addition, each element of the matroid is colored with one of m colors and there are upper and lower bound restrictions on the number of elements of B with color i, for i = 1,2,..., m. This problem is a special case of matroid intersection. An algorithm exploits special structure, and is applied to two optimization problems on graphs. When applied to the weighted bipartite matching problem, the algorithm has complexity O(abs val E abs val V+ abs val V-sq log abs val V). Here V denotes the node set of the underlying bipartite graph, and E denotes its edge set. The second application is defined on a general connected graph G = (V, E) whose edges have a weight and a color. One seeks a minimum weight spanning tree with upper and lower bound restrictions on the number of edges with color i in the tree, for each i. Our algorithm for this problem has complexity O(abs val E abs val V+m-sq abs val V-sq). A special case of this constrained spanning tree problem occurs when V is a set of pairwise nonadjacent nodes of G. One must find a minimum weight spanning tree with upper and lower bound restrictions on each node of V. Then the complexity of our algorithm is O(abs val E abs val V+m-sq abs val V-sq). Finally, we discuss a new relaxation of the traveling salesman problem. GRA

N88-26839# RAND Corp., Santa Monica, Calif.
WHY IS IT DIFFICULT TO PROGRAM IN VON NEUMANN LANGUAGES Interim Report
Sanjai Narain Nov. 1987 25 p
(Contract MDA903-85-C-0030)
(AD-A192830; RAND/N-2660-DARPA) Avail: NTIS HC A03/MF A01 CSCL 12E

Often the assertion is made that programs in von Neumann languages like Fortran, Pascal, or C are difficult to synthesize, analyze, modify, or extend. While the assertion appears to be correct, usual arguments given in this support are not very convincing. This Note focuses on one part of this assertion, namely, that programs in von Neumann languages are difficult to synthesize, and develops a new argument in this support. Frequently it is necessary to express in a programming language statements of the form each of functions f1,...., fn are to be computed for the same entity. The presence of destructive assignment in von Neumann languages gives rise to the possibility that programs modify their inputs. This makes it difficult to express statements

of the above form in them. Applicative languages such as pure Lisp or pure Prolog do not contain destructive assignment, so such statements can be expressed very easily in them. GRA

N88-26840# Pittsburgh Univ., Pa. Dept. of Computer Science.
DISTRIBUTED FAULT TOLERANT EMBEDDINGS OF BINARY TREES IN HYPERCUBES
Foster Provost and Rami Melhem 1988 26 p
(Contract N00014-80-C-04555)
(AD-A192929; TR-88-3) Avail: NTIS HC A03/MF A01 CSCL 12E

This paper presents a distributed algorithm for embedding binary trees in hypercubes. Starting with the root (invoked in some cube node by a host), each node is responsible for determining the addresses of its children, and for invoking the embedding algorithm for the subtree rooted at each child in the proper cube node. This distributed embedding, along with the wealth of communication links in the hypercube, leads to a high potential for fault tolerance. We demonstrate the fault tolerance capability by introducing tree restructuring techniques which may be used to tolerate faults during the initial embedding, as well as to remap nodes that fail at run-time. The distributed nature of the embedding eliminates the need for global knowledge of faulty nodes; each node must only know the status of its neighbors. GRA

N88-26841# Carnegie-Mellon Univ., Pittsburgh, Pa. Dept. of Electrical and Computer Engineerin G.
OPTICAL DATA PROCESSING Annual Report, Jan. 1987 - Mar. 1988
David Casasent Apr. 1988 136 p
(Grant AF AFOSR-0293-84)
(AD-A193024; AFOSR-88-0550TR) Avail: NTIS HC A07/MF A01 CSCL 12I

This research concerns optical data processing for missile guidance and target recognition. It uses pattern recognition techniques with an increased use of knowledge base, inference machine and associative processor techniques. This work concerns new algorithms, real time and practical realizations of such systems, and new initial work on associative processors, symbolic rule-based processors and directed graph processors (with new attention to unique optical realizations of such systems). GRA

N88-26842*# National Aeronautics and Space Administration, Washington, D.C.
DIRECTIONS FOR PROGRAMMING IN FORTRAN 77
Hildegard Schuster Jul. 1988 41 p Transl. into ENGLISH of Richtlinien zur Programmierung in FORTRAN 77 (Oberpfaffenhofen, Fed. Republic of Germany, DFVLR), 1987 p 1-41 Original language document was announced as N88-15487 Transl. by Scientific Translation Service, Santa Barbara, Calif.
(Contract NASw-4307)
(NASA-TT-20317; NAS 1.77:20317; DFVLR-Mitt-87-10) Avail: NTIS HC A03/MF A01 CSCL 09B

Programming rules for FORTRAN 77 are introduced in order to reduce long-term costs of software development and maintenance. General rules are given for the preparation of programs and subroutines, for arithmetic expressions, character quantities, DO-instruction, instruction number, forbidden FORTRAN 77 instructions, input/output functions, code boxes, software and hardware-dependent functions, and program documentation.
Author

N88-26843# Ecole Nationale Superieure des Telecommunications, Paris (France). Dept. Informatique.
COLORED STOCHASTIC PETRI NETS. APPLICATION TO REAL TIME DISTRIBUTED SYSTEMS Ph.D. Thesis - Paris VI Univ. [LES RESEAUX DE PETRI STOCHASTIQUES COLORES. APPLICATION A L'ANALYSE DES SYSTEMES REPARTIS EN TEMPS REEL]
Alexandre Zenie Jun. 1987 199 p In FRENCH
(ENST-87E017; ISSN-0751-1353; ETN-88-92179) Avail: NTIS HC A09/MF A01

A computer program in PASCAL language, which is applicable to Markovian models was developed. It allows colored stochastic Petri networks theory application to real time distributed systems including distributed control, distributed data bases, and access to local networks. The procedure is modular and easily parametrable. ESA

N88-26844# National Aerospace Lab., Amsterdam (Netherlands). Informatics Div.
ENUMERATION, COMMENTS AND DISCUSSION CONCERNING PAPERS PRESENTED DURING THE CONFERENCE ON COMPUTER APPLICATIONS IN PRODUCTION AND ENGINEERING (CAPE) 87
W. Loeve and J. Vlietstra 1 Feb. 1987 14 p In DUTCH; ENGLISH summary Conference held in Amsterdam, Netherlands, Mar. 1987
(NLR-MP-87015-U; JNL208.B87-046; B8731729; ETN-88-92228)
Avail: NTIS HC A03/MF A01

Comments on contributions on CAPE 87 are given with a view to all interconnected operations in an enterprise (preliminary studies, design, manufacturing, marketing, servicing). The different aspects of industrial automation treated during CAPE 87 are summarized. The different methods and computer aided techniques are overviewed. ESA

N88-26845# Technische Hogeschool, Delft (Netherlands). Faculty of Mathematics and Informatics/Computer Science.
DELFI-3 AS A DEVELOPMENT ENVIRONMENT FOR EXPERT SYSTEMS [DELFI-3 ALS ONTWIKKELOMGEVING VOOR EXPERT SYSTEMEN]
W. Jonker and H. deSwaanArons 1987 26 p In DUTCH
(Rept-8767; B8735223; ISSN-0920-2358; ETN-88-92443) Avail: NTIS HC A03/MF A01

The status of the Delfi-3 development environment for complex expert systems is presented. Delfi-3 disposes of a number of advanced knowledge representation techniques and inference mechanisms. The structure of Delfi-3 is uniform and transparant, and therefore simple to use. The use of the knowledge representation language Lore allows the compilation of knowledge banks. The user possibilities of Delfi-3 are demonstrated by an example. Ideas for further developments are given. ESA

N88-26846# Technische Hogeschool, Delft (Netherlands). Faculty of Mathematics and Informatics/Computer Science.
SCRIPT EDITOR: AN EDITOR FOR THE SPECIFICATION PHASE IN THE DEVELOPMENT OF COMPUTER BASED LEARNING [SCRIPT-EDITOR: EEN EDITOR VOOR DE SPECIFICATIE FASE BIJ HET ONTWIKKELEN VAN COMPUTER ONDERSTEUND ONDERWIJS]
B. R. Sodoyer and C. A. P. G. vanderMast 1987 22 p In DUTCH
(Rept-87-68; B8735224; ISSN-0920-2358; ETN-88-92444) Avail: NTIS HC A03/MF A01

The software development for a prototype script editor is reviewed. The methods used for the development computer aided learning are presented. The standard components used to compose a script are given. The functional requirements for the use of a script editor are explained. The user interface of the script editor, the scriptfile manager, and the printer manager are presented. The status of use and evaluation of the prototype is given. ESA

N88-26847# Technische Hogeschool, Delft (Netherlands). Faculty of Mathematics and Informatics/Computer Science.
A SURVEY OF FREEFORM SOLID MODELING METHODS
J. J. Steketee 1987 71 p
(Rept-87-81; B8803158; ISSN-0920-8577; ETN-88-92573)
Copyright Avail: NTIS HC A04/MF A01

Freeform solid modeling is introduced by describing its role in Computer Aided Design/Computer Aided Manufacturing (CAD/CAM). Blending with implementation by rolling sphere, curve rounding, and recursive subdivision are discussed, followed by deformation with freeform deformation as an implementation; offsetting and the application to solids; sweeping and contour orientation; cross sectional design and the interpolation of cross

sections; meshing and the concept of hyperpatches; and surface arrangement, including surface intersection and an implementation for the representation of trimmed surface patches. A classification of objects; an evaluation of freeform solid modeling methods, an integrated view on these methods; and research issues are presented. ESA

N88-26848# Technische Hogeschool, Delft (Netherlands). Faculty of Mathematics and Informatics/Computer Science.
A NEW TRAJECTORY FOLLOWING POLYNOMIAL-TIME ALGORITHM FOR THE LINEAR PROGRAMMING PROBLEM
C. Roos 1987 41 p
(Rept-87-87; B8803797; ISSN-0920-8577; ETN-88-92577)
Copyright Avail: NTIS HC A03/MF A01

An interior point method for the solution of the linear programming problem is presented. It is shown that the method admits a polynomial time bound. The method is based on the use of the trajectory of the problem, which makes it conceptually very simple. It has the advantage over related methods that it requires no problem transformation (either affine or projective) and that the feasible region may be unbounded, so that no normalization constraint is needed. A practical version of the algorithm is presented. ESA

N88-26849# Center for Mathematics and Computer Science, Amsterdam (Netherlands). Dept. of Computer Science/Dept. of Algorithms and Architecture.
FIXPOINT REPRESENTATIONS OF CHARACTERISTIC SETS OF LINEAR-TIME TEMPORAL FORMULAS
Evangelos Kranakis and Kostas N. Oikonomou (Bell Telephone Labs., Inc., Holmdel, N. J.) Nov. 1987 16 p Submitted for publication
(CWI-CS-R8754; B8805677; ETN-88-92587) Copyright Avail: NTIS HC A03/MF A01

An algebraic-axiomatic method for computing existential and universal characteristic sets of linear-time temporal logic formulas on directed graphs is presented. The set of all nodes v of a given graph (model) such that all (respectively, some) infinite walks starting from v satisfy a formula is called the universal (respectively, existential) characteristic set of the formula. Computation of the characteristic set is reduced to finding the least or greatest fixpoint of a system of set equations. Representations of the characteristic set of the logic L obtained are model-independent, in the sense that the same representation holds for all graphs, and regardless of whether or not they are finite or infinite. ESA

N88-26850# Center for Mathematics and Computer Science, Amsterdam (Netherlands). Dept. of Computer Science/Dept. of Software Technology.
CONTRACTIONS IN COMPARING CONCURRENCY SEMANTICS
Joost N. Kok and Jan J. M. M. Rutten Nov. 1987 43 p Sponsored by the European Economic Commission ESPRIT Project 415
(CWI-CS-R8755; B8805678; ETN-88-92588) Copyright Avail: NTIS HC A03/MF A01

Concurrent imperative languages (both operational and denotational semantic models) are defined as fixed points of contractions on complete metric spaces. A general method for comparing different semantic models by relating their defining contractions and exploiting the fact that contractions have a unique fixed point is developed. ESA

N88-26851# Center for Mathematics and Computer Science, Amsterdam (Netherlands). Dept. of Computer Science/Dept. of Interactive Systems.
INTERACTION MANAGEMENT IN CAD SYSTEMS WITH A HISTORY MECHANISM
Yasushi Yamaguchi, Fumihiko Kimura (Tokyo Univ., Japan), and Paul J. W. tenHagen Nov. 1987 15 p Submitted for publication Sponsored by the Japan Society of Precision Engineering and the Ricoh Co. Ltd.
(CWI-CS-R8756; B8805679; ETN-88-92589) Copyright Avail: NTIS HC A03/MF A01

User friendliness in computer aided design systems is considered. A concept called model derivation, which describes how the user treats the model in terms of its evolution is introduced. To construct and use model derivation a history mechanism which keeps and manipulates the history of the modeling process is proposed. The history mechanism manages high level interactions by introducing powerful symbolic computation to manipulate the history. Since the history representation is based on the operation's syntax and separated from the internal model representation, it is easy to apply the history mechanism to any modeling system which uses established techniques. Thus the system designer can easily introduce model derivation without reducing efficiency of the implementation. ESA

N88-26852# Center for Mathematics and Computer Science, Amsterdam (Netherlands). Dept. of Computer Science/Dept. of Software Technology.
A NETWORK APPROACH TO THE CERTAINTY FACTOR MODEL
L. C. vanderGaag Nov. 1987 20 p
(CWI-CS-R8757; B8805680; ETN-88-92590) Copyright Avail: NTIS HC A03/MF A01

So-called inference networks are used to demonstrate the application of the MYCIN expert system certainty model in a rule-based top-down reasoning expert system. This approach shows inadequacies of the notational convention used by the creators of the model. A syntactically correct formalism is proposed and used to discuss properties of the model. ESA

N88-26853# Center for Mathematics and Computer Science, Amsterdam (Netherlands). Dept. of Computer Science.
A SEMANTIC APPROACH TO FAIRNESS
J. J. M. M. Rutten and J. I. Zucker (State Univ. of New York, Buffalo.) Nov. 1987 28 p Sponsored in cooperation with the European Economic Commission ESPRIT Project 415
(Grant NSF DCR-85-04296)
(CWI-CS-R8759; B8805682; ETN-88-92592) Copyright Avail: NTIS HC A03/MF A01

In the semantic framework of metric process theory, fairness of processes are investigated from two points of view: (1) intrinsic fairness of processes, and (2) fair operations on processes. Regarding (1) a fairification operation on processes called Fair such that for every (generally unfair) process p the process Fair(p) is fair, and contains precisely those paths of p that are fair, is defined. The definition uses systematic alternation of random choices. The notion of fair operations on processes is treated. Suppose given an operator on processes (like merge, or infinite iteration), one wants to define a fair version of it. For the operation of infinite iteration a fair version is defined, again by a fair scheduling technique. ESA

N88-26854# Center for Mathematics and Computer Science, Amsterdam (Netherlands). Dept. of Pure Mathematics.
MINIMUM DISCLOSURE PROOFS OF KNOWLEDGE
Gilles Brassard, David Chaum, and Claude Crepeau (Massachusetts Inst. of Tech., Cambridge.) Dec. 1987 49 p Revised
(Grants NSERC-A4107; NSF DCR-MCS-85-09905)
(CWI-PM-R8710; B8805665; ETN-88-92598) Copyright Avail: NTIS HC A03/MF A01

Protocols for allowing a prover to convince a verifier that the prover knows verifiable secret information, without allowing the verifier to learn anything about the secret are given. The secret can be probabilistically or deterministically verifiable, and only one of the prover or verifier need have constrained resources. ESA

N88-26855# Oak Ridge National Lab., Tenn.
AN EXPEDITIOUS TECHNIQUE FOR KEYBOARD INPUT OF INFORMATION TO FORTRAN COMPUTER PROGRAMS
D. H. Smith and D. E. Goeringer May 1988 29 p
(Contract DE-AC05-84OR-21400)
(DE88-009617; ORNL/TM-10770) Avail: NTIS HC A03

A technique for rapid and accurate input of information via a video display terminal to FORTRAN computer programs has been developed. The overall approach is described; it is applicable to any programming environment based on a similar system with only the most rudimentary control of graphics functions. The specific application in the laboratory, using DEC VT-100-compatible terminals, is also described and illustrated with examples. Listings of the graphics subroutines for use with a DEC RT-11 system are provided. DOE

N88-26856# Lawrence Livermore National Lab., Calif.
EFFICIENT BIT-LEVEL, WORD-LEVEL AND BLOCK-LEVEL SYSTOLIC ARRAYS FOR MATRIX-MATRIX MULTIPLICATION
A. J. DeGroot, S. R. Parker, and E. M. Johansson Feb. 1988 10 p Presented at SPIE O-E Lase '88: Optoelectronics and Laser Applications in Science and Engineering, Los Angeles, Calif., 10 Jan. 1988
(Contract W-7405-eng-48)
(DE88-011331; UCRL-98086; CONF-880110-33; CONF-880110) Avail: NTIS HC A02/MF A01

The mapping of matrix-matrix multiplication onto bit level, word level and block level systolic arrays is investigated. Highly efficient and regular bit level, word level and block level systolic arrays are described. Efficiencies of many block level and word level systolic arrays reported in this paper approach 100 percent, three times the efficiencies of systolic arrays reported previously. Bit level systolic arrays reported require less computation time than do bit level systolic arrays reported previously and, for special matrices, require less cells. Execution times of block level systolic algorithms on sixty-four-element multiprocessors agree with theory. DOE

N88-26857# Vrije Universiteit, Amsterdam (Netherlands). Subfaculteit Wiskunde en Informatica.
PROGRAMMER-FRIENDLY LL(1) PARSER GENERATOR
D. Grune and C. J. H. Jacobs 1986 11 p
(PB88-126933; IR-127) Avail: NTIS HC E03/MF E01; copy not available from STI Facility CSCL 09B

LL(1) grammars have the conceptual and practical advantage that they allow the compiler writer to view the grammar as a program; this allows a more natural positioning of semantic actions and a single attribute mechanism. Resulting parsers can be constructed that do fully automatic error recovery, which allows the compiler writer to ignore totally the issue of syntax errors. Measurement shows that such parsers can be reasonably efficient. GRA

N88-26858*# Colorado Univ., Boulder. Dept. of Aerospace Engineering Sciences.
SOLUTION OF THE ORR-SOMMERFELD EQUATION FOR THE BLAUSIUS BOUNDARY-LAYER DOCUMENTATION OF PROGRAM ORRBL AND A TEST CASE
S. Biringen and G. Danabasoglu Aug. 1988 19 p
(Grant NAG1-798)
(NASA-CR-4169; NAS 1.26:4169) Avail: NTIS HC A03/MF A01 CSCL 09B

A Chebyshev matrix collocation method is outlined for the solution of the Orr-Sommerfeld equation for the Blausius boundary layer. User information is provided for FORTRAN program ORRBL which solves the equation by the QR method. Author

N88-26859*# Jet Propulsion Lab., California Inst. of Tech., Pasadena.
DIAGNOSING FAULTS IN AUTONOMOUS ROBOT PLAN EXECUTION
Raymond K. Lam, Rajkumar S. Doshi, David J. Atkinson, and Denise M. Lawson 1 Mar. 1988 31 p
(Contract NAS7-918)
(NASA-CR-182480; JPL-Publ-88-14; NAS 1.26:182480) Avail: NTIS HC A03/MF A01 CSCL 09B

A major requirement for an autonomous robot is the capability to diagnose faults during plan execution in an uncertain environment. Many diagnostic researches concentrate only on hardware failures within an autonomous robot. Taking a different approach, the implementation of a Telerobot Diagnostic System that addresses, in addition to the hardware failures, failures caused by unexpected event changes in the environment or failures due to plan errors, is described. One feature of the system is the utilization of task-plan knowledge and context information to deduce fault symptoms. This forward deduction provides valuable information on past activities and the current expectations of a robotic event, both of which can guide the plan-execution inference process. The inference process adopts a model-based technique to recreate the plan-execution process and to confirm fault-source hypotheses. This technique allows the system to diagnose multiple faults due to either unexpected plan failures or hardware errors. This research initiates a major effort to investigate relationships between hardware faults and plan errors, relationships which were not addressed in the past. The results of this research will provide a clear understanding of how to generate a better task planner for an autonomous robot and how to recover the robot from faults in a critical environment. Author

N88-26327# Fujitsu Ltd., Kawasaki (Japan).
CELLULAR ARRAY PROCESSOR CAP AND ITS APPLICATION TO COMPUTER GRAPHICS
Hiroyuki Sato, Kouichi Murakami, Morio Ikesaka, Hiroaki Ishihata, and Mitsuo Ishii *In* National Aerospace Lab., Proceedings of the 5th NAL Symposium on Aircraft Computational Aerodynamics Nov. 1987 p 262-271 In JAPANESE; ENGLISH summary Original contains color illustrations (For primary document see N88-26290 20-01)
Avail: NTIS HC A12/MF A01

N88-26519# Technische Hochschule, Darmstadt (West Germany). Inst. fuer Regelungstechnik.
PARAMETER ESTIMATION OF DYNAMICAL SYSTEMS
R. Isermann *In* DFVLR, System Identification in Vehicle Dynamics 1987 p 9-49 In GERMAN; ENGLISH summary (For primary document see N88-26518 20-31)
Avail: NTIS HC A18/MF A01; DFVLR, VB-PL-DO, 90 60 58, 5000 Cologne, Fed. Republic of Germany, 109 Deutsche marks

62 COMPUTER SYSTEMS

Includes computer networks and special application computer systems.

N88-26860*# Illinois Univ., Urbana-Champaign. Coordinated Science Lab.
DEFINITION OF AN AUXILIARY PROCESSOR DEDICATED TO REAL-TIME OPERATING SYSTEM KERNELS
Wolfgang A. Halang Jun. 1988 78 p
(Grant NAG1-613)
(NASA-CR-183070; NAS 1.26:183070; UILU-ENG-88-2228; CSG-87) Avail: NTIS HC A05/MF A01 CSCL 09B

In order to increase the efficiency of process control data processing, it is necessary to enhance the productivity of real time high level languages and to automate the task administration, because presently 60 percent or more of the applications are still programmed in assembly languages. This may be achieved by migrating apt functions for the support of process control oriented languages into the hardware, i.e., by new architectures. Whereas numerous high level languages have already been defined or realized, there are no investigations yet on hardware assisted implementation of real time features. The requirements to be fulfilled by languages and operating systems in hard real time environment are summarized. A comparison of the most prominent languages, viz. Ada, HAL/S, LTR, Pearl, as well as the real time extensions of FORTRAN and PL/1, reveals how existing languages meet these demands and which features still need to be incorporated to enable the development of reliable software with predictable program behavior, thus making it possible to carry out a technical safety approval. Accordingly, Pearl proved to be the closest match to the mentioned requirements. Author

N88-26861# Sandia National Labs., Albuquerque, N. Mex.
A HIGH SPEED SERIAL LINK INTERFACE FOR SANDAC-V
V. G. Grafe, G. S. Davidson, and M. G. Wilde Jan. 1988 23 p
(Contract DE-AC04-76DP-00789)
(DE88-007694; SAND-87-1088) Avail: NTIS HC A03/MF A01

A need has been identified for high speed communications between embedded computers and their associated gateway computers. To this end, a high speed serial link has been developed in Sandia National Laboratories' Electronics Subsystems Department for interfacing the SANDAC-V embedded computer to an IBM-PC gateway. The resulting 20 Mbit/second serial link is shown to be suitable for direct interfaces to sensors, actuators, and other computers in the embedded environment. Characteristics of this link and previous methods are presented. Complete schematics and directions for use are included as appendices. DOE

N88-26862# Oak Ridge National Lab., Tenn. Engineering Physics and Mathematics Div.
A LINEAR-PROGRAMMING METHOD INSPIRED BY THE NEURAL NETWORKS FRAMEWORK
J. C. Culioli and V. Protopopescu 1988 9 p Presented at the IEEE Annual International Conference on Neural Networks, San Diego, Calif., 24 Jul. 1988
(Contract DE-AC05-84OR-21400)
(DE88-008688; CONF-880745-2; CONF-880745) Avail: NTIS HC A02

A discrete numerical algorithm is proposed for linear programming that has common features with nonlinear optimization algorithms and with neural network models. The computation energy of the algorithm is not quadratic, but linear, which greatly simplifies the model. The collective computational properties are obtained by dividing the neurons in two classes: primal and dual. The algorithm is parallelisable, easier to code than most classical linear-programming algorithms, and implementable in YLSI. The relationship with other neural network models is discussed. DOE

N88-26863# SRI International Corp., Menlo Park, Calif.
AN EVALUATION METHODOLOGY FOR DEPENDABLE MULTIPROCESSORS Final Technical Report, Jul. - Sep. 1987
Jack Goldberg Mar. 1988 73 p
(Contract F19628-86-D-0003)
(AD-A192799; SRI-ESU-2918; RADC-TR-88-23) Avail: NTIS HC A04/MF A01 CSCL 12F

This report outlines an approach to a methodology for evaluating high performance, reliable computers. The purpose of the methodology is to provide a framework and a basis for tool development that will make it possible to conduct such evaluations systematically and efficiently. The increasing complexities of high performance computer systems and the stringent requirement for high reliability in harsh environments (e.g., space) make such an evaluation methodology an absolute necessity. The report discusses sources of difficulty in evaluation, such as the many complexities of multiprocessing, the difficulty of distinguishing various factor (algorithms, software), operating systems, fault diagnostics, etc.) that affect performance and fault tolerance, the use of formal and experimental analyses, and the special problems of computer security. Criteria and suggestions are given for the design of unified working environments and specific classes of tools that support the methodology. GRA

N88-26864# Technische Hogeschool, Delft (Netherlands). Faculty of Mathematics and Informatics/Computer Science.
EXTENSIBLE NETWORKS. PART 1: PRINCIPLES AND CONSTRUCTIONS
F. Peper 1987 20 p
(Rept-87-91-Pt-1; B8805148; ISSN-0920-8577; ETN-88-92579)
Copyright Avail: NTIS HC A03/MF A01

A construction method for networks which maintain their properties upon extension, such as a highly regular structure, fixed degree, high connectivity, and low diameter is described. Optimal routing functions for these networks appear to be invariant under extension. The method is used to construct an infinite class of extensible networks satisfying the above requirements. ESA

63 CYBERNETICS

Includes feedback and control theory, artificial intelligence, robotics and expert systems.

For related information see also *54 Man/System Technology and Life Support.*

N88-26865 Stanford Univ., Calif.
EXPERIMENTS IN ADAPTIVE CONTROL OF A VERY FLEXIBLE ONE LINK MANIPULATOR Ph.D. Thesis
Daniel Mark Rovner 1987 125 p
Avail: Univ. Microfilms Order No. DA8801017

Experiments conducted to advance the science of adaptive control as applied to mechanical systems with distributed flexibility, very low inherent damping, and non-collocated sensors and actuators are described. The experimental apparatus employed is a very flexible one link robotic manipulator. The adaptive controllers described maintain stable, high-bandwidth tip position control by adjusting themselves to compensate for these changes. Self-Tuning Regulator algorithms were developed in which the controller explicitly identifies system models from input/output data and uses them in a subsequent control law design step. The sensitivity of pole placement and Linear Quadratic Gaussian control law design to identification inaccuracies is examined. The experimental performance of identification algorithms is then discussed in the context of the accuracy required for control law design. The performance of an adaptive controller using a modified least squares identification algorithm and a pole placement control law design algorithm is demonstrated. An identification algorithm is proposed and demonstrated that directly estimates the physical parameter subject to variation, in this case the mass of the manipulator load. Extensions of the technique to other parameters and to more than one parameter are indicated. Dissert. Abstr.

N88-26866# Los Alamos National Lab., N. Mex.
BUILDING AN ARTIFICIAL INTELLIGENCE CAPABILITY AT LOS ALAMOS
J. G. Marinuzzi 1988 5 p Presented at the Artificial Intelligence Applications for Military Logistics Conference, Williamsburg, Va., 29 Mar. 1988
(Contract W-7405-eng-36)
(DE88-009155; LA-UR-88-1166; CONF-880393-1) Avail: NTIS HC A02/MF A01

In 1985, after three years of preliminary work, Management of the Los Alamos National Laboratory started an ambitious program to develop a strong technical capability in the rapidly emerging field of Artificial Intelligence/Knowledge Based Systems (AI/KBS). When this AI development program began, except for a few staff members doing basic AI research, AI was essentially nonexistent at the laboratory. The basics, including such things as AI computer hardware and software, literature, books, knowledgeable personnel, or even a general knowledge of what AI was, were most difficult if not impossible to find. For this reason, we had to approach the problem with a very broad perspective, which strongly addressed the basics while aiming toward more advanced AI program elements. Broad, intensive education was the bootstrapping tool used in this five year, multi-million dollar AI capability development program. Halfway through the program, our accomplishments indicate that the program is extremely successful. In terms of trained staff, active programs and state-of-the-art equipment, we have developed one of the strongest AI technical capabilities within the Department of Energy (DOE) and the Department of Defense (DOD). However, a great deal more must be done before the full potential of the program can be realized. DOE

N88-26867*# University of Central Florida, Orlando. Dept. of Computer Engineering.
EXPERT SYSTEM APPLICATION EDUCATION PROJECT Final Report, 10 Aug. 1987 - 10 Aug. 1988
Avelino J. Gonzelez and James M. Ragusa 8 Aug. 1988 5 p
(Grant NAG10-0043)
(NASA-CR-183089; NAS 1.26:183089) Avail: NTIS HC A02/MF A01 CSCL 09B

Artificial intelligence (AI) technology, and in particular expert systems, has shown potential applicability in many areas of operation at the Kennedy Space Center (KSC). In an era of limited resources, the early identification of good expert system applications, and their segregation from inappropriate ones can result in a more efficient use of available NASA resources. On the other hand, the education of students in a highly technical area such as AI requires an extensive hands-on effort. The nature of expert systems is such that proper sample applications for the educational process are difficult to find. A pilot project between NASA-KSC and the University of Central Florida which was designed to simultaneously address the needs of both institutions at a minimum cost. This project, referred to as Expert Systems Prototype Training Project (ESPTP), provided NASA with relatively inexpensive development of initial prototype versions of certain applications. University students likewise benefit by having expertise on a non-trivial problem accessible to them at no cost. Such expertise is indispensible in a hands-on training approach to developing expert systems. Author

N88-26868# JAYCOR, Vienna, Va.
NARRATIVE DOMAIN IMPLEMENTATION
Jun. 1988 35 p
(Contract N00014-85-C-2044)
(AD-A192265) Avail: NTIS HC A03/MF A01 CSCL 05B

The SUMMARY expert system was developed to summarize (pick out particular pieces of information) Navy Casualty Report (CASREP) narrative sections. This task of summarization requires several steps which we will describe here, in a cursory manner. The first step is to obtain a normalized parse of each sentence in the message. The second step is to transform each parse into an Information Format. These information formats are then passed to the SUMMARY expert system where rules representing general linguistic rules of summarization, domain-specific rules of classification, and rules of emphasis on particular types of information are applied to the formats. The format(s) with the highest emphasis (score) is then chosen as the summary. In this report, the concern lies in the third phase of this process where summaries are chosen by the SUMMARY expert system. GRA

N88-26869# Air Force Weapons Lab., Kirtland AFB, N. Mex.
TIME-OPTIMAL ADAPTIVE SHAPED TORQUE (TOAST) TECHNICAL NOTE Final Report, 1 Jul. 1985 - 15 Nov. 1986
D. L. Cate Jan. 1988 58 p
(AD-A192719; AFWL-TN-86-72) Avail: NTIS HC A04/MF A01 CSCL 17K

A discussion of time-optimal retargeting of beam steering mirrors is given. The argument for a bang-bang waveform is given first along with a simple 2nd order regulator problem as an example. The method of solution for a 2nd order tracker problem is given with an example. An argument is then put forth for using the time-optimal bang bang method on closed-loop control systems. The solution for the general multiple-order complex eigenvalue bang-bang boundary value problem is derived and an example is shown. This is followed by the demonstration of the time savings of the time-optimal retargeting technique, in which a lead compensator with a pure inertia is used to show the relationship between the ratio of maximum torque to the torque required by a classical set-point change and the savings in time for general retargeting problems. Finally, the time-optimal retargeting solution is applied to general retargeting problems. From this analysis several conclusions about using time optimal control on real systems are drawn. GRA

N88-26870*# National Aeronautics and Space Administration. Langley Research Center, Hampton, Va.
KINEMATICS OF HOOKE UNIVERSAL JOINT ROBOT WRISTS
William S. McKinney, Jr. Jun. 1988 33 p
(NASA-TM-100567; NAS 1.15:100567) Avail: NTIS HC A03/MF A01 CSCL 09B

The singularity problem associated with wrist mechanisms commonly found on industrial manipulators can be alleviated by redesigning the wrist so that it functions as a three-axis gimbal system. This paper discussess the kinematics of gimbal robot wrists made of one and two Hooke universal joints. Derivations of the resolved rate motion control equations for the single and double Hooke universal joint wrists are presented using the three-axis gimbal system as a theoretical wrist model. Author

N88-26871# National Aerospace Lab., Amsterdam (Netherlands). Informatics Div.
NEXT: AN EXPERT SYSTEM DEVELOPMENT TOOL TO SUPPORT ENGINEERING DESIGN
J. C. Donker and P. J. Kat 17 Nov. 1986 24 p Presented at the Conference on Computer Applications in Production and Engineering (CAPE) 87, Amsterdam, Netherlands, 17-19 Mar. 1987
(NLR-MP-86070-U; B8803801; ETN-88-92604) Avail: NTIS HC A03/MF A01

A knowledge based system shell called NEXT was developed. Its main features are an inference mechanism incorporating a mixture of forward and backward reasoning, facilities for iteration, and a good user interface. One of the applications, developed as a test case for the system, will form part of the user interface to the engineering data base system EDIPAS. Its helps the designer to initialize his data base in the right way. It is expected that this application will be extended to include other parts of the user interface. ESA

64 NUMERICAL ANALYSIS

Includes iteration, difference equations, and numerical approximation.

N88-26872 Mississippi State Univ., Mississippi State.
THE CONSTRUCTION OF COMPOSITE GRIDS FOR GENERAL THREE-DIMENSIONAL REGIONS Ph.D. Thesis
Yeon Seok Chae 1987 258 p
Avail: Univ. Microfilms Order No. DA8728921

The construction of a two dimensional, two block and four block system for a coastal grid; a three dimensional single block system for a wing-body configuration, a three dimensionsl 37-block and 13-block system for a wing-body-pylon-store configuration are discussed. Eglin's EAGLE code, which has a surface and grid generation systems for general, three dimensional, composite or multiblock grids based on algebraic and elliptic grid generation techniques, is used for this research. Introduced are several symbolic surface and grid generation runstreams for single block wing-body configurations and, 37-block and 13-block wing-body-pylon-store configurations. These runstreams can be used for other types of wing-body-pylon-store configurations. The detailed construction and the editing procedure of each surface and grid generation runstream are also discussed. The purpose of this research included the generation of various grids without obtaining solutions with a flow solver. Dissert. Abstr.

N88-26873*# Harris Corp., Melbourne, Fla. Government Aerospace Systems Div.
FINITE-DIMENSIONAL APPROXIMATION FOR OPTIMAL FIXED-ORDER COMPENSATION OF DISTRIBUTED PARAMETER SYSTEMS Final Report
Dennis S. Bernstein and I. G. Rosen (University of Southern California, Los Angeles.) Jun. 1988 25 p Submitted for publication
(Contracts NAS1-18107; F49620-86-C-0002; Grant

AF-AFOSR-0351-87)
(NASA-CR-181674; ICASE-88-36; NAS 1.26:181674) Avail: NTIS HC A03/MF A01 CSCL 12A

In controlling distributed parameter systems it is often desirable to obtain low-order, finite-dimensional controllers in order to minimize real-time computational requirements. Standard approaches to this problem employ model/controller reduction techniques in conjunction with LQG theory. In this paper we consider the finite-dimensional approximation of the infinite-dimensional Berstein/Hyland optimal projection theory. This approach yields fixed-finite-order controllers which are optimal with respect to high-order, approximating, finite-dimensional plant models. The technique is illustrated by computing a sequence of first-order controllers for one-dimensional, single-input/single-output, parabolic (heat/diffusion) and hereditary systems using spline-based, Ritz-Galerkin, finite element approximation. Numerical studies indicate covergence of the feedback gains with less than 2 percent performance degradation over full-order LQG controllers for the parabolic system and 10 percent degradation for the hereditary system. Author

N88-26874# Los Alamos National Lab., N. Mex.
EIGENMODES OF A RANDOM WALK ON A 2-D LATTICE TORUS WITH ONE TRAP
D. C. Torney 14 Mar. 1988 15 p Presented at the Conference on Transport Theory, Invariant Imbedding and Integral Equations, Santa Fe, N. Mex., 20 Jan. 1988
(Contract W-7405-eng-36)
(DE88-007830; LA-UR-88-915; CONF-880123-2) Avail: NTIS HC A03/MF A01

The complete set of eigenvalues and eigenmodes is elaborated for a random walk on a two-dimensional N (times) N square lattice torus with one trap site. The eigenvalue closest to unity is found to have an asymptotic expansion in N; the leading behavior is lambda (approximately) 1 - (2N log N) + O(N log N)(sup -2). In general, the eigenvalues and eigenmodes for this problem are constructed from those for a random walk on the same lattice containing no trap. The degeneracy of the latter eigenmodes is a prominent feature of this construction, and a formula is derived for this degeneracy. DOE

N88-26875# Sandia National Labs., Albuquerque, N. Mex.
THE SCALED-SIZED MODEL: A REVISION OF AMDAHL'S LAW
J. L. Gustafson 1988 11 p Presented at the 3rd International Conference on Supercomputing, Boston, Mass., 15 May 1988
(Contract DE-AC04-76DP-00789)
(DE88-008114; SAND-88-0372C; CONF-880567-4) Avail: NTIS HC A03/MF A01

The conventional argument, generally attributed to Amdahl, is that vector and parallel architectures should not be carried to extremes because the scalar or serial portion of the code will eventually dominate. Since pipeline stages and extra processors obviously add hardware cost, a corollary to this argument is that the most cost-effective computer is one based on uniprocessor, scalar principles. For architectures that are both parallel and vector, the argument is compounded, making it appear that near-optimal performance on such architectures is a near-impossibility. We present an argument based on the assumption that program execution time, not problem size, is constant for various amounts of vectorization and parallelism. This has a dramatic effect on Amdahl's argument, revealing that one can be much more optimistic about achieving high speedups on massively-parallel and highly-vectorized machines. The revised argument is supported by recent results of over 1000 times speedup on 1024 processors on several practical scientific applications. DOE

N88-26876# Sandia National Labs., Albuquerque, N. Mex.
A NODAL METHOD FOR TIME-DEPENDENT TRANSPORT EQUATION
A. Badruzzaman 1987 11 p Presented at the American Nuclear Society Annual Meeting, San Diego, Calif., 12 Jun. 1988
(Contract DE-AC04-76DP-00789)
(DE88-004285; SAND-87-3054C; CONF-880601-4) Avail: NTIS HC A03/MF A01

Numerical time-dependent transport methods implicit in the time variable yield unconditionally stable solutions with the mesh ratio, r = v delta t/ delta x, greater than unity, thereby allowing large time steps. An explicit scheme, on the other hand, requires r less than 1 for stability. It has been showed, however, that the basic difference scheme in the implicit approach can lead to large errors in the solution while being stable. They demonstrated that appropriate explicit algorithms are considerably more accurate, although restricted to small time steps. In this paper we report a nodal procedure applied to both the temporal and the spatial variables. Nodal methods, which retain higher-order moments of the solution, have been utilized to solve the static transport equation with much larger cell widths than required by the standard differencing schemes to attain the same accuracy. DOE

N88-26877# California Univ., Berkeley. Lawrence Berkeley Lab.
USING COMMON SUBEXPRESSIONS TO OPTIMIZE MULTIPLE QUERIES
J. Park and A. Segev Feb. 1988 10 p Presented at the 4th International Conference on Data Engineering, Los Angeles, Calif., 1 Feb. 1988
(Contract DE-AC03-76SF-00098)
(DE88-008210; LBL-23597; CONF-880245-2) Avail: NTIS HC A02

This paper deals with the problem of identifying common subexpressions and using them in the simultaneous optimization of multiple queries. In particular, we emphasize the strategy of selecting access plans for the single queries and their integration into a global access plan that takes advantage of common tasks. We present a dynamic programming algorithm for the selection of individual access plans such that the resulting global access plan is of minimum processing cost. The computational complexity of this algorithm represents a significant improvement over existing algorithms. DOE

N88-26878# Lawrence Livermore National Lab., Calif.
PROCEDURE FOR CONVERTING A WILSON-FOWLER SPLINE TO A CUBIC B-SPLINE WITH DOUBLE KNOTS
F. N. Fritsch 14 Oct. 1987 14 p
(Contract W-7405-eng-48)
(DE88-008971; UCID-21325) Avail: NTIS HC A03/MF A01

The Wilson-Fowler spline (WF-spline) has been used by the DOE Weapons Complex for over twenty years to represent point-defined smooth curves. Most modern CADCAM systems use parametric B-spline curves (or, more recently, rational B-splines) for this same purpose. The WF-spline is a parametric piecewise cubic curve. It has been shown that a WF-spline can be reparametrized so that its components are C^1 piecewise cubic functions (functions that are cubic polynomials on each parameter interval, joined so the function and first derivative are continuous). The purpose of these notes is to show explicitly how to convert a given WF-spline to a cubic B-spline with double knots. DOE

N88-26879# Argonne National Lab., Ill.
CHALLENGE PROBLEMS FOCUSING ON EQUALITY AND COMBINATORY LOGIC: EVALUATING AUTOMATED THEOREM-PROVING PROGRAMS
L. Wos and W. McCune 1988 12 p Presented at the 9th International Conference on Automated Deduction (CAD-9), Argonne, Ill., 23 May 1988
(Contract W-31-109-eng-38)
(DE88-010057; CONF-8805110-2) Avail: NTIS HC A03/MF A01

A set of problems for evaluating the power of automated theorem-proving programs and the potential of new ideas is presented. Since the problems published in the proceedings of the first CADE conference proved to be so useful, and since researchers are now far more disposed to implementing and testing their ideas, a new set of problems to complement those that

have been widely studied is in order. In general, the new problems provide a far greater challenge for an automated theorem-proving program than those in the first set do. Indeed, to our knowledge, five of the six problems we propose for study have never been proved with a theorem-proving program. For each problem, we give a set of statements that can easily be translated into a standard set of clauses. We also state each problem in its mathematical and logical form. In many cases, we also provide a proof of the theorem from which a problem is taken so that one can measure a program's progress in its attempt to solve the problem. Two of the theorems we discuss are of especial interest in that they answer questions that had been open concerning the constructability of two types of combinator. Also included is a brief description of a new strategy for restricting the application of paramodulation. All of the problems proposed for study emphasize the role of equality. This paper is tutorial in nature. DOE

N88-26880# International Centre for Theoretical Physics, Trieste (Italy).
ACCURATE SOLUTION OF PARABOLIC EQUATIONS BY EXPANSION IN ULTRASPHERICAL POLYNOMIALS
E. H. Doha Nov. 1986 26 p
(DE88-701829; IC-86/317) Avail: NTIS (US Sales Only) HC A03/MF A01

An ultraspherical expansion technique is applied to obtain numerically the solution of the third boundary value problem for linear parabolic partial differential equation in one space variable. The differential equation with its boundary and initial conditions is reduced to a system of ordinary differential equations for the coefficients of the expansion. This system may be solved analytically or numerically in a step-by-step manner. The method in its present form may be considered as a generalization of that of Dew and Scraton. The extension of the method to the polar type equations is also considered. DOE

N88-26881# International Centre for Theoretical Physics, Trieste (Italy).
NONTRIVIAL CRITICAL POINTS FOR ASYMPTOTICALLY QUADRATIC FUNCTION
Shujie Li and J. Q. Liu Dec. 1986 11 p
(DE88-101851; IC-86/390) Avail: NTIS (US Sales Only) HC A03/MF A01

The existence of some nontrivial critical points are studied. As applications, the existence of nontrivial solutions of the Dirichlet problem is studied for nonlinear elliptic partial differential equations and periodic boundary value problem for nonlinear ordinary differential equations. DOE

N88-26882# International Centre for Theoretical Physics, Trieste (Italy).
CANONICAL CONSTRUCTION OF DIFFERENTIAL OPERATORS INTERTWINING REPRESENTATIONS OF REAL SEMISIMPLE LIE GROUPS
V. K. Dobrev Nov. 1986 32 p
(DE88-701852; IC-86/393) Avail: NTIS (US Sales Only) HC A03/MF A01

Let G be a real linear connected semisimple Lie group. We present a canonical construction of the differential operators intertwining elementary (ident to generalized principal series) representations of G. The results are easily extended to real linear reductive Lie groups. DOE

N88-26883# International Centre for Theoretical Physics, Trieste (Italy).
THEORY OF PSEUDO-DIFFERENTIAL OPERATORS OVER C*-ALGEBRAS
N. Mohammad Jun. 1987 14 p
(DE88-701860; IC-87/117) Avail: NTIS (US Sales Only) HC A03/MF A01

In this article the behaviour of adjoints and composition of pseudo-differential operators in the framework of a C*-algebra is studied. It results that the class of pseudo-differential operators of order zero is a C*-algebra. DOE

N88-26884# Argonne National Lab., Ill. Mathematics and Computer Science Div.
COMPARISON THEOREMS AND THEIR USE IN THE ANALYSIS OF SOME NONLINEAR DIFFUSION PROBLEMS
H. G. Kaper and Man Kam Kwong 1988 14 p Presented at the Conference on Transport Theory, Invariant Imbedding and Integral Equations, Santa Fe, N. Mex. 20 Jan. 1988
(Contract W-31109-eng-38)
(DE88-010032; CONF-880123-3) Avail: NTIS HC A03/MF A01

This article is concerned with concavity and monotonicity properties of radial solutions of nonlinear diffusion equations of the type u(sub t) = Delta u - Lambda u(sup q) R(sup N); lambda is a positive constant and O less than q less than 1. It is shown that the Sturm-Picone theorem of classical linear oscillation theory can be used effectively in the study of nonlinear differential equations. DOE

N88-26885*# National Aeronautics and Space Administration. Lewis Research Center, Cleveland, Ohio.
EVOLUTION OF HAIRPIN VORTICES IN A SHEAR FLOW
T.-L. Hon (Lehigh Univ., Bethlehem, Pa.) and J. D. A. Walker Jul. 1988 23 p
(NASA Order C-99066-G)
(NASA-TM-100858; ICOMP-88-9; E-4062; NAS 1.15:100858)
Avail: NTIS HC A03/MF A01 CSCL 12A

Recent experimental studies suggest that the hairpin vortex plays an important (and perhaps dominant) role in the dynamics of turbulent flows near walls. In this study a numerical procedure is developed to allow the accurate computation of the trajectory of a 3-D vortex having a small core radius. For hairpin vortices which are convected in a shear flow above a wall, the calculated results show that a 2-D vortex containing a small 3-D disturbance distorts into a complex shape with subsidiary hairpin vortices forming outboard of the original hairpin vortex. As the vortex moves above the wall, it induces unsteady motion in the viscous flow near the wall: numerical solutions suggest that the boundary-layer flow near the wall will ultimately erupt in response to the motion of the hairpin vortex and in the process a secondary hairpin vortex will be created. The computer results agree with recent experimental investigations. Author

N88-26886# Technische Hogeschool, Delft (Netherlands). Faculty of Mathematics and Informatics/Computer Science.
LINEARIZATION ALONG INVARIANT MANIFOLDS AND A GENERALIZATION OF THE HARTMAN-GROBMAN THEOREMS FOR DEGENERATE SINGULARITIES OF VECTOR FIELDS IN R CUBED
Sebastian vanStrien 1987 22 p
(Rept-87-80; B8801071; ISSN-0920-8577; ETN-88-92572)
Copyright Avail: NTIS HC A03/MF A01

The phase-portrait at a singularity of a vectorfield in R sup n when the singularity is nonhyperbolic is considered. The approach is to blow-up the singularity and apply linearization theorems along invariant manifolds which are not necessarily normally hyperbolic. Extending a result of Bonckaert, Dumortier, and van Strien on singularities of vector fields determined by their first nonvanishing jet slightly, a generalization of the Hartman-Grobman theorem in R cubed is given. This result holds for nonhyperbolic singularities and also gives nice smoothness of the homeomorphisms without requiring nonresonance conditions. ESA

N88-26887# Technische Hogeschool, Delft (Netherlands). Faculty of Mathematics and Informatics/Computer Science.
A FULL BUT ELEMENTARY TREATMENT OF SYSTEMS OF HOMOGENEOUS ORDINARY LINEAR DIFFERENTIAL EQUATIONS WITH CONSTANT COEFFICIENTS
J. G. Besjes 1987 12 p
(Rept-87-82; B8801072; ISSN-0920-8577; ETN-88-92574)
Copyright Avail: NTIS HC A03/MF A01

Construction of the general solution of homogeneous linear

differential equations with constant coefficients is considered. It is shown that only the most elementary results from linear algebra are needed to give a full treatment. It is also shown that Fulmer's (1975) method for calculating the fundamental solution can be proved without assuming the Cayley-Hamilton theorem from linear algebra. ESA

N88-26888# Technische Hogeschool, Delft (Netherlands). Faculty of Mathematics and Informatics/Computer Science.
SEMILINEAR ELLIPTIC PROBLEMS ON DOMAINS WITH CORNERS
Guido Sweers 1987 22 p
(Rept-87-83; B8801073; ISSN-0920-8577; ETN-88-92575)
Copyright Avail: NTIS HC A03/MF A01

It is shown that there exist sign-changing stable solutions of semilinear elliptic problems with Dirichlet boundary condition, if the (smooth) boundary is close to a cone somewhere. For problems with these nonlinear right hand sides, there is a critical angle for corners of the domain if one wants existence of a positive solution. ESA

N88-26889# Technische Hogeschool, Delft (Netherlands). Faculty of Mathematics and Informatics/Computer Science.
PROLONGATION, RESTRICTION AND COARSE GRID APPROXIMATION IN A THREE-DIMENSIONAL CELL-CENTERED MULTIGRID METHOD
M. Khalil, J. J. I. M. vanKan, and P. Wesseling 1987 55 p
(Rept-88-02; B8805149; ISSN-0920-8577; ETN-88-92581)
Copyright Avail: NTIS HC A04/MF A01

The notions of cell-centered and vertex-centered multigrid methods are discussed. Prolongation, restriction, and coarse grid approximation for cell-centered multigrid are studied. It is found that preferable combinations are: zeroth order interpolation for prolongation, linear or multilinear interpolation for the adjoint of the restriction, and coarse grid Galerkin approximation. If chosen properly, these combinations lead to a coarse grid matrix that has not more non-zero elements per row than the fine grid matrix. Methods and computer programs are presented for the derivation of the structure and of explicit formulas for the coarse grid matrix. ESA

N88-26890# National Research Inst. for Mathematical Sciences, Pretoria (South Africa).
TWO FAMILIES OF GRAPHS SATISFYING THE CYCLE BASIS INTERPOLATION PROPERTY
E. B. Jarrett Sep. 1986 19 p
(PB88-127808; CSIR-TWISK-485) Avail: NTIS HC E04/MF E04; copy not available from STI Facility CSCL 12A

The length of a cycle basis of a graph G is the sum of the lengths of its c-, c+ cycles. Let c-, c+ be the lengths of the minimal and maximal cycle basis, respectively. Then G has the cycle basis interpolation property (cbip) if for all integers c, c- much smaller than c much smaller than c+, there exists a cycle basis of length c. Two families of graphs with the cbip, namely snake-graphs and kite-graphs are constructed. GRA

N88-26891# National Research Inst. for Mathematical Sciences, Pretoria (South Africa).
ALGORITHM FOR GENERATING THE MINIMAL CYCLE BASIS OF A GRAPH
E. B. Jarrett Sep. 1986 15 p
(PB88-126610; CSIR-TWISK-483) Avail: NTIS HC E04/MF E04; copy not available from STI Facility CSCL 12A

A method is given for finding the minimum cycle basis of a simple, undirected, 2-connected graph. The algorithm described starts from the fundamental cycle set and proceeding through a series of exchanges of cycles with smaller cycles, results in a minimal cycle basis. GRA

N88-26892# National Research Inst. for Mathematical Sciences, Pretoria (South Africa).
LINEAR PROGRAMMING IN R SUP 3 AND THE SKELETON AND LARGEST INCIRCLE OF A CONVEX POLYGON
M. Orlowski and M. Pachter Aug. 1986 17 p
(PB88-124664; CSIR-TWISK-480) Avail: NTIS HC E04/MF E04; copy not available from STI Facility CSCL 12A

The geometrical problem of constructing the largest circle inscribed in a (given) convex polygon is solved in 0(n) time. The problem is related to the construction of the skeleton of the polygon, which construction is shown to be accomplishable in 0(n log n) time. GRA

N88-26318# National Aerospace Lab., Tokyo (Japan).
ON THE PROPAGATING SPEED IN DIFFERENCE APPROXIMATIONS FOR CONSERVATION LAWS
Hideaki Aiso *In its* Proceedings of the 5th NAL Symposium on Aircraft Computational Aerodynamics Nov. 1987 p 201-207
In JAPANESE; ENGLISH summary (For primary document see N88-26290 20-01)
Avail: NTIS HC A12/MF A01

65 STATISTICS AND PROBABILITY

Includes data sampling and smoothing; Monte Carlo method; and stochastic processes.

N88-26893# Michigan Univ., Ann Arbor. Communications and Signal Processing Lab.
ASYMPTOTICALLY EFFICIENT ADAPTIVE ALLOCATION SCHEMES FOR CONTROLLED MARKOV CHAINS: FINITE PARAMETER SPACE
Rajeev Agrawal, Demosthenis Teneketzis, and Venkatachalam Anantharam Feb. 1988 38 p Prepared in cooperation with Cornell Univ., Ithaca, N.Y.
(Contract N00014-87-K-0540; Grant NSF ECS-85-17708)
(AD-A192228; TR-254) Avail: NTIS HC A03/MF A01 CSCL 12C

Consider a controlled Markov chain whose transition probabilities and initial distribution are parametrized by an unknown parameter Theta belonging to some known parameter space Theta. There is a one-step reward associated with each pair of control and the following state of the process. The objective is to maximize the expected value of the sum of one step rewards over an infinite horizon. By introducing the Loss associated with a control scheme, the problem is equivalent to minimizing this Loss. Define a uniformly good adaptive control schemes and restrict attention to these schemes. A lower bound is developed on the Loss associated with any uniformly good control scheme. Finally, an adaptive control scheme is constructed whose Loss equals the lower bound, and is therefore optimal. GRA

N88-26894# North Carolina Univ., Chapel Hill. Center for Stochastic Processes.
TWO CLASSES OF SELF-SIMILAR STABLE PROCESSES WITH STATIONARY INCREMENTS Report, Sep. 1987 - Aug. 1988
Stamatis Cambanis and Makoto Maejima Jan. 1988 34 p
(Contract F49620-85-C-0144)
(AD-A192842; TR-220; AFOSR-88-0357TR) Avail: NTIS HC A03/MF A01 CSCL 12C

Two disjoint classes of self-similar symmetric stable processes with stationary increments are studied. The first class consists of linear fractional stable processes, which are related to moving average stable processes, and the second class consists of harmonizable fractional stable processes, which are connected to harmonizable stationary stable processes. The domain of attraction of the harmonizable fractional stable processes is also discussed. GRA

N88-26895# Technische Hogeschool, Delft (Netherlands). Faculty of Mathematics and Informatics/Computer Science.
COMBINING EXPERT OPINIONS: AN OPTIMIZATION FRAMEWORK
Janos Pinter (Research Inst. for Water Resources Development,

Budapest, Hungary) and Roger Cooke 1987 46 p
(Rept-87-84; B8803156; ISSN-0920-8577; ETN-88-92576)
Copyright Avail: NTIS HC A03/MF A01

An optimization approach for aggregating individual opinions (point estimates, probability distributions, etc) in a quantitatively best sense is presented. The framework suggested permits a great variety of problem-dependent concretizations, several of which are presented. Numerical solution aspects of the introduced model variants are also treated. ESA

N88-26896# Technische Hogeschool, Delft (Netherlands). Faculty of Mathematics and Informatics/Computer Science.
MARKOV CHAIN COMPUTATIONS TO A SOLUTION OF THE MUTUAL-EXCLUSION PROBLEM IN CONCURRENCY
J. E. Mebius 1987 18 p
(Rept-87-89; B8803798; ISSN-0920-8577; ETN-88-92578)
Copyright Avail: NTIS HC A03/MF A01

A Markov chain model of a mutual-exclusion protocol is presented. A performance concept for synchronization protocols in general is formulated. A personal-computer implementation is described. Computational results are given. In case of interference, the slower of the two processes has a smaller performance degradation. If there is interference, performance and interference overhead are optimal at a dispatching probability of 25 percent, not at 50 percent, as one intuitively expects. The performance varies by 30 percent over the observed interval (0.01 ..0.99); the performance degradation is minimally 0.2857 to 0.2101 = 0.0756 and maximally 0.2587 to 0.1376 = 0.1211, so it varies by a factor of 1.6 over the observed interval. From the performance viewpoint, Dijkstra's Fourth Attempt is not a very good protocol. ESA

N88-26897# Technische Hogeschool, Delft (Netherlands). Onderafdeling der Wiskunde en Informatica.
RANGE OF A CONSTRAINED RANDOM WALK
W. T. F. denHollander and G. H. Weiss 1987 30 p
(PB88-126867; Rept-87-26) Avail: NTIS HC E03/MF E01; copy not available from STI Facility CSCL 12A

The report examines the statistical properties of the range (equal to the number of distinct sites visited) of a lattice random walk in discrete time. In particular, the authors calculate the mean and obtain a bound on the variance of the range in the large time limit. The results are applied to a problem involving an unconstrained random walk in the presence of randomly distributed traps. GRA

66 SYSTEMS ANALYSIS

Includes mathematical modeling; network analysis; and operations research.

N88-26898# RAND Corp., Santa Monica, Calif.
AN AGENDA FOR THE STRATEGIC DEFENSE INITIATIVE
Glenn A. Kent Jan. 1988 9 p Presented at a Colloqium of the American Association for the Advancement of Science, 14 May 1987
(RAND-P-7404) Avail: NTIS HC A02/MF A01

The goal of moving from an offense-dominated to a defense-dominated international strategic scene is desirable and feasible, and can best be achieved in cooperation with the U.S.S.R. Such a shared goal implies that deploying strategic defenses is clearly subordinate to the more encompassing matter of reducing ballistic missiles to zero or near zero. In addition to seeking Soviet cooperation, the U.S. should continue to discuss the pros and cons of such a direction with its allies, continue to conduct the strategic defense initiative (SDI) technology program aimed at an earth-based defense with passive defense, and continue to adhere to the 1972 ABM treaty. J.P.B.

N88-26899# Oak Ridge National Lab., Tenn.
THE OAK RIDGE NATIONAL LABORATORY STRATEGIC DEFENSE INITIATIVE SHIELD OPTIMIZATION PROGRAM: EXECUTIVE SUMMARY
R. T. Santoro and T. A. Gabriel Apr. 1988 21 p
(Contract DE-AC05-84OR-21400)
(DE88-008016; ORNL/TM-10629) Avail: NTIS HC A03/MF A01

Scoping studies have been completed to estimate radiation-induced damage in silicon-based electronic components carried on a satellite. The analyses were completed for natural (Van Allen belt protons and electrons, solar flares, and galactic cosmic rays) and man-made (nuclear and directed neutral particle beam weapons) radiation expected to be encountered by an SDI satellite or weapon platform. The Van Allen belt protons, depending on altitude and orbital inclination, were found to be the most stressing natural radiation threat. Nuclear weapon radiation, depending upon the weapon yield and distance of the detonation from the satellite, and neutral particle beam radiation were found to terminally destroy electronic components. Calculations were also made to estimate the amount of local shielding required to extend mission performance. These shields were optimized for minimum weight for specified damage thresholds. All of the calculations were carried out assuming the presence of a thin primary shield tailored specifically for survivability against an incident low mass kinetic energy weapon projectile and which affords minimal protection against energetic radiation. DOE

N88-26900# Los Alamos National Lab., N. Mex. Center for National Security Studies.
MONITORING SPACE WEAPONRY: DETECTION AND VERIFICATION ISSUES
P. J. Garrity, R. A. Gore, R. E. Pendley, and J. F. Pilat Apr. 1988 37 p
(Contract W-7405-eng-36)
(DE88-008726; LA-11278) Avail: NTIS HC A03/MF A01

If agreements that affect the research, development, testing, or deployment of space weapons are to be reached, the United States must be able to monitor the treaty-limited systems and verify compliance with the agreement. This report attempts to establish guidelines for future space monitoring technologies by briefly examining key types of potential arms control constraints on space weapons; considering the impact of those constraints on current and potential U. S. military capabilities, including the consequences of treaty violations; defining generic monitoring/verification requirements and difficulties for these arms control regimes; and deriving future verification and intelligence collection requirements and technology challenges. DOE

N88-26901# Los Alamos National Lab., N. Mex.
SDI: MYTH OR REALITY
G. H. Canavan 1988 15 p Presented at the 4th National Space Symposium, Colorado Springs, Colo., 12 Apr. 1988
(Contract W-7405-eng-36)
(DE88-009121; LA-UR-88-1326; CONF-8804105-1) Avail: NTIS HC A03/MF A01

This report reviews previous attempt to develop strategic defenses, the technologies currently under consideration, their main unknowns, and their likely performance relative to evolving threats. DOE

N88-26902# Army Weapons Command, Rock Island, Ill.
THE STRATEGIC DEFENSE INITIATIVE: STRATEGIC IMPLICATIONS
Thomas L. Russell 31 Mar. 1988 41 p
(AD-A192341; AD-E801594) Avail: NTIS HC A03/MF A01 CSCL 05D

In March 1983, during this address to the nation, President Reagan initiated a major shift in U.S. strategic policy, as he indicated his desire to move away from the condition of mutual vulnerability as the primary deterrent to nuclear war. The Strategic Defense Initiative (SDI), as the vehicle for this shift, has become the focus of debate over implications of a new strategic policy. This study

seeks to examine the strategic relationship, and the role of arms control during a transition from an offensive-dominant strategy to a defensive-dominant strategy. The methodology for the study is to present arguments for and against SDI, as they relate to the issues of stability and arms control, evaluate their validity, draw conclusions, and provide recommendations that may enhance international security during a transition period of SDI. GRA

N88-26903# RAND Corp., Santa Monica, Calif.
SDI AND/OR ARMS CONTROL
David A. Ochmanek Aug. 1987 15 p
(RAND-P-7357) Avail: NTIS HC A03/MF A01

A frame of reference is established which relates U.S. policies regarding both strategic defense and arms control to the deterrence of aggression and the limiting of damage should deterrence fail. Early deployment of an extensive but only partially effective strategic defense system could actually reduce security. However, strategic defense, if deployed in such a way that it did not damage the deterrent effect of assured retaliation, can make a profound contribution to national survival if deterrence failed and nuclear weapons were launched by accident or against all reason. Assured national survival, a more modest goal than perfect population defense, still presents problems of technical feasibility and possible destabilization if engaged in unilaterally. The U.S. should plan on the continued need for cooperation with the U.S.S.R. and for arms control. Policy implications include: (1) the need to reverse the erosion of the ABM treaty; (2) the desirability of enacting the 50 percent reduction negotiated in Reykjavik; and (3) during arms negotiations, the U.S. should maintain a vigorous strategic defense initiative (SDI) technology program. J.P.B.

67 THEORETICAL MATHEMATICS

Includes topology and number theory.

N88-26904# Center for Mathematics and Computer Science, Amsterdam (Netherlands). Dept. of Pure Mathematics.
ALGEBRAIC AND ARITHMETIC GEOMETRY IN STRING THEORY
Dirk-Jan Smit (Utrecht State Univ., Netherlands) Nov. 1987 16 p Sponsored by the Stichting voor Fundamenteel Onderzoek der Materie, Netherlands
(CWI-PM-R8708; B8805666; ETN-88-92597) Copyright Avail: NTIS HC A03/MF A01

Ways in which elements of algebraic geometry can be used to give an algebraic formula for the string partition function are reviewed. Ideas are generalized to include arithmetic surfaces, i.e., surfaces defined over an algebraic number field K. The volume of the lattice formed by K-rational tangent vectors at a K-rational point in moduli space, with respect to the Polyakov measure, is calculated explicitly. ESA

70 PHYSICS (GENERAL)

For precision time and time interval (PTTI) see *35 Instrumentation and Photography;* for geophysics, astrophysics or solar physics see *46 Geophysics, 90 Astrophysics,* or *92 Solar Physics.*

N88-26905# International Centre for Theoretical Physics, Trieste (Italy).
ON THE SELF-FOCUSING OF ELECTRIC HELICONS
N. L. Tsintadze, M. Y. El-Ashry, and D. P. Garuchava Jul. 1987 8 p
(DE88-701870; IC-87/127) Avail: NTIS (US Sales Only) HC A02/MF A01

The present work is devoted to the investigation of the stationary self-focusing of circularly polarized helicons in a magnetized plasma in the case of ultra-relativistic intensities. It is shown that the larger intensity and effective width at the boundary is the much faster growing self-focusing. DOE

N88-26906# University Coll., London (England). Dept. of Computer Science.
QUALITATIVE REASONING FOR PHYSICISTS
J. A. Campbell May 1987 13 p
(PB88-116298; UCL-CS-TR-133) Avail: NTIS HC E04/MF E04; copy not available from STI Facility CSCL 20C

Qualitative reasoning is introduced as a potentially new field of study with relevance to physicists' practice and experience. It has arisen from the need, in artificial intelligence (an area of advanced computer science), to model common sense and intuitive notions of the physical world in ways which are formal enough to allow representation in computer programs. Equation-based and axiom-based examples of work in qualitative reasoning are given, together with indications of open problem areas to which physicists may be able to contribute. GRA

71 ACOUSTICS

Includes sound generation, transmission and attenuation. For noise pollution see *45 Environmental Pollution.*

N88-26907*# National Aeronautics and Space Administration. Langley Research Center, Hampton, Va.
HELICOPTER MAIN-ROTOR NOISE: DETERMINATION OF SOURCE CONTRIBUTIONS USING SCALED MODEL DATA
Thomas F. Brooks, J. Ralph Jolly, Jr. (Planning Research Corp., Hampton, Va.), and Michael A. Marcolini Aug. 1988 66 p
(NASA-TP-2825; L-16399; NAS 1.60:2825) Avail: NTIS HC A04/MF A01 CSCL 20A

Acoustic data from a test of a 40 percent model MBB BO-105 helicopter main rotor are scaled to equivalent full-scale flyover cases. The test was conducted in the anechoic open test section of the German-Dutch Windtunnel (DNW). The measured data are in the form of acoustic pressure time histories and spectra from two out-of-flow microphones underneath and foward of the model. These are scaled to correspond to measurements made at locations 150 m below the flight path of a full-scale rotor. For the scaled data, a detailed analysis is given for the identification in the data of the noise contributions from different rotor noise sources. Key results include a component breakdown of the noise contributions, in terms of noise criteria calculations of a weighted sound pressure level (dBA) and perceived noise level (PNL), as functions of rotor advance ratio and descent angle. It is shown for the scaled rotor that, during descent, impulsive blade-vortex interaction (BVI) noise is the dominant contributor to the noise. In level flight and mild climb, broadband blade-turbulent wake interaction (BWI) noise is dominant due to the absence of BVI activity. At high climb angles, BWI is reduced and self-noise from blade boundary-layer turbulence becomes the most prominent.
Author

N88-26908 Yale Univ., New Haven, Conn.
QUANTITATIVE PARTICLE CHARACTERIZATION BY SCATTERED ULTRASOUND Ph.D. Thesis
Ronald Aurele Roy 1987 147 p
Avail: Univ. Microfilms Order No. DA8729140

An acoustic scattering technique for determining the compressibility and density of individual particles is discussed. The particles, which have diameters on the order of 10 micron, are modeled as fluid spheres. Ultrasonic tone bursts of 2 microsec duration and 30 MHz center frequency scatter from individual particles as they transverse the focal region of two confocally positioned transducers. One transducer acts as a receiver while the other both transmits and receives acoustic signals. The resulting scattered bursts are detected at 90 deg and to 180 deg. Using either the long wavelength (Rayleigh) or the weak scatterer (Born) approximations, it is possible to determine the compressibility and density of the particle provided a priori knowledge of the particle size and host properties are possessed. An experiment was run first to assess the feasibility of using polystyrene polymer microspheres to calibrate the instrument. A second study was performed on the buffy coat harvested from whole human blood.

Finally, chinese hamster ovary cells which were subjected to hyperthermia treatment were studied in order to see if the instrument could detect heat induced membrane bleeding.
Dissert. Abstr.

N88-26909*# Duke Univ., Durham, N. C. Dept. of Mechanical Engineering and Materials Science.
AIRCRAFT INTERIOR NOISE REDUCTION BY ALTERNATE RESONANCE TUNING Semiannual Progress Report, period ending Jun. 1988
Donald B. Bliss, James A. Gottwald, Mark B. Gustaveson, and James R. Burton, III Jul. 1988 35 p
(Grant NAG1-722)
(NASA-CR-182540; NAS 1.26:182540) Avail: NTIS HC A03/MF A01 CSCL 20A

Model problem development and analysis continues with the Alternate Resonance Tuning (ART) concept. The various topics described are presently at different stages of completion: investigation of the effectiveness of the ART concept under an external propagating pressure field associated with propeller passage by the fuselage; analysis of ART performance with a double panel wall mounted in a flexible frame model; development of a data fitting scheme using a branch analysis with a Newton-Raphson scheme in multiple dimensions to determine values of critical parameters in the actual experimental apparatus; and investigation of the ART effect with real panels as opposed to the spring-mass-damper systems currently used in much of the theory. Author

N88-26910# Swedish Inst. for Materials Testing, Boras. Acoustics Lab.
SOUND POWER MEASUREMENTS IN SITU USING A REFERENCE SOUND SOURCE
H. G. Jonasson 1988 113 p
(PB88-182571; SP-RAPP-1988:03; ISBN-91-7848-089-2) Avail: NTIS HC A06/MF A01 CSCL 20A

A new method to determine sound power levels of large noise sources in situ is proposed. It is based on comparison measurements with a reference sound source; but certain improvements were made, especially concerning the handling of the reference sound source. The reference sound source must be placed close to important noise radiating parts of the source under test and only calibrated positions may be used. A calibrated position is a position which is well defined relative to reflecting surfaces and one in which the reference sound source has been tested by having 4 different measurement teams carrying out measurements on a water turbine and connected electric generator in two different acoustical environments. The results indicate that the standard deviation of the A weighted sound power level is less than 0.2 B, i.e., the method can be rated as an ISO engineering method. Author

N88-26911*# Georgia Inst. of Tech., Atlanta. School of Mechanical Engineering.
SOUND PROPAGATION OVER UNEVEN GROUND AND IRREGULAR TOPOGRAPHY Semiannual Status Report No. 7, Jan. - Jul. 1988
Yves H. Berthelot, Allan D. Pierce, James A. Kearns, and Ji-Xun Zhou Aug. 1988 55 p
(Grant NAG1-566)
(NASA-CR-182956; NAS 1.26:182956) Avail: NTIS HC A04/MF A01 CSCL 20A

Theoretical, computational, and experimental techniques were developed for predicting the effects of irregular topography on long range sound propagation in the atmosphere. Irregular topography is understood to imply a ground surface that: (1) is not idealizable as being perfectly flat, or (2) that is not idealizable as having a constant specific acoustic impedance. The focus is on circumstances where the propagation is similar to what might be expected for noise from low altitude air vehicles flying over suburban or rural terrain, such that rays from the source arrive at angles close to grazing incidence. Author

N88-26912# Quaid-i-Azam Univ., Islamabad (Pakistan). Dept. of Mathematics.
ACOUSTIC DIFFRACTION BY AN ABSORBING FINITE STRIP IN A MOVING FLUID
S. Asghar Aug. 1987 18 p
(PB88-191382; QAUM-87/27) Avail: NTIS HC A03/MF A01 CSCL 20A

The diffraction of a line source of sound by an absorbing finite strip in the presence of a fluid flow is investigated. The problem is solved by a method due to Jones based on the Wiener-Hopf technique. The diffracted field is shown to be the sum of a field produced by the two edges of the strip and a field due to the interaction of the two edges. The far field is then calculated using asymptotic approximations. GRA

N88-26913*# National Aeronautics and Space Administration. Langley Research Center, Hampton, Va.
EVALUATION OF A MULTI-POINT METHOD FOR DETERMINING ACOUSTIC IMPEDANCE
Michael G. Jones (Planning Research Corp., Hampton, Va.) and Tony L. Parrott Jun. 1988 37 p
(NASA-TM-100637; NAS 1.15:100637) Avail: NTIS HC A03/MF A01 CSCL 20A

An investigation was conducted to explore potential improvements provided by a Multi-Point Method (MPM) over the Standing Wave Method (SWM) and Two-Microphone Method (TMM) for determining acoustic impedance. A wave propagation model was developed to model the standing wave pattern in an impedance tube. The acoustic impedance of a test specimen was calculated from a best fit of this standing wave pattern to pressure measurements obtained along the impedance tube centerline. Three measurement spacing distributions were examined: uniform, random, and selective. Calculated standing wave patterns match the point pressure measurement distributions with good agreement for a reflection factor magnitude range of 0.004 to 0.999. Comparisons of results using 2, 3, 6, and 18 measurement points showed that the most consistent results are obtained when using at least 6 evenly spaced pressure measurements per half-wavelength. Also, data were acquired with broadband noise added to the discrete frequency noise and impedances were calculated using the MPM and TMM algorithms. The results indicate that the MPM will be superior to the TMM in the presence of significant broadband noise levels associated with mean flow.
Author

N88-26914# Texas Univ., Austin. Applied Research Lab.
AN ANALYSIS OF THE EFFICIENCY AND DIRECTIVITY OF THE SOUND GENERATED BY A MOVING LASER SOURCE Final Report, 1 Sep. 1985 - 30 Sep. 1987
Rao J. Chandrasekhar, Luis J. Gonzalez, and Ilene J. Busch-Vishniac 13 Aug. 1987 119 p
(Contract N00014-85-K-0819)
(AD-A192220; ARL-TR-87-42) Avail: NTIS HC A06/MF A01 CSCL 20A

In the past decade there has been much work on the sound generated underwater by a moving laser source. In particular, a great deal of effort has been directed toward understanding the thermoacoustic sound generation process, in which the laser heats the fluid medium and radiates sound as a result of the induced volumetric expansion. Theoretical predictions of the laser generated sound and experimental measurements have been shown to agree well for a wide range of source velocities, and source-receiver geometries. The notable exception to this agreement between theory and experiment is for laser beams which are moved at velocities near Mach one. It was found in earlier experimental studies on moving thermoacoustic sources that transonic motion of the source produces significantly higher sound pressure levels than predicted by linear theory. This report examines some possible explanations of that observation. In particular, we study the effect of non-linearities in the equation of state due to entropy generation, the variation of sound generating efficiency with time for subsonic and transonic sources, and the validity of linear superposition for

a moving thermoacoustic source. In Part 2 of this report we discuss how the sound signal generated by a laser source is affected by various source and receiver parameters. GRA

N88-26915# Yale Univ., New Haven, Conn. Dept. of Mechanical Engineering.
STUDYING MATERIALS USING ACOUSTIC WAVES Final Report, Feb. 1985 - Feb. 1988
R. E. Apfel 1 Mar. 1988 23 p
(Contract N00014-85-K-0215)
(AD-A192234) Avail: NTIS HC A03/MF A01 CSCL 20A

This final report summarizes the activity of the contractor in meeting the objectives of the contract. A comprehensive bibliography and list of participants on the contract work are included along with a discussion including: microcavitation, microparticle characterization, interfacial characterization using acoustic levitation, measurements of the acoustic nonlinear parameter for determining the composition of mixtures. GRA

N88-26916# Naval Ocean Systems Center, San Diego, Calif.
A MODAL APPROACH TO ARCTIC NOISE MODELLING WITH IMPLIED VERTICAL COHERENCE
R. B. Williams Feb. 1988 2 p
(AD-A192966) Avail: NTIS HC A02/MF A01 CSCL 20B

Analytic formulas of the modal attenuation coefficients appropriate for deep Arctic under-ice conditions, and modal energy partitioning of ambient noise sources are proposed. These functions can be used, together with various assumed spatial and temporal distribution functions to calculate various statistical ambient noise functions, such as vertical coherence. Vertical noise data between 15 and 50 Hz have been analyzed for model comparison, using a bandwidth of about 5 Hz. These data show that the vertical coherence usually has a sin x/x dependence, with the first zero crossing at one wavelength. Sometimes, however zero crossing lengths of more than two wavelengths are observed. Longer correlation lengths are consistent with much of the noise energy radiating from a small region, although other interpretations are possible. Initial simple model calculations show agreement with the data. A strong nearby source of noise will cause the correlation to lengthen, while several more distant sources support the one wavelength zero crossing result. Initial sensitivity calculations, however, show that the vertical coherence function by itself is not a good validator of the model functions. Other statistics will be sought to further examine model validity. GRA

N88-26917# Physics and Electronics Lab. TNO, The Hague (Netherlands).
OUTDOOR SOUND PROPAGATION, ITS IMPLICATIONS FOR UNATTENDED GROUND SENSORS
H. A. J. M. vanHoof Dec. 1986 44 p
(Contract A80/KL/138)
(FEL-1986-64; ETN-88-92566) Avail: NTIS HC A03/MF A01

Effects which influence sound propagation are reviewed. The propagation medium affects the original source spectrum and might be considered as a transfer function. The sound pressure of a point source in free space decays with 6 dB for doubling the distance, independent of the frequency. The presence of the ground changes the transfer function: at low frequencies sound pressure doubles; it decreases at intermediate frequencies; and oscillates at high frequencies causing sharp dips in the magnitude. Atmospheric turbulence is of minor importance. Atmospheric absorption can be neglected for the source-receiver ranges involved and for frequencies below a few kHz. Upward refraction causes shadow zones: extra attenuation of 5 to 20 dB may occur. When a large obstacle is in between the source and the receiver (e.g., an earth barrier) the sound reaches the receiver by diffraction: extra attenuation of 10 dB at low frequencies up to 20 dB at high frequencies may be expected. Topography and vegetation influence the transfer function. ESA

72 ATOMIC AND MOLECULAR PHYSICS

Includes atomic structure, electron properties, and molecular spectra.

N88-26918# Tokyo Univ. (Japan). Inst. of Space and Astronautical Science.
FAST ATOM BOMBARDMENT STUDY ON INTERACTION OF ANTICODONIC NUCLEOTIDES AND THEIR COGNATE AMINO ACID
Mikio Shimizu Dec. 1986 13 p
(ISAS-RN-355) Avail: NTIS HC A03/MF A01

It can be shown by molecular model building and semi-empirical calculation that a complex of four nucleotides (C4N) composed of three anticodonic bases and a discriminator base can discriminate its cognate amino acid by the lock and key relationships. Possible evidence for the detection of such complexes (the C4N and the C4N-amino acid complexes) are presented by using fast atom bombardment-mass spectroscopy. Author

N88-26919# Tokyo Univ. (Japan). Inst. of Space and Astronautical Science.
LOW ENERGY MOLECULAR COLLISIONS
Kazuo Takayanagi Jul. 1987 33 p Presented at the UK-Japan Seminar on the Theory of Atomic Collisions, Royal Holloway and Bedford New College, 3-6 Aug. 1987
(ISAS-RN-366) Avail: NTIS HC A03/MF A01

A brief review is given of the present status of knowledge of low-energy molecular collisions. Theoretical works on the rotational and vibrational transitions and the collision-induced dissociation are surveyed. In the Appendix a list of references is given for theoretical works on collision processes relevant, particularly, to interstellar cloud physics. Author

N88-26920# Lund Univ. (Sweden). Dept. of Physics.
CHARGED PION PRODUCTION AND PROJECTILE BREAKUP IN 85A MeV(SUP)12C INDUCED HEAVY ION REACTIONS
B. Noren, B. Jakobsson, A. Kristiansson, L. Karlsson, A. Oskarsson, M. Westenius, J. Julien, V. Bellini, R. Fonte, and T. Johansson (Uppsala Univ., Sweden) [1988] 30 p
(LUIP-8802; LUNFD6/(NFFK-7085)1-29; ISSN-0348-9329) Avail: NTIS HC A03/MF A01

Charged pions have been measured at 70 deg in coincidence with projectile-like fragments in Carbon-12(+)Carbon-12, Carbon-12(+)Tin-116, and Carbon-12(+) Tin-124 reactions at 85A MeV. Neither the pi(sup +) emission nor the pi(sup +) pi(sup -) ratio exhibit differences for Tin-124 and Tin-116 targets outside those expected from the isospin difference. Inconsistencies in the target mass dependence of the pion yield disappear if a correction for reabsorption is included. After this correction, a strong, approx A sup 1.05, mass dependence is observed. The projectile breakup is significantly stronger for pion producing collisions than for the average collision indicating a much stronger abundance of central collisions. Author

N88-26921# Los Alamos National Lab., N. Mex. Theoretical Div.
FLUID DYNAMICAL MODEL OF ULTRARELATIVISTIC HEAVY ION COLLISIONS
L. Csernai, M. Gong (Michigan State Univ., East Lansing.), and D. D. Strottman 1988 6 p Presented at the 5th Winter Workshop on Nuclear Dynamics, Sun Valley, Ida., 22 Feb. 1988 Prepared in cooperation with Los Alamos National Lab., NM.
(Contract W-7405-eng-36)
(DE88-007905; LA-UR-88-748; CONF-880260-2) Avail: NTIS HC A02/MF A01

The aim of the present paper is to investigate a phase transition to a quark-gluon plasma. During the phase transition a large portion of the initial kinetic energy is invested in the latent heat. At late expansion stages we gain back this energy as random thermal motion and not as directed collective flow. In the framework of a three-dimensional relativistic fluid dynamical model the sensitivity of dN (sub B/dy), and less than p(sup z/a) greater than on the equation of state are pointed out. DOE

N88-26922# Brookhaven National Lab., Upton, N. Y.
COMPARISON OF EXCLUSIVE REACTIONS AT LARGE MOMENTUM TRANSFER
A. S. Carroll 1987 12 p Presented at the 2nd International Conference on Elastic and Diffractive Scattering, New York, N.Y., 15 Oct. 1987
(Contract DE-AC02-76CH-00016)
(DE88-007544; BNL-41003; CONF-8710274-4) Avail: NTIS HC A03/MF A01

This paper discusses exclusive reactions at large momentum transfer: namely two-body reactions where all of the final state particles have been kinematically identified. In particular pp yields px, pi(+) p yields p(+) x, pi(+) p yield p X(+), pi(+) p yield K(+) X and pp yields pp reactions are discussed. DOE

N88-26923# Los Alamos National Lab., N. Mex.
THE ELECTRONIC STRUCTURE OF CONDENSED MOLECULAR SYSTEMS
R. A. LeSar 1988 21 p Presented at the NATO Advanced Study Institute on Simple Molecular Systems at Very High Densities, Les Houches, France, 29 Mar. 1988
(Contract W-7405-eng-36)
(DE88-007823; LA-UR-88-1015; CONF-880372-1) Avail: NTIS HC A03/MF A01

Some of the basic properties of the electronic structure of condensed molecular systems are reviewed. For the rare-gas solids, we concentrated our discussion on changes in the ground- and excited-state crystal-atomic wave functions as calculated with an approximate theoretical method. Compression of these wave functions leads to a softening of the equation of state at high densities, which seems to account for much of the total many-body effects. This compression is a true many-body effect and cannot be easily decomposable into a sum of 3-body and higher terms. We reviewed the electronic properties of four molecular systems, each manifesting different behavior at high densities. Because of a general lack of theory of the electronic structure of molecular solids, we restricted ourselves to a descriptive account. Solid oxygen, for instance, seems to exhibit the beginnings of covalent bonding between the pi orbitals on adjacent molecules in its epsilon phase. It was a combination of optical-absorption data and infrared and Raman spectroscopy that led to these conclusions. Iodine is unique in that it becomes metallic as a molecular crystal at pressures easily obtainable experimentally. It is interesting that the X-ray data, which indicates a transition to a monatomic lattice at 21 GPa, and the Moessbauer spectra, which implies that molecular character is retained to 30 GPa, are in such disagreement. DOE

N88-26924# Pittsburgh Univ., Pa. Dept. of Chemistry.
HIGH RESOLUTION SPECTROSCOPY OF DISSOCIATING MOLECULES Final Report, 15 Dec. 1986 - 14 Oct. 1987
K. C. Janda 15 Mar. 1988 39 p
(Contract DE-FG02-87ER-13655)
(DE88-007959; DOE/ER-13655/3) Avail: NTIS HC A03/MF A01

The goal of this project has been to study the structure and dynamics of rare gas-halogen van der Waals molecules. These molecules are important because they provide the only chemical dynamics problem for which precise state-to-state dynamics can be determined by both experiment and full, three-dimensional quantum mechanics theory. DOE

N88-26925# Lawrence Livermore National Lab., Calif.
SHOCK WAVE COMPRESSION AND METALLIZATION OF SIMPLE MOLECULES
M. Ross and H. B. Radousky Mar. 1988 40 p Presented at the NATO Advanced Study Institute on Simple Molecular Systems At Very High Densities, Les Houches, France, 29 Mar. 1988
(DE88-008031; UCRL-98441; CONF-880372-2) Avail: NTIS HC A03/MF A01

In this paper we combine shock wave studies and metallization of simple molecules in a single overview. The unifying features are provided by the high shock temperatures which lead to a metallic-like state in the rare gases and to dissociation of diatomic molecules. In the case of the rare gases, electronic excitation into the conduction band leads to a metallic-like inert gas state at lower than metallic densities and provides information regarding the closing of the band gap. Diatomic dissociation caused by thermal excitation also leads to a final metallic-like or monatomic state. In addition, shock wave data can provide information concerning the short range intermolecular force of the insulator that can be useful for calculating the metallic phase transition as for example in the case of hydrogen. DOE

N88-26926# Illinois Inst. of Tech., Chicago.
THEORETICAL STUDIES IN ELEMENTARY PARTICLE PHYSICS
J. C. Collins 1988 12 p
(Contract DE-FG02-85ER-40235)
(DE88-006929; DOE/ER-40235/1) Avail: NTIS HC A03/MF A01

This report briefly discusses the elementary particle physics research being done at Illinois Institute of Technology. Some of the work in progress is: understanding the foundations of perturbative QCD in its applications to hadron-hadron scattering; studies of the QCD predictions for the angular distribution of the muons produced in the Drell-Yan process; the small-x regime and cosmic ray signals from Cygnus X-3. DOE

N88-26927# Kansas Univ., Lawrence. Dept. of Physics and Astronomy.
RESEARCH IN THEORETICAL PARTICLE PHYSICS Progress Report, 1 Jan. - 21 Dec. 1987
D. McKay, H. Munczek, A. Melott, and J. Ralston 1987 13 p
(Contract DE-FG02-85ER-40214)
(DE88-008230; DOE/ER-40214/2) Avail: NTIS HC A03/MF A01

This paper briefly discusses topics in High Energy Physics. Some topics discussed are: symmetry breaking in weak interactions; chiral symmetry breaking; radiative decay of neutrinos; topology studies; generation-changing interactions; and charge asymmetry in production of a photon and a meson in electron-positron annihilation. DOE

N88-26928# International Centre for Theoretical Physics, Trieste (Italy).
INELASTIC TWO COMPOSITE PARTICLE SYSTEMS SCATTERING AT HIGH ENERGY
Yushun Zhang Nov. 1986 19 p
(DE88-701841; IC-86/371) Avail: NTIS (US Sales Only) HC A03/MF A01

By using the collective coordinate of Bohr and phenomenological deformed optical potentials, the scattering amplitudes of two composite particle systems can be obtained and the collective excitation for two composite particle systems in the scattering process is discussed. DOE

N88-26929# Oak Ridge National Lab., Tenn.
INELASTIC MEAN FREE PATHS OF ELECTRONS AND POSITRONS IN MATTER
R. H. Ritchie and J. C. Ashley 1987 12 p Presented at the 10th Werner Brandt Workshop on Penetration Phenomena: Dynamic Actions of Energetic Probes with Condensed Matter, Alicante, Spain, 7 Jan. 1987
(Contract DE-AC05-84OR-21400)
(DE88-008086; CONF-870155-7) Avail: NTIS HC A03/MF A01

This paper discusses the energy losses processes involved when electrons and positrons pass through matter. Functional relationships for the Mean Free Paths (MFP) are determined. Differences between electron and positron MFP are discussed. DOE

N88-26930# Clemson Univ., S.C. Dept. of Physics and Astronomy.
RECOIL SATURATION OF THE SELF-ENERGY IN ATOMIC SYSTEMS

J. R. Manson and R. H. Ritchie 1988 10 p Presented at the 11th Werner Brandt Workshop on Penetration Phenomena of Charged Particles in Matter, Oak Ridge, Tenn., 14 Apr. 1988 Prepared in cooperation with Oak Ridge National Lab., Tenn.
(Contract DE-AC05-84OR-21400)
(DE88-010450; CONF-8804141-1; CONF-8804141) Avail: NTIS HC A02/MF A01

Within the framework of the general self-energy problem for the interaction of a projectile with a many-body system, we consider the dispersion force between two atoms or between a charge and an atom. Since the Born-Oppenheimer approximation is not made, this is a useful approach for exhibiting non-adiabatic effects. We find compact expressions in terms of matrix elements of operators in the atomic displacement which are not limited by multipole expansions. DOE

N88-26931# Los Alamos National Lab., N. Mex.
SOURCES OF POLARIZED IONS AND ATOMS
W. D. Cornelius 1988 22 p Presented at the 7th International Conference on Ion Implantation Technology, Kyoto, Japan, 7 Jun. 1988
(Contract W-7405-eng-36)
(DE88-010910; LA-UR-88-1446; CONF-880614-2) Avail: NTIS HC A03/MF A01

In this presentation we discuss methods of producing large quantities of polarized atoms and ions (Stern-Gerlach separation, optical pumping, and spin-exchange) as well as experimental methods of measuring the degree of polarization of atomic systems. The usefulness of polarized atoms in probing the microscopic magnetic surface properties of materials will also be discussed. DOE

N88-26932# Los Alamos National Lab., N. Mex.
DEVELOPMENT OF NUCLEAR MODELS FOR HIGHER ENERGY CALCULATIONS
M. Bozoian, E. R. Siciliano, and R. D. Smith 1988 9 p Presented at the International Conference on Nuclear Data for Science and Technology, Mito, Japan, 30 May 1988
(Contract W-7405-eng-36)
(DE88-010919; LA-UR-88-1695; CONF-880546-3) Avail: NTIS HC A02

Two nuclear models for higher energy calculations have been developed in the regions of high and low energy transfer, respectively. In the former, a relativistic hybrid-type preequilibrium model is compared with data ranging from 60 to 800 MeV. Also, the GNASH exciton preequilibrium-model code with higher energy improvements is compared with data at 200 and 318 MeV. In the region of low energy transfer, nucleon-nucleus scattering is predominately a direct reaction involving quasi-elastic collisions with one or more target nucleons. We discuss various aspects of quasi-elastic scattering which are important in understanding features of cross sections and spin observables. These include (1) contributions from multi-step processes; (2) damping of the continuum response from 2p-2h excitations; (3) the optimal choice of frame in which to evaluate the nucleon-nucleon amplitudes; and (4) the effect of optical and spin-orbit distortions, which are included in a model based on the RPA the DWIA and the eikonal approximation. DOE

N88-26933# Aerospace Corp., El Segundo, Calif. Aerophysics Lab.
NASCENT VIBRATIONAL/ROTATIONAL DISTRIBUTION PRODUCED BY HYDROGEN ATOM RECOMBINATION
A. O. Woodin 1 Feb. 1988 26 p
(Contract F04701-85-C-0086)
(AD-A193005; TR-0086A(2930-02)-1; SD-TR-87-61) Avail: NTIS HC A03/MF A01 CSCL 20E

The nascent vibrational/rotational distribution produced by the reaction H + H + H yields H2(v, J) + H is calculated using resonance complex theory. The calculations are performed using the accurate Siegbahn-Liu-Truhlar-Horowitz surface. Results are presented for the dependence of the total recombination rate coefficient on temperature, and specific rate coefficients into individual vibrational/rotational states. GRA

N88-26934# California Univ., Berkeley. Lawrence Berkeley Lab.
DEVELOPMENT OF HIGH CURRENT AND HIGH BRIGHTNESS NEGATIVE HYDROGEN ION SOURCES
K. N. Leung Apr. 1988 21 p Presented at the 7th International Conference on Ion Implantation Technology, Kyoto, Japan, 7 Jun. 1988
(Contract DE-AC03-76SF-00098)
(DE88-010882; LBL-24686; CONF-880614-1; CONF-880614) Avail: NTIS HC A03/MF A01

Negative hydrogen ions have found important applications in particle accelerators and in fusion research. These ions can be generated from two different types of ion sources, the surface conversion source and the volume production source. Recent experiments demonstrate that H(-) current exceeding 1 A can be obtained from both types of ion sources. Because of the lower H(-) ion temperature and the fact that they can be operated without cesium, volume H(-) sources are highly desired. However, further technology must be developed on the control of electrons and the reduction of gas flow before these types of sources become practical units of a multiampere neutral beam injection system. DOE

73 NUCLEAR AND HIGH-ENERGY PHYSICS

Includes elementary and nuclear particles; and reactor theory.

For space radiation see *93 Space Radiation.*

N88-26935*# National Aeronautics and Space Administration. Langley Research Center, Hampton, Va.
NUCLEON-NUCLEUS INTERACTION DATA BASE: TOTAL NUCLEAR AND ABSORPTION CROSS SECTIONS
J. W. Wilson, L. W. Townsend, W. W. Buck, S. Y. Chun, B. S. Hong, and S. L. Lamkin (Planning Research Corp., Hampton, Va.) Aug. 1988 26 p
(NASA-TM-4053; L-16461; NAS 1.15:4053) Avail: NTIS HC A03/MF A01 CSCL 20H

Neutron total cross sections are represented for Li to Pu targets at energies above 0.1 MeV and less than 100 MeV using a modified nuclear Ramsauer formalism. The formalism is derived for energies above 100 MeV by fitting theoretical cross sections. Neutron absorption cross sections are represented by analytic expressions of similar form, but shape resonance phenomena of the Ramsauer effect is not present. Elastic differential cross sections are given as a renormalized impulse approximation. These cross section data bases are useful for nucleon transport applications. Author

N88-26936# Continuous Electron Beam Accelerator Facility, Newport New, Va.
SUPERCONDUCTING RF AND BEAM-CAVITY INTERACTIONS
J. J. Bisognano 1987 13 p
(Contract DE-AC05-84ER-40150)
(DE88-008598; DOE/ER-40150/46; CEBAF-PR-88-004) Avail: NTIS HC A03/MF A01

Beam-cavity interactions can limit the beam quality and current handling capability of linear and circular accelerators. These collective effects include cumulative and regenerative transverse beam breakup (BBU) in linacs, transverse multipass beam breakup in recirculating linacs and microtrons, longitudinal and transverse coupled-bunch instabilities in storage rings, and a variety of transverse and longitudinal single-bunch phenomena (instabilities, beam breakup, and energy deposition). The superconducting radio frequency (SRF) environment has a number of features which distinguish it from room temperature configuration with regard to these beam-cavity interactions. Typically the unloaded Qs of the lower Higher Order Modes (HOM) are at the 10 to the 9th level and require significant damping through couplers. High gradient

CW operation, which is a principal advantage of SRF, allows for better control of beam quality, which for its preservation requires added care which respect to collective phenomena. Gradients are significantly higher than those attainable with copper in CW operation but remain significantly lower than those obtainable with pulsed copper cavities. Finally, energy deposition by the beam into the cavity can occur in a cryogenic environment. In this note those characteristics of beam-cavity interactions which are of particular importance for superconducting RF cavities are highlighted. DOE

N88-26937# California Univ., Berkeley. Lawrence Berkeley Lab.
ENHANCEMENT OF VOLUME H(-) PRODUCTION BY VIBRATIONALLY PRE-EXCITING THE HYDROGEN MOLECULES
K. N. Leung, S. R. Walther, and W. B. Kunkel Feb. 1988 7 p Presented at the 3rd European Workshop on Production and Applications of Light Negative Ions, Amersfoort, Netherlands, 17 Feb. 1988
(Contract DE-AC03-76SF-00098)
(DE88-010783; LBL-24452; CONF-880256-4) Avail: NTIS HC A02/MF A01

H(-) and D(-) ions have useful applications in high-energy accelerators and in neutral beam heating, or for current drive of fusion plasmas. Among the different techniques for producing H(-) ions, direct extraction from a hydrogen discharge is the most attractive. This method requires no cesium and the H(-) ions generated by volume processes have lower average energy than those formed by surface conversion or by charge exchange processes. For this reason, intensive research and development of volume H(-) sources are now being conducted at various accelerator and fusion laboratories. DOE

N88-26938# Fermi National Accelerator Lab., Batavia, Ill.
Rf CAVITY PRIMER FOR CYCLIC PROTON ACCELERATORS
J. E. Griffin Apr. 1988 37 p Presented at the 4th INFN ELOISATRON Project Workshop: Very High Energy Proton-Proton Physics, Erice, Italy, 31 May 1987
(Contract DE-AC02-76CH-03000)
(DE88-010655; FNAL-TM-1519; CONF-8705291) Avail: NTIS HC A03/MF A01

The electrical and mechanical properities of particle accelerator rf cavities are described in a manner which will be useful to physics and engineering graduates entering the accelerator field. The discussion is limited to proton (or antiproton) synchrotron accelerators or storage rings operating roughly in the range of 20 to 200 MHz. The very high gradient, fixed frequency UHF or microwave devices appropriate for electron machines and the somewhat lower frequency and broader bandwidth devices required for heavy ion accelerators are discussed extensively in other papers in this series. While it is common practice to employ field calculation programs such as SUPERFISH, URMEL, or MAFIA as design aids in the development of rf cavities, we attempt here to elucidate various of the design parameters commonly dealt with in proton machines through the use of simple standing wave coaxial resonator expressions. In so doing, we treat only standing wave structures. Although low-impedance, moderately broad pass-band travelling wave accelerating systems are used in the CERN SPS, such systems are more commonly found in linacs, and they have not been used widely in large cyclic accelerators. Two appendices providing useful supporting material regarding relativistic particle dynamics and synchrotron motion in cyclic accelerators are added to supplement the text. DOE

N88-26939# Los Alamos National Lab., N. Mex.
MILLIWATT GENERATOR PROJECT Progress Report, Apr. 1983 - Mar. 1984
G. H. Rinehart and T. W. Latimer May 1988 27 p
(Contract W-7405-eng-36)
(DE88-011261; LA-11220-PR) Avail: NTIS HC A03/MF A01

This report covers progress on the Milliwatt Generator Project during April 1983--March 1984. Activities included plutonium 238 oxide fuel processing and characterization, production of heat sources, fabrication of pressure-burst test units, compatibility studies, impact testing, examination of surveillance units, Inconel weld development, and quality assurance. DOE

N88-26940# Institut National Polytechnique, Grenoble (France).
SIMULATION OF THE NEUTRONIC CHARACTERISTICS OF LARGE FAST NEUTRON REACTORS Ph.D. Thesis [SIMULATION DES CARACTERES NEUTRONIQUES DES RNR DE GRANDE TAILLE]
Young-Cheol Kim 1987 234 p In FRENCH
(ETN-88-92305) Avail: NTIS HC A11/MF A01

An experimental program was designed to estimate critical parameters of fast nuclear reactors. Almost 2000 kg of plutonium will be employed. The parameters studied include the reactivity of the control bars, the neutron flow distribution, and the validation of the computation methods. The detailed definition of the experimental set-up is discussed. ESA

74 OPTICS

Includes light phenomena; and optical devices.
For lasers see *36 Lasers and Masers.*

N88-26941*# Stanford Univ., Calif. Center for Space Science and Astrophysics.
THE EVALUATION OF A DEFORMABLE DIFFRACTION GRATING FOR A STIGMATIC EUV SPECTROHELIOMETER Progress Report, 1 Dec. 1987 - 31 May 1988
J. G. Timothy 21 Jul. 1988 7 p
(Grant NAGw-540)
(NASA-CR-183064; NAS 1.26:183064) Avail: NTIS HC A02/MF A01 CSCL 20F

The primary activities of the development program were the preparations for the detailed laboratory tests of the first two toroidal gratings, and the initial tests in the optical laboratory of the more complex elastically deformable substrate for the fabrication of aspheric gratings. Author

N88-26942# Sandia National Labs., Albuquerque, N. Mex.
A NEW APPROACH TO MACHINE-BASED PERCEPTION OF MONOCULAR IMAGES
G. C. Osbourn 1988 31 p Presented at the IEEE Computer Society Conference on Computer Vision and Pattern Recognition, Ann Arbor, Mich., 5 Jun. 1988
(Contract DE-AC04-76DP-00789)
(DE88-002418; SAND-87-2728C; CONF-880637-1) Avail: NTIS HC A03/MF A01

A new approach to machine-based visual perception of monocular images is presented and demonstrated. The approach employs a recursive procedure to generate a series of reconstructed versions of the raw video image. The procedure is designed to imitate certain perceptual organization functions of the human visual system. Recognition of object categories is attempted at each step by comparing the newly generated regions to stored object categories. These generated regions may have relatively few edges or region pixels in common with any of the regions in the raw video image. Category retrieval is carried out using a software-based content-addressing scheme which provides access to complete object representations in memory using incomplete portions of the representation. The category representation scheme is sufficiently general to allow a variety of poorly correlated images of specific category examples to be represented and recognized by a single general category representation. These properties are illustrated using a group of distorted, defective and idealized images of ascii A's and handguns. DOE

N88-26943# Los Alamos National Lab., N. Mex.
USE OF FIBER OPTIC EQUIPMENT FOR SECURITY
R. W. Schalm 1988 6 p Presented at the Carnahan Conference, Lexington, Ky., 1 May 1988

(Contract W-7405-eng-36)
(DE88-007898; LA-UR-88-798; CONF-880584-1) Avail: NTIS HC A02/MF A01

This paper discusses the many applications of fiber optics equipment. DOE

N88-26944# Hughes Aircraft Co., Long Beach, Calif. Advanced Products Lab.
VISIBLE TUNABLE SOURCE
Oct. 1987 60 p
(Contract DE-FG03-85ER-13448)
(DE88-006442; DOE/ER-13448/T3) Avail: NTIS HC A04/MF A01

We planned four tasks for the second phase of this project; these are: study the effect of different grating materials; study the effect of different grating shapes; study the effect of anisotropic conductivity, and optimize the resonator configuration. Because the measurement techniques involved in the first two tasks are similar, the studies on different grating materials and shapes are discussed together. We are conducting two more experiments which were not originally planned. An experiment with a high current pulsed e-beam generator is presented and a measurement of radiation as a function of beam thickness is reported. DOE

N88-26945# Edgerton, Germeshausen and Grier, Inc., Los Alamos, N. Mex.
AN OVERVIEW OF THE DEVELOPMENT OF A LINEAR BROADBAND ANALOG FIBER-OPTIC LINK
R. L. Ramsey 1988 24 p Presented at the DOD Fiber-optics Conference, McLean, Va., 22 Mar. 1988
(Contract DE-AC08-88NV-10617)
(DE88-008668; CONF-880384-1) Avail: NTIS HC A03/MF A01

Data recording requirements for SDI and nuclear weapons tests have increased the demands placed on analog data links. The development of a low-distortion, 100-MHz fiber-optic link for these applications is described. DOE

N88-26946# Lawrence Livermore National Lab., Calif.
OPTICAL CHARACTERIZATION OF SILICA AEROGEL
L. W. Hrubesh and C. T. Alviso Mar. 1988 6 p Presented at the Spring Meeting of the Materials Research Society, Reno, Nev., 4 Apr. 1988
(Contract W-7405-eng-48)
(DE88-008916; UCRL-97327; CONF-880408-13) Avail: NTIS HC A02

Two optical methods are described for mapping the local variations of refractive index within monoliths of porous silica aerogel. One is an interferometric measurement that produces iso-index fringes in a two-dimensional image; an orthogonal view gives the third dimension information. The other method uses the deflection of a He-Ne laser beam to map the gradient index within a sample. The quantification of the measurements is described and the accuracy of the results is discussed. DOE

N88-26947# Brookhaven National Lab., Upton, N. Y.
IN-SITU REACTIVE OF X-RAY OPTICS BY GLOW DISCHARGE
E. D. Johnson and R. F. Garrett 1987 17 p Presented at the 5th National Synchrotron Radiation Instrumentation Conference, Madison, Wis., 21 Jun. 1987
(Contract DE-AC02-76CH-00016)
(DE88-009840; BNL-41167; CONF-870610-22) Avail: NTIS HC A03/MF A01

We have developed a method of in-situ reactive glow discharge cleaning of X-ray optical surfaces which is capable of complete removal of carbon contamination. Our work is the first to successfully clean an entire optical system in-situ and characterize its performance at short wavelengths (as low as 10 angstroms). The apparatus required is quite simple and can easily be fitted to most existing UHV (Ultra High Vacuum) mirror boxes of monochromators. The advantages of this technique over previously available methods include dramatic improvements in instrument performance and reductions in down time since the whole process typically takes a few days. This paper will briefly describe our results and detail the experimental considerations for application of the technique on different monochromator geometries. Possible improvements and extensions of the technique are also discussed. DOE

N88-26948# Rochester Univ., N. Y. Lab. for Laser Energetics.
LIQUID CRYSTAL OPTICS FOR LASER SYSTEMS
S. D. Jacobs, K. A. Cerqua, K. L. Marshall, A. Schmid, M. J. Guardalben, and K. J. Skerrett Jan. 1988 32 p Presented at SPIE O-E Lase '88: Optoelectronics and Laser Applications in Science and Engineering, Los Angeles, Calif., 10 Jan. 1988
(Contract DE-FC08-85DP-40200)
(DE88-008475; DOE/DP-40200/66; CONF-880110-29) Avail: NTIS HC A03

We present an overview of the development of laser optics utilizing liquid crystals. Devices discussed include wave plates, circular polarizers, optical isolators, laser blocking notch filters and laser beam apodizers. Issues addressesed include fabrication methods and laser damage resistance. DOE

N88-26949# Los Alamos National Lab., N. Mex.
STRESS-RELATED PHENOMENA IN TRANSIENT RADIATION-INDUCED ABSORPTION IN OPTICAL FIBERS
L. D. Looney, P. B. Lyons, and R. E. Kelly 1988 12 p Presented at the OPTO '88, Paris, France, 17 May 1988
(Contract W-7405-eng-36)
(DE88-010956; LA-UR-88-1458; CONF-8805121-1; CONF-8805121) Avail: NTIS HC A03/MF A01

The optical properties of materials can be modified by exposure to radiation. Research to investigate these radiation-induced phenomena has intensified over the last several decades. The advent of optical fiber technology and the many applications of optical fiber for information transmission have sharply increased the interest in these investigations. Optical fibers present a long optical transmission path and that path may traverse different adverse environments, including radiation areas. The long transmission path provides increased potential for interactions between the optical information signal and the optical medium. DOE

N88-26950# Litton Systems, Inc., Van Nuys, Calif. Data Systems Div.
OPTICAL CORRELATION USING THE MAGNETO-OPTIC DEVICE Final Technical Report, Oct. 1985 - Feb. 1987
William E. Ross Dec. 1987 41 p
(Contract F08635-85-C-0137)
(AD-A192342; AD-E801594; AFATL-TR-87-26) Avail: NTIS HC A03/MF A01 CSCL 17E

This report describes binary filters and applications of the Magneto-Optic Device (MOD) to pattern recognition. Three issues concerning use of the MOD in pattern recognition are reported herein: (1) the use of the MOD as an input device and as a spatial filter in a Vander Lugt correlator; (2) algorithms to generate binary filters for multiple images recognition; (3) the use of MOD for multiple bit-slice correlations. GRA

N88-26951# Technische Univ., Berlin (West Germany). Fachbereich fuer Elektrotechnik.
EXCITATION OF SINGLE-MODE GLASS FIBER BY PARTIALLY COHERENT SOURCES Ph.D. Thesis [DIE ANREGUNG EINWELLIGER GLASFASERN DURCH QUELLEN BELIEBIGER KOHAERENZ]
Bernd Hillerich 1987 155 p In GERMAN
(ETN-88-92121) Avail: NTIS HC A08/MF A01

Coherent light sources for single mode glass fibers on distances up to 10 km luminescence diodes are shown to be more appropriate than semiconductor laser diodes. Mathematical models are given for the computation of coherence function of partially coherent sources like luminescence diodes. The coupling efficiency between radiation source and monomode fibers with or without optical coupling is studied. Comparison of results between numerical simulation and measured coupling efficiency is concordant. ESA

N88-26952# Cologne Univ. (West Germany). Mathematisch-Naturwissenschaftlichen Fakultaet.
GROUND LEVEL HYDROXYL (OH) CONCENTRATION MEASUREMENTS BY LONG PATH DIFFERENTIAL OPTICAL LASER ABSORPTION Ph.D. Thesis [MESSUNG DER BODENNAHEN HYDROXYL-(OH)-KONZENTRATION MITTELS DIFFERENTIELLER OPTISCHER LASERLANGFADABSORPTION]
Gerhard Huebler 1987 95 p In GERMAN
(ETN-88-92124) Avail: NTIS HC A05/MF A01

Optical long path absorption spectroscopy is studied for the measurement of trophospheric hydroxyl (OH) concentrations in the range 500,000 to 2.6 million OH molecules/CC. A laser light source provides UV radiation emitted in the free atmosphere by mirror reflection on a determined measurement length. Spectral scattering is examined in the OH band lines region. Atmospheric effects like intensity oscillations due to turbulence are avoided by the rapid determination of 160 microsec. ESA

N88-26953# Erlangen-Nuremberg Univ. (West Germany). Naturwissenschaftlichen Fachbereichen.
DIGITAL IMAGE PROCESSING FROM SPECKLE INTERFEROGRAMS BY CORRELATION METHODS: APPLICATION IN ATMOSPHERIC OPTICS, ASTRONOMY, AND BIOLOGY Ph.D. Thesis [DIGITALE BILDVERARBEITUNG VON SPECKLE-INTERFEROGRAMMEN DURCH KORRELATIONSMETHODEN: ANWENDUNGEN IN ATMOSPHAERISCHER OPTIK, ASTRONOMIE UND BIOLOGIE]
Johannes Ebersberger 1986 77 p In GERMAN
(ETN-88-92125) Avail: NTIS HC A05/MF A01

Statistical and optical properties of speckle interferometry by selected measurement methods are studied and used in three applications: in atmospheric optics for the determination of various parameters of astronomical speckle interferograms like speckle lifetime and isoplanatism grade; in astronomy for the elimination of atmospheric image disturbances and the determination of mass-to-light ratios; in biology for the motion measurement of microorganisms. Digital space-time cross correlation analyses are performed for the digital processing of bidimensional information of speckle interferograms. ESA

N88-26954# Physics and Electronics Lab. TNO, The Hague (Netherlands).
DESCRIPTION OF THE MPTR SYSTEM: MULTI PATH TRANSMISSOMETER RADIOMETER Final Report
A. N. deJong and M. J. J. Roos Mar. 1987 67 p
(FEL-1987-14; ETN-88-92568) Avail: NTIS HC A04/MF A01

A multipath transmissometer radiometer system which enables the measurement of transmittance and emittance values along 12 lines of sight in 4 spectral bands over a field of view of 60 deg simultaneously through smoke clouds/obscurants under investigation was developed. The system proves to be successful during tests, and gives the smoke-developer and evaluator quick data upon the smoke screens. ESA

N88-26955# Lawrence Livermore National Lab., Calif.
FABRICATION TECHNOLOGY
May 1988 31 p
(Contract W-7405-eng-48)
(DE88-010598; UCID-21391) Avail: NTIS HC A03/MF A01

Many laboratory programs continue to need optical components of ever-increasing size and accuracy. Unfortunately, optical surfaces produced by the conventional sequence of grinding, lapping, and polishing can become prohibitively expensive. Research in the Fabrication Technology area focuses on methods of fabricating components with heretofore unrealized levels of precision. In FY87, researchers worked to determine the fundamental mechanical limits of material removal, experimented with unique material removal and deposition processes, developed servo systems for controlling the geometric position of ultraprecise machine tools, and advanced the ability to precisely measure contoured workpieces. Continued work in these areas will lead to more cost-effective processes to fabricate even higher quality optical components for advanced lasers and for visible, ultraviolet, and X-ray diagnostic systems. DOE

N88-27005# Corning Glass Works, N.Y. Research and Development Lab.
SEMICONDUCTOR MICROCRYSTALLITES IN POROUS GLASS AND THEIR APPLICATIONS IN OPTICS Abstract Only
John C. Luong *In* Illinois Univ., Third International Conference on Superlattices, Microstructures and Microdevices 1987 p 21 (For primary document see N88-26995 20-76)
Avail: NTIS HC A08/MF A01 CSCL 20F

N88-27025# Arizona Univ., Tucson. Dept. of Physics.
PROPERTIES OF MULTILAYERS FOR SOFT X-RAY OPTICS Abstract Only
Charles M. Falco and Felix E. Fernandez *In* Illinois Univ., Third International Conference on Superlattices, Microstructures and Microdevices 1987 p 41 (For primary document see N88-26995 20-76)
(Contract F49620-85-C-0039; Grant AF-AFOSR-0347-86)
Avail: NTIS HC A08/MF A01 CSCL 20F

75 PLASMA PHYSICS

Includes magnetohydrodynamics and plasma fusion.
For ionospheric plasmas see *46 Geophysics*. For space plasmas see *90 Astrophysics*.

N88-26956# Nagoya Univ. (Japan). Inst. of Plasma Physics.
SYMMETRIZED MAGNETIC FIELD CONFIGURATION OF LOW ASPECT RATIO HELICAL SYSTEM
Kiyohiko Nishimura and Masami Fujiwara May 1988 17 p
(IPPJ-869; ISSN-0469-4732) Avail: NTIS HC A03/MF A01

A helical system has the attractive feature such that it can generate the closed magnetic surface by externally wound coils alone. However, there are many problems to be solved for the confinement of a reactor grade plasma in helical systems. A new method is proposed for coil width modulation (modulation of the helical coil current distribution) to meet with the requirement for the magnetic configuration of a high temperature plasma confinement. This method can reduce multi-helicity (higher or satellite harmonics of the fundamental helical field) which brings many demerits into the conventional stellerator/torsatron/heliotron configuration. Author

N88-26957# Nagoya Univ. (Japan). Inst. of Plasma Physics.
PROCEEDINGS OF THE 2ND US-JAPAN WORKSHOP ON ADVANCED PLASMA MODELING, VOLUME 3
Apr. 1988 51 p Workshop held in Nagoya, Japan, 23-27 Mar. 1987
(IPPJ-867; ISSN-0469-4732) Avail: NTIS HC A04/MF A01

Topics addressed include: mass electron model for plasma simulations and modeling of kinetic processes in plasma simulation. For individual titles, see N88-26958 through N88-26959.

N88-26958# California Univ., Los Angeles. Dept. of Physics.
A VLASOV ION ZERO MASS ELECTRON MODEL FOR PLASMA SIMULATIONS
John M. Dawson and F. Kazeminezhad *In* Nagoya Univ., Proceedings of the 2nd US-Japan Workshop on Advanced Plasma Modeling, Volume 3 Apr. 1988 23 p (For primary document see N88-26957 20-75)
Avail: NTIS HC A04/MF A01

A model which treated ions as fluid elements and electrons as a massless fluid is presented. It is shown how the two and three dimensional versions of the code predicted most of the MHD waves and their excellent agreements with the linear analytic predictions. The model was generalized to include kinetic effects rather than simply treating them as a fluid. B.G.

N88-26959# California Univ., Los Angeles. Dept. of Physics.
MODELING OF SUBTLE KINETIC PROCESSES IN PLASMA SIMULATION
Richard D. Sydora, Viktor K. Decyk, and John M. Dawson *In* Nagoya Univ., Proceedings of the 2nd US-Japan Workshop on Advanced Plasma Modeling, Volume 3 Apr. 1988 25 p (For primary document see N88-26957 20-75)
Avail: NTIS HC A04/MF A01

A diagnostic method for plasma simulation models is presented which enables one to probe the subtle dielectric properties of the plasma medium. The procedure involves the removal of the background plasma response in order to isolate the effects of small perturbing influences which are externally added. It was found that the technique accurately describes fundamental kinetic plasma behavior such as the shielding of individual test charges and currents. Wave emission studies and drag of test particles was performed in explicit particle algorithms as well as large time step implicit and gyrokinetic models. Accurate plasma behavior is produced and it is possible to investigate in detail, processes which can be compared with plasma kinetic theory. The technique of subtraction is not only limited to particle simulation models but also can be used in MHD or fluid models where resolution is difficult due to the intensity of the background response relative to the phenomena one is interested in measuring, such as a weakly growing instability or nonlinear mode coupling effect. Author

N88-26960# Sandia National Labs., Albuquerque, N. Mex.
FIELD-ENHANCED LITHIUM ION SOURCES FOR PBFA 2
R. W. Stinnett, R. E. Olson, J. O. Dritt, K. W. Bieg, R. A. Gerber, P. F. McKay, J. A. Panitz, A. L. Pregenzer, and J. R. Woodworth 1988 9 p Presented at the 13th International Symposium on Discharges and Electrical Insulation in Vacuum, Paris, France, 27 Jun. 1988
(Contract DE-AC04-76DP-00789)
(DE88-007195; SAND-88-0625C; CONF-880687-2) Avail: NTIS HC A02/MF A01

Inertial Confinement Fusion (ICF) experiments at 30 MeV on the Particle Beam Fusion Accelerator (PBFA) 2 at Sandia National Laboratories will require the use of high intensity, high purity beams of singly ionized lithium ions. One approach which is being tested to produce such beams is the use of field-enhanced lithium ion sources. We have identified several ion production mechanisms which may be active in this source. DOE

N88-26961# Sandia National Labs., Albuquerque, N. Mex.
AN ELLIPTICAL SPECTROGRAPH/GATED MICROCHANNEL PLATE DETECTOR FOR TIME-RESOLVED SPECTRAL MEASUREMENTS IN THE X-RAY REGION
B. A. Hammel and L. E. Ruggles 1988 17 p Presented at the 7th Topical Conference on High Temperature Plasma Diagnostics, Napa, Calif., 13 Mar. 1988
(Contract DE-AC04-76DP-00789)
(DE88-007590; SAND-87-3084C; CONF-880364-6) Avail: NTIS HC A03/MF A01

Time-resolved measurements from an elliptical crystal spectrograph are used to diagnose X-ray laser experiments on a gas puff Z-pinch. The elliptical spectrograph (1.2 m working distance, eccentricity = 0.9586) observes the 1 keV region, covering a range of lambda/2d = 0.5 - 0.9. A thin filter (0.2 micron Al on 2 micron Kimfol) stretched across the spectrograph exit slit acts as a low energy x-ray cutoff and as a vacuum window, allowing the detector to be at high vacuum regardless of the pressure in the experimental chamber. The detector consists of a 7-frame microchannel plate intensifier system. A pulser is used to gate each of 7 striplines on the microchannel plate, providing nanosecond resolution. With this instrument we are able to measure the pump radiation from the imploding plasma (Ne or Ar) and converter layer (Al), and to study the lasant ionization state (Ne-like Ni or Cu). DOE

N88-26962# Oak Ridge National Lab., Tenn. Fusion Engineering Design Center.
THERMAL AND MECHANICAL ANALYSIS OF THE FARADAY SHIELD FOR THE COMPACT IGNITION TOKAMAK
R. A. Vesey Feb. 1988 40 p
(Contract DE-AC05-84OR-21400)
(DE88-007855; ORNL/FEDC-87/5) Avail: NTIS HC A03/MF A01

The antenna for the Ion Cyclotron Resonance Heating (ICRH) system of the Compact Ignition Tokamak (CIT) is protected from the plasma environment by a Faraday shield, an array of gas-cooled metallic tubes. The plasma side of the tubes is armored with graphite tiles, which can be either brazed or mechanically attached to the tube. The Faraday shield has been analyzed using finite element codes to model thermal and mechanical responses to typical CIT heating and disruption loads. Four representative materials (Inconel 718, tantalum-10 tungsten, copper alloy C17510, and molybdenum alloy TZM) and several combinations of tube and armor thicknesses were used in the thermal analysis, which revealed that maximum allowable temperatures were not exceeded for any of the four materials considered. The 2-D thermal stress analysis indicated Von Mises stresses greater than twice the yield stress for a tube constructed of Inconel 718 (the original design material) for the brazed-graphite design. Analysis of stresses caused by plasma disruption (rvec J X rvec B) loads eliminated the copper and molybdenum alloys as candidate tube materials.Of the four materials considered, tantulum-10 tungsten performed the best for a brazed graphite design, showing acceptable thermal stresses (69 percent of yield) and disruption stresses (42 percent of yield). A preliminary thermal analysis of the mechanically attached graphite scheme predicts minimal thermal stresses in the tube. The survivability of the graphite tubes in this scheme is yet to be analyzed. DOE

N88-26963# General Atomic Co., San Diego, Calif.
POLOIDAL FIELD MEASUREMENTS USING LASER ENHANCED ATTENUATION OF AN ENERGETIC LITHIUM BEAM
W. P. West, D. M. Thomas, and M. P. Thomas Feb. 1988 13 p Presented at the 7th Topical Conference, on High Temperature Plasma Diagnostics, Napa, Calif., 13 Mar. 1988
(Contract DE-AC03-84ER-53158)
(DE88-008360; GA-A-19217; CONF-880364-18) Avail: NTIS HC A03/MF A01

The current density profile diagnostic system presently operating on the Texas Experimental Tokamak (TEXT) employs a cw dye laser system to induce fluorescence in a lithium beam injected into the discharge. Systematic effects due to the finite lifetime of the excited state and enhancement of the beam attenuation during laser excitation limit the application of this technique to plasma densities approx lt 1 times 10 to the 13/cu cm cm sup minus 3. Laser enhancement of beam attenuation results from the large collisional ionization cross sections of the excited Li 2P state compared to the 2S ground state. This effect is exploited in a new diagnostic scheme which uses the polarization modulation of the present technique, but monitors the enhanced attenuation as opposed to the fluorescence. Detailed modeling indicates that a collinear beams configuration, with a short pulse laser and time of flight signal analysis, will provide a measurement of the complete poloidal field profile on TEXT at plasma densities up to 3 times 10 to the 13/cu cm sup minus 3 with 16 ms averaging times. DOE

N88-26964# General Atomic Co., San Diego, Calif.
FUSION PROGRAMS IN APPLIED PLASMA PHYSICS AND DEVELOPMENT AND TECHNOLOGY AT GA TECHNOLOGIES, INC. Annual Report, Fiscal Year 1987
D. O. Overskei Jan. 1988 89 p
(Contract DE-AC03-84ER-53158)
(DE88-008406; GA-A-19100) Avail: NTIS HC A05/MF A01

Research carried out by GA for the Department of Energy Office of Fusion Energy provides key information and insight necessary for the development of fusion power systems. Highlights

of the fusion theory effort described in this report include progress in numerical simulations of turbulent transport in tokamak plasmas, extension of novel theories of the H-mode, development and application of advanced codes for evaluating ECRF current drive efficiency, and new understanding and techniques for dealing with high beta tokamak equilibria. Experimental plasma research efforts are addresssing several important issues in fusion research. Neutron and alpha particle spectroscopy and triton confinement diagnostics are being developed to enable fusion researchers to understand alpha particle confinement and slowdown in burning plasmas. Development of Li beam diagnostic systems continued and has shown a capability for measuring both magnetic field pitch angle and relative current density profiles. Experiments on Ergodic Magnetic Divertor (EMD) phenomena on the Texas Experimental Tokamak (TEXT) continued to demonstrate low plasma edge temperatures and impurity reduction that make the concept attractive for reactor applications. GA led efforts continuing the Resonant Island Divertor (RID) experiments on TEXT using the EMD as a controlled magnetic perturbation. Research carried out in GA's Development and Technology programs included reactor systems design studies, and development of ferritic steels suitable for use as a structural material in fusion reactors. In the reactor systems design area, GA participated in the TITAN Reserved Field Pinch (RFP) Reactor Design Study. GA is responsible for project operation, safety design and analysis, and blanket shield neutronics calculations for this study. DOE

N88-26965# Oak Ridge National Lab., Tenn.
A CO2 LASER THOMSON SCATTERING DIAGNOSTIC FOR FUSION PRODUCT ALPHA PARTICLE MEASUREMENT
R. K. Richards, C. A. Bennett, L. K. Fletcher, H. T. Hunter, and D. P. Hutchinson 1988 13 p Presented at the 7th Topical Conference on High Temperature Plasma Diagnostics, Napa, Calif., 13 Mar. 1988
(Contract DE-AC05-84OR-21400)
(DE88-007683; CONF-880364-13) Avail: NTIS HC A03/MF A01

A description of a CO2 laser Thomson scattering diagnostic for fusion alpha particles is presented. Scattering calculations based on CIT plasma parameters are presented and compared to previous work based on TFTR parameters. Systems components are described and a proof-of-principle test in a nonburning plasma is discussed. DOE

N88-26966# General Atomic Co., San Diego, Calif.
OVERVIEW OF THE TITAN-2 REVERSED-FIELD PINCH AQUEOUS FUSION POWER CORE DESIGN
C. P. C. Wong, R. L. Creedon, S. Grotz, E. T. Cheng, S. Sharafat, and P. I. H. Cooke Mar. 1988 15 p Presented at the International Symposium on Fusion Nuclear Technology, Tokyo, Japan, 10 Apr. 1988 Prepared in cooperation with California Univ., Los Angeles
(Contract DE-AC03-84ER-53158)
(DE88-008170; GA-A-19239; CONF-880417-6) Avail: NTIS HC A03/MF A01

TITAN-2 is a compact, high power density Reversed-Field Pinch fusion power reactor design based on the aqueous lithium solution fusion power core concept. The selected breeding and structural materials are LiNO3 and 9-C low activation ferritic steel, respectively. TITAN-2 is a viable alternative to the TITAN-1 lithium self-cooled design for the Reversed-Field Pinch reactor to operate at a neutron wall loading of 18 MW/sq m. Submerging the complete fusion power core and the primary loop in a large pool of cool water will minimize the probability of radioactivity release. Since the protection of the large pool integrity is the only requirement for the protection of the public, TITAN-2 is a passive safety assurance design. DOE

N88-26967# Lawrence Livermore National Lab., Calif.
PLASMA ARMATURE FORMATION IN HIGH-PRESSURE, HIGH-VELOCITY HYDROGEN
R. S. Hawke, A. R. Susoeff, J. R. Asay, C. A. Hall, C. H. Konrad, R. J. Hickman, and J. L. Sauve 1 Mar. 1988 5 p Presented at the 4th Symposium on Electromagnetic Launch Technology, Austin, Tex., 12 Apr. 1988 Prepared in cooperation with Sandia National Labs., Albuquerque, N. Mex., Ktech Corp., Albuquerque, N. Mex. and Edgerton, Germeshausen and Grier, Inc., Albuquerque, N. Mex.
(Contract W-7405-eng-48)
(DE88-008347; UCRL-97385; CONF-880478-11) Avail: NTIS HC A02/MF A01

The use of a two-stage light-gas gun (2SLGG) as a preaccelerator in combination with a railgun is expected to significantly reduce barrel ablation and improve overall performance. In particular, the use of a hydrogen 2SLGG provides injection velocities of 6 to 8 km/s and a pure hydrogen environment immediately behind the projectile as it enters a railgun. To continue acceleration of the projectile, a plasma armature must be formed. We explored two methods of converting a portion of the fast-moving hydrogen gas into a plasma armature capable of supporting currents exceeding 100 kA. We report on the results of these studies. This work is part of STARFIRE, the joint Sandia National Laboratories/Lawrence Livermore National Laboratory project to develop a hypervelocity railgun. DOE

N88-26968# Colorado Univ., Boulder.
NEOCLASSICAL DIFFUSION DUE TO TRAPPING/DETRAPPING ORBITS IN STELLARATORS Annual Progress Report, 15 Sep. 1987 - 14 Sep. 1988
J. R. Cary Mar. 1988 38 p
(Contract DE-FG02-85ER-53207)
(DE88-008566; DOE/NE-53207/T1) Avail: NTIS HC A03/MF A01

In the last funding year significant progress was made in understanding the orbits of charged particles in stellarators and rippled tokamaks. Averaged equations of motion were derived for the invariants found in previous work. The first-order corrections to the ripple-averaged invariants were found. A code for testing the analytical theory was developed. The phase change between successive separatrix crossings was derived. A code for testing the effect of quantum quenching of the separatrix crossing induced spreading of the adiabatic invariant was nearly completed. The completed work allows significant savings in computer time for Monte Carlo codes. It will also reduce the dimensionality of linearized collision operator theory. DOE

N88-26969# General Atomic Co., San Diego, Calif.
MULTIPOINT THOMSON SCATTERING DIAGNOSTIC FOR DIII-D
C. L. Hsieh, R. Chase, J. C. DeBoo, R. G. Evanko, P. Gohil, R. T. Snider, and R. E. Stockdale Feb. 1988 14 p Presented at the 7th Topical Conference on High Temperature Plasma Diagnostics, Napa, Calif., 13 Mar. 1988
(Contract DE-AC03-84ER-51044)
(DE88-008737; GA-A-19192; CONF-880364-19) Avail: NTIS HC A03/MF A01

The multipoint Thomson scattering diagnostic for DIII-D has been in operation since early 1987. Its capability of measuring electron temperatures as low as 50 eV at densities of a few times 10 to the 12th/cu cm and a spatial resolution of 1.4 cm in the plasma edge region has been essential in the study of H-mode plasmas. The major components of the diagnositc system consist of a 10-J ruby laser, many stages of funnel shaped beam baffles, stacks of razor blades for viewing and stray light dumps, two wide-angle lenses for the collection of scattered light through re-entrant window ports with protection shutters, 88 fiber bundles 15 m in length for light transmission to an focal length/1.9 spectrometer, an intensified CCD camera system capable of single photon detection, and a VAX computer for hardware control and data processing. The input end of the fiber bundle is made demountable so the view locations can be reconfigured to optimize the spatial resolution for the plasma region of interest. DOE

N88-26970# Lawrence Livermore National Lab., Calif.
TIBER (TOKAMAK IGNITION/BURN EXPERIMENTAL REACTOR) 2 AS A PRECURSOR TO AN INTERNATIONAL THERMONUCLEAR EXPERIMENTAL REACTOR
C. D. Henning and J. R. Gilleland Apr. 1988 14 p Presented at the International Symposium on Fusion Nuclear Technology, Tokyo, Japan, 10 Apr. 1988
(Contract W-7405-eng-48)
(DE88-008906; UCRL-98306; CONF-880417-9) Avail: NTIS HC A03/MF A01

The Tokamak Ignition/Burn Experimental Reactor (TIBER) was pursued in the U.S. as one option for an International Thermonuclear Experimental Reactor (ITER). This concept evolved from earlier work on the Tokamak Fusion Core Experiment (TFCX) to develop a small, ignited tokamak. While the copper-coil versions of TFCX became the short-pulsed, 1.23-m radius, Compact Ignition Tokamak (CIT), the superconducting TIBER with long pulse or steady state and a 2.6-m radius was considered for international collaboration. Recently the design was updated to TIBER 2, to accommodate more conservative confinement scaling, double-poloidal divertors for impurity control, steady-state current drive, and nuclear testing. DOE

N88-26971# California Univ., Berkeley. Coll. of Engineering.
EFFECTS OF SECONDARY ELECTRON EMISSION ON THE COLLECTOR AND SOURCE SHEATHS OF A FINITE ION TEMPERATURE PLASMA
L. A. Schwager 13 Apr. 1988 62 p
(Contract DE-FG03-86ER-53220)
(DE88-008930; UCB/ERL-M-88/24) Avail: NTIS HC A04/MF A01

The region between a Maxwellian plasma source and an absorbing surface which emits cool secondary electrons is modeled numerically with dynamic, electrostatic particle simulation and theoretically with a static, kinetic plasma-sheath model. The coefficient of secondary electron emission is varied up to and beyond critical emission which causes electric field reversal at the collector. Results from these models agree very well over this range of emission coefficients. Increasing the secondary emission coefficient reduces the collector potential which increases the total energy flux to the collector while decreasing the ion energy deposited. In the simulation, some heating of the secondary electron stream is observed to gradually evolve over many Debye lengths, possibly because of a beam-plasma interaction. This heating increases potential fluctuations but causes only small deviations from the predictions with static theory. DOE

N88-26972# Lawrence Livermore National Lab., Calif.
THE EFFECT OF ICRF ON THE ALCATOR C SCRAPE-OFF LAYER PLASMA
A. S. Wan, B. Lipschultz, F. S. McDermott, and J. L. Terry May 1988 18 p Presented at the 8th International Conference on Plasma Surface Interactions in Controlled Fusions Devices, Julich, Fed. Republic of Germany, 2 May 1988
(Contracts W-7405-eng-48; DE-AC02-78ET-51013)
(DE88-009821; UCRL-98600; CONF-880512-1; CONF-880512) Avail: NTIS HC A03/MF A01

This paper presents a characterization of the Alcator C Scrape-Off Layer (SOL) plasma during ICRF hydrogen-minority fast wave heating experiments. The SOL plasma parameters were measured using a multifunctional probe, JANUS, which is capable of simultaneously measuring the ion and electron parameters both parallel and antiparallel with respect to the toroidal magnetic field. The probe data indicate, at low value of injected rf power, there is direct edge heating and density increases at radii greater than that of the antenna Faraday shield. Increasing the injected rf power spreads both the temperature and density increases throughout the edge region, flattening the radial profiles. Varying the position of the resonance layer in the main plasma does not significantly change the effect of ICRF on the SOL parameters. Given this single spatial point characterization of the SOL, a crude estimate of power flow into and through the edge plasma indicate that (approximately)20 percent of the ICRF power launched from the antenna is absorbed directly in the SOL plasma. Additional observation of the impurity source rates confirms the conclusions of an earlier paper, which attributed increasing central densities of high-Z impurities to the increase in physical sputtering rate at both the ICRF antenna's Faraday shield and the limiter surface. DOE

N88-26973# Edgerton, Germeshausen and Grier, Inc., Idaho Falls, Idaho.
DEVELOPING DIAGNOSTIC METHODS FOR PLASMA-PARTICLE INTERACTION
C. B. Shaw, Jr. 1987 8 p Presented at the 5th Symposium on Energy Engineering Sciences, Argonne, Ill., 17 Jun. 1987
(Contract DE-AC07-76ID-01570)
(TI88-007726; EGG-M-17287; CONF-870679-4) Avail: NTIS HC A02/MF A01

Three diagnostic methods for study of plasma-particle interactions are described. The first, the single-line method of emission spectroscopy for measurement of plasma temperature, is well established but required careful implementation of automatic methods for data reduction and analysis, and will need to be extended at a later date. The second, laser-induced fluorescence (LIF) for measurement of density of species vaporized from the particles, has been found to require substantial modification in experimental detail and data analysis from its origin in flame diagnostics. The third, Doppler-shifted Rayleigh scattering for direct measurement of plasma velocity, is a new undertaking suggested by a single published report of successful measurements on a very high current arc. DOE

N88-26974# International Centre for Theoretical Physics, Trieste (Italy).
ON THE SELF-TRAPPING OF AN ELECTROMAGNETIC WAVE IN MAGNETIZED PLASMA
M. Y. El-Ashry, V. I. Berezhiani, and Sh. D. Pichkhadze Jun. 1987 6 p
(DE88-701872; IC-87/129) Avail: NTIS (US Sales Only) HC A02/MF A01

The possibility of relativistic self-trapping of an electromagnetic wave in magnetized plasma is studied. It is shown that in the case of propagation of fast wave packet of electromagnetic wave in plasma, self-trapping is possible due to the effect of relativistic non-linearity, which is effective even for small amplitudes of the pumping wave. DOE

N88-26975# International Centre for Theoretical Physics, Trieste (Italy).
FACTORS WHICH AFFECT OPERATION OF A PLASMA FOCUS IN VARIOUS GASES
A. J. Smith Jun. 1987 6 p
(DE88-701882; IC-87/140) Avail: NTIS (US Sales Only) HC A02/MF A01

It is shown that the axial transit time t(sub a) and gamma, the ratio of specific heats, are the main factors which affect the operation of a plasma focus in various gases. An energy balance theory is used to explore this dependence. The results are consistent with previous calculations and with experiment. DOE

N88-26976# International Centre for Theoretical Physics, Trieste (Italy).
MODULATIONAL INSTABILITY OF ELECTRIC HELICONS IN A MAGNETIZED COLLISIONAL PLASMA
M. Y. El-Ashry and N. A. Papuashvili Jun. 1987 8 p
(DE88-701885; IC-87/143) Avail: NTIS (US Sales Only) HC A02/MF A01

The interaction of a rf electromagnetic wave with a magnetized collisional plasma in the ultra-relativistic case has been investigated to show the effect of the collisions on the modulational instability growth rate. DOE

N88-26977# International Centre for Theoretical Physics, Trieste (Italy).
THERMAL INHIBITION BY MEGAGAUSS FIELD DUE TO VARIATION OF ELECTRON TEMPERATURE IN LASER PLASMA
L. N. Jha Jun. 1987 10 p
(DE88-701887; IC-87/145) Avail: NTIS (US Sales Only) HC A02/MF A01

The magnetic field evolution equation is solved by the Transform method and the variation of megagauss fields due to perturbation in temperature has been shown. The influence of B sub max-variation on ICF target due to thermal inhibition has also been discussed. DOE

N88-26978# International Centre for Theoretical Physics, Trieste (Italy).
KINETIC MODULATIONAL INSTABILITY OF ELECTRON CYCLOTRON WAVES IN PLASMAS
P. K. Shukla and G. S. Lakhina Jul. 1987 8 p
(DE88-701893; IC-87/151) Avail: NTIS (US Sales Only) HC A02/MF A01

The modulation of a large amplitude electron cyclotron wave by non-resonant ion quasi-modes is considered. The growth rate of the kinetic modulational instability is derived. Our results can have relevance to the magnetic fusion as well as to space plasmas with equal electron and ion temperatures. DOE

N88-26979# International Centre for Theoretical Physics, Trieste (Italy).
MEGAGAUSS FIELD VARIATION ALONG AXIS OF WIRE TARGET IN LASER PRODUCED PLASMA
L. N. Jha and M. P. Srivastava Jul. 1987 8 p
(DE88-701895; IC-87/153) Avail: NTIS (US Sales Only) HC A02/MF A01

Analytical results for megagauss magnetic field variation for laser produced plasmas are obtained. Laser is irradiated on an Al wire target. The exponential electron density variation is taken as is observed in the experiment of Raven et al. (Appl. Phys. Lett. 1979). The variation of magnetic field along the axis of wire is computed with experimentally observed variation and the results obtained by computer simulation. B sub max and its variation is found to agree fairly well with experiment. DOE

N88-26980# Oak Ridge National Lab., Tenn.
REQUIREMENTS FOR NEUTRAL BEAM CURRENT DRIVE IN TOKAMAKS
R. A. Dory 1988 15 p Presented at the US/Japan Workshop on Advanced Current Drive, Livermore, Calif., 8 Feb. 1988
(Contract DE-AC05-84OR-21400)
(DE88-006180; CONF-880249-1) Avail: NTIS HC A03/MF A01

This paper contains viewgraphs on the use of neutral beam current drive in future tokamaks. Current profiles, slowing down distributions, beam destabilization of alfven waves and plasma parameters are some items covered in this paper. DOE

N88-26981# TRW Space Technology Labs., Redondo Beach, Calif.
PLASMA SEPARATION PROCESS. BETACELL (BCELL) CODE, USER'S MANUAL
M. Taherzadeh 13 Nov. 1987 147 p
(Contract DE-AC03-77ET-33006)
(DE88-006955; DOE/ET-33006/025; PSP-R1-1438) Avail: NTIS HC A07/MF A01

The emergence of clearly defined applications for (small or large) amounts of long-life and reliable power sources has given the design and production of betavoltaic systems a new life. Moreover, because of the availability of the Plasma Separation Program, (PSP) at TRW, it is now possible to separate the most desirable radioisotopes for betacell power generating devices. A computer code, named BCELL, has been developed to model the betavoltaic concept by utilizing the available up-to-date source/cell parameters. In this program, attempts have been made to determine the betacell energy device maximum efficiency, degradation due to the emitting source radiation and source/cell lifetime power reduction processes. Additionally, comparison is made between the Schottky and PN junction devices for betacell battery design purposes. Certain computer code runs have been made to determine the JV distribution function and the upper limit of the betacell generated power for specified energy sources. A Ni beta emitting radioisotope was used for the energy source and certain semiconductors were used for the converter subsystem of the betacell system. Some results for a Promethium source are also given here for comparison. DOE

N88-26982# Texas Univ., Austin. Inst. for Fusion Studies.
DRIFT WAVE VORTICES AND ANOMALOUS TRANSPORT
W. Horton Apr. 1988 40 p
(Contract DE-FG05-80ET-53088)
(DE88-009562; DOE/ET-53088/312; IFSR-312) Avail: NTIS HC A03/MF A01

Theory and computer simulations are used to describe the inelastic vortex-vortex and vortex-wave interactions that lead to the quasi-coherent transport of plasma across the magnetic field. Monopole and dipole drift wave vortices with radii r sub o large compared with the ion inertial scale length rho (sub s) are shown to produce transport at the rate un(sub upsilon) integral of d sigma(b) less than or equal to n(sub upsilon)Upsilon(sub de)r(sub o) where n(sub upsilon) is the vortex line density and d sigma(b) is the inelastic collision cross-section for impact parameter b. The transport during collisions and mergings is evaluated from the evolution of a passively convected scalar concentration of test particles. DOE

N88-26983# Argonne National Lab., Ill.
THE HOLE OF A BLANKET TRITIUM SYSTEM ON THE FUSION FUEL CYCLE
D. K. Sze, P. Finn, R. Clemmer, J. Anderson, J. Bartlit, Y. Naruse, and H. Yoshida Feb. 1988 20 p Presented at the International Symposium on Fusion Nuclear Technology, Tokyo, Japan, 10 Apr. 1988 Prepared in cooperation with Los Alamos National Lab., N. Mex.; Japan Atomic Energy Research Inst., Tokyo
(Contract W-31109-eng-38)
(DE88-010007; CONF-880417-17) Avail: NTIS HC A03/MF A01

The requirements of tritium technology are centered in three main areas, i.e., (1) fuel processing, (2) breeder tritium extraction, and (3) tritium containment. The gaseous tritium stream from the breeder tritium extraction system is significantly different from the plasma exhaust stream and, therefore, may have important impact on the operation of the fuel processing system. For some blankets, such as aqueous solution blanket, the blanket tritium stream may dominate the fuel processing system in terms of component size and power consumption. The importance of the blanket interface to a fuel processing experiment, such as TSTA, has been identified. The initial work to define the blanket processing system, which is proposed to be added as part of TSTA, will be discussed here. DOE

N88-26984# Argonne National Lab., Ill.
IMPURITY TRANSPORT CALCULATIONS FOR A DRIFT-DEPENDENT TOKAMAK SCRAPE-OFF PLASMA
J. N. Brooks, M. Petravic, and G. K. Petravic Apr. 1988 7 p Presented at the International Workshop on Plasma Edge Theory, Augustusburg, German Democratic Republic, 26 Apr. 1988
(Contract W-31109-eng-38)
(DE88-010053; CONF-8804123-1) Avail: NTIS HC A02/MF A01

Two dimensional calculations of impurtiy transport in a high recycling divertor scrape-off region have been made with an updated version of the ZTRANS Monte Carlo computer code. The calculations use plasma parameters for the Doublet 3 divertor, as computed by the Planet Fluid Transport Code. The effects of electric field, particle drift velocities, and thermal forces are included in the calculations. For all impurity species studied, it is found that impurity transport is dominated by frictional forces, over most of the scrape-off region. Light impurities, however, impinge

substantially closer to the divertor plate center than do heavy impurities, which tend to impinge at the outer plate boundary. DOE

N88-26985# Oak Ridge National Lab., Tenn.
FULL-WAVE CALCULATIONS IN FLUX COORDINATES FOR TOROIDAL GEOMETRY
B. A. Carreras, V. E. Lynch, E. F. Jaeger, and D. B. Batchelor 1988 18 p Presented at the Sherwood Theory Conference, Gatlinburg, Tenn., 18 Apr. 1988
(Contract DE-AC05-84OR-21400)
(DE88-010131; CONF-8804103-3-Vugraphs) Avail: NTIS HC A03/MF A01

A new 2-D full-wave code, HYPERION, employing a poloidal and toroidal mode expansion and including the toroidal terms arising in the wave equation has been developed. It is based on the existing modules developed for the MHD stability codes and uses as input the tokamak equilibria calculated with the RSTEQ code. At present the plasma response is described by the collisionally broadened cold plasma conductivity. However, the code is written in straight field line coordinates, this permits the accurate representation of k (sub parallel) and as a consequence allows the incorporation of the plasma Z functions. This code also retains the E(sub parallel) component of the electric field which will allow the study of the low density region of the plasma. We have done detailed benchmarking of the HYPERION code in the cold plasma limit with the existing finite difference ORION full-wave code. The agreement is very good. DOE

N88-26986# General Atomic Co., San Diego, Calif.
TOROIDAL AND POLOIDAL SOFT X-RAY IMAGING SYSTEM ON THE D3-D TOKAMAK
R. Snider, R. Evanko, and J. Haskovec Feb. 1988 14 p Presented at the 7th Topical Conference on High Temperature Plasma Diagnostics, Napa, Calif., 13 Mar. 1988
(Contract DE-AC03-84ER-51044)
(DE88-010585; GA-A-19159; CONF-880364-23) Avail: NTIS HC A03/MF A01

A toroidal soft X-ray imaging system is being added to the currently installed poloidal soft X-ray system on the D3-D tokamak. The poloidal array is used to determine the poloidal mode structure and location of internal helical MHD perturbations in the plasma. The new array will add toroidal mode identification capability. The four detector arrays are toroidally spaced in a manner which allows identification of toroidal mode numbers of up to 24. Beryllium vacuum windows separate the detectors from the tokamak vacuum and also serve as low energy filters. The separate detector vacuum chambers can be filled with a gas which changes the low energy cutoff of the system. By proper selection of the gas and pressure the low energy cutoff can be chosen over the entire range of the detector sensitivity (500 eV to 1200 eV). This capability can be used to produce crude X-ray spectra for the entire imaging system or for gain control. DOE

N88-26987# General Atomic Co., San Diego, Calif.
VERTICAL VIEWING ECE DIAGNOSTIC FOR THE D3-D TOKAMAK
R. James, S. Janz, R. Ellis, D. Boyd, and J. Lohr Feb. 1988 15 p Presented at the 7th Topical Conference on High Temperature Plasma Diagnostics, Napa, Calif., 13 Mar. 1988
(Contract DE-AC03-84ER-51044)
(DE88-010586; GA-A-19174; CONF-880364-22) Avail: NTIS HC A03/MF A01

The vertical viewing ECE diagnostic on the D3-D tokamak will be used to assess the non-thermal electron distributions resulting from ECRH and Electron Cyclotron Current Drive experiments. Electron cyclotron emission along a vertical chord is collected using an ellipsodal focusing mirror and retro-reflector (the latter to minimize wall reflections). The emission is then transported approximately 20m using a quasi-optical transport system comprised of 8 lenses and 3 mirrors, and detected between the 2nd and the 10th harmonics by a fast scanning (40 Hz) Michelson interferometer. The entire system has been aligned using a Gaussian beam simulator and absolutely calibrated, in-situ using a cold liquid nitrogen bath. Details of the design, installation, and calibration are given. DOE

N88-26988# Mission Research Corp., Albuquerque, N. Mex.
MACH2: A TWO-DIMENSIONAL MAGNETOHYDRODYNAMIC SIMULATION CODE FOR COMPLEX EXPERIMENTAL CONFIGURATIONS Interim Report
Michael H. Frese Sep. 1987 93 p
(Contract F29601-86-C-0216)
(AD-A192285; AMRC-R-874) Avail: NTIS HC A05/MF A01 CSCL 20I

MACH2 is a flexible and powerful two-dimensional magnetohydrodynamic simulation code designed specifically to handle complex experimental configurations. The code's capabilities include a numerically generated solution-adaptive grid which permits it to be used for either Eulerian or Lagrangian flow problems, use of real equations of state and transport properties from the Los Alamos National Laboratory SESAME package, and a multigrid implicit magnetic field diffusion solver which can be used to simulate problems with vacuum. The descriptive power of the namelist-based problem input language is sufficient that no code modifications are required to set up any of a broad class of problems. Almost no knowledge of the internal data structures and numerical techniques is required to do simulations that realistically model complex experiments. This is made possible by the code's multiblock architecture and table-driven control structure. Code reliability and flexibility are ensured and enhanced by a structured and modular implementation of boundary conditions and block coupling. This report details the physical model, including boundary conditions; permissible problem geometries; time differencing; and spatial discretization, centering, and differencing of MACH2. GRA

N88-26989# California Univ., Los Angeles.
ELECTROSTATIC WHISTLER MODE CONVERSION AT PLASMA RESONANCE
J. E. Maggs and G. J. Morales Feb. 1988 47 p
(Contract N00014-84-K-0583)
(AD-A192951; PPG-1131) Avail: NTIS HC A03/MF A01 CSCL 20I

The mode conversion of an electrostatic whistler wave into a Bohm-Gross mode at plasma resonance is analyzed for a magnetized plasma with a longitudinal density gradient (i.e., Vno x B = 0). It is found that a whistler incident upon plasma resonance from inside the plasma converts, without producing a reflected wave, into a short wavelength Bohm-Groiss mode that carries energy down the density gradient away from resonance. The detailed structure of the electric field near the resonance is found analytically. It is shown that the production of the Bohm-Gross wave by mode conversion can be described by a model of plasma resonance driven by a K = 0 electric field (i.e., the capacitor plate model). The relation between the driver amplitude and the amplitude of the incident whistler is derived. GRA

N88-26990# Aerospace Corp., El Segundo, Calif. Aerophysics Lab.
ULTRAVIOLET-VISIBLE SPECTROSCOPY OF LASER-PRODUCED ALUMINUM PLASMAS Final Report
J. T. Knudtson, William B. Green, and David G. Sutton 22 Jan. 1988 45 p
(Contract F04701-85-C-0086)
(AD-A193004; TR-0086(6930-01)-14; SD-TR-87-57) Avail: NTIS HC A03/MF A01 CSCL 09C

The optical emission spectra (180 to 760 nm) of plasmas produced by a flashlamp-pumped dye laser focused on an aluminum target have been recorded and analyzed. In the incident intensity range from near plasma threshold to 5 x 107 W/sq cm, the electron temperature was calculated from the relative emission intensity of Al(II) states (Te = 8.0 x 103 K). The electron density was determined from Stark broadened linewidths of four Al(II) lines. Both the spatial and temporal dependence of the emission spectra

were obtained, providing a map of the electron density and temperature. GRA

N88-26991# California Univ., Berkeley.
LASER SPECTOSCOPY OF PLASMAS Annual Report, Dec. 1986 - Dec. 1987
John W. Daily 10 Feb. 1988 13 p
(Grant AF AFOSR-0067-86)
(AD-A193009; AFOSR-88-0299TR) Avail: NTIS HC A03/MF A01 CSCL 07D

During the past year, work was continued developing novel advanced laser spectroscopy plasma diagnostic methods. The methods are based on observing the doppler shift in the absorption lines of ionic species. Two methods under study are Velocity Modulated Laser Spectroscopy and Two-Beam Doppler Shift Laser Spectroscopy. The scientific goal of the work is to increase understanding of plasmas by making in-situ measurements of ion drift velocities, concentrations and temperatures in a non-intrusive fashion. The scientific approach is to combine conventional laser spectroscopies with velocity detection. Using a method such as Rayleigh, fluorescence, or Raman scattering, one probes the Doppler profile of the specie of interest, observing shifts in the Doppler profile that arise because of the presence of a electric field. The shift may be related to the ion mobility, and thus conductivity, if the electric field is known, or to the electric field if the mobility is known. Temperature and concentration may be recovered by the conventional means. GRA

N88-26992# Technische Hogeschool, Eindhoven (Netherlands).
PLASMA DEPOSITION: INVESTIGATIONS ON A NEW APPROACH Ph.D. Thesis
Gerardus Maria Wilhe Kroesen 1988 116 p Sponsored by the Netherlands Technology Foundation
(ETN-88-92619) Avail: NTIS HC A06/MF A01

A plasma deposition process in which dissociation and ionization of the original material, transport of the produced reactive particles towards the substrate, and the creation of surface conditions that favor an efficient incorporation of the supplied particles in the growing film are spatially separated, and each of them is optimized separately, was developed. A cascaded arc plasma in argon is used to dissociate and ionize the injected methane and acetylene molecules. The produced reactive particles are transported efficiently towards the substrate by a supersonic expansion into vacuum and a subsonic plasma beam. On the substrate an amorphous carbon film is growing. The flowing plasma in the cascaded arc is analyzed with diagnostics and models. The deposition rates obtained exceed the highest values (for amorphous carbon coatings) in the literature by a factor of 30. ESA

N88-26993# Lawrence Livermore National Lab., Calif.
MTX (MICROWAVE TOKAMAK EXPERIMENT) PLASMA DIAGNOSTIC SYSTEM
B. W. Rice, E. B. Hooper, and C. A. Brooksby Oct. 1987 5 p Presented at the 12th Symposium on Fusion Engineering, Monterey, Calif., 12 Oct. 1987
(Contract W-7405-eng-48)
(DE88-011326; UCRL-96654; CONF-871007-97; CONF-871007)
Avail: NTIS HC A02/MF A01

In this paper, a general overview of the MTX plasma diagnostics system is given. This includes a description of the MTX machine configuration and the overall facility layout. The data acquisition system and techniques for diagnostic signal transmission are also discussed. In addition, the diagnostic instruments planned for both an initial ohmic-heating set and a second FEL-heating set are described. The expected range of plasma parameters along with the planned plasma measurements will be reviewed. DOE

N88-26994# Lawrence Livermore National Lab., Calif. Physics Dept.
BREMSSTRAHLUNG FROM HIGH Z IMPURITIES IN HOT PLASMAS
H. DeWitt, F. Rogers, and C. Iglesias May 1988 19 p
(Contract W-7405-eng-48)
(DE88-011755; UCID-21403) Avail: NTIS HC A03/MF A01

This is a study of the effect of core electron and plasma screening on Bremsstrahlung from high-Z impurities in hot plasmas. DOE

N88-26504# Gunma Univ., Maebashi (Japan). Faculty of Engineering.
ABSORPTION CHARACTERISTICS OF SI3N4 ABLATION LAYER PLASMA
Hiroyuki Shirai *In* Tokyo Univ., The Proceedings of the Symposium on Mechanics for Space Flight 1987 Mar. 1988 p 37-45 (For primary document see N88-26499 20-31)
Avail: NTIS HC A07/MF A01

76 SOLID-STATE PHYSICS

Includes superconductivity.

For related information, see also *33 Electronics and Electrical Engineering* and *36 Lasers and Masers.*

N88-26995# Illinois Univ., Champaign.
THIRD INTERNATIONAL CONFERENCE ON SUPERLATTICES, MICROSTRUCTURES AND MICRODEVICES Final Report, 11-20 Aug. 1987
Bruce Vojak 1987 175 p Conference held in Chicago, Ill., 17-20 Aug. 1987; sponsored by Amoco Corp., NSF, ONR and AFOSR
(AF Proj. 2305)
(AD-A191416; AFOSR-88-0005TR) Avail: NTIS HC A08/MF A01 CSCL 20L

Topics addressed include: transport and tunneling; spectroscopy; microstructures and microdevices; metallic superlattices; photons and hot electrons; and structural studies. For individual titles, see N88-26996 through N88-27057.

N88-26996# Sony Corp., Yokohama (Japan). Research Center.
HOT ELECTRON TRANSISTORS GROWN BY MOCVD Abstract Only
K. Kawai, I. Hase, S. Imanaga, K. Kaneko, and N. Watanabe *In* Illinois Univ., Third International Conference on Superlattices, Microstructures and Microdevices 1987 p 11 (For primary document see N88-26995 20-76)
Avail: NTIS HC A08/MF A01 CSCL 20L

Monolayer precision superstructure devices such as ultrathin superlattices and quantum wells can be fabricated by metallorganic chemical vapor deposition (MOCVD) and their structural quality is favorably confirmed. Energetic electron transport in III-V semiconductors is also investigated through the analysis of MOCVD grown single barrier diodes and hot electron transistors as well as MBE grown ones. The characteristic behavior of injected hot electrons in a narrow base of AlGaAs/GaAs HETs was reported by Heiblum. There are, however, still many issues which should deeply be discussed on the hot electron transport. To better understand the mechanism of the hot electron transport, a series of HETs were fabricated using the MOCVD in which the values of several of the parameters, collector barrier height, base width, base doping concentration, and base depth by incorporating In were changed. The results are discussed. Author

N88-26997# Purdue Univ., Indianapolis, Ind. Dept. of Physics.
RAMAN, PHOTOLUMINESCENCE AND MODULATION SPECTROSCOPY OF SEMICONDUCTOR HETEROSTRUCTURES Abstract Only
A. K. Ramdas *In* Illinois Univ., Third International Conference on Superlattices, Microstructures and Microdevices 1987 p 13 (For primary document see N88-26995 20-76)
Avail: NTIS HC A08/MF A01 CSCL 20L

Collective and localized excitations in semiconductor heterostructures can be discovered and delineated with a number of spectroscopic techniques. When subjected to an alternating strain, the piezomodulated optical properties display signatures

characteristic of electronic transitions. Results for single, double, and multiple quantum wells in GaAs/Al(x)Ga(1-x)As quantum well structures reveal electronic transitions in the wells, the barriers, and the buffer layer with exceptional clarity. Raman scattering in a single quantum well of GaAs sandwiched between Al(x)Ga(1-x)As layers reveals longitudinal optical (LO) phonons confined to the well, resonance of the scattered radiation with the electronic transitions of the well being exploited. The frequencies of the confined LO phonons agree well with these deduced from the bulk dispersion of GaAs. Also observed in the Raman spectrum of superlattices of such structures are the interface optical phonons. Raman spectroscopy applied to heterostructures of diluted magnetic semiconductors show zone folded acoustic phonons, propagating and confined optical phonons, and interface optical phonons. The large magnetic field shifts in the photoluminescence associated with the electron transition in the quantum wells demonstrate the existence of large exchange interaction between the band electrons and the magnetic ions, as in the bulk. Magnetic excitations in diluted magnetic semiconductor heterostructure will be discussed. Author

N88-26998# State Univ. of New York, Buffalo.
FAR-INFRARED STUDIES OF DOPED AlGaAs/GaAs MULTIPLE-QUANTUM-WELL STRUCTURES Abstract Only
J.-M. Mercy, Y.-H. Chang, A. A. Reeder, G. Brozak, and B. D. McCombe *In* Illinois Univ., Third International Conference on Superlattices, Microstructures and Microdevices 1987 p 14 Sponsored in part by ONR, Washington, D.C., Army Research Office, Washington, D.C. and NSF, Washington, D.C. (For primary document see N88-26995 20-76)
Avail: NTIS HC A08/MF A01 CSCL 20L

Recent far infrared (FIR) experiments on doped AlGaAs/GaAs multiple quantum well (MQW) structures will be reviewed. Experiments were carried out between 4.2 and 70 K in magnetic fields up to 9 T with a FIR Fourier transform spectrometer. The MQW structures were grown by MBE with well-widths between 80 and 450 A and barrier widths between 125 and 150 A. The structures were selectively doped with Si impurities in the center of the walls, or both in the center of the barrier and in the center of the wells. Magnetoabsorption measurements on the latter samples show three absorption lines in the vicinity of the hydrogenic donor 1s- 2p (m-+1) transition. The highest frequency line is due to neutral donor impurities in the well centers. The strongest line, the lower frequency of the two new lines, is attributed to electrons in the wells bound to their positively charged parent donors in the center of the barriers. Experiments on the widest-well center-doped sample with the magnetic field in the plane of the sample and light propagation perpendicular to the magnetic field have permitted the observation and identification of the 2p state for the hydrogenic donors that is associated with the first excited confinement subband. The energy of this state is in good agreement with calculations. Experiments were also performed under optical excitation with the pump photon energy greater than the gap of the AlGaAs. All MQW structures studied exhibited large excess free electron concentrations at low pump intensities. Author

N88-26999# Massachusetts Inst. of Tech., Lexington. Lincoln Lab.
ELECTRO-OPTICAL STUDIES OF Al(X)Ga(1-x)As/GaAs COUPLED QUANTUM WELLS Abstract Only
H. Q. Le, J. J. Zayhowski, W. D. Goodhue, J. V. Hryniewicz, and V. A. Mims *In* Illinois Univ., Third International Conference on Superlattices, Microstructures and Microdevices 1987 p 15 Sponsored in part by the Department of the Air Force, Washington, D.C. (For primary document see N88-26995 20-76)
Avail: NTIS HC A08/MF A01 CSCL 20L

The interest in semiconductor quantum wells (QWs) is based, in part, on their promise for optoelectronic applications. For the majority of these applications, the key physical effects result from quantum confinement. The engineering of quantum confinement systems can benefit from more complex structures whose wavefunctions can be designed with more flexibility than in square QWs. The Al(x)Ga(1-x)As/GaAs coupled quantum well structures consisting of a pair of square QWs were investigated experimentally. The influence of electric field on the optical properties differs significantly in this type of structure from that of square QWs, and in fact, effects appear that do not exist for square QWs. Analysis indicates that some of the observed properties are due to the shapes of the confinement wavefunctions. The effects also arise from the electrically tunable crossing of the quantized light hole and heavy hole levels in the valence band, and the shifting of Fermi levels in doped structures. These effects promise applications beyond those of square QWs. . Author

N88-27000# Missouri Univ., Columbia.
QUANTUM WELLS AND BULK AlGaAs UNDER HYDROSTATIC PRESSURE Abstract Only
Meera Chandrasekhar, H. R. Chandrasekhar, H. Venkateswaran, and A. Kangarlu *In* Illinois Univ., Third International Conference on Superlattices, Microstructures and Microdevices 1987 p 16 (For primary document see N88-26995 20-76)
(Contracts DAAL03-86-K-0083; DE-AC02-84ER-45048)
Avail: NTIS HC A08/MF A01 CSCL 20L

Excitonic and staggered transitions in quantum wells and deep donor levels tied to indirect bands in Al(x)Ga(1-x)As are studied using spectroscopic techniques such as photoluminescence (PL) and photoreflectance (PR) under high pressure and low temperatures. In the quantum wells, valence band offsets were determined using the staggered transition between the electron in the AlGaAs X well and the hole in GaAs VB well. The valence offset is found to be 30 + or - 3 percent. The pressure coefficients of confined transitions were studied as a function of well width L sub z using PL and as a function of quantum number n using PR. These transitions are found to have pressure coefficients up to 10 percent lower than that of GaAs host as L sub z decreases or n increases. While there are several competing factors, the major effect is due to change in the electron effective mass m sub e as a function of pressure and the nonparabolicity of the gamma conduction band (CB). Deep donor levels observed in AlGaAs are seen to be resonant states tied to initially the L CB and at high pressures to the X CB. A detailed study for a series of temperatures and excitation intensity reveals luminescence from the DX center, and its behavior under pressure. Author

N88-27001# Stuttgart Univ. (West Germany). Physikalisches Inst.
AUGER RECOMBINATION IN GaSb/AlSb-MULTI QUANTUM WELL HETEROSTRUCTURES Abstract Only
E. Zielinski, H. Schweizer, R. Stuber, G. Griffiths, H. Kroemer, and S. Subbanna (California Univ., Santa Barbara.) *In* Illinois Univ., Third International Conference on Superlattices, Microstructures and Microdevices 1987 p 17 (For primary document see N88-26995 20-76)
Avail: NTIS HC A08/MF A01 CSCL 20L

The experimental determination of Auger recombination coefficients in GaSb/AlSb multi quantum well heterostructures is reported. The samples investigated were grown by molecular beam epitaxy and consist of a 1 micron thick multi quantum well structure. Auger recombination reduces the carrier lifetime and therefore strongly influences devices which are operated at high carrier density levels like semiconductor lasers. Especially in GaSb, where the spin-orbit splitting and the band gap energy are comparable, strongest Auger recombination rates are expected due to the negligible activation energy for the CHSH-process. This process, where a recombining electron-hole pair transfers energy and momentum to a heavy holes which is excited into the split-off band, gives rise to a weak emission at the energy of E sub q + delta sub o. This luminescence is used to monitor the population processes of the split-off band via carrier scattering and intervalence band absorption. The most important results are: the dominant population process of the split-off band is the CHSH-Auger process as compared to the intervalence bond absorption; the Auger coefficients exhibit a dependence on the well width; and no resonance of the Auger recombination is observed tuning the band gap energy over the spin-orbit splitting with temperature, as in bulk GaSb. Author

N88-27002# Los Alamos National Lab., N. Mex.
PIEZOELECTRIC EFFECTS IN STRAINED LAYER SUPERLATTICES Abstract Only
D. L. Smith and C. Mailhiot (Xerox Webster Research Center, N.Y.) *In* Illinois Univ., Third International Conference on Superlattices, Microstructures and Microdevices 1987 p 18 (For primary document see N88-26995 20-76)
Avail: NTIS HC A08/MF A01 CSCL 20L

Because zincblende structure semiconductors are piezoelectric, polarization fields can be generated in the constituent materials of strained layer superlattices by lattice mismatch induced strain. The orientation of the polarization fields depends on the superlattice growth axis. For a (111) growth axis, the polarization fields are parallel to the growth axis; for a (110) growth axis, the polarization fields are perpendicular to the growth axis; and for a (100) growth axis, no polarization fields are generated. Because one of the constituent layers of the superlattice is in biaxial tension and the other is in biaxial compression, the sign of the polarization field is opposite in the two constituent layers making up the superlattice period. Thus, sheets of divergence of polarization occur at the interfaces of a (111) growth axis superlattice and sheets of curl of polarization occur at the interfaces of a (110) growth axis superlattice. The sheets of divergence of polarization generate internal electric fields and the sheets of curl of polarization generate electric displacement fields. The magnitude of these fields can be very large. These fields significantly change the electronic structure of the superlattices. As a result the optical response of these supperlattices is strongly modified by the fields. Author

N88-27003# Hiroshima Univ. (Japan). Dept. of Physical Electronics.
ULTRAFAST OPTICAL NONLINEARITY IN QUANTUM WELL STRUCTURES WITH ELECTRIC FIELD Abstract Only
Masamichi Yamanishi *In* Illinois Univ., Third International Conference on Superlattices, Microstructures and Microdevices 1987 p 19 (For primary document see N88-26995 20-76)
Avail: NTIS HC A08/MF A01 CSCL 20L

A new concept on field-induced optical nonlinearity due to virtual transitions in quantum well (QW) structures is proposed, showing some examples of theoretical results on the nonlinearity. In a QW structure subjected to dc electric field E sub O, negative and positive electric charges of which spatial profiles are given by wave functions at the subbands induced by the virtual transitions due to an intense pump light with a photon energy far below the band gap may produce a screening field E sub s, cancelling out, to some extent, the external bias field R sub O. As a consequence of numerical estimations, the following results are obtained for a Ga(1-x)Al(x)As graded gap QW structure. An increase in the 1e-1hh transition oscillator strength, 3.6 percent, and a blue shift of the band gap, 0.17 meV are expected for a pump power density of 10 to the 8th W/sq cm with a photon energy, 100 meV below the energy gap and for an electric field E sub O of 90,000 V/cm. The variation in the oscillator strength is significantly larger than that (bleaching) due to conventional phase filling mechanisms. The amount of the blue shift is comparable to that due to dressed exciton mechanism. The field-induced optical nonlinearity seems to be observable and quite useful for designing an ultrafast optical gate. Author

N88-27004# North Carolina State Univ., Raleigh.
STRAINED LAYER AND LATTICE MATCHED TRANSVERSE JUNCTION STRIPE QUANTUM WELL LASERS FOR CONTINUOUS ROOM TEMPERATURE OPERATION Abstract Only
Y. J. Yang, K. Y. Hsieh, and R. M. Kolbas *In* Illinois Univ., Third International Conference on Superlattices, Microstructures and Microdevices 1987 p 20 (For primary document see N88-26995 20-76)
Avail: NTIS HC A08/MF A01 CSCL 20L

Two Transverse Junction Stripe (TJS) laser structures using lattice matched AlGaAs-GaAs and strained layer InGaAs-GaAs-AlGaAs quantum wells were demonstrated. The lasers are grown by molecular beam epitaxy and the junction is produced by a two step zinc diffusion and anneal. The diffusion process produces a lateral heterojunction by diffusion enchanced computational disordering of the quantum well active region. Both lasers exhibit low thresholds and single mode operation. The excellent performance of both lasers indicates that high quality lateral p(+)-p-n junctions and heterojunctions can be formed by zinc diffusion enhanced compositional disordering of both lattice matched GaAs-AlGaAs and strain layer InGaAs-GaAs-AlGaAs quantum well structures. Data are presented on the growth, processing, and characterization of the lasers which confirms the claim of high quality lateral heterojunctions in a quantum well structure. The temperature dependence of the threshold current T sub o = 120 K for 77 K is less than T is less than 240 K; T sub o = 100 K at 300 K are comparable to double heterostructure lasers. Preliminary lifetime data for the strained layer laser shows no observable degradation in the power-current characteristics. Also, the InGaAs-GaAs-AlGaAs laser result is the first demonstration of a continuous wave room temperature strained layer laser grown by molecular beam epitaxy. Author

N88-27005# Corning Glass Works, N.Y. Research and Development Lab.
SEMICONDUCTOR MICROCRYSTALLITES IN POROUS GLASS AND THEIR APPLICATIONS IN OPTICS Abstract Only c74
John C. Luong *In* Illinois Univ., Third International Conference on Superlattices, Microstructures and Microdevices 1987 p 21 (For primary document see N88-26995 20-76)
Avail: NTIS HC A08/MF A01 CSCL 20F

Fabrication of semiconductor microcrystallites is of such current interest in the rapidly advancing field of artificial superlattices and quantum well structures. The utilization of the semiconductors of groups II-VI, IV-VI, and layered transition metal chalcogenides is presented. Based on electronic spectral evidence, quantum confinement effects were observed in some of the semiconductors when confined spatially within the pores of the porous glass. Nonlinear optical applicaitons of the porous glass doped with semiconductors microcrystallites will be discussed. Author

N88-27006# Leoben Univ. of Mining and Metallurgy (Austria).
CONTROL OF CARRIER LIFETIME IN PbTe NIPI SUPERLATTICES BY EXTERNAL PHOTOINJECTION Abstract Only
G. Bauer, J. Oswald, W. Goltsos, and A. V. Nurmikko (Brown Univ., Providence, R. I.) *In* Illinois Univ., Third International Conference on Superlattices, Microstructures and Microdevices 1987 p 22 (For primary document see N88-26995 20-76)
Avail: NTIS HC A08/MF A01 CSCL 20L

Versatile PbTe nipi superlattices were recently demonstrated to reach near theoretical limits as infrared detectors. Apart from their epitaxial material quality, increased sensitivity arises from large enhancement of nonequilibrium carrier lifetimes due to electron and hole separation in real space by the built-in nipi potential. Methods of time resolved photoconductivity were employed to investigate the influence of photoinjected electron hole pairs on recombination rates over a wide range of experimental conditions. Large photoinduced lifetime changes from approximately 50 microsec to 1 nanosec were observed. At very low excess carrier densities, two dominant recombination mechanisms can be identified. At low temperature, recombination rates are determined by the probability for tunneling into the nipi barrier while at higher temperatures thermal activation above the barrier leads to direct recombination by vertical transitions. For typical superlattice parameters the two mechanisms are comparable at about 130 K. At high excess carrier densities approaching the static space charge density of the ionized dopants, the nipi potential can in principle be neutralized with lifetime approaching the bulk PbTe limits. The nipi potential was solved self-consistently to provide a good theoretical description to the experimental observations. The transition from the usual electric potential dominated regime to one controlled by an external magnetic field was investigated.
Author

N88-27007# Hamburg Univ. (West Germany). Inst. fuer Angewandte Physik.
SPECTROSCOPY OF ONE-DIMENSIONAL SUBBANDS ON InSb Abstract Only
U. Merkt, Ch. Sikorski, and J. P. Kotthaus *In* Illinois Univ., Third International Conference on Superlattices, Microstructures and Microdevices 1987 p 23 (For primary document see N88-26995 20-76)
Avail: NTIS HC A08/MF A01 CSCL 20L

Periodic metal stripes were prepared with grating constants a (approximately 250 nm) and small free widths w (approximately 100 nm) between stripes on InSb surfaces of metal-oxide-semiconductor structures. In such microstructures, electrons of fairly high mobility mu (approximately 20000 sq cm/V/s) are induced by a gate voltage into the channels between the metal stripes. The optical excitations are studied by far-infrared laser and Fourier spectroscopy. Cyclotron resonance experiments in quantizing magnetic fields show the importance of a lateral confining potential and a transition from two-dimensional to one-dimensional (1D) behavior when the magnetic field strength is decreased. Resonance energies are measured in zero magnetic fields as a function of the applied gate voltage V sub g and are discussed with the aid of simple theoretical pictures of the 1D quantization. The experimental results and their comparison with theoretically expected values demonstrate that quasi 1D subbands were created on InSb. Author

N88-27008# Katholieke Universiteit te Leuven (Belgium). Lab. voor Vaste Stof-Fysika en Magnetisme.
AHARONOV-BOHM EFFECTS IN DISORDERED METALS Abstract Only
Y. Bruynseraede and C. VanHaesendonck *In* Illinois Univ., Third International Conference on Superlattices, Microstructures and Microdevices 1987 p 24 (For primary document see N88-26995 20-76)
Avail: NTIS HC A08/MF A01 CSCL 20L

After the discovery of weak electron localization, it became clear that interference processes between diffusing electron waves in disordered metal films can not be neglected. Due to inelastic scattering and spin scattering by magnetic impurities, the interference only occurs over distances shorter than a characteristic phase breaking length L sub phi. In thin metal films with a size much larger than L sub phi, ensemble averaging largely destroys the influence of the interference processes. For backscattering along time-reversed paths, the destruction does not occur, since the phase difference between the two partial electron waves is always equal to zero. In a magnetic field perpendicular to the time-reversed paths, the backscattering probability oscillates with flux-period h/2e. When the size of a metal film is smaller than L sub phi, ensemble averaging is not complete. In this mesoscopic regime, interference between split electron waves traveling along different paths, can no longer be neglected. For a ring geometry, the direct interference gives rise to experimentally observable magnetoresistance oscillations with the fundamental Aharonov-Bohm period h/e. Author

N88-27009# Ecole Normale Superieure, Paris (France). Groupe de Physique des Solides.
ENERGY LEVELS AND MAGNETO-ELECTRIC EFFECTS IN SOME QUASI UNI-DIMENSIONAL SEMICONDUCTOR HETEROSTRUCTURES Abstract Only
J. A. Brum and G. Bastard *In* Illinois Univ., Third International Conference on Superlattices, Microstructures and Microdevices 1987 p 25 (For primary document see N88-26995 20-76)
Avail: NTIS HC A08/MF A01 CSCL 20L

Quantum wires were considered in the quasi-decoupled situation: the side lengths L sub z, L sub z are characterized by L sub x is much greater than L sub z. In this approximation the Schroedinger equation for the envelope functions becomes quasi-separable in the x and z for states energetically close from the Gamma sub 6 edges of the host materials. Accordingly, the eigenvalues are approximately classified in terms of closely spaced L sub x levels derived from well separated L sub z levels. To each of these eigenvalues is attached 8 one-dimensional subbands due to the free motion along the y axis. For the Gamma sub 8 valence states the subband structure is more complicated. In a rectangular quantum wire, the confinement in the x-direction introduces a mixing in the J sub z = + or - 3/2 and J sub z = + or - 1/2 levels. This mixing increases with increasing quantization along the x axis. The case of the rectangular quantum wires assumed to be n-type spike- and modulation-doped on one of the L sub x sides is considered. A self-consistent calculation is performed and the energy levels and the charge transfer are calculated. Finally, the quantum wires subjected to crossed electric and magnetic fields perpendicular to the wire axis are considered. Author

N88-27010# Bell Telephone Labs., Inc., Holmdel, N. J.
QUANTUM TRANSPORT IN AN ELECTRON WAVEGUIDE Abstract Only
A. M. Chang and G. L. Timp *In* Illinois Univ., Third International Conference on Superlattices, Microstructures and Microdevices 1987 p 26 (For primary document see N88-26995 20-76)
Avail: NTIS HC A08/MF A01 CSCL 20L

High mobility, one dimensional wires were fabricated in GaAs/AlGaAs heterostructures in which the width of the conducting channel is comparable to the electronic wavelength, and the ohmic, four terminal, and electrical resistance were measured as a function of magnetic field and temperature. Because of the size of the devices and the high mobility, a few transverse channels carry the current at 35 mK with minimal scattering. Fluctuations in the resistance are observed as a function of the magnetic field. At low temperature the frequency and amplitude of the fluctuation decreases as the magnetic field approaches the extreme quantum limit where only the lower Landau level is occupied. It was proposed that the fluctuations in the resistance of the wire are due to the Aharonov-Bohm effect, and that the change in the frequency of oscillation is due to the change in the probability amplitude of the electronic wavefunction acrose the wire as the Landau level index changes with the field. At sufficiently high fields in the regime of well developed quantized Hall effect, the fluctuations may arise from finite size percolation effects in the electron wavefunction. Author

N88-27011# Cambridge Univ. (England).
TRANSPORT IN GaAs HETEROJUNCTION RING STRUCTURES Abstract Only
C. J. B. Ford, T. J. Thornton, R. Newbury, M. Pepper, H. Ahmed, G. J. Davies, and D. Andrews (British Telecom Research Labs., Ipswich, England) *In* Illinois Univ., Third International Conference on Superlattices, Microstructures and Microdevices 1987 p 27 (For primary document see N88-26995 20-76)
Avail: NTIS HC A08/MF A01 CSCL 20L

In an earlier work it was shown that the split gate GaAs-AlGaAs heterojunstion FET was a very useful system for obtaining 1D transport. This work was extended to the construction of ring structures. Here, a ring of resist (outside diameter 2.2 micron, inside diameter 0.1 micron) is formed on the AlGaAs surface using electron beam lithography, and is covered with metal, thereby forming a Schottky gate inside and outside the ring. Application of a negative voltage to the gates depletes the high-mobility 2D electron gas at the interface, except in a narrow annulus between the gates. The width of this ring-shaped 2D electron gas can be varied by changing the gate voltage. The magnetoresistance was measured down to approximately mK and magnetic fields up to 10 Tesla. Results are presented on the Aharonov-Bohm effect and conductance fluctuations at low fields, and on magnetic quantization at high fields. Author

N88-27012# Argonne National Lab., Ill. Materials Science Div.
METALLIC SUPERLATTICES Abstract Only
Ivan K. Schuller *In* Illinois Univ., Third International Conference on Superlattices, Microstructures and Microdevices 1987 p 28 (For primary document see N88-26995 20-76)
(Contracts N0014-83-F-0031; W-31-109-eng-38)
Avail: NTIS HC A08/MF A01 CSCL 20L

The preparation, characterization, and physical properties of metallic superlattices are described. The structure and growth of metallic superlattices is determined by a variety of epitaxial considerations, including the structure of the constituents as well as their equilibrium thermodynamic phase diagram. The structural properties determined using surface analytical and diffraction techniques will be related to numerical simulation studies, particularly molecular dynamics. The physical properties including transport, elastic, magnetic, and superconduction properties will be related to structural properties. It will be shown that the physical properties depend strongly on the length scale of the physical phenomenon under study and that different structural characteristics should be emphasized accordingly. Some of the unusual physical properties such as anomalous elastic constants, electron localization, dimensional crossover, and magnetic coupling will be described to illustrate the richness of phenomena present in these microstructures. Author

N88-27013# Naval Research Lab., Washington, D.C.
FERROMAGNETIC/SEMICONDUCTOR HYBRID STRUCTURES Abstract Only
G. A. Prinz *In* Illinois Univ., Third International Conference on Superlattices, Microstructures and Microdevices 1987 p 29 (For primary document see N88-26995 20-76)
Avail: NTIS HC A08/MF A01 CSCL 20L

Recent work has shown that single crystal ferromagnetic films can be grown epitaxially on compound semiconductor surfaces using molecular beam epitaxy. These heterostructures can provide the basis for new hybrid device structures which could exploit the properties of both the semiconductor as well as the ferromagnet. In particular it permits the growth of monolithic structures in which a magnetic field, provided by the ferromagnetic element of the structure, may act upon the semiconductor component of the structure. This may affect either the electronic transport properties or radiation propagating through the semiconductor. A number of these heterostructures will be discussed, including Fe and Co grown on GaAs, ZnSe, and Zn(1-x)Mn(x)Se. The growth conditions and interface properties will be described. Finally, several applications of these heterostructures will be illustrated, including high frequency and magneto-optical device applications. Author

N88-27014# Bell Telephone Labs., Inc., Murray Hill, N. J.
PROPERTIES OF SYNTHETIC MAGNETIC SUPERLATTICES Abstract Only
J. Kwo *In* Illinois Univ., Third International Conference on Superlattices, Microstructures and Microdevices 1987 p 30 (For primary document see N88-26995 20-76)
Avail: NTIS HC A08/MF A01 CSCL 20L

Recent advances in the metal molecular beam epitaxy technique have produced high quality synthetic magnetic spin superlattices. The basic building blocks of the superlattices consist of magnetic rare earths, e.g., Gd, Dy, and Ho and their nonmagnetic analog, e.g., Y. Systems studied to date include Gd-Y, D(z)-Y, Ho-Y, Gd-D(y), periodic superlattices, as well as quasi-periodic Gd-Y superlattices in the Fibonacci sequence. The growth mode of rare earth metals follows the layer-by-layer type, and oscillations in the RHEED intensities were observed at low growth temperature. The structural perfection of the superlattice crystals including the in-plane coherence length and the interfacial width of the chemical modulation are approaching those achieved in the semiconductor superlattices. Magnetization measurements and polarized neutron diffration studies have demonstrated that the overall magnetic order of the superlattice as a whole is modulated by the superlattice periodicities. This long range magnetic correlation is caused by the coherent propagation of the Ruderman-Kittel-Kasuya-Yosida (RKKY) coupling through the conduction electrons of the nonmagnetic intervening Y layer. These results will be presented along with an intriguing interplay between ferromagnetic and helimagnetic order recently observed in the Gd-Dy superlattices. Author

N88-27015# Oxford Univ. (England).
OBSERVATION OF FERROMAGNETISM IN ULTRATHIN f.c.c. FILMS BY SPIN POLARISED NEUTRON REFLECTION Abstract Only
J. A. C. Bland, D. Pescia, and R. F. Willis (Cambridge Univ., England) *In* Illinois Univ., Third International Conference on Superlattices, Microstructures and Microdevices 1987 p 31 (For primary document see N88-26995 20-76)
Avail: NTIS HC A08/MF A01 CSCL 20L

Polarized neutron near critical reflection was used to probe for ferromagnetism in ultrathin f.c.c. Fe and Co films epitaxed to single crystal nonmagnetic substrates. The films are overcoated with Cu(001) overlayers of thicknesses between 40 and 130 A in order to enhance the spin dependence of the neutron reflectivity via wave interference within the sandwich structures. A strong ferromagnetic (FM) response for f.c.c. Co films of thicknesses 2,4,6, and 10 monolayers (ML) epitaxed to Cu(001) substrates with a magnetic moment per atom mu close to that of bulk (hcp) Co (1.7 mu sub 3). The temperature dependence of mu in the range 0 to 300 K is very weak for all the Co films investigated, in agreement with recent spin resolved photoemission experiments on uncoated Co films in the same thickness range. The results for f.c.c. Fe films epitaxed to Rh(001) and Cu(001) substrates contrast sharply with these obtained for the f.c.c. Co films. The 300 K spin dependent response is very weak if present and not experimentally detectable. At 4 K, a 9 A Fe/Rh(001) film displays a significant FM response which is, however, substantially smaller than that anticipated for a saturated film with the bulk phase value of mu. The results are discussed in the context of recent theories which model the roles of lattice strain and surface anisotropy on moment formation in thin films. Author

N88-27016# Thomson-CSF, Orsay (France). Lab. Central de Recherches.
THEORETICAL ASPECTS OF ELECTRON TRANSPORT IN MODULATED STRUCTURES Abstract Only
B. Vinter and T. Weil *In* Illinois Univ., Third International Conference on Superlattices, Microstructures and Microdevices 1987 p 32 (For primary document see N88-26995 20-76)
Avail: NTIS HC A08/MF A01 CSCL 20L

In the theory of transport in modulated structures, both transport perpendicular and parallel to the heterojunction interfaces were studied. In perpendicular transport models were investigated for tunneling through double barriers and it was found that resonant tunneling and sequential tunneling lead to the same expression for the current as long as the width of the energy distribution of the injected electrons are larger than the width of the resonant level in the diode. Results are presented for phonon assisted tunneling between two wells in a model which remains valid even when the barrier shrinks and the tunneling probability becomes very high. Proposals for practical schemes for incorporating this model in programs for calculating the transport in generalized band-engineered structures are given. In parallel transport it was shown that very satisfactory agreement with extensive measurements of the mobility in modulation doped structures in the whole temperature range from 4 to 300 K can be obtained if the complete quasi-two-dimensional subband structure and all the relevant scattering mechanisms are taken into account. Having established this, the program is applied to systems with more complicated double channel structures, and it is shown how the conductivity of a channel in which perpendicular resonant tunneling affects parallel transport can be tailored. Author

N88-27017# Texas Instruments, Inc., Dallas.
QUANTUM TRANSPORT THEORY OF RESONANT-TUNNELING HETEROSTRUCTURE DEVICES Abstract Only
William R. Frensley *In* Illinois Univ., Third International Conference on Superlattices, Microstructures and Microdevices 1987 p 33 (For primary document see N88-26995 20-76)
Avail: NTIS HC A08/MF A01 CSCL 20L

The ability to fabricate very small semiconductor heterostructures has led to the development of devices which exploit quantum-mechanical effects in their operation. The quantum

device which has received the most attention recently is the quantum-well resonant-tunneling diode. This device shows a negative-resistance characteristic which is manifestly quantum-mechanical in origin, and is potentially a very fast device. Existing techniques for analyzing and modeling devices are not able to adequately describe the transient behavior of such a device. A form of quantum transport theory was developed to model the resonant-tunneling diode and similar devices. The internal state of the device is represented by the Wigner distribution function. The boundary conditions applied to the Wigner function model the open-system nature of the device by coupling it to electron reservoirs. This coupling introduces irreversibility into the model, permitting meaningful calculations of the transient behavior of any physical observable. The steady-state I-V curves derived from this model show the expected negative resistance. Calculations of the frequency-domain linear and nonlinear response of the resonant-tunneling diode show that the maximum oscillation frequency is in the low Terahertz range, and that the rectification response extends to even higher frequencies. Author

N88-27018# Bell Telephone Labs., Inc., Murray Hill, N. J.
RESONANT TUNNELING TRANSISTORS AND RESONANT TUNNELING HOT ELECTRON SPECTROSCOPY Abstract Only
F. Capasso, S. Sen, A. Y. Cho, and A. C. Gossard *In* Illinois Univ., Third International Conference on Superlattices, Microstructures and Microdevices 1987 p 34 (For primary document see N88-26995 20-76)
Avail: NTIS HC A08/MF A01 CSCL 20L

Results are presented on a variety of new resonant tunneling (RT) structures; both the under lying physical phenomena and the devices applications will be emphasized. These include: RT gate field-effect transistors; RT devices with multiple negative differential resistance (NDR) regions and 3-state memory circuits; RT bipolar transistors; and RT hot electron spectrometers. Author

N88-27019# Naval Research Lab., Washington, D.C.
SUPERLATTICE DOPING INTERFACES Abstract Only
S. W. Kirchoefer, H. S. Newman, J. M. Pond, and P. Uppal (Martin Marietta Labs., Baltimore, Md.) *In* Illinois Univ., Third International Conference on Superlattices, Microstructures and Microdevices 1987 p 35 (For primary document see N88-26995 20-76)
Avail: NTIS HC A08/MF A01 CSCL 20L

The effect of background doping on current transport in quantum well structures is of great technological importance. Complicated doping - quantum well interactions are known to exist, yet remain poorly understood. The effect of doping on current vs. voltage characteristics in resonant tunneling devices (due to undoped spacer layer thickness) and in quantum well barrier devices serve as examples of these interactions. The use of n(+)-n junctions superimposed on superlattices as a simplified system for such effects is examined. Four samples were grown and tested. The difference between each of the four samples was the particular doping combination of the 50 A well and the 30 A well superlattices. The samples were grown as a sequential set by MBE so as to minimize uncontrolled variations. Data are presented which show that the applied bias appears across only lightly doped and depleted regions. Slight symmetry effects about the origin are observed which are consistent with expected electron barriers for these supperlattice structures. Negative differential resistance effects and conductance oscillation effects are also observed, and are discussed in light of the present understanding of these devices. Author

N88-27020# Institut National des Sciences Appliquees, Toulouse (France). Dept. de Genie Physique.
PRESSURE-DEPENDENT MEASUREMENT ON n+GaAs (Si, Sn): THE EFFECT OF DEEP DONOR (DX) STATES ON THE ELECTRICAL PROPERTIES AND PRESISTENT PHOTOCONDUCTIVITY EFFECTS Abstract Only
J. C. Portal, D. K. Maude, L. Dmowski, T. Foster, L. Eaves, M. Nathan, M. Heiblum, G. G. Harris, and R. S. Beall (Philips Research Labs., Redhill, England) *In* Illinois Univ., Third International Conference on Superlattices, Microstructures and Microdevices 1987 p 36 (For primary document see N88-26995 20-76)
Avail: NTIS HC A08/MF A01 CSCL 20L

Shubnikov-de Haas measurements up to magnetic fields of 20 T are used to study the effects of hydrostatic pressure on the free electron concentration (n) and mobility (mu) of MBE-grown n(+)GaAs layers heavily doped with either Si or Sn. This type of layer forms the electrical contacts to a variety of (AlGa)As/GaAs tunneling devices and superlattices that were investigated under hydrostatic pressure. Increasing the pressure from zero causes an immediate and large decrease of n and increase of mu in n(+) samples doped at 1.8 x 10 to the 19th/cu cm. Illumination with red light at low temperatures (40 K) leads to a persistent restoration of n to its zero pressure level. This is accompanied by a decrease in mu. It is concluded that the trap involved is a deep donor with DX character, present in the n(+)GaAs layers, at concentrations comparable to the doping level. It was found that the energy of the level relative to the L-minima decreases with increasing doping and that its pressure coefficient is close to that of the L-minima. At doping levels above 1.8 x 10 to the 19th/cu cm, the level is partially occupied even at atmospheric pressure. The properties of the deep donor level appear to be very similar for both Si-and Sn-doping. Examples of how these DX centers affect the current-voltage characteristics of tunneling devices as a function of hydrostatic pressure are given. Author

N88-27021# Bell Telephone Labs., Inc., Holmdel, N. J.
RANDOM QUANTUM INTERFERENCE IN MICRODEVICES Abstract Only
W. J. Skocpol *In* Illinois Univ., Third International Conference on Superlattices, Microstructures and Microdevices 1987 p 37 (For primary document see N88-26995 20-76)
Avail: NTIS HC A08/MF A01 CSCL 20L

Experiments on narrow silicon MOSFETs, metal wires and rings, and III-V devices of various sorts prove that the conductance of small electronic devices at low temperatures is affected by random quantum interference of a surprisingly universal character. The quantum phase information of electron waves is not destroyed by elastic scattering. If the inelastic diffusion length L sub phi is much greater than the mean free path, diffusing electrons will interfere in random patterns determined by the specific microscopic configuration of scatterers. As a result, the conductance of each quantum domain of size L sub phi is changed by random amounts with a rms average deviation of just e (sup 2)/h, and is sensitive to changing even a single scatterer. The range of possible interference patterns in a single device can be investigated by applying magnetic flux, or by changing the Fermi energy. In the experiments, the conductance of submicron patterned silicon inversion layers (MOSFETs) with narrow channels and sidebranches used as potential probes was measured. In typical semiconductor devices at room temperature, the mean free path is limited by inelastic scattering, so that these quantum diffusion effects are not significant. Author

N88-27022# Yale Univ., New Haven, Conn. Section of Applied Physics.
QUANTUM INTERFERENCE AND TRANSPORT IN MICROSTRUCTURES Abstract Only
S. Wind, V. Chandrasekhar, M. J. Rooks, and D. E. Prober *In* Illinois Univ., Third International Conference on Superlattices, Microstructures and Microdevices 1987 p 38 (For primary document see N88-26995 20-76)
Avail: NTIS HC A08/MF A01 CSCL 20L

Advances in microfabrication technology have made possible the production of structures with ever decreasing dimensions. As the size of these structures approaches certain characteristic lengths, quantum mechanical effects become evident. Electron interference phenomena may be observed in systems whose size is on the order of the electorn phase coherence length, l sub phi (which can be 1 micron or more at 1 K). For a wire of width less than l sub phi, the interference of electron partial waves which are elastically scattered by impurities leads to one-dimensional localization. This effect manifests itself in the form of a small

correction to the low temperature residual resistance. For ring structures of diameter of approximately l sub phi, electron quantum interference leads to oscillations in the magnetoresistance of the ring with periods h/e and h/2e. These oscillations are the solid state analog of the Aharonov-Bohm effect. Experimental studies of these quantum interference effects in ultrasmall metal wires and rings fabricated by high resolution microlithographic techniques are reviewed. The mechanisms which determine electron energy and phase relaxation in these systems, as determined from these effects, are also discussed. These relaxation mechanisms may be relevant for new classes of semiconductor devices, such as the hot electron transistor. Author

N88-27023# Bell Communications Research, Inc., Red Bank, N.J.
EXCITONIC PROPERTIES OF GaAs-AlGaAs NANOSTRUCTURES Abstract Only
K. Kash, H. G. Craighead, A. Scherer, P. S. D. Lin, P. Grabbe, J. Harbison, and L. Schiavone *In* Illinois Univ., Third International Conference on Superlattices, Microstructures and Microdevices 1987 p 39 (For primary document see N88-26995 20-76)
Avail: NTIS HC A08/MF A01 CSCL 20L

Recent advances in electron beam lithography and the etching of nanostructure features in semiconductor quantum wells have made possible the fabrication of structures in which excitons can be confined, in all three dimensions, to lengths of the order of a few times the exciton diameter. These achievements have led to structures with optical properties strikingly different from those of the original quantum wells. The first observation of exciton energy shifts due to lateral confinement in nanostructures etched from GaAs-AlGaAs quantum wells is presented. The first luminescence measurements from arrays of structures of varying lateral sizes etched from quantum wells is also presented. Surprisingly efficient photoluminescence of excitons, measured over five orders of magnitude in excitation intensity, was observed from structures as small in lateral dimension as 40 nm. A blue shift of several meV in the ground state exciton was observed for the smallest structures, which were attributed to lateral carrier confinement. The luminescence spectra of the structure was measured at 10 K for excitation intensities ranging from approximately 0.1 Watt/sq cm through saturation of the exciton recombination. Measurements of the excitation and luminescence spectra under picosecond and steady state excitation show a dramatic size dependence of the exciton saturation. Author

N88-27024# Bell Telephone Labs., Inc., Murray Hill, N. J.
INFRARED DETECTORS BASED ON THE PHOTON DRAG EFFECT AND INTERSUBBAND ABSORPTION BY A TWO-DIMENSIONAL ELECTRON GAS Abstract Only
Serge Luryi *In* Illinois Univ., Third International Conference on Superlattices, Microstructures and Microdevices 1987 p 40 (For primary document see N88-26995 20-76)
Avail: NTIS HC A08/MF A01 CSCL 20L

Intersubband transitions stimulated by an infrared lightwave propagating in the plane of a two-dimensional electron gas (2DEG) are accompanied by a photon-drag current due to the momentum imparted by the absorbed photons. If the momentum relaxation times in the ground and the excited subbands are equal, then the resultant current density corresponds to electrons moving in the direction of the incident photons. The photon-drag current considered represents a small net difference between two oppositely directed larger currents: one due to excited electrons in the upper subband, the other due to remaining holes in the lower subband. In the presence of radiation both subbands acquire an electron distribution disturbed from cylindrical symmetry, but carriers in the upper subband equilibrate much faster. The photon-drag effect permits a new type of spectroscopy containing information about the momentum-relaxation kinetics in 2D subbands. It also allows the implementation of longwave infrared detectors. Estimates predict the possibility of achieving a detector sensitivity of order 1 A/W (or quantum efficiencies of order of a few percent) at an incident photon wavelength of approximately 10 microns. Performance of this detector at a given frequency is limited mainly by the thermal noise. Author

N88-27025# Arizona Univ., Tucson. Dept. of Physics.
PROPERTIES OF MULTILAYERS FOR SOFT X-RAY OPTICS Abstract Only **c74**
Charles M. Falco and Felix E. Fernandez *In* Illinois Univ., Third International Conference on Superlattices, Microstructures and Microdevices 1987 p 41 (For primary document see N88-26995 20-76)
(Contract F49620-85-C-0039; Grant AF-AFOSR-0347-86)
Avail: NTIS HC A08/MF A01 CSCL 20F

Appropriate physical description of multilayer structures to be used as soft X-ray optical elements is necessary to ensure agreement of predicted and actual performance. Deviation of the fabricated structures from an ideal design (interfacial roughness and diffusion, microvoids, impurities, thickness errors) degrade the reflectance properties. In addition, deviations of the physical properties of very thin films from those of the bulk materials can limit the validity of reflectance calculations. These difficulties and how a particular fabrication-characterization procedure can help solve them are described. Characterization techniques used include a variety of X-ray diffraction techniques, Rutherford Backscattering Spectroscopy and Transmission Electron Microscopy are described. Examples of results obtained for samples prepared by triode magnetically confined dc sputtering will be given, as will a discussion of the implication of these results for other multilayer materials. Author

N88-27026# Bell Telephone Labs., Inc., Murray Hill, N. J.
A 10 MICRONS PHOTOEXCITED AVALANCHE GAIN DUE TO ELECTRON IMPACT IONIZATION FROM GaAs QUANTUM WELL SUPERLATTICES Abstract Only
B. F. Levine, K. K. Choi, C. G. Bethea, J. Walker, and R. J. Malik *In* Illinois Univ., Third International Conference on Superlattices, Microstructures and Microdevices 1987 p 42 (For primary document see N88-26995 20-76)
Avail: NTIS HC A08/MF A01 CSCL 20L

The first demonstration of far infrared photoinduced impact ionization of electrons out of GaAs/Al(x)Ga(1-x)As quantum well superlattices is presented. The photoexcited electron efficiently tunnels out in 150 fsec and travels a hot electron mean free path through the superlattice and produces a large photocurrent before being recaptured by the quantum wells. The measured absolute responsivity R, increases with bias voltage and is in excellent agreement with the theory (which neglects avalanche gain) over three orders of magnitude from 0 to 9 V. A more complete theory which includes infrared photoelectron initiated impact ionization of carriers out of the doped quantum wells is in excellent agreement with the data and quantitatively explains the responsibility increase of 300 percent from 9 to 12 V, and the large measured value of R = 7 A/W at 12 V bias. The responsivity of these GaAs/Al(x)Ga(1-x)As supperlattice detectors at wavelength = 10 micron is comparable to that of HgCdTe alloys and has the advantages of a more advanced technology, a narrow bandwidth delta wavelength/wavelength = 10 percent and importantly the wavelength of operation can be readily tuned from less than 5 to over 100 microns by simply changing the superlattice parameters (i.e., the well widths and barrier heights). Author

N88-27027# Allgeimeine Elektrizitaets-Gesellschaft, Ulm (West Germany).
TRANSPORT STUDY ON Si/Si(1-x)Ge(x) SUPERLATTICES SELECTIVELY DOPED BY SECONDARY IMPLANTATION OF Sb Abstract Only
H. Jorke, H.-J. Herzog, and E. Kasper *In* Illinois Univ., Third International Conference on Superlattices, Microstructures and Microdevices 1987 p 43 (For primary document see N88-26995 20-76)
Avail: NTIS HC A08/MF A01 CSCL 20L

Strained layer superlattices made of lattice mismatched semiconductor materials offer possibilities of tailoring bandgaps and band offsets by strain adjustment. This was demonstrated

impressively for Si/Si(1-x)Ge(x) superlattices and heterostructures, grown by molecular beam epitaxy. The built-in strain leads to a split-off of the sixfold degeneracy of the conduction band minima and influences dominantly band ordering. However, the full electronic potential of these structures becomes accessible only by methods which allow selective doping in a range comparable to the superlattice period length. Particularly doping by secondary implantation was found to enable sharp and precisely localized structures. In the present study MBE grown Si/Si(1-x)Ge(x) heterostructures were selectively doped by secondary implantation of Sb. Transport properties and dopant concentrations are determined by Hall measurements and secondary ion mass spectroscopy, respectively. The results demonstrate that: full dopant activation is achieved; room temperature electron mobility of selectively doped Si/Si(1-x)Ge(x) superlattices is considerably enhanced compared to equally doped Si bulk material; and electron transport properties are dominantly influenced by the strain adjustment within the layers. These properties of selectively doped Si/Si(1-x)Ge(x) strained layer heterostructures open new facilities for electronic devices. Author

N88-27028# Bell Telephone Labs., Inc., Holmdel, N. J.
NOVEL QUANTUM WELL OPTICAL DEVICES Abstract Only
D. A. B. Miller *In* Illinois Univ., Third International Conference on Superlattices, Microstructures and Microdevices 1987 p 45 (For primary document see N88-26995 20-76)
Avail: NTIS HC A08/MF A01 CSCL 20L

Some of the recent work on quantum well (QW) optical devices based on quantum-confined Stark effect (QCSE) electroabsorption is reviewed. The QCSE is seen for electric fields perpendicular to the QW layers, and it is physically now well understood, with good quantitative agreement with experiment for both GaAs/AlGaAs and recently also InGaAs/AnP QWs that are compatible with long-wavelength optical communications. The flexibility of the layered growth technique has also made possible a variety of sophisticated QCSE device structures. A high-contrast waveguide modulator based on pairs of coupled wells, demonstrated the potential of electroabsorption in nonrectangular QW structures. The epitaxial growth was also used to construct an integral multilayer dielectric mirror, giving a reflecting modulator. In the so-called self-electro-optic effect devices (SEEDs), the QCSE modulation is combined with photodetection to make devices that can operate with both optical inputs and outputs. Such devices become particularly attractive if they can be integrated so that they have no electrical parasitics, allowing scaling to small, efficient devices. Another recent development was the symmetric SEED that can operate as a set-reset latch, and can also show time-sequential optical signal gain. These developments show the potential of QW structures for practical optical devices with characteristics that can be tailored to the application, and represent only the beginning of a family of opto-electrical devices. Author

N88-27029# Tokyo Inst. of Tech. (Japan). Dept. of Physical Electronics.
ELECTRICAL PROPERTIES OF p-TYPE AND n-TYPE ZnSe-ZnTe STRAINED-LAYER SUPERLATTICES Abstract Only
Masakazu Kobayashi, Shiro Dosho, Akira Imai, Ryuhei Kimura, Makoto Konagai, and Kiyoshi Takahashi *In* Illinois Univ., Third International Conference on Superlattices, Microstructures and Microdevices 1987 p 46 (For primary document see N88-26995 20-76)
Avail: NTIS HC A08/MF A01 CSCL 20L

ZnSe and ZnTe are semiconducting materials ideally suited for the fabrication of short wavelength light emitting devices. The realization of this potential hinges on obtaining low-resistivity material of controlled conduction type, carrier density, and carrier mobility. Superlattice structures using these materials, and introduction of modulation doping technique may prove to be a good technique to fabricate p-n junctions from wide-gap II-VI compound semiconductor materials. ZnSe-ZnTe strained-layer superlattices (SLSs) were grown on InP substrates by MBE. Two kinds of modulation doped SLS samples were prepared. The van der Pauw measurements of the SLS samples at room temperature showed that their electrical properties could be controlled by using modulation doping technique. The results serve as a major step toward the realization of p-n junctions from wide bandgap II-VI semiconductor materials using strained-layer superlattice structures. Author

N88-27030# Technische Univ., Berlin (West Germany). Inst. fuer Festkoerperphysik.
DIRECT IMAGING OF THE COLUMNAR STRUCTURE OF GaAs QUANTUM WELLS Abstract Only
D. Bimberg, J. Christen, T. Fukunaga, H. Nakashima, D. E. Mars, and J. N. Miller (Hewlett-Packard Labs., Palo Alto, Calif.) *In* Illinois Univ., Third International Conference on Superlattices, Microstructures and Microdevices 1987 p 47 (For primary document see N88-26995 20-76)
Avail: NTIS HC A08/MF A01 CSCL 20L

Direct images of growth islands differing by 2.8 A (one monolayer) height at GaAs/AlGaAs heterointerfaces and of the columnar structure of quantum wells are reported. The structures are grown by MBE with interruptions of the growth of approximately 2 min at the interfaces. The method used to obtain these images is scanning cathodoluminescence. The dependence of the lateral extension of these islands on growth conditions is investigated. For fixed growth rate r sub s is approximately 0.5 monolayer/s the mean island size decreases from 6 to 7 microns upon an increase of growth temperature from T sub g = 600 to 660 C. Apparently the growth process changes from a planar to a three-dimensional one. For low growth temperature and rate the lateral extension of such islands can be larger than the carrier diffusion length. Under these conditions inter-island thermalization of carriers is largely suppressed. Time resolved cathodoluminescence images directly visualize the extent of thermalization. Author

N88-27031# Notre Dame Univ., Ind.
EXAFS STUDIES OF THE MICROSTRUCTURE OF SEMICONDUCTOR ALLOYS, DEFECTS AND SEMICONDUCTOR-METAL INTERFACES Abstract Only
Bruce A. Bunker *In* Illinois Univ., Third International Conference on Superlattices, Microstructures and Microdevices 1987 p 48 (For primary document see N88-26995 20-76)
(Contract N00014-85-K-0614)
Avail: NTIS HC A08/MF A01 CSCL 20L

The Extended X-ray Absorption Fine Structure (EXAFS) technique is an extremely useful probe of atomic-scale structure, revealing bond lengths, types and number of neighbors, and vibronic motion of atoms. Further, this information is available for the various constituent atomic species separately. The technique is applicable to microcrystalline materials, amorphous, or glassy materials, to disordered alloys. The applications of EXAFS to the study of disordered semiconductor alloys and to semiconductor surfaces and interfaces are shown. Results are presented for four different systems. First, it is shown that bond lengths are essentially constant as a function of composition x in the dilute magnetic semiconductor Zn(1-x)Mn(x)Se, where the lattice constant changes by over 0.1 wavelength and the alloy undergoes a zincblende-to-wurtzite transition as a function of composition. This result implies a large local distortion in the alloy structure. In the second example, it is shown that the local alloy disorder in the IV-VI alloy Pb(1-x)Ge(x)Te is enough to induce a ferroelectric phase transition. The third example concerns Fe-implanted in Si. Using EXAFS, it is shown that the lattice expands in a breathing-mode distortion about the Fe, while the second-shell actually contracts. Finally, it is shown that by using total external reflection of X-rays and EXAFS, buried interfaces such as Al-GaAs interface may be studied. Author

N88-27032# Electrotechnical Lab., Ibaraki (Japan).
LATTICE STRAIN IN HETEROEPITAXIAL FILMS Abstract Only
T. Yao *In* Illinois Univ., Third International Conference on Superlattices, Microstructures and Microdevices 1987 p 49 (For primary document see N88-26995 20-76)
Avail: NTIS HC A08/MF A01 CSCL 20L

Lattice strain in heteroepitaxial films is discussed. There are two dominant causes for the lattice strain. One is the lattice misfit between the epilayer and the substrate. The lattice strain due to the lattice misfit is caused as a result of the matching in the in-plane lattice constant at the heterointerface. However, dislocations will be induced in the epitaxial films when the film thickness exceeds a critical thickness and the misfit strain is relaxed as the film thickness exceeds the critical thickness. The other is the difference in thermal expansion coefficients of the epilayer and the substrate. The thermal stress was investigated in terms of the bimetallic strip model and becomes dominant after the misfit stress is relaxed by the introduction of dislocations. There are four cases of the relations between lattice parameter and the thermal expansion coefficients of the epilayer and the substrate. A model calculation was done for each of the four cases and the residual lattice strain is calculated as a function of the film thickness. Lattice strain was discussed in terms of the model and at least qualitative agreement was obtained between the measured lattice strain and the calculation. The influence of the lattice strain on the energy band structure in the heteroepitaxial systems was discussed. Author

N88-27033# Hughes Research Labs., Malibu, Calif.
MBE GROWTH OF HgTe/CdTe SUPERLATTICES ON Si(100) SUBSTRATES Abstract Only
Owen K. Wu, Fred A. Shirland, James P. Baukus, Andrew T. Hunter, and Irnee J. DHaenens *In* Illinois Univ., Third International Conference on Superlattices, Microstructures and Microdevices 1987 p 50 (For primary document see N88-26995 20-76)
Avail: NTIS HC A08/MF A01 CSCL 20L

Molecular Beam Epitaxy (MBE) growth of Hg(1-x)Cd(x)Te alloys and HgTe/CdTe superlattices are of great interest because of their potential applications in infrared imaging systems and fiber optical communication devices. Recently, there was a great deal of interest in growing Hg(1-x)Cd(x)Te alloys and HgTe/CdTe superlattices on foreign substrates such as GaAs, InSb, and sapphire. An epitaxial layer of Hg(1-x)Cd(x)Te alloys or HgTe/CdTe superlattices on silicon could provide the basis for a monolithic focal plane array with the signal processing devices fabricated on the silicon. Molecular Beam Epitaxy growth of HgTe/CdTe superlattices on Si(001) substrates is reported. Abount 3 microns of GaAs as the first buffer layer was deposited on silicon (001) substrate in the III-V MBE system. Then the sample was moved to the II-Vi MBE system for a 0.5 micron of CdTe deposition as the second buffer layer prior to the HgTe/CdTe superlattice growth. One hundred and fifty periods of HgTe (33 A)/CdTe (78 A) superlattices were grown at 175 C. The RHEED pattern was observed during the superlattice growth. Infrared photoluminescence measurements showed luminescence signals occurred at 2000/cm. A comparison of HgTe/CdTe superlattices grown on CdTe(111) and (100) substrates will be made. In addition, structural and electrical properties are discussed. Author

N88-27034# Eidgenoessische Technische Hochschule, Zurich (Switzerland). Lab. fuer Festkoerperphysik.
GROWTH OF HIGH QUALITY CoSi2/Si SUPERSTRUCTURES ON Si(111) Abstract Only
H. vonKaenel, J. Henz, M. Ospelt, and P. Wachter *In* Illinois Univ., Third International Conference on Superlattices, Microstructures and Microdevices 1987 p 51 (For primary document see N88-26995 20-76)
Avail: NTIS HC A08/MF A01 CSCL 20L

The growth of epitaxial films of CoSi2 on Si (111) with excellent crystallinity was demonstrated in the past few years. Films with a thickness of the order of 100 A or less (usually grown by solid phase epitaxy) seemed, however, to be always characterized by an extraordinary large density of pinholes (typically 1 million/sq cm). Now for the first time CoSi2 layers as thin as 30 A were grown with a detectable pinhole density of essentially zero. This was achieved by a modified solid phase epitaxy (SPE) technique, in which Co and Si are coevaporated near room temperature, followed by an anneal up to typically 450 C. Complete elimination of pinholes is rigorously required for the subsequent overgrowth of untwinned Si. Whereas the silicide is well known to grow with type B orientation (rotated by 180 degrees about the surface normal) on Si(111), the overgrowth silicon can unambiguously be shown to have the same orientation as the underlying CoSi2 (type A orientation). Hence, Si on top of CoSi2 is rotated with respect to the Si substrate. This explains the mixed type A and B grains obtained on a silicide containing pinholes. Author

N88-27035# Consiglio Nazionale delle Ricerche, Rome (Italy). Inst. di Acustica.
PHONONS IN SEMICONDUCTOR SUPERLATTICES Abstract Only
E. Molinari and A. Fasolino (SISSA, Trieste, Italy) *In* Illinois Univ., Third International Conference on Superlattices, Microstructures and Microdevices 1987 p 52 (For primary document see N88-26995 20-76)
Avail: NTIS HC A08/MF A01 CSCL 20L

The phonon spectra of semiconductor superlattices along the growth direction are calculated using a new approach which provides realistic dispersions and displacement patterns for both acoustical and optical modes at the same time. The method is based on an exact mapping to one dimension of the full three-dimensional problem. The difference in lattice dynamics of the two components is shown to be accurately described by keeping the same interactions and by assigning masses and effective charges appropriate to each material. The interfaces are then simply treated as changes localized on the atomic planes and not affecting the interactions between planes. The results are shown for GaAs/AlAs, InAs/GaSb, and Si/Ge (001) superlattices, with particular emphasis on the following features: longitudinal and transverse optical modes; interface modes of microscopic origin; and acoustic modes. Finally the one-dimensional character of the method allows the treatment of superlattices with a great number of atomic planes: preliminary results will be presented for superlattices with surfaces and for superlattices with non-periodic distributions of layer thicknesses (disordered and quasi-periodic). Author

N88-27036# Illinois Univ., Urbana. Coordinated Science Lab.
MONTE CARLO SIMULATIONS OF FEMTOSECOND RELAXATION OF PHOTOEXCITED ELECTRONS IN AlGaAs/GaAs QUANTUM WELLS Abstract Only
C. J. Stanton, D. W. Bailey, K. Hess, Y. C. Chang, F. W. Wise, and C. L. Tang (Cornell Univ., Ithaca, N.Y.) *In* Illinois Univ., Third International Conference on Superlattices, Microstructures and Microdevices 1987 p 53 (For primary document see N88-26995 20-76)
Avail: NTIS HC A08/MF A01 CSCL 20L

The development of femtosecond lasers has enabled the study of ultrafast energy relaxation processes in semiconductors. The results of ensemble Monte Carlo simulation of the femtosecond energy relaxation of the electrons photoexcited with a 2 eV laser in AlGaAs/GaAs quantum well structures at room temperature are compared with bulk GaAs. The simulations include self-consistent two-dimensional numerical eigenfunctions for up to five electron subbands, taken into account Pauli exclusion, and electron-electron, electron-phonon, and electron-ionized impurity scattering. A short relaxation component was found in both bulk and quantum wells due to electron-electron and gamma-L intervalley scattering as previously suggested. The simulations indicate that gamma-L scattering is the dominant process. An intermediate relaxation component associated with polar optical phonon scattering in bulk GaAs was found, but not in the quantum well structures. The results are in agreement with the experimental data of Rosker et al. Author

N88-27037# Royal Signals and Radar Establishment, Malvern (England).
ELECTRON-PHONON INTERACTIONS IN In(0.53)Ga(0.47)As AND IN In(0.53)Ga(0.47)As/InP QUANTUM WELLS Abstract Only
K. J. Nash, M. S. Skolnick, P. R. Tapster, S. J. Bass, P. A. Claxton, and J. S. Roberts (Sheffield Univ., England) *In* Illinois Univ.,

Third International Conference on Superlattices, Microstructures and Microdevices 1987 p 54 (For primary document see N88-26995 20-76)
Avail: NTIS HC A08/MF A01 CSCL 20L

Studies of the longitudinal optic (LO) phonon sideband X sub LO of the low-temperature exciton photoluminescence (PL) line X in (In,Ga)As/InP quantum wells (QWs) are presented. The theory of LO phonon satellites is extended to the multi-mode low-dimensional system. Electron-phonon interactions in the bulk alloy In(0.53)Ga(0.47)As are considered. The Froehlich interaction and the Lyddane-Sachs-Teller splittings of the optic modes of mixed crystals are discussed. The existing theory of these properties and the experimental results for In(0.53)Ga(0.47)As, including the studies of phonon satellies of recombination in QWs are described. The phonon sideband X sub LO of recombination in (In,Ga)As/InP QWs consists of separate lines arising from LO modes of the InP and GaAs-like and InAs-like LO modes of the (In,Ga)As. The intensity of each phonon satellite was calculated, taking into account the contribution of interface modes. Experimental results were obtained for (In,Ga)As/InP QWa grown by Molecular Beam Epitaxy (MBE) with well widths from 10 to 110 A. The satellite spectrum is dominated for the wider wells by the GaAs-like modes of the (In,Ga)As, and for the narrower wells by the InP modes. Author

N88-27038# IBM Watson Research Center, Yorktown Heights, N.Y.
ELECTRONIC STRUCTURE OF QUANTUM-WELL STATES REVEALED UNDER HIGH PRESSURES Abstract Only
D. J. Wolford, T. F. Kuech, T. Steiner, J. A. Bradley, M. A. Gell, D. Ninno, and M. Jaros (Newcastle-upon-Tyne Univ., England) *In* Illinois Univ., Third International Conference on Superlattices, Microstructures and Microdevices 1987 p 55 (For primary document see N88-26995 20-76)
Avail: NTIS HC A08/MF A01 CSCL 20L

High pressure has become a powerful tool in electronic structure of semiconductors. In the bulk, band states formed from the periodic atomic potential and bound states formed from isolated potentials were shown to depend, often sensitively, on pressure-induced changes in interatomic distance. And since in multi-valley semiconductors, both free and localized states may contain momentum values from across the reduced zones, pressure has become particularly useful in revealing secondary electronic structure and inducing mixing between states of differing k-value. Such studies were extended, focussing on electronic and optical properties under pressure, from the bulk to two dimensions, using isolated quantum wells and superlattices. Sample systems were studied at low temperature, versus percent, layer thickness, and hydrostatic pressure using photoluminescence, PL-excitation, and fast time-resolved PL, together with full-scale pseudopotential simulation of the electronic structure. Complete and accurate description was obtained of the electronic and optical properties of these structures in all interesting ranges of energy, taking into account the complete multi-valley band structure and heterojunction band offsets of the hosts. Using pressure the intervalley mixing was also examined connecting the quantized electron states of differing k-value, but identical symmetry, as crossings between them are induced. It was shown that the intervalley mixings become increasingly pronounced as well widths become narrow. Author

N88-27039# Oxford Univ. (England).
MAGNETO-OPTICAL STUDIES OF GaInAs-InP QUANTUM WELLS Abstract Only
D. J. Mowbray, N. A. Pulsford, J. Singleton, M. S. Skolnick, S. J. Bass (Royal Signals and Radar Establishment, Malvern, England), R. J. Nicholas, and W. Hayes *In* Illinois Univ., Third International Conference on Superlattices, Microstructures and Microdevices 1987 p 57 (For primary document see N88-26995 20-76)
Avail: NTIS HC A08/MF A01 CSCL 20L

A study was performed on the optical properties of a series of Ga(0.47)In(0.53)As-InP quantum wells grown by Atmospheric Pressure Metal Organic Chemical Vapor Deposition (AP-MOCVD) in magnetic fields from 0 to 16 T. Both single (SQW) and multiple quantum well (MQW) samples were studied with well widths from 50 to 200 A and sheet electron concentrations of zero to N sub s = 10 to the 12th/sq cm. A comparison of low temperature photoluminescence (PL) and photoconductivity (PC) spectra in magnetic fields up to 9.5 T shows the existence of a Stokes' shift between features in PL and PC, indicating that the hole states associated with the PL recombination are localized, probably at fluctuations in the alloy composition of the well material. The observation of the Stokes' shift in a highly doped sample having N sub s = 10 to the 12th/sq cm shows that this hole localization is not screened out by the high electron density. In addition, a measurement of the diamagnetic shift for the ground state of HH1-E1 exciton in a 100 A MQW shows a large value in PC than PL, providing further evidence for a localized hole state observed in the PL. Author

N88-27040# Sheffield Univ. (England). Dept. of Physics.
ON a-Si:H/a-SiN(x):H SUPERLATTICES: CONFINEMENT OR CONTAMINATION Abstract Only
S. Kalem *In* Illinois Univ., Third International Conference on Superlattices, Microstructures and Microdevices 1987 p 58 (For primary document see N88-26995 20-76)
Avail: NTIS HC A08/MF A01 CSCL 20L

Changes in the optical and electronic properties of the a-Si:H/a-SiN(x):H superlattices are commonly observed when the a-Si:H sublayer thickness (d sub Si) is reduced below approximately 40 A. However, there is not yet a clear evidence for quantum confinement effects in these structures. Photothermal deflection spectroscopy (PDS) and infrared photoluminescence excitation are used to study the size effects in the plasma deposited a-Si:H/a-SiN(x):H superlattices with d sub Si as small as 11 A. Thickness induced changes in the band gap, Urbach energy, and defect density are observed for d sub Si is less than 30 A and the results are analyzed in order to clarify the origin of the effects. It is found that despite the explanation of the blue shift in the band gap by a Kronig-Penney model, the results suggest that the variations in the optical parameters may instead be due to the nitrogen contamination of the quantum well layer. The properties of these amorphous superlattices are compared with those of hydrogen rich a-Si:H deposited at low temperatures and a-SiN(x):H alloys contaminated deliberately by nitrogen. Also, new IR-excitation results in the same structures will be reported and discussed in terms of the size effects. In addition the first double beam photoluminescence measurements on these modulated structures are presented. Author

N88-27041# Hamburg Univ. (West Germany). Inst. fuer Angewandte Physik.
EXTENDED AND LOCAL PLASMONS IN A LATERAL SUPERLATTICE Abstract Only
D. Heitmann and U. Mackens (Max-Planck-Inst. fuer Festkoerperforschung, Stuttgart, West Germany) *In* Illinois Univ., Third International Conference on Superlattices, Microstructures and Microdevices 1987 p 59 (For primary document see N88-26995 20-76)
Avail: NTIS HC A08/MF A01 CSCL 20L

Si-metal-oxide-semiconductor (MOS) structures were prepared with a periodically varying oxide thickness. Via a continuous gate the originally two-dimensional (2D) charge density (N sub s) is spatially modulated N (sub s) = N (sub s)(x). For the investigations discussed samples were prepared where the region t sub 2 of high density N (sub s2) is about 3 to 4 times larger than the lower density region t sub 1. Using far infrared spectroscopy the excitation of 2D plasmons propagating perpendicular to the grating grooves of the microstructure was studied. For small plasmon wavevectors q = 2 pi/a, where the plasmon oscillation extends over several superlattice periods, minigaps were observed in the plasmon dispersion due to the superlattice effect of the periodic charge density modulation. For this q the plasmon frequency is governed by the averaged charge density. For higher wave vectors the plasmon frequency increases significantly stronger with q than expected from the classical square root of q dependence for the plasmon frequency of a 2D-electronic system. Author

N88-27042# IBM Watson Research Center, Yorktown Heights, N.Y.
HOT ELECTRONS IN SILICON DIOXIDE: BALLISTIC TO STEADY-STATE TRANSPORT Abstract Only
D. J. DiMaria and M. V. Fischetti *In* Illinois Univ., Third International Conference on Superlattices, Microstructures and Microdevices 1987 p 61 (For primary document see N88-26995 20-76)
Avail: NTIS HC A08/MF A01 CSCL 20L

Hot electron transport in silicon dioxide is examined with emphasis on current experimental and theoretical results. For oxide layers thicker than 100 A, steady-state transport was shown to control the carrier flow at all fields studies. The steady-state transition from a nearly thermal electron distribution at electric fields less than approximately 1.5 MV/cm to significantly hot distributions with average energies between 2 and 6 eV at higher fields of up to 16 MV/cm is discussed. The significance of non-polar phonon scattering in controlling the dispersive transport at higher electric fields, thereby preventing run-away and avalanche breakdown, is reviewed. With very thin oxides, total ballistic transport of the electrons is observed for voltages of less than to approximately 1 V dropped across the remaining oxide portion after tunneling. For voltage drops of greater than 1 V, a transition from the ballistic to the steady-state regime is seen. Monte-Carlo simulations are used to predict the observed experimental behavior including quantum mechanical interference effects and phonon-induced side bands in the electron distribution. This latter effect is the first direct observation in any material of the interaction of ballistic electrons with single phonons of the lattice. Author

N88-27043# Illinois Univ., Urbana-Champaign.
THE THEORY OF ELECTRON-POLAR PHONON SCATTERING RATES IN SEMICONDUCTOR MICRO-STRUCTURES Abstract Only
Bruce Mason *In* Illinois Univ., Third International Conference on Superlattices, Microstructures and Microdevices 1987 p 62 (For primary document see N88-26995 20-76)
Avail: NTIS HC A08/MF A01 CSCL 20L

The scattering of electrons by the optical phonon modes in polar semiconductors is the most important energy loss mechanism for an electron gas at temperatures above 100 K. This polar interaction is effectively stronger when the electrons are confined in narrow wells than it is in the bulk, making the study of the electron-phonon interaction of even greater importance in quasi-two-dimensional electron systems. The effects of confinement, screening, and electronic degeneracy can cause significant qualitative and quantitative changes in the electronic scattering rates. A many-body method of calculating the scattering rates is presented which can include the effects of degeneracy, screening, temperature, and well size and shape. Both phonon absorption and emission rates are obtained explicitly by this method. It is found that the inclusion of the quantum well size and shape and electronic population and degeneracy are vital for accurate calculations. Results are presented to show the effects of various parameters on the scattering rates. These results will be discussed with consideration of their implications for experimental systems. Author

N88-27044# City Coll. of the City Univ. of New York. Dept. of Physics.
DIRECT MEASUREMENT OF ULTRAFAST ELECTRON-HOLE PLASMA EXPANSION AT HIGH DENSITY AT AN ASYMMETRIC GaAs QUANTUM WELL Abstract Only
Kai Shum, M. R. Junnarkar, H. S. Chao, and R. R. Alfano *In* Illinois Univ., Third International Conference on Superlattices, Microstructures and Microdevices 1987 p 63 Sponsored in part by AFOSR, Bolling AFB, Washington, D.C. (For primary document see N88-26995 20-76)
Avail: NTIS HC A08/MF A01 CSCL 20L

The ultrafast spatial expansion of photoexcited electron-hole plasma created by a femtosecond laser pulse excitation in an asymmetric GaAs single quantum well at 4.3 K was directly measured using a 3ps time resolution streak camera system. The experimental results show that the diffusion D is four orders of magnitude larger than the conventional ambipolar diffusivity and the ballistic velocity of the plasma is about four times larger than its Fermi-velocity. The mechanism which causes the photoexcited carriers to be so diffusive is discussed. Author

N88-27045# Texas Instruments, Inc., Dallas. Central Research Labs.
VERTICAL ELECTRONIC TRANSPORT IN NOVEL SEMICONDUCTOR HETEROJUNCTION STRUCTURES Abstract Only
Mark A. Reed *In* Illinois Univ., Third International Conference on Superlattices, Microstructures and Microdevices 1987 p 64 Sponsored in part by ONR, Washington, D.C., Army Research Office, Washington, D.C. and AFWAL, Wright-Patterson AFB, Ohio (For primary document see N88-26995 20-76)
Avail: NTIS HC A08/MF A01 CSCL 20L

The investigation of vertical transport in semiconductor heterojunction systems has recently undergone a renaissance due to improved epitaxial techniques in a number of material systems. These systems are suitable for electronic spectroscopy to determine the band structure, effective masses, and space charge layers of the heterojunction systems. Investigations in a number of bandgap engineered structures, devices, and material systems are presented. For example, one of the intriguing systems investigated is a multi-component resonant tunneling structure consisting of a GaAs contact-AlGaAs barrier-InGaAs quantum well structure. In this structure, the high electron affinity of the quantum well creates a deep quantum well, in which it is demonstrated that quantum well states can be hidden from transport. The high field magnetotransport measurements of these structures yields an anomolously small effective mass of electrons tunneling through the quantum well, which is resolved by a correct modeling of the structure involving the space charge layers of the structure. Results are also presented for vertical transport in a semiconductor-semimetal system, HgCdTe/HgTe, where the physics of this heterojunction system is distinctly different from that of the now familiar GaAs/AlGaAs. Analysis of transport through various multilayer structures verifies the existence of the proposed intrinsic interface state model. Author

N88-27046# Illinois Univ., Urbana-Champaign. Coordinated Science Lab.
RECENT APPLICATIONS OF MONTE CARLO METHODS FOR SEMICONDUCTOR MICRODEVICE SIMULATION Abstract Only
U. Ravaioli *In* Illinois Univ., Third International Conference on Superlattices, Microstructures and Microdevices 1987 p 65 (For primary document see N88-26995 20-76)
Avail: NTIS HC A08/MF A01 CSCL 20L

Ensemble Monte Carlo (EMC) calculations offer probably the most accurate tool for the investigation of the behavior of submicron devices, since nonlinear hot electrons effects are naturally included and, due to the stochastic nature of the method, no assumptions are needed for the particle distribution function. The EMC techniques are, however, extemely time consuming and the available computational resources are mainly limiting their applications. Some new techniques which address the vectorization of the EMC programs, and the extension of EMC calculations to include overshoot effects in more conventional drift-diffusion simulations are presented. Author

N88-27047# Princeton Univ., N. J. Dept. of Electrical Engineering.
RESONANT TUNNELING IN InGaAs-InP DOUBLE-BARRIER STRUCTURES AND SUPERLATTICES Abstract Only
T. H. H. Vuong, D. C. Tsui, and W. T. Tsang (Bell Telephone Labs., Inc., Holmdel, N. J.) *In* Illinois Univ., Third International Conference on Superlattices, Microstructures and Microdevices 1987 p 66 (For primary document see N88-26995 20-76)
Avail: NTIS HC A08/MF A01 CSCL 20L

In the last few years, there was a great deal of renewed interest in the vertical, tunneling transport in double-barrier tunneling structures (DBTS), which were shown to be possible microwave oscillators. To date, most of the work on DBTS was performed

using GaAs-AlGaAs structures because of the excellent control in both the growth and the device processing of this system. The first study of DBTS of the In(0.53)Ga(0.47)As-InP system, which is an important one in optoelectronics, is presented. The first devices fabricated using the usual mesa-etching procedure showed a large non-tunneling current which was ascribed to surface leakage current at the sides of the mesas, since this was often a problem with similar devices of this system. By additional mesa-etching which selectively etch the InGaAs layer faster than the InP layer, the surface leakage current was greatly reduced, and the characteristic current peaks associated with resonant tunneling become well developed. The voltage values at the resonances are in fair agreement with the theoretical predictions. The transport properties of the InGaAs-InP DBTS show interesting differences with those of the GaAs-AlGaAs system, of which the most remarkable is the symmetry about zero bias voltage in the former device. These results will be discussed with preliminary results related to the vertical transport in superlattices of the InGaAs-InP system. Author

N88-27048# Fujitsu Ltd., Atsugi (Japan).
EXCELLENT NEGATIVE DIFFERENTIAL RESISTANCE OF InGaAs/InAlAs RESONANT TUNNELING BARRIER STRUCTURES AND APPLICATIONS TO A NEW FUNCTIONAL DEVICE, RHET Abstract Only
S. Hiyamizu, S. Muto, T. Inata, T. Fujii, and K. Imamura *In* Illinois Univ., Third International Conference on Superlattices, Microstructures and Microdevices 1987 p 67 Sponsored by Ministry of International Trade and Industry, Japan (For primary document see N88-26995 20-76)
Avail: NTIS HC A08/MF A01 CSCL 20L

Since the first proposal of negative differential resistance (NDR) for GaAs-AlGaAs resonant tunneling barrier (RTS) structures, extensive study of NDR has followed, mainly based on GaAs-AlGaAs RTB structures. The NDR characteristics of a GaAs-AlGaAs RTB structure, however, is still unsatisfactory for practical device applications. Recently, excellent NDR characteristics were achieved using an InGaAs/In AlAs RTB structure, lattice-matched to an InP substrate, grown by MBE, which opened the door to the development of a new functional device, resonant tunneling hot electron transistor (RHET), with practical high-speed performance capability. The RHET is briefly described. Author

N88-27049# Ohio State Univ., Columbus. Dept. of Electrical Engineering.
NON-EFFECTIVE-MASS MATCHING IN SUPERLATTICES Abstract Only
Patrick Roblin *In* Illinois Univ., Third International Conference on Superlattices, Microstructures and Microdevices 1987 p 68 (For primary document see N88-26995 20-76)
Avail: NTIS HC A08/MF A01 CSCL 20L

An analytic theory for the matching of the bandstructure of different crystals at the interface of a heterojunction is presented. The Generalized Wannier functions serve as a basis. For a simple uniform band, the Hamiltonian matrix elements then reduce to the k-space Fourier coefficients of the bandstructure along the superlattice direction. The technique therefore accounts for noneffective mass effects, and the lower and upper valleys, and enables both the quasi-k-space periodicity together with the spatial variations of the bandstructure to be invoked. The superlattice Hamiltonian is a system of difference equations taking the form of a band matrix. A new definition of current not effective-mass based is introduced and for this higher-order Schroedinger equation. The enforcement of current continuity leads to analytic connection rules for the overlap Hamiltonian matrix elements. The latter can be expressed in terms of a single ideality coefficient measuring the transparency of the heterojunction. A maximum transparency for all energies is achieved only for geometrically related bandstructures. Non-effective mass effects are demonstrated for the two-dimensional electron-gas and resonant tunneling systems. The technique presented offers theoretical insights together with efficient numerical tools for the study of non-effective mass superlattices. Author

N88-27050# Brown Univ., Providence, R. I.
INFLUENCE OF INTERFACES ON ELECTRONIC AND MAGNETIC PROPERTIES OF MnSe/ZnSe SUPERLATTICES NEAR MONOLAYER LIMIT Abstract Only
D. Lee, S.-K. Chang, H. Nakata, A. V. Nurmikko, L. A. Kolodziejski, and R. L. Gunshor (Purdue Univ., Indianapolis, Ind.) *In* Illinois Univ., Third International Conference on Superlattices, Microstructures and Microdevices 1987 p 69 (For primary document see N88-26995 20-76)
Avail: NTIS HC A08/MF A01 CSCL 20L

The preparation of semiconductor superlattices in which layer thicknesses approach molecular monolayer limits presents a situation where effects of heterointerfaces can become a key factor in determining the physical properties of these artificial microstructures. A so far unexploited possibility is to use magnetic phenomena as a complement to conventional electronic probes for interface specific information. The development of advanced epitaxial preparation methods are paving the way for microstructures at high concentration at high concentration of the magnetic constituent. In particular, versatile superlattice structures based on the MnSe/ZnSe heteropair were recently grown. Direct magnetization and optical measurements in structures containing ultrathins are examined. The experimental results show dramatically the importance of real interfaces to magnetic properties which probe atomic arrangements of the scale of chemical bondlengths. Author

N88-27051# Electrotechnical Lab., Ibaraki (Japan).
STRUCTURAL STUDIES OF (Ga,In)(As,P) ALLOYS AND (InAs) SUB m (GaAs) SUB n STRAINED-LAYER SUPERLATTICES BY FLUORESCENCE-DETECTED EXAFS Abstract Only
H. Oyanagi, Y. Takeda, T. Matsushita, T. Yao, T. Ishiguro, and A. Sasaki (Kyoto Univ., Japan) *In* Illinois Univ., Third International Conference on Superlattices, Microstructures and Microdevices 1987 p 70 (For primary document see N88-26995 20-76)
Avail: NTIS HC A08/MF A01 CSCL 20L

Local structures of (Ga,In)(As,P) alloys and (InAs) sub m (GaAs) sub n strained-layer superlattices were studied as grown by fluorescence-detected extended X-ray absorption fine structure (EXAFS) using synchrotron radiation from the 2.5 GeV storage ring. The Ga K- and As K-edge EXAFS data were Fourier-analyzed to obtain bond lengths. In (Ga,In)(As,P) quarternary alloys lattice-matched to InP, the deviation of bondlengths between cation (Ga,In) and anions (As,P) species from virtual crystal approximation (VCA) are more than three times larger that those from binary compounds and are nearly constant for a wide range in composition, indicating that the lattice relaxation is primarily due to bond-bending. The composition-weighted average bond length determined from EXAFS results agreed well with the average interatomic distance based on X-ray diffraction data and VCA. On the other hand, a large amount of bond-stretching relaxation was found for the Ga-As distance in (InAs) sub m (GaAs) sub n strained-layer superlattices with $m = 6.45$ and $n = 0.51$ while the In-As distance showed no appreciable change on going from a binary compound to the strained-layer superlattices. These results suggest the existence of bond stretching relaxation localized at the interface region between the two alternating layers. Author

N88-27052# Illinois Univ., Chicago.
TYPE 3 - TYPE 1 TRANSITION AND STRAIN EFFECT IN Hg(1-x)Cd(x)Te-CdTe AND Hg(1-x)Zn(x)Te-CdTe SUPERLATTICES Abstract Only
S. Sivananthan, X. Chu, and J. P. Faurie *In* Illinois Univ., Third International Conference on Superlattices, Microstructures and Microdevices 1987 p 71 (For primary document see N88-26995 20-76)
Avail: NTIS HC A08/MF A01 CSCL 20L

Most of the superlattices grown exhibit a n to p-type transition. Hall measurements were performed on several p-type superlattices. In order to investigate the high hole mobility problem,

Hg(1-x)Cd(x)Te-CdTe and Hg(1-x)Zn(x)Te-CdTe superlattices in which the valence band structure is expected to change with x were grown. The superlattices were characterized by electron and X-ray diffraction, infrared transmission and Hall measurements. The presence of satellite peaks in the X-ray spectra show that the superlattices have narrower bandgaps than the equivalent alloys. These superlattices are p-type. The superlattices were investigated for the effect of strain in the system. The Hall characterization, along with magnetotransport experiments, seem to indicate that high hole mobilities observed in p-type HgTe-CdTe superlattices are due to some kind of relationship between the 2D heavy hole gas and the interface state existing in Type 3 superlattices.
Author

N88-27053# Sandia National Labs., Albuquerque, N. Mex.
ATOMISTIC SIMULATION OF STABILITY, METASTABILITY AND GROWTH OF STRAINED LAYER STRUCTURES Abstract Only
Brian W. Dodson and Paul A. Taylor *In* Illinois Univ., Third International Conference on Superlattices, Microstructures and Microdevices 1987 p 72 (For primary document see N88-26995 20-76)
(Contract DE-AC04-76DP-00789)
Avail: NTIS HC A08/MF A01 CSCL 20L

The potential importance of strained-layer heterostructure is, at this point, well established for both semiconductor and metal systems. It is clear from the experiment that structures which are formally metastable, but which persist for long periods can be grown. The increase in strained-layer thickness and/or mismatch made possible by metastability is often of practical importance. It is therefore desirable to understand the material and growth factors which control the production of equilibrium and metastable strained-layer structures. A comprehensive program to study the structural energetics of semiconductor and metal strained-layer heterostructures was in progress for almost two years. The thermodynamic stability of coherently strained overlayers in metal and semiconductor systems was studied using Monte Carlo based microscopic techniques and accurate many-body empirical potentials. It was found that earlier continuum models represent the asymptotic limit of the atomistic calculations for large film thicknesses, but that thin layers are generally less stable than predicted by the continuum models. Metastability against nucleation of misfit dislocations in an initially perfect stained layer was also investigated for semiconductors. The growth of strained-layer heterostructures was simulated for atoms interacting through a Lennard-Jones potential to study the influence of lattice mismatch and substrate temperature of vapor phase growth of mismatched systems.
Author

N88-27054# Notre Dame Univ., Ind. Dept. of Physics.
ORDERING TRANSITIONS OF TERNARY ALLOYS A(1-x)B(x)C Abstract Only
Kathie E. Newman and Jun Shen *In* Illinois Univ., Third International Conference on Superlattices, Microstructures and Microdevices 1987 p 73 (For primary document see N88-26995 20-76)
(Contracts N00014-85-K-0158; N00014-85-K-0352)
Avail: NTIS HC A08/MF A01 CSCL 20L

Alloys of the form A(1-x)B(x)C may form ordered structures for special values of the composition x. This possibility was investigated by considering alloys that have in their disordered high temperature form the zincblende crystal structure. That is, compounds that have a tetrahedral bonding of the type sp3, e.g., alloys of III-V compounds, II-VI compounds (including the diluted magnetic semiconductors), and alloys that are mixtures of the natural chalcopyrites (e.g., II-IV-V sub 2 compounds such as ZnGeAs2) with natural zincblende-structure materials were considered. Possible ordered forms of the alloys A(1-x)B(x)C include, for x = 0.5, a superlattice structure of alternating layers ACBC oriented along the (001) axis, such as was seen in the III-V compound GaAlAs2. Alternatively, for x = 0.5, alloys A(1-x)B(x)C may order in a low temperature phase as an ABC2 chalcopyrite structure, e.g., ZnGeAs2. The question of the relative stabilities of the possible ordered and disordered phases of A(1-x)B(x)C compounds was addressed by using the Kikuchi approximation. The calculations include chemical energies as well as the strain effects. Calculated phase diagrams are shown that exhibit the ordered phases of this type of alloy.
Author

N88-27055# Exxon Research and Engineering Co., Annandale, N.J.
APERIODIC SUPERLATTICES: STRUCTURED RANDOMNESS Abstract Only
Roy Clarke, T. D. Moustakas, and R. Merlin (Michigan Univ., Ann Arbor.) *In* Illinois Univ., Third International Conference on Superlattices, Microstructures and Microdevices 1987 p 74 (For primary document see N88-26995 20-76)
(Contract DAAG29-85-K-0175; Grant NSF DMR-86-02675)
Avail: NTIS HC A08/MF A01 CSCL 20L

The successful realization of quasiperiodic superlattices was recently demonstrated using MBE techniques. These experiments opened the way to studies on a wide variety of model systems in which the multilayers are not periodic but are deposited according to some predetermined mathematical sequence. Such aperiodic systems are of interest because they offer the potential to fabricate materials whose physical properties are quite unlike those of either crystalline of amorphous solids. The results of extensive X-ray and Raman scattering experiments which probe the unusual structural and vibrational properties of aperiodic superlattices are presented. Specifically, the behavior of quasiperiodic (Fibonacci) GaAs-AlAs superlattices were compared with similar MBE-grown samples in which some disorder was deliberately introduced during growth. It appears that different kinds of disorder have markedly different effects on the structural properties. The question of what constitutes randomness in a finite size system (thin film) is important in this context. With this in mind, various strategies were explored for introducing randomness into the superlattices. The experiments take advantage of the high degree of control that is possible with a computerized MBE system. Moreover, atomically abrupt interfaces with perfect periodicity in the plane of the film ensure that the randomness is one-dimensional.
Author

N88-27056# Illinois Univ., Urbana-Champaign. Dept. of Physics.
CHARACTERIZATION OF STRUCTURAL AND MAGNETIC ORDER OF Er/Y SUPERLATTICES
J. Borchers, M. B. Salamon, R. Du, C. P. Flynn, R. W. Erwin, and J. J. Rhyne (National Bureau of Standards, Gaithersburg, Md.) *In* Illinois Univ., Third International Conference on Superlattices, Microstructures and Microdevices 1987 p 75 (For primary document see N88-26995 20-76)
(Grant NSF DMR-85-21616)
Avail: NTIS HC A08/MF A01 CSCL 20L

As an extension of previous studies of magnetic Dy/Y superlattices, crystalline superlattices of erbium and yttrium were prepared epitaxially with layer thicknesses on the scale of the magnetic periodicity of Er. X-ray characterization of these samples reveals that, although the lattice mismatch between Er and Y is 2.5 percent and the crystal structures are highly strained, they are still coherent and exhibit sharp interfaces. Neutron diffraction and magnetometer measurements show that the magnetic properties of these systems differ from the pure Er. In zero field, the spins are c-axis modulated (CAM) in a sinusoidal manner below the Neel temperature. Unlike pure Er, however, the superlattice does not develop a conical spin structure at low temperatures. Overall, the transition temperatures are lower than those for pure Ef, and the first order transition to the conical phase is suppressed, possibly due to the lattice clamping effects such as observed in Dy/Y superlattices. Neutron diffraction data for one sample with 23 Er layers per bilayer show little variation of the modulation wavevector with temperature. This behavior suggests a lock-in of the modulated spins to one of the commensurate spin-slip structures.
Author

N88-27057# Northwestern Univ., Evanston, Ill. Materials Research Center.
SUPERCONDUCTIVITY OF Cr/V SUPERLATTICES Abstract Only
Bradley M. Davis, Paul R. Auvil, John B. Ketterson, and John E. Hilliard *In* Illinois Univ., Third International Conference on Superlattices, Microstructures and Microdevices 1987 p 76 (For primary document see N88-26995 20-76)
Avail: NTIS HC A08/MF A01 CSCL 20L

Cr(m)V(n) superlattices, where m and n denote the number of atomic planes of Cr or V, were grown in an ultrahigh vacuum unit containing two e-guns and a rotating substrate table. Up to 20 samples could be made in each run. Samples were grown on c cut sapphire substrates at 520 K at deposition rates of approximately 2 l/s. Samples consisted of between 7 and 10 wavelengths and were characterized using X-ray diffraction and stylus profilometry. All specimens were found to have a strong (110) texture. The zero field transition temperature and upper critical field were measured. The zero field transition temperature of the sample will be discussed in terms of various proximity effect theories. These include the procedures of Werthamer and Menon-Arnold. In addition a detailed numerical solution was performed based on de Gennes method of expanding the kernel of the linearized self-consistency condition in terms of the eigenfunctions of the diffusion equation. Results of this modeling will be presented including findings on the pair breaking strength of thin Cr layers. Author

N88-27058# Joint Inst. for Nuclear Research, Dubna (USSR). Lab. of Theoretical Physics.
TO THE TWINNING PLANE SUPERCONDUCTIVITY THEORY
T. M. Mishonov 1987 19 p In RUSSIAN; ENGLISH summary (DE88-702195; JINR-R-17-87-497) Avail: NTIS (US Sales Only) HC A03/MF A01

The thermodynamic potential for narrow superconductive layer near the Twinning Plane (TP) for type-1 superconductors was found. A correction is found also to the surface tension which is proportional to the square root of the Ginzburg-Landau (GL) parameter k. A rule of corresponding states is found for supercooling field for Twinning Plane Superconductivity (TPS) type-1. Conditions for Berezinskii-Kosteriiz-Thouless transtition are considered for proximity effect and also a possible mechanism for conducting transitions TPS and pinning-force near the TP. It was found that work distribution for order parameter is also suitable for describing magnetisation in layered structures of type Ge-Fe and for superlattices from normal-superconducting metal. DOE

N88-27059 Stanford Univ., Calif.
ELECTRICAL STUDY OF METAL/GROUP 3-5 SEMICONDUCTOR INTERFACES: COMPARISON WITH THE ATOMIC-LEVEL STUDIES Ph.D. Thesis
Nathan Newman 1987 247 p
Avail: Univ. Microfilms Order No. DA8723059

The results of a systematic study designed to investigate the physical mechanisms involved in Fermi level pinning on Group 3 to 5 semiconductor surfaces are presented. Diodes were fabricated on clean cleaved GaAs and InP (110) surfaces under ultrahigh-vacuum conditions with in situ metal depositions. Using current-voltage (I-V) and capacitance-voltage (C-V) measuring techniques, very reliable and consistent determinations of the barrier height and ideality factor n were obtained. Using valence-band and core-level photoemission spectroscopy, as well as transmission electron microscopy (TEM) and electrical device measurements, the effects of annealing Ag, Al, and Au/GaAs (110) Schottky diodes were also studied. The results of this study show that the annealing induced microscopic changes in the electronic and chemical structure of the metal/semiconductor interface can be strongly correlated with the macroscopic changes in the electrical properties of thick metal/semiconductor Schottky barriers. Dissert. Abstr.

N88-27060# Louisiana State Univ., Baton Rouge. Dept. of Electrical and Computer Engineering.
GROWTH AND CHARACTERIZATION OF THIN FILMS OF ZnSnP(SUB)2 Final Report, 15 Oct. 1983 - 31 May 1987
P. K. Ajmera and H. Y. Shin Feb. 1988 59 p
(Contract DE-AC02-83CH-10093)
(DE88-001164; SERI/STR-211-3216) Avail: NTIS HC A04/MF A01

This research involved the vacuum deposition of thin films of ZnSnP2. This ternary chalcopyrite semiconductor has a direct energy gap of 1.66 eV. Its constituent elements, zinc and phosphorus, are plentiful in the U.S. and tin is readily available from abroad. This makes ZnSnP2 an attractive material for low-cost terrestrial photovoltaic applications. Growth conditions were experimentally determined to obtain near-stoichiometric vacuum growth of thin films of ZnSnP2 on GaAs, quartz, and molybdenum substrates utilizing elemental sources. The grown films were characterized by chemical, electrical, and optical measurements and by morphological studies. Attempts were made to fabricate simple heterostructure devices on the grown layers. This research provides information on the relevant properties of vacuum-grown thin films of ZnSnP2 for its potential application in polycrystalline thin-film PV devices. DOE

N88-27061# Tennessee Univ., Knoxville.
RAMAN AND ABSORPTION SPECTROPHOTOMETRIC STUDIES OF SELECTED LANTHANIDE, CALIFORNIUM-DOPED LANTHANIDE, AND ACTINIDE TRIHALIDES IN THE SOLID STATE Ph.D. Thesis
W. R. Wilmarth Mar. 1988 131 p
(Contracts DE-AS05-76ER-04447; DE-AC05-84OR-21400)
(DE88-008234; DOE/ER-04447/235) Avail: NTIS HC A07/MF A01

The solid-state absorption spectra of Cf(3) ions as a dopant in lanthanide trihalide hosts (LnCl3: Ln = Ce, Sm, and Y; LnBr3: Ln = Ce, Sm, Tb, and Y; LnI3: Ln = Ce and Y) have been recorded. The spectra of Cf(3) have been correlated with the various crystal structures. The phonon Raman spectra and solid-state absorption spectra of PmF3, PmCl3, PmBr3, and two crystal modifications of PmI3 have been recorded. Symmetry assignments have been made for the Raman-active bands for these trihalides and also the sesquioxide. The room-temperature absorption spectra have been correlated to crystal field effects. The symmetry assignments of the Raman-active phonon modes have been made based on polarized Raman spectra from single crystals of YF3-type orthorhombic TbF3 and PuBr3-type orthorhombic NdBr3. Raman spectra of other isostructural lanthanide compounds have been recorded and compared. Symmetry assignments for these compounds have been made by analogy to the single-crystal assignments. Raman spectra have been obtained and catalogued for a number of actinide compounds. Symmetry assignments have been made for the observed Raman-active phonon bands in this work based on the assignments made for isostructural lanthanide compounds. DOE

N88-27062# Sandia National Labs., Albuquerque, N. Mex.
PHOTOLUMINESCENCE STUDIES OF InGaAlAs QUATERNARY ALLOYS
E. D. Jones and L. R. Dawson Mar. 1988 11 p Presented at the Advances in Semiconductors and Superconductors: Physics and Device Applications, Newport Beach, Calif., 13 Mar. 1988
(Contract DE-AC04-76DP-00789)
(DE88-007197; CONF-880311-1) Avail: NTIS HC A03/MF A01

Photoluminescence data are used to obtain the concentration and temperature dependence of the bandgap energies of epitaxial layers of quaternary alloy In0.1GaxAlyAs for Al concentrations less than 0.6. The samples were grown by MBE without an intervening buffer layer. For an In concentration of 0.1, the transition from a direct to an indirect bandgap material occurs for an Al concentration of about 0.5. Coefficients of the temperature dependence of the bandgap energy are also presented. DOE

N88-27063# Los Alamos National Lab., N. Mex.
PREPARATION OF OXIDE SUPERCONDUCTORS
D. E. Peterson 1988 5 p Presented at the 10th Annual Ideas in Science and Electronics Exposition, Albuquerque, N. Mex., 10 May 1988
(Contract W-7405-eng-36)
(DE88-009136; LA-UR-88-1226; CONF-880579-3) Avail: NTIS HC A02/MF A01

Preparation of bulk superconductors by cold pressing and sintering of metal oxides has been optimized in this study. A knowledge of phase behavior was used in developing a flux method for growing superconducting single crystals of yttrium and gadolinium based superconductors. Means of achieving single-phase, high-density samples of (Rare Earth)-Ba2Cu3O7 with optimal electronic properties are reviewed. DOE

N88-27064# Oak Ridge National Lab., Tenn.
EFFECTS OF GRAIN BOUNDARY COMPOSITION ON PROPERTIES OF YBa2Cu3O/SUB 7-x/
D. M. Kroeger, J. Brynestad, R. K. Williams, R. A. Padgett, and J. O. Scarbrough 1988 6 p Presented at the MRS High Temperature Superconductors, Reno, Nev., 4 Apr. 1988
(Contract DE-AC05-84OR-21400)
(DE88-007679; CONF-880481-2) Avail: NTIS HC A02/MF A01

Results strongly suggest that the source of grain boundary resistance in sintered YBa2Cu3O(sub 7-x) is a layer of material at grain boundaries which differs from the bulk in composition. If it is not superconducting as the composition determinations suggest, then transport between grains is by a tunneling process, as others have surmised from the field dependence of J(sub c). The composition of the grain boundary layer is affected by small deviations from the stoichiometric composition. It is likely that the variations of J(sub c)(H) and rho (T) with sample composition are reflections of these changes in grain boundary composition. The variation of grain size with composition may be due to changes in grain boundary diffusion rates. We conclude that control of grain boundary composition is essential to improvement of J(sub c). Sample homogeneity may be an important issue since local composition variations would be expected to lead to variations in grain boundary composition. DOE

N88-27065# Los Alamos National Lab., N. Mex.
SUPERCONDUCTIVITY OF HEAVY-ELECTRON URANIUM COMPOUNDS
Z. Fisk, H. Borges, M. McElfresh, J. L. Smith, J. D. Thompson, H. R. Ott, G. Aeppli, H. Bucher, S. E. Lambert, and M. B. Maple et al. 1988 8 p Presented at the International Conference on High Temperature Superconductors and Materials and Mechanisms of Superconductivity, Interlaken, Switzerland, 29 Feb. 1988 Prepared in cooperation with Eidgenoessische Technische Hochschule, Zurich, Switzerland, Bell Labs., Murray Hill, N.J., California Univ., San Diego and Risoe National Lab., Roskilde, Denmark
(Contract W-7405-eng-36)
(DE88-007901; LA-UR-88-788; CONF-880206-4) Avail: NTIS HC A02/MF A01

This paper reviews the status of the understanding of superconductivity in uranium heavy-electron compounds. DOE

N88-27066# California Univ., Berkeley. Lawrence Berkeley Lab.
FERMI LEVEL DEPENDENT NATIVE DEFECT FORMATION: CONSEQUENCES FOR METAL-SEMICONDUCTOR AND SEMICONDUCTOR-SEMICONDUCTOR INTERFACES
W. Walukiewicz Feb. 1988 25 p Presented at the 15th Annual Conference on Physics and Chemistry of Semiconductor Interfaces, Asilomar, Calif., 1 Feb. 1988
(Contract DE-AC03-76SF-00098)
(DE88-008247; LBL-24157; CONF-880208-1) Avail: NTIS HC A03/MF A01

The amphoteric native defect model of the Schottky barrier formation is used to analyze the Fermi level pinning at metal/semiconductor interfaces for submonolayer metal coverages. It is assumed that the energy required for defect generation is released in the process of surface back-relaxation. Model calculations for metal/GaAs interfaces show a weak dependence of the Fermi level pinning on the thickness of metal deposited at room temperature. This weak dependence indicates a strong dependence of the defect formation energy on the Fermi level, a unique feature of amphoteric native defects. This result is in very good agreement with experimental data. It is shown that a very distinct asymmetry in the Fermi level pinning on p- and n-type GaAs observed at liquid nitrogen temperatures can be understood in terms of much different recombination rates for amphoteric native defects in those two types of materials. Also, it is demonstrated that the Fermi level stabilization energy, a central concept of the amphoteric defect system, plays a fundamental role in other phenomena in semiconductors such as semiconductor/semiconductor heterointerface intermixing and saturation of free carrier concentration. DOE

N88-27067# Lawrence Livermore National Lab., Calif.
NONLINEAR MATERIALS FOR FREQUENCY CONVERSION
S. P. Velsko and D. Eimerl 22 Mar. 1988 13 p Presented at SPIE O-E Lase '88: Optoelectronics and Laser Applications in Science and Engineering, Los Angeles, Calif., 10 Jan. 1988
(Contract W-7405-eng-48)
(DE88-008343; UCRL-98470; CONF-880110-28) Avail: NTIS HC A03/MF A01

Two figures of merit, the threshold power (P sub th) and the limiting volume (5 sub min) can be used to compare the relative efficiency and economy of new harmonic generating crystals. The properties of barium metaborate and L-Arginine phosphate are used to illustrate the effect of nonlinearity, birefringence, and damage threshold on these figures of merit. DOE

N88-27068# Colorado School of Mines, Golden. Dept. of Physics.
FUNDAMENTAL OPTICAL STUDIES OF COMPETITIVE ADSORPTION AND THIN FILM PHENOMENA Progress Report, 1 Jul. 1987 - 30 Jun. 1988
T. E. Furtak Apr. 1988 17 p
(Contract DE-FG02-86ER-45253)
(DE88-008780; DOE/ER-45253/2) Avail: NTIS HC A03/MF A01

We have developed optical second harmonic generation into a powerful new surface structure probe that is ideal for problems such as the electrolyte-solid interface. We have determined the geometry of electrodeposited metal monolayers of Cd, Zn, and Tl on Ag(111) while the sample was under electrochemical control. The initial experiments were performed with the CW technique using a tightly focussed laser beam. We have now acquired the capability to perform the experiment with a wider variety of optical configurations and as a function of the incident photon energy. The latter is important to study and exploit electronic resonances in the overlayer system. We have also succeeded in obtaining our first plasmon-assisted Raman spectrum of an adsorbed molecule on a smooth Ag surface using our newly developed plasmon excitation/emission apparatus. DOE

N88-27069# Sandia National Labs., Albuquerque, N. Mex.
CHARACTERIZATION OF THE SURFACE AREA AND POROSITY OF SOL-GEL FILMS USING SAW DEVICES
G. C. Frye, A. J. Ricco, S. J. Martin, and C. J. Brinker 1988 11 p Presented at the Spring Meeting of the Materials Research Society, Reno, Nev., 4 Apr. 1988
(Contract DE-AC04-76DP-00789)
(DE88-008794; SAND-87-2673C; CONF-880408-1) Avail: NTIS HC A03/MF A01

A novel technique for accurately obtaining nitrogen adsorption isotherms on thin porous films has been developed. These isotherms are useful for characterizing the surface area and pore size distribution of porous samples. The sensitivity to adsorbed nitrogen is increased by several orders of magnitude over conventional techniques by forming the test film on the substrate of a surface acoustic wave (SAW) device. This device functions

as a microbalance able to detect less than 100 pg of adsorbed nitrogen per sq cm of film. Surface areas and pore size distributions were calculated from adsorption isotherms obtained with this technique on silicate sol-gel films. The results are compared to those for bulk samples prepared from similar sol-gel solutions. DOE

N88-27070# Sandia National Labs., Albuquerque, N. Mex.
RECENT ADVANCES IN ATOM-PROBE FIELD ION MICROSCOPY
G. L. Kellogg 1988 26 p Presented at the Scanning Microscopy Meeting, St. Louis, Mo., 2 May 1988
(Contract DE-AC04-76DP-00789)
(DE88-008799; SAND-88-0748C; CONF-880588-1) Avail: NTIS HC A03/MF A01

The techniques of field ion microscopy and atom-probe mass spectroscopy are reviewed. Recent advances in instrumentation are discussed and selected applications are presented. Emphasis is placed on more recent investigations such as surface reconstructions, mixed-metal cluster formation, surface chemical reactions, and the microscopic properties of ceramic superconductors. DOE

N88-27071# Oak Ridge National Lab., Tenn.
HEFLOW: A PROGRAM FOR CALCULATING PRESSURE AND TEMPERATURE OF HELIUM IN FORCED-FLOW SUPERCONDUCTORS. PART 1: NUMERICAL SOLUTIONS. PART 2: HEFLOW USER'S MANUAL
M. W. Keller Mar. 1988 35 p
(Contract DE-AC05-84OR-21400)
(DE88-008941; ORNL/TM-10743-Pt-1/2) Avail: NTIS HC A03/MF A01

HeFlow, a program to calculate the pressure and temperature of supercritical helium flowing in a heated channel, has been used to model the flow in the Westinghouse (WH) Large Coil Program (LCP) coil. The passage of the helium both at normal operating conditions and near the critical point has been shown to be isenthalpic to better than 1 or 2 parts in 1000. The effect of changing the sign of the Joule-Thomson (J-T) coefficient is discussed, and a useful approximation for temperature changes in helium flow is developed. DOE

N88-27072# Argonne National Lab., Ill.
CHALLENGE EQUALITY PROBLEMS IN LATTICE THEORY
W. McCune 1988 5 p Presented at the 9th International Conference on Automated Deduction (CAD-9), Argonne, Ill., 23 May 1988
(Contract W-31-109-eng-38)
(DE88-010094; CONF-8805110-1) Avail: NTIS HC A02/MF A01

This note contains five problems which should be useful for experimentation with equality-oriented automated theorem-proving programs. The problems are formally stated and proved in first-order predicate calculus with equality. The problems are taken from the often-overlooked paper Semi-automated mathematics by Guard et al. All of the theorems concern the existence and uniqueness of complements in modular lattices with 0 and 1. DOE

N88-27073# International Centre for Theoretical Physics, Trieste (Italy).
LATTICE THEORY OF FRACTURE OF SOLIDS WITH LAYERED STRUCTURE
Decheng Tian, Yinhua Xu, Guoming Li, and Weiho Guan Jun. 1987 18 p
(DE88-701867; IC-87/124) Avail: NTIS (US Sales Only) HC A03/MF A01

The lattice trapping effect of a crack in solids with layered structure has been studied with Thomson's chain model. It is shown that the difference in physico-mechanical properties between different atomic planes has significant influence upon this effect and the stress range for stability of a crack can be enhanced by increasing the difference. This perhaps provides a way for the lattice trapping effect to be made observable by appropriately synthesizing solids with superlattice of special design. DOE

N88-27074# International Centre for Theoretical Physics, Trieste (Italy).
PHENOMENOLOGICAL APPROACH TO HIGH T/SUB c/ OXIDE SUPERCONDUCTORS
J. Chela-Flores, M. P. Das, and A. G. Saif Jun. 1987 11 p
(DE88-701868; IC-87/125) Avail: NTIS (US Sales Only) HC A03/MF A01

Oxide superconductors are described in terms of macroscopic wave functions PSI and PHI corresponding, respectively, to electron pairs of the superconducting and insulating states. In terms of the total free energy of the system, including the effect of interaction, we discuss the electrodynamic responses of the oxide superconductors in relation with the experiments to data. DOE

N88-27075# International Centre for Theoretical Physics, Trieste (Italy).
ON THE POSSIBILITY OF THE SOLITON DESCRIPTION OF ACOUSTIC EMISSION DURING PLASTIC DEFORMATION OF CRYSTALS
A. Pawelek Jun. 1987 20 p
(DE88-701878; IC-87/136) Avail: NTIS (US Sales Only) HC A03/MF A01

Two basic sources of acoustic emission (AE) during plastic deformation of pure crystals are discussed. One is related to non-stationary dislocation motion (the bremsstrahlung type of acoustic radiation), and the other to dislocation annihilation processes (the main component of the transition type of acoustic radiation). The possible soliton description of the bremsstrahlung acoustic radiation by oscillating dislocation kink and by bound kink-antikink pair (dislocation breather) is considered on the basis of Eshelby's theory (Proc. Roy. Soc. London A266, 222 (1962)). The dislocation annihilation component of transition acoustic emission is considered only in relation to the Frank-Read source operation. A soliton model for this type of acoustic radiation is proposed and the simple quantum-mechanical hypothesis is advanced for the purpose. Both soliton descriptions are discussed on the basis of available experimental data on the AE intensity behaviour during tensile deformation of crystals. DOE

N88-27076# International Centre for Theoretical Physics, Trieste (Italy).
DERIVATION OF SPACE GROUPS IN mm2, 222 AND mmm CRYSTAL CLASSES
G. D. Nigam Aug. 1987 16 p
(DE88-701881; IC-87/139) Avail: NTIS (US Sales Only) HC A03/MF A01

An algebraic approach is developed to derive space groups using 4x4 Seitz matrices for the crystal classes mm2, 222 and mmm in the orthorhombic system. The advantage of the present method is that it is relatively simple and can be adapted to introduce space groups to beginners. One of the advantages of the present method is that it admits a geometrical visualization of the symmetry elements of space group. The method can easily be extended to other crystal classes in a straightforward way. DOE

N88-27077# Continuous Electron Beam Accelerator Facility, Newport New, Va.
PROGRESS IN DIAGNOSTIC TECHNIQUES FOR SC (SUPERCONDUCTING) CAVITIES
C. E. Reece 1988 19 p
(Contract DE-AC05-84ER-40150)
(DE88-008600; DOE/ER-40150/45) Avail: NTIS HC A03/MF A01

Despite the very real progress that has been made, the routine performance of superconducting cavities still falls far short of both the theoretical expectations and the performance of a few exceptional examples. It is the task of systematically applied diagnostic techniques to reveal additional information concerning the response of superconducting surfaces to applied RF fields. In

this paper we will direct our attention to discussions of recent developments in diagnostic techniqeus, such as thermometry in superfluid helium, and scanning laser acoustic microscopy. DOE

N88-27078# Bethlehem Steel Co., Pa.
HIGH RESOLUTION DETECTION OF SOLUTE SEGREGATION TO THE CORES OF DISLOCATIONS IN GRAIN BOUNDARIES
J. R. Michael, C. H. Lin, and S. L. Sass (Cornell Univ., Ithaca, N.Y.) Mar. 1988 5 p Prepared in cooperation with Cornell Univ., Ithaca, NY.
(Contract DE-FG02-85ER-45211)
(DE88-009168; DOE/ER-45211/8; MSC-6391) Avail: NTIS HC A02/MF A01

Thin film Fe -0.8 at. percent Au bicrystals, approximately 60 nm thick, containing (001) twist boundaries were prepared. The average compositon of the bicrystal was determined by Rutherford backscattering spectroscopy (RBS), which also showed that the Au was nonuniformly distributed along the direction normal to the interface, with a large amount concentrated at the (001) twist boundary. This observation constitutes direct evidence that the Au is segregated to the vicinity of the grain boundary. The Au distribution within the plane of the interface was analyzed in a Vacuum Generators HB-501 Scanning Transmission Electron Microscope (STEM) equipped with a field emission electron source and a Link Analytical windowless X-ray detector. The boundary plane was oriented perpendicular to the electron beam. Digital line scans were performed across the dislocation network. Au segregates extensively to the cores of the (100)-type dislocations in small angle (001) twist boundaries in Fe-Au alloys. Our observations demonstrate that the (110) network is favored in pure Fe, which leads to the suggestion that the dislocation core energy plays an important role in determining the stable boundary structure. DOE

N88-27079# Illinois Univ., Chicago. Dept. of Physics.
THE SUPERCONDUCTING TRANSITION IN OXYGEN DEFICIENT YBa2Cu3O(SUB 7-DELTA)
H. Claus, G. W. Crabtree, W. K. Kwok, and B. W. Veal (Argonne National Lab., Ill.) 1988 2 p Presented at the International Conference on High Temperature Superconductors and Materials and Mechanisms of Superconductivity, Interlaken, Switzerland, 29 Feb. - 4 Mar. 1988 Prepared in cooperation with Argonne National Lab., IL.
(Contract W-31109-eng-38)
(DE88-009957; CONF-880206-12; CONF-880206) Avail: NTIS HC A02/MF A01

In this paper we compare the superconductive transition of several oxygen deficient samples measured inductively to that measured resistively and point out important systematic differences between the results of the two types of measurements. Fully oxygenated samples were prepared. The oxygen stoichiometry was reduced by heat treatment at 500 C for 22 hours in an O2Ar mixture containing various amounts of O2 flowing over the sample. Samples were then quenched in liquid nitrogen to prevent any change in the oxygen stoichiometry upon cooling. The oxygen content of the samples was determined by weighing. Superconducting transition temperatures were determined by magnetic shielding measurements in a low field SQUID magnetometer in fields of 2 Gauss. The measurements were carried out by cooling the sample to 4.2 K in zero field, applying the measuring field and taking data on warming. Resistivity measurements were made by the four probe ac technique at frequency of 100 Hz and with a measuring current of 1.5mA. DOE

N88-27080# Argonne National Lab., Ill. Materials Science Div.
ANISOTROPIC CHARACTERISTIC LENGTHS IN SINGLE CRYSTAL YBa2Cu3O(SUB 7-DELTA)
A. Umezawa, G. W. Crabtree, and J. Z. Liu Feb. 1988 9 p Presented at the International Conference on High Temperature Superconductors and Materials and Mechanisms of Superconductivity, Interlaken, Switzerland, 29 Feb. - 4 Mar. 1988
(Contract W-31109-eng-38)
(DE88-009959; CONF-880206-10; CONF-880206) Avail: NTIS HC A02/MF A01

The available data on the upper critical field in single crystal samples of YBa2Cu3O(sub 7-delta) is reviewed, and values for the slope near T(sub c) extracted. We report new measurements of the lower critical field at low temperature from magnetization data on several single crystals with varying strength of flux pinning. We then infer the anisotropy of the Ginzburg-Landau parameter, coherence length, and penetration depth from the measured upper and lower critical field data using London electrodynamics. DOE

N88-27081# Argonne National Lab., Ill. Materials Science Div.
ANISOTROPY OF THE LOWER CRITICAL FIELD IN YBa2Cu3O(SUB 7-DELTA)
A. Umezawa, G. W. Crabtree, J. Z. Liu, and L. H. Nunez Feb. 1988 7 p Presented at the Discussion Meeting on High-/Tc/ Superconductors, Mauterndorf, Austria, 7-11 Feb. 1988
(Contract W-31109-eng-38)
(DE88-009971; CONF-880207-3) Avail: NTIS HC A02/MF A01

We report the first careful measurements of the two dimensional anisotropy of the lower critical field H(sub c1). We compare the anisotropy in our values of H(sub c1) with the anisotropy observed in H(sub c2) and derive values for the anisotropy of the effective mass. The single crystals used in this study were grown by a solid state annealing method. Y2O3, BaCO3, and CuO powders were mixed in the stoichiometric 1:2:3 ratio, ground with a mortar and pestle, placed in a platinum crucible and heated to 975 C for 3-5 days. The reaction product contained many small crystals up to typical dimensions of 0.5 mm. The crystals showed a sharp inductive onset at 91.5 K as measured in a dc shielding experiment in a field of 10 Oe. In general the crystals were not oxygen annealed before measurement. Three crystals were selected for measurements of H(sub c1). One of the crystals was used as-grown, one was annealed for 24 hours at 500 C in a pure oxygen environment, and one was irradiated with neutrons to a fluence of 8.16 X 10 to the 17 neutrons/sq cm. Results are discussed. DOE

N88-27082# Argonne National Lab., Ill.
PREPARATION OF HIGH-T(SUB)c Y1Ba2Cu3O(SUB 7-DELTA) SUPERCONDUCTING THIN FILMS BY MBE (MOLECULAR-BEAM-EPITAXY) TECHNIQUES
K. Y. Yang, H. Homma, R. Lee, R. Bhadra, J. P. Locquet, Y Bruynseraede, and I. K. Schuller Feb. 1988 6 p Presented at the Spring Meeting of the Materials Research Society, Reno, Nev., 4 Apr. 1988 Prepared in cooperation with Louvain Univ. (Belgium); California Univ., San Diego, La Jolla.
(Contract W-31109-eng-38)
(DE88-009999; CONF-880408-21; CONF-880408) Avail: NTIS HC A02

We report here the fabrication of high temperature superconducting thin films of Ya-Ba-Cu-O by metal Molecular-Beam-Epitaxy technique. X-ray analysis of the films grown on SrTiO3(100) substrate indicates a preferred orientation with a-axis normal to the surface. Raman scattering was used as an effective tool in the determination of the oxygen stoichiometry and impurity phases in these Y-Ba-Cu-O thin films. DOE

N88-27083# Argonne National Lab., Ill.
OXYGEN VACANCY ORDERING AND SUPERCONDUCTIVITY IN YBa2Cu3O(SUB 7-x)
J. D. Jorgensen, H. Shaked, D. G. Hinks, B. Dabrowski, B. W. Veal, A. P. Paulikas, L. J. Nowicki, G. W. Crabtree, W. K. Kwok, and L. N. Nunez et al. Mar. 1988 12 p Presented at the International Conference on High Temperature Superconductors and Materials and Mechanisms of Superconductivity, Interlaken, Switzerland, 29 Feb. - 4 Mar. 1988
(Contract W-31109-eng-38)
(DE88-010005; CONF-880206-11) Avail: NTIS HC A03/MF A01

The superconducting properties of YBa2Cu3O(sub 7-x) have been shown to depend markedly on the overall oxygen

stoichiometry and on the ordering of oxygen vacancies on the available sites. YBa2Cu3O(sub 7-x) has been studied in situ by high-temperature neutron powder diffraction in controlled oxygen atmospheres in order to learn the structural properties of the system in thermodynamic equilibrium. Additionally, metastable, oxygen-deficient samples produced by quenching into liquid nitrogen from high temperature and various oxygen partial pressures have been studied at room temperature or low temperature in order to correlate the structural and superconducting properties. Such experiments have shown that a systematic relationship exists between the superconducting transition temperature, T(sub c), the number of oxygen vacancies, and the degree of oxygen vacancy ordering. This brief paper reviews our work in these areas. DOE

N88-27084# Argonne National Lab., Ill.
PURE METALLIC BRIDGE AND POINT-CONTACT TUNNELING INTO SINGLE- AND POLYCRYSTAL YBa2Cu3O(SUB 7-y)
K. E. Gray, E. R. Moog, and M. E. Hawley Jan. 1988 5 p Presented at the Discussion Meeting on High-/Tc/ Superconductors, Mauterndorf, Austria, 7-11 Feb. 1988
(Contract W-31109-eng-38)
(DE88-010030; CONF-880207-6) Avail: NTIS HC A02/MF A01

It is known theoretically and experimentally that when the resistance of a point-contact is decreased the current-voltage characteristic, 1(5), changes from that of an insulating barrier to that of a pure metallic bridge. Such an 1(5) still shows the energy gap but, because of its much lower resistance, it is less sensitive to extraneous conduction mechanisms. Values of between 25 and 35 MeV are reported here for YBa2Cu3O(sub 7-y), and these are in agreement with our results for low-resistance point-contact tunneling in both single- and poly-crystal samples. Examples of 1(5) and the conductance, dI/dV, will also be presented for pure metallic bridges as well as higher resistance point-contact tunneling. An electrically insulating layer is found on the surface of all samples, including single-crystals showing no evidence of impurities measured by Raman scattering. Consequently, contact of the tunneling tip is necessary to mechanically scrape, and thus clean, the surface before a measurable current can be obtained. Although this represents a disadvantage, a more serious drawback of point-contact tunneling is the inability to measure the 1(5) continuously through the transition temperature T(sub c) due to thermal expansion of the mechanical apparatus. We will argue that thin film tunnel junctions are thus desirable both to unambiguously identify the energy gap with the 90 K bulk material, and to subtract the background conductance to evaluate the electron coupling mechanism in the high-T(sub c) superconductors(HTS), that is analogous to electron-phonon coupling in traditional superconductors. DOE

N88-27085# Argonne National Lab., Ill. Materials Science Div.
ELECTRON IRRADIATION EFFECTS IN YBa2Cu3O7-DELTA SINGLE CRYSTALS
M. A. Kirk, M. C. Baker, J. Z. Liu, D. J. Lam, and H. W. Weber (Atominstitut der Oesterreichischen Hochschulen, Vienna.) Apr. 1988 8 p Presented at the Discussion Meeting on High-/Tc/ Superconductors, Mauterndorf, Austria, 7-11 Feb. 1988
(Contract W-31109-eng-38)
(DE88-010050; CONF-880207-5) Avail: NTIS HC A02/MF A01

Defect structures in YBa2Cu3O(sub 7- delta) produced by electron irradiation at 300 K, were investigated by transmission electron microscopy. Threshold energies for the production of visible defects were determined to b 152 keV and 131 keV (+ or -7 keV) in directions near the a- and b-axes, respectively (b greater than a, both perpendicular to c, the long axis in the orthorhombic structure). During above-threshold irradiations in an electron flux of 3 x 10 to the 18th/sq cm/sec, extended defects were observed to form and grow to sizes of 10-50 nm over 15 minutes, in material thicknesses varying between 20 and 200 nm. Upon irradiation between the a- and b-thresholds, movement of twin plane boundaries and shrinkage of twinned volume were observed. All these findings suggest oxygen atom displacements in the basal plane with recoil energies near 20 eV. Above-threshold irradiations also show the collapse of c-axis long-range order into a planar faulted defect structure with short range order peaks at 1.2 c and 1.07 c, depending on the irradiation direction. DOE

N88-27086# Argonne National Lab., Ill.
PHASE TRANSFORMATIONS AND THERMODYNAMIC BEHAVIOR OF THE YBa2Cu3O(SUB)x SYSTEM VIA EMF MEASUREMENTS
M. Tetenbaum, A. Brown, and M. Blander 1988 13 p Presented at the 90th Annual Meeting of American Ceramic Society, Cincinnati, Ohio, 1 May 1988
(Contract W-31109-eng-38)
(DE88-010054; CONF-880504-2) Avail: NTIS HC A03/MF A01

EMF measurements of oxygen fugacities as a function of stoichiometry in YBa2Cu3Ox were made in the temperature range 650-750 C by means of an oxygen titration technique with a ZrO2 electrolyte doped with Y2O3. From plots of equilibrium oxygen pressures versus x, no sign of a change in curvature or discontinuity was observed at an oxygen stoichiometry of x = 6.5 where copper is divalent. A change in slope was observed when x approximates 6.3. The EMF measurements were extended to an oxygen stoichiometry of x = 6.15; after slow cooling to room temperature, X-ray examination of the samples indicated that the original orthorhombic phase was completely transformed to tetragonal. A rapid increase in the partial molar entropy of oxygen, delta bar S sub O sub 2, was found in the composition range x = 6.3 to 6.15. The increase in delta bar S sub O sub 2 values appears to reflect the differences between distributions of oxygen atoms and vacancies in the relatively disordered tetragonal structure and the more ordered orthorhombic structure. The results to date indicate that the important orthorhombic structure can exist over an extended oxygen composition range, namely, approximates 6.3-7.0 at temperatures in the range of 650-750 C. DOE

N88-27087# Argonne National Lab., Ill.
CERAMIC PROCESSING OF HIGH-T(SUB)c SUPERCONDUCTORS
R. B. Poeppel, J. P. Singh, M. T. Lanagan, K. C. Goretta, J. T. Dusek, and D. W. Capone, II 1988 4 p Presented at the SPIE Conference on Superconducting Materials and Instruments, Los Angeles, Calif., 10 Jan. 1988
(Contract W-31109-eng-38)
(DE88-010090; CONF-880182-1) Avail: NTIS HC A02

The means by which superconducting YBa2Cu3O(sub 7-x) powders can be synthesized are summarized. Methods of forming powders into useful shapes are then described. Lastly, heat treatment schedules used for consolidation of the powders into dense, sound bodies with good superconducting properties are discussed. DOE

N88-27088# Missouri Univ., Rolla.
DEFECT CHARACTERIZATION OF THE REDOX BEHAVIOR AND STABILITY OF CONDUCTING OXIDES
H. U. Anderson, S. A. Howard, and D. M. Sparlin 1988 35 p
(Contract DE-FG02-85ER-45219)
(DE88-010799; DOE/ER-45219/3) Avail: NTIS HC A03/MF A01

Goal was to study the interrelationships between electrical conductivity, oxidation-reduction kinetics, defect structure, and composition of n- and p-type binary and ternary transition metal oxides. Experimental part included thermogravimet, X-ray diffraction, thermally stimulated current, oxygen diffusion, optical absorption, transmission electron microscopy, electrical conductivity, and Seeback effect. Systems studied were La-doped SrTiO3, Mg-doped LaCrO3, Mg-doped LaMnO3, Sr-doped LaMnO3, Nb-doped LaCrO3, and Ba2YCu3O sub 7-x. Results show: 1) that at low oxygen activity donor LaCrO3 is n-type, but becomes p-type as oxidation occurs; 2) the oxidation kinetics of both LaCrO3 and SrTiO3 are dominated by a rapid oxygen uptake followed by a slow uptake which can be attributed to a grain boundary type of process followed by volume diffusion; 3) DLTS and electrode probe measurements suggest that the 0.5eV defect state observed for SrTiO3 is probally due to the grain boundaries; 4) X-ray diffraction

studies have revealed that the degree of cation imperfection in La-doped SrTiO3 is directly related to the lattice strain; 5) Initial results for the Ba2YCu3O sub 7-x system suggests that the electrical conductivity, hole mobility and thermoelectric power are more strongly dependent upon oxygen stoichiometry than upon temperature. DOE

N88-27089# Oxford Univ. (England). Dept. of Theoretical Physics.
DEFECTS AND DISORDER IN AMORPHOUS AND DAMAGED SILICON Final Report, May 1984 - Jun. 1987
Roger J. Elliott Dec. 1987 13 p
(Contract DAJA45-83-C-0056; DA Proj. 1L1-61102-BH-57)
(AD-A192277) Avail: NTIS HC A03/MF A01 CSCL 20L

This study of defects and disorder in Si has focussed on models of excitation near defects in the crystal, in structurally disordered amorphous material, and at interfaces between crystal and amorphous material. The first section deals with the vibrations of Si slabs with (3) faces subject to varying boundary conditions. In particular slabs with free boundaries, with dangling bonds saturated by hydrogen, and slabs embedded in amorphous material were considered. The shift and broadening of the Raman peak was calculated and it was shown how this could be used to obtain estimates of crystallyte size in disordered material. The main work related to a model of electron states at an interface between crystalline Si and amorphous SiO2. The latter material was modelled using a Bethe lattice. The final component of the work was a study of various aspects of electronic energy levels in quantum wells. The detailed form of the hole band structure including the anomalous dispersion of the sub-bands was examined in detail, as was the non-parabolicity of the conduction sub-bands. The effect of these changes on the exciton binding energy was examined in some detail for several systems. GRA

N88-27090# Lund Univ. (Sweden). Dept. of Solid State Physics.
DEFECTS IN HIGH-MOBILITY SEMICONDUCTOR SYSTEMS Interim Report No. 2
Hermann Grimmeiss 23 Dec. 1987 3 p
(Contract DAJA45-87-C-0052)
(AD-A192298) Avail: NTIS HC A02/MF A01 CSCL 20L

Work under subject contract was continued in the period 23 Oct thru 23 Dec 1987 on (1) extensive electrical examination of the Pb center on silicon surfaces; (2) preliminary electrical investigation of the new metastable gallium arsenide (GaAs) defect which competes with the EL-2 center; (3) initial EPR measurements on a high ceramic superconductor; (4) related conceptual studies and tests. The photocapacitance system described in the First Interim Report was applied to an extensive study of the Pb center on oxidized silicon (SI) surfaces. This center is the most important defect in integrated circuit technology, and serves as an ideal reference for study of other less-well characterized defects. GRA

N88-27091# Westinghouse Research and Development Center, Pittsburgh, Pa.
SUPERCONDUCTING ELECTRONIC FILM STRUCTURES Annual Report, 1 Jan. - 31 Dec. 1987
A. I. Braginski, J. R. Gavaler, and J. Talvacchio 24 Jan. 1988 26 p
(Contract F49620-85-C-0043)
(AD-A192907; Rept-88-9S52-SUPER-R1; AFOSR-88-0286TR)
Avail: NTIS HC A03/MF A01 CSCL 20C

Bulk samples of the new oxide superconductors were prepared and some of their properties measured. Thin films of yttrium-barium-copper-oxide, completely superconducting below 85K, were prepared by both sputtering and evaporation. The sputtered films on (100) and (110) strontium-titanium-oxide substrates were epitaxial. A correlation between oxygen content in as-deposited films and the formation of non-superconducting surface layers was established. The thickness of these layers was greatly reduced by sputtering in argon and oxygen gas mixtures. The presence of fluorine in the evaporated films was also found effective in minimizing the barium segregation which produces such layers. Zero resistance gold contact layers were obtained on Y-Ba-Cu-O-sputtered films which were processed entirely in situ. Tunneling data using a low-temperature tunneling microscope were obtained on both evaporated and sputtered Y-Ba-Cu-O films. A new surface characterization capability based on the analysis of (Low Energy Electron Diffraction) or (Reflection High Energy Electron Diffraction) diffraction spot intensity was developed. GRA

N88-27092# Virginia Univ., Charlottesville.
SIS (SUPERCONDUCTOR-INSULATOR-SUPERCONDUCTOR) MIXER RESEARCH Annual Technical Report, Nov. 1986 - Nov. 1987
M. J. Feldman Feb. 1988 12 p
(Grant AF AFOSR-0056-86)
(AD-A192908; UVA/525658/EE88/102; AFOSR-88-0289TR)
Avail: NTIS HC A03/MF A01 CSCL 20C

Theoretical and experimental research has been conducted to elucidate the basic physics behind the properties of Superconductor-Insulator-Superconductor (SIS) tunnel junction receiving devices. The saturation of the gain of the SIS mixer was measured using both monochromatic and thermal signals, and these experiments dramatically verified the theoretical expression derived in the previous report period. A study of the role of the image termination for SIS mixer behavior found that the nonlinear quantum reactance results in an effective time delay at the input port of the mixer. Many aspects of the operation of SIS mixers at submillimeter wavelengths were clarified, including a discussion of the potential of the new oxide superconductors for this field. The goal of the realization of high quality niobium nitride edge junctions was advanced by optimizing the edge profile and by improving the insulating barrier. GRA

N88-27093# Technische Univ., Berlin (West Germany). Fachbereich fuer Physik.
ELECTRONIC AND GEOMETRIC STRUCTURE OF SILVER AND PALLADIUM ON ALUMINUM (111) IN MONOATOMIC SURFACE LAYERS Ph.D. Thesis [DIE ELEKTRONISCHE UND GEOMETRISCHE STRUKTUR VON SILBER UND PALLADIUM AUF ALUMINIUM (111) IM MONOLAGENBEREICH]
Bjoern Frick Oct. 1987 105 p In GERMAN
(ETN-88-92120) Avail: NTIS HC A06/MF A01

Geometric and electronic structures of Ag and Pd on Al (111) are observed by low energy electron diffraction, by Auger electron spectroscopy, and angle resolved UV photoelectron spectroscopy. The Al (111) substrate is well adapted for the observation of crystal formation. Vapor deposited Ag and Pd lead to 2D-crystal formation by the growth of a monoatomic surface layer. Both systems show a similar electronic transfer of atomic character to the 3D-band. ESA

N88-27094# Stuttgart Univ. (West Germany). Inst. fuer Physik.
EPITAXY AND PROPERTIES OF TWO DIMENSIONAL GaInAs SEMICONDUCTOR STRUCTURES Ph.D. Thesis [EPITAXIE UND EIGENSCHAFTEN VON ZWEIDIMENSIONALEN GAINAS-HALBLEITERSTRUKTUREN]
Ferdinand Scholz 1986 134 p In GERMAN
(ETN-88-92357) Avail: NTIS HC A07/MF A01

Fabrication and investigation of two-dimensional GaInAs-InP structures are described. Crystal growth process in organometallic gas phase epitaxy is studied and appropriate equipment is developed where organometallic adducts as In and Ga sources are inserted. Preparation of InP-epitaxy layers serves to study the fabrication procedure and the final material. Quantum well structures are prepared and analyzed by photoluminescence, excitation spectroscopy, secondary emission mass spectroscopy, and X-ray diffractometry. ESA

N88-27095# Office National d'Etudes et de Recherches Aerospatiales, Paris (France).
CONTRIBUTION TO THE STUDY OF ORDER EFFECTS IN THE ISING MODEL FRAMEWORK: GROUND STATES AND PHASE DIAGRAMS Thesis
Alphonse Finel 1987 238 p In FRENCH; ENGLISH summary Report will also be announced as translation (ESA-TT-1118)
(ONERA-NT-1987; ISSN-0078-3781; ETN-88-92727) Avail: NTIS HC A11/MF A01

Order phenomena on a fixed underlying lattice are studied. The ground states at zero temperature are determined using an algorithm, the linear chain ground states with pair and multiple interactions up to the fifth neighbor. It does it partially for centered cubic lattices. At finite temperature approximate methods are used, including the cluster variation method. The introduction of a hierarchy of approximations for three-dimensional lattices allows a monotonic convergence towards the exact solution. Frustration and degeneracy effects and the ANNNI model are also discussed. ESA

N88-27096# Lawrence Livermore National Lab., Calif.
ON THE CHEMISTRY OF SUPERCONDUCTIVITY
R. More and E. Teller Aug. 1987 19 p Presented at the 7th Session of the International Seminars on Nuclear War, Erice, Italy, 19 Aug. 1987
(Contract W-7405-eng-48)
(DE88-010714; UCRL-98684; CONF-8708201-2; CONF-8708201) Avail: NTIS HC A03/MF A01

High-temperature superconductivity is observed in ceramics with complex crystal structures. In each case, perovskite-like layers (CuO2) are found next to cation-monoxide layers (LaO or CuO). We suggest that Bloch wave functions in these two layers are hybridized. The interaction of the bottom of an energy band in the monoxide layer with the top of the perovskite band gives rise to states with a low group velocity within these layers. Superconductivity is explained by the strong interaction of these electrons with loosely-bound oxygen ions which leads to pairing and ordering of the electrons. Experimental verification of this model may be obtained by observing the variation of the current due to the dependence of the group velocity on the location of oxygen ions. DOE

77 THERMODYNAMICS AND STATISTICAL PHYSICS

Includes quantum mechanics; theoretical physics; and Bose and Fermi statistics.

For related information see also *25 Inorganic and Physical Chemistry* and *34 Fluid Mechanics and Heat Transfer.*

N88-27097# Los Alamos National Lab., N. Mex.
EXTENSION OF BOLTZMANN'S THEORY TO A LIQUID
D. C. Wallace 1988 6 p Presented at the 3rd University of California Conference on Statistical Mechanics, Lake Arrowhead, Calif., 27 Mar. 1988
(Contract W-7405-eng-36)
(DE88-009153; LA-UR-88-1126; CONF-880307-2) Avail: NTIS HC A02/MF A01

A theory for the nonequilibrium statistical mechanics of a liquid is presented. This theory consists of coupled evolution equations for the one-particle momentum distribution, and for the two-particle correlation function, and it possesses the same important properties as does Boltzmann's theory, namely the local conservation laws, the local h theorem, and the correct equilibrium solution. DOE

N88-27098# Lawrence Livermore National Lab., Calif.
NON-EQUILIBRIUM PHASES AND PHASE DIAGRAMS
T. B. Massalski and H. F. Rizzo Mar. 1988 9 p Presented at the International Symposium on Nonequilibrium Solid Phase of Metals and Alloys, Kyoto, Japan, 14 Mar. 1988
(Contract W-7405-eng-48)
(DE88-008896; UCRL-98460; CONF-880310-2) Avail: NTIS HC A02/MF A01

The degree of usefulness of the phase diagram and the related thermodynamics is considered in predicting and understanding the formation of metastable phases during quenching, or during low-temperature solid-state interdiffusion, or during co-deposition. Recent research has demonstrated that many of such metastable phases are formed because the more stable intermediate phases that are favored thermodynamically are nevertheless bypassed kinetically. The kinetic elimination of intermediate phases provides conditions where a metastable equilibrium can be established at low temperatures between the supercooled liquid and the terminal solid solutions, leading to metastable partitioned two-phase regions. Alternatively, the range of the metastable phases may be governed by the T sub 0 principle related to the crossover of the respective free energy curves, or may be controlled mainly by kinetic considerations. Which particular thermodynamic conditions apply appears to depend on the initial form of the phase diagram and the specific technique used. The occurrence of massive transformations also is discussed. DOE

N88-27099# International Centre for Theoretical Physics, Trieste (Italy).
ON LINEAR RELATIONSHIP BETWEEN SHOCK VELOCITY AND PARTICLE VELOCITY
H. Dandache Nov. 1986 12 p
(DE88-701827; IC-86/287) Avail: NTIS (US Sales Only) HC A03/MF A01

We attempt to derive the linear relationship between shock velocity, U sub s, and particle velocity, U sub p, from thermodynamic considerations, taking into account an ideal gas equation of state and a Mie-Gruneisen equation of state for solids. DOE

N88-27100# International Centre for Theoretical Physics, Trieste (Italy).
THEORY OF RELATIVITY AND SUPER-LIGHT-SPEEDS-I: KINEMATICAL PART
Shenglin Cao May 1987 14 p
(DE88-701832; IC-86/328) Avail: NTIS (US Sales Only) HC A03/MF A01

According to some local properties of Lorentz transformation, Einstein stated: Velocities greater than that of light have no possibility of existence. He neglected to point out the applicable range of the special theory of relativity. In fact, it could only be applied to the sub-light-speed. This paper shows that if we think of the possibility of the existence of the super-light-speed and redescribe the special theory of relativity following Einstein's way, a new kinematical theory would be founded. The new theory would retain all kinematical meaning of the special theory of relativity when matters move with sub-light-speed and would give new content when matters move with super-light-speed. The paper also discusses the observation principle for the motions with the super-light-speed. DOE

N88-27101# International Centre for Theoretical Physics, Trieste (Italy).
FINITELY MANY DELTA-INTERACTIONS WITH SUPPORTS ON CONCENTRIC SPHERES
J. Shabani Dec. 1986 17 p
(DE88-701834; IC-86/336) Avail: NTIS (US Sales Only) HC A03/MF A01

Using the theory of self adjoint extensions of symmetric operators we give the precise methematical definition of the quantum Hamiltonian describing a finite number of delta interactions with supports of concentric spheres. We also derive its resolvent, describe its spectral properties and show how this Hamiltonian can be obtained as a norm resolvent limit of a family of local scaled short range Hamiltonians. DOE

N88-27102# International Centre for Theoretical Physics, Trieste (Italy).
COMBINING RELATIVITY AND QUANTUM MECHANICS: SCHROEDINGER'S INTERPRETATION OF PSI

A. O. Barut Jul. 1987 12 p
(DE88-701899; IC-87/157) Avail: NTIS (US Sales Only) HC A03/MF A01

The incongruence between quantum theory and relativity theory is traced to the probability interpretation of the former. The classical continium interpretation of psi removes the difficulty. How quantum properties of matter and light, and in particular the radiative problems, like spontaneous emission and Lamb shift, may be accounted in a first quantized Maxwell-Dirac system is discussed. DOE

N88-27103# Technische Univ., Munich (West Germany). Lehrstuhl fuer Thermodynamik.
THERMAL CONDUCTIVITY OF PURE FLUIDS IN A LARGE REGION AROUND THE CRITICAL POINT Ph.D. Thesis [DIE TEMPERATURLEITFAEHIGKEIT REINER FLUIDE IM WEITEN ZUSTANDSBEREICH UM DEN KRITISCHEN PUNKT]
Peter Jany 1986 133 p In GERMAN
(ETN-88-92135) Avail: NTIS HC A07/MF A01

Temperature conductivity from -35 K to +50 K of 5 pure fluids is studied: sulfur hexafluoride, ethane, dinitrogen oxide, CCIF3, and xenon. Data are obtained along the critical isochores and isotherms and on the binary phases curves. Light scattering and photon correlation spectroscopy are used in the region near the critical point. Auxiliary data obtained are pressure and refractive index allowing the determination of density and isothermal compressibility. ESA

N88-27104# Oak Ridge National Lab., Tenn.
TRANSIENT THERMAL ANALYSIS OF THREE LATENT HEAT STORAGE CONFIGURATIONS FOR RAPID THERMAL CHARGING
T. K. Stovall 28 Jun. 1988 72 p
(Contract DE-AC05-84OR-21400)
(DE88-008943; ORNL/TM-10719) Avail: NTIS HC A04/MF A01

A space-based thermal storage applicaton must accept large quantities of heat in a short period of time at an elevated temperature. An approximate model of a lithium hydride phase change energy storage system was used to estimate reasonable physical dimensions for this application which included the use of a liquid metal heat transfer fluid. A finite difference computer code was developed and used to evaluate three methods of enhancing heat transfer in the PCM energy storage system. None of these three methods, inserting thin fins, reticulated nickel, or liquid lithium, improved the system performance by a significantly large amount. The use of a 95 percent void fraction reticulated nickel insert was found to increase the storage capacity of the system slightly with a small decrease in the system energy density. The addition of 10 percent liquid lithium was found to cause minor increases in both storage density and storage capacity with the added benefit of reducing the hydrogen pressure of the lithium hydride. DOE

80 SOCIAL SCIENCES (GENERAL)

Includes educational matters.

N88-27105# Technische Hogeschool, Delft (Netherlands). Faculty of Technical Mathematics and Informatics.
THE SINE AND COSINE FUNCTION FOR CLASS 4-VWO. EXPLORATION OF POSSIBLE BOTTLENECKS [DE SINUS- EN COSINUSFUNCTIE VOOR 4-VWO. EEN VERKENNING VAN MOGELIJKE KNELPUNTEN]
W. M. G. Jochems, C. A. P. G. vanderMast, H. J. Smid, J. Vastenhouw, and A. Verweij 1987 65 p In DUTCH
(Rept-87-72; B8736946; ISSN-0920-2358; ETN-88-92448) Avail: NTIS HC A04/MF A01

Tests in goniometry were given to students in the frameworks of computer aided learning. The specific difficulties encountered by the students, as well as the basic levels of performance were determined. The results of the tests were quantitatively and qualitatively analyzed. Based on these results advice on the implementation of computer aided learning is given. ESA

N88-27106# Technische Hogeschool, Delft (Netherlands). Faculty of Technical Mathematics and Informatics.
DESIGN AND DEVELOPMENT OF COURSEWARE FOR GONIOMETRY [ONTWERP EN ONTWIKKELING VAN COURSEWARE VOOR GONIOMETRIE]
W. M. G. Jochems, C. A. P. G. vanderMast, H. J. Smid, J. Vastenhouw, G. Verveld, A. Verweij, and F. R. vanderVlugt 1987 50 p In DUTCH
(Rept-87-73; B8736947; ISSN-0920-2358; ETN-88-92449)
Copyright Avail: NTIS HC A03/MF A01

Computer programs for computer aided learning in goniometry were developed. The development took into account the dominating effects of the textbook on the programming of the courses. The choice of the content of the computerized lessons is explained. The structure of the different computerized lessons is presented. The didactic and technical difficulties encountered during the development of the programs are outlined. The evaluation of the lessons by the students is summarized. ESA

81 ADMINISTRATION AND MANAGEMENT

Includes management planning and research.

N88-27107# Air Command and Staff Coll., Maxwell AFB, Ala.
LAUNCH OPERATIONS TO SUPPORT FUTURE SPACE FORCES
John B. Sullivan Apr. 1988 23 p
(AD-A192679; ACSC-88-2520) Avail: NTIS HC A03/MF A01 CSCL 22A

Currently, military space launch operations are managed by Air Force Systems Command. The research and development perspective of Air Force Systems Command limits the flexibility and responsiveness of the U.S.'s space launch capability. The paper advocates that space launch operations should be managed by Air Force Space Command. The mission-accomplishment perspective of Air Force Space Command will be needed to achieve an operational space launch capability. Military doctrine identifies the need for an operational space launch capability and operational commands to manage other weapon systems such as the ballistic missile. GRA

82 DOCUMENTATION AND INFORMATION SCIENCE

Includes information management; information storage and retrieval technology; technical writing; graphic arts; and micrography.

For computer documentation see *61 Computer Programming and Software.*

N88-27108*# National Academy of Sciences - National Research Council, Washington, D. C. Space Science Board.
ISSUES AND RECOMMENDATIONS ASSOCIATED WITH DISTRIBUTED COMPUTATION AND DATA MANAGEMENT SYSTEMS FOR THE SPACE SCIENCES
1986 124 p
(Contract NASw-3482)
(NASA-CR-183026; NAS 1.26:183026; PB88-188446) Avail: NTIS HC A06/MF A01 CSCL 05B

The primary purpose of the report is to explore management approaches and technology developments for computation and data management systems designed to meet future needs in the space sciences.The report builds on work presented in previous reports on solar-terrestrial and planetary reports, broadening the outlook to all of the space sciences, and considering policy issues aspects related to coordiantion between data centers, missions,

and ongoing research activities, because it is perceived that the rapid growth of data and the wide geographic distribution of relevant facilities will present especially troublesome problems for data archiving, distribution, and analysis. GRA

N88-27109# National Bureau of Standards, Gaithersburg, Md. Information Systems Engineering Div.
COMPUTER SCIENCE AND TECHNOLOGY: KNOWLEDGE-BASED SYSTEM FOR PHYSICAL DATABASE DESIGN Final Report
C. E. Dabrowski and D. K. Jefferson Feb. 1988 62 p
(PB88-193289; NBS/SP-500/151) Avail: NTIS HC A04/MF A01; also available SOD HC $3.25 as 003-003-02849-5 CSCL 05B

A knowledge-based system for physical database design has been developed at the Institute for Computer Sciences and Technology. The system processes large multi-entity databases with complex workload requirements and identifies near-optimal physical designs. It employs heuristics developed by physical design experts and cost modeling algorithms to reduce the large number of design alternatives available in large complex problems to a few select designs. The system is implemented in LISP. GRA

N88-27110# Kent Univ., Canterbury (England). Computing Lab.
TOWARDS KNOWLEDGE BASES-SEMANTICS, RULES AND OBJECT-ORIENTED PROGRAMMING
E. A. Oxborrow 1987 19 p
(PB88-108154; UKC/COMPUTING LAB-45) Avail: NTIS HC E03/MF E04; copy not available from STI Facility CSCL 05B

The data modeling aspects of a knowledge base management system is studied. After identifying the problems with existing systems, the objectives of a knowledge base description language is investigated, and some work which has been carried out in fields related to the objectives is considered. A language called KBZ is then introduced. The main features which KBZ is designed to support are: full conceptual model semantics, dynamic and static rules, object oriented concepts, and a unified approach to the description of both data model and functional model aspects of an application. The emphasis is on the data modeling capabilities of KBZ, but its ability to support other features is also discussed. Author

N88-27111# Lund Univ. (Sweden). Research Policy Inst.
CONTEXT OF NATIONAL INFORMATION SYSTEMS IN DEVELOPING COUNTRIES: INDIA AND CHINA IN A COMPARATIVE PERSPECTIVE Ph.D. Thesis
E. Baark 1986 221 p
(PB88-109954; ISBN-91-86002-58-9) Avail: NTIS HC E10/MF E10; copy not available from STI Facility CSCL 05B

The problem, theoretical framework, conceptual models and main propositions, research approach and methodology of the topic are discussed. National information systems in China and India are also discussed. This includes dissimination structures, types of information and information flow, organizational framework, information policy and the modernization of services. Information needs and utilization; both a general survey and a case study is presented. A basic information source, and intrinsic limitations to information utilization is included. The availability of standard documents in India and China along with extrinsic limitations to information utilization and problems of quality control in both countries were studied. Author

N88-27112# Technische Hogeschool, Delft (Netherlands). Faculteit der Geodesie.
KNOWLEDGE REPRESENTATION IN GEOGRAPHIC INFORMATION SYSTEMS Thesis [KENNISREPRESENTATIE IN GEOGRAFISCHE INFORMATIESYSTEMEN]
N. P. vanderBeek May 1987 60 p In DUTCH
(ETN-88-92470) Avail: NTIS HC A04/MF A01

Information systems and knowledge representation in geography are presented. The information paradigm and the recursion principle are given. In knowledge representation semantic networks, modeling of the real system, operations in a model, and properties and values of models are discussed. The specific aspects of geographic information systems are given. The characteristics of the modeling of spatial data in a geographic information system are treated. ESA

N88-27113# Lawrence Livermore National Lab., Calif.
AN INTEGRATED, MULTI-VENDOR DISTRIBUTED DATA ACQUISITION SYSTEM
D. N. Butner, M. Drlik, W. H. Meyer, J. M. Moller, and G. G. Preckshot 3 Mar. 1988 14 p Presented at the 7th Topical Conference on High Temperature Plasma Diagnostics, Napa, Calif., 13 Mar. 1988
(Contract W-7405-eng-48)
(DE88-008900; UCRL-97871; CONF-880364-21) Avail: NTIS HC A03/MF A01

A distributed data acquisition system that uses various computer hardware and software is being developed to support magnetic fusion experiments at Lawrence Livermore National Laboratory (LLNL). The experimental sequence of operations is controlled by a supervisory program, which coordinates software running on Digital Equipment Corporation (DEC) VAX computers, Hewlett-Packard (HP) UNIX-based workstations, and HP BASIC desk-top computers. An interprocess communication system (IPCS) allows programs to communicate with one another in a standard manner regardless of program location in the network or of operating system and hardware differences. We discuss the design and implementation of this data acquisition system with particular emphasis on the coordination model and the IPCS. DOE

N88-27114# Vrije Universiteit, Amsterdam (Netherlands). Subfaculteit Wiskunde en Informatica.
HIDING IN STREAM SEMANTICS OF UNIFORM CONCURRENCY
J. J. C. Meyer and E. R. Olderog 1986 22 p Prepared in cooperation with Kiel Univ., Fed. Republic of Germany
(PB88-121579; IR-125) Avail: NTIS HC E03/MF E01; copy not available from STI Facility CSCL 05B

A stream semantics is given for a language with recursion, parallelism, and a hiding operator. Among the technical results, the continuity of the hiding operator in the framework is proved. For this, several lemmas are used dealing with topological and order-theoretical properties of the semantical model. Finally the hiding operator is considered a syntactical transformation, and a calculus is given for it by means of fixed point transformations. GRA

N88-26326# Tokyo Metropolitan Univ. (Japan). Coll. of Aeronautical Engineering.
THEORY OF NUMERICAL INFORMATION ENVIRONMENT AND ITS APPLICATIONS
Masayuki Hatakeyama *In* National Aerospace Lab., Proceedings of the 5th NAL Symposium on Aircraft Computational Aerodynamics Nov. 1987 p 255-259 In JAPANESE; ENGLISH summary (For primary document see N88-26290 20-01)
Avail: NTIS HC A12/MF A01

83 ECONOMICS AND COST ANALYSIS

Includes cost effectiveness studies.

N88-27115# Edgerton, Germeshausen and Grier, Inc., Idaho Falls, Idaho.
MUTUALLY EXCLUSIVE ALTERNATIVES BY CLUSTERING
E. Mooney and T. Ross 1988 5 p Presented at the Institute of Industrial Engineers Meeting, Orlando, Fla., 22 May 1988
(Contract DE-AC07-76ID-01570)
(DE88-007707; EGG-M-00388; CONF-880591-1) Avail: NTIS HC A02

This paper begins with a brief introduction to cluster analysis and an overview of its application in the identification of mutually exclusive alternatives for economic analysis. The approach is then

illustrated with an example, followed by some concluding remarks. The example involves maintenance of minicomputers at INEL.
DOE

N88-27116# Oak Ridge National Lab., Tenn.
KNOWLEDGE-BASED COST ESTIMATING VS TRADITIONAL SOFTWARE COST MODELS
L. F. Arrowood, M. L. Emrich, A. R. Sadlowe, K. A. Jones, B. D. Watson, and R. Surapaneni 12 Apr. 1988 25 p Presented at the 2nd Annual Engineering Society of Detroit SMI Expert Systems 88 Solutions in Manufacturing Conference and Exhibition, Detroit, Mich., 12 Apr. 1988
(Contract DE-AC05-84OR-21400)
(DE88-009707; CONF-8804115-1) Avail: NTIS HC A03/MF A01

A knowledge-based system, ADP-Estimator, is under development to perform ADP project cost estimating. Designed to retain crucial expertise held by experienced project leaders, this system allows new project leaders to interactively generate cost estimates. Initially, project leaders indicate constraints (e.g. personnel levels, equipment, and facilities) placed upon a project. The system uses these to identify resources and procedures required for project completion. The efficacy of this system is compared with manual efforts and traditional software cost models. DOE

N88-27117# Army Engineer Div., Huntsville, Ala.
PAX ECONOPACK ECONOMIC ANALYSIS PACKAGE USERS MANUAL
Hugh W. Mason Feb. 1988 444 p Supersedes HNDSP-86-117-ED-ES-Rev
(AD-A192949; HNDSP-86-117-ED-ES-Rev) Avail: NTIS HC A19/MF A01 CSCL 05C

This users manual provides information on the use of the ECONPACK Computer Program, an interactive computer system which assists the Department of Defense in the preparation of life cycle costs analysis reports in support of funding requests for construction programs as well as many other types of programs. The program is in accordance with AR 11-28 Economic Analysis and Program Evaluation for Resource Management. GRA

84 LAW, POLITICAL SCIENCE AND SPACE POLICY

Includes NASA appropriation hearings; aviation law; space law and policy; international law; international cooperation; and patent policy.

N88-27118# Bundesministerium fuer Forschung und Technologie, Bonn (West Germany).
SPACE POLICY OF COMMON SENSE AND MODERATION [WELTRAUMPOLITIK DER VERNUNFT UND DES MASSES]
3 Nov. 1987 14 p In GERMAN
(Rept-49/87; ETN-88-91950) Avail: NTIS HC A03/MF A01

The space policy of the government of the Federal Republic of Germany is presented. It is explained in what sense this policy contributes to securing the future of the country. The thirst for knowledge as a stimulus for internationally enhanced space activities is presented. The importance of present space activities is depicted. The policy in the field of space research and technology is outlined. The economic burdens imposed by space research and technology are presented. ESA

85 URBAN TECHNOLOGY AND TRANSPORTATION

Includes applications of space technology to urban problems; technology transfer; technology assessment; and surface and mass transportation.

For related information see also *03 Air Transportation and Safety, 16 Space Transportation,* and *44 Energy Production and Conversion.*

N88-27119*# Sverdrup Technology, Inc., Cleveland, Ohio.
RESOURCES: NASA FOR ENTREPRENEURS
Mary Ann Jannazo May 1988 44 p Sponsored by NASA, Washington, D. C. Original contains color illustrations
(NASA-CR-182152; NAS 1.26:182152) Avail: NTIS HC A03/MF A01 CSCL 05A

The services of NASA's Technology Utilization Program are detailed and highlights of spinoff products in various stages of completion are described. Areas discussed include: Stirling engines for automotive applications, klystron tubes used to reduce power costs at UHF television stations, sports applications of riblet film (e.g., boat racing), reinforced plastic for high-temperature applications, coating technology appropriate for such applications similar to the renovation of the Statue of Liberty, and medical uses of fuel pump technology (e.g., heart pumps). J.P.B.

88 SPACE SCIENCES (GENERAL)

N88-27120*# Martin Marietta Aerospace, Denver, Colo.
STUDY OF COMET NUCLEUS GAMMA-RAY SPECTROMETER PENETRATION SYSTEM
G. L. Adams, R. J. Amundsen, R. W. Beardsley, R. H. Cash, B. C. Clark, T. C. D. Knight, J. P. Martin, P. Monti, D. A. Outteridge, and W. D. Plaster Mar. 1986 244 p
(Contract NAS2-12130)
(NASA-CR-177393; NAS 1.26:177393) Avail: NTIS HC A11/MF A01 CSCL 03A

A penetrator system has been suggested as an approach for making in situ measurements of the composition and physical properties of the nucleus of a comet. This study has examined in detail the feasibility of implementing the penetrator concept. The penetrator system and mission designs have been developed and iterated in sufficient detail to provide a high level of confidence that the concept can be implemented within the constraints of the Mariner Mark 2 spacecraft. Author

89 ASTRONOMY

Includes radio, gamma-ray, and infrared astronomy, and astrometry.

N88-27121*# Hawaii Univ., Honolulu. Inst. for Astronomy.
SPACE INFRARED TELESCOPE FACILITY PROJECT Final Technical Report, 1 Aug. 1986 - 8 Jan. 1988
Dale P. Cruikshank 25 Jul. 1988 35 p
(Grant NAG2-424)
(NASA-CR-183058; NAS 1.26:183058) Avail: NTIS HC A03/MF A01 CSCL 03A

The functions undertaken during this reporting period were: to inform the planetary science community of the progress and status of the Space Infrared Telescope Facility (SIRTF) Project; to solicit input from the planetary science community on needs and requirements of planetary science in the use of SIRTF at such time that it becomes an operational facility; and a white paper was prepared on the use of the SIRTF for solar system studies. B.G.

N88-27122# Technische Hochschule, Aachen (West Germany). Inst. fuer Physik.
OBSERVATION OF A POINT SOURCE IN CYGNUS CONSTELLATION WITH THE UNDERGROUND DETECTOR AT FREJUS (FRANCE) Ph.D. Thesis [SUCHE NACH EINER PUNKTQUELLE IM STERNBILD SCHWAN MIT DEM FREJUS UNTERGRUNDDETEKTOR]
Anton Hofmann 1987 105 p In GERMAN
(PITHA-87/02; ETN-88-92091) Avail: NTIS HC A06/MF A01

The double star Cygnus X-3 in Cygnus constellation is the first high energetic cosmic radiation to be observed. An underground detector allows by the presence of muons to study neutral light particles. Astronomical principles are given for the ground level and underground observation of Cygnus X-3. ESA

N88-27123# Leiden Univ. (Netherlands).
THE POLARIZATION OF RADIO GALAXIES: ITS STRUCTURE AT LOW FREQUENCIES Ph.D. Thesis
Willem Joseph Jaegers 1986 269 p In CHINESE, DUTCH and ENGLISH
(B8681611; ETN-88-92623) Avail: NTIS HC A12/MF A01

The 0.6 GHz mapping of extended radio galaxies: edge-brightened double sources; edge-darkened double sources; 3C66B, NGC1265, 3C129, DA240, 3C236, 4C48.29, IC708 and IC711, 4CT51.29.1, 3C310, Abell2256, 3C402 and 3C465; systematics of spectral index distributions of radio sources at low frequencies, and systematics of polarization distributions (evidence for excess gas associated with giant elliptical galaxies) is summarized. A multifrequency polarization study of 3C66B is described. Low frequency polarization observations of the radio galaxy 4C73.48; radio observations of the giant quasar 4C34.47; the cluster around 3C130; the radio structure of 3C130 interpreted with a dynamical model; and possible one-sized ejection in the prototype tailed radio galaxy 3C129 are considered. ESA

N88-27124# Office National d'Etudes et de Recherches Aerospatiales, Paris (France).
METHODS FOR INDIRECT IMAGING THROUGH THE ATMOSPHERE Ph.D. Thesis - Nice Univ.
Alain Seve 1987 154 p In FRENCH; ENGLISH summary Report will also be announced as translation (ESA-TT-1115)
(ONERA-NT-1987-4; ISSN-0078-3781; ETN-88-92728) Avail: NTIS HC A08/MF A01

Speckle methods are reviewed and the speckle interferometry technique and the Knox-Thompson algorithm are detailed. The main maximum likelihood algorithms are also reviewed and compared. These methods are applied to astronomical and simulation data. The results show that the algorithms should be tested using complex structure images in order to estimate their performance. The Skilling algorithm is clearly the most promising. ESA

N88-27125# Lawrence Livermore National Lab., Calif.
PROBING THE POSSIBILITY OF A (12)C/(13)C ABUNDANCE GRADIENT FROM OBSERVATIONS OF INTERSTELLAR CH+
Isabel Hawkins 16 Sep. 1987 15 p Presented at the 194th American Chemical Society National Meeting, New Orleans, La., 31 Aug. - 4 Sep. 1987
(Contract W-7405-eng-48)
(DE88-008908; UCRL-96433; CONF-870802-40) Avail: NTIS HC A03/MF A01

High signal-to-noise (S/N= 300 to 500) observations have been performed of interstellar CH(+) at Lick Observatory and at CTIO of the reddened, early-type stars HD 183143, HD 24432, and HD 157038 in an effort to probe the existence of a C-12/C-13 abundance gradient in our Galaxy. DOE

N88-27126 Arizona Univ., Tucson.
THE APPLICATION OF IMAGING TO THE ATMOSPHERIC CERENKOV TECHNIQUE: OBSERVATIONS OF THE CRAB NEBULA Ph.D. Thesis
Kenneth Gerard Gibbs 1987 112 p
Avail: Univ. Microfilms Order No. DA8803254

Gamma-ray astronomy is generally viewed as an adjunct to cosmic ray physics. As such, the observation of very high energy gamma rays will allow a new and complementary means of examining the origin and evolution of cosmic rays. However, at present the atmospheric Cerenkov technique (the technique by which very high energy gamma rays are observed) is seriously hampered by limited flux sensitivity. Monte Carlo simulations suggest that the application of imaging to the atmospheric Cerenkov technique will provide a much needed increase in sensitivity. The successful application of imaging to very high energy gamma-ray observations of the Crab nebula is discussed, as are improved techniques for calibration and noise rejection. These observations permit an improved estimate of the nebular magnetic field strength. Dissert. Abstr.

N88-27127 Wisconsin Univ., Madison.
A SURVEY OF THE Ap STARS FOR RAPID VARIABILITY Ph.D. Thesis
Matthew Jon Nelson 1987 194 p
Avail: Univ. Microfilms Order No. DA8727249

The construction of a two-star high-speed photometer for Washburn Observatory is described.The ability of the instrument to detect coherent variability at levels of 1 nMag or less in the presence of much larger noise levels is demonstrated. This demonstration proves its effectiveness in searching the Ap stars for rapid variability. A survey of the Ap stars is presented which was done with the Washburn two-star photometer. Forty-five Ap stars in the temperature range from B8 to F6 spectral type were searched for rapid variability. No definite detections of pulsations are seen in this sample, although most of the stars in the survey need further observations due to the variable nature of their pulsations. Several interesting stars are discussed and suggestions are presented for further observations of the Ap stars. Dissert. Abstr.

90 ASTROPHYSICS

Includes cosmology; celestial mechanics; space plasmas; and interstellar and interplanetary gases and dust.
For related information see also *75 Plasma Physics*.

N88-27128# Lawrence Livermore National Lab., Calif.
TIME-DEPENDENT MASS LOSS FROM HOT STARS WITH AND WITHOUT RADIATIVE DRIVING
J. I. Castor, S. P. Owocki, and G. B. Rybicki 29 Jan. 1988 19 p Presented at the Trieste Workshop on Pulsation and Mass Loss in Stars, Trieste, Italy, 14 Sep. 1987 Prepared in cooperation with Franklin Inst., Newark, Del. and Harvard-Smithsionian Center for Astrophysics, Cambridge, Mass.
(Contract W-7405-eng-48)
(DE88-008899; UCRL-98097; CONF-8709261-1) Avail: NTIS HC A03/MF A01

A numerical hydrodynamics code is used to investigate two aspects of the winds of hot stars. The first is the question of the instability of the massive radiatively-driven wind of an O star that is caused by the line shape mechanism: modulation of the radiation force by velocity fluctuations. The evolution of this instability is8studied in a model O star wind, and is found, modulo some numerical uncertainty, to lead to wave structures that are compatible with observations of wind instabilities. The other area of investigation is of main-sequence B star winds. Attempts were made to simulate a radiatively-driven and a pulsation-driven wind in a B star, but in each case the wind turned out to be very weak. It is argued that the pulsation-driven wind model is not likely to apply to B stars. DOE

N88-27129# International Centre for Theoretical Physics, Trieste (Italy).
COSMIC WAVEFUNCTION WITH INDUCED GRAVITY
H. J. Mo and L. Z. Fang Jun. 1987 9 p
(DE88-701873; IC-87/130) Avail: NTIS (US Sales Only) HC A02/MF A01

The Hartle-Hawking cosmic wavefunction is calculated in a model with induced potential. It is found that quantum cosmology can explain the existences of physical constants such as gravitational constant and cosmological constant. DOE

N88-27130# Stevens Inst. of Tech., Hoboken, N.J.
COSMOLOGICAL HELIUM PRODUCTION SIMPLIFIED
Jeremy Bernstein, Lowell S. Brown, and G. Feinberg (Columbia Univ., New York, N.Y.) 1988 39 p Prepared in cooperation with Rockefeller Univ., New York.
(Contract DE-AS06-88ER-40423)
(DE88-009578; DOE/ER-40423/02-P8) Avail: NTIS HC A03/MF A01

Presented is a simplified model of helium synthesis in the early universe, the purpose of which is to explain the physical ideas relevant to the cosmological helium synthesis, in a manner that does not overlay these ideas with complex computer calculations. The model closely follows the standard calculation, except that it neglects the small effect of Fermi-Dirac statistics for the leptons. Also neglected is the temperature difference between photons and neutrinos during the period in which neutrons and protons interconvert. These approximations allow us to express the neutron-proton conversion rates in a closed form, which agrees to 10 percent accuracy or better with the exact rates. Using these analytic expressions for the rates, we reduce the calculation of the neutron-proton ratio as a function of temperature to a simple numerical integral. We also estimate the effect of neutron decay on the helium abundance. Results agree well with precise computer calculations. We use our semi-analytic formulas to determine how the predicted helium abundance varies with such parameters as the neutron lifetime, the baryon to photon ratio, the number of neutrino species, and a possible electron-neutrino chemical potential. DOE

N88-27131# Paris VI Univ. (France).
PROCESSING AND ANALYSIS OF IMAGES TRANSMITTED BY VEGA SPACE PROBES OVER HALLEY'S COMET Ph.D. Thesis [TRAITEMENT ET ANALYSE DES IMAGES TRANSMISES LORS DES SURVOLS DE LA COMETE HALLEY PAR LES SONDES VEGA]
Alain Abergel 1987 234 p In FRENCH
(ETN-88-92291) Avail: NTIS HC A11/MF A01

The numerical methods leading to the identification of the Halley comet nucleus parameters are discussed. An algorithm was developed to visualize the nucleus contours from the images transmitted by the Vega probes. The three-dimensional shape is determined from the contours and the complex rotation parameters. The albedo and dust jets distribution are also estimated. The dimensions found are 7.5 km, 8.3 km, and 16 km with precisions of 0,5, 0.5 and 1.5 km respectively. ESA

N88-27132# Leiden Univ. (Netherlands).
THE VELOCITY FIELD OF THE OUTER GALAXY Ph.D. Thesis
Jan Brand 1986 215 p Sponsored in part by the Netherlands Foundation for Astronomical Research
(B8681472; ETN-88-92622) Avail: NTIS HC A10/MF A01

The determination of the velocity field of the (outer) Galaxy and the determination of the rotation curve of our star system beyond the Sun are discussed. Perturbations in the rotation of stars and gas in the Galaxy (i.e., with respect to circular rotation) were mapped by expanding the sample of available objects to the Southern Hemisphere, in order to cover as large a part of the Galaxy as possible, to confirm the gentle rise determined mainly from Northern Hemisphere objects. A catalog of nebulous objects; CO observations of galactic nebulae; determination of distances to O, B, and A type stars in the Walraven photometric system; distances to galactic nebulae; and the velocity field of the outer galaxy and the distance to the galactic center are considered. ESA

91 LUNAR AND PLANETARY EXPLORATION

Includes planetology; and manned and unmanned flights. For spacecraft design or space stations see *18 Spacecraft Design, Testing and Performance.*

N88-27133*# National Aeronautics and Space Administration, Washington, D.C.
REPORTS OF PLANETARY GEOLOGY AND GEOPHYSICS PROGRAM, 1987
Jun. 1988 602 p
(NASA-TM-4041; NAS 1.15:4041) Avail: NTIS HC A99/MF A01 CSCL 03B

This is a compilation of abstracts of reports from Principal Investigators of NASA's PLanetary Geology and Geophysics program, Office of Space Science and Applications. The purpose is to document in summary form research work conducted in this program during 1987. Each report reflects significant accomplishments in the area of the author's funded grant or contract. Author

N88-27134*# Arizona State Univ., Tempe. Dept. of Geology.
A BIBLIOGRAPHY OF DUNES: EARTH, MARS, AND VENUS
N. Lancaster Jun. 1988 118 p
(Contract NCC2-346)
(NASA-CR-4149; NAS 1.26:4149) Avail: NTIS HC A06/MF A01 CSCL 03B

Dunes are important depositional landforms and sedimentary environments on Earth and Mars, and may be important on Venus. The similarity of dune forms on Earth and Mars, together with the dynamic similarity of aeolian processes on the terrestrial planets indicates that it is appropriate to interpret dune forms and processes on Mars and Venus by using analog studies. However, the literature on dune studies is large and scattered. The aim of this bibliography is to assist investigators by providing a literature resource on techniques which have proved successful in elucidating dune characteristics and processes on Earth, Mars, and Venus. This bibliography documents the many investigations of dunes undertaken in the last century. It concentrates on studies of inland dunes in both hot and cold desert regions on Earth and includes investigations of coastal dunes only if they discuss matters of general significance for dune sediments, processes, or morphology. Author

N88-27135*# Eagle Engineering, Inc., Webster, Tex.
LUNAR BASE LAUNCH AND LANDING FACILITY CONCEPTUAL DESIGN, 2ND EDITION
25 Mar. 1988 111 p
(Contract NAS9-17878)
(NASA-CR-172049; NAS 1.26:172049; EEI-88-178) Avail: NTIS HC A06/MF A01 CSCL 03B

This report documents the Lunar Base Launch and Landing Facility Conceptual Design study. The purpose of this study was to examine the requirements for launch and landing facilities for early lunar bases and to prepare conceptual designs for some of these facilities. The emphasis of this study is on the facilities needed from the first manned landing until permanent occupancy. Surface characteristics and flight vehicle interactions are described, and various facility operations are related. Specific recommendations for equipment, facilities, and evolutionary planning are made, and effects of different aspects of lunar development scenarios on facilities and operations are detailed. Finally, for a given scenario, a specific conceptual design is developed and presented. Author

N88-27136*# Iowa Univ., Iowa City. Dept. of Physics and Astronomy.
ULTRAVIOLET GEOMETRIC ALBEDO OF URANUS Final Technical Report
John S. Neff 1 Aug. 1988 4 p
(Grant NAG5-544)

(NASA-CR-183099; NAS 1.26:183099) Avail: NTIS HC A02/MF A01 CSCL 03B

The purpose was to obtain ultraviolet flux measurements of Uranus before and after the January 1986 flyby past Uranus by Voyager. These measurements were used to determine absolute flux distributions in the wavelength range 1950 to 3200 A. This wavelength range is an important region to observe since the model atmospheres for Uranus indicate that the albedo spectrum in this region can tightly constrain the height of the photochemical haze layer. Author

N88-27137*# Carnegie Institution of Washington, D. C. Geophysical Lab.

EXPERIMENTAL STUDY OF PLANETARY GASES WITH APPLICATIONS TO PLANETARY INTERIOR MODELS Final Project Report, 1 Jun. 1983 - 30 Nov. 1987

Peter M. Bell and Ho-kwang Mao 8 Aug. 1988 10 p
(Grant NAGw-214)
(NASA-CR-183098; NAS 1.26:183098) Avail: NTIS HC A02/MF A01 CSCL 03B

High-pressure experimental data on planetary materials are critical in developing planetary models and in addressing otherwise insoluble problems of the internal structure of the major planets. Progress in the last five years has been particularly marked. Maximum static pressure of 550 GPa was achieved. For the first time, X-ray diffraction of solidified gases (Ne, Xe) and ices (H2O) were obtained at pressures above one megabar, single-crystal diffraction of ultralight elements (H2, He) were detected up to 25 GPa, pressures over 200 GPa at 77 K were reached in solid hydrogen, including the discovery of a phase transformation in the molecular solid. Advances in instrumentation and new measurements performed during 1983 to 1988 are summarized. Author

92 SOLAR PHYSICS

Includes solar activity, solar flares, solar radiation and sunspots.

For related information see *93 Space Radiation.*

N88-27138# National Geophysical Data Center, Boulder, Colo.

SOLAR-GEOPHYSICAL DATA NUMBER 522, FEBRUARY 1988. PART 2: (COMPREHENSIVE REPORTS). DATA FOR AUGUST 1987 AND MISCELLANEA

Helen E. Coffey, ed. and John A. McKinnon, ed. Aug. 1987 56 p
(Contract N00014-86-F-0049)
(PB88-194741; SGD-522-Pt-2; ISSN-0038-0911; LC-79-640375) Avail: NTIS HC A04/MF A01 CSCL 03B

Solar-Geophysical Data Number 522, February 1988. Part 2 (Comprehensive Reports), contains the following: Data for August 1987; Meudon Carte Synoptique; Solar flares, solar radio bursts at fixed frequencies; Solar X-ray radiation from GOES satellite; Mass ejection from the Sun; and Active prominences and filaments. GRA

N88-27139# National Geophysical Data Center, Boulder, Colo.

SOLAR-GEOPHYSICAL DATA NUMBER 522, FEBRUARY 1988. PART 1: (PROMPT REPORTS). DATA FOR JANUARY 1988, DECEMBER 1987 AND LATE DATA

Helen E. Coffey, ed. and John A. McKinnon, ed. Dec. 1987 105 p
(Contract N00014-86-F-0049)
(PB88-194733; SGD-522-Pt-1; ISSN-0038-0911; LC-79-640375) Avail: NTIS HC A06/MF A01 CSCL 03B

Solar-Geophysical Data Number 522, February 1988, Part 1 (Prompt Reports), contains the following: Data for January 1988; IUWDS alert periods (Advanced and Worldwide); Solar activity indices; Solar flares; Solar radio emission; and Stanford mean solar magnetic field. GRA

N88-27140# Science Research Council, Chilton (England).

GENERATION OF ADLAM-ALLEN WAVES BY PLASMA RELEASE EXPERIMENTS IN THE SOLAR WIND

C. M. C. Nairn, R. Bingham, and J. E. Allen Mar. 1987 24 p
(PB88-106000; RAL-87-015) Avail: NTIS HC E03/MF E03; copy not available from STI Facility CSCL 03B

Recent experiments in space plasma physics involved the release of lithium and barium plasmas in the solar wind. The resulting expanding artificial plasmas created diamagnetic cavities which were bounded on the sunward-side by a large shock-like magnetic field structure. Observations made by two spacecraft of the AMPTE mission revealed the presence of large amplitude magnetic field oscillations. It is shown that these oscillations, which resemble finite amplitude magnetosonic waves and have the characteristics of Adlam-Allen waves, can be described by a nonlinear wave equation, namely the Korteweg-de Vries equation. Author

N88-27141# Aerospace Corp., El Segundo, Calif. Space Sciences Lab.

THE PROPERTIES OF SOLAR CORONAL ACTIVE REGIONS DEDUCED FROM X-RAY LINE SPECTRA

D. L. McKenzie 5 Feb. 1988 34 p
(Contract F04701-85-C-0086)
(AD-A193026; TR-0086A(2940-01)-1; SD-TR-88-04) Avail: NTIS HC A03/MF A01 CSCL 03B

Coronal active regions, the sites of energetic solar flares, have temperatures higher than 10 K and emit strongly in the X-ray region of the spectrum. In this report X-ray emission line-ratio diagnostics for electron density and temperature are applied to over 100 spectra of nonflaring active regions taken by the SOLEX B spectrometer aboard the U.S. Department of Defense Space Test Program's P78-1 Satellite from March to November 1979. The purpose is to draw general conclusions from analysis of the spectra of a large variety of regions. In the course of the study, we were also able to evaluate existing theoretical calculations of the helium-like ion line ratios. A number of them can now be rejected as inconsistent with the data. Future work may modify the conclusions of the study, but not significantly. GRA

93 SPACE RADIATION

Includes cosmic radiation; and inner and outer earth's radiation belts.

For biological effects of radiation see *52 Aerospace Medicine.* For theory see *73 Nuclear and High-Energy Physics.*

N88-27142*# National Aeronautics and Space Administration. Langley Research Center, Hampton, Va.

STUDIES OF HZE PARTICLE INTERACTIONS AND TRANSPORT FOR SPACE RADIATION PROTECTION PURPOSES Abstract Only

Lawrence W. Townsend, John W. Wilson, Walter Schimmerling, and Mervyn Wong (California Univ., Berkeley. Lawrence Berkeley Lab.) [1987] 6 p Presented at the NASA Space Life Sciences Symposium, Washington, D.C., 21-26 Jun. 1987
(NASA-TM-101159; NAS 1.15:101159) Avail: NTIS HC A02/MF A01 CSCL 03B

The main emphasis is on developing general methods for accurately predicting high-energy heavy ion (HZE) particle interactions and transport for use by researchers in mission planning studies, in evaluating astronaut self-shielding factors, and in spacecraft shield design and optimization studies. The two research tasks are: (1) to develop computationally fast and accurate solutions to the Boltzmann (transport) equation; and (2) to develop accurate HZE interaction models, from fundamental physical considerations, for use as inputs into these transport codes. Accurate solutions to the HZE transport problem have been formulated through a combination of analytical and numerical techniques. In addition, theoretical models for the input interaction

parameters are under development: stopping powers, nuclear absorption cross sections, and fragmentation parameters. Author

N88-27143# Tokyo Univ. (Japan). Inst. of Space and Astronautical Science.
DETECTION OF ABSORPTION LINES IN THE SPECTRA OF X-RAY BURSTS FROM X1608-52
Norio Nakamura, Hajime Inoue, and Yasuo Tanaka Mar. 1987 20 p Submitted for publication
(ISAS-RN-360) Avail: NTIS HC A03/MF A01

X-ray bursts from X1608-52 were observed with the gas scintillation proportional counters onboard Tenma. Absorption features were detected in the spectra of three bursts among the 17 observed. These absorption features are consistent with a common absorption line at 4.1 keV. The energy and the properties of the absorption lines of the X1608-52 bursts are similar to those observed from the X1636-53 bursts previously reported. The absorption lines are most probably redshifted by the effect of the strong gravitational field near the neutron star surface. Near equality of the absorption line energies for X1636-53 and X1608-52 would then imply that the neutron stars in these two systems are very similar to each other. In addition, the detection of an absorption line from the second X-ray burst source suggests that absorption lines may be present in the burst spectra from other sources. Author

N88-27144*# National Aeronautics and Space Administration. Goddard Space Flight Center, Greenbelt, Md.
THE HARD X-RAY BURST SPECTROMETER EVENT LISTING 1980-1987
B. R. Dennis, L. E. Orwig, A. L. Kiplinger, R. A. Schwartz, B. R. Gibson, G. S. Kennard, A. K. Tolbert, D. A. Biesecker, G. J. Labow, and A. Shaver (Science Applications Research, Lanham, Md.) Feb. 1988 158 p
(NASA-TM-4036; Rept-88B0124; NAS 1.15:4036) Avail: NTIS HC A08/MF A01 CSCL 03B

This event listing is a comprehensive reference for the Hard X-ray bursts detected with the Hard X-ray Burst Spectrometer on the Solar Maximum Mission from the time of launch 14 February 1980 to December 1987. Over 8600 X-ray events were detected in the energy range from 30 to approx. 600 keV with the vast majority being solar flares. The listing includes the start time, peak time, duration and peak rate of each event. Author

N88-27145# California Univ., Berkeley. Lawrence Berkeley Lab.
COSMIONS AND STARS
P. Salati Dec. 1987 12 p Presented at the Extra Solar Neutrino Astronomy Workshop, Los Angeles, Calif., 30 Sep. 1987
(Contract DE-AC03-76SF-00098)
(DE88-010886; LBL-24417; CONF-8709275-1; UCB-PTH-87/52)
Avail: NTIS HC A03/MF A01

Hypothetical particles such as the heavy neutrino, the photino (lambda dash), or the sneutrino(nu dash) generically called cosmions may solve the so called missing mass problem. If they exist, the cosmions may close the Universe. In addition to their gravitational effect on cosmological scales, the cosmions may also be captured by stars and concentrate in their cores. Since cosmions are able to transport heat outside stellar cores much more efficiently than photons, they may seriously affect the thermodynamics of the inner layer of stars. We have done an exact calculation of the accretion rate of cosmions by main sequence stars and we have studied the suppression of their central convection. We concluded that central convection inside stars between 0.3 Msub solar and 1 Msub solar is broken in the presence of cosmions. DOE

N88-27146*# California Inst. of Tech., Pasadena. Space Radiation Lab.
RESEARCH IN PARTICLE AND GAMMA-RAY ASTROPHYSICS Semiannual Status Report, 1 Apr. 1987 - 31 Mar. 1988
E. C. Stone, L. Davis, Jr., R. A. Mewaldt, and T. A. Prince 8 Aug. 1988 25 p
(Grant NGR-05-002-160)
(NASA-CR-183111; NAS 1.26:183111) Avail: NTIS HC A03/MF A01 CSCL 09B

This research program is directed toward the investigation of the astrophysical aspects of cosmic rays and gamma rays and of the radiation and electromagnetic field environment of the Earth and other planets. The emphasis was on precice measurements with high resolution in charge, mass and energy. These investigations were carried out by means of energetic particle and photon detector systems flown on spacecraft and balloons. Author

99 GENERAL

No abstracts in this category.

Typical Subject Index Listing

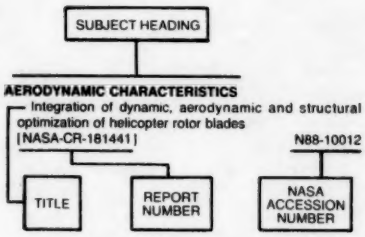

The subject heading is the key to the subject content of the document. Titles, report numbers, and accession numbers of pertinent documents are provided under each subject heading. When the title is insufficiently descriptive of the document content, a title extension has been added, separated from the title by three hyphens. The report number helps to indicate the type of document cited (e.g., NASA report, NASA translation, NASA contractor report). The NASA accession number is the number by which the document abstracts are arranged in this journal and by which the document is sold or requested. The titles, with title extensions if present, are arranged under each subject heading in ascending accession number order. The subject headings have been selected from the latest revision of the *NASA Thesaurus* (NASA SP-7053).

A

ABLATION
Why plasma armature railguns don't work (and what can be done about it)
[DE88-007900] N88-26384
Absorption characteristics of Si3N4 ablation layer plasma N88-26504

ABORT TRAJECTORIES
The effects of RCS jet firing on the isolated Orbiter and mated coast phases of the glide return to launch site maneuver at Mach number 6 (IA302B)
[NASA-CR-180223] N88-26403

ABSORPTION CROSS SECTIONS
Nucleon-nucleus interaction data base: Total nuclear and absorption cross sections
[NASA-TM-4053] N88-26935
Studies of HZE particle interactions and transport for space radiation protection purposes
[NASA-TM-101159] N88-27142

ABSORPTION SPECTRA
Absorption characteristics of Si3N4 ablation layer plasma N88-26504
Raman and absorption spectrophotometric studies of selected lanthanide, californium-doped lanthanide, and actinide trihalides in the solid state
[DE88-008234] N88-27061
Detection of absorption lines in the spectra of X-ray bursts from X1608-52
[ISAS-RN-360] N88-27143

ABSORPTION SPECTROSCOPY
Laser spectoscopy of plasmas
[AD-A193009] N88-26991

ABSTRACTS
Reports of planetary geology and geophysics program, 1987
[NASA-TM-4041] N88-27133

ABUNDANCE
Fine-scale traverses in cumulate rocks, Stillwater Complex: A lunar analogue study
[NASA-CR-183066] N88-26747
Probing the possibility of a (12)C/(13)C abundance gradient from observations of interstellar CH+
[DE88-008908] N88-27125

ACCELERATED LIFE TESTS
A statistical treatment of accelerated life test data for copper-water heat pipes N88-26509

ACCELERATION TOLERANCE
Significance of sensory signal phase mismatch in mechanisms of motion sickness development N88-26787

ACCEPTOR MATERIALS
Modeling the primary events of photosynthesis using chlorophyll containing fixed distance donor-acceptor molecules
[DE88-010033] N88-26793

ACCESS CONTROL
Using common subexpressions to optimize multiple queries
[DE88-008210] N88-26877

ACCIDENTS
Book analysis. Challenger: A major malfunction
[AD-A192458] N88-26388

ACCURACY
On the accuracy of upwind biased finite volume method N88-26316

ACID RAIN
Acid Precipitation: A current awareness bulletin
[DE88-007987] N88-26738

ACOUSTIC EMISSION
An analysis of the efficiency and directivity of the sound generated by a moving laser source
[AD-A192220] N88-26914
On the possibility of the soliton description of acoustic emission during plastic deformation of crystals
[DE88-701878] N88-27075

ACOUSTIC IMPEDANCE
Evaluation of a multi-point method for determining acoustic impedance
[NASA-TM-100637] N88-26913

ACOUSTIC LEVITATION
Program for the feasibility of developing a high pressure acoustic levitator
[NASA-CR-182154] N88-26498

ACOUSTIC MEASUREMENT
Sound power measurements in situ using a reference sound source
[PB88-182571] N88-26910
Evaluation of a multi-point method for determining acoustic impedance
[NASA-TM-100637] N88-26913

ACOUSTIC PROPAGATION
Sound propagation over uneven ground and irregular topography
[NASA-CR-182956] N88-26911

ACOUSTIC SCATTERING
Quantitative particle characterization by scattered ultrasound N88-26908
Studying materials using acoustic waves
[AD-A192234] N88-26915

ACOUSTIC SOUNDING
Remote sensing of temperature profiles. Performance test of PASS
[DE88-753108] N88-26768

ACOUSTIC VELOCITY
Dynamics and stability of combustion driven self oscillations in presence of various frequencies. Extensive stability criteria
[ETN-88-92123] N88-26432

ACOUSTICS
Local free-space mapping and path guidance for mobile robots
[AD-A192970] N88-26674
Acoustic diffraction by an absorbing finite strip in a moving fluid
[PB88-191382] N88-26912
An analysis of the efficiency and directivity of the sound generated by a moving laser source
[AD-A192220] N88-26914
Studying materials using acoustic waves
[AD-A192234] N88-26915

ACTIVE CONTROL
Active phase compensation system for fiber optic holography
[NASA-TM-101295] N88-26641

ADAPTIVE CONTROL
Experiments in adaptive control of a very flexible one link manipulator N88-26865
Asymptotically efficient adaptive allocation schemes for controlled Markov chains: Finite parameter space
[AD-A192228] N88-26893

ADDITIVES
Grain boundary structure in Ni3Al
[DE88-009164] N88-26444

ADHESION
The adherence of nickel oxide on nickel during high temperature oxidation
[DE88-011194] N88-26450
Reducing adhesion and agglomeration within a cloud of combustible particles
[NASA-TM-100902] N88-26539

ADHESIVES
Initial adhesive screening of novel polyamide-imides and their copolymers
[NASA-TM-100641] N88-26481

ADMIXTURES
Development of an equation of state for computation of supercompressibility factors, critical flow factors and other properties for wet, sour natural gases, synthetic gases and admixtures
[PB88-202676] N88-26602

ADSORPTION
Heat pump augmented radiator for low-temperature space applications
[DE88-008369] N88-26393
Fundamental optical studies of competitive adsorption and thin film phenomena
[DE88-008780] N88-27068

AERIAL EXPLOSIONS
Australian structures response evaluation: Ground shock and air blast measurements for site investigation survey
[MRL-TN-526] N88-26685

AEROACOUSTICS
Outdoor sound propagation, its implications for unattended ground sensors
[FEL-1986-64] N88-26917

AERODYNAMIC CHARACTERISTICS
Proceedings of the 5th NAL Symposium on Aircraft Computational Aerodynamics
[NAL-SP-8] N88-26290
Numerical simulations of aerodynamic contribution of flows about a space-plane-type configuration N88-26292
Numerical solutions of the Euler equations for the flow field around counter-rotating propellers N88-26296
Influence of wind shear on the aerodynamic characteristics of airplanes
[NASA-TP-2827] N88-26344
Airbus 1987: Success in Europe
[ETN-88-92099] N88-26364
Surface disturbances produced by low-level, subsonic B-1 aircraft
[AD-A192257] N88-26752

AERODYNAMIC CONFIGURATIONS
Ludwig Prandtl collected treatises on applied mechanics, hydro- and aerodynamics, part 1
[NASA-TT-20316] N88-26337

AERODYNAMIC LOADS
Calculations of unsteady aerodynamics for a full aircraft configuration using boundary element method N88-26303
An initial investigation into methods of computing transonic aerodynamic sensitivity coefficients
[NASA-CR-183061] N88-26332

AERODYNAMICS
Ludwig Prandtl collected treatises on applied mechanics, hydro- and aerodynamics, part 2, IV interfaces and resistance
[NASA-TT-20315] N88-26338
A two-point aerodynamic model for identification N88-26526

Parametric estimation of aerodynamic nonlinearities in rolling moment due to sideslip using maximum likelihood method N88-26528

AERONAUTICAL ENGINEERING

The role of computational fluid dynamics in aeronautical engineering (5): Improvements and applications of implicit TVD finite volume code N88-26313

Flight research and testing [NASA-TM-100439] N88-26361

AEROSOLS

Studies of the mechanisms and rates with which nitrogen species are incorporated into cloud water and precipitation [PB88-193065] N88-26764

AEROSPACE MEDICINE

JPRS report: Science and technology. USSR: Life sciences [JPRS-ULS-88-009] N88-26785

Does dihydroergotamine used in therapeutical doses influence the physical and psychomotor performance of young pilots or other traffic drivers subjected to hypotonia? [ETN-88-92136] N88-26799

Aerospace medicine and biology: A continuing bibliography with indexes (supplement 313) [NASA-SP-7011(313)] N88-26800

AEROSPACE PLANES

Numerical simulations of aerodynamic contribution of flows about a space-plane-type configuration N88-26292

High speed and high angle of attack wind tunnel test results of the winged space vehicle C-2 [ISAS-RN-623] N88-26329

AEROSPACE SCIENCES

Issues and recommendations associated with distributed computation and data management systems for the space sciences [NASA-CR-183026] N88-27108

AEROSPACE VEHICLES

Study of the influence of metallurgical factors on fatigue and fracture of aerospace structural materials [AD-A192909] N88-26452

AEROTHERMODYNAMICS

Analysis of gas turbine test cell number 1, Lemoore Naval Air Station, California [AD-A192870] N88-26380

AFRICA

Westward moving atmospheric wave disturbances over the African tropics: Dynamic and energetic aspects [MITT-57] N88-26774

AGGLOMERATION

Reducing adhesion and agglomeration within a cloud of combustible particles [NASA-TM-100902] N88-26539

AGING (MATERIALS)

High temperature resins for injection. High temperature pre-impregnated [RC-648676] N88-26486

AGREEMENTS

Monitoring space weaponry: Detection and verification issues [DE88-006726] N88-26900

AIR CONDITIONING

Enhanced emergency smoke venting [DOT/FAA/CT-88/22] N88-26350

AIR COOLING

Computational study on thermal efficiency of ceramic gas turbine [DE88-753114] N88-26667

Study on the heat resisting and cooling property of the ceramics-metal hybrid stator vanes [DE88-753117] N88-26668

AIR FILTERS

Characteristics of pressure loss during filtration using a porous ceramic filter [DE88-752547] N88-26604

AIR MASSES

Parametric methodologies of cloud vertical transport for acid deposition models [PB88-191374] N88-26782

AIR NAVIGATION

A positioning system based on NAVSAT [NLR-MP-87018-U] N88-26358

AIR POLLUTION

Overview of the PRECP (processing of emissions by clouds and precipitation) Program [DE88-008205] N88-26741

An efficient model for changes of global climate and composition of the atmosphere due to human activities [ETN-88-92359] N88-26775

AIR TRAFFIC CONTROL

Statistical properties of real time events in an ATC (Air Traffic Control) system [PB88-118781] N88-26353

AIR WATER INTERACTIONS

Physical oceanography and tracer chemistry of the southern ocean [DE88-006852] N88-26779

AIRBORNE EQUIPMENT

Trajectory measurement of the Fokker 100 aircraft during autoland testing [NLR-MP-88010-U] N88-26366

AIRBORNE/SPACEBORNE COMPUTERS

Development of an airborne facility for advanced avionics research [NLR-MP-87012-U] N88-26368

A cockpit natural language study - selected transcripts [AD-A192972] N88-26808

AIRCRAFT ACCIDENT INVESTIGATION

Aircraft accident report: Joe Foster Excavating, Inc., Bell 206B, N49606, in-flight collision with trees, Alamo, California, August 3, 1986 [PB88-910405] N88-26345

Aircraft accident report: Midair collision of SkyWest Airlines Swearingen METRO 2, N163SW, and Mooney M20, N6485U, Kearns, Utah, January 15, 1987 [PB88-910404] N88-26346

AIRCRAFT COMPARTMENTS

Aircraft interior noise reduction by alternate resonance tuning [NASA-CR-182540] N88-26909

AIRCRAFT CONFIGURATIONS

Aerodynamic simulation for complete ASKA aircraft configuration N88-26301

Numerical simulation of viscous flows over transonic aircraft configurations N88-26302

Calculations of unsteady aerodynamics for a full aircraft configuration using boundary element method N88-26303

AIRCRAFT CONTROL

Influence of wind shear on the aerodynamic characteristics of airplanes [NASA-TP-2827] N88-26344

Propfan test assessment testbed aircraft stability and control/performance 1/9-scale wind tunnel tests [NASA-CR-182121] N88-26360

Low-speed wind-tunnel test of a STOL supersonic-cruise fighter concept [NASA-TM-4050] N88-26374

Nonlinear identification of an aircraft for the direct calculation of an anticipatory control N88-26535

AIRCRAFT DESIGN

An initial investigation into methods of computing transonic aerodynamic sensitivity coefficients [NASA-CR-183061] N88-26332

Flight research and testing [NASA-TM-100439] N88-26361

Flight Mechanics Panel Symposium on Rotorcraft Design for Operations: Technical evaluation report [AGARD-AR-243] N88-26362

A new method for the estimation of aircraft inertia characteristics N88-26530

AIRCRAFT DETECTION

Surface disturbances produced by low-level, subsonic B-1 aircraft [AD-A192257] N88-26752

AIRCRAFT EQUIPMENT

Tactical Rubidium Frequency Standard (TRFS), volume 1 [AD-A192981] N88-26640

A cockpit natural language study - selected transcripts [AD-A192972] N88-26808

AIRCRAFT FUELS

Feasibility of producing jet fuel from GPGP (Great Plains Gasification Plant) by-products [DE88-010233] N88-26492

Biodegradation of JP-5 aviation fuel by subsurface microbial communities [AD-A192743] N88-26493

AIRCRAFT HAZARDS

Intelligent guidance and control for wind shear encounter [NASA-CR-183060] N88-26347

AIRCRAFT MANEUVERS

Flight simulator: Field of view utilized in performing tactical maneuvers [AD-A192412] N88-26379

AIRCRAFT MODELS

A two-point aerodynamic model for identification N88-26526

AIRCRAFT NOISE

Helicopter main-rotor noise: Determination of source contributions using scaled model data [NASA-TP-2825] N88-26907

AIRCRAFT PERFORMANCE

Propfan test assessment testbed aircraft stability and control/performance 1/9-scale wind tunnel tests [NASA-CR-182121] N88-26360

AIRCRAFT SAFETY

Enhanced emergency smoke venting [DOT/FAA/CT-88/22] N88-26350

Corrosion in aircraft structures. Part 1: Text [LR-527-PT-1] N88-26458

Corrosion in aircraft structures. Part 2: Figures [LR-527-PT-2] N88-26459

AIRCRAFT STABILITY

Propfan test assessment testbed aircraft stability and control/performance 1/9-scale wind tunnel tests [NASA-CR-182121] N88-26360

Low-speed wind-tunnel test of a STOL supersonic-cruise fighter concept [NASA-TM-4050] N88-26374

AIRCRAFT STRUCTURES

Sensitivity to crack initiation in thick assemblies. Test report 48-444 [REPT-48-444] N88-26365

Corrosion in aircraft structures. Part 1: Text [LR-527-PT-1] N88-26458

Corrosion in aircraft structures. Part 2: Figures [LR-527-PT-2] N88-26459

AIRFOIL PROFILES

Finite element analysis of incompressible viscous flow around multi-element aerofoils N88-26294

Computation of flow around NACA0012 airfoil at high angle of attack N88-26300

Parallelization on a multiprocessor system of a solution method for the unsteady Navier-Stokes equations at high Reynolds numbers [ONERA-NT-1987-8] N88-26632

Treatment of the separated flow around profiles (nonviscous, incompressible, two dimensional flow) by the singularities method [ISL-R-106/87] N88-26633

AIRFOILS

Wall interference assessment/correction of data from tests of a CAST 10-2/DOA 2 airfoil in the Langley 0.3-m transonic cryogenic tunnel N88-26331

Improved potential flow computational methods with Euler corrections for airfoil and wing/body design [AD-A192303] N88-26334

ALBEDO

Ultraviolet geometric albedo of Uranus [NASA-CR-183099] N88-27136

ALGORITHMS

An implicit, high order accurate, upwind scheme for unsteady Euler equations N88-26317

Relaxation scheme for compressible flows N88-26323

The modified-fluid-in-cell method to which adaptive mesh and multigrid were applied N88-26324

Simple 2-D navigation for wheeled vehicles [DE88-007115] N88-26351

Microwave image understanding and its application to radar cross section management N88-26542

Multi-target tracking algorithms for cluttered environments N88-26543

A random access algorithm for environments with capture and limited feedback capabilities [AD-A192233] N88-26552

Effects of atmospheric model layering on LOWTRAN 6 calculations of 8-12 micrometers near-horizon sky radiances [AD-A192969] N88-26559

Improved 3-D turbomachinery CFD algorithm [NASA-CR-179364] N88-26619

Parallelization on a multiprocessor system of a solution method for the unsteady Navier-Stokes equations at high Reynolds numbers [ONERA-NT-1987-8] N88-26632

Optimization of performance criteria with bounded joint velocities for robots with one degree of redundancy [DE88-003915] N88-26670

An assessment of modelling techniques for the finite element analysis of reinforced concrete plate and shell structures [AD-A192263] N88-26697

Image pyramid motion detection applied to sea ice N88-26713

Computer science research, 1987: Computation Directorate [DE88-008637] N88-26812

Tuning a major part of a clustering algorithm [AD-A191446] N88-26821

SEGMERGE: A scanline visible surface algorithm with adaptive span selection and inexpensive antialiasing [DE88-009186] N88-26826

Computing small singular values of bidiagonal matrices with guaranteed high relative accuracy: LAPACK working note number 3 [DE88-008465] N88-26829

A practical shifted Adams algorithm [DE88-008573] N88-26830

Conditions for finite convergence of algorithms for nonlinear programs and variational inequalities
[AD-A192355] N88-26834
A matroid algorithm and its application to the efficient solution of two optimization problems on graphs, revision
[AD-A192709] N88-26838
A new trajectory following polynomial-time algorithm for the linear programming problem
[REPT-87-87] N88-26848
Algorithm for generating the minimal cycle basis of a graph
[PB88-126610] N88-26891
A new approach to machine-based perception of monocular images
[DE88-002418] N88-26942
Methods for indirect imaging through the atmosphere
[ONERA-NT-1987-4] N88-27124
Processing and analysis of images transmitted by Vega space probes over Halley's comet
[ETN-88-92291] N88-27131

ALKYL COMPOUNDS
A study of solvent effects on the synthesis of pure component and composite ceramic powders by metal alkoxide hydrolysis
[DE88-008381] N88-26470

ALLOYING
Shape memory alloys: New materials for future engineering
[NASA-TT-20193] N88-26455

ALLOYS
Plastic deformation and roughness of free metal surfaces
[PB88-196621] N88-26439
EXAFS studies of the microstructure of semiconductor alloys, defects and semiconductor-metal interfaces N88-27031
Non-equilibrium phases and phase diagrams
[DE88-008896] N88-27098

ALPHA PARTICLES
A CO2 laser Thomson scattering diagnostic for fusion product alpha particle measurement
[DE88-007683] N88-26965

ALUMINIDES
Nickel aluminides: A new family of nickel + aluminum alloys featuring simple composition, low density, excellent oxidation resistance and high yield strength that increases with temperature
[DE88-010692] N88-26461

ALUMINUM
A numerical study of Rayleigh-Taylor instability in aluminum and steel plates
[DE88-010475] N88-26449
A finite element analysis for the hydroforming of aluminum
[DE88-008050] N88-26516
Crystallization of aluminum hydroxide in the aluminum-air battery: Literature review, crystallizer design and results of integrated system tests
[DE88-010510] N88-26594
Ultraviolet-visible spectroscopy of laser-produced aluminum plasmas
[AD-A193004] N88-26990
Electronic and geometric structure of silver and palladium on aluminum (111) in monoatomic surface layers
[ETN-88-92120] N88-27093

ALUMINUM ALLOYS
Precipitation study by electrical resistivity measurement in Ni-Al alloys
[DE88-701877] N88-26440
Grain boundary structure in Ni3Al
[DE88-009184] N88-26444
Optimizing superplastic response in lithium containing aluminum-magnesium alloys
[AD-A192217] N88-26451
Fatigue of lithium-aluminum alloys: An example of localization of the plastic deformation
[ETN-88-92309] N88-26456
Analysis of the perforation of monolithic and simple laminate aluminium targets as a test of analytical deformation models
[MRL-R-1111] N88-26686

ALUMINUM ARSENIDES
Photoluminescence studies of InGaAlAs quaternary alloys
[DE88-007197] N88-27062

ALUMINUM GALLIUM ARSENIDES
Far-infrared studies of doped AlGaAs/GaAs multiple-quantum-well structures N88-26998
Electro-optical studies of Al(x)Ga(1-x)As/GaAs coupled quantum wells N88-26999
Quantum wells and bulk AlGaAs under hydrostatic pressure N88-27000

ALUMINUM OXIDES
The protonic Beta double prime aluminas: Preparation, stability, conductivity and structure
[DE88-008442] N88-26415

AMBIENT TEMPERATURE
Ambient temperature secondary lithium batteries using LiAl lithium insertion anodes
[DE88-008394] N88-26574

AMINES
Structural study of impregnating resins of TGMDA/DDS type
[ETN-88-92167] N88-26488

AMINO ACIDS
Fast atom bombardment study on interaction of anticodonic nucleotides and their cognate amino acid
[ISAS-RN-355] N88-26918

AMORPHOUS MATERIALS
Glass forming ranges of amorphous alloys
[DE88-007897] N88-26438
Plasma deposition: Investigations on a new approach
[ETN-88-92619] N88-26992

AMORPHOUS SEMICONDUCTORS
Defects and disorder in amorphous and damaged silicon
[AD-A192277] N88-27089

AMORPHOUS SILICON
Defects and disorder in amorphous and damaged silicon
[AD-A192277] N88-27089

AMPLIFICATION
Model for pulse amplification by a gaseous laser amplifier
[DE88-011729] N88-26657

ANALOG DATA
An overview of the development of a linear broadband analog fiber-optic link
[DE88-008668] N88-26945

ANALYZERS
Computer-aided writing
[AD-A192516] N88-26837

ANEMOMETERS
A microcomputer based frequency-domain processor for laser Doppler anemometry
[NASA-TM-100998] N88-26634

ANGLE OF ATTACK
Computation of flow around NACA0012 airfoil at high angle of attack N88-26300
High speed and high angle of attack wind tunnel test results of the winged space vehicle C-2
[ISAS-RN-623] N88-26329
The effect of a turbulent airstream on a vertically-launched missile at high angles of attack
[AD-A192408] N88-26363

ANGULAR MOMENTUM
Nutational stability of a satellite equipped with an active magnetic momentum wheel N88-26513

ANISOTROPY
Stress concentration around circular hole in a composite material specimen representative of the X-29A forward-swept wing aircraft
[NASA-CR-179435] N88-26694
Anisotropic characteristic lengths in single crystal YBa2Cu3O(sub 7-Delta)
[DE88-009959] N88-27080
Anisotropy of the lower critical field in YBa2Cu3O(sub 7-Delta)
[DE88-009971] N88-27081

ANNEALING
Electrical study of metal/group 3-5 semiconductor interfaces: Comparison with the atomic-level studies N88-27059

ANNIHILATION REACTIONS
Research in theoretical particle physics
[DE88-008230] N88-26927

ANNUAL VARIATIONS
The seasonal exchange of carbon dioxide between the atmosphere and the terrestrial biosphere: Extrapolation from site-specific models to regional models
[DE88-007870] N88-26740
Circulation statistics from seasonal and perpetual January and July simulations with the NCAR (National Center for Atmospheric Research) Community Climate Model (CCM1):R15
[PB88-192620] N88-26748
The 1985 Meteorological Yearbook of Ispra (27th)
[PB88-125729] N88-26777

ANODES
Ambient temperature secondary lithium batteries using LiAl lithium insertion anodes
[DE88-008394] N88-26574

ANOMALIES
A severe spacecraft-charging event on SCATHA in September 1982
[AD-A193007] N88-26396
Drift wave vortices and anomalous transport
[DE88-009582] N88-26982

ANTARCTIC OCEAN
Physical oceanography and tracer chemistry of the southern ocean
[DE88-006852] N88-26779

ANTENNA DESIGN
Radar cross section studies/compact range research
[NASA-CR-183124] N88-26585

ANTENNA RADIATION PATTERNS
Antenna heights for the optimum utilization of the oceanic evaporation duct. Part 3: Results from the Mediterranean measurements, volume 2
[AD-A192311] N88-26554
Antenna heights for the optimum utilization of the oceanic evaporation duct. Part 1: Results from the Pacific measurements. Part 2: Results from the Key West measurements, volume 1
[AD-A192358] N88-26555

ANTENNAS
Antenna heights for the optimum utilization of the oceanic evaporation duct. Part 3: Results from the Mediterranean measurements, volume 2
[AD-A192311] N88-26554
Antenna heights for the optimum utilization of the oceanic evaporation duct. Part 1: Results from the Pacific measurements. Part 2: Results from the Key West measurements, volume 1
[AD-A192358] N88-26555
A model for insulated wires in the method of moments code NEC (Numerical Electromagnetics Code)
[DE88-008920] N88-26577

ANTIMISSILE DEFENSE
The Oak Ridge National Laboratory strategic defense initiative shield optimization program: Executive summary
[DE88-008016] N88-26899
SDI: Myth or reality
[DE88-009121] N88-26901
The strategic defense initiative: Strategic implications
[AD-A192341] N88-26902

ANTIMISSILE MISSILES
A simulation of post boost vehicle deployment of multiple reentry vehicles
[DE88-009537] N88-26391

ANTIMISTING FUELS
Antimisting kerosene: Low temperature degradation and blending
[NASA-CR-182725] N88-26495

ANTIREFLECTION COATINGS
Optical coatings for high average power XeF lasers
[DE88-011356] N88-26656

APPLICATIONS PROGRAMS (COMPUTERS)
Intelligent guidance and control for wind shear encounter
[NASA-CR-183060] N88-26347

APPROXIMATION
On the propagating speed in difference approximations for conservation laws N88-26318
Finite element approximation to a model problem of transonic flow
[DE88-701835] N88-26333
L(sub infinity symbol)-approximations of complex functions and robust controllers for large flexible space structures
[PB88-186226] N88-26390
Finite-dimensional approximation for optimal fixed-order compensation of distributed parameter systems
[NASA-CR-181674] N88-26873
Prolongation, restriction and coarse grid approximation in a three-dimensional cell-centered multigrid method
[REPT-88-02] N88-26889

ARC WELDING
Physical-chemical reactions at welding arc/molten pool interfaces
[DE88-007717] N88-26662

ARCHITECTURE (COMPUTERS)
The UMAC simulator N88-26811
Research in VLSI computer systems
[AD-A192915] N88-26816
Design of high performance microcomputers for numerical data processing
[ETN-88-92371] N88-26818
The scaled-sized model: A revision of Amdahl's law
[DE88-008114] N88-26875

ARCTIC OCEAN
Arctic ice island and sea ice movements and mechanical properties
[DE88-004267] N88-26782

ARCTIC REGIONS
A modal approach to Arctic noise modelling with implied vertical coherence
[AD-A192966] N88-26916

ARMATURES
Why plasma armature railguns don't work (and what can be done about it)
[DE88-007900] N88-26384

Plasma armature formation in high-pressure, high-velocity hydrogen
[DE88-006347] N88-26967

ARTIFICIAL GRAVITY
Some operational aspects of a rotating advanced-technology space station for the year 2025
[NASA-CR-181617] N88-26397

ARTIFICIAL INTELLIGENCE
A cockpit natural language study - selected transcripts
[AD-A192972] N88-26808
Direct manipulation and the design of user interfaces
[PB88-126354] N88-26810
SIMS: Single Interface to Multiple Systems
[AD-A192264] N88-26832
Building an artificial intelligence capability at Los Alamos
[DE88-009155] N88-26866
Expert system application education project
[NASA-CR-183089] N88-26867
Narrative domain implementation
[AD-A192265] N88-26868
NEXT: An expert system development tool to support engineering design
[NLR-MP-86070-U] N88-26871
Qualitative reasoning for physicists
[PB88-116298] N88-26906
Challenge equality problems in lattice theory
[DE88-010094] N88-27072

ASSAYING
Methods and techniques of NDA (nondestructive assay)
[DE88-009145] N88-26682

ASSOCIATIVE PROCESSING (COMPUTERS)
Optical data processing
[AD-A193024] N88-26841

ASTRONOMICAL MODELS
Observation of a point source in Cygnus constellation with the underground detector at Frejus (France)
[PITHA-87/02] N88-27122

ASTRONOMICAL PHOTOGRAPHY
Methods for indirect imaging through the atmosphere
[ONERA-NT-1987-4] N88-27124

ASTRONOMY
Digital image processing from speckle interferograms by correlation methods: Application in atmospheric optics, astronomy, and biology
[ETN-88-92125] N88-26953

ASTROPHYSICS
Research in particle and gamma-ray astrophysics
[NASA-CR-183111] N88-27146

ASYMPTOTIC METHODS
Asymptotically efficient adaptive allocation schemes for controlled Markov chains: Finite parameter space
[AD-A192228] N88-26893

ATMOSPHERIC ATTENUATION
Ground level hydroxyl (OH) concentration measurements by long path differential optical laser absorption
[ETN-88-92124] N88-26952

ATMOSPHERIC BOUNDARY LAYER
Ground level hydroxyl (OH) concentration measurements by long path differential optical laser absorption
[ETN-88-92124] N88-26952

ATMOSPHERIC CHEMISTRY
Overview of the PRECP (processing of emissions by clouds and precipitation) Program
[DE88-008205] N88-26741
Studies of the mechanisms and rates with which nitrogen species are incorporated into cloud water and precipitation
[PB88-193065] N88-26764
Ground level hydroxyl (OH) concentration measurements by long path differential optical laser absorption
[ETN-88-92124] N88-26952

ATMOSPHERIC CIRCULATION
Tracer water transport and subgrid precipitation variation within atmospheric general circulation models
[NASA-CR-182897] N88-26745
Circulation statistics from seasonal and perpetual January and July simulations with the NCAR (National Center for Atmospheric Research) Community Climate Model (CCM1):R15
[PB88-192620] N88-26748

ATMOSPHERIC COMPOSITION
Measurement of HO2 and other trace gases in the stratosphere using a high resolution far-infrared spectrometer at 28 KM
[NASA-CR-180400] N88-26737
Wavenumber spectra from THIR 6.7 micron water vapor data N88-26756
An efficient model for changes of global climate and composition of the atmosphere due to human activities
[ETN-88-92359] N88-26775
Space infrared telescope facility project
[NASA-CR-183058] N88-27121
Ultraviolet geometric albedo of Uranus
[NASA-CR-183099] N88-27136

ATMOSPHERIC DIFFUSION
Development of an atmospheric diffusion evaluation method incorporating topographical effects. Part 1: Literature review of atmospheric diffusion models incorporating terrain effects
[DE88-753104] N88-26742
Wind tunnel study of atmospheric diffusion in unstable stratified boundary layer. Part 2: Characteristic scale and diffusion
[DE88-753109] N88-26749

ATMOSPHERIC MODELS
Effects of atmospheric model layering on LOWTRAN 6 calculations of 8-12 micrometers near-horizon sky radiances
[AD-A192969] N88-26559
Rocket measurements within a polar cap arc: Ionospheric modelling
[AD-A192381] N88-26754
Diffusion of slight solar induced disturbances in the middle atmosphere
[MITT-53] N88-26758
The NASA Marshall engineering thermosphere model
[NASA-CR-179350] N88-26760
Influence of stable stratification on atmospheric turbulence: An experimental contribution
[ETN-88-92292] N88-26772

ATMOSPHERIC RADIATION
Review of methods for remote sensing of atmospheric emissions from stationary sources
[PB88-190483] N88-26739
A control program for global radiation measurements
[KNMI-TR-100] N88-26757

ATMOSPHERIC SOUNDING
High latitude ionospheric radio studies
[AD-A192270] N88-26753
Influence of stable stratification on atmospheric turbulence: An experimental contribution
[ETN-88-92292] N88-26772

ATMOSPHERIC STRATIFICATION
Influence of stable stratification on atmospheric turbulence: An experimental contribution
[ETN-88-92292] N88-26772

ATMOSPHERIC TEMPERATURE
Satellite remote sensing of the wet bulb globe temperature heat stress index, phase 2
[AD-A192798] N88-26717
Our climate in danger
[DE88-701824] N88-26743
An efficient model for changes of global climate and composition of the atmosphere due to human activities
[ETN-88-92359] N88-26775

ATMOSPHERIC TURBULENCE
Influence of stable stratification on atmospheric turbulence: An experimental contribution
[ETN-88-92292] N88-26772

ATOMIC BEAMS
Fast atom bombardment study on interaction of anticodonic nucleotides and their cognate amino acid
[ISAS-RN-355] N88-26918

ATOMIC COLLISIONS
Recoil saturation of the self-energy in atomic systems
[DE88-010450] N88-26930

ATOMIC EXCITATIONS
Excitation of single-mode glass fiber by partially coherent sources
[ETN-88-92121] N88-26951

ATOMIC INTERACTIONS
Contribution to the study of order effects in the Ising model framework: Ground states and phase diagrams
[ONERA-NT-1987] N88-27095

ATOMIC RECOMBINATION
Nascent vibrational/rotational distribution produced by hydrogen atom recombination
[AD-A193005] N88-26933

ATOMIC STRUCTURE
The electronic structure of condensed molecular systems
[DE88-007823] N88-26923
Piezoelectric effects in strained layer superlattices N88-27002
Electronic structure of quantum-well states revealed under high pressures N88-27038
Ordering transitions of ternary alloys A(1-x)B(x)C N88-27054

ATOMIZING
Pulsed spray structure and atomisation techniques
[AD-A192280] N88-26614
Small-droplet spray measurements with a scattered-light scanner
[NASA-TM-100973] N88-26645

ATOMS
Sources of polarized ions and atoms
[DE88-010910] N88-26931

ATTENUATION
Poloidal field measurements using laser enhanced attenuation of an energetic lithium beam
[DE88-006360] N88-26963

ATTITUDE CONTROL
Spacecraft applications of advanced global positioning system technology
[NASA-CR-172063] N88-26359

AUDIOMETRY
Auditory evoked magnetic fields in man
[PB88-193446] N88-26796

AUDITORY STIMULI
Auditory evoked magnetic fields in man
[PB88-193446] N88-26796

AUGMENTATION
Enhancement of volume H(-) production by vibrationally pre-exciting the hydrogen molecules
[DE88-010783] N88-26937

AURORAL ZONES
On the conjugacy of the aurora: High and low latitudes
[AD-A193008] N88-26755

AURORAS
High latitude ionospheric radio studies
[AD-A192270] N88-26753

AUSTENITIC STAINLESS STEELS
Reduced-activation austenitic stainless steels: The Fe-Cr-C system
[DE88-008091] N88-26442
Helium induced degradation in the weldability of an austenitic stainless steel
[DE88-009062] N88-26443

AUTOMATIC CONTROL
Technical instructions for a control operating system of the gas flow installation for the solid fuel combustion chamber
[LR-507] N88-26537
Automated measurement of crack length and load line displacement at elevated temperature
[AGARD-R-751] N88-26695

AUTOMATIC LANDING CONTROL
Trajectory measurement of the Fokker 100 aircraft during autoland testing
[NLR-MP-86010-U] N88-26366

AUTOMATIC TEST EQUIPMENT
Automated measurement of crack length and load line displacement at elevated temperature
[NLR-MP-87049-U] N88-26706

AUTOMATION
Enumeration, comments and discussion concerning papers presented during the Conference on Computer Applications in Production and Engineering (CAPE) 87
[NLR-MP-87015-U] N88-26844

AUTOMOBILE ENGINES
The influence of foreign particles on bearing metals
[NASA-TT-20155] N88-26454

AUTONOMOUS NAVIGATION
Local free-space mapping and path guidance for mobile robots
[AD-A192970] N88-26674

AVIONICS
Fiber optics for advanced aircraft
[NASA-TM-101294] N88-26328
Development of an airborne facility for advanced avionics research
[NLR-MP-87012-U] N88-26368
A cockpit natural language study - selected transcripts
[AD-A192972] N88-26808

AXIAL MODES
Permanent magnet excitation of axial flow synchronous machines with high rotation moment
[ETN-88-92385] N88-26592

AXIOMS
Fixpoint representations of characteristic sets of linear-time temporal formulas
[CWI-CS-R8754] N88-26849

AXISYMMETRIC BODIES
Influence of rear body geometry on the velocity characteristics of the near wake
[ISL-R-113/87] N88-26339

AXISYMMETRIC FLOW
Simulation of axisymmetric flow with H2O2 reactions N88-26311

B

B-1 AIRCRAFT
Surface disturbances produced by low-level, subsonic B-1 aircraft
[AD-A192257] N88-26752

BACKSCATTERING
Sources of scattering in vegetarian and other surfaces and objects
[NASA-CR-182975] N88-26710
BACTERIA
Biodegradation of JP-5 aviation fuel by subsurface microbial communities
[AD-A192743] N88-26493
BALLISTICS
Contact force history and dynamic response due to the impact of a soft projectile
[NASA-TM-100961] N88-26679
BALLOON FLIGHT
On the dynamic behavior of balloon during its launch; application of panel method and extension to unsteady problem
[ISAS-RN-622] N88-26330
BAND STRUCTURE OF SOLIDS
Non-effective-mass matching in superlattices N88-27049
BARIUM
Electron irradiation effects in YBa2Cu3O7-Delta single crystals
[DE88-010050] N88-27085
Generation of Adlam-Allen waves by plasma release experiments in the solar wind
[PB88-106000] N88-27140
BARIUM OXIDES
Effects of grain boundary composition on properties of YBa2Cu3O/sub 7-x/
[DE88-007679] N88-27064
The superconducting transition in oxygen deficient YBa2Cu3O(sub 7-Delta)
[DE88-009957] N88-27079
Anisotropic characteristic lengths in single crystal YBa2Cu3O(sub 7-Delta)
[DE88-009959] N88-27080
Anisotropy of the lower critical field in YBa2Cu3O(sub 7-Delta)
[DE88-009971] N88-27081
Preparation of high-T(sub)c Y1Ba2Cu3O(sub 7-Delta) superconducting thin films by MBE (Molecular-Beam-Epitaxy) techniques
[DE88-009999] N88-27082
Oxygen vacancy ordering and superconductivity in YBa2Cu3O(sub 7-x)
[DE88-010005] N88-27083
Pure metallic bridge and point-contact tunneling into single- and polycrystal YBa2Cu3O(sub 7-y)
[DE88-010030] N88-27084
Phase transformations and thermodynamic behavior of the YBa2Cu3O(sub)x system via EMF measurements
[DE88-010054] N88-27086
Ceramic processing of high-T(sub)c superconductors
[DE88-010090] N88-27087
BAROCLINIC WAVES
Westward moving atmospheric wave disturbances over the African tropics: Dynamic and energetic aspects
[MITT-57] N88-26774
BARRIER LAYERS
A 10 microns photoexcited avalanche gain due to electron impact ionization from GaAs quantum well superlattices N88-27026
Resonant tunneling in InGaAs-InP double-barrier structures and superlattices N88-27047
BARS
Vibration frequencies of tapered bars with nonclassical boundary conditions
[NASA-CR-183059] N88-26688
BAYS (STRUCTURAL UNITS)
FEB structural analysis, revision H
[AD-A192302] N88-26698
BEACONS
COSPAS/SARSAT 406-MHz emergency beacon digital controller
[NASA-TM-100859] N88-26566
BEAM CURRENTS
Requirements for neutral beam current drive in tokamaks
[DE88-006180] N88-26980
BEAMS (RADIATION)
Time-Optimal Adaptive Shaped Torque (TOAST) technical note
[AD-A192719] N88-26869
BEAMS (SUPPORTS)
Mobile remote manipulator system for a tetrahedral truss
[NASA-CASE-MSC-20985-1] N88-26398
BEARING ALLOYS
The influence of foreign particles on bearing metals
[NASA-TT-20155] N88-26454
BENDING
Vertical ship motions and sea loads considering nonlinear effects
[TAE-592] N88-26515
BETA PARTICLES
Plasma separation process. Betacell (BCELL) code, user's manual
[DE88-006955] N88-26981
BIBLIOGRAPHIES
A bibliography and author index for electrical discharges in vacuum (1897-1986)
[DE88-008744] N88-26579
Aerospace medicine and biology: A continuing bibliography with indexes (supplement 313)
[NASA-SP-7011(313)] N88-26800
BIDIRECTIONAL REFLECTANCE
Determination and application of bidirectional solar-optical properties of fenestration systems
[DE88-010364] N88-26727
BINARY DATA
Distributed fault tolerant embeddings of binary trees in hypercubes
[AD-A192929] N88-26840
BINDERS (MATERIALS)
Determination of binder distributions in green-state ceramics by NMR imaging
[DE88-009990] N88-26474
BINOCULAR VISION
Biorhythms of binocular vision N88-26788
BIOCHEMISTRY
JPRS report: Science and technology. USSR: Life sciences
[JPRS-ULS-88-009] N88-26785
Regulatory biochemical and metabolic responses in photoreceptors
[AD-A192898] N88-26794
BIODEGRADATION
Biodegradation of JP-5 aviation fuel by subsurface microbial communities
[AD-A192743] N88-26493
BIOLOGICAL EFFECTS
Interaction of biological systems with static and ELF electric and magnetic fields
[DE88-007951] N88-26792
Aerospace medicine and biology: A continuing bibliography with indexes (supplement 313)
[NASA-SP-7011(313)] N88-26800
BIOMAGNETISM
Auditory evoked magnetic fields in man
[PB88-193446] N88-26796
BIOPHYSICS
JPRS report: Science and technology. USSR: Life sciences
[JPRS-ULS-88-009] N88-26785
BIOSPHERE
The seasonal exchange of carbon dioxide between the atmosphere and the terrestrial biosphere: Extrapolation from site-specific models to regional models
[DE88-007870] N88-26740
BIPOLAR TRANSISTORS
Resonant tunneling transistors and resonant tunneling hot electron spectroscopy N88-27018
BIRDS
Survey for least bell's vireo in riparian habitat on Vandenberg Air Force Base, Santa Barbara County, California
[NASA-TM-100984] N88-26744
BIT ERROR RATE
Error performance of voice band data signals with an overloaded delta modulator
[FEL-1987-05] N88-26562
BLADE SLAP NOISE
Helicopter main-rotor noise: Determination of source contributions using scaled model data
[NASA-TP-2825] N88-26907
BLOOD CIRCULATION
Respiration and oxygen tension in the blood of animals exposed to high pressures N88-26790
BLOWING
Numerical study of delta wing leading edge blowing
[NASA-CR-183101] N88-26335
BLUFF BODIES
Vortex methods for separated flows
[NASA-TM-100068] N88-26342
BO-105 HELICOPTER
Helicopter main-rotor noise: Determination of source contributions using scaled model data
[NASA-TP-2825] N88-26907
BODY-WING AND TAIL CONFIGURATIONS
The determination of the topological structure of skin friction lines on a rectangular wing-body combination
[NASA-CR-4168] N88-26343
BODY-WING CONFIGURATIONS
Improved potential flow computational methods with Euler corrections for airfoil and wing/body design
[AD-A192303] N88-26334
BOHR THEORY
Inelastic two composite particle systems scattering at high energy
[DE88-701841] N88-26928
BOILING
Investigation on refrigerant R12 critical boiling point in narrow flow pipes considered as model fluid
[ETN-88-92374] N88-26626
BOLTS
FEB structural analysis, revision H
[AD-A192302] N88-26698
BOLTZMANN DISTRIBUTION
Extension of Boltzmann's theory to a liquid
[DE88-009153] N88-27097
BOLTZMANN TRANSPORT EQUATION
On microphysical principles of thermofluid dynamics
[ETN-88-92095] N88-26620
BOREHOLES
Reaming experiments for the lethality test system
[DE88-007902] N88-26383
BORON
Grain boundary structure in Ni3Al
[DE88-009164] N88-26444
BOUNDARY ELEMENT METHOD
Calculations of unsteady aerodynamics for a full aircraft configuration using boundary element method N88-26303
Boundary element method for contact heat transfer
[DE88-011013] N88-26613
Time-domain boundary element analysis of dynamic near-tip fields for impact-loaded collinear cracks
[AD-A192930] N88-26700
Off-boundary approach to the boundary element method
[AD-A192931] N88-26701
BOUNDARY INTEGRAL METHOD
A new boundary integral equation formulation for elastodynamic and elastostatic crack analysis
[AD-A192967] N88-26702
BOUNDARY LAYER TRANSITION
Turbulence transition in a circular pipe N88-26503
BOUNDARY LAYERS
Prediction of continental shelf sediment transport using a theoretical model of the wave-current boundary layer
[AD-A192272] N88-26783
Solution of the Orr-Sommerfeld equation for the Blasius boundary-layer documentation of program ORRBL and a test case
[NASA-CR-4169] N88-26858
BOUNDARY VALUE PROBLEMS
Vortex methods for separated flows
[NASA-TM-100068] N88-26342
Vibration frequencies of tapered bars with nonclassical boundary conditions
[NASA-CR-183059] N88-26688
Off-boundary approach to the boundary element method
[AD-A192931] N88-26701
BRAIN
Effect of weightlessness on brain development (results of flight of pregnant rats on Kosmos-1514 biosatellite and study of subsequent development of their progeny on earth N88-26786
BREMSSTRAHLUNG
Bremsstrahlung from high Z impurities in hot plasmas
[DE88-011755] N88-26994
BRITTLENESS
Ductile-brittle transition of cutting behavior in diamond turning of single crystal Si
[DE88-008890] N88-26664
BROKEN SYMMETRY
Research in theoretical particle physics
[DE88-008230] N88-26927
BUCKLING
Three-dimensional analysis of a postbuckled embedded delamination
[NASA-TP-2823] N88-26684
BUOYANCY
Nonlinear equation of state effects and the momentum-dilution trade-off in a turbulent buoyant jet
[DE88-701839] N88-26510
BUOYS
Arctic ice island and sea ice movements and mechanical properties
[DE88-004267] N88-26782
BURNERS
Dynamics and stability of combustion driven self oscillations in presence of various frequencies. Extensive stability criteria
[ETN-88-92123] N88-26432
BURSTS
Detection of absorption lines in the spectra of X-ray bursts from X1608-52
[ISAS-RN-360] N88-27143
The hard X-ray burst spectrometer event listing 1980-1987
[NASA-TM-4036] N88-27144

BY-PRODUCTS
Feasibility of producing jet fuel from GPGP (Great Plains Gasification Plant) by-products
[DE88-010233] N88-26492

C

C (PROGRAMMING LANGUAGE)
FASTRUN phase sequencer descriptor language (PDL)
[DE88-007966] N88-26828
CADMIUM TELLURIDES
MBE growth of HgTe/CdTe superlattices on Si(100) substrates N88-27033
Type 3 - type 1 transition and strain effect in Hg(1-x)Cd(x)Te-CdTe and Hg(1-x)Zn(x)Te-CdTe superlattices N88-27052
CALIBRATING
Time-resolved doubly bent crystal X-ray spectrometer
[DE88-007899] N88-26637
Microwave calibration system 2
[AD-A192976] N88-26639
Fiber optic sensors with internal referencing
[NASA-TM-100893] N88-26644
Surface disturbances produced by low-level, subsonic B-1 aircraft
[AD-A192257] N88-26752
CALIFORNIA
Survey for least bell's vireo in riparian habitat on Vandenberg Air Force Base, Santa Barbara County, California
[NASA-TM-100984] N88-26744
CALIFORNIUM COMPOUNDS
Raman and absorption spectrophotometric studies of selected lanthanide, californium-doped lanthanide, and actinide trihalides in the solid state
[DE88-008234] N88-27061
CAMERAS
Stress analysis using infrared thermography
[ETN-88-92169] N88-26705
CANONICAL FORMS
Canonical construction of differential operators intertwining representations of real semisimple Lie groups
[DE88-701852] N88-26882
CANOPIES (VEGETATION)
Hydrologic models for land-atmosphere retrospective studies of the use of LANDSAT and AVHRR data
[NASA-CR-182662] N88-26716
CAPACITANCE
Defects in high-mobility semiconductor systems
[AD-A192298] N88-27090
CAPILLARY FLOW
Liquid motions in partially filled containers: Preliminary results of the D-1 mission — Spacelab
[NLR-MP-86042-U] N88-26629
CARBON
Reduced-activation austenitic stainless steels: The Fe-Cr-C system
[DE88-008091] N88-26442
CARBON DIOXIDE
A shock-tube experiment on gases mixing processes associated with CO2/N2 mixing gasdynamic laser
[ISAS-RN-350] N88-26598
The seasonal exchange of carbon dioxide between the atmosphere and the terrestrial biosphere: Extrapolation from site-specific models to regional models
[DE88-007870] N88-26740
CARBON DIOXIDE LASERS
A CO2 laser Thomson scattering diagnostic for fusion product alpha particle measurement
[DE88-007683] N88-26965
CARBON FIBER REINFORCED PLASTICS
High temperature resins for injection. High temperature pre-impregnated
[RC-646676] N88-26486
CARBON FIBERS
Thermoplastic coating of carbon fibers
[NASA-CR-183067] N88-26407
The crystallization of tough thermoplastic resins in the presence of carbon fibers
[NASA-CR-182984] N88-26484
CARBON 12
Probing the possibility of a (12)C/(13)C abundance gradient from observations of interstellar CH+
[DE88-006908] N88-27125
CARBON 13
Probing the possibility of a (12)C/(13)C abundance gradient from observations of interstellar CH+
[DE88-006908] N88-27125
CARBON-CARBON COMPOSITES
Electrical resistivity of carbon-carbon composites
[AD-A193008] N88-26410
High temperature testing of C/C (Carbon/Carbon) composites
[AD-A193012] N88-26411
CARIBBEAN REGION
The role of aviation technology in the Caribbean Basin
[NASA-CR-183069] N88-26289
CARRIER DENSITY (SOLID STATE)
Development of a model procedure for the determination of volume diffusion lengths by transient measurements on monocrystal silicon solar cells
[ETN-88-92119] N88-26733
Auger recombination in GaSb/AlSb-multi quantum well heterostructures N88-27001
CARRIER LIFETIME
Auger recombination in GaSb/AlSb-multi quantum well heterostructures N88-27001
Control of carrier lifetime in PbTe nipi superlattices by external photoinjection N88-27006
CARTESIAN COORDINATES
Spatial dynamics of deformable multibody systems with variable kinematic structure N88-26687
CASCADE FLOW
Numerical analysis of three dimensional cascade flow by solving Navier-Stokes equations N88-26310
Application of computational fluid dynamics to design of compressor cascade N88-26315
CASTING
Fluid flow modeling in casting processes and its implications
[DE88-010009] N88-26671
CATALYTIC ACTIVITY
Production of powdered sodium hydride with large specific surface by the catalyzed reaction of molten sodium with hydrogen-1
[NASA-TT-20185] N88-26462
CATHODES
Degradation of beam brightness by field emission from a cathode shroud
[DE88-008345] N88-26576
CATHODIC COATINGS
Extinction behavior of low voltage switching arc under consideration of cathodic coatings and dynamic arc column
[ETN-88-92384] N88-26591
CAVITATION FLOW
Pulsed spray structure and atomisation techniques
[AD-A192280] N88-26614
CAVITIES
Research in electromagnetic shielding theory. Part1. Shielding by rectangular enclosures
[AD-A192881] N88-26557
Rf cavity primer for cyclic proton accelerators
[DE88-010655] N88-26938
CAVITY RESONATORS
Superconducting rf and beam-cavity interactions
[DE88-008598] N88-26936
Rf cavity primer for cyclic proton accelerators
[DE88-010655] N88-26938
Progress in diagnostic techniques for SC (superconducting) cavities
[DE88-008600] N88-27077
CENTER OF GRAVITY
A new method for the estimation of aircraft inertia characteristics N88-26530
CERAMIC COATINGS
Development of protective coatings for ceramic tubular components
[PB88-197165] N88-26463
CERAMIC MATRIX COMPOSITES
Manufacturing of a ceramic-ceramic composite matrix using the sol-gel procedure
[ETN-88-92157] N88-26414
CERAMICS
Application of electron microscopy for the analysis of the mechanical behavior of advanced ceramics
[DE88-005049] N88-26469
A study of solvent effects on the synthesis of pure component and composite ceramic powders by metal alkoxide hydrolysis
[DE88-008381] N88-26470
Observations on residual stresses in ceramic composites by neutron diffraction techniques
[DE88-009937] N88-26472
Application of magnification xeroradiography to advanced ceramics
[DE88-009965] N88-26473
Determination of binder distributions in green-state ceramics by NMR imaging
[DE88-009990] N88-26474
The outlook for ceramics in heat engines, 1990-2010: Results of a worldwide Delphi survey
[DE88-010075] N88-26475
Factors influencing the toughening behavior of whisker reinforced ceramics
[DE88-011396] N88-26479
Fracture resistance of a TiB2 particle/SiC matrix composite at elevated temperature
[NASA-TM-100967] N88-26482
Ceramic Technology for Advanced Heat Engines Program data base
[DE88-008954] N88-26489
Characteristics of pressure loss during filtration using a porous ceramic filter
[DE88-752547] N88-26604
Computational study on thermal efficiency of ceramic gas turbine
[DE88-753114] N88-26667
Study on the heat resisting and cooling property of the ceramics-metal hybrid stator vanes
[DE88-753117] N88-26668
Ceramic processing of high-T(sub)c superconductors
[DE88-010090] N88-27087
CEREBRAL CORTEX
Method for observing changes in functional state of human operator N88-26789
CERENKOV RADIATION
The application of imaging to the atmospheric Cerenkov technique: Observations of the Crab nebula N88-27126
CHAOS
Stationary, wave type, and chaos type convection in spherical symmetry geometries
[ETN-88-92358] N88-26625
CHARACTERIZATION
GTAW characterization for weld penetration on 304L stainless steel
[DE88-010611] N88-26672
CHARGE EFFICIENCY
Nickel hydrogen cell positive-electrode studies: Cobalt segregation in reducing environments
[AD-A193025] N88-26587
Computer controlled procedures for traction battery power performance tests
[ETN-88-92352] N88-26589
CHARGED PARTICLES
JFET/SOS (Junction Field-Effect Transistor/Silicon-on-Sapphire) devices: Gamma-radiation-induced effects
[AD-A193001] N88-26586
Charged pion production and projectile breakup in 85A MeV(sup)12C induced heavy ion reactions
[LUIP-8802] N88-26920
Neoclassical diffusion due to trapping/detrapping orbits in stellarators
[DE88-008566] N88-26968
CHEBYSHEV APPROXIMATION
Solution of the Orr-Sommerfeld equation for the Blausius boundary-layer documentation of program ORRBL and a test case
[NASA-CR-4169] N88-26858
CHEMICAL ANALYSIS
Surface phases and their influence on metal-oxide interfaces
[DE88-007938] N88-26420
CHEMICAL BONDS
Fundamental studies of elastomers
[DE88-009679] N88-26471
Structural studies of (Ga,In)(As,P) alloys and (InAs) sub m (GaAs) sub n strained-layer superlattices by fluorescence-detected EXAFS N88-27051
CHEMICAL COMPOSITION
The structure and properties of grain boundaries in B2 ordered alloys
[DE88-009890] N88-26447
Nickel aluminides: A new family of nickel + aluminum alloys featuring simple composition, low density, excellent oxidation resistance and high yield strength that increases with temperature
[DE88-010692] N88-26461
Physical-chemical reactions at welding arc/molten pool interfaces
[DE88-007717] N88-26662
Fine-scale traverses in cumulate rocks, Stillwater Complex: A lunar analogue study
[NASA-CR-183066] N88-26747
Effects of grain boundary composition on properties of YBa2Cu3O/sub 7-x/
[DE88-007679] N88-27064
Defect characterization of the redox behavior and stability of conducting oxides
[DE88-010799] N88-27088
Space infrared telescope facility project
[NASA-CR-183058] N88-27121
CHEMICAL ENERGY
Thermodynamic analysis of chemical heat storage system for heat pump
[DE88-753121] N88-26728
CHEMICAL FUELS
Technical instructions for a control operating system of the gas flow installation for the solid fuel combustion chamber
[LR-507] N88-26537

CHEMICAL PROPERTIES
Synthesis of model polymers and related structures in support of vinyl monomer grafting studies
[DE88-010245] N88-26476
Refractory Materials of Zirconate. Part 2: Synthesis and some properties of strontium, zirconate, calcium zirconate and barium zirconate
[NASA-TT-20186] N88-26483
CHEMICAL REACTIONS
The protonic Beta double prime aluminas: Preparation, stability, conductivity and structure
[DE88-008442] N88-26415
Structural study of impregnating resins of TGMDA/DDS type
[ETN-88-92167] N88-26488
Freely expanding detonation products: Scaling of rate processes
[DE88-007827] N88-26606
Physical-chemical reactions at welding arc/molten pool interfaces
[DE88-007717] N88-26662
Ion and electron interactions of atmospheric importance
[AD-A192255] N88-26751
On the chemistry of superconductivity
[DE88-010714] N88-27096
CHIRP
The chirped-pulse free-electron laser
[DE88-009269] N88-26651
CHLORIDES
Rare Gas Halide (RGH) kinetics
[AD-A192352] N88-26425
CHLOROPHYLLS
Mechanisms of photochemical energy conversion by chlorophyll
[DE88-008763] N88-26725
Modeling the primary events of photosynthesis using chlorophyll containing fixed distance donor-acceptor molecules
[DE88-010033] N88-26793
CHROMIUM
Superconductivity of Cr/V superlattices N88-27057
CHROMIUM ALLOYS
Reduced-activation austenitic stainless steels: The Fe-Cr-C system
[DE88-008091] N88-26442
The T-T-T curve in Cu-Cr alloy
[NASA-TT-20167] N88-26453
CHROMIUM STEELS
Investigation of structure and surface state effect on hydrogen embrittlement of steels, under consideration of acoustic emission analysis
[ETN-88-92350] N88-26457
CIRCADIAN RHYTHMS
Biorhythms of binocular vision N88-26788
CIRCLES (GEOMETRY)
Linear programming in R sup 3 and the skeleton and largest incircle of a convex polygon
[PB88-124664] N88-26892
CIRCULAR CYLINDERS
Liquid motions in partially filled containers: Preliminary results of the D-1 mission — Spacelab
[NLR-MP-86042-U] N88-26629
CLASSIFICATIONS
Interpreting forest biome productivity and cover utilizing nested scales of image resolution and biogeographical analysis
[NASA-CR-183036] N88-26711
CLEANING
In-situ reactive of X-ray optics by glow discharge
[DE88-009840] N88-26947
CLIMATE
Our climate in danger
[DE88-701824] N88-26743
Circulation statistics from seasonal and perpetual January and July simulations with the NCAR (National Center for Atmospheric Research) Community Climate Model (CCM1):R15
[PB88-192620] N88-26748
Vegetation studies on Vandenberg Air Force Base, California
[NASA-TM-100985] N88-26795
CLIMATOLOGY
An efficient model for changes of global climate and composition of the atmosphere due to human activities
[ETN-88-92359] N88-26775
Evaluation of surface energy and radiation balance systems for FIFE
[NASA-CR-183118] N88-26778
CLOUD PHYSICS
Studies of the mechanisms and rates with which nitrogen species are incorporated into cloud water and precipitation
[PB88-193065] N88-26764
Present status of artificial rain making
[DE88-701823] N88-26769
Dynamic interaction of convective cumulus with large-scale environment
[MITT-55] N88-26773
CLOUD SEEDING
Present status of artificial rain making
[DE88-701823] N88-26769
CLOUDS
Overview of the PRECP (processing of emissions by clouds and precipitation) Program
[DE88-008205] N88-26741
Studies of the mechanisms and rates with which nitrogen species are incorporated into cloud water and precipitation
[PB88-193065] N88-26764
CLUSTER ANALYSIS
Tuning a major part of a clustering algorithm
[AD-A191446] N88-26821
Mutually exclusive alternatives by clustering
[DE88-007707] N88-27115
CLUTTER
Multi-target tracking algorithms for cluttered environments N88-26543
Method and apparatus for measuring distance
[NASA-CASE-MSC-20912-1] N88-26568
COAL
Experiments on densely-loaded non-Newtonian slurries in laminar and turbulent pipe flows
[DE88-010579] N88-26612
COATINGS
Thermoplastic coating of carbon fibers
[NASA-CR-183067] N88-26407
Interface modification in Nicalon (trademark)/SiC composites
[DE88-009708] N88-26409
The effects of Hertzian stress and test ambient on the friction coefficient of MoS2 coatings
[DE88-008118] N88-26467
Characterization of coating wear phenomena in nitride and carbide coated tool inserts
[DE88-011196] N88-26478
COBALT
Nickel hydrogen cell positive-electrode studies: Cobalt segregation in reducing environments
[AD-A193025] N88-26587
COBALT COMPOUNDS
Growth of high quality CoSi2/Si superstructures on Si(111) N88-27034
COCKPITS
Checklist interruption and resumption: A linguistic study
[NASA-CR-177460] N88-26348
A cockpit natural language study - selected transcripts
[AD-A192972] N88-26808
COEFFICIENT OF FRICTION
The effects of Hertzian stress and test ambient on the friction coefficient of MoS2 coatings
[DE88-008118] N88-26467
COGNITION
Direct manipulation and the design of user interfaces
[PB88-126354] N88-26810
COHERENT LIGHT
Excitation of single-mode glass fiber by partially coherent sources
[ETN-88-92121] N88-26951
COHERENT RADIATION
Interferometric recording of holographic optical elements using partially coherent light N88-26636
COLD PRESSING
Preparation of oxide superconductors
[DE88-009136] N88-27063
COLLINEARITY
Time-domain boundary element analysis of dynamic near-tip fields for impact-loaded collinear cracks
[AD-A192930] N88-26700
COLLISIONAL PLASMAS
Modulational instability of electric helicons in a magnetized collisional plasma
[DE88-701885] N88-26976
COMBINATORIAL ANALYSIS
Challenge problems focusing on equality and combinatory logic: Evaluating automated theorem-proving programs
[DE88-010057] N88-26879
COMBUSTIBLE FLOW
Ignition and flame spread of PMMA
[NASA-TT-20290] N88-26431
COMBUSTION
Modelling of premixed combustion using a thin flame sheet and the effect of the hydrodynamic instability
[DE88-009467] N88-26423
Asynchronous optical sampling for laser-based combustion diagnostics in high pressure flames
[AD-A192920] N88-26428
Pulsed spray structure and atomisation techniques
[AD-A192280] N88-26614
COMBUSTION CHAMBERS
An efficient computational tool for ramjet combustor research
[DE88-010034] N88-26369
Dynamics and stability of combustion driven self oscillations in presence of various frequencies. Extensive stability criteria
[ETN-88-92123] N88-26432
Technical instructions for a control operating system of the gas flow installation for the solid fuel combustion chamber
[LR-507] N88-26537
COMBUSTION PHYSICS
Study of the local behavior of a flame
[ETN-88-92300] N88-26433
COMBUSTION PRODUCTS
Freely expanding detonation products: Scaling of rate processes
[DE88-007827] N88-26606
COMBUSTION STABILITY
Dynamics and stability of combustion driven self oscillations in presence of various frequencies. Extensive stability criteria
[ETN-88-92123] N88-26432
Study of the local behavior of a flame
[ETN-88-92300] N88-26433
COMET NUCLEI
Study of comet nucleus gamma-ray spectrometer penetration system
[NASA-CR-177393] N88-27120
Processing and analysis of images transmitted by Vega space probes over Halley's comet
[ETN-88-92291] N88-27131
COMMAND AND CONTROL
An evaluation methodology for dependable multiprocessors
[AD-A192799] N88-26863
Launch operations to support future space forces
[AD-A192679] N88-27107
COMMUNICATION
Communication training for aircrews: A review of theoretical and pragmatic aspects of training program design
[NASA-CR-177459] N88-26349
COMMUNICATION EQUIPMENT
Digital communication transmitter and receiver test procedures
[AD-A191218] N88-26540
COMMUNICATION NETWORKS
The performance of Eurocom error correction schemes for data communications
[FEL-1987-56] N88-26563
An integrated circuit for error protection in modern data communication systems conforming to Eurocom specifications
[FEL-1987-48] N88-26593
Extensible networks. Part 1: Principles and constructions
[REPT-87-91-PT-1] N88-26864
COMMUTATORS
Loss evaluation of self-commutated power conditioner for battery energy storage system
[DE88-752075] N88-26575
COMPACTING
Sintering of the heterogeneous MgO compacts
[DE88-010357] N88-26408
COMPARISON
The influence of uncompensated solution resistance on the determination and standard electrochemical rate constants using cyclic voltammetry and some comparisons with AC voltammetry
[AD-A192825] N88-26427
Comparison theorems and their use in the analysis of some nonlinear diffusion problems
[DE88-010032] N88-26884
COMPENSATORS
Time-Optimal Adaptive Shaped Torque (TOAST) technical note
[AD-A192719] N88-26869
COMPILERS
Nebula support software
[AD-A192281] N88-26833
Programmer-friendly LL(1) parser generator
[PB88-126933] N88-26857
COMPOSITE MATERIALS
Instability-related delamination growth of embedded and edge delaminations N88-26406
Interface modification in Nicalon (trademark)/SiC composites
[DE88-009708] N88-26409
A micromechanics model of the stiffness and strength of laminates with fiber waviness
[NASA-CR-181670] N88-26413
Observations on residual stresses in ceramic composites by neutron diffraction techniques
[DE88-009937] N88-26472

Stress concentration around circular hole in a composite material specimen representative of the X-29A forward-swept wing aircraft
[NASA-CR-179435] N88-26694
COMPOSITE STRUCTURES
The construction of composite grids for general three-dimensional regions N88-26672
COMPRESSED GAS
Shock wave compression and metallization of simple molecules
[DE88-008031] N88-26025
COMPRESSIBILITY
The effects of thin compressive films on indentation fracture toughness measurements
[AD-A192243] N88-26480
Development of an equation of state for computation of supercompressibility factors, critical flow factors and other properties for wet, sour natural gases, synthetic gases and admixtures
[PB88-202676] N88-26002
Quantitative particle characterization by scattered ultrasound N88-26908
COMPRESSIBLE BOUNDARY LAYER
Compressible boundary layers — atmospheric reentry
[CERT-OA-13/5005-AYD] N88-26623
COMPRESSIBLE FLOW
Relaxation scheme for compressible flows N88-26323
The modified-fluid-in-cell method to which adaptive mesh and multigrid were applied N88-26324
COMPRESSING
The electronic structure of condensed molecular systems
[DE88-007823] N88-26023
COMPRESSION LOADS
Compression creep of filamentary composites
[NASA-CR-182550] N88-26601
COMPRESSIVE STRENGTH
A micromechanics model of the stiffness and strength of laminates with fiber waviness
[NASA-CR-181670] N88-26413
Compression creep of filamentary composites
[NASA-CR-182550] N88-26601
COMPRESSOR EFFICIENCY
Experimental and theoretical study of the dynamic operational behavior of a three stage radial compressor
[ETN-88-92129] N88-26676
COMPRESSORS
Experimental and theoretical study of the dynamic operational behavior of a three stage radial compressor
[ETN-88-92129] N88-26676
COMPUTATION
High speed inlet calculations with real gas effects
[NASA-CR-182167] N88-26336
Off-boundary approach to the boundary element method
[AD-A192931] N88-26701
Numerical model for the computation of radiance distributions in natural waters with wind-roughened surfaces
[PB88-192703] N88-26765
Fully implicit splitting method for accurate tidal computations
[PB88-183637] N88-26781
The role of working memory in language comprehension
[AD-A192721] N88-26805
COMPUTATIONAL ASTROPHYSICS
Numerical simulations of astrophysical jets N88-26295
COMPUTATIONAL FLUID DYNAMICS
Proceedings of the 5th NAL Symposium on Aircraft Computational Aerodynamics
[NAL-SP-8] N88-26290
Computation of flow around NACA0012 airfoil at high angle of attack N88-26300
The role of computational fluid dynamics in aeronautical engineering (5): Improvements and applications of implicit TVD finite volume code N88-26313
Extensive verification of blade-to-blade flow code based on Denton scheme N88-26314
Application of computational fluid dynamics to design of compressor cascade N88-26315
On the accuracy of upwind biased finite volume method N88-26316
An initial investigation into methods of computing transonic aerodynamic sensitivity coefficients
[NASA-CR-183061] N88-26332
The Proceedings of the Symposium on Mechanics for Space Flight 1987
[ISAS-SP-6] N88-26499
Use of direct solvers for multidimensional fluid flow computations
[DE88-010063] N88-26611
Three-dimensional viscous flow computations of a circular jet in subsonic and supersonic cross flow
[NASA-CR-182153] N88-26616
A study of flow separation in transonic flow using inviscid and viscous computational fluid dynamics (CFD) schemes
[NASA-CR-183119] N88-26618
Improved 3-D turbomachinery CFD algorithm
[NASA-CR-179364] N88-26619
Study of a water-steam two phase flow in a T-branch
[ETN-88-92306] N88-26624
Preliminary design and analysis of procedures for the numerical generation of 3D block-structured grids
[NLR-TR-86102-U] N88-26628
Parallelization on a multiprocessor system of a solution method for the unsteady Navier-Stokes equations at high Reynolds numbers
[ONERA-NT-1987-8] N88-26632
COMPUTATIONAL GRIDS
Proceedings of the 5th NAL Symposium on Aircraft Computational Aerodynamics
[NAL-SP-8] N88-26290
On the accuracy of upwind biased finite volume method N88-26316
The modified-fluid-in-cell method to which adaptive mesh and multigrid were applied N88-26324
Grid generation of a helicopter rotary-wing N88-26325
A diagonally inverted LU implicit multigrid scheme
[NASA-TM-100911] N88-26340
Numerical solution of weak forms of conservation laws on optimal unstructured triangular grids N88-26597
Multigrid computation of practical fluid flows and heat transfer
[TI88-010064] N88-26609
Preliminary design and analysis of procedures for the numerical generation of 3D block-structured grids
[NLR-TR-86102-U] N88-26628
The construction of composite grids for general three-dimensional regions N88-26672
Prolongation, restriction and coarse grid approximation in a three-dimensional cell-centered multigrid method
[REPT-88-02] N88-26689
COMPUTER AIDED DESIGN
Extensive verification of blade-to-blade flow code based on Denton scheme N88-26314
Research in VLSI computer systems
[AD-A192915] N88-26816
The knowledge based automatic extraction of the machinable surfaces for automatic CAD-CAM system
[INPE-4542-PRE/1288] N88-26824
Enumeration, comments and discussion concerning papers presented during the Conference on Computer Applications in Production and Engineering (CAPE) 87
[NLR-MP-87015-U] N88-26844
A survey of freeform solid modeling methods
[REPT-87-81] N88-26847
Interaction management in CAD systems with a history mechanism
[CWI-CS-R8756] N88-26851
NEXT: An expert system development tool to support engineering design
[NLR-MP-86070-U] N88-26871
COMPUTER AIDED MANUFACTURING
The knowledge based automatic extraction of the machinable surfaces for automatic CAD-CAM system
[INPE-4542-PRE/1288] N88-26824
Enumeration, comments and discussion concerning papers presented during the Conference on Computer Applications in Production and Engineering (CAPE) 87
[NLR-MP-87015-U] N88-26844
A survey of freeform solid modeling methods
[REPT-87-81] N88-26847
COMPUTER AIDED MAPPING
The transition from traditional to modern map reproduction
[B8735128] N88-26718
Graphical communication and symbolism in a computerized cartography and map compilation system
[PB88-124672] N88-26720
COMPUTER ASSISTED INSTRUCTION
Computer-aided writing
[AD-A192516] N88-26837
Script editor: An editor for the specification phase in the development of computer based learning
[REPT-87-68] N88-26846
The sine and cosine function for class 4-VWO. Exploration of possible bottlenecks
[REPT-87-72] N88-27105
Design and development of courseware for goniometry
[REPT-87-73] N88-27106
COMPUTER DESIGN
Design of high performance microcomputers for numerical data processing
[ETN-88-92371] N88-26618
COMPUTER GRAPHICS
Cellular array processor CAP and its application to computer graphics N88-26327
The transition from traditional to modern map reproduction
[B8735128] N88-26718
Graphical communication and symbolism in a computerized cartography and map compilation system
[PB88-124672] N88-26720
XDATAP
[DE88-007161] N88-26827
Interactive computer programme for the analysis of a two-way Wilkinson divider/combiner
[PB88-105424] N88-26831
Editfont: An interactive font editing system
[AD-A192373] N88-26836
A survey of freeform solid modeling methods
[REPT-87-81] N88-26847
An expeditious technique for keyboard input of information to FORTRAN computer programs
[DE88-009617] N88-26855
COMPUTER INFORMATION SECURITY
An evaluation methodology for dependable multiprocessors
[AD-A192799] N88-26863
COMPUTER NETWORKS
Cellular array processor CAP and its application to computer graphics N88-26327
Computer science research, 1987: Computation Directorate
[DE88-008637] N88-26812
A linear-programming method inspired by the neural networks framework
[DE88-008688] N88-26862
COMPUTER PROGRAM INTEGRITY
Nebula support software
[AD-A192281] N88-26833
COMPUTER PROGRAMMING
Research in computer science 1985/6
[PB88-113840] N88-26815
Nebula support software
[AD-A192281] N88-26833
Why is it difficult to program in von Neumann languages
[AD-A192830] N88-26839
Directions for programming in FORTRAN 77
[NASA-TT-20317] N88-26842
Diagnosing faults in autonomous robot plan execution
[NASA-CR-182480] N88-26859
Definition of an auxiliary processor dedicated to real-time operating system kernels
[NASA-CR-183070] N88-26860
PAX ECONOPACK economic analysis package users manual
[AD-A192949] N88-27117
COMPUTER PROGRAMS
High speed inlet calculations with real gas effects
[NASA-CR-182167] N88-26336
An interactive computer code for preliminary design of solid propellant rocket motors
[AD-A192869] N88-26399
Experimental and theoretical analysis of the radiative transfer within a sooty pool fire
[DE88-007099] N88-26419
A numerical study of Rayleigh-Taylor instability in aluminum and steel plates
[DE88-010475] N88-26449
Vertical ship motions and sea loads considering nonlinear effects
[TAE-592] N88-26515
Parameter identification of the passenger simulation model MADYMO: Methods and experience N88-26536
MAXWELL3: A 3D finite element electromagnetic modeling code
[DE88-010602] N88-26551
The Oak Ridge Heat Pump Design Model: Mark 3 version program documentationon
[DE88-007863] N88-26607
A study of flow separation in transonic flow using inviscid and viscous computational fluid dynamics (CFD) schemes
[NASA-CR-183119] N88-26618
Improved 3-D turbomachinery CFD algorithm
[NASA-CR-179364] N88-26619
A general-purpose approach to computer-aided dynamic analysis of a flexible helicopter
[NASA-TM-101002] N88-26709
A control program for global radiation measurements
[KNMI-TR-100] N88-26757
Computer controlled data acquisition system for the NASA 1986 Rocket Triggered Lightning Program
[DE88-008335] N88-26766
Managing microcomputer applications: A primer and guide to good practice
[AD-A192992] N88-26817

Common Data Format (CDF) to store images
[NASA-CR-179366] N88-26825
XDATAP
[DE88-007161] N88-26827
Interactive computer programme for the analysis of a two-way Wilkinson divider/combiner
[PB88-105424] N88-26831
SIMS: Single Interface to Multiple Systems
[AD-A192264] N88-26832
Nebula support software
[AD-A192281] N88-26833
Computer programs for high-current beam transport in accelerators
[AD-A192356] N88-26835
Computer-aided writing
[AD-A192516] N88-26837
Colored stochastic Petri nets. Application to real time distributed systems
[ENST-87E017] N88-26843
An expeditious technique for keyboard input of information to FORTRAN computer programs
[DE88-009617] N88-26855
An evaluation methodology for dependable multiprocessors
[AD-A192799] N88-26863
The construction of composite grids for general three-dimensional regions N88-26872
Qualitative reasoning for physicists
[PB88-116298] N88-26906
Recent applications of Monte Carlo methods for semiconductor microdevice simulation N88-27046
Knowledge-based cost estimating vs traditional software cost models
[DE88-009707] N88-27116

COMPUTER STORAGE DEVICES

The role of working memory in language comprehension
[AD-A192721] N88-26805
Common Data Format (CDF) to store images
[NASA-CR-179366] N88-26825

COMPUTER SYSTEMS DESIGN

A multiprocess operating system for 16 bit microcomputers or porting Unix (trademark) to a NS32016 with enhancements N88-26822
Computer science and technology: Knowledge-based system for physical database design
[PB88-193289] N88-27109
An integrated, multi-vendor distributed data acquisition system
[DE88-008900] N88-27113

COMPUTER SYSTEMS PERFORMANCE

On the NAL numerical simulator system N88-26291
Extensive verification of blade-to-blade flow code based on Denton scheme N88-26314
A multiprocess operating system for 16 bit microcomputers or porting Unix (trademark) to a NS32016 with enhancements N88-26822

COMPUTER SYSTEMS PROGRAMS

Nebula support software
[AD-A192281] N88-26833

COMPUTER TECHNIQUES

On the NAL numerical simulator system N88-26291
Theory of numerical information environment and its applications N88-26326
Application of Moment Iteration Method (MIM) to electromagnetic field computation
[PB88-194139] N88-26546
Graphical communication and symbolism in a computerized cartography and map compilation system
[PB88-124672] N88-26720
Inference and discovery in an exploratory laboratory
[AD-A192231] N88-26801
Managing microcomputer applications: A primer and guide to good practice
[AD-A192992] N88-26817
Computer-aided writing
[AD-A192516] N88-26837

COMPUTER VISION

Sensor fusion for robot navigation
[DE88-008383] N88-26663

COMPUTERIZED SIMULATION

The role of aviation technology in the Caribbean Basin
[NASA-CR-183069] N88-26289
Computer simulation of a single pilot flying a modern high-performance helicopter
[NASA-TM-100182] N88-26376
Computer simulation of multiple pilots flying a modern high performance helicopter
[NASA-TM-100183] N88-26377
A simulation of post boost vehicle deployment of multiple reentry vehicles
[DE88-009537] N88-26391
Computation equipment for damage simulation in laminated composites
[AD-A193013] N88-26412
Rare Gas Halide (RGH) kinetics
[AD-A192352] N88-26425
Grain boundaries
[DE88-009889] N88-26446
Fundamental studies of elastomers
[DE88-009679] N88-26471
Statistical mechanics of polymer systems
[DE88-011172] N88-26477
Vortex filament simulation for the crosslinking rings N88-26501
MAXWELL3: A 3D finite element electromagnetic modeling code
[DE88-010602] N88-26551
Freely expanding detonation products: Scaling of rate processes
[DE88-007827] N88-26606
Axisymmetric liquid sloshing under low-g conditions: Numerical simulation method (reference manual)
[NLR-TR-86057-4] N88-26627
Fluid flow modeling in casting processes and its implications
[DE88-010009] N88-26671
Analytical and experimental investigation of ringless piston concept
[AD-A192835] N88-26673
Microstructural effects in static and dynamic numerical experiments
[DE88-004289] N88-26690
Circulation statistics from seasonal and perpetual January and July simulations with the NCAR (National Center for Atmospheric Research) Community Climate Model (CCM1):R15
[PB88-192620] N88-26748
Synoptic patterns related to tropical cyclone recurvature
[AD-A192338] N88-26771
Automated system for mathematical processing of the data from a hybrid spectrometer
[DE87-702995] N88-26820
Proceedings of the 2nd US-Japan Workshop on Advanced Plasma Modeling, volume 3
[IPPJ-867] N88-26957
A Vlasov ion zero mass electron model for plasma simulations N88-26958
Modeling of subtle kinetic processes in plasma simulation N88-26959
Drift wave vortices and anomalous transport
[DE88-009562] N88-26982
MACH2: A two-dimensional magnetohydrodynamic simulation code for complex experimental configurations
[AD-A192285] N88-26988
Cosmological helium production simplified
[DE88-009578] N88-27130

CONCENTRATORS

Photovoltaic concentrator technology: Recent results
[DE88-009588] N88-26726

CONCENTRIC CYLINDERS

Study of temperature and stress fields of two sliding cylinders
[ETN-88-92134] N88-26704

CONCENTRIC SPHERES

Finitely many delta-interactions with supports on concentric spheres
[DE88-701834] N88-27101

CONCRETES

An assessment of modelling techniques for the finite element analysis of reinforced concrete plate and shell structures
[AD-A192263] N88-26697

CONCURRENT PROCESSING

Modeling and optimum time performance for concurrent processing
[NASA-CR-4167] N88-26595
Contractions in comparing concurrency semantics
[CWI-CS-R8755] N88-26850
Markov chain computations to a solution of the mutual-exclusion problem in concurrency
[REPT-87-89] N88-26896

CONDUCTIVITY

The protonic Beta double prime aluminas: Preparation, stability, conductivity and structure
[DE88-008442] N88-26415
Theoretical aspects of electron transport in modulated structures N88-27016

CONFERENCES

Flight Mechanics Panel Symposium on Rotorcraft Design for Operations: Technical evaluation report
[AGARD-AR-243] N88-26362
System identification in vehicle dynamics
[DFVLR-MITT-87-22] N88-26518
Proceedings of the Array Signal Processing Symposium: Treaty Verification Program
[DE88-008346] N88-26548
Proceedings of the 2nd US-Japan Workshop on Advanced Plasma Modeling, volume 3
[IPPJ-867] N88-26957
Third International Conference on Superlattices, Microstructures and Microdevices
[AD-A191416] N88-26995

CONFORMAL MAPPING

Image force expression for the dislocation near a crack
[DE88-701894] N88-26692

CONSERVATION EQUATIONS

Simulation of axisymmetric flow with H2O2 reactions N88-26311
A new boundary integral equation formulation for elastodynamic and elastostatic crack analysis
[AD-A192967] N88-26702

CONSERVATION LAWS

On the propagating speed in difference approximations for conservation laws N88-26318
Numerical solution of weak forms of conservation laws on optimal unstructured triangular grids N88-26597

CONSTANTS

A simulation analysis of errors in the measurement of standard electrochemical rate constants from phase-selective impedance data
[AD-A192739] N88-26426

CONSTRAINTS

Range of a constrained random walk
[PB88-126867] N88-26897

CONTAINERLESS MELTS

Program for the feasibility of developing a high pressure acoustic levitator
[NASA-CR-182154] N88-26498

CONTAMINANTS

Overview of the PRECP (processing of emissions by clouds and precipitation) Program
[DE88-008205] N88-26741

CONTINENTAL SHELVES

Effects of a temperature-dependent rheology on large scale continental extension
[NASA-CR-183117] N88-26759
Prediction of continental shelf sediment transport using a theoretical model of the wave-current boundary layer
[AD-A192272] N88-26783
Stability of a coastal upwelling front over topography
[AD-A192354] N88-26784

CONTINUOUS WAVE LASERS

Strained layer and lattice matched transverse junction stripe quantum well lasers for continuous room temperature operation N88-27004

CONTINUOUS WAVE RADAR

Method and apparatus for measuring distance
[NASA-CASE-MSC-20912-1] N88-26568

CONTINUUM MECHANICS

On microphysical principles of thermofluid dynamics
[ETN-88-92095] N88-26620

CONTROL SYSTEMS DESIGN

Fiber optics for advanced aircraft
[NASA-TM-101294] N88-26328
Computer simulation of multiple pilots flying a modern high performance helicopter
[NASA-TM-100183] N88-26377
A reusable rocket engine intelligen control
[NASA-TM-100963] N88-26401
Nonlinear identification of an aircraft for the direct calculation of an anticipatory control N88-26535
Design of a controller to reduce residual vibration in the positioning control of flexible robotic manipulators N88-26658
An introduction to robot joint control methods
[NLR-TR-86080-U] N88-26677
Expert system application education project
[NASA-CR-183089] N88-26867

CONTROL THEORY

An introduction to robot joint control methods
[NLR-TR-86080-U] N88-26677

CONTROLLERS

L(sub infinity symbol)-approximations of complex functions and robust controllers for large flexible space structures
[PB88-186226] N88-26390
COSPAS/SARSAT 406-MHz emergency beacon digital controller
[NASA-TM-100859] N88-26566
Design of a controller to reduce residual vibration in the positioning control of flexible robotic manipulators N88-26658

CONVECTION

Cosmions and stars
[DE88-010686] N88-27145

CONVECTION CLOUDS

Parametric methodologies of cloud vertical transport for acid deposition models
[PB88-191374] N88-26762
Dynamic interaction of convective cumulus with large-scale environment
[MITT-55] N88-26773

CONVECTIVE FLOW
Stationary, wave type, and chaos type convection in spherical symmetry geometries
[ETN-88-92358] N88-26625
CONVECTIVE HEAT TRANSFER
An arranging method on L/D of two-phase closed thermosyphons N88-26508
Forced-convective boiling in small diameter tube N88-26510
CONVERGENCE
Application of Moment Iteration Method (MIM) to electromagnetic field computation
[PB88-194139] N88-26546
Conditions for finite convergence of algorithms for nonlinear programs and variational inequalities
[AD-A192355] N88-26834
CONVEXITY
Linear programming in R sup 3 and the skeleton and largest incircle of a convex polygon
[PB88-124664] N88-26802
COOLING
Heat pump augmented radiator for low-temperature space applications
[DE88-008369] N88-26393
COORDINATES
Full-wave calculations in flux coordinates for toroidal geometry
[DE88-010131] N88-26985
COPOLYMERS
Synthesis of model polymers and related structures in support of vinyl monomer grafting studies
[DE88-010245] N88-26476
Initial adhesive screening of novel polyamide-imides and their copolymers
[NASA-TM-100641] N88-26481
COPPER
The T-T-T curve in Cu-Cr alloy
[NASA-TT-20167] N88-26453
Oxygen vacancy ordering and superconductivity in YBa2Cu3O(sub 7-x)
[DE88-010005] N88-27083
Pure metallic bridge and point-contact tunneling into single- and polycrystal YBa2Cu3O(sub 7-y)
[DE88-010030] N88-27084
Electron irradiation effects in YBa2Cu3O7-Delta single crystals
[DE88-010050] N88-27085
COPPER OXIDES
Phase transformations and thermodynamic behavior of the YBa2Cu3O(sub)x system via EMF measurements
[DE88-010054] N88-27086
CORES
High resolution detection of solute segregation to the cores of dislocations in grain boundaries
[DE88-009168] N88-27078
CORNERS
Semilinear elliptic problems on domains with corners
[REPT-87-83] N88-26888
CORONAS
The properties of solar coronal active regions deduced from X-ray line spectra
[AD-A193026] N88-27141
CORRELATORS
Optical correlation using the magneto-optic device
[AD-A192342] N88-26950
CORROSION
Corrosion in aircraft structures. Part 1: Text
[LR-527-PT-1] N88-26458
Corrosion in aircraft structures. Part 2: Figures
[LR-527-PT-2] N88-26459
CORROSION PREVENTION
Guide to the control of high temperature corrosion and protection of gas turbine materials
[PB88-107412] N88-26370
Corrosion prevention in gas turbines
[NLR-MP-87029-U] N88-26373
Development of protective coatings for ceramic tubular components
[PB88-197165] N88-26483
CORROSION RESISTANCE
Guide to the control of high temperature corrosion and protection of gas turbine materials
[PB88-107412] N88-26370
Nickel aluminides: A new family of nickel + aluminum alloys featuring simple composition, low density, excellent oxidation resistance and high yield strength that increases with temperature
[DE88-010692] N88-26481
CORRUGATING
Characteristics of long size thermosyphons made of corrugated tube N88-26511
Variational analysis of dielectrically loaded multidepth corrugated waveguides
[PB88-193602] N88-26573
COSMIC RAYS
Effects of cosmic rays on single event upsets
[NASA-CR-183053] N88-26569
Observation of a point source in Cygnus constellation with the underground detector at Frejus (France)
[PITHA-87/02] N88-27122
Time-dependent mass loss from hot stars with and without radiative driving
[DE88-008899] N88-27128
Studies of HZE particle interactions and transport for space radiation protection purposes
[NASA-TM-101159] N88-27142
Research in particle and gamma-ray astrophysics
[NASA-CR-183111] N88-27146
COSMOLOGY
Cosmic wavefunction with induced gravity
[DE88-701873] N88-27129
Cosmological helium production simplified
[DE88-009578] N88-27130
Cosmions and stars
[DE88-010886] N88-27145
COSPAS
COSPAS/SARSAT 406-MHz emergency beacon digital controller
[NASA-TM-100859] N88-26566
COST ANALYSIS
Engine component retirement for cause. Volume 1: Executive summary
[AD-A192730] N88-26371
COST ESTIMATES
Knowledge-based cost estimating vs traditional software cost models
[DE88-009707] N88-27116
COUNTER ROTATION
Numerical solutions of the Euler equations for the flow field around counter-rotating propellers N88-26298
COUPLERS
Study and implementation of ultrahigh frequency coupling devices using the fin line technology — millimeter waves
[ETN-88-92307] N88-26588
CRAB NEBULA
The application of imaging to the atmospheric Cerenkov technique: Observations of the Crab nebula N88-27126
CRACK GEOMETRY
Sensitivity to crack initiation in thick assemblies. Test report 48-444
[REPT-48-444] N88-26365
CRACK PROPAGATION
Accelerated fatigue crack growth behavior of PWA 1480 single crystal alloy and its dependence on the deformation mode
[NASA-TM-100943] N88-26436
Study of the influence of metallurgical factors on fatigue and fracture of aerospace structural materials
[AD-A192909] N88-26452
Irreversible deformations during fracture in polymers
[W-7/88] N88-26485
Fatigue crack growth under far-field cyclic compression
[DE88-011215] N88-26689
Automated measurement of crack length and load line displacement at elevated temperature
[AGARD-R-751] N88-26695
A new boundary integral equation formulation for elastodynamic and elastostatic crack analysis
[AD-A192967] N88-26702
Prediction of fatigue growth
[NLR-MP-87052-U] N88-26707
CRACKING (FRACTURING)
Automated measurement of crack length and load line displacement at elevated temperature
[AGARD-R-751] N88-26695
CRACKS
Helium induced degradation in the weldability of an austenitic stainless steel
[DE88-009062] N88-26443
Image force expression for the dislocation near a crack
[DE88-701894] N88-26692
Time-domain boundary element analysis of dynamic near-tip fields for impact-loaded collinear cracks
[AD-A192930] N88-26700
A new boundary integral equation formulation for elastodynamic and elastostatic crack analysis
[AD-A192967] N88-26702
CRAY COMPUTERS
The performance of the NEC SX-2 and Cray X-MP supercomputers
[DE88-009177] N88-26813
CREEP PROPERTIES
Compression creep of filamentary composites
[NASA-CR-182550] N88-26601
CREEP TESTS
Automated measurement of crack length and load line displacement at elevated temperature
[AGARD-R-751] N88-26695
Automated measurement of crack length and load line displacement at elevated temperature
[NLR-MP-87049-U] N88-26706
CREW PROCEDURES (PREFLIGHT)
Checklist interruption and resumption: A linguistic study
[NASA-CR-177460] N88-26348
CREWS
Checklist interruption and resumption: A linguistic study
[NASA-CR-177460] N88-26348
CRITICAL FLOW
Development of an equation of state for computation of supercompressibility factors, critical flow factors and other properties for wet, sour natural gases, synthetic gases and admixtures
[PB88-202676] N88-26602
CRITICAL POINT
Critical point wetting drop tower experiment
[NASA-CR-183062] N88-26603
Investigation on refrigerant R12 critical boiling point in narrow flow pipes considered as model fluid
[ETN-88-92374] N88-26626
Nontrivial critical points for asymptotically quadratic function
[DE88-101851] N88-26881
Thermal conductivity of pure fluids in a large region around the critical point
[ETN-88-92135] N88-27103
CROSS CORRELATION
Development of advanced flow simulation system by water flow model. New method of velocity measurement using cross-correlation
[DE88-753120] N88-26608
CROSS FLOW
Three-dimensional viscous flow computations of a circular jet in subsonic and supersonic cross flow
[NASA-CR-182153] N88-26616
Cross flow induced vibrations in tube bundle by displaced and misaligned tube configurations
[ETN-88-92132] N88-26621
CRYOGENIC TEMPERATURE
Low noise cryogenic dielectric resonator oscillator
[NASA-CASE-NPO-17157-1-CU] N88-26596
CRYOGENIC WIND TUNNELS
Wall interference assessment/correction of data from tests of a CAST 10-2/DOA 2 airfoil in the Langley 0.3-m transonic cryogenic tunnel N88-26331
CRYOGENICS
Electrodynamic driver for the space thermoacoustic refrigerator (STAR)
[AD-A192337] N88-26517
Development of external cooling cryo-resistive cable systems. Part 2: Insulation characteristics on 68 kV rated cryo-resistive testing cable
[DE88-770191] N88-26571
CRYPTOGRAPHY
Minimum disclosure proofs of knowledge
[CWI-PM-R8710] N88-26854
CRYSTAL DEFECTS
Aharonov-Bohm effects in disordered metals N88-27008
EXAFS studies of the microstructure of semiconductor alloys, defects and semiconductor-metal interfaces N88-27031
Aperiodic superlattices: Structured randomness N88-27055
Fermi level dependent native defect formation: Consequences for metal-semiconductor and semiconductor-semiconductor interfaces
[DE88-008247] N88-27066
Electron irradiation effects in YBa2Cu3O7-Delta single crystals
[DE88-010050] N88-27085
Defect characterization of the redox behavior and stability of conducting oxides
[DE88-010799] N88-27088
CRYSTAL DISLOCATIONS
Image force expression for the dislocation near a crack
[DE88-701894] N88-26692
On the possibility of the soliton description of acoustic emission during plastic deformation of crystals
[DE88-701878] N88-27075
CRYSTAL GROWTH
The structure and properties of grain boundaries in B2 ordered alloys
[DE88-009890] N88-26447
Preparation of oxide superconductors
[DE88-009136] N88-27063

CRYSTAL LATTICES
Abnormal diffusion of vacancies in metals
[DE88-701880] N88-26441
Lattice strain in heteroepitaxial films N88-27032
Lattice theory of fracture of solids with layered structure
[DE88-701867] N88-27073
Derivation of space groups in mm2, 222 and mmm crystal classes
[DE88-701881] N88-27076
Contribution to the study of order effects in the Ising model framework: Ground states and phase diagrams
[ONERA-NT-1987] N88-27095
CRYSTAL OPTICS
Liquid crystal optics for laser systems
[DE88-008475] N88-26948
CRYSTAL STRUCTURE
Phase stability and alloy design of ordered intermetallics
[DE88-007479] N88-26435
Strained layer and lattice matched transverse junction stripe quantum well lasers for continuous room temperature operation N88-27004
Metallic superlattices N88-27012
Growth of high quality CoSi2/Si superstructures on Si(111) N88-27034
Characterization of structural and magnetic order of Er/Y superlattices N88-27056
Raman and absorption spectrophotometric studies of selected lanthanide, californium-doped lanthanide, and actinide trihalides in the solid state
[DE88-008234] N88-27061
Lattice theory of fracture of solids with layered structure
[DE88-701867] N88-27073
Derivation of space groups in mm2, 222 and mmm crystal classes
[DE88-701881] N88-27076
Electronic and geometric structure of silver and palladium on aluminum (111) in monoatomic surface layers
[ETN-88-92120] N88-27093
Epitaxy and properties of two dimensional GaInAs semiconductor structures
[ETN-88-92357] N88-27094
Contribution to the study of order effects in the Ising model framework: Ground states and phase diagrams
[ONERA-NT-1987] N88-27095
CRYSTALLITES
The crystallization of tough thermoplastic resins in the presence of carbon fibers
[NASA-CR-182984] N88-26464
CRYSTALLIZATION
The crystallization of tough thermoplastic resins in the presence of carbon fibers
[NASA-CR-182984] N88-26464
Crystallization of aluminum hydroxide in the aluminum-air battery: Literature review, crystallizer design and results of integrated system tests
[DE88-010510] N88-26594
CRYSTALS
Time-resolved doubly bent crystal X-ray spectrometer
[DE88-007899] N88-26637
CUBES (MATHEMATICS)
Procedure for converting a Wilson-Fowler spline to a cubic B-spline with double knots
[DE88-008971] N88-26878
CUMULUS CLOUDS
Dynamic interaction of convective cumulus with large-scale environment
[MITT-55] N88-26773
CURRENT DENSITY
Poloidal field measurements using laser enhanced attenuation of an energetic lithium beam
[DE88-008360] N88-26963
CURVATURE
Synoptic patterns related to tropical cyclone recurvature
[AD-A192338] N88-26771
CURVES
The T-T-T curve in Cu-Cr alloy
[NASA-TT-20167] N88-26453
CUTTERS
Characterization of coating wear phenomena in nitride and carbide coated tool inserts
[DE88-011196] N88-26478
CUTTING
Characterization of coating wear phenomena in nitride and carbide coated tool inserts
[DE88-011196] N88-26478
Ductile-brittle transition of cutting behavior in diamond turning of single crystal Si
[DE88-008890] N88-26664
CYCLES
The influence of uncompensated solution resistance on the determination and standard electrochemical rate constants using cyclic voltammetry and some comparisons with AC voltammetry
[AD-A192825] N88-26427
Two families of graphs satisfying the cycle basis interpolation property
[PB88-127808] N88-26890
Algorithm for generating the minimal cycle basis of a graph
[PB88-126610] N88-26891
CYCLIC ACCELERATORS
Rf cavity primer for cyclic proton accelerators
[DE88-010655] N88-26938
CYCLIC LOADS
Fatigue crack growth under far-field cyclic compression
[DE88-011215] N88-26689
Damage in a perforated graphite-epoxy plate under monotonic, cyclic biaxial loading
[ONERA-NT-1987-5] N88-26708
CYCLOBUTANE
Research in energetic compounds
[AD-A192953] N88-26494
CYCLOTRON RADIATION
Kinetic modulational instability of electron cyclotron waves in plasmas
[DE88-701893] N88-26978
CYCLOTRON RESONANCE
Kinetic modulational instability of electron cyclotron waves in plasmas
[DE88-701893] N88-26978
CYGNUS CONSTELLATION
Observation of a point source in Cygnus constellation with the underground detector at Frejus (France)
[PITHA-87/02] N88-27122

D

DAMAGE
Stiffness degradation of composite laminates N88-26405
Computation equipment for damage simulation in laminated composites
[AD-A193013] N88-26412
The influence of foreign particles on bearing metals
[NASA-TT-20155] N88-26454
Irreversible deformations during fracture in polymers
[W-7/86] N88-26485
Mobile robot survival
[DE88-009108] N88-26665
Damage in a perforated graphite-epoxy plate under monotonic, cyclic biaxial loading
[ONERA-NT-1987-5] N88-26708
DAMAGE ASSESSMENT
Principles of a nondestructive evaluation process for damage location, damage profile, and damage extension in welded joints by radiometric measurements
[MPA-86-02] N88-26683
DATA ACQUISITION
Measurement of HO2 and other trace gases in the stratosphere using a high resolution far-infrared spectrometer at 28 KM
[NASA-CR-180400] N88-26737
Computer controlled data acquisition system for the NASA 1986 Rocket Triggered Lightning Program
[DE88-008335] N88-26786
An expeditious technique for keyboard input of information to FORTRAN computer programs
[DE88-009617] N88-26855
An overview of the development of a linear broadband analog fiber-optic link
[DE88-008668] N88-26945
An integrated, multi-vendor distributed data acquisition system
[DE88-008900] N88-27113
DATA BASE MANAGEMENT SYSTEMS
Issues and recommendations associated with distributed computation and data management systems for the space sciences
[NASA-CR-183026] N88-27108
Computer science and technology: Knowledge-based system for physical database design
[PB88-193289] N88-27109
Towards knowledge bases-semantics, rules and object-oriented programming
[PB88-106154] N88-27110
DATA BASES
SIMS: Single Interface to Multiple Systems
[AD-A192264] N88-26832
Nucleon-nucleus interaction data base: Total nuclear and absorption cross sections
[NASA-TM-4053] N88-26935
DATA FLOW ANALYSIS
Statistical properties of real time events in an ATC (Air Traffic Control) system
[PB88-118781] N88-26353
DATA MANAGEMENT
The role of working memory in language comprehension
[AD-A192721] N88-26805
DATA PROCESSING
On the NAL numerical simulator system N88-26291
Theory of numerical information environment and its applications N88-26326
Treatment of systematic errors in the processing of wide angle sonar sensor data for robotic navigation
[DE88-008961] N88-26352
Statistical properties of real time events in an ATC (Air Traffic Control) system
[PB88-118781] N88-26353
Laser ranging data analysis
[NASA-CR-183115] N88-26567
Automated system for mathematical processing of the data from a hybrid spectrometer
[DE87-702995] N88-26820
Narrative domain implementation
[AD-A192265] N88-26868
Knowledge-based cost estimating vs traditional software cost models
[DE88-009707] N88-27116
DATA REDUCTION
Data volume reduction for imaging radar polarimetry
[NASA-CASE-NPO-17184-1-CU] N88-26541
DATA STORAGE
Theory of numerical information environment and its applications N88-26326
DATA STRUCTURES
Design of high performance microcomputers for numerical data processing
[ETN-88-92371] N88-26818
DATA TRANSMISSION
The performance of Eurocom error correction schemes for data communications
[FEL-1987-56] N88-26563
An integrated circuit for error protection in modern data communication systems conforming to Eurocom specifications
[FEL-1987-48] N88-26593
A high speed serial link interface for SANDAC-V
[DE88-007694] N88-26881
Use of fiber optic equipment for security
[DE88-007898] N88-26943
DEAD RECKONING
Simple 2-D navigation for wheeled vehicles
[DE88-007115] N88-26351
DECISION MAKING
A semantic approach to fairness
[CWI-CS-R8759] N88-26853
Expert system application education project
[NASA-CR-183089] N88-26867
DECISION THEORY
Combining expert opinions: An optimization framework
[REPT-87-84] N88-26895
DEFECTS
Application of magnification xeroradiography to advanced ceramics
[DE88-009965] N88-26473
Microfocus X-ray techniques for flaw location
[DE88-008636] N88-26880
Defects and disorder in amorphous and damaged silicon
[AD-A192277] N88-27089
Defects in high-mobility semiconductor systems
[AD-A192298] N88-27090
DEFENSE PROGRAM
An agenda for the strategic defense initiative
[RAND-P-7404] N88-26898
The Oak Ridge National Laboratory strategic defense initiative shield optimization program: Executive summary
[DE88-009016] N88-26899
Monitoring space weaponry: Detection and verification issues
[DE88-008726] N88-26900
SDI: Myth or reality
[DE88-009121] N88-26901
SDI and/or arms control
[RAND-P-7357] N88-26903
DEFORMATION
Accelerated fatigue crack growth behavior of PWA 1480 single crystal alloy and its dependence on the deformation mode
[NASA-TM-100943] N88-26436
Irreversible deformations during fracture in polymers
[W-7/86] N88-26485
Spatial dynamics of deformable multibody systems with variable kinematic structure N88-26687

DELAMINATING
Instability-related delamination growth of embedded and edge delaminations N88-26406
Three-dimensional analysis of a postbuckled embedded delamination
[NASA-TP-2823] N88-26684
DELTA FUNCTION
Finitely many delta-interactions with supports on concentric spheres
[DE88-701834] N88-27101
DELTA WINGS
Numerical study of delta wing leading edge blowing
[NASA-CR-183101] N88-26335
DENSITY WAVE MODEL
Electrostatic whistler mode conversion at plasma resonance
[AD-A192951] N88-26969
DEPLOYMENT
A simulation of post boost vehicle deployment of multiple reentry vehicles
[DE88-009537] N88-26391
DEPOSITION
Electrophoretic coatings. Part 1: Sandia applications
[DE88-008668] N88-26465
The effects of Hertzian stress and test ambient on the friction coefficient of MoS2 coatings
[DE88-008118] N88-26467
Overview of the PRECP (processing of emissions by clouds and precipitation) Program
[DE88-008205] N88-26741
DEPTH
Variational analysis of dielectrically loaded multidepth corrugated waveguides
[PB88-193602] N88-26573
DESIGN ANALYSIS
Some operational aspects of a rotating advanced-technology space station for the year 2025
[NASA-CR-181617] N88-26397
Radar cross section studies/compact range research
[NASA-CR-183124] N88-26565
The Oak Ridge Heat Pump Design Model: Mark 3 version program documentationon
[DE88-007863] N88-26607
Improvement of head-up display standards. Volume 1: Head-up display design guide, appendix
[AD-A192973] N88-26809
DETECTION
Evaluation of engineering leak before break assessment methods by piping tests
[PB88-126982] N88-26538
Laser spectoscopy of plasmas
[AD-A193009] N88-26991
High resolution detection of solute segregation to the cores of dislocations in grain boundaries
[DE88-009168] N88-27078
Detection of absorption lines in the spectra of X-ray bursts from X1608-52
[ISAS-RN-360] N88-27143
DEUTERIUM
Factors which affect operation of a plasma focus in various gases
[DE88-701882] N88-26975
DIAGNOSIS
Asynchronous optical sampling for laser-based combustion diagnostics in high pressure flames
[AD-A192920] N88-26428
Laser diagnostics applied to advanced combustion systems
[DE88-753119] N88-26649
DIELECTRIC PROPERTIES
Development of external cooling cryo-resistive cable systems. Part 2: Insulation characteristics on 66 kV rated cryo-resistive testing cable
[DE88-770191] N88-26571
Variational analysis of dielectrically loaded multidepth corrugated waveguides
[PB88-193602] N88-26573
Low noise cryogenic dielectric resonator oscillator
[NASA-CASE-NPO-17157-1-CU] N88-26596
Modeling of subtle kinetic processes in plasma simulation N88-26959
DIELECTRICS
Visible tunable source
[DE88-006442] N88-26944
DIESEL ENGINES
Pulsed spray structure and atomisation techniques
[AD-A192280] N88-26814
DIFFERENTIAL EQUATIONS
Propagation of inernio-acoustic gravity waves in a rotating and radiating opaque atmosphere
[DE88-701866] N88-26750
A practical shifted Adams algorithm
[DE88-008573] N88-26830
Canonical construction of differential operators intertwining representations of real semisimple Lie groups
[DE88-701852] N88-26882
Theory of pseudo-differential operators over C*-algebras
[DE88-701860] N88-26883
A full but elementary treatment of systems of homogeneous ordinary linear differential equations with constant coefficients
[REPT-87-82] N88-26887
DIFFRACTION
Scattering patterns of dihedral corner reflectors with impedance surface impedances
[NASA-CR-183078] N88-26545
Acoustic diffraction by an absorbing finite strip in a moving fluid
[PB88-191382] N88-26912
The evaluation of a deformable diffraction grating for a stigmatic EUV spectroheliometer
[NASA-CR-183064] N88-26941
DIFFRACTION PATHS
Sound propagation over uneven ground and irregular topography
[NASA-CR-182956] N88-26911
DIFFUSION
Abnormal diffusion of vacancies in metals
[DE88-701880] N88-26441
Comparison theorems and their use in the analysis of some nonlinear diffusion problems
[DE88-010032] N88-26884
Neoclassical diffusion due to trapping/detrapping orbits in stellarators
[DE88-008566] N88-26968
DIFFUSION COEFFICIENT
Development of a model procedure for the determination of volume diffusion lengths by transient measurements on monocrystal silicon solar cells
[ETN-88-92119] N88-26733
DIFFUSION FLAMES
Heterogeneous diffusion flame stabilization
[AD-A193014] N88-26429
DIGITAL DATA
Theory of numerical information environment and its applications N88-26326
DIGITAL SIMULATION
Proceedings of the 5th NAL Symposium on Aircraft Computational Aerodynamics
[NAL-SP-8] N88-26290
On the NAL numerical simulator system N88-26291
Numerical simulations of aerodynamic contribution of flows about a space-plane-type configuration N88-26292
Numerical simulations of flow around shuttle orbiter N88-26293
Numerical simulations of astrophysical jets N88-26295
Numerical simulation of supersonic free-jets N88-26299
Aerodynamic simulation for complete ASKA aircraft configuration N88-26301
Numerical simulation of viscous flows over transonic aircraft configurations N88-26302
A numerical analysis of flow characteristics in laser propulsion system N88-26305
Numerical simulation of the shock tube flows by TVD scheme N88-26308
Numerical calculation of three dimensional flow by TVD scheme N88-26309
Numerical analysis of three dimensional cascade flow by solving Navier-Stokes equations N88-26310
Simulation of axisymmetric flow with H2O2 reactions N88-26311
Application of computational fluid dynamics to design of compressor cascade N88-26315
Numerical simulation of transition to turbulence in plane Poiseuille flow by a spectral method N88-26321
Numerical simulation of turbulent flow using the exponential expression of k-epsilon equation N88-26322
Theory of numerical information environment and its applications N88-26326
A high fidelity real-time simulation of a small turboshaft engine
[NASA-TM-100991] N88-26378
A simulation analysis of errors in the measurement of standard electrochemical rate constants from phase-selective impedance data
[AD-A192739] N88-26426
The influence of uncompensated solution resistance on the determination and standard electrochemical rate constants using cyclic voltammetry and some comparisons with AC voltammetry
[AD-A192825] N88-26427
Simulation models for the dynamics of tracked vehicle systems: State-of-the-art and open problems N88-26522
Parameter identification of the passenger simulation model MADYMO: Methods and experience N88-26536
DIGITAL SYSTEMS
Digital communication transmitter and receiver test procedures
[AD-A191218] N88-26540
COSPAS/SARSAT 406-MHz emergency beacon digital controller
[NASA-TM-100859] N88-26566
DIHEDRAL ANGLE
Scattering patterns of dihedral corner reflectors with impedance surface impedances
[NASA-CR-183078] N88-26545
DIMENSIONAL ANALYSIS
Display and processing of multidimensional signals with the aid of fractal image sequences
[ETN-88-92131] N88-26642
DIMENSIONS
Analysis of gas turbine test cell number 1, Lemoore Naval Air Station, California
[AD-A192870] N88-26380
Vertical viewing ECE diagnostic for the D3-D tokamak
[DE88-010586] N88-26987
DIODES
Electrical study of metal/group 3-5 semiconductor interfaces: Comparison with the atomic-level studies N88-27059
DIRECTIVITY
An analysis of the efficiency and directivity of the sound generated by a moving laser source
[AD-A192220] N88-26914
DIRICHLET PROBLEM
Nontrivial critical points for asymptotically quadratic function
[DE88-101851] N88-26881
Semilinear elliptic problems on domains with corners
[REPT-87-83] N88-26888
DISORDERS
Defects and disorder in amorphous and damaged silicon
[AD-A192277] N88-27089
DISPLAY DEVICES
XDATAP
[DE88-007161] N88-26827
Editfont: An interactive font editing system
[AD-A192373] N88-26836
DISSOCIATION
High resolution spectroscopy of dissociating molecules
[DE88-007959] N88-26924
DISTANCE
Modeling the primary events of photosynthesis using chlorophyll containing fixed distance donor-acceptor molecules
[DE88-010033] N88-26793
DISTANCE MEASURING EQUIPMENT
Method and apparatus for measuring distance
[NASA-CASE-MSC-20912-1] N88-26568
DISTILLATION
Feasibility of producing jet fuel from GPGP (Great Plains Gasification Plant) by-products
[DE88-010233] N88-26492
DISTRIBUTED PARAMETER SYSTEMS
Finite-dimensional approximation for optimal fixed-order compensation of distributed parameter systems
[NASA-CR-181674] N88-26873
DISTRIBUTED PROCESSING
Research in computer science 1985/6
[PB88-113840] N88-26815
Correctness criteria for process migration
[NASA-CR-182939] N88-26823
Distributed fault tolerant embeddings of binary trees in hypercubes
[AD-A192929] N88-26840
Issues and recommendations associated with distributed computation and data management systems for the space sciences
[NASA-CR-183026] N88-27108
An integrated, multi-vendor distributed data acquisition system
[DE88-008900] N88-27113
DISTRIBUTION FUNCTIONS
A modal approach to Arctic noise modelling with implied vertical coherence
[AD-A192966] N88-26916
DO-28 AIRCRAFT
Flight test preparation and measuring data validation for parameter identification N88-26529
DOMAINS
A microcomputer based frequency-domain processor for laser Doppler anemometry
[NASA-TM-100998] N88-26634

DONOR MATERIALS
Modeling the primary events of photosynthesis using chlorophyll containing fixed distance donor-acceptor molecules
[DE88-010033] N88-26793
DOPED CRYSTALS
Superlattice doping interfaces N88-27019
DOPPLER EFFECT
Developing diagnostic methods for plasma-particle interaction
[TI88-007726] N88-26973
Laser spectoscopy of plasmas
[AD-A193009] N88-26991
DOUBLE STARS
Observation of a point source in Cygnus constellation with the underground detector at Frejus (France)
[PITHA-87/02] N88-27122
DRAG
Ludwig Prandtl collected treatises on applied mechanics, hydro- and aerodynamics, part 2, IV interfaces and resistance
[NASA-TT-20315] N88-26338
Why plasma armature railguns don't work (and what can be done about it)
[DE88-007900] N88-26384
Experimental investigation of turbulent flow in smooth and longitudinal grooved tubes
[NASA-TM-77480] N88-26615
Infrared detectors based on the photon drag effect and intersubband absorption by a two-dimensional electron gas N88-27024
DRAG REDUCTION
Drag reduction of turbulent boundary layers by means of grooved surfaces
[ETN-88-92618] N88-26630
DRAINAGE PATTERNS
Hydrologic models for land-atmosphere retrospective studies of the use of LANDSAT and AVHRR data
[NASA-CR-182862] N88-26716
DRIFT (INSTRUMENTATION)
Testing of a gravimeter LCR G 785
[B8735061] N88-26643
DROP SIZE
Small-droplet spray measurements with a scattered-light scanner
[NASA-TM-100973] N88-26645
DROP TOWERS
Critical point wetting drop tower experiment
[NASA-CR-183062] N88-26603
DROPS (LIQUIDS)
Small-droplet spray measurements with a scattered-light scanner
[NASA-TM-100973] N88-26645
DRYING
Prospects for hot dry rock in the future
[DE88-010909] N88-26730
DUCTED FLOW
Numerical analysis of duct flow using three-dimensional parabolized Navier-Stokes equation N88-26312
Antenna heights for the optimum utilization of the oceanic evaporation duct. Part 3: Results from the Mediterranean measurements, volume 2
[AD-A192311] N88-26554
Antenna heights for the optimum utilization of the oceanic evaporation duct. Part 1: Results from the Pacific measurements. Part 2: Results from the Key West measurements, volume 1
[AD-A192358] N88-26555
DUCTILITY
Optimizing superplastic response in lithium containing aluminum-magnesium alloys
[AD-A192217] N88-26451
Ductile-brittle transition of cutting behavior in diamond turning of single crystal Si
[DE88-008890] N88-26664
DUNES
A bibliography of dunes: Earth, Mars, and Venus
[NASA-CR-4149] N88-27134
DUST COLLECTORS
Characteristics of pressure loss during filtration using a porous ceramic filter
[DE88-752547] N88-26604
DYNAMIC CHARACTERISTICS
On the dynamic behavior of balloon during its launch; application of panel method and extension to unsteady problem
[ISAS-RN-622] N88-26330
DYNAMIC PROGRAMMING
SIMS: Single Interface to Multiple Systems
[AD-A192264] N88-26832
DYNAMIC RESPONSE
Vehicle dynamics: Identification in the frequency domain N88-26523
Frequency domain identification of the dynamics of a scaled remotely-piloted helicopter N88-26524
Multivariable identification of a flexible transport aircraft N88-26525
Identification methods for transport dynamical investigations N88-26531
Instrumentation for the measurement of penetrator dynamic response to permit force estimation
[DE88-010608] N88-26666
Experimental and theoretical study of the dynamic operational behavior of a three stage radial compressor
[ETN-88-92129] N88-26676
Contact force history and dynamic response due to the impact of a soft projectile
[NASA-TM-100961] N88-26679
DYNAMIC STRUCTURAL ANALYSIS
Design of a controller to reduce residual vibration in the positioning control of flexible robotic manipulators N88-26658
Contact force history and dynamic response due to the impact of a soft projectile
[NASA-TM-100961] N88-26679
A general-purpose approach to computer-aided dynamic analysis of a flexible helicopter
[NASA-TM-101002] N88-26709
DYNAMICAL SYSTEMS
System identification in vehicle dynamics
[DFVLR-MITT-87-22] N88-26518
Parameter estimation of dynamical systems N88-26519
Simulation models for the dynamics of tracked vehicle systems: State-of-the-art and open problems N88-26522

E

EARTH (PLANET)
Research in particle and gamma-ray astrophysics
[NASA-CR-183111] N88-27146
EARTH ATMOSPHERE
High spatial frequency thermal blooming instability: A linear stability analysis
[DE88-010711] N88-26655
The seasonal exchange of carbon dioxide between the atmosphere and the terrestrial biosphere: Extrapolation from site-specific models to regional models
[DE88-007870] N88-26740
Our climate in danger
[DE88-701824] N88-26743
The NASA Marshall engineering thermosphere model
[NASA-CR-179359] N88-26760
The application of imaging to the atmospheric Cerenkov technique: Observations of the Crab nebula N88-27126
EARTH GRAVITATION
Program for the feasibility of developing a high pressure acoustic levitator
[NASA-CR-182154] N88-26498
EARTH IONOSPHERE
High latitude ionospheric radio studies
[AD-A192270] N88-26753
Rocket measurements within a polar cap arc: Ionospheric modelling
[AD-A192381] N88-26754
EARTH ORBITAL ENVIRONMENTS
Application of superconducting technology to earth-to-orbit electromagnetic launch systems
[DE88-010022] N88-26386
EARTH RESOURCES
Survey for least bell's vireo in riparian habitat on Vandenberg Air Force Base, Santa Barbara County, California
[NASA-TM-100984] N88-26744
EARTH SURFACE
A bibliography of dunes: Earth, Mars, and Venus
[NASA-CR-4149] N88-27134
ECONOMIC ANALYSIS
Mutually exclusive alternatives by clustering
[DE88-007707] N88-27115
PAX ECONOPACK economic analysis package users manual
[AD-A192949] N88-27117
ECONOMIC FACTORS
Corrosion in aircraft structures. Part 1: Text
[LR-527-PT-1] N88-26458
Corrosion in aircraft structures. Part 2: Figures
[LR-527-PT-2] N88-26459
ECONOMICS
A basis of settlement: Economic foundations of permanent pioneer communities
[DE88-010907] N88-26382
EDDY CURRENTS
Sensitivity to crack initiation in thick assemblies. Test report 48-444
[REPT-48-444] N88-26365
EDGES
Instability-related delamination growth of embedded and edge delaminations N88-26406
EDITING
Editfont: An interactive font editing system
[AD-A192373] N88-26836
Script editor: An editor for the specification phase in the development of computer based learning
[REPT-87-68] N88-26846
EDITING ROUTINES (COMPUTERS)
Editfont: An interactive font editing system
[AD-A192373] N88-26836
EDUCATION
Communication training for aircrews: A review of theoretical and pragmatic aspects of training program design
[NASA-CR-177459] N88-26349
Inference and discovery in an exploratory laboratory
[AD-A192231] N88-26601
EFFICIENCY
An efficient computational tool for ramjet combustor research
[DE88-010034] N88-26389
Heat pump augmented radiators for spacecraft thermal management
[DE88-007890] N88-26392
A matroid algorithm and its application to the efficient solution of two optimization problems on graphs, revision
[AD-A192709] N88-26838
EIGENVALUES
Eigenmatrix representations of radiance distributions in layered natural waters with wind-roughened surfaces
[PB88-188701] N88-26780
Computing small singular values of bidiagonal matrices with guaranteed high relative accuracy: LAPACK working note number 3
[DE88-008465] N88-26829
Eigenmodes of a random walk on a 2-D lattice torus with one trap
[DE88-007830] N88-26874
Superconducting rf and beam-cavity interactions
[DE88-008598] N88-26936
ELASTIC CYLINDERS
Study of temperature and stress fields of two sliding cylinders
[ETN-88-92134] N88-26704
ELASTIC PROPERTIES
Time-domain boundary element analysis of dynamic near-tip fields for impact-loaded collinear cracks
[AD-A192930] N88-26700
Off-boundary approach to the boundary element method
[AD-A192931] N88-26701
ELASTIC SCATTERING
Comparison of exclusive reactions at large momentum transfer
[DE88-007544] N88-26922
ELASTOMERS
Fundamental studies of elastomers
[DE88-009679] N88-26471
ELASTOSTATICS
A new boundary integral equation formulation for elastodynamic and elastostatic crack analysis
[AD-A192967] N88-26702
ELECTRIC ARCS
Extinction behavior of low voltage switching arc under consideration of cathodic coatings and dynamic arc column
[ETN-88-92384] N88-26591
Physical-chemical reactions at welding arc/molten pool interfaces
[DE88-007717] N88-26662
ELECTRIC BATTERIES
Advanced photovoltaic power system technology for lunar base applications
[NASA-TM-100965] N88-26402
Loss evaluation of self-commutated power conditioner for battery energy storage system
[DE88-752075] N88-26575
Exploratory battery technology development and testing report for 1986
[DE88-009870] N88-26578
Modeling and thermal management of advanced batteries
[DE88-010023] N88-26580
Molten salt electrolytes for high-temperature lithium cells
[DE88-010058] N88-26581
Computer controlled procedures for traction battery power performance tests
[ETN-88-92352] N88-26589
ELECTRIC BRIDGES
Pure metallic bridge and point-contact tunneling into single- and polycrystal YBa2Cu3O(sub 7-y)
[DE88-010030] N88-27084
ELECTRIC CHARGE
A severe spacecraft-charging event on SCATHA in September 1982
[AD-A193007] N88-26396

ELECTRIC CURRENT
Computer programs for high-current beam transport in accelerators
[AD-A192356] N88-26835
ELECTRIC DISCHARGES
A severe spacecraft-charging event on SCATHA in September 1982
[AD-A193007] N88-26396
Electron-impact-ionization and electron-attachment cross sections of radicals important in transient gaseous discharges
[AD-A192248] N88-26424
A bibliography and author index for electrical discharges in vacuum (1897-1986)
[DE88-008744] N88-26579
ELECTRIC FIELDS
Degradation of beam brightness by field emission from a cathode shroud
[DE88-008345] N88-26576
High spatial frequency thermal blooming instability: A linear stability analysis
[DE88-010711] N88-26655
Interaction of biological systems with static and ELF electric and magnetic fields
[DE88-007951] N88-26792
Sources of polarized ions and atoms
[DE88-010910] N88-26931
Field-enhanced lithium ion sources for PBFA 2
[DE88-007195] N88-26960
Ultrafast optical nonlinearity in quantum well structures with electric field N88-27003
ELECTRIC GENERATORS
Analysis of the electrical characteristics of a Westinghouse variable speed generating system for wind turbine applications
[DE88-001139] N88-26721
ELECTRIC MOTOR VEHICLES
Computer controlled procedures for traction battery power performance tests
[ETN-88-92352] N88-26589
ELECTRIC MOTORS
Contribution to speed regulation of small motors with phase-locked loops
[ETN-88-92373] N88-26590
ELECTRIC POTENTIAL
Transport study on Si/Si(1-x)Ge(x) superlattices selectively doped by secondary implantation of Sb N88-27027
ELECTRIC POWER PLANTS
An analysis of gas-steam total power recovery energy system N88-26512
ELECTRIC POWER SUPPLIES
Advanced photovoltaic power system technology for lunar base applications
[NASA-TM-100965] N88-26402
ELECTRICAL ENGINEERING
Center for Electronics and Electrical Engineering technical publication announcements covering Center programs, July to September 1987
[PB88-196530] N88-26572
Analytical determination of critical crack size in solar cells
[NASA-CR-183128] N88-26736
ELECTRICAL INSULATION
Development of external cooling cryo-resistive cable systems. Part 2: Insulation characteristics on 66 kV rated cryo-resistive testing cable
[DE88-770191] N88-26571
A model for insulated wires in the method of moments code NEC (Numerical Electromagnetics Code)
[DE88-006920] N88-26577
ELECTRICAL MEASUREMENT
The influence of uncompensated solution resistance on the determination and standard electrochemical rate constants using cyclic voltammetry and some comparisons with AC voltammetry
[AD-A192825] N88-26427
ELECTRICAL PROPERTIES
Electrodynamic driver for the space thermoacoustic refrigerator (STAR)
[AD-A192337] N88-26517
Analysis of the electrical characteristics of a Westinghouse variable speed generating system for wind turbine applications
[DE88-001139] N88-26721
Pressure-dependent measurement on n+ GaAs (Si, Sn): The effect of deep donor (DX) states on the electrical properties and presistent photoconductivity effects N88-27020
Electrical properties of p-type and n-type ZnSe-ZnTe strained-layer superlattices N88-27029
MBE growth of HgTe/CdTe superlattices on Si(100) substrates N88-27033
On a-Si:H/a-SiN(x):H superlattices: Confinement or contamination N88-27040
Influence of interfaces on electronic and magnetic properties of MnSe/ZnSe superlattices near monolayer limit N88-27050
Electrical study of metal/group 3-5 semiconductor interfaces: Comparison with the atomic-level studies N88-27059
ELECTRICAL RESISTANCE
The influence of uncompensated solution resistance on the determination and standard electrochemical rate constants using cyclic voltammetry and some comparisons with AC voltammetry
[AD-A192825] N88-26427
ELECTRICAL RESISTIVITY
Electrical resistivity of carbon-carbon composites
[AD-A193006] N88-26410
Precipitation study by electrical resistivity measurement in Ni-Al alloys
[DE88-701877] N88-26440
Visible tunable source
[DE88-006442] N88-26944
Defect characterization of the redox behavior and stability of conducting oxides
[DE88-010799] N88-27088
ELECTRICITY
Inference and discovery in an exploratory laboratory
[AD-A192231] N88-26801
ELECTRO-OPTICS
Integrated optoelectronic circuits utilizing InGaAsP grown by molecular beam epitaxy (erbium doping of MBE GaAs)
[AD-A192269] N88-26584
The evaluation of a deformable diffraction grating for a stigmatic EUV spectroheliometer
[NASA-CR-183064] N88-26941
Electro-optical studies of Al(x)Ga(1-x)As/GaAs coupled quantum wells N88-26999
Novel quantum well optical devices N88-27028
ELECTROCATALYSTS
In situ spectroscopic studies of transition metal macrocycles as catalysts for the electrochemical reduction of oxygen
[PB88-203195] N88-26416
Electrocatalysts for oxygen electrodes
[DE88-006397] N88-26724
ELECTROCHEMICAL CELLS
Photovoltaic cells with n-silicon and conductive polymers
[ETN-88-92133] N88-26734
ELECTROCHEMICAL CORROSION
Effect of double layer structure on the determination of corrosion rates from polarization measurements
[DE88-010097] N88-26448
ELECTROCHEMISTRY
In situ spectroscopic studies of transition metal macrocycles as catalysts for the electrochemical reduction of oxygen
[PB88-203195] N88-26416
A simulation analysis of errors in the measurement of standard electrochemical rate constants from phase-selective impedance data
[AD-A192739] N88-26426
The influence of uncompensated solution resistance on the determination and standard electrochemical rate constants using cyclic voltammetry and some comparisons with AC voltammetry
[AD-A192825] N88-26427
ELECTRODES
Performance of lightweight nickel electrodes
[NASA-TM-100958] N88-26430
Nickel hydrogen cell positive-electrode studies: Cobalt segregation in reducing environments
[AD-A193025] N88-26587
Electrocatalysts for oxygen electrodes
[DE88-006397] N88-26724
ELECTRODYNAMICS
Electrodynamic driver for the space thermoacoustic refrigerator (STAR)
[AD-A192337] N88-26517
ELECTROLYTIC CELLS
Oxygen reduction in fuel cell electrolytes
[DE88-006240] N88-26723
ELECTROMAGNETIC FIELDS
Application of Moment Iteration Method (MIM) to electromagnetic field computation
[PB88-194139] N88-26546
A maximum entropy solution for the underdetermined electromagnetic field within a volume
[DE88-007020] N88-26550
MAXWELL3: A 3D finite element electromagnetic modeling code
[DE88-010602] N88-26551
Research in electromagnetic shielding theory. Part1. Shielding by rectangular enclosures
[AD-A192881] N88-26557
Computer programs for high-current beam transport in accelerators
[AD-A192356] N88-26835
Research in particle and gamma-ray astrophysics
[NASA-CR-183111] N88-27146
ELECTROMAGNETIC INTERFERENCE
Random quantum interference in microdevices N88-27021
Quantum interference and transport in microstructures N88-27022
ELECTROMAGNETIC PROPULSION
Application of superconducting technology to earth-to-orbit electromagnetic launch systems
[NASA-TM-101134] N88-26385
ELECTROMAGNETIC PULSES
High bandwidth optoelectronic signal link for use in an EMP (electromagnetic pulse) plus radiation environment
[DE88-009254] N88-26549
The use of commercial off-the-shelf equipment and its impact on C3 (Command, Control and Communications EMP (electromagnetic pulse) survivability
[AD-A192614] N88-26556
Research in electromagnetic shielding theory. Part 2: EMP (electromagnetic pulse) simulation using small loops
[AD-A192882] N88-26558
ELECTROMAGNETIC RADIATION
Method and apparatus for measuring distance
[NASA-CASE-MSC-20912-1] N88-26568
ELECTROMAGNETIC SCATTERING
New hybrid method for solving time-domain integral equations (one-dimensional scattering problems)
[PB88-186192] N88-26547
Stochastic modeling of EM scattering from foliage
[AD-A192258] N88-26553
ELECTROMAGNETIC SHIELDING
Research in electromagnetic shielding theory. Part1. Shielding by rectangular enclosures
[AD-A192881] N88-26557
Research in electromagnetic shielding theory. Part 2: EMP (electromagnetic pulse) simulation using small loops
[AD-A192882] N88-26558
ELECTROMAGNETIC WAVE TRANSMISSION
New hybrid method for solving time-domain integral equations (one-dimensional scattering problems)
[PB88-186192] N88-26547
On the self-trapping of an electromagnetic wave in magnetized plasma
[DE88-701872] N88-26974
ELECTROMAGNETISM
A model for insulated wires in the method of moments code NEC (Numerical Electromagnetics Code)
[DE88-006920] N88-26577
ELECTRON ATTACHMENT
Ion and electron interactions of atmospheric importance
[AD-A192255] N88-26751
ELECTRON BEAMS
Electron-impact-ionization and electron-attachment cross sections of radicals important in transient gaseous discharges
[AD-A192248] N88-26424
The free-electron laser: Theoretical innovations and gas-loaded experiment N88-26646
Results from the SLAC lasertron
[DE88-007816] N88-26647
Inelastic mean free paths of electrons and positrons in matter
[DE88-008086] N88-26929
Visible tunable source
[DE88-006442] N88-26944
Excitonic properties of GaAs-AlGaAs nanostructures N88-27023
ELECTRON BUNCHING
Results from the SLAC lasertron
[DE88-007816] N88-26647
ELECTRON DENSITY (CONCENTRATION)
Megagauss field variation along axis of wire target in laser produced plasma
[DE88-701895] N88-26979
Ultraviolet-visible spectroscopy of laser-produced aluminum plasmas
[AD-A193004] N88-26990
Far-infrared studies of doped AlGaAs/GaAs multiple-quantum-well structures N88-26998
ELECTRON DISTRIBUTION
On the conjugacy of the aurora: High and low latitudes
[AD-A193008] N88-26755
ELECTRON EMISSION
Degradation of beam brightness by field emission from a cathode shroud
[DE88-008345] N88-26576
Effects of secondary electron emission on the collector and source sheaths of a finite ion temperature plasma
[DE88-006930] N88-26971

ELECTRON ENERGY
Thermal inhibition by megagauss field due to variation of electron temperature in laser plasma
[DE88-701887] N88-26977
ELECTRON IRRADIATION
Electron irradiation effects in YBa2Cu3O7-Delta single crystals
[DE88-010050] N88-27085
ELECTRON MOBILITY
Transport study on Si/Si(1-x)Ge(x) superlattices selectively doped by secondary implantation of Sb N88-27027
ELECTRON PHONON INTERACTIONS
Electron-phonon interactions in In(0.53)Ga(0.47)As and in In(0.53)Ga(0.47)As/InP quantum wells N88-27037
Hot electrons in silicon dioxide: Ballistic to steady-state transport N88-27042
The theory of electron-polar phonon scattering rates in semiconductor micro-structures N88-27043
ELECTRON PRECIPITATION
Rocket measurements within a polar cap arc: Ionospheric modelling
[AD-A192381] N88-26754
On the conjugacy of the aurora: High and low latitudes
[AD-A193008] N88-26755
ELECTRON SCATTERING
Ion and electron interactions of atmospheric importance
[AD-A192255] N88-26751
ELECTRON TRANSFER
Mechanisms of photochemical energy conversion by chlorophyll
[DE88-008763] N88-26725
Ferromagnetic/semiconductor hybrid structures N88-27013
Hot electrons in silicon dioxide: Ballistic to steady-state transport N88-27042
Vertical electronic transport in novel semiconductor heterojunction structures N88-27045
ELECTRON TUNNELING
Third International Conference on Superlattices, Microstructures and Microdevices
[AD-A191416] N88-26995
Theoretical aspects of electron transport in modulated structures N88-27016
Resonant tunneling transistors and resonant tunneling hot electron spectroscopy N88-27018
Pressure-dependent measurement on n+ GaAs (Si, Sn): The effect of deep donor (DX) states on the electrical properties and presistent photoconductivity effects N88-27020
Resonant tunneling in InGaAs-InP double-barrier structures and superlattices N88-27047
Excellent negative differential resistance of InGaAs/InAlAs resonant tunneling barrier structures and applications to a new functional device, RHET N88-27048
Pure metallic bridge and point-contact tunneling into single- and polycrystal YBa2Cu3O(sub 7-y)
[DE88-010030] N88-27084
ELECTRONIC EQUIPMENT
High bandwidth optoelectronic signal link for use in an EMP (electromagnetic pulse) plus radiation environment
[DE88-009254] N88-26549
The Oak Ridge National Laboratory strategic defense initiative shield optimization program: Executive summary
[DE88-006016] N88-26899
Superconducting electronic film structures
[AD-A192907] N88-27091
ELECTRONIC EQUIPMENT TESTS
Development of an airborne facility for advanced avionics research
[NLR-MP-87012-U] N88-26368
ELECTRONICS
Center for Electronics and Electrical Engineering technical publication announcements covering Center programs, July to September 1987
[PB88-196530] N88-26572
ELECTRONS
Infrared detectors based on the photon drag effect and intersubband absorption by a two-dimensional electron gas N88-27024
A 10 microns photoexcited avalanche gain due to electron impact ionization from GaAs quantum well superlattices N88-27026
Monte Carlo simulations of femtosecond relaxation of photoexcited electrons in AlGaAs/GaAs quantum wells N88-27036
Direct measurement of ultrafast electron-hole plasma expansion at high density at an asymmetric GaAs quantum well N88-27044
Superconductivity of heavy-electron uranium compounds
[DE88-007901] N88-27065
ELECTROPHORESIS
Electrophoretic coatings. Part 1: Sandia applications
[DE88-008666] N88-26485
ELECTROSTATIC WAVES
Electrostatic whistler mode conversion at plasma resonance
[AD-A192951] N88-26989
ELECTROSTATICS
A severe spacecraft-charging event on SCATHA in September 1982
[AD-A193007] N88-26396
ELEMENTARY PARTICLE INTERACTIONS
Nucleon-nucleus interaction data base: Total nuclear and absorption cross sections
[NASA-TM-4053] N88-26935
ELLIPTIC FUNCTIONS
Semilinear elliptic problems on domains with corners
[REPT-87-83] N88-26888
EMBEDDED COMPUTER SYSTEMS
A high speed serial link interface for SANDAC-V
[DE88-007694] N88-26861
EMBEDDING
Instability-related delamination growth of embedded and edge delaminations N88-26406
Distributed fault tolerant embeddings of binary trees in hypercubes
[AD-A192929] N88-26840
EMERGENCY LOCATOR TRANSMITTERS
COSPAS/SARSAT 406-MHz emergency beacon digital controller
[NASA-TM-100859] N88-26566
EMISSION
Review of methods for remote sensing of atmospheric emissions from stationary sources
[PB88-190483] N88-26739
EMISSION SPECTRA
Ultraviolet-visible spectroscopy of laser-produced aluminum plasmas
[AD-A193004] N88-26990
ENCLOSURES
Research in electromagnetic shielding theory. Part1. Shielding by rectangular enclosures
[AD-A192881] N88-26557
ENDANGERED SPECIES
Survey for least bell's vireo in riparian habitat on Vandenberg Air Force Base, Santa Barbara County, California
[NASA-TM-100984] N88-26744
ENERGY CONVERSION
Mechanisms of photochemical energy conversion by chlorophyll
[DE88-008763] N88-26725
ENERGY CONVERSION EFFICIENCY
Photovoltaic concentrator technology: Recent results
[DE88-009588] N88-26726
ENERGY DISTRIBUTION
Evaluation of surface energy and radiation balance systems for FIFE
[NASA-CR-183118] N88-26778
ENERGY LEVELS
Energy levels and magneto-electric effects in some quasi uni-dimensional semiconductor heterostructures N88-27009
Superconducting electronic film structures
[AD-A192907] N88-27091
ENERGY STORAGE
Loss evaluation of self-commutated power conditioner for battery energy storage system
[DE88-752075] N88-26575
ENERGY TECHNOLOGY
Fuel cell systems program plan: Fiscal year 1988
[DE88-011080] N88-26731
ENERGY TRANSFER
Electrodynamic driver for the space thermoacoustic refrigerator (STAR)
[AD-A192337] N88-26517
Effects of cosmic rays on single event upsets
[NASA-CR-183053] N88-26569
ENGINE DESIGN
Analysis of flow through pump of large rocket engine N88-26306
Permanent magnet excitation of axial flow synchronous machines with high rotation moment
[ETN-88-92385] N88-26592
Analytical and experimental investigation of ringless piston concept
[AD-A192835] N88-26673
The design and fabrication of a Stirling engine heat exchanger module with an integral heat pipe
[NASA-TM-101296] N88-26732
ENGINE PARTS
Guide to the control of high temperature corrosion and protection of gas turbine materials
[PB88-107412] N88-26370
Engine component retirement for cause. Volume 1: Executive summary
[AD-A192730] N88-26371
The outlook for ceramics in heat engines, 1990-2010: Results of a worldwide Delphi survey
[DE88-010075] N88-26475
Ceramic Technology for Advanced Heat Engines Program data base
[DE88-008954] N88-26489
ENGINE TESTS
Analysis of flow through pump of large rocket engine N88-26306
Environmental monitoring of a titan 34D 5 1/2 segment solid rocket motor static firing
[AD-A192975] N88-26400
Ceramic Technology for Advanced Heat Engines Program data base
[DE88-008954] N88-26489
ENGINEERING MANAGEMENT
Pyrotechnic system failures: Causes and prevention
[NASA-TM-100833] N88-26394
The NASA Marshall engineering thermosphere model
[NASA-CR-179359] N88-26760
ENTROPY
Improved potential flow computational methods with Euler corrections for airfoil and wing/body design
[AD-A192303] N88-26334
ENVIRONMENT POLLUTION
Acid Precipitation: A current awareness bulletin
[DE88-007987] N88-26738
ENVIRONMENT PROTECTION
Vegetation studies on Vandenberg Air Force Base, California
[NASA-TM-100985] N88-26795
ENVIRONMENTAL MONITORING
Environmental monitoring of a titan 34D 5 1/2 segment solid rocket motor static firing
[AD-A192975] N88-26400
The role of space borne imaging radars in environmental monitoring: Some shuttle imaging radar results in Asia
[NASA-TM-101175] N88-26544
Advanced life support control/monitor instrumentation concepts for flight application
[NASA-CR-177378] N88-26807
ENVIRONMENTS
Thermal conductivity of selected foams and systems from 100 to 300 K
[PB88-201553] N88-26466
EPITAXY
Growth of high quality CoSi2/Si superstructures on Si(111) N88-27034
Epitaxy and properties of two dimensional GaInAs semiconductor structures
[ETN-88-92357] N88-27094
EPOXY COMPOUNDS
Structural study of impregnating resins of TGMDA/DDS type
[ETN-88-92167] N88-26488
EPOXY RESINS
High temperature resins for injection. High temperature pre-impregnated
[RC-648676] N88-26486
Polymerization of epoxy matrix composites using pulsed microwaves
[CERT-3/1324-MO] N88-26487
Structural study of impregnating resins of TGMDA/DDS type
[ETN-88-92167] N88-26488
EQUATIONS OF MOTION
Random vibration analysis of rattling structures
[DE88-007196] N88-26691
Neoclassical diffusion due to trapping/detrapping orbits in stellarators
[DE88-008566] N88-26968
EQUATIONS OF STATE
Development of an equation of state for computation of supercompressibility factors, critical flow factors and other properties for wet, sour natural gases, synthetic gases and admixtures
[PB88-202676] N88-26602
Freely expanding detonation products: Scaling of rate processes
[DE88-007827] N88-26606
Nonlinear equation of state effects and the momentum-dilution trade-off in a turbulent buoyant jet
[DE88-701839] N88-26610
An analysis of the efficiency and directivity of the sound generated by a moving laser source
[AD-A192220] N88-26914
Shock wave compression and metallization of simple molecules
[DE88-008031] N88-26925
On linear relationship between shock velocity and particle velocity
[DE88-701827] N88-27099

ERBIUM
Integrated optoelectronic circuits utilizing InGaAsP grown by molecular beam epitaxy (erbium doping of MBE GaAs)
[AD-A192269] N88-26584
Characterization of structural and magnetic order of Er/Y superlattices N88-27056
ERGOTAMINE
Does dihydroergotamine used in therapeutical doses influence the physical and psychomotor performance of young pilots or other traffic drivers subjected to hypotonia?
[ETN-88-92136] N88-26799
ERROR ANALYSIS
A simulation analysis of errors in the measurement of standard electrochemical rate constants from phase-selective impedance data
[AD-A192739] N88-26426
Coherent RF error statistics
[AD-A193002] N88-26560
A control program for global radiation measurements
[KNMI-TR-100] N88-26757
ERROR CORRECTING DEVICES
The performance of Eurocom error correction schemes for data communications
[FEL-1987-56] N88-26563
An integrated circuit for error protection in modern data communication systems conforming to Eurocom specifications
[FEL-1987-48] N88-26593
ESTERS
Dual mechanism bifunctional polymers: Design, synthesis and application of a new category of metal ion complexing agents
[DE88-008233] N88-26468
ESTIMATES
Instrumentation for the measurement of penetrator dynamic response to permit force estimation
[DE88-010608] N88-26666
Hydrologic models for land-atmosphere retrospective studies of the use of LANDSAT and AVHRR data
[NASA-CR-182861] N88-26712
ETCHING
Excitonic properties of GaAs-AlGaAs nanostructures N88-27023
EULER EQUATIONS OF MOTION
Numerical simulations of flow around shuttle orbiter N88-26293
Numerical solutions of the Euler equations for the flow field around counter-rotating propellers N88-26298
Aerodynamic simulation for complete ASKA aircraft configuration N88-26301
Numerical calculation of three dimensional flow by TVD scheme N88-26309
An implicit, high order accurate, upwind scheme for unsteady Euler equations N88-26317
On the stationary solutions of three-dimensional Euler equations by the TVD difference schemes N88-26320
Improved potential flow computational methods with Euler corrections for airfoil and wing/body design
[AD-A192303] N88-26334
A diagonally inverted LU implicit multigrid scheme
[NASA-TM-100911] N88-26340
Vortex methods for separated flows
[NASA-TM-100068] N88-26342
EUROPEAN AIRBUS
Airbus 1987: Success in Europe
[ETN-88-92099] N88-26364
EVALUATION
Evaluation of engineering leak before break assessment methods by piping tests
[PB88-126982] N88-26538
Loss evaluation of self-commutated power conditioner for battery energy storage system
[DE88-752075] N88-26575
Australian structures response evaluation: Ground shock and air blast measurements for site investigation survey
[MRL-TN-526] N88-26685
EVAPORATION
Antenna heights for the optimum utilization of the oceanic evaporation duct. Part 3: Results from the Mediterranean measurements, volume 2
[AD-A192311] N88-26554
Antenna heights for the optimum utilization of the oceanic evaporation duct. Part 1: Results from the Pacific measurements. Part 2: Results from the Key West measurements, volume 1
[AD-A192358] N88-26555
EVAPORATORS
An experimental investigation of transient characteristics in a gravity-assisted heat pipe N88-26506
Forced-convective boiling in small diameter tube N88-26510
EVOKED RESPONSE (PSYCHOPHYSIOLOGY)
Auditory evoked magnetic fields in man
[PB88-193446] N88-26796
EVOLUTION (DEVELOPMENT)
Evolution of hairpin vortices in a shear flow
[NASA-TM-100858] N88-26885
EXCITATION
Enhancement of volume H(-) production by vibrationally pre-exciting the hydrogen molecules
[DE88-010783] N88-26937
EXCITONS
Excitonic properties of GaAs-AlGaAs nanostructures N88-27023
EXCLUSION
Markov chain computations to a solution of the mutual-exclusion problem in concurrency
[REPT-87-89] N88-26896
EXOBIOLOGY
Aerospace medicine and biology: A continuing bibliography with indexes (supplement 313)
[NASA-SP-7011(313)] N88-26800
EXPERIMENT DESIGN
Study of flow tracer behavior models and experimental validation with multiple exposure holographic velocimetry
[IMFL-87/30] N88-26622
Simulation of the neutronic characteristics of large fast neutron reactors
[ETN-88-92305] N88-26940
EXPERT SYSTEMS
Intelligent guidance and control for wind shear encounter
[NASA-CR-183060] N88-26347
A reusable rocket engine intelligen control
[NASA-TM-100963] N88-26401
Preliminary study within a project for the development of intelligent assistance to piloting: Formal description of combat pilot expertise and implementation of an interactive system to represent operations
[CERMA-87-31] N88-26806
Delfi-3 as a development environment for expert systems
[REPT-8767] N88-26845
A network approach to the certainty factor model — expert systems
[CWI-CS-R8757] N88-26852
Expert system application education project
[NASA-CR-183089] N88-26867
NEXT: An expert system development tool to support engineering design
[NLR-MP-86070-U] N88-26871
Combining expert opinions: An optimization framework
[REPT-87-84] N88-26895
Computer science and technology: Knowledge-based system for physical database design
[PB88-193289] N88-27109
Knowledge representation in geographic information systems
[ETN-88-92470] N88-27112
EXPLOSIVES
Research in energetic compounds
[AD-A192953] N88-26494
EXTERNAL TANKS
The effects of RCS jet firing on the isolated Orbiter and mated coast phases of the glide return to launch site maneuver at Mach number 6 (IA302B)
[NASA-CR-180223] N88-26403
EXTINCTION
Extinction behavior of low voltage switching arc under consideration of cathodic coatings and dynamic arc column
[ETN-88-92384] N88-26591
EXTREMELY LOW FREQUENCIES
Interaction of biological systems with static and ELF electric and magnetic fields
[DE88-007951] N88-26792

F

FABRICATION
Interface modification in Nicalon (trademark)/SiC composites
[DE88-009708] N88-26409
Fabrication technology
[DE88-010598] N88-26955
Epitaxy and properties of two dimensional GaInAs semiconductor structures
[ETN-88-92357] N88-27094
FACSIMILE COMMUNICATION
Document transfer by a digital satellite link
[NLR-MP-86071-U] N88-26564
FAILURE
Aircraft accident report: Midair collision of SkyWest Airlines Swearingen METRO 2, N163SW, and Mooney M20, N6485U, Kearns, Utah, January 15, 1987
[PB88-910404] N88-26348
FAILURE ANALYSIS
Pyrotechnic system failures: Causes and prevention
[NASA-TM-100633] N88-26394
Diagnosing faults in autonomous robot plan execution
[NASA-CR-182480] N88-26859
FALLOUT
Acute radiation syndrones and their management
[DE88-009839] N88-26797
FAR FIELDS
Fatigue crack growth under far-field cyclic compression
[DE88-011215] N88-26689
FARADAY EFFECT
Thermal and mechanical analysis of the Faraday shield for the compact ignition tokamak
[DE88-007855] N88-26962
FAST NEUTRONS
Simulation of the neutronic characteristics of large fast neutron reactors
[ETN-88-92305] N88-26940
FAST NUCLEAR REACTORS
Simulation of the neutronic characteristics of large fast neutron reactors
[ETN-88-92305] N88-26940
FATIGUE (BIOLOGY)
Method for observing changes in functional state of human operator N88-26789
FATIGUE (MATERIALS)
Study of the influence of metallurgical factors on fatigue and fracture of aerospace structural materials
[AD-A192909] N88-26452
Fatigue of lithium-aluminum alloys: An example of localization of the plastic deformation
[ETN-88-92309] N88-26458
FATIGUE LIFE
Engine component retirement for cause. Volume 1: Executive summary
[AD-A192730] N88-26371
Stiffness degradation of composite laminates N88-26405
Accelerated fatigue crack growth behavior of PWA 1480 single crystal alloy and its dependence on the deformation mode
[NASA-TM-100943] N88-26436
Fatigue crack growth under far-field cyclic compression
[DE88-011215] N88-26689
Prediction of fatigue growth
[NLR-MP-87052-U] N88-26707
FATIGUE TESTS
Automated measurement of crack length and load line displacement at elevated temperature
[AGARD-R-751] N88-26695
FAULT TOLERANCE
Distributed fault tolerant embeddings of binary trees in hypercubes
[AD-A192929] N88-26840
Diagnosing faults in autonomous robot plan execution
[NASA-CR-182480] N88-26859
An evaluation methodology for dependable multiprocessors
[AD-A192799] N88-26863
FEASIBILITY ANALYSIS
Feasibility of producing jet fuel from GPGP (Great Plains Gasification Plant) by-products
[DE88-010233] N88-26492
Program for the feasibility of developing a high pressure acoustic levitator
[NASA-CR-182154] N88-26498
SDI: Myth or reality
[DE88-009121] N88-26901
Study of comet nucleus gamma-ray spectrometer penetration system
[NASA-CR-177393] N88-27120
FEEDBACK
A random access algorithm for environments with capture and limited feedback capabilities
[AD-A192233] N88-26552
Force servo control of a commercial gantry robot
[DE88-006649] N88-26660
FEEDBACK CONTROL
RRSAS (Robotic Radiation Survey and Analysis System) Project: A real time sensor driven robotic system
[DE88-006625] N88-26661
FERMI SURFACES
Fermi level dependent native defect formation: Consequences for metal-semiconductor and semiconductor-semiconductor interfaces
[DE88-008247] N88-27068
FERROMAGNETISM
Ferromagnetic/semiconductor hybrid structures N88-27013
Properties of synthetic magnetic superlattices N88-27014
Observation of ferromagnetism in ultrathin f.c.c. films by spin polarised neutron reflection N88-27015
Contribution to the study of order effects in the Ising model framework: Ground states and phase diagrams
[ONERA-NT-1987] N88-27095

FIBER COMPOSITES
Structural optimization of fiber composite turbomachine blades
[ETN-88-92351] N88-26372
FIBER OPTICS
Fiber optics for advanced aircraft
[NASA-TM-101294] N88-26328
Active phase compensation system for fiber optic holography
[NASA-TM-101295] N88-26641
Fiber optic sensors with internal referencing
[NASA-TM-100893] N88-26644
Use of fiber optic equipment for security
[DE88-007898] N88-26943
An overview of the development of a linear broadband analog fiber-optic link
[DE88-008668] N88-26945
FIBERS
Interface modification in Nicalon (trademark)/SiC composites
[DE88-009708] N88-26409
A micromechanics model of the stiffness and strength of laminates with fiber waviness
[NASA-CR-181670] N88-26413
FIELD EFFECT TRANSISTORS
Microwave amplifiers
[AD-A192974] N88-26585
Transport in GaAs heterojunction ring structures N88-27011
Resonant tunneling transistors and resonant tunneling hot electron spectroscopy N88-27018
Random quantum interference in microdevices N88-27021
FIELD EMISSION
Degradation of beam brightness by field emission from a cathode shroud
[DE88-008345] N88-26576
Development of liquid metal field-emission sources for use in fast repetitive opening switches
[AD-A192230] N88-26583
Progress in diagnostic techniques for SC (superconducting) cavities
[DE88-008600] N88-27077
FIELD OF VIEW
Flight simulator: Field of view utilized in performing tactical maneuvers
[AD-A192412] N88-26379
FIELD THEORY (ALGEBRA)
Algebraic and arithmetic geometry in string theory
[CWI-PM-R8708] N88-26904
FIELD THEORY (PHYSICS)
Combining relativity and quantum mechanics: Schroedinger's interpretation of psi
[DE88-701899] N88-27102
FILTRATION
Characteristics of pressure loss during filtration using a porous ceramic filter
[DE88-752547] N88-26604
FINE STRUCTURE
EXAFS studies of the microstructure of semiconductor alloys, defects and semiconductor-metal interfaces N88-27031
Structural studies of (Ga,In)(As,P) alloys and (InAs) sub m (GaAs) sub n strained-layer superlattices by fluorescence-detected EXAFS N88-27051
FINITE DIFFERENCE THEORY
An implicit, high order accurate, upwind scheme for unsteady Euler equations N88-26317
On the propagating speed in difference approximations for conservation laws N88-26318
On symmetric TVD schemes N88-26319
On the stationary solutions of three-dimensional Euler equations by the TVD difference schemes N88-26320
Axisymmetric liquid sloshing under low-g conditions: Numerical simulation method (reference manual)
[NLR-TR-86057-4] N88-26627
FINITE ELEMENT METHOD
Finite element analysis of incompressible viscous flow around multi-element aerofoils N88-26294
Finite element approximation to a model problem of transonic flow
[DE88-701835] N88-26333
A finite element analysis for the hydroforming of aluminum
[DE88-008050] N88-26516
MAXWELL3: A 3D finite element electromagnetic modeling code
[DE88-010602] N88-26551
Velocity-pressure integrated versus penalty finite element methods for high Reynolds number flows
[NASA-CR-179357] N88-26635
Finite element welding computations using general purpose nonlinear analysis codes
[DE88-005398] N88-26659
Three-dimensional analysis of a postbuckled embedded delamination
[NASA-TP-2823] N88-26684
An assessment of modelling techniques for the finite element analysis of reinforced concrete plate and shell structures
[AD-A192263] N88-26697
FINITE VOLUME METHOD
The role of computational fluid dynamics in aeronautical engineering (5): Improvements and applications of implicit TVD finite volume code N88-26313
On the accuracy of upwind biased finite volume method N88-26316
Navier-Stokes simulation of shock-tube flows over a wedge-type step by finite volume method
[ISAS-RN-628] N88-26599
Preliminary design and analysis of procedures for the numerical generation of 3D block-structured grids
[NLR-TR-86102-U] N88-26628
FINLAND
On the global radiation incident variously orientated surfaces on the South Coast of Finland
[FMI-5] N88-26746
FINS
Study and implementation of ultrahigh frequency coupling devices using the fin line technology --- millimeter waves
[ETN-89-92307] N88-26588
FIRES
Experimental and theoretical analysis of the radiative transfer within a sooty pool fire
[DE88-007099] N88-26419
FLAME PROPAGATION
Ignition and flame spread of PMMA
[NASA-TT-20290] N88-26431
FLAMES
Ultraviolet imaging of hydrogen flames
[DE88-009152] N88-26422
Asynchronous optical sampling for laser-based combustion diagnostics in high pressure flames
[AD-A192920] N88-26428
Study of the local behavior of a flame
[ETN-88-92300] N88-26433
Reducing adhesion and agglomeration within a cloud of combustible particles
[NASA-TM-100902] N88-26539
FLAMMABILITY
Reducing adhesion and agglomeration within a cloud of combustible particles
[NASA-TM-100902] N88-26539
FLANGES
GTAW characterization for weld penetration on 304L stainless steel
[DE88-010611] N88-26672
FEB structural analysis, revision H
[AD-A192302] N88-26698
FLAPS (CONTROL SURFACES)
The identification of the direct lift control flap system of the research aircraft ATTAS N88-26527
FLAT PLATES
Drag reduction of turbulent boundary layers by means of grooved surfaces
[ETN-88-92618] N88-26630
FLEXIBLE BODIES
Experiments in adaptive control of a very flexible one link manipulator N88-26885
FLEXIBLE SPACECRAFT
L(sub infinity symbol)-approximations of complex functions and robust controllers for large flexible space structures
[PB88-186226] N88-26390
FLIGHT CHARACTERISTICS
Airbus 1987: Success in Europe
[ETN-88-92099] N88-26364
FLIGHT CONTROL
Control of flight through microburst wind shear using deterministic trajectory optimization N88-26375
Computer simulation of a single pilot flying a modern high-performance helicopter
[NASA-TM-100182] N88-26376
FLIGHT CREWS
Communication training for aircrews: A review of theoretical and pragmatic aspects of training program design
[NASA-CR-177459] N88-26349
FLIGHT MANAGEMENT SYSTEMS
Development of an airborne facility for advanced avionics research
[NLR-MP-87012-U] N88-26368
FLIGHT PATHS
Geographical information for design purposes
[NLR-MP-87014-U] N88-26719
FLIGHT SAFETY
System identification in vehicle dynamics
[DFVLR-MITT-87-22] N88-26518
FLIGHT SIMULATION
On the dynamic behavior of balloon during its launch; application of panel method and extension to unsteady problem
[ISAS-RN-622] N88-26330
A high fidelity real-time simulation of a small turboshaft engine
[NASA-TM-100991] N88-26378
FLIGHT SIMULATORS
Flight simulator: Field of view utilized in performing tactical maneuvers
[AD-A192412] N88-26379
FLIGHT TEST INSTRUMENTS
Trajectory measurement of the Fokker 100 aircraft during autoland testing
[NLR-MP-86010-U] N88-26366
Development of an airborne facility for advanced avionics research
[NLR-MP-87012-U] N88-26368
FLIGHT TESTS
Flight research and testing
[NASA-TM-100439] N88-26361
Flight test preparation and measuring data validation for parameter identification N88-26529
Utilization of identification methods in the time and frequency domain for the determination of the XV-15 (tilt-rotor) dynamics for lateral motion in hover flight N88-26532
Application of complementary parameter identification techniques to flight test data of a transport aircraft N88-26533
FLIGHT TRAINING
Flight simulator: Field of view utilized in performing tactical maneuvers
[AD-A192412] N88-26379
FLIGHT VEHICLES
Flight vehicle system identification: Status and prospects N88-26520
FLOW DEFLECTION
Computation of flow around NACA0012 airfoil at high angle of attack N88-26300
FLOW DISTORTION
Cross flow induced vibrations in tube bundle by displaced and misaligned tube configurations
[ETN-88-92132] N88-26621
FLOW DISTRIBUTION
Proceedings of the 5th NAL Symposium on Aircraft Computational Aerodynamics
[NAL-SP-8] N88-26290
Numerical simulations of aerodynamic contribution of flows about a space-plane-type configuration N88-26292
Numerical simulations of flow around shuttle orbiter N88-26293
Numerical calculation of supersonic flow by the PNS equations N88-26296
Navier-Stokes analysis of transonic transport aircraft empennage N88-26297
Computation of flow around NACA0012 airfoil at high angle of attack N88-26300
Numerical simulation of viscous flows over transonic aircraft configurations N88-26302
Numerical simulation of the shock tube flows by TVD scheme N88-26308
Numerical calculation of three dimensional flow by TVD scheme N88-26309
Numerical analysis of three dimensional cascade flow by solving Navier-Stokes equations N88-26310
Numerical analysis of duct flow using three-dimensional parabolized Navier-Stokes equation N88-26312
The role of computational fluid dynamics in aeronautical engineering (5): Improvements and applications of implicit TVD finite volume code N88-26313
Numerical simulation of turbulent flow using the exponential expression of k-epsilon equation N88-26322
Relaxation scheme for compressible flows N88-26323
The modified-fluid-in-cell method to which adaptive mesh and multigrid were applied N88-26324
Heterogeneous diffusion flame stabilization
[AD-A193014] N88-26429
The Proceedings of the Symposium on Mechanics for Space Flight 1987
[ISAS-SP-6] N88-26499
Numerical analysis of reconnection of vortex rings N88-26500
Vortex filament simulation for the crosslinking rings N88-26501
Crosslinking of two vortex rings side by side N88-26502
Forced-convective boiling in small diameter tube N88-26510

Wind tunnel study of atmospheric diffusion in unstable stratified boundary layer. Part 2: Characteristic scale and diffusion
[DE88-753109] N88-26749

FLOW EQUATIONS
The modified-fluid-in-cell method to which adaptive mesh and multigrid were applied N88-26324

FLOW MEASUREMENT
Study of flow tracer behavior models and experimental validation with multiple exposure holographic velocimetry
[IMFL-87/30] N88-26622

FLOW STABILITY
Cross flow induced vibrations in tube bundle by displaced and misaligned tube configurations
[ETN-88-92132] N88-26621
Stationary, wave type, and chaos type convection in spherical symmetry geometries
[ETN-88-92358] N88-26625

FLOW VELOCITY
Development of advanced flow simulation system by water flow model. New method of velocity measurement using cross-correlation
[DE88-753120] N88-26608

FLOW VISUALIZATION
The determination of the topological structure of skin friction lines on a rectangular wing-body combination
[NASA-CR-4168] N88-26343
Development of advanced flow simulation system by water flow model. New method of velocity measurement using cross-correlation
[DE88-753120] N88-26608
Study of flow tracer behavior models and experimental validation with multiple exposure holographic velocimetry
[IMFL-87/30] N88-26622

FLUID DYNAMICS
Stationary, wave type, and chaos type convection in spherical symmetry geometries
[ETN-88-92358] N88-26625
Computer science research, 1987: Computation Directorate
[DE88-008637] N88-26812
Fluid dynamical model of ultrarelativistic heavy ion collisions
[DE88-007905] N88-26921

FLUID FILLED SHELLS
Quantitative particle characterization by scattered ultrasound N88-26908

FLUID FILMS
The use of liquid films for spacecraft survivability to laser radiation
[AD-A192954] N88-26395

FLUID FLOW
Multigrid computation of practical fluid flows and heat transfer
[TI88-010064] N88-26609
Use of direct solvers for multidimensional fluid flow computations
[DE88-010063] N88-26611
Fluid flow modeling in casting processes and its implications
[DE88-010009] N88-26671
Acoustic diffraction by an absorbing finite strip in a moving fluid
[PB88-191382] N88-26912

FLUID INJECTION
Numerical simulation of ignition of hydrogen jet in hot air N88-26307

FLUID JETS
Small-droplet spray measurements with a scattered-light scanner
[NASA-TM-100973] N88-26645

FLUORESCENCE
Laser fluorescence spectroscopy of zinc neutrals originating from laser-irradiated and ion-bombarded zinc sulfide and zinc surfaces
[DE88-008037] N88-26418
Physical-chemical reactions at welding arc/molten pool interfaces
[DE88-007717] N88-26662

FLUOROCARBONS
Substituted 1,1,1-Triaryl-2,2,2-Trifluoroethanes and processes for their synthesis
[NASA-CASE-LEW-14345-1] N88-26404

FLUOROPOLYMERS
Substituted 1,1,1-Triaryl-2,2,2-Trifluoroethanes and processes for their synthesis
[NASA-CASE-LEW-14345-1] N88-26404

FOCUSING
Microfocus X-ray techniques for flaw location
[DE88-008636] N88-26680

FOLIAGE
Stochastic modeling of EM scattering from foliage
[AD-A192258] N88-26553

FORCED CONVECTION
Forced-convective boiling in small diameter tube N88-26510

FORCED VIBRATION
Experimental and theoretical investigation of passive damping concepts for member forced and free vibration
[NASA-CR-183082] N88-26693

FORECASTING
Prospects for hot dry rock in the future
[DE88-010909] N88-26730
An interagency working group on lightning threat warning
[DE88-009828] N88-26767

FOREIGN BODIES
The influence of foreign particles on bearing metals
[NASA-TT-20155] N88-26454

FORESTS
Interpreting forest biome productivity and cover utilizing nested scales of image resolution and biogeographical analysis
[NASA-CR-183036] N88-26711

FORTRAN
An interactive computer code for preliminary design of solid propellant rocket motors
[AD-A192889] N88-26399
Directions for programming in FORTRAN 77
[NASA-TT-20317] N88-26842
An expeditious technique for keyboard input of information to FORTRAN computer programs
[DE88-009617] N88-26855

FOURIER TRANSFORMATION
Numerical simulation of transition to turbulence in plane Poiseuille flow by a spectral method N88-26321

FRACTALS
Display and processing of multidimensional signals with the aid of fractal image sequences
[ETN-88-92131] N88-26642

FRACTURE MECHANICS
The effects of thin compressive films on indentation fracture toughness measurements
[AD-A192243] N88-26480
Research on the kinetics of phase changes in solids
[AD-A192222] N88-26696
Prediction of fatigue growth
[NLR-MP-87052-U] N88-26707
Analytical determination of critical crack size in solar cells
[NASA-CR-183128] N88-26736

FRACTURE STRENGTH
The effects of thin compressive films on indentation fracture toughness measurements
[AD-A192243] N88-26480
Fracture resistance of a TiB2 particle/SiC matrix composite at elevated temperature
[NASA-TM-100967] N88-26482

FRACTURES (MATERIALS)
Irreversible deformations during fracture in polymers
[W-7/86] N88-26485
Principles of a nondestructive evaluation process for damage location, damage profile, and damage extension in welded joints by radiometric measurements
[MPA-86-02] N88-26683

FRACTURING
Lattice theory of fracture of solids with layered structure
[DE88-701867] N88-27073

FRAGMENTATION
Milliwatt generator project
[DE88-011261] N88-26939
Studies of HZE particle interactions and transport for space radiation protection purposes
[NASA-TM-101159] N88-27142

FREE ELECTRON LASERS
The free-electron laser: Theoretical innovations and gas-loaded experiment N88-26646
The propagation of irradiance moments of an aberrated, apodized FEL beam
[DE88-006972] N88-26648
The chirped-pulse free-electron laser
[DE88-009289] N88-26651
Novel magnetic materials research using free electron lasers
[DE88-009959] N88-26652

FREE ELECTRONS
Inelastic mean free paths of electrons and positrons in matter
[DE88-008086] N88-26929

FREE JETS
Numerical simulation of supersonic free-jets N88-26299

FREE VIBRATION
Experimental and theoretical investigation of passive damping concepts for member forced and free vibration
[NASA-CR-183082] N88-26693

FREON
Investigation on refrigerant R12 critical boiling point in narrow flow pipes considered as model fluid
[ETN-88-92374] N88-26626

FREQUENCIES
A microcomputer based frequency-domain processor for laser Doppler anemometry
[NASA-TM-100998] N88-26634

FREQUENCY CONVERTERS
Electrostatic whistler mode conversion at plasma resonance
[AD-A192951] N88-26989
Nonlinear materials for frequency conversion
[DE88-008343] N88-27067

FREQUENCY DIVIDERS
Interactive computer programme for the analysis of a two-way Wilkinson divider/combiner
[PB88-105424] N88-26831

FREQUENCY STANDARDS
Tactical Rubidium Frequency Standard (TRFS), volume 1
[AD-A192981] N88-26640

FRICTION FACTOR
Drag reduction of turbulent boundary layers by means of grooved surfaces
[ETN-88-92618] N88-26630

FUEL CELLS
Phosphoric acid electric utility fuel cell technology development
[DE88-010187] N88-26582
Oxygen reduction in fuel cell electrolytes
[DE88-008240] N88-26723
Electrocatalysts for oxygen electrodes
[DE88-008397] N88-26724
Fuel cell systems program plan: Fiscal year 1988
[DE88-011080] N88-26731

FUEL COMBUSTION
Laser diagnostics applied to advanced combustion systems
[DE88-753119] N88-26649

FUEL FLOW
Analysis of flow through pump of large rocket engine N88-26306

FUEL INJECTION
Heterogeneous diffusion flame stabilization
[AD-A193014] N88-26429
Pulsed spray structure and atomisation techniques
[AD-A192280] N88-26614

FURNACES
High temperature testing of C/C (Carbon/Carbon) composites
[AD-A193012] N88-26411

FUSION REACTORS
Development of high current and high brightness negative hydrogen ion sources
[DE88-010882] N88-26934

G

GALACTIC COSMIC RAYS
The application of imaging to the atmospheric Cerenkov technique: Observations of the Crab nebula N88-27126

GALACTIC ROTATION
The velocity field of the outer galaxy
[B8681472] N88-27132

GALLIUM ARSENIDE LASERS
New semiconductor laser structure for an optical communication system
[ETN-88-92353] N88-26654

GALLIUM ARSENIDES
Integrated optoelectronic circuits utilizing InGaAsP grown by molecular beam epitaxy (erbium doping of MBE GaAs)
[AD-A192269] N88-26584
Transport in GaAs heterojunction ring structures N88-27011
Pressure-dependent measurement on n+ GaAs (Si, Sn): The effect of deep donor (DX) states on the electrical properties and presistent photoconductivity effects N88-27020
Direct imaging of the columnar structure of GaAs quantum wells N88-27030
Direct measurement of ultrafast electron-hole plasma expansion at high density at an asymmetric GaAs quantum well N88-27044
Photoluminescence studies of InGaAlAs quaternary alloys
[DE88-007197] N88-27062
Defects in high-mobility semiconductor systems
[AD-A192298] N88-27090

GAMMA RAY ASTRONOMY
The application of imaging to the atmospheric Cerenkov technique: Observations of the Crab nebula N88-27126

GAMMA RAY SPECTROMETERS
Study of comet nucleus gamma-ray spectrometer penetration system
[NASA-CR-177393] N88-27120

GAMMA RAYS
JFET/SOS (Junction Field-Effect Transistor/Silicon-on-Sapphire) devices: Gamma-radiation-induced effects
[AD-A193001] N88-26586
Research in particle and gamma-ray astrophysics
[NASA-CR-183111] N88-27146
GANTRY CRANES
Force servo control of a commercial gantry robot
[DE88-006649] N88-26660
GAS COOLING
Thermal and mechanical analysis of the Faraday shield for the compact ignition tokamak
[DE88-007855] N88-26962
GAS DETECTORS
Method for the isotopically selective detection of inert gases
[TI88-008370] N88-26421
GAS DISCHARGES
Electron-impact-ionization and electron-attachment cross sections of radicals important in transient gaseous discharges
[AD-A192248] N88-26424
GAS DYNAMICS
A shock-tube experiment on gases mixing processes associated with CO2/N2 mixing gasdynamic laser
[ISAS-RN-350] N88-26598
GAS FLOW
Remote sensing and satellite applications to the needs of the gas and pipeline industry
[PB88-202668] N88-26714
GAS INJECTION
Three-dimensional viscous flow computations of a circular jet in subsonic and supersonic cross flow
[NASA-CR-182153] N88-26616
GAS JETS
Numerical simulations of astrophysical jets
N88-26295
Numerical simulation of ignition of hydrogen jet in hot air N88-26307
GAS LASERS
A shock-tube experiment on gases mixing processes associated with CO2/N2 mixing gasdynamic laser
[ISAS-RN-350] N88-26598
Model for pulse amplification by a gaseous laser amplifier
[DE88-011729] N88-26657
GAS MIXTURES
Antimisting kerosene: Low temperature degradation and blending
[NASA-CR-182725] N88-26495
A shock-tube experiment on gases mixing processes associated with CO2/N2 mixing gasdynamic laser
[ISAS-RN-350] N88-26598
GAS PIPES
Remote sensing and satellite applications to the needs of the gas and pipeline industry
[PB88-202668] N88-26714
GAS RECOVERY
An analysis of gas-steam total power recovery energy system N88-26512
GAS TURBINE ENGINES
Corrosion prevention in gas turbines
[NLR-MP-87029-U] N88-26373
GAS TURBINES
Engine component retirement for cause. Volume 1: Executive summary
[AD-A192730] N88-26371
Analysis of gas turbine test cell number 1, Lemoore Naval Air Station, California
[AD-A192870] N88-26380
GASES
Factors which affect operation of a plasma focus in various gases
[DE88-701882] N88-26975
Infrared detectors based on the photon drag effect and intersubband absorption by a two-dimensional electron gas N88-27024
Experimental study of planetary gases with applications to planetary interior models
[NASA-CR-183098] N88-27137
GASIFICATION
Feasibility of producing jet fuel from GPGP (Great Plains Gasification Plant) by-products
[DE88-010233] N88-26492
GEARS
A review of gear housing dynamics and acoustics literature
[NASA-CR-183110] N88-26675
GELS
Characterization of the surface area and porosity of sol-gel films using saw devices
[DE88-008794] N88-27069
GEODESY
Research project Loran-C of the Geometric Service of the Ministry of Public Works
[B8735055] N88-26356
GEODETIC ACCURACY
Research project Loran-C of the Geometric Service of the Ministry of Public Works
[B8735055] N88-26356
GEOGRAPHIC INFORMATION SYSTEMS
Hydrologic models for land-atmosphere retrospective studies of the use of LANDSAT and AVHRR data
[NASA-CR-182861] N88-26712
Hydrologic models for land-atmosphere retrospective studies of the use of LANDSAT and AVHRR data
[NASA-CR-182862] N88-26716
Geographical information for design purposes
[NLR-MP-87014-U] N88-26719
Knowledge representation in geographic information systems
[ETN-88-92470] N88-27112
GEOLOGY
Vegetation studies on Vandenberg Air Force Base, California
[NASA-TM-100985] N88-26795
GEOMETRY
Development of liquid metal field-emission sources for use in fast repetitive opening switches
[AD-A192230] N88-26583
Full-wave calculations in flux coordinates for toroidal geometry
[DE88-010131] N88-26985
Aharonov-Bohm effects in disordered metals
N88-27008
Design and development of courseware for goniometry
[REPT-87-73] N88-27106
GEOPHYSICS
Reports of planetary geology and geophysics program, 1987
[NASA-TM-4041] N88-27133
Solar-geophysical data number 522, February 1988. Part 2: (Comprehensive reports). Data for August 1987 and miscellanea
[PB88-194741] N88-27138
Solar-geophysical data number 522, February 1988. Part 1: (Prompt reports). Data for January 1988, December 1987 and late data
[PB88-194733] N88-27139
GEOTHERMAL ENERGY UTILIZATION
Prospects for hot dry rock in the future
[DE88-010909] N88-26730
GEOTHERMAL RESOURCES
Prospects for hot dry rock in the future
[DE88-010909] N88-26730
GEOTHERMAL TECHNOLOGY
Prospects for hot dry rock in the future
[DE88-010909] N88-26730
GLASS
Glass forming ranges of amorphous alloys
[DE88-007897] N88-26438
Statistical mechanics of polymer systems
[DE88-011172] N88-26477
Semiconductor microcrystallites in porous glass and their applications in optics N88-27005
GLASS FIBERS
Excitation of single-mode glass fiber by partially coherent sources
[ETN-88-92121] N88-26951
GLIDE LANDINGS
The effects of RCS jet firing on the isolated Orbiter and mated coast phases of the glide return to launch site maneuver at Mach number 6 (IA302B)
[NASA-CR-180223] N88-26403
GLOBAL POSITIONING SYSTEM
NAVSTAR global positioning system
[AD-A192609] N88-26354
Position and velocity determination using a Global Positioning System: An outline
[B8735052] N88-26355
The Sercel TR5S Global Positioning System (GPS) receiver
[ETN-88-92473] N88-26357
A positioning system based on NAVSAT
[NLR-MP-87018-U] N88-26358
Spacecraft applications of advanced global positioning system technology
[NASA-CR-172063] N88-26359
GLOW DISCHARGES
In-situ reactive of X-ray optics by glow discharge
[DE88-009840] N88-26947
GOAL THEORY
Plans for discourse
[AD-A192242] N88-26802
GOLD
Grain boundaries
[DE88-009889] N88-26446
GOLD ALLOYS
High resolution detection of solute segregation to the cores of dislocations in grain boundaries
[DE88-009168] N88-27078
GOVERNMENT PROCUREMENT
The use of commercial off-the-shelf equipment and its impact on C3 (Command, Control and Communications EMP (electromagnetic pulse) survivability
[AD-A192614] N88-26556
GRADIENT INDEX OPTICS
Optical characterization of silica aerogel
[DE88-008916] N88-26948
GRADIENTS
Probing the possibility of a (12)C/(13)C abundance gradient from observations of interstellar CH+
[DE88-008908] N88-27125
GRAIN BOUNDARIES
Phase stability and alloy design of ordered intermetallics
[DE88-007479] N88-26435
Grain boundary structure in Ni3Al
[DE88-009164] N88-26444
The effects of gradients on boundary stability
[DE88-009592] N88-26445
Grain boundaries
[DE88-009889] N88-26446
The structure and properties of grain boundaries in B2 ordered alloys
[DE88-009890] N88-26447
Effects of grain boundary composition on properties of YBa2Cu3O/sub 7-x/
[DE88-007679] N88-27064
High resolution detection of solute segregation to the cores of dislocations in grain boundaries
[DE88-009168] N88-27078
GRANULAR MATERIALS
Granulation of pyrotechnic tracer composition R284T
[MRL-TN-528] N88-26490
GRAPH THEORY
Extensible networks. Part 1: Principles and constructions
[REPT-87-91-PT-1] N88-26864
Two families of graphs satisfying the cycle basis interpolation property
[PB88-127808] N88-26890
GRAPHIC ARTS
Editfont: An interactive font editing system
[AD-A192373] N88-26836
GRAPHITE-EPOXY COMPOSITES
Stiffness degradation of composite laminates
N88-26405
Compression creep of filamentary composites
[NASA-CR-182550] N88-26601
Damage in a perforated graphite-epoxy plate under monotonic, cyclic biaxial loading
[ONERA-NT-1987-5] N88-26708
GRAPHS (CHARTS)
A matroid algorithm and its application to the efficient solution of two optimization problems on graphs, revision
[AD-A192709] N88-26838
Algorithm for generating the minimal cycle basis of a graph
[PB88-126610] N88-26891
GRATINGS (SPECTRA)
The evaluation of a deformable diffraction grating for a stigmatic EUV spectroheliometer
[NASA-CR-183064] N88-26941
GRAVIMETERS
Testing of a gravimeter LCR G 785
[B8735061] N88-26643
GRAVITATIONAL CONSTANT
Cosmic wavefunction with induced gravity
[DE88-701873] N88-27129
GRAVITATIONAL EFFECTS
Industrial processes influenced by gravity
[NASA-CR-182140] N88-26497
Thermostatistical estimations of vapor-state molecules affected by gravity in a heat pipe N88-26505
An experimental investigation of transient characteristics in a gravity-assisted heat pipe N88-26506
GRAVITY WAVES
Propagation of inernio-acoustic gravity waves in a rotating and radiating opaque atmosphere
[DE88-701866] N88-26750
GRID GENERATION (MATHEMATICS)
Numerical simulations of flow around shuttle orbiter
N88-26293
Grid generation of a helicopter rotary-wing
N88-26325
Finite element welding computations using general purpose nonlinear analysis codes
[DE88-005398] N88-26659
GRINDING (MATERIAL REMOVAL)
Reaming experiments for the lethality test system
[DE88-007902] N88-26383

GROOVES
Drag reduction of turbulent boundary layers by means of grooved surfaces
[ETN-88-92618] N88-26630
GROOVING
Experimental investigation of turbulent flow in smooth and longitudinal grooved tubes
[NASA-TM-77480] N88-26615
GROUND STATE
Contribution to the study of order effects in the Ising model framework: Ground states and phase diagrams
[ONERA-NT-1987] N88-27095
GROUND TESTS
Australian structures response evaluation: Ground shock and air blast measurements for site investigation survey
[MRL-TN-526] N88-26685
GROUP THEORY
Nontrivial critical points for asymptotically quadratic function
[DE88-101851] N88-26881
Algebraic and arithmetic geometry in string theory
[CWI-PM-R8708] N88-26904
GUIDANCE (MOTION)
Local free-space mapping and path guidance for mobile robots
[AD-A192970] N88-26574
GUN LAUNCHERS
Reaming experiments for the lethality test system
[DE88-007902] N88-26383

H

HALIDES
Rare Gas Halide (RGH) kinetics
[AD-A192352] N88-26425
HALL EFFECT
Quantum transport in an electron waveguide N88-27010
HALLEY'S COMET
Processing and analysis of images transmitted by Vega space probes over Halley's comet
[ETN-88-92291] N88-27131
HAMILTONIAN FUNCTIONS
Non-effective-mass matching in superlattices N88-27049
Finitely many delta-interactions with supports on concentric spheres
[DE88-701834] N88-27101
HARDNESS
Initial development of high-temperature titanium silicide alloys
[DE88-007860] N88-26437
HARMONIC OSCILLATION
Off-boundary approach to the boundary element method
[AD-A192931] N88-26701
HEAD-UP DISPLAYS
Improvement of head-up display standards. Volume 1: Head-up display design guide, appendix
[AD-A192973] N88-26809
HEARING
Auditory evoked magnetic fields in man
[PB88-193446] N88-26796
HEAT EXCHANGERS
Cross flow induced vibrations in tube bundle by displaced and misaligned tube configurations
[ETN-88-92132] N88-26621
The design and fabrication of a Stirling engine heat exchanger module with an integral heat pipe
[NASA-TM-101296] N88-26732
HEAT FLUX
Surface temperature thermal fluxmeters for shock tubes
[NASA-TT-20319] N88-26381
Evaluation of surface energy and radiation balance systems for FIFE
[NASA-CR-183118] N88-26778
HEAT MEASUREMENT
Surface temperature thermal fluxmeters for shock tubes
[NASA-TT-20319] N88-26381
HEAT PIPES
The Proceedings of the Symposium on Mechanics for Space Flight 1987
[ISAS-SP-6] N88-26499
Thermostatistical estimations of vapor-state molecules affected by gravity in a heat pipe N88-26505
An experimental investigation of transient characteristics in a gravity-assisted heat pipe N88-26506
Heat transfer of mesh-wick heat-pipes (bottom heat mode) N88-26507
A statistical treatment of accelerated life test data for copper-water heat pipes N88-26509
The design and fabrication of a Stirling engine heat exchanger module with an integral heat pipe
[NASA-TM-101296] N88-26732
HEAT PUMPS
Heat pump augmented radiators for spacecraft thermal management
[DE88-007890] N88-26392
Heat pump augmented radiator for low-temperature space applications
[DE88-008369] N88-26393
Magnetic heat pump design
[DE88-007730] N88-26605
The Oak Ridge Heat Pump Design Model: Mark 3 version program documentationon
[DE88-007863] N88-26607
Thermodynamic analysis of chemical heat storage system for heat pump
[DE88-753121] N88-26728
HEAT RESISTANT ALLOYS
A constitutive model with damage for high-temperature superalloys N88-26434
Accelerated fatigue crack growth behavior of PWA 1480 single crystal alloy and its dependence on the deformation mode
[NASA-TM-100943] N88-26436
Initial development of high-temperature titanium silicide alloys
[DE88-007860] N88-26437
HEAT SHIELDING
Thermal and mechanical analysis of the Faraday shield for the compact ignition tokamak
[DE88-007855] N88-26962
HEAT SOURCES
Milliwatt generator project
[DE88-011261] N88-26939
HEAT STORAGE
Thermodynamic analysis of chemical heat storage system for heat pump
[DE88-753121] N88-26728
Transient thermal analysis of three latent heat storage configurations for rapid thermal charging
[DE88-008943] N88-27104
HEAT TOLERANCE
Satellite remote sensing of the wet bulb globe temperature heat stress index, phase 2
[AD-A192798] N88-26717
HEAT TRANSFER
Design and testing of a high power spacecraft thermal management system
[NASA-TM-4051] N88-26389
Heat transfer of mesh-wick heat-pipes (bottom heat mode) N88-26507
Magnetic heat pump design
[DE88-007730] N88-26605
Multigrid computation of practical fluid flows and heat transfer
[TI88-010064] N88-26609
Boundary element method for contact heat transfer
[DE88-011013] N88-26613
Overview of the TITAN-2 reversed-field pinch aqueous fusion power core design
[DE88-008170] N88-26966
HEAT TRANSFER COEFFICIENTS
Characteristics of long size thermosyphons made of corrugated tube N88-26511
HEAT TREATMENT
Development of protective coatings for ceramic tubular components
[PB88-197165] N88-26463
HEAVY IONS
Charged pion production and projectile breakup in 85A MeV(sup)12C induced heavy ion reactions
[LUIP-8802] N88-26920
Fluid dynamical model of ultrarelativistic heavy ion collisions
[DE88-007905] N88-26921
Studies of HZE particle interactions and transport for space radiation protection purposes
[NASA-TM-101159] N88-27142
HEAVY NUCLEI
Cosmions and stars
[DE88-010886] N88-27145
HEIGHT
Antenna heights for the optimum utilization of the oceanic evaporation duct. Part 1: Results from the Pacific measurements. Part 2: Results from the Key West measurements, volume 1
[AD-A192358] N88-26555
HELICAL INDUCERS
Symmetrized magnetic field configuration of low aspect ratio helical system
[IPPJ-869] N88-26956
HELICOPTER CONTROL
Frequency domain identification of the dynamics of a scaled remotely-piloted helicopter N88-26524
HELICOPTER PERFORMANCE
Grid generation of a helicopter rotary-wing N88-26325
HELICOPTERS
Aircraft accident report: Joe Foster Excavating, Inc., Bell 206B, N49606, in-flight collision with trees, Alamo, California, August 3, 1986
[PB88-910405] N88-26345
Flight Mechanics Panel Symposium on Rotorcraft Design for Operations: Technical evaluation report
[AGARD-AR-243] N88-26362
Computer simulation of a single pilot flying a modern high-performance helicopter
[NASA-TM-100182] N88-26376
Computer simulation of multiple pilots flying a modern high performance helicopter
[NASA-TM-100183] N88-26377
A high fidelity real-time simulation of a small turboshaft engine
[NASA-TM-100991] N88-26378
A general-purpose approach to computer-aided dynamic analysis of a flexible helicopter
[NASA-TM-101002] N88-26709
HELIUM
Helium induced degradation in the weldability of an austenitic stainless steel
[DE88-009062] N88-26443
HeFlow: A program for calculating pressure and temperature of helium in forced-flow superconductors. Part 1: Numerical solutions. Part 2: HeFlow user's manual
[DE88-008941] N88-27071
Cosmological helium production simplified
[DE88-009578] N88-27130
HETEROGENEITY
Sintering of the heterogeneous MgO compacts
[DE88-010357] N88-26408
Off-boundary approach to the boundary element method
[AD-A192931] N88-26701
HETEROJUNCTION DEVICES
Transport in GaAs heterojunction ring structures N88-27011
Vertical electronic transport in novel semiconductor heterojunction structures N88-27045
HETEROJUNCTIONS
Theoretical aspects of electron transport in modulated structures N88-27016
HIGH ENERGY INTERACTIONS
Theoretical studies in elementary particle physics
[DE88-006929] N88-26926
HIGH LEVEL LANGUAGES
Definition of an auxiliary processor dedicated to real-time operating system kernels
[NASA-CR-183070] N88-26860
HIGH POWER LASERS
Optical coatings for high average power XeF lasers
[DE88-011356] N88-26656
HIGH PRESSURE
Asynchronous optical sampling for laser-based combustion diagnostics in high pressure flames
[AD-A192920] N88-26428
Respiration and oxygen tension in the blood of animals exposed to high pressures N88-26790
Electronic structure of quantum-well states revealed under high pressures N88-27038
Experimental study of planetary gases with applications to planetary interior models
[NASA-CR-183098] N88-27137
HIGH RESOLUTION
High resolution detection of solute segregation to the cores of dislocations in grain boundaries
[DE88-009168] N88-27078
HIGH REYNOLDS NUMBER
Velocity-pressure integrated versus penalty finite element methods for high Reynolds number flows
[NASA-CR-179357] N88-26635
HIGH SPEED
High speed inlet calculations with real gas effects
[NASA-CR-182167] N88-26336
A high speed serial link interface for SANDAC-V
[DE88-007694] N88-26861
A survey of the Ap stars for rapid variability N88-27127
HIGH TEMPERATURE
The adherence of nickel oxide on nickel during high temperature oxidation
[DE88-011194] N88-26450
Fracture resistance of a TiB2 particle/SiC matrix composite at elevated temperature
[NASA-TM-100967] N88-26482
Feasibility of producing jet fuel from GPGP (Great Plains Gasification Plant) by-products
[DE88-010233] N88-26492
Molten salt electrolytes for high-temperature lithium cells
[DE88-010058] N88-26581

On the chemistry of superconductivity
[DE88-010714] N88-27096

HIGH TEMPERATURE AIR
Numerical simulation of ignition of hydrogen jet in hot air N88-26307

HIGH TEMPERATURE ENVIRONMENTS
High speed inlet calculations with real gas effects
[NASA-CR-182167] N88-26336

HIGH TEMPERATURE PLASMAS
Bremsstrahlung from high Z impurities in hot plasmas
[DE88-011755] N88-26994

HIGH TEMPERATURE TESTS
Automated measurement of crack length and load line displacement at elevated temperature
[NLR-MP-87049-U] N88-26706

HILBERT SPACE
Theory of pseudo-differential operators over C*-algebras
[DE88-701860] N88-26883

HOLE DISTRIBUTION (MECHANICS)
Stress concentration around circular hole in a composite material specimen representative of the X-29A forward-swept wing aircraft
[NASA-CR-179435] N88-26694

HOLE GEOMETRY (MECHANICS)
Dynamical stress concentration problems, from every side, bordered and perforated plates
[ETN-88-92128] N88-26703

HOLES
Compression creep of filamentary composites
[NASA-CR-182550] N88-26601

HOLES (ELECTRON DEFICIENCIES)
Direct measurement of ultrafast electron-hole plasma expansion at high density at an asymmetric GaAs quantum well N88-27044
Oxygen vacancy ordering and superconductivity in YBa2Cu3O(sub 7-x)
[DE88-010005] N88-27083

HOLOGRAPHY
Study of flow tracer behavior models and experimental validation with multiple exposure holographic velocimetry
[IMFL-87/30] N88-26622
Interferometric recording of holographic optical elements using partially coherent light N88-26636
Active phase compensation system for fiber optic holography
[NASA-TM-101295] N88-26641
Optical data processing
[AD-A193024] N88-26841

HOMOGENEITY
Off-boundary approach to the boundary element method
[AD-A192931] N88-26701

HOOKES LAW
Kinematics of Hooke universal joint robot wrists
[NASA-TM-100567] N88-26870

HOT CORROSION
Guide to the control of high temperature corrosion and protection of gas turbine materials
[PB88-107412] N88-26370

HOT ELECTRONS
Third International Conference on Superlattices, Microstructures and Microdevices
[AD-A191416] N88-26995
Hot electron transistors grown by MOCVD N88-26996
Hot electrons in silicon dioxide: Ballistic to steady-state transport N88-27042
Recent applications of Monte Carlo methods for semiconductor microdevice simulation N88-27046

HOT STARS
Time-dependent mass loss from hot stars with and without radiative driving
[DE88-008899] N88-27128

HOUSINGS
A review of gear housing dynamics and acoustics literature
[NASA-CR-183110] N88-26675

HOVERING
Hover performance tests of baseline metal and Advanced Technology Blade (ATB) rotor systems for the XV-15 tilt rotor aircraft
[NASA-CR-177436] N88-26367

HUMAN FACTORS ENGINEERING
Computer simulation of multiple pilots flying a modern high performance helicopter
[NASA-TM-100183] N88-26377

HUMAN REACTIONS
Computer simulation of a single pilot flying a modern high-performance helicopter
[NASA-TM-100182] N88-26376

HYDRODYNAMICS
Ludwig Prandtl collected treatises on applied mechanics, hydro- and aerodynamics, part 2, IV interfaces and resistance
[NASA-TT-20315] N88-26338
Modelling of premixed combustion using a thin flame sheet and the effect of the hydrodynamic instability
[DE88-009467] N88-26423
Numerical modeling of the effect of particle size of explosives on shock initiation properties
[DE88-010479] N88-26491
Vertical ship motions and sea loads considering nonlinear effects
[TAE-592] N88-26515
Freely expanding detonation products: Scaling of rate processes
[DE88-007827] N88-26606

HYDROFORMING
A finite element analysis for the hydroforming of aluminum
[DE88-008050] N88-26516

HYDROGEN
Ultraviolet imaging of hydrogen flames
[DE88-009152] N88-26422
Production of powdered sodium hydride with large specific surface by the catalyzed reaction of molten sodium with hydrogen-1
[NASA-TT-20185] N88-26482
Shock wave compression and metallization of simple molecules
[DE88-008031] N88-26925
Enhancement of volume H(-) production by vibrationally pre-exciting the hydrogen molecules
[DE88-010783] N88-26937

HYDROGEN ATOMS
Nascent vibrational/rotational distribution produced by hydrogen atom recombination
[AD-A193005] N88-26933

HYDROGEN EMBRITTLEMENT
Investigation of structure and surface state effect on hydrogen embrittlement of steels, under consideration of acoustic emission analysis
[ETN-88-92350] N88-26457
Research on the kinetics of phase changes in solids
[AD-A192222] N88-26696

HYDROGEN FUELS
Numerical simulation of ignition of hydrogen jet in hot air N88-26307

HYDROGEN IONS
Development of high current and high brightness negative hydrogen ion sources
[DE88-010882] N88-26934

HYDROGEN PEROXIDE
Simulation of axisymmetric flow with H2O2 reactions N88-26311

HYDROGEN PLASMA
Plasma armature formation in high-pressure, high-velocity hydrogen
[DE88-008347] N88-26967

HYDROGEN PRODUCTION
Photosynthetic water splitting
[DE88-007809] N88-26791

HYDROGEN RECOMBINATIONS
Nascent vibrational/rotational distribution produced by hydrogen atom recombination
[AD-A193005] N88-26933

HYDROLOGY
Surface hydrology, sediment transport dynamics and remote sensing of disturbed watersheds in a humid temperate region
[DE88-008719] N88-26715
Vegetation studies on Vandenberg Air Force Base, California
[NASA-TM-100985] N88-26795

HYDROLOGY MODELS
Hydrologic models for land-atmosphere retrospective studies of the use of LANDSAT and AVHRR data
[NASA-CR-182861] N88-26712
Hydrologic models for land-atmosphere retrospective studies of the use of LANDSAT and AVHRR data
[NASA-CR-182862] N88-26716

HYDROLYSIS
A study of solvent effects on the synthesis of pure component and composite ceramic powders by metal alkoxide hydrolysis
[DE88-008381] N88-26470

HYDROSTATIC PRESSURE
Quantum wells and bulk AlGaAs under hydrostatic pressure N88-27000
Pressure-dependent measurement on n+GaAs (Si, Sn): The effect of deep donor (DX) states on the electrical properties and presistent photoconductivity effects N88-27020

HYDROXIDES
Crystallization of aluminum hydroxide in the aluminum-air battery: Literature review, crystallizer design and results of integrated system tests
[DE88-010510] N88-26594

HYDROXYL RADICALS
Ground level hydroxyl (OH) concentration measurements by long path differential optical laser absorption
[ETN-88-92124] N88-26952

HYPERCUBE MULTIPROCESSORS
Relay approach message routing in hypercube multiprocessors
[DE88-009973] N88-26814
Distributed fault tolerant embeddings of binary trees in hypercubes
[AD-A192929] N88-26840

HYPERFINE STRUCTURE
Sources of polarized ions and atoms
[DE88-010910] N88-26931

HYPERSONIC FLIGHT
Compressible boundary layers --- atmospheric reentry
[CERT-OA-13/5005-AYD] N88-26623

HYPERSONIC FLOW
The Proceedings of the Symposium on Mechanics for Space Flight 1987
[ISAS-SP-6] N88-26499

HYPERVELOCITY LAUNCHERS
Application of superconducting technology to earth-to-orbit electromagnetic launch systems
[NASA-TM-101134] N88-26385
Application of superconducting technology to earth-to-orbit electromagnetic launch systems
[DE88-010022] N88-26386

HYSTERESIS
Experimental and theoretical study of the dynamic operational behavior of a three stage radial compressor
[ETN-88-92129] N88-26676

I

ICEBERGS
Arctic ice island and sea ice movements and mechanical properties
[DE88-004267] N88-26782

IGNITION
Ignition and flame spread of PMMA
[NASA-TT-20290] N88-26431
Thermal and mechanical analysis of the Faraday shield for the compact ignition tokamak
[DE88-007855] N88-26962

IGNITION LIMITS
Numerical simulation of ignition of hydrogen jet in hot air N88-26307

IMAGE ANALYSIS
Image pyramid motion detection applied to sea ice N88-26713
Processing and analysis of images transmitted by Vega space probes over Halley's comet
[ETN-88-92291] N88-27131

IMAGE PROCESSING
Data volume reduction for imaging radar polarimetry
[NASA-CASE-NPO-17184-1-CU] N88-26541
Microwave image understanding and its application to radar cross section management N88-26542
Microfocus X-ray techniques for flaw location
[DE88-008636] N88-26680
The interaction of sensory and perceptual variables: Spatial, temporal and orientation response to figure and ground
[AD-A192897] N88-26798
Research in computer science 1985/6
[PB88-113840] N88-26815
Automated system for mathematical processing of the data from a hybrid spectrometer
[DE87-702995] N88-26820
Common Data Format (CDF) to store images
[NASA-CR-179366] N88-26825
SEGMERGE: A scanline visible surface algorithm with adaptive span selection and inexpensive antialiasing
[DE88-009186] N88-26826
A new approach to machine-based perception of monocular images
[DE88-002418] N88-26942
Digital image processing from speckle interferograms by correlation methods: Application in atmospheric optics, astronomy, and biology
[ETN-88-92125] N88-26953
Direct imaging of the columnar structure of GaAs quantum wells N88-27030
Methods for indirect imaging through the atmosphere
[ONERA-NT-1987-4] N88-27124
The application of imaging to the atmospheric Cerenkov technique: Observations of the Crab nebula N88-27126
Processing and analysis of images transmitted by Vega space probes over Halley's comet
[ETN-88-92291] N88-27131

IMAGE RECONSTRUCTION
Display and processing of multidimensional signals with the aid of fractal image sequences
[ETN-88-92131] N88-26642
A new approach to machine-based perception of monocular images
[DE88-002418] N88-26942
IMAGE RESOLUTION
Ultraviolet imaging of hydrogen flames
[DE88-009152] N88-26422
Interpreting forest biome productivity and cover utilizing nested scales of image resolution and biogeographical analysis
[NASA-CR-183036] N88-26711
IMAGING RADAR
Data volume reduction for imaging radar polarimetry
[NASA-CASE-NPO-17184-1-CU] N88-26541
IMAGING TECHNIQUES
Ultraviolet imaging of hydrogen flames
[DE88-009152] N88-26422
Methods for indirect imaging through the atmosphere
[ONERA-NT-1987-4] N88-27124
IMPACT LOADS
Contact force history and dynamic response due to the impact of a soft projectile
[NASA-TM-100961] N88-26679
IMPACT TESTS
Contact force history and dynamic response due to the impact of a soft projectile
[NASA-TM-100961] N88-26679
Analysis of the perforation of monolithic and simple laminate aluminium targets as a test of analytical deformation models
[MRL-R-1111] N88-26686
Milliwatt generator project
[DE88-011261] N88-26939
IMPEDANCE
Scattering patterns of dihedral corner reflectors with impedance surface impedances
[NASA-CR-183078] N88-26545
IMPEDANCE MEASUREMENT
A simulation analysis of errors in the measurement of standard electrochemical rate constants from phase-selective impedance data
[AD-A192739] N88-26426
IMPEDANCE PROBES
Evaluation of a multi-point method for determining acoustic impedance
[NASA-TM-100637] N88-26913
IMPLANTATION
Transport study on Si/Si(1-x)Ge(x) superlattices selectively doped by secondary implantation of Sb N88-27027
IMPURITIES
Impurity transport calculations for a drift-dependent tokamak scrape-off plasma
[DE88-010053] N88-26984
Bremsstrahlung from high Z impurities in hot plasmas
[DE88-011755] N88-26994
INCENDIARY AMMUNITION
Granulation of pyrotechnic tracer composition R284T
[MRL-TN-528] N88-26490
INCIDENCE
On the global radiation incident variously orientated surfaces on the South Coast of Finland
[FMI-5] N88-26746
INCOMPRESSIBLE FLOW
Finite element analysis of incompressible viscous flow around multi-element aerofoils N88-26294
INCONEL (TRADEMARK)
Milliwatt generator project
[DE88-011261] N88-26939
INDEPENDENT VARIABLES
Studies of HZE particle interactions and transport for space radiation protection purposes
[NASA-TM-101159] N88-27142
INDIUM ANTIMONIDES
Spectroscopy of one-dimensional subbands on InSb N88-27007
INDIUM ARSENIDES
Photoluminescence studies of InGaAlAs quaternary alloys
[DE88-007197] N88-27062
INDUSTRIES
Resources: NASA for entrepreneurs
[NASA-CR-182152] N88-27119
INELASTIC SCATTERING
Inelastic two composite particle systems scattering at high energy
[DE88-701841] N88-26926
INEQUALITIES
Conditions for finite convergence of algorithms for nonlinear programs and variational inequalities
[AD-A192355] N88-26834
INERTIA
A new method for the estimation of aircraft inertia characteristics N88-26530
INERTIAL CONFINEMENT FUSION
The effect of ICRF on the Alcator C Scrape-Off Layer plasma
[DE88-009821] N88-26972
INFERENCE
A network approach to the certainty factor model — expert systems
[CWI-CS-R8757] N88-26852
INFORMATION DISSEMINATION
Context of national information systems in developing countries: India and China in a comparative perspective
[PB88-109954] N88-27111
INFORMATION FLOW
Context of national information systems in developing countries: India and China in a comparative perspective
[PB88-109954] N88-27111
Hiding in stream semantics of uniform concurrency
[PB88-121579] N88-27114
INFORMATION PROCESSING (BIOLOGY)
Working memory capacity: An individual differences approach
[AD-A192359] N88-26803
INFORMATION RETRIEVAL
A cockpit natural language study - selected transcripts
[AD-A192972] N88-26808
INFORMATION SYSTEMS
The role of working memory in language comprehension
[AD-A192721] N88-26805
SIMS: Single Interface to Multiple Systems
[AD-A192264] N88-26832
Computer-aided writing
[AD-A192516] N88-26837
Context of national information systems in developing countries: India and China in a comparative perspective
[PB88-109954] N88-27111
INFORMATION TRANSFER
A cockpit natural language study - selected transcripts
[AD-A192972] N88-26808
INFRARED DETECTORS
Infrared detectors based on the photon drag effect and intersubband absorption by a two-dimensional electron gas N88-27024
INFRARED IMAGERY
Stress analysis using infrared thermography
[ETN-88-92169] N88-26705
INFRARED RADIATION
Regulatory biochemical and metabolic responses in photoreceptors
[AD-A192898] N88-26794
INFRARED SPECTROSCOPY
Spectroscopy of one-dimensional subbands on InSb N88-27007
INFRASONIC FREQUENCIES
Surface disturbances produced by low-level, subsonic B-1 aircraft
[AD-A192257] N88-26752
INJECTION MOLDING
High temperature resins for injection. High temperature pre-impregnated
[RC-648676] N88-26486
INLET FLOW
High speed inlet calculations with real gas effects
[NASA-CR-182167] N88-26336
INPUT
Why is it difficult to program in von Neumann languages
[AD-A192830] N88-26839
INSULATION
SIS (Superconductor-Insulator-Superconductor) mixer research
[AD-A192908] N88-27092
INTEGRAL EQUATIONS
New hybrid method for solving time-domain integral equations (one-dimensional scattering problems)
[PB88-186192] N88-26547
Time-domain boundary element analysis of dynamic near-tip fields for impact-loaded collinear cracks
[AD-A192930] N88-26700
A new boundary integral equation formulation for elastodynamic and elastostatic crack analysis
[AD-A192967] N88-26702
INTEGRATED CIRCUITS
Effects of cosmic rays on single event upsets
[NASA-CR-183053] N88-26569
Analysis of networks with parameters S: Generalization of junction matrix
[INPE-4535-PRE/1282] N88-26570
Integrated optoelectronic circuits utilizing InGaAsP grown by molecular beam epitaxy (erbium doping of MBE GaAs)
[AD-A192269] N88-26584
An integrated circuit for error protection in modern data communication systems conforming to Eurocom specifications
[FEL-1987-48] N88-26593
Research in VLSI computer systems
[AD-A192915] N88-26816
Defects in high-mobility semiconductor systems
[AD-A192298] N88-27090
INTERFACE STABILITY
Stability of a coastal upwelling front over topography
[AD-A192354] N88-26784
INTERFACES
Ludwig Prandtl collected treatises on applied mechanics, hydro- and aerodynamics, part 2, IV interfaces and resistance
[NASA-TT-20315] N88-26338
Interface modification in Nicalon (trademark)/SiC composites
[DE88-009708] N88-26409
Surface phases and their influence on metal-oxide interfaces
[DE88-007938] N88-26420
Direct manipulation and the design of user interfaces
[PB88-126354] N88-26810
Common Data Format (CDF) to store images
[NASA-CR-179366] N88-26825
A high speed serial link interface for SANDAC-V
[DE88-007694] N88-26861
Superlattice doping interfaces N88-27019
Fermi level dependent native defect formation: Consequences for metal-semiconductor and semiconductor-semiconductor interfaces
[DE88-008247] N88-27066
Fundamental optical studies of competitive adsorption and thin film phenomena
[DE88-008780] N88-27068
INTERFEROMETRY
Interferometric recording of holographic optical elements using partially coherent light N88-26636
Digital image processing from speckle interferograms by correlation methods: Application in atmospheric optics, astronomy, and biology
[ETN-88-92125] N88-26953
INTERMETALLICS
Phase stability and alloy design of ordered intermetallics
[DE88-007479] N88-26435
Nickel aluminides: A new family of nickel + aluminum alloys featuring simple composition, low density, excellent oxidation resistance and high yield strength that increases with temperature
[DE88-010692] N88-26461
Superconductivity of heavy-electron uranium compounds
[DE88-007901] N88-27065
INTERNAL COMBUSTION ENGINES
The outlook for ceramics in heat engines, 1990-2010: Results of a worldwide Delphi survey
[DE88-010075] N88-26475
Ceramic Technology for Advanced Heat Engines Program data base
[DE88-008954] N88-26489
INTERNATIONAL COOPERATION
An agenda for the strategic defense initiative
[RAND-P-7404] N88-26898
Simulation of the neutronic characteristics of large fast neutron reactors
[ETN-88-92305] N88-26940
INTERNATIONAL TRADE
A basis of settlement: Economic foundations of permanent pioneer communities
[DE88-010907] N88-26382
INTERPLANETARY MAGNETIC FIELDS
On the conjugacy of the aurora: High and low latitudes
[AD-A193008] N88-26755
INTERPOLATION
A practical shifted Adams algorithm
[DE88-008573] N88-26830
Prolongation, restriction and coarse grid approximation in a three-dimensional cell-centered multigrid method
[REPT-88-02] N88-26889
Two families of graphs satisfying the cycle basis interpolation property
[PB88-127808] N88-26890
INTERPROCESSOR COMMUNICATION
Relay approach message routing in hypercube multiprocessors
[DE88-009973] N88-26814
Correctness criteria for process migration
[NASA-CR-182939] N88-26823
INTERSTELLAR MATTER
Probing the possibility of a (12)C/(13)C abundance gradient from observations of interstellar CH+
[DE88-008908] N88-27125

INVERSIONS
A diagonally inverted LU implicit multigrid scheme
[NASA-TM-100911] N88-26340
INVISCID FLOW
On the stationary solutions of three-dimensional Euler equations by the TVD difference schemes N88-26320
A study of flow separation in transonic flow using inviscid and viscous computational fluid dynamics (CFD) schemes
[NASA-CR-183119] N88-26618
ION EXCHANGING
Dual mechanism bifunctional polymers: Design, synthesis and application of a new category of metal ion complexing agents
[DE88-006233] N88-26468
ION IMPLANTATION
Development of high current and high brightness negative hydrogen ion sources
[DE88-010882] N88-26934
ION PROBES
Laser spectoscopy of plasmas
[AD-A193009] N88-26991
ION SOURCES
Sources of polarized ions and atoms
[DE88-010910] N88-26931
Development of high current and high brightness negative hydrogen ion sources
[DE88-010882] N88-26934
Enhancement of volume H(-) production by vibrationally pre-exciting the hydrogen molecules
[DE88-010783] N88-26937
Field-enhanced lithium ion sources for PBFA 2
[DE88-007195] N88-26960
ION TEMPERATURE
Effects of secondary electron emission on the collector and source sheaths of a finite ion temperature plasma
[DE88-008930] N88-26971
IONIC COLLISIONS
Fluid dynamical model of ultrarelativistic heavy ion collisions
[DE88-007905] N88-26921
IONIZATION
Rare Gas Halide (RGH) kinetics
[AD-A192352] N88-26425
Laser desorption/ablation studies by resonance ionization mass spectrometry
[DE88-009124] N88-26650
A 10 microns photoexcited avalanche gain due to electron impact ionization from GaAs quantum well superlattices N88-27026
IONOSPHERIC DRIFT
High latitude ionospheric radio studies
[AD-A192270] N88-26753
IONS
Sources of polarized ions and atoms
[DE88-010910] N88-26931
Recent advances in atom-probe field ion microscopy
[DE88-008799] N88-27070
IRON ALLOYS
Reduced-activation austenitic stainless steels: The Fe-Cr-C system
[DE88-008091] N88-26442
IRRADIANCE
The propagation of irradiance moments of an aberrated, apodized FEL beam
[DE88-008972] N88-26648
IRRADIATION
Laser fluorescence spectroscopy of zinc neutrals originating from laser-irradiated and ion-bombarded zinc sulfide and zinc surfaces
[DE88-008037] N88-26418
Fast atom bombardment study on interaction of anticodonic nucleotides and their cognate amino acid
[ISAS-RN-355] N88-26918
ISOCYANATES
Research in energetic compounds
[AD-A192953] N88-26494
ISOTHERMAL PROCESSES
The crystallization of tough thermoplastic resins in the presence of carbon fibers
[NASA-CR-182984] N88-26484
ISOTOPIC LABELING
Method for the isotopically selective detection of inert gases
[TI88-006370] N88-26421
ISOTROPIC MEDIA
Wave propagation in locally isotropic turbulent medium with smoothly changing characteristics
[NASA-TT-20312] N88-26617
ISOTROPIC TURBULENCE
Wave propagation in locally isotropic turbulent medium with smoothly changing characteristics
[NASA-TT-20312] N88-26617
ITALY
The 1985 Meteorological Yearbook of Iapra (27th)
[PB88-125729] N88-26777
ITERATION
Application of Moment Iteration Method (MIM) to electromagnetic field computation
[PB85-194139] N88-26546

J

JAPAN
Survey on utility technology of a tidal and ocean current energy
[DE88-770148] N88-26722
JAPANESE SPACE PROGRAM
High speed and high angle of attack wind tunnel test results of the winged space vehicle C-2
[ISAS-RN-623] N88-26329
JET ENGINE FUELS
Feasibility of producing jet fuel from GPGP (Great Plains Gasification Plant) by-products
[DE88-010233] N88-26492
Biodegradation of JP-5 aviation fuel by subsurface microbial communities
[AD-A192743] N88-26493
JET ENGINES
Engine component retirement for cause. Volume 1: Executive summary
[AD-A192730] N88-26371
JET FLOW
Three-dimensional viscous flow computations of a circular jet in subsonic and supersonic cross flow
[NASA-CR-182153] N88-26616
JET LIFT
Numerical study of delta wing leading edge blowing
[NASA-CR-183101] N88-26335
JET MIXING FLOW
Numerical simulation of ignition of hydrogen jet in hot air N88-26307
JFET
JFET/SOS (Junction Field-Effect Transistor/Silicon-on-Sapphire) devices: Gamma-radiation-induced effects
[AD-A193001] N88-26586
JOINTS (JUNCTIONS)
Optimization of performance criteria with bounded joint velocities for robots with one degree of redundancy
[DE88-003915] N88-26670
FEB structural analysis, revision H
[AD-A192302] N88-26698
Kinematics of Hooke universal joint robot wrists
[NASA-TM-100567] N88-26870
JP-5 JET FUEL
Biodegradation of JP-5 aviation fuel by subsurface microbial communities
[AD-A192743] N88-26493

K

KALMAN FILTERS
A positioning system based on NAVSAT
[NLR-MP-87018-U] N88-26358
KELVIN-HELMHOLTZ INSTABILITY
Numerical simulation of supersonic free-jets N88-26299
KERNEL FUNCTIONS
Definition of an auxiliary processor dedicated to real-time operating system kernels
[NASA-CR-183070] N88-26860
KEROSENE
Antimisting kerosene: Low temperature degradation and blending
[NASA-CR-182725] N88-26495
KINEMATICS
Spatial dynamics of deformable multibody systems with variable kinematic structure N88-26687
Kinematics of Hooke universal joint robot wrists
[NASA-TM-100567] N88-26870
Theory of relativity and super-light-speeds-I: Kinematical part
[DE88-701832] N88-27100
KINETICS
The crystallization of tough thermoplastic resins in the presence of carbon fibers
[NASA-CR-182984] N88-26484
Research on the kinetics of phase changes in solids
[AD-A192222] N88-26696
Proceedings of the 2nd US-Japan Workshop on Advanced Plasma Modeling, volume 3
[IPPJ-867] N88-26957
Modeling of subtle kinetic processes in plasma simulation N88-26959
KNOWLEDGE
Minimum disclosure proofs of knowledge
[CWI-PM-R8710] N88-26854
Knowledge representation in geographic information systems
[ETN-88-92470] N88-27112
KNOWLEDGE REPRESENTATION
The knowledge based automatic extraction of the machinable surfaces for automatic CAD-CAM system
[INPE-4542-PRE/1288] N88-26824
Delfi-3 as a development environment for expert systems
[REPT-8767] N88-26845
Computer science and technology: Knowledge-based system for physical database design
[PB88-193289] N88-27109
Knowledge-based cost estimating vs traditional software cost models
[DE88-009707] N88-27116

L

LABORATORIES
Inference and discovery in an exploratory laboratory
[AD-A192231] N88-26801
Experimental study of planetary gases with applications to planetary interior models
[NASA-CR-183098] N88-27137
LAKES
Eigenmatrix representations of radiance distributions in layered natural waters with wind-roughened surfaces
[PB88-188701] N88-26780
LAMINAR FLOW
Numerical simulation of transition to turbulence in plane Poiseuille flow by a spectral method N88-26321
Experiments on densely-loaded non-Newtonian slurries in laminar and turbulent pipe flows
[DE88-010579] N88-26612
Velocity-pressure integrated versus penalty finite element methods for high Reynolds number flows
[NASA-CR-179357] N88-26635
LAMINATES
Stiffness degradation of composite laminates N88-26405
Instability-related delamination growth of embedded and edge delaminations N88-26406
Computation equipment for damage simulation in laminated composites
[AD-A193013] N88-26412
A micromechanics model of the stiffness and strength of laminates with fiber waviness
[NASA-CR-181670] N88-26413
Compression creep of filamentary composites
[NASA-CR-182550] N88-26601
Three-dimensional analysis of a postbuckled embedded delamination
[NASA-TP-2823] N88-26684
Analysis of the perforation of monolithic and simple laminate aluminium targets as a test of analytical deformation models
[MRL-R-1111] N88-26686
Properties of multilayers for soft X-ray optics N88-27025
LAND USE
Hydrologic models for land-atmosphere retrospective studies of the use of LANDSAT and AVHRR data
[NASA-CR-182861] N88-26712
LARGE SPACE STRUCTURES
L(sub infinity symbol)-approximations of complex functions and robust controllers for large flexible space structures
[PB88-186226] N88-26390
Mobile remote manipulator system for a tetrahedral truss
[NASA-CASE-MSC-20985-1] N88-26398
Experimental and theoretical investigation of passive damping concepts for member forced and free vibration
[NASA-CR-183082] N88-26693
LASER ANEMOMETERS
Study of the local behavior of a flame
[ETN-88-92300] N88-26433
LASER APPLICATIONS
Asynchronous optical sampling for laser-based combustion diagnostics in high pressure flames
[AD-A192920] N88-26428
Interferometric recording of holographic optical elements using partially coherent light N88-26636
LASER DOPPLER VELOCIMETERS
Influence of rear body geometry on the velocity characteristics of the near wake
[ISL-R-113/87] N88-26339
Experiments on densely-loaded non-Newtonian slurries in laminar and turbulent pipe flows
[DE88-010579] N88-26612
Study of flow tracer behavior models and experimental validation with multiple exposure holographic velocimetry
[IMFL-87/30] N88-26622

A microcomputer based frequency-domain processor for laser Doppler anemometry
[NASA-TM-100998] N88-26634
LASER GUIDANCE
Tracking a monochromatic light source
[DE88-011260] N88-26653
LASER INDUCED FLUORESCENCE
Developing diagnostic methods for plasma-particle interaction
[TI88-007726] N88-26973
LASER MATERIALS
Liquid crystal optics for laser systems
[DE88-008475] N88-26948
Nonlinear materials for frequency conversion
[DE88-008343] N88-27067
LASER OUTPUTS
The use of liquid films for spacecraft survivability to laser radiation
[AD-A192954] N88-26395
Laser fluorescence spectroscopy of zinc neutrals originating from laser-irradiated and ion-bombarded zinc sulfide and zinc surfaces
[DE88-008037] N88-26418
Electron-impact-ionization and electron-attachment cross sections of radicals important in transient gaseous discharges
[AD-A192248] N88-26424
Results from the SLAC lasertron
[DE88-007816] N88-26647
The propagation of irradiance moments of an aberrated, apodized FEL beam
[DE88-008972] N88-26648
Laser desorption/ablation studies by resonance ionization mass spectrometry
[DE88-009124] N88-26650
Poloidal field measurements using laser enhanced attenuation of an energetic lithium beam
[DE88-008360] N88-26963
LASER PLASMAS
A numerical analysis of flow characteristics in laser propulsion system N88-26305
On the self-focusing of electric helicons
[DE88-701870] N88-26905
Thermal inhibition by megagauss field due to variation of electron temperature in laser plasma
[DE88-701687] N88-26977
Megagauss field variation along axis of wire target in laser produced plasma
[DE88-701695] N88-26979
Ultraviolet-visible spectroscopy of laser-produced aluminum plasmas
[AD-A193004] N88-26990
Laser spectoscopy of plasmas
[AD-A193009] N88-26991
LASER PROPULSION
A numerical analysis of flow characteristics in laser propulsion system N88-26305
LASER RANGE FINDERS
Laser ranging data analysis
[NASA-CR-183115] N88-26567
LASER SPECTROSCOPY
Laser fluorescence spectroscopy of zinc neutrals originating from laser-irradiated and ion-bombarded zinc sulfide and zinc surfaces
[DE88-008037] N88-26418
Laser diagnostics applied to advanced combustion systems
[DE88-753119] N88-26649
Ground level hydroxyl (OH) concentration measurements by long path differential optical laser absorption
[ETN-88-92124] N88-26952
An elliptical spectrograph/gated microchannel plate detector for time-resolved spectral measurements in the X-ray region
[DE88-007590] N88-26961
LASER WEAPONS
High spatial frequency thermal blooming instability: A linear stability analysis
[DE88-010711] N88-26655
LASERS
Laser desorption/ablation studies by resonance ionization mass spectrometry
[DE88-009124] N88-26650
Liquid crystal optics for laser systems
[DE88-008475] N88-26948
LATENT HEAT
Transient thermal analysis of three latent heat storage configurations for rapid thermal charging
[DE88-008943] N88-27104
LATTICE VIBRATIONS
Defects and disorder in amorphous and damaged silicon
[AD-A192277] N88-27089
LATTICES (MATHEMATICS)
Fixpoint representations of characteristic sets of linear-time temporal formulas
[CWI-CS-R8754] N88-26849
Eigenmodes of a random walk on a 2-D lattice torus with one trap
[DE88-007830] N88-26874
Challenge equality problems in lattice theory
[DE88-010094] N88-27072
LAUNCH VEHICLES
Application of superconducting technology to earth-to-orbit electromagnetic launch systems
[DE88-010022] N88-26386
LAUNCHING BASES
Lunar base launch and landing facility conceptual design, 2nd edition
[NASA-CR-172049] N88-27135
LAYERS
Eigenmatrix representations of radiance distributions in layered natural waters with wind-roughened surfaces
[PB88-188701] N88-26780
LEADING EDGES
Numerical study of delta wing leading edge blowing
[NASA-CR-183101] N88-26335
LEAKAGE
Evaluation of engineering leak before break assessment methods by piping tests
[PB88-126982] N88-26538
Remote sensing and satellite applications to the needs of the gas and pipeline industry
[PB88-202668] N88-26714
LEARNING
Inference and discovery in an exploratory laboratory
[AD-A192231] N88-26801
Script editor: An editor for the specification phase in the development of computer based learning
[REPT-87-68] N88-26846
The sine and cosine function for class 4-VWO. Exploration of possible bottlenecks
[REPT-87-72] N88-27105
LEAST SQUARES METHOD
Parameter estimation of dynamical systems N88-26519
LEAVES
Sources of scattering in vegetarian and other surfaces and objects
[NASA-CR-182975] N88-26710
LENGTH
Automated measurement of crack length and load line displacement at elevated temperature
[AGARD-R-751] N88-26695
LETHALITY
Reaming experiments for the lethality test system
[DE88-007902] N88-26383
LIE GROUPS
Canonical construction of differential operators intertwining representations of real semisimple Lie groups
[DE88-701852] N88-26882
LIFE CYCLE COSTS
Engine component retirement for cause. Volume 1: Executive summary
[AD-A192730] N88-26371
PAX ECONOPACK economic analysis package users manual
[AD-A192949] N88-27117
LIFE SUPPORT SYSTEMS
Advanced life support control/monitor instrumentation concepts for flight application
[NASA-CR-177378] N88-26807
LIFT DEVICES
The role of computational fluid dynamics in aeronautical engineering (5): Improvements and applications of implicit TVD finite volume code N88-26313
The identification of the direct lift control flap system of the research aircraft ATTAS N88-26527
LIGHT EMISSION
Development of liquid metal field-emission sources for use in fast repetitive opening switches
[AD-A192230] N88-26583
LIGHT EMITTING DIODES
Excitation of single-mode glass fiber by partially coherent sources
[ETN-88-92121] N88-26951
LIGHT SCATTERING
Effects of atmospheric model layering on LOWTRAN 6 calculations of 8-12 micrometers near-horizon sky radiances
[AD-A192969] N88-26559
LIGHT SOURCES
Tracking a monochromatic light source
[DE88-011260] N88-26653
LIGHT SPEED
Theory of relativity and super-light-speeds-I: Kinematical part
[DE88-701832] N88-27100
LIGHT TRANSMISSION
Stress-related phenomena in transient radiation-induced absorption in optical fibers
[DE88-010956] N88-26949
LIGHTNING
Computer controlled data acquisition system for the NASA 1986 Rocket Triggered Lightning Program
[DE88-008335] N88-26766
A radar study of the interaction between lightning and precipitation
[DE88-009120] N88-26770
LIGHTNING SUPPRESSION
An interagency working group on lightning threat warning
[DE88-009828] N88-26767
LINE SPECTRA
Detection of absorption lines in the spectra of X-ray bursts from X1608-52
[ISAS-RN-360] N88-27143
LINEAR ACCELERATORS
Results from the SLAC lasertron
[DE88-007816] N88-26647
LINEAR FILTERS
Optical correlation using the magneto-optic device
[AD-A192342] N88-26950
LINEAR PREDICTION
An analysis of the efficiency and directivity of the sound generated by a moving laser source
[AD-A192220] N88-26914
LINEAR PROGRAMMING
A new trajectory following polynomial-time algorithm for the linear programming problem
[REPT-87-87] N88-26848
A linear-programming method inspired by the neural networks framework
[DE88-008688] N88-26862
Linear programming in R sup 3 and the skeleton and largest incircle of a convex polygon
[PB88-124664] N88-26892
LINEAR QUADRATIC GAUSSIAN CONTROL
Experiments in adaptive control of a very flexible one link manipulator N88-26865
LINEARITY
A full but elementary treatment of systems of homogeneous ordinary linear differential equations with constant coefficients
[REPT-87-82] N88-26867
On linear relationship between shock velocity and particle velocity
[DE88-701827] N88-27099
LINEARIZATION
Linearization along invariant manifolds and a generalization of the Hartman-Grobman theorems for degenerate singularities of vector fields in R cubed
[REPT-87-80] N88-26886
LIQUID ALLOYS
Fluid flow modeling in casting processes and its implications
[DE88-010009] N88-26671
LIQUID CRYSTALS
Liquid crystal optics for laser systems
[DE88-008475] N88-26948
LIQUID FILLED SHELLS
Liquid motions in partially filled containers: Preliminary results of the D-1 mission — Spacelab
[NLR-MP-86042-U] N88-26629
LIQUID METALS
Development of liquid metal field-emission sources for use in fast repetitive opening switches
[AD-A192230] N88-26583
LIQUID PROPELLANT ROCKET ENGINES
Analysis of flow through pump of large rocket engine N88-26306
LIQUID SLOSHING
Axisymmetric liquid sloshing under low-g conditions: Numerical simulation method (reference manual)
[NLR-TR-86057-4] N88-26627
LIQUID SURFACES
Liquid motions in partially filled containers: Preliminary results of the D-1 mission — Spacelab
[NLR-MP-86042-U] N88-26629
LIQUIDS
The use of liquid films for spacecraft survivability to laser radiation
[AD-A192954] N88-26395
Extension of Boltzmann's theory to a liquid
[DE88-009153] N88-27097
LITHIUM
Optimizing superplastic response in lithium containing aluminum-magnesium alloys
[AD-A192217] N88-26451
Ambient temperature secondary lithium batteries using LiAl lithium insertion anodes
[DE88-008394] N88-26574

Molten salt electrolytes for high-temperature lithium cells
[DE88-010058] N88-26581
Field-enhanced lithium ion sources for PBFA 2
[DE88-007195] N88-26960
Poloidal field measurements using laser enhanced attenuation of an energetic lithium beam
[DE88-008360] N88-26963
Generation of Adlam-Allen waves by plasma release experiments in the solar wind
[PB88-106000] N88-27140

LITHIUM ALLOYS
Fatigue of lithium-aluminum alloys: An example of localization of the plastic deformation
[ETN-88-92309] N88-26456

LITHOGRAPHY
Excitonic properties of GaAs-AlGaAs nanostructures N88-27023

LITHOSPHERE
Effects of a temperature-dependent rheology on large scale continental extension
[NASA-CR-183117] N88-26759

LOAD TESTING MACHINES
Automated measurement of crack length and load line displacement at elevated temperature
[NLR-MP-87049-U] N88-26706

LOADS (FORCES)
Vertical ship motions and sea loads considering nonlinear effects
[TAE-592] N88-26515
Instrumentation for the measurement of penetrator dynamic response to permit force estimation
[DE88-010608] N88-26666

LONG DURATION SPACE FLIGHT
Studies of HZE particle interactions and transport for space radiation protection purposes
[NASA-TM-101159] N88-27142

LOOP ANTENNAS
Research in electromagnetic shielding theory. Part 2: EMP (electromagnetic pulse) simulation using small loops
[AD-A192882] N88-26558

LORAN C
Research project Loran-C of the Geometric Service of the Ministry of Public Works
[B8735055] N88-26356

LOSSES
Loss evaluation of self-commutated power conditioner for battery energy storage system
[DE88-752075] N88-26575

LOW ASPECT RATIO
Symmetrized magnetic field configuration of low aspect ratio helical system
[IPPJ-869] N88-26956

LOW FREQUENCIES
Aircraft interior noise reduction by alternate resonance tuning
[NASA-CR-182540] N88-26909
The polarization of radio galaxies: Its structure at low frequencies
[B8681611] N88-27123

LOW NOISE
Low noise cryogenic dielectric resonator oscillator
[NASA-CASE-NPO-17157-1-CU] N88-26596

LOW TEMPERATURE
Antimisting kerosene: Low temperature degradation and blending
[NASA-CR-182725] N88-26495
Superconducting electronic film structures
[AD-A192907] N88-27091

LOW VOLTAGE
Extinction behavior of low voltage switching arc under consideration of cathodic coatings and dynamic arc column
[ETN-88-92384] N88-26591

LUNAR BASES
Advanced photovoltaic power system technology for lunar base applications
[NASA-TM-100965] N88-26402
Lunar base launch and landing facility conceptual design, 2nd edition
[NASA-CR-172049] N88-27135

LUNAR SURFACE
Lunar base launch and landing facility conceptual design, 2nd edition
[NASA-CR-172049] N88-27135

M

MACH NUMBER
The effects of RCS jet firing on the isolated Orbiter and mated coast phases of the glide return to launch site maneuver at Mach number 6 (IA302B)
[NASA-CR-180223] N88-26403

MACHINING
Ductile-brittle transition of cutting behavior in diamond turning of single crystal Si
[DE88-008890] N88-26664
The knowledge based automatic extraction of the machinable surfaces for automatic CAD-CAM system
[INPE-4542-PRE/1288] N88-26824

MAGMA
Fine-scale traverses in cumulate rocks, Stillwater Complex: A lunar analogue study
[NASA-CR-183066] N88-26747

MAGNESIUM ALLOYS
Optimizing superplastic response in lithium containing aluminum-magnesium alloys
[AD-A192217] N88-26451

MAGNESIUM OXIDES
Sintering of the heterogeneous MgO compacts
[DE88-010357] N88-26408

MAGNETIC EFFECTS
Energy levels and magneto-electric effects in some quasi uni-dimensional semiconductor heterostructures N88-27009

MAGNETIC FIELD CONFIGURATIONS
MACH2: A two-dimensional magnetohydrodynamic simulation code for complex experimental configurations
[AD-A192285] N88-26988

MAGNETIC FIELDS
Application of superconducting technology to earth-to-orbit electromagnetic launch systems
[NASA-TM-101134] N88-26385
Magnetic heat pump design
[DE88-007730] N88-26605
Magnetohydrodynamic squeeze film
[DE88-701876] N88-26669
Interaction of biological systems with static and ELF electric and magnetic fields
[DE88-007951] N88-26792
Sources of polarized ions and atoms
[DE88-010910] N88-26931
Symmetrized magnetic field configuration of low aspect ratio helical system
[IPPJ-869] N88-26956
Thermal inhibition by megagauss field due to variation of electron temperature in laser plasma
[DE88-701887] N88-26977
Megagauss field variation along axis of wire target in laser produced plasma
[DE88-701895] N88-26979

MAGNETIC FLUX
Permanent magnet excitation of axial flow synchronous machines with high rotation moment
[ETN-88-92385] N88-26592

MAGNETIC MATERIALS
Novel magnetic materials research using free electron lasers
[DE88-009989] N88-26652

MAGNETIC PROPERTIES
Magneto-optical studies of GaInAs-InP quantum wells N88-27039
Influence of interfaces on electronic and magnetic properties of MnSe/ZnSe superlattices near monolayer limit N88-27050
Characterization of structural and magnetic order of Er/Y superlattices N88-27056

MAGNETIC SUSPENSION
Nutational stability of a satellite equipped with an active magnetic momentum wheel N88-26513

MAGNETICALLY TRAPPED PARTICLES
On the self-trapping of an electromagnetic wave in magnetized plasma
[DE88-701872] N88-26974

MAGNETO-OPTICS
Optical correlation using the magneto-optic device
[AD-A192342] N88-26950

MAGNETOHYDRODYNAMIC FLOW
Full-wave calculations in flux coordinates for toroidal geometry
[DE88-010131] N88-26985

MAGNETOHYDRODYNAMIC STABILITY
Modulational instability of electric helicons in a magnetized collisional plasma
[DE88-701885] N88-26976
Kinetic modulational instability of electron cyclotron waves in plasmas
[DE88-701893] N88-26978

MAGNETOHYDRODYNAMICS
Magnetohydrodynamic squeeze film
[DE88-701876] N88-26669
Proceedings of the 2nd US-Japan Workshop on Advanced Plasma Modeling, volume 3
[IPPJ-867] N88-26957
MACH2: A two-dimensional magnetohydrodynamic simulation code for complex experimental configurations
[AD-A192285] N88-26988

MAGNIFICATION
Application of magnification xeroradiography to advanced ceramics
[DE88-009965] N88-26473

MAINTENANCE
Mutually exclusive alternatives by clustering
[DE88-007707] N88-27115

MAN ENVIRONMENT INTERACTIONS
An efficient model for changes of global climate and composition of the atmosphere due to human activities
[ETN-88-92359] N88-26775

MAN MACHINE SYSTEMS
Preliminary study within a project for the development of intelligent assistance to piloting: Formal description of combat pilot expertise and implementation of an interactive system to represent operations
[CERMA-87-31] N88-26806
Interaction management in CAD systems with a history mechanism
[CWI-CS-R8756] N88-26851

MAN-COMPUTER INTERFACE
SIMS: Single Interface to Multiple Systems
[AD-A192264] N88-26832

MANAGEMENT METHODS
Overview of the TITAN-2 reversed-field pinch aqueous fusion power core design
[DE88-008170] N88-26966

MANAGEMENT PLANNING
Engine component retirement for cause. Volume 1: Executive summary
[AD-A192730] N88-26371
Managing microcomputer applications: A primer and guide to good practice
[AD-A192992] N88-26817

MANEUVERS
The effects of RCS jet firing on the isolated Orbiter and mated coast phases of the glide return to launch site maneuver at Mach number 6 (IA302B)
[NASA-CR-180223] N88-26403

MANGANESE ALLOYS
Reduced-activation austenitic stainless steels: The Fe-Cr-C system
[DE88-008091] N88-26442

MANIFOLDS (MATHEMATICS)
Linearization along invariant manifolds and a generalization of the Hartman-Grobman theorems for degenerate singularities of vector fields in R cubed
[REPT-87-80] N88-26886

MANIPULATORS
Mobile remote manipulator system for a tetrahedral truss
[NASA-CASE-MSC-20985-1] N88-26398
Design of a controller to reduce residual vibration in the positioning control of flexible robotic manipulators N88-26658
Optimization of performance criteria with bounded joint velocities for robots with one degree of redundancy
[DE88-003915] N88-26670
An introduction to robot joint control methods
[NLR-TR-86080-U] N88-26677
Simulation of space manipulator operations (EUROSIM)
[NLR-MP-87017-U] N88-26678
Experiments in adaptive control of a very flexible one link manipulator N88-26865

MANUALS
Technical instructions for a control operating system of the gas flow installation for the solid fuel combustion chamber
[LR-507] N88-26537

MANUFACTURING
Manufacturing of a ceramic-ceramic composite matrix using the sol-gel procedure
[ETN-88-92157] N88-26414
Preparation technology for thin film solid electrolyte fuel cells
[PB88-131925] N88-26735

MANY BODY PROBLEM
Spatial dynamics of deformable multibody systems with variable kinematic structure N88-26687
Atomistic simulation of stability, metastability and growth of strained layer structures N88-27053

MAPPING
Efficient bit-level, word-level and block-level systolic arrays for matrix-matrix multiplication
[DE88-011331] N88-26856

MARINE CHEMISTRY
Physical oceanography and tracer chemistry of the southern ocean
[DE88-006852] N88-26779

MARINE METEOROLOGY
Mariners weather log, volume 31, number 4, Fall 1987
[PB88-173851] N88-26761
Stability of a coastal upwelling front over topography
[AD-A192354] N88-26784

MARKING
Study of flow tracer behavior models and experimental validation with multiple exposure holographic velocimetry
[IMFL-87/30] N88-26622

MARKOV CHAINS
Colored stochastic Petri nets. Application to real time distributed systems
[ENST-87E017] N88-26643
Asymptotically efficient adaptive allocation schemes for controlled Markov chains: Finite parameter space
[AD-A192228] N88-26693
Markov chain computations to a solution of the mutual-exclusion problem in concurrency
[REPT-87-89] N88-26696

MARS (PLANET)
A bibliography of dunes: Earth, Mars, and Venus
[NASA-CR-4149] N88-27134

MASS
A Vlasov ion zero mass electron model for plasma simulations N88-26958

MASS SPECTROSCOPY
Laser desorption/ablation studies by resonance ionization mass spectrometry
[DE88-009124] N88-26650
Recent advances in atom-probe field ion microscopy
[DE88-008799] N88-27070

MASS TRANSFER
Parametric methodologies of cloud vertical transport for acid deposition models
[PB88-191374] N88-26762

MATERIALS HANDLING
RRSAS (Robotic Radiation Survey and Analysis System) Project: A real time sensor driven robotic system
[DE88-006825] N88-26661
Expert system application education project
[NASA-CR-183089] N88-26667

MATHEMATICAL MODELS
A numerical analysis of flow characteristics in laser propulsion system N88-26305
Finite element approximation to a model problem of transonic flow
[DE88-701835] N88-26333
Stiffness degradation of composite laminates N88-26405
Experimental and theoretical analysis of the radiative transfer within a sooty pool fire
[DE88-007099] N88-26419
A constitutive model with damage for high-temperature superalloys N88-26434
A numerical study of Rayleigh-Taylor instability in aluminum and steel plates
[DE88-010475] N88-26449
Numerical modeling of the effect of particle size of explosives on shock initiation properties
[DE88-010479] N88-26491
Dynamics of satellites with radial wire antennas N88-26514
Vertical ship motions and sea loads considering nonlinear effects
[TAE-592] N88-26515
Modeling and parameter identification of motor vehicles N88-26521
A two-point aerodynamic model for identification N88-26526
Utilization of identification methods in the time and frequency domain for the determination of the XV-15 (tilt-rotor) dynamics for lateral motion in hover flight N88-26532
A random access algorithm for environments with capture and limited feedback capabilities
[AD-A192233] N88-26552
Modeling and thermal management of advanced batteries
[DE88-010023] N88-26580
Microwave amplifiers
[AD-A192974] N88-26585
The Oak Ridge Heat Pump Design Model: Mark 3 version program documentationon
[DE88-007863] N88-26607
Nonlinear equation of state effects and the momentum-dilution trade-off in a turbulent buoyant jet
[DE88-701839] N88-26610
Axisymmetric liquid sloshing under low-g conditions: Numerical simulation method (reference manual)
[NLR-TR-86057-4] N88-26627
Vibration frequencies of tapered bars with nonclassical boundary conditions
[NASA-CR-183059] N88-26688
Microstructural effects in static and dynamic numerical experiments
[DE88-004289] N88-26690
Random vibration analysis of rattling structures
[DE88-007196] N88-26691
An assessment of modelling techniques for the finite element analysis of reinforced concrete plate and shell structures
[AD-A192263] N88-26697
Interpreting forest biome productivity and cover utilizing nested scales of image resolution and biogeographical analysis
[NASA-CR-183036] N88-26711
Surface hydrology, sediment transport dynamics and remote sensing of disturbed watersheds in a humid temperate region
[DE88-008719] N88-26715
Development of a model procedure for the determination of volume diffusion lengths by transient measurements on monocrystal silicon solar cells
[ETN-88-92119] N88-26733
Development of an atmospheric diffusion evaluation method incorporating topographical effects. Part 1: Literature review of atmospheric diffusion models incorporating terrain effects
[DE88-753104] N88-26742
Effects of a temperature-dependent rheology on large scale continental extension
[NASA-CR-183117] N88-26759
Parametric methodologies of cloud vertical transport for acid deposition models
[PB88-191374] N88-26762
Synoptic patterns related to tropical cyclone recurvature
[AD-A192338] N88-26771
Evaluation of surface energy and radiation balance systems for FIFE
[NASA-CR-183118] N88-26778
Prediction of continental shelf sediment transport using a theoretical model of the wave-current boundary layer
[AD-A192272] N88-26783
Stability of a coastal upwelling front over topography
[AD-A192354] N88-26784
Aircraft interior noise reduction by alternate resonance tuning
[NASA-CR-182540] N88-26909
A modal approach to Arctic noise modelling with implied vertical coherence
[AD-A192966] N88-26916
Proceedings of the 2nd US-Japan Workshop on Advanced Plasma Modeling, volume 3
[IPPJ-867] N88-26957
A Vlasov ion zero mass electron model for plasma simulations N88-26958
Modeling of subtle kinetic processes in plasma simulation N88-26959
Atomistic simulation of stability, metastability and growth of strained layer structures N88-27053
Superconductivity of Cr/V superlattices N88-27057

MATRICES (MATHEMATICS)
A diagonally inverted LU implicit multigrid scheme
[NASA-TM-100911] N88-26340
Eigenmatrix representations of radiance distributions in layered natural waters with wind-roughened surfaces
[PB88-188701] N88-26780
Computing small singular values of bidiagonal matrices with guaranteed high relative accuracy: LAPACK working note number 3
[DE88-008465] N88-26829
A matroid algorithm and its application to the efficient solution of two optimization problems on graphs, revision
[AD-A192709] N88-26838
Derivation of space groups in mm2, 222 and mmm crystal classes
[DE88-701881] N88-27076

MATRIX METHODS
Efficient bit-level, word-level and block-level systolic arrays for matrix-matrix multiplication
[DE88-011331] N88-26856

MATTER (PHYSICS)
Inelastic mean free paths of electrons and positrons in matter
[DE88-008086] N88-26929

MAXIMUM ENTROPY METHOD
A maximum entropy solution for the underdetermined electromagnetic field within a volume
[DE88-007020] N88-26550

MAXIMUM LIKELIHOOD ESTIMATES
System identification in vehicle dynamics
[DFVLR-MITT-87-22] N88-26518
Parameter estimation of dynamical systems N88-26519
Parametric estimation of aerodynamic nonlinearities in rolling moment due to sideslip using maximum likelihood method N88-26528
Tuning a major part of a clustering algorithm
[AD-A191446] N88-26821

MAXWELL EQUATION
Stochastic modeling of EM scattering from foliage
[AD-A192258] N88-26553

MEAN FREE PATH
Inelastic mean free paths of electrons and positrons in matter
[DE88-008086] N88-26929

MEASURING INSTRUMENTS
Surface temperature thermal fluxmeters for shock tubes
[NASA-TT-20319] N88-26381
Instrumentation for the measurement of penetrator dynamic response to permit force estimation
[DE88-010608] N88-26666

MECHANICAL PROPERTIES
Interface modification in Nicalon (trademark)/SiC composites
[DE88-009706] N88-26409
A constitutive model with damage for high-temperature superalloys N88-26434
Phase stability and alloy design of ordered intermetallics
[DE88-007479] N88-26435
Investigation of structure and surface state effect on hydrogen embrittlement of steels, under consideration of acoustic emission analysis
[ETN-88-92350] N88-26457
Application of electron microscopy for the analysis of the mechanical behavior of advanced ceramics
[DE88-005049] N88-26469
Resistance of polyamide-6 against long time effects of various media at various temperatures
[NASA-TT-20297] N88-26484
Polymerization of epoxy matrix composites using pulsed microwaves
[CERT-3/1324-MO] N88-26487
A finite element analysis for the hydroforming of aluminum
[DE88-008050] N88-26516
Electrodynamic driver for the space thermoacoustic refrigerator (STAR)
[AD-A192337] N88-26517
Research on the kinetics of phase changes in solids
[AD-A192222] N88-26696

MELTING POINTS
The crystallization of tough thermoplastic resins in the presence of carbon fibers
[NASA-CR-182984] N88-26464

MEMORY
Working memory capacity: An individual differences approach
[AD-A192359] N88-26803

MENTAL PERFORMANCE
Method for observing changes in functional state of human operator N88-26789

MERCURY TELLURIDES
MBE growth of HgTe/CdTe superlattices on Si(100) substrates N88-27033
Type 3 - type 1 transition and strain effect in Hg(1-x)Cd(x)Te-CdTe and Hg(1-x)Zn(x)Te-CdTe superlattices N88-27052

MESSAGE PROCESSING
A cockpit natural language study - selected transcripts
[AD-A192972] N88-26808
Relay approach message routing in hypercube multiprocessors
[DE88-009973] N88-26814

METABOLISM
Regulatory biochemical and metabolic responses in photoreceptors
[AD-A192898] N88-26794

METAL AIR BATTERIES
Crystallization of aluminum hydroxide in the aluminum-air battery: Literature review, crystallizer design and results of integrated system tests
[DE88-010510] N88-26594

METAL FILMS
Aharonov-Bohm effects in disordered metals N88-27008

METAL IONS
Field-enhanced lithium ion sources for PBFA 2
[DE88-007195] N88-26960

METAL MATRIX COMPOSITES
Fracture resistance of a TiB2 particle/SiC matrix composite at elevated temperature
[NASA-TM-100967] N88-26482

METAL OXIDE SEMICONDUCTORS
Extended and local plasmons in a lateral superlattice N88-27041

METAL OXIDES
Surface phases and their influence on metal-oxide interfaces
[DE88-007938] N88-26420
Defect characterization of the redox behavior and stability of conducting oxides
[DE88-010799] N88-27088

METAL PLATES
A numerical study of Rayleigh-Taylor instability in aluminum and steel plates
[DE88-010475] N88-26449
Analysis of the perforation of monolithic and simple laminate aluminium targets as a test of analytical deformation models
[MRL-R-1111] N88-26686
Vibration response of constrained viscoelastically damped plates: Analyses and experiments
[AD-A192329] N88-26699

METALLIC PLASMAS
Ultraviolet-visible spectroscopy of laser-produced aluminum plasmas
[AD-A193004] N88-26990

METALLIZING
Shock wave compression and metallization of simple molecules
[DE88-008031] N88-26925

METALLOGRAPHY
The adherence of nickel oxide on nickel during high temperature oxidation
[DE88-011194] N88-26450

METALS
Plastic deformation and roughness of free metal surfaces
[PB88-196621] N88-26439
Abnormal diffusion of vacancies in metals
[DE88-701880] N88-26441
Shock wave compression and metallization of simple molecules
[DE88-008031] N88-26925
Metallic superlattices N88-27012
Pure metallic bridge and point-contact tunneling into single- and polycrystal YBa2Cu3O(sub 7-y)
[DE88-010030] N88-27084

METEOROLOGICAL CHARTS
Mariners weather log, volume 31, number 4, Fall 1987
[PB88-173851] N88-26761
Meteorological atlas of the Southern Hemisphere lower stratosphere for August and September 1987
[NASA-TM-4049] N88-26763
The 1985 Meteorological Yearbook of Ispra (27th)
[PB88-125729] N88-26777

METEOROLOGICAL PARAMETERS
Effects of atmospheric model layering on LOWTRAN 6 calculations of 8-12 micrometers near-horizon sky radiances
[AD-A192969] N88-26559
The 1985 Meteorological Yearbook of Ispra (27th)
[PB88-125729] N88-26777

METEOROLOGICAL RADAR
Remote sensing of temperature profiles. Performance test of PASS
[DE88-753108] N88-26768
A radar study of the interaction between lightning and precipitation
[DE88-009120] N88-26770

METEOROLOGICAL SATELLITES
Satellite remote sensing of the wet bulb globe temperature heat stress index, phase 2
[AD-A192798] N88-26717

METEOROLOGY
Our climate in danger
[DE88-701824] N88-26743

METHANE
Probing the possibility of a (12)C/(13)C abundance gradient from observations of interstellar CH+
[DE88-008908] N88-27125

MICROBIOLOGY
Digital image processing from speckle interferograms by correlation methods: Application in atmospheric optics, astronomy, and biology
[ETN-88-92125] N88-26953

MICROBURSTS (METEOROLOGY)
Influence of wind shear on the aerodynamic characteristics of airplanes
[NASA-TP-2827] N88-26344
Control of flight through microburst wind shear using deterministic trajectory optimization N88-26375

MICROCHANNEL PLATES
An elliptical spectrograph/gated microchannel plate detector for time-resolved spectral measurements in the X-ray region
[DE88-007590] N88-26961

MICROCOMPUTERS
A microcomputer based frequency-domain processor for laser Doppler anemometry
[NASA-TM-100998] N88-26634
Managing microcomputer applications: A primer and guide to good practice
[AD-A192992] N88-26817
Design of high performance microcomputers for numerical data processing
[ETN-88-92371] N88-26818
A multiprocess operating system for 16 bit microcomputers or porting Unix (trademark) to a NS32016 with enhancements N88-26822

MICROCRACKS
Time-domain boundary element analysis of dynamic near-tip fields for impact-loaded collinear cracks
[AD-A192930] N88-26700

MICROCRYSTALS
Semiconductor microcrystallites in porous glass and their applications in optics N88-27005

MICROHARDNESS
Characterization of coating wear phenomena in nitride and carbide coated tool inserts
[DE88-011196] N88-26478

MICROMECHANICS
A micromechanics model of the stiffness and strength of laminates with fiber waviness
[NASA-CR-181670] N88-26413

MICROORGANISMS
Biodegradation of JP-5 aviation fuel by subsurface microbial communities
[AD-A192743] N88-26493

MICROPHONES
Outdoor sound propagation, its implications for unattended ground sensors
[FEL-1986-64] N88-26917

MICROPROCESSORS
FASTRUN phase sequencer descriptor language (PDL)
[DE88-007966] N88-26828
Mutually exclusive alternatives by clustering
[DE88-007707] N88-27115

MICROPROGRAMMING
The UMAC simulator N88-26811

MICROSCOPY
Recent advances in atom-probe field ion microscopy
[DE88-008799] N88-27070
Progress in diagnostic techniques for SC (superconducting) cavities
[DE88-008600] N88-27077

MICROSTRUCTURE
Initial development of high-temperature titanium silicide alloys
[DE88-007860] N88-26437
Helium induced degradation in the weldability of an austenitic stainless steel
[DE88-009062] N88-26443
The structure and properties of grain boundaries in B2 ordered alloys
[DE88-009890] N88-26447
Application of electron microscopy for the analysis of the mechanical behavior of advanced ceramics
[DE88-005049] N88-26469
Microstructural effects in static and dynamic numerical experiments
[DE88-004289] N88-26690
Third International Conference on Superlattices, Microstructures and Microdevices
[AD-A191416] N88-26995
Hot electron transistors grown by MOCVD N88-26996
Spectroscopy of one-dimensional subbands on InSb N88-27007
Metallic superlattices N88-27012
Quantum interference and transport in microstructures N88-27022
EXAFS studies of the microstructure of semiconductor alloys, defects and semiconductor-metal interfaces N88-27031
The theory of electron-polar phonon scattering rates in semiconductor micro-structures N88-27043
Influence of interfaces on electronic and magnetic properties of MnSe/ZnSe superlattices near monolayer limit N88-27050
Type 3 - type 1 transition and strain effect in Hg(1-x)Cd(x)Te-CdTe and Hg(1-x)Zn(x)Te-CdTe superlattices N88-27052

MICROWAVE AMPLIFIERS
Microwave amplifiers
[AD-A192974] N88-26585

MICROWAVE CIRCUITS
Analysis of networks with parameters S: Generalization of junction matrix
[INPE-4535-PRE/1282] N88-26570

MICROWAVE EQUIPMENT
Study and implementation of ultrahigh frequency coupling devices using the fin line technology — millimeter waves
[ETN-88-92307] N88-26588

MICROWAVE FREQUENCIES
Polymerization of epoxy matrix composites using pulsed microwaves
[CERT-3/1324-MO] N88-26487

MICROWAVE IMAGERY
Microwave image understanding and its application to radar cross section management N88-26542

MICROWAVE LANDING SYSTEMS
Development of an airborne facility for advanced avionics research
[NLR-MP-87012-U] N88-26368

MICROWAVE OSCILLATORS
Low noise cryogenic dielectric resonator oscillator
[NASA-CASE-NPO-17157-1-CU] N88-26596

MICROWAVE SCATTERING
Microwave amplifiers
[AD-A192974] N88-26585

MICROWAVE SENSORS
Microwave calibration system 2
[AD-A192976] N88-26639

MICROWAVES
Antenna heights for the optimum utilization of the oceanic evaporation duct. Part 3: Results from the Mediterranean measurements, volume 2
[AD-A192311] N88-26554
MTX (Microwave Tokamak Experiment) plasma diagnostic system
[DE88-011326] N88-26993

MIDAIR COLLISIONS
Aircraft accident report: Midair collision of SkyWest Airlines Swearingen METRO 2, N163SW, and Mooney M20, N6485U, Kearns, Utah, January 15, 1987
[PB88-910404] N88-26346

MIDDLE ATMOSPHERE
Diffusion of slight solar induced disturbances in the middle atmosphere
[MITT-53] N88-26758

MILITARY AIR FACILITIES
Vegetation studies on Vandenberg Air Force Base, California
[NASA-TM-100985] N88-26795

MILITARY OPERATIONS
NAVSTAR global positioning system
[AD-A192609] N88-26354
The strategic defense initiative: Strategic implications
[AD-A192341] N88-26902
Launch operations to support future space forces
[AD-A192679] N88-27107

MILITARY SPACECRAFT
Launch operations to support future space forces
[AD-A192679] N88-27107

MILKY WAY GALAXY
The velocity field of the outer galaxy
[B8681472] N88-27132

MILLIMETER WAVES
Study and implementation of ultrahigh frequency coupling devices using the fin line technology — millimeter waves
[ETN-88-92307] N88-26588

MINIATURIZATION
Tactical Rubidium Frequency Standard (TRFS), volume 1
[AD-A192981] N88-26640

MISMATCH (ELECTRICAL)
Atomistic simulation of stability, metastability and growth of strained layer structures N88-27053

MISSILE CONTROL
Optical data processing
[AD-A193024] N88-26841

MISSILE DEFENSE
A simulation of post boost vehicle deployment of multiple reentry vehicles
[DE88-009537] N88-26391
SDI: Myth or reality
[DE88-009121] N88-26901
An overview of the development of a linear broadband analog fiber-optic link
[DE88-008668] N88-26945

MISSILE DETECTION
A cockpit natural language study - selected transcripts
[AD-A192972] N88-26808

MISSILES
Launch operations to support future space forces
[AD-A192679] N88-27107

MISSION PLANNING
Flight Mechanics Panel Symposium on Rotorcraft Design for Operations: Technical evaluation report
[AGARD-AR-243] N88-26362

MIXERS
SIS (Superconductor-Insulator-Superconductor) mixer research
[AD-A192908] N88-27092

MODELS
Stochastic modeling of EM scattering from foliage
[AD-A192258] N88-26553
Modeling and optimum time performance for concurrent processing
[NASA-CR-4167] N88-26595
Numerical model for the computation of radiance distributions in natural waters with wind-roughened surfaces
[PB88-192703] N88-26765

Prediction of continental shelf sediment transport using a theoretical model of the wave-current boundary layer
[AD-A192272] N88-26783
Experimental study of planetary gases with applications to planetary interior models
[NASA-CR-183098] N88-27137

MODULATION
Kinetic modulational instability of electron cyclotron waves in plasmas
[DE88-701893] N88-26978

MODULATORS
Error performance of voice band data signals with an overloaded delta modulator
[FEL-1987-05] N88-26562

MOISTURE CONTENT
Studies of the mechanisms and rates with which nitrogen species are incorporated into cloud water and precipitation
[PB88-193065] N88-26764

MOLECULAR BEAM EPITAXY
Analysis of the performance of the space ultravacuum research facility in attached and free-flyer mode
[NASA-TM-100325] N88-26387
Integrated optoelectronic circuits utilizing InGaAsP grown by molecular beam epitaxy (erbium doping of MBE GaAs)
[AD-A192269] N88-26584
MBE growth of HgTe/CdTe superlattices on Si(100) substrates N88-27033
Preparation of high-T(sub)c Y1Ba2Cu3O(sub 7-Delta) superconducting thin films by MBE (Molecular-Beam-Epitaxy) techniques
[DE88-009999] N88-27082

MOLECULAR BEAMS
Electron-impact-ionization and electron-attachment cross sections of radicals important in transient gaseous discharges
[AD-A192248] N88-26424

MOLECULAR COLLISIONS
Low energy molecular collisions
[ISAS-RN-366] N88-26919

MOLECULAR GASES
Thermostatistical estimations of vapor-state molecules affected by gravity in a heat pipe N88-26505

MOLECULAR INTERACTIONS
Fast atom bombardment study on interaction of anticodonic nucleotides and their cognate amino acid
[ISAS-RN-355] N88-26918
Low energy molecular collisions
[ISAS-RN-366] N88-26919

MOLECULAR RELAXATION
Monte Carlo simulations of femtosecond relaxation of photoexcited electrons in AlGaAs/GaAs quantum wells N88-27036

MOLECULAR ROTATION
Low energy molecular collisions
[ISAS-RN-366] N88-26919

MOLECULAR STRUCTURE
High resolution spectroscopy of dissociating molecules
[DE88-007959] N88-26924

MOLECULES
Modeling the primary events of photosynthesis using chlorophyll containing fixed distance donor-acceptor molecules
[DE88-010033] N88-26793
Shock wave compression and metallization of simple molecules
[DE88-008031] N88-26925

MOLTEN SALT ELECTROLYTES
Molten salt electrolytes for high-temperature lithium cells
[DE88-010058] N88-26581

MOLTEN SALTS
Production of powdered sodium hydride with large specific surface by the catalyzed reaction of molten sodium with hydrogen-1
[NASA-TT-20185] N88-26462

MOLYBDENUM DISULFIDES
The effects of Hertzian stress and test ambient on the friction coefficient of MsS2 coatings
[DE88-008118] N88-26467

MOMENTS
Application of Moment Iteration Method (MIM) to electromagnetic field computation
[PB88-194139] N88-26546

MOMENTS OF INERTIA
A new method for the estimation of aircraft inertia characteristics N88-26530

MOMENTUM TRANSFER
Comparison of exclusive reactions at large momentum transfer
[DE88-007544] N88-26922

MONOCULAR VISION
Biorhythms of binocular vision N88-26768
A new approach to machine-based perception of monocular images
[DE88-002418] N88-26942

MONOMERS
Substituted 1,1,1-Triaryl-2,2,2-Trifluoroethanes and processes for their synthesis
[NASA-CASE-LEW-14345-1] N88-26404
Synthesis of model polymers and related structures in support of vinyl monomer grafting studies
[DE88-010245] N88-26476

MONTE CARLO METHOD
Rarefied gas numerical wind tunnel 3: Universal code for three dimensional bodies N88-26304
Statistical mechanics of polymer systems
[DE88-011172] N88-26477
Theoretical studies in elementary particle physics
[DE88-006929] N88-26926
Monte Carlo simulations of femtosecond relaxation of photoexcited electrons in AlGaAs/GaAs quantum wells N88-27036
Hot electrons in silicon dioxide: Ballistic to steady-state transport N88-27042
Recent applications of Monte Carlo methods for semiconductor microdevice simulation N88-27046
Atomistic simulation of stability, metastability and growth of strained layer structures N88-27053

MOON
A basis of settlement: Economic foundations of permanent pioneer communities
[DE88-010907] N88-26382

MOTION PERCEPTION
Image pyramid motion detection applied to sea ice N88-26713

MOTION SICKNESS
Significance of sensory signal phase mismatch in mechanisms of motion sickness development N88-26787

MOTION SIMULATION
Parameter identification of the passenger simulation model MADYMO: Methods and experience N88-26536

MOTION STABILITY
Stability of a coastal upwelling front over topography
[AD-A192354] N88-26784

MOTOR VEHICLES
System identification in vehicle dynamics
[DFVLR-MITT-87-22] N88-26518
Modeling and parameter identification of motor vehicles N88-26521
Identification methods for transport dynamical investigations N88-26531
Parameter identification of the passenger simulation model MADYMO: Methods and experience N88-26536

MULTIPATH TRANSMISSION
A random access algorithm for environments with capture and limited feedback capabilities
[AD-A192233] N88-26552
Description of the MPTR system: Multi Path Transmissometer Radiometer
[FEL-1987-14] N88-26954

MULTIPHASE FLOW
Study of a water-steam two phase flow in a T-branch
[ETN-88-92306] N88-26624

MULTIPROCESSING (COMPUTERS)
Cellular array processor CAP and its application to computer graphics N88-26327
A multiprocess operating system for 16 bit microcomputers or porting Unix (trademark) to a NS32016 with enhancements N88-26822
Definition of an auxiliary processor dedicated to real-time operating system kernels
[NASA-CR-183070] N88-26860
An evaluation methodology for dependable multiprocessors
[AD-A192799] N88-26863

MYOCARDIAL INFARCTION
Aircraft accident report: Joe Foster Excavating, Inc., Bell 206B, N49606, in-flight collision with trees, Alamo, California, August 3, 1986
[PB88-910405] N88-26345

N

N-TYPE SEMICONDUCTORS
Photovoltaic cells with n-silicon and conductive polymers
[ETN-88-92133] N88-26734
Electrical properties of p-type and n-type ZnSe-ZnTe strained-layer superlattices N88-27029

NASA PROGRAMS
Resources: NASA for entrepreneurs
[NASA-CR-182152] N88-27119

NATURAL GAS
Development of an equation of state for computation of supercompressibility factors, critical flow factors and other properties for wet, sour natural gases, synthetic gases and admixtures
[PB88-202676] N88-26602

NATURAL LANGUAGE (COMPUTERS)
A cockpit natural language study - selected transcripts
[AD-A192972] N88-26808

NAVIER-STOKES EQUATION
Finite element analysis of incompressible viscous flow around multi-element aerofoils N88-26294
Numerical calculation of supersonic flow by the PNS equations N88-26296
Navier-Stokes analysis of transonic transport aircraft empennage N88-26297
Numerical calculation of three dimensional flow by TVD scheme N88-26309
Numerical analysis of three dimensional cascade flow by solving Navier-Stokes equations N88-26310
Numerical analysis of duct flow using three-dimensional parabolized Navier-Stokes equation N88-26312
Vortex methods for separated flows
[NASA-TM-100068] N88-26342
Numerical analysis of reconnection of vortex rings N88-26500
Navier-Stokes simulation of shock-tube flows over a wedge-type step by finite volume method
[ISAS-RN-828] N88-26599
Spectral resolution of the Navier-Stokes equations in multi-domain curved complex geometries
[ONERA-NT-1987-2] N88-26631

NAVIGATION
Aircraft accident report: Midair collision of SkyWest Airlines Swearingen METRO 2, N163SW, and Mooney M20, N6485U, Kearns, Utah, January 15, 1987
[PB88-910404] N88-26346
Treatment of systematic errors in the processing of wide angle sonar sensor data for robotic navigation
[DE88-008961] N88-26352
Spacecraft applications of advanced global positioning system technology
[NASA-CR-172063] N88-26359
Sensor fusion for robot navigation
[DE88-008383] N88-26663

NAVIGATION AIDS
Geographical information for design purposes
[NLR-MP-87014-U] N88-26719

NAVIGATION INSTRUMENTS
Simple 2-D navigation for wheeled vehicles
[DE88-007115] N88-26351

NAVSTAR SATELLITES
NAVSTAR global positioning system
[AD-A192609] N88-26354

NAVY
Analysis of gas turbine test cell number 1, Lemoore Naval Air Station, California
[AD-A192870] N88-26380

NEAR WAKES
Influence of rear body geometry on the velocity characteristics of the near wake
[ISL-R-113/87] N88-26339

NEGATIVE IONS
Development of high current and high brightness negative hydrogen ion sources
[DE88-010882] N88-26934

NEGATIVE RESISTANCE DEVICES
Quantum transport theory of resonant-tunneling heterostructure devices N88-27017
Resonant tunneling transistors and resonant tunneling hot electron spectroscopy N88-27018
Excellent negative differential resistance of InGaAs/InAlAs resonant tunneling barrier structures and applications to a new functional device, RHET N88-27048

NETWORK ANALYSIS
Analysis of networks with parameters S: Generalization of junction matrix
[INPE-4535-PRE/1282] N88-26570
A network approach to the certainty factor model --- expert systems
[CWI-CS-R8757] N88-26852

NEURAL NETS
A linear-programming method inspired by the neural networks framework
[DE88-008688] N88-26862

NEUTRAL BEAMS
Requirements for neutral beam current drive in tokamaks
[DE88-006180] N88-26980

NEUTRON BEAMS
Tracking a monochromatic light source
[DE88-011260] N88-26853

NEUTRON CROSS SECTIONS
Nucleon-nucleus interaction data base: Total nuclear and absorption cross sections
[NASA-TM-4053] N88-26935
NEUTRON DIFFRACTION
Observations on residual stresses in ceramic composites by neutron diffraction techniques
[DE88-009937] N88-26472
NEUTRON STARS
Detection of absorption lines in the spectra of X-ray bursts from X1608-52
[ISAS-RN-360] N88-27143
NEUTRONS
Observation of ferromagnetism in ultrathin f.c.c. films by spin polarised neutron reflection N88-27015
NICKEL
Performance of lightweight nickel electrodes
[NASA-TM-100958] N88-26430
Grain boundary structure in NiAl
[DE88-009164] N88-26444
The adherence of nickel oxide on nickel during high temperature oxidation
[DE88-011194] N88-26450
NICKEL ALLOYS
Glass forming ranges of amorphous alloys
[DE88-007897] N88-26438
Precipitation study by electrical resistivity measurement in Ni-Al alloys
[DE88-701877] N88-26440
Shape memory alloys: New materials for future engineering
[NASA-TT-20193] N88-26455
The preparation of mechanically alloyed powders for TEM (Transmission Electron Microscopy) examination
[DE88-008043] N88-26460
Nickel aluminides: A new family of nickel + aluminum alloys featuring simple composition, low density, excellent oxidation resistance and high yield strength that increases with temperature
[DE88-010692] N88-26461
NICKEL HYDROGEN BATTERIES
Performance of lightweight nickel electrodes
[NASA-TM-100958] N88-26430
Nickel hydrogen cell positive-electrode studies: Cobalt segregation in reducing environments
[AD-A193025] N88-26587
NICKEL OXIDES
The adherence of nickel oxide on nickel during high temperature oxidation
[DE88-011194] N88-26450
NIOBIUM
Rocket-propellant burn tests of silicide-coated niobium and tantalum
[DE88-010729] N88-26496
NIOBIUM ALLOYS
The preparation of mechanically alloyed powders for TEM (Transmission Electron Microscopy) examination
[DE88-008043] N88-26460
NITRATES
Studies of the mechanisms and rates with which nitrogen species are incorporated into cloud water and precipitation
[PB88-193065] N88-26764
NITRATION
Research in energetic compounds
[AD-A192953] N88-26494
NITROGEN
Thermal conductivity of selected foams and systems from 100 to 300 K
[PB88-201553] N88-26466
A shock-tube experiment on gases mixing processes associated with CO2/N2 mixing gasdynamic laser
[ISAS-RN-350] N88-26598
NODES (STANDING WAVES)
A nodal method for time-dependent transport equation
[DE88-004285] N88-26876
NOISE (SOUND)
A modal approach to Arctic noise modelling with implied vertical coherence
[AD-A192966] N88-26916
NOISE INTENSITY
Sound power measurements in situ using a reference sound source
[PB88-182571] N88-26910
NOISE MEASUREMENT
Sound power measurements in situ using a reference sound source
[PB88-182571] N88-26910
NOISE PROPAGATION
Sound propagation over uneven ground and irregular topography
[NASA-CR-182956] N88-26911
NOISE REDUCTION
Signal processing in digital speech transmission systems
[ETN-88-92122] N88-26561
A review of gear housing dynamics and acoustics literature
[NASA-CR-183110] N88-26675
Aircraft interior noise reduction by alternate resonance tuning
[NASA-CR-182540] N88-26909
NOISE SPECTRA
Sound power measurements in situ using a reference sound source
[PB88-182571] N88-26910
NONDESTRUCTIVE TESTS
Sensitivity to crack initiation in thick assemblies. Test report 48-444
[REPT-48-444] N88-26385
Microfocus X-ray techniques for flaw location
[DE88-008636] N88-26680
Development of an automated X-ray gauge for nondestructive quantitative analysis
[DE88-008633] N88-26681
Methods and techniques of NDA (nondestructive assay)
[DE88-009145] N88-26682
Principles of a nondestructive evaluation process for damage location, damage profile, and damage extension in welded joints by radiometric measurements
[MPA-86-02] N88-26683
Stress analysis using infrared thermography
[ETN-88-92169] N88-26705
NONEQUILIBRIUM CONDITIONS
Non-equilibrium phases and phase diagrams
[DE88-008896] N88-27098
NONLINEAR EQUATIONS
Nonlinear equation of state effects and the momentum-dilution trade-off in a turbulent buoyant jet
[DE88-701839] N88-26610
NONLINEAR OPTICS
Liquid crystal optics for laser systems
[DE88-008475] N88-26948
NONLINEAR PROGRAMMING
Conditions for finite convergence of algorithms for nonlinear programs and variational inequalities
[AD-A192355] N88-26834
NONLINEAR SYSTEMS
Parametric estimation of aerodynamic nonlinearities in rolling moment due to sideslip using maximum likelihood method N88-26528
Identification of lateral operation dynamics of rail vehicles using roll test stand tests N88-26534
Nonlinear identification of an aircraft for the direct calculation of an anticipatory control N88-26535
Studying materials using acoustic waves
[AD-A192234] N88-26915
NONLINEARITY
Finite element welding computations using general purpose nonlinear analysis codes
[DE88-005398] N88-26659
Comparison theorems and their use in the analysis of some nonlinear diffusion problems
[DE88-010032] N88-26884
Ultrafast optical nonlinearity in quantum well structures with electric field N88-27003
Nonlinear materials for frequency conversion
[DE88-008343] N88-27067
NORTH DAKOTA
Feasibility of producing jet fuel from GPGP (Great Plains Gasification Plant) by-products
[DE88-010233] N88-26492
NUCLEAR EXPLOSIONS
Acute radiation syndromes and their management
[DE88-009839] N88-26797
NUCLEAR FUEL ELEMENTS
Methods and techniques of NDA (nondestructive assay)
[DE88-009145] N88-26682
NUCLEAR FUELS
The hole of a blanket tritium system on the fusion fuel cycle
[DE88-010007] N88-26983
NUCLEAR FUSION
Fusion programs in applied plasma physics and development and technology at GA Technologies, Inc.
[DE88-008406] N88-26964
Overview of the TITAN-2 reversed-field pinch aqueous fusion power core design
[DE88-008170] N88-26966
NUCLEAR INTERACTIONS
Nucleon-nucleus interaction data base: Total nuclear and absorption cross sections
[NASA-TM-4053] N88-26935
NUCLEAR MAGNETIC RESONANCE
Determination of binder distributions in green-state ceramics by NMR imaging
[DE88-009990] N88-26474
NUCLEAR MODELS
Development of nuclear models for higher energy calculations
[DE88-010919] N88-26932
NUCLEAR REACTIONS
Automated system for mathematical processing of the data from a hybrid spectrometer
[DE87-702995] N88-26820
Development of nuclear models for higher energy calculations
[DE88-010919] N88-26932
NUCLEAR REACTORS
Principles of a nondestructive evaluation process for damage location, damage profile, and damage extension in welded joints by radiometric measurements
[MPA-86-02] N88-26683
Fusion programs in applied plasma physics and development and technology at GA Technologies, Inc.
[DE88-008406] N88-26964
TIBER (Tokamak Ignition/Burn Experimental Reactor) 2 as a precursor to an international thermonuclear experimental reactor
[DE88-008906] N88-26970
NUCLEAR VULNERABILITY
The strategic defense initiative: Strategic implications
[AD-A192341] N88-26902
NUCLEAR WEAPONS
An agenda for the strategic defense initiative
[RAND-P-7404] N88-26898
Monitoring space weaponry: Detection and verification issues
[DE88-008726] N88-26900
SDI and/or arms control
[RAND-P-7357] N88-26903
NUCLEATE BOILING
Forced-convective boiling in small diameter tube N88-26510
NUCLEOTIDES
Fast atom bombardment study on interaction of anticodonic nucleotides and their cognate amino acid
[ISAS-RN-355] N88-26918
NUMERICAL ANALYSIS
Analysis of gas turbine test cell number 1, Lemoore Naval Air Station, California
[AD-A192870] N88-26380
Numerical analysis of reconnection of vortex rings N88-26500
Numerical solution of weak forms of conservation laws on optimal unstructured triangular grids N88-26597
Navier-Stokes simulation of shock-tube flows over a wedge-type step by finite volume method
[ISAS-RN-628] N88-26599
A numerical simulation of two-dimensional transient shear flow
[ISAS-RN-627] N88-26600
Off-boundary approach to the boundary element method
[AD-A192931] N88-26701
Numerical model for the computation of radiance distributions in natural waters with wind-roughened surfaces
[PB88-192703] N88-26765
Prediction of continental shelf sediment transport using a theoretical model of the wave-current boundary layer
[AD-A192272] N88-26783
Superconductivity of Cr/V superlattices N88-27057
NUMERICAL INTEGRATION
Analysis of gas turbine test cell number 1, Lemoore Naval Air Station, California
[AD-A192870] N88-26380
NUMERICAL STABILITY
Semilinear elliptic problems on domains with corners
[REPT-87-83] N88-26888
Two classes of self-similar stable processes with stationary increments
[AD-A192842] N88-26894
NUTATION DAMPERS
Nutational stability of a satellite equipped with an active magnetic momentum wheel N88-26513

O

OBJECT PROGRAMS
Towards knowledge bases-semantics, rules and object-oriented programming
[PB88-108154] N88-27110
OCEAN CURRENTS
Survey on utility technology of a tidal and ocean current energy
[DE88-770148] N88-26722
OCEAN DYNAMICS
Physical oceanography and tracer chemistry of the southern ocean
[DE88-006852] N88-26779

OCEANOGRAPHY
Mariners weather log, volume 31, number 4, Fall 1987
[PB88-173851] N88-26761
Physical oceanography and tracer chemistry of the southern ocean
[DE88-006852] N88-26779
OPERATOR PERFORMANCE
Method for observing changes in functional state of human operator N88-26789
OPERATORS (MATHEMATICS)
Canonical construction of differential operators intertwining representations of real semisimple Lie groups
[DE88-701852] N88-26882
Theory of pseudo-differential operators over C*-algebras
[DE88-701860] N88-26883
OPTICAL COMMUNICATION
Fiber optics for advanced aircraft
[NASA-TM-101294] N88-26328
New semiconductor laser structure for an optical communication system
[ETN-88-92353] N88-26654
Use of fiber optic equipment for security
[DE88-007898] N88-26943
OPTICAL DATA PROCESSING
Optical data processing
[AD-A193024] N88-26841
OPTICAL EQUIPMENT
Use of fiber optic equipment for security
[DE88-007898] N88-26943
In-situ reactive of X-ray optics by glow discharge
[DE88-009840] N88-26947
Fabrication technology
[DE88-010598] N88-26955
Novel quantum well optical devices N88-27028
OPTICAL FIBERS
Stress-related phenomena in transient radiation-induced absorption in optical fibers
[DE88-010956] N88-26949
OPTICAL FILTERS
Optical correlation using the magneto-optic device
[AD-A192342] N88-26950
OPTICAL MEASURING INSTRUMENTS
Fiber optics for advanced aircraft
[NASA-TM-101294] N88-26328
OPTICAL PROPERTIES
Development of liquid metal field-emission sources for use in fast repetitive opening switches
[AD-A192230] N88-26583
Interferometric recording of holographic optical elements using partially coherent light N88-26636
Optical coatings for high average power XeF lasers
[DE88-011356] N88-26656
Determination and application of bidirectional solar-optical properties of fenestration systems
[DE88-010364] N88-26727
Stress-related phenomena in transient radiation-induced absorption in optical fibers
[DE88-010956] N88-26949
Ultrafast optical nonlinearity in quantum well structures with electric field N88-27003
Semiconductor microcrystallites in porous glass and their applications in optics N88-27005
Properties of multilayers for soft X-ray optics N88-27025
Magneto-optical studies of GaInAs-InP quantum wells N88-27039
On a-Si:H/a-SiN(x):H superlattices: Confinement or contamination N88-27040
OPTICAL PUMPING
Sources of polarized ions and atoms
[DE88-010910] N88-26931
Far-infrared studies of doped AlGaAs/GaAs multiple-quantum-well structures N88-26998
OPTICAL RESONANCE
Laser desorption/ablation studies by resonance ionization mass spectrometry
[DE88-009124] N88-26650
OPTICAL SCANNERS
Development of an automated X-ray gauge for nondestructive quantitative analysis
[DE88-009633] N88-26681
OPTICAL TRACKING
Tracking a monochromatic light source
[DE88-011260] N88-26653
OPTIMIZATION
Structural optimization of fiber composite turbomachine blades
[ETN-88-92351] N88-26372
Modeling and optimum time performance for concurrent processing
[NASA-CR-4167] N88-26595
Optimization of performance criteria with bounded joint velocities for robots with one degree of redundancy
[DE88-003915] N88-26670
A matroid algorithm and its application to the efficient solution of two optimization problems on graphs, revision
[AD-A192709] N88-26838
Using common subexpressions to optimize multiple queries
[DE88-008210] N88-26877
Combining expert opinions: An optimization framework
[REPT-87-84] N88-26895
Visible tunable source
[DE88-006442] N88-26944
ORBITAL ASSEMBLY
Mobile remote manipulator system for a tetrahedral truss
[NASA-CASE-MSC-20985-1] N88-26398
ORDER-DISORDER TRANSFORMATIONS
The structure and properties of grain boundaries in B2 ordered alloys
[DE88-009890] N88-26447
Ordering transitions of ternary alloys A(1-x)B(x)C N88-27054
Defects and disorder in amorphous and damaged silicon
[AD-A192277] N88-27089
ORR-SOMMERFELD EQUATIONS
Solution of the Orr-Sommerfeld equation for the Blausius boundary-layer documentation of program ORRBL and a test case
[NASA-CR-4169] N88-26858
OXIDATION
The adherence of nickel oxide on nickel during high temperature oxidation
[DE88-011194] N88-26450
Research in energetic compounds
[AD-A192953] N88-26494
OXIDATION-REDUCTION REACTIONS
Oxygen reduction in fuel cell electrolytes
[DE88-008240] N88-26723
Defect characterization of the redox behavior and stability of conducting oxides
[DE88-010799] N88-27088
OXIDE FILMS
Superconducting electronic film structures
[AD-A192907] N88-27091
OXIDES
Development of protective coatings for ceramic tubular components
[PB88-197165] N88-26463
Preparation of oxide superconductors
[DE88-009136] N88-27063
Phenomenological approach to high T/sub c/ oxide superconductors
[DE88-701868] N88-27074
OXYGEN
In situ spectroscopic studies of transition metal macrocycles as catalysts for the electrochemical reduction of oxygen
[PB88-203195] N88-26416
Electrocatalysts for oxygen electrodes
[DE88-008397] N88-26724
The superconducting transition in oxygen deficient YBa2Cu3O(sub 7-Delta)
[DE88-009957] N88-27079
Oxygen vacancy ordering and superconductivity in YBa2Cu3O(sub 7-x)
[DE88-010005] N88-27083
OXYGEN PRODUCTION
Photosynthetic water splitting
[DE88-007809] N88-26791
OXYGEN TENSION
Respiration and oxygen tension in the blood of animals exposed to high pressures N88-26790
OZONE DEPLETION
Meteorological atlas of the Southern Hemisphere lower stratosphere for August and September 1987
[NASA-TM-4049] N88-26763

P

P-TYPE SEMICONDUCTORS
Electrical properties of p-type and n-type ZnSe-ZnTe strained-layer superlattices N88-27029
PALLADIUM
Electronic and geometric structure of silver and palladium on aluminum (111) in monoatomic surface layers
[ETN-88-92120] N88-27093
PANEL METHOD (FLUID DYNAMICS)
On the dynamic behavior of balloon during its launch; application of panel method and extension to unsteady problem
[ISAS-RN-622] N88-26330
PARABOLIC DIFFERENTIAL EQUATIONS
Numerical calculation of supersonic flow by the PNS equations N88-26296
Numerical analysis of duct flow using three-dimensional parabolized Navier-Stokes equation N88-26312
Accurate solution of parabolic equations by expansion in ultraspherical polynomials
[DE88-701829] N88-26880
PARALLEL PROCESSING (COMPUTERS)
Cellular array processor CAP and its application to computer graphics N88-26327
Parallelization on a multiprocessor system of a solution method for the unsteady Navier-Stokes equations at high Reynolds numbers
[ONERA-NT-1987-8] N88-26832
Computer science research, 1987: Computation Directorate
[DE88-008637] N88-26812
The performance of the NEC SX-2 and Cray X-MP supercomputers
[DE88-009177] N88-26813
Efficient bit-level, word-level and block-level systolic arrays for matrix-matrix multiplication
[DE88-011331] N88-26856
Extensible networks. Part 1: Principles and constructions
[REPT-87-91-PT-1] N88-26864
The scaled-sized model: A revision of Amdahl's law
[DE88-008114] N88-26875
PARAMETER IDENTIFICATION
System identification in vehicle dynamics
[DFVLR-MITT-87-22] N88-26518
Parameter estimation of dynamical systems N88-26519
Flight vehicle system identification: Status and prospects N88-26520
Modeling and parameter identification of motor vehicles N88-26521
Parametric estimation of aerodynamic nonlinearities in rolling moment due to sideslip using maximum likelihood method N88-26528
Flight test preparation and measuring data validation for parameter identification N88-26529
Application of complementary parameter identification techniques to flight test data of a transport aircraft N88-26533
Parameter identification of the passenger simulation model MADYMO: Methods and experience N88-26536
PARAMETERIZATION
Parametric methodologies of cloud vertical transport for acid deposition models
[PB88-191374] N88-26762
Lattice strain in heteroepitaxial films N88-27032
PARSING ALGORITHMS
Programmer-friendly LL(1) parser generator
[PB88-126933] N88-26857
PARTIAL DIFFERENTIAL EQUATIONS
Computer science research, 1987: Computation Directorate
[DE88-008637] N88-26812
Nontrivial critical points for asymptotically quadratic function
[DE88-101851] N88-26881
PARTIAL PRESSURE
Phase transformations and thermodynamic behavior of the YBa2Cu3O(sub)x system via EMF measurements
[DE88-010054] N88-27086
PARTICLE ACCELERATOR TARGETS
Development of nuclear models for higher energy calculations
[DE88-010919] N88-26932
PARTICLE ACCELERATORS
Computer programs for high-current beam transport in accelerators
[AD-A192356] N88-26835
Superconducting rf and beam-cavity interactions
[DE88-008598] N88-26936
PARTICLE BEAMS
Electron-impact-ionization and electron-attachment cross sections of radicals important in transient gaseous discharges
[AD-A192248] N88-26424
Computer programs for high-current beam transport in accelerators
[AD-A192356] N88-26835
PARTICLE COLLISIONS
Charged pion production and projectile breakup in 85A MeV(sup)12C induced heavy ion reactions
[LUIP-8802] N88-26920
PARTICLE DENSITY (CONCENTRATION)
Quantitative particle characterization by scattered ultrasound N88-26908
PARTICLE ENERGY
Inelastic two composite particle systems scattering at high energy
[DE88-701841] N88-26928
PARTICLE IN CELL TECHNIQUE
The modified-fluid-in-cell method to which adaptive mesh and multigrid were applied N88-26324

Computer programs for high-current beam transport in accelerators
[AD-A192356] N88-26835
PARTICLE INTERACTIONS
Ion and electron interactions of atmospheric importance
[AD-A192255] N88-26751
Charged pion production and projectile breakup in 85A MeV(sup)12C induced heavy ion reactions
[LUIP-8802] N88-26920
Comparison of exclusive reactions at large momentum transfer
[DE88-007544] N88-26922
Inelastic two composite particle systems scattering at high energy
[DE88-701841] N88-26928
Recoil saturation of the self-energy in atomic systems
[DE88-010450] N88-26930
PARTICLE PRODUCTION
Charged pion production and projectile breakup in 85A MeV(sup)12C induced heavy ion reactions
[LUIP-8802] N88-26920
PARTICLE SIZE DISTRIBUTION
The preparation of mechanically alloyed powders for TEM (Transmission Electron Microscopy) examination
[DE88-008043] N88-26460
Numerical modeling of the effect of particle size of explosives on shock initiation properties
[DE88-010479] N88-26491
PARTICLES
The influence of foreign particles on bearing metals
[NASA-TT-20155] N88-26454
Reducing adhesion and agglomeration within a cloud of combustible particles
[NASA-TM-100902] N88-26539
Research in theoretical particle physics
[DE88-008230] N88-26927
On linear relationship between shock velocity and particle velocity
[DE88-701827] N88-27099
PASSENGER AIRCRAFT
Enhanced emergency smoke venting
[DOT/FAA/CT-88/22] N88-26350
PASSIVITY
Experimental and theoretical investigation of passive damping concepts for member forced and free vibration
[NASA-CR-183082] N88-26693
PATTERN RECOGNITION
Treatment of systematic errors in the processing of wide angle sonar sensor data for robotic navigation
[DE88-008961] N88-26352
Synoptic patterns related to tropical cyclone recurvature
[AD-A192338] N88-26771
Optical data processing
[AD-A193024] N88-26841
Optical correlation using the magneto-optic device
[AD-A192342] N88-26950
PEEK
The crystallization of tough thermoplastic resins in the presence of carbon fibers
[NASA-CR-182984] N88-26464
Compression creep of filamentary composites
[NASA-CR-182550] N88-26601
PENALTY FUNCTION
Velocity-pressure integrated versus penalty finite element methods for high Reynolds number flows
[NASA-CR-179357] N88-26635
PENETRATION
Instrumentation for the measurement of penetrator dynamic response to permit force estimation
[DE88-010608] N88-26666
GTAW characterization for weld penetration on 304L stainless steel
[DE88-010611] N88-26672
Study of comet nucleus gamma-ray spectrometer penetration system
[NASA-CR-177393] N88-27120
PERCEPTION
The interaction of sensory and perceptual variables: Spatial, temporal and orientation response to figure and ground
[AD-A192897] N88-26798
PERFORATED PLATES
Dynamical stress concentration problems, from every side, bordered and perforated plates
[ETN-88-92128] N88-26703
PERFORATION
Analysis of the perforation of monolithic and simple laminate aluminium targets as a test of analytical deformation models
[MRL-R-1111] N88-26686
PERFORMANCE PREDICTION
Prediction of fatigue growth
[NLR-MP-87052-U] N88-26707
PERFORMANCE TESTS
Hover performance tests of baseline metal and Advanced Technology Blade (ATB) rotor systems for the XV-15 tilt rotor aircraft
[NASA-CR-177436] N88-26367
Digital communication transmitter and receiver test procedures
[AD-A191218] N88-26540
Computer controlled procedures for traction battery power performance tests
[ETN-88-92352] N88-26589
Evaluation of thermophosphor temperature technique
[DE88-007654] N88-26638
Testing of a gravimeter LCR G 785
[B8735061] N88-26643
Automated system for mathematical processing of the data from a hybrid spectrometer
[DE87-702995] N88-26820
The evaluation of a deformable diffraction grating for a stigmatic EUV spectroheliometer
[NASA-CR-183064] N88-26941
Plasma armature formation in high-pressure, high-velocity hydrogen
[DE88-008347] N88-26967
PERIODICALS
Wind Energy Technology: Generating power from the wind, a current awareness bulletin
[DE88-008292] N88-26729
PERIPHERAL EQUIPMENT (COMPUTERS)
Definition of an auxiliary processor dedicated to real-time operating system kernels
[NASA-CR-183070] N88-26860
PERMEABILITY
Characteristics of pressure loss during filtration using a porous ceramic filter
[DE88-752547] N88-26604
PERSONNEL SELECTION
USAF flying screening: First step on the road to wings
[AD-A192613] N88-26804
PERTURBATION
An initial investigation into methods of computing transonic aerodynamic sensitivity coefficients
[NASA-CR-183061] N88-26332
PERTURBATION THEORY
On the propagating speed in difference approximations for conservation laws N88-26318
Magnetohydrodynamic squeeze film
[DE88-701876] N88-26669
Recoil saturation of the self-energy in atomic systems
[DE88-010450] N88-26930
PETN
Freely expanding detonation products: Scaling of rate processes
[DE88-007827] N88-26606
PETRI NETS
Colored stochastic Petri nets. Application to real time distributed systems
[ENST-87E017] N88-26843
PHARMACOLOGY
JPRS report: Science and technology. USSR: Life sciences
[JPRS-ULS-88-009] N88-26785
Does dihydroergotamine used in therapeutical doses influence the physical and psychomotor performance of young pilots or other traffic drivers subjected to hypotonia?
[ETN-88-92136] N88-26799
PHASE CONTROL
Active phase compensation system for fiber optic holography
[NASA-TM-101295] N88-26641
PHASE DIAGRAMS
Non-equilibrium phases and phase diagrams
[DE88-008895] N88-27098
PHASE ERROR
Coherent RF error statistics
[AD-A193002] N88-26560
PHASE LOCKED SYSTEMS
Contribution to speed regulation of small motors with phase-locked loops
[ETN-88-92373] N88-26590
PHASE MATCHING
Significance of sensory signal phase mismatch in mechanisms of motion sickness development N88-26787
PHASE SHIFT KEYING
Error performance of voice band data signals with an overloaded delta modulator
[FEL-1987-05] N88-26562
PHASE TRANSFORMATIONS
Refractory Materials of Zirconate. Part 2: Synthesis and some properties of strontium, zirconate, calcium zirconate and barium zirconate
[NASA-TT-20186] N88-26483
Fluid dynamical model of ultrarelativistic heavy ion collisions
[DE88-007905] N88-26921
The electronic structure of condensed molecular systems
[DE88-007823] N88-26923
Shock wave compression and metallization of simple molecules
[DE88-008031] N88-26925
Phase transformations and thermodynamic behavior of the YBa2Cu3O(sub)x system via EMF measurements
[DE88-010054] N88-27086
PHASED ARRAYS
Proceedings of the Array Signal Processing Symposium: Treaty Verification Program
[DE88-008346] N88-26548
PHONONS
Phonons in semiconductor superlattices N88-27035
Monte Carlo simulations of femtosecond relaxation of photoexcited electrons in AlGaAs/GaAs quantum wells N88-27036
PHOSPHATES
Growth and characterization of thin films of ZnSnP(sub)2
[DE88-001164] N88-27060
PHOSPHORIC ACID FUEL CELLS
Phosphoric acid electric utility fuel cell technology development
[DE88-010187] N88-26582
PHOSPHORUS
Evaluation of thermophosphor temperature technique
[DE88-007654] N88-26638
PHOTOCHEMICAL REACTIONS
Ultraviolet geometric albedo of Uranus
[NASA-CR-183099] N88-27136
PHOTOCONDUCTIVITY
Control of carrier lifetime in PbTe nipi superlattices by external photoinjection N88-27006
Pressure-dependent measurement on n+ GaAs (Si, Sn): The effect of deep donor (DX) states on the electrical properties and presistent photoconductivity effects N88-27020
Magneto-optical studies of GaInAs-InP quantum wells N88-27039
PHOTOELECTRIC CELLS
Photovoltaic cells with n-silicon and conductive polymers
[ETN-88-92133] N88-26734
PHOTOELECTRICITY
Defects in high-mobility semiconductor systems
[AD-A192298] N88-27090
PHOTOELECTRON SPECTROSCOPY
Electronic and geometric structure of silver and palladium on aluminum (111) in monoatomic surface layers
[ETN-88-92120] N88-27093
PHOTOGRAPHIC EQUIPMENT
Trajectory measurement of the Fokker 100 aircraft during autoland testing
[NLR-MP-86010-U] N88-26366
PHOTOLUMINESCENCE
Raman, photoluminescence and modulation spectroscopy of semiconductor heterostructures N88-26997
Magneto-optical studies of GaInAs-InP quantum wells N88-27039
Photoluminescence studies of InGaAlAs quaternary alloys
[DE88-007197] N88-27062
PHOTOLYSIS
Photosynthetic water splitting
[DE88-007809] N88-26791
PHOTOMETERS
A survey of the Ap stars for rapid variability N88-27127
PHOTOMICROGRAPHY
Microstructural effects in static and dynamic numerical experiments
[DE88-004289] N88-26690
PHOTONS
Third International Conference on Superlattices, Microstructures and Microdevices
[AD-A191416] N88-26995
Infrared detectors based on the photon drag effect and intersubband absorption by a two-dimensional electron gas N88-27024
PHOTORECEPTORS
Regulatory biochemical and metabolic responses in photoreceptors
[AD-A192898] N88-26794
PHOTOSYNTHESIS
Mechanisms of photochemical energy conversion by chlorophyll
[DE88-008763] N88-26725
Photosynthetic water splitting
[DE88-007809] N88-26791

Modeling the primary events of photosynthesis using chlorophyll containing fixed distance donor-acceptor molecules
[DE88-010033] N88-26793
PHOTOVOLTAIC CELLS
Advanced photovoltaic power system technology for lunar base applications
[NASA-TM-100965] N88-26402
Photovoltaic concentrator technology: Recent results
[DE88-009588] N88-26726
Photovoltaic cells with n-silicon and conductive polymers
[ETN-88-92133] N88-26734
Growth and characterization of thin films of ZnSnP(sub)2
[DE88-001164] N88-27060
PHYSIOLOGICAL RESPONSES
Regulatory biochemical and metabolic responses in photoreceptors
[AD-A192898] N88-26794
PHYSIOLOGY
JPRS report: Science and technology. USSR: Life sciences
[JPRS-ULS-88-009] N88-26785
PIEZOELECTRICITY
Piezoelectric effects in strained layer superlattices N88-27002
PILOT PERFORMANCE
Aircraft accident report: Joe Foster Excavating, Inc., Bell 206B, N49606, in-flight collision with trees, Alamo, California, August 3, 1986
[PB88-910405] N88-26345
Aircraft accident report: Midair collision of SkyWest Airlines Swearingen METRO 2, N163SW, and Mooney M20, N6485U, Kearns, Utah, January 15, 1987
[PB88-910404] N88-26346
Checklist interruption and resumption: A linguistic study
[NASA-CR-177460] N88-26348
Control of flight through microburst wind shear using deterministic trajectory optimization N88-26375
Computer simulation of a single pilot flying a modern high-performance helicopter
[NASA-TM-100182] N88-26376
Computer simulation of multiple pilots flying a modern high performance helicopter
[NASA-TM-100183] N88-26377
Flight simulator: Field of view utilized in performing tactical maneuvers
[AD-A192412] N88-26379
Does dihydroergotamine used in therapeutical doses influence the physical and psychomotor performance of young pilots or other traffic drivers subjected to hypotonia?
[ETN-88-92136] N88-26799
Preliminary study within a project for the development of intelligent assistance to piloting: Formal description of combat pilot expertise and implementation of an interactive system to represent operations
[CERMA-87-31] N88-26806
PILOT TRAINING
Intelligent guidance and control for wind shear encounter
[NASA-CR-183060] N88-26347
USAF flying screening: First step on the road to wings
[AD-A192613] N88-26804
Preliminary study within a project for the development of intelligent assistance to piloting: Formal description of combat pilot expertise and implementation of an interactive system to represent operations
[CERMA-87-31] N88-26806
PILOTS (PERSONNEL)
USAF flying screening: First step on the road to wings
[AD-A192613] N88-26804
PIONS
Charged pion production and projectile breakup in 85A MeV(sup)12C induced heavy ion reactions
[LUIP-8802] N88-26920
PIPE FLOW
Turbulence transition in a circular pipe N88-26503
Characteristics of long size thermosyphons made of corrugated tube N88-26511
Experiments on densely-loaded non-Newtonian slurries in laminar and turbulent pipe flows
[DE88-010579] N88-26612
Investigation on refrigerant R12 critical boiling point in narrow flow pipes considered as model fluid
[ETN-88-92374] N88-26626
PIPELINING (COMPUTERS)
The performance of the NEC SX-2 and Cray X-MP supercomputers
[DE88-009177] N88-26813
PIPES (TUBES)
Forced-convective boiling in small diameter tube N88-26510
Evaluation of engineering leak before break assessment methods by piping tests
[PB88-126982] N88-26538
Experimental investigation of turbulent flow in smooth and longitudinal grooved tubes
[NASA-TM-77480] N88-26615
Cross flow induced vibrations in tube bundle by displaced and misaligned tube configurations
[ETN-88-92132] N88-26621
Thermal and mechanical analysis of the Faraday shield for the compact ignition tokamak
[DE88-007855] N88-26962
PISTONS
Analytical and experimental investigation of ringless piston concept
[AD-A192835] N88-26673
PITOT TUBES
Heterogeneous diffusion flame stabilization
[AD-A193014] N88-26429
PIXELS
SEGMERGE: A scanline visible surface algorithm with adaptive span selection and inexpensive antialiasing
[DE88-009186] N88-26826
PLANETARY ATMOSPHERES
Experimental study of planetary gases with applications to planetary interior models
[NASA-CR-183098] N88-27137
PLANETARY EVOLUTION
Reports of planetary geology and geophysics program, 1987
[NASA-TM-4041] N88-27133
PLANETARY GEOLOGY
Reports of planetary geology and geophysics program, 1987
[NASA-TM-4041] N88-27133
PLANETARY LANDING
Lunar base launch and landing facility conceptual design, 2nd edition
[NASA-CR-172049] N88-27135
PLANETARY RADIATION
Research in particle and gamma-ray astrophysics
[NASA-CR-183111] N88-27146
PLANETARY STRUCTURE
Experimental study of planetary gases with applications to planetary interior models
[NASA-CR-183098] N88-27137
PLANNING
Plans for discourse
[AD-A192242] N88-26802
PLASMA COMPRESSION
Factors which affect operation of a plasma focus in various gases
[DE88-701882] N88-26975
PLASMA CONTROL
Symmetrized magnetic field configuration of low aspect ratio helical system
[IPPJ-869] N88-26956
Neoclassical diffusion due to trapping/detrapping orbits in stellarators
[DE88-008566] N88-26968
The effect of ICRF on the Alcator C Scrape-Off Layer plasma
[DE88-009821] N88-26972
PLASMA DENSITY
Poloidal field measurements using laser enhanced attenuation of an energetic lithium beam
[DE88-008360] N88-26963
PLASMA DIAGNOSTICS
An elliptical spectrograph/gated microchannel plate detector for time-resolved spectral measurements in the X-ray region
[DE88-007590] N88-26961
Poloidal field measurements using laser enhanced attenuation of an energetic lithium beam
[DE88-008360] N88-26963
Fusion programs in applied plasma physics and development and technology at GA Technologies, Inc.
[DE88-008406] N88-26964
A CO2 laser Thomson scattering diagnostic for fusion product alpha particle measurement
[DE88-007983] N88-26965
Multipoint Thomson scattering diagnostic for DIII-D
[DE88-008737] N88-26969
Developing diagnostic methods for plasma-particle interaction
[TI88-007726] N88-26973
Vertical viewing ECE diagnostic for the D3-D tokamak
[DE88-010586] N88-26987
MTX (Microwave Tokamak Experiment) plasma diagnostic system
[DE88-011326] N88-26993
PLASMA FOCUS
On the self-focusing of electric helicons
[DE88-701870] N88-26905
Factors which affect operation of a plasma focus in various gases
[DE88-701882] N88-26975
PLASMA HEATING
The effect of ICRF on the Alcator C Scrape-Off Layer plasma
[DE88-009821] N88-26972
PLASMA INTERACTIONS
Fluid dynamical model of ultrarelativistic heavy ion collisions
[DE88-007905] N88-26921
The effect of ICRF on the Alcator C Scrape-Off Layer plasma
[DE88-009821] N88-26972
PLASMA JETS
Plasma deposition: Investigations on a new approach
[ETN-88-92619] N88-26992
PLASMA LAYERS
Absorption characteristics of Si3N4 ablation layer plasma N88-26504
The effect of ICRF on the Alcator C Scrape-Off Layer plasma
[DE88-009821] N88-26972
PLASMA PHYSICS
Fusion programs in applied plasma physics and development and technology at GA Technologies, Inc.
[DE88-008406] N88-26964
PLASMA PINCH
Factors which affect operation of a plasma focus in various gases
[DE88-701882] N88-26975
PLASMA RESONANCE
Electrostatic whistler mode conversion at plasma resonance
[AD-A192951] N88-26989
PLASMA SHEATHS
Effects of secondary electron emission on the collector and source sheaths of a finite ion temperature plasma
[DE88-008930] N88-26971
PLASMA SPECTRA
Time-resolved doubly bent crystal X-ray spectrometer
[DE88-007899] N88-26637
PLASMA SPRAYING
Plasma deposition: Investigations on a new approach
[ETN-88-92619] N88-26992
PLASMA WAVES
On the self-focusing of electric helicons
[DE88-701870] N88-26905
Kinetic modulational instability of electron cyclotron waves in plasmas
[DE88-701893] N88-26978
Drift wave vortices and anomalous transport
[DE88-009562] N88-26982
Generation of Adlam-Allen waves by plasma release experiments in the solar wind
[PB88-106000] N88-27140
PLASMA-PARTICLE INTERACTIONS
Developing diagnostic methods for plasma-particle interaction
[TI88-007726] N88-26973
PLASMAS (PHYSICS)
Why plasma armature railguns don't work (and what can be done about it)
[DE88-007900] N88-26384
Proceedings of the 2nd US-Japan Workshop on Advanced Plasma Modeling, volume 3
[IPPJ-867] N88-26957
A Vlasov ion zero mass electron model for plasma simulations N88-26958
Modeling of subtle kinetic processes in plasma simulation N88-26959
Effects of secondary electron emission on the collector and source sheaths of a finite ion temperature plasma
[DE88-008930] N88-26971
On the self-trapping of an electromagnetic wave in magnetized plasma
[DE88-701872] N88-26974
Plasma separation process. Betacell (BCELL) code, user's manual
[DE88-006955] N88-26981
Impurity transport calculations for a drift-dependent tokamak scrape-off plasma
[DE88-010053] N88-26984
MACH2: A two-dimensional magnetohydrodynamic simulation code for complex experimental configurations
[AD-A192285] N88-26988
Electrostatic whistler mode conversion at plasma resonance
[AD-A192951] N88-26989
PLASMONS
Extended and local plasmons in a lateral superlattice N88-27041
Fundamental optical studies of competitive adsorption and thin film phenomena
[DE88-008780] N88-27068

PLASTIC DEFORMATION
Plastic deformation and roughness of free metal surfaces
[PB88-196621] N88-26439
Shape memory alloys: New materials for future engineering
[NASA-TT-20193] N88-26455
Fatigue of lithium-aluminum alloys: An example of localization of the plastic deformation
[ETN-88-92309] N88-26456
On the possibility of the soliton description of acoustic emission during plastic deformation of crystals
[DE88-701878] N88-27075
PLASTIC MEMORY
Shape memory alloys: New materials for future engineering
[NASA-TT-20193] N88-26455
PLASTICS
Statistical mechanics of polymer systems
[DE88-011172] N88-26477
PLUTONIUM ISOTOPES
Milliwatt generator project
[DE88-011261] N88-26939
POINT SOURCES
Observation of a point source in Cygnus constellation with the underground detector at Frejus (France)
[PITHA-87/02] N88-27122
POINTING CONTROL SYSTEMS
Time-Optimal Adaptive Shaped Torque (TOAST) technical note
[AD-A192719] N88-26869
POINTS (MATHEMATICS)
Procedure for converting a Wilson-Fowler spline to a cubic B-spline with double knots
[DE88-008971] N88-26878
Evaluation of a multi-point method for determining acoustic impedance
[NASA-TM-100637] N88-26913
POLAR CAPS
High latitude ionospheric radio studies
[AD-A192270] N88-26753
Rocket measurements within a polar cap arc: Ionospheric modelling
[AD-A192381] N88-26754
On the conjugacy of the aurora: High and low latitudes
[AD-A193008] N88-26755
POLARIMETRY
Data volume reduction for imaging radar polarimetry
[NASA-CASE-NPO-17184-1-CU] N88-26541
POLARIZATION (SPIN ALIGNMENT)
Observation of ferromagnetism in ultrathin f.c.c. films by spin polarised neutron reflection N88-27015
POLARIZATION CHARACTERISTICS
Effect of double layer structure on the determination of corrosion rates from polarization measurements
[DE88-010097] N88-26448
POLICIES
An agenda for the strategic defense initiative
[RAND-P-7404] N88-26898
SDI and/or arms control
[RAND-P-7357] N88-26903
Space policy of common sense and moderation
[REPT-49/87] N88-27118
POLITICS
Book analysis. Challenger: A major malfunction
[AD-A192458] N88-26388
POLLUTION CONTROL
Acid Precipitation: A current awareness bulletin
[DE88-007987] N88-26738
POLOIDAL FLUX
Toroidal and poloidal soft X-ray imaging system on the D3-D tokamak
[DE88-010585] N88-26986
POLYAMIDE RESINS
Initial adhesive screening of novel polyamide-imides and their copolymers
[NASA-TM-100641] N88-26481
Resistance of polyamide-6 against long time effects of various media at various temperatures
[NASA-TT-20297] N88-26484
POLYCRYSTALS
The effects of thin compressive films on indentation fracture toughness measurements
[AD-A192243] N88-26480
Pure metallic bridge and point-contact tunneling into single- and polycrystal YBa2Cu3O(sub 7-y)
[DE88-010030] N88-27084
POLYETHYLENES
Combustion of PMMA (polymethylmethacrylate), PE (polyethylene) and PS (polystyrene) in a ramjet
[PB88-186572] N88-26417
POLYGONS
Linear programming in R sup 3 and the skeleton and largest incircle of a convex polygon
[PB88-124664] N88-26892
POLYIMIDE RESINS
High temperature resins for injection. High temperature pre-impregnated
[RC-648676] N88-26486
POLYIMIDES
Substituted 1,1,1-Triaryl-2,2,2-Trifluoroethanes and processes for their synthesis
[NASA-CASE-LEW-14345-1] N88-26404
Initial adhesive screening of novel polyamide-imides and their copolymers
[NASA-TM-100641] N88-26481
POLYMER CHEMISTRY
Substituted 1,1,1-Triaryl-2,2,2-Trifluoroethanes and processes for their synthesis
[NASA-CASE-LEW-14345-1] N88-26404
Fundamental studies of elastomers
[DE88-009679] N88-26471
Statistical mechanics of polymer systems
[DE88-011172] N88-26477
Initial adhesive screening of novel polyamide-imides and their copolymers
[NASA-TM-100641] N88-26481
POLYMER MATRIX COMPOSITES
Thermoplastic coating of carbon fibers
[NASA-CR-183067] N88-26407
Irreversible deformations during fracture in polymers
[W-7/86] N88-26485
POLYMERIZATION
Fundamental studies of elastomers
[DE88-009679] N88-26471
Polymerization of epoxy matrix composites using pulsed microwaves
[CERT-3/1324-MO] N88-26487
Structural study of impregnating resins of TGMDA/DDS type
[ETN-88-92167] N88-26488
The electronic structure of condensed molecular systems
[DE88-007823] N88-26923
POLYMETHYL METHACRYLATE
Combustion of PMMA (polymethylmethacrylate), PE (polyethylene) and PS (polystyrene) in a ramjet
[PB88-186572] N88-26417
Ignition and flame spread of PMMA
[NASA-TT-20290] N88-26431
Irreversible deformations during fracture in polymers
[W-7/86] N88-26485
POLYNOMIALS
A new trajectory following polynomial-time algorithm for the linear programming problem
[REPT-87-87] N88-26848
Accurate solution of parabolic equations by expansion in ultraspherical polynomials
[DE88-701829] N88-26880
POLYPHENYLS
The crystallization of tough thermoplastic resins in the presence of carbon fibers
[NASA-CR-182984] N88-26464
POLYSTYRENE
Combustion of PMMA (polymethylmethacrylate), PE (polyethylene) and PS (polystyrene) in a ramjet
[PB88-186572] N88-26417
POLYURETHANE FOAM
Thermal conductivity of selected foams and systems from 100 to 300 K
[PB88-201553] N88-26486
POROSITY
A model for insulated wires in the method of moments code NEC (Numerical Electromagnetics Code)
[DE88-008920] N88-26577
Characterization of the surface area and porosity of sol-gel films using saw devices
[DE88-008794] N88-27069
POROUS WALLS
Heterogeneous diffusion flame stabilization
[AD-A193014] N88-26429
POSITION (LOCATION)
NAVSTAR global positioning system
[AD-A192609] N88-26354
POSITION ERRORS
A positioning system based on NAVSAT
[NLR-MP-87018-U] N88-26358
POSITIONING
Position and velocity determination using a Global Positioning System: An outline
[B8735052] N88-26355
Research project Loran-C of the Geometric Service of the Ministry of Public Works
[B8735055] N88-26356
The Sercel TR5S Global Positioning System (GPS) receiver
[ETN-88-92473] N88-26357
POSITRONS
Inelastic mean free paths of electrons and positrons in matter
[DE88-008086] N88-26929
POTENTIAL FLOW
The role of computational fluid dynamics in aeronautical engineering (5): Improvements and applications of implicit TVD finite volume code N88-26313
Improved potential flow computational methods with Euler corrections for airfoil and wing/body design
[AD-A192303] N88-26334
Calculation of 2-D unsteady transonic full potential flow about oscillating airfoils by two complementary approaches
[PB88-127519] N88-26341
POWDER (PARTICLES)
Production of powdered sodium hydride with large specific surface by the catalyzed reaction of molten sodium with hydrogen-1
[NASA-TT-20185] N88-26462
A study of solvent effects on the synthesis of pure component and composite ceramic powders by metal alkoxide hydrolysis
[DE88-008381] N88-26470
Ceramic processing of high-T(sub)c superconductors
[DE88-010090] N88-27087
POWDER METALLURGY
The preparation of mechanically alloyed powders for TEM (Transmission Electron Microscopy) examination
[DE88-006043] N88-26460
POWER EFFICIENCY
Computer controlled procedures for traction battery power performance tests
[ETN-88-92352] N88-26589
POWER LINES
Development of external cooling cryo-resistive cable systems. Part 2: Insulation characteristics on 66 kV rated cryo-resistive testing cable
[DE88-770191] N88-26571
PRANDTL NUMBER
Ludwig Prandtl collected treatises on applied mechanics, hydro- and aerodynamics, part 1
[NASA-TT-20316] N88-26337
Ludwig Prandtl collected treatises on applied mechanics, hydro- and aerodynamics, part 2, IV interfaces and resistance
[NASA-TT-20315] N88-26338
PRECIPITATION (CHEMISTRY)
Dual mechanism bifunctional polymers: Design, synthesis and application of a new category of metal ion complexing agents
[DE88-008233] N88-26468
PRECIPITATION (METEOROLOGY)
A radar study of the interaction between lightning and precipitation
[DE88-009120] N88-26770
PRECIPITATION HARDENING
Precipitation study by electrical resistivity measurement in Ni-Al alloys
[DE88-701877] N88-26440
PRECISION
Fabrication technology
[DE88-010598] N88-26955
PREDICTION ANALYSIS TECHNIQUES
Experimental and theoretical analysis of the radiative transfer within a sooty pool fire
[DE88-007099] N88-26419
Interpreting forest biome productivity and cover utilizing nested scales of image resolution and biogeographical analysis
[NASA-CR-183036] N88-26711
Synoptic patterns related to tropical cyclone recurvature
[AD-A192338] N88-26771
PREDICTIONS
Intelligent guidance and control for wind shear encounter
[NASA-CR-183060] N88-26347
Prediction of continental shelf sediment transport using a theoretical model of the wave-current boundary layer
[AD-A192272] N88-26783
Hot electrons in silicon dioxide: Ballistic to steady-state transport N88-27042
PREMIXED FLAMES
Modelling of premixed combustion using a thin flame sheet and the effect of the hydrodynamic instability
[DE88-009467] N88-26423
PRESSURE DISTRIBUTION
Calculations of unsteady aerodynamics for a full aircraft configuration using boundary element method N88-26303
PRESSURE GRADIENTS
HeFlow: A program for calculating pressure and temperature of helium in forced-flow superconductors. Part 1: Numerical solutions. Part 2: HeFlow user's manual
[DE88-008941] N88-27071
PRESSURE MEASUREMENT
Velocity-pressure integrated versus penalty finite element methods for high Reynolds number flows
[NASA-CR-179357] N88-26835

Evaluation of a multi-point method for determining acoustic impedance
[NASA-TM-100637] N88-26913
PRESSURE OSCILLATIONS
Dynamics and stability of combustion driven self oscillations in presence of various frequencies. Extensive stability criteria
[ETN-88-92123] N88-26432
PRESSURE REDUCTION
Characteristics of pressure loss during filtration using a porous ceramic filter
[DE88-752547] N88-26604
PROBABILITY THEORY
Antenna heights for the optimum utilization of the oceanic evaporation duct. Part 3: Results from the Mediterranean measurements, volume 2
[AD-A192311] N88-26554
PROBLEM SOLVING
An initial investigation into methods of computing transonic aerodynamic sensitivity coefficients
[NASA-CR-183061] N88-26332
Use of direct solvers for multidimensional fluid flow computations
[DE88-010063] N88-26611
Vibration frequencies of tapered bars with nonclassical boundary conditions
[NASA-CR-183059] N88-26688
Inference and discovery in an exploratory laboratory
[AD-A192231] N88-26801
Challenge problems focusing on equality and combinatory logic: Evaluating automated theorem-proving programs
[DE88-010057] N88-26879
Combining expert opinions: An optimization framework
[REPT-87-84] N88-26895
PROCESS CONTROL (INDUSTRY)
Granulation of pyrotechnic tracer composition R284T
[MRL-TN-528] N88-26490
Industrial processes influenced by gravity
[NASA-CR-182140] N88-26497
The knowledge based automatic extraction of the machinable surfaces for automatic CAD-CAM system
[INPE-4542-PRE/1288] N88-26824
The hole of a blanket tritium system on the fusion fuel cycle
[DE88-010007] N88-26983
Ceramic processing of high-T(sub)c superconductors
[DE88-010090] N88-27067
PRODUCT DEVELOPMENT
New semiconductor laser structure for an optical communication system
[ETN-88-92353] N88-26654
Design of high performance microcomputers for numerical data processing
[ETN-88-92371] N88-26818
Delfi-3 as a development environment for expert systems
[REPT-8767] N88-26845
PROGRAMMERS
Programmer-friendly LL(1) parser generator
[PB88-126933] N88-26857
PROGRAMMING LANGUAGES
FASTRUN phase sequencer descriptor language (PDL)
[DE88-007966] N88-26828
Why is it difficult to program in von Neumann languages
[AD-A192830] N88-26839
Contractions in comparing concurrency semantics
[CWI-CS-R8755] N88-26850
A semantic approach to fairness
[CWI-CS-R8759] N88-26853
PROJECT PLANNING
Fuel cell systems program plan: Fiscal year 1988
[DE88-011080] N88-26731
PROJECTILES
Contact force history and dynamic response due to the impact of a soft projectile
[NASA-TM-100961] N88-26679
Analysis of the perforation of monolithic and simple laminate aluminium targets as a test of analytical deformation models
[MRL-R-1111] N88-26686
Charged pion production and projectile breakup in 85A MeV(sup)12C induced heavy ion reactions
[LUIP-8802] N88-26920
PROP-FAN TECHNOLOGY
Propfan test assessment testbed aircraft stability and control/performance 1/9-scale wind tunnel tests
[NASA-CR-182121] N88-26360
PROPAGATION MODES
On the propagating speed in difference approximations for conservation laws N88-26318
PROPELLANT COMBUSTION
Rocket-propellant burn tests of silicide-coated niobium and tantalum
[DE88-010729] N88-26496
PROPELLERS
Numerical solutions of the Euler equations for the flow field around counter-rotating propellers N88-26298
PROPULSION SYSTEM CONFIGURATIONS
A reusable rocket engine intelligen control
[NASA-TM-100963] N88-26401
PROTECTION
The use of liquid films for spacecraft survivability to laser radiation
[AD-A192954] N88-26395
PROTECTIVE COATINGS
Corrosion prevention in gas turbines
[NLR-MP-87029-U] N88-26373
Electrophoretic coatings. Part 1: Sandia applications
[DE88-008666] N88-26465
The effects of thin compressive films on indentation fracture toughness measurements
[AD-A192243] N88-26480
Rocket-propellant burn tests of silicide-coated niobium and tantalum
[DE88-010729] N88-26496
PROTOCOL (COMPUTERS)
Minimum disclosure proofs of knowledge
[CWI-PM-R8710] N88-26854
Markov chain computations to a solution of the mutual-exclusion problem in concurrency
[REPT-87-89] N88-26896
PROTONS
The protonic Beta double prime aluminas: Preparation, stability, conductivity and structure
[DE88-008442] N88-26415
Rf cavity primer for cyclic proton accelerators
[DE88-010655] N88-26938
PROTOTYPES
Analytical and experimental investigation of ringless piston concept
[AD-A192835] N88-26673
Expert system application education project
[NASA-CR-183089] N88-26867
PROVING
Minimum disclosure proofs of knowledge
[CWI-PM-R8710] N88-26854
PSYCHOMOTOR PERFORMANCE
Does dihydroergotamine used in therapeutical doses influence the physical and psychomotor performance of young pilots or other traffic drivers subjected to hypotonia?
[ETN-88-92136] N88-26799
PSYCHOPHYSICS
Does dihydroergotamine used in therapeutical doses influence the physical and psychomotor performance of young pilots or other traffic drivers subjected to hypotonia?
[ETN-88-92136] N88-26799
PULSE AMPLITUDE MODULATION
Polymerization of epoxy matrix composites using pulsed microwaves
[CERT-3/1324-MO] N88-26487
PULSE GENERATORS
Research in electromagnetic shielding theory. Part 2: EMP (electromagnetic pulse) simulation using small loops
[AD-A192882] N88-26558
PULSED LASERS
The chirped-pulse free-electron laser
[DE88-009289] N88-26651
Model for pulse amplification by a gaseous laser amplifier
[DE88-011729] N88-26657
PYROTECHNICS
Pyrotechnic system failures: Causes and prevention
[NASA-TM-100633] N88-26394
Granulation of pyrotechnic tracer composition R284T
[MRL-TN-528] N88-26490

Q

QUALITATIVE ANALYSIS
Qualitative reasoning for physicists
[PB88-116296] N88-26906
QUALITY CONTROL
Analytical determination of critical crack size in solar cells
[NASA-CR-183128] N88-26736
Milliwatt generator project
[DE88-011261] N88-26939
Optical characterization of silica aerogel
[DE88-008916] N88-26946
QUANTITATIVE ANALYSIS
Development of an automated X-ray gauge for nondestructive quantitative analysis
[DE88-008633] N88-26681
QUANTUM CHROMODYNAMICS
Comparison of exclusive reactions at large momentum transfer
[DE88-007544] N88-26922
Theoretical studies in elementary particle physics
[DE88-006929] N88-26926
QUANTUM EFFICIENCY
Results from the SLAC lasertron
[DE88-007816] N88-26647
QUANTUM ELECTRONICS
Random quantum interference in microdevices N88-27021
Defects and disorder in amorphous and damaged silicon
[AD-A192277] N88-27089
QUANTUM MECHANICS
High resolution spectroscopy of dissociating molecules
[DE88-007959] N88-26924
Quantum transport theory of resonant-tunneling heterostructure devices N88-27017
Quantum interference and transport in microstructures N88-27022
Combining relativity and quantum mechanics: Schroedinger's interpretation of psi
[DE88-701899] N88-27102
QUANTUM THEORY
Cosmic wavefunction with induced gravity
[DE88-701873] N88-27129
QUANTUM WELLS
Far-infrared studies of doped AlGaAs/GaAs multiple-quantum-well structures N88-26998
Electro-optical studies of Al(x)Ga(1-x)As/GaAs coupled quantum wells N88-26999
Quantum wells and bulk AlGaAs under hydrostatic pressure N88-27000
Auger recombination in GaSb/AlSb-multi quantum well heterostructures N88-27001
Ultrafast optical nonlinearity in quantum well structures with electric field N88-27003
Strained layer and lattice matched transverse junction stripe quantum well lasers for continuous room temperature operation N88-27004
Quantum transport theory of resonant-tunneling heterostructure devices N88-27017
Superlattice doping interfaces N88-27019
Excitonic properties of GaAs-AlGaAs nanostructures N88-27023
A 10 microns photoexcited avalanche gain due to electron impact ionization from GaAs quantum well superlattices N88-27026
Novel quantum well optical devices N88-27028
Direct imaging of the columnar structure of GaAs quantum wells N88-27030
Monte Carlo simulations of femtosecond relaxation of photoexcited electrons in AlGaAs/GaAs quantum wells N88-27036
Electron-phonon interactions in In(0.53)Ga(0.47)As and in In(0.53)Ga(0.47)As/InP quantum wells N88-27037
Electronic structure of quantum-well states revealed under high pressures N88-27038
Magneto-optical studies of GaInAs-InP quantum wells N88-27039
On a-Si:H/a-SiN(x):H superlattices: Confinement or contamination N88-27040
Direct measurement of ultrafast electron-hole plasma expansion at high density at an asymmetric GaAs quantum well N88-27044
QUARKS
Theoretical studies in elementary particle physics
[DE88-006929] N88-26926
QUATERNARY ALLOYS
Photoluminescence studies of InGaAlAs quaternary alloys
[DE88-007197] N88-27062
QUENCHING (COOLING)
The T-T-T curve in Cu-Cr alloy
[NASA-TT-20167] N88-26453
QUERY LANGUAGES
Using common subexpressions to optimize multiple queries
[DE88-008210] N88-26877

R

RADAR CORNER REFLECTORS
Scattering patterns of dihedral corner reflectors with impedance surface impedances
[NASA-CR-183078] N88-26545

RADAR CROSS SECTIONS
Microwave image understanding and its application to radar cross section management N88-26542
Scattering patterns of dihedral corner reflectors with impedance surface impedances
[NASA-CR-183078] N88-26545
Radar cross section studies/compact range research
[NASA-CR-183124] N88-26565
RADAR IMAGERY
Sources of scattering in vegetarian and other surfaces and objects
[NASA-CR-182975] N88-26710
Image pyramid motion detection applied to sea ice N88-26713
RADAR RESOLUTION
Sources of scattering in vegetarian and other surfaces and objects
[NASA-CR-182975] N88-26710
RADAR SCATTERING
Scattering patterns of dihedral corner reflectors with impedance surface impedances
[NASA-CR-183078] N88-26545
RADIAL FLOW
Experimental and theoretical study of the dynamic operational behavior of a three stage radial compressor
[ETN-88-92129] N88-26676
RADIANCE
Effects of atmospheric model layering on LOWTRAN 6 calculations of 8-12 micrometers near-horizon sky radiances
[AD-A192969] N88-26559
Numerical model for the computation of radiance distributions in natural waters with wind-roughened surfaces
[PB88-192703] N88-26765
Eigenmatrix representations of radiance distributions in layered natural waters with wind-roughened surfaces
[PB88-188701] N88-26780
RADIATION ABSORPTION
Absorption characteristics of Si3N4 ablation layer plasma N88-26504
RADIATION DAMAGE
JFET/SOS (Junction Field-Effect Transistor/Silicon-on-Sapphire) devices: Gamma-radiation-induced effects
[AD-A193001] N88-26586
Acute radiation syndrones and their management
[DE88-009839] N88-26797
The Oak Ridge National Laboratory strategic defense initiative shield optimization program: Executive summary
[DE88-008016] N88-26899
Electron irradiation effects in YBa2Cu3O7-Delta single crystals
[DE88-010050] N88-27085
RADIATION DOSAGE
Acute radiation syndrones and their management
[DE88-009839] N88-26797
RADIATION EFFECTS
Abnormal diffusion of vacancies in metals
[DE88-701880] N88-26441
Helium induced degradation in the weldability of an austenitic stainless steel
[DE88-009062] N88-26443
Effects of cosmic rays on single event upsets
[NASA-CR-183053] N88-26569
RADIATION HARDENING
Electrophoretic coatings. Part 1: Sandia applications
[DE88-008666] N88-26465
High bandwidth optoelectronic signal link for use in an EMP (electromagnetic pulse) plus radiation environment
[DE88-009254] N88-26549
RADIATION HAZARDS
Studies of HZE particle interactions and transport for space radiation protection purposes
[NASA-TM-101159] N88-27142
RADIATION MEASUREMENT
Evaluation of surface energy and radiation balance systems for FIFE
[NASA-CR-183118] N88-26778
RADIATION PRESSURE
Time-dependent mass loss from hot stars with and without radiative driving
[DE88-008699] N88-27128
RADIATION PROTECTION
The use of liquid films for spacecraft survivability to laser radiation
[AD-A192954] N88-26395
Mobile robot survival
[DE88-009108] N88-26665
Studies of HZE particle interactions and transport for space radiation protection purposes
[NASA-TM-101159] N88-27142
RADIATIVE HEAT TRANSFER
Experimental and theoretical analysis of the radiative transfer within a sooty pool fire
[DE88-007099] N88-26419
Ignition and flame spread of PMMA
[NASA-TT-20290] N88-26431
RADICALS
Probing the possibility of a (12)C/(13)C abundance gradient from observations of interstellar CH+
[DE88-008908] N88-27125
RADIO ASTRONOMY
The polarization of radio galaxies: Its structure at low frequencies
[B8681611] N88-27123
RADIO CONTROL
Frequency domain identification of the dynamics of a scaled remotely-piloted helicopter N88-26524
RADIO EQUIPMENT
A random access algorithm for environments with capture and limited feedback capabilities
[AD-A192233] N88-26552
RADIO FREQUENCIES
Coherent RF error statistics
[AD-A193002] N88-26560
Microwave calibration system 2
[AD-A192976] N88-26639
Superconducting rf and beam-cavity interactions
[DE88-008598] N88-26936
Rf cavity primer for cyclic proton accelerators
[DE88-010655] N88-26938
RADIO FREQUENCY INTERFERENCE
Method and apparatus for measuring distance
[NASA-CASE-MSC-20912-1] N88-26568
RADIO GALAXIES
The polarization of radio galaxies: Its structure at low frequencies
[B8681611] N88-27123
RADIO NAVIGATION
NAVSTAR global positioning system
[AD-A192609] N88-26354
RADIO RECEIVERS
The Sercel TR5S Global Positioning System (GPS) receiver
[ETN-88-92473] N88-26357
RADIOACTIVE MATERIALS
RRSAS (Robotic Radiation Survey and Analysis System) Project: A real time sensor driven robotic system
[DE88-006825] N88-26661
RADIOISOTOPE BATTERIES
Plasma separation process. Betacell (BCELL) code, user's manual
[DE88-006955] N88-26981
RADIOMETERS
Description of the MPTR system: Multi Path Transmissometer Radiometer
[FEL-1987-14] N88-26954
RAIL TRANSPORTATION
Identification of lateral operation dynamics of rail vehicles using roll test stand tests N88-26534
RAILGUN ACCELERATORS
Reaming experiments for the lethality test system
[DE88-007902] N88-26383
Why plasma armature railguns don't work (and what can be done about it)
[DE88-007900] N88-26384
Application of superconducting technology to earth-to-orbit electromagnetic launch systems
[DE88-010022] N88-26386
Plasma armature formation in high-pressure, high-velocity hydrogen
[DE88-008347] N88-26967
RAIN
Present status of artificial rain making
[DE88-701823] N88-26769
RAINMAKING
Present status of artificial rain making
[DE88-701823] N88-26769
RAMAN LASERS
Laser spectoscopy of plasmas
[AD-A193009] N88-26991
RAMAN SPECTRA
Raman and absorption spectrophotometric studies of selected lanthanide, californium-doped lanthanide, and actinide trihalides in the solid state
[DE88-008234] N88-27061
RAMAN SPECTROSCOPY
Raman, photoluminescence and modulation spectroscopy of semiconductor heterostructures N88-26997
RAMJET ENGINES
An efficient computational tool for ramjet combustor research
[DE88-010034] N88-26369
Combustion of PMMA (polymethylmethacrylate), PE (polyethylene) and PS (polystyrene) in a ramjet
[PB88-186572] N88-26417
Heterogeneous diffusion flame stabilization
[AD-A193014] N88-26429
RANDOM ACCESS MEMORY
A random access algorithm for environments with capture and limited feedback capabilities
[AD-A192233] N88-26552
RANDOM VIBRATION
Random vibration analysis of rattling structures
[DE88-007196] N88-26691
RANDOM WALK
Eigenmodes of a random walk on a 2-D lattice torus with one trap
[DE88-007830] N88-26874
Range of a constrained random walk
[PB88-126867] N88-26897
RANKINE CYCLE
Analytical and experimental investigation of ringless piston concept
[AD-A192835] N88-26673
RAPID TRANSIT SYSTEMS
Simulation models for the dynamics of tracked vehicle systems: State-of-the-art and open problems N88-26522
RARE GASES
Method for the isotopically selective detection of inert gases
[TI88-008370] N88-26421
Rare Gas Halide (RGH) kinetics
[AD-A192352] N88-26425
The electronic structure of condensed molecular systems
[DE88-007823] N88-26923
RAREFIED GAS DYNAMICS
Rarefied gas numerical wind tunnel 3: Universal code for three dimensional bodies N88-26304
RATES (PER TIME)
A simulation analysis of errors in the measurement of standard electrochemical rate constants from phase-selective impedance data
[AD-A192739] N88-26426
Effect of double layer structure on the determination of corrosion rates from polarization measurements
[DE88-010097] N88-26448
RAYLEIGH SCATTERING
Developing diagnostic methods for plasma-particle interaction
[TI88-007726] N88-26973
REACTION KINETICS
Simulation of axisymmetric flow with H2O2 reactions N88-26311
Rare Gas Halide (RGH) kinetics
[AD-A192352] N88-26425
The influence of uncompensated solution resistance on the determination and standard electrochemical rate constants using cyclic voltammetry and some comparisons with AC voltammetry
[AD-A192825] N88-26427
Oxygen reduction in fuel cell electrolytes
[DE88-008240] N88-26723
Defect characterization of the redox behavior and stability of conducting oxides
[DE88-010799] N88-27088
REACTION WHEELS
Nutational stability of a satellite equipped with an active magnetic momentum wheel N88-26513
REACTIVITY
In-situ reactive of X-ray optics by glow discharge
[DE88-009840] N88-26947
REACTOR DESIGN
Fusion programs in applied plasma physics and development and technology at GA Technologies, Inc.
[DE88-008406] N88-26964
REACTOR MATERIALS
Helium induced degradation in the weldability of an austenitic stainless steel
[DE88-009062] N88-26443
REACTOR SAFETY
Overview of the TITAN-2 reversed-field pinch aqueous fusion power core design
[DE88-006170] N88-26966
READING
Working memory capacity: An individual differences approach
[AD-A192359] N88-26803
The role of working memory in language comprehension
[AD-A192721] N88-26805
REAL GASES
High speed inlet calculations with real gas effects
[NASA-CR-182167] N88-26336
REAL TIME OPERATION
A high fidelity real-time simulation of a small turboshaft engine
[NASA-TM-100991] N88-26378
Environmental monitoring of a titan 34D 5 1/2 segment solid rocket motor static firing
[AD-A192975] N88-26400

Laser ranging data analysis
[NASA-CR-183115] N88-26567
RRSAS (Robotic Radiation Survey and Analysis System) Project: A real time sensor driven robotic system
[DE88-006825] N88-26661
Colored stochastic Petri nets. Application to real time distributed systems
[ENST-87E017] N88-26843
Definition of an auxiliary processor dedicated to real-time operating system kernels
[NASA-CR-183070] N88-26860

RECEIVERS
Digital communication transmitter and receiver test procedures
[AD-A191218] N88-26540
SIS (Superconductor-Insulator-Superconductor) mixer research
[AD-A192906] N88-27092

RECOMBINATION COEFFICIENT
Nascent vibrational/rotational distribution produced by hydrogen atom recombination
[AD-A193005] N88-26833

RECOMBINATION REACTIONS
Auger recombination in GaSb/AlSb-multi quantum well heterostructures N88-27001
Control of carrier lifetime in PbTe nipi superlattices by external photoinjection N88-27006

RECORDING
Computer controlled data acquisition system for the NASA 1986 Rocket Triggered Lightning Program
[DE88-006335] N88-26766

RECTANGULAR PLANFORMS
The determination of the topological structure of skin friction lines on a rectangular wing-body combination
[NASA-CR-4168] N88-26343

REDUCED GRAVITY
Industrial processes influenced by gravity
[NASA-CR-182140] N88-26497

REDUCTION
Reducing adhesion and agglomeration within a cloud of combustible particles
[NASA-TM-100902] N88-26539

REDUCTION (CHEMISTRY)
In situ spectroscopic studies of transition metal macrocycles as catalysts for the electrochemical reduction of oxygen
[PB88-203195] N88-26416
Nickel hydrogen cell positive-electrode studies: Cobalt segregation in reducing environments
[AD-A193025] N88-26587

REENTRY PHYSICS
Compressible boundary layers — atmospheric reentry
[CERT-OA-13/5005-AYD] N88-26623

REENTRY VEHICLES
A simulation of post boost vehicle deployment of multiple reentry vehicles
[DE88-009537] N88-26391

REFINING
Feasibility of producing jet fuel from GPGP (Great Plains Gasification Plant) by-products
[DE88-010233] N88-26492

REFLECTANCE
Numerical model for the computation of radiance distributions in natural waters with wind-roughened surfaces
[PB88-192703] N88-26765
Observation of ferromagnetism in ultrathin f.c.c. films by spin polarised neutron reflection N88-27015

REFLECTION
The use of liquid films for spacecraft survivability to laser radiation
[AD-A192954] N88-26395

REFRACTIVITY
Optical characterization of silica aerogel
[DE88-008916] N88-26946

REFRACTORY MATERIALS
Refractory Materials of Zirconate. Part 2: Synthesis and some properties of strontium, zirconate, calcium zirconate and barium zirconate
[NASA-TT-20186] N88-26483

REFRIGERANTS
Investigation on refrigerant R12 critical boiling point in narrow flow pipes considered as model fluid
[ETN-88-92374] N88-26626
Thermal conductivity of pure fluids in a large region around the critical point
[ETN-88-92135] N88-27103

REFRIGERATORS
Electrodynamic driver for the space thermoacoustic refrigerator (STAR)
[AD-A192337] N88-26517

REGENERATION (ENGINEERING)
Advanced life support control/monitor instrumentation concepts for flight application
[NASA-CR-177378] N88-26807

REGISTERS (COMPUTERS)
Simple multireader registers using time-stamp schemes
[CWI-CS-R8758] N88-26819

REGRESSION ANALYSIS
A statistical treatment of accelerated life test data for copper-water heat pipes N88-26509

REINFORCEMENT (STRUCTURES)
An assessment of modelling techniques for the finite element analysis of reinforced concrete plate and shell structures
[AD-A192263] N88-26697

RELATIVISTIC THEORY
On the self-trapping of an electromagnetic wave in magnetized plasma
[DE88-701872] N88-26974

RELATIVITY
On microphysical principles of thermofluid dynamics
[ETN-88-92095] N88-26620
Theory of relativity and super-light-speeds-I: Kinematical part
[DE88-701832] N88-27100
Combining relativity and quantum mechanics: Schroedinger's interpretation of psi
[DE88-701899] N88-27102

RELAXATION METHOD (MATHEMATICS)
Relaxation scheme for compressible flows N88-26323

RELIABILITY
Pyrotechnic system failures: Causes and prevention
[NASA-TM-100633] N88-26394
An evaluation methodology for dependable multiprocessors
[AD-A192799] N88-26863

REMOTE HANDLING
Mobile remote manipulator system for a tetrahedral truss
[NASA-CASE-MSC-20985-1] N88-26398

REMOTE SENSING
The role of space borne imaging radars in environmental monitoring: Some shuttle imaging radar results in Asia
[NASA-TM-101175] N88-26544
Remote sensing and satellite applications to the needs of the gas and pipeline industry
[PB88-202668] N88-26714
Surface hydrology, sediment transport dynamics and remote sensing of disturbed watersheds in a humid temperate region
[DE88-008719] N88-26715
Satellite remote sensing of the wet bulb globe temperature heat stress index, phase 2
[AD-A192798] N88-26717
Review of methods for remote sensing of atmospheric emissions from stationary sources
[PB86-190483] N88-26739
Remote sensing of temperature profiles. Performance test of PASS
[DE88-753108] N88-26768

REMOTE SENSORS
Satellite remote sensing of the wet bulb globe temperature heat stress index, phase 2
[AD-A192798] N88-26717

REPORTS
Acid Precipitation: A current awareness bulletin
[DE88-007987] N88-26738

REPRESENTATIONS
Knowledge representation in geographic information systems
[ETN-88-92470] N88-27112

REPRODUCTION (COPYING)
The transition from traditional to modern map reproduction
[B8735128] N88-26718

REQUIREMENTS
The free-electron laser: Theoretical innovations and gas-loaded experiment N88-26646

RESEARCH AIRCRAFT
The identification of the direct lift control flap system of the research aircraft ATTAS N88-26527

RESEARCH AND DEVELOPMENT
Exploratory battery technology development and testing report for 1986
[DE88-009870] N88-26578
Space policy of common sense and moderation
[REPT-49/87] N88-27118

RESEARCH FACILITIES
Building an artificial intelligence capability at Los Alamos
[DE88-009155] N88-26866

RESEARCH MANAGEMENT
Flight research and testing
[NASA-TM-100439] N88-26361
Plastic deformation and roughness of free metal surfaces
[PB88-196621] N88-26439
Novel magnetic materials research using free electron lasers
[DE88-009989] N88-26652
Building an artificial intelligence capability at Los Alamos
[DE88-009155] N88-26866
Issues and recommendations associated with distributed computation and data management systems for the space sciences
[NASA-CR-183026] N88-27108

RESIDUAL STRESS
Observations on residual stresses in ceramic composites by neutron diffraction techniques
[DE88-009937] N88-26472
Lattice strain in heteroepitaxial films N88-27032

RESINS
Electrophoretic coatings. Part 1: Sandia applications
[DE88-008666] N88-26485

RESONANCE
Aircraft interior noise reduction by alternate resonance tuning
[NASA-CR-182540] N88-26909
Resonant tunneling in InGaAs-InP double-barrier structures and superlattices N88-27047
Excellent negative differential resistance of InGaAs/InAlAs resonant tunneling barrier structures and applications to a new functional device, RHET N88-27048

RESONANT FREQUENCIES
FEB structural analysis, revision H
[AD-A192302] N88-26698
Vibration response of constrained viscoelastically damped plates: Analyses and experiments
[AD-A192329] N88-26699

RESONATORS
Low noise cryogenic dielectric resonator oscillator
[NASA-CASE-NPO-17157-1-CU] N88-26596

RESPIRATION
Respiration and oxygen tension in the blood of animals exposed to high pressures N88-26790

RESPONSES
The interaction of sensory and perceptual variables: Spatial, temporal and orientation response to figure and ground
[AD-A192897] N88-26798

RETENTION (PSYCHOLOGY)
Working memory capacity: An individual differences approach
[AD-A192359] N88-26803

RETIREMENT FOR CAUSE
Engine component retirement for cause. Volume 1: Executive summary
[AD-A192730] N88-26371

REUSABLE ROCKET ENGINES
A reusable rocket engine intelligen control
[NASA-TM-100963] N88-26401

REVERSE FIELD PINCH
Overview of the TITAN-2 reversed-field pinch aqueous fusion power core design
[DE88-008170] N88-26966

RHEOLOGY
Experiments on densely-loaded non-Newtonian slurries in laminar and turbulent pipe flows
[DE88-010579] N88-26612
Effects of a temperature-dependent rheology on large scale continental extension
[NASA-CR-183117] N88-26759

RING STRUCTURES
Analytical and experimental investigation of ringless piston concept
[AD-A192835] N88-26673
Transport in GaAs heterojunction ring structures N88-27011

ROADWAY POWERED VEHICLES
Simulation models for the dynamics of tracked vehicle systems: State-of-the-art and open problems N88-26522

ROBOTICS
Treatment of systematic errors in the processing of wide angle sonar sensor data for robotic navigation
[DE88-008961] N88-26352
Design of a controller to reduce residual vibration in the positioning control of flexible robotic manipulators N88-26658
RRSAS (Robotic Radiation Survey and Analysis System) Project: A real time sensor driven robotic system
[DE88-006825] N88-26661
An introduction to robot joint control methods
[NLR-TR-86080-U] N88-26677
Simulation of space manipulator operations (EUROSIM)
[NLR-MP-87017-U] N88-26678
Experiments in adaptive control of a very flexible one link manipulator N88-26865
Kinematics of Hooke universal joint robot wrists
[NASA-TM-100567] N88-26870

ROBOTS
Simple 2-D navigation for wheeled vehicles
[DE88-007115] N88-26351
Force servo control of a commercial gantry robot
[DE88-006649] N88-26660
Sensor fusion for robot navigation
[DE88-008383] N88-26663
Mobile robot survival
[DE88-009108] N88-26665
Optimization of performance criteria with bounded joint velocities for robots with one degree of redundancy
[DE88-003915] N88-26670
Local free-space mapping and path guidance for mobile robots
[AD-A192970] N88-26674
Diagnosing faults in autonomous robot plan execution
[NASA-CR-182480] N88-26859
ROCKET EXHAUST
Environmental monitoring of a titan 34D 5 1/2 segment solid rocket motor static firing
[AD-A192975] N88-26400
ROCKET SOUNDING
Rocket measurements within a polar cap arc: Ionospheric modelling
[AD-A192381] N88-26754
ROCKS
Prospects for hot dry rock in the future
[DE88-010909] N88-26730
Fine-scale traverses in cumulate rocks, Stillwater Complex: A lunar analogue study
[NASA-CR-183066] N88-26747
ROLLING MOMENTS
Parametric estimation of aerodynamic nonlinearities in rolling moment due to sideslip using maximum likelihood method N88-26528
ROOTS OF EQUATIONS
A full but elementary treatment of systems of homogeneous ordinary linear differential equations with constant coefficients
[REPT-87-82] N88-26887
ROTARY WING AIRCRAFT
Grid generation of a helicopter rotary-wing N88-26325
Hover performance tests of baseline metal and Advanced Technology Blade (ATB) rotor systems for the XV-15 tilt rotor aircraft
[NASA-CR-177436] N88-26367
A general-purpose approach to computer-aided dynamic analysis of a flexible helicopter
[NASA-TM-101002] N88-26709
ROTARY WINGS
Helicopter main-rotor noise: Determination of source contributions using scaled model data
[NASA-TP-2825] N88-26907
ROTATION
Some operational aspects of a rotating advanced-technology space station for the year 2025
[NASA-CR-181617] N88-26397
ROTOR AERODYNAMICS
A review of gear housing dynamics and acoustics literature
[NASA-CR-183110] N88-26675
ROTOR BLADES
Hover performance tests of baseline metal and Advanced Technology Blade (ATB) rotor systems for the XV-15 tilt rotor aircraft
[NASA-CR-177436] N88-26367
ROTORCRAFT AIRCRAFT
The role of aviation technology in the Caribbean Basin
[NASA-CR-183069] N88-26289
RUBIDIUM
Tactical Rubidium Frequency Standard (TRFS), volume 1
[AD-A192981] N88-26640
RUBY LASERS
Multipoint Thomson scattering diagnostic for DIII-D
[DE88-008737] N88-26969
RULES
Directions for programming in FORTRAN 77
[NASA-TT-20317] N88-26842
Towards knowledge bases-semantics, rules and object-oriented programming
[PB88-108154] N88-27110
RUN TIME (COMPUTERS)
Modeling and optimum time performance for concurrent processing
[NASA-CR-4167] N88-26595

S

S MATRIX THEORY
Analysis of networks with parameters S: Generalization of junction matrix
[INPE-4535-PRE/1282] N88-26570
SAFETY FACTORS
Control of flight through microburst wind shear using deterministic trajectory optimization N88-26375
SAMPLING
Asynchronous optical sampling for laser-based combustion diagnostics in high pressure flames
[AD-A192920] N88-26428
SARSAT
COSPAS/SARSAT 406-MHz emergency beacon digital controller
[NASA-TM-100859] N88-26566
SATELLITE ANTENNAS
Dynamics of satellites with radial wire antennas N88-26514
SATELLITE ATTITUDE CONTROL
Nutational stability of a satellite equipped with an active magnetic momentum wheel N88-26513
Dynamics of satellites with radial wire antennas N88-26514
SATELLITE IMAGERY
Interpreting forest biome productivity and cover utilizing nested scales of image resolution and biogeographical analysis
[NASA-CR-183036] N88-26711
Hydrologic models for land-atmosphere retrospective studies of the use of LANDSAT and AVHRR data
[NASA-CR-182861] N88-26712
Hydrologic models for land-atmosphere retrospective studies of the use of LANDSAT and AVHRR data
[NASA-CR-182862] N88-26716
SATELLITE NAVIGATION SYSTEMS
A positioning system based on NAVSAT
[NLR-MP-87018-U] N88-26358
SATELLITE NETWORKS
Document transfer by a digital satellite link
[NLR-MP-86071-U] N88-26564
SATELLITE OBSERVATION
Remote sensing and satellite applications to the needs of the gas and pipeline industry
[PB88-202668] N88-26714
Diffusion of slight solar induced disturbances in the middle atmosphere
[MITT-53] N88-26758
SATELLITE-BORNE INSTRUMENTS
The Oak Ridge National Laboratory strategic defense initiative shield optimization program: Executive summary
[DE88-008016] N88-26899
SATELLITE-BORNE RADAR
The role of space borne imaging radars in environmental monitoring: Some shuttle imaging radar results in Asia
[NASA-TM-101175] N88-26544
SCALE EFFECT
Dynamic interaction of convective cumulus with large-scale environment
[MITT-55] N88-26773
SCALE MODELS
Frequency domain identification of the dynamics of a scaled remotely-piloted helicopter N88-26524
SCALING LAWS
The scaled-sized model: A revision of Amdahl's law
[DE88-008114] N88-26675
SCANNING
SEGMERGE: A scanline visible surface algorithm with adaptive span selection and inexpensive antialiasing
[DE88-009186] N88-26826
SCATHA SATELLITE
A severe spacecraft-charging event on SCATHA in September 1982
[AD-A193007] N88-26396
SCATTERING
Microwave image understanding and its application to radar cross section management N88-26542
The theory of electron-polar phonon scattering rates in semiconductor micro-structures N88-27043
SCATTERING CROSS SECTIONS
Inelastic two composite particle systems scattering at high energy
[DE88-701841] N88-26928
SCHROEDINGER EQUATION
Combining relativity and quantum mechanics: Schroedinger's interpretation of psi
[DE88-701899] N88-27102
SEA LAUNCHING
The effect of a turbulent airstream on a vertically-launched missile at high angles of attack
[AD-A192408] N88-26363
SEAS
Eigenmatrix representations of radiance distributions in layered natural waters with wind-roughened surfaces
[PB88-188701] N88-26780
SECONDARY EMISSION
Effects of secondary electron emission on the collector and source sheaths of a finite ion temperature plasma
[DE88-008930] N88-26971
SECURITY
Use of fiber optic equipment for security
[DE88-007898] N88-26943
SEDIMENT TRANSPORT
Surface hydrology, sediment transport dynamics and remote sensing of disturbed watersheds in a humid temperate region
[DE88-008719] N88-26715
Prediction of continental shelf sediment transport using a theoretical model of the wave-current boundary layer
[AD-A192272] N88-26783
SEISMIC WAVES
Proceedings of the Array Signal Processing Symposium: Treaty Verification Program
[DE88-008346] N88-26548
SELF FOCUSING
On the self-focusing of electric helicons
[DE88-701870] N88-26905
SEMANTICS
Contractions in comparing concurrency semantics
[CWI-CS-R8755] N88-26850
A semantic approach to fairness
[CWI-CS-R8759] N88-26853
Towards knowledge bases-semantics, rules and object-oriented programming
[PB88-108154] N88-27110
Hiding in stream semantics of uniform concurrency
[PB88-121579] N88-27114
SEMICONDUCTOR DEVICES
Plasma separation process. Betacell (BCELL) code, user's manual
[DE88-006955] N88-26981
Raman, photoluminescence and modulation spectroscopy of semiconductor heterostructures N88-26997
Energy levels and magneto-electric effects in some quasi uni-dimensional semiconductor heterostructures N88-27009
Quantum transport in an electron waveguide N88-27010
Random quantum interference in microdevices N88-27021
Recent applications of Monte Carlo methods for semiconductor microdevice simulation N88-27046
Excellent negative differential resistance of InGaAs/InAlAs resonant tunneling barrier structures and applications to a new functional device, RHET N88-27048
Fermi level dependent native defect formation: Consequences for metal-semiconductor and semiconductor-semiconductor interfaces
[DE88-008247] N88-27066
SEMICONDUCTOR LASERS
New semiconductor laser structure for an optical communication system
[ETN-88-92353] N88-26654
SEMICONDUCTORS (MATERIALS)
Auger recombination in GaSb/AlSb-multi quantum well heterostructures N88-27001
Piezoelectric effects in strained layer superlattices N88-27002
Semiconductor microcrystallites in porous glass and their applications in optics N88-27005
Ferromagnetic/semiconductor hybrid structures N88-27013
Properties of synthetic magnetic superlattices N88-27014
EXAFS studies of the microstructure of semiconductor alloys, defects and semiconductor-metal interfaces N88-27031
Phonons in semiconductor superlattices N88-27035
Electron-phonon interactions in In(0.53)Ga(0.47)As and in In(0.53)Ga(0.47)As/InP quantum wells N88-27037
Electronic structure of quantum-well states revealed under high pressures N88-27038
The theory of electron-polar phonon scattering rates in semiconductor micro-structures N88-27043
Vertical electronic transport in novel semiconductor heterojunction structures N88-27045
Influence of interfaces on electronic and magnetic properties of MnSe/ZnSe superlattices near monolayer limit N88-27050
Atomistic simulation of stability, metastability and growth of strained layer structures N88-27053
Electrical study of metal/group 3-5 semiconductor interfaces: Comparison with the atomic-level studies N88-27059
Growth and characterization of thin films of ZnSnP(sub)2
[DE88-001164] N88-27060
Defects in high-mobility semiconductor systems
[AD-A192298] N88-27090
Epitaxy and properties of two dimensional GaInAs semiconductor structures
[ETN-88-92357] N88-27094

SENSE ORGANS
Regulatory biochemical and metabolic responses in photoreceptors
[AD-A192898] N88-26794
SENSITIVITY
The T-T-T curve in Cu-Cr alloy
[NASA-TT-20167] N88-26453
SENSORS
Fiber optic sensors with internal referencing
[NASA-TM-100893] N88-26644
RRSAS (Robotic Radiation Survey and Analysis System) Project: A real time sensor driven robotic system
[DE88-006825] N88-26661
SENSORY STIMULATION
Significance of sensory signal phase mismatch in mechanisms of motion sickness development N88-26787
SEPARATED FLOW
Vortex methods for separated flows
[NASA-TM-100068] N88-26342
A study of flow separation in transonic flow using inviscid and viscous computational fluid dynamics (CFD) schemes
[NASA-CR-183119] N88-26618
Treatment of the separated flow around profiles (nonviscous, incompressible, two dimensional flow) by the singularities method
[ISL-R-106/87] N88-26633
SERIES EXPANSION
Accurate solution of parabolic equations by expansion in ultraspherical polynomials
[DE88-701829] N88-26580
SERVICE LIFE
Engine component retirement for cause. Volume 1: Executive summary
[AD-A192730] N88-26371
A statistical treatment of accelerated life test data for copper-water heat pipes N88-26509
SERVOMECHANISMS
Force servo control of a commercial gantry robot
[DE88-006649] N88-26660
SHALLOW WATER
Fully implicit splitting method for accurate tidal computations
[PB88-183637] N88-26781
SHAPE MEMORY ALLOYS
Shape memory alloys: New materials for future engineering
[NASA-TT-20193] N88-26455
SHEAR FLOW
Influence of wind shear on the aerodynamic characteristics of airplanes
[NASA-TP-2627] N88-26344
A numerical simulation of two-dimensional transient shear flow
[ISAS-RN-627] N88-26600
Stability of a coastal upwelling front over topography
[AD-A192354] N88-26784
Evolution of hairpin vortices in a shear flow
[NASA-TM-100858] N88-26885
SHEAR LAYERS
Stability of a coastal upwelling front over topography
[AD-A192354] N88-26784
SHEAR PROPERTIES
Pulsed spray structure and atomisation techniques
[AD-A192260] N88-26614
SHIPS
Vertical ship motions and sea loads considering nonlinear effects
[TAE-592] N88-26515
SHOCK LAYERS
Absorption characteristics of Si3N4 ablation layer plasma N88-26504
SHOCK LOADS
Numerical simulation of supersonic free-jets N88-26299
SHOCK TUBES
Numerical simulation of the shock tube flows by TVD scheme N88-26308
Surface temperature thermal fluxmeters for shock tubes
[NASA-TT-20319] N88-26381
A shock-tube experiment on gases mixing processes associated with CO2/N2 mixing gasdynamic laser
[ISAS-RN-350] N88-26598
Navier-Stokes simulation of shock-tube flows over a wedge-type step by finite volume method
[ISAS-RN-628] N88-26599
SHOCK WAVE INTERACTION
Compressible boundary layers --- atmospheric reentry
[CERT-OA-13/5005-AYD] N88-26623
SHOCK WAVES
On symmetric TVD schemes N88-26319
Numerical modeling of the effect of particle size of explosives on shock initiation properties
[DE88-010479] N88-26491
Australian structures response evaluation: Ground shock and air blast measurements for site investigation survey
[MRL-TN-526] N88-26685
Shock wave compression and metallization of simple molecules
[DE88-008031] N88-26925
On linear relationship between shock velocity and particle velocity
[DE88-701827] N88-27099
SHORT TAKEOFF AIRCRAFT
Aerodynamic simulation for complete ASKA aircraft configuration N88-26301
Low-speed wind-tunnel test of a STOL supersonic-cruise fighter concept
[NASA-TM-4050] N88-26374
SHROUDS
Degradation of beam brightness by field emission from a cathode shroud
[DE88-008345] N88-26576
SHUTTLE IMAGING RADAR
The role of space borne imaging radars in environmental monitoring: Some shuttle imaging radar results in Asia
[NASA-TM-101175] N88-26544
SIDESLIP
Parametric estimation of aerodynamic nonlinearities in rolling moment due to sideslip using maximum likelihood method N88-26528
SIGNAL DETECTION
Proceedings of the Array Signal Processing Symposium: Treaty Verification Program
[DE88-008346] N88-26548
Surface disturbances produced by low-level, subsonic B-1 aircraft
[AD-A192257] N88-26752
SIGNAL DETECTORS
Local free-space mapping and path guidance for mobile robots
[AD-A192970] N88-26674
SIGNAL MEASUREMENT
An analysis of the efficiency and directivity of the sound generated by a moving laser source
[AD-A192220] N88-26914
SIGNAL PROCESSING
Proceedings of the Array Signal Processing Symposium: Treaty Verification Program
[DE88-008346] N88-26548
Signal processing in digital speech transmission systems
[ETN-88-92122] N88-26561
A microcomputer based frequency-domain processor for laser Doppler anemometry
[NASA-TM-100998] N88-26634
Display and processing of multidimensional signals with the aid of fractal image sequences
[ETN-88-92131] N88-26642
SIGNAL RECEPTION
Digital communication transmitter and receiver test procedures
[AD-A191218] N88-26540
SIGNAL TO NOISE RATIOS
Signal processing in digital speech transmission systems
[ETN-88-92122] N88-26561
SILICA GEL
A model for insulated wires in the method of moments code NEC (Numerical Electromagnetics Code)
[DE88-008920] N88-26577
Optical characterization of silica aerogel
[DE88-008916] N88-26946
SILICIDES
Initial development of high-temperature titanium silicide alloys
[DE88-007860] N88-26437
Rocket-propellant burn tests of silicide-coated niobium and tantalum
[DE88-010729] N88-26496
SILICON
Ductile-brittle transition of cutting behavior in diamond turning of single crystal Si
[DE88-008890] N88-26664
SILICON CARBIDES
Interface modification in Nicalon (trademark)/SiC composites
[DE88-009708] N88-26409
Observations on residual stresses in ceramic composites by neutron diffraction techniques
[DE88-009937] N88-26472
Factors influencing the toughening behavior of whisker reinforced ceramics
[DE88-011396] N88-26479
SILICON NITRIDES
Application of electron microscopy for the analysis of the mechanical behavior of advanced ceramics
[DE88-005049] N88-26469
Application of magnification xeroradiography to advanced ceramics
[DE88-009965] N88-26473
Absorption characteristics of Si3N4 ablation layer plasma N88-26504
SILICON OXIDES
Hot electrons in silicon dioxide: Ballistic to steady-state transport N88-27042
SILICON POLYMERS
Photovoltaic cells with n-silicon and conductive polymers
[ETN-88-92133] N88-26734
SILVER
Electronic and geometric structure of silver and palladium on aluminum (111) in monoatomic surface layers
[ETN-88-92120] N88-27093
SIMULATION
A simulation analysis of errors in the measurement of standard electrochemical rate constants from phase-selective impedance data
[AD-A192739] N88-26426
Research in electromagnetic shielding theory. Part 2: EMP (electromagnetic pulse) simulation using small loops
[AD-A192882] N88-26558
Navier-Stokes simulation of shock-tube flows over a wedge-type step by finite volume method
[ISAS-RN-628] N88-26599
A numerical simulation of two-dimensional transient shear flow
[ISAS-RN-627] N88-26600
Monte Carlo simulations of femtosecond relaxation of photoexcited electrons in AlGaAs/GaAs quantum wells N88-27036
Atomistic simulation of stability, metastability and growth of strained layer structures N88-27053
SIMULATORS
On the NAL numerical simulator system N88-26291
Research in electromagnetic shielding theory. Part 2: EMP (electromagnetic pulse) simulation using small loops
[AD-A192882] N88-26558
The UMAC simulator N88-26811
SINGLE CRYSTALS
Accelerated fatigue crack growth behavior of PWA 1480 single crystal alloy and its dependence on the deformation mode
[NASA-TM-100943] N88-26436
Development of a model procedure for the determination of volume diffusion lengths by transient measurements on monocrystal silicon solar cells
[ETN-88-92119] N88-26733
Anisotropic characteristic lengths in single crystal YBa2Cu3O(sub 7-Delta)
[DE88-009959] N88-27080
Pure metallic bridge and point-contact tunneling into single- and polycrystal YBa2Cu3O(sub 7-y)
[DE88-010030] N88-27084
Electron irradiation effects in YBa2Cu3O7-Delta single crystals
[DE88-010050] N88-27085
SINGLE EVENT UPSETS
Effects of cosmic rays on single event upsets
[NASA-CR-183053] N88-26569
SINGULARITY (MATHEMATICS)
Linearization along invariant manifolds and a generalization of the Hartman-Grobman theorems for degenerate singularities of vector fields in R cubed
[REPT-87-80] N88-26886
SINTERING
Sintering of the heterogeneous MgO compacts
[DE88-010357] N88-26408
Manufacturing of a ceramic-ceramic composite matrix using the sol-gel procedure
[ETN-88-92157] N88-26414
Preparation of oxide superconductors
[DE88-009136] N88-27063
SITE SELECTION
Australian structures response evaluation: Ground shock and air blast measurements for site investigation survey
[MRL-TN-526] N88-26685
SIZE DISTRIBUTION
Small-droplet spray measurements with a scattered-light scanner
[NASA-TM-100973] N88-26645
SKIN FRICTION
The determination of the topological structure of skin friction lines on a rectangular wing-body combination
[NASA-CR-4168] N88-26343
SKY
Effects of atmospheric model layering on LOWTRAN 6 calculations of 8-12 micrometers near-horizon sky radiances
[AD-A192969] N88-26559

SKY SURVEYS (ASTRONOMY)
A survey of the Ap stars for rapid variability N88-27127
SLIDING FRICTION
Study of temperature and stress fields of two sliding cylinders
[ETN-88-92134] N88-26704
SLOTTED WIND TUNNELS
Wall interference assessment/correction of data from tests of a CAST 10-2/DOA 2 airfoil in the Langley 0.3-m transonic cryogenic tunnel N88-26331
SLURRIES
Experiments on densely-loaded non-Newtonian slurries in laminar and turbulent pipe flows
[DE88-010579] N88-26612
SMOKE
Enhanced emergency smoke venting
[DOT/FAA/CT-88/22] N88-26350
SODIUM
Production of powdered sodium hydride with large specific surface by the catalyzed reaction of molten sodium with hydrogen-1
[NASA-TT-20185] N88-26462
SODIUM HYDRIDES
Production of powdered sodium hydride with large specific surface by the catalyzed reaction of molten sodium with hydrogen-1
[NASA-TT-20185] N88-26462
SOFTWARE ENGINEERING
Position and velocity determination using a Global Positioning System: An outline
[B8735052] N88-26355
Research in computer science 1985/6
[PB88-113840] N88-26815
Script editor: An editor for the specification phase in the development of computer based learning
[REPT-87-68] N88-26846
Fixpoint representations of characteristic sets of linear-time temporal formulas
[CWI-CS-R8754] N88-26849
NEXT: An expert system development tool to support engineering design
[NLR-MP-86070-U] N88-26871
Design and development of courseware for goniometry
[REPT-87-73] N88-27106
SOFTWARE TOOLS
The UMAC simulator N88-26811
A multiprocess operating system for 16 bit microcomputers or porting Unix (trademark) to a NS32016 with enhancements N88-26822
SOI (SEMICONDUCTORS)
JFET/SOS (Junction Field-Effect Transistor/Silicon-on-Sapphire) devices: Gamma-radiation-induced effects
[AD-A193001] N88-26586
SOILS
Vegetation studies on Vandenberg Air Force Base, California
[NASA-TM-100985] N88-26795
SOL-GEL PROCESSES
Manufacturing of a ceramic-ceramic composite matrix using the sol-gel procedure
[ETN-88-92157] N88-26414
Characterization of the surface area and porosity of sol-gel films using saw devices
[DE88-008794] N88-27069
SOLAR ACTIVITY
Diffusion of slight solar induced disturbances in the middle atmosphere
[MITT-53] N88-26758
Solar-geophysical data number 522, February 1988. Part 2: (Comprehensive reports). Data for August 1987 and miscellanea
[PB88-194741] N88-27138
Solar-geophysical data number 522, February 1988. Part 1: (Prompt reports). Data for January 1988, December 1987 and late data
[PB88-194733] N88-27139
SOLAR ACTIVITY EFFECTS
Diffusion of slight solar induced disturbances in the middle atmosphere
[MITT-53] N88-26758
SOLAR CELLS
Electrophoretic coatings. Part 1: Sandia applications
[DE88-008666] N88-26485
Photovoltaic concentrator technology: Recent results
[DE88-009588] N88-26726
Development of a model procedure for the determination of volume diffusion lengths by transient measurements on monocrystal silicon solar cells
[ETN-88-92119] N88-26733
Photovoltaic cells with n-silicon and conductive polymers
[ETN-88-92133] N88-26734
Analytical determination of critical crack size in solar cells
[NASA-CR-183128] N88-26736
SOLAR CORONA
The properties of solar coronal active regions deduced from X-ray line spectra
[AD-A193026] N88-27141
SOLAR FLARES
The properties of solar coronal active regions deduced from X-ray line spectra
[AD-A193026] N88-27141
The hard X-ray burst spectrometer event listing 1980-1987
[NASA-TM-4036] N88-27144
SOLAR NEUTRINOS
Cosmions and stars
[DE88-010886] N88-27145
SOLAR RADIATION
Determination and application of bidirectional solar-optical properties of fenestration systems
[DE88-010364] N88-26727
On the global radiation incident variously orientated surfaces on the South Coast of Finland
[FMI-5] N88-26746
Solar-geophysical data number 522, February 1988. Part 1: (Prompt reports). Data for January 1988, December 1987 and late data
[PB88-194733] N88-27139
SOLAR SPECTROMETERS
The hard X-ray burst spectrometer event listing 1980-1987
[NASA-TM-4036] N88-27144
SOLAR SYSTEM
Space infrared telescope facility project
[NASA-CR-183058] N88-27121
SOLAR TERRESTRIAL INTERACTIONS
Diffusion of slight solar induced disturbances in the middle atmosphere
[MITT-53] N88-26758
SOLAR WIND
Generation of Adlam-Allen waves by plasma release experiments in the solar wind
[PB88-106000] N88-27140
SOLAR X-RAYS
The properties of solar coronal active regions deduced from X-ray line spectra
[AD-A193026] N88-27141
SOLID ELECTROLYTES
Preparation technology for thin film solid electrolyte fuel cells
[PB88-131925] N88-26735
SOLID MECHANICS
Analytical determination of critical crack size in solar cells
[NASA-CR-183128] N88-26736
SOLID PROPELLANT COMBUSTION
Combustion of PMMA (polymethylmethacrylate), PE (polyethylene) and PS (polystyrene) in a ramjet
[PB88-186572] N88-26417
SOLID PROPELLANT ROCKET ENGINES
An interactive computer code for preliminary design of solid propellant rocket motors
[AD-A192869] N88-26399
Environmental monitoring of a titan 34D 5 1/2 segment solid rocket motor static firing
[AD-A192975] N88-26400
SOLID PROPELLANTS
Technical instructions for a control operating system of the gas flow installation for the solid fuel combustion chamber
[LR-507] N88-26537
SOLID STATE
Raman and absorption spectrophotometric studies of selected lanthanide, californium-doped lanthanide, and actinide trihalides in the solid state
[DE88-008234] N88-27061
SOLIDS
Research on the kinetics of phase changes in solids
[AD-A192222] N88-26696
Lattice theory of fracture of solids with layered structure
[DE88-701867] N88-27073
SOLUBILITY
Synthesis of model polymers and related structures in support of vinyl monomer grafting studies
[DE88-010245] N88-26476
Critical point wetting drop tower experiment
[NASA-CR-183062] N88-26603
SOLUTES
High resolution detection of solute segregation to the cores of dislocations in grain boundaries
[DE88-009168] N88-27078
SOLUTION
Numerical solution of weak forms of conservation laws on optimal unstructured triangular grids N88-26597
Solution of the Orr-Sommerfeld equation for the Blausius boundary-layer documentation of program ORRBL and a test case
[NASA-CR-4169] N88-26858
SOLUTIONS
The influence of uncompensated solution resistance on the determination and standard electrochemical rate constants using cyclic voltammetry and some comparisons with AC voltammetry
[AD-A192825] N88-26427
A matroid algorithm and its application to the efficient solution of two optimization problems on graphs, revision
[AD-A192709] N88-26838
SOLVENTS
A study of solvent effects on the synthesis of pure component and composite ceramic powders by metal alkoxide hydrolysis
[DE88-008381] N88-26470
SONAR
Treatment of systematic errors in the processing of wide angle sonar sensor data for robotic navigation
[DE88-008961] N88-26352
Sensor fusion for robot navigation
[DE88-008383] N88-26663
SOOT
Experimental and theoretical analysis of the radiative transfer within a sooty pool fire
[DE88-007099] N88-26419
SOS (SEMICONDUCTORS)
JFET/SOS (Junction Field-Effect Transistor/Silicon-on-Sapphire) devices: Gamma-radiation-induced effects
[AD-A193001] N88-26586
SOUND FIXING AND RANGING
Outdoor sound propagation, its implications for unattended ground sensors
[FEL-1986-64] N88-26917
SOUND INTENSITY
Sound power measurements in situ using a reference sound source
[PB88-182571] N88-26910
SOUND PRESSURE
An analysis of the efficiency and directivity of the sound generated by a moving laser source
[AD-A192220] N88-26914
SOUND PROPAGATION
Outdoor sound propagation, its implications for unattended ground sensors
[FEL-1986-64] N88-26917
SOUND TRANSMISSION
Signal processing in digital speech transmission systems
[ETN-88-92122] N88-26561
Aircraft interior noise reduction by alternate resonance tuning
[NASA-CR-182540] N88-26909
Acoustic diffraction by an absorbing finite strip in a moving fluid
[PB88-191382] N88-26912
SOUND WAVES
Dynamics and stability of combustion driven self oscillations in presence of various frequencies. Extensive stability criteria
[ETN-88-92123] N88-26432
Studying materials using acoustic waves
[AD-A192234] N88-26915
On the possibility of the soliton description of acoustic emission during plastic deformation of crystals
[DE88-701878] N88-27075
SOUTHERN HEMISPHERE
Meteorological atlas of the Southern Hemisphere lower stratosphere for August and September 1987
[NASA-TM-4049] N88-26763
SPACE CHARGE
Results from the SLAC lasertron
[DE88-007816] N88-26647
SPACE FLIGHT STRESS
Effect of weightlessness on brain development (results of flight of pregnant rats on Kosmos-1514 biosatellite and study of subsequent development of their progeny on earth N88-26786
SPACE INFRARED TELESCOPE FACILITY
Space infrared telescope facility project
[NASA-CR-183058] N88-27121
SPACE LABORATORIES
Simulation of space manipulator operations (EUROSIM)
[NLR-MP-87017-U] N88-26678
SPACE MANUFACTURING
Some operational aspects of a rotating advanced-technology space station for the year 2025
[NASA-CR-181617] N88-26397
SPACE MISSIONS
Launch operations to support future space forces
[AD-A192679] N88-27107

SPACE PERCEPTION
The interaction of sensory and perceptual variables: Spatial, temporal and orientation response to figure and ground
[AD-A192897] N88-26798
SPACE PLASMAS
Kinetic modulational instability of electron cyclotron waves in plasmas
[DE88-701893] N88-26978
Generation of Adlam-Allen waves by plasma release experiments in the solar wind
[PB88-106000] N88-27140
SPACE PROCESSING
Analysis of the performance of the space ultravacuum research facility in attached and free-flyer mode
[NASA-TM-100325] N88-26387
Industrial processes influenced by gravity
[NASA-CR-182140] N88-26497
SPACE PROGRAMS
Space policy of common sense and moderation
[REPT-49/87] N88-27118
SPACE SHUTTLE ORBITERS
Numerical simulations of flow around shuttle orbiter N88-26293
The effects of RCS jet firing on the isolated Orbiter and mated coast phases of the glide return to launch site maneuver at Mach number 6 (IA302B)
[NASA-CR-180223] N88-26403
SPACE SHUTTLES
Book analysis. Challenger: A major malfunction
[AD-A192458] N88-26388
SPACE STATION STRUCTURES
Mobile remote manipulator system for a tetrahedral truss
[NASA-CASE-MSC-20985-1] N88-26396
SPACE STATIONS
Some operational aspects of a rotating advanced-technology space station for the year 2025
[NASA-CR-181617] N88-26397
SPACE TOOLS
An introduction to robot joint control methods
[NLR-TR-86080-U] N88-26677
SPACE WEAPONS
Monitoring space weaponry: Detection and verification issues
[DE88-008726] N88-26900
SDI and/or arms control
[RAND-P-7357] N88-26903
Launch operations to support future space forces
[AD-A192679] N88-27107
SPACECRAFT COMMUNICATION
Document transfer by a digital satellite link
[NLR-MP-86071-U] N88-26564
SPACECRAFT COMPONENTS
The use of liquid films for spacecraft survivability to laser radiation
[AD-A192954] N88-26395
SPACECRAFT CONFIGURATIONS
Ludwig Prandtl collected treatises on applied mechanics, hydro- and aerodynamics, part 1
[NASA-TT-20316] N88-26337
SPACECRAFT CONTROL
Spacecraft applications of advanced global positioning system technology
[NASA-CR-172063] N88-26359
SPACECRAFT DESIGN
Design and testing of a high power spacecraft thermal management system
[NASA-TM-4051] N88-26389
SPACECRAFT EQUIPMENT
Heat pump augmented radiator for low-temperature space applications
[DE88-008369] N88-26393
Transient thermal analysis of three latent heat storage configurations for rapid thermal charging
[DE88-008943] N88-27104
SPACECRAFT LANDING
Lunar base launch and landing facility conceptual design, 2nd edition
[NASA-CR-172049] N88-27135
SPACECRAFT LAUNCHING
Launch operations to support future space forces
[AD-A192679] N88-27107
SPACECRAFT PERFORMANCE
Design and testing of a high power spacecraft thermal management system
[NASA-TM-4051] N88-26389
SPACECRAFT POWER SUPPLIES
The design and fabrication of a Stirling engine heat exchanger module with an integral heat pipe
[NASA-TM-101296] N88-26732
SPACECRAFT RADIATORS
Heat pump augmented radiators for spacecraft thermal management
[DE88-007890] N88-26392
SPACECRAFT STABILITY
The Proceedings of the Symposium on Mechanics for Space Flight 1987
[ISAS-SP-6] N88-26499
Nutational stability of a satellite equipped with an active magnetic momentum wheel N88-26513
SPACECRAFT STRUCTURES
Study of the influence of metallurgical factors on fatigue and fracture of aerospace structural materials
[AD-A192909] N88-26452
SPACECRAFT SURVIVABILITY
The use of liquid films for spacecraft survivability to laser radiation
[AD-A192954] N88-26395
SPACECRAFT TEMPERATURE
Design and testing of a high power spacecraft thermal management system
[NASA-TM-4051] N88-26389
SPACELAB PAYLOADS
Liquid motions in partially filled containers: Preliminary results of the D-1 mission --- Spacelab
[NLR-MP-86042-U] N88-26629
SPANWISE BLOWING
Numerical study of delta wing leading edge blowing
[NASA-CR-183101] N88-26335
SPATIAL FILTERING
Optical correlation using the magneto-optic device
[AD-A192342] N88-26950
SPECIFICATIONS
Analytical determination of critical crack size in solar cells
[NASA-CR-183128] N88-26736
Script editor: An editor for the specification phase in the development of computer based learning
[REPT-87-68] N88-26846
The evaluation of a deformable diffraction grating for a stigmatic EUV spectrohelioimeter
[NASA-CR-183064] N88-26941
SPECIMEN GEOMETRY
Damage in a perforated graphite-epoxy plate under monotonic, cyclic biaxial loading
[ONERA-NT-1987-5] N88-26708
SPECKLE PATTERNS
Digital image processing from speckle interferograms by correlation methods: Application in atmospheric optics, astronomy, and biology
[ETN-88-92125] N88-26953
Methods for indirect imaging through the atmosphere
[ONERA-NT-1987-4] N88-27124
SPECTRA
Wavenumber spectra from THIR 6.7 micron water vapor data N88-26756
SPECTRAL METHODS
Study and implementation of ultrahigh frequency coupling devices using the fin line technology --- millimeter waves
[ETN-88-92307] N88-26588
Spectral resolution of the Navier-Stokes equations in multi-domain curved complex geometries
[ONERA-NT-1987-2] N88-26631
Solution of the Orr-Sommerfeld equation for the Blausius boundary-layer documentation of program ORRBL and a test case
[NASA-CR-4169] N88-26858
SPECTRAL RESOLUTION
Spectral resolution of the Navier-Stokes equations in multi-domain curved complex geometries
[ONERA-NT-1987-2] N88-26631
Time-resolved doubly bent crystal X-ray spectrometer
[DE88-007899] N88-26637
SPECTROHELIOGRAPHS
The evaluation of a deformable diffraction grating for a stigmatic EUV spectrohelioimeter
[NASA-CR-183064] N88-26941
SPECTROSCOPIC ANALYSIS
In situ spectroscopic studies of transition metal macrocycles as catalysts for the electrochemical reduction of oxygen
[PB88-203195] N88-26416
SPECTRUM ANALYSIS
Measurement of HO2 and other trace gases in the stratosphere using a high resolution far-infrared spectrometer at 28 KM
[NASA-CR-180400] N88-26737
SPEECH RECOGNITION
Signal processing in digital speech transmission systems
[ETN-88-92122] N88-26561
SPEED CONTROL
Contribution to speed regulation of small motors with phase-locked loops
[ETN-88-92373] N88-26590
SPEED REGULATORS
Contribution to speed regulation of small motors with phase-locked loops
[ETN-88-92373] N88-26590
SPIN DYNAMICS
Dynamics of satellites with radial wire antennas N88-26514
Properties of synthetic magnetic superlattices N88-27014
SPIN STABILIZATION
Dynamics of satellites with radial wire antennas N88-26514
SPLINES
Procedure for converting a Wilson-Fowler spline to a cubic B-spline with double knots
[DE88-008971] N88-26878
SPLITTING
Fully implicit splitting method for accurate tidal computations
[PB88-183637] N88-26781
SPRAYERS
Pulsed spray structure and atomisation techniques
[AD-A192280] N88-26614
SPRAYING
Small-droplet spray measurements with a scattered-light scanner
[NASA-TM-100973] N88-26645
SPUTTERING
The effects of thin compressive films on indentation fracture toughness measurements
[AD-A192243] N88-26480
Laser desorption/ablation studies by resonance ionization mass spectrometry
[DE88-009124] N88-26650
SQUEEZE FILMS
Magnetohydrodynamic squeeze film
[DE88-701876] N88-26669
STABILITY
Instability-related delamination growth of embedded and edge delaminations N88-26406
The protonic Beta double prime aluminas: Preparation, stability, conductivity and structure
[DE88-008442] N88-26415
Modelling of premixed combustion using a thin flame sheet and the effect of the hydrodynamic instability
[DE88-009467] N88-26423
Phase stability and alloy design of ordered intermetallics
[DE88-007479] N88-26435
The effects of gradients on boundary stability
[DE88-009592] N88-26445
A numerical study of Rayleigh-Taylor instability in aluminum and steel plates
[DE88-010475] N88-26449
Resistance of polyamide-6 against long time effects of various media at various temperatures
[NASA-TT-20297] N88-26484
STABILIZATION
Heterogeneous diffusion flame stabilization
[AD-A193014] N88-26429
STACKS
Phosphoric acid electric utility fuel cell technology development
[DE88-010187] N88-26582
STAINLESS STEELS
The effects of Hertzian stress and test ambient on the friction coefficient of MoS2 coatings
[DE88-008118] N88-26467
GTAW characterization for weld penetration on 304L stainless steel
[DE88-010611] N88-26672
STANDARD DEVIATION
Coherent RF error statistics
[AD-A193002] N88-26560
STANDARDS
Center for Electronics and Electrical Engineering technical publication announcements covering Center programs, July to September 1987
[PB88-196530] N88-26572
Fiber optic sensors with internal referencing
[NASA-TM-100893] N88-26644
Improvement of head-up display standards. Volume 1: Head-up display design guide, appendix
[AD-A192973] N88-26809
STARK EFFECT
Novel quantum well optical devices N88-27028
STARS
Cosmions and stars
[DE88-010886] N88-27145
STATIC FIRING
Environmental monitoring of a titan 34D 5 1/2 segment solid rocket motor static firing
[AD-A192975] N88-26400
STATISTICAL ANALYSIS
Circulation statistics from seasonal and perpetual January and July simulations with the NCAR (National Center for Atmospheric Research) Community Climate Model (CCM1):R15
[PB88-192620] N88-26748

STATISTICAL DISTRIBUTIONS
Interpreting forest biome productivity and cover utilizing nested scales of image resolution and biogeographical analysis
[NASA-CR-183036] N88-26711
Range of a constrained random walk
[PB88-126867] N88-26897
Aperiodic superlattices: Structured randomness N88-27055

STATISTICAL MECHANICS
On microphysical principles of thermofluid dynamics
[ETN-88-92095] N88-26620
Extension of Boltzmann's theory to a liquid
[DE88-009153] N88-27097

STATOR BLADES
Computational study on thermal efficiency of ceramic gas turbine
[DE88-753114] N88-26667

STATORS
Study on the heat resisting and cooling property of the ceramics-metal hybrid stator vanes
[DE88-753117] N88-26668

STEAM FLOW
Study of a water-steam two phase flow in a T-branch
[ETN-88-92306] N88-26624

STEELS
A numerical study of Rayleigh-Taylor instability in aluminum and steel plates
[DE88-010475] N88-26449

STEERING
Local free-space mapping and path guidance for mobile robots
[AD-A192970] N88-26674
Time-Optimal Adaptive Shaped Torque (TOAST) technical note
[AD-A192719] N88-26869

STELLAR WINDS
Time-dependent mass loss from hot stars with and without radiative driving
[DE88-008899] N88-27128

STELLARATORS
Neoclassical diffusion due to trapping/detrapping orbits in stellarators
[DE88-008566] N88-26968

STIFFNESS
Stiffness degradation of composite laminates N88-26405
A micromechanics model of the stiffness and strength of laminates with fiber waviness
[NASA-CR-181670] N88-26413

STIRLING CYCLE
Magnetic heat pump design
[DE88-007730] N88-26605

STIRLING ENGINES
The design and fabrication of a Stirling engine heat exchanger module with an integral heat pipe
[NASA-TM-101296] N88-26732

STOCHASTIC PROCESSES
Stochastic modeling of EM scattering from foliage
[AD-A192258] N88-26553
Two classes of self-similar stable processes with stationary increments
[AD-A192842] N88-26894

STOPPING POWER
Studies of HZE particle interactions and transport for space radiation protection purposes
[NASA-TM-101159] N88-27142

STORAGE BATTERIES
Ambient temperature secondary lithium batteries using LiAl lithium insertion anodes
[DE88-008394] N88-26574
Exploratory battery technology development and testing report for 1986
[DE88-009870] N88-26578

STRAIN DISTRIBUTION
Compression creep of filamentary composites
[NASA-CR-182550] N88-26601

STRAIN ENERGY METHODS
Vibration response of constrained viscoelastically damped plates: Analyses and experiments
[AD-A192329] N88-26699

STRAIN ENERGY RELEASE RATE
Three-dimensional analysis of a postbuckled embedded delamination
[NASA-TP-2823] N88-26684

STRATEGY
SDI: Myth or reality
[DE88-009121] N88-26901
The strategic defense initiative: Strategic implications
[AD-A192341] N88-26902

STRATOSPHERE
Meteorological atlas of the Southern Hemisphere lower stratosphere for August and September 1987
[NASA-TM-4049] N88-26763

STREAMLINING
The determination of the topological structure of skin friction lines on a rectangular wing-body combination
[NASA-CR-4168] N88-26343

STREAMS
Hiding in stream semantics of uniform concurrency
[PB88-121579] N88-27114

STRESS (PHYSIOLOGY)
Satellite remote sensing of the wet bulb globe temperature heat stress index, phase 2
[AD-A192798] N88-26717
Effect of weightlessness on brain development (results of flight of pregnant rats on Kosmos-1514 biosatellite and study of subsequent development of their progeny on earth N88-26786

STRESS ANALYSIS
A constitutive model with damage for high-temperature superalloys N88-26434
Observations on residual stresses in ceramic composites by neutron diffraction techniques
[DE88-009937] N88-26472
Vertical ship motions and sea loads considering nonlinear effects
[TAE-592] N88-26515
Stress concentration around circular hole in a composite material specimen representative of the X-29A forward-swept wing aircraft
[NASA-CR-179435] N88-26694
Dynamical stress concentration problems, from every side, bordered and perforated plates
[ETN-88-92128] N88-26703
Study of temperature and stress fields of two sliding cylinders
[ETN-88-92134] N88-26704
Stress analysis using infrared thermography
[ETN-88-92169] N88-26705
Stress-related phenomena in transient radiation-induced absorption in optical fibers
[DE88-010956] N88-26949
Lattice strain in heteroepitaxial films N88-27032

STRESS CONCENTRATION
Stress concentration around circular hole in a composite material specimen representative of the X-29A forward-swept wing aircraft
[NASA-CR-179435] N88-26694
Dynamical stress concentration problems, from every side, bordered and perforated plates
[ETN-88-92128] N88-26703

STRESS DISTRIBUTION
Study of temperature and stress fields of two sliding cylinders
[ETN-88-92134] N88-26704

STRESS FUNCTIONS
Dynamical stress concentration problems, from every side, bordered and perforated plates
[ETN-88-92128] N88-26703

STRESS INTENSITY FACTORS
Lattice theory of fracture of solids with layered structure
[DE88-701867] N88-27073

STRESS PROPAGATION
Instability-related delamination growth of embedded and edge delaminations N88-26406

STRESSES
A new boundary integral equation formulation for elastodynamic and elastostatic crack analysis
[AD-A192967] N88-26702

STRING THEORY
Algebraic and arithmetic geometry in string theory
[CWI-PM-R8708] N88-26904
Research in theoretical particle physics
[DE88-008230] N88-26927

STRONGLY COUPLED PLASMAS
MACH2: A two-dimensional magnetohydrodynamic simulation code for complex experimental configurations
[AD-A192285] N88-26988

STRUCTURAL ANALYSIS
Sensitivity to crack initiation in thick assemblies. Test report 48-444
[REPT-48-444] N88-26365
Surface phases and their influence on metal-oxide interfaces
[DE88-007938] N88-26420
Australian structures response evaluation: Ground shock and air blast measurements for site investigation survey
[MRL-TN-526] N88-26685
FEB structural analysis, revision H
[AD-A192302] N88-26698

STRUCTURAL MEMBERS
Experimental and theoretical investigation of passive damping concepts for member forced and free vibration
[NASA-CR-183082] N88-26693

STRUCTURAL VIBRATION
Modeling and parameter identification of motor vehicles N88-26521

STUDENTS
The sine and cosine function for class 4-VWO. Exploration of possible bottlenecks
[REPT-87-72] N88-27105

SUBSONIC FLOW
Influence of rear body geometry on the velocity characteristics of the near wake
[ISL-R-113/87] N88-26339
Three-dimensional viscous flow computations of a circular jet in subsonic and supersonic cross flow
[NASA-CR-182153] N88-26616

SUBSTRATES
Plasma deposition: Investigations on a new approach
[ETN-88-92619] N88-26992
MBE growth of HgTe/CdTe superlattices on Si(100) substrates N88-27033
Preparation of high-T(sub)c Y1Ba2Cu3O(sub 7-Delta) superconducting thin films by MBE (Molecular-Beam-Epitaxy) techniques
[DE88-009999] N88-27082

SULFIDES
The crystallization of tough thermoplastic resins in the presence of carbon fibers
[NASA-CR-182984] N88-26484

SUMMARIES
Narrative domain implementation
[AD-A192265] N88-26868

SUPERCOMPUTERS
Computer science research, 1987: Computation Directorate
[DE88-008637] N88-26812
The performance of the NEC SX-2 and Cray X-MP supercomputers
[DE88-009177] N88-26813

SUPERCONDUCTIVITY
Application of superconducting technology to earth-to-orbit electromagnetic launch systems
[NASA-TM-101134] N88-26385
Application of superconducting technology to earth-to-orbit electromagnetic launch systems
[DE88-010022] N88-26386
Superconducting rf and beam-cavity interactions
[DE88-008598] N88-26936
Superconductivity of Cr/V superlattices N88-27057
To the twinning plane superconductivity theory
[DE88-702195] N88-27058
Effects of grain boundary composition on properties of YBa2Cu3O/sub 7-x/
[DE88-007679] N88-27064
Superconductivity of heavy-electron uranium compounds
[DE88-007901] N88-27065
The superconducting transition in oxygen deficient YBa2Cu3O(sub 7-Delta)
[DE88-009957] N88-27079
Anisotropy of the lower critical field in YBa2Cu3O(sub 7-Delta)
[DE88-009971] N88-27081
Preparation of high-T(sub)c Y1Ba2Cu3O(sub 7-Delta) superconducting thin films by MBE (Molecular-Beam-Epitaxy) techniques
[DE88-009999] N88-27082
Oxygen vacancy ordering and superconductivity in YBa2Cu3O(sub 7-x)
[DE88-010005] N88-27083
Superconducting electronic film structures
[AD-A192907] N88-27091
On the chemistry of superconductivity
[DE88-010714] N88-27096

SUPERCONDUCTORS
Preparation of oxide superconductors
[DE88-009136] N88-27063
Recent advances in atom-probe field ion microscopy
[DE88-008799] N88-27070
HeFlow: A program for calculating pressure and temperature of helium in forced-flow superconductors. Part 1: Numerical solutions. Part 2: HeFlow user's manual
[DE88-008941] N88-27071
Phenomenological approach to high T/sub c/ oxide superconductors
[DE88-701868] N88-27074
Anisotropic characteristic lengths in single crystal YBa2Cu3O(sub 7-Delta)
[DE88-009959] N88-27080
Ceramic processing of high-T(sub)c superconductors
[DE88-010090] N88-27087
SIS (Superconductor-Insulator-Superconductor) mixer research
[AD-A192908] N88-27092

SUPERCRITICAL AIRFOILS
Calculation of 2-D unsteady transonic full potential flow about oscillating airfoils by two complementary approaches
[PB88-127519] N88-26341

SUPERLATTICES
Third International Conference on Superlattices, Microstructures and Microdevices
[AD-A191416] N88-26995
Piezoelectric effects in strained layer superlattices N88-27002
Control of carrier lifetime in PbTe nipi superlattices by external photoinjection N88-27006
Metallic superlattices N88-27012
Properties of synthetic magnetic superlattices N88-27014
Superlattice doping interfaces N88-27019
A 10 microns photoexcited avalanche gain due to electron impact ionization from GaAs quantum well superlattices N88-27026
Transport study on Si/Si(1-x)Ge(x) superlattices selectively doped by secondary implantation of Sb N88-27027
Electrical properties of p-type and n-type ZnSe-ZnTe strained-layer superlattices N88-27029
MBE growth of HgTe/CdTe superlattices on Si(100) substrates N88-27033
Growth of high quality CoSi2/Si superstructures on Si(111) N88-27034
Phonons in semiconductor superlattices N88-27035
Electronic structure of quantum-well states revealed under high pressures N88-27038
On a-Si:H/a-SiN(x):H superlattices: Confinement or contamination N88-27040
Extended and local plasmons in a lateral superlattice N88-27041
Resonant tunneling in InGaAs-InP double-barrier structures and superlattices N88-27047
Non-effective-mass matching in superlattices N88-27049
Influence of interfaces on electronic and magnetic properties of MnSe/ZnSe superlattices near monolayer limit N88-27050
Structural studies of (Ga,In)(As,P) alloys and (InAs) sub m (GaAs) sub n strained-layer superlattices by fluorescence-detected EXAFS N88-27051
Type 3 - type 1 transition and strain effect in Hg(1-x)Cd(x)Te-CdTe and Hg(1-x)Zn(x)Te-CdTe superlattices N88-27052
Ordering transitions of ternary alloys A(1-x)B(x)C N88-27054
Aperiodic superlattices: Structured randomness N88-27055
Characterization of structural and magnetic order of Er/Y superlattices N88-27056
Superconductivity of Cr/V superlattices N88-27057

SUPERPLASTICITY
Optimizing superplastic response in lithium containing aluminum-magnesium alloys
[AD-A192217] N88-26451

SUPERSONIC AIRCRAFT
Navier-Stokes analysis of transonic transport aircraft empennage N88-26297
Numerical simulation of viscous flows over transonic aircraft configurations N88-26302
Low-speed wind-tunnel test of a STOL supersonic-cruise fighter concept
[NASA-TM-4050] N88-26374

SUPERSONIC FLOW
Numerical simulations of aerodynamic contribution of flows about a space-plane-type configuration N88-26292
Numerical calculation of supersonic flow by the PNS equations N88-26296
Numerical simulation of supersonic free-jets N88-26299
Three-dimensional viscous flow computations of a circular jet in subsonic and supersonic cross flow
[NASA-CR-182153] N88-26616

SUPERSONIC JET FLOW
Numerical simulations of astrophysical jets N88-26295

SUPERSONIC SPEED
High speed and high angle of attack wind tunnel test results of the winged space vehicle C-2
[ISAS-RN-623] N88-26329

SUPPORT SYSTEMS
Engine component retirement for cause. Volume 1: Executive summary
[AD-A192730] N88-26371

SURFACE CRACKS
Boundary element method for contact heat transfer
[DE88-011013] N88-26613

SURFACE DIFFUSION
On the global radiation incident variously orientated surfaces on the South Coast of Finland
[FMI-5] N88-26746

SURFACE FINISHING
The knowledge based automatic extraction of the machinable surfaces for automatic CAD-CAM system
[INPE-4542-PRE/1288] N88-26824
Fabrication technology
[DE88-010598] N88-26955

SURFACE LAYERS
Surface phases and their influence on metal-oxide interfaces
[DE88-007938] N88-26420
Fundamental optical studies of competitive adsorption and thin film phenomena
[DE88-006780] N88-27068
Electronic and geometric structure of silver and palladium on aluminum (111) in monoatomic surface layers
[ETN-88-92120] N88-27093

SURFACE PROPERTIES
Production of powdered sodium hydride with large specific surface by the catalyzed reaction of molten sodium with hydrogen-1
[NASA-TT-20185] N88-26482
Scattering patterns of dihedral corner reflectors with impedance surface impedances
[NASA-CR-183078] N88-26545
Evaluation of surface energy and radiation balance systems for FIFE
[NASA-CR-183118] N88-26778
Eigenmatrix representations of radiance distributions in layered natural waters with wind-roughened surfaces
[PB88-188701] N88-26780
SEGMERGE: A scanline visible surface algorithm with adaptive span selection and inexpensive antialiasing
[DE88-009186] N88-26826
Sound propagation over uneven ground and irregular topography
[NASA-CR-182956] N88-26911
Fermi level dependent native defect formation: Consequences for metal-semiconductor and semiconductor-semiconductor interfaces
[DE88-008247] N88-27066

SURFACE REACTIONS
Numerical model for the computation of radiance distributions in natural waters with wind-roughened surfaces
[PB88-192703] N88-26785

SURFACE ROUGHNESS
Plastic deformation and roughness of free metal surfaces
[PB88-196621] N88-26439
Numerical model for the computation of radiance distributions in natural waters with wind-roughened surfaces
[PB88-192703] N88-26785
Eigenmatrix representations of radiance distributions in layered natural waters with wind-roughened surfaces
[PB88-188701] N88-26780

SURFACE TEMPERATURE
Surface temperature thermal fluxmeters for shock tubes
[NASA-TT-20319] N88-26381

SURFACE TO AIR MISSILES
The effect of a turbulent airstream on a vertically-launched missile at high angles of attack
[AD-A192408] N88-26363

SURFACE VEHICLES
Local free-space mapping and path guidance for mobile robots
[AD-A192970] N88-26674

SURVEILLANCE RADAR
Multi-target tracking algorithms for cluttered environments N88-26543

SURVEYS
RRSAS (Robotic Radiation Survey and Analysis System) Project: A real time sensor driven robotic system
[DE88-006825] N88-26661
Australian structures response evaluation: Ground shock and air blast measurements for site investigation survey
[MRL-TN-526] N88-26685

SURVIVAL
Mobile robot survival
[DE88-009108] N88-26665

SUSPENSION SYSTEMS (VEHICLES)
A review of gear housing dynamics and acoustics literature
[NASA-CR-183110] N88-26675

SWITCHES
Electron-impact-ionization and electron-attachment cross sections of radicals important in transient gaseous discharges
[AD-A192248] N88-26424
Development of liquid metal field-emission sources for use in fast repetitive opening switches
[AD-A192230] N88-26583

SWITCHING CIRCUITS
Extinction behavior of low voltage switching arc under consideration of cathodic coatings and dynamic arc column
[ETN-88-92384] N88-26591

SYMMETRY
On symmetric TVD schemes N88-26319
Symmetrized magnetic field configuration of low aspect ratio helical system
[IPPJ-869] N88-26956

SYNCHRONISM
Asynchronous optical sampling for laser-based combustion diagnostics in high pressure flames
[AD-A192920] N88-26428

SYNCHRONOUS MOTORS
Permanent magnet excitation of axial flow synchronous machines with high rotation moment
[ETN-88-92385] N88-26592

SYNOPTIC MEASUREMENT
The role of space borne imaging radars in environmental monitoring: Some shuttle imaging radar results in Asia
[NASA-TM-101175] N88-26544

SYNOPTIC METEOROLOGY
Synoptic patterns related to tropical cyclone recurvature
[AD-A192338] N88-26771
Solar-geophysical data number 522, February 1988. Part 2: (Comprehensive reports). Data for August 1987 and miscellanea
[PB88-194741] N88-27138

SYNTHESIS (CHEMISTRY)
Substituted 1,1,1-Triaryi-2,2,2-Trifluoroethanes and processes for their synthesis
[NASA-CASE-LEW-14345-1] N88-26404
Glass forming ranges of amorphous alloys
[DE88-007897] N88-26438
Dual mechanism bifunctional polymers: Design, synthesis and application of a new category of metal ion complexing agents
[DE88-008233] N88-26488
A study of solvent effects on the synthesis of pure component and composite ceramic powders by metal alkoxide hydrolysis
[DE88-008381] N88-26470
Fundamental studies of elastomers
[DE88-009679] N88-26471
Refractory Materials of Zirconate. Part 2: Synthesis and some properties of strontium, zirconate, calcium zirconate and barium zirconate
[NASA-TT-20186] N88-26483
Cosmological helium production simplified
[DE88-009578] N88-27130

SYNTHETIC APERTURE RADAR
Data volume reduction for imaging radar polarimetry
[NASA-CASE-NPO-17184-1-CU] N88-26541
The role of space borne imaging radars in environmental monitoring: Some shuttle imaging radar results in Asia
[NASA-TM-101175] N88-26544

SYNTHETIC FUELS
Development of an equation of state for computation of supercompressibility factors, critical flow factors and other properties for wet, sour natural gases, synthetic gases and admixtures
[PB88-202676] N88-26602

SYSTEM IDENTIFICATION
System identification in vehicle dynamics
[DFVLR-MITT-87-22] N88-26518
Flight vehicle system identification: Status and prospects N88-26520
Vehicle dynamics: Identification in the frequency domain N88-26523
Frequency domain identification of the dynamics of a scaled remotely-piloted helicopter N88-26524
Multivariable identification of a flexible transport aircraft N88-26525
A two-point aerodynamic model for identification N88-26526
The identification of the direct lift control flap system of the research aircraft ATTAS N88-26527
Identification methods for transport dynamical investigations N88-26531
Utilization of identification methods in the time and frequency domain for the determination of the XV-15 (tilt-rotor) dynamics for lateral motion in hover flight N88-26532
Identification of lateral operation dynamics of rail vehicles using roll test stand tests N88-26534
Nonlinear identification of an aircraft for the direct calculation of an anticipatory control N88-26535

SYSTEMS ANALYSIS
Diagnosing faults in autonomous robot plan execution
[NASA-CR-182480] N88-26859
Finite-dimensional approximation for optimal fixed-order compensation of distributed parameter systems
[NASA-CR-181674] N88-26873

SYSTEMS ENGINEERING
Improvement of head-up display standards. Volume 1: Head-up display design guide, appendix
[AD-A192973] N88-26809

An overview of the development of a linear broadband analog fiber-optic link
[DE88-008668] N88-26945
SYSTEMS SIMULATION
Simulation of space manipulator operations (EUROSIM)
[NLR-MP-87017-U] N88-26678
SYSTOLIC ARRAYS
Efficient bit-level, word-level and block-level systolic arrays for matrix-matrix multiplication
[DE88-011331] N88-26856

T

T SHAPE
Study of a water-steam two phase flow in a T-branch
[ETN-88-92306] N88-26624
TACTICS
Flight simulator: Field of view utilized in performing tactical maneuvers
[AD-A192412] N88-26379
TAIL ASSEMBLIES
Navier-Stokes analysis of transonic transport aircraft empennage N88-26297
TANTALUM
Rocket-propellant burn tests of silicide-coated niobium and tantalum
[DE88-010729] N88-26496
TARGET RECOGNITION
Multi-target tracking algorithms for cluttered environments N88-26543
Optical data processing
[AD-A193024] N88-26841
Outdoor sound propagation, its implications for unattended ground sensors
[FEL-1986-64] N88-26917
TARGETS
Analysis of the perforation of monolithic and simple laminate aluminium targets as a test of analytical deformation models
[MRL-R-1111] N88-26686
TASKS
Diagnosing faults in autonomous robot plan execution
[NASA-CR-182480] N88-26859
TECHNICAL WRITING
Computer-aided writing
[AD-A192516] N88-26837
TECHNOLOGIES
Center for Electronics and Electrical Engineering technical publication announcements covering Center programs, July to September 1987
[PB88-196530] N88-26572
Resources: NASA for entrepreneurs
[NASA-CR-182152] N88-27119
TECHNOLOGY ASSESSMENT
Flight Mechanics Panel Symposium on Rotorcraft Design for Operations: Technical evaluation report
[AGARD-AR-243] N88-26362
Pyrotechnic system failures: Causes and prevention
[NASA-TM-100633] N88-26394
The outlook for ceramics in heat engines, 1990-2010: Results of a worldwide Delphi survey
[DE88-010075] N88-26475
Photovoltaic concentrator technology: Recent results
[DE88-009588] N88-26726
TECHNOLOGY TRANSFER
Wind Energy Technology: Generating power from the wind, a current awareness bulletin
[DE88-008292] N88-26729
TECHNOLOGY UTILIZATION
The role of aviation technology in the Caribbean Basin
[NASA-CR-183069] N88-26289
Resources: NASA for entrepreneurs
[NASA-CR-182152] N88-27119
TECTONICS
Effects of a temperature-dependent rheology on large scale continental extension
[NASA-CR-183117] N88-26759
TELEOPERATORS
Simulation of space manipulator operations (EUROSIM)
[NLR-MP-87017-U] N88-26678
TELEVISION CAMERAS
Sensor fusion for robot navigation
[DE88-008383] N88-26663
TELEVISION SYSTEMS
Optical data processing
[AD-A193024] N88-26841
TEMPERATURE CONTROL
Design and testing of a high power spacecraft thermal management system
[NASA-TM-4051] N88-26389
Heat pump augmented radiators for spacecraft thermal management
[DE88-007890] N88-26392
Modeling and thermal management of advanced batteries
[DE88-010023] N88-26580
TEMPERATURE DEPENDENCE
Effects of a temperature-dependent rheology on large scale continental extension
[NASA-CR-183117] N88-26759
Photoluminescence studies of InGaAlAs quaternary alloys
[DE88-007197] N88-27062
TEMPERATURE DISTRIBUTION
A statistical treatment of accelerated life test data for copper-water heat pipes N88-26509
Characteristics of long size thermosyphons made of corrugated tube N88-26511
Study of temperature and stress fields of two sliding cylinders
[ETN-88-92134] N88-26704
TEMPERATURE EFFECTS
Critical point wetting drop tower experiment
[NASA-CR-183062] N88-26603
Our climate in danger
[DE88-701824] N88-26743
Photosynthetic water splitting
[DE88-007809] N88-26791
Thermal inhibition by megagauss field due to variation of electron temperature in laser plasma
[DE88-701887] N88-26977
Phase transformations and thermodynamic behavior of the YBa2Cu3O(sub)x system via EMF measurements
[DE88-010054] N88-27086
TEMPERATURE GRADIENTS
The effects of gradients on boundary stability
[DE88-009592] N88-26445
An experimental investigation of transient characteristics in a gravity-assisted heat pipe N88-26506
HeFlow: A program for calculating pressure and temperature of helium in forced-flow superconductors. Part 1: Numerical solutions. Part 2: HeFlow user's manual
[DE88-008941] N88-27071
TEMPERATURE MEASUREMENT
Evaluation of thermophosphor temperature technique
[DE88-007654] N88-26638
Remote sensing of temperature profiles. Performance test of PASS
[DE88-753108] N88-26768
TEMPERATURE PROFILES
An arranging method on L/D of two-phase closed thermosyphons N88-26508
Remote sensing of temperature profiles. Performance test of PASS
[DE88-753108] N88-26768
TENSILE PROPERTIES
Initial development of high-temperature titanium silicide alloys
[DE88-007860] N88-26437
Helium induced degradation in the weldability of an austenitic stainless steel
[DE88-009062] N88-26443
Nickel aluminides: A new family of nickel + aluminum alloys featuring simple composition, low density, excellent oxidation resistance and high yield strength that increases with temperature
[DE88-010692] N88-26461
TENSILE STRENGTH
High temperature testing of C/C (Carbon/Carbon) composites
[AD-A193012] N88-26411
TENSILE TESTS
High temperature testing of C/C (Carbon/Carbon) composites
[AD-A193012] N88-26411
Investigation of structure and surface state effect on hydrogen embrittlement of steels, under consideration of acoustic emission analysis
[ETN-88-92350] N88-26457
TERNARY ALLOYS
Ordering transitions of ternary alloys A(1-x)B(x)C N88-27054
TERRAIN
Development of an atmospheric diffusion evaluation method incorporating topographical effects. Part 1: Literature review of atmospheric diffusion models incorporating terrain effects
[DE88-753104] N88-26742
Sound propagation over uneven ground and irregular topography
[NASA-CR-182956] N88-26911
TERRESTRIAL PLANETS
A bibliography of dunes: Earth, Mars, and Venus
[NASA-CR-4149] N88-27134
TEST FACILITIES
Development of a model procedure for the determination of volume diffusion lengths by transient measurements on monocrystal silicon solar cells
[ETN-88-92119] N88-26733
TEST RANGES
Radar cross section studies/compact range research
[NASA-CR-183124] N88-26565
TEST STANDS
Identification of lateral operation dynamics of rail vehicles using roll test stand tests N88-26534
TEST VEHICLES
Vehicle dynamics: Identification in the frequency domain N88-26523
TESTS
The design and fabrication of a Stirling engine heat exchanger module with an integral heat pipe
[NASA-TM-101296] N88-26732
THEOREM PROVING
Challenge problems focusing on equality and combinatory logic: Evaluating automated theorem-proving programs
[DE88-010057] N88-26879
THEOREMS
Comparison theorems and their use in the analysis of some nonlinear diffusion problems
[DE88-010032] N88-26884
Challenge equality problems in lattice theory
[DE88-010094] N88-27072
THEORETICAL PHYSICS
Theoretical studies in elementary particle physics
[DE88-008929] N88-26926
Research in theoretical particle physics
[DE88-008230] N88-26927
THERMAL ANALYSIS
Thermal and mechanical analysis of the Faraday shield for the compact ignition tokamak
[DE88-007855] N88-26962
Transient thermal analysis of three latent heat storage configurations for rapid thermal charging
[DE88-008943] N88-27104
THERMAL BLOOMING
High spatial frequency thermal blooming instability: A linear stability analysis
[DE88-010711] N88-26655
THERMAL CONDUCTIVITY
Thermal conductivity of selected foams and systems from 100 to 300 K
[PB88-201553] N88-26486
An experimental investigation of transient characteristics in a gravity-assisted heat pipe N88-26506
Boundary element method for contact heat transfer
[DE88-011013] N88-26613
Physical-chemical reactions at welding arc/molten pool interfaces
[DE88-007717] N88-26862
Thermal conductivity of pure fluids in a large region around the critical point
[ETN-88-92135] N88-27103
THERMAL DEGRADATION
Antimisting kerosene: Low temperature degradation and blending
[NASA-CR-182725] N88-26495
THERMAL DIFFUSION
High spatial frequency thermal blooming instability: A linear stability analysis
[DE88-010711] N88-26655
THERMAL RESISTANCE
High temperature testing of C/C (Carbon/Carbon) composites
[AD-A193012] N88-26411
Heat transfer of mesh-wick heat-pipes (bottom heat mode) N88-26507
THERMAL SHOCK
An analysis of the efficiency and directivity of the sound generated by a moving laser source
[AD-A192220] N88-26914
THERMAL STABILITY
Defect characterization of the redox behavior and stability of conducting oxides
[DE88-010799] N88-27088
THERMAL STRESSES
Study on the heat resisting and cooling property of the ceramics-metal hybrid stator vanes
[DE88-753117] N88-26668
THERMODYNAMIC EFFICIENCY
Computational study on thermal efficiency of ceramic gas turbine
[DE88-753114] N88-26667
An analysis of the efficiency and directivity of the sound generated by a moving laser source
[AD-A192220] N88-26914
THERMODYNAMICS
Thermostatistical estimations of vapor-state molecules affected by gravity in a heat pipe N88-26505
Electrodynamic driver for the space thermoacoustic refrigerator (STAR)
[AD-A192337] N88-26517
On microphysical principles of thermofluid dynamics
[ETN-88-92095] N88-26620

Thermodynamic analysis of chemical heat storage system for heat pump
[DE88-753121] N88-26728
Non-equilibrium phases and phase diagrams
[DE88-006896] N88-27098

THERMOGRAPHY
Stress analysis using infrared thermography
[ETN-88-92169] N88-26705

THERMOHYDRAULICS
Study of a water-steam two phase flow in a T-branch.
[ETN-88-92306] N88-26624

THERMOMETERS
Evaluation of thermophosphor temperature technique
[DE88-007654] N88-26638

THERMONUCLEAR REACTIONS
TIBER (Tokamak Ignition/Burn Experimental Reactor) 2 as a precursor to an international thermonuclear experimental reactor
[DE88-006906] N88-26970

THERMOPLASTIC RESINS
Thermoplastic coating of carbon fibers
[NASA-CR-183067] N88-26407
Irreversible deformations during fracture in polymers
[W-7/86] N88-26485

THERMOPLASTICITY
The crystallization of tough thermoplastic resins in the presence of carbon fibers
[NASA-CR-182984] N88-26484

THERMOSIPHONS
Heat transfer of mesh-wick heat-pipes (bottom heat mode) N88-26507
An arranging method on L/D of two-phase closed thermosyphons N88-26508
Characteristics of long size thermosyphons made of corrugated tube N88-26511

THERMOSPHERE
The NASA Marshall engineering thermosphere model
[NASA-CR-179350] N88-26760

THICK FILMS
The effects of thin compressive films on indentation fracture toughness measurements
[AD-A192243] N88-26480
Superconducting electronic film structures
[AD-A192907] N88-27091

THICKNESS
GTAW characterization for weld penetration on 304L stainless steel
[DE88-010611] N88-26672

THIN FILMS
The use of liquid films for spacecraft survivability to laser radiation
[AD-A192954] N88-26395
The effects of thin compressive films on indentation fracture toughness measurements
[AD-A192243] N88-26480
Preparation technology for thin film solid electrolyte fuel cells
[PB88-131925] N88-26735
Properties of multilayers for soft X-ray optics N88-27025
Growth and characterization of thin films of ZnSnP(sub)2
[DE88-001164] N88-27060
Fundamental optical studies of competitive adsorption and thin film phenomena
[DE88-006780] N88-27068
Characterization of the surface area and porosity of sol-gel films using saw devices
[DE88-006794] N88-27069
Preparation of high-T(sub)c Y1Ba2Cu3O(sub 7-Delta) superconducting thin films by MBE (Molecular-Beam-Epitaxy) techniques
[DE88-009999] N88-27082

THOMSON SCATTERING
A CO2 laser Thomson scattering diagnostic for fusion product alpha particle measurement
[DE88-007683] N88-26965
Multipoint Thomson scattering diagnostic for DIII-D
[DE88-006737] N88-26969

THREE DIMENSIONAL BODIES
Rarefied gas numerical wind tunnel 3: Universal code for three dimensional bodies N88-26304
Relaxation scheme for compressible flows N88-26323
A survey of freeform solid modeling methods
[REPT-87-81] N88-26847
The construction of composite grids for general three-dimensional regions N88-26872

THREE DIMENSIONAL FLOW
Numerical calculation of three dimensional flow by TVD scheme N88-26309
Numerical analysis of three dimensional cascade flow by solving Navier-Stokes equations N88-26310
Numerical analysis of duct flow using three-dimensional parabolized Navier-Stokes equation N88-26312
On the stationary solutions of three-dimensional Euler equations by the TVD difference schemes N88-26320
Use of direct solvers for multidimensional fluid flow computations
[DE88-010063] N88-26611
Three-dimensional viscous flow computations of a circular jet in subsonic and supersonic cross flow
[NASA-CR-182153] N88-26616
Improved 3-D turbomachinery CFD algorithm
[NASA-CR-179364] N88-26619

THRUST
Low-speed wind-tunnel test of a STOL supersonic-cruise fighter concept
[NASA-TM-4050] N88-26374

THRUST VECTOR CONTROL
The effects of RCS jet firing on the isolated Orbiter and mated coast phases of the glide return to launch site maneuver at Mach number 6 (IA302B)
[NASA-CR-180223] N88-26403

THUNDERSTORMS
A radar study of the interaction between lightning and precipitation
[DE88-009120] N88-26770

TIDEPOWER
Survey on utility technology of a tidal and ocean current energy
[DE88-770148] N88-26722

TIDES
Fully implicit splitting method for accurate tidal computations
[PB88-183637] N88-26781

TILT ROTOR AIRCRAFT
The role of aviation technology in the Caribbean Basin
[NASA-CR-183069] N88-26289

TILT ROTOR RESEARCH AIRCRAFT PROGRAM
Hover performance tests of baseline metal and Advanced Technology Blade (ATB) rotor systems for the XV-15 tilt rotor aircraft
[NASA-CR-177436] N88-26367

TIME DEPENDENCE
Resistance of polyamide-6 against long time effects of various media at various temperatures
[NASA-TT-20297] N88-26484
A new trajectory following polynomial-time algorithm for the linear programming problem
[REPT-87-87] N88-26848
A nodal method for time-dependent transport equation
[DE88-004285] N88-26876

TIME FUNCTIONS
Simple multireader registers using time-stamp schemes
[CWI-CS-R8758] N88-26819

TIME MARCHING
Extensive verification of blade-to-blade flow code based on Denton scheme N88-26314

TIME MEASUREMENT
A simulation analysis of errors in the measurement of standard electrochemical rate constants from phase-selective impedance data
[AD-A192739] N88-26426

TIME OPTIMAL CONTROL
Time-Optimal Adaptive Shaped Torque (TOAST) technical note
[AD-A192719] N88-26889

TITANIUM ALLOYS
Initial development of high-temperature titanium silicide alloys
[DE88-007660] N88-26437
Glass forming ranges of amorphous alloys
[DE88-007897] N88-26438

TOKAMAK DEVICES
Thermal and mechanical analysis of the Faraday shield for the compact ignition tokamak
[DE88-007855] N88-26962
Fusion programs in applied plasma physics and development and technology at GA Technologies, Inc.
[DE88-006406] N88-26964
Multipoint Thomson scattering diagnostic for DIII-D
[DE88-006737] N88-26969
TIBER (Tokamak Ignition/Burn Experimental Reactor) 2 as a precursor to an international thermonuclear experimental reactor
[DE88-006906] N88-26970
Requirements for neutral beam current drive in tokamaks
[DE88-006180] N88-26980
Impurity transport calculations for a drift-dependent tokamak scrape-off plasma
[DE88-010053] N88-26984
Full-wave calculations in flux coordinates for toroidal geometry
[DE88-010131] N88-26985
Toroidal and poloidal soft X-ray imaging system on the D3-D tokamak
[DE88-010585] N88-26986
Vertical viewing ECE diagnostic for the D3-D tokamak
[DE88-010586] N88-26987
MTX (Microwave Tokamak Experiment) plasma diagnostic system
[DE88-011326] N88-26993

TOMOGRAPHY
XDATAP
[DE88-007161] N88-26827

TOPOGRAPHY
Development of an atmospheric diffusion evaluation method incorporating topographical effects. Part 1: Literature review of atmospheric diffusion models incorporating terrain effects
[DE88-753104] N88-26742

TOPOLOGY
The determination of the topological structure of skin friction lines on a rectangular wing-body combination
[NASA-CR-4168] N88-26343

TOROIDAL PLASMAS
Full-wave calculations in flux coordinates for toroidal geometry
[DE88-010131] N88-26985
Toroidal and poloidal soft X-ray imaging system on the D3-D tokamak
[DE88-010585] N88-26986

TORQUE
Time-Optimal Adaptive Shaped Torque (TOAST) technical note
[AD-A192719] N88-26889

TORUSES
Eigenmodes of a random walk on a 2-D lattice torus with one trap
[DE88-007830] N88-26874

TOTAL ENERGY SYSTEMS
An analysis of gas-steam total power recovery energy system N88-26512

TOXICOLOGY
JPRS report: Science and technology. USSR: Life sciences
[JPRS-ULS-88-009] N88-26785

TRACE ELEMENTS
Review of methods for remote sensing of atmospheric emissions from stationary sources
[PB88-190483] N88-26739
Tracer water transport and subgrid precipitation variation within atmospheric general circulation models
[NASA-CR-182897] N88-26745
Physical oceanography and tracer chemistry of the southern ocean
[DE88-006852] N88-26779

TRACKING (POSITION)
Multi-target tracking algorithms for cluttered environments N88-26543

TRACKING NETWORKS
Surface disturbances produced by low-level, subsonic B-1 aircraft
[AD-A192257] N88-26752

TRAJECTORIES
A simulation of post boost vehicle deployment of multiple reentry vehicles
[DE88-009537] N88-26391
Multi-target tracking algorithms for cluttered environments N88-26543

TRAJECTORY ANALYSIS
A new trajectory following polynomial-time algorithm for the linear programming problem
[REPT-87-87] N88-26848

TRAJECTORY MEASUREMENT
Trajectory measurement of the Fokker 100 aircraft during autoland testing
[NLR-MP-86010-U] N88-26386

TRANSFORMATIONS (MATHEMATICS)
Thermal inhibition by megagauss field due to variation of electron temperature in laser plasma
[DE88-701887] N88-26977

TRANSIENT HEATING
Transient thermal analysis of three latent heat storage configurations for rapid thermal charging
[DE88-008943] N88-27104

TRANSIENT RESPONSE
An experimental investigation of transient characteristics in a gravity-assisted heat pipe N88-26506

TRANSISTORS
Hot electron transistors grown by MOCVD N88-26996
Excellent negative differential resistance of InGaAs/InAlAs resonant tunneling barrier structures and applications to a new functional device, RHET N88-27046

TRANSITION FLOW
Numerical simulation of transition to turbulence in plane Poiseuille flow by a spectral method N88-26321
Turbulence transition in a circular pipe N88-26503

TRANSITION METALS
In situ spectroscopic studies of transition metal macrocycles as catalysts for the electrochemical reduction of oxygen
[PB88-203195] N88-26416
TRANSITION TEMPERATURE
The superconducting transition in oxygen deficient YBa2Cu3O(sub 7-Delta)
[DE88-009957] N88-27079
TRANSLATING
The UMAC simulator N88-26811
TRANSMISSOMETERS
Description of the MPTR system: Multi Path Transmissometer Radiometer
[FEL-1987-14] N88-26954
TRANSMITTER RECEIVERS
Digital communication transmitter and receiver test procedures
[AD-A191218] N88-26540
TRANSONIC FLOW
Navier-Stokes analysis of transonic transport aircraft empennage N88-26297
Aerodynamic simulation for complete ASKA aircraft configuration N88-26301
Numerical simulation of the shock tube flows by TVD scheme N88-26308
An initial investigation into methods of computing transonic aerodynamic sensitivity coefficients
[NASA-CR-183061] N88-26332
Finite element approximation to a model problem of transonic flow
[DE88-701835] N88-26333
Calculation of 2-D unsteady transonic full potential flow about oscillating airfoils by two complementary approaches
[PB88-127519] N88-26341
A study of flow separation in transonic flow using inviscid and viscous computational fluid dynamics (CFD) schemes
[NASA-CR-183119] N88-26618
TRANSONIC WIND TUNNELS
Wall interference assessment/correction of data from tests of a CAST 10-2/DOA 2 airfoil in the Langley 0.3-m transonic cryogenic tunnel N88-26331
TRANSPORT AIRCRAFT
Navier-Stokes analysis of transonic transport aircraft empennage N88-26297
Multivariable identification of a flexible transport aircraft N88-26525
Application of complementary parameter identification techniques to flight test data of a transport aircraft N88-26533
TRANSPORT PROPERTIES
Drift wave vortices and anomalous transport
[DE88-009562] N88-26982
Impurity transport calculations for a drift-dependent tokamak scrape-off plasma
[DE88-010053] N88-26984
Third International Conference on Superlattices, Microstructures and Microdevices
[AD-A191416] N88-26995
Transport in GaAs heterojunction ring structures N88-27011
Theoretical aspects of electron transport in modulated structures N88-27016
Transport study on Si/Si(1-x)Ge(x) superlattices selectively doped by secondary implantation of Sb N88-27027
Resonant tunneling in InGaAs-InP double-barrier structures and superlattices N88-27047
Type 3 - type 1 transition and strain effect in Hg(1-x)Cd(x)Te-CdTe and Hg(1-x)Zn(x)Te-CdTe superlattices N88-27052
Studies of HZE particle interactions and transport for space radiation protection purposes
[NASA-TM-101159] N88-27142
TRANSPORT THEORY
Tracer water transport and subgrid precipitation variation within atmospheric general circulation models
[NASA-CR-182897] N88-26745
Eigenmodes of a random walk on a 2-D lattice torus with one trap
[DE88-007830] N88-26874
A nodal method for time-dependent transport equation
[DE88-004285] N88-26876
Quantum transport theory of resonant-tunneling heterostructure devices N88-27017
Quantum interference and transport in microstructures N88-27022
TRAPPED PARTICLES
JFET/SOS (Junction Field-Effect Transistor/Silicon-on-Sapphire) devices: Gamma-radiation-induced effects
[AD-A193001] N88-26586
TRITIUM
The hole of a blanket tritium system on the fusion fuel cycle
[DE88-010007] N88-26983
TROPICAL METEOROLOGY
Dynamic interaction of convective cumulus with large-scale environment
[MITT-55] N88-26773
Westward moving atmospheric wave disturbances over the African tropics: Dynamic and energetic aspects
[MITT-57] N88-26774
TRUSSES
Mobile remote manipulator system for a tetrahedral truss
[NASA-CASE-MSC-20985-1] N88-26398
TUBE HEAT EXCHANGERS
Development of protective coatings for ceramic tubular components
[PB88-197165] N88-26483
TUNING
Tuning a major part of a clustering algorithm
[AD-A191446] N88-26821
Aircraft interior noise reduction by alternate resonance tuning
[NASA-CR-182540] N88-26909
Visible tunable source
[DE88-006442] N88-26944
TUNNEL DIODES
SIS (Superconductor-Insulator-Superconductor) mixer research
[AD-A192908] N88-27092
TURBINE BLADES
Extensive verification of blade-to-blade flow code based on Denton scheme N88-26314
Computational study on thermal efficiency of ceramic gas turbine
[DE88-753114] N88-26667
TURBINE ENGINES
A high fidelity real-time simulation of a small turboshaft engine
[NASA-TM-100991] N88-26378
TURBINE PUMPS
Analysis of flow through pump of large rocket engine N88-26306
TURBOCOMPRESSORS
Application of computational fluid dynamics to design of compressor cascade N88-26315
TURBOMACHINE BLADES
Structural optimization of fiber composite turbomachine blades
[ETN-88-92351] N88-26372
TURBOMACHINERY
A diagonally inverted LU implicit multigrid scheme
[NASA-TM-100911] N88-26340
Improved 3-D turbomachinery CFD algorithm
[NASA-CR-179364] N88-26619
TURBOSHAFTS
A high fidelity real-time simulation of a small turboshaft engine
[NASA-TM-100991] N88-26378
TURBULENCE
Wind flow study: July 1987 and November-December 1987
[DE88-008969] N88-26776
TURBULENT BOUNDARY LAYER
Drag reduction of turbulent boundary layers by means of grooved surfaces
[ETN-88-92618] N88-26630
Wind tunnel study of atmospheric diffusion in unstable stratified boundary layer. Part 2: Characteristic scale and diffusion
[DE88-753109] N88-26749
TURBULENT DIFFUSION
Development of an atmospheric diffusion evaluation method incorporating topographical effects. Part 1: Literature review of atmospheric diffusion models incorporating terrain effects
[DE88-753104] N88-26742
Wind tunnel study of atmospheric diffusion in unstable stratified boundary layer. Part 2: Characteristic scale and diffusion
[DE88-753109] N88-26749
TURBULENT FLOW
Numerical simulation of transition to turbulence in plane Poiseuille flow by a spectral method N88-26321
Numerical simulation of turbulent flow using the exponential expression of k-epsilon equation N88-26322
Influence of rear body geometry on the velocity characteristics of the near wake
[ISL-R-113/87] N88-26339
The effect of a turbulent airstream on a vertically-launched missile at high angles of attack
[AD-A192408] N88-26363
An efficient computational tool for ramjet combustor research
[DE88-010034] N88-26389
Heterogeneous diffusion flame stabilization
[AD-A193014] N88-26429
Turbulence transition in a circular pipe N88-26503
Nonlinear equation of state effects and the momentum-dilution trade-off in a turbulent buoyant jet
[DE88-701839] N88-26610
Experiments on densely-loaded non-Newtonian slurries in laminar and turbulent pipe flows
[DE88-010579] N88-26612
Experimental investigation of turbulent flow in smooth and longitudinal grooved tubes
[NASA-TM-77480] N88-26615
Treatment of the separated flow around profiles (nonviscous, incompressible, two dimensional flow) by the singularities method
[ISL-R-106/87] N88-26633
Evolution of hairpin vortices in a shear flow
[NASA-TM-100858] N88-26685
TURING MACHINES
Simple multireader registers using time-stamp schemes
[CWI-CS-R8758] N88-26819
TWINNING
To the twinning plane superconductivity theory
[DE88-702195] N88-27058
TWO DIMENSIONAL FLOW
An initial investigation into methods of computing transonic aerodynamic sensitivity coefficients
[NASA-CR-183061] N88-26332
Calculation of 2-D unsteady transonic full potential flow about oscillating airfoils by two complementary approaches
[PB88-127519] N88-26341
Heterogeneous diffusion flame stabilization
[AD-A193014] N88-26429
A numerical simulation of two-dimensional transient shear flow
[ISAS-RN-627] N88-26600
Treatment of the separated flow around profiles (nonviscous, incompressible, two dimensional flow) by the singularities method
[ISL-R-106/87] N88-26633
TWO PHASE FLOW
An arranging method on L/D of two-phase closed thermosyphons N88-26508
Characteristics of long size thermosyphons made of corrugated tube N88-26511

U

ULTRAHIGH VACUUM
Analysis of the performance of the space ultravacuum research facility in attached and free-flyer mode
[NASA-TM-100325] N88-26387
ULTRASONICS
Quantitative particle characterization by scattered ultrasound N88-26908
ULTRAVIOLET RADIATION
Ultraviolet imaging of hydrogen flames
[DE88-009152] N88-26422
UNDERWATER ACOUSTICS
A modal approach to Arctic noise modelling with implied vertical coherence
[AD-A192966] N88-26916
UNITED STATES
Monitoring space weaponry: Detection and verification issues
[DE88-008726] N88-26900
UNSTEADY AERODYNAMICS
Calculations of unsteady aerodynamics for a full aircraft configuration using boundary element method N88-26303
UNSTEADY FLOW
Numerical simulation of the shock tube flows by TVD scheme N88-26308
An implicit, high order accurate, upwind scheme for unsteady Euler equations N88-26317
On the dynamic behavior of balloon during its launch; application of panel method and extension to unsteady problem
[ISAS-RN-622] N88-26330
Calculation of 2-D unsteady transonic full potential flow about oscillating airfoils by two complementary approaches
[PB88-127519] N88-26341
UPSTREAM
On the accuracy of upwind biased finite volume method N88-26316
An implicit, high order accurate, upwind scheme for unsteady Euler equations N88-26317

UPWELLING WATER
Stability of a coastal upwelling front over topography
[AD-A192354] N88-26784
URANUS (PLANET)
Ultraviolet geometric albedo of Uranus
[NASA-CR-183099] N88-27136
USER MANUALS (COMPUTER PROGRAMS)
Axisymmetric liquid sloshing under low-g conditions: Numerical simulation method (reference manual)
[NLR-TR-86057-4] N88-26627
PAX ECONOPACK economic analysis package users manual
[AD-A192949] N88-27117
USER REQUIREMENTS
Flight Mechanics Panel Symposium on Rotorcraft Design for Operations: Technical evaluation report
[AGARD-AR-243] N88-26362
Direct manipulation and the design of user interfaces
[PB88-126354] N88-26810
SIMS: Single Interface to Multiple Systems
[AD-A192264] N88-26832
Interaction management in CAD systems with a history mechanism
[CWI-CS-R8756] N88-26851
Programmer-friendly LL(1) parser generator
[PB88-126933] N88-26857
UTILITIES
Phosphoric acid electric utility fuel cell technology development
[DE88-010187] N88-26582

V

VACANCIES (CRYSTAL DEFECTS)
Abnormal diffusion of vacancies in metals
[DE88-701880] N88-26441
VACUUM
A bibliography and author index for electrical discharges in vacuum (1897-1986)
[DE88-008744] N88-26579
VACUUM APPARATUS
High temperature testing of C/C (Carbon/Carbon) composites
[AD-A193012] N88-26411
VACUUM DEPOSITION
Plasma deposition: Investigations on a new approach
[ETN-88-92619] N88-26992
Growth and characterization of thin films of ZnSnP(sub)2
[DE88-001164] N88-27060
VAN DER WAAL FORCES
High resolution spectroscopy of dissociating molecules
[DE88-007959] N88-26924
VANADIUM
Superconductivity of Cr/V superlattices N88-27057
VANES
Study on the heat resisting and cooling property of the ceramics-metal hybrid stator vanes
[DE88-753117] N88-26668
VAPOR DEPOSITION
Hot electron transistors grown by MOCVD
N88-26996
VAPOR PHASES
Thermostatistical estimations of vapor-state molecules affected by gravity in a heat pipe N88-26505
VAPOR PRESSURE
Physical-chemical reactions at welding arc/molten pool interfaces
[DE88-007717] N88-26662
VARIABILITY
Wave propagation in locally isotropic turbulent medium with smoothly changing characteristics
[NASA-TT-20312] N88-26617
VARIABLE STARS
A survey of the Ap stars for rapid variability
N88-27127
VARIATIONAL PRINCIPLES
Variational analysis of dielectrically loaded multidepth corrugated waveguides
[PB88-193602] N88-26573
VECTOR SPACES
Linearization along invariant manifolds and a generalization of the Hartman-Grobman theorems for degenerate singularities of vector fields in R cubed
[REPT-87-80] N88-26886
VEGETATION
Sources of scattering in vegetarian and other surfaces and objects
[NASA-CR-182975] N88-26710
VELOCITY
On linear relationship between shock velocity and particle velocity
[DE88-701827] N88-27099
VELOCITY DISTRIBUTION
The velocity field of the outer galaxy
[B8681472] N88-27132
VELOCITY MEASUREMENT
Position and velocity determination using a Global Positioning System: An outline
[B8735052] N88-26355
Heterogeneous diffusion flame stabilization
[AD-A193014] N88-26429
Crosslinking of two vortex rings side by side
N88-26502
Development of advanced flow simulation system by water flow model. New method of velocity measurement using cross-correlation
[DE88-753120] N88-26608
Velocity-pressure integrated versus penalty finite element methods for high Reynolds number flows
[NASA-CR-179357] N88-26635
VENTING
Enhanced emergency smoke venting
[DOT/FAA/CT-88/22] N88-26350
VENUS (PLANET)
A bibliography of dunes: Earth, Mars, and Venus
[NASA-CR-4149] N88-27134
VERTICAL MOTION
Vertical ship motions and sea loads considering nonlinear effects
[TAE-592] N88-26515
VERTICAL ORIENTATION
The effect of a turbulent airstream on a vertically-launched missile at high angles of attack
[AD-A192408] N88-26363
Stability of a coastal upwelling front over topography
[AD-A192354] N88-26784
A modal approach to Arctic noise modelling with implied vertical coherence
[AD-A192966] N88-26916
Vertical viewing ECE diagnostic for the D3-D tokamak
[DE88-010586] N88-26987
VERY LARGE SCALE INTEGRATION
Effects of cosmic rays on single event upsets
[NASA-CR-183053] N88-26569
Research in VLSI computer systems
[AD-A192915] N88-26816
VESTIBULES
Significance of sensory signal phase mismatch in mechanisms of motion sickness development
N88-26787
VIBRATION
Rare Gas Halide (RGH) kinetics
[AD-A192352] N88-25425
A review of gear housing dynamics and acoustics literature
[NASA-CR-183110] N88-26675
Vibration frequencies of tapered bars with nonclassical boundary conditions
[NASA-CR-183059] N88-26688
FEB structural analysis, revision H
[AD-A192302] N88-26698
Low energy molecular collisions
[ISAS-RN-366] N88-26919
Enhancement of volume H(-) production by vibrationally pre-exciting the hydrogen molecules
[DE88-010783] N88-26937
Aperiodic superlattices: Structured randomness
N88-27055
VIBRATION DAMPING
Design of a controller to reduce residual vibration in the positioning control of flexible robotic manipulators
N88-26658
Experimental and theoretical investigation of passive damping concepts for member forced and free vibration
[NASA-CR-183082] N88-26693
Vibration response of constrained viscoelastically damped plates: Analyses and experiments
[AD-A192329] N88-26699
VIBRATION TESTS
Cross flow induced vibrations in tube bundle by displaced and misaligned tube configurations
[ETN-88-92132] N88-26621
VIDEO DATA
Cellular array processor CAP and its application to computer graphics N88-26327
VIEWING
Vertical viewing ECE diagnostic for the D3-D tokamak
[DE88-010586] N88-26987
VISCOELASTICITY
Compression creep of filamentary composites
[NASA-CR-182550] N88-26601
Vibration response of constrained viscoelastically damped plates: Analyses and experiments
[AD-A192329] N88-26699
VISCOSITY
Synthesis of model polymers and related structures in support of vinyl monomer grafting studies
[DE88-010245] N88-26476
VISCOUS FLOW
Numerical simulations of aerodynamic contribution of flows about a space-plane-type configuration
N88-26292
Finite element analysis of incompressible viscous flow around multi-element aerofoils N88-26294
Numerical simulation of viscous flows over transonic aircraft configurations N88-26302
Numerical analysis of reconnection of vortex rings
N88-26500
Three-dimensional viscous flow computations of a circular jet in subsonic and supersonic cross flow
[NASA-CR-182153] N88-26616
A study of flow separation in transonic flow using inviscid and viscous computational fluid dynamics (CFD) schemes
[NASA-CR-183119] N88-26618
Spectral resolution of the Navier-Stokes equations in multi-domain curved complex geometries
[ONERA-NT-1987-2] N88-26631
VISUAL PERCEPTION
Biorhythms of binocular vision N88-26788
The interaction of sensory and perceptual variables: Spatial, temporal and orientation response to figure and ground
[AD-A192897] N88-26796
A new approach to machine-based perception of monocular images
[DE88-002418] N88-26942
VOICE COMMUNICATION
Error performance of voice band data signals with an overloaded delta modulator
[FEL-1987-05] N88-26562
A cockpit natural language study - selected transcripts
[AD-A192972] N88-26808
VOLUME
A maximum entropy solution for the underdetermined electromagnetic field within a volume
[DE88-007020] N88-26550
VORTEX FILAMENTS
Vortex filament simulation for the crosslinking rings
N88-26501
VORTEX RINGS
Numerical analysis of reconnection of vortex rings
N88-26500
Vortex filament simulation for the crosslinking rings
N88-26501
Crosslinking of two vortex rings side by side
N88-26502
VORTICES
Numerical study of delta wing leading edge blowing
[NASA-CR-183101] N88-26335
Vortex methods for separated flows
[NASA-TM-100068] N88-26342
Evolution of hairpin vortices in a shear flow
[NASA-TM-100858] N88-26885
Drift wave vortices and anomalous transport
[DE88-009562] N88-26982
VORTICITY
The Proceedings of the Symposium on Mechanics for Space Flight 1987
[ISAS-SP-6] N88-26499
VULNERABILITY
The use of commercial off-the-shelf equipment and its impact on C3 (Command, Control and Communications EMP (electromagnetic pulse) survivability
[AD-A192614] N88-26556

W

WALL FLOW
Evolution of hairpin vortices in a shear flow
[NASA-TM-100858] N88-26885
WALLS
Research in electromagnetic shielding theory. Part1. Shielding by rectangular enclosures
[AD-A192881] N88-26557
On the global radiation incident variously orientated surfaces on the South Coast of Finland
[FMI-5] N88-26748
Aircraft interior noise reduction by alternate resonance tuning
[NASA-CR-182540] N88-26909
WARNING SYSTEMS
An interagency working group on lightning threat warning
[DE88-009828] N88-26767
Synoptic patterns related to tropical cyclone recurvature
[AD-A192338] N88-26771
WASTE ENERGY UTILIZATION
An analysis of gas-steam total power recovery energy system N88-26512

WASTE HEAT
An analysis of gas-steam total power recovery energy system N88-26512
WASTES
Overview of the TITAN-2 reversed-field pinch aqueous fusion power core design
[DE88-008170] N88-26966
WATER FLOW
Development of advanced flow simulation system by water flow model. New method of velocity measurement using cross-correlation
[DE88-753120] N88-26608
WATER VAPOR
Tracer water transport and subgrid precipitation variation within atmospheric general circulation models
[NASA-CR-182897] N88-26745
Wavenumber spectra from THIR 6.7 micron water vapor data N88-26756
WATERSHEDS
Surface hydrology, sediment transport dynamics and remote sensing of disturbed watersheds in a humid temperate region
[DE88-008719] N88-26715
WATERWAVE ENERGY
Survey on utility technology of a tidal and ocean current energy
[DE88-770148] N88-26722
WAVE EQUATIONS
High spatial frequency thermal blooming instability: A linear stability analysis
[DE88-010711] N88-26655
Propagation of inernio-acoustic gravity waves in a rotating and radiating opaque atmosphere
[DE88-701866] N88-26750
WAVE FUNCTIONS
Quantum transport in an electron waveguide N88-27010
To the twinning plane superconductivity theory
[DE88-702195] N88-27058
Phenomenological approach to high T/sub c/ oxide superconductors
[DE88-701868] N88-27074
Cosmic wavefunction with induced gravity
[DE88-701873] N88-27129
WAVE PROPAGATION
Proceedings of the Array Signal Processing Symposium: Treaty Verification Program
[DE88-008346] N88-26548
Variational analysis of dielectrically loaded multidepth corrugated waveguides
[PB88-193602] N88-26573
Wave propagation in locally isotropic turbulent medium with smoothly changing characteristics
[NASA-TT-20312] N88-26617
The propagation of irradiance moments of an aberrated, apodized FEL beam
[DE88-008972] N88-26648
Propagation of inernio-acoustic gravity waves in a rotating and radiating opaque atmosphere
[DE88-701866] N88-26750
Westward moving atmospheric wave disturbances over the African tropics: Dynamic and energetic aspects
[MITT-57] N88-26774
XDATAP
[DE88-007161] N88-26827
On the self-focusing of electric helicons
[DE88-701870] N88-26905
WAVEFORMS
Time-Optimal Adaptive Shaped Torque (TOAST) technical note
[AD-A192719] N88-26869
WAVEGUIDES
Variational analysis of dielectrically loaded multidepth corrugated waveguides
[PB88-193602] N88-26573
Quantum transport in an electron waveguide N88-27010
WAVELENGTHS
Wavenumber spectra from THIR 6.7 micron water vapor data N88-26756
WEAR RESISTANCE
Characterization of coating wear phenomena in nitride and carbide coated tool inserts
[DE88-011196] N88-26478
WEAR TESTS
Characterization of coating wear phenomena in nitride and carbide coated tool inserts
[DE88-011196] N88-26478
WEATHER FORECASTING
Mariners weather log, volume 31, number 4, Fall 1987
[PB88-173851] N88-26761
Synoptic patterns related to tropical cyclone recurvature
[AD-A192338] N88-26771
WEDGE FLOW
Navier-Stokes simulation of shock-tube flows over a wedge-type step by finite volume method
[ISAS-RN-628] N88-26599
WEIGHT REDUCTION
Performance of lightweight nickel electrodes
[NASA-TM-100958] N88-26430
WEIGHTLESSNESS
Axisymmetric liquid sloshing under low-g conditions: Numerical simulation method (reference manual)
[NLR-TR-86057-4] N88-26627
Liquid motions in partially filled containers: Preliminary results of the D-1 mission --- Spacelab
[NLR-MP-86042-U] N88-26629
Effect of weightlessness on brain development (results of flight of pregnant rats on Kosmos-1514 biosatellite and study of subsequent development of their progeny on earth N88-26786
WELD TESTS
Principles of a nondestructive evaluation process for damage location, damage profile, and damage extension in welded joints by radiometric measurements
[MPA-86-02] N88-26683
WELDABILITY
Helium induced degradation in the weldability of an austenitic stainless steel
[DE88-009062] N88-26443
WELDED JOINTS
Principles of a nondestructive evaluation process for damage location, damage profile, and damage extension in welded joints by radiometric measurements
[MPA-86-02] N88-26683
WELDING
Finite element welding computations using general purpose nonlinear analysis codes
[DE88-005398] N88-26659
Milliwatt generator project
[DE88-011261] N88-26939
WEST GERMANY
Space policy of common sense and moderation
[REPT-49/87] N88-27118
WETTING
Critical point wetting drop tower experiment
[NASA-CR-183062] N88-26603
WHISKER COMPOSITES
Factors influencing the toughening behavior of whisker reinforced ceramics
[DE88-011396] N88-26479
WHISTLERS
Electrostatic whistler mode conversion at plasma resonance
[AD-A192951] N88-26989
WICKS
Heat transfer of mesh-wick heat-pipes (bottom heat mode) N88-26507
WIDE ANGLE LENSES
Treatment of systematic errors in the processing of wide angle sonar sensor data for robotic navigation
[DE88-008961] N88-26352
WIGGLER MAGNETS
The free-electron laser: Theoretical innovations and gas-loaded experiment N88-26646
WIND (METEOROLOGY)
A radar study of the interaction between lightning and precipitation
[DE88-009120] N88-26770
Wind flow study: July 1987 and November-December 1987
[DE88-008969] N88-26776
WIND EFFECTS
Numerical model for the computation of radiance distributions in natural waters with wind-roughened surfaces
[PB88-192703] N88-26765
Eigenmatrix representations of radiance distributions in layered natural waters with wind-roughened surfaces
[PB88-188701] N88-26780
WIND SHEAR
Influence of wind shear on the aerodynamic characteristics of airplanes
[NASA-TP-2827] N88-26344
Intelligent guidance and control for wind shear encounter
[NASA-CR-183060] N88-26347
WIND TUNNEL MODELS
Heterogeneous diffusion flame stabilization
[AD-A193014] N88-26429
WIND TUNNEL TESTS
High speed and high angle of attack wind tunnel test results of the winged space vehicle C-2
[ISAS-RN-623] N88-26329
Propfan test assessment testbed aircraft stability and control/performance 1/9-scale wind tunnel tests
[NASA-CR-182121] N88-26360
Low-speed wind-tunnel test of a STOL supersonic-cruise fighter concept
[NASA-TM-4050] N88-26374
Wind tunnel study of atmospheric diffusion in unstable stratified boundary layer. Part 2: Characteristic scale and diffusion
[DE88-753109] N88-26749
Helicopter main-rotor noise: Determination of source contributions using scaled model data
[NASA-TP-2825] N88-26907
WIND TUNNEL WALLS
Wall interference assessment/correction of data from tests of a CAST 10-2/DOA 2 airfoil in the Langley 0.3-m transonic cryogenic tunnel N88-26331
WIND TUNNELS
Rarefied gas numerical wind tunnel 3: Universal code for three dimensional bodies N88-26304
WIND TURBINES
Analysis of the electrical characteristics of a Westinghouse variable speed generating system for wind turbine applications
[DE88-001139] N88-26721
WIND VELOCITY
Wind flow study: July 1987 and November-December 1987
[DE88-008969] N88-26776
WINDOWS (APERTURES)
Determination and application of bidirectional solar-optical properties of fenestration systems
[DE88-010364] N88-26727
WINDPOWER UTILIZATION
Analysis of the electrical characteristics of a Westinghouse variable speed generating system for wind turbine applications
[DE88-001139] N88-26721
Wind Energy Technology: Generating power from the wind, a current awareness bulletin
[DE88-008292] N88-26729
WINDPOWERED GENERATORS
Analysis of the electrical characteristics of a Westinghouse variable speed generating system for wind turbine applications
[DE88-001139] N88-26721
WING PROFILES
Numerical simulation of turbulent flow using the exponential expression of k-epsilon equation N88-26322
Improved potential flow computational methods with Euler corrections for airfoil and wing/body design
[AD-A192303] N88-26334
WIRE
A model for insulated wires in the method of moments code NEC (Numerical Electromagnetics Code)
[DE88-008920] N88-26577
WORKING FLUIDS
Heat transfer of mesh-wick heat-pipes (bottom heat mode) N88-26507
WORKLOADS (PSYCHOPHYSIOLOGY)
Method for observing changes in functional state of human operator N88-26789
WRIST
Kinematics of Hooke universal joint robot wrists
[NASA-TM-100567] N88-26870

X

X RAY ABSORPTION
EXAFS studies of the microstructure of semiconductor alloys, defects and semiconductor-metal interfaces N88-27031
Structural studies of (Ga,In)(As,P) alloys and (InAs) sub m (GaAs) sub n strained-layer superlattices by fluorescence-detected EXAFS N88-27051
X RAY ANALYSIS
Development of an automated X-ray gauge for nondestructive quantitative analysis
[DE88-008633] N88-26681
X RAY IMAGERY
Toroidal and poloidal soft X-ray imaging system on the D3-D tokamak
[DE88-010585] N88-26986
X RAY INSPECTION
Damage in a perforated graphite-epoxy plate under monotonic, cyclic biaxial loading
[ONERA-NT-1987-5] N88-26708
X RAY LASERS
An elliptical spectrograph/gated microchannel plate detector for time-resolved spectral measurements in the X-ray region
[DE88-007590] N88-26961
X RAY SPECTRA
The properties of solar coronal active regions deduced from X-ray line spectra
[AD-A193026] N88-27141

Detection of absorption lines in the spectra of X-ray bursts from X1608-52
[ISAS-RN-360] N88-27143
X RAY SPECTROSCOPY
Time-resolved doubly bent crystal X-ray spectrometer
[DE88-007899] N88-26637
X RAYS
Microfocus X-ray techniques for flaw location
[DE88-008636] N88-26680
In-situ reactive of X-ray optics by glow discharge
[DE88-009840] N88-26947
Properties of multilayers for soft X-ray optics
N88-27025
The hard X-ray burst spectrometer event listing 1980-1987
[NASA-TM-4036] N88-27144
XENON
Rare Gas Halide (RGH) kinetics
[AD-A192352] N88-26425
XENON FLUORIDE LASERS
Optical coatings for high average power XeF lasers
[DE88-011356] N88-26656
XEROGRAPHY
Application of magnification xeroradiography to advanced ceramics
[DE88-009965] N88-26473
XV-15 AIRCRAFT
Hover performance tests of baseline metal and Advanced Technology Blade (ATB) rotor systems for the XV-15 tilt rotor aircraft
[NASA-CR-177436] N88-26367
Utilization of identification methods in the time and frequency domain for the determination of the XV-15 (tilt-rotor) dynamics for lateral motion in hover flight
N88-26532

Y

YTTRIUM
Characterization of structural and magnetic order of Er/Y superlattices N88-27056
Pure metallic bridge and point-contact tunneling into single- and polycrystal YBa2Cu3O(sub 7-y)
[DE88-010030] N88-27084
YTTRIUM OXIDES
Effects of grain boundary composition on properties of YBa2Cu3O/sub 7-x/
[DE88-007679] N88-27054
The superconducting transition in oxygen deficient YBa2Cu3O(sub 7-Delta)
[DE88-009957] N88-27079
Anisotropic characteristic lengths in single crystal YBa2Cu3O(sub 7-Delta)
[DE88-009959] N88-27080
Anisotropy of the lower critical field in YBa2Cu3O(sub 7-Delta)
[DE88-009971] N88-27081
Preparation of high-T(sub)c Y1Ba2Cu3O(sub 7-Delta) superconducting thin films by MBE (Molecular-Beam-Epitaxy) techniques
[DE88-009999] N88-27082
Oxygen vacancy ordering and superconductivity in YBa2Cu3O(sub 7-x)
[DE88-010005] N88-27083
Electron irradiation effects in YBa2Cu3O7-Delta single crystals
[DE88-010050] N88-27085
Phase transformations and thermodynamic behavior of the YBa2Cu3O(sub)x system via EMF measurements
[DE88-010054] N88-27086
Ceramic processing of high-T(sub)c superconductors
[DE88-010090] N88-27087

Z

ZINC
Laser fluorescence spectroscopy of zinc neutrals originating from laser-irradiated and ion-bombarded zinc sulfide and zinc surfaces
[DE88-008037] N88-26418
ZINC SELENIDES
Growth and characterization of thin films of ZnSnP(sub)2
[DE88-001164] N88-27060
ZINC SULFIDES
Laser fluorescence spectroscopy of zinc neutrals originating from laser-irradiated and ion-bombarded zinc sulfide and zinc surfaces
[DE88-008037] N88-26418
ZIRCONATES
Refractory Materials of Zirconate. Part 2: Synthesis and some properties of strontium, zirconate, calcium zirconate and barium zirconate
[NASA-TT-20186] N88-26483

Typical Personal Author Index Listing

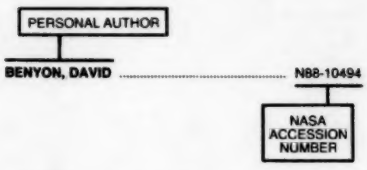

Listings in this index are arranged alphabetically by personal author. The NASA accession number denotes the number by which the citation is identified.

A

ABDURAKHIMOV, A. U. N88-26820
ABE, TAKASHI N88-26305
ABE, TOSHIO N88-26608
N88-26667
N88-26668
ABERGEL, ALAIN N88-27131
ABRAHAM, K. M. N88-26574
ACHENBACH, J. D. N88-26700
N88-26701
N88-26702
ACKERMAN, J. L. N88-26474
ADAIR, DESMOND N88-26634
ADAMOVSKY, GRIGORY N88-26644
ADAMS, G. L. N88-27120
ADAMS, NIGEL G. N88-26751
AEPPLI, G. N88-27065
AGRAWAL, OM P. N88-26709
AGRAWAL, RAJEEV N88-26893
AGUIARNETO, BENEDITO G. N88-26561
AHMED, H. N88-27011
AHN, D. N88-26585
AISO, HIDEAKI N88-26318
AJMERA, P. K. N88-27060
AKAI, YUKIO N88-26768
AKI, TAKAYUKI N88-26319
AKITA, K. N88-26431
AKITA, SHIGE N88-26571
AL-KHAYYAL, FAIZ A. N88-26834
ALEXANDER, H. N88-26367
ALEXANDRATOS, S. D. N88-26488
ALFANO, R. R. N88-27044
ALJABRI, A. S. N88-26360
ALLARD, L. F. N88-26469
ALLEN, J. E. N88-27140
ALLEN, L. E. N88-26407
ALLISON, S. W. N88-26638
ALSTON, WILLIAM B. N88-26404
ALVISO, C. T. N88-26946
AMALBERTI, R. N88-26806
AMANO, KANICHI N88-26297
N88-26313
AMUNDSEN, R. J. N88-27120
ANANTHARAM, VENKATACHALAM N88-26893
ANDERSON, H. U. N88-27088
ANDERSON, J. N88-26983
ANDERSON, L. E. N88-26792
ANDO, TSUNEYO N88-26324
ANDREWS, D. N88-27011
ANGELINI, P. N88-26479
ANSARI, M. I. N88-26440
AOKI, SUNAO N88-26314
APFEL, R. E. N88-26915
ARAI, K. N88-26509
ARCHIBALD, T. A. N88-26494
ARELLANO, J. M. N88-26766
ARLINGHAUS, H. F. N88-26418
ARROWOOD, L. F. N88-27116
ASAY, J. R. NC8-26967
ASGHAR, S. N88-26912
ASHLEY, J. C. N88-26929
ASKEW, A. L. N88-26613
ATKINSON, DAVID J. N88-26859
AUPOIX, B. N88-26623
AUSSUDRE, SERGE N88-26487
AUVIL, PAUL R. N88-27057
AYERS, THEODORE G. N88-26361

B

BAARK, E. N88-27111
BABCOCK, S. M. N88-26670
BADER, S. D. N88-26652
BADRUZZAMAN, A. N88-26876
BAILEY, D. W. N88-27036
BAKER, I. N88-26447
BAKER, M. C. N88-27085
BAKER, W. N88-26763
BALANIS, CONSTANTINE A. N88-26545
BALCH, T. N88-26826
BALDWIN, J. D. N88-26717
BALGASUREN, YA. N88-26820
BALLIN, MARK G. N88-26378
BALLUFFI, R. W. N88-26446
BAMLER, RICHARD N88-26642
BARNARD, J. J. N88-26655
BARNES, CHARLES E. N88-26586
BARTH, JOHN A. N88-26784
BARTIE, K. N88-26367
BARTLIT, J. N88-26983
BARUT, A. O. N88-27102
BASS, S. J. N88-27037
N88-27039
BASTARD, G. N88-27009
BATCHELOR, D. B. N88-26985
BATEMAN, V. I. N88-26666
BATES, RAYMOND L. N88-26832
BAUER, G. N88-27006
BAUKUS, JAMES P. N88-27033
BAUMBICK, ROBERT J. N88-26328
BEALL, R. S. N88-27020
BEARDSLEY, R. W. N88-27120
BECHER, P. F. N88-26479
BECKERMAN, M. N88-26352
BECKERT, DIETER N88-26734
BEHEIM, GLENN N88-26641
BELL, PETER M. N88-27137
BELLINI, V. N88-26920
BEMENT, LAURENCE J. N88-26394
BENNER, STEVE N88-26389
BENNETT, C. A. N88-26965
BERCHTOLD, GERD N88-26372
BEREZHIANI, V. I. N88-26974
BERGER, M. E. N88-26730
BERLINRUT, DANIEL D. N88-26400
BERNER, C. N88-26339
BERNSTEIN, DENNIS S. N88-26373
BERNSTEIN, JEREMY N88-27130
BERTHELOT, YVES H. N88-26911
BESJES, J. G. N88-26887
BESTMAN, A. R. N88-26750
BETHEA, C. G. N88-27026
BEVENSEE, R. M. N88-26550
BHADRA, R. N88-27082
BIBL, KLAUS N88-26753
BIEG, K. W. N88-26960
BIESECKER, D. A. N88-27144
BIMBERG, D. N88-27030
BINGHAM, R. N88-27140
BIRINGEN, S. N88-26858
BISHOP, H. N88-26367
BISOGNANO, J. J. N88-26936
BLACKBURN, P. S. N88-26738
BLAKE, R. L. N88-26637
BLAKELY, J. M. N88-26420
BLAND, J. A. C. N88-27015
BLANDER, M. N88-27086
BLANEY, JOSEPH I. N88-26752
BLANKENSHIP, GILMORE N88-26553
BLISS, DONALD B. N88-26909
BOCK, H.-G. N88-26536
BOERSTOEL, J. W. N88-26628
BOES, E. C. N88-26726
BOLEY, C. D. N88-26657
BOLLINI, G. N88-26777
BONSU, F. O. N88-26494
BOOKER, M. K. N88-26489
BORCHERS, J. N88-27056
BORGES, H. N88-27065
BOULONNAIS, D. N88-26487
BOX, PHILLIP N88-26685
BOYD, D. N88-26987
BOYD, J. K. N88-26576
BOZOIAN, M. N88-26932
BRADLEY, J. A. N88-27038
BRAGINSKI, A. I. N88-27091
BRAITHWAITE, J. W. N88-26578
BRAND, JAN N88-27132
BRASSARD, GILLES N88-26854
BRECHET, YVES N88-26456
BREEMAN, J. H. N88-26533
BREININGER, DAVID R. N88-26744
BREZOVEC, CARL N88-26838
BRINKER, C. J. N88-27069
BRINKER, DAVID J. N88-26402
BRISTOWE, P. D. N88-26446
BRITTON, DORIS L. N88-26430
BROCKHAUS, RUDOLF N88-26518
BROECKER, WALLACE S. N88-26745
BROOKS, J. N. N88-26984
BROOKS, THOMAS F. N88-26907
BROOKSBY, C. A. N88-26993
BROWN, A. N88-27086
BROWN, LOWELL S. N88-27130
BROZAK, G. N88-26998
BRUEHL, CHRISTOPH N88-26775
BRUENING, ULRICH N88-26818
BRUM, J. A. N88-27009
BRUNSON, R. R. N88-26470
BRUYNSERAEDE, Y N88-27082
BRUYNSERAEDE, Y. N88-27008
BRYNESTAD, J. N88-27064
BUCHANAN, T. D. N88-26403
BUCHARLES, A. N88-26525
BUCHELE, DONALD R. N88-26645
BUCHER, H. N88-27065
BUCK, W. W. N88-26935
BUNKER, BRUCE A. N88-27031
BUNSHAH, R. F. N88-26478
BURKE, G. J. N88-26577
BURNSIDE, W. D. N88-26565
BURTON, JAMES R., III N88-26909
BUSCH-VISHNIAC, ILENE J. N88-26914
BUSH, D. M. N88-26578
BUTLER, G. B. N88-26476
BUTLER, P. C. N88-26578
BUTNER, D. N. N88-27113
BUTTERFIELD, A. J. N88-26397
BUZDAVINA, N. A. N88-26820
BYERS, C. H. N88-26470

C

CAIRNS, E. J. N88-26723
CALAWAY, W. F. N88-26418
CAMBANIS, STAMATIS N88-26894
CAMBRAY, P. N88-26433
CAMPBELL, J. A. N88-26906
CAMPBELL, NANCY L. N88-26674
CANAVAN, G. H. N88-26901
CAO, SHENGLIN N88-27100
CAPASSO, F. N88-27018
CAPONE, D. W., II N88-27087
CARCASSES, ALAIN N88-26325
CARLSON, LELAND A. N88-26332
CARNEY, L. M. N88-26385
N88-26386
CARPENTER, PATRICIA A. N88-26805
CARRERAS, B. A. N88-26985
CARROLL, A. S. N88-26922
CARY, J. R. N88-26968
CASASENT, DAVID N88-26841
CASH, R. H. N88-27120
CASTOR, J. I. N88-27128
CASTRO, R. N88-26460

CATE, D. L. N88-26869
CAUGHEY, DAVID A. N88-26340
CERQUA, K. A. N88-26948
CHAE, YEON SEOK N88-26872
CHAN, KWAI S. N88-26452
CHANCE, KELLY V. N88-26737
CHANDRASEKHAR, H. R. N88-27000
CHANDRASEKHAR, MEERA N88-27000
CHANDRASEKHAR, RAO J. N88-26914
CHANDRASEKHAR, V. N88-27022
CHANG, A. M. N88-27010
CHANG, CHE-WEI N88-26687
CHANG, S.-K. N88-27050
CHANG, Y. C. N88-27036
CHANG, Y.-H. N88-26998
CHAO, H. S. N88-27044
CHAPMAN, K. R. N88-26776
CHASE, L. L. N88-26418
CHASE, R. N88-26969
CHATROU, J. P. H. N88-26356
CHAUM, DAVID N88-26854
CHELA-FLORES, J. N88-27074
CHEN, C. P. N88-26736
CHEN, H. L. N88-26500
CHEN, L. T. N88-26334
CHEN, Y. J. N88-26576
CHENG, E. T. N88-26966
CHIBA, KAORU N88-26315
CHIMA, RODRICK V. N88-26340
CHINL, B. A. N88-26443
CHO, A. Y. N88-27018
CHOI, K. K. N88-27026
CHOUDHURY, A. M. N88-26743
N88-26769
CHRISTEN, J. N88-27030
CHU, X. N88-27052
CHUANG, S. L. N88-26585
CHUBB, LUCY N88-26822
CHUN, S. Y. N88-26935
CLARK, B. C. N88-27120
CLARK, R. P. N88-26578
CLARKE, ROY N88-27055
CLAUS, H. N88-27079
CLAXTON, P. A. N88-27037
CLEMMER, R. N88-26983
CLIQUE, M. N88-26525
COE, PAUL L., JR. N88-26374
COFFEY, HELEN E. N88-27138
N88-27139
COFFEY, S. J. N88-26739
COGGIOLA, MICHAEL J. N88-26583
COIRIER, WILLIAM J. N88-26336
COLLINS, J. C. N88-26926
COOK, ELIZABETH A. N88-26711
COOKE, P. I. H. N88-26966
COOKE, ROGER N88-26895
CORNELIUS, W. D. N88-26931
CORNUEJOLS, GERARD N88-26836
CRABTREE, G. W. N88-27079
N88-27080
N88-27081
N88-27083
CRAIGHEAD, H. G. N88-27023
CRAVER, W. LIONEL, JR. N88-26688
CREEDON, R. L. N88-26966
CREPEAU, CLAUDE N88-26854
CRONKITE, E. P. N88-26797
CROSKEY, CHARLES L. N88-26698
CROUCH, I. G. N88-26686
CROWLEY, FRANCIS A. N88-26752
CRUIKSHANK, DALE P. N88-27121
CSERNAI, L. N88-26921
CUDDIHY, W. F. N88-26397
CULIOLI, J. C. N88-26862
CURTAIN, R. F. N88-26390
CURTIS, P. G. N88-26496

D

DABROWSKI, B. N88-27083
DABROWSKI, C. E. N88-27109
DACUS, M. W. N88-26605
DADI, M. N88-26622
DADRAS, PARVIS N88-26411
DAHLHAUSEN, M. J. N88-26807
DAILY, JOHN W. N88-26991
DALAUDIER, FRANCIS N88-26772
DALY, B. J. N88-26449
DAM, N. N88-26695
N88-26706
DAMERIS, MARTIN N88-26758
DANABASOGLU, G. N88-26858
DANDACHE, H. N88-27099
DANG, T. Q. N88-26334
DANILOV, A. R. N88-26786
DAS, M. P. N88-27074
DAVIDSON, DAVID L. N88-26452
DAVIDSON, G. S. N88-26861
DAVIES, G. J. N88-27011
DAVIS, BRADLEY M. N88-27057
DAVIS, L., JR. N88-27146
DAWSON, JOHN M. N88-26958
N88-26959
DAWSON, L. R. N88-27062
DEANGELIS, D. L. N88-26740
DEBOO, J. C. N88-26969
DEBRIEDER, E. N. N88-26563
DEBSKI, W. N88-26484
DECYK, VIKTOR K. N88-26959
DEGROOT, A. J. N88-26856
DEJONG, A. N. N88-26954
DEJONG, H. E. N88-26459
DEJONG, H. F. N88-26458
DEJONG, R. C. N88-26530
DEKONING, A. U. N88-26707
DELMOTTE, MICHEL N88-26487
DELONEY, THURMON LAWRENCE, II N88-26646
DEMMEL, J. N88-26829
DEMUTH, G. N88-26639
DENHOLLANDER, W. T. F. N88-26897
DENNIS, B. R. N88-27144
DERESKIEWICZ, J. P. N88-26672
DEREUS, N. M. N88-26358
DESAIN, P. N88-26810
DESHAIES, B. N88-26433
DESWAANARONS, H. N88-26845
DEVENISH, LINDA N88-26349
DEWITT, H. N88-26994
DEWITTE, T. D. N88-26719
DEZERN, JAMES F. N88-26481
DHAENENS, IRNEE J. N88-27033
DICK, G. JOHN N88-26596
DICKEY, DANIEL W. N88-26673
DIJK, J. N88-26564
DIMARIA, D. J. N88-27042
DMOWSKI, L. N88-27020
DOBREV, V. K. N88-26882
DODSON, BRIAN W. N88-27053
DOHA, E. H. N88-26880
DOHERR, KARL-FRIEDRICH N88-26518
DOMINEK, A. K. N88-26565
DONALDSON, R. R. N88-26664
DONKER, J. C. N88-26871
DORY, R. A. N88-26980
DOSHI, RAJKUMAR S. N88-26859
DOSHO, SHIRO N88-27029
DOZOIS, CLAUDE G. N88-26753
DREWS, M. J. N88-26407
DRITT, J. O. N88-26960
DRLIK, M. N88-27113
DROTNING, W. D. N88-26681
DU, R. N88-27056
DUBE, W. P. N88-26466
DUBEY, R. V. N88-26670
DUBOIS, PASCALE C. N88-26541
DUCHON, CLAUDE E. N88-26712
N88-26716
DURETTHUAL, C. N88-26370
DUSEK, J. T. N88-27087
DYBDAL, R. B. N88-26560

E

EAGLESON, PETER S. N88-26745
EAVES, L. N88-27020
EBEL, A. N88-26756
N88-26773
N88-26774
EBERSBERGER, JOHANNES N88-26953
EBERWIJN, C. N88-26562
EBERZ, BERNHARD N88-26774
EDIE, D. D. N88-26407
EICHINGER, B. E. N88-26471
EIMERL, D. N88-27067
EISEN, STEFAN, JR. N88-26804
EL-ASHRY, M. Y. N88-26905
N88-26974
N88-26976
ELDEM, C. N88-26823
ELFVING, A. N88-26678
ELLINGSON, W. A. N88-26473
N88-26474
ELLIOTT, ROGER J. N88-27089
ELLIS, R. N88-26987
ELLISON, M. S. N88-26407
ELTHON, DONALD N88-26747
EMRICH, M. L. N88-27116
ENGLAND, PHILIP C. N88-26759
ENGLE, RANDALL W. N88-26803
ENGLMEIER, H. P. N88-26353
ERNEST, T. L. N88-26691
ERSU, E. N88-26678
ERWIN, R. W. N88-27056
ESFAHANIAN, A. H. N88-26614
ESTLER, R. C. N88-26650
ETORI, KANJI N88-26505
EULER, J. A. N88-26670
EVANKO, R. N88-26986
EVANKO, R. G. N88-26969
EVANS, D. S. N88-26755

F

FALCO, CHARLES M. N88-27025
FANG, L. Z. N88-27129
FARRINGTON, G. C. N88-26415
FARTHING, W. E. N88-26739
FASOLINO, A. N88-27035
FAURIE, J. P. N88-27052
FEAREY, B. L. N88-26650
FEARN, RICHARD L. N88-26343
FEINBERG, G. N88-27130
FELDMAN, M. J. N88-27092
FELL, R. B. N88-26807
FENNELL, J. F. N88-26396
FENSKE, G. R. N88-26478
FERNANDEZ, FELIX E. N88-27025
FINEL, ALPHONSE N88-27095
FINN, P. N88-26983
FISCHER, S. K. N88-26607
FISCHETTI, M. V. N88-27042
FISHER, H. M. N88-26827
FISK, Z. N88-27065
FITZPATRICK, MICHELE N88-26517
FLETCHER, L. K. N88-26965
FLOOD, DENNIS J. N88-26402
FLORY, DAN E. N88-26808
FLYNN, C. P. N88-27056
FOKKEMA, G. A. N88-26781
FONTE, R. N88-26920
FORD, C. J. B. N88-27011
FOSTER, G. W. N88-26533
FOSTER, T. N88-27020
FRANK, THOMAS D. N88-26711
FREESE, J. M. N88-26578
FRENSLEY, WILLIAM R. N88-27017
FRESE, MICHAEL H. N88-26988
FRICK, BJOERN N88-27093
FRIEDRICH, RUDOLF N88-26825
FRITSCH, F. N. N88-26878
FRITSCHEN, LEO J. N88-26778
FRYBERGER, P. E. N88-26403
FRYE, G. C. N88-27069
FUJII, KOZO N88-26292
N88-26302
FUJII, T. N88-27048
FUJIWARA, MASAMI N88-26956
FUJIWARA, TOSHITAKA N88-26307
FUKUDA, MASAHIRO N88-26291
FUKUNAGA, T. N88-27030
FUNABIKI, KATSUSHI N88-26598
FURTAK, T. E. N88-27068
FURUKAWA, MASAO N88-26510

G

GABRIEL, T. A. N88-26899
GALVA, A. N88-26777
GAMACHE, ROBERT R. N88-26753
GANDINO, C. N88-26777
GARCIA, P. N88-26549
GARDINER, J. G. N88-26831
GARN, P. A. N88-26397
GARRETT, L. V. N88-26403
GARRETT, R. F. N88-26947
GARRIDO, L. N88-26474
GARRITY, P. J. N88-26900
GARUCHAVA, D. P. N88-26905
GARVER, L. C. N88-26494
GAVALER, J. R. N88-27091
GELB N88-26395
GELL, M. A. N88-27038
GELMAN, M. N88-26763
GEORGE, D. N88-26656
GERBER, R. A. N88-26960
GESSLEIN, GEORGE N88-26833
GEX, WILLIAM T. N88-26674
GHONIEM, A. F. N88-26423
GHOSN, LOUIS J. N88-26436
GIBBS, F. E. N88-26516
GIBBS, KENNETH GERARD N88-27126
GIBSON, B. R. N88-27144
GILES, G. E. N88-26613
GILLELAND, J. R. N88-26970

GLASER, ROBERT N88-26801
GLOVER, FRED N88-26838
GODFREY, BRENDAN B. N88-26835
GOERINGER, D. E. N88-26855
GOERTLER, HENRY N88-26337
N88-26338
GOGUEN, JOSEPH N88-26348
N88-26349
GOHIL, P. N88-26969
GOLD, PHILLIP I. N88-26410
GOLDBERG, JACK N88-26863
GOLTSOS, W. N88-27006
GOMAN, V. S. N88-26820
GONG, M. N88-26921
GONZALEZ, LUIS J. N88-26914
GONZELEZ, AVELINO J. N88-26867
GOODHUE, W. D. N88-26999
GOODS, S. H. N88-26443
GORE, R. A. N88-26900
GORETTA, K. C. N88-27087
GORNEY, D. J. N88-26755
GOSSARD, A. C. N88-27018
GOTTWALD, JAMES A. N88-26909
GOUD, MARGARET R. N88-26783
GOUVEIA, F. J. N88-26776
GOVORUN, N. N. N88-26820
GRABBE, P. N88-27023
GRADY, J. E. N88-26679
GRAESSER, D. L. N88-26601
GRAFE, V. G. N88-26661
GRAHAM, ROBIN L. N88-26711
GRANT, J. B. N88-26551
GRATZ, ROY F. N88-26404
GRAY, K. E. N88-27084
GRAY, L. J. N88-26613
GRAY, N. T. N88-26637
GREEN, WILLIAM B. N88-26990
GREENBAUM, E. N88-26791
GREINER, N. R. N88-26606
GRENIER-LOUSTALOT, M. F. N88-26488
GRENIER, P. N88-26488
GRIESSER, TIMOTHY N88-26545
GRIFFIN, J. E. N88-26938
GRIFFITHS, G. N88-27001
GRIMLEY, T. A. N88-26612
GRIMMEISS, HERMANN N88-27090
GROEP, F. F. N88-26695
N88-26706
GROSSBECK, M. L. N88-26443
GROSZ, BARBARA J. N88-26802
GROTHAUS, K. R. N88-26578
GROTZ, S. N88-26966
GRUEN, D. M. N88-26418
GRUNE, D. N88-26857
GRUPE, K. F. N88-26812
GUAN, WEIHO N88-27073
GUARDALBEN, M. J. N88-26948
GUMBERT, CLYDE R. N88-26331
GUNSHOR, R. L. N88-27050
GUPTA, I. J. N88-26565
GUSELLAJUNIOR, EDSON N88-26570
GUSTAFSON, J. L. N88-26875
GUSTAVESON, MARK B. N88-26909
GUTHRIE, J. W. N88-26680

H

HACKNEY, S. A. N88-26445
HALANG, WOLFGANG A. N88-26860
HALES, JEREMY M. N88-26741
HALL, C. A. N88-26967
HALL, THOMAS M. N88-26388
HALLE, LINDA F. N88-26586
HAMAMATSU, TERUHIDE N88-26667
N88-26668
N88-26728
HAMEL, P. G. N88-26520
HAMMARLUND, GREGORY R. N88-26498
HAMMEL, B. A. N88-26961
HAMZA, E. A. N88-26669
HANSEN, KATHERINE M. N88-26821
HARBISON, J. N88-27023
HARKER, A. B. N88-26480
HARLOFF, G. J. N88-26616
HARRIS, CHARLES E. N88-26413
HARRIS, D. B. N88-26548
HARRIS, G. G. N88-27020
HARRIS, JOHN A., JR. N88-26371
HARRIS, M. T. N88-26470
HASBROUCK, R. T. N88-26766
N88-26767
HASE, I. N88-26996
HASEGAWA, TOSHIAKI N88-26608
HASKOVEC, J. N88-26986
HATAKEYAMA, M. N88-26599
HATAKEYAMA, MASAHIRO N88-26598
HATAKEYAMA, MASAYUKI N88-26304
N88-26326
HAVERLAND, M. N88-26535
HAWKE, R. S. N88-26967
HAWKINS, ISABEL N88-27125
HAWLEY, M. E. N88-27084
HAWS, R. C. N88-26762
HAYASHI, KOICHI N88-26307
HAYER, L. K. N88-26516
HAYES, W. N88-27039
HECKENDORN, F. N88-26665
HEGG, D. A. N88-26764
HEIBLUM, M. N88-27020
HEITMANN, D. N88-27041
HELD, DANIEL N. N88-26541
HELM, F. H. N88-26496
HENDRICKS, K. N88-26639
HENNESSY, JOHN N88-26816
HENNING, C. D. N88-26970
HENSON, T. J. N88-26437
HENZ, J. N88-27034
HEPPNER, D. B. N88-26807
HERRERA, J. I. N88-26721
HERZOG, H.-J. N88-27027
HESS, K. N88-27036
HEYM, K. N88-26534
HICKEY, MICHAEL PHILIP N88-26760
HICKMAN, R. J. N88-26967
HICKSON, DIANA E. N88-26795
HILLERICH, BERND N88-26951
HILLIARD, JOHN E. N88-27057
HINADA, MOTOKI N88-26514
HINATSU, MUNEHIKO N88-26322
HINKLE, C. ROSS N88-26795
HINKS, D. G. N88-27083
HIRANO, T. N88-26431
HIRASHIMA, MASAO N88-26508
N88-26511
HIROSE, MANABU N88-26722
HIRTH, J. P. N88-26696
HISAMATSU, TORU N88-26608
N88-26667
N88-26668
HITNEY, H. V. N88-26554
N88-26555
HIYAMIZU, S. N88-27048
HOBBS, P. V. N88-26764
HOCKADAY, M. P. N88-26637
HOELZEMAN, RONALD G. N88-26376
N88-26377
HOFMANN, ANTON N88-27122
HOGEN-ESCH, T. E. N88-26476
HOKE, MELVIN D., JR. N88-26556
HOLDEN, D. N. N88-26770
HOLLIS, BRYON T. N88-26808
HOMMA, H. N88-27082
HON, T.-L. N88-26885
HONG, B. S. N88-26935
HOOPER, E. B. N88-26993
HOOTEN, D. N88-26383
HORNBOGEN, E. N88-26455
HORNE, W. CLIFTON N88-26634
HORTON, W. N88-26992
HOSOKAWA, IWAO N88-26321
HOUNJET, M. H. L. N88-26341
HOWARD, S. A. N88-27088
HRUBESH, L. W. N88-26946
HRYNIEWICZ, J. V. N88-26999
HSIEH, C. L. N88-26969
HSIEH, K. Y. N88-27004
HSU, S. A. N88-26717
HSUEH, CHUNG-HWAY N88-26479
HUANG, ZUQIA N88-26441
HUEBLER, GERHARD N88-26952
HUGHES, THOMAS J. N88-26697
HUH, O. K. N88-26717
HULL, J. R. N88-26385
HUNT, P. N88-26353
HUNTER, ANDREW T. N88-27033
HUNTER, H. T. N88-26965
HUTCHINSON, D. P. N88-26965

I

ICHIKAWA, YOICHI N88-26742
N88-26749
IGLESIAS, C. N88-26994
IIJIMA, SHIRO N88-26667
IKEDA, YOSHIO N88-26507
IKESAKA, MORIO N88-26327
IMAI, AKIRA N88-27029
IMAMURA, K. N88-27048
IMANAGA, S. N88-26996
IMBERT, ERIC N88-26588
IMHOFF, M. N88-26544
INATA, T. N88-27048
INATANI, YOSHIFUMI N88-26329
N88-26330
INGEBO, ROBERT D. N88-26645
INIZAN, G. N88-26708
INOUE, HAJIME N88-27143
INOUE, MASAO N88-26513
INOUE, O. N88-26599
INUMARU, JUN N88-26606
ISERMANN, R. N88-26519
ISHIGURO, T. N88-27051
ISHIGURO, TOMIKO N88-26293
N88-26309
N88-26320
ISHIHARA, KAORU N88-26571
ISHIHATA, HIROAKI N88-26327
ISHII, MITSUO N88-26327
ISHII, RYUJI N88-26295
N88-26299
ISHII, YOSHIO N88-26503
ISHIKAWA, TADAO N88-26575
ISOBE, TOSHIO N88-26304
ISRAELI, AMOS N88-26819
ITO, SHIGEO N88-26604
ITOH, KATSUHIRO N88-26308
IVANCIC, WILLIAM D. N88-26566
IVANOV, V. G. N88-26820
IVERSON, LOUIS R. N88-26711
IWATSUBO, TETSUSHIRO N88-26728
IZIMA, SHIRO N88-26668
IZUTSU, NAOKI N88-26502

J

JACKSON, W. L. N88-26607
JACOBS, C. J. H. N88-26857
JACOBS, S. D. N88-26948
JAEGER, E. F. N88-26985
JAEGERS, WILLEM JOSEPH N88-27123
JAGODA, JECHIEL I. N88-26429
JAKOBSSON, B. N88-26920
JAMES, R. N88-26987
JANDA, K. C. N88-26924
JANNAZO, MARY ANN N88-27119
JANUS, J. MARK N88-26619
JANY, PETER N88-27103
JANZ, S. N88-26987
JAROS, M. N88-27038
JARRETT, E. B. N88-26890
N88-26891
JASCHINSKI, J. N88-26522
JATEGAONKAR, R. V. N88-26528
JEFFERSON, D. K. N88-27109
JEFFRIES, M. O. N88-26782
JENKINS, MICHAEL G. N88-26482
JHA, L. N. N88-26977
N88-26979
JOCHEMS, W. M. G. N88-27105
N88-27106
JOHANSSON, E. M. N88-26856
JOHANSSON, T. N88-26920
JOHNSON, D. G. N88-26793
JOHNSON, E. D. N88-26947
JOHNSON, J. P. N88-26766
JOLLAY, D. M. N88-26663
JOLLY, J. RALPH, JR. N88-26907
JONASSON, H. G. N88-26910
JONES, E. D. N88-27062
JONES, ERIC M. N88-26382
JONES, J. F. N88-26660
JONES, K. A. N88-27116
JONES, MICHAEL G. N88-26913
JONKER, W. N88-26845
JORGENSEN, J. D. N88-27083
JORKE, H. N88-27027
JOULIN, G. N88-26433
JULIEN, J. N88-26920
JULLIEN, HENRI N88-26487
JUNNARKAR, M. R. N88-27044
JUST, MARCEL A. N88-26805

K

KADOYU, MASATAKA N88-26722
KAHAN, W. N88-26829
KAI, FEI N88-26376
N88-26377
KAKISHIMA, SHINJI N88-26749
KALEM, S. N88-27040
KALETKA, J. N88-26532
KAMENETZKY, E. A. N88-26460
KAMINAGA, F. N88-26506
KAMO, KEISUKE N88-26297

KANAI, ERIYA N88-26324
KANEKO, K. N88-26996
KANEKO, KEN-ICHI N88-26508
KANERO, KEN-ICHI N88-26511
KANGARLU, A. N88-27000
KANNDA, HIDESADA N88-26503
KANNO, MOTOHIRO N88-26453
KAPER, H. G. N88-26684
KARASHIMA, KEIICHI N88-26329
KARLSSON, L. N88-26920
KARSTEN, P. C. A. M. N88-26593
KASH, K. N88-27023
KASPER, E. N88-27027
KAT, P. J. N88-26871
KAUFHERR, N. N88-26478
KAULKER, WILLIAM F. N88-26603
KAUN, T. D. N88-26581
KAWAI, K. N88-26996
KAWAIKE, KAZUHIKO N88-26667
KAZEMINEZHAD, F. N88-26958
KEARNS, JAMES A. N88-26911
KECHTER, G. E. N88-26701
KELLER, M. W. N88-27071
KELLOGG, G. L. N88-27070
KELLY, R. E. N88-26949
KELMAN, B. J. N88-26792
KENNARD, G. S. N88-27144
KENNON, STEPHEN RAY N88-26597
KENT, GLENN A. N88-26898
KERN, RICHARD N88-26733
KERSHNER, J. D. N88-26491
KETTERSON, JOHN B. N88-27057
KEY, J. F. N88-26662
KHALIL, M. N88-26889
KHOE, T.J. H. N88-26562
KIKSTRA, O. J. N88-26355
KIKUCHI, KAZUO N88-26312
KIM, SANG-WOOK N88-26535
KIM, YOUNG-CHEOL N88-26940
KIMURA, FUMIHIKO N88-26851
KIMURA, RYUHEI N88-27029
KIMURA, WAYNE D. N88-26425
KING, A. W. N88-26740
KING, C. B. N88-26397
KING, DAVID A. N88-26837
KING, GALEN B. N88-26428
KING, N. N88-26422
KIPLINGER, A. L. N88-27144
KIRCHOEFER, S. W. N88-27019
KIRK, M. A. N88-27085
KIROL, L. D. N88-26605
KITROSSER, DAVID F. N88-26753
KLARER, P. R. N88-26351
KLEMS, J. N88-26727
KLUEH, R. L. N88-26442
KNIGHT, T. C. D. N88-27120
KNIO, O. M. N88-26423
KNUDSON, C. L. N88-26492
KNUDTSON, J. T. N88-26990
KOBAYAKAWA, MAKOTO N88-26298
KOBAYASHI, HERBERT S. N88-26568
KOBAYASHI, KENJI N88-26315
KOBAYASHI, MASAKAZU N88-27029
KOBRIN, P. H. N88-26480
KOCHETKOVA, L. P. N88-26788
KOCK, MARTIN ERNST MAX N88-26457
KODAMA, YOSHIAKI N88-26322
KOENCZOEL, L. N88-26485
KOENIG, WINFRIED N88-26773
KOJIMA, Y. N88-26509
KOK, JOOST N. N88-26850
KOLBAS, R. M. N88-27004
KOLODZIEJSKI, L. A. N88-27050
KONAGAI, MAKOTO N88-27029
KONNO, M. N88-26506
KONRAD, C. H. N88-26967
KOONS, H. C. N88-26396
KORTING, P. A. O. G. N88-26417
KORTUEM, W. N88-26522
KOSHIOKA, YASUHIRO N88-26297
N88-26600
KOSTER, RANDAL D. N88-26745
KOTTHAUS, J. P. N88-27007
KOURA, KATSUHISA N88-26304
KOVAC, J. N88-26477
KOYADA, KAZUO N88-26649
KRAG, B. N88-26533
KRAMER, B. M. N88-26478
KRANAKIS, EVANGELOS N88-26849
KRANKOTA, J. L. N88-26516
KRASNOV, I. B. N88-26786
KRAZINSKI, J. L. N88-26369
KRIJN, R. N88-26366
KRIKORIAN, O. H. N88-26496
KRISTIANSSON, A. N88-26920
KRIZ, PETR N88-26462
KRIZ, R. J. N88-26473
KROEGER, D. M. N88-27064
KROEMER, H. N88-27001
KROESEN, GERARDUS MARIA WILHELMUS
N88-26992
KRUEGER, A. J. N88-26763
KRYUCHKOVA, T. A. N88-26786
KU, JENTUNG N88-26389
KUECH, T. F. N88-27038
KUIJPER, M. N88-26677
KUNKEL, W. B. N88-26937
KUPPERMAN, D. S. N88-26472
KURIYMA, YOSHIO N88-26510
KUWAHARA, KUNIO N88-26300
KUZMA, T. J. N88-26714
KWO, J. N88-27014
KWOK, W. K. N88-27079
N88-27083
KWONG, MAN KAM N88-26884
KYPARISIS, JERZY N88-26834

L

LABARRERE, M. N88-26525
N88-26533
LABOW, G. J. N88-27144
LAFON, A. N88-26623
LAKHINA, G. S. N88-26978
LALESSE, A. J. N88-26716
LAM, D. J. N88-27085
LAM, RAYMOND K. N88-26859
LAMB, J. W. N88-26766
LAMBERT, S. E. N88-27065
LAMICH, D. J. N88-26763
LAMKIN, S. L. N88-26935
LAMMERTSVANBUEREN, G. M. N88-26357
LAMON, S. N88-26367
LAN, Y. N88-26814
LANAGAN, M. T. N88-27087
LANCASTER, N. N88-27134
LANG, WALTER N88-26432
LANKFORD, JAMES N88-26452
LARNAC, G. N88-26414
LARSEN, R. P. N88-26475
LATIMER, T. W. N88-26939
LAURENDEAU, NORMAND M. N88-26428
LAWSON, DENISE M. N88-26859
LE, H. Q. N88-26999
LECURU, D. N88-26365
LEE, D. N88-27050
LEE, E. H. N88-26437
LEE, J. N88-26580
LEE, J. K. N88-26445
LEE, JONG-WON N88-26413
LEE, LONG C. N88-26424
LEE, R. N88-27082
LEE, R. H. N88-26478
LEE, S. M. N88-26585
LEE, S. W. N88-26585
LEON, STACY CUEVAS N88-26636
LEPI, S. M. N88-26516
LESAR, R. A. N88-26923
LEUNG, K. N. N88-26934
N88-26937
LEVERANT, GERALD R. N88-26452
LEVINE, B. F. N88-27026
LI, GUOMING N88-27073
LI, HSUEH-JYH N88-26542
LI, MING N88-26819
LI, SHUJIE N88-26881
LICHTENBERG, CHRISTOPHER L. N88-26568
LICKFIELD, G. C. N88-26407
LIM, TEIK CHIN N88-26675
LIN, C. H. N88-27078
LIN, H. T. N88-26443
LIN, MARK KIN-FU N88-26408
LIN, P. S. D. N88-27023
LINDE, CHARLOTTE N88-26348
N88-26349
LINDELL, I. V. N88-26546
LINDEMANN, U. N88-26535
LING, ZHI-GUANG N88-26512
LIPPAY, A. L. N88-26678
LIPSCHULTZ, B. N88-26972
LITTLE, B. H., JR. N88-26360
LIU, C. T. N88-26435
N88-26437
LIU, J. Q. N88-26881
LIU, J. W. S. N88-26823
LIU, J. Z. N88-27080
N88-27081
N88-27085
LIU, KEFENG N88-26545
LIU, YUNG Y. N88-26450
LOCQUET, J. P. N88-27082
LOEHLE, MICHAEL N88-26876
LOEVE, W. N88-26844
LOHR, J. N88-26987
LONGENBAUGH, R. S. N88-26419
LOONEY, L. D. N88-26949
LORENZO, CARL F. N88-26401
LOWDEN, R. A. N88-26409
LOWE, CALVIN W. N88-26569
LU, CHIN N88-26823
LUBECK, O. M. N88-26813
LUNG, C. W. N88-26692
LUONG, JOHN C. N88-27005
LURYI, SERGE N88-27024
LYNCH, THOMAS J. N88-26640
LYNCH, V. E. N88-26985
LYONS, DANIEL F. N88-26552
LYONS, P. B. N88-26949
LYTLE, FRED E. N88-26428
LYTLE, J. K. N88-26616

M

MAASS, MATHIAS N88-26703
MACIASZEK, THIERRY N88-26624
MACKENS, U. N88-27041
MACKENZIE, R. A. D. N88-26444
MADER, C. L. N88-26491
MAEDA, MINORU N88-26483
MAEJIMA, MAKOTO N88-26894
MAEKELAE, J. N88-26796
MAGGS, J. E. N88-26989
MAGNANI, N. J. N88-26578
MAILHIOT, C. N88-27002
MAIMONI, A. N88-26594
MAITLAND, DUNCAN J., IV N88-26644
MAJUMDAR, S. N88-26472
MAKINO, HISAO N88-26604
MALES, RICHARD M. N88-26817
MALIK, A. A. N88-26494
MALIK, R. J. N88-27026
MANE, LAURE N88-26632
MANNAN, M. N88-26602
MANNEY, GLORIA L. N88-26756
MANNHEIMER, R. J. N88-26612
MANSON, J. R. N88-26930
MAO, HO-KWANG N88-27137
MAPLE, M. B. N88-27065
MARCOLINI, MICHAEL A. N88-26907
MARINUZZI, J. G. N88-26866
MARS, D. E. N88-27030
MARSHALL, K. L. N88-26948
MARTIN, J. P. N88-27120
MARTIN, S. J. N88-27069
MASON, BRUCE N88-27043
MASON, C. A. N88-26360
MASON, HUGH W. N88-27117
MASSALSKI, T. B. N88-27098
MATSUDA, TAKUYA N88-26295
N88-26299
MATSUNO, KENICHI N88-26317
MATSUOKA, TAKAYOSHI N88-26508
N88-26511
MATSUSHIMA, KISA N88-26292
N88-26302
MATSUSHITA, T. N88-27051
MATTHEWS, L. K. N88-26419
MATYUSHIN, A. T. N88-26820
MAUDE, D. K. N88-27020
MAULARD, JEAN N88-26381
MAURER, GERALD J. N88-26699
MAYER, ROLF N88-26592
MAYLOR, ELLIOTT L. N88-26350
MAYOR, MARCO ANTONIO N88-26543
MAZIASZ, P. J. N88-26442
MCCABE, MICHAEL E., JR. N88-26389
MCCOLLUM, J. R. N88-26407
MCCOMBE, B. D. N88-26998
MCCUNE, W. N88-26879
N88-27072
MCDERMOTT, F. S. N88-26972
MCELFRESH, M. N88-27065
MCGRAW, J. R. N88-26812
MCILWAIN, M. E. N88-26662
MCKAY, D. N88-26927
MCKAY, P. F. N88-26960
MCKENZIE, D. L. N88-27141
MCKINNEY, WILLIAM S., JR. N88-26870
MCKINNON, JOHN A. N88-27138
N88-27139
MCLARNON, F. R. N88-26723
MCVEIGH, M. N88-26367
MEBIUS, J. E. N88-26896
MEEKS, E. L. N88-26584
MELHEM, RAMI N88-26840
MELOTT, A. N88-26927

MENDEZ, R. N88-26813
MENU, J.-P. N88-26806
MERCER, CAROLYN R. N88-26641
MERCY, J.-M. N88-26998
MERKLEY, DENNIS R. N88-26498
MERKT, U. N88-27007
MERLIN, R. N88-27055
MERRIGAN, M. A. N88-26392
MERRILL, WALTER C. N88-26401
MESSURI, ANTHONY PAUL N88-26658
METIVET, BRIGITTE N88-26631
MEWALDT, R. A. N88-27146
MEYER, J. J. C. N88-27114
MEYER, W. H. N88-27113
MGOMBELO, M. R. N88-26831
MICHAEL, J. R. N88-27078
MICKLE, MARLIN H. N88-26376
N88-26377
MIELKE, ROLAND R. N88-26595
MIHALOEW, JAMES R. N88-26376
N88-26377
MILAM, D. N88-26656
MILLER, C. M. N88-26650
MILLER, D. A. B. N88-27028
MILLER, H. C. N88-26579
MILLER, J. N. N88-27030
MILNER, D. F. N88-26426
MILNER, DAVID F. N88-26427
MIMS, V. A. N88-26999
MISHONOV, T. M. N88-27058
MIYATA, HIROSHI N88-26667
N88-26668
MIYAZAKI, YOSHIRO N88-26510
MIYOSHI, HAJIME N88-26291
MIZERA, P. F. N88-26396
N88-26755
MO, H. J. N88-27129
MOBLEY, C. D. N88-26765
MOEK, G. N88-26358
MOENNICH, W. N88-26526
N88-26527
MOHAMMAD, N. N88-26883
MOLINARI, E. N88-27035
MOLLER, J. M. N88-27113
MOM, A. J. A. N88-26373
MONNIER, G. N88-26525
MONROE, RICHARD L. N88-26557
N88-26558
MONTI, P. N88-27120
MOOG, E. R. N88-27084
MOONEY, E. N88-27115
MOORE, G. T. N88-26651
MOORE, J. W. N88-26813
MOORE, R. K. N88-26710
MORALES, G. J. N88-26989
MORBIOLI, R. N88-26370
MORE, R. N88-27096
MOREAU, J. A. N88-26486
MORI, HEDETAKA N88-26314
MORI, SANAE N88-26454
MORITA, TOSHIYUKI N88-26303
MORROW, T. B. N88-26612
MOTODA, KENTARO N88-26324
MOURAD, A. G. N88-26714
MOUSTAKAS, T. D. N88-27055
MOWBRAY, D. J. N88-27039
MUELLER-MENZEL, THOMAS N88-26626
MUELLER, GUSTAV N88-26654
MULDER, J. A. N88-26530
MUNCZEK, H. N88-26927
MUNGER, MICHAEL P. N88-26808
MUNRO, IAN G. N88-26451
MURAKAMI, CHIKARA N88-26513
MURAKAMI, KOUICHI N88-26327
MURAKAMI, M. N88-26509
MURANAKA, NOBORU N88-26514
MURPHY, H. D. N88-26730
MURPHY, K. D. N88-26578
MUTO, S. N88-27048
MYKINS, DAVID W. N88-26693

N

NAGAYAMA, TSUTOMU N88-26604
NAGY, Z. N88-26448
NAIRN, C. M. C. N88-27140
NAKAHASHI, KAZUHIRO N88-26310
NAKAJIMA, ATSUSHI N88-26513
NAKAMURA, KAZUO N88-26483
NAKAMURA, KINUYO N88-26304
NAKAMURA, NORIO N88-27143
NAKAMURA, YOSHIAKI N88-26296
NAKAO, MASAHIRO N88-26298
NAKASHIMA, H. N88-27030
NAKATA, H. N88-27050
NAKATA, TOSHIHIKO N88-26649
NAKATANI, ICHIRO N88-26514
NAMERA, TAKAKAZU N88-26514
NARAIN, SANJAI N88-26839
NARUSE, Y. N88-26983
NASH, K. J. N88-27037
NATESAN, K. N88-26450
NATHAN, M. N88-27020
NAUMANN, ROBERT J. N88-26387
NEDROW, P. T. N88-26637
NEFF, JOHN S. N88-27136
NEGISHI, A. N88-26735
NEGISHI, KANJI N88-26508
N88-26511
NEJAD, A. S. N88-26369
NELSON, MATTHEW JON N88-27127
NEMOTO, MINORU N88-26571
NEUBAUER, F. M. N88-26758
N88-26773
N88-26774
NEWBURY, R. N88-27011
NEWMAN, E. H. N88-26565
NEWMAN, H. S. N88-27019
NEWMAN, KATHIE E. N88-27054
NEWMAN, NATHAN N88-27059
NEWMAN, P. A. N88-26763
NEWMAN, RICHARD L. N88-26809
NI, L. M. N88-26814
NICHOLAS, R. J. N88-27039
NICKS, ARLIN D. N88-26712
N88-26716
NIGAM, G. D. N88-27076
NIKOSKINEN, K. I. N88-26546
NINNO, D. N88-27038
NINOMIYA, KEIKEN N88-26514
NISHIKAWA, NOBUHIDE N88-26323
NISHIKAWA, YUUJI N88-26508
N88-26511
NISHIMURA, KIYOHIKO N88-26956
NISHINOMIYA, SHO N88-26742
N88-26766
NITSCHKE, P. N88-26615
NOGAR, N. S. N88-26650
NOLAN, T. A. N88-26469
NOREN, B. N88-26920
NORIKANE, LYNNE N88-26541
NOWICKI, L. J. N88-27083
NOZAKI, OSAMU N88-26310
NUNEZ, L. H. N88-27081
NUNEZ, L. N. N88-27083
NURMIKKO, A. V. N88-27006
N88-27050

O

OBAYASHI, SHIGERU N88-26292
N88-26302
OBLOW, E. M. N88-26352
OCHMANEK, DAVID A. N88-26903
ODORICO, J. N88-26365
OGATA, JUNICHI N88-26571
OGAWA, SATORU N88-26293
N88-26309
N88-26320
OGUCHI, H. N88-26599
OGUCHI, HAKURO N88-26598
OGURA, NAOTO N88-26514
OIKONOMOU, KOSTAS N. N88-26849
OKAMOTO, Y. N88-26506
OKHRIMENKO, L. S. N88-26820
OKUBO, TSUTOMO N88-26483
OLADIPUPO, ADEBISI O. N88-26569
OLDEROG, E. R. N88-27114
OLENEV, S. N. N88-26786
OLIVERA, HECTOR J. N88-26836
OLSDER, G. J. N88-26358
OLSON, JERRY S. N88-26711
OLSON, R. E. N88-26960
OLSZEWSKI, M. N88-26393
ONO, IKUO N88-26324
ONUMA, SADAYUKI N88-26507
ORLOWSKI, M. N88-26892
ORWIG, L. E. N88-27144
OSBOURN, G. C. N88-26942
OSHIMA, K. N88-26499
N88-26500
OSHIMA, RYOICHIRO N88-26667
N88-26668
OSHIMA, YUKO N88-26501
N88-26502
OSKANEN, M. I. N88-26573
OSKARSSON, A. N88-26920
OSPELT, M. N88-27034
OSTRACH, SIMON N88-26497
OSWALD, J. N88-27006
OTT, H. R. N88-27065
OTT, R. H. N88-26560
OUTTERIDGE, D. A. N88-27120
OVERSKEI, D. O. N88-26964
OWOCKI, S. P. N88-27128
OXBORROW, E. A. N88-27110
OYANAGI, H. N88-27051

P

PAC, J. L. N88-26525
PACHTER, M. N88-26892
PADGETT, R. A. N88-27064
PAEZ, T. L. N88-26691
PANITZ, J. A. N88-26960
PANITZ, J. K. G. N88-26465
N88-26467
PAPAMICHAEL, K. N88-26727
PAPANTONI-KAZAKOS, P. N88-26552
PAPUASHVILI, N. A. N88-26976
PARIKH, P. N88-26495
PARK, J. N88-26877
PARK, J. T. N88-26612
PARKER, J. V. N88-26384
PARKER, S. R. N88-26656
PARROTT, TONY L. N88-26913
PATHAK, P. H. N88-26565
PATTON, R. J. N88-26524
PAULIKAS, A. P. N88-27083
PAVLIN, JASMINA N88-26932
PAWELEK, A. N88-27075
PAYNE, M. G. N88-26421
PELLIN, M. J. N88-26418
PELTOMAA, AULIS N88-26746
PENDLEY, R. E. N88-26900
PEPER, F. N88-26864
PEPPER, M. N88-27011
PESCIA, D. N88-27015
PETERS, L., JR. N88-26565
PETERSON, D. E. N88-27063
PETITDEMANGE, V. N88-26339
PETRAVIC, G. K. N88-26984
PETRAVIC, M. N88-26984
PETTERSON, B. J. N88-26660
PHALIPPOU, J. N88-26414
PICHKHADZE, SH. D. N88-26974
PIERCE, ALLAN D. N88-26911
PIETARINEN, MAIJA N88-26746
PILAT, J. F. N88-26900
PINTER, JANOS N88-26895
PLASTER, W. D. N88-27120
PLICHTA, M. R. N88-26445
POEMP, KURT N88-26799
POEPPEL, R. B. N88-27087
PONCE, T. C. N88-26610
POND, J. M. N88-27019
POPE, L. E. N88-26467
PORRATI, E. N88-26777
PORTAL, J. C. N88-27020
POST, W. M. N88-26740
PRECKSHOT, G. G. N88-27113
PREGENZER, A. L. N88-26960
PREISENDORFER, R. W. N88-26765
N88-26780
PRICE, J. R. N88-26463
PRINCE, T. A. N88-27146
PRINZ, G. A. N88-27013
PRIOU, ALAIN N88-26487
PROBER, D. E. N88-27022
PROCHAZKA, VLADIMIR N88-26462
PROGAR, DONALD J. N88-26481
PRONK, C. N. A. N88-26678
PROSKAWETZ, K.-O. N88-26529
PROTOPOPESCU, V. N88-26862
PROVOST, FOSTER N88-26840
PRZYLECKA, M. N88-26484
PSIAKI, MARK LOCKWOOD N88-26375
PULLES, CORNELIS JOHANNES ADRIANUS N88-26630
PULSFORD, N. A. N88-27039
PUTNAM, TERRILL W. N88-26361

Q

QIAN, PING N88-26778
QUEIJO, M. J. N88-26397
QUIRK, F. W. N88-26717

R

RAAFF, W. R. N88-26757
RADOUSKY, H. B. N88-26925
RAGHAVAN, KALYANI N88-26801
RAGUSA, JAMES M. N88-26867
RALSTON, J. N88-26927

RAMDAS, A. K. N88-26997
RAMSEY, R. L. N88-26945
RASCHKE, E. N88-26758
N88-26773
N88-26774
RAVAIOLI, U. N88-27046
RAWLINS, M. H. N88-26469
RAZZAQ, ZIA N88-26693
REDDOCH, T. W. N88-26721
REDEY, L. N88-26581
REECE, C. E. N88-27077
REED, MARK A. N88-27045
REEDER, A. A. N88-26998
REICHELT, W. N88-26531
REID, R. S. N88-26392
REID, T. B. N88-26602
REILLY, T. D. N88-26682
REIMANN, NORBERT N88-26591
REINA, F. N88-26362
REINERS, TH. N88-26536
REINISCH, BODO W. N88-26753
REY, CHARLES A. N88-26498
RHODES, J. A. N88-26618
RHYNE, J. J. N88-27056
RICCO, A. J. N88-27069
RICE, B. W. N88-26993
RICE, C. K. N88-26607
RICHARDS, R. K. N88-26965
RICHTER, J. H. N88-26554
N88-26555
RICKS, R. E. N88-26663
RILEY, DONALD R. N88-26374
RILEY, WILLIAM J. N88-26640
RINDT, J. R. N88-26492
RINEHART, G. H. N88-26939
RINEHART, GRAHAM W. N88-26400
RITCHIE, R. H. N88-26929
N88-26930
RIZZO, H. F. N88-27096
ROANE, DONALD P., JR. N88-26363
ROBERTS, J. S. N88-27037
ROBERTS, LEONARD N88-26335
ROBLIN, PATRICK N88-27049
ROCKENFELLER, U. N88-26393
RODRIGUES, VALTER N88-26824
ROEDER, J. L. N88-26396
ROGERS, F. N88-26994
ROHLF, D. N88-26527
ROOKS, M. J. N88-27022
ROOS, C. N88-26848
ROOS, M. J. J. N88-26954
ROSEN, I. G. N88-26873
ROSS, HOWARD D. N88-26539
ROSS, M. N88-26925
ROSS, T. N88-27115
ROSS, WILLIAM E. N88-26950
ROVNER, DANIEL MARK N88-26865
ROWE, M. W. N88-26650
ROY, RONALD AURELE N88-26908
RUGGLES, L. E. N88-26961
RUSSELL, THOMAS L. N88-26902
RUTTEN, J. J. M. M. N88-26853
RUTTEN, JAN J. M. M. N88-26850
RYBICKI, G. B. N88-27126

S

SACKINGER, W. M. N88-26782
SADA, KOICHI N88-26749
SADASIVAN, S. N88-26602
SADLOWE, A. R. N88-27116
SAEGER, M. L. N88-26739
SAIF, A. G. N88-27074
SAIKAWA, MICHIYUKI N88-26728
SAILLEAU, D. N88-26487
SAITO, T. N88-26506
SAITOV, I. S. N88-26820
SAKURAI, AKIRA N88-26307
SALAMON, M. B. N88-27056
SALATI, P. N88-27145
SALEM, JONATHAN A. N88-26482
SAMADANI, RAMIN N88-26713
SANTORO, R. T. N88-26899
SAROHIA, V. N88-26495
SASAKI, A. N88-27051
SASS, S. L. N88-26444
N88-27078
SATO, HIROYUKI N88-26327
SATO, KIYOSHI N88-26329
SATO, MIKIO N88-26649
SATO, SHUNITSU N88-26596
SATO, TOMIHIKO N88-26314
SAUVE, J. L. N88-26967
SAVIDGE, J. L. N88-26602
SAWADA, KEISUKE N88-26295
N88-26299
N88-26301
N88-26316
SCARBROUGH, J. O. N88-27064
SCHAFFAR, M. N88-26633
SCHALM, R. W. N88-26943
SCHATZLE, F. J. N88-26717
SCHEEPERS, C. F. N88-26720
SCHERER, A. N88-27023
SCHERSON, D. A. N88-26416
SCHIAVONE, L. N88-27023
SCHIEHLEN, W. N88-26521
SCHILLING, L. N88-26653
SCHIMMERLING, WALTER N88-27142
SCHIPPERS, H. N88-26341
SCHLICHTING, HERMANN N88-26337
N88-26338
SCHMALZER, PAUL A. N88-26795
SCHMID, A. N88-26948
SCHNEIDER, WILLIAM C. N88-26398
SCHOEBERL, M. R. N88-26763
SCHOLZ, FERDINAND N88-27094
SCHRA, L. N88-26695
N88-26706
SCHREIBER, JEFFREY G. N88-26732
SCHULLER, I. K. N88-27082
SCHULLER, IVAN K. N88-27012
SCHULTZ, P. F. N88-26448
SCHUSTER, HILDEGARD N88-26842
SCHWAB, RUDOLPH T. N88-26354
SCHWAGER, L. A. N88-26971
SCHWARTZ, R. A. N88-27144
SCHWARZ, R. B. N88-26438
SCHWEIZER, H. N88-27001
SEGEV, A. N88-26877
SELKOWITZ, S. N88-26727
N88-27018
SEN, S. N88-26482
SESHADRI, SRINIVASA G. N88-27124
SEVE, ALAIN N88-26671
SHA, W. T. N88-27101
SHABANI, J. N88-26515
SHACHAM, I. N88-27083
SHAKED, H. N88-26966
SHARAFAT, S. N88-26465
SHARP, D. J. N88-27144
SHAVER, A. N88-26973
SHAW, C. B., JR. N88-26754
SHEEHAN, ROBERT E. N88-27054
SHEN, JUN N88-26833
SHENKER, ABRAHAM N88-26771
SHERMAN, BRETT T. N88-26434
SHERWOOD, JAMES ALLEN N88-26300
SHIDA, YOSHIFUMI N88-26294
SHIGEMI, MASASHI N88-26295
SHIMA, EIJI N88-26299
N88-26313
SHIMADA, S. N88-26664
SHIMADA, TORU N88-26305
SHIMIZU, ATSUSHI N88-26315
SHIMIZU, MIKIO N88-26918
SHIMOJI, TOSHIYUKI N88-26304
SHIN, H. Y. N88-27060
SHIRAI, HIROYUKI N88-26504
SHIRLAND, FRED A. N88-27033
SHOEMAKER, P. E. N88-26578
SHOLL, P. L. N88-26391
SHORES, PAUL W. N88-26568
SHREVE, LOY W., II N88-26825
SHUKLA, P. K. N88-26978
SHUM, KAI N88-27044
SHUTE, VALERIE N88-26801
SIAS, F. R., JR. N88-26665
SICILIANO, E. R. N88-26932
SIDNER, CANDACE L. N88-26802
SIKORSKI, CH. N88-27007
SILVER, LEONARD N88-26833
SIMONS, H. J. N88-26564
SINGH, J. P. N88-26472
N88-27087
SINGH, RAJENDRA N88-26675
SINGLETON, J. N88-27039
SIVANANTHAN, S. N88-27052
SKERRETT, K. J. N88-26948
SKOCPOL, W. J. N88-27021
SKOLNICK, M. S. N88-27037
N88-27039
SLIFKA, A. J. N88-26466
SMALL, RONALD L. N88-26808
SMID, H. J. N88-27105
N88-27106
SMIT, DIRK-JAN N88-26904
SMITH, A. J. N88-26975
SMITH, D. H. N88-26855
SMITH, D. L. N88-27002
SMITH, DAVID N88-26751
SMITH, J. L. N88-27065
SMITH, KEVIN D. N88-26380
SMITH, L. N88-26729
SMITH, R. D. N88-26932
SMITH, ROBERT W. N88-26289
SNIDER, R. N88-26986
SNIDER, R. T. N88-26969
SODOYER, B. R. N88-26846
SOKOL, C. K. N88-26739
SOM, SUKHAMOY N88-26595
SONDER, LESLIE J. N88-26759
SOROKINA, L. M. N88-26786
SPALART, PHILIPPE R. N88-26342
SPARKS, L. L. N88-26466
SPARLIN, D. M. N88-27088
SPETH, P. N88-26758
N88-26773
N88-26774
SPROUL, W. D. N88-26478
SRIVASTAVA, M. P. N88-26979
SRIVASTAVA, SANTOSH K. N88-26424
STANFORD, JOHN L. N88-26756
STANLEY, P. N88-26383
STANTON, C. J. N88-27036
STARLING, K. E. N88-26602
STEELE, B. C. N88-26729
STEIN, PETER J. N88-26794
STEINER, T. N88-27038
STEINMETZ, P. N88-26370
STEKETEE, J. J. N88-26847
STELLING, G. S. N88-26781
STENGEL, ROBERT F. N88-26347
STINNETT, R. W. N88-26960
STINTON, D. P. N88-26409
STOCKDALE, R. E. N88-26969
STONE, E. C. N88-27146
STONE, R. W. N88-26397
STOUGHTON, JOHN W. N88-26595
STOVALL, T. K. N88-27104
STRAHLE, WARREN C. N88-26429
STRAUB, DIETER N88-26620
STRIEBEL, K. A. N88-26723
STROTTMAN, D. D. N88-26921
STUBER, R. N88-27001
SUBBANNA, S. N88-27001
SUEMATSU, KAZUYO N88-26304
SULLIVAN, JOHN B. N88-27107
SURAPANENI, R. N88-27116
SURESH, S. N88-26689
SUSOEFF, A. R. N88-26967
SUTTON, DAVID G. N88-26990
SUZUKI, AKIRA N88-26323
SUZUKI, HIROSHI N88-26571
SUZUKI, HISASHI N88-26453
SVEC, W. A. N88-26793
SWEELY, D. N88-26828
SWEERS, GUIDO N88-26888
SWINDOLL, CHARLES M. N88-26493
SYDORA, RICHARD D. N88-26059
SYN, C. K. N88-26664
SZE, D. K. N88-26983

T

TAGUCHI, MASAKAZU N88-26508
N88-26511
TAHERZADEH, M. N88-26981
TAKAHASHI, KIYOSHI N88-27029
TAKAHASHI,, ICHIRO N88-26668
TAKAKURA, YOKO N88-26293
N88-26309
N88-26320
TAKANASHI, SUSUME N88-26292
TAKANASHI, SUSUMU N88-26301
N88-26302
N88-26316
TAKAYAMA, FUMIO N88-26307
TAKAYAMA, KAZUYOSHI N88-26308
TAKAYANAGI, KAZUO N88-26919
TAKEDA, Y. N88-27051
TAKI, SHIROU N88-26307
TALJA, H. N88-26538
TALVACCHIO, J. N88-27091
TAM, HON-WAH N88-26830
TAMAKI, TEIICHI N88-26315
TAMMELIN, BENGT N88-26746
TAMURA, ATSUHIRO N88-26310
N88-26312
TANAKA, HIROYOSHI N88-26722
TANAKA, TAKASHI N88-26804
TANAKA, YASUO N88-27143
TANG, C. L. N88-27036
TANGMANEE, S. N88-26333
TANNER, L. E. N88-26480
TAPSTER, P. R. N88-27037
TATARSKIY, V. I. N88-26617

TATSUMI, SHIGEFUMI N88-26303
TAVEAU, P. N88-26486
TAVELLA, DOMINGO N88-26335
TAYLOR, J. S. N88-26664
TAYLOR, L. N88-26653
TAYLOR, PAUL A. N88-27053
TEAGUE, M. R. N88-26648
TELESMAN, JACK N88-26436
TELLER, E. N88-27096
TENEKETZIS, DEMOSTHENIS N88-26893
TENHAGEN, PAUL J. W. N88-26851
TENNERY, V. J. N88-26469
TERRY, J. L. N88-26972
TETENBAUM, M. N88-27086
TETERINA, T. P. N88-26788
TEWS, V. N88-26523
THEIL, MICHAEL H. N88-26464
THOMAS, D. M. N88-26963
THOMAS, H. L. N88-26407
THOMAS, I. N88-26656
THOMAS, M. P. N88-26963
THOMPSON, J. D. N88-27065
THORNTON, T. J. N88-27011
THUILLIER, FRANCOIS-MARIE N88-26487
TH1NBORG, SIEGFRIED N88-26661
TIAN, DECHENG N88-27073
TIEGS, T. N. N88-26479
TIMOTHY, J. G. N88-26941
TIMP, G. L. N88-27010
TISCHLER, M. B. N88-26532
TIWARI, S. N. N88-26618
TLASKAL, JAROSLAV N88-26462
TOLBERT, A. K. N88-27144
TOLLIN, G. N88-26725
TOLLMIEN, WALTER N88-26337
TOLMIEN, WALTER N88-26338
TOMLIN, K. H. N88-26360
TORNEY, D. C. N88-26874
TORRACA, L. N88-26639
TOWNSEND, L. W. N88-26935
TOWNSEND, LAWRENCE W. N88-27142
TRAUB, WESLEY A. N88-26737
TRENT, B. C. N88-26690
TROIDL, HUBERT N88-26621
TSANG, W. T. N88-27047
TSINTADZE, N. L. N88-26905
TSUCHIYA, KAZUO N88-26513
TSUI, D. C. N88-27047
TSUYUZAKI, N. N88-26506
TUKEY, JOHN W. N88-26821
TULBAYEVA, F. P. N88-26790
TURNER, W. C. N88-26576
TUTTLE, M. E. N88-26601
TZENG, D. D. N88-26494

U

ULBRICH, C. W. N88-26770
UMEDA, YOSHIKUNI N88-26295
N88-26299
UMEZAWA, A. N88-27080
N88-27081
UO, MASAHI N88-26514
UPATISING, VIRIYA N88-26811
UPPAL, P. N88-27019

V

VACCARO, FRANK T. N88-26379
VALKONEN, A. E. N88-26439
VALOT, C. N88-26806
VALOT, HENRI N88-26487
VANDENBERG, R. P. N88-26537
VANDERBEEK, N. P. N88-27112
VANDERGAAG, L. C. N88-26852
VANDERGELD, C. W. M. N88-26417
VANDERMAST, C. A. P. G. N88-26846
N88-27105
N88-27106
VANDERVEEN, J. C. T. N88-26366
VANDERVLUGT, F. R. N88-27106
VANDRIEL, N. N88-26368
VANESS, PIETER J. N88-26643
VANGULICK, L. A. N88-26659
VANHAESENDONCK, C. N88-27008
VANHOOF, H. A. J. M. N88-26917
VANINETTI, J. N88-26637
VANKA, S. P. N88-26389
N88-26609
N88-26611
VANKAN, J. J. I. M. N88-26889
VANLEEUWEN, H. P. N88-26695
N88-26706
VANROODE, M. N88-26463
VANSTIJN, T. L. N88-26781
VANSTRIEN, SEBASTIAN N88-26886
VANZYL, JAKOB J. N88-26541
VASTENHOUW, J. N88-27105
N88-27106
VAUDIN, M. D. N88-26444
VEAL, B. W. N88-27079
N88-27083
VELDMANN, A. E. P. N88-26627
VELDS, C. A. N88-26757
VELSKO, S. P. N88-27067
VENABLE, DEMETRIUS D. N88-26569
VENKATESWARAN, H. N88-27000
VERLIJSDONK, A. P. N88-26564
VERMILLION, C. N88-26544
VERSMISSEN, J. N88-26537
VERVELD, G. N88-27106
VERWEIJ, A. N88-27105
N88-27106
VESCOVI, MARCOS REGIS N88-26824
VESEY, R. A. N88-26962
VICROY, DAN D. N88-26344
VINTER, B. N88-27016
VISSERS, D. R. N88-26581
VITANYI, PAUL M. B. N88-26819
VLADIMIRSKIY, B. M. N88-26789
VLASKINA, L. A. N88-26789
VLIETSTRA, J. N88-26844
VOGELS, M. E. S. N88-26627
N88-26629
VOGT, WILLIAM G. N88-26376
N88-26377
VOJAK, BRUCE N88-26995
VOLKOV, V. V. N88-26788
VONKAENEL, H. N88-27034
VONLAVANTE, E. N88-26618
VOROBYEV, O. A. N88-26787
VREEBURG, J. P. B. N88-26629
VUKOVICH, F. M. N88-26762
VUONG, T. H. H. N88-27047
VYAS, A. D. N88-26475

W

WACHTER, P. N88-27034
WAGNER, ULRICH N88-26589
WALKER, J. N88-27026
WALKER, J. D. A. N88-26885
WALL, M. N88-26480
WALLACE, D. C. N88-27097
WALSH, MICHAEL R. N88-26817
WALTERS, E. J. N88-26572
WALTHER, S. R. N88-26937
WALUKIEWICZ, W. N88-27086
WAN, A. S. N88-26972
WANG, A. S. N88-26412
WANG, DONG P. N88-26424
WARNER, B. E. N88-26657
WASIELEWSKI, M. R. N88-26793
WATANABE, MASATOSHI N88-26604
WATANABE, N. N88-26996
WATANABE, SHIZUI N88-26311
WATANABE, YOSHIAKI N88-26306
WATSON, B. D. N88-27116
WEAVER, M. J. N88-26426
WEAVER, MICHAEL J. N88-26427
WEBER, H. W. N88-27085
WEIGEL, R. J. N88-26792
WEIL, T. N88-27016
WEISS, G. H. N88-26897
WEISSTEIN, NAOMI N88-26798
WELCH, J. J. N88-26647
WELLER, T. N88-26515
WESSELING, P. N88-26889
WESSELSKI, CLARENCE J. N88-26398
WEST, W. P. N88-26963
WESTENIUS, M. N88-26920
WEYAND, J. D. N88-26474
WHITCOMB, JOHN D. N88-26406
N88-26684
WHITFIELD, DAVID L. N88-26619
WIEKHORST, LINDA A. N88-26379
WIEMANS, R. N88-26547
WIJCHERS, T. N88-26417
WILDE, M. G. N88-26861
WILDER, J. N88-26656
WILDERS, P. N88-26781
WILKE, M. N88-26422
WILKE, M. D. N88-26637
WILLIAMS, R. B. N88-26916
WILLIAMS, R. K. N88-27064
WILLIAMS, T. H. LEE N88-26712
N88-26716
WILLIAMSON, D. L. N88-26748
WILLIAMSON, DAVID T. N88-26808
WILLIAMSON, G. S. N88-26748
WILLIS, R. F. N88-27015
WILLSON, W. G. N88-26492
WILMARTH, W. R. N88-27061
WILSON, J. W. N88-26935
WILSON, JOHN W. N88-27142
WILSON, M. A. N88-26490
WIND, S. N88-27022
WINKLER, HUBERTUS N88-26704
WISE, F. W. N88-27036
WOLFORD, D. J. N88-27038
WOLLENWEBER, F. G. N88-26559
WONG, C. P. C. N88-26966
WONG, MERVYN N88-27142
WOOD, CHARLES D. N88-26673
WOODIN, A. O. N88-26933
WOODWARD, R. L. N88-26686
WOODWORTH, J. R. N88-26960
WOS, L. N88-26879
WRIGHT, R. S. N88-26739
WROBEL, J. R. N88-26397
WU, CHEN T. N88-26836
WU, OWEN K. N88-27033
WUENSCH, WOLFGANG N88-26683

X

XU, Y.-L. N88-26701
XU, YINHUA N88-27073

Y

YAMADA, HITOSHI N88-26306
YAMAGUCHI, YASUSHI N88-26851
YAMAMOTO, KIYOSHI N88-26321
YAMANISHI, MASAMICHI N88-27003
YAMASHITA, AKIKO N88-26501
YANAGIZAWA, MITSUNORI N88-26303
YANG, K. Y. N88-27082
YANG, SE HOON N88-26405
YANG, Y. J. N88-27004
YAO, T. N88-27032
N88-27051
YASUDA, ATSUHIKO N88-26295
N88-26299
YASUHARA, MICHIRU N88-26296
YATES, G. J. N88-26422
YATES, LESLIE A. N88-26343
YAVROUIAN, A. N88-26495
YEAGER, E. N88-26724
YEAGER, E. B. N88-26416
YEH, DAVID N88-26335
YEH, HSIEN-YANG N88-26694
YING, KE N88-26711
YOKOTA, JEFFREY W. N88-26340
YONEMOCHI, OSAMU N88-26483
YOSHIDA, H. N88-26983
YOSHIDA, KENJI N88-26313
YOSHIDA, MASAHIRO N88-26302
YOSHIZAWA, Y. N88-26325
YOUNG, C. E. N88-26418
YOUNG, P. N88-26524
YUAN, CHUNG-I. N88-26399
YULE, A. J. N88-26614

Z

ZAYHOWSKI, J. J. N88-26999
ZEBKER, HOWARD A. N88-26541
ZENIE, ALEXANDRE N88-26843
ZHANG, C. N88-26700
ZHANG, CH. N88-26702
ZHANG, WEITANG N88-26590
ZHANG, YUSHUN N88-26928
ZHOU, JI-XUN N88-26911
ZHOU, S. J. N88-26692
ZHU, HUILONG N88-26441
ZIELINSKI, E. N88-27001
ZIETLOW, THOMAS C. N88-26586
ZIMMERMAN, ALBERT H. N88-26587
ZIPF, MARK E. N88-26376
N88-26377
ZOBEL, R. N88-26536
ZUCKER, J. I. N88-26853
ZYDA, MICHAEL J. N88-26836

Typical Corporate Source Index Listing

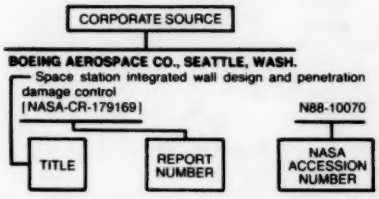

Listings in this index are arranged alphabetically by corporate source. The title of the document provides the user with a brief description of the subject matter. The report number helps to indicate the type of document cited (e.g., NASA report, translation, NASA contractor report). The NASA accession number denotes the number by which the citation is identified. The titles are arranged under each corporate source in ascending accession number order.

A

ADVISORY GROUP FOR AEROSPACE RESEARCH AND DEVELOPMENT, NEUILLY-SUR-SEINE (FRANCE).
Flight Mechanics Panel Symposium on Rotorcraft Design for Operations: Technical evaluation report
[AGARD-AR-243] N88-26362
Automated measurement of crack length and load line displacement at elevated temperature
[AGARD-R-751] N88-26695

AEROSPACE CORP., EL SEGUNDO, CALIF.
A severe spacecraft-charging event on SCATHA in September 1982
[AD-A193007] N88-26396
Electrical resistivity of carbon-carbon composites
[AD-A193006] N88-26410
Coherent RF error statistics
[AD-A193002] N88-26560
JFET/SOS (Junction Field-Effect Transistor/Silicon-on-Sapphire) devices: Gamma-radiation-induced effects
[AD-A193001] N88-26586
Nickel hydrogen cell positive-electrode studies: Cobalt segregation in reducing environments
[AD-A193025] N88-26587
On the conjugacy of the aurora: High and low latitudes
[AD-A193008] N88-26755
Nascent vibrational/rotational distribution produced by hydrogen atom recombination
[AD-A193005] N88-26933
Ultraviolet-visible spectroscopy of laser-produced aluminum plasmas
[AD-A193004] N88-26990
The properties of solar coronal active regions deduced from X-ray line spectra
[AD-A193026] N88-27141

AIR COMMAND AND STAFF COLL., MAXWELL AFB, ALA.
NAVSTAR global positioning system
[AD-A192609] N88-26354
Book analysis. Challenger: A major malfunction
[AD-A192458] N88-26388
The use of commercial off-the-shelf equipment and its impact on C3 (Command, Control and Communications EMP (electromagnetic pulse) survivability
[AD-A192614] N88-26556
USAF flying screening: First step on the road to wings
[AD-A192613] N88-26804
Computer-aided writing
[AD-A192516] N88-26837
Launch operations to support future space forces
[AD-A192679] N88-27107

AIR FORCE ASTRONAUTICS LAB., EDWARDS AFB, CALIF.
Environmental monitoring of a titan 34D 5 1/2 segment solid rocket motor static firing
[AD-A192975] N88-26400

AIR FORCE HUMAN RESOURCES LAB., BROOKS AFB, TEX.
Flight simulator: Field of view utilized in performing tactical maneuvers
[AD-A192412] N88-26379

AIR FORCE WEAPONS LAB., KIRTLAND AFB, N. MEX.
Microwave calibration system 2
[AD-A192976] N88-26639
Time-Optimal Adaptive Shaped Torque (TOAST) technical note
[AD-A192719] N88-26869

ALABAMA UNIV., HUNTSVILLE.
Critical point wetting drop tower experiment
[NASA-CR-183062] N88-26603

ALASKA UNIV., FAIRBANKS.
Arctic ice island and sea ice movements and mechanical properties
[DE88-004267] N88-26782

ALLGEIMEINE ELEKTRIZITAETS-GESELLSCHAFT, ULM (WEST GERMANY).
Transport study on Si/Si(1-x)Ge(x) superlattices selectively doped by secondary implantation of Sb
N88-27027

ALLIED BENDIX AEROSPACE, KANSAS CITY, MO.
GTAW characterization for weld penetration on 304L stainless steel
[DE88-010611] N88-26672

ALUMINUM CO. OF AMERICA, ALCOA CENTER, PA.
Determination of binder distributions in green-state ceramics by NMR imaging
[DE88-009990] N88-26474

ARGONNE NATIONAL LAB., ILL.
An efficient computational tool for ramjet combustor research
[DE88-010034] N88-26369
Application of superconducting technology to earth-to-orbit electromagnetic launch systems
[DE88-010022] N88-26386
Laser fluorescence spectroscopy of zinc neutrals originating from laser-irradiated and ion-bombarded zinc sulfide and zinc surfaces
[DE88-008037] N88-26418
Effect of double layer structure on the determination of corrosion rates from polarization measurements
[DE88-010097] N88-26448
The adherence of nickel oxide on nickel during high temperature oxidation
[DE88-011194] N88-26450
Observations on residual stresses in ceramic composites by neutron diffraction techniques
[DE88-009937] N88-26472
Determination of binder distributions in green-state ceramics by NMR imaging
[DE88-009990] N88-26474
The outlook for ceramics in heat engines, 1990-2010: Results of a worldwide Delphi survey
[DE88-010075] N88-26475
Characterization of coating wear phenomena in nitride and carbide coated tool inserts
[DE88-011196] N88-26478
Modeling and thermal management of advanced batteries
[DE88-010023] N88-26580
Molten salt electrolytes for high-temperature lithium cells
[DE88-010058] N88-26581
Multigrid computation of practical fluid flows and heat transfer
[TI88-010064] N88-26609
Use of direct solvers for multidimensional fluid flow computations
[DE88-010063] N88-26611
Novel magnetic materials research using free electron lasers
[DE88-009989] N88-26652
Fluid flow modeling in casting processes and its implications
[DE88-010009] N88-26671
Modeling the primary events of photosynthesis using chlorophyll containing fixed distance donor-acceptor molecules
[DE88-010033] N88-26793
Relay approach message routing in hypercube multiprocessors
[DE88-009973] N88-26814
Computing small singular values of bidiagonal matrices with guaranteed high relative accuracy: LAPACK working note number 3
[DE88-008465] N88-26829
Challenge problems focusing on equality and combinatory logic: Evaluating automated theorem-proving programs
[DE88-010057] N88-26879
Comparison theorems and their use in the analysis of some nonlinear diffusion problems
[DE88-010032] N88-26884
The hole of a blanket tritium system on the fusion fuel cycle
[DE88-010007] N88-26983
Impurity transport calculations for a drift-dependent tokamak scrape-off plasma
[DE88-010053] N88-26984
Metallic superlattices N88-27012
Challenge equality problems in lattice theory
[DE88-010094] N88-27072
Anisotropic characteristic lengths in single crystal YBa2Cu3O(sub 7-Delta)
[DE88-009959] N88-27080
Anisotropy of the lower critical field in YBa2Cu3O(sub 7-Delta)
[DE88-009971] N88-27081
Preparation of high-T(sub)c Y1Ba2Cu3O(sub 7-Delta) superconducting thin films by MBE (Molecular-Beam-Epitaxy) techniques
[DE88-009999] N88-27082
Oxygen vacancy ordering and superconductivity in YBa2Cu3O(sub 7-x)
[DE88-010005] N88-27083
Pure metallic bridge and point-contact tunneling into single- and polycrystal YBa2Cu3O(sub 7-y)
[DE88-010030] N88-27084
Electron irradiation effects in YBa2Cu3O7-Delta single crystals
[DE88-010050] N88-27085
Phase transformations and thermodynamic behavior of the YBa2Cu3O(sub)x system via EMF measurements
[DE88-010054] N88-27086
Ceramic processing of high-T(sub)c superconductors
[DE88-010090] N88-27087

ARIZONA STATE UNIV., TEMPE.
Scattering patterns of dihedral corner reflectors with impedance surface impedances
[NASA-CR-183078] N88-26545
A bibliography of dunes: Earth, Mars, and Venus
[NASA-CR-4149] N88-27134

ARIZONA UNIV., TUCSON.
Mechanisms of photochemical energy conversion by chlorophyll
[DE88-008763] N88-26725
Properties of multilayers for soft X-ray optics
N88-27025
The application of imaging to the atmospheric Cerenkov technique: Observations of the Crab nebula N88-27126

ARMY ENGINEER DIV., HUNTSVILLE, ALA.
PAX ECONOPACK economic analysis package users manual
[AD-A192949] N88-27117

ARMY TEST AND EVALUATION COMMAND, ABERDEEN PROVING GROUND, MD.
Digital communication transmitter and receiver test procedures
[AD-A191218] N88-26540

ARMY WEAPONS COMMAND, ROCK ISLAND, ILL.
The strategic defense initiative: Strategic implications
[AD-A192341] N88-26902

ARNOLD ENGINEERING DEVELOPMENT CENTER, ARNOLD AIR FORCE STATION, TENN.
The effects of RCS jet firing on the isolated Orbiter and mated coast phases of the glide return to launch site maneuver at Mach number 6 (IA302B)
[NASA-CR-180223] N88-26403
AUBURN UNIV., ALA.
Helium induced degradation in the weldability of an austenitic stainless steel
[DE88-009062] N88-26443

B

BATTELLE COLUMBUS LABS., OHIO.
Remote sensing and satellite applications to the needs of the gas and pipeline industry
[PB88-202668] N88-26714
BELL COMMUNICATIONS RESEARCH, INC., RED BANK, N.J.
Excitonic properties of GaAs-AlGaAs nanostructures N88-27023
BELL TELEPHONE LABS., INC., HOLMDEL, N. J.
Quantum transport in an electron waveguide N88-27010
Random quantum interference in microdevices N88-27021
Novel quantum well optical devices N88-27028
BELL TELEPHONE LABS., INC., MURRAY HILL, N. J.
Properties of synthetic magnetic superlattices N88-27014
Resonant tunneling transistors and resonant tunneling hot electron spectroscopy N88-27018
Infrared detectors based on the photon drag effect and intersubband absorption by a two-dimensional electron gas N88-27024
A 10 microns photoexcited avalanche gain due to electron impact ionization from GaAs quantum well superlattices N88-27026
Superconductivity of heavy-electron uranium compounds
[DE88-007901] N88-27065
BETHLEHEM STEEL CO., PA.
High resolution detection of solute segregation to the cores of dislocations in grain boundaries
[DE88-009168] N88-27078
BIONETICS CORP., HAMPTON, VA.
Some operational aspects of a rotating advanced-technology space station for the year 2025
[NASA-CR-181617] N88-26397
BIRMINGHAM UNIV. (ENGLAND).
Ion and electron interactions of atmospheric importance
[AD-A192255] N88-26751
BOEING COMMERCIAL AIRPLANE CO., SEATTLE, WASH.
Enhanced emergency smoke venting
[DOT/FAA/CT-88/22] N88-26350
BOEING VERTOL CO., PHILADELPHIA, PA.
Hover performance tests of baseline metal and Advanced Technology Blade (ATB) rotor systems for the XV-15 tilt rotor aircraft
[NASA-CR-177436] N88-26367
BOLT, BERANEK, AND NEWMAN, INC., CAMBRIDGE, MASS.
Plans for discourse
[AD-A192242] N88-26802
BOSTON COLL., CHESTNUT HILL, MASS.
Rocket measurements within a polar cap arc: Ionospheric modelling
[AD-A192381] N88-26754
BRADFORD UNIV. (ENGLAND).
Interactive computer programme for the analysis of a two-way Wilkinson divider/combiner
[PB88-105424] N88-26831
BROOKHAVEN NATIONAL LAB., UPTON, N. Y.
Acute radiation syndromes and their management
[DE88-009639] N88-26797
FASTRUN phase sequencer descriptor language (PDL)
[DE88-007966] N88-26828
Comparison of exclusive reactions at large momentum transfer
[DE88-007544] N88-26922
In-situ reactive of X-ray optics by glow discharge
[DE88-009840] N88-26947
BROWN UNIV., PROVIDENCE, R. I.
Fatigue crack growth under far-field cyclic compression
[DE88-011215] N88-26689
Influence of interfaces on electronic and magnetic properties of MnSe/ZnSe superlattices near monolayer limit N88-27050
BUNDESMINISTERIUM FUER FORSCHUNG UND TECHNOLOGIE, BONN (WEST GERMANY).
Space policy of common sense and moderation
[REPT-49/87] N88-27118

C

CALIFORNIA INST. OF TECH., PASADENA.
Effects of a temperature-dependent rheology on large scale continental extension
[NASA-CR-183117] N88-26759
Research in particle and gamma-ray astrophysics
[NASA-CR-183111] N88-27146
CALIFORNIA STATE UNIV., LONG BEACH.
Stress concentration around circular hole in a composite material specimen representative of the X-29A forward-swept wing aircraft
[NASA-CR-179435] N88-26694
CALIFORNIA UNIV., BERKELEY.
Effects of secondary electron emission on the collector and source sheaths of a finite ion temperature plasma
[DE88-006930] N88-26971
Laser spectoscopy of plasmas
[AD-A193009] N88-26991
CALIFORNIA UNIV., BERKELEY. LAWRENCE BERKELEY LAB.
Sintering of the heterogeneous MgO compacts
[DE88-010357] N88-26408
The preparation of mechanically alloyed powders for TEM (Transmission Electron Microscopy) examination
[DE88-008043] N88-26460
Ambient temperature secondary lithium batteries using LiAl lithium insertion anodes
[DE88-008394] N88-26574
Oxygen reduction in fuel cell electrolytes
[DE88-008240] N88-26723
Electrocatalysts for oxygen electrodes
[DE88-008397] N88-26724
Determination and application of bidirectional solar-optical properties of fenestration systems
[DE88-010364] N88-26727
Using common subexpressions to optimize multiple queries
[DE88-008210] N88-26877
Development of high current and high brightness negative hydrogen ion sources
[DE88-010882] N88-26934
Enhancement of volume H(-) production by vibrationally pre-exciting the hydrogen molecules
[DE88-010783] N88-26937
Fermi level dependent native defect formation: Consequences for metal-semiconductor and semiconductor-semiconductor interfaces
[DE88-008247] N88-27066
Cosmions and stars
[DE88-010886] N88-27145
CALIFORNIA UNIV., LOS ANGELES.
A Vlasov ion zero mass electron model for plasma simulations N88-26958
Modeling of subtle kinetic processes in plasma simulation N88-26959
Overview of the TITAN-2 reversed-field pinch aqueous fusion power core design
[DE88-008170] N88-26966
Electrostatic whistler mode conversion at plasma resonance
[AD-A192951] N88-26989
CALIFORNIA UNIV., SAN DIEGO.
Superconductivity of heavy-electron uranium compounds
[DE88-007901] N88-27065
CALIFORNIA UNIV., SAN DIEGO, LA JOLLA.
Preparation of high-T(sub)c Y1Ba2Cu3O(sub 7-Delta) superconducting thin films by MBE (Molecular-Beam-Epitaxy) techniques
[DE88-009999] N88-27082
CALSPAN FIELD SERVICES, INC., ARNOLD AFS, TENN.
The effects of RCS jet firing on the isolated Orbiter and mated coast phases of the glide return to launch site maneuver at Mach number 6 (IA302B)
[NASA-CR-180223] N88-26403
CAMBRIDGE UNIV. (ENGLAND).
Transport in GaAs heterojunction ring structures N88-27011
CARNEGIE INSTITUTION OF WASHINGTON, D. C.
Experimental study of planetary gases with applications to planetary interior models
[NASA-CR-183098] N88-27137
CARNEGIE-MELLON UNIV., PITTSBURGH, PA.
The role of working memory in language comprehension
[AD-A192721] N88-26805
A matroid algorithm and its application to the efficient solution of two optimization problems on graphs, revision
[AD-A192709] N88-26838
Optical data processing
[AD-A193024] N88-26841
CASE WESTERN RESERVE UNIV., CLEVELAND, OHIO.
In situ spectroscopic studies of transition metal macrocycles as catalysts for the electrochemical reduction of oxygen
[PB88-203195] N88-26416
Industrial processes influenced by gravity
[NASA-CR-182140] N88-26497
CENTER FOR MATHEMATICS AND COMPUTER SCIENCE, AMSTERDAM (NETHERLANDS).
Simple multireader registers using time-stamp schemes
[CWI-CS-R8758] N88-26819
Fixpoint representations of characteristic sets of linear-time temporal formulas
[CWI-CS-R8754] N88-26849
Contractions in comparing concurrency semantics
[CWI-CS-R8755] N88-26850
Interaction management in CAD systems with a history mechanism
[CWI-CS-R8756] N88-26851
A network approach to the certainty factor model
[CWI-CS-R8757] N88-26852
A semantic approach to fairness
[CWI-CS-R8759] N88-26853
Minimum disclosure proofs of knowledge
[CWI-PM-R8710] N88-26854
Algebraic and arithmetic geometry in string theory
[CWI-PM-R8708] N88-26904
CENTRAL RESEARCH INST. OF ELECTRIC POWER INDUSTRY, TOKYO (JAPAN).
Development of external cooling cryo-resistive cable systems. Part 2: Insulation characteristics on 66 kV rated cryo-resistive testing cable
[DE88-770191] N88-26571
Loss evaluation of self-commutated power conditioner for battery energy storage system
[DE88-752075] N88-26575
Characteristics of pressure loss during filtration using a porous ceramic filter
[DE88-752547] N88-26604
Development of advanced flow simulation system by water flow model. New method of velocity measurement using cross-correlation
[DE88-753120] N88-26608
Laser diagnostics applied to advanced combustion systems
[DE88-753119] N88-26649
Computational study on thermal efficiency of ceramic gas turbine
[DE88-753114] N88-26667
Study on the heat resisting and cooling property of the ceramics-metal hybrid stator vanes
[DE88-753117] N88-26668
Survey on utility technology of a tidal and ocean current energy
[DE88-770148] N88-26722
Thermodynamic analysis of chemical heat storage system for heat pump
[DE88-753121] N88-26728
Development of an atmospheric diffusion evaluation method incorporating topographical effects. Part 1: Literature review of atmospheric diffusion models incorporating terrain effects
[DE88-753104] N88-26742
Wind tunnel study of atmospheric diffusion in unstable stratified boundary layer. Part 2: Characteristic scale and diffusion
[DE88-753109] N88-26749
Remote sensing of temperature profiles. Performance test of PASS
[DE88-753108] N88-26768
CENTRE D'ETUDES ET DE RECHERCHES, TOULOUSE (FRANCE).
Polymerization of epoxy matrix composites using pulsed microwaves
[CERT-3/1324-MO] N88-26487
Multivariable identification of a flexible transport aircraft N88-26525
Compressible boundary layers
[CERT-OA-13/5005-AYD] N88-26623
CENTRE D'ETUDES ET DE RECHERCHES DE MEDECINE AEROSPATIALE, PARIS (FRANCE).
Preliminary study within a project for the development of intelligent assistance to piloting: Formal description of combat pilot expertise and implementation of an interactive system to represent operations
[CERMA-87-31] N88-26806
CENTRE NATIONAL DE LA RECHERCHE SCIENTIFIQUE, GRENOBLE (FRANCE).
Pressure-dependent measurement on n+GaAs (Si, Sn): The effect of deep donor (DX) states on the electrical properties and presistent photoconductivity effects N88-27020

CENTRE NATIONAL DE LA RECHERCHE SCIENTIFIQUE, MARSEILLES (FRANCE).
Stress analysis using infrared thermography
[ETN-88-92169] N88-26705
CENTRE NATIONAL DE LA RECHERCHE SCIENTIFIQUE, MONTPELLIER (FRANCE).
Manufacturing of a ceramic-ceramic composite matrix using the sol-gel procedure
[ETN-88-92157] N88-26414
CHIBA UNIV. (JAPAN).
Relaxation scheme for compressible flows
N88-26323
CINCINNATI UNIV., OHIO.
A constitutive model with damage for high-temperature superalloys N88-26434
CITY COLL. OF THE CITY UNIV. OF NEW YORK.
Direct measurement of ultrafast electron-hole plasma expansion at high density at an asymmetric GaAs quantum well N88-27044
CLEMSON UNIV., S.C.
Thermoplastic coating of carbon fibers
[NASA-CR-183067] N88-26407
Mobile robot survival
[DE88-009108] N88-26665
A radar study of the interaction between lightning and precipitation
[DE88-009120] N88-26770
Recoil saturation of the self-energy in atomic systems
[DE88-010450] N88-26930
CLEVELAND STATE UNIV., OHIO.
Design of a controller to reduce residual vibration in the positioning control of flexible robotic manipulators
N88-26658
COLOGNE UNIV. (WEST GERMANY).
Diffusion of slight solar induced disturbances in the middle atmosphere
[MITT-53] N88-26758
Dynamic interaction of convective cumulus with large-scale environment
[MITT-55] N88-26773
Westward moving atmospheric wave disturbances over the African tropics: Dynamic and energetic aspects
[MITT-57] N88-26774
Ground level hydroxyl (OH) concentration measurements by long path differential optical laser absorption
[ETN-88-92124] N88-26952
COLORADO SCHOOL OF MINES, GOLDEN.
Fundamental optical studies of competitive adsorption and thin film phenomena
[DE88-008780] N88-27068
COLORADO UNIV., BOULDER.
Solution of the Orr-Sommerfeld equation for the Blausius boundary-layer documentation of program ORRBL and a test case
[NASA-CR-4169] N88-26858
Neoclassical diffusion due to trapping/detrapping orbits in stellarators
[DE88-008566] N88-26968
COMMISSION OF THE EUROPEAN COMMUNITIES (LUXEMBOURG).
Guide to the control of high temperature corrosion and protection of gas turbine materials
[PB88-107412] N88-26370
The 1985 Meteorological Yearbook of Ispra (27th)
[PB88-125729] N88-26777
CONSIGLIO NAZIONALE DELLE RICERCHE, ROME (ITALY).
Phonons in semiconductor superlattices N88-27035
CONTINUOUS ELECTRON BEAM ACCELERATOR FACILITY, NEWPORT NEW, VA.
Superconducting rf and beam-cavity interactions
[DE88-008598] N88-26936
Progress in diagnostic techniques for SC (superconducting) cavities
[DE88-008600] N88-27077
CORNELL UNIV., ITHACA, N.Y.
Surface phases and their influence on metal-oxide interfaces
[DE88-007938] N88-26420
Grain boundary structure in Ni3Al
[DE88-009164] N88-26444
Asymptotically efficient adaptive allocation schemes for controlled Markov chains: Finite parameter space
[AD-A192228] N88-26893
CORNING GLASS WORKS, N.Y.
Semiconductor microcrystallites in porous glass and their applications in optics N88-27005
CREW SYSTEMS CONSULTANTS, YELLOW SPRINGS, OHIO.
Improvement of head-up display standards. Volume 1: Head-up display design guide, appendix
[AD-A192973] N88-26809

D

DAIMLER-BENZ A.G., STUTTGART (WEST GERMANY).
Identification methods for transport dynamical investigations N88-26531
DAR-ES-SALAAM UNIV. (TANZANIA).
Interactive computer programme for the analysis of a two-way Wilkinson divider/combiner
[PB88-105424] N88-26831
DARTMOUTH COLL., HANOVER, N.H.
The structure and properties of grain boundaries in B2 ordered alloys
[DE88-009890] N88-26447
DEPARTMENT OF ENERGY, OAK RIDGE, TENN.
Acid Precipitation: A current awareness bulletin
[DE88-007987] N88-26738
DEPARTMENT OF ENERGY, WASHINGTON, D. C.
Wind Energy Technology: Generating power from the wind, a current awareness bulletin
[DE88-008292] N88-26729
Fuel cell systems program plan: Fiscal year 1988
[DE88-011080] N88-26731
DEUTSCHE AIRBUS G.M.B.H., MUNICH (WEST GERMANY).
Airbus 1987: Success in Europe
[ETN-88-92099] N88-26364
DEUTSCHE FORSCHUNGS- UND VERSUCHSANSTALT FUER LUFT- UND RAUMFAHRT, BRUNSWICK (WEST GERMANY).
System identification in vehicle dynamics
[DFVLR-MITT-87-22] N88-26518
Flight vehicle system identification: Status and prospects N88-26520
A two-point aerodynamic model for identification N88-26526
The identification of the direct lift control flap system of the research aircraft ATTAS N88-26527
Parametric estimation of aerodynamic nonlinearities in rolling moment due to sideslip using maximum likelihood method N88-26528
Flight test preparation and measuring data validation for parameter identification N88-26529
Utilization of identification methods in the time and frequency domain for the determination of the XV-15 (tilt-rotor) dynamics for lateral motion in hover flight N88-26532
Application of complementary parameter identification techniques to flight test data of a transport aircraft N88-26533
DEUTSCHE FORSCHUNGS- UND VERSUCHSANSTALT FUER LUFT- UND RAUMFAHRT, OBERPFAFFENHOFEN (WEST GERMANY).
Simulation models for the dynamics of tracked vehicle systems: State-of-the-art and open problems N88-26522
DREXEL UNIV., PHILADELPHIA, PA.
Computation equipment for damage simulation in laminated composites
[AD-A193013] N88-26412
DU PONT DE NEMOURS (E. I.) AND CO., AIKEN, S.C.
Mobile robot survival
[DE88-009108] N88-26665
DUKE UNIV., DURHAM, N. C.
Aircraft interior noise reduction by alternate resonance tuning
[NASA-CR-182540] N88-26909

E

EAGLE ENGINEERING, INC., WEBSTER, TEX.
Lunar base launch and landing facility conceptual design, 2nd edition
[NASA-CR-172049] N88-27135
ECOLE NATIONALE SUPERIEURE DE MECANIQUE ET D'AEROTECHNIQUE, POITIERS (FRANCE).
Study of the local behavior of a flame
[ETN-88-92300] N88-26433
ECOLE NATIONALE SUPERIEURE DES TELECOMMUNICATIONS, PARIS (FRANCE).
Colored stochastic Petri nets. Application to real time distributed systems
[ENST-87E017] N88-26843
ECOLE NORMALE SUPERIEURE, PARIS (FRANCE).
Energy levels and magneto-electric effects in some quasi uni-dimensional semiconductor heterostructures N88-27009
EDGERTON, GERMESHAUSEN AND GRIER, INC., ALBUQUERQUE, N. MEX.
Plasma armature formation in high-pressure, high-velocity hydrogen
[DE88-008347] N88-26967
EDGERTON, GERMESHAUSEN AND GRIER, INC., IDAHO FALLS, IDAHO.
Magnetic heat pump design
[DE88-007730] N88-26605
Physical-chemical reactions at welding arc/molten pool interfaces
[DE88-007717] N88-26662
Developing diagnostic methods for plasma-particle interaction
[TI88-007726] N88-26973
Mutually exclusive alternatives by clustering
[DE88-007707] N88-27115
EDGERTON, GERMESHAUSEN AND GRIER, INC., LOS ALAMOS, N. MEX.
An overview of the development of a linear broadband analog fiber-optic link
[DE88-008668] N88-26945
EDGERTON, GERMESHAUSEN AND GRIER, INC., SALEM, MASS.
Tactical Rubidium Frequency Standard (TRFS), volume 1
[AD-A192981] N88-26640
EG AND G ENERGY MEASUREMENTS, INC., LOS ALAMOS, N. MEX.
Time-resolved doubly bent crystal X-ray spectrometer
[DE88-007899] N88-26637
EIDGENOESSISCHE TECHNISCHE HOCHSCHULE, ZURICH (SWITZERLAND).
Growth of high quality CoSi2/Si superstructures on Si(111) N88-27034
Superconductivity of heavy-electron uranium compounds
[DE88-007901] N88-27065
ELECTROTECHNICAL LAB., IBARAKI (JAPAN).
Lattice strain in heteroepitaxial films N88-27032
Structural studies of (Ga,In)(As,P) alloys and (InAs) sub m (GaAs) sub n strained-layer superlattices by fluorescence-detected EXAFS N88-27051
ELECTROTECHNICAL LAB., SAKURA (JAPAN).
Preparation technology for thin film solid electrolyte fuel cells
[PB88-131925] N88-26735
ELECTROTEK CONCEPTS, INC., KNOXVILLE, TENN.
Analysis of the electrical characteristics of a Westinghouse variable speed generating system for wind turbine applications
[DE88-001139] N88-26721
ERLANGEN-NUREMBERG UNIV. (WEST GERMANY).
Digital image processing from speckle interferograms by correlation methods: Application in atmospheric optics, astronomy, and biology
[ETN-88-92125] N88-26953
EUROCONTROL EXPERIMENTAL CENTRE, BRETIGNY (FRANCE).
Statistical properties of real time events in an ATC (Air Traffic Control) system
[PB88-118781] N88-26353
EXXON RESEARCH AND ENGINEERING CO., ANNANDALE, N.J.
Aperiodic superlattices: Structured randomness N88-27055

F

FERMI NATIONAL ACCELERATOR LAB., BATAVIA, ILL.
Rf cavity primer for cyclic proton accelerators
[DE88-010655] N88-26938
FINNISH METEOROLOGICAL INST., HELSINKI.
On the global radiation incident variously orientated surfaces on the South Coast of Finland
[FMI-5] N88-26746
FLORIDA INTERNATIONAL UNIV., MIAMI.
Conditions for finite convergence of algorithms for nonlinear programs and variational inequalities
[AD-A192355] N88-26834
FLORIDA UNIV., GAINESVILLE.
The determination of the topological structure of skin friction lines on a rectangular wing-body combination
[NASA-CR-4168] N88-26343
Synthesis of model polymers and related structures in support of vinyl monomer grafting studies
[DE88-010245] N88-26476
FLUOROCHEM, INC., AZUSA, CALIF.
Research in energetic compounds
[AD-A192953] N88-26494
FRANKLIN INST., NEWARK, DEL.
Time-dependent mass loss from hot stars with and without radiative driving
[DE88-008899] N88-27128
FRAUNHOFER INST. FUER WERKSTOFFMECHANIK, FREIBURG (WEST GERMANY).
Irreversible deformations during fracture in polymers
[W-7/86] N88-26485

FUJI HEAVY INDUSTRIES LTD., UTSUNOMIYA (JAPAN).
Navier-Stokes analysis of transonic transport aircraft empennage N88-26297
FUJITSU LTD., ATSUGI (JAPAN).
Excellent negative differential resistance of InGaAs/InAlAs resonant tunneling barrier structures and applications to a new functional device, RHET N88-27048
FUJITSU LTD., KAWASAKI (JAPAN).
Cellular array processor CAP and its application to computer graphics N88-26327
FUJITSU LTD., TOKYO (JAPAN).
On the stationary solutions of three-dimensional Euler equations by the TVD difference schemes N88-26320

G

GAS RESEARCH INST., CHICAGO, ILL.
Photosynthetic water splitting
[DE88-007809] N88-26791
GENERAL ATOMIC CO., SAN DIEGO, CALIF.
Poloidal field measurements using laser enhanced attenuation of an energetic lithium beam
[DE88-006360] N88-26963
Fusion programs in applied plasma physics and development and technology at GA Technologies, Inc.
[DE88-006406] N88-26964
Overview of the TITAN-2 reversed-field pinch aqueous fusion power core design
[DE88-006170] N88-26966
Multipoint Thomson scattering diagnostic for DIII-D
[DE88-006737] N88-26969
Toroidal and poloidal soft X-ray imaging system on the D3-D tokamak
[DE88-010585] N88-26986
Vertical viewing ECE diagnostic for the D3-D tokamak
[DE88-010586] N88-26987
GENERAL ELECTRIC CO., LARGO, FLA.
A bibliography and author index for electrical discharges in vacuum (1897-1986)
[DE88-008744] N88-26579
GEORGE WASHINGTON UNIV., WASHINGTON, D.C.
Stiffness degradation of composite laminates N88-26405
Multi-target tracking algorithms for cluttered environments N88-26543
GEORGIA INST. OF TECH., ATLANTA.
Wall interference assessment/correction of data from tests of a CAST 10-2/DOA 2 airfoil in the Langley 0.3-m transonic cryogenic tunnel N88-26331
Heterogeneous diffusion flame stabilization
[AD-A193014] N88-26429
Conditions for finite convergence of algorithms for nonlinear programs and variational inequalities
[AD-A192355] N88-26834
Sound propagation over uneven ground and irregular topography
[NASA-CR-182956] N88-26911
GEORGIA TECH RESEARCH INST., ATLANTA.
Integrated optoelectronic circuits utilizing InGaAsP grown by molecular beam epitaxy (erbium doping of MBE GaAs)
[AD-A192269] N88-26584
GLOBAL PATTERNS ASSOCIATES, LENOIR CITY, TENN.
Interpreting forest biome productivity and cover utilizing nested scales of image resolution and biogeographical analysis
[NASA-CR-183036] N88-26711
GRONINGEN RIJKSUNIVERSITEIT (NETHERLANDS).
L(sub infinity symbol)-approximations of complex functions and robust controllers for large flexible space structures
[PB88-186226] N88-26390
GULF WEATHER CORP., BAY SAINT LOUIS, MISS.
Satellite remote sensing of the wet bulb globe temperature heat stress index, phase 2
[AD-A192798] N88-26717
GUNMA UNIV., MAEBASHI (JAPAN).
Absorption characteristics of Si3N4 ablation layer plasma N88-26504

H

HAMBURG UNIV. (WEST GERMANY).
Spectroscopy of one-dimensional subbands on InSb N88-27007
Extended and local plasmons in a lateral superlattice N88-27041
HAMPTON INST., VA.
Effects of cosmic rays on single event upsets
[NASA-CR-183053] N88-26569
HARRIS CORP., MELBOURNE, FLA.
Finite-dimensional approximation for optimal fixed-order compensation of distributed parameter systems
[NASA-CR-181674] N88-26873
HARVARD-SMITHSONIAN CENTER FOR ASTROPHYSICS, CAMBRIDGE, MASS.
Time-dependent mass loss from hot stars with and without radiative driving
[DE88-006899] N88-27128
HAWAII UNIV., HONOLULU.
Space infrared telescope facility project
[NASA-CR-183058] N88-27121
HELSINKI UNIV. (FINLAND).
Evaluation of engineering leak before break assessment methods by piping tests
[PB88-126982] N88-26538
HELSINKI UNIV. OF TECHNOLOGY, ESPOO (FINLAND).
Plastic deformation and roughness of free metal surfaces
[PB88-196621] N88-26439
Application of Moment Iteration Method (MIM) to electromagnetic field computation
[PB88-194139] N88-26546
Variational analysis of dielectrically loaded multidepth corrugated waveguides
[PB88-193602] N88-26573
Auditory evoked magnetic fields in man
[PB88-193446] N88-26796
HIROSHIMA UNIV. (JAPAN).
Ultrafast optical nonlinearity in quantum well structures with electric field N88-27003
HOUSTON UNIV., TEX.
Fine-scale traverses in cumulate rocks, Stillwater Complex: A lunar analogue study
[NASA-CR-183066] N88-26747
HUGHES AIRCRAFT CO., LONG BEACH, CALIF.
Visible tunable source
[DE88-006442] N88-26944
HUGHES RESEARCH LABS., MALIBU, CALIF.
MBE growth of HgTe/CdTe superlattices on Si(100) substrates N88-27033

I

IBARAKI UNIV., HITACHI (JAPAN).
An experimental investigation of transient characteristics in a gravity-assisted heat pipe N88-26506
IBM WATSON RESEARCH CENTER, YORKTOWN HEIGHTS, N.Y.
Electronic structure of quantum-well states revealed under high pressures N88-27038
Hot electrons in silicon dioxide: Ballistic to steady-state transport N88-27042
ILLINOIS INST. OF TECH., CHICAGO.
Theoretical studies in elementary particle physics
[DE88-006929] N88-26926
ILLINOIS NATURAL HISTORY SURVEY, CHAMPAIGN.
Interpreting forest biome productivity and cover utilizing nested scales of image resolution and biogeographical analysis
[NASA-CR-183036] N88-26711
ILLINOIS UNIV., CHAMPAIGN.
Third International Conference on Superlattices, Microstructures and Microdevices
[AD-A191416] N88-26995
ILLINOIS UNIV., CHICAGO.
Application of magnification xeroradiography to advanced ceramics
[DE88-009965] N88-26473
Spatial dynamics of deformable multibody systems with variable kinematic structure N88-26687
Type 3 - type 1 transition and strain effect in Hg(1-x)Cd(x)Te-CdTe and Hg(1-x)Zn(x)Te-CdTe superlattices N88-27052
The superconducting transition in oxygen deficient YBa2Cu3O(sub 7-Delta)
[DE88-009957] N88-27079
ILLINOIS UNIV., URBANA.
Microwave amplifiers
[AD-A192974] N88-26585
Interpreting forest biome productivity and cover utilizing nested scales of image resolution and biogeographical analysis
[NASA-CR-183036] N88-26711
Correctness criteria for process migration
[NASA-CR-182939] N88-26823
A practical shifted Adams algorithm
[DE88-008573] N88-26830
Monte Carlo simulations of femtosecond relaxation of photoexcited electrons in AlGaAs/GaAs quantum wells N88-27036
ILLINOIS UNIV., URBANA-CHAMPAIGN.
Definition of an auxiliary processor dedicated to real-time operating system kernels
[NASA-CR-183070] N88-26860
The theory of electron-polar phonon scattering rates in semiconductor micro-structures N88-27043
Recent applications of Monte Carlo methods for semiconductor microdevice simulation N88-27046
Characterization of structural and magnetic order of Er/Y superlattices N88-27056
INSTITUT DE MECANIQUE DES FLUIDES DE MARSEILLE (FRANCE).
Study of flow tracer behavior models and experimental validation with multiple exposure holographic velocimetry
[IMFL-87/30] N88-26822
INSTITUT FRANCO-ALLEMAND DE RECHERCHES, ST. LOUIS (FRANCE).
Influence of rear body geometry on the velocity characteristics of the near wake
[ISL-R-113/87] N88-26339
Treatment of the separated flow around profiles (nonviscous, incompressible, two dimensional flow) by the singularities method
[ISL-R-106/87] N88-26633
INSTITUT NATIONAL DES SCIENCES APPLIQUEES, TOULOUSE (FRANCE).
Pressure-dependent measurement on n+ GaAs (Si, Sn): The effect of deep donor (DX) states on the electrical properties and presistent photoconductivity effects N88-27020
INSTITUT NATIONAL POLYTECHNIQUE, GRENOBLE (FRANCE).
Fatigue of lithium-aluminum alloys: An example of localization of the plastic deformation
[ETN-88-92309] N88-26456
Study and implementation of ultrahigh frequency coupling devices using the fin line technology
[ETN-88-92307] N88-26588
Study of a water-steam two phase flow in a T-branch
[ETN-88-92306] N88-26624
Simulation of the neutronic characteristics of large fast neutron reactors
[ETN-88-92305] N88-26940
INSTITUTE FOR WATER RESOURCES, FORT BELVOIR, VA.
Managing microcomputer applications: A primer and guide to good practice
[AD-A192992] N88-26817
INSTITUTO DE PESQUISAS ESPACIAIS, SAO JOSE DOS CAMPOS (BRAZIL).
Analysis of networks with parameters S: Generalization of junction matrix
[INPE-4535-PRE/1282] N88-26570
The knowledge based automatic extraction of the machinable surfaces for automatic CAD-CAM system
[INPE-4542-PRE/1288] N88-26824
INTERNATIONAL CENTRE FOR THEORETICAL PHYSICS, TRIESTE (ITALY).
Finite element approximation to a model problem of transonic flow
[DE88-701835] N88-26333
Precipitation study by electrical resistivity measurement in Ni-Al alloys
[DE88-701877] N88-26440
Abnormal diffusion of vacancies in metals
[DE88-701880] N88-26441
Nonlinear equation of state effects and the momentum-dilution trade-off in a turbulent buoyant jet
[DE88-701839] N88-26610
Magnetohydrodynamic squeeze film
[DE88-701876] N88-26669
Image force expression for the dislocation near a crack
[DE88-701894] N88-26692
Our climate in danger
[DE88-701824] N88-26743
Propagation of inernio-acoustic gravity waves in a rotating and radiating opaque atmosphere
[DE88-701866] N88-26750
Present status of artificial rain making
[DE88-701823] N88-26769
Accurate solution of parabolic equations by expansion in ultraspherical polynomials
[DE88-701829] N88-26880
Nontrivial critical points for asymptotically quadratic function
[DE88-101851] N88-26881
Canonical construction of differential operators intertwining representations of real semisimple Lie groups
[DE88-701852] N88-26882
Theory of pseudo-differential operators over C*-algebras
[DE88-701880] N88-26883
On the self-focusing of electric helicons
[DE88-701870] N88-26905
Inelastic two composite particle systems scattering at high energy
[DE88-701841] N88-26928

On the self-trapping of an electromagnetic wave in magnetized plasma
[DE88-701872] N88-26974
Factors which affect operation of a plasma focus in various gases
[DE88-701882] N88-26975
Modulational instability of electric helicons in a magnetized collisional plasma
[DE88-701885] N88-26976
Thermal inhibition by megagauss field due to variation of electron temperature in laser plasma
[DE88-701887] N88-26977
Kinetic modulational instability of electron cyclotron waves in plasmas
[DE88-701893] N88-26978
Megagauss field variation along axis of wire target in laser produced plasma
[DE88-701895] N88-26979
Lattice theory of fracture of solids with layered structure
[DE88-701867] N88-27073
Phenomenological approach to high T/sub c/ oxide superconductors
[DE88-701868] N88-27074
On the possibility of the soliton description of acoustic emission during plastic deformation of crystals
[DE88-701878] N88-27075
Derivation of space groups in mm2, 222 and mmm crystal classes
[DE88-701881] N88-27076
On linear relationship between shock velocity and particle velocity
[DE88-701827] N88-27099
Theory of relativity and super-light-speeds-I: Kinematical part
[DE88-701832] N88-27100
Finitely many delta-interactions with supports on concentric spheres
[DE88-701834] N88-27101
Combining relativity and quantum mechanics: Schroedinger's interpretation of psi
[DE88-701899] N88-27102
Cosmic wavefunction with induced gravity
[DE88-701873] N88-27129

INTERNATIONAL FUEL CELLS CORP., SOUTH WINDSOR, CONN.
Phosphoric acid electric utility fuel cell technology development
[DE88-010187] N88-26582

INTERSONICS, INC., NORTHBROOK, ILL.
Program for the feasibility of developing a high pressure acoustic levitator
[NASA-CR-182154] N88-26498

IOWA STATE UNIV. OF SCIENCE AND TECHNOLOGY, AMES.
Wavenumber spectra from THIR 6.7 micron water vapor data N88-26756

IOWA UNIV., IOWA CITY.
Ultraviolet geometric albedo of Uranus
[NASA-CR-183099] N88-27136

ISHIKAWAJIMA-HARIMA HEAVY INDUSTRIES CO. LTD., TOKYO (JAPAN).
Application of computational fluid dynamics to design of compressor cascade N88-26315

IWAKI MEISEI UNIV. (JAPAN).
Numerical simulation of ignition of hydrogen jet in hot air N88-26307

J

JAPAN ATOMIC ENERGY RESEARCH INST., TOKYO.
The hole of a blanket tritium system on the fusion fuel cycle
[DE88-010007] N88-26983

JAYCOR, VIENNA, VA.
Narrative domain implementation
[AD-A192265] N88-26868

JET PROPULSION LAB., CALIFORNIA INST. OF TECH., PASADENA.
Antimisting kerosene: Low temperature degradation and blending
[NASA-CR-182725] N88-26495
Analytical determination of critical crack size in solar cells
[NASA-CR-183128] N88-26736
Diagnosing faults in autonomous robot plan execution
[NASA-CR-182480] N88-26859

JOINT INST. FOR NUCLEAR RESEARCH, DUBNA (USSR).
Automated system for mathematical processing of the data from a hybrid spectrometer
[DE87-702995] N88-26820
To the twinning plane superconductivity theory
[DE88-702195] N88-27058

JOINT PUBLICATIONS RESEARCH SERVICE, ARLINGTON, VA.
JPRS report: Science and technology. USSR: Life sciences
[JPRS-ULS-88-009] N88-26785
Effect of weightlessness on brain development (results of flight of pregnant rats on Kosmos-1514 biosatellite and study of subsequent development of their progeny on earth N88-26786
Significance of sensory signal phase mismatch in mechanisms of motion sickness development N88-26787
Biorhythms of binocular vision N88-26788
Method for observing changes in functional state of human operator N88-26789
Respiration and oxygen tension in the blood of animals exposed to high pressures N88-26790

K

KANSAS UNIV., LAWRENCE.
Research in theoretical particle physics
[DE88-008230] N88-26927

KANSAS UNIV. CENTER FOR RESEARCH, INC., LAWRENCE.
Sources of scattering in vegetarian and other surfaces and objects
[NASA-CR-182975] N88-26710

KARLSRUHE UNIV. (WEST GERMANY).
Dynamical stress concentration problems, from every side, bordered and perforated plates
[ETN-88-92128] N88-26703

KATHOLIEKE UNIVERSITEIT, NIJMEGEN (NETHERLANDS).
Direct manipulation and the design of user interfaces
[PB88-126354] N88-26810

KATHOLIEKE UNIVERSITEIT TE LEUVEN (BELGIUM).
Aharonov-Bohm effects in disordered metals N88-27008

KAWASAKI HEAVY INDUSTRIES LTD., KAGAMIHARA (JAPAN).
The role of computational fluid dynamics in aeronautical engineering (5): Improvements and applications of implicit TVD finite volume code N88-26313
On the accuracy of upwind biased finite volume method N88-26316

KEIO UNIV., TOKYO (JAPAN).
The modified-fluid-in-cell method to which adaptive mesh and multigrid were applied N88-26324

KENT UNIV., CANTERBURY (ENGLAND).
Towards knowledge bases-semantics, rules and object-oriented programming
[PB88-108154] N88-27110

KIEL UNIV. (WEST GERMANY).
Hiding in stream semantics of uniform concurrency
[PB88-121579] N88-27114

KRAUSS-MAFFEI A.G., MUNICH (WEST GERMANY).
Identification of lateral operation dynamics of rail vehicles using roll test stand tests N88-26534

KTECH CORP., ALBUQUERQUE, N. MEX.
Plasma armature formation in high-pressure, high-velocity hydrogen
[DE88-008347] N88-26967

KYOTO UNIV. (JAPAN).
Numerical simulations of astrophysical jets N88-26295
Numerical solutions of the Euler equations for the flow field around counter-rotating propellers N88-26298
Numerical simulation of supersonic free-jets N88-26299

L

LAWRENCE LIVERMORE NATIONAL LAB., CALIF.
A simulation of post boost vehicle deployment of multiple reentry vehicles
[DE88-009537] N88-26391
Laser fluorescence spectroscopy of zinc neutrals originating from laser-irradiated and ion-bombarded zinc sulfide and zinc surfaces
[DE88-008037] N88-26418
The preparation of mechanically alloyed powders for TEM (Transmission Electron Microscopy) examination
[DE88-008043] N88-26460
Rocket-propellant burn tests of silicide-coated niobium and tantalum
[DE88-010729] N88-26496
Proceedings of the Array Signal Processing Symposium: Treaty Verification Program
[DE88-008346] N88-26548
A maximum entropy solution for the underdetermined electromagnetic field within a volume
[DE88-007020] N88-26550
MAXWELL3: A 3D finite element electromagnetic modeling code
[DE88-010602] N88-26551
Degradation of beam brightness by field emission from a cathode shroud
[DE88-008345] N88-26576
A model for insulated wires in the method of moments code NEC (Numerical Electromagnetics Code)
[DE88-008920] N88-26577
Crystallization of aluminum hydroxide in the aluminum-air battery: Literature review, crystallizer design and results of integrated system tests
[DE88-010510] N88-26594
The propagation of irradiance moments of an aberrated, apodized FEL beam
[DE88-008972] N88-26648
High spatial frequency thermal blooming instability: A linear stability analysis
[DE88-010711] N88-26655
Optical coatings for high average power XeF lasers
[DE88-011356] N88-26656
Model for pulse amplification by a gaseous laser amplifier
[DE88-011729] N88-26657
Ductile-brittle transition of cutting behavior in diamond turning of single crystal Si
[DE88-008890] N88-26664
Computer controlled data acquisition system for the NASA 1986 Rocket Triggered Lightning Program
[DE88-008335] N88-26766
An interagency working group on lightning threat warning
[DE88-009828] N88-26767
Wind flow study: July 1987 and November-December 1987
[DE88-008969] N88-26776
Computer science research, 1987: Computation Directorate
[DE88-008637] N88-26812
SEGMERGE: A scanline visible surface algorithm with adaptive span selection and inexpensive antialiasing
[DE88-009186] N88-26826
Efficient bit-level, word-level and block-level systolic arrays for matrix-matrix multiplication
[DE88-011331] N88-26856
Procedure for converting a Wilson-Fowler spline to a cubic B-spline with double knots
[DE88-008971] N88-26878
Shock wave compression and metallization of simple molecules
[DE88-008031] N88-26925
Optical characterization of silica aerogel
[DE88-008916] N88-26946
Fabrication technology
[DE88-010598] N88-26955
Plasma armature formation in high-pressure, high-velocity hydrogen
[DE88-008347] N88-26967
TIBER (Tokamak Ignition/Burn Experimental Reactor) 2 as a precursor to an international thermonuclear experimental reactor
[DE88-008906] N88-26970
The effect of ICRF on the Alcator C Scrape-Off Layer plasma
[DE88-009821] N88-26972
MTX (Microwave Tokamak Experiment) plasma diagnostic system
[DE88-011326] N88-26993
Bremsstrahlung from high Z impurities in hot plasmas
[DE88-011755] N88-26994
Nonlinear materials for frequency conversion
[DE88-008343] N88-27067
On the chemistry of superconductivity
[DE88-010714] N88-27096
Non-equilibrium phases and phase diagrams
[DE88-008896] N88-27098
An integrated, multi-vendor distributed data acquisition system
[DE88-008900] N88-27113
Probing the possibility of a (12)C/(13)C abundance gradient from observations of interstellar CH+
[DE88-008908] N88-27125
Time-dependent mass loss from hot stars with and without radiative driving
[DE88-008899] N88-27128

LEIDEN UNIV. (NETHERLANDS).
The polarization of radio galaxies: Its structure at low frequencies
[B8681611] N88-27123
The velocity field of the outer galaxy
[B8681472] N88-27132

LEOBEN UNIV. OF MINING AND METALLURGY (AUSTRIA).
Control of carrier lifetime in PbTe nipi superlattices by external photoinjection N88-27006

LIFE SYSTEMS, INC., CLEVELAND, OHIO.
Advanced life support control/monitor instrumentation concepts for flight application
[NASA-CR-177378] N88-26807
LITTON SYSTEMS, INC., VAN NUYS, CALIF.
Optical correlation using the magneto-optic device
[AD-A192342] N88-26950
LOCKHEED AERONAUTICAL SYSTEMS CO., MARIETTA, GA.
Propfan test assessment testbed aircraft stability and control/performance 1/9-scale wind tunnel tests
[NASA-CR-182121] N88-26360
LOS ALAMOS NATIONAL LAB., N. MEX.
A basis of settlement: Economic foundations of permanent pioneer communities
[DE88-010907] N88-26382
Reaming experiments for the lethality test system
[DE88-007902] N88-26383
Why plasma armature railguns don't work (and what can be done about it)
[DE88-007900] N88-26384
Heat pump augmented radiators for spacecraft thermal management
[DE88-007890] N88-26392
Ultraviolet imaging of hydrogen flames
[DE88-009152] N88-26422
Glass forming ranges of amorphous alloys
[DE88-007897] N88-26438
A numerical study of Rayleigh-Taylor instability in aluminum and steel plates
[DE88-010475] N88-26449
Numerical modeling of the effect of particle size of explosives on shock initiation properties
[DE88-010479] N88-26491
Freely expanding detonation products: Scaling of rate processes
[DE88-007827] N88-26606
Time-resolved doubly bent crystal X-ray spectrometer
[DE88-007899] N88-26637
Laser desorption/ablation studies by resonance ionization mass spectrometry
[DE88-009124] N88-26650
Tracking a monochromatic light source
[DE88-011260] N88-26653
Finite element welding computations using general purpose nonlinear analysis codes
[DE88-005398] N88-26659
Methods and techniques of NDA (nondestructive assay)
[DE88-009145] N88-26682
Microstructural effects in static and dynamic numerical experiments
[DE88-004289] N88-26690
Prospects for hot dry rock in the future
[DE88-010909] N88-26730
A radar study of the interaction between lightning and precipitation
[DE88-009120] N88-26770
The performance of the NEC SX-2 and Cray X-MP supercomputers
[DE88-009177] N88-26813
XDATAP
[DE88-007161] N88-26827
Building an artificial intelligence capability at Los Alamos
[DE88-009155] N88-26866
Eigenmodes of a random walk on a 2-D lattice torus with one trap
[DE88-007830] N88-26874
Monitoring space weaponry: Detection and verification issues
[DE88-006726] N88-26900
SDI: Myth or reality
[DE88-009121] N88-26901
Fluid dynamical model of ultrarelativistic heavy ion collisions
[DE88-007905] N88-26921
The electronic structure of condensed molecular systems
[DE88-007823] N88-26923
Sources of polarized ions and atoms
[DE88-010910] N88-26931
Development of nuclear models for higher energy calculations
[DE88-010919] N88-26932
Milliwatt generator project
[DE88-011261] N88-26939
Use of fiber optic equipment for security
[DE88-007898] N88-26943
Stress-related phenomena in transient radiation-induced absorption in optical fibers
[DE88-010956] N88-26949
The hole of a blanket tritium system on the fusion fuel cycle
[DE88-010007] N88-26983
Piezoelectric effects in strained layer superlattices N88-27002
Preparation of oxide superconductors
[DE88-009136] N88-27063
Superconductivity of heavy-electron uranium compounds
[DE88-007901] N88-27065
Extension of Boltzmann's theory to a liquid
[DE88-009153] N88-27097
LOUISIANA STATE UNIV., BATON ROUGE.
Growth and characterization of thin films of ZnSnP(sub)2
[DE88-001164] N88-27060
LOUVAIN UNIV. (BELGIUM).
Preparation of high-T(sub)c Y1Ba2Cu3O(sub 7-Delta) superconducting thin films by MBE (Molecular-Beam-Epitaxy) techniques
[DE88-009999] N88-27082
LOWELL UNIV., MASS.
High latitude ionospheric radio studies
[AD-A192270] N88-26753
LUND UNIV. (SWEDEN).
Charged pion production and projectile breakup in 85A MeV(sup)12C induced heavy ion reactions
[LUIP-8802] N88-26920
Defects in high-mobility semiconductor systems
[AD-A192298] N88-27090
Context of national information systems in developing countries: India and China in a comparative perspective
[PB88-109954] N88-27111

M

MAINZ UNIV. (WEST GERMANY).
An efficient model for changes of global climate and composition of the atmosphere due to human activities
[ETN-88-92359] N88-26775
MANCHESTER UNIV. (ENGLAND).
Pulsed spray structure and atomisation techniques
[AD-A192280] N88-26614
MARTIN MARIETTA AEROSPACE, DENVER, COLO.
Study of comet nucleus gamma-ray spectrometer penetration system
[NASA-CR-177393] N88-27120
MARTIN MARIETTA ENERGY SYSTEMS, INC., OAK RIDGE, TENN.
Boundary element method for contact heat transfer
[DE88-011013] N88-26613
MASSACHUSETTS GENERAL HOSPITAL, BOSTON.
Determination of binder distributions in green-state ceramics by NMR imaging
[DE88-009990] N88-26474
MASSACHUSETTS INST. OF TECH., CAMBRIDGE.
Modelling of premixed combustion using a thin flame sheet and the effect of the hydrodynamic instability
[DE88-009467] N88-26423
Grain boundaries
[DE88-009889] N88-26446
Tracer water transport and subgrid precipitation variation within atmospheric general circulation models
[NASA-CR-182897] N88-26745
MASSACHUSETTS INST. OF TECH., LEXINGTON.
Electro-optical studies of Al(x)Ga(1-x)As/GaAs coupled quantum wells N88-26999
MATERIALPRUEFUNGSANSTALT, STUTTGART (WEST GERMANY).
Principles of a nondestructive evaluation process for damage location, damage profile, and damage extension in welded joints by radiometric measurements
[MPA-86-02] N88-26683
MATERIALS RESEARCH LABS., MELBOURNE (AUSTRALIA).
Granulation of pyrotechnic tracer composition R284T
[MRL-TN-528] N88-26490
Australian structures response evaluation: Ground shock and air blast measurements for site investigation survey
[MRL-TN-526] N88-26685
Analysis of the perforation of monolithic and simple laminate aluminium targets as a test of analytical deformation models
[MRL-R-1111] N88-26686
MCDONNELL-DOUGLAS CORP., LONG BEACH, CALIF.
Improved potential flow computational methods with Euler corrections for airfoil and wing/body design
[AD-A192303] N88-26334
MICHIGAN STATE UNIV., EAST LANSING.
Relay approach message routing in hypercube multiprocessors
[DE88-009973] N88-26814
MICHIGAN TECHNOLOGICAL UNIV., HOUGHTON.
The effects of gradients on boundary stability
[DE88-009592] N88-26445
MICHIGAN UNIV., ANN ARBOR.
Interferometric recording of holographic optical elements using partially coherent light N88-26636
Asymptotically efficient adaptive allocation schemes for controlled Markov chains: Finite parameter space
[AD-A192228] N88-26893
MIDWEST SYSTEMS RESEARCH, INC., DAYTON, OHIO.
A cockpit natural language study - selected transcripts
[AD-A192972] N88-26808
MINISTRY OF TRANSPORTATION, TOKYO (JAPAN).
Numerical simulation of turbulent flow using the exponential expression of k-epsilon equation N88-26322
MISSION RESEARCH CORP., ALBUQUERQUE, N. MEX.
Computer programs for high-current beam transport in accelerators
[AD-A192356] N88-26835
MACH2: A two-dimensional magnetohydrodynamic simulation code for complex experimental configurations
[AD-A192285] N88-26988
MISSISSIPPI STATE UNIV., MISSISSIPPI STATE.
Improved 3-D turbomachinery CFD algorithm
[NASA-CR-179364] N88-26819
The construction of composite grids for general three-dimensional regions N88-26872
MISSOURI UNIV., COLUMBIA.
Quantum wells and bulk AlGaAs under hydrostatic pressure N88-27000
MISSOURI UNIV., ROLLA.
Defect characterization of the redox behavior and stability of conducting oxides
[DE88-010799] N88-27088
MITSUBISHI ELECTRIC CO., AMAGASAKI (JAPAN).
Nutational stability of a satellite equipped with an active magnetic momentum wheel N88-26513
MITSUBISHI HEAVY-INDUSTRIES LTD., TOKYO (JAPAN).
Extensive verification of blade-to-blade flow code based on Denton scheme N88-26314
MIYAZAKI UNIV. (JAPAN).
Thermostatistical estimations of vapor-state molecules affected by gravity in a heat pipe N88-26505

N

NAGOYA UNIV. (JAPAN).
Numerical calculation of supersonic flow by the PNS equations N88-26296
Symmetrized magnetic field configuration of low aspect ratio helical system
[IPPJ-869] N88-26956
Proceedings of the 2nd US-Japan Workshop on Advanced Plasma Modeling, volume 3
[IPPJ-867] N88-26957
NASA SCIENTIFIC AND TECHNICAL INFORMATION FACILITY, BALTIMORE-WASHINGTON INTERNATIONAL AIRPORT, MD. 21240.
Aerospace medicine and biology: A continuing bibliography with indexes (supplement 313)
[NASA-SP-7011(313)] N88-26800
NATIONAL ACADEMY OF SCIENCES - NATIONAL RESEARCH COUNCIL, WASHINGTON, D. C.
Physical oceanography and tracer chemistry of the southern ocean
[DE88-006852] N88-26779
Issues and recommendations associated with distributed computation and data management systems for the space sciences
[NASA-CR-183026] N88-27108
NATIONAL AERONAUTICS AND SPACE ADMINISTRATION, WASHINGTON, D.C.
Ludwig Prandtl collected treatises on applied mechanics, hydro- and aerodynamics, part 1
[NASA-TT-20316] N88-26337
Ludwig Prandtl collected treatises on applied mechanics, hydro- and aerodynamics, part 2, IV interfaces and resistance
[NASA-TT-20315] N88-26338
Surface temperature thermal fluxmeters for shock tubes
[NASA-TT-20319] N88-26381
Ignition and flame spread of PMMA
[NASA-TT-20290] N88-26431
The T-T-T curve in Cu-Cr alloy
[NASA-TT-20167] N88-26453
The influence of foreign particles on bearing metals
[NASA-TT-20155] N88-26454
Shape memory alloys: New materials for future engineering
[NASA-TT-20193] N88-26455
Production of powdered sodium hydride with large specific surface by the catalyzed reaction of molten sodium with hydrogen-1
[NASA-TT-20185] N88-26462
Refractory Materials of Zirconate. Part 2: Synthesis and some properties of strontium, zirconate, calcium zirconate and barium zirconate
[NASA-TT-20186] N88-26483

Resistance of polyamide-6 against long time effects of various media at various temperatures
[NASA-TT-20297] N88-26484
Experimental investigation of turbulent flow in smooth and longitudinal grooved tubes
[NASA-TM-77480] N88-26615
Wave propagation in locally isotropic turbulent medium with smoothly changing characteristics
[NASA-TT-20312] N88-26617
Directions for programming in FORTRAN 77
[NASA-TT-20317] N88-26842
Reports of planetary geology and geophysics program, 1987
[NASA-TM-4041] N88-27133

NATIONAL AERONAUTICS AND SPACE ADMINISTRATION. AMES RESEARCH CENTER, MOFFETT FIELD, CALIF.
Numerical simulations of aerodynamic contribution of flows about a space-plane-type configuration N88-26292
Numerical simulation of viscous flows over transonic aircraft configurations N88-26302
Vortex methods for separated flows
[NASA-TM-100068] N88-26342
A high fidelity real-time simulation of a small turboshaft engine
[NASA-TM-100991] N88-26378
A microcomputer based frequency-domain processor for laser Doppler anemometry
[NASA-TM-100998] N88-26634
A general-purpose approach to computer-aided dynamic analysis of a flexible helicopter
[NASA-TM-101002] N88-26709

NATIONAL AERONAUTICS AND SPACE ADMINISTRATION. GODDARD SPACE FLIGHT CENTER, GREENBELT, MD.
Design and testing of a high power spacecraft thermal management system
[NASA-TM-4051] N88-26389
The role of space borne imaging radars in environmental monitoring: Some shuttle imaging radar results in Asia
[NASA-TM-101175] N88-26544
Meteorological atlas of the Southern Hemisphere lower stratosphere for August and September 1987
[NASA-TM-4049] N88-26763
The hard X-ray burst spectrometer event listing 1980-1987
[NASA-TM-4036] N88-27144

NATIONAL AERONAUTICS AND SPACE ADMINISTRATION. HUGH L. DRYDEN FLIGHT RESEARCH FACILITY, EDWARDS, CALIF.
Flight research and testing
[NASA-TM-100439] N88-26361

NATIONAL AERONAUTICS AND SPACE ADMINISTRATION. JOHN F. KENNEDY SPACE CENTER, COCOA BEACH, FLA.
Survey for least bell's vireo in riparian habitat on Vandenberg Air Force Base, Santa Barbara County, California
[NASA-TM-100984] N88-26744
Vegetation studies on Vandenberg Air Force Base, California
[NASA-TM-100985] N88-26795

NATIONAL AERONAUTICS AND SPACE ADMINISTRATION. LYNDON B. JOHNSON SPACE CENTER, HOUSTON, TEX.
Mobile remote manipulator system for a tetrahedral truss
[NASA-CASE-MSC-20985-1] N88-26398
Method and apparatus for measuring distance
[NASA-CASE-MSC-20912-1] N88-26568

NATIONAL AERONAUTICS AND SPACE ADMINISTRATION. LANGLEY RESEARCH CENTER, HAMPTON, VA.
Influence of wind shear on the aerodynamic characteristics of airplanes
[NASA-TP-2827] N88-26344
Low-speed wind-tunnel test of a STOL supersonic-cruise fighter concept
[NASA-TM-4050] N88-26374
Pyrotechnic system failures: Causes and prevention
[NASA-TM-100633] N88-26394
Initial adhesive screening of novel polyamide-imides and their copolymers
[NASA-TM-100641] N88-26481
Three-dimensional analysis of a postbuckled embedded delamination
[NASA-TP-2823] N88-26684
Kinematics of Hooke universal joint robot wrists
[NASA-TM-100567] N88-26870
Helicopter main-rotor noise: Determination of source contributions using scaled model data
[NASA-TP-2825] N88-26907
Evaluation of a multi-point method for determining acoustic impedance
[NASA-TM-100637] N88-26913
Nucleon-nucleus interaction data base: Total nuclear and absorption cross sections
[NASA-TM-4053] N88-26935
Studies of HZE particle interactions and transport for space radiation protection purposes
[NASA-TM-101159] N88-27142

NATIONAL AERONAUTICS AND SPACE ADMINISTRATION. LEWIS RESEARCH CENTER, CLEVELAND, OHIO.
Fiber optics for advanced aircraft
[NASA-TM-101294] N88-26328
A diagonally inverted LU implicit multigrid scheme
[NASA-TM-100911] N88-26340
Computer simulation of a single pilot flying a modern high-performance helicopter
[NASA-TM-100182] N88-26376
Computer simulation of multiple pilots flying a modern high performance helicopter
[NASA-TM-100183] N88-26377
Application of superconducting technology to earth-to-orbit electromagnetic launch systems
[NASA-TM-101134] N88-26385
A reusable rocket engine intelligen control
[NASA-TM-100963] N88-26401
Advanced photovoltaic power system technology for lunar base applications
[NASA-TM-100965] N88-26402
Substituted 1,1,1-Triaryl-2,2,2-Trifluoroethanes and processes for their synthesis
[NASA-CASE-LEW-14345-1] N88-26404
Performance of lightweight nickel electrodes
[NASA-TM-100958] N88-26430
Accelerated fatigue crack growth behavior of PWA 1480 single crystal alloy and its dependence on the deformation mode
[NASA-TM-100943] N88-26436
Fracture resistance of a TiB2 particle/SiC matrix composite at elevated temperature
[NASA-TM-100967] N88-26482
Reducing adhesion and agglomeration within a cloud of combustible particles
[NASA-TM-100902] N88-26539
COSPAS/SARSAT 406-MHz emergency beacon digital controller
[NASA-TM-100859] N88-26566
Active phase compensation system for fiber optic holography
[NASA-TM-101295] N88-26641
Fiber optic sensors with internal referencing
[NASA-TM-100893] N88-26644
Small-droplet spray measurements with a scattered-light scanner
[NASA-TM-100973] N88-26645
Contact force history and dynamic response due to the impact of a soft projectile
[NASA-TM-100961] N88-26679
The design and fabrication of a Stirling engine heat exchanger module with an integral heat pipe
[NASA-TM-101296] N88-26732
Evolution of hairpin vortices in a shear flow
[NASA-TM-100858] N88-26885

NATIONAL AERONAUTICS AND SPACE ADMINISTRATION. MARSHALL SPACE FLIGHT CENTER, HUNTSVILLE, ALA.
Analysis of the performance of the space ultravacuum research facility in attached and free-flyer mode
[NASA-TM-100325] N88-26387

NATIONAL AERONAUTICS AND SPACE ADMINISTRATION. PASADENA OFFICE, CALIF.
Data volume reduction for imaging radar polarimetry
[NASA-CASE-NPO-17184-1-CU] N88-26541
Low noise cryogenic dielectric resonator oscillator
[NASA-CASE-NPO-17157-1-CU] N88-26596

NATIONAL AEROSPACE LAB., AMSTERDAM (NETHERLANDS).
Calculation of 2-D unsteady transonic full potential flow about oscillating airfoils by two complementary approaches
[PB88-127519] N88-26341
A positioning system based on NAVSAT
[NLR-MP-87018-U] N88-26358
Trajectory measurement of the Fokker 100 aircraft during autoland testing
[NLR-MP-86010-U] N88-26366
Development of an airborne facility for advanced avionics research
[NLR-MP-87012-U] N88-26368
Corrosion prevention in gas turbines
[NLR-MP-87029-U] N88-26373
Document transfer by a digital satellite link
[NLR-MP-86071-U] N88-26564
Axisymmetric liquid sloshing under low-g conditions: Numerical simulation method (reference manual)
[NLR-TR-86057-4] N88-26627
Preliminary design and analysis of procedures for the numerical generation of 3D block-structured grids
[NLR-TR-86102-U] N88-26628
Liquid motions in partially filled containers: Preliminary results of the D-1 mission
[NLR-MP-86042-U] N88-26629
An introduction to robot joint control methods
[NLR-TR-86080-U] N88-26677
Simulation of space manipulator operations (EUROSIM)
[NLR-MP-87017-U] N88-26678
Automated measurement of crack length and load line displacement at elevated temperature
[NLR-MP-87049-U] N88-26706
Prediction of fatigue growth
[NLR-MP-87052-U] N88-26707
Geographical information for design purposes
[NLR-MP-87014-U] N88-26719
Enumeration, comments and discussion concerning papers presented during the Conference on Computer Applications in Production and Engineering (CAPE) 87
[NLR-MP-87015-U] N88-26844
NEXT: An expert system development tool to support engineering design
[NLR-MP-86070-U] N88-26871

NATIONAL AEROSPACE LAB., KAKUDA (JAPAN).
Analysis of flow through pump of large rocket engine N88-26306

NATIONAL AEROSPACE LAB., TOKYO (JAPAN).
Proceedings of the 5th NAL Symposium on Aircraft Computational Aerodynamics
[NAL-SP-8] N88-26290
On the NAL numerical simulator system N88-26291
Numerical simulations of flow around shuttle orbiter N88-26293
Finite element analysis of incompressible viscous flow around multi-element aerofoils N88-26294
Aerodynamic simulation for complete ASKA aircraft configuration N88-26301
Calculations of unsteady aerodynamics for a full aircraft configuration using boundary element method N88-26303
Rarefied gas numerical wind tunnel 3: Universal code for three dimensional bodies N88-26304
Numerical calculation of three dimensional flow by TVD scheme N88-26309
Numerical analysis of three dimensional cascade flow by solving Navier-Stokes equations N88-26310
Numerical analysis of duct flow using three-dimensional parabolized Navier-Stokes equation N88-26312
An implicit, high order accurate, upwind scheme for unsteady Euler equations N88-26317
On the propagating speed in difference approximations for conservation laws N88-26318
On symmetric TVD schemes N88-26319
Numerical simulation of transition to turbulence in plane Poiseuille flow by a spectral method N88-26321

NATIONAL BUREAU OF STANDARDS, BOULDER, COLO.
Thermal conductivity of selected foams and systems from 100 to 300 K
[PB88-201553] N88-26466

NATIONAL BUREAU OF STANDARDS, GAITHERSBURG, MD.
Center for Electronics and Electrical Engineering technical publication announcements covering Center programs, July to September 1987
[PB88-196530] N88-26572
Computer science and technology: Knowledge-based system for physical database design
[PB88-193289] N88-27109

NATIONAL CENTER FOR ATMOSPHERIC RESEARCH, BOULDER, COLO.
Circulation statistics from seasonal and perpetual January and July simulations with the NCAR (National Center for Atmospheric Research) Community Climate Model (CCM1):R15
[PB88-192620] N88-26748

NATIONAL GEOPHYSICAL DATA CENTER, BOULDER, COLO.
Solar-geophysical data number 522, February 1988. Part 2: (Comprehensive reports). Data for August 1987 and miscellanea
[PB88-194741] N88-27138
Solar-geophysical data number 522, February 1988. Part 1: (Prompt reports). Data for January 1988, December 1987 and late data
[PB88-194733] N88-27139

NATIONAL OCEANIC AND ATMOSPHERIC ADMINISTRATION, SEATTLE, WASH.
Numerical model for the computation of radiance distributions in natural waters with wind-roughened surfaces
[PB88-192703] N88-26765

Eigenmatrix representations of radiance distributions in layered natural waters with wind-roughened surfaces
[PB88-188701] N88-26780

NATIONAL OCEANOGRAPHIC DATA CENTER, WASHINGTON, D. C.
Mariners weather log, volume 31, number 4, Fall 1987
[PB88-173851] N88-26761

NATIONAL RESEARCH INST. FOR MATHEMATICAL SCIENCES, PRETORIA (SOUTH AFRICA).
Graphical communication and symbolism in a computerized cartography and map compilation system
[PB88-124672] N88-26720
Two families of graphs satisfying the cycle basis interpolation property
[PB88-127808] N88-26890
Algorithm for generating the minimal cycle basis of a graph
[PB88-126810] N88-26891
Linear programming in R sup 3 and the skeleton and largest incircle of a convex polygon
[PB88-124664] N88-26892

NATIONAL TRANSPORTATION SAFETY BOARD, WASHINGTON, D. C.
Aircraft accident report: Joe Foster Excavating, inc., Bell 206B, N49606, in-flight collision with trees, Alamo, California, August 3, 1986
[PB88-910405] N88-26345
Aircraft accident report: Midair collision of SkyWest Airlines Swearingen METRO 2, N163SW, and Mooney M20, N6485U, Kearns, Utah, January 15, 1987
[PB88-910404] N88-26346

NAVAL CIVIL ENGINEERING LAB., PORT HUENEME, CALIF.
Biodegradation of JP-5 aviation fuel by subsurface microbial communities
[AD-A192743] N88-26493

NAVAL OCEAN SYSTEMS CENTER, SAN DIEGO, CALIF.
Antenna heights for the optimum utilization of the oceanic evaporation duct. Part 3: Results from the Mediterranean measurements, volume 2
[AD-A192311] N88-26554
Antenna heights for the optimum utilization of the oceanic evaporation duct. Part 1: Results from the Pacific measurements. Part 2: Results from the Key West measurements, volume 1
[AD-A192356] N88-26555
Effects of atmospheric model layering on LOWTRAN 6 calculations of 8-12 micrometers near-horizon sky radiances
[AD-A192969] N88-26559
Local free-space mapping and path guidance for mobile robots
[AD-A192970] N88-26674
A modal approach to Arctic noise modelling with implied vertical coherence
[AD-A192966] N88-26916

NAVAL POSTGRADUATE SCHOOL, MONTEREY, CALIF.
The effect of a turbulent airstream on a vertically-launched missile at high angles of attack
[AD-A192408] N88-26363
Analysis of gas turbine test cell number 1, Lemoore Naval Air Station, California
[AD-A192870] N88-26380
An interactive computer code for preliminary design of solid propellant rocket motors
[AD-A192969] N88-26399
Optimizing superplastic response in lithium containing aluminum-magnesium alloys
[AD-A192217] N88-26451
Electrodynamic driver for the space thermoacoustic refrigerator (STAR)
[AD-A192337] N88-26517
Vibration response of constrained viscoelastically damped plates: Analyses and experiments
[AD-A192329] N88-26699
Synoptic patterns related to tropical cyclone recurvature
[AD-A192338] N88-26771
The performance of the NEC SX-2 and Cray X-MP supercomputers
[DE88-009177] N88-26813
Editfont: An interactive font editing system
[AD-A192373] N88-26836

NAVAL RESEARCH LAB., WASHINGTON, D.C.
Ferromagnetic/semiconductor hybrid structures
N88-27013
Superlattice doping interfaces N88-27019

NEW MEXICO STATE UNIV., LAS CRUCES.
Experimental and theoretical analysis of the radiative transfer within a sooty pool fire
[DE88-007099] N88-26419

NEW MEXICO UNIV., ALBUQUERQUE.
The chirped-pulse free-electron laser
[DE88-009289] N88-26651

NEW SOUTH WALES UNIV., KENSINGTON (AUSTRALIA).
The UMAC simulator N88-26811
A multiprocess operating system for 16 bit microcomputers or porting Unix (trademark) to a NS32016 with enhancements N88-26822

NIPPON ELECTRIC CO. LTD., YOKOHAMA (JAPAN).
Dynamics of satellites with radial wire antennas
N88-26514

NIPPON INST. OF TECH. (JAPAN).
Heat transfer of mesh-wick heat-pipes (bottom heat mode) N88-26507

NISSAN MOTOR CO. LTD., TOKYO (JAPAN).
A numerical analysis of flow characteristics in laser propulsion system N88-26305

NORTH CAROLINA STATE UNIV., RALEIGH.
The crystallization of tough thermoplastic resins in the presence of carbon fibers
[NASA-CR-182984] N88-26484
Strained layer and lattice matched transverse junction stripe quantum well lasers for continuous room temperature operation N88-27004

NORTH CAROLINA UNIV., CHAPEL HILL.
Two classes of self-similar stable processes with stationary increments
[AD-A192842] N88-26894

NORTH DAKOTA UNIV., GRAND FORKS.
Feasibility of producing jet fuel from GPGP (Great Plains Gasification Plant) by-products
[DE88-010233] N88-26492

NORTHWESTERN UNIV., EVANSTON, ILL.
Time-domain boundary element analysis of dynamic near-tip fields for impact-loaded collinear cracks
[AD-A192930] N88-26700
Off-boundary approach to the boundary element method
[AD-A192931] N88-26701
A new boundary integral equation formulation for elastodynamic and elastostatic crack analysis
[AD-A192967] N88-26702
Superconductivity of Cr/V superlattices N88-27057

NOTRE DAME UNIV., IND.
EXAFS studies of the microstructure of semiconductor alloys, defects and semiconductor-metal interfaces
N88-27031
Ordering transitions of ternary alloys A(1-x)B(x)C
N88-27054

O

OAK RIDGE GASEOUS DIFFUSION PLANT, TENN.
Evaluation of thermophosphor temperature technique
[DE88-007654] N88-26638

OAK RIDGE NATIONAL LAB., TENN.
Treatment of systematic errors in the processing of wide angle sonar sensor data for robotic navigation
[DE88-008961] N88-26352
Heat pump augmented radiator for low-temperature space applications
[DE88-008369] N88-26393
Interface modification in Nicalon (trademark)/SiC composites
[DE88-009706] N88-26409
Method for the isotopically selective detection of inert gases
[TI88-008370] N88-26421
Phase stability and alloy design of ordered intermetallics
[DE88-007479] N88-26435
Initial development of high-temperature titanium silicide alloys
[DE88-007860] N88-26437
Reduced-activation austenitic stainless steels: The Fe-Cr-C system
[DE88-008091] N88-26442
Helium induced degradation in the weldability of an austenitic stainless steel
[DE88-009062] N88-26443
Nickel aluminides: A new family of nickel + aluminum alloys featuring simple compositon, low density, excellent oxidation resistance and high yield strength that increases with temperature
[DE88-010892] N88-26461
Application of electron microscopy for the analysis of the mechanical behavior of advanced ceramics
[DE88-005049] N88-26469
A study of solvent effects on the synthesis of pure component and composite ceramic powders by metal alkoxide hydrolysis
[DE88-008381] N88-26470
Factors influencing the toughening behavior of whisker reinforced ceramics
[DE88-011396] N88-26479
Ceramic Technology for Advanced Heat Engines Program data base
[DE88-008954] N88-26489
The Oak Ridge Heat Pump Design Model: Mark 3 version program documentationon
[DE88-007863] N88-26607
Boundary element method for contact heat transfer
[DE88-011013] N88-26613
Sensor fusion for robot navigation
[DE88-008383] N88-26683
Optimization of performance criteria with bounded joint velocities for robots with one degree of redundancy
[DE88-003915] N88-26670
Interpreting forest biome productivity and cover utilizing nested scales of image resolution and biogeographical analysis
[NASA-CR-183036] N88-26711
The seasonal exchange of carbon dioxide between the atmosphere and the terrestrial biosphere: Extrapolation from site-specific models to regional models
[DE88-007870] N88-26740
An expeditious technique for keyboard input of information to FORTRAN computer programs
[DE88-009617] N88-26855
A linear-programming method inspired by the neural networks framework
[DE88-008688] N88-26862
The Oak Ridge National Laboratory strategic defense initiative shield optimization program: Executive summary
[DE88-008016] N88-26899
Inelastic mean free paths of electrons and positrons in matter
[DE88-008086] N88-26929
Recoil saturation of the self-energy in atomic systems
[DE88-010450] N88-26930
Thermal and mechanical analysis of the Faraday shield for the compact ignition tokamak
[DE88-007855] N88-26962
A CO2 laser Thomson scattering diagnostic for fusion product alpha particle measurement
[DE88-007683] N88-26965
Requirements for neutral beam current drive in tokamaks
[DE88-006180] N88-26980
Full-wave calculations in flux coordinates for toroidal geometry
[DE88-010131] N88-26985
Effects of grain boundary composition on properties of YBa2Cu3O/sub 7-x/
[DE88-007679] N88-27064
HeFlow: A program for calculating pressure and temperature of helium in forced-flow superconductors. Part 1: Numerical solutions. Part 2: HeFlow user's manual
[DE88-008941] N88-27071
Transient thermal analysis of three latent heat storage configurations for rapid thermal charging
[DE88-008943] N88-27104
Knowledge-based cost estimating vs traditional software cost models
[DE88-009707] N88-27116

OCHANOMIZU WOMEN'S UNIV., TOKYO (JAPAN).
Crosslinking of two vortex rings side by side
N88-26502

ODYSSEY RESEARCH ASSOCIATES, INC., ITHACA, N.Y.
Nebula support software
[AD-A192281] N88-26833

OFFICE NATIONAL D'ETUDES ET DE RECHERCHES AEROSPATIALES, PARIS (FRANCE).
Spectral resolution of the Navier-Stokes equations in multi-domain curved complex geometries
[ONERA-NT-1987-2] N88-26631
Parallelization on a multiprocessor system of a solution method for the unsteady Navier-Stokes equations at high Reynolds numbers
[ONERA-NT-1987-8] N88-26632
Damage in a perforated graphite-epoxy plate under monotonic, cyclic biaxial loading
[ONERA-NT-1987-5] N88-26708
Contribution to the study of order effects in the Ising model framework: Ground states and phase diagrams
[ONERA-NT-1987] N88-27095
Methods for indirect imaging through the atmosphere
[ONERA-NT-1987-4] N88-27124

OHIO STATE UNIV., COLUMBUS.
Plastic deformation and roughness of free metal surfaces
[PB88-196621] N88-26439
Radar cross section studies/compact range research
[NASA-CR-183124] N88-26565
A review of gear housing dynamics and acoustics literature
[NASA-CR-183110] N88-26675
Research on the kinetics of phase changes in solids
[AD-A192222] N88-26696

Non-effective-mass matching in superlattices N88-27049

OKLAHOMA UNIV., NORMAN.
Development of an equation of state for computation of supercompressibility factors, critical flow factors and other properties for wet, sour natural gases, synthetic gases and admixtures
[PB88-202676] N88-26602
Hydrologic models for land-atmosphere retrospective studies of the use of LANDSAT and AVHRR data
[NASA-CR-182861] N88-26712
Hydrologic models for land-atmosphere retrospective studies of the use of LANDSAT and AVHRR data
[NASA-CR-182862] N88-26716

OLD DOMINION UNIV., NORFOLK, VA.
Modeling and optimum time performance for concurrent processing
[NASA-CR-4167] N88-26595
A study of flow separation in transonic flow using inviscid and viscous computational fluid dynamics (CFD) schemes
[NASA-CR-183119] N88-26618
Experimental and theoretical investigation of passive damping concepts for member forced and free vibration
[NASA-CR-183082] N88-26693

OSAKA UNIV. (JAPAN).
An arranging method on L/D of two-phase closed thermosyphons N88-26508
Ductile-brittle transition of cutting behavior in diamond turning of single crystal Si
[DE88-008890] N88-26664

OXFORD UNIV. (ENGLAND).
Observation of ferromagnetism in ultrathin f.c.c. films by spin polarised neutron reflection N88-27015
Magneto-optical studies of GaInAs-InP quantum wells N88-27039
Defects and disorder in amorphous and damaged silicon
[AD-A192277] N88-27089

P

PACIFIC NORTHWEST LABS., RICHLAND, WASH.
Overview of the PRECP (processing of emissions by clouds and precipitation) Program
[DE88-006205] N88-26741
Interaction of biological systems with static and ELF electric and magnetic fields
[DE88-007951] N88-26792

PARIS VI UNIV. (FRANCE).
Influence of stable stratification on atmospheric turbulence: An experimental contribution
[ETN-88-92292] N88-26772
Processing and analysis of images transmitted by Vega space probes over Halley's comet
[ETN-88-92291] N88-27131

PAU UNIV. (FRANCE).
Structural study of impregnating resins of TGMDA/DDS type
[ETN-88-92167] N88-26488

PENNSYLVANIA STATE UNIV., UNIVERSITY PARK.
FEB structural analysis, revision H
[AD-A192302] N88-26698
Surface hydrology, sediment transport dynamics and remote sensing of disturbed watersheds in a humid temperate region
[DE88-006719] N88-26715

PENNSYLVANIA UNIV., PHILADELPHIA.
The protonic Beta double prime aluminas: Preparation, stability, conductivity and structure
[DE88-008442] N88-26415
Microwave image understanding and its application to radar cross section management N88-26542

PHILIPS INTERNATIONAL B.V., EINDHOVEN (NETHERLANDS).
Fully implicit splitting method for accurate tidal computations
[PB88-183637] N88-26781

PHYSICAL SCIENCES, INC., ANDOVER, MASS.
The use of liquid films for spacecraft survivability to laser radiation
[AD-A192954] N88-26395

PHYSICS AND ELECTRONICS LAB. TNO, THE HAGUE (NETHERLANDS).
Error performance of voice band data signals with an overloaded delta modulator
[FEL-1987-05] N88-26562
The performance of Eurocom error correction schemes for data communications
[FEL-1987-56] N88-26563
An integrated circuit for error protection in modern data communication systems conforming to Eurocom specifications
[FEL-1987-48] N88-26593
Outdoor sound propagation, its implications for unattended ground sensors
[FEL-1986-64] N88-26917
Description of the MPTR system: Multi Path Transmissometer Radiometer
[FEL-1987-14] N88-26954

PITTSBURGH UNIV., PA.
Inference and discovery in an exploratory laboratory
[AD-A192231] N88-26801
Distributed fault tolerant embeddings of binary trees in hypercubes
[AD-A192929] N88-26840
High resolution spectroscopy of dissociating molecules
[DE88-007959] N88-26924

PRATT AND WHITNEY AIRCRAFT, WEST PALM BEACH, FLA.
Engine component retirement for cause. Volume 1: Executive summary
[AD-A192730] N88-26371

PRINCETON UNIV., N. J.
Intelligent guidance and control for wind shear encounter
[NASA-CR-183060] N88-26347
Control of flight through microburst wind shear using deterministic trajectory optimization N88-26375
Tuning a major part of a clustering algorithm
[AD-A191446] N88-26821
Resonant tunneling in InGaAs-InP double-barrier structures and superlattices N88-27047

PRINS MAURITS LAB. TNO, RIJSWIJK (NETHERLANDS).
Combustion of PMMA (polymethylmethacrylate), PE (polyethylene) and PS (polystyrene) in a ramjet
[PB88-186572] N88-26417
Technical instructions for a control operating system of the gas flow installation for the solid fuel combustion chamber
[LR-507] N88-26537

PUERTO RICO UNIV., MAYAGUEZ.
The role of aviation technology in the Caribbean Basin
[NASA-CR-183068] N88-26289

PURDUE UNIV., INDIANAPOLIS, IND.
Raman, photoluminescence and modulation spectroscopy of semiconductor heterostructures N88-26997

PURDUE UNIV., WEST LAFAYETTE, IND.
A simulation analysis of errors in the measurement of standard electrochemical rate constants from phase-selective impedance data
[AD-A192739] N88-26426
The influence of uncompensated solution resistance on the determination and standard electrochemical rate constants using cyclic voltammetry and some comparisons with AC voltammetry
[AD-A192825] N88-26427
Asynchronous optical sampling for laser-based combustion diagnostics in high pressure flames
[AD-A192920] N88-26428

Q

QUAID-I-AZAM UNIV., ISLAMABAD (PAKISTAN).
Acoustic diffraction by an absorbing finite strip in a moving fluid
[PB88-191382] N88-26912

R

RAND CORP., SANTA MONICA, CALIF.
Why is it difficult to program in von Neumann languages
[AD-A192830] N88-26839
An agenda for the strategic defense initiative
[RAND-P-7404] N88-26898
SDI and/or arms control
[RAND-P-7357] N88-26903

RESEARCH TRIANGLE INST., RESEARCH TRIANGLE PARK, N.C.
Review of methods for remote sensing of atmospheric emissions from stationary sources
[PB88-190483] N88-26739
Parametric methodologies of cloud vertical transport for acid deposition models
[PB88-191374] N88-26762

RIJKSWATERSTAAT, THE HAGUE (NETHERLANDS).
Fully implicit splitting method for accurate tidal computations
[PB88-183637] N88-26781

RISO NATIONAL LAB., ROSKILDE (DENMARK).
Superconductivity of heavy-electron uranium compounds
[DE88-007901] N88-27065

ROCHESTER UNIV., N. Y.
Liquid crystal optics for laser systems
[DE88-008475] N88-26948

ROCKEFELLER UNIV., NEW YORK.
Cosmological helium production simplified
[DE88-009578] N88-27130

ROCKWELL INTERNATIONAL CORP., GOLDEN, COLO.
A finite element analysis for the hydroforming of aluminum
[DE88-008050] N88-26516

ROCKWELL INTERNATIONAL CORP., THOUSAND OAKS, CALIF.
The effects of thin compressive films on indentation fracture toughness measurements
[AD-A192243] N88-26480

ROCKY RESEARCH CORP., BOULDER CITY, NEV.
Heat pump augmented radiator for low-temperature space applications
[DE88-008369] N88-26393

ROYAL NETHERLANDS METEOROLOGICAL INST., DE BILT.
A control program for global radiation measurements
[KNMI-TR-100] N88-26757

ROYAL SIGNALS AND RADAR ESTABLISHMENT, MALVERN (ENGLAND).
Electron-phonon interactions in In(0.53)Ga(0.47)As and in In(0.53)Ga(0.47)As/InP quantum wells N88-27037

S

SAN DIEGO STATE UNIV., CALIF.
Electron-impact-ionization and electron-attachment cross sections of radicals important in transient gaseous discharges
[AD-A192248] N88-26424

SANDIA LABS., LIVERMORE, CALIF.
Helium induced degradation in the weldability of an austenitic stainless steel
[DE88-009062] N88-26443

SANDIA NATIONAL LABS., ALBUQUERQUE, N. MEX.
Simple 2-D navigation for wheeled vehicles
[DE88-007115] N88-26351
Experimental and theoretical analysis of the radiative transfer within a sooty pool fire
[DE88-007099] N88-26419
Electrophoretic coatings. Part 1: Sandia applications
[DE88-008666] N88-26485
The effects of Hertzian stress and test ambient on the friction coefficient of MoS2 coatings
[DE88-008118] N88-26487
High bandwidth optoelectronic signal link for use in an EMP (electromagnetic pulse) plus radiation environment
[DE88-009254] N88-26549
Exploratory battery technology development and testing report for 1986
[DE88-009870] N88-26578
Force servo control of a commercial gantry robot
[DE88-006649] N88-26660
RRSAS (Robotic Radiation Survey and Analysis System) Project: A real time sensor driven robotic system
[DE88-006825] N88-26661
Instrumentation for the measurement of penetrator dynamic response to permit force estimation
[DE88-010608] N88-26666
Microfocus X-ray techniques for flaw location
[DE88-008636] N88-26680
Development of an automated X-ray gauge for nondestructive quantitative analysis
[DE88-008633] N88-26681
Random vibration analysis of rattling structures
[DE88-007196] N88-26691
Photovoltaic concentrator technology: Recent results
[DE88-009588] N88-26726
Computer controlled data acquisition system for the NASA 1986 Rocket Triggered Lightning Program
[DE88-008335] N88-26766
A high speed serial link interface for SANDAC-V
[DE88-007694] N88-26861
The scaled-sized model: A revision of Amdahl's law
[DE88-008114] N88-26875
A nodal method for time-dependent transport equation
[DE88-004285] N88-26876
A new approach to machine-based perception of monocular images
[DE88-002418] N88-26942
Field-enhanced lithium ion sources for PBFA 2
[DE88-007195] N88-26960
An elliptical spectrograph/gated microchannel plate detector for time-resolved spectral measurements in the X-ray region
[DE88-007590] N88-26961
Plasma armature formation in high-pressure, high-velocity hydrogen
[DE88-008347] N88-26967

Atomistic simulation of stability, metastability and growth of strained layer structures N88-27053

Photoluminescence studies of InGaAlAs quaternary alloys
[DE88-007197] N88-27062

Characterization of the surface area and porosity of sol-gel films using saw devices
[DE88-008794] N88-27069

Recent advances in atom-probe field ion microscopy
[DE88-008799] N88-27070

SCIENCE APPLICATIONS INTERNATIONAL CORP., LA JOLLA, CALIF.

Computer programs for high-current beam transport in accelerators
[AD-A192356] N88-26835

SCIENCE RESEARCH COUNCIL, CHILTON (ENGLAND).

Generation of Adlam-Allen waves by plasma release experiments in the solar wind
[PB88-106000] N88-27140

SCIENTIFIC RESEARCH ASSOCIATES, INC., GLASTONBURY, CONN.

Improved 3-D turbomachinery CFD algorithm
[NASA-CR-179364] N88-26619

SHANGHAI INST. OF ENERGY (CHINA).

An analysis of gas-steam total power recovery energy system N88-26512

SHEFFIELD UNIV. (ENGLAND).

On a-Si:H/a-SiN(x):H superlattices: Confinement or contamination N88-27040

SMITHSONIAN ASTROPHYSICAL OBSERVATORY, CAMBRIDGE, MASS.

Measurement of HO2 and other trace gases in the stratosphere using a high resolution far-infrared spectrometer at 26 KM
[NASA-CR-180400] N88-26737

SOCIETE EUROPEENNE DE PROPULSION, BORDEAUX (FRANCE).

High temperature resins for injection. High temperature pre-impregnated
[RC-648676] N88-26486

SOCIETE NATIONALE INDUSTRIELLE AEROSPATIALE, SURESNES (FRANCE).

Sensitivity to crack initiation in thick assemblies. Test report 48-444
[REPT-48-444] N88-26365

SOL TELECOMMUNICATIONS SERVICES, INC., MCLEAN, VA.

Research in electromagnetic shielding theory. Part1. Shielding by rectangular enclosures
[AD-A192881] N88-26557

Research in electromagnetic shielding theory. Part 2: EMP (electromagnetic pulse) simulation using small loops
[AD-A192882] N88-26558

SOLAR TURBINES INTERNATIONAL, SAN DIEGO, CALIF.

Development of protective coatings for ceramic tubular components
[PB88-197165] N88-26483

SONY CORP., YOKOHAMA (JAPAN).

Hot electron transistors grown by MOCVD N88-26996

SOUTH CAROLINA UNIV., COLUMBIA.

Working memory capacity: An individual differences approach
[AD-A192359] N88-26803

SOUTHERN RESEARCH INST., BIRMINGHAM, ALA.

Review of methods for remote sensing of atmospheric emissions from stationary sources
[PB88-190483] N88-26739

SOUTHWEST RESEARCH INST., SAN ANTONIO, TEX.

Study of the influence of metallurgical factors on fatigue and fracture of aerospace structural materials
[AD-A192909] N88-26452

Experiments on densely-loaded non-Newtonian slurries in laminar and turbulent pipe flows
[DE88-010579] N88-26612

Analytical and experimental investigation of ringless piston concept
[AD-A192635] N88-26673

SPECTRA TECHNOLOGY, INC., BELLEVUE, WASH.

Rare Gas Halide (RGH) kinetics
[AD-A192352] N88-26425

SRI INTERNATIONAL CORP., MENLO PARK, CALIF.

Development of liquid metal field-emission sources for use in fast repetitive opening switches
[AD-A192230] N88-26583

An evaluation methodology for dependable multiprocessors
[AD-A192799] N88-26863

STANFORD LINEAR ACCELERATOR CENTER, CALIF.

Results from the SLAC lasertron
[DE88-007816] N88-26647

STANFORD UNIV., CALIF.

Numerical study of delta wing leading edge blowing
[NASA-CR-183101] N88-26335

The free-electron laser: Theoretical innovations and gas-loaded experiment N88-26646

An assessment of modelling techniques for the finite element analysis of reinforced concrete plate and shell structures
[AD-A192263] N88-26697

Image pyramid motion detection applied to sea ice N88-26713

Research in VLSI computer systems
[AD-A192915] N88-26816

Experiments in adaptive control of a very flexible one link manipulator N88-26865

The evaluation of a deformable diffraction grating for a stigmatic EUV spectrohelioimeter
[NASA-CR-183064] N88-26941

Electrical study of metal/group 3-5 semiconductor interfaces: Comparison with the atomic-level studies N88-27059

STATE UNIV. OF NEW YORK, BUFFALO.

Far-infrared studies of doped AlGaAs/GaAs multiple-quantum-well structures N88-26998

STATE UNIV. OF NEW YORK AT BUFFALO, AMHERST.

The interaction of sensory and perceptual variables: Spatial, temporal and orientation response to figure and ground
[AD-A192897] N88-26798

STEVENS INST. OF TECH., HOBOKEN, N.J.

Cosmological helium production simplified
[DE88-009578] N88-27130

STRUCTURAL SEMANTICS, PALO ALTO, CALIF.

Checklist interruption and resumption: A linguistic study
[NASA-CR-177460] N88-26348

Communication training for aircrews: A review of theoretical and pragmatic aspects of training program design
[NASA-CR-177459] N88-26349

STUTTGART UNIV. (WEST GERMANY).

Modeling and parameter identification of motor vehicles N88-26521

Stationary, wave type, and chaos type convection in spherical symmetry geometries
[ETN-88-92358] N88-26625

Experimental and theoretical study of the dynamic operational behavior of a three stage radial compressor
[ETN-88-92129] N88-26676

Auger recombination in GaSb/AlSb-multi quantum well heterostructures N88-27001

Epitaxy and properties of two dimensional GaInAs semiconductor structures
[ETN-88-92357] N88-27094

SVERDRUP TECHNOLOGY, INC., CLEVELAND, OHIO.

High speed inlet calculations with real gas effects
[NASA-CR-182167] N88-26336

Three-dimensional viscous flow computations of a circular jet in subsonic and supersonic cross flow
[NASA-CR-182153] N88-26616

Resources: NASA for entrepreneurs
[NASA-CR-182152] N88-27119

SWEDISH INST. FOR MATERIALS TESTING, BORAS.

Sound power measurements in situ using a reference sound source
[PB88-182571] N88-26910

SYSTEMS ENGINEERING LABS., INC., GREENBELT, MD.

Stochastic modeling of EM scattering from foliage
[AD-A192258] N88-26553

T

TAI CORP., HUNTSVILLE, ALA.

Common Data Format (CDF) to store images
[NASA-CR-179366] N88-26825

TAKUMA RESEARCH AND DEVELOPMENT CO. LTD., DOJIMA (JAPAN).

Characteristics of long size thermosyphons made of corrugated tube N88-26511

TECHNION - ISRAEL INST. OF TECH., HAIFA.

Vertical ship motions and sea loads considering nonlinear effects
[TAE-592] N88-26515

TECHNISCHE HOCHSCHULE, AACHEN (WEST GERMANY).

Observation of a point source in Cygnus constellation with the underground detector at Frejus (France)
[PITHA-87/02] N88-27122

TECHNISCHE HOCHSCHULE, DARMSTADT (WEST GERMANY).

Parameter estimation of dynamical systems N88-26519

Vehicle dynamics: Identification in the frequency domain N88-26523

TECHNISCHE HOGESCHOOL, DELFT (NETHERLANDS).

Position and velocity determination using a Global Positioning System: An outline
[B8735052] N88-26355

Research project Loran-C of the Geometric Service of the Ministry of Public Works
[B8735055] N88-26356

The Sercel TR5S Global Positioning System (GPS) receiver
[ETN-88-92473] N88-26357

Combustion of PMMA (polymethylmethacrylate), PE (polyethylene) and PS (polystyrene) in a ramjet
[PB88-186572] N88-26417

Corrosion in aircraft structures. Part 1: Text
[LR-527-PT-1] N88-26458

Corrosion in aircraft structures. Part 2: Figures
[LR-527-PT-2] N88-26459

A new method for the estimation of aircraft inertia characteristics N88-26530

Technical instructions for a control operating system of the gas flow installation for the solid fuel combustion chamber
[LR-507] N88-26537

New hybrid method for solving time-domain integral equations (one-dimensional scattering problems)
[PB88-186192] N88-26547

Testing of a gravimeter LCR G 785
[B8735061] N88-26643

The transition from traditional to modern map reproduction
[B8735128] N88-26718

Fully implicit splitting method for accurate tidal computations
[PB88-183637] N88-26781

Delfi-3 as a development environment for expert systems
[REPT-8767] N88-26845

Script editor: An editor for the specification phase in the development of computer based learning
[REPT-87-68] N88-26846

A survey of freeform solid modeling methods
[REPT-87-81] N88-26847

A new trajectory following polynomial-time algorithm for the linear programming problem
[REPT-87-87] N88-26848

Extensible networks. Part 1: Principles and constructions
[REPT-87-91-PT-1] N88-26864

Linearization along invariant manifolds and a generalization of the Hartman-Grobman theorems for degenerate singularities of vector fields in R cubed
[REPT-87-80] N88-26886

A full but elementary treatment of systems of homogeneous ordinary linear differential equations with constant coefficients
[REPT-87-82] N88-26887

Semilinear elliptic problems on domains with corners
[REPT-87-83] N88-26888

Prolongation, restriction and coarse grid approximation in a three-dimensional cell-centered multigrid method
[REPT-88-02] N88-26889

Combining expert opinions: An optimization framework
[REPT-87-84] N88-26895

Markov chain computations to a solution of the mutual-exclusion problem in concurrency
[REPT-87-89] N88-26896

Range of a constrained random walk
[PB88-126867] N88-26897

The sine and cosine function for class 4-VWO. Exploration of possible bottlenecks
[REPT-87-72] N88-27105

Design and development of courseware for goniometry
[REPT-87-73] N88-27106

Knowledge representation in geographic information systems
[ETN-88-92470] N88-27112

TECHNISCHE HOGESCHOOL, EINDHOVEN (NETHERLANDS).

Drag reduction of turbulent boundary layers by means of grooved surfaces
[ETN-88-92618] N88-26630

Plasma deposition: Investigations on a new approach
[ETN-88-92619] N88-26992

TECHNISCHE UNIV., BERLIN (WEST GERMANY).

Signal processing in digital speech transmission systems
[ETN-88-92122] N88-26581

Contribution to speed regulation of small motors with phase-locked loops
[ETN-88-92373] N88-26590

Development of a model procedure for the determination of volume diffusion lengths by transient measurements on monocrystal silicon solar cells
[ETN-88-92119] N88-26733

Design of high performance microcomputers for numerical data processing
[ETN-88-92371] N88-26818
Excitation of single-mode glass fiber by partially coherent sources
[ETN-88-92121] N88-26951
Direct imaging of the columnar structure of GaAs quantum wells N88-27030
Electronic and geometric structure of silver and palladium on aluminum (111) in monoatomic surface layers
[ETN-88-92120] N88-27093

TECHNISCHE UNIV., BRUNSWICK (WEST GERMANY).
Nonlinear identification of an aircraft for the direct calculation of an anticipatory control N88-26535
Extinction behavior of low voltage switching arc under consideration of cathodic coatings and dynamic arc column
[ETN-88-92384] N88-26591
Permanent magnet excitation of axial flow synchronous machines with high rotation moment
[ETN-88-92385] N88-26592
Investigation on refrigerant R12 critical boiling point in narrow flow pipes considered as model fluid
[ETN-88-92374] N88-26626

TECHNISCHE UNIV., MUNICH (WEST GERMANY).
Structural optimization of fiber composite turbomachine blades
[ETN-88-92351] N88-26372
Dynamics and stability of combustion driven self oscillations in presence of various frequencies. Extensive stability criteria
[ETN-88-92123] N88-26432
Investigation of structure and surface state effect on hydrogen embrittlement of steels, under consideration of acoustic emission analysis
[ETN-88-92350] N88-26457
Computer controlled procedures for traction battery power performance tests
[ETN-88-92352] N88-26589
Cross flow induced vibrations in tube bundle by displaced and misaligned tube configurations
[ETN-88-92132] N88-26621
Display and processing of multidimensional signals with the aid of fractal image sequences
[ETN-88-92131] N88-26642
New semiconductor laser structure for an optical communication system
[ETN-88-92353] N88-26654
Study of temperature and stress fields of two sliding cylinders
[ETN-88-92134] N88-26704
Photovoltaic cells with n-silicon and conductive polymers
[ETN-88-92133] N88-26734
Does dihydroergotamine used in therapeutical doses influence the physical and psychomotor performance of young pilots or other traffic drivers subjected to hypotonia?
[ETN-88-92136] N88-26799
Thermal conductivity of pure fluids in a large region around the critical point
[ETN-88-92135] N88-27103

TENNESSEE UNIV., KNOXVILLE.
Dual mechanism bifunctional polymers: Design, synthesis and application of a new category of metal ion complexing agents
[DE88-006233] N88-26468
Statistical mechanics of polymer systems
[DE88-011172] N88-26477
Optimization of performance criteria with bounded joint velocities for robots with one degree of redundancy
[DE88-003915] N88-26670
Raman and absorption spectrophotometric studies of selected lanthanide, californium-doped lanthanide, and actinide trihalides in the solid state
[DE88-008234] N88-27061

TEXAS A&M UNIV., COLLEGE STATION.
An initial investigation into methods of computing transonic aerodynamic sensitivity coefficients
[NASA-CR-183061] N88-26332
A micromechanics model of the stiffness and strength of laminates with fiber waviness
[NASA-CR-181670] N88-26413

TEXAS INSTRUMENTS, INC., DALLAS.
Quantum transport theory of resonant-tunneling heterostructure devices N88-27017
Vertical electronic transport in novel semiconductor heterojunction structures N88-27045

TEXAS INSTRUMENTS, INC., PLANO, TEX.
Spacecraft applications of advanced global positioning system technology
[NASA-CR-172063] N88-26359

TEXAS UNIV., AUSTIN.
Laser ranging data analysis
[NASA-CR-183115] N88-26567
Numerical solution of weak forms of conservation laws on optimal unstructured triangular grids N88-26597
An analysis of the efficiency and directivity of the sound generated by a moving laser source
[AD-A192220] N88-26914
Drift wave vortices and anomalous transport
[DE88-009562] N88-26982

TEXAS UNIV., EL PASO.
Vibration frequencies of tapered bars with nonclassical boundary conditions
[NASA-CR-183059] N88-26688

THOMSON-CSF, ORSAY (FRANCE).
Theoretical aspects of electron transport in modulated structures N88-27016

TOHOKU UNIV., SENDAI (JAPAN).
Numerical simulation of the shock tube flows by TVD scheme N88-26308

TOKYO INST. OF TECH. (JAPAN).
Electrical properties of p-type and n-type ZnSe-ZnTe strained-layer superlattices N88-27029

TOKYO METROPOLITAN UNIV. (JAPAN).
Simulation of axisymmetric flow with H2O2 reactions N88-26311
Theory of numerical information environment and its applications N88-26326

TOKYO UNIV. (JAPAN).
Computation of flow around NACA0012 airfoil at high angle of attack N88-26300
High speed and high angle of attack wind tunnel test results of the winged space vehicle C-2
[ISAS-RN-623] N88-26329
On the dynamic behavior of balloon during its launch; application of panel method and extension to unsteady problem
[ISAS-RN-622] N88-26330
The Proceedings of the Symposium on Mechanics for Space Flight 1987
[ISAS-SP-6] N88-26499
Numerical analysis of reconnection of vortex rings N88-26500
Vortex filament simulation for the crosslinking rings N88-26501
Turbulence transition in a circular pipe N88-26503
A shock-tube experiment on gases mixing processes associated with CO2/N2 mixing gasdynamic laser
[ISAS-RN-350] N88-26596
Navier-Stokes simulation of shock-tube flows over a wedge-type step by finite volume method
[ISAS-RN-628] N88-26599
A numerical simulation of two-dimensional transient shear flow
[ISAS-RN-627] N88-26600
Fast atom bombardment study on interaction of anticodonic nucleotides and their cognate amino acid
[ISAS-RN-355] N88-26918
Low energy molecular collisions
[ISAS-RN-366] N88-26919
Detection of absorption lines in the spectra of X-ray bursts from X1608-52
[ISAS-RN-360] N88-27143

TOSHIBA CORP., TOKYO (JAPAN).
Forced-convective boiling in small diameter tube N88-26510

TRW SPACE TECHNOLOGY LABS., REDONDO BEACH, CALIF.
Plasma separation process. Betacell (BCELL) code, user's manual
[DE88-006955] N88-26981

TSUKUBA UNIV., IBARAKI (JAPAN).
Grid generation of a helicopter rotary-wing N88-26325
A statistical treatment of accelerated life test data for copper-water heat pipes N88-26509

U

UNIVERSITAET DER BUNDESWEHR, NEUBIBERG (WEST GERMANY).
On microphysical principles of thermofluid dynamics
[ETN-88-92095] N88-26620

UNIVERSITIES SPACE RESEARCH ASSOCIATION, HUNTSVILLE, ALA.
Velocity-pressure integrated versus penalty finite element methods for high Reynolds number flows
[NASA-CR-179357] N88-26635
The NASA Marshall engineering thermosphere model
[NASA-CR-179359] N88-26760

UNIVERSITY COLL., LONDON (ENGLAND).
Research in computer science 1985/6
[PB88-113840] N88-26815
Qualitative reasoning for physicists
[PB88-116298] N88-26906

UNIVERSITY OF CENTRAL FLORIDA, ORLANDO.
Expert system application education project
[NASA-CR-183089] N88-26867

UNIVERSITY OF SOUTHERN CALIFORNIA, MARINA DEL REY.
SIMS: Single Interface to Multiple Systems
[AD-A192264] N88-26832

V

VIRGINIA POLYTECHNIC INST. AND STATE UNIV., BLACKSBURG.
Instability-related delamination growth of embedded and edge delaminations N88-26406

VIRGINIA UNIV., CHARLOTTESVILLE.
A random access algorithm for environments with capture and limited feedback capabilities
[AD-A192233] N88-26552
SIS (Superconductor-Insulator-Superconductor) mixer research
[AD-A192908] N88-27092

VOLKSWAGEN A.G., WOLFSBURG (WEST GERMANY).
Parameter identification of the passenger simulation model MADYMO: Methods and experience N88-26536

VRIJE UNIVERSITEIT, AMSTERDAM (NETHERLANDS).
Programmer-friendly LL(1) parser generator
[PB88-126933] N88-26857
Hiding in stream semantics of uniform concurrency
[PB88-121579] N88-27114

W

WASHINGTON UNIV., SEATTLE.
Fundamental studies of elastomers
[DE88-009679] N88-26471
Compression creep of filamentary composites
[NASA-CR-182550] N88-26601
Studies of the mechanisms and rates with which nitrogen species are incorporated into cloud water and precipitation
[PB88-193065] N88-26764
Numerical model for the computation of radiance distributions in natural waters with wind-roughened surfaces
[PB88-192703] N88-26765
Evaluation of surface energy and radiation balance systems for FIFE
[NASA-CR-183118] N88-26778

WESTINGHOUSE RESEARCH AND DEVELOPMENT CENTER, PITTSBURGH, PA.
Superconducting electronic film structures
[AD-A192907] N88-27091

WESTON OBSERVATORY, MASS.
Surface disturbances produced by low-level, subsonic B-1 aircraft
[AD-A192257] N88-26752

WISCONSIN UNIV., MADISON.
A survey of the Ap stars for rapid variability N88-27127

WOODS HOLE OCEANOGRAPHIC INSTITUTION, MASS.
Prediction of continental shelf sediment transport using a theoretical model of the wave-current boundary layer
[AD-A192272] N88-26783
Stability of a coastal upwelling front over topography
[AD-A192354] N88-26784

WRIGHT STATE UNIV., DAYTON, OHIO.
High temperature testing of C/C (Carbon/Carbon) composites
[AD-A193012] N88-26411

Y

YALE UNIV., NEW HAVEN, CONN.
Regulatory biochemical and metabolic responses in photoreceptors
[AD-A192898] N88-26794
Quantitative particle characterization by scattered ultrasound N88-26908
Studying materials using acoustic waves
[AD-A192234] N88-26915
Quantum interference and transport in microstructures N88-27022

YORK UNIV. (ENGLAND).
Frequency domain identification of the dynamics of a scaled remotely-piloted helicopter N88-26524

Typical Contract Number Index Listing

Listings in this index are arranged alphanumerically by contract number. Under each contract number the NASA accession numbers denoting documents that have been produced as a result of research done under that contract are arranged in ascending order. The NASA accession number denotes the number by which the citation is identified.

AF AFOSR-0013-87 ..... N88-26412
AF AFOSR-0056-86 ..... N88-27092
AF AFOSR-0067-86 ..... N88-26991
AF AFOSR-0069-87 ..... N88-26803
AF AFOSR-0095-82 ..... N88-26751
AF AFOSR-0115-84 ..... N88-26798
AF AFOSR-0171-84 ..... N88-26794
AF AFOSR-0224-86 ..... N88-26411
AF AFOSR-0293-84 ..... N88-26841
AF AFOSR-0323-84 ..... N88-26428
AF AFOSR-0356-83 ..... N88-26429
AF PROJ. 2305 ..... N88-26995
AF-AFOSR-0347-86 ..... N88-27025
AF-AFOSR-0351-87 ..... N88-26873
A73/KL/035 ..... N88-26562
A80/KL/138 ..... N88-26917
A82/KL/060 ..... N88-26583
N88-26593
C-21066-G N88-26497
DA PROJ. 1L1-61102-BH-57 ..... N88-26614
N88-27089
DA PROJ. 1L1-62120-AH-25 ..... N88-26557
N88-26558
DAAG29-85-K-0175 ..... N88-27055
DAAJ02-86-C-0030 ..... N88-26673
DAAK70-85-C-0007 ..... N88-26673
DAAL02-86-C-0052 ..... N88-26557
N88-26558
DAAL03-86-K-0073 ..... N88-26821
DAAL03-86-K-0083 ..... N88-27000
DAJA45-83-C-0058 ..... N88-27089
DAJA45-83-C-0061 ..... N88-26614
DAJA45-87-C-0052 ..... N88-27090
DAMD17-86-C-6004 ..... N88-26717
DE-AC02-76CH-00016 ..... N88-26797
N88-26828
N88-26922
N88-26947
DE-AC02-76CH-03000 ..... N88-26938
DE-AC02-78ET-51013 ..... N88-26972
DE-AC02-80ER-10597 ..... N88-26415
DE-AC02-83CH-10093 ..... N88-26721
N88-27060
DE-AC02-84ER-45048 ..... N88-27000
DE-AC03-76SF-00098 ..... N88-26408
N88-26460
N88-26574
N88-26723
N88-26724
N88-26877
N88-26934
N88-26937
N88-27066
N88-27145
DE-AC03-76SF-00515 ..... N88-26647
DE-AC03-77ET-33006 ..... N88-26981
DE-AC03-84ER-51044 ..... N88-26969
N88-26986
N88-26987
DE-AC03-84ER-53158 ..... N88-26963
N88-26964
N88-26966
DE-AC04-76DP-00613 ..... N88-26672
DE-AC04-76DP-00656 ..... N88-26579
DE-AC04-76DP-00789 ..... N88-26351
N88-26419
N88-26465
N88-26467
N88-26549
N88-26578
N88-26651
N88-26660
N88-26661
N88-26666
N88-26680
N88-26681
N88-26691
N88-26726
N88-26766
N88-26861
N88-26875
N88-26876
N88-26942
N88-26960
N88-26961
N88-27053
N88-27062
N88-27069
N88-27070
DE-AC04-76DP-03533 ..... N88-26516
DE-AC04-81AL-16310 ..... N88-26423
DE-AC05-84ER-40150 ..... N88-26936
N88-27077
DE-AC05-84OR-21400 ..... N88-26352
N88-26393
N88-26409
N88-26421
N88-26435
N88-26437
N88-26442
N88-26443
N88-26461
N88-26469
N88-26470
N88-26479
N88-26489
N88-26607
N88-26613
N88-26663
N88-26670
N88-26740
N88-26791
N88-26855
N88-26862
N88-26899
N88-26929
N88-26930
N88-26962
N88-26965
N88-26980
N88-26985
N88-27061
N88-27064
N88-27071
N88-27104
N88-27116
DE-AC05-84OT-21400 ..... N88-26638
DE-AC06-76RL-01830 ..... N88-26741
N88-26792
DE-AC07-76ID-01570 ..... N88-26605
N88-26662
N88-26973
N88-27115
DE-AC08-88NV-10617 ..... N88-26945
DE-AC09-76SR-00001 ..... N88-26665
DE-AC21-83FE-60338 ..... N88-26582
DE-AC21-83MC-20037 ..... N88-26782
DE-AC22-87PC-90016 ..... N88-26492
DE-AS05-76ER-04447 ..... N88-27061
DE-AS06-88ER-40423 ..... N88-27130
DE-FC08-85DP-40200 ..... N88-26948
DE-FG01-84ER-60266 ..... N88-26779
DE-FG02-84ER-45167 ..... N88-26689
DE-FG02-85ER-40214 ..... N88-26927
DE-FG02-85ER-40235 ..... N88-26926
DE-FG02-85ER-45211 ..... N88-26444
N88-27078
DE-FG02-85ER-45219 ..... N88-27088
DE-FG02-85ER-53207 ..... N88-26968
DE-FG02-86ER-13631 ..... N88-26725
DE-FG02-86ER-45253 ..... N88-27066
DE-FG02-87ER-13655 ..... N88-26924
DE-FG02-87ER-25026 ..... N88-26830
DE-FG02-87ER-45310 ..... N88-26446
DE-FG02-87ER-45311 ..... N88-26447
DE-FG02-87ER-45315 ..... N88-26445
DE-FG02-87ER-45328 ..... N88-26420
DE-FG02-87ER-60594 ..... N88-26715
DE-FG03-85ER-13448 ..... N88-26944
DE-FG03-86ER-53220 ..... N88-26971
DE-FG05-80ET-53088 ..... N88-26982
DE-FG05-84ER-45104 ..... N88-26476
DE-FG05-84ER-45114 ..... N88-26477
DE-FG05-86ER-13591 ..... N88-26468
DE-FG06-84ER-45123 ..... N88-26471
DE-FG22-86PC-90962 ..... N88-26612
DFG-EB-56/7-2.3 ..... N88-26758
DFG-KO/883/1-1 ..... N88-26485
DRET-84-003-5 ..... N88-26622
DRET-84-439 ..... N88-26486
DRET-84-1183 ..... N88-26705
DRET-85-34-355-00470501 ..... N88-26488
DRET-85-002 ..... N88-26487
DRET-85-130 ..... N88-26433
DRET-85-183 ..... N88-26414
DRET-86-002 ..... N88-26623
DRET-86-1021 ..... N88-26806
DTFA03-80-A-00215 ..... N88-26495
DTFA03-87-C-00038 ..... N88-26350
EPA-68-02-4059 ..... N88-26762
EPA-68-02-4442 ..... N88-26739
ESA-5826/84-NL-PB(SC) N88-26707
ESA-6482/85 ..... N88-26678
F04701-85-C-0086 ..... N88-26396
N88-26410
N88-26560
N88-26598
N88-26587
N88-26755
N88-26933
N88-26990
N88-27141
F08635-85-C-0137 ..... N88-26950
F19628-83-C-0092 ..... N88-26753
F19628-83-C-0175 ..... N88-26640
F19628-85-C-0180 ..... N88-26553
F19628-85-K-0051 ..... N88-26754
F19628-86-C-0055 ..... N88-26752
F19628-86-D-0003 ..... N88-26863
F29601-86-C-0216 ..... N88-26968
F30602-84-C-0182 ..... N88-26833
F33615-80-C-5160 ..... N88-26371
F33615-84-K-1557 ..... N88-26585
F33615-85-C-3602 ..... N88-26809
F33615-85-C-3623 ..... N88-26806
F49620-84-C-0102 ..... N88-26395
F49620-85-C-0039 ..... N88-27025
F49620-85-C-0043 ..... N88-27091
F49620-85-C-0144 ..... N88-26894
F49620-86-C-0002 ..... N88-26873
F49620-86-C-0024 ..... N88-26452
GRI-5084-260-1010 ..... N88-26802
GRI-5086-232-1233 ..... N88-26463
GRI-5086-260-1403 ..... N88-26416
GRI-5087-271-1520 ..... N88-26714
GRI-5883-260-0880 ..... N88-26791
MDA903-81-C-0335 ..... N88-26832
MDA903-83-C-0335 ..... N88-26816
MDA903-85-C-0030 ..... N88-26839
NAGW-214 ..... N88-27137
NAGW-540 ..... N88-26941
NAG1-336 ..... N88-26693
NAG1-363 ..... N88-26618
NAG1-368 ..... N88-26343
NAG1-525 ..... N88-26464
NAG1-562 ..... N88-26545
NAG1-566 ..... N88-26911

NAG1-613 ..... N88-26823, N88-26860
NAG1-621 ..... N88-26601
NAG1-680 ..... N88-26407
NAG1-683 ..... N88-26595
NAG1-711 ..... N88-26413
NAG1-722 ..... N88-26909
NAG1-793 ..... N88-26332
NAG1-798 ..... N88-26858
NAG1-834 ..... N88-26347
NAG2-424 ..... N88-27121
NAG3-729 ..... N88-26376, N88-26377
NAG3-773 ..... N88-26675
NAG5-271 ..... N88-26710
NAG5-544 ..... N88-27136
NAG5-743 ..... N88-26745
NAG5-842 ..... N88-26759
NAG5-901 ..... N88-26778
NAG5-929 ..... N88-26569
NAG5-1021 ..... N88-26567
NAG8-511 ..... N88-26603
NAG9-146 ..... N88-26686
NAG9-212 ..... N88-26747
NAG10-0043 ..... N88-26867
NASA ORDER C-99066-G N88-26885
NASW-3482 ..... N88-27108
NASW-3541 ..... N88-26615
NASW-4307 ..... N88-26337, N88-26338, N88-26381, N88-26431, N88-26453, N88-26454, N88-26455, N88-26483, N88-26484, N88-26617, N88-26642
NASW-4703 ..... N88-26462
NAS1-18107 ..... N88-26873
NAS1-18267 ..... N88-26397
NAS2-11052 ..... N88-26348
NAS2-11250 ..... N88-26367
NAS2-11758 ..... N88-26807
NAS2-12130 ..... N88-27120
NAS2-12379 ..... N88-26349
NAS3-24105 ..... N88-26336
NAS3-24339 ..... N88-26360
NAS3-25115 ..... N88-26498
NAS3-25266 ..... N88-26616
NAS5-27344 ..... N88-26567
NAS5-28626 ..... N88-26389
NAS5-28781 ..... N88-26711
NAS7-100 ..... N88-26495
NAS7-918 ..... N88-26541, N88-26736, N88-26859
NAS8-35918 ..... N88-26635
NAS8-36185 ..... N88-26619
NAS8-36400 ..... N88-26760
NAS8-36992 ..... N88-26825
NAS9-17781 ..... N88-26359
NAS9-17876 ..... N88-27135
NAS10-10285 ..... N88-26744, N88-26795
NCC2-341 ..... N88-26335
NCC2-346 ..... N88-27134
NCC2-496 ..... N88-26289
NCC3-558 ..... N88-26644
NGR-05-002-160 ..... N88-27146
NGT-05020412 ..... N88-26694
NIVR-311.1-1101/01604N N88-26628
NIVR-1860/1999 ..... N88-26627
NIVR-1999 ..... N88-26629
NSERC-A4107 ..... N88-26854
NSF ATM-87-09659 ..... N88-26748
NSF DCR-MCS-85-09905 ..... N88-26854
NSF DCR-83-01766 ..... N88-26819
NSF DCR-85-04296 ..... N88-26853
NSF DCR-86-06366 ..... N88-26819
NSF DMR-83-11620 ..... N88-26439
NSF DMR-85-21616 ..... N88-27056
NSF DMR-86-02675 ..... N88-27055
NSF ECS-85-17708 ..... N88-26693
NSF ECS-86-01660 ..... N88-26838
NSF OCE-84-03249 ..... N88-26783
NSF OCE-84-08563 ..... N88-26784
NSG-1613 ..... N88-26565
NSG-5175 ..... N88-26737
N0014-83-F-0031 ..... N88-27012
N00014-78-C-0147 ..... N88-26494
N00014-80-C-04555 ..... N88-26840
N00014-83-K-2017 ..... N88-26584
N00014-84-C-0134 ..... N88-26784
N00014-84-K-0542 ..... N88-26801
N00014-84-K-0583 ..... N88-26969
N00014-85-C-0079 ..... N88-26802
N00014-85-C-0140 ..... N88-26480
N00014-85-C-0843 ..... N88-26425
N00014-85-C-2044 ..... N88-26868
N00014-85-K-0158 ..... N88-27054
N00014-85-K-0196 ..... N88-26696
N00014-85-K-0198 ..... N88-26836
N00014-85-K-0215 ..... N88-26915
N00014-85-K-0352 ..... N88-27054
N00014-85-K-0401 ..... N88-26700, N88-26701, N88-26702
N00014-85-K-0445 ..... N88-26819
N00014-85-K-0584 ..... N88-26805
N00014-85-K-0614 ..... N88-27031
N00014-85-K-0819 ..... N88-26914
N00014-86-F-0049 ..... N88-27136, N88-27139
N00014-86-K-0061 ..... N88-26783
N00014-86-K-0173 ..... N88-26834
N00014-86-K-0556 ..... N88-26426, N88-26427
N00014-86-K-0558 ..... N88-26424
N00014-86-K-0596 ..... N88-26583
N00014-86-K-0742 ..... N88-26552
N00014-87-K-0540 ..... N88-26893
N00014-87-K-0828 ..... N88-26816
N00167-85-C-0134 ..... N88-26334
N60921-85-C-0044 ..... N88-26835
N62583-86-M-R195 ..... N88-26697
PEO-90753.140 ..... N88-26537
RR0-4206 ..... N88-26801, N88-26805
STPA-85-96-032 ..... N88-26365
STW-DLR-11.0120 ..... N88-26537
W-31-109-ENG-38 ..... N88-26369, N88-26418, N88-26472, N88-26609, N88-26793, N88-26829, N88-26879, N88-27012, N88-27072
W-7405-ENG-36 ..... N88-26382, N88-26383, N88-26384, N88-26392, N88-26422, N88-26438, N88-26449, N88-26491, N88-26606, N88-26637, N88-26650, N88-26653, N88-26659, N88-26682, N88-26690, N88-26730, N88-26813, N88-26827, N88-26866, N88-26874, N88-26900, N88-26901, N88-26921, N88-26923, N88-26931, N88-26932, N88-26939, N88-26943, N88-26949, N88-27063, N88-27065, N88-27097
W-7405-ENG-48 ..... N88-26391, N88-26418, N88-26460, N88-26496, N88-26548, N88-26550, N88-26551, N88-26576, N88-26577, N88-26594, N88-26648, N88-26655, N88-26656, N88-26657, N88-26664, N88-26767, N88-26770, N88-26776, N88-26812
W-31109-ENG-38 ..... N88-26826, N88-26856, N88-26878, N88-26946, N88-26955, N88-26967, N88-26970, N88-26972, N88-26993, N88-26994, N88-27067, N88-27096, N88-27098, N88-27113, N88-27125, N88-27128, N88-26385, N88-26386, N88-26448, N88-26450, N88-26473, N88-26474, N88-26475, N88-26478, N88-26580, N88-26581, N88-26611, N88-26652, N88-26671, N88-26814, N88-26884, N88-26983, N88-26984, N88-27079, N88-27080, N88-27081, N88-27082, N88-27083, N88-27084, N88-27085, N88-27086, N88-27087
W23-03 ..... N88-26334
142-20-10 ..... N88-26498
142-50-10 ..... N88-26497
199-22-76-01 ..... N88-26935, N88-27142
422-00-00-03-07 ..... N88-26736
505-60-11-03 ..... N88-26343
505-60-21-01 ..... N88-26858
505-61-01 ..... N88-26634
505-61-11-02 ..... N88-26913
505-61-51 ..... N88-26367, N88-26378
505-61-71-07 ..... N88-26374
505-62-01 ..... N88-26328, N88-26644
505-62-21 ..... N88-26336, N88-26340, N88-26616, N88-26645, N88-26885
505-63-1B N88-26436, N88-26482
505-63-01-05 ..... N88-26684
505-63-11 ..... N88-26679
505-63-51 ..... N88-26907
505-66-41-02 ..... N88-26344
505-67-11 ..... N88-26349
505-67-51 ..... N88-26348
505-90-01 ..... N88-26376, N88-26377
505-90-21-01 ..... N88-26873
506-41-11 ..... N88-26402
506-41-21 ..... N88-26430
506-43-11-01 ..... N88-26481
506-43-11-04 ..... N88-26413
506-49-31-01 ..... N88-26397
506-64-31 ..... N88-26807
533-02-51 ..... N88-26694
549-02-31-02 ..... N88-26859
549-02-41-01 ..... N88-26870
582-01-11 ..... N88-26641
582-01-41 ..... N88-26401
584-02-11-01 ..... N88-26595
586-01-11 ..... N88-26732
669-00-00 ..... N88-26566
694-00-03 ..... N88-26539
927-11-01-01 ..... N88-26394
992-21-01 ..... N88-26709

REPORT/ACCESSION NUMBER INDEX

Typical Report Number Index Listing

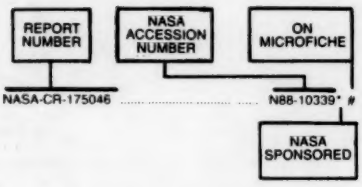

Listings in this index are arranged alphanumerically by report number. The NASA accession number denotes the number by which the citation is identified. An asterisk (*) indicates that the item is a NASA report. A pound sign (#) indicates that the item is available on microfiche.

A-88097 ..... N88-26342* #
A-88151 ..... N88-26378* #
A-88173 ..... N88-26634* #
A-88183 ..... N88-26709* #

ACSC-88-0850 ..... N88-26804 #
ACSC-88-1135 ..... N88-26388 #
ACSC-88-1250 ..... N88-26556 #
ACSC-88-1465 ..... N88-26837 #
ACSC-88-2355 ..... N88-26354 #
ACSC-88-2520 ..... N88-27107 #

AD-A191218 ..... N88-26540 #
AD-A191416 ..... N88-26995 #
AD-A191446 ..... N88-26821 #
AD-A192217 ..... N88-26451 #
AD-A192220 ..... N88-26914 #
AD-A192222 ..... N88-26696 #
AD-A192228 ..... N88-26893 #
AD-A192230 ..... N88-26583 #
AD-A192231 ..... N88-26801 #
AD-A192233 ..... N88-26552 #
AD-A192234 ..... N88-26915 #
AD-A192242 ..... N88-26802 #
AD-A192243 ..... N88-26480 #
AD-A192248 ..... N88-26424 #
AD-A192255 ..... N88-26751 #
AD-A192257 ..... N88-26752 #
AD-A192258 ..... N88-26553 #
AD-A192263 ..... N88-26697 #
AD-A192264 ..... N88-26832 #
AD-A192265 ..... N88-26868 #
AD-A192269 ..... N88-26584 #
AD-A192270 ..... N88-26753 #
AD-A192272 ..... N88-26783 #
AD-A192277 ..... N88-27089 #
AD-A192280 ..... N88-26614 #
AD-A192281 ..... N88-26833 #
AD-A192285 ..... N88-26988 #
AD-A192298 ..... N88-27090 #
AD-A192302 ..... N88-26698 #
AD-A192303 ..... N88-26334 #
AD-A192311 ..... N88-26554 #
AD-A192329 ..... N88-26699 #
AD-A192337 ..... N88-26517 #
AD-A192338 ..... N88-26771 #
AD-A192341 ..... N88-26902 #
AD-A192342 ..... N88-26950 #
AD-A192352 ..... N88-26425 #
AD-A192354 ..... N88-26784 #
AD-A192355 ..... N88-26834 #
AD-A192356 ..... N88-26835 #
AD-A192358 ..... N88-26555 #
AD-A192359 ..... N88-26803 #
AD-A192373 ..... N88-26836 #
AD-A192381 ..... N88-26754 #
AD-A192408 ..... N88-26363 #
AD-A192412 ..... N88-26379 #
AD-A192458 ..... N88-26388 #
AD-A192516 ..... N88-26837 #
AD-A192609 ..... N88-26354 #
AD-A192613 ..... N88-26804 #
AD-A192614 ..... N88-26556 #
AD-A192679 ..... N88-27107 #
AD-A192709 ..... N88-26838 #
AD-A192719 ..... N88-26869 #
AD-A192721 ..... N88-26805 #
AD-A192730 ..... N88-26371 #
AD-A192739 ..... N88-26426 #
AD-A192743 ..... N88-26493 #
AD-A192798 ..... N88-26717 #
AD-A192799 ..... N88-26863 #
AD-A192825 ..... N88-26427 #
AD-A192830 ..... N88-26839 #
AD-A192835 ..... N88-26673 #
AD-A192842 ..... N88-26894 #
AD-A192869 ..... N88-26399 #
AD-A192870 ..... N88-26380 #
AD-A192881 ..... N88-26557 #
AD-A192882 ..... N88-26558 #
AD-A192897 ..... N88-26798 #
AD-A192898 ..... N88-26794 #
AD-A192907 ..... N88-27091 #
AD-A192908 ..... N88-27092 #
AD-A192909 ..... N88-26452 #
AD-A192915 ..... N88-26816 #
AD-A192920 ..... N88-26428 #
AD-A192929 ..... N88-26840 #
AD-A192930 ..... N88-26700 #
AD-A192931 ..... N88-26701 #
AD-A192949 ..... N88-27117 #
AD-A192951 ..... N88-26989 #
AD-A192953 ..... N88-26494 #
AD-A192954 ..... N88-26395 #
AD-A192966 ..... N88-26916 #
AD-A192967 ..... N88-26702 #
AD-A192969 ..... N88-26559 #
AD-A192970 ..... N88-26674 #
AD-A192972 ..... N88-26808 #
AD-A192973 ..... N88-26809 #
AD-A192974 ..... N88-26585 #
AD-A192975 ..... N88-26400 #
AD-A192976 ..... N88-26639 #
AD-A192981 ..... N88-26640 #
AD-A192992 ..... N88-26617 #
AD-A193001 ..... N88-26586 #
AD-A193002 ..... N88-26560 #
AD-A193004 ..... N88-26990 #
AD-A193005 ..... N88-26933 #
AD-A193006 ..... N88-26410 #
AD-A193007 ..... N88-26396 #
AD-A193008 ..... N88-26755 #
AD-A193009 ..... N88-26991 #
AD-A193012 ..... N88-26411 #
AD-A193013 ..... N88-26412 #
AD-A193014 ..... N88-26429 #
AD-A193024 ..... N88-26841 #
AD-A193025 ..... N88-26587 #
AD-A193026 ..... N88-27141 #

AD-E801594 ..... N88-26517 #
AD-E801594 ..... N88-26554 #
AD-E801594 ..... N88-26699 #
AD-E801594 ..... N88-26771 #
AD-E801594 ..... N88-26902 #
AD-E801594 ..... N88-26950 #

AEDC-TSR-88-V7 ..... N88-26403* #

AFAL-TR-88-029 ..... N88-26400 #

AFATL-TR-87-26 ..... N88-26950 #

AFGL-TR-87-0056 ..... N88-26753 #
AFGL-TR-87-0325 ..... N88-26752 #
AFGL-TR-87-0326 ..... N88-26754 #
AFGL-TR-88-0021 ..... N88-26751 #

AFHRL-TP-86-29 ..... N88-26379 #
AFHRL-TP-87-50 ..... N88-26379 #

AFOSR-88-0005TR ..... N88-26995 #
AFOSR-88-0265TR ..... N88-26803 #
AFOSR-88-0282TR ..... N88-26798 #
AFOSR-88-0286TR ..... N88-27091 #
AFOSR-88-0289TR ..... N88-27092 #
AFOSR-88-0294TR ..... N88-26452 #
AFOSR-88-0297TR ..... N88-26428 #
AFOSR-88-0299TR ..... N88-26991 #
AFOSR-88-0304TR ..... N88-26395 #
AFOSR-88-0309TR ..... N88-26411 #
AFOSR-88-0311TR ..... N88-26412 #
AFOSR-88-0328TR ..... N88-26429 #
AFOSR-88-0357TR ..... N88-26894 #
AFOSR-88-0550TR ..... N88-26841 #
AFOSR-88-0567TR ..... N88-26794 #

AFWAL-TR-87-1144 ..... N88-26585 #
AFWAL-TR-87-3055-VOL-1 ..... N88-26809 #
AFWAL-TR-87-4069-VOL-1 ..... N88-26371 #
AFWAL-TR-88-3009 ..... N88-26808 #

AFWL-TN-86-72 ..... N88-26869 #

AFWL-TR-87-119 ..... N88-26639 #

AGARD-AR-243 ..... N88-26382 #

AGARD-R-751 ..... N88-26695 #

AIAA-88-0060 ..... N88-26389 #
AIAA-88-3076 ..... N88-26336* #
AIAA-88-3114 ..... N88-26401* #
AIAA-88-3567 ..... N88-26340* #

AMRC-R-874 ..... N88-26988 #
AMRC-R-1012 ..... N88-26835 #

ANL/MCS-TM-110 ..... N88-26829 #

AR-005-198 ..... N88-26685 #
AR-005-208 ..... N88-26490 #
AR-005-219 ..... N88-26688 #

ARL-TR-87-42 ..... N88-26914 #

ARO-23360.8-MA ..... N88-26821 #

BBN-6728 ..... N88-26802 #

BDX-613-3931 ..... N88-26672 #

BFLRF-247 ..... N88-26673 #

BIO-1 ..... N88-26744* #

BNL-40991 ..... N88-26828 #
BNL-41003 ..... N88-26922 #
BNL-41167 ..... N88-26947 #
BNL-41186 ..... N88-26797 #

B8681472 ..... N88-27132 #
B8681611 ..... N88-27123 #
B8725693 ..... N88-26757 #
B8731729 ..... N88-26844 #
B8733279 ..... N88-26458 #
B8733281 ..... N88-26459 #
B8733285 ..... N88-26537 #
B8735052 ..... N88-26355 #
B8735055 ..... N88-26356 #
B8735061 ..... N88-26643 #
B8735128 ..... N88-26718 #
B8735223 ..... N88-26845 #
B8735224 ..... N88-26846 #
B8736946 ..... N88-27105 #
B8736947 ..... N88-27106 #
B8801071 ..... N88-26886 #
B8801072 ..... N88-26887 #
B8801073 ..... N88-26888 #
B8803156 ..... N88-26895 #
B8803158 ..... N88-26847 #
B8803797 ..... N88-26848 #
B8803798 ..... N88-26896 #
B8803801 ..... N88-26871 #
B8803802 ..... N88-26719 #
B8803803 ..... N88-26366 #
B8803804 ..... N88-26366 #

B8803893 ..... N88-26358 #
B8803894 ..... N88-26677 #
B8803895 ..... N88-26626 #
B8803896 ..... N88-26627 #
B8805148 ..... N88-26864 #
B8805149 ..... N88-26889 #
B8805302 ..... N88-26707 #
B8805303 ..... N88-26706 #
B8805304 ..... N88-26564 #
B8805305 ..... N88-26678 #
B8805306 ..... N88-26629 #
B8805308 ..... N88-26373 #
B8805665 ..... N88-26854 #
B8805666 ..... N88-26904 #
B8805677 ..... N88-26849 #
B8805678 ..... N88-26850 #
B8805679 ..... N88-26851 #
B8805680 ..... N88-26852 #
B8805681 ..... N88-26819 #
B8805682 ..... N88-26853 #

C-11-333 ..... N88-26425 #

CEBAF-PR-88-004 ..... N88-26936 #

CERMA-87-31 ..... N88-26806 #

CERT-OA-13/5005-AYD ..... N88-26623 #

CERT-3/1324-MO ..... N88-26487 #

CESAR-87/41 ..... N88-26670 #
CESAR-88/07 ..... N88-26352 #

CONF-841041 ..... N88-26792 #
CONF-870155-7 ..... N88-26929 #
CONF-870610-22 ..... N88-26947 #
CONF-870679-4 ..... N88-26973 #
CONF-870793-7 ..... N88-26444 #
CONF-870802-40 ..... N88-27125 #
CONF-871007 ..... N88-26993 #
CONF-871007-97 ..... N88-26993 #
CONF-871047-1 ..... N88-26657 #
CONF-871124-99 ..... N88-26460 #
CONF-880110 ..... N88-26856 #
CONF-880110-28 ..... N88-27067 #
CONF-880110-29 ..... N88-26948 #
CONF-880110-33 ..... N88-26856 #
CONF-880118 ..... N88-26472 #
CONF-880118 ..... N88-26473 #
CONF-880118-5 ..... N88-26409 #
CONF-880118-6 ..... N88-26473 #
CONF-880118-7 ..... N88-26474 #
CONF-880118-8 ..... N88-26472 #
CONF-880122-10 ..... N88-26392 #
CONF-880123-2 ..... N88-26874 #
CONF-880123-3 ..... N88-26884 #
CONF-880133-3 ..... N88-26580 #
CONF-880139-4 ..... N88-26369 #
CONF-880181-1 ..... N88-26793 #
CONF-880182-1 ..... N88-27087 #
CONF-880206 ..... N88-27079 #
CONF-880206 ..... N88-27080 #
CONF-880206-4 ..... N88-27065 #
CONF-880206-10 ..... N88-27080 #
CONF-880206-11 ..... N88-27083 #
CONF-880206-12 ..... N88-27079 #
CONF-880207-3 ..... N88-27081 #
CONF-880207-5 ..... N88-27085 #
CONF-880207-6 ..... N88-27084 #
CONF-880208-1 ..... N88-27066 #
CONF-880245-2 ..... N88-26877 #
CONF-880249-1 ..... N88-26960 #
CONF-880256-4 ..... N88-26937 #
CONF-880260-2 ..... N88-26921 #
CONF-880279-1 ..... N88-26475 #
CONF-880307-2 ..... N88-27097 #
CONF-880310-1 ..... N88-26438 #
CONF-880310-2 ..... N88-27098 #
CONF-880311-1 ..... N88-27062 #
CONF-880318-2 ..... N88-26852 #
CONF-880351-3 ..... N88-26741 #
CONF-880364-6 ..... N88-26961 #
CONF-880364-13 ..... N88-26965 #
CONF-880364-14 ..... N88-26637 #
CONF-880364-18 ..... N88-26963 #
CONF-880364-19 ..... N88-26969 #
CONF-880364-21 ..... N88-27113 #
CONF-880364-22 ..... N88-26967 #
CONF-880364-23 ..... N88-26966 #
CONF-880372-1 ..... N88-26923 #
CONF-880372-2 ..... N88-26925 #
CONF-880383-1 ..... N88-26465 #
CONF-880384-1 ..... N88-26945 #
CONF-880390-1 ..... N88-26664 #
CONF-880393-1 ..... N88-26666 #

CONF-880394-2 ..... N88-26797 #
CONF-880408 ..... N88-26470 #
CONF-880408 ..... N88-27082 #
CONF-880408-1 ..... N88-27069 #
CONF-880408-9 ..... N88-26470 #
CONF-880408-13 ..... N88-26946 #
CONF-880408-21 ..... N88-27082 #
CONF-880417-6 ..... N88-26966 #
CONF-880417-9 ..... N88-26970 #
CONF-880417-17 ..... N88-26983 #
CONF-880433-5 ..... N88-26665 #
CONF-880435-6 ..... N88-26421 #
CONF-880435-12 ..... N88-26650 #
CONF-880438-6 ..... N88-26609 #
CONF-880438-7 ..... N88-26611 #
CONF-880462-7 ..... N88-26422 #
CONF-880466-1 ..... N88-26385 #
CONF-880477-5 ..... N88-26730 #
CONF-880478-8 ..... N88-26383 #
CONF-880478-9 ..... N88-26384 #
CONF-880478-11 ..... N88-26967 #
CONF-880478-13 ..... N88-26386 #
CONF-880481-2 ..... N88-27064 #
CONF-880488 ..... N88-26478 #
CONF-880488-1 ..... N88-26467 #
CONF-880488-5 ..... N88-26478 #
CONF-880493-1 ..... N88-26766 #
CONF-880493-2 ..... N88-26767 #
CONF-880494-1 ..... N88-26576 #
CONF-880499 ..... N88-26663 #
CONF-880499-1 ..... N88-26663 #
CONF-880504-2 ..... N88-27086 #
CONF-880512 ..... N88-26972 #
CONF-880512-1 ..... N88-26972 #
CONF-880513-1 ..... N88-26726 #
CONF-880546-3 ..... N88-26932 #
CONF-880549-2 ..... N88-26448 #
CONF-880567-4 ..... N88-26875 #
CONF-880567-6 ..... N88-26814 #
CONF-880579-3 ..... N88-27063 #
CONF-880579-4 ..... N88-26549 #
CONF-880584-1 ..... N88-26943 #
CONF-880588-1 ..... N88-27070 #
CONF-880591-1 ..... N88-27115 #
CONF-880598-3 ..... N88-26581 #
CONF-880601-4 ..... N88-26876 #
CONF-880607-1 ..... N88-26469 #
CONF-880613-2 ..... N88-26442 #
CONF-880613-4 ..... N88-26443 #
CONF-880614 ..... N88-26934 #
CONF-880614-1 ..... N88-26934 #
CONF-880614-2 ..... N88-26931 #
CONF-880615 ..... N88-26727 #
CONF-880615-3 ..... N88-26727 #
CONF-880637-1 ..... N88-26942 #
CONF-880654-3 ..... N88-26690 #
CONF-880658-2 ..... N88-26550 #
CONF-880661-1 ..... N88-26659 #
CONF-880683-1 ..... N88-26660 #
CONF-880683-2 ..... N88-26661 #
CONF-880687-2 ..... N88-26960 #
CONF-880689-1 ..... N88-26351 #
CONF-880693-1 ..... N88-26606 #
CONF-880702-2 ..... N88-26393 #
CONF-880721-1 ..... N88-26670 #
CONF-880745 ..... N88-26862 #
CONF-880745-2 ..... N88-26862 #
CONF-8705291 ..... N88-26938 #
CONF-8706103-8 ..... N88-26435 #
CONF-8707152-VUGRAPHS ..... N88-26548 #
CONF-8708201 ..... N88-27096 #
CONF-8708201-2 ..... N88-27096 #
CONF-8708237-1 ..... N88-26605 #
CONF-8709261-1 ..... N88-27126 #
CONF-8709275-1 ..... N88-27145 #
CONF-8710165-13 ..... N88-26418 #
CONF-8710274-4 ..... N88-26922 #
CONF-8803106-1 ..... N88-26655 #
CONF-8804103-3-VUGRAPHS ..... N88-26985 #
CONF-8804104-1-REV ..... N88-26382 #
CONF-8804105-1 ..... N88-26901 #
CONF-8804109-1 ..... N88-26682 #
CONF-8804115-1 ..... N88-27116 #
CONF-8804117-2 ..... N88-26450 #
CONF-8804117-2 ..... N88-26450 #
CONF-8804123-1 ..... N88-26984 #
CONF-8804124-1 ..... N88-26671 #
CONF-8804141 ..... N88-26930 #
CONF-8804141-1 ..... N88-26930 #
CONF-8805110-1 ..... N88-27072 #
CONF-8805110-2 ..... N88-26879 #
CONF-8805121 ..... N88-26949 #
CONF-8805121-1 ..... N88-26949 #
CONF-8805129-1 ..... N88-26613 #
CONF-8806103-1 ..... N88-26479 #
CONF-8806113-1 ..... N88-26770 #

CONTRIB-813 ..... N88-26765 #

CRC-APRAC-AP-7 ..... N88-26764 #

CRIE-T-86032 ..... N88-26575 #
CRIE-T-86073-PT-1 ..... N88-26742 #
CRIE-T-86080-PT-2 ..... N88-26571 #
CRIE-T-86092 ..... N88-26766 #
CRIE-T-86095-PT-2 ..... N88-26749 #

CRIE-U-86033 ..... N88-26722 #

CRIE-W-86015 ..... N88-26667 #
CRIE-W-86025 ..... N88-26604 #
CRIE-W-86033 ..... N88-26668 #
CRIE-W-86035 ..... N88-26649 #
CRIE-W-86036 ..... N88-26608 #
CRIE-W-87005 ..... N88-26728 #

CSG-87 ..... N88-26860* #

CSIR-TWISK-479 ..... N88-26720 #
CSIR-TWISK-480 ..... N88-26892 #
CSIR-TWISK-483 ..... N88-26891 #
CSIR-TWISK-485 ..... N88-26890 #

CWI-CS-R8754 ..... N88-26849 #
CWI-CS-R8755 ..... N88-26850 #
CWI-CS-R8756 ..... N88-26851 #
CWI-CS-R8757 ..... N88-26852 #
CWI-CS-R8758 ..... N88-26819 #
CWI-CS-R8759 ..... N88-26853 #

CWI-PM-R8708 ..... N88-26904 #
CWI-PM-R8710 ..... N88-26854 #

DE87-702995 ..... N88-26820 #
DE88-001139 ..... N88-26721 #
DE88-001164 ..... N88-27060 #
DE88-002418 ..... N88-26942 #
DE88-003915 ..... N88-26670 #
DE88-004267 ..... N88-26782 #
DE88-004285 ..... N88-26876 #
DE88-004289 ..... N88-26690 #
DE88-005049 ..... N88-26469 #
DE88-005398 ..... N88-26659 #
DE88-006180 ..... N88-26980 #
DE88-006442 ..... N88-26944 #
DE88-006649 ..... N88-26660 #
DE88-006825 ..... N88-26661 #
DE88-006852 ..... N88-26779 #
DE88-006929 ..... N88-26926 #
DE88-006955 ..... N88-26981 #
DE88-007020 ..... N88-26550 #
DE88-007099 ..... N88-26419 #
DE88-007115 ..... N88-26351 #
DE88-007161 ..... N88-26827 #
DE88-007195 ..... N88-26960 #
DE88-007196 ..... N88-26691 #
DE88-007197 ..... N88-27062 #
DE88-007479 ..... N88-26435 #
DE88-007544 ..... N88-26922 #
DE88-007590 ..... N88-26961 #
DE88-007654 ..... N88-26636 #
DE88-007679 ..... N88-27064 #
DE88-007683 ..... N88-26965 #
DE88-007694 ..... N88-26861 #
DE88-007707 ..... N88-27115 #
DE88-007717 ..... N88-26662 #
DE88-007730 ..... N88-26605 #
DE88-007809 ..... N88-26791 #
DE88-007816 ..... N88-26647 #
DE88-007823 ..... N88-26923 #
DE88-007827 ..... N88-26606 #
DE88-007830 ..... N88-26874 #
DE88-007855 ..... N88-26962 #
DE88-007860 ..... N88-26437 #
DE88-007863 ..... N88-26607 #
DE88-007870 ..... N88-26740 #
DE88-007890 ..... N88-26392 #
DE88-007897 ..... N88-26438 #
DE88-007898 ..... N88-26943 #
DE88-007899 ..... N88-26637 #
DE88-007900 ..... N88-26384 #
DE88-007901 ..... N88-27065 #
DE88-007902 ..... N88-26383 #
DE88-007905 ..... N88-26921 #
DE88-007938 ..... N88-26420 #
DE88-007951 ..... N88-26792 #
DE88-007959 ..... N88-26924 #
DE88-007966 ..... N88-26628 #
DE88-007987 ..... N88-26738 #
DE88-008016 ..... N88-26899 #
DE88-008031 ..... N88-26925 #
DE88-008037 ..... N88-26418 #
DE88-008043 ..... N88-26460 #

DE88-008050 ..... N88-26516 #
DE88-008086 ..... N88-26929 #
DE88-008091 ..... N88-26442 #
DE88-008114 ..... N88-26875 #
DE88-008118 ..... N88-26467 #
DE88-008170 ..... N88-26966 #
DE88-008205 ..... N88-26741 #
DE88-008210 ..... N88-26877 #
DE88-008230 ..... N88-26927 #
DE88-008233 ..... N88-26468 #
DE88-008234 ..... N88-27061 #
DE88-008240 ..... N88-26723 #
DE88-008247 ..... N88-27066 #
DE88-008292 ..... N88-26729 #
DE88-008335 ..... N88-26766 #
DE88-008343 ..... N88-27067 #
DE88-008345 ..... N88-26576 #
DE88-008346 ..... N88-26548 #
DE88-008347 ..... N88-26967 #
DE88-008360 ..... N88-26963 #
DE88-008369 ..... N88-26393 #
DE88-008381 ..... N88-26470 #
DE88-008383 ..... N88-26663 #
DE88-008394 ..... N88-26574 #
DE88-008397 ..... N88-26724 #
DE88-008406 ..... N88-26964 #
DE88-008442 ..... N88-26415 #
DE88-008465 ..... N88-26829 #
DE88-008475 ..... N88-26948 #
DE88-008566 ..... N88-26968 #
DE88-008573 ..... N88-26830 #
DE88-008596 ..... N88-26936 #
DE88-008600 ..... N88-27077 #
DE88-008633 ..... N88-26681 #
DE88-008636 ..... N88-26680 #
DE88-008637 ..... N88-26812 #
DE88-008666 ..... N88-26465 #
DE88-008668 ..... N88-26945 #
DE88-008688 ..... N88-26862 #
DE88-008719 ..... N88-26715 #
DE88-008726 ..... N88-26900 #
DE88-008737 ..... N88-26969 #
DE88-008744 ..... N88-26579 #
DE88-008763 ..... N88-26725 #
DE88-008780 ..... N88-27068 #
DE88-008794 ..... N88-27069 #
DE88-008799 ..... N88-27070 #
DE88-008890 ..... N88-26664 #
DE88-008898 ..... N88-27098 #
DE88-008899 ..... N88-27128 #
DE88-008900 ..... N88-27113 #
DE88-008906 ..... N88-26970 #
DE88-008908 ..... N88-27125 #
DE88-008916 ..... N88-26946 #
DE88-008920 ..... N88-26577 #
DE88-008930 ..... N88-26971 #
DE88-008941 ..... N88-27071 #
DE88-008943 ..... N88-27104 #
DE88-008954 ..... N88-26489 #
DE88-008961 ..... N88-26352 #
DE88-008969 ..... N88-26776 #
DE88-008971 ..... N88-26878 #
DE88-008972 ..... N88-26648 #
DE88-009062 ..... N88-26443 #
DE88-009108 ..... N88-26665 #
DE88-009120 ..... N88-26770 #
DE88-009121 ..... N88-26901 #
DE88-009124 ..... N88-26650 #
DE88-009136 ..... N88-27063 #
DE88-009145 ..... N88-26682 #
DE88-009152 ..... N88-26422 #
DE88-009153 ..... N88-27097 #
DE88-009155 ..... N88-26866 #
DE88-009164 ..... N88-26444 #
DE88-009168 ..... N88-27076 #
DE88-009177 ..... N88-26813 #
DE88-009186 ..... N88-26826 #
DE88-009254 ..... N88-26549 #
DE88-009269 ..... N88-26651 #
DE88-009467 ..... N88-26423 #
DE88-009537 ..... N88-26391 #
DE88-009562 ..... N88-26982 #
DE88-009578 ..... N88-27130 #
DE88-009588 ..... N88-26726 #
DE88-009592 ..... N88-26445 #
DE88-009617 ..... N88-26855 #
DE88-009679 ..... N88-26471 #
DE88-009707 ..... N88-27116 #
DE88-009708 ..... N88-26409 #
DE88-009821 ..... N88-26972 #
DE88-009828 ..... N88-26767 #
DE88-009839 ..... N88-26797 #
DE88-009840 ..... N88-26947 #
DE88-009870 ..... N88-26578 #
DE88-009889 ..... N88-26446 #
DE88-009890 ..... N88-26447 #
DE88-009937 ..... N88-26472 #
DE88-009955 ..... N88-26385 #
DE88-009957 ..... N88-27079 #
DE88-009959 ..... N88-27080 #
DE88-009965 ..... N88-26473 #
DE88-009971 ..... N88-27081 #
DE88-009973 ..... N88-26814 #
DE88-009989 ..... N88-26652 #
DE88-009990 ..... N88-26474 #
DE88-009999 ..... N88-27082 #
DE88-010005 ..... N88-27083 #
DE88-010007 ..... N88-26983 #
DE88-010009 ..... N88-26671 #
DE88-010022 ..... N88-26386 #
DE88-010023 ..... N88-26580 #
DE88-010030 ..... N88-27084 #
DE88-010032 ..... N88-26884 #
DE88-010033 ..... N88-26793 #
DE88-010034 ..... N88-26369 #
DE88-010050 ..... N88-27085 #
DE88-010053 ..... N88-26984 #
DE88-010054 ..... N88-27086 #
DE88-010057 ..... N88-26879 #
DE88-010058 ..... N88-26581 #
DE88-010063 ..... N88-26611 #
DE88-010075 ..... N88-26475 #
DE88-010090 ..... N88-27087 #
DE88-010094 ..... N88-27072 #
DE88-010097 ..... N88-26448 #
DE88-010131 ..... N88-26985 #
DE88-010187 ..... N88-26582 #
DE88-010233 ..... N88-26492 #
DE88-010245 ..... N88-26476 #
DE88-010357 ..... N88-26408 #
DE88-010364 ..... N88-26727 #
DE88-010450 ..... N88-26930 #
DE88-010475 ..... N88-26449 #
DE88-010479 ..... N88-26491 #
DE88-010510 ..... N88-26594 #
DE88-010579 ..... N88-26612 #
DE88-010585 ..... N88-26986 #
DE88-010586 ..... N88-26987 #
DE88-010598 ..... N88-26955 #
DE88-010602 ..... N88-26551 #
DE88-010608 ..... N88-26666 #
DE88-010611 ..... N88-26672 #
DE88-010655 ..... N88-26938 #
DE88-010692 ..... N88-26461 #
DE88-010711 ..... N88-26655 #
DE88-010714 ..... N88-27096 #
DE88-010729 ..... N88-26496 #
DE88-010783 ..... N88-26937 #
DE88-010799 ..... N88-27088 #
DE88-010882 ..... N88-26934 #
DE88-010886 ..... N88-27145 #
DE88-010907 ..... N88-26382 #
DE88-010909 ..... N88-26730 #
DE88-010910 ..... N88-26931 #
DE88-010919 ..... N88-26932 #
DE88-010956 ..... N88-26949 #
DE88-011013 ..... N88-26613 #
DE88-011080 ..... N88-26731 #
DE88-011172 ..... N88-26477 #
DE88-011194 ..... N88-26450 #
DE88-011196 ..... N88-26478 #
DE88-011215 ..... N88-26689 #
DE88-011260 ..... N88-26653 #
DE88-011261 ..... N88-26939 #
DE88-011326 ..... N88-26993 #
DE88-011331 ..... N88-26856 #
DE88-011356 ..... N88-26656 #
DE88-011396 ..... N88-26479 #
DE88-011729 ..... N88-26657 #
DE88-011755 ..... N88-26994 #
DE88-101851 ..... N88-26881 #
DE88-701823 ..... N88-26769 #
DE88-701824 ..... N88-26743 #
DE88-701827 ..... N88-27099 #
DE88-701829 ..... N88-26880 #
DE88-701832 ..... N88-27100 #
DE88-701834 ..... N88-27101 #
DE88-701835 ..... N88-26333 #
DE88-701839 ..... N88-26610 #
DE88-701841 ..... N88-26928 #
DE88-701852 ..... N88-26882 #
DE88-701860 ..... N88-26883 #
DE88-701866 ..... N88-26750 #
DE88-701867 ..... N88-27073 #
DE88-701868 ..... N88-27074 #
DE88-701870 ..... N88-26905 #
DE88-701872 ..... N88-26974 #
DE88-701873 ..... N88-27129 #
DE88-701876 ..... N88-26669 #
DE88-701877 ..... N88-26440 #
DE88-701878 ..... N88-27075 #
DE88-701880 ..... N88-26441 #
DE88-701881 ..... N88-27078 #
DE88-701882 ..... N88-26975 #
DE88-701885 ..... N88-26976 #
DE88-701887 ..... N88-26977 #
DE88-701893 ..... N88-26978 #
DE88-701894 ..... N88-26692 #
DE88-701895 ..... N88-26979 #
DE88-701899 ..... N88-27102 #
DE88-702195 ..... N88-27058 #
DE88-752075 ..... N88-26575 #
DE88-752547 ..... N88-26604 #
DE88-753104 ..... N88-26742 #
DE88-753108 ..... N88-26768 #
DE88-753109 ..... N88-26749 #
DE88-753114 ..... N88-26667 #
DE88-753117 ..... N88-26688 #
DE88-753119 ..... N88-26649 #
DE88-753120 ..... N88-26606 #
DE88-753121 ..... N88-26728 #
DE88-770148 ..... N88-26722 #
DE88-770191 ..... N88-26571 #

DFVLR-MITT-87-10 ..... N88-26842* #
DFVLR-MITT-87-22 ..... N88-26518 #

DOE/AL-16310/T2 ..... N88-26423 #

DOE/APC-88-1 ..... N88-26738 #

DOE/DP-40200/66 ..... N88-26948 #

DOE/ER-04447/235 ..... N88-27061 #
DOE/ER-10597/1 ..... N88-26415 #
DOE/ER-13448/T3 ..... N88-26944 #
DOE/ER-13591/2 ..... N88-26468 #
DOE/ER-13631/2 ..... N88-26725 #
DOE/ER-13655/3 ..... N88-26924 #
DOE/ER-13788/1 ..... N88-26651 #
DOE/ER-25026/20 ..... N88-26830 #
DOE/ER-40150/45 ..... N88-27077 #
DOE/ER-40150/46 ..... N88-26938 #
DOE/ER-40214/2 ..... N88-26927 #
DOE/ER-40235/1 ..... N88-26926 #
DOE/ER-40423/02-P8 ..... N88-27130 #
DOE/ER-45104/3 ..... N88-26476 #
DOE/ER-45114/5 ..... N88-26477 #
DOE/ER-45123/4 ..... N88-26471 #
DOE/ER-45167/8 ..... N88-26689 #
DOE/ER-45211/4 ..... N88-26444 #
DOE/ER-45211/6 ..... N88-27076 #
DOE/ER-45219/3 ..... N88-27088 #
DOE/ER-45253/2 ..... N88-27068 #
DOE/ER-45310/8 ..... N88-26446 #
DOE/ER-45311/T1 ..... N88-26447 #
DOE/ER-45315/1 ..... N88-26445 #
DOE/ER-45328/1 ..... N88-26420 #
DOE/ER-60266/T2 ..... N88-26779 #
DOE/ER-60594/1 ..... N88-26715 #

DOE/ET-33006/025 ..... N88-26981 #
DOE/ET-53088/312 ..... N88-26982 #

DOE/FE-0105 ..... N88-26731 #
DOE/FE-60336/2557 ..... N88-26582 #

DOE/MC-20037/T1 ..... N88-26782 #

DOE/NE-53207/T1 ..... N88-26968 #

DOE/PC-90016/T2 ..... N88-26492 #
DOE/PC-90962/T6 ..... N88-26612 #

DOE/WET-88-1 ..... N88-26729 #

DOT/FAA/CT-86/3 ..... N88-26495* #
DOT/FAA/CT-88/22 ..... N88-26350 #

DOT/FAA/PS-88/15 ..... N88-26344* #

DP-MS-88-37 ..... N88-26665 #

DTRC-AD-CR-01-87 ..... N88-26334 #

D210-12380-1 ..... N88-26367* #

E-3759 ..... N88-26376* #
E-3760 ..... N88-26377* #
E-3842-1 ..... N88-26482* #
E-4035 ..... N88-26679* #
E-4062 ..... N88-26885* #
E-4064 ..... N88-26566* #
E-4082 ..... N88-26539* #
E-4101 ..... N88-26732* #
E-4134 ..... N88-26644* #
E-4163 ..... N88-26340* #
E-4223 ..... N88-26616* #

E-4231 ..... N88-26436* #
E-4236 ..... N88-26645* #
E-4252 ..... N88-26430* #
E-4256 ..... N88-26401* #
E-4258 ..... N88-26402* #
E-4276 ..... N88-26328* #
E-4277 ..... N88-26641* #
E-4287 ..... N88-26336* #

EEC-205 ..... N88-26353 #

EEI-88-178 ..... N88-27135* #

EGG-M-00388 ..... N88-27115 #
EGG-M-12987 ..... N88-26605 #
EGG-M-17287 ..... N88-26973 #

EGG-MS-7858 ..... N88-26662 #

ENST-87E017 ..... N88-26843 #

EPA/600/3-88/011 ..... N88-26762 #
EPA/600/4-88/014 ..... N88-26739 #

ESL-716148-31 ..... N88-26585* #

ETN-88-91805 ..... N88-26757 #
ETN-88-91950 ..... N88-27118 #
ETN-88-92091 ..... N88-27122 #
ETN-88-92092 ..... N88-26683 #
ETN-88-92095 ..... N88-26620 #
ETN-88-92099 ..... N88-26364 #
ETN-88-92100 ..... N88-26485 #
ETN-88-92119 ..... N88-26733 #
ETN-88-92120 ..... N88-27093 #
ETN-88-92121 ..... N88-26951 #
ETN-88-92122 ..... N88-26561 #
ETN-88-92123 ..... N88-26432 #
ETN-88-92124 ..... N88-26952 #
ETN-88-92125 ..... N88-26953 #
ETN-88-92128 ..... N88-26703 #
ETN-88-92129 ..... N88-26676 #
ETN-88-92131 ..... N88-26642 #
ETN-88-92132 ..... N88-26621 #
ETN-88-92133 ..... N88-26734 #
ETN-88-92134 ..... N88-26704 #
ETN-88-92135 ..... N88-27103 #
ETN-88-92136 ..... N88-26799 #
ETN-88-92147 ..... N88-26365 #
ETN-88-92155 ..... N88-26486 #
ETN-88-92157 ..... N88-26414 #
ETN-88-92159 ..... N88-26622 #
ETN-88-92162 ..... N88-26487 #
ETN-88-92164 ..... N88-26623 #
ETN-88-92167 ..... N88-26488 #
ETN-88-92169 ..... N88-26705 #
ETN-88-92179 ..... N88-26843 #
ETN-88-92228 ..... N88-26844 #
ETN-88-92291 ..... N88-27131 #
ETN-88-92292 ..... N88-26772 #
ETN-88-92300 ..... N88-26433 #
ETN-88-92305 ..... N88-26940 #
ETN-88-92306 ..... N88-26624 #
ETN-88-92307 ..... N88-26568 #
ETN-88-92309 ..... N88-26456 #
ETN-88-92314 ..... N88-26518 #
ETN-88-92346 ..... N88-26758 #
ETN-88-92348 ..... N88-26773 #
ETN-88-92349 ..... N88-26774 #
ETN-88-92350 ..... N88-26457 #
ETN-88-92351 ..... N88-26372 #
ETN-88-92352 ..... N88-26569 #
ETN-88-92353 ..... N88-26654 #
ETN-88-92357 ..... N88-27094 #
ETN-88-92358 ..... N88-26625 #
ETN-88-92359 ..... N88-26775 #
ETN-88-92371 ..... N88-26818 #
ETN-88-92373 ..... N88-26590 #
ETN-88-92374 ..... N88-26626 #
ETN-88-92384 ..... N88-26591 #
ETN-88-92385 ..... N88-26592 #
ETN-88-92423 ..... N88-26718 #
ETN-88-92424 ..... N88-26643 #
ETN-88-92429 ..... N88-26355 #
ETN-88-92443 ..... N88-26845 #
ETN-88-92444 ..... N88-26846 #
ETN-88-92448 ..... N88-27105 #
ETN-88-92449 ..... N88-27106 #
ETN-88-92455 ..... N88-26537 #
ETN-88-92467 ..... N88-26458 #
ETN-88-92468 ..... N88-26459 #
ETN-88-92470 ..... N88-27112 #
ETN-88-92472 ..... N88-26356 #
ETN-88-92473 ..... N88-26357 #
ETN-88-92543 ..... N88-26806 #
ETN-88-92566 ..... N88-26917 #

ETN-88-92567 ..... N88-26562 #
ETN-88-92568 ..... N88-26954 #
ETN-88-92570 ..... N88-26593 #
ETN-88-92571 ..... N88-26563 #
ETN-88-92572 ..... N88-26886 #
ETN-88-92573 ..... N88-26847 #
ETN-88-92574 ..... N88-26887 #
ETN-88-92575 ..... N88-26888 #
ETN-88-92576 ..... N88-26895 #
ETN-88-92577 ..... N88-26848 #
ETN-88-92578 ..... N88-26896 #
ETN-88-92579 ..... N88-26864 #
ETN-88-92581 ..... N88-26889 #
ETN-88-92587 ..... N88-26849 #
ETN-88-92588 ..... N88-26850 #
ETN-88-92589 ..... N88-26851 #
ETN-88-92590 ..... N88-26852 #
ETN-88-92591 ..... N88-26819 #
ETN-88-92592 ..... N88-26853 #
ETN-88-92597 ..... N88-26904 #
ETN-88-92596 ..... N88-26854 #
ETN-88-92599 ..... N88-26627 #
ETN-88-92600 ..... N88-26677 #
ETN-88-92601 ..... N88-26628 #
ETN-88-92602 ..... N88-26366 #
ETN-88-92603 ..... N88-26629 #
ETN-88-92604 ..... N88-26871 #
ETN-88-92605 ..... N88-26564 #
ETN-88-92607 ..... N88-26368 #
ETN-88-92608 ..... N88-26719 #
ETN-88-92609 ..... N88-26678 #
ETN-88-92610 ..... N88-26358 #
ETN-88-92611 ..... N88-26373 #
ETN-88-92613 ..... N88-26706 #
ETN-88-92614 ..... N88-26707 #
ETN-88-92618 ..... N88-26630 #
ETN-88-92619 ..... N88-26992 #
ETN-88-92622 ..... N88-27132 #
ETN-88-92623 ..... N88-27123 #
ETN-88-92726 ..... N88-26631 #
ETN-88-92727 ..... N88-27095 #
ETN-88-92728 ..... N88-27124 #
ETN-88-92729 ..... N88-26708 #
ETN-88-92730 ..... N88-26632 #
ETN-88-92732 ..... N88-26633 #
ETN-88-92734 ..... N88-26339 #

EUR-10570-IT ..... N88-26777 #
EUR-10682-EN ..... N88-26370 #

FCR-9206 ..... N88-26582 #

FEL-1986-64 ..... N88-26917 #
FEL-1987-05 ..... N88-26562 #
FEL-1987-14 ..... N88-26954 #
FEL-1987-48 ..... N88-26593 #
FEL-1987-56 ..... N88-26563 #

FMI-5 ..... N88-26746 #

FNAL-TM-1519 ..... N88-26938 #

GA-A-19100 ..... N88-26964 #
GA-A-19159 ..... N88-26986 #
GA-A-19174 ..... N88-26987 #
GA-A-19192 ..... N88-26969 #
GA-A-19217 ..... N88-26963 #
GA-A-19239 ..... N88-26966 #

GEPP-TIS-366E ..... N88-26579 #

GRI-87/0346 ..... N88-26714 #
GRI-88/0001 ..... N88-26602 #
GRI-88/0005 ..... N88-26463 #
GRI-88/0044 ..... N88-26791 #
GRI-88/0066 ..... N88-26416 #

H-1435 ..... N88-26694* #
H-1483 ..... N88-26361* #

HDL-CR-88-052-1 ..... N88-26557 #
HDL-CR-88-052-2 ..... N88-26558 #

HNDSP-86-117-ED-ES-REV ..... N88-27117 #

IC-86/239 ..... N88-26769 #
IC-86/240 ..... N88-26743 #
IC-86/287 ..... N88-27099 #
IC-86/317 ..... N88-26880 #
IC-86/328 ..... N88-27100 #
IC-86/336 ..... N88-27101 #
IC-86/346 ..... N88-26333 #
IC-86/364 ..... N88-26610 #
IC-86/371 ..... N88-26928 #
IC-86/390 ..... N88-26881 #
IC-86/393 ..... N88-26882 #

IC-87/117 ..... N88-26883 #
IC-87/123 ..... N88-26750 #
IC-87/124 ..... N88-27073 #
IC-87/125 ..... N88-27074 #
IC-87/127 ..... N88-26905 #
IC-87/129 ..... N88-26974 #
IC-87/130 ..... N88-27129 #
IC-87/134 ..... N88-26669 #
IC-87/135 ..... N88-26440 #
IC-87/136 ..... N88-27075 #
IC-87/138 ..... N88-26441 #
IC-87/139 ..... N88-27076 #
IC-87/140 ..... N88-26975 #
IC-87/143 ..... N88-26976 #
IC-87/145 ..... N88-26977 #
IC-87/151 ..... N88-26978 #
IC-87/152 ..... N88-26692 #
IC-87/153 ..... N88-26979 #
IC-87/157 ..... N88-27102 #

ICASE-88-36 ..... N88-26873* #

ICOMP-88-9 ..... N88-26885* #

IFSR-312 ..... N88-26982 #

IMFL-87/30 ..... N88-26622 #

INPE-4535-PRE/1282 ..... N88-26570 #
INPE-4542-PRE/1288 ..... N88-26824 #

IPPJ-867 ..... N88-26957 #
IPPJ-869 ..... N88-26956 #

IR-125 ..... N88-27114 #
IR-127 ..... N88-26857 #

ISAS-RN-350 ..... N88-26598 #
ISAS-RN-355 ..... N88-26918 #
ISAS-RN-360 ..... N88-27143 #
ISAS-RN-366 ..... N88-26919 #
ISAS-RN-622 ..... N88-26330 #
ISAS-RN-623 ..... N88-26329 #
ISAS-RN-627 ..... N88-26600 #
ISAS-RN-628 ..... N88-26599 #

ISAS-SP-6 ..... N88-26499 #

ISBN-91-7848-089-2 ..... N88-26910 #
ISBN-91-86002-58-9 ..... N88-27111 #
ISBN-92-825-6541-6 ..... N88-26370 #
ISBN-92-835-0448-1 ..... N88-26695 #
ISBN-92-835-0450-X ..... N88-26362 #
ISBN-951-754-195-3 ..... N88-26538 #
ISBN-951-754-389-1 ..... N88-26573 #
ISBN-951-754-400-6 ..... N88-26439 #
ISBN-951-754-405-7 ..... N88-26546 #
ISBN-951-754-430-8 ..... N88-26796 #

ISI/RR-88-200 ..... N88-26832 #

ISL-R-106/87 ..... N88-26633 #
ISL-R-113/87 ..... N88-26339 #

ISSN-0038-0911 ..... N88-27138 #
ISSN-0038-0911 ..... N88-27139 #
ISSN-0069-5882 ..... N88-26758 #
ISSN-0069-5882 ..... N88-26773 #
ISSN-0069-5882 ..... N88-26774 #
ISSN-0078-3781 ..... N88-26631 #
ISSN-0078-3781 ..... N88-26632 #
ISSN-0078-3781 ..... N88-26708 #
ISSN-0078-3781 ..... N88-27095 #
ISSN-0078-3781 ..... N88-27124 #
ISSN-0169-1708 ..... N88-26757 #
ISSN-0176-7739 ..... N88-26518 #
ISSN-0285-6808 ..... N88-26329 #
ISSN-0285-6808 ..... N88-26330 #
ISSN-0285-6808 ..... N88-26599 #
ISSN-0285-6808 ..... N88-26600 #
ISSN-0288-433X ..... N88-26499 #
ISSN-0348-9329 ..... N88-26920 #
ISSN-0452-2982 ..... N88-26290 #
ISSN-0469-4732 ..... N88-26956 #
ISSN-0469-4732 ..... N88-26957 #
ISSN-0721-4529 ..... N88-26683 #
ISSN-0751-1353 ..... N88-26843 #
ISSN-0920-2358 ..... N88-26845 #
ISSN-0920-2358 ..... N88-26846 #
ISSN-0920-2358 ..... N88-27105 #
ISSN-0920-2358 ..... N88-27106 #
ISSN-0920-8577 ..... N88-26847 #
ISSN-0920-8577 ..... N88-26848 #
ISSN-0920-8577 ..... N88-26864 #
ISSN-0920-8577 ..... N88-26886 #
ISSN-0920-8577 ..... N88-26887 #

ISSN-0920-8577 ..... N88-26888 #
ISSN-0920-8577 ..... N88-26889 #
ISSN-0920-8577 ..... N88-26895 #
ISSN-0920-8577 ..... N88-26896 #

ITOP-6-2-246 ..... N88-26540 #

IWR-88-R-3 ..... N88-26817 #

JIAA-TR-86 ..... N88-26335* #

JINR-R-10-86-612 ..... N88-26820 #
JINR-R-17-87-497 ..... N88-27058 #

JNL206.B87-046 ..... N88-26844 #

JPL-PUB-D-5518 ..... N88-26495* #

JPL-PUBL-88-10 ..... N88-26736* #
JPL-PUBL-88-14 ..... N88-26859* #

JPRS-ULS-88-009 ..... N88-26785 #

K/ETAC-38 ..... N88-26638 #

KNMI-TR-100 ..... N88-26757 #

L-16399 ..... N88-26907* #
L-16422 ..... N88-26374* #
L-16439 ..... N88-26344* #
L-16453 ..... N88-26684* #
L-16461 ..... N88-26935* #

LA-UR-87-227 ..... N88-26813 #
LA-UR-87-4218 ..... N88-26690 #
LA-UR-88-313 ..... N88-26659 #
LA-UR-88-748 ..... N88-26921 #
LA-UR-88-782 ..... N88-26383 #
LA-UR-88-788 ..... N88-27065 #
LA-UR-88-789 ..... N88-26384 #
LA-UR-88-797 ..... N88-26637 #
LA-UR-88-798 ..... N88-26943 #
LA-UR-88-809 ..... N88-26438 #
LA-UR-88-847 ..... N88-26392 #
LA-UR-88-915 ..... N88-26874 #
LA-UR-88-963 ..... N88-26606 #
LA-UR-88-1015 ..... N88-26923 #
LA-UR-88-1077 ..... N88-26682 #
LA-UR-88-1110-REV ..... N88-26382 #
LA-UR-88-1121 ..... N88-26422 #
LA-UR-88-1126 ..... N88-27097 #
LA-UR-88-1166 ..... N88-26866 #
LA-UR-88-1226 ..... N88-27063 #
LA-UR-88-1261 ..... N88-26730 #
LA-UR-88-1281 ..... N88-26650 #
LA-UR-88-1326 ..... N88-26901 #
LA-UR-88-1328 ..... N88-26770 #
LA-UR-88-1446 ..... N88-26931 #
LA-UR-88-1458 ..... N88-26949 #
LA-UR-88-1695 ..... N88-26932 #

LA-11155-MS ..... N88-26827 #
LA-11192-MS ..... N88-26449 #
LA-11220-PR ..... N88-26939 #
LA-11239-MS ..... N88-26491 #
LA-11278 ..... N88-26900 #
LA-11312-MS ..... N88-26653 #

LBL-23597 ..... N88-26877 #
LBL-24157 ..... N88-27066 #
LBL-24340 ..... N88-26723 #
LBL-24417 ..... N88-27145 #
LBL-24452 ..... N88-26937 #
LBL-24647 ..... N88-26574 #
LBL-24686 ..... N88-26934 #
LBL-24788 ..... N88-26724 #
LBL-25124 ..... N88-26727 #
LBL-25165 ..... N88-26408 #

LC-79-640375 ..... N88-27138 #
LC-79-640375 ..... N88-27139 #

LG88ER0056 ..... N88-26360* #

LR-507 ..... N88-26537 #
LR-514 ..... N88-26417 #
LR-527-PT-1 ..... N88-26458 #
LR-527-PT-2 ..... N88-26459 #

LSI-TR-596-28 ..... N88-26807* #

LUIP-8802 ..... N88-26920 #

LUNFD6/(NFFK-7085)1-29 ..... N88-26920 #

MDC-K0445 ..... N88-26334 #

MIT-R88-06 ..... N88-26745* #

MIT-317 ..... N88-26745* #

MITT-53 ..... N88-26758 #
MITT-55 ..... N88-26773 #
MITT-57 ..... N88-26774 #

MPA-86-02 ..... N88-26683 #

MRL-R-1111 ..... N88-26686 #

MRL-TN-526 ..... N88-26685 #
MRL-TN-528 ..... N88-26490 #

MSC-6186 ..... N88-26444 #
MSC-6391 ..... N88-27078 #

MSSR-534(R) ..... N88-26838 #

MTR-1/88 ..... N88-26439 #

NAL-SP-8 ..... N88-26290 #

NAS 1.15:4036 ..... N88-27144* #
NAS 1.15:4041 ..... N88-27133* #
NAS 1.15:4049 ..... N88-26763* #
NAS 1.15:4050 ..... N88-26374* #
NAS 1.15:4051 ..... N88-26389* #
NAS 1.15:4053 ..... N88-26935* #
NAS 1.15:77480 ..... N88-26615* #
NAS 1.15:100068 ..... N88-26342* #
NAS 1.15:100182 ..... N88-26376* #
NAS 1.15:100183 ..... N88-26377* #
NAS 1.15:100325 ..... N88-26387* #
NAS 1.15:100439 ..... N88-26361* #
NAS 1.15:100567 ..... N88-26870* #
NAS 1.15:100633 ..... N88-26394* #
NAS 1.15:100637 ..... N88-26913* #
NAS 1.15:100641 ..... N88-26481* #
NAS 1.15:100858 ..... N88-26885* #
NAS 1.15:100859 ..... N88-26566* #
NAS 1.15:100893 ..... N88-26644* #
NAS 1.15:100902 ..... N88-26539* #
NAS 1.15:100911 ..... N88-26340* #
NAS 1.15:100943 ..... N88-26436* #
NAS 1.15:100958 ..... N88-26430* #
NAS 1.15:100961 ..... N88-26679* #
NAS 1.15:100963 ..... N88-26401* #
NAS 1.15:100965 ..... N88-26402* #
NAS 1.15:100967 ..... N88-26482* #
NAS 1.15:100973 ..... N88-26645* #
NAS 1.15:100984 ..... N88-26744* #
NAS 1.15:100985 ..... N88-26795* #
NAS 1.15:100991 ..... N88-26378* #
NAS 1.15:100998 ..... N88-26634* #
NAS 1.15:101002 ..... N88-26709* #
NAS 1.15:101134 ..... N88-26385 #
NAS 1.15:101159 ..... N88-27142* #
NAS 1.15:101175 ..... N88-26544* #
NAS 1.15:101294 ..... N88-26328* #
NAS 1.15:101295 ..... N88-26641* #
NAS 1.15:101296 ..... N88-26732* #
NAS 1.21:7011(313) ..... N88-26800* #
NAS 1.26:4149 ..... N88-27134* #
NAS 1.26:4167 ..... N88-26595* #
NAS 1.26:4168 ..... N88-26343* #
NAS 1.26:4169 ..... N88-26858* #
NAS 1.26:172049 ..... N88-27135* #
NAS 1.26:172063 ..... N88-26359* #
NAS 1.26:177378 ..... N88-26807* #
NAS 1.26:177393 ..... N88-27120* #
NAS 1.26:177436 ..... N88-26367* #
NAS 1.26:177459 ..... N88-26349* #
NAS 1.26:177460 ..... N88-26348* #
NAS 1.26:179357 ..... N88-26635* #
NAS 1.26:179359 ..... N88-26760* #
NAS 1.26:179364 ..... N88-26619* #
NAS 1.26:179366 ..... N88-26825* #
NAS 1.26:179435 ..... N88-26694* #
NAS 1.26:180223 ..... N88-26403* #
NAS 1.26:180400 ..... N88-26737* #
NAS 1.26:181617 ..... N88-26397* #
NAS 1.26:181670 ..... N88-26413* #
NAS 1.26:181674 ..... N88-26873* #
NAS 1.26:182121 ..... N88-26360* #
NAS 1.26:182140 ..... N88-26497* #
NAS 1.26:182152 ..... N88-27119* #
NAS 1.26:182153 ..... N88-26616* #
NAS 1.26:182154 ..... N88-26498* #
NAS 1.26:182167 ..... N88-26336* #
NAS 1.26:182480 ..... N88-26859* #
NAS 1.26:182540 ..... N88-26909* #
NAS 1.26:182550 ..... N88-26601* #
NAS 1.26:182725 ..... N88-26495* #
NAS 1.26:182861 ..... N88-26712* #
NAS 1.26:182862 ..... N88-26716* #
NAS 1.26:182897 ..... N88-26745* #
NAS 1.26:182939 ..... N88-26823* #
NAS 1.26:182956 ..... N88-26911* #
NAS 1.26:182975 ..... N88-26710* #
NAS 1.26:182984 ..... N88-26464* #
NAS 1.26:183026 ..... N88-27108* #
NAS 1.26:183036 ..... N88-26711* #
NAS 1.26:183053 ..... N88-26569* #
NAS 1.26:183058 ..... N88-27121* #
NAS 1.26:183059 ..... N88-26688* #
NAS 1.26:183060 ..... N88-26347* #
NAS 1.26:183061 ..... N88-26332* #
NAS 1.26:183062 ..... N88-26603* #
NAS 1.26:183064 ..... N88-26941* #
NAS 1.26:183066 ..... N88-26747* #
NAS 1.26:183067 ..... N88-26407* #
NAS 1.26:183069 ..... N88-26289* #
NAS 1.26:183070 ..... N88-26860* #
NAS 1.26:183078 ..... N88-26545* #
NAS 1.26:183082 ..... N88-26693* #
NAS 1.26:183089 ..... N88-26867* #
NAS 1.26:183098 ..... N88-27137* #
NAS 1.26:183099 ..... N88-27136* #
NAS 1.26:183101 ..... N88-26335* #
NAS 1.26:183110 ..... N88-26675* #
NAS 1.26:183111 ..... N88-27146* #
NAS 1.26:183115 ..... N88-26567* #
NAS 1.26:183117 ..... N88-26759* #
NAS 1.26:183118 ..... N88-26778* #
NAS 1.26:183119 ..... N88-26618* #
NAS 1.26:183124 ..... N88-26565* #
NAS 1.26:183128 ..... N88-26736* #
NAS 1.60:2823 ..... N88-26684* #
NAS 1.60:2825 ..... N88-26907* #
NAS 1.60:2827 ..... N88-26344* #
NAS 1.71:NPO-17184-1-CU ..... N88-26541* #
NAS 1.77:20155 ..... N88-26454* #
NAS 1.77:20167 ..... N88-26453* #
NAS 1.77:20185 ..... N88-26462* #
NAS 1.77:20186 ..... N88-26483* #
NAS 1.77:20193 ..... N88-26455* #
NAS 1.77:20290 ..... N88-26431* #
NAS 1.77:20297 ..... N88-26484* #
NAS 1.77:20312 ..... N88-26617* #
NAS 1.77:20315 ..... N88-26338* #
NAS 1.77:20316 ..... N88-26337* #
NAS 1.77:20317 ..... N88-26842* #
NAS 1.77:20319 ..... N88-26381* #

NASA-CASE-LEW-14345-1 ..... N88-26404*

NASA-CASE-MSC-20912-1 ..... N88-26568*
NASA-CASE-MSC-20985-1 ..... N88-26398*

NASA-CASE-NPO-17157-1-CU N88-26596*
NASA-CASE-NPO-17184-1-CU ..... N88-26541* #

NASA-CR-4149 ..... N88-27134* #
NASA-CR-4167 ..... N88-26595* #
NASA-CR-4168 ..... N88-26343* #
NASA-CR-4169 ..... N88-26858* #
NASA-CR-172049 ..... N88-27135* #
NASA-CR-172063 ..... N88-26359* #
NASA-CR-177378 ..... N88-26807* #
NASA-CR-177393 ..... N88-27120* #
NASA-CR-177436 ..... N88-26367* #
NASA-CR-177459 ..... N88-26349* #
NASA-CR-177460 ..... N88-26348* #
NASA-CR-179357 ..... N88-26635* #
NASA-CR-179359 ..... N88-26760* #
NASA-CR-179364 ..... N88-26619* #
NASA-CR-179366 ..... N88-26825* #
NASA-CR-179435 ..... N88-26694* #
NASA-CR-180223 ..... N88-26403* #
NASA-CR-180400 ..... N88-26737* #
NASA-CR-181617 ..... N88-26397* #
NASA-CR-181670 ..... N88-26413* #
NASA-CR-181674 ..... N88-26873* #
NASA-CR-182121 ..... N88-26360* #
NASA-CR-182140 ..... N88-26497* #
NASA-CR-182152 ..... N88-27119* #
NASA-CR-182153 ..... N88-26616* #
NASA-CR-182154 ..... N88-26498* #
NASA-CR-182167 ..... N88-26336* #
NASA-CR-182480 ..... N88-26859* #
NASA-CR-182540 ..... N88-26909* #
NASA-CR-182550 ..... N88-26601* #
NASA-CR-182725 ..... N88-26495* #
NASA-CR-182861 ..... N88-26712* #
NASA-CR-182862 ..... N88-26716* #
NASA-CR-182897 ..... N88-26745* #
NASA-CR-182939 ..... N88-26823* #
NASA-CR-182956 ..... N88-26911* #
NASA-CR-182975 ..... N88-26710* #
NASA-CR-182984 ..... N88-26464* #

NASA-CR-183026 ..... N88-27108* #
NASA-CR-183036 ..... N88-26711* #
NASA-CR-183053 ..... N88-26589* #
NASA-CR-183058 ..... N88-27121* #
NASA-CR-183059 ..... N88-26688* #
NASA-CR-183060 ..... N88-26347* #
NASA-CR-183061 ..... N88-26332* #
NASA-CR-183062 ..... N88-26603* #
NASA-CR-183064 ..... N88-26941* #
NASA-CR-183066 ..... N88-26747* #
NASA-CR-183067 ..... N88-26407* #
NASA-CR-183069 ..... N88-26289* #
NASA-CR-183070 ..... N88-26860* #
NASA-CR-183078 ..... N88-26545* #
NASA-CR-183082 ..... N88-26693* #
NASA-CR-183089 ..... N88-26867* #
NASA-CR-183098 ..... N88-27137* #
NASA-CR-183099 ..... N88-27136* #
NASA-CR-183101 ..... N88-26335* #
NASA-CR-183110 ..... N88-26675* #
NASA-CR-183111 ..... N88-27146* #
NASA-CR-183115 ..... N88-26567* #
NASA-CR-183117 ..... N88-26759* #
NASA-CR-183118 ..... N88-26778* #
NASA-CR-183119 ..... N88-26618* #
NASA-CR-183124 ..... N88-26565* #
NASA-CR-183128 ..... N88-26736* #

NASA-SP-7011(313) N88-26800*

NASA-TM-4036 ..... N88-27144* #
NASA-TM-4041 ..... N88-27133* #
NASA-TM-4049 ..... N88-26763* #
NASA-TM-4050 ..... N88-26374* #
NASA-TM-4051 ..... N88-26389* #
NASA-TM-4053 ..... N88-26935* #
NASA-TM-77480 ..... N88-26615* #
NASA-TM-100068 ..... N88-26342* #
NASA-TM-100182 ..... N88-26376* #
NASA-TM-100183 ..... N88-26377* #
NASA-TM-100325 ..... N88-26387* #
NASA-TM-100439 ..... N88-26361* #
NASA-TM-100567 ..... N88-26870* #
NASA-TM-100633 ..... N88-26394* #
NASA-TM-100637 ..... N88-26913* #
NASA-TM-100641 ..... N88-26481* #
NASA-TM-100658 ..... N88-26885* #
NASA-TM-100659 ..... N88-26566* #
NASA-TM-100893 ..... N88-26644* #
NASA-TM-100902 ..... N88-26539* #
NASA-TM-100911 ..... N88-26340* #
NASA-TM-100943 ..... N88-26436* #
NASA-TM-100958 ..... N88-26430* #
NASA-TM-100961 ..... N88-26679* #
NASA-TM-100963 ..... N88-26401* #
NASA-TM-100965 ..... N88-26402* #
NASA-TM-100967 ..... N88-26482* #
NASA-TM-100973 ..... N88-26645* #
NASA-TM-100984 ..... N88-26744* #
NASA-TM-100985 ..... N88-26795* #
NASA-TM-100991 ..... N88-26378* #
NASA-TM-100998 ..... N88-26634* #
NASA-TM-101002 ..... N88-26709* #
NASA-TM-101134 ..... N88-26385 #
NASA-TM-101159 ..... N88-27142* #
NASA-TM-101175 ..... N88-26544* #
NASA-TM-101294 ..... N88-26328* #
NASA-TM-101295 ..... N88-26641* #
NASA-TM-101296 ..... N88-26732* #

NASA-TP-2823 ..... N88-26684* #
NASA-TP-2825 ..... N88-26907* #
NASA-TP-2827 ..... N88-26344* #

NASA-TT-20155 ..... N88-26454* #
NASA-TT-20167 ..... N88-26453* #
NASA-TT-20185 ..... N88-26462* #
NASA-TT-20186 ..... N88-26483* #
NASA-TT-20193 ..... N88-26455* #
NASA-TT-20290 ..... N88-26431* #
NASA-TT-20297 ..... N88-26484* #
NASA-TT-20312 ..... N88-26617* #
NASA-TT-20315 ..... N88-26338* #
NASA-TT-20316 ..... N88-26337* #
NASA-TT-20317 ..... N88-26842* #
NASA-TT-20319 ..... N88-26381* #

NBS/SP-500/151 ..... N88-27109 #

NBSIR-88/3066 ..... N88-26466 #
NBSIR-88/3748 ..... N88-26572 #

NCAR/TN-302-STR ..... N88-26748 #

NCEL-CR-88.008 ..... N88-26697 #

NLR-MP-86010-U ..... N88-26366 #
NLR-MP-86035-U ..... N88-26341 #
NLR-MP-86042-U ..... N88-26629 #
NLR-MP-86070-U ..... N88-26871 #
NLR-MP-86071-U ..... N88-26564 #
NLR-MP-87012-U ..... N88-26368 #
NLR-MP-87014-U ..... N88-26719 #
NLR-MP-87015-U ..... N88-26844 #
NLR-MP-87017-U ..... N88-26678 #
NLR-MP-87018-U ..... N88-26358 #
NLR-MP-87029-U ..... N88-26373 #
NLR-MP-87049-U ..... N88-26706 #
NLR-MP-87052-U ..... N88-26707 #

NLR-TR-86057-4 ..... N88-26627 #
NLR-TR-86080-U ..... N88-26677 #
NLR-TR-86102-U ..... N88-26628 #

NOAA-TM-ERL-PMEL-75 ..... N88-26765 #
NOAA-TM-ERL-PMEL-76 ..... N88-26780 #

NOSC/TD-1193 ..... N88-26559 #
NOSC/TD-1209-PT-1/2-VOL-1 ..... N88-26555 #
NOSC/TD-1209-PT-3-VOL-2 ..... N88-26554 #
NOSC/TD-1227 ..... N88-26674 #

NPS52-88-001 ..... N88-26836 #

NTSB-AAR-88-03 ..... N88-26346 #
NTSB-AAR-88-04 ..... N88-26345 #

NU-SML-TR-88-1 ..... N88-26700 #
NU-SML-TR-88-2 ..... N88-26701 #
NU-SML-TR-88-3 ..... N88-26702 #

ODU/ICAM-88-102 ..... N88-26618* #

ONERA-NT-1987 ..... N88-27095 #
ONERA-NT-1987-2 ..... N88-26631 #
ONERA-NT-1987-4 ..... N88-27124 #
ONERA-NT-1987-5 ..... N88-26708 #
ONERA-NT-1987-8 ..... N88-26632 #

ONERA-TP-648 ..... N88-26381* #

ONR-2-10 ..... N88-26494 #
ONR-88-1 ..... N88-26805 #

ORNL-6435 ..... N88-26437 #

ORNL/FEDC-87/5 ..... N88-26962 #

ORNL/M-462 ..... N88-26489 #
ORNL/M-548 ..... N88-26461 #

ORNL/TM-10192 ..... N88-26607 #
ORNL/TM-10570 ..... N88-26740 #
ORNL/TM-10629 ..... N88-26899 #
ORNL/TM-10704 ..... N88-26791 #
ORNL/TM-10719 ..... N88-27104 #
ORNL/TM-10743-PT-1/2 ..... N88-27071 #
ORNL/TM-10763 ..... N88-26352 #
ORNL/TM-10770 ..... N88-26855 #

PAPER-LBS-88-016 ..... N88-26382 #

PB88-105424 ..... N88-26831 #
PB88-106000 ..... N88-27140 #
PB88-107412 ..... N88-26370 #
PB88-108154 ..... N88-27110 #
PB88-109954 ..... N88-27111 #
PB88-113840 ..... N88-26815 #
PB88-116298 ..... N88-26906 #
PB88-118781 ..... N88-26353 #
PB88-121579 ..... N88-27114 #
PB88-124664 ..... N88-26892 #
PB88-124672 ..... N88-26720 #
PB88-125729 ..... N88-26777 #
PB88-126354 ..... N88-26810 #
PB88-126610 ..... N88-26891 #
PB88-126867 ..... N88-26897 #
PB88-126933 ..... N88-26857 #
PB88-126982 ..... N88-26536 #
PB88-127519 ..... N88-26341 #
PB88-127606 ..... N88-26890 #
PB88-131925 ..... N88-26735 #
PB88-173851 ..... N88-26761 #
PB88-182571 ..... N88-26910 #
PB88-183637 ..... N88-26781 #
PB88-186192 ..... N88-26547 #
PB88-186226 ..... N88-26390 #
PB88-186572 ..... N88-26417 #
PB88-188446 ..... N88-27108* #
PB88-188701 ..... N88-26780 #
PB88-190483 ..... N88-26739 #
PB88-191374 ..... N88-26762 #
PB88-191382 ..... N88-26912 #
PB88-192620 ..... N88-26748 #
PB88-192703 ..... N88-26765 #
PB88-193065 ..... N88-26764 #
PB88-193289 ..... N88-27109 #
PB88-193446 ..... N88-26796 #
PB88-193602 ..... N88-26573 #
PB88-194139 ..... N88-26546 #
PB88-194733 ..... N88-27139 #
PB88-194741 ..... N88-27138 #
PB88-196530 ..... N88-26572 #
PB88-196621 ..... N88-26439 #
PB88-197165 ..... N88-26463 #
PB88-201553 ..... N88-26466 #
PB88-202668 ..... N88-26714 #
PB88-202676 ..... N88-26602 #
PB88-203195 ..... N88-26416 #
PB88-910404 ..... N88-26346 #
PB88-910405 ..... N88-26345 #

PDRC-88-01 ..... N88-26834 #

PITHA-87/02 ..... N88-27122 #

PML-1987-C-18 ..... N88-26417 #
PML-1987-C1 ..... N88-26537 #

PNL-SA-15688 ..... N88-26741 #

PPG-1131 ..... N88-26989 #

PR-150-6549-1 ..... N88-26347* #

PSP-R1-1438 ..... N88-26981 #

PWA-FR-18301-VOL-1 ..... N88-26371 #

QAUM-87/27 ..... N88-26912 #

QTPR-6 ..... N88-26612 #

RADC-TR-87-166-VOL-1 ..... N88-26840 #
RADC-TR-87-179 ..... N88-26833 #
RADC-TR-87-257 ..... N88-26553 #
RADC-TR-88-23 ..... N88-26863 #

RAL-87-015 ..... N88-27140 #

RAND-P-7357 ..... N88-26903 #
RAND-P-7404 ..... N88-26898 #

RAND/N-2660-DARPA ..... N88-26839 #

RC-648676 ..... N88-26486 #

REPT-1/87 ..... N88-26538 #
REPT-22 ..... N88-26573 #
REPT-23 ..... N88-26546 #
REPT-46-444 ..... N88-26365 #
REPT-49/87 ..... N88-27118 #
REPT-87-FU-01 ..... N88-26810 #
REPT-87-26 ..... N88-26897 #
REPT-87-68 ..... N88-26846 #
REPT-87-72 ..... N88-27105 #
REPT-87-73 ..... N88-27106 #
REPT-87-75 ..... N88-26781
REPT-87-80 ..... N88-26886 #
REPT-87-81 ..... N88-26847 #
REPT-87-82 ..... N88-26887 #
REPT-87-83 ..... N88-26888 #
REPT-87-84 ..... N88-26895 #
REPT-87-87 ..... N88-26848 #
REPT-87-89 ..... N88-26896 #
REPT-87-91-PT-1 ..... N88-26864 #
REPT-88-9S52-SUPER-R1 ..... N88-27091 #
REPT-88-02 ..... N88-26889 #
REPT-88B0124 ..... N88-27144* #
REPT-88B0167 ..... N88-26389* #
REPT-88B0189 ..... N88-26763* #
REPT-1987-27 ..... N88-26547 #
REPT-8767 ..... N88-26845 #

RFP-4208 ..... N88-26516 #

RSL-5870-5 ..... N88-26710* #

RTI/3744/04-01F ..... N88-26739 #

SAND-86-0083 ..... N88-26419 #
SAND-87-0673 ..... N88-26866 #
SAND-87-1088 ..... N88-26861 #
SAND-87-1730C ..... N88-26726 #
SAND-87-1904C ..... N88-26661 #
SAND-87-2167C ..... N88-26660 #
SAND-87-2521C ..... N88-26766 #
SAND-87-2588C ..... N88-26467 #

SAND-87-2673C ..... N88-27069 #
SAND-87-2676C ..... N88-26691 #
SAND-87-2728C ..... N88-26942 #
SAND-87-3054C ..... N88-26876 #
SAND-87-3081C ..... N88-26549 #
SAND-87-3084C ..... N88-26961 #
SAND-87-3094 ..... N88-26578 #
SAND-88-0119 ..... N88-26681 #
SAND-88-0318C ..... N88-26465 #
SAND-88-0372C ..... N88-26875 #
SAND-88-0448 ..... N88-26680 #
SAND-88-0540C ..... N88-26351 #
SAND-88-0625C ..... N88-26960 #
SAND-88-0748C ..... N88-27070 #

SASR-20 ..... N88-26737* #
SASR-21 ..... N88-26737* #
SASR-22 ..... N88-26737* #

SD-TR-87-57 ..... N88-26990 #
SD-TR-87-61 ..... N88-26933 #
SD-TR-87-64 ..... N88-26587 #
SD-TR-88-04 ..... N88-27141 #
SD-TR-88-07 ..... N88-26560 #
SD-TR-88-09 ..... N88-26755 #
SD-TR-88-10 ..... N88-26410 #
SD-TR-88-12 ..... N88-26396 #
SD-TR-88-17 ..... N88-26586 #

SERI/STR-211-3216 ..... N88-27060 #
SERI/STR-217-3133 ..... N88-26721 #

SFCC-30 ..... N88-26537 #

SFCC/PUB-42 ..... N88-26417 #

SGD-522-PT-1 ..... N88-27139 #
SGD-522-PT-2 ..... N88-27138 #

SP-RAPP-1988:03 ..... N88-26910 #

SR-1 ..... N88-26752 #
SR-2 ..... N88-26754 #

SRI-ESU-2918 ..... N88-26863 #

SRI-MP-88-007 ..... N88-26583 #

SR87-R-5334-12 ..... N88-26463 #

SU-SLAC-PUB-4517 ..... N88-26647 #

SWRI-06-1364 ..... N88-26612 #
SWRI-06-8972/2 ..... N88-26452 #

TAE-592 ..... N88-26515 #

TAMRF-5802-88-02 ..... N88-26332* #

TI88-007726 ..... N88-26973 #
TI88-008370 ..... N88-26421 #
TI88-010064 ..... N88-26609 #

TN-1310-NR-01-REV-H ..... N88-26698 #

TPR-33 ..... N88-26582 #

TR-5 ..... N88-26412 #
TR-5 ..... N88-26696 #
TR-63 ..... N88-26426 #
TR-87-15-VOL-1 ..... N88-26809 #
TR-88-3 ..... N88-26840 #
TR-220 ..... N88-26894 #
TR-254 ..... N88-26893 #
TR-294 ..... N88-26821 #
TR-0086(6925-05)-1 ..... N88-26560 #
TR-0086(6925-07)-3 ..... N88-26586 #
TR-0086(6930-01)-14 ..... N88-26990 #
TR-0086A(2930-02)-1 ..... N88-26933 #
TR-0086A(2935-06)-4 ..... N88-26410 #
TR-0086A(2940-01)-1 ..... N88-27141 #
TR-0086A(2940-06)-4 ..... N88-26755 #
TR-0086A(2940-06)-6 ..... N88-26396 #
TR-0086A(2945-01)-4 ..... N88-26587 #

TTC-0642 ..... N88-26419 #

TW-281 ..... N88-26390 #

UB/PSEEE/RR-396 ..... N88-26831 #

UCB-PTH-87/52 ..... N88-27145 #

UCB/ERL-M-88/24 ..... N88-26971 #

UCID-20664-87 ..... N88-26812 #

UCID-21285 ..... N88-26551 #
UCID-21301 ..... N88-26577 #
UCID-21304 ..... N88-26648 #
UCID-21325 ..... N88-26878 #
UCID-21349 ..... N88-26656 #
UCID-21350 ..... N88-26826 #
UCID-21360 ..... N88-26776 #
UCID-21389 ..... N88-26391 #
UCID-21391 ..... N88-26955 #
UCID-21395 ..... N88-26496 #
UCID-21403 ..... N88-26994 #

UCL-CS-TR-125 ..... N88-26815 #
UCL-CS-TR-133 ..... N88-26906 #

UCRL-53843 ..... N88-26594 #
UCRL-96433 ..... N88-27125 #
UCRL-96654 ..... N88-26993 #
UCRL-96753 ..... N88-26657 #
UCRL-97327 ..... N88-26946 #
UCRL-97385 ..... N88-26967 #
UCRL-97871 ..... N88-27113 #
UCRL-98006 ..... N88-26767 #
UCRL-98043 ..... N88-26576 #
UCRL-98068 ..... N88-26655 #
UCRL-98086 ..... N88-26856 #
UCRL-98097 ..... N88-27128 #
UCRL-98100 ..... N88-26664 #
UCRL-98168 ..... N88-26418 #
UCRL-98230 ..... N88-26460 #
UCRL-98245 ..... N88-26550 #
UCRL-98306 ..... N88-26970 #
UCRL-98441 ..... N88-26925 #
UCRL-98460 ..... N88-27096 #
UCRL-98470 ..... N88-27067 #
UCRL-98600 ..... N88-26972 #
UCRL-98684 ..... N88-27096 #

UILU-ENG-88-1725 ..... N88-26830 #
UILU-ENG-88-2228 ..... N88-26860* #

UIUCDCS-R-88-1420 ..... N88-26830 #

UKC/COMPUTING LAB-45 ..... N88-27110 #

ULRF-439/CAR ..... N88-26753 #

UPITT/LRDC/ONR/KBC-10 ..... N88-26801 #

US-PATENT-APPL-SN-116810 ..... N88-26596*
US-PATENT-APPL-SN-195225 ..... N88-26541* #
US-PATENT-APPL-SN-831193 ..... N88-26568*
US-PATENT-APPL-SN-904134 ..... N88-26396*
US-PATENT-APPL-SN-924474 ..... N88-26404*

US-PATENT-CLASS-104-35 ..... N88-26398*
US-PATENT-CLASS-104-49 ..... N88-26398*
US-PATENT-CLASS-104-172.1 ..... N88-26398*
US-PATENT-CLASS-244-159 ..... N88-26398*
US-PATENT-CLASS-260-386 ..... N88-26404*
US-PATENT-CLASS-260-389 ..... N88-26404*
US-PATENT-CLASS-260-395 ..... N88-26404*
US-PATENT-CLASS-331-3 ..... N88-26596*
US-PATENT-CLASS-331-94.1 ..... N88-26596*
US-PATENT-CLASS-331-162 ..... N88-26596*
US-PATENT-CLASS-342-43 ..... N88-26568*
US-PATENT-CLASS-342-51 ..... N88-26568*
US-PATENT-CLASS-342-125 ..... N88-26568*
US-PATENT-CLASS-342-127 ..... N88-26568*
US-PATENT-CLASS-549-241 ..... N88-26404*

US-PATENT-4,757,278 ..... N88-26596*
US-PATENT-4,757,315 ..... N88-26568*
US-PATENT-4,757,767 ..... N88-26398*
US-PATENT-4,758,380 ..... N88-26404*

UVA/525415/EE88/111 ..... N88-26552 #
UVA/525658/EE88/102 ..... N88-27092 #

U1-780130-F ..... N88-26359* #

W-7/86 ..... N88-26485 #

WHOI-87-48 ..... N88-26784 #
WHOI-88-4 ..... N88-26783 #

WP-29-86-87-REV ..... N88-26838 #

☆ U.S. GOVERNMENT PRINTING OFFICE: 1988— 202-150/80018

FEDERAL REGIONAL DEPOSITORY LIBRARIES

ALABAMA

AUBURN UNIV. AT MONTGOMERY LIBRARY
Documents Department
Montgomery, AL 36193
(205) 271-9650

UNIV. OF ALABAMA LIBRARY
Documents Dept.-Box S
University, AL 35486
(205) 348-6046

ARIZONA

DEPT. OF LIBRARY, ARCHIVES AND PUBLIC RECORDS
Third Floor—State Cap.
1700 West Washington
Phoenix, AZ 85007
(602) 255-4121

UNIVERSITY OF ARIZONA LIB.
Government Documents Dept.
Tucson, AZ 85721
(602) 621-6433

ARKANSAS

ARKANSAS STATE LIBRARY
One Capitol Mall
Little Rock, AR 72201
(501) 371-2326

CALIFORNIA

CALIFORNIA STATE LIBRARY
Govt. Publications Section
P.O. Box 2037
Sacramento, CA 95809
(916) 324-4863

COLORADO

UNIV OF COLORADO LIB.
Government Pub. Division
Campus Box 184
Boulder, CO 80309
(303) 492-8834

DENVER PUBLIC LIBRARY
Govt. Pub. Department
1357 Broadway
Denver, CO 80203
(303) 571-2131

CONNECTICUT

CONNECTICUT STATE LIBRARY
Government Documents Unit
231 Capitol Avenue
Hartford, CT 06106
(203) 566-7029

FLORIDA

UNIV. OF FLORIDA LIBRARIES
Library West
Documents Department
Gainesville, FL 32611
(904) 392-0367

GEORGIA

UNIV. OF GEORGIA LIBRARIES
Government Reference Dept.
Athens, GA 30602
(404) 542-8949

HAWAII

UNIV. OF HAWAII LIBRARY
Govt. Documents Collection
2550 The Mall
Honolulu, HI 96822
(808) 948-8230

IDAHO

UNIV. OF IDAHO LIBRARY
Documents Section
Moscow, ID 83843
(208) 885-6344

ILLINOIS

ILLINOIS STATE LIBRARY
Information Services Branch
Centennial Building
Springfield, IL 62756
(217) 782-5185

INDIANA

INDIANA STATE LIBRARY
Serials Documents Section
140 North Senate Avenue
Indianapolis, IN 46204
(317) 232-3686

IOWA

UNIV. OF IOWA LIBRARIES
Govt. Documents Department
Iowa City, IA 52242
(319) 353-3318

KANSAS

UNIVERSITY OF KANSAS
Doc. Collect—Spencer Lib.
Lawrence, KS 66045-2800
(913) 864-4662

KENTUCKY

UNIV. OF KENTUCKY LIBRARIES
Govt. Pub. Department
Lexington, KY 40506-0039
(606) 257-3139

LOUISIANA

LOUISIANA STATE UNIVERSITY
Middleton Library
Govt. Docs. Dept.
Baton Rouge, LA 70803
(504) 388-2570

LOUISIANA TECHNICAL UNIV. LIBRARY
Documents Department
Ruston, LA 71272-0046
(318) 257-4962

MAINE

UNIVERSITY OF MAINE
Raymond H. Fogler Library
Tri-State Regional Documents Depository
Orono, ME 04469
(207) 581-1680

MARYLAND

UNIVERSITY OF MARYLAND
McKeldin Lib.—Doc. Div.
College Park, MD 20742
(301) 454-3034

MASSACHUSETTS

BOSTON PUBLIC LIBRARY
Government Docs. Dept.
Boston, MA 02117
(617) 536-5400 ext.226

MICHIGAN

DETROIT PUBLIC LIBRARY
Sociology Department
5201 Woodward Avenue
Detroit, MI 48202-4093
(313) 833-1409

MICHIGAN STATE LIBRARY
P.O. Box 30007
Lansing, MI 48909
(517) 373-1593

MINNESOTA

UNIVERSITY OF MINNESOTA
Government Pubs. Division
409 Wilson Library
309 19th Avenue South
Minneapolis, MN 55455
(612) 373-7870

MISSISSIPPI

UNIV. OF MISSISSIPPI LIB.
Documents Department
University, MS 38677
(601) 232-5857

MONTANA

UNIV. OF MONTANA
Mansfield Library
Documents Division
Missoula, MT 59812
(406) 243-6700

NEBRASKA

UNIVERSITY OF NEBRASKA - LINCOLN
Love Library
Documents Department
Lincoln, NE 68588-0410
(402) 472-2562

NEVADA

UNIVERSITY OF NEVADA LIB.
Govt. Pub. Department
Reno, NV 89557-0044
(702) 784-6579

NEW JERSEY

NEWARK PUBLIC LIBRARY
5 Washington Street
Newark, NJ 07101-0630
(201) 733-7812

NEW MEXICO

UNIVERSITY OF NEW MEXICO
Zimmerman Library
Government Pub. Dept.
Albuquerque, NM 87131
(505) 277-5441

NEW MEXICO STATE LIBRARY
Reference Department
325 Don Gaspar Avenue
Santa Fe, NM 87503
(505) 827-3826

NEW YORK

NEW YORK STATE LIBRARY
Empire State Plaza
Albany, NY 12230
(518) 474-5563

NORTH CAROLINA

UNIVERSITY OF NORTH CAROLINA AT CHAPEL HILL
Davis Library
BA/SS Documents Division
Chapel Hill, NC 27515
(919) 962-1151

NORTH DAKOTA

UNIVERSITY OF NORTH DAKOTA
Chester Fritz Library
Documents Department
Grand Forks, ND 58202
(701) 777-4629
In cooperation with North Dakota State Univ. Library

OHIO

STATE LIBRARY OF OHIO
Documents Department
65 South Front Street
Columbus, OH 43266-0334
(614) 462-7051

OKLAHOMA

OKLAHOMA DEPT. OF LIB.
Government Documents
200 NE 18th Street
Oklahoma City, OK 73105
(405) 521-2502, ext. 252

OKLAHOMA STATE UNIV. LIB.
Documents Department
Stillwater, OK 74078
(405) 624-6546

OREGON

PORTLAND STATE UNIV. LIB.
Documents Department
P.O. Box 1151
Portland, OR 97207
(503) 229-3673

PENNSYLVANIA

STATE LIBRARY OF PENN.
Government Pub. Section
P.O. Box 1601
Harrisburg, PA 17105
(717) 787-3752

TEXAS

TEXAS STATE LIBRARY
Public Services Department
P.O. Box 12927—Cap. Sta.
Austin, TX 78711
(512) 475-2996

TEXAS TECH. UNIV. LIBRARY
Govt. Documents Department
Lubbock, TX 79409
(806) 742-2268

UTAH

UTAH STATE UNIVERSITY
Merrill Library, U.M.C. 30
Logan, UT 84322
(801) 750-2682

VIRGINIA

UNIVERSITY OF VIRGINIA
Alderman Lib.—Public Doc.
Charlottesville, VA 22903-2498
(804) 924-3133

WASHINGTON

WASHINGTON STATE LIBRARY
Documents Section
Olympia, WA 98504
(206) 753-4027

WEST VIRGINIA

WEST VIRGINIA UNIV. LIB.
Documents Department
Morgantown, WV 26506-6069
(304) 293-3640

WISCONSIN

MILWAUKEE PUBLIC LIBRARY
814 West Wisconsin Avenue
Milwaukee, WI 53233
(414) 278-3065

ST. HIST LIB. OF WISCONSIN
Government Pub. Section
816 State Street
Madison, WI 53706
(608) 262-4347

WYOMING

WYOMING STATE LIBRARY
Supreme Ct. & Library Bld.
Cheyenne, WY 82002
(307) 777-5919

National Aeronautics and
Space Administration
Code NTT-4
Washington, D.C.
20546
Official Business
Penalty for Private Use, $300

SPECIAL FOURTH-CLASS RATE
POSTAGE & FEES PAID
NASA
PERMIT No. G 27

NASA

POSTMASTER: If Undeliverable (Section 158
Postal Manual) Do Not Return